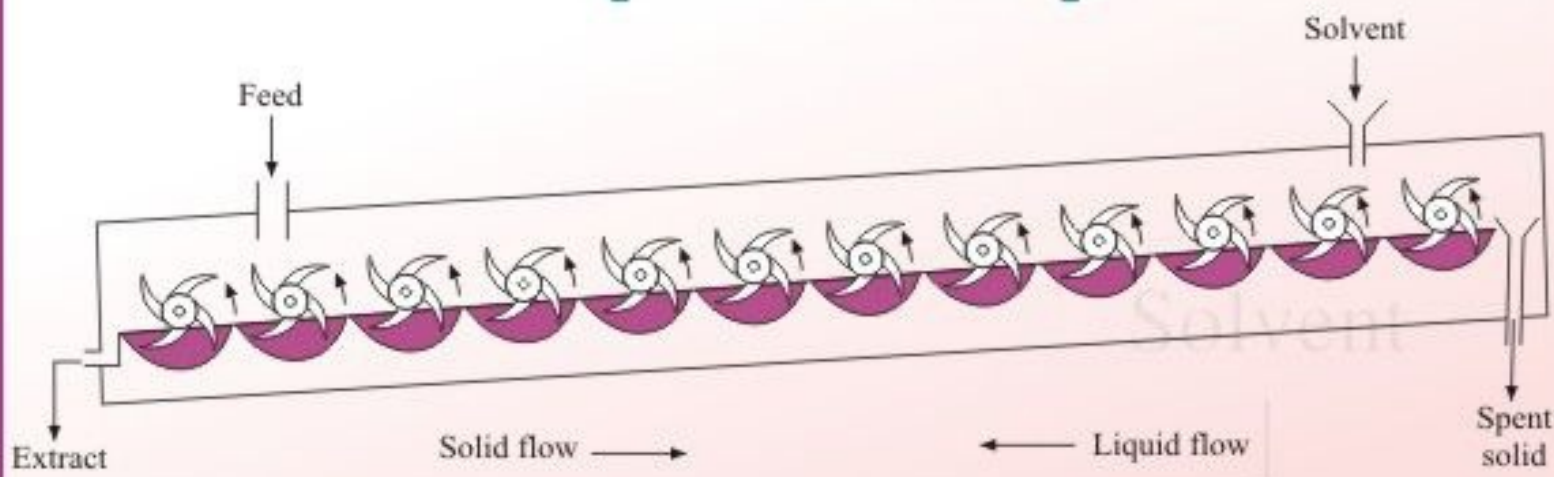


# Mass Transfer

## Principles and Operations



A.P. Sinha  
Parameswar De



**Uploaded by:**

## **Ebooks Chemical Engineering**

<https://www.facebook.com/pages/Ebooks-Chemical-Engineering/238197077030>

For More Books, softwares & tutorials Related to Chemical Engineering  
Join Us

@facebook: <https://www.facebook.com/pages/Ebooks-Chemical-Engineering/238197077030>

@facebook: <https://www.facebook.com/AllAboutChemcalEngineering>

@facebook: <https://www.facebook.com/groups/10436265147/>

**ADMIN:**

**I.W**

**<< If you like this Book, than support the author and BuY it >>**

# **MASS TRANSFER**

## **Principles and Operations**

**A.P. Sinha**

*Former Dean*

Faculty of Engineering

University of Burdwan

Bardhaman

**PARAMESWAR DE**

*Professor*

Department of Chemical Engineering

University of Calcutta

Kolkata

**PHI Learning Private Limited**

New Delhi-110001

2012

**MASS TRANSFER: Principles and Operations**

A.P. Sinha and Parameswar De

© 2012 by PHI Learning Private Limited, New Delhi. All rights reserved. No part of this book may be reproduced in any form, by mimeograph or any other means, without permission in writing from the publisher.

**ISBN-978-81-203-4541-6**

The export rights of this book are vested solely with the publisher.

Published by Asoke K. Ghosh, PHI Learning Private Limited, M-97, Connaught Circus, New Delhi-110001 and Printed by Mohan Makhiiani at Rekha Printers Private Limited, New Delhi-110020.

This book is dedicated by Parameswar De (the coauthor)  
to the memory of his parents  
and to the memory of  
A.P. Sinha (the first author) and his wife  
who both unfortunately expired before the book could be published

# Contents

Preface xv

## 1. Introduction 1–6

- 1.1 Direct Contact of Two Immiscible or Partially Miscible Phases 3
- 1.1.1 Gas/Vapour–Liquid Contact 3
- 1.1.2 Gas–Solid Contact 4
- 1.1.3 Liquid–Liquid Contact 4
- 1.1.4 Liquid–Solid Contact 4
- 1.2 Phases Separated by Membrane 5
- 1.3 Direct Contact of Miscible Phases 5
- 1.4 Classification of Mass Transfer Operations 5
- References 6

## 2. Diffusion 7–72

- 2.1 Introduction 7
- 2.2 Molecular Diffusion 8
  - 2.2.1 Concentration 8
  - 2.2.2 Velocity 8
  - 2.2.3 Frames of Reference 9
  - 2.2.4 Flux 9
- 2.3 Models of Diffusion 11
- 2.4 Fick's Law 12
- 2.5 Molecular Diffusion in Gases 14
  - 2.5.1 Steady-State Molecular Diffusion in a Binary Mixture Through a Constant Area 16
  - 2.5.2 Nonequimolar Counter-Diffusion of Two Components 21
  - 2.5.3 Multi-component Diffusion 21

2.5.4 Diffusion Through Variable Area (Truncated Cone) 23
2.5.5 Diffusion from a Sphere 25
2.6 Diffusion Coefficient or Diffusivity of Gases 26
2.6.1 Equivalence of Diffusivities 27
2.6.2 Determination of Gas Phase Diffusivity 28
2.7 Molecular Diffusion in Liquids 39
2.7.1 Diffusion of Component A Through Non-Diffusing B 40
2.7.2 Equimolar Counter-Diffusion of A and B 41
2.8 Liquid Phase Diffusivity 42
2.8.1 Prediction of Liquid Phase Diffusivity 43
2.8.2 Experimental Determination of Liquid Phase Diffusivity 46
2.9 Diffusion in Turbulent Stream—Eddy Diffusion 46
2.10 Diffusion in Solids 50
2.10.1 Steady-State Diffusion in Solids 50
2.10.2 Transient or Unsteady-State Diffusion 51
2.11 Some Special Types of Diffusion in Solids 60
Nomenclature 63
Numerical Problems 64
Short and Multiple Choice Questions 70
References 71

### **3. Mass Transfer Coefficients and Analogy Equations 73–103**

3.1 Introduction 73
3.2 Types of Mass Transfer Coefficients 74
3.2.1 Diffusion of One Component Through the Stagnant Layer of Another Component 75
3.2.2 Equal Molal Counter-Diffusion of Two Components 76
3.2.3 Volumetric Mass Transfer Coefficients 77
3.2.4 Mass Transfer Coefficient in Laminar Flow 78
3.3 Dimensionless Groups in Mass Transfer 80
3.4 Analogy between Momentum, Heat and Mass Transfer 84
3.4.1 Analogy between Momentum and Heat Transfer—Reynold's Analogy 84
3.4.2 Analogy between Heat and Mass Transfer 86
3.5 Mass Transfer Coefficients for Simple Geometrical Shapes 91
3.5.1 Mass Transfer in Flow Past Flat Plates 91
3.5.2 Mass Transfer in Fluids Flowing Through Pipes 93
3.5.3 Mass Transfer in Single Phase Flow Through Packed Bed 94
3.5.4 Mass Transfer Coefficient for Flow Past a Solid Sphere 95
3.5.5 Mass Transfer in Flow Normal to a Single Cylinder 96
3.5.6 Mass Transfer in the Neighbourhood of a Rotating Disk 96

3.5.7 Mass Transfer to Drops and Bubbles 96

Nomenclature 97

Numerical Problems 99

Short and Multiple Choice Questions 100

References 102

## **4. Interphase Mass Transfer 104–122**

4.1 Introduction 104

4.2 Theories of Interphase Mass Transfer 111

4.2.1 The Two-Film or Two Resistance Theory 111

4.2.2 The Penetration Theory 113

4.2.3 Surface Renewal Theory 115

4.2.4 Film Penetration Model 115

4.2.5 Surface-Stretch Theory 115

4.2.6 The Boundary Layer Theory 115

Nomenclature 117

Numerical Problems 118

Short and Multiple Choice Questions 121

References 122

## **5. Methods of Operation and Computation 123–158**

5.1 Introduction 123

5.2 Stage-wise Contact 124

5.2.1 Single-Stage Operation 124

5.2.2 Batch Operation 126

5.2.3 Multi-Stage Operation 127

5.2.4 Cross-Flow Cascade 127

5.2.5 Counter-Current Multi-Stage Cascade 129

5.2.6 Design Procedure for Concentrated Gases 135

5.3 Continuous Differential Contact 135

5.3.1 Material Balance—The Operating Line 135

5.3.2 Estimation of Tower Height 138

5.4 Relation between Overall and Individual Phase Transfer Units 148

Nomenclature 150

Numerical Problems 151

Short and Multiple Choice Questions 156

References 157

## **6. Equipment for Gas–Liquid Contact 159–208**

6.1 Introduction	159
6.2 Gas Dispersed	159
6.2.1 Sparged Vessel	160
6.2.2 Mechanically Agitated Device	160
6.2.3 Plate Column	160
6.2.4 Plate Efficiencies	173
6.3 Liquid Dispersed	176
6.3.1 Simulated Packed Tower	176
6.3.2 Packed Tower	180
6.3.3 Spray Tower and Spray Chamber	195
6.3.4 Venturi Scrubber	196
6.3.5 Pulsed Column	199
Nomenclature	200
Numerical Problems	202
Short and Multiple Choice Questions	204
References	207

## **7. Gas Absorption 209–255**

7.1 Introduction	209
7.2 Equilibrium Relations	210
7.2.1 Raoult's Law	211
7.2.2 Henry's Law	212
7.3 Nomenclature and Material Balance	213
7.4 Selection of Solvent	215
7.5 Types of Equipment and Methods of Operation	215
7.5.1 Minimum Solvent Rate—Actual Solvent Rate	217
7.5.2 Flooding—Tower Diameter	218
7.6 Stage-wise Contact—Number of Plates (Stages)	221
7.6.1 Graphical Method	221
7.6.2 Algebraic Method	221
7.7 Absorption of Concentrated Gases	224
7.8 Estimation of Packing Height—Mass Transfer Rate Calculations	225
7.8.1 Absorption from Concentrated Gases	226
7.8.2 Simplified Procedure for Lean Gases	227
7.9 Multicomponent Absorption	238
7.9.1 Absorption of Concentrated Gases—Graphical Method	240
7.9.2 Absorption of Lean Gases—Algebraic Method	241
7.10 Absorption with Chemical Reaction	241
7.10.1 Rapid Reaction	242
7.10.2 Slow Reaction	243

7.11 Reactive Absorption and Stripping 244

Nomenclature 245

Numerical Problems 246

Short and Multiple Choice Questions 252

References 255

## **8. Distillation 256–333**

8.1 Introduction 256

8.2 Vapour–Liquid Equilibrium 256

8.2.1 Vapour–Liquid Equilibrium at Constant Pressure 257

8.2.2 Vapour–Liquid Equilibrium at Constant Temperature 259

8.2.3 Raoult’s Law 259

8.2.4 Positive Deviation from Ideality 260

8.2.5 Negative Deviation from Ideality 262

8.3 Prediction of Equilibrium Data 263

8.4 Multicomponent Equilibria 267

8.5 Methods of Distillation 269

8.5.1 Single-Stage Distillation 269

8.5.2 Continuous Multistage Distillation—Binary Systems 279

8.5.3 Rectification—Methods of Calculation 280

8.5.4 Determination of Number of Theoretical Plates 281

8.6 Use of Open Steam 294

8.7 Side Stream 295

8.8 Plate Efficiency 295

8.9 Continuous Differential Contact Distillation—Packed Tower 297

8.10 Multicomponent Distillation 299

8.11 Methods of Calculation 300

8.11.1 Approximate Methods 300

8.11.2 Exact Methods 301

8.12 Distillation Equipment and Energy Conservation Practices 303

8.13 Distillation of Constant Boiling Mixtures 307

8.13.1 Azeotropic Distillation 308

8.13.2 Extractive Distillation 309

8.14 Molecular Distillation 310

8.15 Fractional Distillation 311

8.16 Cryogenic Distillation 312

8.17 Reactive Distillation 314

Nomenclature 316

Numerical Problems 317

Short and Multiple Choice Questions 330

## **9. Humidification Operations 334–370**

- 9.1 Introduction 334
- 9.2 Terminologies Commonly Used 335
- 9.3 Adiabatic Saturation Temperature 338
- 9.4 Wet-Bulb Temperature 339
- 9.5 Operation Involving Gas–Liquid Contact 344
  - 9.5.1 General Equations 345
  - 9.5.2 Enthalpy Balance 345
- 9.6 Water Cooling 346
- 9.7 Adiabatic Humidification—Cooling 350
- 9.8 Cooling Range and Approach 352
- 9.9 Nonadiabatic Operations: Evaporative Cooling 354
- 9.10 Equipment for Air–Water Contact 355
- 9.11 Some Important Accessories and Operational Features of Cooling Towers 360
  - 9.11.1 Accessories 360
  - 9.11.2 Operational Features 362
- Nomenclature 364
- Numerical Problems 365
- Short and Multiple Choice Questions 368
- References 370

## **10. Liquid–Liquid Extraction 371–426**

- 10.1 Introduction 371
- 10.2 Terminologies Used 372
- 10.3 Extraction Equilibrium 373
  - 10.3.1 Ternary Equilibrium 373
  - 10.3.2 System of 3 Liquids, One Pair Partially Miscible 374
  - 10.3.3 System of 3 Liquids, Two Pairs Partially Miscible 375
  - 10.3.4 Liquid–Liquid Equilibria on Solvent-Free Coordinates 375
- 10.4 Selection of Solvent 376
- 10.5 Methods of Extraction 377
  - 10.5.1 Stage-wise Contact 377
  - 10.5.2 Continuous Differential Contact 393
- 10.6 Extraction by Supercritical Fluids 396
- 10.7 Equipment for Liquid–Liquid Extraction 399
  - 10.7.1 Phase Dispersion by Mechanical Agitation 402
  - 10.7.2 Phase Dispersion by Gravity 407

10.7.3 Phase Dispersion by Pulsation	408
10.7.4 Phase Dispersion by Reciprocating Action	409
10.7.5 Phase Dispersion by Centrifugal Force	410
10.8 Estimation of Some Important Parameters in Agitated Liquid Dispersions	411
10.9 Reactive Extraction	414
Nomenclature	414
Numerical Problems	416
Short and Multiple Choice Questions	423
References	425

## **11. Leaching 427–452**

11.1 Introduction	427
11.2 Classification	427
11.3 Terminologies Used	428
11.4 Solid–Liquid Equilibria	428
11.5 Leaching Operation	430
11.6 Methods of Calculation	431
11.6.1 Single Stage Leaching	431
11.6.2 Multistage Cross-current Leaching	432
11.6.3 Multistage Counter-current Leaching	433
11.6.4 Algebraic Method	437
11.7 Leaching Equipment	440
11.7.1 Unsteady-State Equipment	440
11.7.2 Steady-State Equipment	442
Nomenclature	447
Numerical Problems	448
Short and Multiple Choice Questions	450
References	452

## **12. Drying 453–502**

12.1 Introduction	453
12.2 Drying Equilibria	453
12.3 Some Important Terminologies	454
12.4 Mechanism and Theory of Drying	455
12.5 Drying Rate Curve	456
12.5.1 Constant Rate Period	457
12.5.2 Cross Circulation Drying	457
12.5.3 Falling Rate Period	460

12.5.4 Through-Circulation Drying	461
12.6 Continuous Drying	462
12.7 Rate of Batch Drying	463
12.7.1 Cross-Circulation Drying	463
12.7.2 Through-Circulation Drying	469
12.8 Rate of Continuous Drying	469
12.9 Drying Equipment	473
12.10 Batch Driers	473
12.10.1 Direct Driers	474
12.10.2 Indirect Driers	475
12.11 Continuous Driers	478
12.11.1 Direct Driers	478
12.11.2 Indirect Driers	488
12.12 Selection of Drier	488
Nomenclature	491
Numerical Problems	493
Short and Multiple Choice Questions	499
References	501

## **13. Crystallization 503–534**

13.1 Introduction	503
13.1.1 Crystal Form	504
13.1.2 Liquid Crystals	504
13.2 Solid–Liquid Equilibria	505
13.3 Material and Energy Balance	506
13.3.1 Material Balance	506
13.3.2 Heat Balance	508
13.4 The Crystallization Process	508
13.5 Methods of Nucleation	512
13.5.1 Formation of Nuclei in Situ	512
13.5.2 Addition of Nuclei from Outside	512
13.6 Crystal Growth	513
13.6.1 Rate of Crystal Growth	513
13.6.2 Effect of Impurities on Crystal Growth	515
13.6.3 Heat Effects	515
13.6.4 Heat of Crystallization	515
13.6.5 The $\Delta L$ Law	516
13.7 Fractional Crystallization	517
13.8 Crystallization and Precipitation	517
13.9 Caking of Crystals	517

13.10 Crystallization Equipment	518
13.11 Working Principles of Some Important Crystallizers	518
13.11.1 Agitated Batch Crystallizer	518
13.11.2 Swenson–Walker Crystallizer	519
13.11.3 Circulating Liquor Crystallizers	521
13.11.4 Circulating Magma Crystallizers	522
13.12 Melt Crystallization	524
13.12.1 Suspension Based Melt Crystallization	525
13.12.2 Progressive Freezing Crystallization	526
13.13 Purification	528
13.14 Reactive Crystallization	529
Nomenclature	530
Numerical Problems	531
Short and Multiple Choice Questions	532
References	534

## **14. Adsorption and Chromatography 535–593**

14.1 Introduction	535
14.2 Types of Adsorption	535
14.3 Adsorption Equilibrium	536
14.3.1 Langmuir Isotherm	538
14.3.2 Freundlich Isotherm	539
14.3.3 Braunauer-Emmet-Teller Isotherm	541
14.4 Heat of Adsorption	542
14.5 Some Desirable Qualities of Adsorbents	543
14.6 Some Common Adsorbents	543
14.7 Adsorption Operations	547
14.7.1 Single Stage Operation	548
14.7.2 Multistage Cross-current Operation	552
14.7.3 Multistage Counter-Current Operation	553
14.7.4 Continuous Counter-Current Differential Contact Operation	556
14.7.5 Pressure Swing Adsorption	557
14.8 Mechanism of Adsorption	558
14.9 Regeneration of the Adsorbent	564
14.9.1 Temperature Swing Regeneration	565
14.9.2 Pressure Swing Regeneration	566
14.9.3 High Temperature PSA Process	569
14.10 Adsorption Equipment	571
14.10.1 Stage-wise Contact	571
14.10.2 Continuous Contact	572

14.11 Reactive Adsorption 576

Nomenclature 585

Numerical Problems 586

Short and Multiple Choice Questions 590

References 592

## **15. Membrane Separation 594–641**

15.1 Introduction 594

15.2 Membranes 595

15.3 Transport in Membranes 596

15.4 Membrane Materials 598

15.5 Membrane Modules 601

15.6 Membrane Processes 606

15.6.1 Separation of Gases 607

15.6.2 Separation of Liquids 613

15.7 Membrane Filtration 615

15.7.1 Microfiltration 616

15.7.2 Ultrafiltration 617

15.7.3 Nanofiltration 620

15.7.4 Reverse Osmosis 621

15.8 Pervaporation 623

15.9 Design Procedure for Membrane Separation 627

15.10 Membrane Based Reactive Separation 633

15.11 Bioseparations 635

Nomenclature 636

Numerical Problems 637

Short and Multiple Choice Questions 639

References 640

Appendix A 643–648

Appendix B 649–655

Index 657–672

# Preface

The chemical industry involves mass transfer as one of the extensively used unit operations, probably the most creative activity enjoyed by chemical engineering professionals. In recent years there have been significant development of the newer processes, and revision and/or alteration of existing processes are taking place. Also, the equipment of unconventional geometries are being used in process industry now-a-days. The design philosophies of these types of equipment using engineering principles are required to be established in certain cases. Thus the advances during the last few years in the level of understanding of mass transfer theories combined with the availability of equipment with newer designs have led to an enhanced degree of sophistication of the subject. The changing scenario has triggered for the reasonable changes in the content and format of the syllabus of the course to cope up with the requirement. A typical modern syllabus is now composed of core or basic principles with options that would develop the depth and range of experience in certain specialized areas. Needless to say, the study of mass transfer was limited to chemical engineers. But as of now the engineers of other disciplines have become more interested in mass transfer in gases, liquids and solids.

Keeping in view the interest of the beneficiaries, i.e. primarily the undergraduate and postgraduate students of chemical engineering as well as the candidates for Associate Membership Examinations conducted by the Indian Institute of Chemical Engineers [AMIIChE] and the Institution of Engineers [AMIE (Chemical)], this book is aimed at presenting the fundamental principles of mass transfer and its applications in process industry. We believe that the understanding of the basic principles will provide deeper insight into the fundamental processes involving mass transfer operation. Starting with molecular diffusion in gas, liquid and solid including the basic concept developed by Hottel for molecular diffusion in gas, the book has dealt with inter-phase mass transfer. Discussion on operational methods of contact equipment has been made in a comprehensive manner for better understanding of separation aspects. Following chapter has dealt with transport equipment wherein coverage has been on simulated packed tower, i.e. string-of-disks and string-of-spheres columns along with the wetted wall column as laboratory model packed tower. Emphasis has been given on design aspects of mass transfer equipment as well as on the features of newly developed packing for its use in the equipment. The book thereafter contains detailed discussion on gas/vapour–liquid, liquid– liquid, solid–gas/vapour and solid–liquid separations. Adequate coverage has also been made on membrane based separation. Some numerical problems have been worked out in the chapters and the problems with answers have been given at the end of chapters. Moreover, short questions/multiple choice questions with answers have been presented at the end of each chapter for better understanding of the readers. Hopefully, the stake holders will immensely be benefitted. The book also provides extensive coverage on certain other areas like Reactive separation, Melt crystallization, Energy conservation practices in distillation equipment, Operational features of cooling tower, Selection criteria of drier, and application areas of advanced adsorption techniques, e.g. Rapid pressure swing adsorption (RPSA), Vacuum swing adsorption (VSA), Temperature swing sorption enhanced reaction (TSSER) and Pressure swing sorption enhanced reaction (PSSER), which would greatly help to the practicing engineers and also to those engaged in higher studies.

It is unfortunate that Prof. A.P. Sinha passed away on 23rd May 2010 soon after completion of the manuscript. This book is dedicated to the memory of Prof. Sinha, and also to the memory of Mrs. Sinha who expired on 4th December 2009, for providing constant support and inspiration in writing the manuscript.

I, Parameswar De, am indebted to all those who supplied information on certain aspects incorporated in this edition. I convey my sincere gratitude to Prof. Parthasarathi Ray, my teacher and colleague as well as to Ms. Chhayarani Jana, Research Scholar, for their constant support in carrying out the work. I am sincerely indebted to Shri Abhra Shau, Research Scholar, for his extensive help in finalizing the figures. Thanks are due to Shri Pranoy Sinha, Research Scholar, and also to Shri Satyaki Banerjee and Shri Aniket Mukherjee, my undergraduate students for their help. I am personally thankful to Maitreyi, daughter of Prof. Sinha for her untiring efforts in making the job possible. I am also thankful to my wife, Jyotsna and my sons, Ashoke and Anup for their heartfelt co-operation.

Proper checking of the text has been done with the objective of making it factually correct as far as possible. The errors and inaccuracies are, however, difficult to avoid completely. The notification of errors and inaccuracies to the second author will be gratefully acknowledged.

**A.P. Sinha**  
**Parameswar De**

# Introduction

The purification of raw materials, the separation of desirable products from undesirable ones, the treatment of effluent gases and liquids for removal of toxic components from them are some of the common problems frequently faced by engineers working in chemical process and allied industries. Some mixtures can be separated at macroscopic levels by purely mechanical means, for example: the separation of suspended particles from gases by cyclones or bag filters; the separation of suspended solids from liquids by filtration, settling or centrifuging; the separation of solids of different sizes or densities by elutriation; the separation of two immiscible liquids by phase separation followed by decantation; and so on. But there are many other mixtures and solutions the components of which cannot be separated by purely mechanical methods, for example: the removal of ammonia from an air-ammonia mixture, the separation of hydrogen and nitrogen in an ammonia plant, the separation of hydrogen and hydrocarbons in petrochemical applications, the removal of carbon dioxide and water from natural gas, the removal of organic vapour from air or nitrogen streams, the removal of one or more component(s) of a liquid solution as in the concentration of acetic acid from a dilute aqueous solution, or the separation of inhibitory fermentation products such as ethanol and acetone-butanol from a fermentation broth, and so on. In such cases, a group of methods based on diffusion, i.e. ability of certain component(s) to move in molecular scale within a phase or from one phase to another under the influence of a concentration gradient, have been found to be very useful. These methods have been grouped together as *mass transfer operations*.

Numerous examples of mass transfer can be found throughout the biological, chemical, physical and engineering fields. Biological involvement includes respiration mechanism and oxygenation of blood, kidney functions, food and drug assimilation, and so forth. The absorption of atmospheric oxygen into blood occurs in the lungs of living beings. The absorbed oxygen is supplied to the tissues through blood circulation. The carbon dioxide generated in blood is pumped back into the lungs, gets desorbed and then leaves with the exhaled air. Underwater plants, fishes and other living bodies use oxygen dissolved in water. The concentration of oxygen in natural water is usually less than that at saturation. As a result, atmospheric oxygen gets dissolved in the water of lakes, rivers and oceans. The transport of oxygen from air to water is a mass transfer process since it is caused by a concentration driving force. The larger the departure of a system from equilibrium, the greater will be the driving force and hence the higher the rate of transport.

Examples of engineering applications include transpiration and film cooling of rocket and jet-engine exhaust nozzles, the separation of ores and isotopes. Chemical engineering applications consist mainly of diffusional transport of some components within a phase or from one phase to another as in gas absorption, distillation, liquid-liquid extraction, adsorption, drying, crystallization and several other operations.

On the basis of foregoing discussion, we may now define *mass transfer* as the movement of one or more component(s) of a phase in molecular scale either within the phase or to another phase caused by the concentration gradient, the transfer taking place in the direction of decreasing concentration. In industrial operations, the rates of such movements are enhanced by bulk motion of the medium/media through which such movements occur caused either by turbulent flow or by stirring. Accordingly, mass transfer may be of two types—*diffusional* mass transfer and *convective* mass transfer. Diffusional mass transfer occurs in the absence of any macroscopic motion of the medium through which such transfer takes place. As a result, diffusional mass transfer is a very slow process. The movement of moisture within a grain during drying or the transports of a reactant or a product through the pores of a catalyst pellet are examples of diffusional mass transfer. Diffusional mass transfer occurs in quiescent fluids, in fluids moving in laminar motion in a direction perpendicular to the direction of transfer or through microspores of solids. Convective mass transfer, on the other hand, occurs through a fluid which is in turbulent motion or subject to stirring so that bulk motion of the medium takes place. As a result, the rate of transfer increases several times. For increasing the rate of transfer, for reducing the size of equipment and for minimizing the cost, most industrial operations are carried out by convective mass transfer. However, within a narrow region near the phase boundary, the transfer takes place by diffusional process resulting in a very low rate of transfer and this rate then becomes the controlling rate. Therefore, in the design of mass transfer equipment all possible measures should be taken to minimize the role of diffusional mass transfer near the phase boundary. The separation of mixtures and solutions accounts for about 40 to 70% of both capital and operating costs of a chemical process industry (Humphrey and Keller 1997). In exceptional cases, as in the recovery and concentration of high value products, the operating cost may even go up to 90% of the total operating cost. That is why mass transfer operations are of special interest to chemical engineers.

Industrial mass transfer operations involve transfer of one or more components from one phase to another which in turn, depends on transfer within each phase. Like all other transfer processes, the rate of mass transfer depends on two factors, namely, concentration gradient and resistance, the former being the driving force for the transfer which takes place from a higher to a lower concentration. The rate of mass transfer is directly proportional to the concentration gradient and inversely proportional to the resistance offered by the medium through which the transfer takes place. Mass transfer operations are broadly classified into three categories (Treybal 1985).

1. Direct contact of two immiscible or partially miscible phases,
2. Phases separated by membrane, and
3. Direct contact of miscible phases.

## **1.1 Direct Contact of Two Immiscible or Partially Miscible Phases**

The majority of industrial mass transfer operations come under this category in which separation is achieved by taking advantage of the unequal distribution of components in two phases at equilibrium. For example, if a mixture of air and ammonia is brought into intimate contact with water, ammonia passes on to the liquid phase. As the concentration of ammonia in the liquid builds up, the transfer of ammonia from liquid to gas phase starts and increases till the two rates of transfer become equal and a dynamic equilibrium is established within the system. At equilibrium, there is no net transfer of ammonia and no further change in its concentrations in the two phases occurs unless the operating

conditions are changed and a new set of equilibrium established. At equilibrium, the concentrations of ammonia in the two phases will be different, but their chemical potential will be the same. Direct contact of two immiscible or partially miscible phases can further be sub-divided into different unit operations according to the phases involved and the direction in which the transfer takes place. Among the six possible combinations of the three states of aggregation, solid, liquid and gas, two combinations, namely, gas-gas and solid-solid have practically no industrial use since most gases are completely miscible and diffusion in solids is extremely slow. The other four combinations give rise to a number of useful mass transfer operations outlined below.

### 1.1.1 Gas/Vapour–Liquid Contact

The separation of one or more components of a gaseous mixture by preferential dissolution in a liquid (solvent) is called *gas absorption*. If on the other hand, the transfer is from liquid phase to gas phase, the operation is known as *stripping* or *desorption*. The principle involved in both absorption or stripping is the same, the only difference being in the direction of transfer. In these operations, the added solvent or the gas acts as the separating agent. A typical example of gas absorption is the removal of carbon dioxide from ammonia synthesis gas by using aqueous ethanolamine solution or carbonate-bicarbonate solution. The absorbed gas is recovered by stripping when the solvent gets regenerated and becomes fit for reuse. Some other examples are the removal of (i) acetone from air-acetone mixture, (ii) hydrogen sulphide from flue gas, (iii) carbon dioxide from air-carbon dioxide mixture, (iv) sulphur dioxide from the converter gas in sulphuric acid plant, and so forth.

The most common and widely used method for separating a liquid mixture is *distillation* or *rectification* or *fractionation*. In distillation, separation is achieved by taking advantage of the differences in volatilities of the components. The saturated vapour and the boiling liquid are brought into intimate contact within the column so that the more volatile component passes from liquid phase to vapour phase and removed by condensation. The less volatile component, on the other hand, passes from the vapour phase to the liquid phase and is removed as bottoms. In distillation, all the components are present in both the phases at equilibrium and transfer is in both directions. The vapour phase is generated from the liquid by the addition of heat while the liquid is produced by the removal of heat. In distillation, heat acts as the separating agent. Fractionation of petroleum crude to get different cuts with different boiling ranges and separation of air by distillation, are a few examples.

If the liquid phase contains only one component and the gas phase contains two or more components, the operation is termed *humidification* or *dehumidification* depending upon the direction of transfer. In the first case, the liquid is vaporised and passed on to the gas phase, while in the second case, some vapour is condensed and passed on to the liquid phase. In practice, these two terms mostly refer to air-water system.

### 1.1.2 Gas–Solid Contact

Two important applications of gas-solid contact are *drying* and *adsorption*. If a solid moistened with a volatile liquid is exposed to a relatively dry gas, the liquid often vaporises and diffuses into the gas. This operation is called *drying* or sometimes *desorption*. In drying, the liquid in majority of cases is water, the drying gas being air. Drying of wet filter cakes, fruits, ceramic articles, etc. are some common examples of drying. In drying, diffusion is from solid to gas. In adsorption, on the other hand,

diffusion is in the opposite direction, i.e. from gas to solid. If a mixture of air and water vapour is brought into contact with activated silica gel, the gel adsorbs water vapour leaving the air almost dry. If a gas mixture contains several components which are differentially adsorbed by a solid, it is possible to separate them by bringing the solid in contact with the gas. Thus, a mixture of propane and propylene gas may be separated by bringing the gas in contact with activated carbon which is also widely used for wastewater treatment. Ionexchange resins and polymeric adsorbents can be used for protein separations of small organics, for example, a carboxylic acid cation exchange resin is used to recover streptomycin.

### 1.1.3 Liquid–Liquid Contact

If the constituents of a liquid solution are separated by bringing the solution into intimate contact with another liquid which is either insoluble or only partially soluble with the original solution and in which the constituents of the original solution are differentially distributed, then the operation is called *liquid-liquid extraction* or simply *liquid extraction*. If a dilute aqueous solution of acetic acid is brought into intimate contact with ethyl acetate, the acetic acid and only a small amount of water enter the ester layer from which the acetic acid may be easily recovered by simple distillation. Antibiotics are recovered by liquid extraction using amylacetate or isoamylacetate, for example, penicillin is extracted from fermentation broth using isoamylacetate as the solvent. Two phase aqueous extractions of enzymes from microbial cells in fermentation are practised today. In liquid-liquid extraction, the added solvent acts as the separating agent.

### 1.1.4 Liquid–Solid Contact

The important operations in this category are leaching, crystallization and adsorption. The selective dissolution of one or more component(s) from a solid mixture by a liquid solvent is known as *leaching* or *solvent extraction*. Leaching is widely used in metallurgical industries for the concentration of metal bearing minerals or ores. The leaching of gold from its ore by cyanide solution, the extraction of cotton seed oil from the seeds by hexane or other suitable solvents such as super critical fluids, the extraction of soluble proteins such as enzymes between two aqueous phases containing incompatible polymers such as polyethylene glycol and dextran, are some examples of leaching.

When transfer is from liquid to solid with one of the components at equilibrium in both the phases, the operation is known as *crystallization*. In some crystallization operations, however, all the components may be present in both the phases. The removal of penicillin from the fermentation broth by crystallization is an example.

## 1.2 Phases Separated by Membrane

Membrane processes are finding wide applications ranging from water treatment to reactors to advanced bioseparations. The development of separation processes with reduced energy consumption and minimal environmental impact is critical for sustainable operations.

Membranes, in general, prevent intermingling of two miscible phases and separate the components by selectively allowing some of them to pass from one side to the other.

In *gaseous diffusion* or *effusion*, the membranes cause separation by allowing components of different molecular weights to pass through their microspores at different rates. In *permeation*, a gas

or liquid solution is brought into contact with a nonporous membrane in which one of the components is preferentially dissolved. After diffusing to the other side of the membrane, the component is vaporised into the gas phase. The separation of a crystalline substance from a colloid by bringing their mixture in contact with a solvent with an intervening membrane permeable only to the solvent, and the dissolved crystalline solute is known as *dialysis*. If an electromotive force is applied across the membrane to assist diffusion of charged particles, the operation is termed *electrodialysis*. The solute and solvent of a solution can be separated by superimposing a pressure to oppose the osmotic pressure of the solvent and to reverse its flow. This is known as *reverse osmosis* and it has become a very effective strategy for desalination of sea water. In recent years, there have been spectacular developments in the field of membrane technology and it has become a subject by itself.

### 1.3 Direct Contact of Miscible Phases

The separation of components of a single fluid through the creation of a concentration gradient within the fluid by imposing a temperature gradient in the fluid is known as *thermal diffusion*. When a condensable vapour like steam is allowed to diffuse through a gas mixture to preferentially remove one of the components along with it, thus making separation possible, it is called *sweep diffusion*.

### 1.4 Classification of Mass Transfer Operations

Figure 1.1 summarizes the classification of mass transfer operations as discussed in the previous sections.

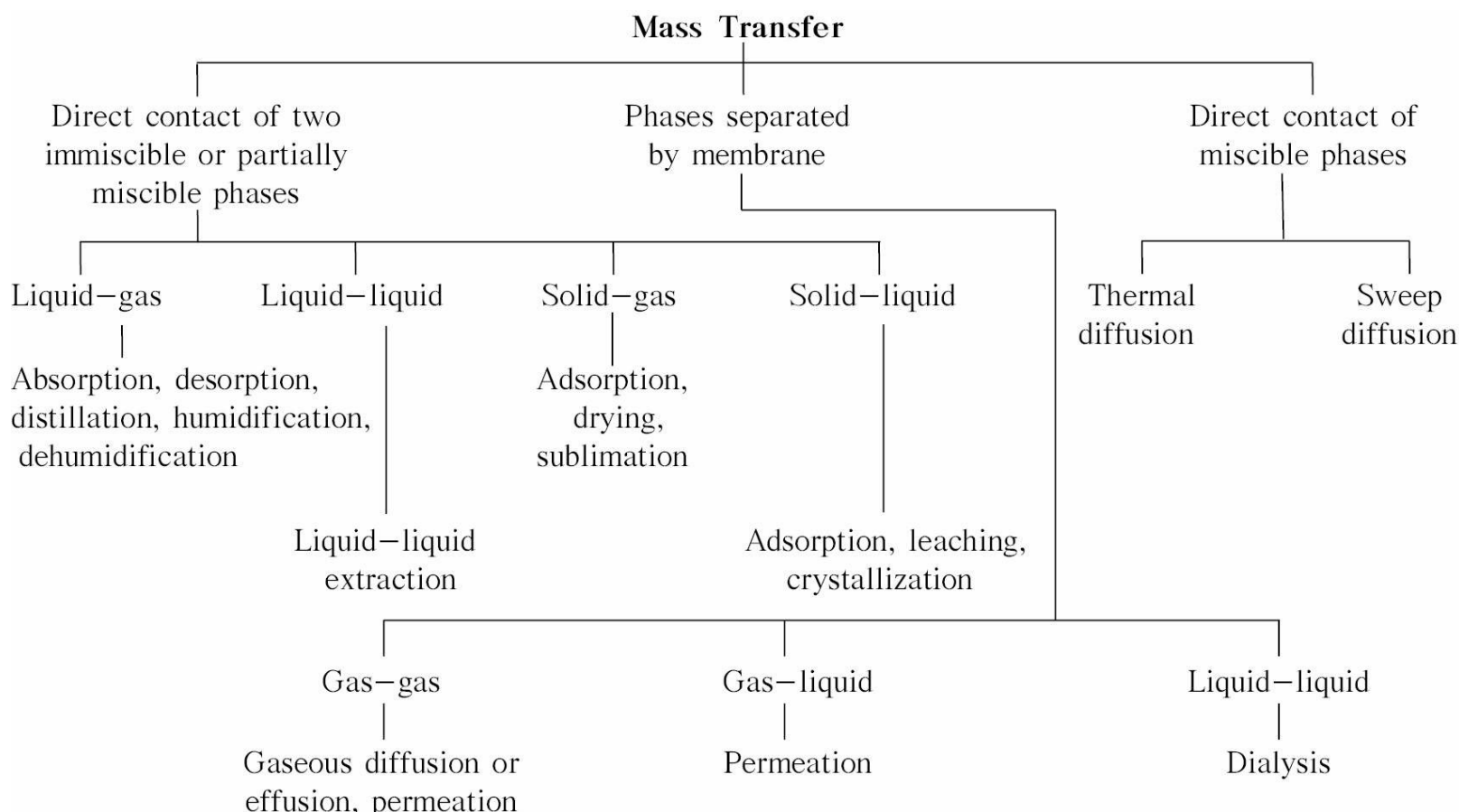


**Figure 1.1** Classification of mass transfer operations.

Process intensification involves the development of radical technologies for the miniaturization of

process plants while achieving the same production objective as in conventional process (Stankiewicz and Moulijn 2000). One of the ways is to replace large scale expensive equipment with one that is smaller, less costly, more efficient and profitable. Reactive separations form a major component of the wider area of process intensification. Reactive separations can be viewed as the integration of reaction and separation in a single unit. This technology has been recognized as one of the main objectives of the future of chemical engineering.

It is highly improbable that the two phases involved in mass transfer are exactly at the same temperature. As a result, some heat transfer is almost always associated with mass transfer. In some cases, the rate of heat transfer controls the rate of mass transfer. This is particularly true in cases where there is phase change of the diffusing component(s). These operations are sometimes categorized as *simultaneous heat and mass transfer*. Distillation, humidification, dehumidification, water-cooling, crystallization, drying, etc. are some of the examples of such operations.

## **References**

- Humphrey, J.L. and G.E. Keller, II, *Separation Process Technology*, McGraw Hill, New York, (1997).
- Stankiewicz, A. and J.A. Moulijn, *Chem. Eng. Prog.*, **96**(1), 22 (2000).
- Treybal, R. E., *Mass Transfer Operations*, 3rd ed., McGraw Hill, Singapore (1985).

# 2

# Diffusion

## 2.1 Introduction

When the composition of a fluid mixture varies from one point to another, each component of the mixture will tend to flow in the direction that will reduce the difference in local concentration. If the bulk fluid is stationary or moving in laminar motion in a direction normal to the direction of concentration gradient, the process reducing the concentration difference is known as *molecular diffusion*. Molecular diffusion takes place because of random movement of individual molecules. It is a very slow process and quite different from bulk transport by eddies which phenomenon is much faster as it takes place in a turbulent fluid.

As an example of molecular diffusion, let us consider a few crystals of copper sulphate placed at the bottom of a tall bottle kept away from any source of disturbance. What we would observe initially is that the colour will concentrate at the bottom of the bottle. After a day, it will penetrate a few centimetres upwards. Ultimately, the solution will become homogeneous only after a very long time. The movement of the coloured solution is the result of molecular diffusion and, as evident, it is extremely slow. In gases molecular diffusion takes place at a rate of about 10 cm/min, in liquids its rate is about 0.05 cm/min, and in solids its rate may be as low as 0.00001 cm/min. In general, the rate of molecular diffusion varies less with temperature in comparison to many other phenomena (Cussler 1997).

Diffusion often occurs sequentially with other phenomena. Being the slowest step in the sequence, it limits the overall rate of the process. For example, diffusion often limits the rate of commercial distillation or the rate of industrial reaction using porous catalyst.

Since mass transfer operations are based on diffusion, the study of diffusion is an essential prerequisite for the proper understanding of mass transfer. In this chapter, we shall discuss the theoretical aspects of molecular diffusion and develop some quantitative relations for the rate of diffusion under different conditions. Since molecular diffusion depends on concentration and molecular velocity of the concerned component as well as the flux of the component at any given point and the frame of reference used for measuring velocity, it will be appropriate to first define all these terms before proceeding with the study of diffusion.

## 2.2 Molecular Diffusion

### 2.2.1 Concentration

A number of methods are available for expressing the concentration of a component in a multi-component system. These are as follows:

1. Mass concentration of a component  $i$ , i.e. mass of component  $i$  per unit volume of solution or

mixture denoted by  $t_i$ , kg/m<sup>3</sup>.

2. Total mass concentration of all the components in a solution or mixture denoted by  $t$ , kg/m<sup>3</sup>. This total mass concentration is the same as the density of the solution or mixture.
3. Mass fraction of a component  $i$  in a solution denoted by  $w_i = t_i/t$ .
4. Molar concentration of a component  $i$  in a solution denoted by  $c_i$  kmol/m<sup>3</sup>.
5. Total molar concentration of the solution, denoted by  $c$  in, kmol/m<sup>3</sup>.
6. Mole fraction of a component  $i$  in a solution denoted by  $x_i = c_i/c$ .

If there are  $n$  components in a solution, we have

$$\sum_{i=1}^n \rho_i = \rho, \quad \sum_{i=1}^n q_i = c, \quad \sum_{i=1}^n w_i = 1, \quad \sum_{i=1}^n x_i = 1$$

In a gaseous mixture, the concentration of a component is usually expressed in terms of its partial pressure  $p_i$  or mole fraction  $y_i$ , where  $y_i = p_i/P$ ,  $P$  being the total pressure. The mole fraction of a component  $i$  is usually denoted by  $x_i$  in liquids and by  $y_i$  in gases.

## 2.2.2 Velocity

Let us consider a nonuniform multi-component fluid mixture, having bulk motion owing to pressure difference, within which the different components are moving with different molecular velocities as a result of diffusion. Two types of average velocities with respect to a stationary observer have been defined for such cases (Bird et al. 1960).

If the statistical average velocity of component  $i$  in the  $x$ -direction with respect to stationary co-ordinates is expressed as  $u_i$ , then the mass flux of component  $i$  through a stationary surface normal to  $u_i$  is  $t_i u_i$ . For an  $n$ -component system, the *mass average velocity* in the  $x$ -direction can be written as

$$u = \frac{1}{\rho} \sum_{i=1}^n \rho_i u_i$$

(2.1)

Another form of average velocity for the mixture is the *molar average velocity* which, in the  $x$ -direction, is given by

$$U = \frac{1}{c} \sum_{i=1}^n c_i u_i$$

(2.2)

The velocities  $u$  and  $U$  are approximately equal at low solute concentrations in binary systems and in nonuniform mixtures of components having the same molecular weight. The velocities  $u$  and  $U$  are also equal in the bulk flow of a mixture with uniform concentration throughout regardless of the relative molecular weights of the components.

## 2.2.3 Frames of Reference

Frames of reference are the co-ordinates on the basis of which the measurements are made. Three

frames of reference or co-ordinates are commonly used for measuring the flux of a diffusing component (Skelland 1974). It is assumed that in a frame of reference there is an observer who observes or measures the velocity or flux of a component in a mixture. If the frame of reference or the observer is stationary with respect to the earth, he notes a velocity  $u_i$  of the  $i$ th component. If the observer is located in a frame of reference that moves with a mass average velocity  $u$  of component  $i$ , he will note a velocity  $(u_i - u)$  of the component  $i$  which is the relative average velocity of the component with respect to the observer who himself is moving with the velocity  $u$  in the same direction. Similarly, if the observer is in a frame of reference moving with the molar average velocity  $U$  of the component  $i$ , he will find the molecules of component  $i$  moving with a velocity  $(u_i - U)$ .

## 2.2.4 Flux

Flux is the net rate at which a component in a solution or in a mixture passes per unit time through a unit area normal to the direction of diffusion. It is expressed in  $\text{kg}/\text{m}^2\text{s}$  or  $\text{kmol}/\text{m}^2\text{s}$ .

The mass and molal fluxes in the  $x$ -direction in the three frames of reference may be expressed as

### Mass Flux

(i) relative to a stationary observer:

$$n_{ix} = t_i u_i \quad (2.3)$$

(ii) relative to an observer moving with the mass average velocity:

$$i_{ix} = t_i(u_i - u) \quad (2.4)$$

(iii) relative to an observer moving with the molar average velocity:

$$j_{ix} = t_i(u_i - U) \quad (2.5)$$

### Molar Flux

(i) relative to a stationary observer:

$$N_{ix} = c_i u_i \quad (2.6)$$

(ii) relative to an observer moving with the mass average velocity:

$$I_{ix} = c_i(u_i - u) \quad (2.7)$$

(iii) relative to an observer moving with the molar average velocity:

$$J_{ix} = c_i(u_i - U) \quad (2.8)$$

**EXAMPLE 2.1** (Estimation of mass average, molar average velocity and volume average velocity): A gas mixture containing 65%  $\text{NH}_3$ , 8%  $\text{N}_2$ , 24%  $\text{H}_2$  and 3% Ar is flowing through a pipe 25 mm in diameter at a total pressure of 4.0 atm. The velocities of the components are as follows:

$\text{NH}_3 = 0.03 \text{ m/s}$ ,  $\text{N}_2 = 0.03 \text{ m/s}$ ,  $\text{H}_2 = 0.035 \text{ m/s}$  and  $\text{Ar} = 0.02 \text{ m/s}$

Calculate the mass average velocity, the molar average velocity and the volume average velocity of the gas mixture.

**Solution:** Let us denote the components of the gas by subscripts as under:

$$\text{NH}_3 = 1, \text{N}_2 = 2, \text{H}_2 = 3 \text{ and } \text{Ar} = 4$$

From Eq. (2.1), the mass average velocity of the mixture is

$$u = \frac{1}{\rho} \sum_{i=1}^n \rho_i u_i$$

or

$$u = \frac{1}{\rho} (t_1 u_1 + t_2 u_2 + t_3 u_3 + t_4 u_4)$$

We know that

$$t_i = \frac{P_i}{RT} M_i \text{ and } t = \frac{P}{RT} M$$

where,

$t_i$  = density of the  $i$ th component

$t$  = total density of the gas mixture

$M_i$  = molecular weight of the  $i$ th component and

$M$  = average molecular weight of the mixture or

$$\frac{\rho_i}{\rho} = \frac{P_i}{P} \frac{M_i}{M} = y_i \frac{M_i}{M}$$

Substituting this in Eq. (2.1), the expression for mass average velocity,  $u$ , becomes

$$u = \frac{1}{M} \sum_{i=1}^4 y_i u_i M_i$$

where,  $M$  the average molecular weight of the mixture is given by

$$\begin{aligned} M &= y_1 M_1 + y_2 M_2 + y_3 M_3 + y_4 M_4 \\ &= (0.65)(17) + (0.08)(28) + (0.24)(2) + (0.03)(40) = 14.97 \end{aligned}$$

Therefore,

$$\begin{aligned} u &= \frac{(0.65)(17)(0.03) + (0.08)(28)(0.03) + (0.24)(2)(0.035) + (0.03)(40)(0.02)}{14.97} \\ &= 0.029 \text{ m/s Ans.} \end{aligned}$$

From Eq. (2.2), the molar average velocity of the mixture is

$$\begin{aligned} U &= \frac{1}{c} (c_1 u_1 + c_2 u_2 + c_3 u_3 + c_4 u_4) \\ &= y_1 u_1 + y_2 u_2 + y_3 u_3 + y_4 u_4 \end{aligned}$$

where  $y_i$  is the mole fraction of the  $i$ th component in the gas mixture.

Substituting the values, we obtain

$$\begin{aligned} U &= (0.65)(0.03) + (0.08)(0.03) + (0.24)(0.035) + (0.03)(0.02) \\ &= 0.0309 \text{ m/s Ans.} \end{aligned}$$

Volume average velocity = Molar average velocity = 0.0309 m/s Ans.

## 2.3 Models of Diffusion

Two mathematical models have been more or less successful in explaining the mechanism of diffusion. The one proposed by Adolf Fick, uses a diffusion coefficient while the other model uses a mass transfer coefficient.

Both the models were verified by a simple experiment shown in Figure 2.1.

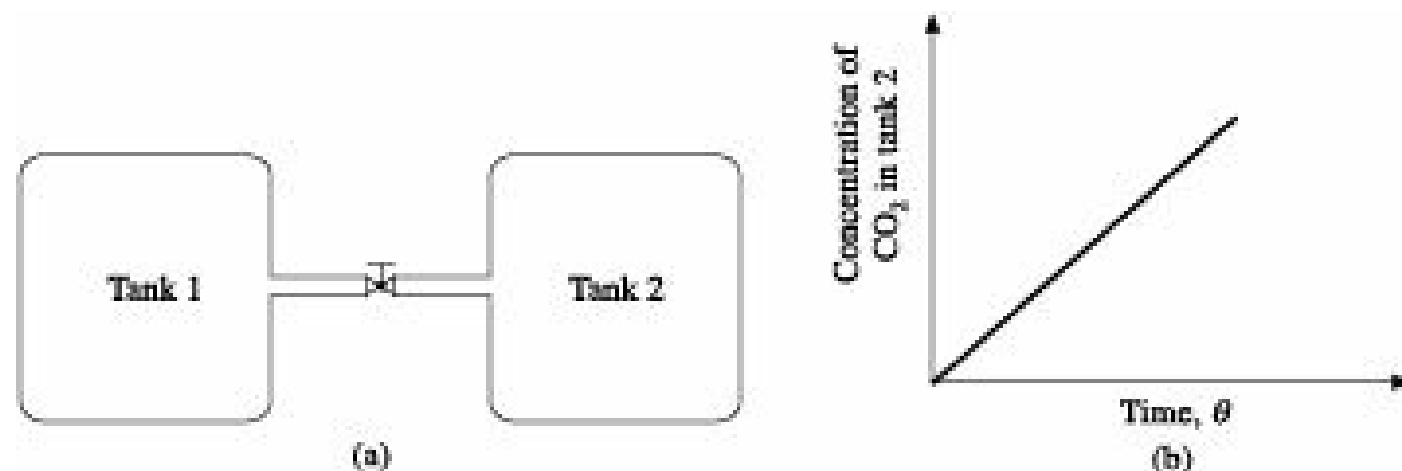


Figure 2.1 Verification of diffusion law.

Tank 1 containing carbon dioxide is connected by a long connecting line to tank 2 containing air [Figure 2.1(a)]. Both tanks of equal volume were sufficiently large. These were kept at constant temperature and pressure. On opening the valve the diffusion proceed, and the concentration of carbon dioxide in tank 2 was measured at a regular interval of time. The concentration of carbon dioxide in tank 2 thus measured was found to vary linearly with time as shown in Figure 2.1(b). Similar observation was made elsewhere (Cussler 1997) for different system. In Fick's model, the results were correlated as

$$\text{Carbon dioxide flux} = D \frac{(\text{Carbon dioxide concentration difference})}{(\text{Capillary length})}$$

where, the proportionality constant  $D$  is the diffusion coefficient. A discussion on Fick's law has been taken up in Section 2.4. The other model assumed the carbon dioxide flux to be proportional to the gas concentration.

$$\text{Carbon dioxide flux} = k (\text{carbon dioxide concentration difference})$$

where, the proportionality constant  $k$  is the mass transfer coefficient. This is a type of reversible rate constant.

Fick's model is commonly used in basic sciences to describe diffusion. In the mass transfer coefficient model, on the other hand the coefficient,  $k$  takes care of several parameters which cannot be directly measured. Mass transfer coefficient leads to the development of correlations commonly used in chemical engineering, chemical kinetics and medicine. Both the models have striking similarity with Ohm's law. The diffusion coefficient is analogous to the reciprocal of resistivity while mass transfer coefficient is analogous to the reciprocal of resistance.

Both the models have some demerits also. For instance, the flux may not be proportional to the concentration difference if the capillary is very thin or if the gases react. The model based on diffusion coefficient gives results of more fundamental value than those obtained using the model based on mass transfer coefficient. The diffusion model has distributed parameters for the dependent variable, i.e. the concentration is allowed to vary with all independent variables like position and

time. In contrast, the mass transfer model has lumped parameters like average values. There is a third way to correlate diffusion by assuming the same to be a first order chemical reaction. However, the idea of treating diffusion as a chemical reaction has many drawbacks. Because the reaction is hypothetical, the rate constant is a composite of physical factors rather than chemical factors. As a result, this model has not been successful.

## 2.4 Fick's Law

Based on his diffusion model (Section 2.3) and series of experiments conducted by Graham (Graham 1850) and himself, Adolf Eugen Fick proposed the basic law of diffusion known as Fick's law (Fick 1885) which is the foundation of all subsequent works on molecular diffusion. According to Fick's law for one-dimensional steady-state molecular diffusion, the molar flux of a component in a frame of reference moving with the molar average velocity is proportional to the concentration gradient of the component. If  $A$  diffuses in a binary mixture of  $A$  and  $B$ , then according to Fick's law

$$J_A \square \frac{dc_A}{dz}, \quad \text{or} \quad J_A = -D_{AB} \frac{dc_A}{dz} \quad (2.9)$$

where,

$J_A$  = molar flux of component  $A$  relative to a frame of reference moving with molar average velocity,

$$\text{M/L}^2\theta$$

$c_A$  = concentration of component  $A$ ,  $\text{M/L}^3$

$z$  = direction or length of diffusion,  $L$

$(dc_A/dz)$  = gradient of concentration of mass and

$D_{AB}$  = proportionality constant known as mass diffusivity or diffusivity or diffusion coefficient of  $A$  with respect to  $B$ ,  $\text{L}^2/\theta$ .

The negative sign in Eq. (2.9) indicates that diffusion takes place in the direction of decreasing concentration. It is interesting to note that Eq. (2.9) is similar to other basic laws of transport, namely Fourier's law of heat conduction and Newton's law of viscosity.

In case of heat conduction, the heat flux is proportional to the temperature gradient, i.e.

$$q_z = -k \frac{dT}{dz} = -\rho c_p \frac{d(\rho c_p T)}{dz} \quad (2.10)$$

where,  $q_z$  is the flux of heat in the  $z$ -direction in which the temperature decreases,  $(k/c_p)$  =  $a$  is the thermal diffusivity,  $\text{L}^2/\theta$  and  $[d(\rho c_p T)/dz]$  is the gradient of concentration of heat.

According to Newton's law of viscosity, the shear stress or momentum flux in a viscous fluid in laminar motion is proportional to the velocity gradient from a faster moving layer to an adjacent slower moving layer, i.e.

$$x_{zx} = -m \frac{du_x}{dz} = -\frac{\mu}{\rho} \frac{d(\rho u_x)}{dz} \quad (2.11)$$

where,  $u_x$  is the velocity in the direction normal to the direction of momentum transfer,  $(du_x/dz)$  is

the gradient of concentration of momentum,  $(m/t) = n$  is the kinematic viscosity or momentum diffusivity,  $L^2/\square$  and  $t_{zx}$  is the flux of momentum in the  $z$ -direction.

Comparing these three Eqs. (2.9) to (2.11), the transport of a property can generally be expressed as  
 $(\text{Flux of a property}) = (-) (\text{Diffusivity of the property})$

# (Gradient of concentration of the property).

It may be observed that the three processes, transport of mass, heat and momentum are similar in nature and are guided by the same principle. Transport of mass takes place in the direction of decreasing concentration, transport of heat occurs in the direction of decreasing temperature and transport of momentum occurs in the direction of decreasing velocity. The analogy between these three transport processes is of considerable importance in chemical engineering. In molecular diffusion, the diffusing molecules move at a velocity higher than the average molar velocity. The relative velocity of a component with respect to a frame of reference moving with molar average velocity  $U$  is called *diffusion velocity*,  $V_{Ad}$  and is given by

$$V_{Ad} = (u_A - U) = \frac{J_A}{c_A} = - \frac{D_{AB}}{c_A} \frac{dc_A}{dx} \quad (2.12)$$

Fick's law for one-dimensional diffusional mass transport in three different co-ordinates can be represented as

(i) For one dimensional diffusion in Cartesian co-ordinates [Eq. (2.9)]

$$J_A = -D_{AB} \frac{dc_A}{dx}$$

(ii) For radial diffusion in Cylindrical co-ordinates

$$J_A = -D_{AB} \frac{dc_A}{dr} \quad (2.13)$$

(iii) For radial diffusion in Spherical co-ordinates

$$J_A = -D_{AB} \frac{dc_A}{dr} \quad (2.14)$$

Although the original form of Fick's law as given in Eq. (2.9) defines molar flux,  $J_A$  with respect to a frame of reference moving with the molar average velocity, molar flux  $N_A$  with respect to stationary frame of reference has been found to be more useful for practical purposes.  $N_A$  can be derived from  $J_A$  in the following way:

From Eq. (2.2) for a binary system,

$$U = \frac{1}{c} (c_A u_A + c_B u_B) \quad (2.15)$$

and from Eq. (2.6),

$$N_A = c_A u_A \quad (2.16)$$

Combining Eqs. (2.15) and (2.16), we get

$$U = \frac{1}{c} (N_A + N_B) \quad (2.17)$$

Fluxes of  $A$  and  $B$  are  $N_A = c_A u_A$  and  $N_B = c_B u_B$

Therefore, from Eqs. (2.8) and (2.9)

$$J_A = -D_{AB} \frac{\frac{dc_A}{dx}}{c} = c_A (u_A - U) = c_A u_A - c_A U$$

Substituting the expression for  $U$  from Eq. (2.15), we obtain

$$J_A = N_A - \frac{c_A}{c} (c_A u_A + c_B u_B)$$

$$= N_A - \frac{c_A}{c} (N_A + N_B)$$

$$\text{or, } N_A = \frac{c_A}{c} (N_A + N_B) - D_{AB} \frac{\frac{dc_A}{dx}}{c} \quad (2.18)$$

Equation (2.18) gives the molar flux of  $A$  in a binary mixture of  $A$  and  $B$  with respect to a stationary frame of reference. The molar flux,  $N_A$  may be considered to consist of two parts, the part

$\left[ \frac{c_A}{c} (N_A + N_B) \right]$  due to bulk motion and the part  $\left[ -D_{AB} \frac{\frac{dc_A}{dx}}{c} \right]$  due to diffusion.

In dilute solutions, bulk motion becomes negligible and the molar flux reduces to

$$N_A = J_A = -D_{AB} \frac{\frac{dc_A}{dx}}{c} \quad (2.19)$$

## 2.5 Molecular Diffusion in Gases

Molecular diffusion in gases is caused by random movement of molecules due to their thermal energy and hence the kinetic theory of gases helps to understand the mechanism of molecular diffusion in gases. According to this theory, molecules of gases move with very high speed. For instance, at 273 K temperature and 101.3 kN/m<sup>2</sup> pressure, the mean speed of oxygen molecules is about 462 m/s. It may, therefore, be expected that the rate of molecular diffusion should be very high. But actually molecular diffusion is an extremely slow process since the molecules undergo several billion collisions per second as a result of which their velocities frequently change both in magnitude and direction, thus making the effective velocity very low.

In case of diffusion in gases, molar flux may be expressed in terms of partial pressure gradient. Assuming the gas mixture to be ideal,

$$c_A = \frac{P_A}{RT} \text{ and } c = \frac{P}{RT}$$

where,  $T$  is the uniform temperature and  $R$  is the universal gas constant.

With the above substitution, Eq. (2.18) becomes

$$N_A = \frac{P'_A}{P} (N_A + N_B) - \frac{D_{AB}}{RT} \frac{dp'_A}{dx} \quad (2.20)$$

It has, however, been argued by some authors (Hines and Madox 1985) that  $J_A$  and  $N_A$  should better be expressed in terms of gradient in mole fraction rather than in terms of gradient in concentration or partial pressure. The reason behind this is that in the absence of mole fraction gradient there will not be any diffusion even if there is partial pressure gradient caused by variation in local temperature. However, partial pressure gradients will be used wherever they are applicable.

Hottel (1949) applied the concept of kinetic theory of gases to develop an expression for molecular diffusion in gases. Considering the diffusion of two components  $A$  and  $B$  of a binary gas mixture across the plane  $PQ$  (Figure 2.2), let  $m$  is the component in the  $z$ -direction of the mean free path of the molecules of  $A$ .

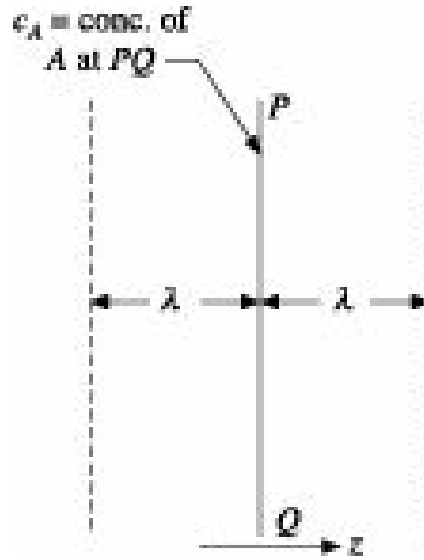


**Figure 2.2** Hottel's analysis of molecular diffusion.

Then within the region  $\pm l$  on either side of  $PQ$ , the gas molecules are free to cross the plane  $PQ$  at their mean speed  $u$  (velocity component in  $z$ -direction). Half the molecules in the narrow region to the left will cross  $PQ$  before colliding, the other half will pass to the left. The total number of molecules of component  $A$  crossing  $PQ$  from left to right will therefore be

$$\frac{\lambda}{2}s \left( c_A - \frac{\lambda}{2} \frac{\partial c_A}{\partial z} \right)$$

where,  $c_A$  = concentration of  $A$  at  $PQ$ , and  $s$  = the cross section of the plane.

Similarly, the total number of molecules of  $A$  passing from right to left will be

$$\frac{\lambda}{2}s \left( c_A + \frac{\lambda}{2} \frac{\partial c_A}{\partial z} \right)$$

In each case, the total distance travelled is  $l$  requiring a time  $(l/u)$ . The net rate of transfer of component  $A$  is therefore

$$N_A \square s = - \frac{(\lambda s/2)(\lambda \partial c_A / \partial z)}{(\lambda/u)} = - \frac{\lambda^2 s}{2} \frac{\partial c_A}{\partial z}$$

where,  $N_A$  = rate of diffusion of  $A$  in moles/(unit area)(unit time)

Since for an ideal gas,  $c_A = p' A / RT$ , we may write

$$N_A = - \frac{\lambda_H}{2RT} \frac{\partial p'_A}{\partial z} = - \frac{D_{AB}}{RT} \frac{\partial p'_A}{\partial z} \quad (2.21)$$

where,  $D_{AB}$  is the diffusivity of component  $A$  with respect to component  $B$ . It may be noted that Eqs. (2.20) and (2.21) become identical if bulk motion is disregarded.

### 2.5.1 Steady-State Molecular Diffusion in a Binary Mixture Through a Constant Area

In many important practical cases, it often becomes necessary to measure the rate of molecular diffusion of a component from one point to another. But a flux equation like Eq. (2.18) cannot be directly used for the purpose since it involves the measurement of concentration gradient at a point which is extremely difficult. On the other hand, the concentration of a component at any two points at a known distance can be measured much easily and accurately. Suitable working equations can conveniently be developed by integrating any of these Eqs. (2.18), (2.19) or (2.20). While developing the working equation, it has been assumed that

- (i) diffusion occurs in steady-state\*,
- (ii) the gas mixture behaves as ideal gas,
- (iii) the temperature is constant throughout,
- (iv) diffusion occurs through constant area.

The following two situations which are commonly encountered in practice have been considered here:

- (a) diffusion of component  $A$  through a stagnant layer of component  $B$ , and
- (b) equal molal counter-diffusion of components  $A$  and  $B$ .

#### ***Diffusion of component $A$ through a stagnant layer of component $B$***

Let us consider a pool of water placed in a tray in contact with a stream of unsaturated air. So long as the air remains unsaturated, water molecules will diffuse into the air. The bulk of air is in motion, but a thin layer of air in contact with water will be stagnant and then moving in laminar motion in a direction normal to the direction of diffusion. Water vapour will diffuse through this layer by molecular diffusion before being carried away by the moving air.

In this case, since the component  $B$  is not diffusing  $N_B = 0$  and Eq. (2.20) becomes

$$N_A = N_A \frac{P}{P} - \frac{D_{AB}}{RT} \frac{dp'_A}{dz} \quad (2.22)$$

$$\text{or, } N_A dz = - \frac{D_{AB} P}{RT(P - p'_A)} dp'_A \quad (2.23)$$

Here,  $N_A$  is constant since diffusion is taking place at steady-state through constant area. Integrating between limits 1 and 2, we get

$$N_A \int_1^2 dz = -\frac{D_{AB}P}{RT} \int_{P'_{A_1}}^{P'_{A_2}} \frac{dp'_A}{(P - p'_A)}$$

$$N_A = \frac{D_{AB}P}{RT(z_2 - z_1)} \ln \frac{P - P'_{A_2}}{P - P'_{A_1}} = \frac{D_{AB}P}{RT(z_2 - z_1)} \ln \frac{P'_{B_2}}{P'_{B_1}} \quad (2.24)$$

or, since the total pressure is uniform,  $P = p \square A_1 + p \square B_1 = p \square A_2 + p \square B_2$

$$\text{or, } p \square B_2 - p \square B_1 = p \square A_1 - p \square A_2.$$

$$\text{Since, } p \square_{BM} = \frac{P'_{B_2} - P'_{B_1}}{\ln(P'_{B_2}/P'_{B_1})}$$

$$\ln \frac{P'_{B_2}}{P'_{B_1}} = \frac{P'_{B_2} - P'_{B_1}}{P'_{BM}} = \frac{P'_{A_1} - P'_{A_2}}{P'_{BM}}$$

so that, we get

$$N_A = \frac{D_{AB}P}{RT(z_2 - z_1)} \frac{P'_{A_1} - P'_{A_2}}{P'_{BM}} \quad (2.25)$$

The molar flux of component  $A$  in a binary mixture of  $A$  and  $B$  where  $B$  is nondiffusing can be calculated from any of these Eqs. (2.24) or (2.25).

After determining the flux  $N_A$ , the partial pressure of  $A$  at any point within the diffusion path can be calculated from Eq. (2.25). The partial pressure of component  $B$  can then be evaluated from the relation  $p \square_B = (P - p \square_A)$ . A typical distribution of partial pressure of components  $A$  and  $B$  during diffusion is shown in Figure 2.3. Component  $A$  diffuses due to the gradient  $(-dp \square_A/dz)$ . Component  $B$  also diffuses relative to the average molar velocity having a flux which depends on  $(-dp \square_B/dz)$ . But it has been assumed that  $B$  is nondiffusing. This apparent anomaly can be explained with the help of the following example:

Let us consider a man swimming in a river against the current, i.e. the velocity of the flowing water. The absolute velocities of the man and the current are equal in magnitude but opposite in direction. To a stationary observer on the river bank, the man appears to be stationary. But an observer moving with the velocity of the current will see the man moving in a direction opposite to that of the current. Similarly, during diffusion of component  $A$  through nondiffusing component  $B$ , the flux of  $B$  to a stationary observer appears to be zero. But an observer moving with the average velocity of  $A$  will find a flux of  $B$  in the opposite direction.

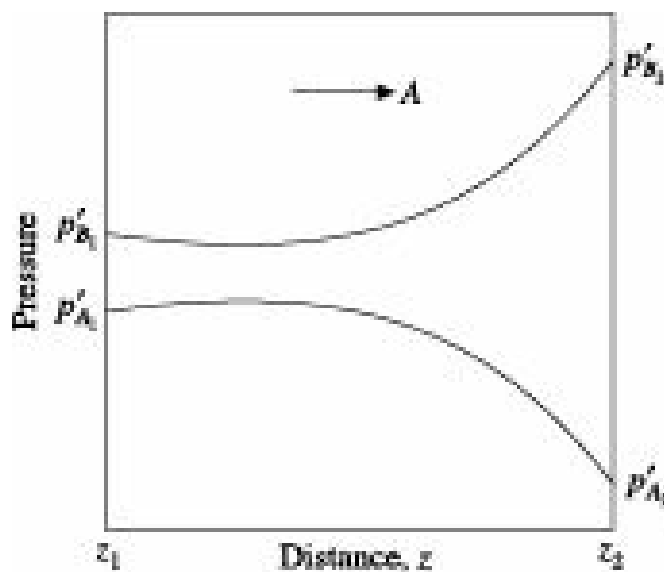


**Figure 2.3** Distribution of partial pressure for diffusion of *A* through stagnant *B*.

**EXAMPLE 2.2** (Diffusion of one component through the stagnant layer of another component): Oxygen is diffusing through a stagnant layer of methane 5 mm thick. The temperature is 20°C and the pressure 100 kN/m<sup>2</sup>. The concentrations of oxygen on the two sides of the film are 15% and 5% by volume. The diffusivity of oxygen in methane at 20°C and 100 kN/m<sup>2</sup> is  $2.046 \times 10^{-5}$  m<sup>2</sup>/s.

- (a) Calculate the rate of diffusion of oxygen in kmol/m<sup>2</sup>s
- (b) What will be the rate of diffusion if the total pressure is raised to 200 kN/m<sup>2</sup>, other conditions remaining unaltered?

**Solution:** This being a case of diffusion of one gas through the stagnant layer of another gas, Eq. (2.25) is applicable.

$$T = 293 \text{ K}, P = 100 \text{ kN/m}^2, \quad z = 5 \text{ mm} = 0.005 \text{ m}$$

$$p_{\square A_1} = 100 \times 0.15 = 15 \text{ kN/m}^2, \quad p_{\square B_1} = (100 - 15) = 85 \text{ kN/m}^2$$

$$p_{\square A_2} = 100 \times 0.05 = 5 \text{ kN/m}^2, \quad p_{\square B_2} = (100 - 5) = 95 \text{ kN/m}^2$$

$$p_{\square B_M} = (95 + 85)/2 = 90 \text{ kN/m}^2;$$

Since the values of  $p_{\square B_1}$  and  $p_{\square B_2}$  are very close, arithmetic average is quite justified. Substituting the values in Eq. (2.25), we obtain

$$N_A = \frac{(2.046 \times 10^{-5})(100)}{(8314)(293)(0.005)} \times \frac{(15 - 5)}{90} = 1.87 \times 10^{-8} \text{ kmol/m}^2 \cdot \text{s}$$

The rate of diffusion of oxygen =  $1.87 \times 10^{-8}$  kmol/s/m<sup>2</sup>

At 200 kN/m<sup>2</sup> pressure:

$$P = 200 \text{ kN/m}^2, D_{AB} = (2.046 \times 10^{-5}) \times (100/200) = 1.023 \times 10^{-5} \text{ m}^2/\text{s}$$

as the diffusivity is inversely proportional to the pressure (Section 2.6).

$$p \square A_1 = 200 \# 0.15 = 30 \text{ kN/m}^2,$$

$$p \square B_1 = (200 - 30) = 170 \text{ kN/m}^2$$

$$p \square A_2 = 200 \# 0.05 = 10 \text{ kN/m}^2,$$

$$p \square B_2 = (200 - 10) = 190 \text{ kN/m}^2$$

$$p \square BM = \frac{(170 + 190)}{2} = 180 \text{ kN/m}^2.$$

From Eq. (2.25),

$$N_A = \frac{(1.023 \times 10^{-5})(200)}{(8314)(293)(0.005)} \times \frac{(30 - 10)}{180} = 1.87 \# 10^{-8} \text{ kmol/ s\$m}^2$$

The rate of diffusion of oxygen at 200 kN/m<sup>2</sup> pressure = 1.87 # 10<sup>-8</sup> kmol/s\\$m<sup>2</sup>. Thus, the rate of diffusion remains unchanged.

**EXAMPLE 2.3** (Calculation of rate of diffusion of one component from data on diffusion of another component): The rate of evaporation of water from a surface maintained at a temperature of 60°C is 2.71 # 10<sup>-4</sup> kg/s\\$m<sup>2</sup>. What will be the rate of evaporation of benzene from a similar surface but maintained at 26°C if the effective film thicknesses are the same in both the cases?

**Given**

Vapour pressure of water at 60°C = 149 mm Hg.

Vapour pressure of benzene at 26°C = 99.5 mm Hg.

Diffusivity of air-water vapour at 60°C = 2.6 # 10<sup>-5</sup> m<sup>2</sup>/s.

Diffusivity of air-benzene vapour at 26°C = 0.98 # 10<sup>-5</sup> m<sup>2</sup>/s.

Atmospheric pressure in both the cases = 1.013 # 10<sup>5</sup> N/m<sup>2</sup>

**Solution:** For evaporation of water

$$\text{Rate of evaporation} = 2.71 \# 10^{-4} \text{ kg/m}^2 \square \text{s} = 1.505 \# 10^{-5} \text{ kmol/s} \square \text{m}^2$$

$$T = 333 \text{ K}, p \square A_1 = 149 \text{ mm Hg} = 0.1986 \# 10^5 \text{ N/m}^2$$

$$p \square B_1 = 1.013 \# 10^5 - 0.1986 \# 10^5 = 0.8144 \# 10^5 \text{ N/m}^2$$

$$p \square A_2 = 0, p \square B_2 = 1.013 \# 10^5 \text{ N/m}^2$$

$$p \square BM = \frac{1.013 \times 10^5 - 0.8144 \times 10^5}{\ln(1.013 \times 10^5 / 0.8144 \times 10^5)} = 0.910 \# 10^5 \text{ N/m}^2$$

From Eq. (2.25), we have

$$z_2 - z_1 = z = \frac{D_{AB}P}{RTN_A} \frac{P_{A_1}}{P_{BM}}$$

Substituting the values, we obtain

$$z = \frac{(2.6 \times 10^{-5})(1.013 \times 10^5)}{(8314)(333)(1.505 \times 10^{-5})} \times \frac{(0.1986 \times 10^5)}{0.9101 \times 10^5} = 0.0138 \text{ m}$$

For evaporation of benzene

$$T = 299 \text{ K}, p_{\square A_1} = 99.5 \text{ mm Hg} = 0.1326 \# 10^5 \text{ N/m}^2$$

$$p_{\square B_1} = 0.8804 \# 10^5 \text{ N/m}^2, p_{\square A_2} = 0, p_{\square B_2} = 1.013 \# 10^5 \text{ N/m}^2$$

$$p_{\square BM} = 0.9451 \# 10^5 \text{ N/m}^2$$

Substituting the values in Eq. (2.25), we get

$$N_A = \frac{(0.98 \times 10^{-5})(1.013 \times 10^5)}{(8314)(299)(0.0138)} \times \frac{(0.1326 \times 10^5 - 0)}{0.9451 \times 10^5}$$

$$= 4.06 \# 10^{-6}$$

The rate of evaporation of benzene =  $4.06 \# 10^{-6} \text{ kmol/s/m}^2$

### ***Equimolar counter-diffusion of two components***

When two components of a mixture of *A* and *B* diffuse at the same rate but in opposite directions, the phenomenon is known as *equimolar counter-diffusion*. In practice, there are numerous examples of equimolar counter-diffusion. Distillation provides a good example of this type of diffusion. Let us consider a mixture of benzene and toluene being rectified. The vapour rising through the column is brought into intimate contact with the liquid flowing down so that mass transfer takes place between the two streams. The less volatile component (toluene) in the vapour condenses and passes on to the liquid phase while the more volatile component (benzene) in the liquid vaporises by utilizing the latent heat of condensation released by toluene. Thus, the vapour phase gets more and more enriched in benzene while the liquid phase gets more and more enriched in toluene. Since the molar latent heats of vaporisation of benzene and toluene are almost equal, one mole of toluene gets condensed while one mole of benzene gets vaporised provided there is no heat loss from the column.

The burning of carbon in air is another example of equimolar counter-diffusion. Assuming complete combustion, carbon dioxide is the only product of combustion and for one mole of oxygen diffusing to the carbon surface through the surrounding air film, one mole of carbon dioxide diffuses out.

For steady-state equimolar counter-diffusion of two components *A* and *B*,

$$N_A = -N_B, \text{ or, } N_A + N_B = 0$$

Substituting the values of  $(N_A + N_B)$  in Eq. (2.20), we have

$$N_A = -\frac{D_{AB}}{RT} \frac{dp'_A}{dz} \quad (2.26)$$

For steady-state diffusion through constant area,  $N_A$  is constant.

Integrating Eq. (2.26) between the limits  $z_1$  and  $z_2$ , and  $p'_A$  and  $p'_A$  yields

$$N_A \int dz = - \frac{D_{AB}}{RT} \int p'_{A_1} dp \square A$$

or,  $N_A = \frac{D_{AB}(p'_{A_1} - p'_{A_2})}{RTz}$  (2.27)

where,  $z = z_2 - z_1$ .

The distribution of partial pressure is shown in Figure 2.4.

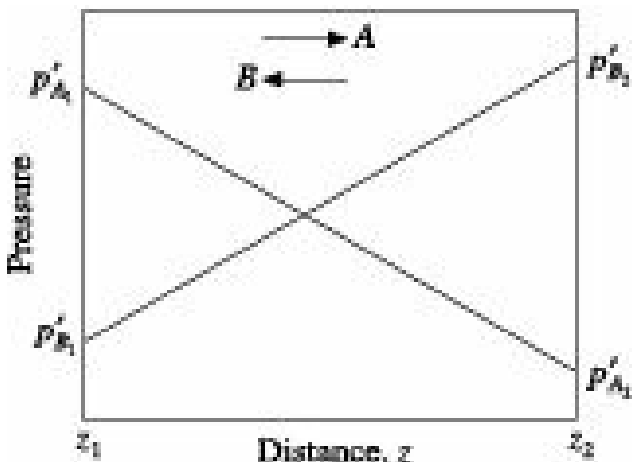


Figure 2.4 Distribution of partial pressure for equimolar counter-diffusion of *A* and *B*.

**EXAMPLE 2.4** (Equimolar counter-diffusion of two components): In a rectification column, toluene is diffusing from gas to liquid and benzene from liquid to gas at 30°C and 101.3 kN/m<sup>2</sup> pressure under conditions of equal molal counter diffusion. At one point in the column, the molal concentrations of toluene on the two sides of a gas film 0.5 mm thick are 70% and 20%, respectively. Assuming the diffusivity of benzene-toluene vapour under the operating conditions to be  $0.38 \times 10^{-5}$  m<sup>2</sup>/s, estimate the rate of diffusion of toluene and benzene in kg/hr across an area of 0.01 m<sup>2</sup>.

**Solution:** This is a case of equal molal counter-diffusion, Eq. (2.27) is applicable.

$$T = 303 \text{ K}, \quad P = 101.3 \text{ kN/m}^2,$$

$$D_{AB} = 0.38 \times 10^{-5} \text{ m}^2/\text{s}, \quad z = 0.0005 \text{ m.}$$

$$p \square_{A_1} = 1.013 \times 10^5 \times 0.70 = 7.091 \times 10^4 \text{ N/m}^2,$$

$$p \square_{A_2} = 1.013 \times 10^5 \times 0.20 = 2.026 \times 10^4 \text{ N/m}^2,$$

Substituting the values in Eq. (2.27), we get

$$N_A = \frac{0.38 \times 10^{-5}}{(8314)(303)(0.0005)} \times (7.091 - 2.026) \times 10^4$$

$$= 1.528 \times 10^{-4} \text{ kmol/s} \cdot \text{m}^2$$

The rate of diffusion of toluene per 0.01 m<sup>2</sup> surface

$$= 1.528 \# 10^{-4} \# 92 \# 3600 \# 0.01 = 0.506 \text{ kg/hr}$$

The rate of diffusion of benzene per  $0.01 \text{ m}^2$  surface

$$= 1.528 \# 10^{-4} \# 78 \# 3600 \# 0.01 = 0.429 \text{ kg/hr}$$

Other diffusional processes sometimes practised in the industry are discussed here.

### 2.5.2 Nonequimolar Counter-Diffusion of Two Components

In practice, we come across many cases where the two components  $A$  and  $B$  diffuse in opposite directions at different molar rates. For instance, in case of incomplete combustion of carbon in air producing carbon monoxide, for each mole of oxygen diffusing through the air film to the surface of carbon particle, two moles of carbon monoxide will diffuse in the opposite direction. This is a case of nonequimolar counter-diffusion where  $N_A = -N_B/2$ . In such a situation, the molar fluxes of  $A$  and  $B$  can be calculated by integrating Eq. (2.20) after expressing  $N_B$  in terms of  $N_A$ . Nonequimolar counter-diffusion is also encountered in distillation where the molar latent heats of vaporisation of the components are different.

### 2.5.3 Multi-component Diffusion

Multi-component diffusion is a complex process and development of equations for such diffusion is quite complicated. However, a relatively simple method can be developed following Maxwell-Stefan approach (Taylor and Krishna 1993). The present discussion has been confined to steady-state diffusion of a single component through a multi-component system.

In case of molecular diffusion in gases, if two components  $A$  and  $B$  follow ideal gas law, the diffusion equation can be written as

$$N_A = \frac{N_A}{N_A + N_B} \frac{D_{AB}P}{RTz} \ln \left( \frac{\frac{N_A}{(N_A + N_B)} (P - p'_{A_2})}{\frac{N_A}{(N_A + N_B)} (P - p'_{A_1})} \right) \quad (2.28)$$

It may be noted that in the special case where  $N_A = \text{constant}$  and  $N_B = 0$ , Eq. (2.28) reduces to Eq. (2.24).

Problems on diffusion of a component  $A$  through a mixture of several nondiffusing components can be solved by using an effective diffusivity in Eq. (2.28). The effective diffusivity can be synthesized from the binary diffusivities of the diffusing component with each of the other components (Bird et al. 1960).

$$\sum_i N_i$$

Thus in Eq. (2.28),  $(N_A + N_B)$  is replaced by  $\sum_i N_i$ , where  $N_i$  is positive if diffusion is in the same direction as that of  $A$  and negative if diffusion is in the opposite direction.

$D_{AB}$  has been replaced by  $D_{Am}$ .

$$D_{A_m} = \frac{y_A - y_{A_m} \sum_{i=A}^n N_i}{\sum_{i=A}^n \frac{1}{D_{A_i}} (y_i N_A - y_{A_m} N_i)} \quad (2.29)$$

where,  $D_{A_i}$  is the binary diffusivity. This indicates that  $D_{A_m}$  may vary considerably along the diffusion path, but a linear variation with distance can easily be assumed for practical calculations. From the simplifying assumption made at the very outset, all the fluxes except the flux of component  $A$  are zero, i.e. all the components except  $A$  are stagnant. Eq. (2.29) then becomes

$$D_{A_m} = \frac{1 - y_A}{\sum_{i=B}^n \frac{y_i}{D_{A_i}}} = \frac{1}{\sum_{i=B}^n \frac{y'_i}{D_{A_i}}} \quad (2.30)$$

where,  $y'_i$  is the mole fraction of component  $i$  on  $A$ -free basis.

If a gas  $A$  is diffusing through a mixture of three gases  $B$ ,  $C$  and  $D$ ;  $y_B$ ,  $y_C$ , and  $y_D$  are their respective mole fractions in the mixture on  $A$ -free basis and  $D_{AB}$ ,  $D_{AC}$  and  $D_{AD}$  are the diffusivities of  $A$  in pure  $B$ ,  $C$  and  $D$ , respectively Eq. (2.30) reduces to

$$D_{A_m} = \frac{1}{\frac{y_B}{D_{AB}} + \frac{y_C}{D_{AC}} + \frac{y_D}{D_{AD}}} \quad (2.31)$$

**EXAMPLE 2.5** (Diffusion of one component through a stagnant layer of a multi-component mixture): Oxygen is diffusing through a stagnant gas mixture containing 50% methane, 30% hydrogen and 20% carbon dioxide by volume. The total pressure is  $1 \times 10^5$  N/m<sup>2</sup> and the temperature is 20°C. The partial pressure of oxygen at two planes 5 mm apart are  $13 \times 10^3$  and  $6.5 \times 10^3$  N/m<sup>2</sup> respectively. Estimate the rate of diffusion of oxygen.

*Given:* At 0°C and pressure at 1 atm, the diffusivities of oxygen with respect to methane, hydrogen and carbon dioxide are:

$$D_{O_2-CH_4} = 0.184 \text{ cm}^2/\text{s}, D_{O_2-H_2} = 0.690 \text{ cm}^2/\text{s}, \text{ and } D_{O_2-CO_2} = 0.139 \text{ cm}^2/\text{s}.$$

**Solution:** Since volume percent = mole percent, mole fractions of the three components of the stagnant gas are:

$$CH_4 = 0.50, H_2 = 0.30 \text{ and } CO_2 = 0.20.$$

The given diffusivity data are converted to diffusivities at 20°C using the relation:

$$\frac{D}{D_0} = \left[ \frac{T}{T_0} \right]^{1.5}$$

$$D_{O_2-CH_4} = 0.184 (293/273)^{1.5} = 0.209 \text{ cm}^2/\text{s}$$

$$D_{O_2-H_2} = 0.690 (293/273)^{1.5} = 0.822 \text{ cm}^2/\text{s}$$

$$D_{O_2-CO_2} = 0.139 (293/273)^{1.5} = 0.158 \text{ cm}^2/\text{s}$$

From Eq. (2.31),

$$D_{Am} = \frac{1}{(0.50/0.209) + (0.30/0.822) + (0.20/0.158)} = 0.248 \text{ cm}^2/\text{s}$$

$$= 2.48 \times 10^{-5} \text{ m}^2/\text{s}$$

Given:  $P = 1 \times 10^5 = 100 \times 10^3 \text{ N/m}^2$ ;  $p_{\square A_1} = 13 \times 10^3 \text{ N/m}^2$ ;  $p_{\square A_2} = 6.5 \times 10^3 \text{ N/m}^2$

$$T = 20^\circ\text{C} = 293 \text{ K}; z = 5 \text{ mm} = 0.005 \text{ m}$$

$$p_{\square A_1} = 13 \times 10^3 \text{ N/m}^2; p_{\square B_1} = (100 \times 10^3 - 13 \times 10^3) = 87 \times 10^3 \text{ N/m}^2$$

$$p_{\square A_2} = 6.5 \times 10^3 \text{ N/m}^2; p_{\square B_1} = (100 \times 10^3 - 6.5 \times 10^3) = 93.5 \times 10^3 \text{ N/m}^2$$

$$p_{\square B_M} = \frac{\frac{(93.5 \times 10^3) - (87 \times 10^3)}{\ln \frac{(93.5 \times 10^3)}{(87 \times 10^3)}}}{= 90.2 \times 10^3 \text{ N/m}^2}$$

Substituting the values in Eq. (2.25), we get

$$N_A = \frac{(2.48 \times 10^{-5})(1 \times 10^5)(13 \times 10^3 - 6.5 \times 10^3)}{(8314)(293)(0.005)(90.2 \times 10^3)} = 1.467 \text{ kmol/m}^2\text{s.}$$

## 2.5.4 Diffusion Through Variable Area (Truncated Cone)

In case of steady flow through a conical channel the flux changes with position. Let us consider two large vessels connected by a truncated conical duct as shown in Figure 2.5.

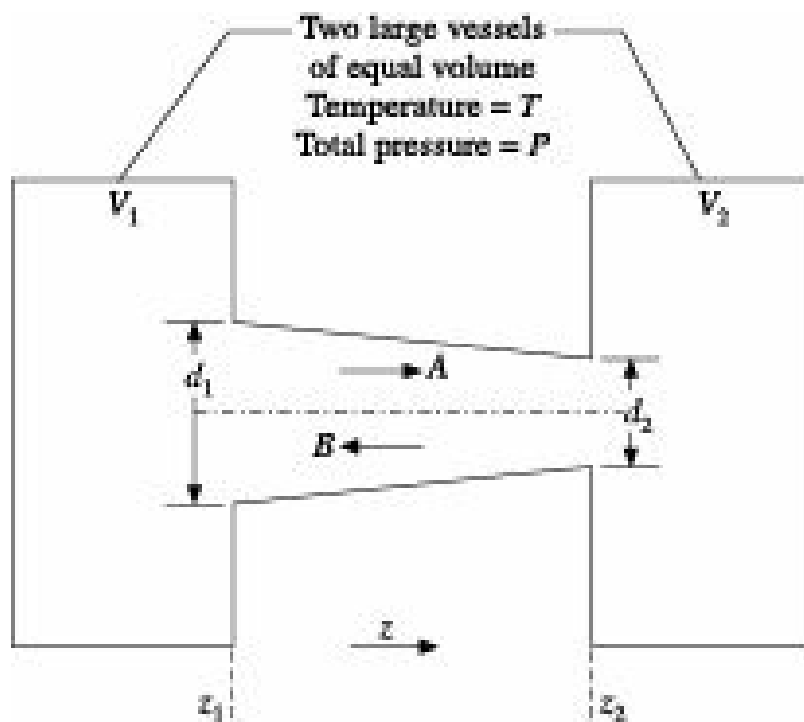


**Figure 2.5** Equal molal counter-diffusion through a truncated cone.

Both the vessels contain components \$A\$ and \$B\$ but in different proportions. \$A\$ and \$B\$ will diffuse in opposite directions depending upon their concentrations in the two vessels so that equimolar counter-diffusion will take place. Since the vessels are very large in comparison with the duct, steady-state transfer may be assumed at the initial stage.

Let us further assume that component \$A\$ diffuses in the \$z\$-direction. According to Eq. (2.26), the rate of transfer at any cross section will be

$$N_{Az} = \frac{q_{Az}}{A} = -\frac{D_{AB}}{RT} \frac{dp'_A}{dz}$$

where, \$q\_{Az}\$ is the rate of transfer of component \$A\$ in the \$z\$-direction in moles/unit time. Denoting the terminal diameters of the truncated cone by \$d\_1\$ and \$d\_2\$ at axial points \$z\_1\$ and \$z\_2\$ respectively (\$d\_1 > d\_2\$), the cross section at a distance \$z\$ from \$z\_1\$ is

$$A = \frac{\pi d^2}{4} = \frac{\pi}{4} \left( d_1 - \frac{(d_1 - d_2)}{(z_2 - z_1)} z \right)^2 \quad (2.32)$$

Substituting the value of \$N\_{Az}\$ from Eq. (2.26) in Eq. (2.32), we get

$$q_{Az} = \frac{\pi D_{AB}}{4RT} \frac{(d_1 - d_2)}{(z_2 - z_1)} \frac{\frac{p'_A - p'_B}{d_1 - \frac{(d_1 - d_2)}{(z_2 - z_1)} z_2} - \frac{1}{d_1 - \frac{(d_1 - d_2)}{(z_2 - z_1)} z_1}}{\frac{1}{d_1 - \frac{(d_1 - d_2)}{(z_2 - z_1)} z_2} - \frac{1}{d_1 - \frac{(d_1 - d_2)}{(z_2 - z_1)} z_1}} \quad (2.33)$$

$$\frac{(d_1 - d_2)}{(z_2 - z_1)}$$

Denoting \$\frac{(d\_1 - d\_2)}{(z\_2 - z\_1)}\$ by \$y\$, a constant,

$$q_{Az} = \frac{\pi D_{AB}}{4RT} \psi \frac{P'_{A_1} - P'_{A_2}}{\frac{1}{(d_1 - \psi z_2)} - \frac{1}{(d_1 - \psi z_1)}} \quad (2.34)$$

**EXAMPLE 2.6** (Diffusion through a truncated cone): Two large vessels are connected by a conical duct 60 cm long having internal diameters of 20 cm and 10 cm at the larger and smaller ends respectively. Vessel 1 contains a uniform mixture of 80 mol% nitrogen and 20 mol% oxygen. Vessel 2 contains 30 mol% nitrogen and 70 mol% oxygen. The temperature throughout is 0°C and the pressure throughout is 1 atm. The diffusivity of N<sub>2</sub>-O<sub>2</sub> under these conditions is 0.181 cm<sup>2</sup>/s.

Determine the rate of transfer of nitrogen between the two vessels during the initial stage of the process assuming the complete absence of convection and that nitrogen diffuses in the direction of decreasing diameter.

**Solution:** As per the given conditions:  $p_{\square A_1} = 0.80 \# 1 = 0.80 \text{ atm}$ ;  $p_{\square A_2} = 0.30 \# 1 = 0.30 \text{ atm}$ .

$$T = 273 \text{ K}; z_1 = 0; z_2 = 60 \text{ cm}; R = 82.06 \text{ cm}^3 \text{ atm/K gmol}$$

$$\gamma = \frac{(d_1 - d_2)}{(z_2 - z_1)} = \frac{(20 - 10)}{(60 - 0)} = 0.167$$

Substituting the values in Eq. (2.34), we obtain

$$q_{Az} = \frac{(3.14)(0.181)}{(4)(82.06)(273)} \times 0.167 \times \frac{(0.80 - 0.30)}{\frac{1}{(20 - 0.167 \times 60)} - \frac{1}{(20 - 0.167 \times 0)}}$$

$$= 1.052 \# 10^{-5} \text{ gmol/s.}$$

Rate of transfer of nitrogen =  $1.052 \# 10^{-5} \text{ gmol/s.}$

## 2.5.5 Diffusion from a Sphere

Diffusion from or to a sphere takes place in several important practical situations. A few typical examples are sublimation from a spherical solid such as naphthalene, iodine, etc., diffusion in a spherical catalyst pellet, evaporation from a droplet in prilling tower, spray dryers, etc.

Let us consider a sphere of radius  $r_s$  placed in a concentric spherical shell of radius  $r_O$ . The partial pressure of a component  $A$  at the surface of the sphere is kept constant at  $p_{\square A_s}$ . The spherical shell contains a stagnant gas  $B$  in which  $D_{AB}$ , the diffusivity of  $A$  is constant. The partial pressure of component  $A$  at the boundary of the spherical shell is uniform at  $p_{\square A_b}$  ( $p_{\square A_b} < p_{\square A_s}$ ). This boundary acts as the sink for component  $A$ . It may be noted that since the diffusion is in steady-state, the material between the surface of the sphere and the boundary of the shell cannot act as a sink.

Equation for steady-state diffusion from the surface of the sphere may be expressed as

$$4pr_s^2 N_{Ar} = 4pr^2 N_{Ar} = - \frac{4\pi r^2 D_{AB} P}{RT(P - p'_A)} \frac{dp'_A}{dr} = \text{constant} \quad (2.35)$$

where,  $N_{Ar}$ , the radial flux at  $r$ , has been replaced by Eq. (2.20) with  $N_{Br} = 0$ . Integrating Eq. (2.35), we have

$$4pr^2 N_{Ar} = \frac{4\pi D_{AB}P}{RT} \frac{(r_I r_o)}{(r_o - r_I)} \ln \frac{(P - P'_{A_s})}{(P - P'_{A_t})} \quad (2.36)$$

Since  $r_o \gg r_s$ , Eq. (2.36) may be written as

$$-\frac{dm_A}{d\theta} = 4pr^2 N_{Ar} = \frac{4\pi D_{AB}P r_s}{RT} \ln \frac{(P - P'_{A_s})}{(P - P'_{A_t})} \quad (2.37)$$

where,  $-\frac{dm_A}{d\theta}$  is the instantaneous rate of evaporation,

$$\text{and } m_A = \frac{4\pi r^3 \rho_A}{3M_A},$$

$$r_s = \left( \frac{3M_A m_A}{4\pi \rho_A} \right)^{1/3}$$

Substituting for  $r_s$  and integrating, we get

$$\theta = \frac{\rho_A r_I^2 RT}{2M_A D_{AB}P \ln[(P - P'_{A_s})/(P - P'_{A_t})]} \quad (2.38)$$

Evaporation from a droplet causes its temperature to fall to a steady-state value called the *wet-bulb temperature*.

**EXAMPLE 2.7** (Diffusion from a sphere): A water drop with an initial diameter of 2.5 mm is suspended on a thin wire in a large volume of air. The air is at a temperature of 26.65°C and a total pressure of 1 atm. Moisture present in the air exerts a partial pressure of 0.01036 atm.

The wet-bulb temperature of the water drop is 15.55°C at which temperature the vapour pressure of water is 0.01743 atm. The diffusivity of water vapour at its average temperature of 21.1°C has been estimated to be 0.2607 cm<sup>2</sup>/s.

Estimate the time required for complete evaporation of the water drop.

The effect of curvature on the vapour pressure of water and convective effect may be neglected.

### Solution:

Initial radius of the water drop =  $2.5/2 = 1.25$  mm = 0.125 cm

Average temperature =  $(26.65 + 15.55)/2 = 21.10^\circ\text{C} = 294.1$  K.

For water,  $M_A = 18$ , Diffusivity in air = 0.2607 cm<sup>2</sup>/s,  $\rho_A = 1$  g/cm<sup>3</sup>,  $P = 1$  atm. Substituting the values in Eq. (2.38), time required for evaporation of the drop is

$$\theta = \frac{(1)(0.125)^2 (82.06)(294.1)}{2(18)(0.2607)(1) \ln \left[ \frac{1 - 0.01036}{1 - 0.01743} \right]}$$

$$= 6217.5 \text{ s} = 1.727 \text{ hr.}$$

## 2.6 Diffusion Coefficient or Diffusivity of Gases

As mentioned in Section 2.4, the constant of proportionality between molar flux and concentration gradient in Fick's equation [Eq. (2.9)] has been defined as diffusion coefficient or diffusivity. Diffusivity is a property of the diffusing component and the medium through which diffusion takes place. Gas phase diffusivity depends on the temperature and pressure of the system. Diffusivity also depends on the presence of other components, the intra-molecular forces in the mixture and the number of collisions of the diffusing molecules with other molecules present in the system.

The kinetic theory of gases expresses diffusivity as

$$D_{AB} = \frac{\lambda u}{2} \quad (2.39)$$

where,  $\lambda$  is the mean free path of the diffusing molecules, and  $u$  is their mean speed.

Higher temperature increases the mean speed,  $u$  and hence increases  $D_{AB}$  which generally varies with the absolute temperature raised to the power 1.50 to 1.75. Higher pressure on the other hand reduces the mean free path of the molecules, increases the number of collisions and reduces the diffusivity which varies inversely to the total pressure up to a pressure of about 10 atm.

**Dimension of Diffusivity:** The dimension of diffusivity can be derived both from Eq. (2.9) and Eq. (2.39).

From Eq. (2.9), we have

$$[D_{AB}] = \frac{[\text{ML}^{-2} \cdot \theta^{-1}][\text{L}]}{[\text{ML}^{-3}]} = \frac{\text{L}^2}{\theta}$$

and from Eq. (2.39),

$$[D_{AB}] = [\text{L}] [\text{L} \square \theta^{-1}] = \text{L}^2/\theta.$$

Generally, diffusivity is expressed in  $\text{cm}^2/\text{s}$  or  $\text{m}^2/\text{s}$ .

It may be noted that kinematic viscosity or momentum diffusivity ( $\eta$ ), thermal diffusivity ( $a$ ) and molecular diffusivity ( $D$ ) have the same dimension of  $(\text{L}^2/\text{i})$ . These three are the coefficients of momentum, heat and mass transport respectively, and their analogy, which constitutes the basis of transport phenomena, is of considerable importance in chemical engineering (Bird et al. 2006).

### 2.6.1 Equivalence of Diffusivities

As molar density of a binary gas mixture does not depend on composition, we have for an ideal gas mixture

$$c_A + c_B = t_M = \frac{P}{RT} \quad (2.40)$$

where,  $c_A$  and  $c_B$  are concentrations of components  $A$  and  $B$  respectively,

Differentiating Eq. (2.40), we get

$$dc_A + dc_B = dt_M = 0$$

whence,  $dc_A = -dc_B$

Considering a reference plane for which volume flow is zero, the sum of the molar diffusion fluxes of  $A$  and  $B$  also becomes zero,

$$-D_{AB} \frac{dc_A}{dx} - D_{BA} \frac{dc_B}{dx} = 0 \quad (2.41)$$

Since  $dc_A = -dc_B$ , it follows that  $D_{AB} = D_{BA}$

Thus, the diffusivity of a gas  $A$  through another gas  $B$  is equal to the diffusivity of  $B$  through  $A$ . The above relation may also be extended to liquid diffusivities provided all mixtures of  $A$  and  $B$  have the same density.

## 2.6.2 Determination of Gas Phase Diffusivity

Values of diffusivities of gases may be obtained from literature, predicted from available equations or by conducting suitable experiments.

### Data available in literature

Experimental values of gas phase diffusivities at different temperatures and pressures for a number of systems are available in the International Critical Tables (ICT 1929). Some selected values are also available in several books (Perry et al. 1997 and Treybal 1985). These values are quite reliable and can be used wherever available.

A list of some gas phase diffusivities for some common systems is given in Table 2.1.

**Table 2.1** Diffusivities of Some Common Gas Pairs at 1 atm Pressure

Gas pair <i>A-B</i>	Temperature °C	$D_{AB} \# 10$ cm <sup>2</sup> /s	Gas Pair <i>A-B</i>	Temperature °C	$D_{AB} \# 10$ cm <sup>2</sup> /s
Air-Ammonia	0	1.98	CO <sub>2</sub> -H <sub>2</sub> O	34.5	2.02
Air-Benzene	25.2	0.96	CO <sub>2</sub> -N <sub>2</sub>	25.2	1.65
Air-CH <sub>4</sub>	0	1.96	CO <sub>2</sub> -O <sub>2</sub>	0	1.39
Air-C <sub>2</sub> H <sub>5</sub> OH	0	1.02	H <sub>2</sub> -He	25.2	11.32
Air-CO <sub>2</sub>	3.2	1.42	H <sub>2</sub> -H <sub>2</sub> O	34.1	9.15
Air-H <sub>2</sub>	0	6.11	H <sub>2</sub> -NH <sub>3</sub>	25	7.83
Air-H <sub>2</sub> O	25.9	2.58	H <sub>2</sub> -N <sub>2</sub>	24.2	7.73
Air-O <sub>2</sub>	0	1.775	H <sub>2</sub> -O <sub>2</sub>	0.2	6.97
Air-Toluene	25.9	0.86	H <sub>2</sub> -SO <sub>2</sub>	12.5	5.25
CH <sub>4</sub> -He	25	6.75	N <sub>2</sub> -SO <sub>2</sub>	-10	1.04
CH <sub>4</sub> -H <sub>2</sub>	0	6.25	O <sub>2</sub> -CO	0	1.85
CO-H <sub>2</sub>	22.6	7.43	O <sub>2</sub> -H <sub>2</sub> O	35.1	2.82
CO <sub>2</sub> -H <sub>2</sub>	25	6.46	He-H <sub>2</sub> O	25.2	9.08

### Prediction from available equations

A number of equations, mostly empirical have been proposed for the prediction of gas phase diffusivities. Some of them are quite reliable.

Based on the kinetic theory of gases, Jeans and co-workers (Bird et al. 1960) developed an expression for diffusivities of monoatomic gases. Gilliland (1934) determined the constants of their expression from published experimental data and proposed the following simple empirical equation for prediction of diffusivities of binary gas mixtures:

$$D_{AB} = 435.7 \frac{T^{1.5}}{P(V_A^{1/3} + V_B^{1/3})^2} \left( \frac{1}{M_A} + \frac{1}{M_B} \right)^{0.5} \quad (2.42)$$

where,

$D_{AB}$  = diffusivity of components  $A$  in  $B$ ,  $\text{cm}^2/\text{s}$

$T$  = temperature, K

$P$  = total pressure,  $\text{N/m}^2$

$V_A$  and  $V_B$  = molar volumes of  $A$  and  $B$  respectively,  $\text{m}^3/\text{kmol}$

$M_A$  and  $M_B$  = molecular weights of  $A$  and  $B$ , respectively.

Molar volumes of compounds may be estimated from Kopp's law of additive volumes.

**EXAMPLE 2.8** (Estimation of diffusivity in gases using Gilliland equation): Estimate the diffusivity of ammonia in air at standard atmospheric pressure and 0°C by using Gilliland equation.

*Given:* Molecular volume of ammonia and air are 25.8 and 29.9, respectively.

**Solution:**  $T = 273 \text{ K}$ ,  $P = 1.013 \times 10^5 \text{ N/m}^2$

For ammonia:  $M_A = 17$ ,  $V_A = 25.8$

For air:  $M_B = 29$ ,  $V_B = 29.9$

Substituting these values in Eq. (2.42), we obtain

$$D_{AB} = 435.7 \times 10^{-4} \frac{(273)^{1.5}}{(1.013 \times 10^5)(25.8^{1/3} + 29.9^{1/3})^2} \left( \frac{1}{17} + \frac{1}{29} \right)^{0.5}$$

$$= 1.615 \times 10^{-5} \text{ m}^2/\text{s}$$

Fuller et al. (1966) had proposed the following empirical equation for predicting binary gas phase diffusivities up to moderate pressures:

$$D_{AB} = 0.00100 \frac{T^{1.75}}{P[(\Sigma V_A)^{1/3} + (\Sigma V_B)^{1/3}]^2} \left( \frac{1}{M_A} + \frac{1}{M_B} \right)^{0.5} \quad (2.43)$$

where,

$D_{AB}$  = diffusivity of components  $A$  and  $B$ ,  $\text{cm}^2/\text{s}$

$T$  = temperature, K

$P$  = total pressure, atm

$\sum y_A$  and  $\sum y_B$  = sum of atomic diffusion volumes of  $A$  and  $B$  respectively

$M_A$  and  $M_B$  = molecular weights of  $A$  and  $B$ , respectively.

Equation (2.43) is simple but quite reliable. In most cases, the error is within  $\pm 5\%$ .

Atomic diffusion volumes for some common molecules and structural groups have been presented in Table 2.2.

**Table 2.2** Atomic diffusion volumes for use in Eq. (2.43)

Atomic and Structural diffusion volume increments,  $u$

Carbon	16.5	Chlorine	19.5
Hydrogen	1.98	Sulphur	17.0
Oxygen	5.48	Aromatic and heterocyclic rings	-20.2
Nitrogen	5.69		

### Diffusion volumes of simple molecules, $S_u$

(H <sub>2</sub> ) Hydrogen	7.07	CO	18.9
(D <sub>2</sub> ) Deuterium	6.70	CO <sub>2</sub>	26.9
(He) Helium	2.88	N <sub>2</sub> O	35.9
(O <sub>2</sub> ) Oxygen	16.6	H <sub>2</sub> O	12.7
Air	20.1	SF <sub>6</sub>	69.7
(Ne) Neon	5.59	Cl <sub>2</sub>	37.7
(Ar) Argon	16.1	Br <sub>2</sub>	67.2
(Kr) Krypton	22.8	SO <sub>2</sub>	41.1
(Xe) Xenon	37.9		

**EXAMPLE 2.9** (Estimation of diffusivity in gases using Fuller et al. equation): Using Equation of Fuller et al., estimate the diffusivity of naphthalene vapour in air at a temperature of 0°C and a total pressure of 1 atm.

**Solution:** Let us call naphthalene (C<sub>10</sub>H<sub>8</sub>)  $A$  and air  $B$ . Hence,  $M_A = 128.16$ ,  $M_B = 29$ .

From Table 2.2, atomic diffusion volume increments are as follows:

For naphthalene ( $A$ ):  $(\sum u)_A = (10 \# 16.5) + (8 \# 1.98) - (2 \# 20.2) = 140.44$

For air ( $B$ ):  $(\sum u)_B = 20.1$

Substituting the values in Eq. (2.43), we get

$$D_{AB} = 0.00100 \frac{(273)^{1.75}}{1[(140.44)^{1/3} + (20.1)^{1/3}]^2} \left( \frac{1}{128.16} + \frac{1}{29} \right)^{0.5}$$

$$= 0.0605 \text{ cm}^2/\text{s.}$$

Chapman and Enskog independently proposed an equation for prediction of binary gas-phase diffusivities. This equation is a theoretical equation based on the kinetic theory of gases and gives fairly reliable values of  $D_{AB}$ . The diffusivity strongly depends upon binary interaction parameters of the two components. Chapman and Enskog used the Lennard-Jones potential function (Chapman and Cowling 1970) to calculate the interaction parameters.

The equation proposed by Chapman and Enskog is as follows:

$$D_{AB} = \frac{1.858 \times 10^{-7} T^{1.5} \left( \frac{1}{M_A} + \frac{1}{M_B} \right)^{0.5}}{P \sigma_{AB}^2 \Omega} \quad (2.44)$$

where,

$D_{AB}$  = diffusivity of components  $A$  and  $B$ ,  $\text{m}^2/\text{s}$

$T$  = temperature, K

$P$  = total pressure, atm.

$M_A$  and  $M_B$  = molecular weights of  $A$  and  $B$ , respectively

$v_{AB}$  = molecular separation at collision =  $(v_A + v_B)/2$

$v_A$  and  $v_B$  = molecular diameters of  $A$  and  $B$ , respectively, Å

$\Omega$  = collision integral, function of  $(kT/f_{AB})$ , where  $k$  is the Boltzmann's constant

$f_{AB}$  = energy of molecular attraction between molecules of  $A$  and  $B$  =  $\sqrt{\epsilon_A \epsilon_B}$ .

Values of  $v$  and  $f$  for some common substances are given in Table 2.3, and values of collision integral  $\Omega$  are given in Table 2.4.

If values of  $v$  and  $f$  are not available, the same may be estimated from the properties of the fluid at the critical point ( $c$ ), the liquid at the normal boiling point ( $b$ ), or the solid at the melting point ( $m$ ), by following very approximate relations (Bird et al. 2006):

$$f/k = 0.77 T_c \text{ and } v = 0.841 V_c^{1/3} \text{ or, } v = 2.44 (T_c/P_c)^{1/3}$$

$$f/k = 1.15 T_b \text{ and } v = 1.166 V_b^{1/3}$$

$$f/k = 1.92 T_m \text{ and } v = 1.222 V_m^{1/3}$$

where,  $f/k$  and  $T$  are in K,  $v$  is in Å,  $V$  is in  $\text{cm}^3/\text{gmol}$ , and  $P_c$  is in atm.

**Table 2.3** Lennard-Jones potential for some common substances

Compound	$v, \text{\AA}$	$f/k_B, \text{K}$
Argon	3.542	93.3
Helium	2.551	10.22
Air	3.711	78.6
Bromine	4.296	507.9
Carbon tetrachloride	5.947	322.7
Chloroform	5.389	340.2
Methyl chloride	4.182	481.8
Methyl bromide	4.118	449.2
Methanol	3.626	481.8
Methane	3.758	148.6
Carbon monoxide	3.690	91.7

Carbon dioxide	3.941	195.2
Carbon disulphide	4.483	467
Acetylene	4.033	231.8
Ethylene	4.163	224.7
Ethane	4.443	215.7
Ethanol	4.530	362.6
Methyl ether	4.307	395.0
Propylene	4.678	298.9
Propane	5.118	237.1
Acetone	4.600	560.2
Ethyl ether	5.678	313.8
Ethyl acetate	5.205	521.3
Benzene	5.349	412.3
Cyclohexane	6.182	297.1
<i>n</i> -Hexane	5.949	399.3
Chlorine	4.217	316.0
Fluorine	3.357	112.6
Hydrogen bromide	3.353	449
Hydrogen cyanide	3.630	569.1
Hydrogen chloride	3.339	344.7
Hydrogen fluoride	3.148	330
Hydrogen iodide	4.211	288.7
Hydrogen	2.827	59.7
Water	2.641	809.1
Hydrogen peroxide	4.196	289.3
Hydrogen sulphide	3.623	301.1
Mercury	2.969	750
Mercuric chloride	4.550	750
Mercuric iodide	5.625	695.6
Mercuric bromide	5.080	686.2
Iodine	5.160	474.2
Ammonia	2.900	558.3
Nitric oxide	3.492	116.7
Nitrogen	3.798	71.4
Nitrous oxide	3.828	232.4
Oxygen	3.467	106.7
Phosphine	3.981	251.5
Sulphur dioxide	4.112	335.4
Uranium hexafluoride	5.967	236.8

**Table 2.4** Values of collision integral,  $\Omega$

$k_B T/f_{AB}$	$\square_{D,AB}$	$k_B T/f_{AB}$	$\square_{D,AB}$
0.30	2.662	2.00	1.075
0.35	2.476	2.10	1.057
0.40	2.318	2.20	1.041
0.45	2.184	2.30	1.026

0.50	2.066	2.40	1.012
0.55	1.966	2.50	0.9996
0.60	1.877	2.60	0.9878
0.65	1.798	2.70	0.9770
0.70	1.729	2.80	0.9672
0.75	1.667	2.90	0.9576
0.80	1.612	3.00	0.9490
0.85	1.562	3.20	0.9328
0.90	1.517	3.40	0.9186
0.95	1.476	3.60	0.9058
1.00	1.439	3.80	0.8942
1.05	1.406	4.00	0.8836
1.10	1.375	5.00	0.8422
1.15	1.346	6.00	0.8124
1.20	1.320	7.00	0.7896
1.25	1.296	8.00	0.7712
1.30	1.273	9.00	0.7556
1.35	1.253	10.00	0.7424
1.40	1.233	20.00	0.6640
1.45	1.215	30.00	0.6232
1.50	1.198	40.00	0.5960
1.55	1.182	50.00	0.5756
1.60	1.167	60.00	0.5596
1.65	1.153	70.00	0.5464
1.70	1.140	80.00	

0.5352			
1.75	1.128	90.00	0.5256
1.80	1.116	100.00	0.5130
1.85	1.105	200.00	0.4644
1.90	1.094	400.00	0.4170
1.95	1.084		

**EXAMPLE 2.10** (Estimation of binary gas diffusivity using Chapman-Enskog equation): Estimate the diffusivity of sulphur dioxide in air at standard atmospheric pressure and 400°C by using Equation of Chapman-Enskog.

**Solution:** Let SO<sub>2</sub> = A, and Air = B.

From Table 2.3,

For air:

$$f_A/k_B = 78.6 \text{ K}, \quad v_A = 3.711 \text{ \AA} = 3.711 \times 10^{-10} \text{ m} = 0.3711 \text{ nm}$$

$$\text{For SO}_2: \quad f_B/k_B = 335.4 \text{ K}, \quad v_B = 4.112 \text{ \AA} = 4.112 \times 10^{-10} \text{ m} = 0.4112 \text{ nm}$$

and for the system:

$$v_{AB} = \frac{1}{2}(v_A + v_B) = \frac{1}{2}(3.711 + 4.112) = 3.9115 \text{ \AA} = 0.39115 \text{ nm}$$

$$f_{AB} = k_B(78.6 \square 335.4)^{1/2}$$

$$\frac{k_B T}{\varepsilon_{AB}} = \frac{k_B (673)}{k_B [(78.6)(335.4)]^{1/2}} = 4.14$$

From Table 2.4,  $\Omega = 0.88$

Using Chapman-Enskog Eq. (2.44)

$$D_{\text{SO}_2\text{-air}} = \frac{(1.858 \times 10^{-7})(673)^{1.5} \sqrt{\frac{1}{64} + \frac{1}{28.9}}}{(1)(3.9115)^2(0.88)}$$

$$= 5.40 \times 10^{-5} \text{ m}^2/\text{s} = 0.54 \text{ cm}^2/\text{s}$$

**EXAMPLE 2.11** (Rate of diffusion of a gas through the pores of a catalyst): A nickel catalyst for the hydrogenation of ethylene has a mean pore diameter of 100 Å. Calculate the diffusivities of hydrogen for this catalyst at (i) temperature 100°C, pressure 1 atm and (ii) temperature 100 °C, pressure 10 atm in a hydrogen-ethane mixture.

**Solution:** Let hydrogen = A and ethane = B.

From Table 2.3,

$$\text{For H}_2 \text{ (A): } f_A/k_B = 59.7 \text{ K}; \quad v_A = 2.827 \text{ \AA} = 2.827 \times 10^{-10} \text{ m}$$

$$\text{For C}_2\text{H}_6 \text{ (B): } f_B/k_B = 215.7 \text{ K}; \quad v_B = 4.443 \text{ \AA} = 4.443 \times 10^{-10} \text{ m}$$

and for the system:

$$v_{AB} = \frac{1}{2}(v_A + v_B) = \frac{1}{2}(2.827 + 4.443) = 3.635 \text{ \AA}$$

$$f_{AB} = k_B (59.7 \# 215.7)]^{1/2}$$

$$\frac{k_B T}{\varepsilon_{AB}} = \frac{k_B(373)}{k_B(59.7 \times 215.7)^{1/2}} = 3.287.$$

From Table 2.4,  $\square = 0.92$

Given,  $T = 100^\circ\text{C} = 373 \text{ K}$ ,  $M_A = 2.016$ ,  $M_B = 30.05$ .

Substituting the values in Chapman-Enskog Eq. (2.44), we get

$$D_{\text{H}_2\text{-C}_2\text{H}_6} = \frac{(1.858 \times 10^{-7})(373)^{1.5} \sqrt{\frac{1}{2.016} + \frac{1}{30.05}}}{P(3.635)^2(0.92)} = \frac{8.01 \times 10^{-5}}{P}$$

(i) when  $P = 1 \text{ atm}$ ,  $D_{\text{H}_2\text{-C}_2\text{H}_6} = 8.01 \# 10^{-5} \text{ m}^2/\text{s} = 0.801 \text{ cm}^2/\text{s}$

(ii) when  $P = 10 \text{ atm}$ ,  $D_{\text{H}_2\text{-C}_2\text{H}_6} = 8.01 \# 10^{-6} \text{ m}^2/\text{s} = 0.0801 \text{ cm}^2/\text{s}$

**EXAMPLE 2.12** (From the value of gas phase diffusivity at a given temperature, prediction of diffusivity for the system at another temperature): The diffusion coefficient of  $\text{H}_2\text{-N}_2$  system is  $7.84 \# 10^{-5} \text{ m}^2/\text{s}$  at 1 atm and 298 K.

(i) Find out the diffusivity at 350 K and 500 K using Chapman-Enskog equation.

(ii) Using equation  $D = D_0 (P_0/P)(T/T_0)^n$ , find the diffusion coefficients at the above temperatures assuming  $n = 1.75$  and  $1.5$ .

**Solution:**

(i) For  $\text{H}_2(A)$ :  $f_A/k_B = 59.7 \text{ K}$ ,  $v_A = 2.827 \text{ \AA} = 2.827 \# 10^{-10} \text{ m}$ ,  $M_A = 2.016$

(ii) For  $\text{N}_2(B)$ :  $f_B/k_B = 71.4 \text{ K}$ ,  $v_B = 3.798 \text{ \AA} = 3.798 \# 10^{-10} \text{ m}$ ,  $M_B = 28.0134$

and for the system:

$$v_{AB} = \frac{1}{2}(v_A + v_B) = \frac{1}{2}(2.827 + 3.798) = 3.3125 \text{ \AA}$$

$$f_{AB} = k_B(f_A f_B)^{1/2} = k_B(59.7 \# 71.4)^{1/2}$$

$$\frac{k_B T}{\varepsilon_{AB}} = \frac{k_B(350)}{k_B(59.7 \times 71.4)^{1/2}} = 5.36.$$

From Table 2.4,  $\square_{AB} = 0.8314$ .

Using Chapman-Enskog Eq. (2.44), we have

$$\frac{(1.858 \times 10^{-7})(350)^{1.5} \sqrt{\frac{1}{2.016} + \frac{1}{28.0134}}}{(1.0)(3.3125)^2(0.8314)}$$

$$D_{\text{H}_2\text{-N}_2} \text{ at } 350 \text{ K} =$$

$$= 9.724 \# 10^{-5} \text{ m}^2/\text{s} = 0.972 \text{ cm}^2/\text{s}$$

Similarly,

$$D_{\text{H}_2\text{-N}_2} \text{ at } 500 \text{ K} (\text{when } k_B T/f_{AB} = 7.66, \square_{AB} = 0.7775) = 17.76 \# 10^{-5} \text{ m}^2/\text{s}.$$

$$(ii) D_{350} = D_{298} \frac{1}{1} \left( \frac{350}{298} \right)^{1.75} = 10.388 \# 10^{-5} \text{ m}^2/\text{s}$$

$$\text{and } D_{500} = D_{298} \frac{1}{1} \left( \frac{500}{298} \right)^{1.75} = 19.392 \# 10^{-5} \text{ m}^2/\text{s}$$

Proceeding in the same way, the values of diffusivity at 350 K and 500 K with  $n = 1.5$  are found to be  $D_{350} = 9.979 \# 10^{-5} \text{ m}^2/\text{s}$ , and  $D_{500} = 17.039 \# 10^{-5} \text{ m}^2/\text{s}$ , respectively.

Comparison of the computed values using different methods as above, shows that the diffusivity values obtained assuming  $n = 1.5$  are in good agreement with those obtained from Chapman-Enskog Equation.

Prediction of the diffusivity using Eq. (2.44) gives rise to values within 6% for nonpolar gas pairs at low density, if the collision constants are available from viscosity data. However, the error increases to about 10% if the Lennard-Jones parameters are estimated from thermodynamic data (Hirschfelder et al. 1949; Tee et al. 1966). The Chapman-Enskog theory fails to predict a variation in the diffusion coefficient with concentration. For example, diffusivity in some binary gas mixtures such as chloroform-air may vary as much as 9% with concentration, whereas in other systems like methanol-air, the diffusivity is independent of the concentration.

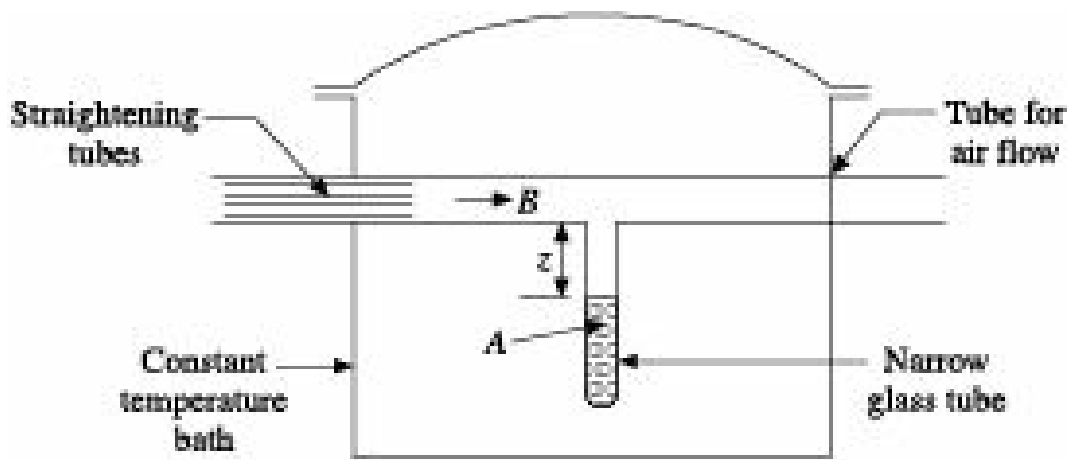


Figure 2.6 Determination of diffusivity by Stefan tube.

The Chapman-Enskog Equation for the transport coefficients is valid for the range 200-1000 K. Below 200 K, quantum effects become important (Hirschfelder et al. 1954), and above 1000 K the Lennard-Jones potential function is no longer applicable. If the force constants are derived from diffusion data instead of the usual viscosity data, the equations may be extended to 1200 K. Above 1200 K, the force constants should be evaluated from molecular beam scattering experiments.

The equations were developed for dilute gases composed of nonpolar, spherical, monoatomic molecules. Empirical functions and correlations, i.e. the Lennard-Jones potential must be used, with

the net result that the equations are remarkable for their ability to predict diffusivity for many gas mixtures. Agreement in nonpolar gas mixtures is excellent, even for polyatomic molecules. For polar-nonpolar gas mixtures the same equations are used with different combining laws (Hirschfelder et al. 1954).

### **Experimental determination of gas phase diffusivity**

Several methods are available for experimental determination of gas phase diffusivity. Two of them are discussed here.

**Stefan tube method:** This method is suitable for measuring gas phase diffusivity of binary mixtures where one of the components (*A*) is available as a liquid at the conditions of the experiment. The other component (*B*) is a gas not soluble in *A*.

As shown in Figure 2.6, the experimental set-up consists of a narrow glass tube 5-6 mm id, sealed at the bottom, held vertically and joined at the top with a larger diameter horizontal tube. The horizontal tube is sometimes provided with straighteners to avoid turbulence. The vertical tube is filled with the experimental liquid *A* up to a certain distance from the top while the gas *B* flows through the horizontal tube. The entire system is maintained at a constant temperature. The molecules of evaporated *A* diffuse through a mixture of *A* and *B*, reaches the top and is swept away by the gas *B*. Being insoluble in liquid *A*, *B* is not diffusing. Hence, this is a case of diffusion of one component through the stagnant layer of another component, i.e. gas. Assuming pseudo-steady state operation, the liquid level in the vertical tube varies very slowly. The experiment should be continued for a long time to reduce experimental error. The distances of the liquid level from the top open end at start and end of the experiment, and also the duration of the experiment along with the ambient temperature and barometric pressure are to be measured. The drop in the liquid level should be accurately measured, preferably with a travelling microscope.

Let *z* be the distance of the liquid level from top open end at any instant *i*, then from Eq. (2.25), the diffusional flux may be expressed as

$$N_A = \frac{D_{AB}P(p'_{A_1} - p'_{A_2})}{RTz p'_{BM}}$$

Equating the above flux with the drop *dz* in liquid level over time *di*,

$$\frac{a dz p_A}{M_A} = a N_A d\theta = \frac{a D_{AB} P (p'_{A_1} - p'_{A_2})}{R T p'_{BM} z} d\theta \quad (2.45)$$

Integrating and rearranging, we get

$$D_{AB} = \frac{RT p_A (z_2^2 - z_1^2) p'_{BM}}{2PM_A (p'_{A_1} - p'_{A_2}) \theta} \quad (2.46)$$

where, *z*<sub>1</sub> and *z*<sub>2</sub> are the distances of the liquid surface from the top at the beginning and at the end of the experiment.

The partial pressure (*p*<sub>A1</sub>) of component *A* at the liquid surface is the vapour pressure of *A* at the temperature of experiment. At the top open end of the tube, *p*<sub>A2</sub> may be assumed zero since vapours

of  $A$  are swept away by  $B$ .

**EXAMPLE 2.13** (Experimental determination of diffusivity of a gas by Stefan-tube method): A narrow vertical glass tube is filled with liquid toluene up to a depth of 2 cm from the top open end placed in a gentle current of air. After 150 hr, the liquid level has dropped to 4.4 cm from the top. The temperature is 25°C and the total pressure  $1.013 \times 10^5 \text{ N/m}^2$ .

At 25°C, the vapour pressure of toluene is 29.2 mm Hg and the density of liquid toluene is  $850 \text{ kg/m}^3$ . Neglecting the effects of convective currents and counter diffusion of air, calculate the diffusivity of toluene in air at 25°C and  $1.013 \times 10^5 \text{ N/m}^2$  pressure.

**Solution:** From Eq. (2.46), we get

$$D_{AB} = \frac{\rho}{M\Theta} \frac{RT}{P \ln(p_{B_2}'/p_{B_1}')} \frac{(z_2^2 - z_1^2)}{2}$$

$$T = 25^\circ\text{C} = 298 \text{ K}, \quad P = 1.013 \times 10^5 \text{ N/m}^2,$$

$$q = 150 \text{ hr} = 5.4 \times 10^5 \text{ s}, \quad z_1 = 0.02 \text{ m},$$

$$z_2 = 0.044 \text{ m}, \quad R = 8314 \text{ Nm/(kmol)(K)}.$$

Molecular weight of toluene = 92

For toluene at 25°C:

$$\text{Vapour pressure} = 29.2 \text{ mm Hg} = 3.89 \times 10^3 \text{ N/m}^2,$$

$$\text{Density} = 850 \text{ kg/m}^3, p_{A1} = 29.2 \text{ mm Hg} = 3.89 \times 10^3 \text{ N/m}^2,$$

$$p_{B_1} = 101.3 \times 10^3 - 3.89 \times 10^3 = 97.41 \times 10^3 \text{ N/m}^2$$

$$p_{A2} = 0, p_{B2} = 101.3 \times 10^3 \text{ N/m}^2.$$

Substituting the values in Eq. (2.46):

$$D_{AB} = \frac{\frac{850}{92 \times 5.4 \times 10^5}}{\frac{8314 \times 298}{(1.013 \times 10^5) \ln\left(\frac{101.3 \times 10^3}{97.41 \times 10^3}\right)}} \frac{(0.044)^2 - (0.02)^2}{2}$$

$$= 0.82 \times 10^{-5}$$

Diffusivity of toluene in air =  $0.82 \times 10^{-5} \text{ m}^2/\text{s}$ .

**Twin Bulb Method:** This method is suitable for measuring the diffusivities of permanent gases or of components that are gases at least at the conditions of the experiment.

As shown in Figure 2.7, the experimental set-up consists of two large bulbs of volumes  $V_1$  and  $V_2$ , connected by a narrow tube fitted with a stop cock or a plug type valve. Let the cross sectional area and the length of the connecting tube be  $a$  and  $z$  respectively.

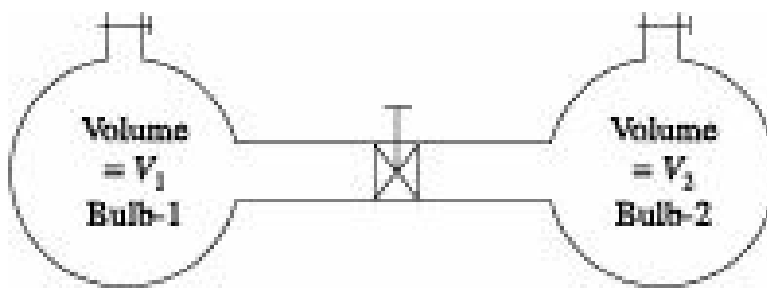


Figure 2.7 The twin bulb set-up.

Before starting the experiment the valve in the connecting tube is closed, the two bulbs are evacuated, washed several times with the respective gases to be filled in that bulb. Then one bulb is filled with pure *A* while the other with pure *B*, both being at the same pressure.

The experiment is then started by opening the valve in the connecting tube. During the experiment the contents of the two bulbs should be constantly stirred to maintain uniform concentration and the entire system should be kept at constant temperature and pressure. Since the two bulbs are large and are at equal and constant pressure, equimolar counter-diffusion takes place through the connecting tube. Concentrations (or partial pressures) of these two components will change only very slowly so that pseudo-steady state conditions may be assumed. The total pressure (*P*) in the bulbs, the duration of the experiment (*q*), and the partial pressures of component *A* in the two bulbs ( $p\Box_{A1}$  and  $p\Box_{A2}$ ) are to be noted.

If  $p\Box_{A1}$  and  $p\Box_{A2}$  ( $p\Box_{A1} > p\Box_{A2}$ ) be the partial pressures of component *A* in bulb 1 and bulb 2 at any instant *q*, the steady state rate of transport of *A* from bulb 1 to bulb 2 can be expressed as follows in terms of Eq. (2.27):

$$aN_A = \frac{aD_{AB}(p'_{A_1} - p'_{A_2})}{RTz} = -aN_B \quad (2.47)$$

Since  $p\Box_{A1}$  and  $p\Box_{A2}$  are the instantaneous partial pressures of component *A* in the two bulbs, the rates of change of partial pressures are given by

$$aN_A = -\frac{V_1}{RT} \frac{dp'_{A_1}}{d\theta} \quad (2.48)$$

$$aN_A = \frac{V_2}{RT} \frac{dp'_{A_2}}{d\theta} \quad (2.49)$$

Combining Eqs. (2.48) and (2.49), we obtain

$$\begin{aligned} -\frac{d}{d\theta} (p\Box_{A1} - p\Box_{A2}) &= aRT \left( \frac{1}{V_1} + \frac{1}{V_2} \right) N_A \\ &= \frac{aD_{AB}(p'_{A_1} - p'_{A_2})}{z} \left( \frac{1}{V_1} + \frac{1}{V_2} \right) \\ \frac{d(p'_{A_1} - p'_{A_2})}{(p'_{A_1} - p'_{A_2})} &= \frac{aD_{AB}}{z} \left( \frac{1}{V_1} + \frac{1}{V_2} \right) d\theta \end{aligned} \quad (2.50)$$

or,

Integrating Eq. (2.50) with the following limits:

$q = 0, (p \square A_1 - p \square A_2) = (P - 0) = P$ ; and  $q = q \square, (p \square A_1 - p \square A_2) = (p \square A_1 - p \square A_2)$  yields

$$\ln \frac{P}{(p'_{A_1} - p'_{A_2})} = \frac{aD_{AB}}{z} \left( \frac{1}{V_1} + \frac{1}{V_2} \right) \theta' \quad (2.51)$$

On the basis of the measurements made,  $D_{AB}$  can be estimated from Eq. (2.51).

## 2.7 Molecular Diffusion in Liquids

Diffusion in liquids is very slow being about ten thousand times slower than diffusion in gases. For instance the diffusivity of ammonia in air at 0°C and 1 atm is  $1.98 \times 10^{-5} \text{ m}^2/\text{s}$  while its diffusivity in water at 5°C and solute concentration of 3.5 kmol/m<sup>3</sup> is only  $1.24 \times 10^{-9} \text{ m}^2/\text{s}$ . The molecular diffusion in gases being due to the kinetic motion of gas molecules about which quantitative relations have been developed, molecular diffusion in gases is amenable to precise mathematical treatment. No such precise relation has yet been developed for diffusion in liquids.

Moreover, both concentration and diffusivity of liquids vary widely which make the situation still more complex.

The flux equation [Eq. (2.18)] reproduced below is applicable to both gases and liquids:

$$N_A = \frac{c_A}{c} (N_A + N_B) - D_{AB} \left( \frac{\frac{dc_A}{dx}}{c} \right)$$

To put it in a workable form, the integration of Eq. (2.18) requires that concentration and diffusivity are constant. This is true for binary gas mixtures but not so in case of liquids where both may vary considerably. Moreover, the viscosity of a liquid often changes with the change in concentration, which may affect the diffusivity. To overcome the situation, it is customary to integrate Eq. (2.18) with average values of total molar concentration and diffusivity between two points. In addition to that, analogy with corresponding type of diffusion in gases has been found to give the equation its final form.

As in case of gases, two common types of diffusion have been considered here.

### 2.7.1 Diffusion of Component A Through Non-Diffusing B

$$N_A = \text{constant}, N_B = 0.$$

Integrating Eq. (2.18) and rearranging, we have

$$N_A = \frac{D_{AB} c_{BM}}{z c_{BM}} (c_{A1} - c_{A2}) \quad (2.52)$$

where,  $c_{BM}$  is the logarithmic mean concentration difference (LMCD) given by

$$c_{BM} = \frac{c_{B_2} - c_{B_1}}{\ln(c_{B_2}/c_{B_1})}$$

Alternatively, putting  $(c_A/c) = x_A$  in Eq. (2.18), we get

$$N_A = (N_A + N_B) x_A - D_{AB} \left( \frac{\rho}{M} \right)_{av} \frac{dx_A}{dz} \quad (2.53)$$

where,  $\rho$  is the density of the liquid and  $M$  is its molecular weight.  
Integrating Eq. (2.53) and rearranging, we obtain

$$N_A = \frac{D_{AB}}{z x_{BM}} \left( \frac{\rho}{M} \right)_{av} (x_{A1} - x_{A2}) \quad (2.54)$$

where,  $x_{BM}$  is the logarithmic mean mole fraction difference given by

$$x_{BM} = \frac{x_{B_2} - x_{B_1}}{\ln(x_{B_2}/x_{B_1})}$$

### 2.7.2 Equimolar Counter-Diffusion of A and B

$$N_A = -N_B$$

From Eq. (2.18), we obtain

$$N_A = -D_{AB} \frac{dc_A}{dz}$$

which on integrating gives

$$N_A = \frac{D_{AB}}{z} (c_{A1} - c_{A2}) \quad (2.55)$$

Alternatively,

$$N_A = \frac{D_{AB}}{z} \left( \frac{\rho}{M} \right)_{av} (x_{A1} - x_{A2}) \quad (2.56)$$

**EXAMPLE 2.14** (Estimation of rate of diffusion of a liquid through a stagnant layer of another liquid): Calculate the rate of diffusion of trichloroacetic acid across nondiffusing methanol solution 2 mm thick at 20°C when the concentrations of the acid on the two opposite sides of the methanol film are 6% and 2% by weight of acid. The densities of 6% and 2% acid solutions are 1012 kg/m<sup>3</sup> and 1003 kg/m<sup>3</sup> respectively. The diffusivity at infinite dilution of trichloroacetic acid in methanol at 20°C is  $1.862 \times 10^{-9}$  m<sup>2</sup>/s.

**Solution:** This is a case of diffusion of one liquid through a stagnant layer of another liquid. Hence, Eq. (2.54) is applicable.

$$T = 293 \text{ K}, z = 2 \text{ mm} = 0.002 \text{ m}, D_{AB} = 1.862 \times 10^{-9} \text{ m}^2/\text{s},$$

$$M_A = 163.5, M_B = 32, \text{Density of 6\% acid} = 1012 \text{ kg/m}^3,$$

$$\text{Density of 2\% acid} = 1003 \text{ kg/m}^3$$

$$\frac{0.06}{163.5}$$

$$\frac{0.06}{163.5} + \frac{0.94}{32}$$

For 6% acid,  $x_{A1} = \frac{0.06}{163.5} + \frac{0.94}{32} = 0.01234$  mol fraction.

$x_{B1} = (1 - 0.01234) = 0.9876$  mol fraction.

$$\frac{0.02}{163.5}$$

$$\frac{0.02}{163.5} + \frac{0.98}{32}$$

For 2% acid,  $x_{A2} = \frac{0.02}{163.5} + \frac{0.98}{32} = 0.00397$  mol fraction.

$x_{B2} = (1 - 0.00397) = 0.9960$  mol fraction.

$$x_{BM} = \frac{\frac{0.9960 - 0.9876}{\ln(\frac{0.9960}{0.9876})}}{= 0.9918}$$

$$\frac{1}{\frac{0.06}{163.5} + \frac{0.94}{32}}$$

For 6% acid,  $M = \frac{1}{\frac{0.06}{163.5} + \frac{0.94}{32}} = 33.62$  kg/kmol,

$$\frac{\rho}{M} = \frac{101.2}{33.62} = 30.10 \text{ kmol/m}^3$$

$$\frac{1}{\frac{0.02}{163.5} + \frac{0.98}{32}}$$

For 2% acid,  $M = \frac{1}{\frac{0.02}{163.5} + \frac{0.98}{32}} = 32.57$  kg/kmol,

$$\frac{\rho}{M} = \frac{100.3}{32.57} = 30.79 \text{ kmol/m}^3$$

$$\left( \frac{\rho}{M} \right)_{av} = \frac{30.10 + 30.79}{2} = 30.445 \text{ kmol/m}^3$$

where,  $M$  represents the molecular weight of the mixture.

Substituting the values in Eq. (2.54),

$$N_A = \frac{1.862 \times 10^{-9}}{(0.002)(0.9918)} \# (30.445) \# (0.01234 - 0.00397)$$

$$= 2.392 \# 10^{-7}$$

The rate of diffusion of trichloroacetic acid =  $2.392 \# 10^{-7}$  kmol/ s\$ m<sup>2</sup>

## 2.8 Liquid Phase Diffusivity

Diffusivities of liquids are very small, usually being in the range of  $0.5 \# 10^{-9}$  to  $2.5 \# 10^{-9}$  m<sup>2</sup>/s at 25°C. On the other hand, diffusivities of gases at 25°C and 1 atm pressure lie between  $0.1 \# 10^{-4}$  and

$1.0 \times 10^{-4} \text{ m}^2/\text{s}$ . In contrast to gaseous diffusivities, diffusivities of liquids often change appreciably with concentration. The molecular theory of liquids has not yet reached a stage to permit precise prediction of liquid diffusivities. A list of experimental values of liquid phase diffusivities of some common substances is given in Table 2.5.

**Table 2.5** Liquid phase diffusivities of some common compounds at infinite dilution at 25°C

Solute	Solvent	$D^{\circ}AB \times 10^5 \text{ cm}^2/\text{s}$
Acetic acid	Water	1.26
Acetone	Water	1.28
Ammonia	Water	1.64
Benzoic acid	Water	1.21
Carbon dioxide	Water	1.92
Chlorine	Water	1.25
Ethanol	Water	1.28
Formic acid	Water	1.50
Hydrogen sulphide	Water	1.41
Methanol	Water	1.60
Nitric acid	Water	2.60
Nitric oxide	Water	2.60
Oxygen	Water	2.41
Sulphuric acid	Water	1.73
Acetic acid	Benzene	2.09
Acetone	Chloroform	2.35
Benzene	Chloroform	2.89
Benzene	Ethyl alcohol	1.81
Benzoic acid	Benzene	1.38
Iodine	Ethyl alcohol	1.32
Water	Acetone	4.56
Water	Ethyl alcohol	1.13
Water	<i>n</i> -Butyl alcohol	0.988
Water	Ethyl acetate	3.20

### 2.8.1 Prediction of Liquid Phase Diffusivity

A number of empirical and semi empirical correlations have been proposed for the prediction of liquid phase diffusivity. But the accuracy of prediction is not as good as in case of gases. The reason for this is that the molecular theory of liquids has not yet reached a stage so as to permit precise prediction of liquid diffusivities.

The prediction of liquid phase diffusivity has become much more complex because of the effect of concentration on liquid diffusivity. Diffusivity of a solute in a concentrated solution may sometimes become quite different from diffusion in a dilute solution since concentrated solutions may differ widely from ideality and solute-solvent interactions may be more complex. Change in viscosity with change in concentration may also affect liquid diffusivity.

Poling et al. (2001) have given detailed account of several available equations for prediction of liquid phase diffusivity along with their applicability.

While developing expressions for prediction of liquid diffusivity, nonelectrolytes and electrolytes have been treated separately.

### **Nonelectrolytes**

By considering Brownian movement of colloids where the particles of radius  $r_p$  are very large in comparison with that of solvent  $B$  and assuming Stokes' law of drag, Einstein developed the so called Stokes-Einstein equation (Brodkey and Hershey 1988) as

$$D_{AB} = \frac{kT}{6\pi r_p \mu_B} \quad (2.57)$$

where,

$D_{AB}$  = diffusivity of  $A$  in dilute  $B$

$k$  = Boltzmann constant

$T$  = absolute temperature

$\mu_B$  = viscosity of solvent

$r_p$  = radius of particles of  $A$ .

Equation (2.57) fails to predict diffusivities of solutes of relatively smaller size. Sutherland (1905) found that if the particles are of like size and there is no tendency for the fluid to stick at the surface of the diffusing particle, i.e. coefficient of sliding friction is zero, then Eq. (2.57) becomes

$$D_{AB} = \frac{kT}{4\pi r_p \mu_B} \quad (2.58)$$

For pure liquids, where the molecules are of the same size and are arranged in a closely packed cubic lattice with all molecules just touching (Bird et al. 1960)

$$r_p = \frac{1}{2} \left( \frac{V_A}{n} \right)^{1/3} \quad (2.59)$$

where,  $n$  = Avogadro's number so that for self diffusion,

$$D_{AA} = \frac{kT}{2\pi \mu_A} \left( \frac{n}{V_A} \right)^{1/3} \quad (2.60)$$

Wilke and Chang (1955) had modified the above equation and proposed the following semiempirical equation for prediction of liquid diffusivity, but the values are not always very reliable

$$D_{AB} = 1.173 \times 10^{-16} (z M_B)^{0.5} \left( \frac{T}{\mu V_A^{1.6}} \right) \quad (2.61)$$

where,

$D_{AB}$  = diffusivity of solute  $A$  in solvent  $B$  in infinitely dilute solution,  $m^2/s$

$z$  = association parameter for solvent (some values of  $z$  are: water = 2.26, methanol = 1.9, nonassociated solvent = 1.0)

$v_A$  = molar volume of solute at normal boiling point,  $\text{m}^3/\text{kmol}$

$T$  = absolute temperature, K

$n$  = viscosity of solution,  $\text{kg}/\text{m}\cdot\text{s}$

$V_A$  = molal volume of solute  $A$  at its normal boiling point,  $\text{cm}^3/\text{gmol}$

Equation (2.61) is not dimensionally consistent and is usually accurate to within 10 to 15% in the temperature range of 10 to 30°C. Although the correlation was proposed for both aqueous and nonaqueous system, later studies have shown that it is satisfactory for most cases of organic solute diffusing in water and fails for many systems when water is diffusing through organic solvent. However, it is the most general and requires minimum supplementary data.

### Electrolytes

In dilute solutions, liquid diffusivity is given by

$$D_{AB}(\text{dil}) = \frac{RT u^+ u^-}{u^+ + u^-} \left( \frac{1}{z^+} + \frac{1}{z^-} \right) \quad (2.62)$$

where,

$D_{AB}(\text{dil})$  = diffusivity in dilute solution,  $\text{cm}^2/\text{s}$

$u^+$  and  $u^-$  = absolute velocities of cations and anions respectively,  $\text{cm}/\text{s}$

$z^+$  and  $z^-$  = valencies of cations and anions respectively

$T$  = absolute temperature, K

$R$  = gas constant =  $8.314 \times 10^7$  ergs/(gmol) (K)

In concentrated solutions, diffusivity is obtained from the relation

$$D_{AB}(\text{conc}) = D_{AB}(\text{dil}) + \left( 1 + \frac{m \delta \ln f}{\delta m} \right) f(m) \quad (2.63)$$

where,

$D_{AB}(\text{conc})$  = diffusivity in concentrated solution,  $\text{cm}^2/\text{s}$

$m$  = molality of solution

$f$  = mean ionic activity coefficient referred to molality

$f(m)$  = a correction factor for effect of concentration on ionic mobility, given by

$$f(m) = \frac{1}{C_B V'_B} \frac{\mu}{\mu_B} \quad (2.64)$$

$V'_B$  = partial molal volume of water in solution

$n$  = viscosity of water

$n_B$  = viscosity of solvent

**EXAMPLE 2.15** (Estimation of liquid diffusivity by Wilke-Chang equation): Estimate the diffusivity of ethyl alcohol in dilute aqueous solution at 20°C.

For water as solvent,  $z = 2.26$

Atomic volumes of C, H and O are 14.8, 3.7 and 7.4 cm<sup>3</sup>/gmol, respectively.

**Solution:** Molecular weight of water,  $M_B = 18.02$ , Temperature,  $T = 20^\circ\text{C} = 293\text{ K}$ .

Molar volume of ethyl alcohol =  $2(14.8) + 6(3.7) + 7.4 = 59.2\text{ cm}^3/\text{gmol}$ .  
=  $0.0592\text{ m}^3/\text{kmol}$

For dilute solution, viscosity may be taken as that of water.

At  $20^\circ\text{C}$ , viscosity of water,  $\eta = 0.001005\text{ kg/m\$s}$ .

Substituting the values in Eq. (2.61),

$$D_{AB} = \frac{(1.173 \times 10^{-16})(2.26 \times 18.02)^{0.5}(293)}{(0.001005)(0.0592)^{0.6}} \text{ m}^2/\text{s}$$
$$= 1.19 \# 10^{-9} \text{ m}^2/\text{s}$$

Diffusivity of ethyl alcohol =  $1.19 \# 10^{-9} \text{ m}^2/\text{s}$

## 2.8.2 Experimental Determination of Liquid Phase Diffusivity

Reports available on experimentation by investigators using various methods for prediction of diffusivity of different liquids are as follows:

- (i) Taylor dispersion technique
- (ii) Rotating disk technique
- (iii) Quasi-elastic light scattering technique
- (iv) Laminar jet method
- (v) Wetted-wall column
- (vi) Diaphragm cell

These are presented elsewhere (Therm et al. 1967, Bulicka and Prochazka 1976, Ramprasad et al. 1990, 1991, Ramakanth et al. 1991, Ghosh et al. 1991, Lee and Li 1991, Chin, et al. 1991; Riede and Schlüder, 1991, Ghorai, 1994). Wise and Houghton (1966) measured diffusion coefficient for dissolved gases like hydrogen, oxygen, helium, argon, methane, ethane, etc. in water by the following rate of collapse of small bubbles in gas-free water.

Amongst these, the diaphragm cell method is widely used as it is the only successful method based on Fick's first law and combines experimental simplicity with accuracy. The apparatus as shown in Figure 2.8 used in laboratory for measurement of diffusivity in binary hydrocarbon systems, consisted of two compartments separated by a G-4 diaphragm (sintered glass or porous membrane).

The concentrated solution and the comparatively dilute solution were kept in two compartments. The liquid layers adjacent to the surfaces of the diaphragm were stirred by magnetic stirrers which was operated by the permanent bar magnets fitted outside the shell. Potassium chloride solution was used as a standard for calibration of the diaphragm cell. The same was analysed by conductivity measurement whereas the concentrations of unknown components were measured by Abbe refractometer. The diffusivity was then determined using Fick's first law in convenient form described by Geankoplis (2005).

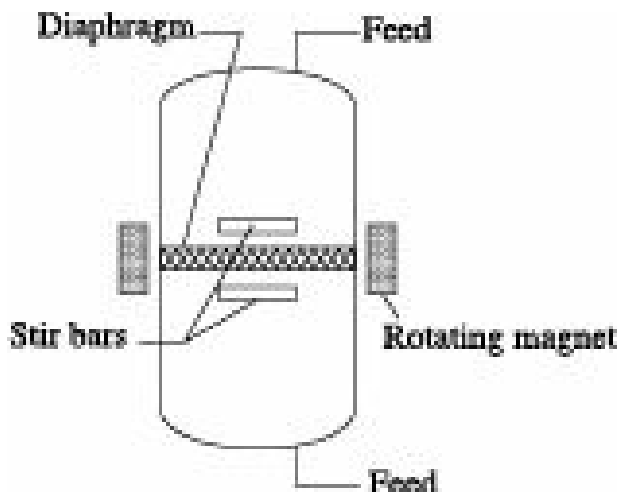


**Figure 2.8** The diaphragm cell for measuring diffusivity of liquids.

## 2.9 Diffusion in Turbulent Stream—Eddy Diffusion

Let us refer to Section 2.1 and consider the case of copper sulphate crystals placed at the bottom of a glass bottle containing water. As the water was quiescent without any disturbance, the copper sulphate crystals took unusually long time to get dissolved in water. If, on the other hand, the contents of the bottle are vigorously stirred, the copper sulphate crystals will be completely dissolved within very short time may be within a minute. Another similar example may be taken from our daily life with which most of us are well acquainted. When we add a sugar cube in a cup of tea and leave it as such, the sugar cube takes very long time to get completely dissolved. If, on the other hand, the contents of the cup are vigorously stirred with a spoon, the sugar cube gets dissolved within a very short time, may be within a minute.

The above examples distinguish two distinct types of diffusion, molecular diffusion and eddy diffusion or convective mass transfer. In Sections 2.3 and 2.4, we have already discussed molecular diffusion in fluids. In this section, we shall briefly discuss eddy diffusion or convective mass transfer. Eddy diffusion or convective mass transfer occurs in turbulent fluids and its rate is much faster than that of molecular diffusion because of high velocity of the medium that reduces the thickness of the laminar film at the phase boundary as well as due to random motion of small lumps of fluid which physically carry the solute from one position to another.

As in case of convective heat transfer, there may be two types of convective mass transfer (i) forced convection mass transfer and (ii) natural convection or free convection mass transfer. As the names imply, in forced convection mass transfer turbulence is created in the medium by external agencies such as pump, blower, stirrer, etc. In natural convection mass transfer, on the other hand, turbulence in the medium is generated mainly due to variation in local conditions such as variation in solute concentration in the solution which causes variation in local density. For instance, when a solid gets dissolved in a liquid, the liquid adjacent to the solid surface becomes saturated almost immediately and as a result, becomes heavier than the bulk of liquid. If this phenomenon takes place at the bottom of the container, then the heavier fluid remains at the bottom and natural convection will not take place. If, on the other hand, dissolution takes place at a certain height above the bottom of the container, then the heavier fluid being above the lighter fluid, natural convection starts. The influence of natural convection on mass transfer may be considerable, particularly in the absence of forced convection.

Natural convection arising from gravitation is also of importance in mass transfer studies. Natural

convection may also occur from centrifugal effects or an electrically conducting fluid exposed to magnetic field.

Turbulence is characterized by random motion of fluid particles which are irregular with respect to both direction and time. For a fluid flowing in the turbulent motion through a duct in the axial or  $x$ -direction, the time average of velocity may be  $u_x$ , at any particular instant, the actual velocity will be  $u_x + u'_{ix}$ , where  $u'_{ix}$  is the fluctuating or deviating velocity. Values of  $u'_{ix}$  will vary with time through a range of positive and negative values, the time average being zero. Since flow is in  $x$ -direction only, the time average of  $u_z$  is zero, but at any instant the deviating velocity in the  $z$ -direction will be  $u'_{iz}$ .

A turbulent fluid is assumed to consist of small lumps of fluid or eddies of a wide size range (Hinze 1959, Davies 1972). Large eddies which contain about 20% of turbulent kinetic energy, produce smaller eddies to which they transfer their energy. The medium eddies make the maximum contribution to the turbulent kinetic energy. The smallest eddies which ultimately dissipate their energy through viscosity are substantially regenerated by large eddies and a state of equilibrium is established. At this stage the energy distribution becomes independent of the conditions by which the turbulence was originally produced and depends only upon the rate at which energy is supplied and dissipated.

Kolmogoroff (1941) defined the velocity  $u'_d$  and length  $l_d$  of the small eddies in terms of the power input per unit mass of the fluid,  $P/m$ :

$$u'_d = \left( \frac{\nu P g_c}{m} \right)^{1/4} \quad (2.65)$$

$$\text{and} \quad l_d = \left( \frac{\nu^3 m}{P g_c} \right)^{1/4} \quad (2.66)$$

Eliminating  $\nu$  from Eqs. (2.65) and (2.66), we get

$$\frac{P g_c}{m} = \frac{u_d^3}{l_d} \quad (2.67)$$

The kinetic theory of gases provides sound theoretical basis for the study of molecular diffusion in gases and by analogy, fairly reliable equations have been proposed for molecular diffusion in liquids. In case of eddy diffusion, no such theoretical relations could, however, be developed because of our limited knowledge about turbulence. Some promising mathematical expressions for turbulence have recently been developed from statistical principles, which may be of use in mass transfer calculations.

Due to the deviating velocity, an eddy from layer 1, having concentration  $c_A$  moves to layer 2 as shown in Figure 2.9 and loses its identity. The next eddy, having a concentration  $(c_A + Dc_A)$  moves from layer 2 to layer 1 and brings with it an additional amount of solute  $Dc_A$ .

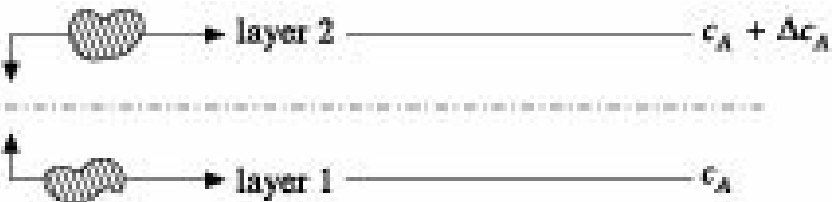


**Figure 2.9** Diffusion in turbulent stream (Eddy diffusion).

The average concentration gradient between layer 1 and layer 2 is  $Dc_A/l$ , where  $l$  is Prandtl Mixing length given by the relation.

$$u'_x = Du_x = -l \frac{du_x}{dz} \quad (2.68)$$

The average concentration gradient is proportional to the local gradient ( $-dc_A/dz$ ). By analogy with eddy viscosity, an eddy diffusivity  $E_D$  may be defined as the ratio of the transfer of component  $A$  to the concentration gradient.

$$E_D = K \frac{u'_x \Delta c_A}{\Delta c_A / l} = \frac{J_A(\text{turb})}{-dc_A/dz} \quad (2.69)$$

where,  $K$  is the proportionality constant.

From Eq. (2.69),

$$J_A(\text{turb}) = -E_D \left( \frac{dc_A}{dz} \right) \quad (2.70)$$

Equation (2.70) is very similar to Eq. (2.9) for molecular diffusion.

The total flux of component  $A$  due to both molecular and eddy diffusion may therefore be expressed as

$$J_A = -(D_{AB} + E_D) \left( \frac{dc_A}{dz} \right) \quad (2.71)$$

where,  $E_D$  is the Eddy diffusivity,  $L^2/\theta$ .

$D_{AB}$  is constant for a particular system at fixed conditions of temperature and pressure but  $E_D$  depends, in addition to temperature and pressure, on the local intensity of turbulence.  $D_{AB}$  predominates within a narrow region near solid wall or phase boundary where the flow is laminar while  $E_D$  predominates in the main turbulent core.

Heat flux and momentum flux in turbulent streams can also be determined by expressions similar to Eq. (2.71).

$$\text{For heat flux: } q = -(a + E_H) \left[ \frac{d(\rho c_p T)}{dz} \right] \quad (2.72)$$

$$\text{and for momentum flux: } x = -(o + E_V) \left[ \frac{d(\rho u_{av})}{dz} \right] \quad (2.73)$$

where,

$E_H$ = eddy thermal diffusivity,  $L^2/\theta$

$E_V$ = eddy viscosity,  $L^2/\theta$

$E_D$ ,  $E_H$  and  $E_V$  are very large, may be several hundred times larger compared to  $D_{AB}$ , a and o respectively.

**EXAMPLE 2.16** (Velocity and length scale of small eddies in a turbulent stream): Water at 25 °C is flowing through a 30 mm id pipe at an average velocity of 2.5 m/s. Determine the velocity and the length scale of the small eddies in the universal range.

For water at 25°C, viscosity is  $8.937 \times 10^{-4}$  kg/m s and density is 997 kg/m<sup>3</sup>.

The value of Fanning's friction factor,  $f$  may be calculated from the relation  $f = 5.62 \# 10^{-8} Re$ .

**Solution:**

$$d = 30 \text{ mm} = 0.03 \text{ m } u = 2.5 \text{ m/s}$$

$$Re = \frac{\frac{du\rho}{\mu}}{8.937 \times 10^{-4}} = 83670$$

$$f = 5.62 \# 10^{-8} \# 83670 = 0.0047.$$

The pressure drop  $Dp$  is given by the relation

$$Dp = \frac{2\rho f L u^2}{dg_e}$$

Considering 1 m length of the pipe

$$Dp = \frac{(2)(997)(0.0047)(1)(2.5)^2}{(0.03)(1)} = 1952 \text{ N/m}^2.$$

Power spent =  $Dp \# \text{volumetric flow rate}$

$$\begin{aligned} &= Dp \# \frac{(\pi d^2 \times u)}{4} = \frac{(1952) \pi (0.03)^2 (2.5)}{4} \\ &= 3.45 \text{ N\$m/s for 1 m pipe} \end{aligned}$$

$$\text{Associated mass} = \frac{\pi d^2 L \rho}{4} = \frac{\pi (0.03)^2 (1) (997)}{4} = 0.704 \text{ kg}$$

$$\frac{P}{m} = \frac{3.45}{0.704} = 4.90 \text{ N\$m/kg\$s}$$

From Eq. (2.65), we obtain

$$u'_d = \left( \frac{\nu P g_e}{m} \right)^{1/4} = \left( \frac{(8.937 \times 10^{-4})(4.90)}{997} \right)^{1/4} = 0.0458 \text{ m/s.}$$

And from Eq. (2.66), we get

$$l_d = \left( \frac{V^3 m}{P g_c} \right)^{1/4} = \left( \frac{(8.937 \times 10^{-4})^3}{(997)^3 (4.90)} \right)^{1/4} = 1.958 \# 10^{-5} \text{ m}$$

## 2.10 Diffusion in Solids

Operations such as leaching, drying, adsorption, dialysis, reverse osmosis, etc. involve diffusion through solid phase. The mechanism of diffusion in solids is much more complicated than diffusion in fluids. Diffusion in solids is broadly classified into two major groups, *structure sensitive diffusion* and *structure insensitive diffusion*. In structure sensitive diffusion, porous solids permit flow of fluid through their interstices and capillaries. In the structure insensitive diffusion, on the other hand, the diffusing substance dissolves in the solid to form solid solution. The actual mechanism may be different in different cases. Thus during diffusion through palladium, hydrogen molecules dissociate and enter the crystal lattice as atoms, while nitrogen and oxygen form unstable compounds during diffusion through metals.

### 2.10.1 Steady-State Diffusion in Solids

With a few exceptions, it is possible to describe steady-state transfer of solute through solids by an equation equivalent to Fick's law. If diffusivity is independent of concentration and there is no bulk flow, the rate of diffusion  $N_A$  of component  $A$  per unit cross section of the solid is given by

$$N_A = -D_A \frac{\delta c_A}{\delta z} \quad (2.74)$$

where,  $D_A$  is the diffusivity of  $A$  through the solid and  $(dc_A/dz)$  is the concentration gradient of the solute in the direction of diffusion. If  $D_A$  is constant, Eq. (2.74) may be integrated for steady-state diffusion through a flat slab of thickness  $z$  to give

$$N_A = \frac{D_A (c_{A1} - c_{A2})}{z} \quad (2.75)$$

where,  $c_{A1}$  and  $c_{A2}$  are the concentrations of the solute at the two faces of the slab.

**EXAMPLE 2.17** (Steady-state diffusion of a gas through a solid wall): Hydrogen gas at 25°C and 1 atm pressure is diffusing through an unglazed neoprene rubber wall 12.5 mm thick. The solubility of hydrogen in the rubber has been estimated to be  $0.053 \text{ cm}^3$  (at STP) per cubic centimetre. The diffusivity of hydrogen through the rubber wall is  $1.8 \# 10^{-6} \text{ cm}^2/\text{s}$ .

Estimate the rate of diffusion of hydrogen per square metre of the wall.

**Solution:** Concentration of hydrogen at the inner side of the rubber wall is

$$c_{A1} = \frac{0.053}{22.41} = 2.37 \# 10^{-3} \text{ kmol/m}^3$$

Assuming the resistance to diffusion of hydrogen at the outside surface of the wall is negligible, the concentration of hydrogen at the outer surface of the wall is  $c_{A2} = 0$ .

Given:  $D_A = 1.8 \times 10^{-6} \text{ cm}^2/\text{s} = 1.8 \times 10^{-10} \text{ m}^2/\text{s}$ .

Thickness of the rubber wall,  $z = 12.5 \text{ mm} = 1.25 \times 10^{-2} \text{ m}$

From Eq. (2.75),

$$N_A = \frac{D_A(c_{A_1} - c_{A_2})}{z}$$

Substituting the values,

$$N_A = \frac{(1.8 \times 10^{-10})(2.37 \times 10^{-3} - 0)}{1.25 \times 10^{-2}}$$
$$= 3.41 \times 10^{-11} \text{ kmol/m}^2\text{s} = 3.41 \times 10^{-8} \text{ mol/m}^2\text{s}$$

The rate of diffusion of hydrogen per square metre =  $3.41 \times 2 \times 10^{-8}$   
 $= 6.82 \times 10^{-8} \text{ kg/m}^2\text{s}$

## 2.10.2 Transient or Unsteady-State Diffusion

Unsteady-state operations, in general, are those in which the operating conditions at a particular point change with time. Unsteady-state mass transfer are those where the concentration at a given point varies with time.

Most of the industrial mass transfer operations such as gas-absorption, distillation, extraction, drying, etc. are conducted in the steady-state. However, during start-up and sometimes during shut down all of them undergo unsteady-state operation.

Majority of mass transfer operations involve transfer between two phases one of which is dispersed as thin film or droplets or bubbles in the other phase. On the basis of various theoretical studies, it has been established that these droplets or bubbles assume spherical shape in which mass transfer takes place by transient or unsteady-state molecular diffusion.

Transient diffusion plays very important role in case of mass transfer in solids. In view of the difficulties in transporting solids through continuous equipment, they are frequently handled in batch or semi-batch equipment. Some common examples are leaching or adsorption in packed beds, drying of porous solids, etc. Moreover, even in steady-state mass transfer equipment, each individual piece of solid often experiences unsteady-state diffusion. For example, during drying of a porous solid bar through one large surface only, the movement of moisture within the solid is by unsteady-state diffusion.

From the above discussion, it is evident that knowledge about unsteady-state diffusion is indispensable in the study of mass transfer, particularly in the study of diffusion through solids.

### ***Rate of unsteady-state diffusion***

Unsteady-state diffusion in a slab becomes important during drying of some colloids or gel-like materials where it is necessary to know the distribution of moisture in the slab as a function of position and time or to know the relation between the average moisture content of the slab and the drying time.

Unsteady-state diffusion in sphere plays an important role in the study of mass transfer to droplets or bubbles of the dispersed phase which assume spherical shape and through which mass transfer takes

place by unsteady-state diffusion.

The three common geometries involved in industrial operations are plane, spherical and cylindrical surfaces. For each of them, equations for unsteady-state diffusion can be developed by making mass balance over a selected differential volume (Crank 1956). In this section, we shall deal with the working equations for the above three geometries in the order of plane, spherical and cylindrical surfaces.

### **Unsteady-state diffusion in a slab through both of the large surfaces**

The section of a slab in which mass transfer is taking place by unsteady-state diffusion, is shown in Figure 2.10.

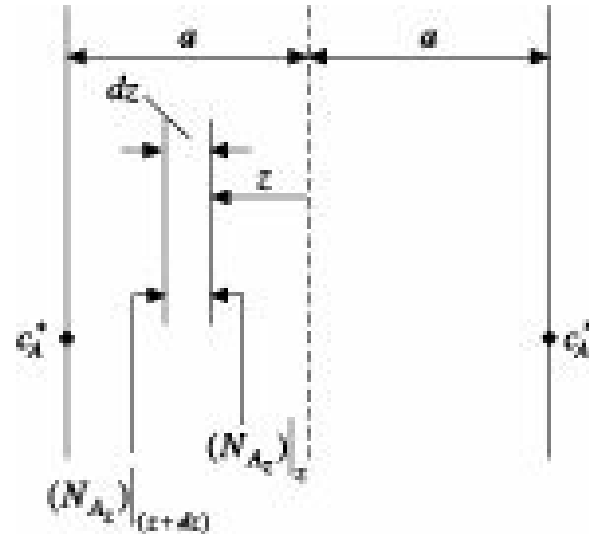


**Figure 2.10** Unsteady-state molecular diffusion in a slab.

The following assumptions are made to facilitate further calculations:

- (i) Uniform concentration of component  $A$ ,  $c_{A0}$  throughout the slab at  $i = 0$ .
- (ii) Constant concentration  $c_A^*$  at the two large surfaces of the slab which are both permeable to solute  $A$ .
- (iii) Diffusion of solute  $A$  only in the direction normal to the two large faces of the slab.
- (iv) Constant physical properties.

The co-ordinates originate at the mid-plane of the slab which has area  $A$  normal to  $z$ . Let us consider a control volume defined by the elements of the slab at  $z$ , having thickness  $dz$  as shown in Figure 2.10. The concentration gradient at  $(z + dz)$  at any given instant is

$$\frac{\delta c_A}{\delta z} + \frac{\delta}{\delta z} \left( \frac{\delta c_A}{\delta z} \right) dz \quad (2.76)$$

and the flow rate of solute into the control volume is given by

$$(N_{Az})_{z+dz} \$A = D\$A \left( \frac{\delta c_A}{\delta z} + \frac{\delta}{\delta z} \left[ \frac{\delta c_A}{\delta z} \right] dz \right) \quad (2.77)$$

The flow rate of solute out of the control volume at the same instant across the face at  $z$  is

$$(N_{A_z})_z \$A = D\$A \frac{\delta c_A}{\delta z} \quad (2.78)$$

The net flow rate into the control volume, as obtained by subtracting Eq. (2.78) from Eq. (2.77), is given by

$$DA \frac{\delta^2 c_A}{\delta z^2} dz \quad (2.79)$$

The rate of accumulation of solute in the control volume is given by

$$Adz \frac{\delta c_A}{\delta \theta} \quad (2.80)$$

Equations (2.79) and (2.80) may therefore be equated, and solved for  $dc_A/di$  to obtain Fick's second law of molecular diffusion, namely

$$\frac{\delta c_A}{\delta \theta} = D \frac{\delta^2 c_A}{\delta z^2} \quad (2.81)$$

For general three-dimensional diffusion with constant  $D$  the expression corresponding to Eq. (2.81) may be obtained in a similar manner by considering the rates at which solute enters, leaves and accumulates in a cubic control volume of differential dimensions ( $dxdydz$ ). The resulting expression becomes,

$$\begin{aligned} \frac{\delta c_A}{\delta \theta} &= D \left( \frac{\delta^2 c_A}{\delta x^2} + \frac{\delta^2 c_A}{\delta y^2} + \frac{\delta^2 c_A}{\delta z^2} \right) \\ &= D \square^2 c_A \end{aligned} \quad (2.82)$$

where,  $\square$  the Laplace operator.

For diffusion through two opposite faces of a slab,  $(d^2c_A/dx^2)$  and  $(d^2c_A/dy^2)$  are zero and from the initial assumptions the boundary conditions become

$$\begin{aligned} c_A(a, i) &= c_A^* \\ c_A(z, 0) &= c_{A0} \\ \frac{\delta c_A}{\delta z}(0, i) &= 0 \end{aligned}$$

Let  $y' = (c_A - c_A^*)$ ,  $y' = y'(z, i)$ . Then

$$\frac{\delta y'}{\delta \theta} = D \frac{\delta^2 y'}{\delta z^2} \quad (2.83)$$

and the boundary condition becomes

$$y'(a, i) = 0, y'(z, 0) = (c_{A0} - c_A^*) = y'_0 \text{ and } \frac{\delta y'}{\delta z}(0, i) = 0$$

Equation (2.83) may be solved both by the method of separation of variables and by using Laplace transformation. The first method is suitable for large diffusion times because the series rapidly converges under such conditions. The second method yields results suitable for small diffusion times. Solving Eq. (2.83) by the method of separation of variables, the following expression is obtained for the local concentration:

$$\frac{(c_A - c_A^*)}{(c_{A0} - c_A^*)} = \frac{4}{\pi} \sum_{n=0}^{\infty} \frac{(-1)^n}{(2n+1)} \cos\left(\frac{(2n+1)\pi z}{2a}\right) \exp\left(\frac{-D(2n+1)^2 \pi^2 \theta}{4a^2}\right) \quad (2.84)$$

and for average concentration:

$$\frac{\langle c_A \rangle - c_A^*}{(c_{A0} - c_A^*)} = \frac{8}{\pi^2} \sum_{n=0}^{\infty} \frac{1}{(2n+1)^2} \exp\left(\frac{-D(2n+1)^2 \pi^2 \theta}{4a^2}\right) \quad (2.85)$$

### ***Diffusion through a single large surface of a slab***

In some cases, for instance during the tray drying of some colloidal or gel-like substances, diffusion may take place only through one large surface of the slab, the other being impermeable to transfer. The concentration gradient ( $dc_A/dz$ ) is zero at the impermeable surface which therefore coincides with the mid-plane of the slab in which diffusion takes place symmetrically through the two large surfaces of the slab having identical concentration,  $c_A^*$ .

The solution for symmetrical diffusion is therefore applicable here with the permeable surface at  $z = a$ , and the impermeable surface at  $z = 0$ .

### ***Unsteady-state diffusion in a sphere***

Let us consider a sphere of radius  $r_s$  through which unsteady-state diffusion takes place.

The following assumptions are made to facilitate calculations:

- (i) The concentration of solute is uniform at  $c_{A0}$  throughout the sphere at the start of diffusion ( $i = 0$ ).
- (ii) The resistance to transfer in the medium around the sphere is negligible, so that surface concentration of the sphere is constant at  $c_A^*$ .
- (iii) The diffusion is radial, there being no variation in concentration with angular position.
- (iv) The physical properties of the material for sphere are constant.

Making a shell balance within a control volume bounded by the surfaces at  $r$  and  $(r + dr)$  as shown in Figure 2.11.

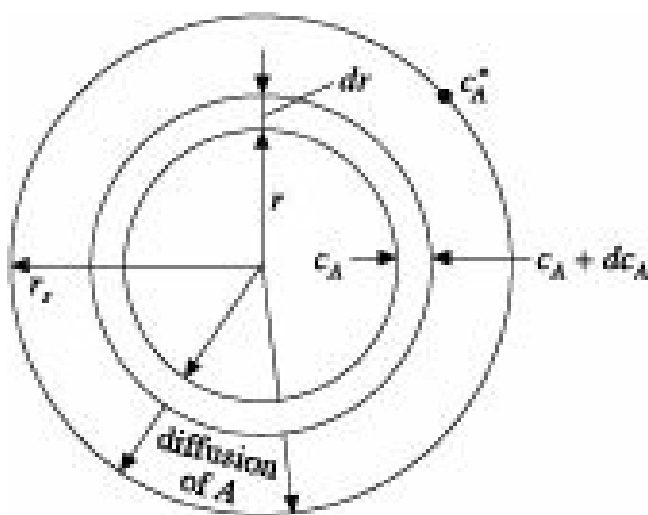


**Figure 2.11** Unsteady-state molecular diffusion in a sphere.

The rate of flow of solute into the control volume =  $-D(4\pi r^2) \frac{\delta c_A}{\delta r}$  (2.86)  
and the rate of flow out of the control volume is

$$-D[4\pi(r+dr)^2 \left( \frac{\delta c_A}{\delta r} + \frac{\delta}{\delta r} \left( \frac{\delta c_A}{\delta r} \right) dr \right)] \quad (2.87)$$

The net flow rate of solute into the control volume as obtained by subtracting Eq. (2.87) from Eq. (2.86), and neglecting second and higher order differentials, is

$$4\pi D \left( r^2 \frac{\delta^2 c_A}{\delta r^2} dr + 2r \frac{\delta c_A}{\delta r} dr \right) \quad (2.88)$$

The rate of accumulation of solute in the control volume is given by

$$(4\pi r^2 dr) \frac{\delta c_A}{\delta t} \quad (2.89)$$

Equating Eqs. (2.88) and (2.89) and solving for  $dc_A/dt$ , we get

$$\frac{\delta c_A}{\delta t} = D \left( \frac{\delta^2 c_A}{\delta r^2} + \frac{2}{r} \frac{\delta c_A}{\delta r} \right) \quad (2.90)$$

From the initial assumptions, the boundary conditions are:

$$c_A(r, 0) = c_{A0}$$

$$c_A(r_s, i) = c_A^*$$

$$\lim_{r \rightarrow 0} c_A(r, i) = \text{bounded}$$

Solving Eq. (2.90) by the method of separation of variables, the following expression may be obtained for the local concentration

$$\frac{c_A - c_A^*}{c_{A_0} - c_A^*} = \frac{2r_I}{\pi} \sum_{n=1}^{\infty} \frac{(-1)^{n+1}}{n} \frac{1}{r_I} \sin\left(\frac{n\pi r}{r_I}\right) \exp\left(-\frac{Dn^2\pi^2\theta}{r_I^2}\right) \quad (2.91)$$

and for the average concentration:

$$\frac{\bar{c}_A - c_A^*}{c_{A_0} - c_A^*} = \frac{6}{\pi^2} \sum_{n=1}^{\infty} \frac{1}{n^2} \exp\left(-\frac{Dn^2\pi^2\theta}{r_I^2}\right) \quad (2.92)$$

### Unsteady-state diffusion in a cylinder

A section of a cylinder is shown in Figure 2.12.

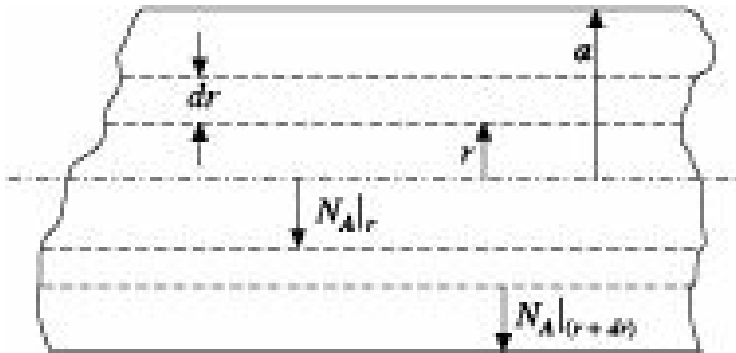


Figure 2.12 Unsteady-state molecular diffusion in a cylinder.

The following assumptions are made to facilitate mathematical analysis:

- (i) The plane ends of the cylinder are sealed so that diffusion takes place only in the radial direction.
- (ii) The physical properties of the material for cylinder are constant.

By making a mass balance for component  $A$  entering, leaving and accumulating in an annular cylindrical volume element, we get

$$\frac{\delta c_A}{\delta \theta} = D \left( \frac{\delta^2 c_A}{\delta r^2} + \frac{1}{r} \frac{\delta c_A}{\delta r} \right) \quad (2.93)$$

The boundary conditions are:

$$c_A(r, 0) = c_{A0}$$

$$c_A(a, i) = c_A^*$$

$$\lim_{r \rightarrow 0} c_A(r, i) = \text{bounded.}$$

By adapting the solution of the differential equation for diffusion into a fluid in plug flow through a cylindrical tube having the walls at constant solute concentration, Eq. (2.93) may be solved for local concentration as

$$\frac{c_A - c_A^*}{c_{A0} - c_A^*} = \frac{2}{a} \sum_{n=1}^{\infty} \frac{J_0(b_n r)}{b_n J_1(b_n a)} \exp(-Db_n^2 \theta) \quad (2.94)$$

where,  $b_n$ 's are roots of  $J_0(b_n a) = 0$ , and  $J_0(br)$  is the Bessel function of the first kind of order zero. The average concentration is given by

$$\frac{\bar{c}_A - \bar{c}_A^*}{c_{A_0} - \bar{c}_A^*} = \frac{4}{a^2} \sum_{n=1}^{\infty} \frac{1}{b_n^2} \exp(-Db_n^2 \theta) \quad (2.95)$$

Solutions to Eqs. (2.85), (2.92) and (2.95) for slab, sphere and cylinder respectively are quite complex and time consuming. However, Newman (1931) had worked out graphical solutions to these

$$\left(1 - \frac{(c_{A_0} - \bar{c}_A)}{(c_{A_0} - \bar{c}_A^*)}\right)$$

equations by plotting  $\left(1 - \frac{(c_{A_0} - \bar{c}_A)}{(c_{A_0} - \bar{c}_A^*)}\right) = \square$  which represents solute unremoved as ordinate against Fourier Number, Fo as the abscissa as shown in Figure 2.13.

The Fourier number, the dimensionless number, is expressed as  $\left(\frac{D\theta}{a^2}\right)$ ,  $\left(\frac{D\theta}{r^2}\right)$  and  $\left(\frac{D\theta}{4a^2}\right)$  for slab, sphere and cylinder respectively.

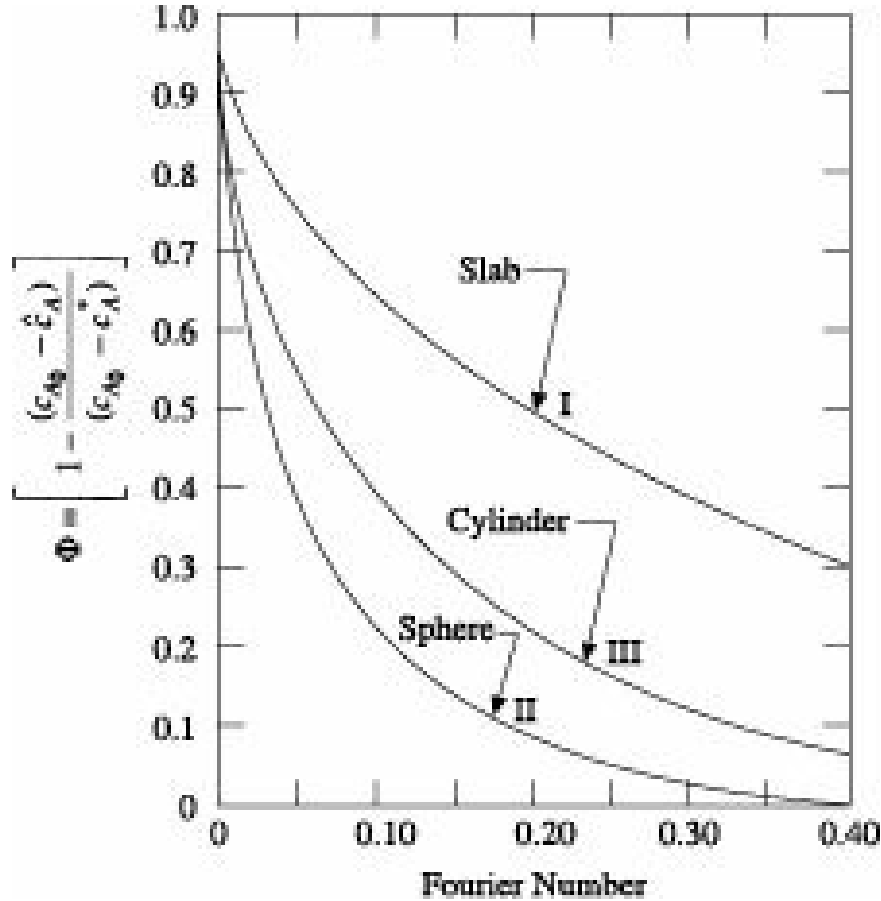


Figure 2.13 Plot of  $F$  vs  $Fo$  for unsteady diffusion.

Newman's work has much simplified the procedure for unsteady-state diffusion through some specific solids.

Some hints on use of the curve (Figure 2.13) depicting  $\square$  vs. Fourier number,  $Fo$  have been presented below:

- (i) Unsteady-state diffusion from two large faces of a solid slab of thickness '2a'

$$\square = f(Fo)_a = F_a$$

where,  $F_a$  is the ordinate of curve-I corresponding to  $(Fo)_a$  expressed as  $(Di/a^2)$

- (ii) Unsteady-state diffusion through one large face of a slab with the other large face made impermeable to the solute.

(iii) Unsteady-state diffusion in a rectangular bar of thickness  $2a_1$  and width  $2a_2$  with both ends sealed

$$F = f(Fo)_{a1} f'(Fo)_{a2} = F_{a1} \$ F_{a2}$$

$F_{a1}$  and  $F_{a2}$  being ordinates of the curve-I corresponding to  $(Fo)_{a1}$  and  $(Fo)_{a1}$  being expressed as  $(D\theta/a_1^2)$  and  $(D\theta/a_2^2)$  respectively.

(iv) Unsteady-state diffusion in a brick shaped solid of thickness  $2a_1$ , width  $2a_2$  and length  $2a_3$

$$F = f(Fo)_{a1} f'(Fo)_{a2} f''(Fo)_{a3} = F_{a1} \$ F_{a2} \$ F_{a3}$$

$F_{a1}$ ,  $F_{a2}$  and  $F_{a3}$  being ordinates of the curve-I corresponding to  $(Fo)_{a1}$ ,  $(Fo)_{a2}$  and  $(Fo)_{a3}$  being expressed as  $(D\theta/a_1^2)$ ,  $(D\theta/a_2^2)$  and  $(D\theta/a_3^2)$  respectively.

(v) Unsteady-state diffusion through a sphere of radius  $r$

$$F = f(Fo)_r = F_r$$

where,  $F_r$  is the ordinate of curve II corresponding to  $(Fo)_r$  expressed as  $(Di/r^2)$

(vi) Unsteady-state diffusion through a cylinder of radius  $a$  and length  $2b$  with one end sealed

$$F = f(Fo)_{cyl} \$ f'(Fo)_{2b} = F_{cyl} \$ F_{2b}$$

where,  $F_{cyl}$  is the ordinate of curve-III corresponding to  $(Fo)_{cyl}$  expressed as  $(Di/a^2)$  and  $F_{2b}$  is the ordinate of curve-I corresponding to  $(Fo)_{2b}$  expressed as  $(Di/(2b))^2$

(vii) Unsteady-state diffusion through a cylinder of radius  $a$  and length  $2b$  with both ends exposed

$$F = f(Fo)_{cyl} f'(Fo)_b = F_{cyl} F_b$$

where,  $F_{cyl}$  is the ordinate of curve-III corresponding to  $(Fo)_{cyl}$  expressed as  $(Di/a^2)$  and  $F_b$  is the ordinate of curve-I corresponding to  $(Fo)_b$  expressed as  $(Di/b^2)$ .

**EXAMPLE 2.18** (Diffusion from both the large faces of a solid slab): A slab of clay 40 mm thick with the four thin edges sealed, is being dried from the two flat faces by exposure to dry air. The initial moisture content is 18%. Drying takes place by internal diffusion of liquid water followed by evaporation at the surface. The surface moisture content is 2.5%. The average moisture content has fallen to 9.75% in 6 hr.

Assuming the diffusivity to be independent of moisture content and uniform in all directions, calculate

(a) the diffusivity in  $\text{m}^2/\text{s}$  (Assume  $Fo = 0.47$  F)

(b) how much time will be required to reduce the average moisture content to 6% under the same drying conditions. (Assume  $Fo = 2.3$  F)

**Solution:**

(a)  $c_{A0} = 0.18$ ,  $\bar{c}_A = 0.0975$ ,  $c_A^* = 0.025$ ,  $a = 0.02 \text{ m}$ ,  $i = 6 \text{ hr} = 21600 \text{ s}$

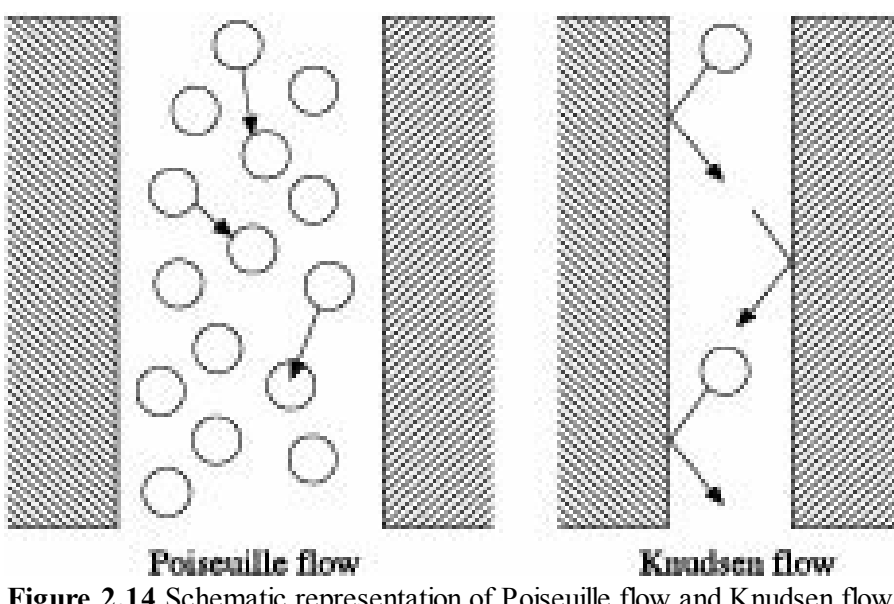


**Figure 2.14** Schematic representation of Poiseuille flow and Knudsen flow.

Hence,

$$F = \frac{\bar{c}_A - c_A^*}{c_{A_0} - c_A^*} = \frac{0.0975 - 0.025}{0.18 - 0.025} = 0.468$$

$$Fo = \frac{D\theta}{a^2} = 0.47F = 0.47 \# 0.468 = 0.22$$

$$D = \frac{(0.22)(0.02)^2}{21600} = 4.07 \# 10^{-9} \text{ m}^2/\text{s}$$

(b) In this case,

$$F = \frac{\bar{c}_A - c_A^*}{c_{A_0} - c_A^*} = \frac{0.06 - 0.025}{0.18 - 0.025} = 0.226$$

$$\text{Hence, } Fo = \frac{D\theta}{a^2} = 2.3F = 2.3 \# 0.226 = 0.52$$

$$\text{or, } i = \frac{(0.52)(0.02)^2}{4.07 \times 10^{-9}} = 51106 \text{ s} = 14.2 \text{ hr}$$

Time required = 14.2 hr.

**EXAMPLE 2.19** (Diffusion from a porous solid sphere): Spheres of porous clay 12 mm diameter were thoroughly impregnated with an aqueous solution of sodium chloride, concentration being 0.15 g/cm<sup>3</sup>. When exposed to a running supply of fresh water at 18°C, the spheres lost 60% of their salt content in 2.25 hr.

At 18°C, the average diffusivity of NaCl in water is  $1.36 \# 10^{-9} \text{ m}^2/\text{s}$

Assume  $Fo = 0.1175F$ .

Estimate the time for removal of 80% of the dissolved solute if the spheres were impregnated with an aqueous solution of ethanol, concentration being 0.17 g/cm<sup>3</sup> when exposed to a running supply of water containing 0.01 g/cm<sup>3</sup> of ethanol at 18°C.

The average diffusivity of ethanol in water at 18°C is  $0.53 \times 10^{-9} \text{ m}^2/\text{s}$ .

Assume  $Fo = 0.933F$ .

**Solution:** For NaCl solution

$$c_{A0} = 0.15, \bar{c}_A = 0.15 \# (1 - 0.6) = 0.06, c_A^* = 0$$

$$a = 6 \text{ mm} = 0.006 \text{ m}, i = 2.25 \# 3600 \text{ s} = 8100 \text{ s}$$

$$\text{Hence, } F = \frac{\frac{\bar{c}_A - c_A^*}{c_{A0} - c_A^*}}{= \frac{0.06 - 0.0}{0.15 - 0.0}} = 0.40,$$

$$\text{or, } Fo = \frac{\frac{D\theta}{a^2}}{= 0.1175F} = 0.1175 \# 0.40 = 0.047$$

$$D_{\text{eff}} = \frac{\frac{(0.047)(0.006)^2}{8100}}{= 2.09 \times 10^{-10} \text{ m}^2/\text{s}}$$

$$\frac{D_{AB}}{D_{\text{eff}}} = \frac{1.36 \times 10^{-9}}{2.09 \times 10^{-10}} = 6.507$$

For ethanol solution:

$$D_{\text{eff}} = \frac{\frac{D_{AB}}{6.507}}{= \frac{0.53 \times 10^{-9}}{6.507}} = 8.15 \times 10^{-11} \text{ m}^2/\text{s}$$

$$c_{A0} = 0.17, \bar{c}_A = 0.17 \# (1 - 0.8) = 0.034, c_A^* = 0.01, a = 6 \text{ mm} = 0.006 \text{ m}$$

$$\text{whence, } F = \frac{\frac{\bar{c}_A - c_A^*}{c_{A0} - c_A^*}}{= \frac{0.034 - 0.01}{0.17 - 0.01}} = 0.15$$

$$Fo = D_{\text{eff}} \frac{\theta}{a^2} = 0.933F = (0.933 \# 0.15) = 0.14$$

$$\text{whence, } i = \frac{\frac{(0.14)(0.006)^2}{8.15 \times 10^{-11}}}{= 61840 \text{ s} = 17.18 \text{ hr}}$$

Time required for removal of 80% solute = 17.18 hr

## 2.11 Some Special Types of Diffusion in Solids

Diffusion through a capillary tube or through a porous solid may be of four types as follows: *molecular diffusion*, *transition diffusion*, *Knudsen diffusion* and *surface diffusion*.

**Molecular diffusion:** It occurs when the mean free path of the diffusing component is small compared to the diameter of the tube or of the pores through which they diffuse.

**Transition diffusion:** It occurs in the region between molecular and Knudsen diffusion. This type of diffusion may take place by both the mechanisms of molecular and Knudsen diffusions.

**Knudsen diffusion:** It occurs through capillary tubes or through the fine pores of a porous solid at very low pressure, as a result of which the mean free path of the diffusing component may become

equal to or even larger than the diameter of the tube or pores through which diffusion takes place. The diffusing molecules collide more with the wall of the tube or pore rather than colliding with each other. After collision with the wall, the molecules may bounce off in any direction. Knudsen diffusion becomes important when the number of molecules present is low and the diameter of the tube or pore very low, usually below 50 microns. Knudsen diffusion occurs when Knudsen number,  $N_{kn}$  defined

$$\text{as } N_{kn} = \frac{\lambda_A}{d_0}$$

is  $\geq 100$ .

where,

$\lambda_A$  = mean free path of the diffusing component A, m and

$d_0$  = diameter of the tube or pore in a porous solid, m.

Equation for Knudsen flow in a long capillary tube is

$$w_A = \frac{d_0^3}{6} \left( \frac{2\pi M_A}{RT} \right)^{0.5} \left( \frac{-\Delta p'}{z} \right); N_{kn} > 10$$

where,

$w_A$  = mass flow rate of component A, kg/s

$\Delta p'$  = difference in partial pressure of A in length  $z$ , m

$z$  = length of the capillary or pore, m

$M_A$  = Molecular weight of component A

The mass rate of flow in Knudsen flow depends on  $d_0^3$  while in laminar flow the same depends on  $d_0^4$ . However, Knudsen diffusion is independent of total pressure and viscosity in contrast to Hagen-Poiseuille equation for laminar flow of an ideal gas (Figure 2.14).

A Knudsen diffusion coefficient,  $D_{kA}$  is defined by the following equation:

$$J_k = -D_{kA} \frac{dc_A}{dz} = \frac{D_{kA}}{RT} \frac{dp'_A}{dz} \quad (2.96)$$

The Knudsen diffusion coefficient being

$$D_{kA} = 48.5 d_0 \left( \frac{T}{M_A} \right)^{0.5} \quad (2.97)$$

where

$D_{kA}$  = Knudsen diffusion coefficient,  $\text{m}^2/\text{s}$ , and

$d_0$  = tube or pore diameter, mm.

From Eq. (2.97), it may be concluded that if two compounds are diffusing in Knudsen flow, then their flux ratio will be inversely proportional to the square roots of their molecular weights.

**Surface diffusion:** If the ratio of actual amount of a substance adsorbed on a surface to that required to form a monolayer is less than unity, a part of the active surface remains vacant. Some of the adsorbed molecules tend to migrate from the zone of higher concentration to these empty sites

provided they have sufficient energy to jump the energy barrier.

The flux of surface diffusion may be represented by an equation similar to Fick's law

$$J_S = -D_S \frac{dc_s}{dx} \quad (2.98)$$

where,

$D_S$  = surface diffusion coefficient,  $\text{m}^2/\text{s}$ , and

$c_s$  = surface concentration of the adsorbed molecules,  $\text{kmol}/\text{m}^2$

We have discussed so far the diffusion that occurs due to concentration gradient in the system. There are some other kinds of diffusion encountered in process industries as follows:

- (i) *Forced diffusion* which is caused by unequal external forces acting on the chemical species, e.g. gradient of electrical potential governs the behaviour of ionic systems. Such electrokinetic phenomena are gaining importance day by day due to advent of microelectronic devices.
- (ii) *Pressure diffusion* caused due to pressure gradient in the system, e.g. separation in the ultracentrifuge is affected due to large pressure gradient. The scheme of the barrier-separation process consists of passing a high pressure gaseous mixture over a separative barrier. A fraction of the feed diffuses through it into the low-pressure discharge chamber as enriched gas while the remainder discharges as high-pressure depleted fluid. For example when two gases  $A$  and  $B$  are forced to diffuse through a third gas  $C$ , there is tendency of  $A$  and  $B$  to separate due to difference in their diffusion rates. This phenomenon is known as *atmolysis* or *sweep diffusion* (Keys and Pigford 1957).
- (iii) *Thermal diffusion* occurs due to temperature gradient. The behaviour of solutions under nonisothermal conditions has two manifestations, (i) If two solutions of different composition and initially at the same temperature diffuse together, a transient temperature gradient occurs (*Dufour effect*). (ii) Conversely, if a temperature gradient is applied to a homogeneous solution, a concentration gradient is generally established (*Soret effect*). Thermal diffusion phenomena can be applied for separation of materials. Two basic methods are available, in the *static* method the thermal gradient is established in such a manner that convection currents are eliminated; in the *reflux* method counter-current flow of hot and cold material is provided, thereby greatly increasing the separation in a single piece of equipment. Reflux is usually provided by utilizing the density gradient that results from the imposed temperature gradient. Such an apparatus is known as *thermo-gravitational column* or a *Clusius–Dickel column* (Clusius and Dickel 1939). Unless the temperature gradient is very large, the separation will normally be significantly small. It has been advantageous to combine the thermal diffusion effect with free convection between two vertical walls, one heated and other cooled. The heated stream then ascends and the cooled one descends. The upward stream will be richer in one of the components and the downward stream will be richer in another component. This is the operation principle of the Clusius-Dickel column (Chapman and Cowling 1970). By coupling many of these columns together in a cascade, it is possible to perform a separation.

## Nomenclature

$A$  : area of slab normal to the direction of diffusion,  $\text{L}^2$

$a$  : half thickness of slab,  $\text{L}$

$a$  : cross section of diffusion,  $\text{L}^2$

$b_n$  : the  $n$ th root of  $J_0(b_n a) = 0$

$c$  : concentration,  $\text{M/L}^3$ ,  $\text{mol/L}^3$

$c$  : total molal concentration,  $\text{mol/L}^3$

$c_{BM}$  : log-mean concentration difference, —

$c_i$  : molar concentration of component  $i$  in a mixture,  $\text{mol/L}^3$

$D, D_A$  : diffusivity,  $\text{L}^2/\theta$

$D_{AB}$  : diffusivity of  $A$  in  $B$ ,  $\text{L}^2/\theta$

$D_{Am}$  : diffusivity of component  $A$  in a mixture,  $\text{L}^2/\theta$

$E_D$  : eddy diffusivity,  $\text{L}^2/\theta$

$E_H$  : eddy thermal diffusivity,  $\text{L}^2/\theta$

$E_V$  : eddy viscosity,  $\text{L}^2/\theta$

$F_o$  : Fourier number, —

$I$  : molar flux relative to an observer moving with the mass average velocity,  $\text{mol/L}^2\theta$

$i$  : mass flux relative to an observer moving with the mass average velocity,  $\text{M/L}^2\theta$

$J$  : molar flux relative to an observer moving with the molar average velocity,  $\text{mol/L}^2\theta$

$J_0(b_r)$  : the Bessel function of first kind of order zero

$J_A(\text{turb})$  : flux of component A due to eddy motion

$j$  : mass flux relative to an observer moving with the molar average velocity,  $\text{M/L}^2\theta$

$k$  : Boltzmann constant

$l$  : Prandtl mixing length,  $\text{L}$

$l_d$  : length scale of eddies in the universal range,  $\text{L}$

$M$  : molecular weight,  $\text{M/mol}$

$m$  : mass,  $\text{M}$

$N$  : molar flux relative to a stationary observer,  $\text{mol/L}^2\theta$

$n$  : mass flux relative to a stationary observer,  $\text{M/L}^2\theta$

$n$  : Avogadro's number, an integer

$P$  : total pressure,  $\text{F/L}^2$

$p'_i$  : partial pressure of the component  $i$  in a mixture,  $\text{F/L}^2$

$p'_{BM}$  : log mean partial pressure of component  $B$ ,  $\text{F/L}^2$

$r$  : radial position,  $\text{L}$

$r$  : radius of cylinder, L  
 $r_s$  : radius of a sphere, L  
 $r'_s$  : radius of a sphere at time q  
 $R$  : universal gas constant, FL/mol T  
 $T$  : absolute temperature, K  
 $U$  : molar average velocity of the components in a mixture, L/q  
 $u$  : mass average velocity of the components in a mixture, L/q  
 $u'_d$  : velocity of eddies in the universal range, L/q  
 $u_i$  : molar velocity of the component  $i$  relative to a stationary observer, L/q  
 $V_{Ad}$  : diffusion velocity of component  $A$ , L/q  
 $V$  : volume, L<sup>3</sup>; Molar volume, L<sup>3</sup>/gmol  
 $v$  : molar volume, L<sup>3</sup>/kmol  
 $x$  : mole fraction of component  $i$  in liquid, -  
 $y$  : mole fraction of component  $i$  in gas, -  
 $z$  : longitudinal co-ordinate in the direction of diffusion, length of diffusion path, L

### Greek Letters

$\alpha$  : thermal diffusivity, L<sup>2</sup>/q  
 $f$  : energy of molecular attraction  
 $i$  : time  
 $m$  : mean free path, L  
 $v_{AB}$  : molecular separation at collision [= (v<sub>A</sub> + v<sub>B</sub>)/2]  
 $v_A, v_B$  : molecular diameter of  $A$  and  $B$  respectively, Å  
 $f_{AB}$  : energy of molecular attraction  
 $\Omega$  : collision integral, function of  $kT/f_{AB}$   
 $z$  : association parameter for solvent, —  
 $\eta$  : viscosity, M/Lq  
 $\rho$  : density, M/L<sup>3</sup>  
 $\square$  : Solute unremoved, —  
 $\tau$  : shear stress, F/L<sup>2</sup>  
 $\nu$  : kinematic viscosity, L<sup>2</sup>/q

### Subscripts

$A$  : component A  
 $B$  : component B  
 $i$  : component  $i$   
1 and 2 : beginning and end of diffusion path

### Numerical Problems

**2.1 Calculation of Average Velocities and Fluxes:** Imagine a cubic volume which is 1 cm on each side and is being convected at 1 cm/s in the horizontal direction ( $z$ -direction). Assume that 2 mol of  $A$  (molecular weight = 2), 3 mol of  $B$  (molecular weight = 3) and 4 mol of  $C$  (molecular weight = 4) are present in the cubic volume at steady-state, and also an unequimolar counter-diffusion is superimposed on the flow. Molecules of  $A$  diffuse in the  $+z$  direction at a rate of 2 mol/s; molecules of  $B$  diffuse in the opposite direction at a rate of 1 mol/s. Find mass average velocity and molar average velocity. Also, calculate the fluxes relative to the mass average velocity and relative to molar average velocity.

[Ans: Mass average velocity = 1.034 cm/s, Molar average velocity = 1.11 cm/s; Molar fluxes relative to mass average velocity of:  $A = 1.931$ ,  $B = -1.1034$ ,  $C = -0.1379$  mol/cm $^2$ s; Mass fluxes relative to mass average velocity of:  $A = 3.8621$ ,  $B = -3.3103$ ,  $C = -0.5517$  g/cm $^2$ s; Molar fluxes relative to molar average velocity of:  $A = 1.7778$ ,  $B = -1.3333$ ,  $C = -0.4444$  mol/cm $^2$ s; Mass fluxes relative to molar average velocity of:  $A = 3.5556$ ,  $B = -4.0$ ,  $C = -1.7778$  g/cm $^2$ s.]

**2.2 Molecular Diffusion of Oxygen Through a Stagnant Layer of Methane:** Oxygen is diffusing through a stagnant layer of methane 5 mm thick. The temperature is 20°C and the pressure is 1 atm. Calculate the rate of diffusion of oxygen in kg/hr through 1 m $^2$  of the methane film when the concentrations of oxygen on two sides of the methane film are 15% and 5% by volume, respectively.

The diffusivity of oxygen through methane at 0°C and 1 atm pressure is 0.184 cm $^2$ /s. [Ans: 2.17 kg/hr $\cdot$ m $^2$ ]

**2.3 Diffusion of Ammonia in Stagnant Air:** Ammonia is diffusing through a stagnant air film of 0.25 mm thick. The total pressure is 2 atm and the temperature 50°C. Calculate the rate of diffusion of ammonia in kg/hr through 1 square metre surface if the concentrations of ammonia on the two sides of the film are 10% and 2% by volume, respectively

Diffusivity of ammonia in air at 0°C and 1 atm pressure is 0.198 cm $^2$ /s

[Ans: 20.04 kg/hr $\cdot$ m $^2$ ]

**2.4 Diffusion of Oxygen in Stagnant Nitrogen:** Oxygen is diffusing in a mixture of oxygen-nitrogen at 1 atm pressure and at a temperature of 25°C; concentrations of oxygen at planes 2 mm apart are 10 and 20 volume percent, respectively. Nitrogen is non-diffusing. Calculate the flux of oxygen. Given: diffusivity of oxygen in nitrogen is  $1.89 \times 10^{-3}$  m $^2$ /s

Ans:  $4.55 \times 10^{-3}$  mol/m $^2$ s.

**2.5 Diffusional Flux of Oxygen in Stagnant Carbon Monoxide:** Oxygen ( $A$ ) is diffusing through carbon monoxide ( $B$ ) under steady-state conditions with carbon monoxide non-diffusing. The total pressure is  $1 \times 10^5$  N/m $^2$  and the temperature is 0°C. The partial pressures of oxygen at two planes 2.0 mm apart are 13000 and 6500 N/m $^2$ , respectively. The diffusivity for the mixture is  $1.87 \times 10^{-5}$  m $^2$ /s. Calculate the amount of oxygen diffused in one hour in kmol through each square metre of the two planes. [Ans: 0.107 kmol/hr $\cdot$ m $^2$ ]

**2.6 Rate of Evaporation of Water Through Air Film:** A layer of water 20 mm thick is maintained at a constant temperature of 25°C in contact with dry air at 30°C and 1 atm pressure. Assuming evaporation to take place by molecular diffusion through an air film of 0.5 mm thick, calculate the time necessary for evaporation of 50% of the water.

The diffusivity of water vapour in air may be taken as  $0.258 \text{ cm}^2/\text{s}$ . The vapour pressure of water at 20°C is 17.6 mm Hg. [Ans: 3.04 hr]

**2.7 Diffusion of Oxygen in Stagnant Nitrogen at Elevated Pressure:** The operation as stated in Numerical Problem 2.4 takes place at 10 atm pressure keeping other conditions the same. Calculate the rate of diffusion of oxygen in  $\text{g/cm}^2\text{hr}$ , taking the value of diffusivity of oxygen in nitrogen  $0.181 \text{ cm}^2/\text{s}$  [Ans:  $5.02 \text{ g/cm}^2\text{hr}$ ]

**2.8 Effect of Elevated Pressure on the Rate of Molecular Diffusion of Ammonia in Air:** Ammonia is diffusing through a stagnant air film 2 mm thick at a temperature of 27°C and a pressure of 1 atm. Estimate the effect on the rate of diffusion of raising the total pressure to 10 atm for the following cases:

- the concentration of ammonia is 10% (by volume) on one side of the film and zero on the other side;
- the partial pressure of ammonia is 0.10 atm on one side of the film and zero on the other side.

The diffusivity of ammonia in air at 0°C and 1 atm pressure is  $0.198 \text{ cm}^2/\text{s}$

[Ans: (i) Rate of diffusion remains unchanged, (ii) Rate of diffusion becomes  $4.65 \times 10^{-7} \text{ gmol/cm}^2\text{s}$ ]

**2.9 Equimolar Counter-Diffusion of Two Gases:** Gases *A* and *B* are diffusing through each other under conditions of equal molal counter-diffusion. The concentrations of gas *A*, 4 mm apart, are 10% and 2% by volume. The total pressure is 1 atm and the temperature is 20°C. The diffusivity of the two gases under these conditions is  $0.15 \text{ cm}^2/\text{s}$  Determine the rate of diffusion. [Ans:  $1.248 \text{ gmol/cm}^2\text{s}$ ]

**2.10 Equimolar Counter-Diffusion of Hydrogen and Oxygen at Elevated Pressure:** In a gas mixture of hydrogen and oxygen, steady-state equimolar counter-diffusion is occurring at a total pressure of 100 kPa and temperature of 20°C. If the partial pressure of oxygen at two planes 0.01 m apart, and perpendicular to the direction of diffusion are 15 kPa and 5 kPa, respectively and the mass diffusion flux of oxygen in the mixture is  $1.6 \times 10^{-5} \text{ kmol/m}^2\text{s}$ , calculate the molecular diffusivity for the system. [Ans.  $38.98 \times 10^{-6} \text{ m}^2/\text{s}$ ]

**2.11 Diffusion of a Gas Through a Mixture of Gases:** Hydrogen is diffusing through a stagnant mixture of gases containing 40% nitrogen, 30% ammonia and 30% carbon dioxide by volume. The temperature is 25°C and total pressure is 1 atm. The partial pressure of hydrogen at two planes 6 mm apart in the direction of diffusion are 100 mm Hg and 40 mm Hg, respectively. Determine the rate of diffusion of hydrogen.

*Given:* At 25°C and 1 atm, the diffusivities of hydrogen with respect to the constituents of the gas mixture are as under:

$$D_{\text{H}_2-\text{N}_2} = 0.773 \text{ cm}^2/\text{s}; D_{\text{H}_2-\text{NH}_3} = 0.783 \text{ cm}^2/\text{s}; D_{\text{H}_2-\text{CO}_2} = 0.646 \text{ cm}^2/\text{s}$$

[Ans:  $4.41 \times 10^{-6} \text{ gmol/s}$ ]

**2.12 Diffusion Through Variable Area:** A conical duct 50 cm long having internal diameters of 15 cm and 7.5 cm at the larger and smaller ends respectively, connects two very large flasks *A* and *B*. Flask *A* contains a uniform mixture of 75 mole% ammonia and 25 mole% hydrogen. Flask *B* contains 20 mole% ammonia and 80 mole% hydrogen. The temperature is throughout 25°C and the total pressure is 1 atm. Under these conditions, the diffusivity of  $\text{NH}_3-\text{H}_2$  is  $7.83 \times 10^{-5} \text{ cm}^2/\text{s}$ .

Assuming complete absence of convection and that ammonia diffuses in the direction of decreasing diameter, determine the rate of transfer of ammonia between the two flasks. [Ans:  $3.11 \times 10^{-5} \text{ gmol/s}$ ]

**2.13 Calculation of the Rate of Combustion of Spherical Charcoal Particle:** Spheres of charcoal, 25 mm in diameter are being burnt in a stream of air at 1 atm pressure. Assuming the controlling resistance is equivalent to that for molecular diffusion of oxygen through a stagnant air film 2.0 mm thick and neglecting the effect of back diffusion of the products of combustion, calculate the theoretical combustion rate in  $\text{kg/hr/m}^2$ .

The partial pressures of oxygen are 0.21 atm in the air stream and zero at the carbon-gas interface. The bulk temperature of the gas is 1550 K. The diffusivity of  $\text{O}_2$  in air at 0°C and 1 atm pressure is  $0.18 \text{ cm}^2/\text{s}$  [Ans:  $9.76 \text{ kg/hr/m}^2$ ]

**2.14 Estimation of Loss of Hydrogen from a Spherical Container:** Hydrogen at 10 bar pressure and at 300 K temperature is stored in a spherical steel tank of 100 mm diameter and 2 mm thickness. The concentration of hydrogen in the tank is  $1.5 \text{ kmol/m}^3$  and the diffusion coefficient of hydrogen in steel is  $0.3 \times 10^{-12} \text{ m}^2/\text{s}$ . Calculate the rate of loss of hydrogen from the tank.

[Ans:  $7.35 \times 10^{-12} \text{ kmol/s}$  or  $14.7 \times 10^{-12} \text{ kg/s}$ ]

**2.15 Effect of Temperature on Diffusivity of Gas System:** A diffusivity value of  $0.151 \text{ cm}^2/\text{s}$  has been reported for  $\text{CO}_2$ -air system at 293 K and 1 atm pressure. Using Chapman-Enskog equation, estimate the diffusivity for the system at 1500 K.

[Ans:  $2.49 \text{ cm}^2/\text{s}$ ]

**2.16 Estimation of Diffusivities in Gas Mixtures using Chapman-Enskog Equation:** Calculate the diffusivities of the following pairs of gases using Chapman-Enskog equation:

- (i) Ammonia in air at standard atmospheric pressure and 0°C.
- (ii) Equimolar mixture of  $\text{CO}_2$  and  $\text{N}_2$  at 288.2 K and 40 atm pressure.
- (iii) Methane-ethane system at 40°C and 1 atm pressure.

[Ans. (i)  $1.84 \times 10^{-5} \text{ m}^2/\text{s} = 0.184 \text{ cm}^2/\text{s}$ , (ii)  $7.5 \times 10^{-5} \text{ cm}^2/\text{s} = 7.5 \times 10^{-9} \text{ m}^2/\text{s}$ , (iii)  $1.56 \times 10^{-5} \text{ m}^2/\text{s}$ .]

**2.17 Diffusivity of Acetone in Air:** A narrow test tube 3 mm id, 50 mm long was filled with acetone to

a height of 39 mm from the bottom and maintained at a constant temperature of 20°C in a gentle current of air. The total pressure was atmospheric. After 5 hr, the liquid level was 29.5 mm from the bottom. The barometric pressure was 750 mm Hg.

Calculate the diffusivity of acetone in air under the conditions of the experiment.

Given: Density of liquid acetone at 20°C = 0.79 g/cm<sup>3</sup>,

Vapour pressure of acetone at 20°C = 180 mm Hg.

[Ans: 0.10 cm<sup>2</sup>/s]

**2.18 Rate of Diffusion of Water in Dry Air in a Well:** Calculate the rate of diffusion of water vapour from a thin layer of water at the bottom of a well 6 m in height to dry air flowing over the top of the well. Assume the entire system is at 298 K and 1 atm pressure. If the well diameter is 3 m, find out the total weight of water diffused per second from the surface of the water in the well. The diffusion coefficient of water vapour in dry air at the operating conditions is  $0.256 \times 10^{-4}$  m<sup>2</sup>/s. The partial pressure of water vapour at 298 K is  $0.0323 \times 10^4$  kg/m<sup>2</sup>. [Ans:  $7.0 \times 10^{-4}$  g/s]

**2.19 Calculation of the Amount of *n*-octane evaporated in nitrogen Atmosphere:** Liquid *n*-octane evaporates and diffuses upward through a long tube initially filled with nitrogen. As the liquid evaporates, it pushes the gas upward. How many grams of liquid *n*-octane will evaporate into nitrogen in 24.5 hr in a system kept at 20°C and 1 atm pressure if the area of the liquid surface is 1.29 cm<sup>2</sup>? The vapour pressure of *n*-octane at 20°C is 10.45 mm Hg. [Ans: 6.71 mg]

**2.20 Rate of Evaporation of Chloropicrin in Air:** Find the rate of evaporation (in g/hr) of chloropicrin ( $\text{CCl}_3\text{NO}_2$ ) kept in a long tube into air (considering it a pure substance) at 25°C.

Given: Total pressure = 770 mm Hg, Diffusivity = 0.088 cm<sup>2</sup>/s, Vapour pressure = 23.81 mm Hg, Distance from liquid level to the top of the tube = 11.14 cm, Density of chloropicrin = 1.65 g/cm<sup>3</sup>, and surface area of liquid exposed for evaporation = 2.29 cm<sup>2</sup>. [Ans: 0.014 g/hr]

**2.21 Rate of Absorption of Oxygen in Pyrogallate Solution:** A test tube 2.0 cm in diameter and 15 cm tall is partly filled with a solution of alkaline pyrogallate. The depth of the empty space above the solution is 5 cm. The temperature is 25°C and the total pressure is 1 atm. Air may be assumed to contain 21% O<sub>2</sub> and 79% N<sub>2</sub>. The diffusivity of O<sub>2</sub> in N<sub>2</sub> at the given condition is 0.21 cm<sup>2</sup>/s. Calculate the rate of absorption of O<sub>2</sub> from air in the solution in kg/s at steady-state if air flows gently over the open end of the test tube. [Ans:  $71.38 \times 10^{-9}$  kg/s]

**2.22 Rate of Diffusion of Acetic Acid Through a Stagnant Film:** Acetic acid is diffusing across a 1.5 mm thick stagnant film of aqueous solution at 20°C. The concentrations of acetic acid on the two sides of the film are 11% and 5% acid by weight respectively. Calculate the rate of diffusion of acetic acid.

Given: Densities of 11% and 5% acetic acid solution at 20°C are 1100 and 1010 kg/m<sup>3</sup> respectively. Diffusivity of acetic acid in aqueous solution at 20°C is  $1 \times 10^{-5}$  cm<sup>2</sup>/s. [Ans:  $0.812 \times 10^{-6}$  kmol/m<sup>2</sup>s]

**2.23 Prediction of Self-Diffusivity in Liquid Mercury:** The diffusivity of Hg<sup>203</sup> in normal liquid Hg has been measured along with viscosity and volume per unit mass. Compare the experimentally

measured  $D_{AA}$  with the values calculated using Eq. (2.60).

$T, \text{ K}$	$D_{AA}, \text{ cm}^2/\text{s}$	$n, \text{ cp}$	$V_A, \text{ cm}^3/\text{g}$
275.7	$1.52 \times 10^{-5}$	1.68	0.0736
289.6	$1.68 \times 10^{-5}$	1.56	0.0737
364.2	$2.57 \times 10^{-5}$	1.27	0.0748

**2.24 Estimation of Diffusivity of Liquid:** Calculate the diffusion coefficient for hydrogen sulphide in water at 40°C. [Ans:  $2.7 \times 10^{-8} \text{ m}^2/\text{s}$ ]

**2.25 Estimation of Liquid Diffusivity Using Wilke-Chang Equation:** Estimate the diffusion coefficient for the following situations using Wilke-Chang equation:

- (i) Acetic acid in dilute aqueous solution at 12.5°C. The density of acetic acid at its normal boiling point is  $0.937 \text{ g/cm}^3$ .
- (ii) A dilute solution of methanol in water at 100°C while the diffusivity for the same solution at 15°C is  $1.28 \times 10^{-5} \text{ cm}^2/\text{s}$ .
- (iii) Bromonaphthalene in dilute ethyl alcohol solution at 20°C. Atomic volume: C = 14.8, H = 3.7, Br = 27.0. For naphthalene ring subtract 30. Viscosity of dilute alcohol solution at 20°C = 1.192 cp; z = 1.5.

[Ans: (i) Experimental value:  $0.91 \pm 0.04 \times 10^{-5} \text{ cm}^2/\text{s}$ , (ii)  $6.7 \times 10^{-5} \text{ cm}^2/\text{s}$ , (iii)  $7.0 \times 10^{-6} \text{ cm}^2/\text{s}$ ]

**2.26 Diffusion through a Solid Slab:** A slab of clay 40 mm thick with the four thin edges sealed, is being dried from two flat faces by exposure to dry air. The initial moisture is 18%. Drying takes place by internal diffusion of liquid water followed by evaporation at the surface. The surface moisture content is 2.5%. The average moisture content has fallen to 9.75% in 6 hr.

Assuming diffusivity to be independent of moisture content and uniform in all directions, calculate (i) the diffusivity of clay in  $\text{cm}^2/\text{s}$ , (ii) the time required to reduce the moisture content to 6%. [Ans: (i)  $4.42 \times 10^{-5} \text{ cm}^2/\text{s}$ , (ii) 14.075 hr]

**2.27 Diffusion Through a Solid Sphere:** Spheres of porous clay 12 mm in diameter were thoroughly impregnated with an aqueous solution of sodium chloride of concentration  $0.15 \text{ g/cm}^3$ . When exposed to a running supply of fresh water at 18°C, the spheres lost 60% of their salt content in 2.25 hr. At 18°C, the average diffusivity of NaCl in water is  $1.36 \times 10^{-9} \text{ m}^2/\text{s}$ . Assume  $Di/a^2 = 0.1175F$ .

Estimate the time required for removal of 80% of the dissolved solute if the spheres were impregnated with an aqueous solution of ethyl alcohol of concentration  $0.17 \text{ g/cm}^3$  when exposed to a running supply of water containing  $0.01 \text{ g/cm}^3$  of ethanol. The average solubility of ethanol in water at 18°C is  $0.53 \times 10^{-9} \text{ m}^2/\text{s}$ .

[Ans: 17.18 hr]

**2.28 Calculation of Pressure in Knudsen Diffusion:** A stainless-steel tubing is of  $1.6 \times 10^{-3} \text{ m}$  inside diameter and 4 m long. One end of the tube is evacuated. Calculate the pressure in the other end in order the Knudsen number to be 10. The gas inside is of molecular weight 92, viscosity  $6.5 \times 10^{-$

$^4$  kg/m $\cdot$ s., and temperature 300 K.

[Ans:  $8.43 \times 10^{-4}$  atm]

**2.29 Calculation of Knudsen Diffusion Coefficient and Flux:** Hydrogen gas is kept in a container at 200°C and 1 atm pressure. The mouth of the container is closed with a porous plug of  $5 \times 10^{-3}$  m long with average pore size of 100 Å. Calculate the Knudsen diffusion coefficient and the steady flux through the plug.

[Ans:  $0.0746 \text{ cm}^2/\text{s}$ ,  $3.84 \times 10^{-6} \text{ gmol/cm}^2\text{s}$ ]

### **Short and Multiple Choice Questions**

1. What are the three types of frames of reference used in mass transfer calculations?
2. What is Fick's first law of molecular diffusion in fluids? What are the other laws similar to this law?
3. Under what condition is the approximate form of Fick's law  $N_A = -D_{AB} \left( \frac{dc_A}{dz} \right)$  valid?
4. Under what condition, the rates of equal molal counter-diffusion of two gases and diffusion of one gas through a stagnant layer of the other gas become almost equal?
5. For what kind of mixture or solution  $D_{AB} = D_{BA}$ ?
6. Why molecular diffusion in liquids is very slow compared to that in gases?
7. How does binary diffusivity for molecular diffusion in liquids vary with temperature?
8. Molecular diffusivity in a binary gas mixture is related to the temperature ( $T$ ) as  
(a)  $D \propto T$  (b)  $D \propto T^{0.5}$  (c)  $D \propto T^{1.5}$  (d)  $D \propto T^{-1}$
9. Molecular diffusivity in a binary gas mixture varies with total pressure ( $P$ ) as  
(a)  $D \propto P^{0.5}$  (b)  $D \propto P^{1.5}$  (c)  $D \propto P^{-0.5}$  (d)  $D \propto P^{-1}$
10. The unit of volumetric diffusivity is  
(a) cm/s (b)  $\text{cm}^2/\text{s}$  (c)  $\text{cm}^3/\text{s}$  (d)  $\text{cm}^2/\text{s}^2$ .
11. Molecular diffusion is caused by  
(a) kinetic energy of the molecules  
(b) activation energy of the molecules  
(c) potential energy of the molecules  
(d) none of these.
12. Which of the following has the same dimension as that of molecular diffusivity?  
(a) momentum flux (b) thermal conductivity (c) kinematic viscosity (d) none of these
13. The steady-state gas phase reaction  $3A + B = C + 2D$  takes place on a catalyst surface. What will be the value of the flux ratio  $N_A/N_D$ ?  
(a) -2 (b) -0.5 (c) -1.5 (d) 2
14. Steady-state equimolar counter-diffusion occurs in  
(a) absorption of  $\text{NH}_3$  from air by water  
(b) separation of a binary mixture by distillation

- (c) liquid-liquid extraction  
(d) leaching of solids
- 15.** The binary diffusivity of gases at atmospheric conditions are approximately  
(a)  $10^{-9}$  cm/s (b)  $10^{-1}$  cm $^2$ /s (c)  $10^{-1}$  cm/s (d)  $10^{-4}$  cm $^2$ /s
- 16.** Binary diffusivities in gases do not depend on the  
(a) pressure (b) temperature  
(c) nature of components (d) none of these
- 17.** Component *A* of a binary gas mixture is diffusing from point 1 to point 2. The total pressure is doubled by keeping all other parameters including mole fraction of *A* at points 1 and 2 constant. How will the rate of diffusion change?  
(a) it will be doubled (b) it will be halved  
(c) it will remain unchanged (d) none of these
- 18.** Molecular diffusivity, thermal diffusivity and eddy momentum diffusivity are the same for  
(a)  $\text{Pr} = \text{Sc} = 0$  (b)  $\text{Pr} = \text{Sc} = 0.5$   
(c)  $\text{Pr} = \text{Sc} = 1$  (d)  $\text{Pr} = \text{Sc} = 10$
- 19.** Diffusivity in concentrated solutions differs from that in dilute solutions because of changes in  
(a) viscosity (b) degree of ideality  
(c) both (a) and (b) (d) neither (a) nor (b)
- 20.** Knudsen diffusivity is proportional to  
(a)  $T^{0.5}$  (b)  $T$  (c)  $T^2$  (d)  $T^4$
- 21.** Liquid phase diffusivity varies with the viscosity of the solution as  
(a)  $D_{AB} \propto n^{0.5}$  (b)  $D_{AB} \propto n$  (c)  $D_{AB} \propto n^{-1}$  (d)  $D_{AB} \propto n^2$
- 22.** Two large bulbs containing mixtures of gases *A* and *B* at different proportions but at the same pressure are connected by a tapered tube 10 cm long and end diameters of 2 cm and 4 cm. At which point will the flux of *B* be maximum?  
(a) at the smaller diameter end (b) at the larger diameter end  
(c) at the middle of the tube. (d) none of these
- 23.** The diffusivity of methane in air at 0°C and 1 atm pressure is 0.196 cm $^2$ /s. What will be the diffusivity of air in methane at 50°C and 2.5 atm pressure?  
(a) 0.196 cm $^2$ /s (b) 0.10 cm $^2$ /s (c) 0.078 cm $^2$ /s (d) none of these

#### *Answers to Multiple Choice Questions*

8. (c) 9. (d) 10. (b) 11. (a) 12. (c) 13. (c) 14. (b) 15. (b)  
16. (d) 17. (c) 18. (c) 19. (c) 20. (a) 21. (c) 22. (a) 23. (c)

#### **References**

- Bird, R.B., W.E. Stewart and E.N. Lightfoot, *Transport Phenomena*, Wiley, New York (1960, 2006).  
Brodkey, R.S. and H.C. Hershey, *Transport Phenomena—A Unified Approach*, McGraw-Hill, New York (1988).  
Bulicka, J. and J. Prochazka, *J. Chem. Eng. Data*, **21**(4), 452 (1976).

- Chapman, S. and T.G. Cowling, *The Mathematical Theory of Nonuniform Gases*, 3rd ed., Cambridge University Press, New York (1970).
- Chin, K.K., S.F.Y. Li, Y.J. Yao and L.S. Yue, *J. Chem. Eng. Data*, **36**, 329 (1991).
- Clusius, K. and G. Dickel, *Z. Phys. Chem.*, **B44**, 397, 451 (1939).
- Crank, J., *The Mathematics of Diffusion*, Claventon Press, Oxford (1956).
- Cussler, E.L., *Diffusion: Mass Transfer in Fluid Systems*, 2nd ed., Cambridge University Press, New York (1997).
- Davies, T.T., *Turbulence Phenomena*, Academic, New York (1972).
- Ficks, A.E., *Philos. Mag.*, **10**, 30 (1855).
- Fuller, E.N., P.D. Schettler and J.C. Giddings, *Ind. Eng. Chem.*, **58**(5), 18; **58**(8), 81 (1966).
- Geankolis, C.J., *Transport Processes and Separation Process Principles*, 4th ed., PHI Learning, New Delhi (2005).
- Ghorai, A., *Measurement of transport coefficients of some binary liquid systems*, B. Tech. Project, Univ. of Calcutta, India (1994).
- Ghosh, U.K., S. Kumar and S.N. Upadhyay, *J. Chem. Eng. Data*, **36**, 413 (1991).
- Gilliland, E.R., *Ind. Eng. Chem.*, **26**, 681 (1934).
- Graham, T., *Philos. Trans. of the Royal Society of London*, **140**, 1 (1850).
- Hines, A.L. and R.N. Maddox, *Mass Transfer Fundamentals and Applications*, Prentice Hall (1985).
- Hinze, J.O., *Turbulence*, McGraw-Hill, New York (1959).
- Hirschfelder, J.O., R.B. Bird and E.L. Spotz, *Trans. ASME*, **71**, 921 (1949).
- Hirschfelder, J.O., C.F. Curtiss and R.B. Bird, *Molecular Theory of Gases and Liquids*, Wiley, New York (1954).
- Hottel, H.C., *Personal Communication*, (1949) in *Absorption and Extraction*, Sherwood, T.K. and R.L. Pigford (Eds.), McGraw-Hill (1952).
- International Critical Tables, vol. V, McGraw Hill, New York (1929).
- Keys, J.J. (Jr.) and R.L. Pigford, *Chem. Eng. Sci.*, **6**, 215 (1957).
- Kolmogoroff, A.N., *C.R. Acad. Sci., URSS*, **30**, 301; **32**, 16 (1941).
- Lee, Y.E. and S.F. Li, *J. Chem. Eng. Data*, **36**, 240 (1991).
- Newman, A.B., *Trans. AIChE.*, **27**, 310 (1931).
- Perry, R.H., D.W. Green and J.O. Malony (Eds.), *Perry's Chemical Engineers-Handbook*, 7th ed., McGraw Hill (1997).
- Poling, B.E., J.M. Prausnitz and J.P. O'Connell, *The Properties of Gases and Liquids*, 5th ed., McGraw-Hill, New York (2001).
- Ramakanth, C., A.K. Mukherjee and T.R. Das, *J. Chem. Eng. Data*, **36**, 384 (1991).
- Ramprasad, G., A.K. Mukherjee and T.R. Das, *J. Chem. Eng. Data*, **23**, 443 (1990).
- Ramprasad, G., A.K. Mukherjee and T.R. Das, *J. Chem. Eng. Japan*, **24**(3), 36 (1991).
- Riede, Th. and E.-U. Schlüder, *Chem. Eng. Sci.*, **46**, 609 (1991).
- Skelland, A.H.P., *Diffusional Mass Transfer*, John Wiley & Sons, Inc, New York (1974)

- Sutherland, W., *Philos. Mag.*, **9**, 781(1905).
- Taylor, R. and R. Krishna, *Multi-component Mass Transfer*, Wiley, New York (1993).
- Tee, L.S., S. Gotoh and W.E. Stewart, *Ind. Eng. Chem. Fund.*, **5**, 356, 363 (1966).
- Therm, M-J, K.K. Bhatia and K.E. Gubbin, *Chem. Eng. Sci.*, **22**, 309 (1967).
- Treybal, R.E., *Mass Transfer Operations*, 3rd ed., McGraw Hill, Singapore (1985).
- Wilke, C.R. and P. Chang, *AICHEJ*, **1**, 264 (1955).
- Wise, D.L. and G. Houghton, *Chem. Eng. Sci.*, **21**, 999 (1966).

\*<sup>\*</sup> A system is in steady-state when the associated parameters at any point do not vary with time.





# 3

## Mass Transfer Coefficients and Analogy Equations

### 3.1 Introduction

Molecular diffusion in gases being due to kinetic motion of gas molecules, fairly reliable equations have been developed from the kinetic theory of gases for prediction of the rates of molecular diffusion in gases as discussed in Chapter 2. Rates of molecular diffusion in liquids can also be predicted using equations derived by analogy with similar type of diffusion in gases. But on account of our very limited knowledge about turbulence, it has not been possible to develop such rate equations for eddy diffusion in gases and liquids although, except within a narrow region near solid surface or phase boundary, industrial mass transfer operations are mostly carried out by convective mass transfer in order to achieve the higher rates of transfer and thereby reduce the size of equipment and consequently the cost.

In some cases of convective mass transfer, it may be possible to calculate the rate of mass transfer by solving the differential equations obtained from mass and momentum balance provided the nature of the flow is properly defined. Typical examples are absorption of a gas in a laminar liquid film falling down along a wall (see Section 3.2.4) or dissolution of a solid coated on a flat plate in a liquid flowing over the plate. In more complex situations such as gas-liquid contact in a packed or plate column, dissolution of a solid in a mechanically stirred vessel, theoretical calculations for rate of mass transfer becomes quite difficult and may even be impossible for the complex nature of the flow. In some cases, the simplifying assumptions required to solve the complex partial differential equations make the results unreliable. The concept of mass transfer coefficient has been introduced with the objective of developing simple but useful approaches for solving such problems.

It has been established that rates of both molecular and eddy diffusion depend on concentration gradient. As a result, rates of transfer involving both molecular and eddy diffusion are generally expressed in terms of mass transfer coefficient defined as

$$\text{Flux} = (\text{Mass transfer coefficient}) \# (\text{Concentration difference})$$

$$\text{or, } \text{Mass transfer coefficient} = \frac{\text{Flux}}{\text{Concentration difference}}$$

Mass transfer coefficient has the dimension of moles/(unit time)(unit area)(unit concentration difference, the driving force) and is the inverse of resistance to mass transfer. It is analogous to heat

transfer coefficient which has the dimension of heat transferred/(unit time) (unit area) (unit temperature difference). But unlike heat transfer operation where temperature difference is the only mode of expressing driving force, the driving force in mass transfer operations may be expressed in different ways namely, partial pressure difference (only for gases), concentration difference and mole fraction difference. Accordingly, mass transfer coefficients may have different values and units.

As mentioned earlier, reliable equations are available for predicting the rates of molecular diffusion. Therefore, mass transfer coefficients as such are not required for cases where only molecular diffusion is involved. But in order to have uniformity with eddy diffusion and to develop design equations for some complex situations, mass transfer coefficients are also used in molecular diffusion. Mass transfer coefficients are particularly useful in interphase mass transfer where both molecular and eddy diffusions are involved. In addition, they are frequently used to estimate rates of mass transfer from and to special geometrical shapes. Many of these coefficients have been derived by analogy with heat transfer.

Let us consider the transfer of a component  $A$  from the bulk of a gas to the bulk of a liquid through the gas-liquid interface. The transfer in the bulk of gas which is in turbulent motion, is by eddy diffusion while that near the interface is by molecular diffusion. The rate of transfer may be expressed by a single equation by using mass transfer coefficient

$$N_{AG} = k_G(p'_{AG} - p'_{Ai}) \quad (3.1)$$

Similarly, the rate of transfer of  $A$  from the interface to the bulk of the liquid may be expressed as

$$N_{AL} = k_L(c_{Ai} - c_{AL}) \quad (3.2)$$

where,

$N_{AG}$  and  $N_{AL}$  = rate of transfer of solute  $A$  in gas and liquid phases, respectively in moles/(unit time)  
(unit area)

$k_G$  = gas phase mass transfer coefficient in moles/(unit time)(unit area)(unit partial pressure  
difference)

$k_L$  = liquid phase mass transfer coefficient in moles/(unit time)(unit area)(unit concentration  
difference)

$p'_{AG}$  and  $p'_{Ai}$  = partial pressures of component  $A$  in the bulk of the gas and at the interface,  
respectively in atmospheres

$c_{Ai}$  and  $c_{AL}$  = concentrations of component  $A$  at the interface and in the bulk of the liquid, respectively  
in moles/unit volume.

## 3.2 Types of Mass Transfer Coefficients

Mass transfer coefficients may be of different types depending upon

- (i) whether one component is diffusing through the stagnant layer of another component or there is counter-diffusion of two components,
- (ii) whether mass transfer is taking place in the gas phase or in the liquid phase, and
- (iii) the choice of expressing driving force.

### 3.2.1 Diffusion of One Component Through the Stagnant Layer of Another Component

Depending upon the mode of expression of the driving force three types of mass transfer coefficients in the gas phase and two types of coefficients in the liquid phase are generally used.

### Gas Phase:

$$N_A = k_G(p'A_1 - p'A_2) = k_C(c_{A1} - c_{A2}) = k_y(y_{A1} - y_{A2}) \quad (3.3)$$

### Liquid Phase

$$N_A = k_L(c_{A1} - c_{A2}) = k_x(x_{A1} - x_{A2}) \quad (3.4)$$

where,  $k_G$ ,  $k_C$ ,  $k_y$  are gas phase mass transfer coefficient while  $k_L$  and  $k_x$  are liquid phase mass transfer coefficients.

The expressions for mass transfer coefficients in gas phase can be obtained in terms of diffusivity by comparing Eq. (3.3) with Eq. (2.25) as follows:

#### Gas phase mass transfer coefficients:

$$N_A = k_G(p'A_1 - p'A_2) = \frac{D_{AB}P}{RTz} \frac{(p'_{A_1} - p'_{A_2})}{p'_{BM}} \quad (3.5)$$

$$\text{whence, } k_G = \frac{D_{AB}P}{RTz p'_{BM}} \quad (3.6)$$

$$N_A = k_C(c_{A1} - c_{A2}) = k_C \frac{(p'_{A_1} - p'_{A_2})}{RT} = \frac{D_{AB}P}{RTz} \frac{(p'_{A_1} - p'_{A_2})}{p'_{BM}} \quad (3.7)$$

$$\text{whence, } k_C = \frac{D_{AB}P}{zp'_{BM}} \quad (3.8)$$

$$N_A = k_y(y_{A1} - y_{A2}) = k_y \frac{(p'_{A_1} - p'_{A_2})}{P} = \frac{D_{AB}P}{RTz} \frac{(p'_{A_1} - p'_{A_2})}{p'_{BM}} \quad (3.9)$$

$$\text{whence, } k_y = \frac{D_{AB}P^2}{RTz p'_{BM}} \quad (3.10)$$

Similar expressions for mass transfer coefficients in the liquid phase can be obtained.

#### Liquid phase mass transfer coefficients:

$$N_A = k_L(c_{A1} - c_{A2}) = \frac{D_{AB}(c_{A_1} - c_{A_2})}{z c_{BM}} \quad (3.11)$$

$$\text{whence, } k_L = \frac{D_{AB}}{z c_{BM}} \quad (3.12)$$

$$N_A = k_x(x_{A1} - x_{A2}) = \frac{D_{AB}}{z x_{BM}} \left( \frac{\rho}{M} \right)_{av} (x_{A1} - x_{A2}) \quad (3.13)$$

$$\frac{D_{AB}(\rho/M)_{av}}{RTz}$$

whence,  $k_x = \frac{D_{AB}(\rho/M)_{av}}{RTz}$  (3.14)

### 3.2.2 Equal Molal Counter-Diffusion of Two Components

The mass transfer coefficients for this type of transfer are denoted by  $k'$  to distinguish them from the coefficients for transfer of one component through the stagnant layer of another component.

In this type of mass transfer also three types of mass transfer coefficients for the gas phase and two types of coefficients for the liquid phase are generally used.

**Gas phase:**

$$N_A = k'G(p'A_1 - p'A_2) = k'C(c_{A1} - c_{A2}) = k'y(y_{A1} - y_{A2}) \quad (3.15)$$

**Liquid Phase:**

$$N_A = k'L(c_{A1} - c_{A2}) = k'_x(x_{A1} - x_{A2}) \quad (3.16)$$

Comparing Eq. (3.15) with Eqs. (2.27), (2.55) and (2.56), respectively one can have the expressions for gas phase mass transfer coefficients as follows:

$$k'G = \frac{D_{AB}}{RTz}, k'C = \frac{D_{AB}}{z}, k'y = \frac{D_{AB}P}{RTz} \quad (3.17)$$

Similar expressions for liquid phase mass transfer coefficients are

$$k'L = \frac{D_{AB}}{z}, k'_x = \frac{D_{AB}(\rho/M)_{av}}{z} \quad (3.18)$$

Flux equations, expressions for mass transfer coefficients, nature of driving force and units for different types of mass transfer coefficients have been given in Table 3.1.

**Table 3.1** Different types of mass transfer coefficients

Flux	Expression for mass transfer coefficient	Driving force	Unit of mass transfer coefficient
Diffusion of one component through a stagnant layer of another component:			
<b>Gas phase:</b>			
$kG(p'A_1 - p'A_2)$	$kG = \frac{D_{AB}P}{RTz_{PM}}$	Partial pressure difference	Moles/(unit time) (unit area) (unit partial pressure difference)
$kC(c_{A1} - c_{A2})$	$kC = \frac{D_{AB}P}{z_{PM}}$	Concentration difference	Moles/(unit time) (unit area) (unit concentration difference)
$ky(y_{A1} - y_{A2})$	$ky = \frac{D_{AB}P^2}{RTz_{PM}}$	Mole fraction difference	Moles/(unit time) (unit area) (unit mole fraction difference)
<b>Liquid phase:</b>			
$kL(c_{A1} - c_{A2})$	$kL = \frac{D_{AB}}{z_{SM}}$	Concentration difference	Moles/(unit time) (unit area) (unit concentration difference)
$k_x(x_{A1} - x_{A2})$	$k_x = \frac{D_{AB}(\rho/M)_{av}}{z_{SM}}$	Mole fraction difference	Moles/(unit time) (unit area) (unit mole fraction difference)
Equal molal counter-diffusion:			
<b>Gas phase:</b>			
$k'G = \frac{D_{AB}}{RTz}$		Partial pressure	

$k'G(p'A1 - p'A2)$	difference	Moles/(unit time) (unit area) (unit partial pressure difference)
$k'C(c_{A1} - c_{A2}) \quad k'C = \frac{D_{AB}}{z}$	Concentration difference	Moles/(unit time) (unit area) (unit concentration difference)
$k'y(y_{A1} - y_{A2}) \quad k'y = \frac{D_{AB}}{RT}$	Mole fraction difference	Moles/(unit time) (unit area) (unit mole fraction difference)
<b>Liquid phase:</b>		
$k'L(c_{A1} - c_{A2}) \quad k'L = \frac{D_{AB}}{z}$	Concentration difference	Moles/(unit time) (unit area) (unit concentration difference)
$k'_x(x_{A1} - x_{A2}) \quad k'_x = \frac{D_{AB}(μ/M)_x}{z}$	Mole fraction difference	Moles/(unit time) (unit area) (unit mole fraction difference)

### 3.2.3 Volumetric Mass Transfer Coefficients

Mass transfer coefficients discussed so far are all based on unit surface of contact between the phases and are expressed as moles/(unit time) (unit area) (unit driving force). But in most of the widely used industrial mass transfer equipment like the packed or plate columns, the interfacial area of contact between the phases cannot be measured. In order to overcome this difficulty, volumetric mass transfer coefficients are generally used for calculating the rate of mass transfer. Since both mass transfer coefficient and specific surface ( $m^2/m^3$ ) of packing depend on the type and size of packing as well as flow rates of the concerned fluids, they can be combined into a single product to provide mass transfer coefficient on volumetric basis. Thus, for transfer of a component within the gas phase, the mass flux and the rate equation may be written as

$$N_A a = k_y a (y_{AG} - y_{Ai}) \quad (3.19a)$$

and for transfer within the liquid phase, the equation may be written as

$$N_A a = k_x a (x_{Ai} - x_{AL}) \quad \text{Figure 3.1 Mass transfer in laminar flow.} \quad (3.19b)$$

where,

$N_A a$  = mass flux per unit volume of the equipment

$k_y a$  = volumetric mass transfer coefficient in the gas phase, moles/(unit time) (unit volume) (unit mole fraction)

$k_x a$  = volumetric mass transfer coefficient in the liquid phase, moles/(unit time) (unit volume) (unit mole fraction)

Mass transfer coefficients on volumetric basis have not been included in Table 3.1 since that will be mostly repetition of what has been given, except the following changes:

- (i)  $k_G$  ( $k'_G$ ),  $k_C$  ( $k'_C$ ),  $k_y$  ( $k'_y$ ),  $k_L$  ( $k'_L$ ), and  $k_x$  ( $k'_x$ ), to be replaced by  $k_G a$  ( $k'_G a$ ),  $k_C a$  ( $k'_C a$ ),  $k_y a$  ( $k'_y a$ ),  $k_L a$  ( $k'_L a$ ), and  $k_x a$  ( $k'_x a$ ) respectively;
- (ii) The expression for mass transfer coefficient to be multiplied by  $a$ , where  $a$  is the specific surface of the packing. For instance,

$$k_G = \frac{D_{AB} P}{R T z p'_{BM}} \quad \text{should be } k_G a = \frac{D_{AB} P}{R T z p'_{BM}} a$$

- (iii) The driving force should be in terms of unit volume instead of unit area.

### 3.2.4 Mass Transfer Coefficient in Laminar Flow

As discussed in Section 3.1, mass transfer coefficients are generally not required for mass transfer calculations in laminar flow where molecular diffusion takes place and the relationships developed in Chapter 2 for molecular diffusion in fluids can be used to compute mass transfer rates. However, mass transfer coefficients are required to be used in laminar flows to have a uniform method for treating both molecular and convective mass transfer particularly in case of inter-phase mass transfer where both molecular and convective mass transfers are involved. Moreover, mass transfer coefficients have to be used in laminar flow where the flow is complex and its nature is not properly understood. In such cases, the simplifying assumptions required to solve the complex differential equations often make the results less reliable.

A relatively simple case of determination of mass transfer coefficient in laminar flow (Figure 3.1) has been discussed here to illustrate the general techniques for such computation. Several such cases are available in the literature (Bennet and Myers 1974, Bird et al. 1960).

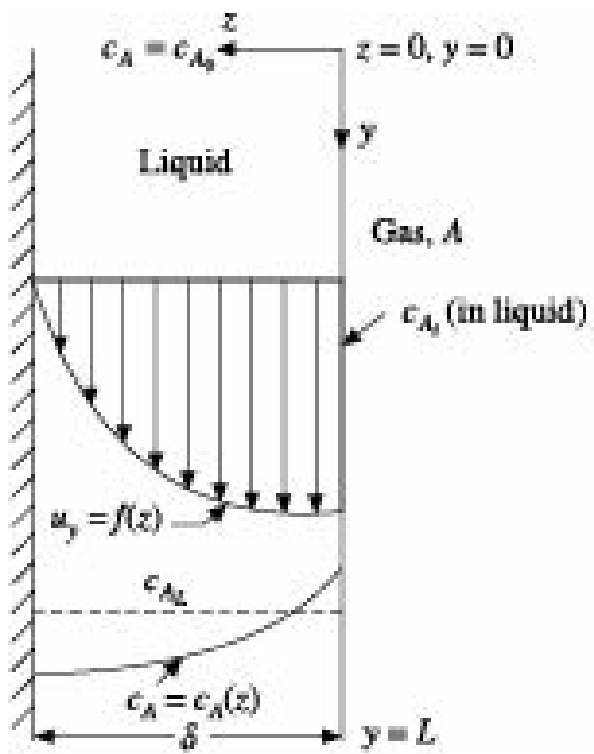


Figure 3.1 Mass transfer in laminar flow.

Let us consider a thin liquid film flowing in laminar motion down a vertical flat surface as shown in the figure and exposed to a gas *A* which dissolves in the liquid. The concentration of *A* in the liquid at the top is  $c_{A0}$ .

Let the concentration of the dissolved gas at the liquid surface be  $c_{Ai}$  in equilibrium with the partial pressure of *A* in the gas. Since  $c_{Ai} > c_{A0}$ , the gas dissolves in the liquid. The value of the mass transfer coefficient  $k_L$  has to be determined for estimating the amount of gas dissolved.

The mass transfer coefficient in such situation can be determined by simultaneous solution of the equation of continuity and the equation of motion as described below.

The equation of continuity for component *A* can be expressed as (Bird, et al, 1960)

$$u_x \frac{\partial c_A}{\partial x} + u_y \frac{\partial c_A}{\partial y} + u_z \frac{\partial c_A}{\partial z} + \frac{\partial c_A}{\partial \theta} = 0$$

$$= D_{AB} \left( \frac{\partial^2 c_A}{\partial x^2} + \frac{\partial^2 c_A}{\partial y^2} + \frac{\partial^2 c_A}{\partial z^2} + R_A \right) \quad (3.20)$$

Considering the physical situation, the following assumptions can be made:

- (i) There is no chemical reaction,  $R_A$  in Eq. (3.20) = 0,
- (ii) Conditions do not change in the  $x$ -direction as the flow has been described considering 2 directions, i.e.  $y$  and  $t$ -directions. Hence, all derivatives with respect to  $x$  of Eq. (3.20) = 0,
- (iii) Steady-state condition prevails, i.e.  $\frac{\partial c_A}{\partial t} = 0$
- (iv) Since the liquid predominantly flows in  $y$ -direction, transport of  $A$  in  $z$ -direction is insignificant and be neglected, i.e.,  $u_z$  in Eq. (3.20) = 0,
- (v) Diffusion of  $A$  in the  $y$ -direction is negligible,  $\frac{\partial^2 c_A}{\partial y^2} = 0$ ,
- (vi) Physical properties like  $D_{AB}$ ,  $t$ ,  $n$  are constant.

With the above simplifying assumptions, Eq. (3.20) becomes

$$u_y \frac{\partial c_A}{\partial y} = D_{AB} \frac{\partial^2 c_A}{\partial z^2} \quad (3.21)$$

The two dimensional equation of motion of the incompressible liquid flowing in laminar and steady-state conditions in such situation reduces to (Bird et al. 1960)

$$n \frac{d^2 u_y}{dz^2} + tg = 0 \quad (3.22)$$

The solution to Eq. (3.22) with the boundary conditions

$$u_y = 0 \text{ at } z = d, \quad \text{and} \quad \frac{du_y}{dz} = 0 \text{ at } z = 0,$$

becomes

$$u_y = \frac{pg\delta^2}{2\mu} \left[ 1 - \left( \frac{z}{\delta} \right)^2 \right] = \frac{3}{2} \bar{u}_y \left[ 1 - \left( \frac{z}{\delta} \right)^2 \right] \quad (3.23)$$

where,  $\bar{u}_y$  is the bulk average velocity.

The film thickness then becomes

$$\delta = \left( \frac{3\bar{u}_y \mu}{\rho g} \right)^{1/2} = \left( \frac{3\mu G}{\rho^2 g} \right)^{1/3} \quad (3.24)$$

where,  $G$  is the mass rate of liquid flow in the  $x$ -direction per unit of film width.

Substituting Eq. (3.23) in Eq. (3.21) gives

$$\frac{3}{2} \bar{u}_y \left[ 1 - \left( \frac{z}{\delta} \right)^2 \right] \frac{\partial c_A}{\partial y} = D_{AB} \frac{\partial^2 c_A}{\partial z^2}$$

(3.25)

The boundary conditions are:

At  $z = 0$ ,  $c_A = c_{A_i}$  for all values of  $y$

At  $z = d$ ,  $\frac{\partial c_A}{\partial z} = 0$  for all values of  $y$ , since there is no diffusion into the solid wall

At  $y = 0$ ,  $c_A = c_{A_0}$  for all values of  $z$ .

The solution to Eq. (3.25) with the above boundary conditions results in an infinite series (Johnstone and Pigford 1942). However, the local mass transfer coefficient may be obtained by combining Eq. (3.4) with Eq. (2.19) for negligible bulk flow considering that mass transfer coefficients use fluxes at the phase boundary ( $z = 0$ ).

$$N_A = -D_{AB} \left( \frac{\partial c_A}{\partial z} \right)_{z=0} = k_L (c_{A_i} - \bar{c}_{AL}) \quad (3.26)$$

and the average coefficient ( $k_L$ ) works out to be

$$\bar{k}_L = \frac{u_f \delta}{L} \ln \frac{c_{A_i} - c_{A_0}}{c_{A_i} - \bar{c}_{AL}} \quad (3.27)$$

where,  $\bar{c}_{AL}$  represents the average concentration of the component in the bulk of the liquid.

For low rates of flow or long time of contact with the liquid,  $\bar{k}_L$  becomes

$$\frac{k_L \delta}{D_{AB}} = Sh_{av} \approx 3.41 \quad (3.28)$$

and for large rates of flow or short time of contact

$$\bar{k}_L = \left( \frac{6 D_{AB} \Gamma}{\rho \pi \delta L} \right)^{0.5} \quad (3.29)$$

$$\text{or, } Sh_{av} = \left( \frac{3}{2} \frac{\delta}{L} Re Sc \right)^{0.5} \quad (3.30)$$

Experimental values of  $\bar{k}_L$  may sometimes be considerably higher than those predicted by the above equations which is due to formation of ripples or waves at the liquid-gas interface.

### 3.3 Dimensionless Groups in Mass Transfer

Dimensionless groups are very frequently used to represent mass and heat transfer coefficients and other relevant data. The main advantage of using the dimensionless groups is that if any transport process in a system is properly described in terms of carefully chosen dimensionless groups, then the expression so developed can be extended to represent other systems provided the conditions are similar and also for scaling up of the equipment. That is why a large number of mass transfer and heat transfer data are represented in terms of dimensionless groups.

Reynold's number is the oldest dimensionless group being used in the study of fluid dynamics and is now widely used in studies of momentum transfer, heat transfer and mass transfer. Heat and mass transfer in fluids largely depend on the hydrodynamic conditions of the media through which such

transfer takes place. Naturally, Reynold's number plays an important role in these transport processes.

**Reynold's number** (Re or  $N_{Re}$ ) is defined as

$$Re = \frac{\text{Inertial force}}{\text{Viscous force}} \text{ and is represented by}$$

$$Re = \frac{Lu\rho}{\mu}$$

where,  $L$  is the characteristic length, and  $u$ ,  $t$ ,  $\rho$  are the average velocity, density and viscosity of the fluid respectively in consistent units.

Let us now briefly discuss the dimensionless groups commonly used in mass transfer along with their counterparts in heat transfer.

**Schmidt number** (Sc or  $N_{Sc}$ ) is defined as

$$Sc = \frac{\text{Momentum diffusivity}}{\text{Mass (Molal) diffusivity}}$$

$$= \frac{\mu/\rho}{D_{AB}} = \frac{\mu}{\rho D_{AB}}$$

where,  $D_{AB}$  is the diffusivity of component  $A$  in  $B$ .

**Prandtl number** (Pr or  $N_{Pr}$ ) in heat transfer is analogous to Schmidt number and is defined as

$$Pr = \frac{\text{Momentum diffusivity}}{\text{Thermal diffusivity}}$$

$$= \frac{\frac{\mu}{\rho}}{\frac{k}{\rho C_p}} = \frac{C_p \mu}{k}$$

where,

$C_p$  is the heat capacity, and

$k$  is the thermal conductivity, all in consistent units.

**Sherwood number** (Sh or  $N_{Sh}$ ) is defined as

$$Sh = \frac{\text{Convective mass (molar) flux}}{\text{Diffusional mass (molar) flux through a stagnant fluid of thickness } L \text{ for the same concentration gradient}}$$

Sh =

$$= \frac{k_G(p'_{A_1} - p'_{A_2})}{(D_{AB}P)(p'_{A_1} - p'_{A_2})} = \frac{k_G RT L p'_{EM}}{D_{AB} P}$$

$$= \frac{k_C L}{D_{AB}} \frac{P'_{EM}}{P}$$

$$\frac{P'_{EM}}{P} \approx 1$$

For low rate of mass transfer from dilute mixtures,

$$\frac{k_C L}{D_{AB}}$$

Hence,  $Sh = \frac{k_C L}{D_{AB}}$

where,  $k_C$  is the gas-side mass transfer coefficient based on log-mean driving force concentration difference, and  $L$  is the characteristic length being diameter ( $d$ ) in case of flow through pipes, flow past spheres and cylinders, and distance from leading edge for flow parallel to flat plates.

**Nusselt number** (Nu or  $N_{Nu}$ ) is the heat transfer analogue of Sherwood number and is defined as

$$Nu = \frac{\text{Convective heat flux}}{\text{Heat flux due to conduction through a stagnant fluid of thickness } L \text{ for the same temperature gradient}}$$

$$= \frac{h\Delta T}{(k/L)\Delta T} = \frac{hL}{k}$$

where,  $h$  and  $k$  represent heat transfer coefficient and thermal conductivity, respectively while  $\Delta T$  represents temperature difference, all being in consistent units.

**Stanton number** in mass transfer [(St) $_M$  or  $N_{(St)M}$ ] is defined as

$$(St)_M = \frac{\text{Convective mass (molar) flux}}{\text{Mass (Molar) flux due to bulk flow}}$$

$$= \frac{k_L}{\bar{u}} = \frac{Sh}{(Re)(Sc)}$$

**Stanton number** in heat transfer [(St) $_H$  or  $N_{(St)H}$ ] is analogous to (St) $_M$  and is defined as

$$(St)_H = \frac{\text{Convective heat flux}}{\text{Heat flux due to bulk flow}}$$

$$= \frac{h}{\bar{u}} = \frac{Nu}{(Re)(Pr)}$$

**Peclet number** in mass transfer [(Pe) $_M$  or  $N_{(Pe)M}$ ] is defined as

$$(Pe)_M = \frac{\text{Mass (molar) flux due to bulk flow}}{\text{Diffusive mass (molar) flux across a layer of thickness } L}$$

$$= \frac{Li}{D_{AB}} = (\text{Re})(\text{Sc})$$

**Peclet number** in heat transfer  $[(\text{Pe})_H \text{ or } N(\text{Pe})_H]$  is analogous to  $(\text{Pe})_M$  and is defined as

$$(\text{Pe})_H =$$

$$\frac{\text{Heat flux due to bulk flow}}{\text{Heat flux due to conduction across a layer of thickness } L}$$

$$= \frac{C_p Li \rho}{k} = (\text{Re})(\text{Pr}) = \frac{Li}{\alpha}$$

where,  $a$  = thermal diffusivity.

**Fourier number** for mass transfer  $[(\text{Fo})_M \text{ or } N(\text{Fo})_M]$ , a nondimensional time parameter, is expressed as

$$(\text{Fo})_M = \frac{D_{AB} \theta}{L^2}$$

where,

$D_{AB}$  = diffusivity of component  $A$  in  $B$

$i$  = time, and

$L$  = characteristic length

**Fourier number** for heat transfer  $[(\text{Fo})_H \text{ or } N(\text{Fo})_H]$ , a nondimensional time parameter, is expressed as

$$(\text{Fo})_H = \frac{\alpha \theta}{L^2}$$

where,  $a$  = thermal diffusivity.

Grashof number,  $\text{Gr}$  is used in transfer processes involving natural convection.

**Grashof number** in mass transfer  $[(\text{Gr})_M \text{ or } N(\text{Gr})_M]$  is defined as

$$(\text{Gr})_M = \frac{gL^3 \Delta \rho}{\rho} \left( \frac{\rho}{\mu} \right)^2$$

**Grashof number** in heat transfer  $[(\text{Gr})_H \text{ or } N(\text{Gr})_H]$  is defined as

$$(\text{Gr})_H = g L^3 b \Delta T \left( \frac{\rho}{\mu} \right)^2$$

where,

$b$  = volumetric coefficient of expansion

$\Delta T$  = temperature difference

**Colburn factor** for mass transfer ( $j_D$ ) is defined as

$$j_D = (\text{St})_M (\text{Sc})^{2/3} \frac{\text{Sh}}{(\text{Re})(\text{Sc})^{1/3}}$$

$$= 0.023 \text{Re}^{-0.2}$$

**Colburn factor** for heat transfer ( $j_H$ ) which is analogous to  $j_D$  is defined as

$$j_H = (\text{St})_H (\text{Pr})^{2/3} \frac{\text{Nu}}{(\text{Re})(\text{Pr})^{1/3}}$$

$$= 0.023 \text{Re}^{-0.2}$$

**Lewis number** (Le or  $N_{Le}$ ) is used in transfer processes involving simultaneous heat and mass transfer like humidification, and is defined as

$$\text{Le} = \frac{\text{Thermal diffusivity}}{\text{Mass diffusivity}} = \frac{k}{(\rho C_p D_{AB})} = \frac{\text{Sc}}{\text{Pr}}$$

Some authors have defined Lewis number as a ratio of Prandtl and Schmidt numbers.

### 3.4 Analogy between Momentum, Heat and Mass Transfer

The following are the analogy between momentum, heat and mass transfer.

#### 3.4.1 Analogy between Momentum and Heat Transfer—Reynold's Analogy

The three processes of momentum, heat and mass transport are analogous to each other, and their analogies have been widely used in the study of mass transfer, particularly in predicting mass transfer coefficients from heat transfer data in many complex systems. Rigorous solution of the equations of mass transfer in turbulent fluids often become very complicated due to unknown fluctuations in velocities. Substantial progress in this field has been achieved by using the analogy equations, particularly heat and mass transfer analogies (Skelland 1974).

The close similarity between the processes of momentum transfer (shear stress), heat transfer and mass transfer is indicated by the fact that the basic equations representing their fluxes have the same form as shown below:

For momentum transfer (Newton's law)

$$\tau_{g_e} = \frac{\nu d(u_x) \rho}{dx} \quad (3.31)$$

For heat transfer (Fourier's law)

$$q = \frac{k}{\rho C_p} \frac{d(\rho C_p T)}{dz} = -\alpha \frac{d(\rho C_p T)}{dz} \quad (3.32)$$

For mass transfer (Fick's law)

$$J_A = -D_{AB} \frac{dc_A}{dz} \quad (3.33)$$

In these equations, the terms  $\alpha$ ,  $a$  and  $D_{AB}$  are the coefficients of momentum, heat and mass transfer

respectively, all having the dimension of  $L^2/q$ .

From Eqs. (3.31) and (3.32), it appears that the same mechanism relates momentum and heat transfer in laminar fluids

$$\text{if } n = \frac{k}{\rho C_p}$$

$$\text{or, if } \frac{C_p \mu}{k} = \text{Pr} = 1.$$

In this way it can also be shown that the same mechanism relates momentum and heat transfer in turbulent fluids if  $(C_p n/k) = 1$ . In other words, both velocity and temperature profiles will have the same shape if Prandtl number is unity. It may be noted that for most of the gases at ordinary pressures, Prandtl number is very close to unity.

Reynolds (1874), who was the pioneer in proposing the analogy equation, used this principle as the basis of his pipe friction-heat transfer analogy which may be stated as under:

$$\frac{\text{Loss of momentum to pipe wall by skin friction}}{\text{Loss of momentum if all the fluid were brought to pipe wall velocity}} = \frac{\text{Heat actually transferred to the fluid}}{\text{Heat to be transferred to the fluid to bring it to pipe wall temperature}}$$

The above relation may be expressed as

$$\frac{x g_c \pi D L}{\pi (D^2/4) L \rho \bar{u}} = \frac{h \pi D L \Delta T}{\pi (D^2/4) L \rho C_p \Delta T} \quad (3.34)$$

Substituting  $x g_c = \frac{1}{2} f \bar{u}^2$  in Eq. (3.34) and rearranging,

$$h = \frac{1}{2} f \bar{u} C_p$$

$$\text{or, } \frac{h}{C_p \bar{u} \rho} = \frac{1}{2} f \quad (3.35)$$

$f$  being the Fanning's friction factor.

Colburn (1933) later proposed the following equation which fits much better with experimental data, and is still widely used for analogy between momentum and heat transfer:

$$\frac{h}{C_p \bar{u} \rho} \left( \frac{C_p \mu}{k} \right)^{2/3} = \frac{1}{2} f = j_H \quad (3.36)$$

**EXAMPLE 3.1** (Estimation of heat transfer coefficient from Reynold's equation): Air is flowing through a smooth pipe of 25 mm internal diameter at a linear velocity of 12 m/s. Under the conditions of flow, the air has the following properties:

Density =  $0.114 \text{ kg/m}^3$ , Viscosity =  $1.85 \times 10^{-5} \text{ kg/m\$s}$ ,

Heat capacity = 1.0 kJ/kg K

Using Reynold's analogy, estimate the heat transfer coefficient of the flowing air.

**Solution:** Internal diameter of pipe = 25 mm = 0.025 m

$$Re = \frac{d_i \rho}{\mu} = \frac{(0.025) \times 0.114}{(1.85 \times 10^{-5})} = 1849$$

The friction factor for smooth pipe may be calculated from the relation

$$f = 0.046 Re^{-0.2}$$

or

$$\frac{1}{2} f = 0.023 Re^{-0.2} = 0.023 (1849)^{-0.2}$$
$$= 5.11 \times 10^{-3}$$

From Reynold's analogy, i.e. Eq. (3.35)

$$\frac{h}{C_p G} = \frac{1}{2} f$$

where,

$h$  = heat transfer coefficient, W/m<sup>2</sup>K

$G = (\dot{m}/A)$  = mass velocity of air, kg/m<sup>2</sup>s

Substituting the values in Eq. (3.35), we get

$$h = \frac{1}{2} f C_p G = (5.11 \times 10^{-3})(1.0 \times 10^3)(0.114 \times 12) = 6.99$$

Heat transfer coefficient,  $h = 6.99$  W/m<sup>2</sup>K

Alternatively,

$$f = \frac{16}{Re} = \frac{16}{1849} = 8.65 \times 10^{-3}$$

$$h = \frac{1}{2} f C_p G = \frac{1}{2} (8.65 \times 10^{-3})(1.0 \times 10^3)(0.114 \times 12)$$
$$= 5.92 \text{ W/m}^2 \text{ K}$$

### 3.4.2 Analogy between Heat and Mass Transfer

As shown in Figure 3.2, let us consider heat transfer from pipe wall to a fluid flowing in turbulent motion through the pipe. The rate of heat transfer in the laminar layer near the pipe wall is given by

$$q = -k \left( \frac{dT}{dx} \right) \quad (3.37)$$

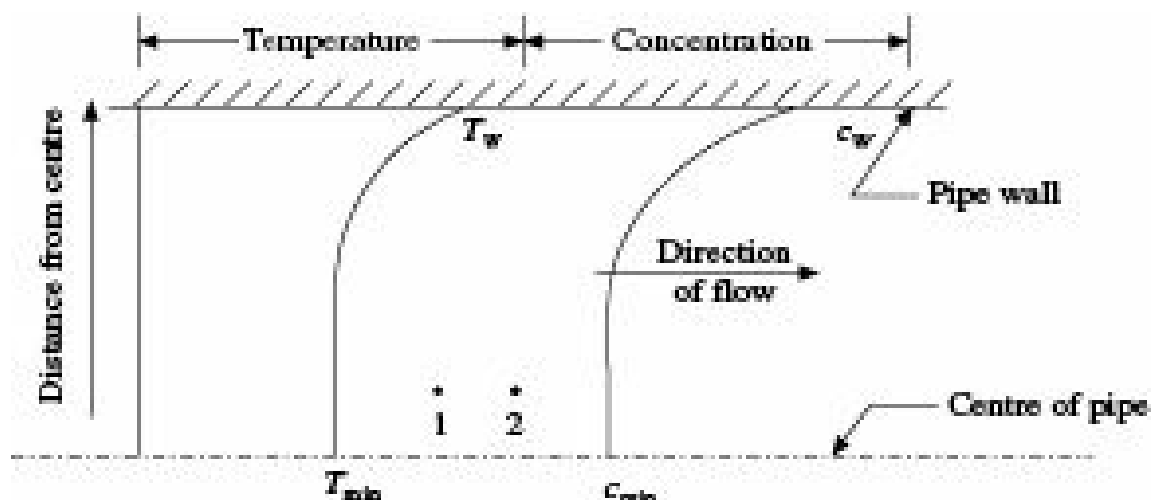


**Figure 3.2** Temperature and concentration profiles in a flowing fluid during simultaneous heat and mass transfer from pipe wall.

Heat transferred between two points 1 and 2 within the turbulent core of the fluid is

$$q = wC_pDT \quad (3.38)$$

where,

$w$  = net interchange of mass per unit time per unit area between points 1 and 2,

$DT$  = the temperature difference between the points 1 and 2.

Let us further assume that mass is being transferred from pipe wall to the fluid due to concentration gradient existing there. Then mass transferred in the laminar zone is given by

$$N_A = -D_{AB} \left( \frac{dc_A}{dz} \right) \quad (3.39)$$

and mass transferred at the turbulent core near the centre of the pipe is given by

$$N_A =$$

$$wDc_A$$

$$M_{av}c$$

(3.40)

Eliminating  $dz$  from Eqs. (3.37) and (3.39), we get

$$\frac{q}{k \Delta T} = \frac{N_A}{D_{AB} dc_A} \quad (3.41)$$

and eliminating  $w$  from Eqs. (3.38) and (3.40), we get

$$\frac{q}{(C_p \Delta T)} = \frac{N_A M_{av} c}{\Delta c_A} \quad (3.42)$$

A comparison of Eqs. (3.41) and (3.42) indicates that the same mechanism holds good for heat and mass transfer both in laminar and turbulent flow provided

$$\frac{1}{M_{av} c D_{AB}} = \frac{C_p}{k} \quad (3.43)$$

Since  $M_{av}c = t$ , it follows that

$$\frac{k}{D_{AB}\rho C_p} = \text{Lewis Number, Le} = 1 \quad (3.44)$$

In other words, both temperature and concentration profiles will have the same shape if  $[k/(D_{AB}tC_p)] = \text{Le} = 1$ . Equation (3.44) is the basis of analogy between heat and mass transfer. In line with Reynold's analogy, we may therefore write

$$\begin{aligned} & \text{Heat actually transferred to the fluid} \\ & \text{Heat to be transferred to bring all the fluid to pipe wall temperature} \\ & \qquad \qquad \qquad = \\ & \qquad \qquad \qquad \text{Mass actually transferred to the fluid} \\ & \text{Mass to be transferred to bring all the fluid in equilibrium with pipe wall concentration} \end{aligned}$$

The above relation may be expressed as

$$\frac{h(\pi DL)dt}{\pi(D^2/4)L\rho C_p\Delta T} = \frac{k_C(\pi DL)dc}{\pi(D^2/4)L\Delta c} \quad (3.45)$$

$$\text{whence, } k_C = \frac{h}{\rho C_p} = \frac{1}{2} f \bar{u} \quad (3.46)$$

$$\text{or } \frac{k_C}{\bar{u}} = \frac{h}{\rho C_p \bar{u}} = \frac{1}{2} f \quad (3.47)$$

where,  $k_C$  is the mass transfer coefficient in moles/(unit time) (unit area) (moles/unit volume). Equations (3.36) and (3.47) can also be expressed in terms of dimensionless groups as follows:

$$\text{From Eq. (3.36)} \quad (\text{St})_H = \frac{\text{Nu}}{\text{Re Pr}} = \frac{1}{2} f \quad (3.48)$$

$$\text{From Eq. (3.47): } (\text{St})_M = \frac{\text{Sh}}{\text{Re Sc}} = \frac{1}{2} f \quad (3.49)$$

where,

$(\text{St})_H$  = Stanton number for heat transfer (dimensionless),

$(\text{St})_M$  = Stanton number for mass transfer (dimensionless).

For flow of a fluid through a pipe, Prandtl (1910, 1928) proposed the following analogy equations:  
For momentum-heat transfer analogy:

$$(\text{St})_H = \frac{\text{Nu}}{\text{Re Pr}} = \frac{f/2}{1 + 5(\text{Pr} - 1)\sqrt{(f/2)}} \quad (3.50)$$

and for momentum-mass transfer analogy:

$$(\text{St})_M = \frac{\text{Sh}}{\text{Re Sc}} = \frac{f/2}{1 + 5(\text{Sc} - 1)\sqrt{(f/2)}} \quad (3.51)$$

It may be noted that for  $\text{Pr} = 1$ , Eq. (3.50) reduces to Reynolds analogy. Likewise for  $\text{Sc} = 1$ , Eq. (3.51) reduces to Reynolds analogy.

Colburn (1933), and Chilton and Colburn (1934) worked with the then available empirical correlations for momentum, heat and mass transfer and proposed analogies between these three processes in terms of 'j' factors.

According to them,

$$j_H = \frac{\text{Nu}}{\text{Re} \text{Pr}^{1/3}} = (\text{St})_H \text{Pr}^{2/3} = 0.023 \text{Re}^{-0.2} \quad (3.52)$$

and  $j_D = \frac{\text{Sh}}{\text{Re} \text{Sc}^{1/3}} = (\text{St})_M \text{Sc}^{2/3} = 0.023 \text{Re}^{-0.2} \quad (3.53)$

Mass transfer coefficients may be calculated from heat transfer data simply by equating  $j_H$  and  $j_D$ .

**EXAMPLE 3.2** (Estimation of mass transfer coefficient by equating  $j_D$  and  $j_H$ ): It is desired to estimate the value of the mass transfer coefficient  $k_G$  for the absorption of ammonia by the wet surface of a streamlined shape placed in a turbulent air-ammonia stream. No data on mass transfer to such a section is available, but experiments under similar conditions indicate the heat transfer coefficient,  $h$  to be  $65 \text{ W/m}^2 \text{ K}$ .

Evaluate  $k_G$  by using an appropriate analogy equation.

The air-NH<sub>3</sub> mixture contains only a small amount of ammonia and its properties under the operating conditions are:

Density =  $1.14 \text{ kg/m}^3$ , Viscosity =  $1.85 \times 10^{-5} \text{ kg/m s}$ ,

Thermal conductivity =  $0.0273 \text{ W/m K}$ , Heat capacity =  $1002 \text{ J/kg K}$

The diffusivity of NH<sub>3</sub> in air may be taken as  $2.4 \times 10^{-5} \text{ m}^2/\text{s}$

The atmospheric pressure is  $101.3 \text{ kN/m}^2$ .

**Solution:** Assuming  $j_D = j_H$

From Eqs. (3.52) and (3.53),

$$(\text{St})_M \text{Sc}^{2/3} = (\text{St})_H \text{Pr}^{2/3}$$

$$\frac{k_G p'_M}{G_M} (\text{Sc})^{2/3} = \frac{h}{C_p \bar{\rho} \rho} (\text{Pr})^{2/3}$$

$$\frac{h}{C_p \bar{\rho} \rho} \frac{G_M}{p'_M} \left( \frac{\text{Pr}}{\text{Sc}} \right)^{2/3}$$

whence,  $k_G =$

$$\frac{G_M}{\bar{\rho} \rho} = \frac{1}{M}, \quad k_G = \frac{h}{C_p M p'_M} \left( \frac{\text{Pr}}{\text{Sc}} \right)^{2/3} \quad (1)$$

Since,

From the given data, we obtain

$$\text{Pr} = \frac{C_p \mu}{k} = \frac{(1002)(1.85 \times 10^{-5})}{(0.0273)} = 0.68$$

$$\text{Sc} = \frac{\mu}{\rho D_{AB}} = \frac{(1.85 \times 10^{-5})}{(1.14)(2.4 \times 10^{-5})} = 0.676$$

The concentration of NH<sub>3</sub> in the air-ammonia stream being very low,

$$p'BM = P = 101.3 \text{ kN/m}^2 \text{ (}P\text{ being the atmospheric pressure)}$$

Substituting the values in Eq. (i), we get

$$k_G = \frac{65}{(1002)(29)(101.3)} \left( \frac{0.68}{0.676} \right)^{2/3} = 2.217 \# 10^{-5}$$

$$\text{Mass transfer coefficient, } k_G = 2.217 \# 10^{-5} \text{ kg/(s)(m}^2\text{)(kN/m}^2\text{)}$$

**EXAMPLE 3.3** (Estimation of mass transfer coefficient for absorption of a gas in a counter-current wetted wall column and comparison of the same with the value obtained from Chilton-Colburn analogy for heat and mass transfer): An air-ammonia mixture containing 5% NH<sub>3</sub> by volume is being scrubbed counter-currently with 2N sulphuric acid in a wetted wall column of 15 mm id and 700 mm in length. The inlet gas rate is 0.20 kmol/hr. The operating temperature and pressure are 20°C and 101.3 kN/m<sup>2</sup>, respectively. Under these conditions, 90% of the incoming NH<sub>3</sub> is absorbed. The change in acid concentration may be neglected.

- (a) Calculate the value of the mass transfer coefficient,  $k_G$ ,
- (b) If the value of the heat transfer coefficient,  $h$  in a similar set-up with identical operating conditions is found to be 75.2 kcal/(hr)(m<sup>2</sup>)(C), estimate  $k_G$  from Chilton-Colburn analogy.

Under the operating conditions, the values of Pr and  $C_p$  for air are 0.70 and 0.238 kcal/(kg)(C), respectively. For air-NH<sub>3</sub>, Sc = 0.67. The diffusivity of NH<sub>3</sub> in air is  $2.20 \# 10^{-5} \text{ m}^2/\text{s}$ .

**Solution:**

$$(a) \quad y_1 = 0.05, Y_1 = \frac{0.05}{1 - 0.05} = 0.0526 \text{ mol NH}_3/\text{mol air.}$$

$$Y_2 = (0.0526 \# 0.1) = 0.00526 \text{ mol NH}_3/\text{mol air,}$$

$$y_2 = \frac{0.00526}{1.00526} = 0.005232$$

$$\text{Air rate} = 0.20 \frac{3600}{3600} = 5.278 \# 10^{-5} \text{ kmol/s}$$

$$\text{NH}_3 \text{ absorbed} = 5.278 \# 10^{-5} (0.0526 - 0.00526) = 2.5 \# 10^{-6} \text{ kmol/s}$$

Since equilibrium partial pressure of NH<sub>3</sub> over sulphuric acid solution is zero,

$$Dp'_1 = p'_A1 = (101.3 \# 0.05) = 5.065 \text{ kN/m}^2$$

and

$$Dp'_2 = p'_A2 = (101.3 \# 0.005232) = 0.530 \text{ kN/m}^2$$

$$Dp'_{lm} = \frac{\frac{(5.065 - 0.530)}{\ln\left(\frac{5.065}{0.530}\right)}}{= 2.009 \text{ kN/m}^2}$$

$$\text{Area available} = (r \# 0.015 \# 0.70) = 0.033 \text{ m}^2$$

$$\text{Hence, } k_G = \frac{2.5 \times 10^{-6}}{(0.033)(2.009)} = 3.77 \# 10^{-5} \text{ kmol/(s)(m}^2\text{)(kN/m}^2\text{)}$$

(b) From Eqs. (3.52) and (3.53), we obtain

$$(St)_M Sc^{2/3} = (St)_H Pr^{2/3}$$

$$\frac{k_G p'_{BM}}{G_M} (Sc)^{2/3} = \frac{h}{C_p \bar{\rho}} Pr^{2/3}$$

$$\text{whence, } k_G = \frac{h}{C_p M p'_{BM}} \left( \frac{Pr}{Sc} \right)^{2/3} \quad (\text{i})$$

$$p'_A1 = 5.065 \text{ kN/m}^2, \quad p'_B1 = (101.3 - 5.065) = 96.235 \text{ kN/m}^2$$

$$p'_A2 = 0.530 \text{ kN/m}^2, \quad p'_B2 = (101.3 - 0.530) = 100.77 \text{ kN/m}^2$$

$$p'_{BM} = \frac{\frac{(100.77 - 96.235)}{\ln\left(\frac{100.77}{96.235}\right)}}{= 98.49 \text{ kN/m}^2}$$

$$M_1 = 17 \# 0.05 + 29 \# 0.95 = 28.40, M_2 = 17 \# 0.005232 + 29 \# 0.9948 = 28.94$$

$$\frac{(28.40 + 28.94)}{2}$$

Molecular weight of the mixture,  $M = \frac{(28.40 + 28.94)}{2} = 28.67$

Substituting the values in Eq. (i), we get

$$k_G = \frac{(75.2/3600)}{(0.238)(28.67)(98.49)} \left( \frac{0.70}{0.67} \right)^{2/3}$$

$$= 3.20 \# 10^{-5} \text{ kmol/(s)(m}^2\text{)(kN/m}^2\text{)}$$

### 3.5 Mass Transfer Coefficients for Simple Geometrical Shapes

Mass transfer coefficients near boundary wall depend on diffusivity ( $D_{AB}$ ) of the system as well as density ( $\rho$ ), viscosity ( $\eta$ ) and velocity ( $u$ ) of the fluid. In addition, the shape of the interface also plays

a role in the transfer. For any given shape, dimensional analysis leads to

$$\frac{k_C d}{D_{AB}} = \Psi\left(\frac{dG}{\mu}, \frac{\mu}{\rho D_{AB}}\right) \quad (3.54)$$

or,

$$Sh = \Psi(Re, Sc) \quad (3.55)$$

The constant of proportionality and indices of the dimensionless groups can be determined by nonlinear regression provided adequate data for different systems under identical conditions are available.

In some boundary layer flows, mass transfer coefficient varies as two-third power of diffusivity and may be represented by  $j_D$  factor analogous to  $j_H$  factor in heat transfer

$$j_D = \frac{k_C}{\bar{u}} \left( \frac{\mu}{\rho D_{AB}} \right)^{2/3} = \frac{k_C}{\bar{u}} Sc^{2/3} \quad (3.56)$$

Most of the data on mass transfer coefficient in literature are presented in terms of either  $Sh$  or  $j_D$ .

Large numbers of correlations, mostly empirical or at best semiempirical, are available for estimation of mass transfer coefficients in fluids or between fluids and solids. Some typical cases have been presented here.

### 3.5.1 Mass Transfer in Flow Past Flat Plates

Most studies on mass transfer to and from solid surfaces have been made in gases by measuring the rates of evaporation of liquids or sublimation of solids.

For low mass transfer rates in boundary layer flow parallel to flat plates with mass transfer beginning at the leading edge and Reynold's number based on the characteristic length,  $Re_L$  less than 50000, the average mass transfer coefficient may be represented by

$$j_D = 0.664 Re_L^{-1/2} \quad (3.57)$$

where,  $Re_L$  = Reynold's number based on the length of the plate.

Combining Eqs. (3.56) and (3.57) and rearranging, we get

$$\frac{k_C L}{D_{AB}} = 0.664 (Re_L)^{1/2} (Sc)^{1/3} \quad (3.58)$$

In case of mass transfer to or from a flat plate and a fluid flowing in turbulent motion parallel to the plate, Rohsenow and Choi (1961) suggested the following equation for the mass transfer coefficient:

$$\frac{K_{Cw} L}{D_{AB}} = 0.037 Sc^{1/3} (Re_L)^{0.8} - 15,500 \quad (3.59)$$

By plotting the data obtained from the experiments carried out by several authors, Sherwood and Pigford (1952) had shown that for  $8,000 < Re_L < 300,000$

$$j_D = (k_C)_{av} \frac{P'_{BM}}{\bar{u} P} Sc^{2/3} = j_H = \frac{f}{2} = 0.037 Re_L^{-0.2} \quad (3.60)$$

**EXAMPLE 3.4** (Estimation of mass transfer coefficient for transfer to a gas flowing past a flat plate): A thin sheet of naphthalene, 10 cm square is placed parallel to an air stream flowing at a uniform velocity of 5 m/s. The air is at 0°C and 101.3 kN/m<sup>2</sup> pressure. Assuming that both the large surfaces are flat and exposed to the air at all times and neglecting evaporation from the edges, calculate the rate of sublimation of naphthalene.

The molecular weight of naphthalene is 128.16. Under the operating conditions, vapour pressure of naphthalene is  $7.86 \times 10^{-4}$  kN/m<sup>2</sup>, diffusivity of air-naphthalene is  $5.1 \times 10^{-6}$  m<sup>2</sup>/s. Density and viscosity of air are 1.29 kg/m<sup>3</sup> and  $1.6 \times 10^{-5}$  kg/m s, respectively.

**Solution:** The mass transfer coefficient for transfer from a flat plate may be represented by Eq. (3.58)

$$\frac{k_C L}{D_{AB}} = 0.664 (\text{Re}_L)^{1/2} (\text{Sc})^{1/3}$$

where  $L$  is the length of the sheet and  $\text{Re}_L$  is the Reynold's number based on the characteristic length of the sheet.

$$\text{Re}_L = \frac{(0.1)(5)(1.29)}{(1.6 \times 10^{-5})} = 40312$$

$$\text{Sc} = \frac{(1.6 \times 10^{-5})}{(1.29)(5.1 \times 10^{-6})} = 2.432$$

Substituting the values in Eq. (3.58), we get

$$\frac{k_C(0.10)}{5.1 \times 10^{-6}} = (0.664)(40312)^{1/2}(2.432)^{1/3}$$

whence,

$$k_C = \frac{5.1 \times 10^{-6}}{0.10} \# 0.664 \# 200.78 \# 1.345 \\ = 9.145 \times 10^{-3} \text{ m/s.}$$

The concentration of naphthalene in vapour phase (when vapour pressure,  $p_A$  becomes equal to partial pressure,  $p'_A$ ) is

$$c_A = \frac{p'_A}{RT} = \frac{7.86 \times 10^{-4}}{(8.314)(273)} = 3.46 \times 10^{-7} \text{ kmol/m}^3$$

Since partial pressure of naphthalene in bulk air is zero,

$$Dc_A = c_A = 3.46 \times 10^{-7} \text{ kmol/m}^3$$

$$\text{Area available} = (0.1)^2 \# 2 = 0.02 \text{ m}^2$$

$$\text{Naphthalene sublimation rate} = 9.145 \times 10^{-3} \# 0.02 \# 3.46 \times 10^{-7}$$

$$= 0.633 \times 10^{-10} \text{ kmol/s}$$

$$= 0.633 \# 10^{-10} \# 128.16 = 8.11 \# 10^{-9} \text{ kg/s}$$

### 3.5.2 Mass Transfer in Fluids Flowing Through Pipes

Correlations for mass transfer inside pipes are similar in nature to those in heat transfer. For laminar flow, Sherwood number shows the same trend as Nusselt number with a limiting value of 3.66 for very long pipes. For short pipes, Sherwood number varies as one-third power of flow rate. In view of inadequate data however, it has not been possible to develop working equations for mass transfer coefficient in laminar flow through pipes.

Several authors have studied gas side coefficients for mass transfer between liquids and gases in wetted wall columns. Most of their data agree approximately with the following equation suggested by Gilliland and Sherwood (1934) on the basis of 400 tests on evaporation of water and eight other organic liquids into air flowing through a wetted wall column of 2.54 cm internal diameter and 117 cm long

$$\frac{k_C d}{D_{AB}} \frac{P_{BM}}{P} = 0.023 Re^{0.83} Sc^{0.44} \quad (3.61)$$

where,

$k_C$  = gas-side mass transfer coefficient based on log-mean driving forces at two ends of the column, cm/s

$Re$  = air stream Reynold's number based on velocity of air relative to the pipe wall.

Both co-current and counter-current flows were used at pressures ranging from 0.1 to 3 atm.

Equation (3.61) is similar to the corresponding equation for heat transfer coefficient except that the term  $(n/n_w)^{0.14}$  has been excluded since its value in mass transfer usually approaches unity.

For engineering calculations, the following equation of Johnstone and Pigford (1942) may be used:

$$j_D = 0.0328 (Re')^{-0.23} \quad (3.62)$$

where  $Re'$  lies between 3000 and 40000,  $Re'$  being Reynolds number based on gas velocity relative to the liquid surface and  $Sc$  lies between 0.5 and 3.0.

**EXAMPLE 3.5** (Estimation of mass transfer coefficient from Gilliland's equation): Estimate the value of the mass transfer coefficient  $k_G$  for the absorption of ammonia by an acid from a turbulent air-NH<sub>3</sub> stream moving at 3 m/s through a counter-current wetted wall tube of 25 mm id. The temperature and pressure are 38°C and 101.3 kN/m<sup>2</sup>, respectively. The inlet gas contains 10% NH<sub>3</sub> by volume and the exit gas contains 1% NH<sub>3</sub> by volume.

Under the operating conditions the gas has the following properties:

Density = 1.14 kg/m<sup>3</sup>, Viscosity = 1.85 # 10<sup>-5</sup> kg/m•s,

Diffusivity of NH<sub>3</sub> in air = 2.4 # 10<sup>-5</sup> m<sup>2</sup>/s.

**Solution:** This being a case of mass transfer between a gas and a liquid film in a wetted wall tower, Eq. (3.61) is applicable subject to  $Re$  and  $Sc$  being within the recommended ranges.

$$\frac{k_C d}{D_{AB}} \frac{P'}{P} = 0.023 \text{Re}^{0.83} \text{Sc}^{0.44}$$

$T = 38^\circ\text{C} = 311 \text{ K}$ ,  $P = 101.3 \text{ kN/m}^2$ ,  $\bar{u} = 3 \text{ m/s}$ ,  $d = 0.025 \text{ m}$

$$p'_{A1} = 101.3 \# 0.1 = 10.13 \text{ kN/m}^2, p'_{B1} = (101.3 - 10.13) = 91.17 \text{ kN/m}^2$$

$$p'_{A2} = 101.3 \# 0.01 = 1.013 \text{ kN/m}^2, p'_{B2} = (101.3 - 1.013) = 100.287 \text{ kN/m}^2$$

$$p'_{BM} = \frac{(100.287 - 91.17)}{\ln \left( \frac{100.287}{91.17} \right)} = 95.66 \text{ kN/m}^2$$

$$\text{Re} = \frac{(0.025)(3)(1.14)}{1.85 \times 10^{-5}} = 4621.6$$

$$\text{Sc} = \frac{1.85 \times 10^{-5}}{(1.14)(2.4 \times 10^{-5})} = 0.676$$

It is found that both Re and Sc are within the recommended ranges.  
Substituting the values in Eq. (3.61), we get

$$\frac{k_C(0.025)}{2.4 \times 10^{-5}} \frac{95.66}{101.3} = 0.023 (4621.6)^{0.83} (0.676)^{0.44}$$

whence,

$$k_C = 0.02167$$

$$k_G = \frac{k_C}{RT} = \frac{0.02167}{(8.314)(311)} = 8.38 \# 10^{-6}$$

Mass transfer coefficient,  $k_G = 8.38 \# 10^{-6} \text{ kmol/(s)(m}^2\text{)(kN/m}^2\text{)}$ .

### 3.5.3 Mass Transfer in Single Phase Flow Through Packed Bed

Data on rate of mass transfer between a gas or liquid and beds of solid particles are important in design of equipment for many major operations such as absorption, leaching, ion exchange as well as heterogeneous catalytic reactions. Numerous studies have therefore been made for determination of mass transfer coefficient in packed beds.

As in other systems, Chilton–Colburn analogy holds very well in single-phase flow through packed beds, and  $j_D$  and  $j_H$  have been found to be essentially equal for the same bed geometry and flux conditions. In many cases, mass transfer coefficient can be estimated from heat transfer data.

The following equation suggested by Sherwood et al. (1975) may be used for engineering calculations both in case of gases and liquids for  $10 < \text{Re} < 2500$ :

$$j_D = 1.17 \left( \frac{d_p \bar{u} P}{\mu} \right)^{-0.415} \quad (3.63)$$

where,

$d_p$  = particle diameter, and

$\bar{u}$  = superficial velocity of the fluid.

### 3.5.4 Mass Transfer Coefficient for Flow Past a Solid Sphere

The flow field around a fixed sphere is very complicated and theoretical calculations are possible only at very low velocities. At higher velocities, separation of boundary layer may take place and wakes may be formed behind the sphere.

In case of forced convection mass transfer to or from an isolated sphere, Harriott (1962) proposed the following equation for  $Re > 1000$  by assuming the terminal velocity as the fluid velocity relative to the particles (slip velocity):

$$Sh = 2.0 + 0.6 Re^{1/2} Sc^{1/3} \quad (3.64)$$

For mass transfer in turbulent stream at high Reynold's number the effect of flow rate increases.

For laminar creeping flow (low  $Re$  and high  $Pe$  but below 10,000) around the sphere, Brian and Halis (1969) suggested

$$Sh = (4.0 + 1.21 Pe^{2/3})^{1/2} \quad (3.65)$$

and for  $Pe > 10000$ ,

$$Sh = 1.01 Pe^{1/3} \quad (3.66)$$

where,  $Pe = \text{Peclet number} = Re \cdot Sc = d_{\bar{u}}/D_{AB}$

In a situation where diffusion occurs in creeping flow around a spherical gas bubble and around a solid sphere, the following equation holds good:

$$Sh = 0.6415 Pe^{1/2} \quad (3.67)$$

For creeping flow around a solid sphere with a slightly soluble coating that dissolves into the approaching fluid,

$$Sh = 0.991 Pe^{1/3} \quad (3.68)$$

Equations (3.76) and (3.68) are not valid in a situation when  $Re = 0$ .

When there is no flow past the solid sphere or the spherical bubble, mass transfer from single drop to stagnant air follows the law for molecular diffusion. Thus, for radial diffusion into a large expanse of stationary medium the partial pressure falls off to zero over an infinite distance. Equation (2.36) shows the expression for mass transfer by steady-state diffusion from the surface of the sphere. Since  $r_o \gg r_s$ , Eq. (2.36) may be written as

$$4\pi r^2 N_{Ar} = \frac{4\pi D_{AB} P r_s}{RT} \ln \frac{(P - p'_A)}{(P - p'_B)} \quad (3.69)$$

The mass transfer rate in terms of mass transfer coefficient,  $k_G$  in such situation can be expressed as

$$4\pi r^2 N_{Ar} = k_G r d_s^2 (p'_A - p'_B), \text{ where } d_s = 2r_s \quad (3.70)$$

Combining Eqs. (3.69) and (3.70) shows the relationship for Sherwood number as

$$Sh = \frac{\frac{k_C P_f' RT d_s}{D_{AB}^P}}{= 2} \quad (3.71)$$

Hence, a satisfactory description of the mass transfer in a situation when  $Re = 0$  can be obtained by using the simple superpositions

$$Sh = 2 + 0.6415 Pe^{1/2} \text{ and } Sh = 2 + 0.991 Pe^{1/3} \quad (3.72)$$

in lieu of Eqs. (3.67) and (3.68), respectively.

### 3.5.5 Mass Transfer in Flow Normal to a Single Cylinder

The following approximate equation may be used for mass transfer coefficient for flow of fluid perpendicular to a cylinder with Reynold's number lying between 10 and 10000:

$$Sh = 0.61 Re^{1/2} Sc^{1/3} \quad (3.73)$$

### 3.5.6 Mass Transfer in the Neighbourhood of a Rotating Disk

For a disk coated with a slightly soluble material and rotating with an angular velocity in a large region of liquid, the mass transfer coefficient can be obtained using the following expression:

$$Sh = 0.62 Re^{1/2} Sc^{1/3} \quad (3.74)$$

where the Reynold's number is to be calculated using the characteristic velocity = (diameter of the disk) # (angular velocity).

### 3.5.7 Mass Transfer to Drops and Bubbles

When bubbles of gas are dispersed in a liquid in an agitated vessel or a sieve-tray column, mass transfer to or from the bubbles takes place at a rate governed by the concentration driving force, the interfacial area for transfer, and the mass transfer coefficient in the liquid phase. There may be some resistance to transfer in the gas phase inside the bubble but this resistance is usually negligible compared with that in the liquid.

The rate of mass transfer between a liquid and a gas as in spray drying can be much enhanced if the liquid is dispersed and suspended in the gas as small drops since that provides large surface of contact between the two phases. Similarly, in liquid-liquid extraction, the rate of mass transfer will be much higher if one liquid is dispersed and suspended in the other liquid as small drops.

Drops of liquid falling through a gas tend to become spherical due to the action of surface tension, and mass transfer coefficients to such drops are often very close to those for solid spheres. Most of the data for mass transfer to and from drops may be approximately represented by

$$Sh = 1.13 Re^{1/2} Sc^{1/2} \quad (3.75)$$

Bubbles behave very much like drops, but their buoyancy and velocity of rise are much higher. Mass transfer within bubbles is relatively rapid since bubbles are filled with gas and molecular diffusion in gases is high.

Although the equation

$$\frac{k_C d_p}{D_{AB}^P} = 1.01 Pe^{1/3} \quad (3.76)$$

gives a fair estimate of  $k_C$ , the following empirical modification by Johnson et al. (1969) gives a more reliable prediction:

$$\frac{k_C d_p}{D_{AB}} = 1.13 \text{ Pe}^{1/2} \left( \frac{d_p}{0.45 + 0.2 d_p} \right) \quad (3.77)$$

The suggested equations are remarkable since these show that the liquid phase mass transfer coefficient is independent of impeller speed, impeller diameter, and power input in an agitated vessel and of gas velocity in a sieve-tray column. In a given system therefore,  $k_C$  is approximately constant; it is usually about five times greater with large bubbles than with small bubbles.

It is an accepted fact that the absorption of a gas by a liquid drop takes place during the period of formation and subsequent movement of the drop through the column. An excellent review (Popovich et al. 1964) is available on theoretical studies on mass transfer during drop formation. The rate of mass transfer in an internally circulating drop forming in a continuous gaseous medium, depends on the residence time of a liquid element on the drop surface with the relation that the rate is inversely proportional to the square root of the contact time, i.e. the residence time of a surface element (Guha et al. 1987). The square root dependence of the mass transfer rate on the time of exposure is in complete agreement with the model as conceived using the modified penetration theories.

## Nomenclature

$c$  : concentration, mass or mol/L<sup>3</sup>

$C_p$  : heat capacity at constant pressure, FL/MT

$D_{AB}$  : molecular diffusivity of component  $A$  in  $B$ , L<sup>2</sup>/□

$f$  : Fanning's friction factor, dimensionless

$G$  : mass velocity, M/L<sup>2</sup>□

$\text{Gr}$  : Grashof number, dimensionless

$h$  : heat transfer coefficient, FL/L<sup>2</sup>□T

$j$  : Colburn factor, dimensionless

$k_C, k_G$ ,

$k_x, k_y$  etc. : individual mass transfer coefficient, mol/(L<sup>2</sup>)(□) (driving force difference)

$k_x a, k_y a$  : mass transfer coefficient on volumetric basis, mol/(L<sup>3</sup>)(□)(mol fraction difference)

$\text{Le}$  : Lewis number, dimensionless

$M$  : molecular weight, M/mol

$N$  : solute flux, M/L<sup>2</sup>□

$P$  : total pressure, F/L<sup>2</sup>

$p$  : vapour pressure, F/L<sup>2</sup>

$p'$  : partial pressure, F/L<sup>2</sup>

$\text{Pe}$  : Peclet number, dimensionless

Pr : Prandtl number, dimensionless  
R : universal gas constant, FL/(mol)(T)  
Re : Reynolds number, dimensionless  
Sc : Schmidt number, dimensionless  
Sh : Sherwood number, dimensionless  
St : Stanton number, dimensionless  
 $T$  : temperature, °C or K  
 $u$  : local velocity, L/ $\square$   
 $\bar{u}$  : average velocity, L/ $\square$   
 $u'_x$  : instantaneous deviating velocity, L/ $\square$

### *Greek Letters*

a : thermal diffusivity, L<sup>2</sup>/ $\square$   
G : mass rate of flow per unit width, M/L $\square$   
d : thickness of a layer, L  
i : time,  $\square$   
n : viscosity, M/L $\square$   
y : kinematic viscosity, L<sup>2</sup>/ $\square$   
t : density, M/L<sup>3</sup>  
x : shear stress, F/L<sup>2</sup>

### *Subscripts*

A : component A  
B : component B  
D : for mass transfer  
H : for heat transfer  
M : for mass transfer  
 $i$  : interface, instantaneous when used with velocity  
lm : logarithmic mean  
Turb : turbulence  
 $x, y, z$  : represent directions respectively

## **Numerical Problems**

**3.1 Determination of Heat Transfer Coefficient Using Analogy Equation:** A gas flowing at a mass velocity of 10,000 kg/(hr)(m<sup>2</sup>) has a Reynold's number of 20,000 in a smooth pipe. If the specific heat, viscosity and thermal conductivity of the gas are 1.675 kJ/kg K, 1.0 # 10<sup>-5</sup> kg/ms, and 0.0249 W/mK respectively, determine the heat transfer coefficient of the flowing gas. [Ans: 19.19 W/m<sup>2</sup>K]

**3.2 Determination of Mass Transfer Coefficient for Absorption of Ammonia in Sulphuric Acid:** An air-ammonia stream containing 4% NH<sub>3</sub> by volume is scrubbed with 2N sulphuric acid in a counter-current wetted wall column of 15 mm id and 750 mm long. The inlet gas rate is 0.20 kmol/hr. The operation is carried out at 20°C and 1 atm pressure. Under these conditions, 90% of the incoming NH<sub>3</sub> is absorbed. The change in acid concentration is negligible.

- (i) Calculate the value of the mass transfer coefficient  $k_G$  in kmol/(hr)(m<sup>2</sup>)(atm).
- (ii) If the heat transfer coefficient in a similar set-up with same gas and liquid flow rates is found to be 68.5 kcal/hr m<sup>2</sup> °C, estimate  $k_G$  from Chilton-Colburn analogy.

*Given:*

For air:  $C_p$  n/k is 0.74, the value of  $C_p$  being 0.24.

For air-NH<sub>3</sub>: n/(rD<sub>AB</sub>) = 0.61, value of  $p'BM$  may be taken as unity.

[Ans: (i) 12.87 kmol/hr m<sup>2</sup> atm, (ii) 10.83 kmol/hr m<sup>2</sup> atm]

**3.3 Rate of Evaporation of Ethanol from a Surface using that of Water from the Surface:** The rate of evaporation of water from a surface maintained at a temperature of 60°C is 3.02 g/s\$cm<sup>2</sup>. What will be the rate of evaporation of ethanol from the surface at 25°C if the effective film thicknesses are the same in both the cases?

*Given:*

Vapour pressure of water at 60°C = 149 mm Hg

Diffusivity of water in air at 60°C = 0.261 cm<sup>2</sup>/s

Vapour pressure of ethanol at 25°C = 93 mm Hg

Diffusivity of ethanol in air at 25°C = 0.127 cm<sup>2</sup>/s

Atmospheric pressure = 760 mm Hg

[Ans: 0.983 g/cm<sup>2</sup>\$s]

**3.4 Gas Film Mass Transfer Coefficient using Gilliland and Sherwood Equation:** The following data were obtained during an experiment on absorption of sulphur dioxide from a dilute air-SO<sub>2</sub> mixture in a wetted wall tower:

Diameter of the tower = 40 mm, Gas velocity = 1.8 m/s,

Gas temperature = 20°C, Gas viscosity = 0.0178 c.p.,

Gas density = 0.0012 g/cm<sup>3</sup>, Diffusivity of SO<sub>2</sub> in air = 0.12 cm<sup>2</sup>/s

Using Gilliland and Sherwood's equation, estimate the gas film mass transfer coefficient for the above experiment.

The mean partial pressure of air may be assumed to be equal to the total pressure.

[Ans: 0.144 cm/s [gmol/cm<sup>2</sup>\$s (gmol/cm<sup>3</sup>)]

**3.5 Enhancement of Mass Transfer Rate:** The mass flux from a 5 cm diameter naphthalene ball placed in stagnant air at 40°C and atmospheric pressure, is 1.47 # 10<sup>-3</sup> mol/m<sup>2</sup>\$s. Assume the vapour pressure of naphthalene to be 0.15 atm at 40°C and negligible bulk concentration of naphthalene in air. If air starts blowing across the surface of naphthalene ball at 3 m/s, by what factor will the

mass transfer rate increase, all other conditions remaining the same?

For spheres:  $Sh = 2.0 + 0.6(Re)^{0.5}(Sc)^{0.33}$

where Sh is the Sherwood number and Sc is the Schmidt number. The viscosity and density of air are  $1.8 \times 10^{-5} \text{ kg/m s}$  and  $1.123 \text{ kg/m}^3$ , respectively and the gas constant is  $82.06 \text{ cm}^3 \text{ atm/mol K}$ .  
[Ans.  $13.9 \times 10^{-3} \text{ mol/m}^2\text{s}$ ]

**3.6 Estimation of Mean Mass Transfer Coefficient and the Instantaneous Rate of Evaporation from the Drop of Water Falling Through Stagnant Air:** A spherical drop of water, 0.5 mm in diameter, is falling at a velocity of 2.15 m/s through dry and stagnant air at 1 atm with no internal circulation. Calculate the mean mass transfer coefficient and the instantaneous rate of evaporation from the drop when the drop surface is at  $21^\circ\text{C}$  and the air far from the drop is at  $60^\circ\text{C}$ . The vapour pressure of water at  $21^\circ\text{C}$  is 0.0247 atm. Assume quasi-steady state conditions. You may use Eq. (3.64) for calculating mean mass transfer coefficient.

[Ans:  $1.35 \times 10^{-3} \text{ gmol/cm}^2\text{s}$ ,  $2.70 \times 10^{-7} \text{ gmol/s}$ ]

## ***Short and Multiple Choice Questions***

1. What are the units of mass transfer coefficients  $k_G$ ,  $k_C$  and  $k_y$ ?
2. How is mass transfer coefficient  $k_y$  and  $k'_y$  related?
3. What are the dimensionless groups in mass transfer corresponding to Prandtl number and Nusselt number in heat transfer?
4. Express Schmidt number as the ratio of two diffusivities.
5. What are the physical significances of Schmidt number and Sherwood number?
6. Write Chilton-Colburn equation regarding analogy between heat and mass transfer.
7. Why neither  $j_D$  nor  $j_H$  are close to  $(1/2)f$  while they are often very close to each other?
8. Write Gilliland's equation for mass transfer in fluids flowing through pipes.
9. Schmidt Number is defined as  
(a)  $n/D_{AB}$  (b)  $n/tD_{AB}$  (c)  $tn/D_{AB}$  (d)  $nD_{AB}/t$
10. Eddy momentum diffusivity, thermal diffusivity and mass diffusivity are the same for  
(a)  $Pr = Sc = 0.7$  (b)  $Pr = Sc = 7.0$  (c)  $Pr = Sc = 1.0$  (d)  $Pr = Sc = 700$ .
11. Lewis number of a mixture is defined as  
(a)  $Pr/Sc$  (b)  $Pr/Sc$  (c)  $Sc/Pr$  (d)  $C_S(Sc/Pr)$
12. Lewis Number is the ratio of  
(a) thermal diffusivity to mass diffusivity  
(b) mass diffusivity to momentum diffusivity  
(c) mass diffusivity to thermal diffusivity  
(d) momentum diffusivity to thermal diffusivity
13. For water at  $20^\circ\text{C}$ , Prandtl Number is  
(a) 0.702 (b) 7.02 (c) 70.2 (d) none of these
14. The probable value of Schmidt number (Sc) for diffusion of ammonia in air at  $0^\circ\text{C}$  is  
(a) 0.35 (b) 0.665 (c) 0.015 (d) none of these

**15.** Rates of mass transfer are directly affected by

- (a) diffusivity (b) hydrodynamic conditions
- (c) interfacial area of contact (d) all of these

**16.** Sherwood number (Sh)

- (a) increases with friction factor,  $f$
- (b) increases with Reynolds Number, Re
- (c) decreases with Reynolds Number, Re
- (d) decreases with friction factor,  $f$

**17.** Stanton number for mass transfer ( $St_M$ ) is expressed as

(a)  $\frac{Sh}{Re Sc}$  (b)  $\frac{Sh}{Re Sc^{1/3}}$  (c)  $\frac{Sh}{Re^{1/2} Sc^{1/2}}$

**18.** Peclet number (Pe) is defined as

- (a)  $Pe = Re Sc$  (b)  $Pe = Re/Sc$  (c)  $Pe = Re^{1/2} Sc^{1/3}$  (d)  $Pe = Re^{1/3} Sc^{1/2}$

**19.** If Lewis number is 1, then

- (a)  $Pr = Sc$  (b)  $Pr = Re$  (c)  $Sc = Re$  (d)  $Sh = Re Sc$

**20.** According to Chilton-Colburn analogy for heat and mass transfer

- (a)  $Sh Sc^{1/3} = f/8$  (b)  $Sh Sc^{2/3} = f/2$
- (c)  $Sh Sc^{3/2} = f/2$  (d)  $Sh Sc^{2/3} = f/8$

**21.** Sherwood number (Sh) is defined as

(a)  $\frac{D_{AB}}{k'_C d}$  (b)  $\frac{k'_C}{d D_{AB}}$  (c)  $\frac{k'_C D_{AB}}{d}$  (d)  $\frac{k'_C d}{D_{AB}}$

**22.** For pure air at atmospheric conditions, Schmidt number (Sc) is

- (a)  $< 1$  (b)  $= 1$  (c)  $> 1$  (d)  $\gg 1$

**23.** For ideal gases, the different mass transfer coefficients are related as

- (a)  $k'_C = k_G RT = k'_y RT/P$  (b)  $k'_C = k_G/RT = k'_y P/RT$
- (c)  $k'_C = k_G RT/P = k'_y RT$  (d)  $k'_C = k_G = k'_y$

**24.** For flow through pipes, Reynolds analogy is valid for

- (a)  $Pr = 1, Sc = 1$  (b)  $Pr > 1, Sc > 1$
- (c)  $Pr < 1, Sc < 1$  (d)  $Pr < 1, Sc > 1$

**25.** The Colburn factor for mass transfer,  $J_D$  can be expressed as

(a)  $\frac{Sh}{Re Sc^{1/3}}$  (b)  $\frac{Sh}{Re Sc}$  (c)  $\frac{St}{Sc^{1/3}}$  (d)  $\frac{St}{Re^{1/3}}$

**26.** In forced mass convection through a tube, Gilliland and Sherwood suggested the relation  $Sh = 0.023 (Re)^{0.83} (Sc)^{0.44}$  for

- (a)  $2000 < Re < 35000$
- (b)  $0.06 < Sc < 2.5$
- (c)  $200 < Re < 35000$  and  $0.06 < Sc < 2.5$
- (d) none of these

## *Answers to Multiple Choice Questions*

- 9. (b) 10. (c) 11. (c) 12. (a) 13. (b)
- 14. (b) 15. (d) 16. (b) 17. (a) 18. (a)
- 19. (a) 20. (b) 21. (d) 22. (a) 23. (a)
- 24. (a) 25. (a) 26. (d)

## **References**

- Bennet, C.O. and J.E. Myers, *Momentum, Heat and Mass Transfer*, 2nd ed., McGraw-Hill, New York (1974).
- Bird, R.B., W.E. Stewart and E.N. Lightfoot, *Transport Phenomena*, John Wiley & Sons, Inc., New York (1960).
- Brian, P.L.T. and H.B. Halis, *AICHE J.*, **15**, 419 (1969).
- Chilton, T.H. and A.P. Colburn, *Ind. Eng. Chem.*, **26**, 1183 (1934).
- Colburn, A.P., *Trans. AIChE.*, **29**, 174 (1933).
- Gilliland, E.R. and T.K. Sherwood, *Ind. Eng. Chem.*, **26**, 516 (1934).
- Guha, D.K., F. Vyarawalla and P. De, *Canad. J. Chem. Eng.*, **65**, 448 (1987).
- Harriott, P., *Chem. Eng. Sci.*, **17**, 149 (1962).
- Johnson, A.I., F. Besic and A.E. Hamielec, *Canad. J. Chem. Eng.*, **47**, 559 (1969).
- Johnstone, H.F. and R.L. Pigford, *Trans. AIChE.*, **38**, 25 (1942).
- Popovich, A.T., R.E. Jervis and O. Träss, *Chem. Eng. Sci.*, **19**, 357 (1964).
- Prandtl, L., *Z. Physik.*, **11**, 1072 (1910); **29**, 487 (1928).
- Reynolds, O., *Proc. Manchester Lit. Phil. Soc.*, **14**, 7 (1874).
- Rohsenow, W.M. and H.Y. Choi, *Heat, Mass and Momentum Transfer*, Prentice Hall, New Jersey (1961).
- Sherwood, T.K. and R.L. Pigford, *Absorption and Extraction*, 2nd ed., McGraw-Hill, New York (1952).
- Sherwood, T.K., R.L. Pigford and C.R. Wilke, *Mass Transfer*, McGraw-Hill, Kogakusha (1975).
- Skelland, A.H.P., *Diffusional Mass Transfer*, John Wiley, New York (1974).

# 4

## Interphase Mass Transfer

### 4.1 Introduction

In Chapter 2, we have discussed transfer of material within a single phase without having to cross any phase boundary. Almost all industrial mass transfer operations however involve transfer of material from one phase to another. For instance, in operations such as gas absorption, liquid extraction, distillation, drying, crystallization, leaching, etc., the diffusing molecules have to travel from the bulk of one phase to the phase boundary or interface, cross the interface and then enter into the bulk of the other phase. In these cases, mass transfer occurs in both the phases on the two sides of the interface. Only in some limited cases, mass transfer takes place in a single phase. For instance, during evaporation of a pure liquid into a gas stream mass transfer is not involved in the liquid phase.

During interphase transfer in fluid systems, both molecular and eddy diffusion are encountered in each of the two phases. Transfer in the bulk of both fluids is usually by eddy diffusion due to the turbulence created there to enhance the rate of transfer. On the other hand, thin layers of fluids on both sides of the interface flow in laminar motion through which transfer is by molecular diffusion. Figure 4.1 shows the steady-state transfer of a solute  $A$  from gas phase to liquid phase as in gas absorption. As figure indicates most of the concentration drops in both the phases are limited within narrow laminar regions on both sides of the interface  $PQ$ . These laminar layers offer maximum resistance to mass transfer, and thus control the overall rate of transfer. A design engineer should therefore create conditions so that the thicknesses of these laminar layers are kept at minimum and their resistances reduced to the extent possible.

The higher location of  $x_{Ai}$  in respect of  $y_{Ai}$  at the interface, as shown in Figure 4.1, does not mean that  $x_{Ai}$  represents a higher potential. This is so because they are differently related to their chemical potential which is the true measure of the driving force. When expressed in terms of chemical potential, their values will be almost the same and they therefore represent equilibrium values of solute A in both the phases at the interface as assumed in the *two resistance theory*.

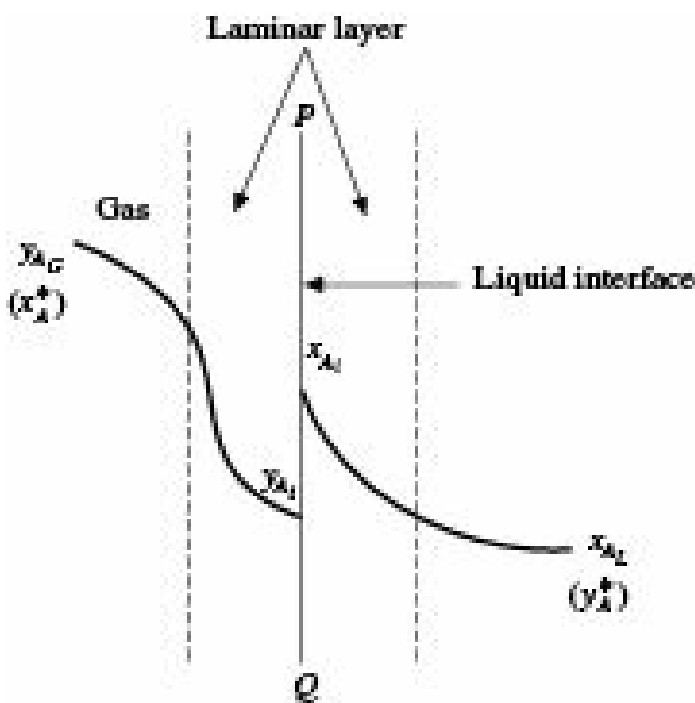


**Figure 4.1** Interphase mass transfer.

In order to visualize the phenomenon of interphase mass transfer, let us consider a simple case of absorption of ammonia ( $A$ ) from an air-ammonia stream in a counter-current wetted wall tower using water as solvent. The air-ammonia mixture enters the tower near its bottom, flows upwards through the central core of the tower and leaves near its top. The water, on the other hand enters the tower near its top, flows down along the inner wall of the tower and leaves near the bottom of the tower as aqueous ammonia solution. As the gas flows upwards, it loses its ammonia content while the liquid picks up more and more ammonia as it flows down.

Let us consider the situation at a particular height somewhere near the middle of the tower. Since ammonia is diffusing from the gas to the liquid phase, there must be some concentration gradient in each phase along the direction of mass transfer, i.e. from the gas side to the liquid side. Let the concentration of ammonia in the bulk of the gas be  $y_{AG}$  mole fraction and that at the interface (phase boundary) be  $y_{Ai}$  mole fraction. Since mass transfer is taking place from gas to liquid through the interface  $y_{AG} > y_{Ai}$ . Similarly in the liquid side, the concentration falls from  $x_{Ai}$  mole fraction at the interface to  $x_{AL}$  mole fraction in the bulk of the liquid. The concentrations  $y_{AG}$  and  $x_{AL}$  are not equilibrium values since diffusion of ammonia is taking place from gas phase to liquid phase.

The situation can be represented graphically as shown in Figure 4.2 having co-ordinates same as those of equilibrium distribution curve. Liquid phase concentrations are represented along the abscissa and gas phase concentrations are plotted along the ordinate. Point  $M$  represents the two concentrations in bulk gas ( $y_{AG}$ ) and bulk liquid ( $x_{AL}$ ), and point  $N$  represents the concentrations at the interface ( $y_{Ai}$  and  $x_{Ai}$ ).

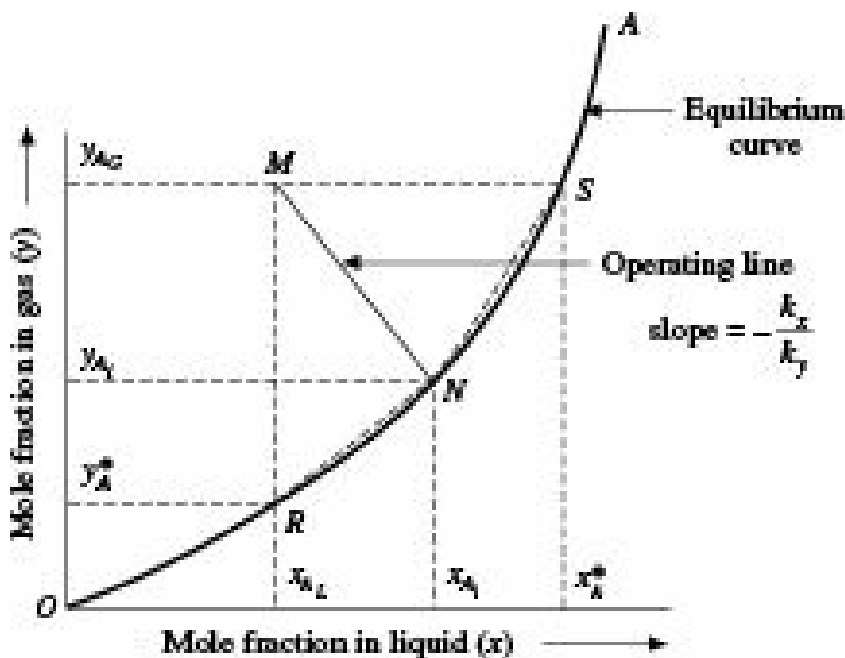


**Figure 4.2** Individual phase and overall concentration gradients in interphase mass transfer.

Let us now examine how to measure the rate of interface mass transfer. One alternative is to determine the rate of transfer within any one of the two phases, i.e. from the bulk gas to the interface in the gas phase or from the interface to the bulk liquid in the liquid phase.

Assuming that there is no chemical reaction and using local mass transfer coefficients  $k_y$  and  $k_x$ , the fluxes in the two phases can be expressed as

$$N_{AG} = k_y(y_{AG} - y_{Ai}) \text{ in the gas phase} \quad (4.1)$$

and  $N_{AL} = k_x(x_{Ai} - x_{AL}) \text{ in the liquid phase} \quad (4.2)$

where,  $N_{AG}$  and  $N_{AL}$  are fluxes of mass of solute  $A$  in gas and liquid phases respectively, moles/(unit time) (unit area)

$k_y$  and  $k_x$  are gas phase and liquid phase mass transfer coefficients respectively, moles/ (unit time) (unit area) (unit mole fraction difference)

$y_{AG}$  and  $y_{Ai}$  are mole fractions of solute  $A$  in the bulk of the gas and at the interface respectively

$x_{AL}$  and  $x_{Ai}$  are mole fractions of solute  $A$  in the bulk of the liquid and at the interface respectively.

The operation being under steady-state conditions, there is no accumulation or depletion of ammonia at the interface. As a result,  $N_{AG}$  will be equal to  $N_{AL}$ , both being equal to the overall rate of transfer.

Denoting the common flux by  $N_A$ , we may therefore write

$$N_A = k_y(y_{AG} - y_{Ai}) = k_x(x_{Ai} - x_{AL}) \quad (4.3)$$

$$\frac{y_{AG} - y_{Ai}}{x_{AL} - x_{Ai}} = -\frac{k_x}{k_y} \quad (4.4)$$

whence,

Equation (4.4) provides the slope of the line  $MN$ , called the *operating line*. If the mass transfer coefficients  $k_y$  and  $k_x$  are known, the interfacial concentrations and hence the flux  $N_A$  can be estimated by solving Eq. (4.4) along with an algebraic expression for equilibrium distribution. Alternatively,  $y_{Ai}$  and  $x_{Ai}$  can be determined graphically from Figure 4.2 by measuring the slope of

the line  $MN$ . A straight line drawn from  $M$  with a slope of  $(-k_x/k_y)$  meets the equilibrium curve  $OA$  at the point  $N$  which represents  $y_{A_i}$  and  $x_{A_i}$ .

Experimental determination of the interfacial concentrations  $y_{A_i}$  and  $x_{A_i}$  are extremely difficult if not impossible. This is because of the fact that the interface itself is so thin and delicate that it is not possible to draw samples from the interface. Introduction of any sampling device at the interface will disturb the interface itself and change the characteristics of the transfer process. In the circumstance, interfacial concentrations are not generally used for experimental determination of the rate of transfer. The other alternative is to estimate the rate of interface mass transfer using bulk concentrations  $y_{AG}$  and  $x_{AL}$  along with overall coefficients. It is relatively easy to measure  $y_{AG}$  and  $x_{AL}$  accurately by sampling and analysing. However, the concentration  $y_{AG}$  and  $x_{AL}$  are not by themselves on the same basis in terms of chemical potential and therefore cannot be directly used for determination of the driving force for mass transfer. In order to overcome this difficulty the concentration  $y_A^*$  which is the equilibrium concentration corresponding to  $x_{AL}$  and has a unique value at any given temperature and pressure, is used in place of  $x_{AL}$ . Moreover,  $y_A^*$  is on the same basis as  $y_{AG}$ . In terms of overall mass transfer coefficients, the rate of transfer can be written as

$$N_A = K_y(y_{AG} - y_A^*) \quad (4.5)$$

and  $N_A = K_x(x_A^* - x_{AL}) \quad (4.6)$

where

$K_y$  = overall mass transfer coefficient based on total driving force expressed as equivalent gas phase mole fraction difference, moles/(unit time) (unit area) (unit mole fraction difference),

$K_x$  = overall mass transfer coefficient based on total driving force expressed as equivalent liquid phase mole fraction difference, moles/(unit time) (unit area) (unit mole fraction difference),

$y_A^*$  = gas phase concentration in equilibrium with liquid phase concentration  $x_{AL}$

$x_A^*$  = liquid phase concentration in equilibrium with gas phase concentration  $y_{AG}$ .

Both  $K_y$  and  $K_x$  represent the same coefficient but their values are different since they are expressed in terms of equivalent driving forces in different phases having different values. Similarly,  $(y_{AG} - y_A^*)$  and  $(x_A^* - x_{AL})$  represent the same driving force but in terms of mole fraction difference in gas and liquid phases respectively.

From the geometry of Figure 4.2,

$$\begin{aligned} (y_{AG} - y_A^*) &= (y_{AG} - y_{A_i}) + (y_{A_i} - y_A^*) \\ &= (y_{AG} - y_{A_i}) + m'(x_{A_i} - x_{AL}) \end{aligned} \quad (4.7)$$

where,  $m'$  is the slope of the chord  $NR$ .

Substituting the value of  $(y_{AG} - y_A^*)$  from Eq. (4.5) and the values of  $(y_{AG} - y_{A_i})$  and  $(x_{A_i} - x_{AL})$  from Eq. (4.3), we have

$$\frac{N_A}{K_y} = \frac{N_A}{k_y} + \frac{m' N_A}{k_x} \quad (4.8)$$

or,  $\frac{1}{K_y} = \frac{1}{k_y} + \frac{m'}{k_x}$  (4.9)

Similarly, it can be shown that

$$\frac{1}{K_x} = \frac{1}{k_x} + \frac{1}{m'' k_y} \quad (4.10)$$

where,  $m''$  is the slope of the chord  $NS$ .

Equations (4.9) and (4.10) can be derived otherwise as follows:

Comparing Eqs. (4.3) and (4.5), one can write

$$\begin{aligned} \frac{1}{K_y} &= \frac{(y_{A_G} - y_A^*)}{k_y(y_{A_G} - y_{A_i})} = \frac{(y_{A_G} - y_{A_i}) + (y_{A_i} - y_A^*)}{k_y(y_{A_G} - y_{A_i})} \\ &= \frac{1}{k_y} + \frac{(y_{A_i} - y_A^*)}{k_y(y_{A_G} - y_{A_i})} \end{aligned}$$

Substituting the expression for  $(y_{A_G} - y_{A_i})$  from Eq. (4.3), we have

$$\frac{1}{K_y} = \frac{1}{k_y} + \frac{(y_{A_i} - y_A^*)}{k_x(x_{A_i} - x_{A_L})} = \frac{1}{k_y} + \frac{m'}{k_x}$$

$$\frac{y_{A_i} - y_A^*}{x_{A_i} - x_{A_L}}$$

where,  $\frac{y_{A_i} - y_A^*}{x_{A_i} - x_{A_L}} = m'$  is the slope of the linear equilibrium line as shown in Figure 4.2.

Similarly, comparing Eqs. (4.3) and (4.6), and thereafter substituting the expression for  $(x_{A_i} - x_{A_L})$  from Eq. (4.3), one can have

$$\frac{1}{K_x} = \frac{1}{k_x} + \frac{1}{m' k_y}$$

$$\frac{y_{A_G} - y_{A_i}}{x_A^* - x_{A_i}}$$

where,  $\frac{y_{A_G} - y_{A_i}}{x_A^* - x_{A_i}} = m''$  is the slope of the equilibrium line as shown in Figure 4.2.

Equations (4.9) and (4.10) show that the relationship between the individual phase mass transfer coefficients and the overall coefficients take the form of addition of resistances.  $K_y$  and  $K_x$  represent the same mass transfer coefficient expressed in terms of gas phase and liquid phase mole fraction difference respectively. As a result, their numerical values are different. Similarly,  $(y_{A_G} - y_A^*)$  and  $(x_A^* - x_{A_L})$  represent the same driving force expressed in terms of gas phase and liquid phase mole fraction difference respectively.

Equations (4.9) and (4.10) provide the following relationship between individual phase and overall mass transfer resistances:

Resistance in gas phase  
Total resistance of both phases

$$= \frac{1/k_y}{1/K_y} \quad (4.11)$$

Resistance in liquid phase  
Total resistance of both phases

$$= \frac{1/k_x}{1/K_x} \quad (4.12)$$

Assuming the numerical values of  $k_y$  and  $k_x$  to be very close to each other, let us examine the role of the slope  $m'$  of the chord  $NR$  (Figure 4.2). If  $m'$  is very small, the equilibrium distribution curve becomes flat and at equilibrium only a small concentration of component  $A$  in the gas produces a very high concentration in the liquid, i.e. the solute  $A$  is highly soluble in the liquid. The term  $m''/k_x$  in Eq. (4.9) becomes very small and negligible in comparison with the term  $1/k_y$ . The major resistance to mass transfer lies in the gas phase. In other words, the mass transfer process is gas phase resistance controlled.

$$\frac{1}{K_y} \approx \frac{1}{k_y}, \text{ or, } k_y \approx K_y \quad (4.13)$$

$$\text{or, } (y_{AG} - y_A^*) \approx (y_{AG} - y_{Ai}) \quad (4.14)$$

In such cases, even large change in liquid phase mass transfer coefficient ( $k_x$ ) will not significantly affect the overall coefficient ( $K_y$ ). Therefore, any attempt to enhance the rate of mass transfer should better be directed towards decreasing the gas phase resistance.

If on the other hand the slope  $m''$  of the chord  $NS$  is very high, the component  $A$  becomes relatively insoluble in the liquid and the term  $1/m'' k_y$  in Eq. (4.10) becomes very small and negligible in comparison with  $1/k_x$ . The main resistance to mass transfer lies in the liquid phase. In other words, the mass transfer process becomes liquid phase resistance controlled.

$$\frac{1}{K_x} \approx \frac{1}{k_x} \text{ or } k_x \approx K_x \quad (4.15)$$

and

$$(x_A^* - x_{AL}) \approx (x_{Ai} - x_{AL}) \quad (4.16)$$

In such cases, large change in gas phase mass transfer coefficient ( $k_y$ ) will not significantly affect the overall coefficient,  $K_x$ . Therefore, any attempt to enhance the rate of mass transfer should better be directed towards decreasing the liquid phase resistance.

Overall mass transfer coefficients are analogous to overall heat transfer coefficients. Just as overall heat transfer coefficients are generally used in the design of heat transfer equipment, overall mass transfer coefficients are generally used in the design of mass transfer equipment. Like overall heat transfer coefficients, overall mass transfer coefficients are often synthesized from individual

coefficients.

Two important conditions have to be remembered while using overall mass transfer coefficients. Firstly, overall mass transfer coefficients are valid only for the hydrodynamic conditions in which they have been determined. Since magnitudes of mass transfer coefficient largely depend on the prevailing hydrodynamic conditions, measurement under one set of conditions and use under another set of conditions will lead to erroneous results. Secondly, for nonlinear equilibrium relations, overall mass transfer coefficients should be used only for the concentration range for which they have been determined. From Eq. (4.9) it may be noted that the value of the overall mass transfer coefficient,  $K_y$  depends on  $m'$ , the slope of the chord  $NR$  (Figure 4.2). So long as  $m'$  remains constant,  $K_y$  has definite relation with  $k_y$  and  $k_x$ . If on the other hand, the value of  $m'$  changes, as often happens in case of nonlinear equilibrium distribution, overall mass transfer coefficient will have different relation with  $k_y$  and  $k_x$ , and its value will change. However, if the equilibrium relationship is linear, the slope  $m'$  remains constant and overall mass transfer coefficient, determined under one concentration can be used at another concentration. The same is applicable for  $K_x$  also.

**EXAMPLE 4.1** (Estimation of overall mass transfer coefficients from individual phase mass transfer coefficients and determination of the ratio of phase resistances): In a gas absorber operating at an absolute pressure of 2278.5 mm Hg, the gas phase and liquid phase mass transfer coefficients have been found to be  $1.07 \text{ kmol}/(\text{m}^2)(\text{hr})(\text{mol fraction})$  and  $22 \text{ kmol}/(\text{m}^2)(\text{hr})$  (mol fraction) respectively. The equilibrium relationship can be represented by the relation:  $p^* = 0.08 \times 10^6 x$ .

- Determine the overall mass transfer coefficients,  $K_x$  and  $K_y$ ,
- Determine the ratio of the diffusional resistances of the liquid and gaseous phases.

**Solution:** The given equilibrium relationship is first transformed to the form:

$$y^* = mx$$

$$y^* = \frac{p^*}{P} = \frac{0.08 \times 10^6}{2278.5} x = 35.1x$$

- The overall mass transfer efficient  $K_y$  may be calculated from Eq. (4.9):

$$K_y = \frac{1}{\frac{1}{1.07} + \frac{1}{22}} = 0.396 \text{ kmol}/(\text{m}^2)(\text{hr})(\text{mol fraction})$$

Similarly, from Eq. (4.10), we get

$$K_x = \frac{1}{\frac{1}{22} + \frac{1}{35.1 \times 1.07}} = 13.9 \text{ kmol}/(\text{m}^2)(\text{hr})(\text{mol fraction})$$

- The ratio of the diffusional resistances of the liquid and gaseous phases is

$$\frac{m}{k_x} : \frac{1}{k_y} = \frac{35.1}{22} : \frac{1}{1.07} = 1.71.$$

**EXAMPLE 4.2** (Estimation of overall mass transfer coefficients): During absorption of carbon tetrachloride from a mixture of air- $\text{CCl}_4$  by an organic oil, the gas and liquid phase mass transfer coefficients have been estimated to be 0.32 and 5.26  $\text{kmol}/(\text{hr})(\text{m}^2)$ (mol fraction), respectively. The equilibrium relation under the operating conditions is given by  $y^* = 20x$ , where  $y$  and  $x$  are mole fractions of  $\text{CCl}_4$  in gas and liquid phases respectively.

Estimate the overall mass transfer coefficients,  $K_y$  and  $K_x$ .

**Solution:**

$$\text{Given: } y^* = 20x; m' \text{ or } m'' = \frac{y^*}{x} = 20.$$

From Eq. (4.9), we have

$$\frac{1}{K_y} = \frac{1}{k_y} + \frac{m'}{k_x}$$

Substituting the values, we obtain

$$\frac{1}{K_y} = \frac{1}{0.32} + \frac{20}{5.26}$$

whence,  $K_y = 0.144 \text{ kmol}/(\text{hr})(\text{m}^2)$ (mol fraction)

From Eq. (4.10), we have

$$\frac{1}{K_x} = \frac{1}{k_x} + \frac{1}{m' k_y}$$

Substituting the values, we obtain

$$\frac{1}{K_x} = \frac{1}{5.26} + \frac{1}{(20)(0.32)}$$

whence,  $K_x = 2.89 \text{ kmol}/(\text{hr})(\text{m}^2)$ (mol fraction).

**EXAMPLE 4.3** (Calculation of individual phase transfer coefficients and interfacial concentration): Ammonia from an aqueous ammonia solution is being stripped into an air stream in a wetted-wall column. At one point in the column, the concentration of  $\text{NH}_3$  in liquid is  $0.3 \text{ kmol}/\text{m}^3$  and the partial pressure of  $\text{NH}_3$  in the gas is 0.06 atm.

The equilibrium relation under the operating conditions is  $p'_A = 0.25c_A$ , where  $p'_A$  is the partial pressure of  $\text{NH}_3$  in atmosphere and  $c_A$  is its concentration in liquid in  $\text{kmol}/\text{m}^3$ . The overall mass transfer coefficient  $K_x$  is  $0.0875 \text{ kmol}/(\text{hr})(\text{m}^2)/(\text{kmol}/\text{m}^3)$ .

If the gas phase resistance is 70% of the total resistance, calculate (i) individual mass transfer coefficients, and (ii) interfacial concentrations of  $\text{NH}_3$ .

**Solution:** From equation (4.10), we have

$$\frac{1}{K_x} = \frac{1}{k_x} + \frac{1}{m' k_y}$$

Given:  $K_x = 0.0875$ ,

$$\text{Overall resistance} = \frac{1}{K_x} = 11.4286$$

$$\text{Resistance of gas phase} = (0.70)(11.4286) = 8.00$$

$$\frac{1}{m' k_y} = 8.00 \text{ or } k_y = \frac{1}{(0.25)(8.00)} = 0.500$$

$$\text{Resistance of liquid phase} = 11.4286 - 8.00 = 3.4286$$

$$\frac{1}{k_x} = 3.4286 \text{ or } k_x = 0.292$$

Gas phase mass transfer coefficient,  $k_y = 0.500 \text{ kmol}/(\text{hr})(\text{m}^2)(\text{atm})$

Liquid phase mass transfer coefficient,  $k_x = 0.292 \text{ kmol}/(\text{hr})(\text{m}^2)(\text{kmol}/\text{m}^3)$

$$\text{Overall mass flux} = K_x (c_{AL} - c_{A^*}) = K_x [c_{AL} - (p'A/0.25)]$$

$$= 0.0875 [0.3 - (0.06/0.25)] = 0.00525 \text{ kmol}/(\text{hr})(\text{m}^2).$$

Considering transfer in gas phase,

$$N_A = k_y(p_{Ai} - p_{AG}),$$

or

$$0.00525 = (0.500)(p_{Ai} - 0.06)$$

whence  $p_{Ai} = 0.0705$

$$c_{Ai} = \frac{p_{Ai}}{m'} = 0.282$$

Interfacial concentration of NH<sub>3</sub>: Gas-side = 0.0705 atm

$$\text{Liquid-side} = 0.282 \text{ kmol}/\text{m}^3$$

## 4.2 Theories of Interphase Mass Transfer

Several theories have been proposed with the objective of explaining the mechanism of interphase mass transfer and develop quantitative relations for the same.

### 4.2.1 The Two-Film or Two Resistance Theory

The credit of being the pioneers in attempting to visualize the mechanism of interphase mass transfer and offer some theoretical basis for the same goes to W.K. Lewis and W.G. Whitman (1924) who proposed the two-film or two-resistance theory of interphase mass transfer. In their theory, Lewis and Whitman assumed the existence of an imaginary film on each side of the interface (phase boundary). Mass was visualized as being transferred by steady-state molecular diffusion through these films each having such thickness that its resistance to molecular diffusion is equal to the total resistance due to both molecular and eddy diffusion actually offered by the respective phase.

When a fluid flows in turbulent motion past a solid surface with mass transfer taking place from solid to fluid, the concentration profile is shown by the continuous line in Figure 4.3.

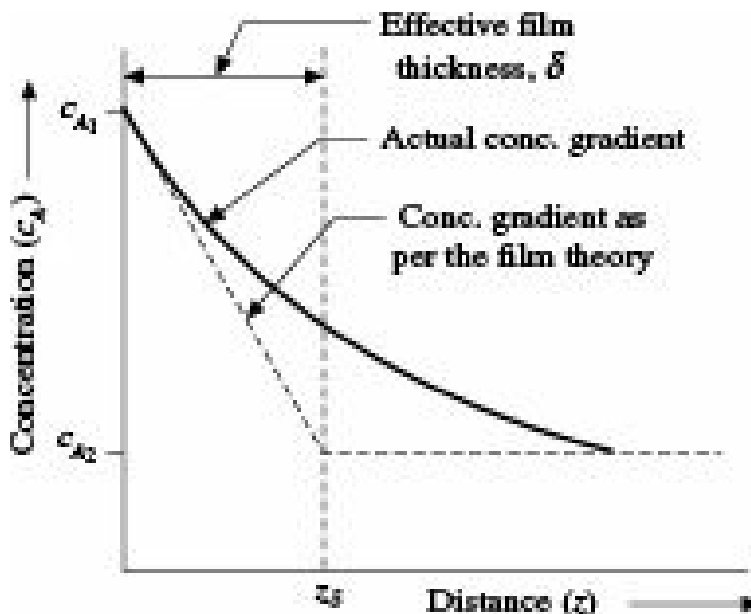


**Figure 4.3** Concentration profile of the diffusing component as proposed by the film theory.

The shape of this curve is controlled by the constantly changing ratio of eddy diffusivity to molecular diffusivity (Treybal 1985). According to the two-film theory, the concentration profile will be as shown by the broken line.

The basic assumptions of this theory are:

- (i) Mass transfer takes place only by molecular diffusion through the two imaginary films on both sides of the interface. Beyond these films, the fluids are well mixed so that its concentration is same as that of the bulk fluid.
- (ii) Mass transfer through the films is by steady-state diffusion.
- (iii) Bulk flow through the films being very small, the fluxes within the films can be represented by the equation

$$N_A = -D_{AB} \frac{dc_A}{dz}$$

- (iv) The interface itself does not offer any resistance to mass transfer so that the diffusing component passes on from one side of the interface to the other side without any resistance and its concentrations on the two sides of the interface are in equilibrium.

Several authors have conducted lots of studies to verify the validity of this hypothesis. Their studies indicate that departure from equilibrium at the interface is rather improbable. According to Schrage (1953), departure from equilibrium may be there if the rate of transfer is very high, much higher than what can be achieved in practice. Careful measurements by some authors (Gordon and Sherwood 1955, Scriven and Pigford, 1959) also support this assumption.

Unexpectedly large or small rates of transfer may sometimes occur at the interface due to heat effects caused by difference in heats of solution in the two phases, which may raise or lower the interface temperature relative to the bulk temperature.

According to the two-film theory, the theoretical concentration profile works out to be

$$c_A = c_{A_i} - (c_{A_i} - c_{AL}) \frac{z}{\delta} \quad (4.17)$$

and the mass transfer coefficient becomes

$$k_L = \frac{D_{AB}}{\delta} \quad (4.18)$$

where,  $d$  is the thickness of the film.

Thus the two-film theory permits calculation of mass transfer coefficient if the diffusivity and the film thickness are known.

This theory is a gross oversimplification of the actual conditions at the phase boundary. The existence of such stationary films near the interface has not been proved conclusively in spite of the findings of several authors in favour of this. Particularly, in commercial equipment like packed or plate towers, the existence of such stationary films is highly improbable. Moreover, this theory predicts first power dependence of  $k_G$  on diffusivity while in practice it has been found to vary approximately as

$D_{AB}^{0.56}$ . In spite of all these drawbacks, this theory gives quite reliable results in many cases and has been very useful in several applications particularly in mass transfer with chemical reaction.

#### 4.2.2 The Penetration Theory

Ralph Higbie (1935) proposed the penetration theory. In this theory, it has been assumed that the principal mechanism of interphase mass transfer involves motion of turbulent eddies from the core of the fluid to the interface, followed by a short interval of unsteady-state molecular diffusion into the other fluid before these eddies are displaced from the surface by subsequent eddies. Higbie further assumed that all eddies that reach the interface have the same exposure time and the diffusing molecules cannot reach the depth  $z_e$  of the eddies due to slow diffusion and short exposure.

According to this theory, in most cases the time of exposure of fluid elements to mass transfer is too short for steady-state concentration gradient to develop, which is the characteristic of the two-film theory.

As shown in Figure 4.4(a), Higbie considered a gas bubble to rise through a liquid which absorbs the gas. A particle or eddy ( $e$ ) of the liquid, initially at the top of the bubble is in contact with the gas for a time  $i$  required by the bubble to raise a distance equal to its diameter. The liquid particle then slips along the surface of the bubble.

Figure 4.4(b) shows an eddy ( $e$ ) rising from the turbulent core of the liquid and remaining exposed to the action of the gas for a time  $i$ . In this theory, the time of exposure has been taken to be the same for all eddies or particles of the liquid.

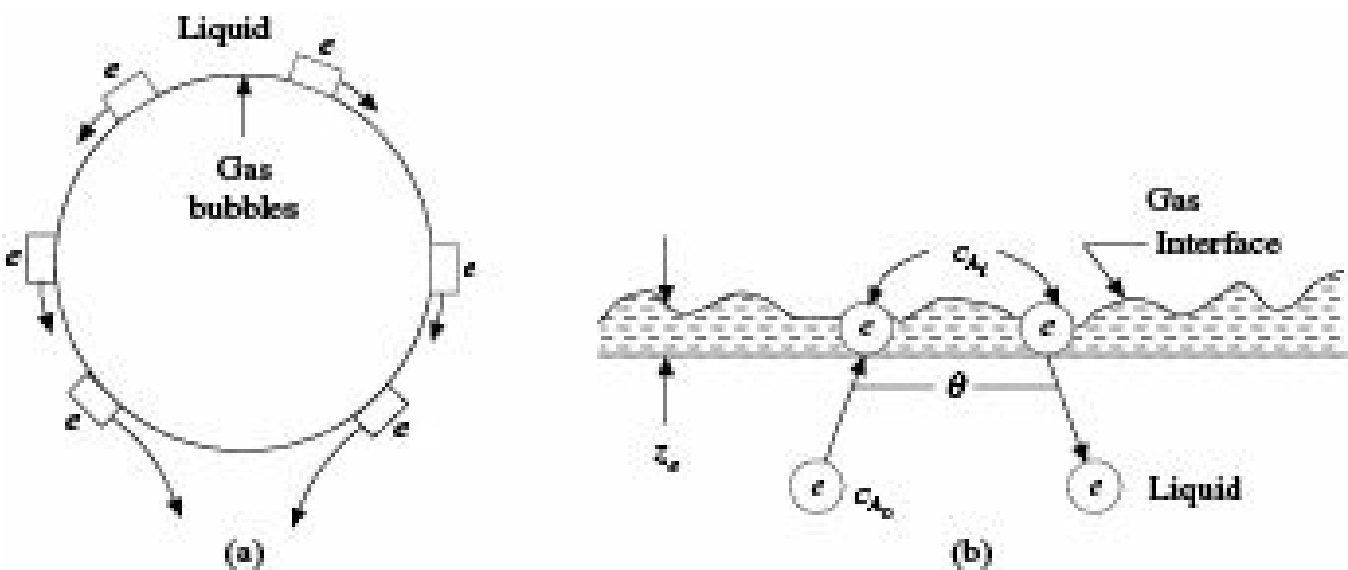


**Figure 4.4** Path of an eddy rising from the core of a turbulent liquid according to the penetration theory.

Initially, the concentration of the dissolved gas in an eddy is uniform at  $c_{A_0}$  and internally the eddy may be considered stagnant. When the eddy is exposed to the gas at the interface, the concentration in the liquid at the gas-liquid surface becomes  $c_{A_i}$  which may be taken as the equilibrium solubility of the gas in the liquid. During the time  $i$ , the liquid particle is subjected to unsteady-state diffusion of solute in the  $z$ -direction. Therefore as an approximation, the situation may be represented by Fick's second law for unidirectional diffusion

$$\frac{\delta c_A}{\delta \theta} = D \frac{\delta^2 c_A}{\delta z^2} \quad (4.19)$$

For short exposure time and slow diffusion in the liquid, the dissolving solute is unable to reach the depth  $z_e$  corresponding to the thickness of the eddy, so that from the solute point of view  $z_e$  may be considered infinite. The boundary conditions for Eq. (4.19) therefore are

$$c_A = c_{A_0} \text{ at } i = 0 \text{ for all } z,$$

$$c_A = c_{A_i} \text{ at } z = 0 \text{ for all } i > 0,$$

$$c_A = c_{A_0} \text{ at } z = \infty \text{ for all } i.$$

Solving Eq. (4.19) with the above conditions provides the average flux for the time of exposure as

$$N_{A\text{av}} = 2(c_{A_i} - c_{A_0}) \left( \frac{D_{AB}}{\pi \theta} \right)^{0.5} \quad (4.20)$$

and the average mass transfer coefficient is given by

$$k_{L\text{av}} = 2 \left( \frac{D_{AB}}{\pi \theta} \right)^{0.5} \quad (4.21)$$

From Eq. (4.21), it may be concluded that according to the penetration theory  $k_L$  varies as  $D_{AB}^{0.5}$ . This is typical for short exposure times. In general, it has been found that  $k_L$  varies as  $(D_{AB})^n$ , where  $n$  may have any value from nearly zero to 0.8 or 0.9.

### 4.2.3 Surface Renewal Theory

The penetration theory was modified by Danckwerts who proposed the surface renewal theory (Danckwerts 1951). According to this theory, the main drawback of the penetration theory is the assumption that all the liquid elements or eddies are exposed to the gas for the same length of time. In a turbulent fluid it is highly probable that some of the eddies are swept away while still young; others continue to be in contact with the gas. As a result, there is a distribution of the eddies present at the interface into different ‘age groups’ depending upon their contact time with the gas. Danckwert assumed random replacement of the eddies by fresh eddies from the bulk of the liquid. At any time, each of the eddies at the interface has equal chance of being replaced by fresh eddies. He further assumed that unsteady-state mass transfer occurs to the eddies during their stay at the interface. Accordingly, he introduced a fractional rate of surface renewal ( $s$ ), where  $s$  is the fraction of the surface area renewed in unit time. He introduced a surface area distribution function and showed the same to be equal to  $se^{si}$ .

According to this theory, the mass transfer coefficient works out to be

$$k_L = \bar{O} \sqrt{D_{AB} \cdot s} \quad (4.22)$$

It may be noted from Eq. (4.22) that according to this theory, the mass transfer coefficient varies as  $D_{AB}^{0.5}$ . The coefficient also varies as  $s^{0.5}$ . Moreover, if turbulence increases,  $s$  also increases thus causing enhancement of the mass transfer coefficient.

### 4.2.4 Film Penetration Model

An objection to the penetration theory and the surface renewal theory is that both the theories have assumed the depth of the liquid element (depth of penetration) to be infinite. In reality, it should have a finite value and the thickness should decrease as turbulence increases.

Toor and Marchelo (1958) proposed the film penetration model according to which the transfer to young elements at the interface with short exposure follows the penetration theory, and transfer to old elements with long exposure follows the film theory. They showed that the Film and penetration theories are but limiting cases of their more general film penetration model.

### 4.2.5 Surface-Stretch Theory

Lightfoot and co-workers (Stewart et al. 1970) in their surface-stretch theory combined the penetration and surface renewal theories by conceiving the interfacial area through which mass transfer takes place, to change periodically with time. Examples of such periodic changes are transfer to bubbles rising through a liquid or transfer to drops and bubbles being formed at a nozzle or to wavy or rippled liquid surfaces.

### 4.2.6 The Boundary Layer Theory

The theories of interphase mass transfer discussed so far are all based on some selected models of mass transfer at the phase boundary without considering the hydrodynamic conditions which largely affect the nature and rate of convective mass transfer. As a result, none of these theories represents a generalized picture of interphase mass transfer although they fit well in some specific cases. The boundary layer theory (Bird, et al. 2006), on the other hand, gives a much more realistic picture of the

mechanism of mass transfer at a phase boundary.

The concept of boundary layer originated in the study of fluid dynamics by Prandtl in the year 1903 and was later extended to studies of heat and mass transfer. Let us consider flow of a fluid past a wide flat plate at zero angle of incidence as shown in Figure 4.5. The fluid velocity is zero at the surface of the plate but increases as the distance from the plate in the  $z$ -direction increases till at sufficiently large distance when the influence of the solid plate disappears and the liquid attains its free stream velocity  $u_0$ . The region above the solid plate where the velocity of the fluid changes from zero to the free-stream velocity, i.e. the velocity of fully developed flow, is called the *hydrodynamic boundary layer* or *velocity boundary layer* or *momentum boundary layer*.

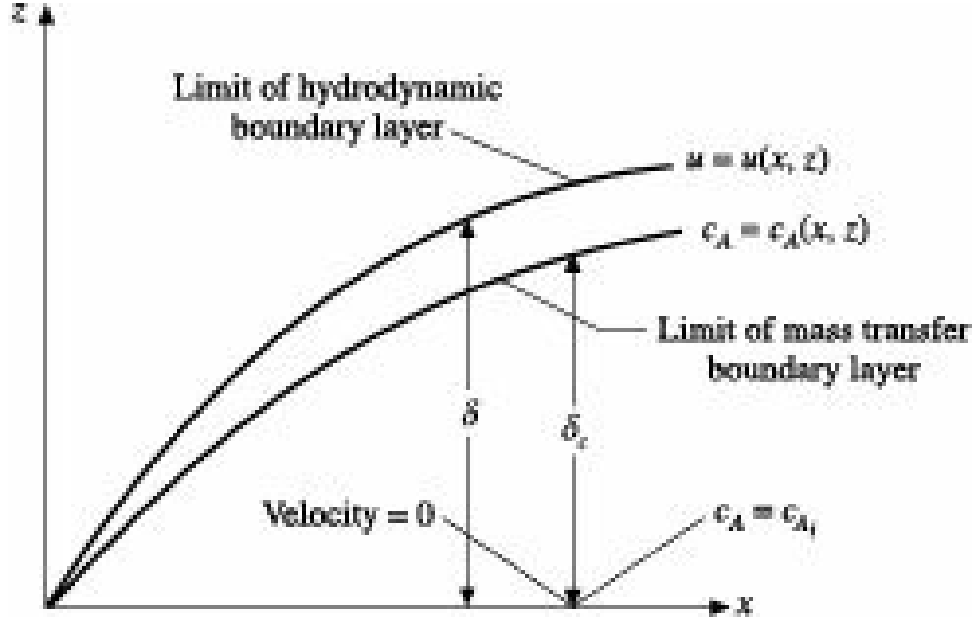


Figure 4.5 Hydrodynamic and mass transfer boundary layers on a flat plate.

Within the hydrodynamic boundary layer,  $du/dz \neq 0$ . However, for all practical purposes the region in which the fluid velocity changes from 0 to 99% of the fully developed velocity is considered to be the hydrodynamic boundary layer. Similarly there may be thermal boundary layer or heat transfer boundary layer  $dT/dz \neq 0$  for heat transfer and concentration or mass transfer boundary layer  $dc_A/dz \neq 0$  for mass transfer.

For zero angle of incidence on a wide flat plate, the fluid motion in the boundary layer is two dimensional,  $u = u(x, z)$ . The characteristics of the boundary layer depends upon the Reynolds number based on length of the solid plate ( $Re_x$ ), expressed as

$$Re_x = \frac{x u_0 \rho}{\mu} \quad (4.23)$$

The flow remains laminar for  $Re < 3-5 \times 10^5$  being the boundary layer extremely stable, even in the presence of turbulence in the external flow. At greater distances from the leading edge, i.e.  $Re > 10^5$ , the stability of the laminar layer decreases rapidly and transition to turbulent flow is more easily provoked. This Reynolds number is called *Critical Reynold's number*.

Having discussed briefly the hydrodynamic nature of the boundary layer, let us now focus our attention to mass transfer. In case of mass transfer two boundary layers are formed, the hydrodynamic boundary layer and the concentration boundary layer. The concentration distribution within the

boundary layer is a function of position,  $c_A = c_A(x, z)$  and its thickness is a function of the distance from the leading edge,  $d = d_C(x)$ , where  $d_C$  is the thickness of the boundary layer within which the concentration drop is 99% of the concentration difference between the surface of the plate and the bulk fluid. The usual boundary conditions on  $c_A$  are that  $c_A = c_{A0}(x)$  at the solid surface, and  $c_A = c_{A\infty}$  at the outer edge of the concentration boundary layer. The relative thicknesses of the hydrodynamic and concentration boundary layers depend upon the value of Schmidt number (Sc) according to the following relation:

$$\frac{\delta_c(x)}{\delta(x)} = Sc^{-1/3}$$

In fluids with constant physical properties and large Schmidt number, i.e.  $Sc > 1$ , the concentration boundary layer usually lies within the hydrodynamic boundary layer which means the thickness of the concentration boundary layer is less than that of the hydrodynamic boundary layer. On the contrary, the concentration boundary layer extends beyond the hydrodynamic boundary layer when  $Sc < 1$ , and both the boundary layers lie on the same line that means the thicknesses of the concentration boundary layer and velocity boundary layer become equal when  $Sc = 1$ .

If there is mass transfer from the plate without chemical reaction, the equation of continuity for the diffusing substance  $A$  reduces to

$$u_x \frac{\partial c_A}{\partial x} + u_z \frac{\partial c_A}{\partial z} = D_{AB} \left( \frac{\partial^2 c_A}{\partial x^2} + \frac{\partial^2 c_A}{\partial z^2} \right) \quad (4.24)$$

Solving the above equation provides the following expression for local Sherwood number in terms of dimensionless groups (Skelland 1974):

$$\frac{Sh_x}{Re_x Sc^{1/3}} = 0.332 Re_x^{-1/2}$$

or,  $Sh_x = 0.332 Re_x^{1/2} Sc^{1/3} \quad (4.25)$

and the equation for the average Sherwood number becomes

$$Sh_{av} = 0.664 Re_L^{1/2} Sc^{1/3} \quad (4.26)$$

where  $Re_L$  is the Reynolds number based on characteristic length of the plate.

## Nomenclature

$A$  : component diffusing

$c$  : solute concentration, mol/L<sup>3</sup>

$D_{AB}$  : molecular diffusivity, L<sup>2</sup>/s

$k_x$  : liquid phase mass transfer coefficient, mol/L<sup>2</sup>s (mol fraction)

$k_y$  : gas phase mass transfer coefficient, mol/L<sup>2</sup>s (mol fraction)

$K_x$  : overall mass transfer coefficient based on liquid phase driving force, mol/L<sup>2</sup> (mol fraction)  
 $K_y$  : overall mass transfer co-efficient based on gas phase driving force, mol/L<sup>2</sup> (mol fraction)  
 $m$  : slope of the equilibrium curve, --  
 $m', m''$  : slopes of chords of the equilibrium curve, --  
 $N$  : mass transfer flux, mol/L<sup>2</sup>  
 $s$  : fractional rate of surface renewal, i.e. fraction of the surface area renewed per unit time, --  
 $T$  : temperature, °C, K  
 $u$  : local velocity, L/ $\square$   
 $u_0$  : free-stream velocity, L/ $\square$   
 $x$  : concentration of a component in a liquid, mol fraction  
 $y$  : concentration of a component in a gas, mol fraction  
 $x, y, z$  : distance in the  $x, y$  and  $z$ -direction respectively, L  
 $z_e$  : depth of penetration, L  
 $d$  : thickness of a layer, L  
 $i$  : time, i

### Subscripts

$A$  : component  $A$   
 $B$  : component  $B$

## Numerical Problems

**4.1 Calculation of Mass Transfer Coefficient in Different Units:** Ammonia ( $A$ ) is being absorbed in water from a mixture of nitrogen ( $B$ ). The partial pressure of the solute in the bulk gas is 40 mm Hg and that at the gas-liquid interface is negligibly small. Diffusion occurs through a stagnant film of thickness 1 mm. The total pressure is 1 atm and temperature is 25°C. Diffusivity of ammonia in nitrogen at the given temperature and pressure is 0.023 cm<sup>2</sup>/s. Calculate the absorption flux of ammonia. Also, calculate the values of mass transfer coefficient if the driving force is expressed in terms of difference in (i) partial pressure of ammonia, (ii) mole fraction of ammonia in gas phase, (iii) concentration of ammonia in kmol/m<sup>3</sup>, (iv) mole fraction of ammonia in liquid phase.

[Ans: 0.00499 mol/(m<sup>2</sup>)(s),  $k_G = 86.99 \text{ mol}/(\text{m}^2)(\text{s})(\text{atm})$ ,  $k_y = 86.99 \text{ mol}/(\text{m}^2)(\text{s})(\text{mol frac})$ ,  $k_C = 0.007 \times 10^{-3} \text{ kmol}/(\text{m}^2)(\text{s})(\text{kmol}/\text{m}^3)$ ,  $k_x = 378.1 \times 10^{-6} \text{ mol}/(\text{m}^2)(\text{s}) (\text{mol frac})$ ]

**4.2 Conversion of the Values of Mass Transfer Coefficient from One Unit to Other:** The overall coefficient of mass transfer in a mass transfer equipment is 10.4 kmol/(m<sup>2</sup>)(hr)(kmol/m<sup>3</sup>). The inert gas is nitrogen. The pressure in the equipment is 760 mm Hg. The temperature is 20°C. Determine the values of the overall coefficient of mass transfer in the following units: (i) kmol/(m<sup>2</sup>)(hr)(Dy = 1), (ii) kmol/(m<sup>2</sup>)(hr)(mm Hg), and (iii) kg/(m<sup>2</sup>) (hr) (kg/kg of inert gas).

[Ans: (i)  $0.433 \text{ kmol}/(\text{m}^2)(\text{hr})(\text{Dy} = 1)$ , (ii)  $5.69 \times 10^{-4} \text{ kmol}/(\text{m}^2)(\text{hr})(\text{mm Hg})$  or  $1.19 \times 10^{-9} \text{ kmol}/(\text{m}^2)(\text{hr})(\text{mm Hg})$ , (iii)  $12.1 \text{ kg}/(\text{m}^2)(\text{hr}) (\text{kg/kg of inert gas})$ ]

**4.3 Gas-film Mass Transfer Coefficient for Ammonia-Water System:** Air with a mixture of ammonia is passed through a scrubber irrigated with water and packed with rings having a unit surface area of  $89.5 \text{ m}^2/\text{m}^3$ . The free volume of the packing is  $0.79 \text{ m}^3/\text{m}^3$ . The temperature of absorption is  $28^\circ\text{C}$  and the absolute pressure is 1 atm. The mean content of ammonia in the gas mixture is 5.8% (by volume). The mass flow rate of the gas related to the total cross-sectional area of the scrubber is  $1.1 \text{ kg}/\text{m}^2 \text{ s}$ . Determine the individual coefficient of mass transfer for the gas considering that the scrubber is operating in film conditions.

[Ans:  $0.038 \text{ m/s}$ ]

**4.4 Liquid-phase Mass Transfer Coefficient for CO<sub>2</sub>-H<sub>2</sub>O System:** Calculate the individual mass transfer coefficient for the liquid phase in a packed absorber in which carbon dioxide is absorbed by water at a temperature of  $20^\circ\text{C}$ . The density of irrigation (fictitious velocity) is  $60 \text{ m}^3/(\text{m}^2)(\text{hr})$ . The packing is dumped ceramic rings  $35 \# 35 \# 4 \text{ mm}$  in size. The coefficient of wetting of the packing is 0.86.

[Ans:  $2.16 \times 10^{-6} \text{ m/s}$ ]

**4.5 Individual Mass Transfer Coefficient for Absorption of Benzene from Coke Gas:** Determine the individual mass transfer coefficient for a gas in a scrubber when benzene vapour is being absorbed from the coke gas in the following conditions: grid packing with bars  $12.5 \# 100 \text{ mm}$  in size having a spacing of  $b = 25 \text{ mm}$  is used (for such packing equivalent diameter =  $2b = 0.05 \text{ m}$ ), the velocity of the gas calculated for the entire cross-section of the scrubber is  $0.95 \text{ m/s}$ , the density of the gas is  $0.5 \text{ kg/m}^3$ , the dynamic viscosity of the gas is  $0.013 \text{ mPa.s}$ , the coefficient of diffusion of benzene in the gas is  $16 \times 10^{-6} \text{ m}^2/\text{s}$ . Consider that the film conditions prevail in the column.

[Ans:  $0.0285 \text{ m/s}$ ]

**4.6 Overall Mass Transfer Coefficient for Air-water System:** Water saturated with oxygen was fed into a tower packed with  $0.9 \text{ m}$  of  $2.54 \text{ cm}$  rings, at a rate  $8.14 \text{ kg/m}^2 \text{ s}$ . Air ( $21\% \text{ O}_2$ ) was supplied to the tower at a rate of  $0.68 \text{ kg/m}^2 \text{ s}$ . The oxygen contents in the water entering and leaving the tower were  $2.9 \times 10^{-3}\%$  and  $1.1 \times 10^{-3}\%$  by weight respectively, and the temperature was  $25^\circ\text{C}$ . Calculate the Overall volumetric mass transfer coefficient. The Henry's coefficient for the system is  $4.38 \times 10^4 \text{ atm/mol fraction}$ .

[Ans:  $0.0086 \text{ kmol}/(\text{s})(\text{m}^3)(\text{kmol}/\text{m}^3)$ ]

**4.7 Overall Mass Transfer Coefficient from Individual Mass Transfer Coefficients:** Determine the overall mass transfer coefficient in an absorber irrigated with water for which the individual gas phase and liquid phase mass transfer coefficients are  $2.76 \times 10^{-3} \text{ kmol}/(\text{m}^2)(\text{hr})(\text{kPa})$  and  $1.17 \times 10^{-4} \text{ m/s}$ , respectively. The operating pressure of the absorber is maintained at 1.07 atm (abs). The equation of the equilibrium line in mole fractions is  $y^* = 1.02x$ .

[Ans: 0.00122 kmol/(m<sup>2</sup>)(hr)(kPa)]

**4.8 Overall Mass Transfer Coefficient For Carbon Dioxide-Water System In Packed Bed Scrubber:** Determine the overall mass transfer coefficient in a water scrubber when carbon dioxide is absorbed from a gas. The scrubber is supplied with 5000 m<sup>3</sup>/hr of a gas mixture, considering it to be at atmospheric pressure and the operating temperature of 20°C. Pure water is fed to the scrubber at a rate of 650 m<sup>3</sup>/hr. The initial content of carbon dioxide in the gas is 28.4% (by volume), the final content (at the top of the scrubber) is 0.2% (by volume). The pressure in the scrubber is 16.5 atm. The bottom part of the scrubber is packed with 3 tons of ceramic rings 50 # 50 # 5 mm in size. Above them are 17 tons of rings 35 # 35 # 4 mm in size. Assume that the coefficient of packing wetting equals unity. The bulk densities of 50 # 50 # 4 mm and 35 # 35 # 4 mm ring packings are 530 and 505 kg/m<sup>3</sup>, respectively; the unit surface areas of 50 # 50 # 4 mm and 35 # 35 # 4 mm ring packings are 87.5 and 140 m<sup>2</sup>/m<sup>3</sup>, respectively. Henry's coefficient for carbon dioxide at 20°C is 1.08 × 10<sup>6</sup> mm Hg, i.e. 0.144 × 10<sup>6</sup> kPa.

[Ans: 0.0095 kg/(m<sup>2</sup>)(hr)(kPa) or 1.02 kg/(m<sup>2</sup>)(hr)(atm) or 0.0013 kg/(m<sup>2</sup>)(hr) (mm Hg)]

**4.9 Calculation of the Rate of Absorption of Carbon Dioxide in Water:** A mixture of 20% carbon dioxide and 80% air at a pressure of 1 atm and a temperature of 293.15 K is absorbed by water in a wetted-wall column of diameter 20 mm and length 200 mm. Calculate the rate of absorption of carbon dioxide in mol/hr, if the flow rate of water is 15.0 kg/hr.

Given: Henry's constant = 0.142 × 10<sup>4</sup> atm, n<sub>L</sub> = 1.0 × 10<sup>-3</sup> Pa·s, t<sub>L</sub> = 1000 kg/m<sup>3</sup>, and diffusivity of CO<sub>2</sub> in H<sub>2</sub>O = 1.7 × 10<sup>-9</sup> m<sup>2</sup>/s.

Following relationship may be used:

$$k(x) = (D/r_i)^{0.5} = (D\$u_{\max}/rx)^{0.5}$$

$$\text{or, } k_{av} = \left(\frac{1}{L}\right) \int_0^L k(x) dx = 1.128 (D\$u_{\max}/L)^{0.5}$$

[Ans: 2.16 × 10<sup>-2</sup> mol/hr]

[Hints: Calculate the thickness (d) of the falling film, and the maximum velocity, u<sub>max</sub>]

**4.10 Estimation of Amount of Oxygen Absorbed by a Bubble:** A 3 mm diameter air bubble is introduced into water from the bottom of a container of depth 0.5 m. Calculate the amount of oxygen absorbed by single bubble if it rises at a velocity of 2 m/s, the pressure inside the bubble is 1 atm (101.325 kPa), and the temperature of water is 20 °C.

Henry's constant for, and Diffusion coefficient of, oxygen in water at 20°C are 4052 MPa and 2.08 × 10<sup>-9</sup> m<sup>2</sup>/s, respectively.

[Ans: 1.65 × 10<sup>-10</sup> mol/bubble]

**4.11 Gas Phase Mass Transfer Coefficient Using Correlation:** Determine the individual mass transfer coefficient for the gaseous phase in a packed absorber used to absorb sulphur dioxide from an inert gas (nitrogen) under atmospheric pressure. The temperature in the absorber is

20°C and it operates in film conditions. The velocity of the gas in the absorber (fictitious) is 0.35 m/s. The absorber is filled with coke (free volume in  $\text{m}^3$  of voids per  $\text{m}^3$  of packed volume, i.e. unit void area in a column section in  $\text{m}^2/\text{m}^2$  is  $0.58 \text{ m}^3/\text{m}^3$  and the unit surface area in  $\text{m}^2$  of dry packing per  $\text{m}^3$  of packed volume is  $42 \text{ m}^2/\text{m}^3$ ). You may use the following correlation:

$$\text{Sh}_g = 0.407 \text{ Re}_G^{0.655} \text{ Sc}_G^{0.33}$$

[Ans:  $144 \# 10^{-4} \text{ m/s}$ ]

### **Short and Multiple Choice Questions**

1. State with reasons which phase resistance controls during absorption of a highly soluble gas.
2. State with reasons whether overall mass transfer coefficients, determined at a given solute concentration, can be used at other solute concentrations when the equilibrium relation is not linear.
3. Why do values of  $K_x$  and  $K_y$  differ although they represent the same overall coefficient?
4. Why do values of  $(y_{AG} - y^*_A)$  and  $(x^*_A - x_{AL})$  of a gas-liquid system differ while they represent the same driving force in terms of mole fraction?
5. What are the main drawbacks of the two-film Theory of interphase mass transfer?
6. What are the main objections against the penetration and surface renewal theories of interphase mass transfer?
7. How does the time of exposure of surface elements of one fluid to the other fluid as assumed in the penetration theory, differ from that assumed in the Surface renewal theory?
8. According to the film theory, mass transfer coefficient ( $k$ ) and diffusivity ( $D$ ) are related as  
 (a)  $k \propto D$  (b)  $k \propto \sqrt{D}$  (c)  $k \propto D^{1.5}$  (d)  $k \propto D^2$ .
9. The penetration theory relates average mass transfer coefficient ( $k$ ) with diffusivity ( $D$ ) as  
 (a)  $k \propto D$  (b)  $k \propto \sqrt{D}$  (c)  $k \propto D^{1.5}$  (d)  $k \propto D^2$ .
10. Which of the following is not a unit of mass transfer coefficient?  
 (a)  $\frac{\text{moles transferred}}{(\text{time})(\text{area})(\text{mole fraction})}$   
 (b)  $\frac{\text{moles transferred}}{(\text{time})(\text{area})(\text{pressure})}$   
 (c)  $\frac{\text{moles transferred}}{(\text{time})(\text{area})(\text{mass A/mass B})}$   
 (d) none of these.
11. Which of the following theories states that the mass transfer coefficient is directly proportional to  $D_{AB}^{0.5}$ ?

- (a) penetration
- (b) surface renewal
- (c) film
- (d) none of these

12. For boundary layer development on a flat plate during convective mass transport the hydrodynamic, thermal and concentration boundary layer will be same if
- (a)  $\text{Pr} = \text{Sc}$
  - (b)  $\text{Pr} = \text{Sc} = \text{Le}$
  - (c)  $\text{Sc} = \text{Le}$
  - (d)  $\text{Pr} = \text{Le}$ .

13. For laminar boundary layer flow past a flat plate oriented at zero angle of incidence, the average mass transfer coefficient,  $(\text{Sh})_{\text{mean}}$  is equal to

- (a)  $0.332(\text{Re})^{0.5} (\text{Sc})^{0.33}$
- (b)  $0.0298(\text{Re})^{0.8} (\text{Sc})^{0.33}$ ,
- (c)  $0.664(\text{Re})^{0.5} (\text{Sc})^{0.33}$
- (d)  $0.036(\text{Re})^{0.8} (\text{Pr})^{0.33}$

*Answer to Multiple Choice Questions*

8. (a) 9. (b) 10. (d) 11. (a) 12. (a)

13. (c)

## **References**

- Bird, R.B., W.E. Stewart and E.N. Lightfoot, *Transport Phenomena*, 2nd ed., Wiley India, New Delhi (2006).
- Danckwerts, P.V., *Ind. Eng. Chem.*, **43**, 1460 (1951).
- Gordon, K.F. and T.K. Sherwood, *AICHE J*, **1**, 129 (1955).
- Higbie, R., *Trans. AICHE*, **31**, 365 (1935).
- Lewis, W.K. and W. Whitman, *Ind. Eng. Chem.*, **16**, 1215 (1924).
- Schrage, R.W., *A Theoretical Study of Interphase Mass Transfer*, Columbia University Press, New York (1953).
- Scriven, L.E. and R.L. Pigford, *AICHE J*, **5**, 397 (1959) .
- Skelland, A.H.P., *Diffusional Mass Transfer*, John Wiley, New York (1974).
- Stewart, W.E., J.B. Angelo and E.N. Lightfoot, *AICHE J*, **16**, 771 (1970).
- Toor, R.L. and J.M. Marchelo, *AICHE J*, **4**, 97 (1958).
- Treybal, R.E., *Mass Transfer Operations*, 3rd ed., McGraw Hill, Singapore (1985).





# 5

# Methods of Operation and Computation

## 5.1 Introduction

Mass transfer operations involve transfer of one or more component(s) from one phase to another which in turn depends on transfer within each phase caused by concentration gradient. Such transfer takes place in the direction of decreasing concentration till attaining equilibrium in the system. There shall be no mass transfer in a system if the phases are in equilibrium. In any mass transfer operation, equilibrium must therefore be initially avoided. Moreover, the rate of mass transfer being proportional to the driving force, which is departure from equilibrium, the farther away the phases are from equilibrium the higher is the rate of transfer. A knowledge about equilibrium between phases is therefore essential in the study of mass transfer.

The phase rule plays an important role in classification of equilibrium and in determination of the number of independent variables available under a given situation. It is expressed as:

$$F = C - P + 2$$

where,

$F$  = degrees of freedom

$C$  = number of components

$P$  = number of phases.

The degree of freedom denotes the independent intensive variables such as temperature, pressure and concentration that must be fixed to define equilibrium of a system. Thus in a gas-liquid system having only two components, if the pressure is fixed then only one of the other variables like temperature, gas composition and liquid composition can be changed independently. For such systems, equilibrium data are usually represented by temperature-composition diagrams at constant pressure or by equilibrium diagrams. The latter is also known as  $y-x$  diagram and presents gas composition as a function of liquid composition at equilibrium. Equilibrium data may be presented in the form of equations, tables and graphs.

Further discussions on equilibrium pertinent to individual operation like absorption, distillation, etc., have been dealt with in respective chapters.

## 5.2 Stage-wise Contact

Mass transfer operations are conducted in two distinct ways, stage-wise contact and continuous differential contact.

A stage is a device or a combination of devices in which two immiscible or partially miscible phases are brought into intimate contact so that interphase mass transfer can take place between them followed by separation of the phases.

An equilibrium or theoretical stage is one in which the time of contact between the two phases is sufficiently large for them to attain equilibrium so that the two streams leaving the stage are in equilibrium.

In continuous contact equipment, on the other hand, mass transfer takes place in continuous differential manner without any intermediate separation and recontacting of the phases. The choice of method depends mainly on the type of equipment being used. For instance, distillation, leaching and sometimes liquid extraction are carried out in equipment like mixer-settlers, diffusion batteries or plate towers which contain a series of discrete units or stages for contact and separation of phases. On the other hand, gas absorption, humidification, water cooling, etc. are generally carried out in packed towers or similar equipment which operate as continuous differential contact units.

The main types of stage-wise and continuous contact operations and the basic principles of their computation have been discussed in the following sections. For their simplicity and wide application, gas absorption and liquid-liquid extraction have been chosen to explain the steps involved in these calculations. The same methods with appropriate modifications can be extended to any other system. Our discussions will be limited to transfer of only one component from one phase to another.

### 5.2.1 Single-Stage Operation

Figure 5.1 represents a single-stage mass transfer operation. The rectangle in the figure is a stage and serves both as a mixer and a settler. In practice, however, these two operations are often carried out in separate units.

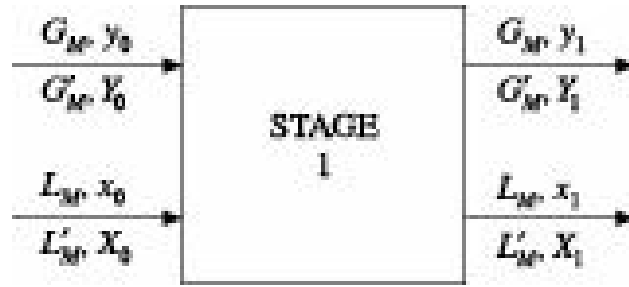


**Figure 5.1** Flow diagram of single-stage mass transfer operation.

The flow rates of solute-free phases  $G$  and  $L$ ,  $G$  being the lighter phase, are  $G'_M$  and  $L'_M$  moles per unit time respectively. The stoichiometric molal ratios of solute in  $G$  and  $L$  are  $Y_0$  and  $X_0$ , respectively during entry and they change to  $Y_1$  and  $X_1$ , respectively at the exit.

From material balance around the stage,

$$G'_M Y_0 + L'_M X_0 = G'_M Y_1 + L'_M X_1 \quad (5.1)$$

and from equilibrium relation, we get

$$Y^* = f(X) \quad (5.2)$$

For removal of a single component from a dilute mixture, the changes in flow rates of the phases may be neglected without much error and Eq. (5.1) may be written as

$$G_M(y_0 - y_1) = L_M(x_1 - x_0) \quad (5.3)$$

where  $G_M$  and  $L_M$  are average flow rates of total  $G$  and total  $L$  respectively, assumed to be constant, and  $y$  and  $x$  are mole fractions of solute in  $G$  and  $L$  respectively.

The operation can be represented graphically on  $y$ - $x$  diagram as shown in Figure 5.2. Point  $A$

represents the composition of phases  $G$  and  $L$  at entrance and their compositions change along the line  $ABC$  having a slope of  $(-L_M/G_M)$  as per Eq. (5.3). If the stage is an equilibrium stage, the line  $ABC$  will meet the equilibrium line at  $C$  and the exit compositions of the two phases will be at equilibrium  $(y_1^*, x_1^*)$ . In practice, equilibrium cannot be attained since that would require infinite time of contact. Depending upon the rate of transfer and the equilibrium relations, the composition will change along  $ABC$  and stop at some intermediate point  $B$  having compositions  $y_1$  and  $x_1$ .

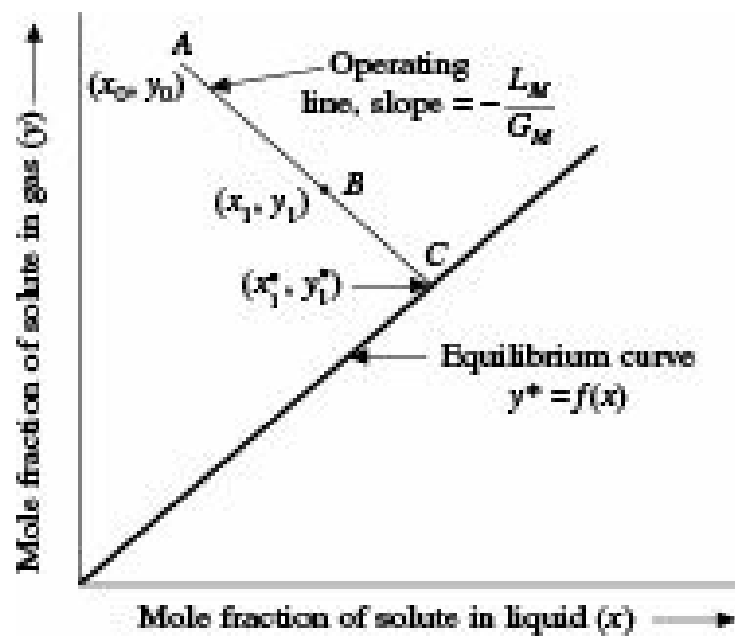


**Figure 5.2** Graphical representation of single-stage mass transfer operation.

The performance of a real stage is expressed in terms of stage efficiency defined as the ratio of actual composition change to that which would occur if equilibrium was reached.

Referring to Figure 5.2,

$$E = \frac{\frac{y_0 - y_1}{y_0 - y_1^*}}{\frac{x_1 - x_0}{x_1^* - x_0}} = \frac{\overline{AB}}{\overline{AC}} \quad (5.4)$$

The concept of equilibrium stage is useful in the mathematical analysis of stage-wise contact. The knowledge of stage efficiency may be obtained from literature or from experimental data.

**EXAMPLE 5.1** (Mass Transfer in a Single-stage Operation): 200 kg of water at 20°C containing 1.0 kg benzoic acid in solution is to be extracted with 80 kg benzene in a single ideal stage. Water and benzene are essentially insoluble.

What percentage of benzoic acid will be extracted?

The following equilibrium data may be used:

$$X': 0.0920 \ 0.1140 \ 0.1530 \ 0.2040 \ 0.2560 \ 0.399$$

$$Y: 0.1030 \ 0.1600 \ 0.2910 \ 0.5530 \ 0.7942 \ 0.010$$

where  $X'$  and  $Y$  are benzoic acid per 100 g of water and benzene, respectively.

**Solution:** 200 kg water contains 1.0 kg benzoic acid.

$$\frac{1.0}{200}$$

Therefore,  $X_F = \frac{1.0}{200} \ # 100 = 0.50$  kg benzoic acid per 100 kg water.

$$A = 200 \text{ kg}, B = 80 \text{ kg}, -\frac{(A)}{B} = -\frac{\frac{200}{100}}{80} = -2.5$$

From the given data the equilibrium line is drawn on Y-X co-ordinates in Figure 5.3.

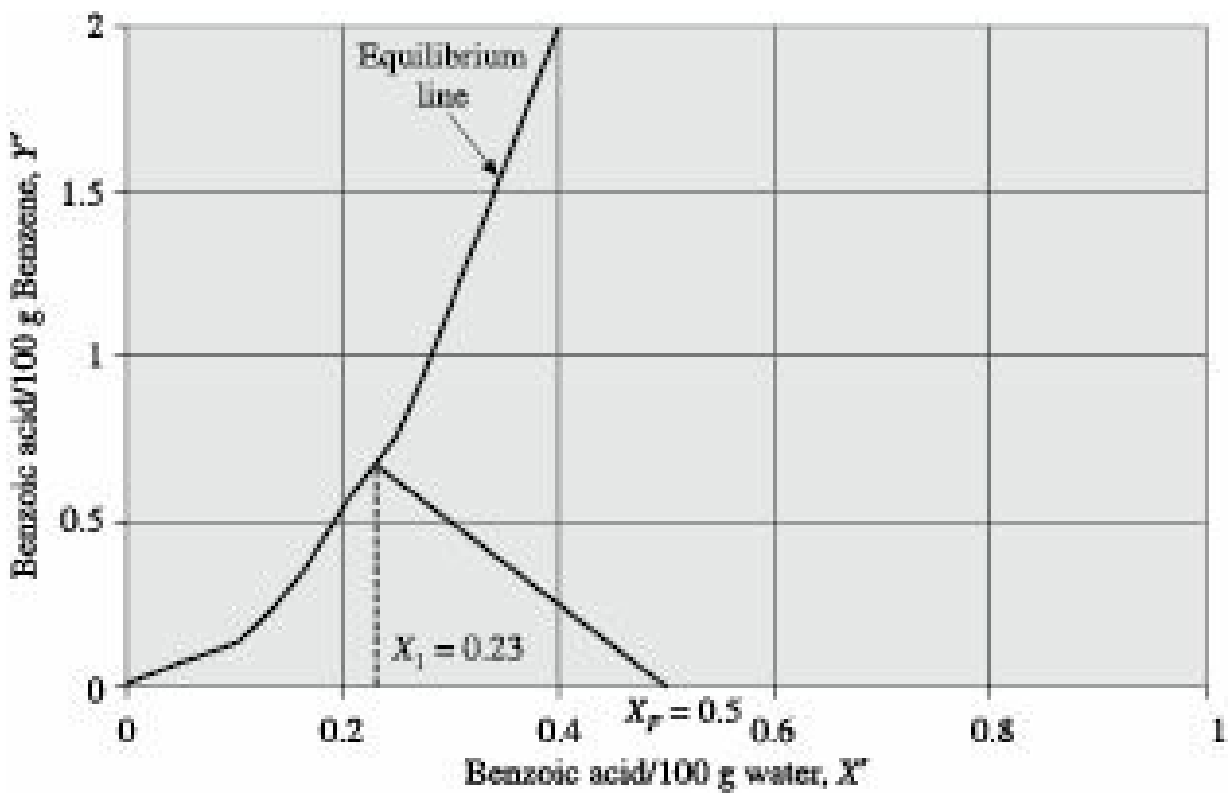


Figure 5.3 Example 5.1

The operating line is drawn from the point  $X_F = 0.50$ ,  $Y_F = 0$  having a slope of -2.5.

$$\frac{0.23 \text{ g benzoic acid}}{100 \text{ g water}}$$

From the figure,  $X_1 = \frac{0.23 \text{ g benzoic acid}}{100 \text{ g water}}$

$$\frac{0.23 \text{ kg benzoic acid}}{100 \text{ kg water}} =$$

$$\text{Benzoic acid in raffinate} = \frac{0.23 \text{ kg}}{100 \text{ kg water}}$$

$$\text{Benzoic acid extracted} = 0.50 - 0.23 = \frac{0.27 \text{ kg}}{100 \text{ kg water}}$$

$$\text{Percentage extraction} = \frac{0.27}{0.500} \# 100 = 54\%$$

## 5.2.2 Batch Operation

In batch operation which is always single stage, the two phases are added to a vessel with provision for stirring and mixed intimately till the desired transfer has taken place. The two phases approach equilibrium as stirring is continued. There is no flow of the phases during mass transfer. The material balance may be written as

$$G'_M (Y_0 - Y_1) = L'_M (X_1 - X_0) \quad (5.5)$$

Equation (5.5) is the equation to the operating line for batch operation and is a straight line when

plotted on  $Y$ - $X$  co-ordinates. For absorption of a single component from a dilute  $G$ , the material balance may be expressed in terms of total flow rates  $G_M$  and  $L_M$  and mole fractions  $y$ ,  $x$  when the equation to the operating line becomes identical with Eq. (5.3).

### 5.2.3 Multi-Stage Operation

The theoretical extent of mass transfer in a single-stage operation is limited by establishment of equilibrium. In practice, even this limit cannot be reached since that requires infinite time. The extent of transfer can, however, be increased by using more than one stage in cascade. A cascade may be defined as a group of inter-connected stages. Cascades may be of two types, cross-flow multi-stage cascades and counter-current multi-stage cascades.

### 5.2.4 Cross-Flow Cascade

Figure 5.4 represents a three stage cross flow cascade, each rectangle representing a stage. The  $G$  phase enters the first stage, flows through subsequent stages and is contacted with fresh  $L$  entering each stage separately. The flow rate of  $L$  may be different for different stages although they are usually kept the same. Each stage may have different stage efficiency. The exit solutions may be collected separately or may be delivered to a single pipe to yield a common solution.

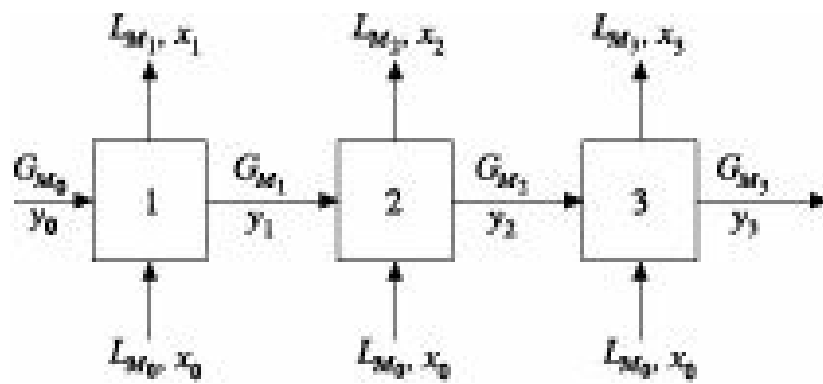


Figure 5.4 Flow diagram of cross-flow cascade for mass transfer.

If the variation in gas and liquid flow rates are neglected and compositions are expressed in terms of mole fractions, the material balance equation for each stage of cross-flow cascade becomes similar to Eq. (5.3) for single-stage operation with necessary modification of notations.

The graphical representation on  $y$ - $x$  diagram of the operation of a cross-flow cascade is shown in Figure 5.5. Cross-flow cascades are rarely used in gas absorption, although they have limited application in extraction, leaching, adsorption and drying.

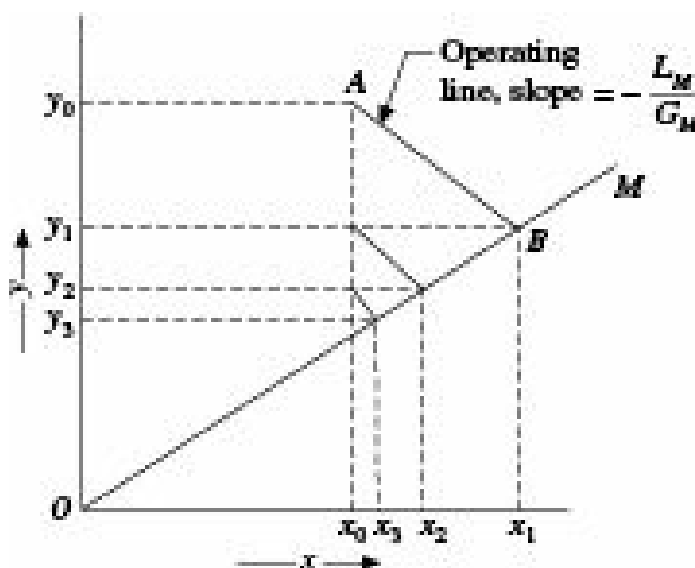


Figure 5.5 Graphical representation of cross-flow mass transfer operation.

**EXAMPLE 5.2** (Mass Transfer in a Three-stage Cross-flow Cascade): 200 kg of water at 20°C containing 1.0 kg benzoic acid in solution is extracted with benzene in three ideal stages using 62.5 kg benzene in each stage. Water and benzene are essentially insoluble.

What percentage of benzoic acid is extracted?

The equilibrium data given in Example 5.1 are applicable.

**Solution:** 200 kg water contains 1.0 kg benzoic acid.

$$\text{Therefore, } X_F = \frac{1.0}{200} \# 100 = 0.50 \text{ kg benzoic acid per 100 kg water.}$$

$$A = 200 \text{ kg}, B = 62.5 \text{ kg}, -\left(\frac{A}{B}\right) = -\left(\frac{200}{62.5}\right) = -3.2$$

From equilibrium data given in Example 5.1, the equilibrium line is drawn on Y-X co-ordinates in Figure 5.6.

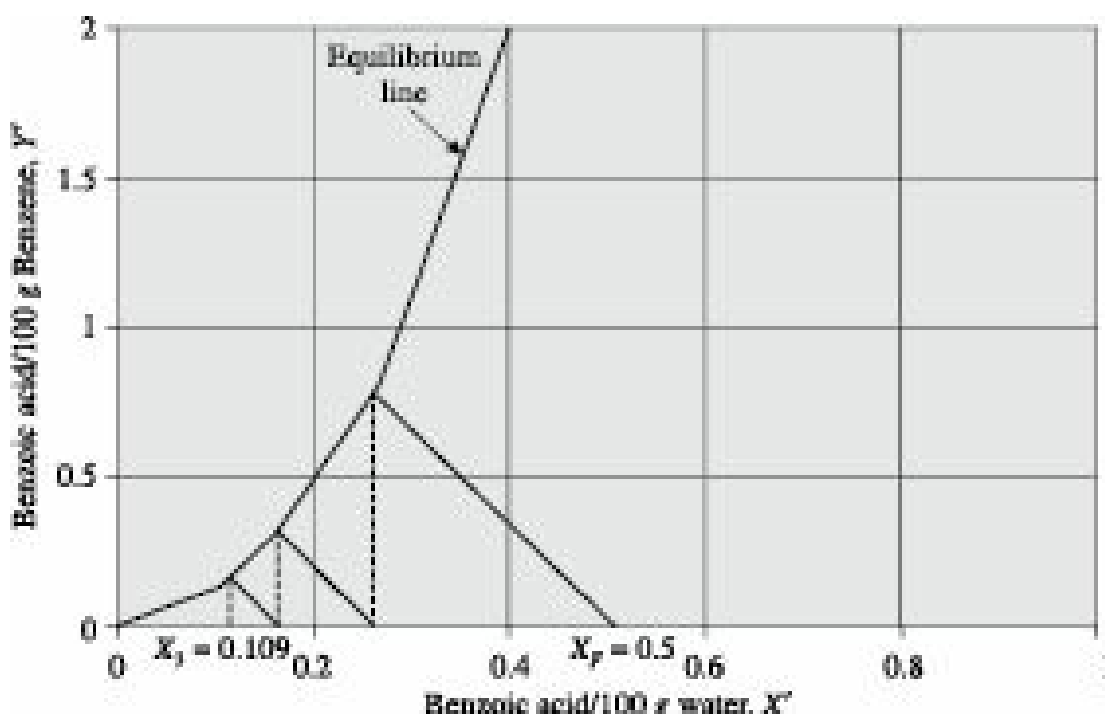


Figure 5.6 Example 5.2

Three parallel operating lines are then drawn starting from the point ( $X_F = 0.50$ ,  $Y_F = 0$ ), each with slope of -3.2.

From the figure,  $X_3 =$

$$= \frac{\frac{0.109 \text{ g benzoic acid}}{100 \text{ g water}}}{\frac{0.109 \text{ kg benzoic acid}}{100 \text{ kg water}}} = \frac{(0.50 - 0.109)}{100} = 0.00301 \text{ kg benzoic acid}$$

$$\text{Benzoic acid extracted} = \frac{0.00301}{100} \# 200 = 0.782 \text{ kg.}$$

$$\text{Percentage extraction} = \frac{0.782}{1.0} \# 100 = 78.2\%$$

### 5.2.5 Counter-Current Multi-Stage Cascade

A common method for appreciably increasing the extent of mass transfer with finite amount of  $L$  is to use multiple stages with counter-current flow of  $G$  and  $L$  streams as shown in Figure 5.7.

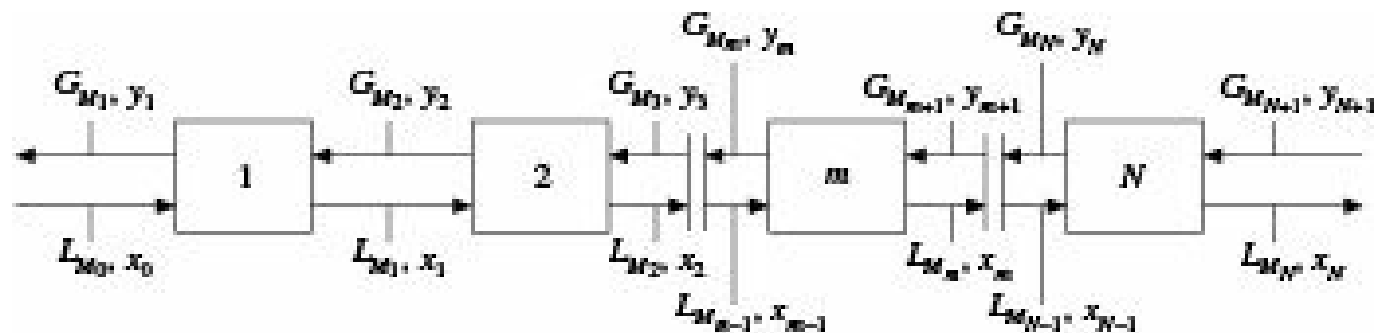


**Figure 5.7** Flow diagram of counter-current multi-stage mass transfer.

Although multi-stage counter-current cascades with separate units for each stage as shown in Figure 5.7 are in use, particularly in operations such as extraction, leaching, etc., the most common form of equipment for multi-stage counter-current contact for gas-liquid systems are plate columns. Each plate acts as a stage with gas-liquid separation taking place in the space between plates.

#### Graphical design method

Let us consider a counter-current absorption unit with  $N$  stages as shown in Figure 5.8.

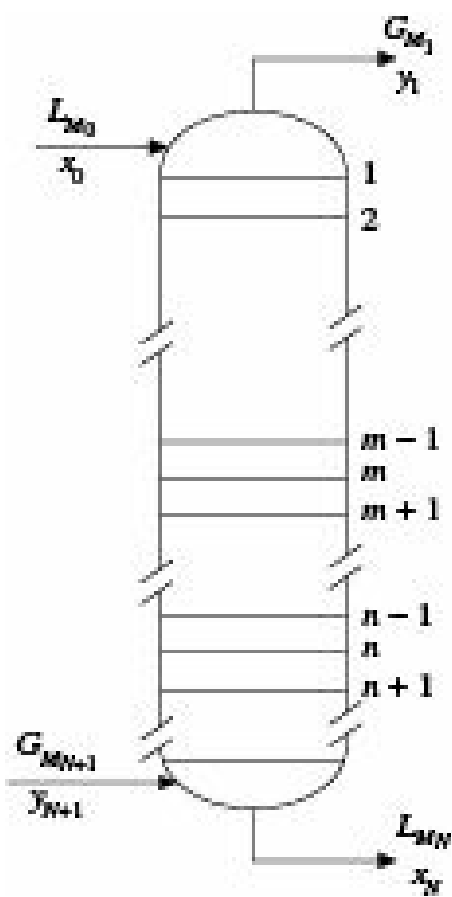


**Figure 5.8** Flow diagram of a multi-stage counter-current equipment (plate column).

Assuming that a single component is being absorbed from the phase  $G$  under steady state conditions at constant temperature and pressure, material balance around any plate  $n$  may be written as

$$G'_M Y_{n+1} + L'_M X_{n-1} = G'_M Y_n + L'_M X_n \quad (5.6)$$

where  $G'_M$  and  $L'_M$  are molal flow rates of solute-free  $G$  and  $L$  respectively which remain constant throughout the process.  $Y$  and  $X$  are molal stoichiometric ratios of solute to solute-free  $G$  and  $L$  respectively,

$$Y = \frac{y}{1-y} \text{ and } X = \frac{x}{1-x}$$

$y$  and  $x$  being mole fractions of solute in  $G$  and  $L$  respectively.

Rearranging Eq. (5.6), we obtain

$$Y_{n+1} = Y_n + \frac{L'_M}{G'_M} (X_n - X_{n-1}) \quad (5.7)$$

For dilute mixtures variations in flow rates of  $G$  and  $L$  may be neglected. Also,  $Y$  and  $X$  may be assumed to be equal to the corresponding mole fractions  $y$  and  $x$  without serious error. Eq. (5.7) then becomes

$$y_{n+1} = y_n + \frac{L_M}{G_M} (x_n - x_{n-1}) \quad (5.8)$$

It is convenient to locate the operating line from knowledge of the terminal compositions since these are set by design specifications. In terms of terminal compositions  $(Y_{N+1}, X_N)$  or  $(y_{N+1}, x_N)$ , Eqs.

(5.7) and (5.8) may be rewritten as

$$Y_{N+1} = Y_N + \frac{L'_M}{G'_M} (X_N - X_{N-1}) \quad (5.9)$$

$$\text{or, } y_{N+1} = y_N + \frac{L_M}{G_M} (x_N - x_{N-1}) \quad (5.10)$$

Similarly equations can be formed in terms of compositions of the other terminal ( $Y_1, X_0$ ) or ( $y_1, x_0$ ). The operating line can be plotted from knowledge of flow rates of the two phases as well as compositions of the entering and exit streams. The compositions of the entering streams are available from design specifications. The composition of the exit  $G$  can be estimated from the stipulated degree of absorption and that of the exit  $L$  can be calculated from material balance as under:

In terms of molal stoichiometric ratio

$$X_N = X_0 + \frac{\frac{G'_M (Y_{N+1} - Y_1)}{L'_M}}{(5.11)}$$

Similarly, in terms of mole fractions

$$\frac{L_M x_0}{L_M y_1} + \frac{G_M y_{N+1} - G_M y_1}{L_M y_1} x_N = (5.12)$$

For dilute systems, the flow rates  $G_M$  and  $L_M$  may be assumed constant or their average values may be used and mole fractions may be assumed to be approximately equal to molal stoichiometric ratios, so that Eq. (5.12) reduces to

$$x_N = x_0 + \frac{\frac{G_M (y_{N+1} - y_1)}{L_M}}{(5.13)}$$

The simplest method of locating the operating line when it is straight, is to draw a straight line through the two terminal points  $(x_0, y_1)$  and  $(x_N, y_{N+1})$ .

For determination of equilibrium stages or theoretical plates, equilibrium and operating lines are drawn on  $y$ - $x$  co-ordinates, the former from appropriate equilibrium relation/data for the system under the operating conditions and the latter by drawing a straight line through the points  $(x_0, y_1)$  and  $(x_N, y_{N+1})$  as shown in Figure 5.9. For concentrated systems which give rise to curved operating lines in mole fraction units, the operating line may be drawn in stoichiometric units by plotting Eq. (5.9) and the equilibrium curve may be drawn in terms of  $Y$  and  $X$ .

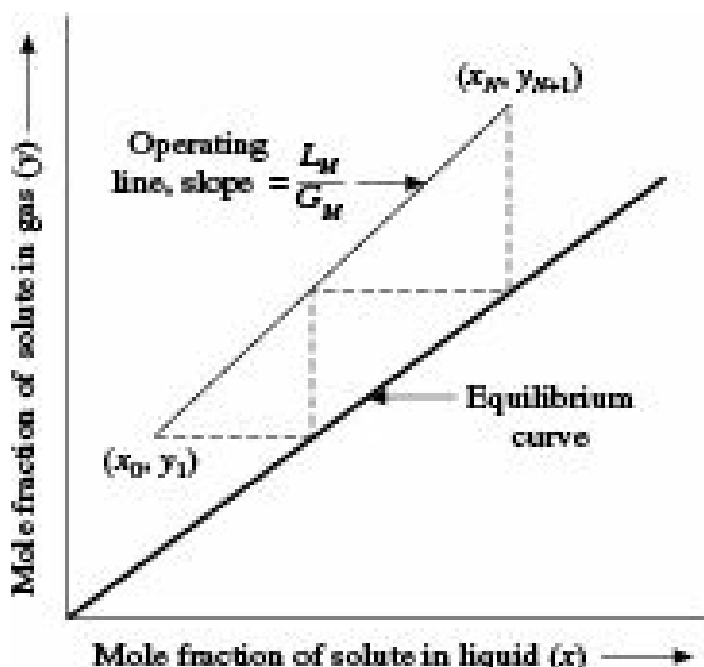


Figure 5.9 Graphical representation of counter-current mass transfer.

After locating the appropriate equilibrium and operating lines, the number of equilibrium stages or theoretical plates may be determined by drawing a vertical line from the point  $(x_N, y_{N+1})$  to the equilibrium line and then moving horizontally to the left to meet the operating line till attaining  $(x_0, y_1)$ . The number of steps so drawn gives the number of theoretical stages or plates required to bring about the change. Alternatively, steps may be drawn by starting at the point  $(x_0, y_1)$  and moving horizontally to the right and vertically upward between the operating and equilibrium lines till attaining  $(x_N, y_{N+1})$ .

**EXAMPLE 5.3** (Determination of Number of Theoretical Stages in Counter-Current Multi-Stage Operation): 1000 kg/hr of a solution of *C* in *A* containing 20% *C* by weight is to be extracted with 400 kg/hr of solvent *B* in a counter-current multi-stage extraction unit. *A* and *B* are mutually insoluble. The equilibrium distribution of component *C* between *A* and *B* at the temperature of extraction are as follows:

kg of *C* / kg of *A*: 0.050.200.300.450.500.54

kg of *C* / kg of *B*: 0.250.400.500.650.700.74

How many theoretical stages will be required to reduce the concentration of *C* in *A* to 5%?

**Solution:**

$$\text{Given, } F = 1000 \text{ kg}, A = 1000 (1 - 0.20) = 800 \text{ kg}$$

$$x_F = 0.20, X_F = \frac{0.20}{(1 - 0.20)} = 0.25$$

$$x_N = 0.05, X_N = \frac{0.05}{(1 - 0.05)} = 0.0526$$

$$B = 400 \text{ kg}, \frac{A}{B} = \frac{800}{400} = 2.0$$

As shown in Figure 5.10, the equilibrium line is drawn from the given data.

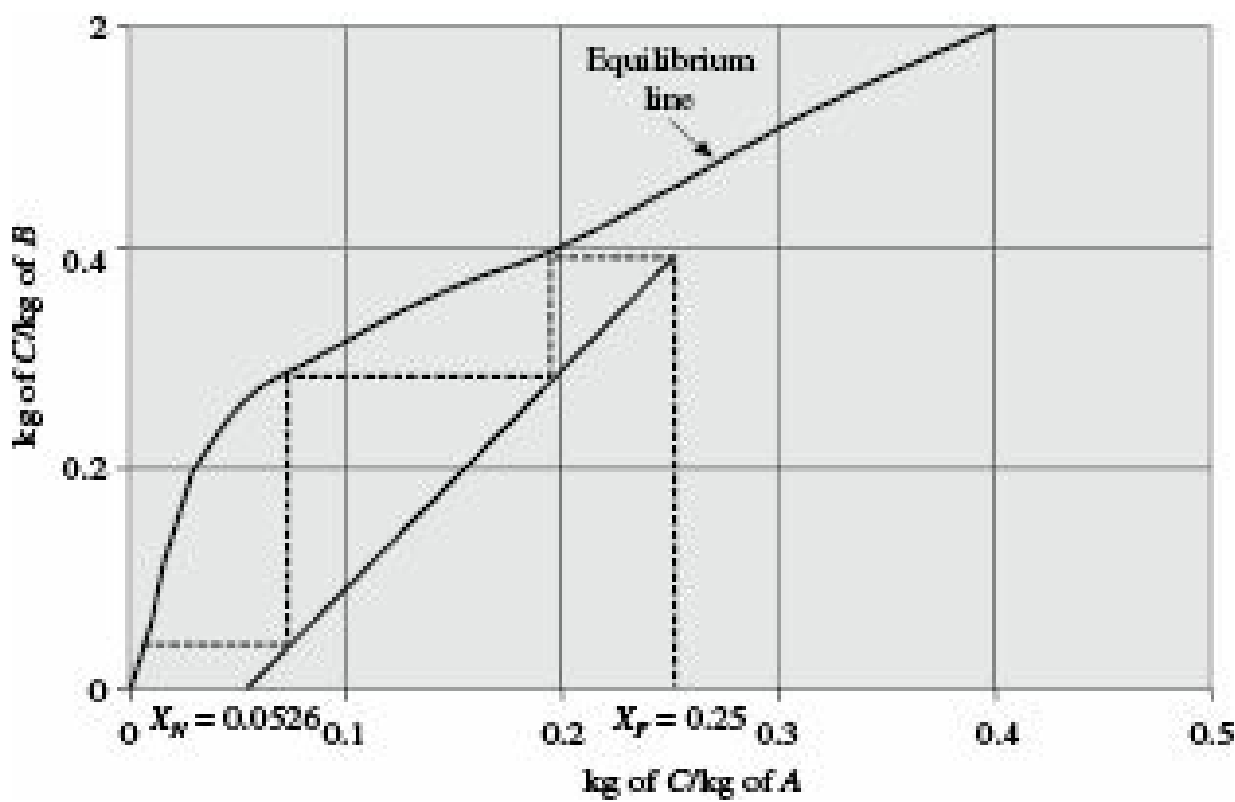


**Figure 5.10** Example 5.3

The operating line is drawn through the point (0.0526, 0) with a slope = 2.0.

By drawing steps between the equilibrium and operating lines, the required number of theoretical stages is found to be 2.25.

### **Algebraic method for lean gases**

In most absorption operations, the equilibrium curve is nonlinear and in some cases, particularly in absorption of rich gases, the operating line may also be curved. In such situations, graphical methods must be used for estimation of number of stages and compositions. However, if both equilibrium and operating lines are straight and the former passes through the origin, analytical solutions are possible. In such cases, the material balance equation around any plate  $n$  [Eq. (5.6)] may be combined with the equilibrium relation  $Y = mX$  and rearranged to give

$$Y_n = Y_{n+1} + \frac{L'_M}{G'_M} X_{n-1} - \frac{L'_M}{G'_M} X_n$$

$$\frac{L'_M}{mG'_M} = Y_{n+1} + \frac{L'_M}{mG'_M} Y_{n-1} - Y_n \quad (5.14)$$

$$\text{or, } Y_n = Y_{n+1} + AY_{n-1} - AY_n \quad (5.15)$$

$$\text{where, } A = \frac{L'_M}{mG'_M}$$

Solving for  $Y_n$ , we get

$$Y_n = \frac{Y_{n+1} + AY_{n-1}}{(A+1)} \quad (5.16)$$

$A$  is known as the *absorption factor* and is the ratio of the slope of the operating line to that of the equilibrium line. Absorption factor has considerable economic significance in gas absorption. For instance, if  $A < 1$ , the equilibrium and operating lines tend to converge near the bottom of the absorber which limits absorption. If on the other hand  $A > 1$ , any extent of absorption is possible if sufficient number of stages or trays are available. There is a value of  $A$  for which absorption is most economical. For rough estimates, the most economical value of  $A$  may be assumed to lie within the range of 1.25 to 2.0 (Colburn 1939).

Equation (5.16) may be rewritten for the entire column having  $N$  plates, using the terminal concentrations, which are usually set by design requirements. Thus referring to Figure 5.8,

$$\frac{Y_{N+1} + AY_{N-1}}{(A+1)} \quad Y_N = (5.17)$$

Considering an absorber with 1 plate ( $N = 1$ ), Eq. (5.17) becomes

$$Y_1 = \frac{Y_2 + AY_0}{(A+1)} \quad (5.18)$$

For an absorber with 2 plates ( $N = 2$ ),

$$Y_2 = \frac{Y_3 + AY_1}{(A+1)} = \frac{(A+1)Y_3 + A^2Y_0}{(A^2 + A + 1)} \quad (5.19)$$

and for an absorber with 3 plates ( $N = 3$ ),

$$Y_3 = \frac{Y_4 + AY_2}{(A+1)} = \frac{(A^2 + A + 1)Y_4 + A^3Y_0}{(A^3 + A^2 + A + 1)} \quad (5.20)$$

In this way, for an absorber with  $N$  plates

$$Y_N = \frac{(A^{N-1} + A^{N-2} + \dots + A^2 + A + 1)Y_{N+1} + A^N Y_0}{(A^N + A^{N-1} + \dots + A^2 + A + 1)} \quad (5.21)$$

Expressing the series in the numerator and denominator in terms of their summations and rearranging, we have

$$Y_N = \frac{(A^N - 1)Y_{N+1} + A^N(A - 1)Y_0}{(A^{N+1} - 1)} \quad (5.22)$$

Referring again to Figure 5.8, material balance between the top and the bottom of the column may be expressed as

$$G'_M Y_{N+1} + L'M X_0 = G'_M Y_1 + L'M X_N \quad (5.23)$$

which by expressing  $X_0$  and  $X_N$  in terms of  $Y_0$  and  $Y_N$  respectively and on rearrangement may be written as

$$Y_{N+1} + \frac{\frac{L'_M}{mG'_M}}{Y_0} Y_0 = Y_1 + \frac{\frac{L'_M}{mG'_M}}{Y_N} Y_N \quad (5.24)$$

$$\text{or, } Y_N = \frac{\frac{Y_{N+1} - Y_1}{A}}{A} \quad (5.25)$$

Equating Eqs. (5.22) and (5.25), we obtain

$$(Y_{N+1} - Y_1)(A^{N+1} - 1) = (Y_{N+1} - Y_0)(A^{N+1} - A) \quad (5.26)$$

$$\frac{Y_{N+1} - Y_1}{Y_{N+1} - Y_0} = \frac{A^{N+1} - A}{A^{N+1} - 1} \quad \text{or, (5.27)}$$

Replacing  $Y_0$  by  $mX_0$ , we get

$$\frac{Y_{N+1} - Y_1}{Y_{N+1} - mX_0} = \frac{A^{N+1} - A}{A^{N+1} - 1} \quad (5.28)$$

For a column with  $N$  theoretical stages or plates, left-hand side of Eq. (5.28) represents the ratio of the actual change in gas composition to the change in composition that would occur if the outgoing gas were in equilibrium with the incoming liquid.

Equation (5.28) is useful in calculating the number of theoretical stages or plates required for a given change in gas composition,

From Eq. (5.23), we have

$$Y_{N+1} + mAX_0 = Y_1 + mAX_N \quad (5.29)$$

$$\text{whence, } A = \frac{\frac{Y_{N+1} - Y_1}{m(X_N - X_0)}}{\frac{Y_{N+1} - Y_1}{Y_N - Y_0}} \quad (5.30)$$

From Eq. (5.28), we get

$$A^{N+1}(Y_{N+1} - Y_1) - Y_{N+1} + Y_1 = A^{N+1}(Y_{N+1} - mX_0) - AY_{N+1} + mAX_0 \quad (5.31)$$

$$\text{or, } A^{N+1}(Y_1 - mX_0) = AY_{N+1} - mAX_0 - Y_{N+1} + Y_1 \quad (5.32)$$

which on rearrangement gives

$$N = \frac{\ln \left[ \left( \frac{Y_{N+1} - mX_0}{Y_1 - mX_0} \right) \left( 1 - \frac{1}{A} \right) + \frac{1}{A} \right]}{\ln A} \quad (5.33)$$

Equation (5.33), suggested by Colburn (1941), permits direct estimation of the number of theoretical stages or plates. This equation is useful when the number of stages or plates is known. It is also useful in visualizing the effect of varying  $(mG_M/L_M)$  or number of plates on the separation. Graphical solutions of Eq. (5.33) in the form of

$$\frac{Y_{N+1} - mX_0}{Y_1 - mX_0} \text{ vs } N$$

for different values of  $(mG_M/L_M)$  are available in the literature (Treybal 1985).

When  $A = 1$ , Eq. (5.28) becomes indeterminate. It may however be shown that for such condition,

$$\frac{Y_{N+1} - Y_1}{Y_{N+1} - mX_0} = \frac{N}{N+1} \quad (5.34)$$

$$\text{whence, } N = \frac{\frac{Y_{N+1} - Y_1}{Y_1 - mX_0}}{\frac{mX_0}{Y_1}} \quad (5.35)$$

Equations (5.28), and (5.33) to (5.35) are known as Kremser equations (Kremser 1930).

In case of low absorption from lean gases, variations in total gas or liquid flow rates may be neglected and average values of  $G_M$  and  $L_M$  may be used along with compositions in mole fraction without any serious error. In such cases, Eqs. (5.28), (5.30), and (5.33) to (5.35) may be expressed in terms of  $G_M$ ,  $L_M$ ,  $x$  and  $y$  for rough estimation of the number of theoretical stages or plates.

### 5.2.6 Design Procedure for Concentrated Gases

For concentrated gases, the graphical method may be applied rigorously for the absorption of a component present in high concentration provided the design diagram takes into account curvature in the operating line due to changes in gas and liquid flow rates and curvature in the equilibrium curve from nonideal solubility. Temperature changes due to high heat of absorption may also have significant effect on the equilibrium relation throughout the column.

## 5.3 Continuous Differential Contact

In contrast to stage-wise contact, there may be continuous contact between the two phases without any intermediate separation. For instance, in packed tower liquid moves over the packing and gas flows through the solid-liquid matrix coming in continuous contact with the liquid so that there is continuous differential mass transfer between them. Packed towers for gas absorption usually operate with counter current flow of gas and liquid.

### 5.3.1 Material Balance—The Operating Line

In steady-state continuous mass transfer processes, as the two phases move through the equipment, the solute concentration in each phase undergoes continuous change because of transfer of solute from one phase to the other. Similarly, in batch processes the concentration in each phase changes with time. These changes cause variation in the driving force which can be followed with the help of material balance as shown below for cocurrent and counter-current processes.

#### *Steady-state co-current process*

Let us consider a steady-state co-current mass transfer process as shown in Figure 5.11. The two insoluble phases  $G$  and  $L$  flow in the same direction,  $G$  being the lighter phase. Let us further assume that only one component A diffuses from phase  $L$  to phase  $G$ .

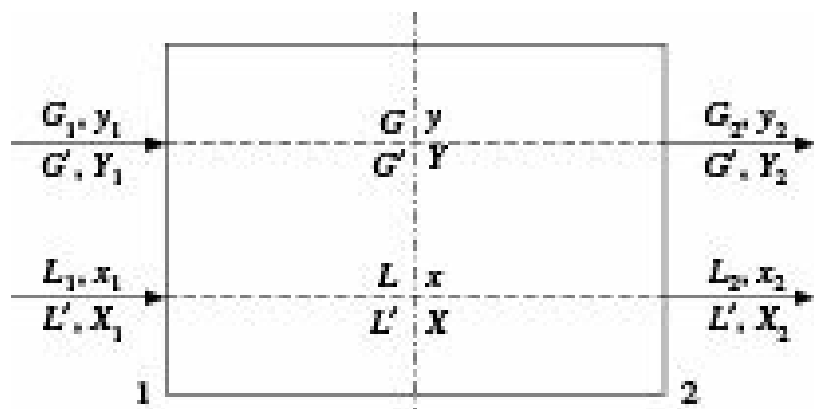


**Figure 5.11** Flow diagram for steady-state differential cocurrent contact.

By a material balance over the entire equipment

$$G_1y_1 + L_1x_1 = G_2y_2 + L_2x_2 \quad (5.36)$$

$$\text{or, } G_1y_1 - G_2y_2 = L_2x_2 - L_1x_1 \quad (5.37)$$

$$\frac{y_1}{1-y_1} \text{ But } G_1y_1 = G' = G'Y_1 \text{ and } G_2y_2 = G'Y_2 \quad (5.38)$$

$$\frac{1-y_1}{y_1} \text{ Similarly, } L_1x_1 = L'X_1 \text{ and } L_2x_2 = L'X_2 \quad (5.39)$$

where,  $y$  and  $x$  are mole fractions of solute  $A$  in phases  $G$  and  $L$  respectively,  $Y$  and  $X$  are mole ratios of solute  $A$  in phases  $G$  and  $L$ , respectively on  $A$ -free basis,  $G'$  and  $L'$  are molal mass velocities of solute-free phases  $G$  and  $L$ , respectively.

Substituting Eqs. (5.38) and (5.39) in Eq. (5.37), we get

$$G'(Y_2 - Y_1) = L'(X_1 - X_2) \quad (5.40)$$

Equation (5.40) is an equation to a straight line having a slope of  $(L'/G')$  and passing through the points  $(X_1, Y_1)$  and  $(X_2, Y_2)$ .

In a similar way, by making a material balance up to any intermediate point of the equipment where the concentrations of  $A$  in the two phases  $G$  and  $L$  are  $Y$  and  $X$  respectively, we get

$$G'(Y - Y_1) = L'(X_1 - X) \quad (5.41)$$

Equation (5.41) is also an equation to a straight line having a slope of  $(L'/G')$  and passing through the points  $(X_1, Y_1)$  and  $(X, Y)$ . Since the two straight lines represented by Eqs. (5.40) and (5.41) have the same slope and one point in common, they are the same straight line.

In Figure 5.12, the equilibrium relationship in terms of  $X$  and  $Y$  is shown by the curve  $OC$ . The straight line  $QP$  represents the material balance and is called the *operating line*.

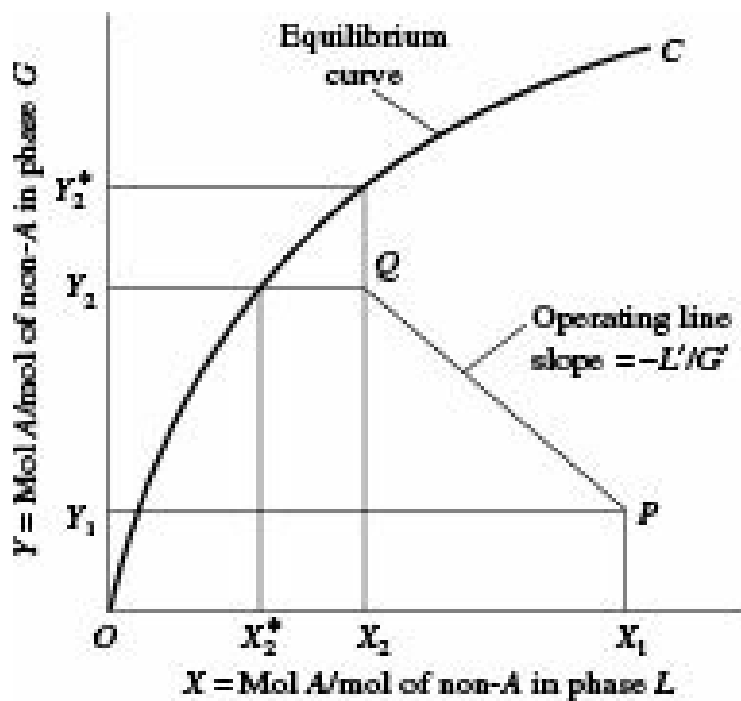


**Figure 5.12** Graphical representation of steady-state differential co-current contact. Transfer from  $L$  phase to  $G$  phase.

The operating line is a graphical representation of the material balance. A point on this line represents the bulk average concentration of the streams in contact with each other at any section of the equipment.

In case of diffusion from phase  $G$  to phase  $L$  as in case of gas absorption, the operating line will lie on the opposite side of the equilibrium curve as shown in Figure 5.12.

### Steady-state counter-current process

The advantage of the counter-current process over the co-current one is that for counter-current process the average driving force for a given situation is higher resulting in either smaller sized equipment for a given set of flow conditions or lower flow rates for a given size of equipment.

If the transfer process is carried out in steady-state counter-current fashion as shown in Figure 5.13, where the subscripts 1 indicate that end of the equipment where phase  $G$  enters.

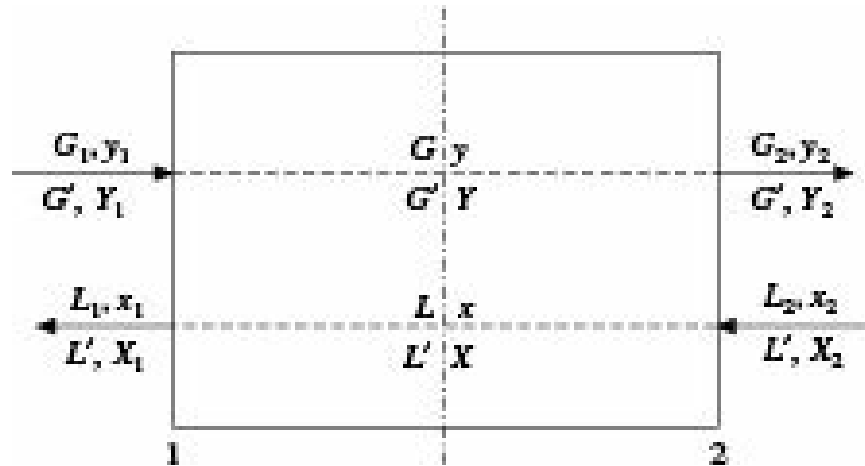


**Figure 5.13** Flow diagram for steady-state differential counter-current contact.

The material balance over the entire unit becomes

$$G_1 y_1 + L_2 x_2 = G_2 y_2 + L_1 x_1 \quad (5.42)$$

$$G'(Y_1 - Y_2) = L'(X_1 - X_2) \quad (5.43)$$

For any section of the equipment where the concentrations are  $X$  and  $Y$ ,

$$Gy + L_1x_1 = G_1y_1 + Lx \quad (5.44)$$

$$\text{and } L'(X_1 - X) = G'(Y_1 - Y) \quad (5.45)$$

Equations (5.42) and (5.43) give the total material balance while Eqs. (5.44) and (5.45) give the general relationship between concentrations in the phases at any section of the equipment. Eq. (5.43) is that of a straight line on  $Y-X$  co-ordinates having a slope of  $(L'/G')$  and passing through the points  $(X_1, Y_1)$  and  $(X_2, Y_2)$  as shown in Figure 5.14.

The line will be above the equilibrium curve if diffusion is from phase  $G$  to phase  $L$ , and below the equilibrium line if diffusion is in the opposite direction. For diffusion from phase  $G$  to phase  $L$ , at a point where the phases are represented by the point  $P$ , the driving force line is given by  $PM$  whose slope depends upon the relative diffusional resistances of the phases. The magnitude of the driving force changes from one end of the equipment to the other. If the operating line touches the equilibrium curve at any point so that the two phases reach equilibrium, the driving force and hence the rate of mass transfer becomes zero and the time required for a finite material transfer becomes infinite.

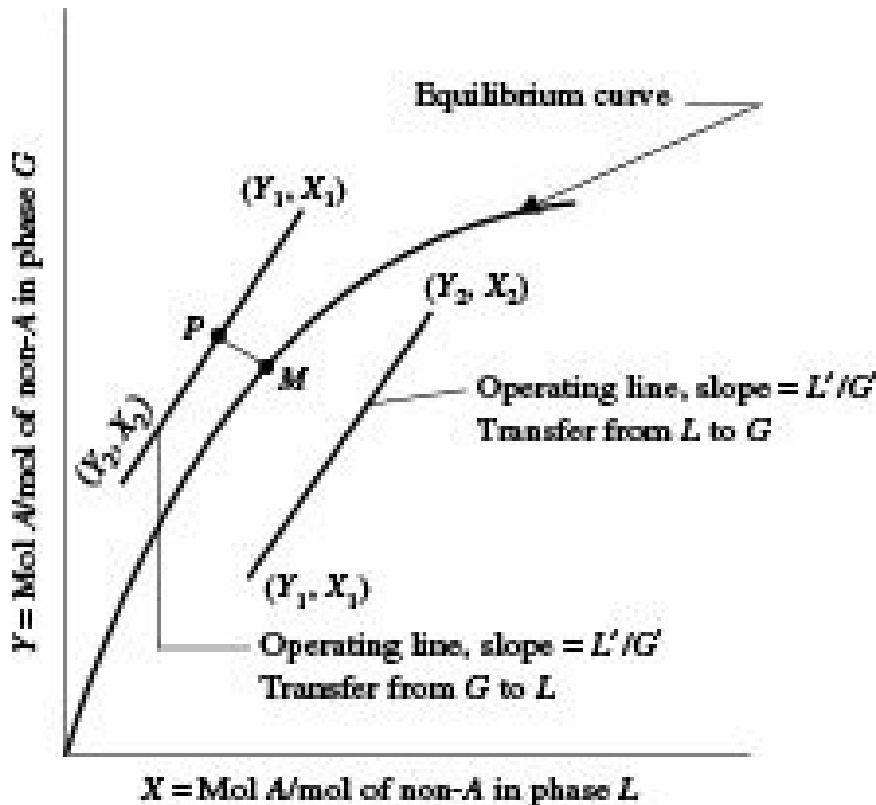


Figure 5.14 Graphical representation of steady-state differential counter-current contact.

Both in cases of co-current and counter-current processes of mass transfer, linearity of the operating line depends upon the method of expressing the concentrations. In the present case, they are straight lines because mole ratio concentrations  $X$  and  $Y$  are based on solute-free flow rates  $G'$  and  $L'$  which do not change during the process. If mole fractions or partial pressures are used to express concentration, the operating lines will be curved.

### 5.3.2 Estimation of Tower Height

The following section discusses estimation of tower height.

## **Height Equivalent to a Theoretical Plate (HETP)**

This is an old method for estimation of tower height. But it ignores the difference between stage-wise and continuous contact. In this method, the number of theoretical plates or trays required for a given change in concentration is first determined by using the method of computation for stage-wise contact. This number is then multiplied by a quantity known as the HETP to get the required height of packing to achieve the same change in concentration

$$Z = (\text{HETP}) \# N (5.46)$$

where  $Z$  and  $N$  represent the total height of packing and number of theoretical or equilibrium stages respectively. Many designers prefer to use the HETP approach because it provides a comparison with the number of theoretical stages determined with tray column.

The HETP is evaluated simply as the ratio of packed height used for a certain degree of separation to the theoretical number of stages. Its relation to the fundamental quantity, HTU- the height of a transfer unit, is

$$\frac{\ln(mG_M/L_M)}{(mG_M/L_M) - 1} \quad \text{HETP} = \text{HTU} \quad (5.47)$$

where,  $m$  is the slope of the equilibrium curve. In distillation, the equilibrium and operating lines diverge below the feed point and converge above it. As a result the value of  $(mG_M/L_M)$  averages approximately unity for distillation so that HETP and HTU become essentially equal. However, this is not true in absorption and stripping processes. Figure 5.15(a) shows that the magnitude of number of theoretical stages per metre depends on the size of packing as well as on the system conditions. The variation of HETP value as shown in Figure 5.15(b), indicates its dependency on the geometry of packing and also on the gas flow rate.

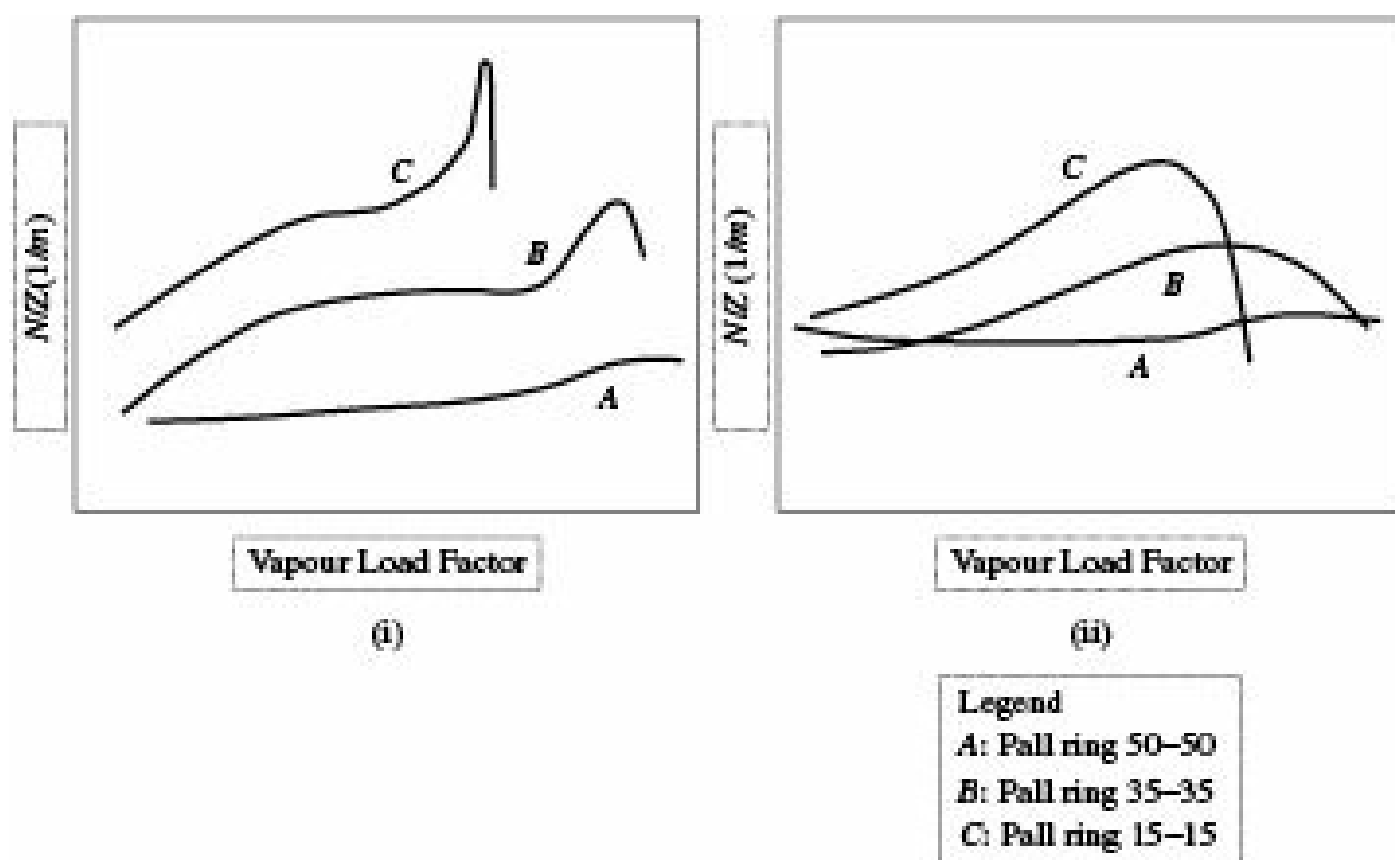


**Figure 5.15(a)** Number of theoretical stages per m. ( $1/\text{HETP}$ ),  $L/G = 1$  for (i) Methanol/Ethanol, and (ii) Ethylbenzene/Styrene system.

This method has also two fundamental drawbacks. Firstly, it ignores the basic difference between stage-wise and continuous contact. Secondly, the HETP must be an experimentally determined quantity which strongly depends on several factors like the system and the concentration changes involved, the flow rates of the fluids and the type and size of packing. Enormous quantity of data must be accumulated to make use of this method. HETP values for a wide range of packing used in industrial separations are available in literature (Kister 1992, Peters and Timmerhaus 1991). A glimpse of some data is given Table 15.1.

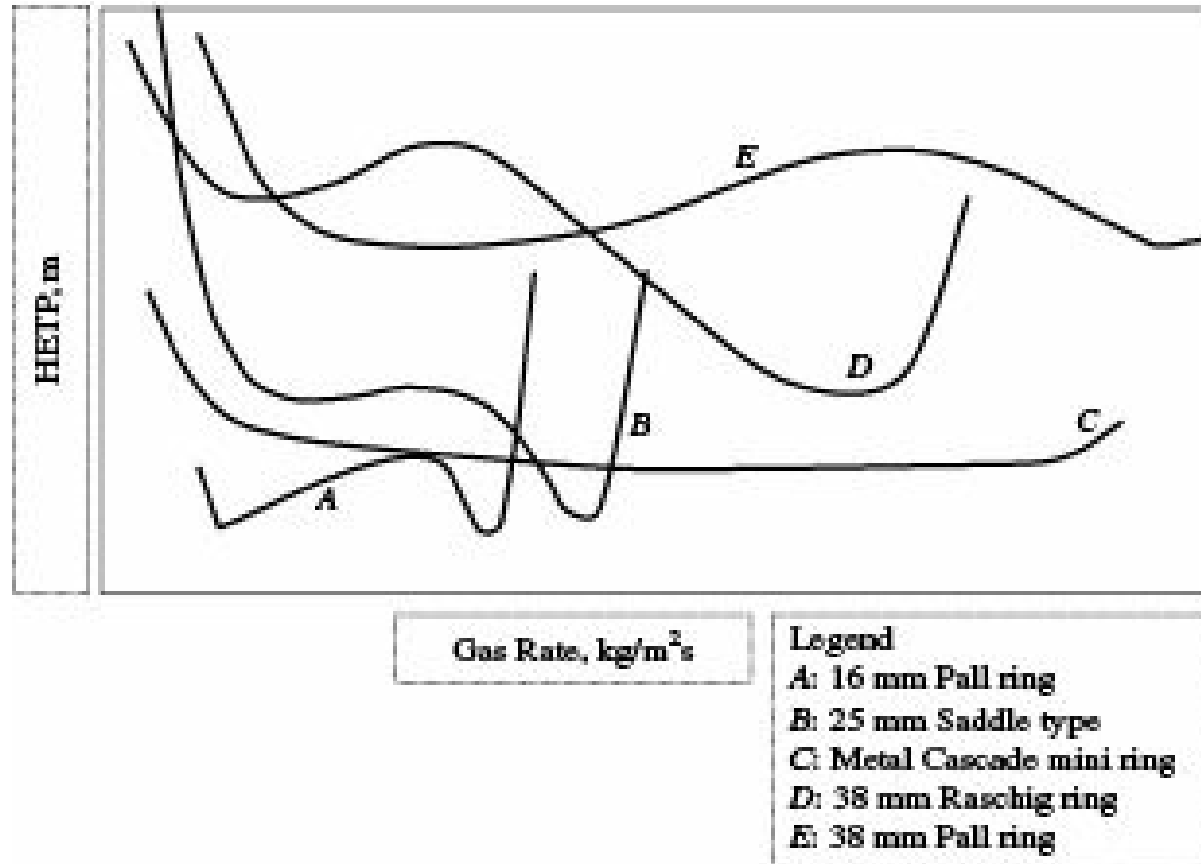


**Figure 5.15(b)** HETP as function of geometry of packing and gas rate.

**Table 5.1** Characteristics of some packings

Type of packing	Void fraction	Surface area per unit volume, m <sup>2</sup> /m <sup>3</sup>	Approx. HETP, m
<b>Random packings</b>			
Ceramic Raschig rings, 25 mm	0.73	190	0.6-0.12
Ceramic Intalox saddles, 25 mm	0.78	256	0.5-0.9
Ceramic Berl saddles, 25 mm	0.69	259	0.6-0.9
Plastic Pall rings, 25 mm	0.90	267	0.4-0.5
Metal Pall rings, 25 mm	0.94	207	0.25-0.3
<b>Structured packings</b>			
Intalox 2T (Norton)	0.96	213	0.2-0.3
Flexipac® 1 (Koch)	0.91	558	0.2-0.3
Flexipac® 2 (Koch)	0.93	249	0.3-0.4
Gempak® 4A (Glitsch)	0.91	525	0.2-0.3
Gempak® 2A (Glitsch)	0.93	262	0.3-0.4
Sulzer BX (Sulzer)	0.90	499	0.2-0.3

If such data are not available, Kister has provided helpful rules of thumb for predicting HETP values with random packings in terms of column diameter,  $D$ :

$$\text{HETP} = D \text{ for } D \leq 0.5 \text{ m}$$

$$= 0.5D^{0.3} \text{ for } D > 0.5 \text{ m}$$

$$= D^{0.3} \text{ for absorption columns with } D > 0.5 \text{ m.}$$

For vacuum distillation, it is recommended that an extra 0.15 m be added to these predicted values of HETP.

A rule of thumb for quick estimation of HETP for structured packing has also been presented (Harrison and France 1989):

$$\text{HETP} = \frac{9.29}{a_p} + 0.10(5.48)$$

where  $a_p$  is the packing surface area per unit volume,  $\text{m}^2/\text{m}^3$  and HETP in metres. A more accurate approach would however be to use the interpolation or extrapolation of packing efficiency data presented by Kister.

**HETP correlations:** The correlation has been developed based on primarily laboratory data which may not be suitable for understanding the large scale behaviour. Some of values pertaining to large scale behaviour are given as (Frank 1977)

Types of packing/Application	HETP, m
25 mm dia packing	0.46
38 mm dia packing	0.66
50 mm dia packing	0.90
Absorption duty	1.5-1.8
Small diameter columns (< 0.6 m dia.)	Column diameter
Vacuum columns	Values as above + 0.1 m

A correlation for Raschig rings and Berl saddles (Murch 1953) covers columns up to 30 in. diameter and 10 ft high is as follows:

$$\text{HETP} = C_1 G' C_2 d_e C_3 Z^{1/3} \frac{\alpha \mu_L}{\rho_L} \quad (5.49)$$

where,

$G'$  = mass velocity of vapour per unit tower area,  $\text{kg}/\text{m}^2\text{s}$

$d_e$  = column diameter, m

$Z$  = packed height, m

$\alpha$  = relative volatility

$\eta_L$  = liquid viscosity,  $\text{N s/m}^2$

$\rho_L$  = liquid density,  $\text{kg}/\text{m}^3$

Values of the constants  $C_i$  are as follows:

Types of packing	Size, mm	$C_1 (\# 10^{-5})$	$C_2$	$C_3$
Rings	6			1.24
	9	0.77	-0.37	1.24
	12.5	7.43	-0.24	1.24
	25	1.26	-0.10	1.24
	50	1.80	0	1.24
Saddles	12.5	0.75	-0.45	1.11
	25	0.80	-0.14	1.11

EMUS (1955) developed a correlation for 25 and 70 mm rasching rings with HETP (m)

$$\left[ \left( \frac{G'_M}{L} \right) - 1 \right] \text{HETP} = 18d_r + 12 m \quad (5.50)$$

where

$d_r$  = diameter of the rings, m

$m$  = average slope of equilibrium curve

$G'_M$  = vapour mass flow rate

$L'M$  = liquid mass flow rate

### Method based on individual phase mass transfer coefficients

Limiting our discussion to transfer of a single component from a binary gas mixture, the required height of packing for a desired change in composition may be estimated by equating the differential form of material balance with the point value of the rate equation.

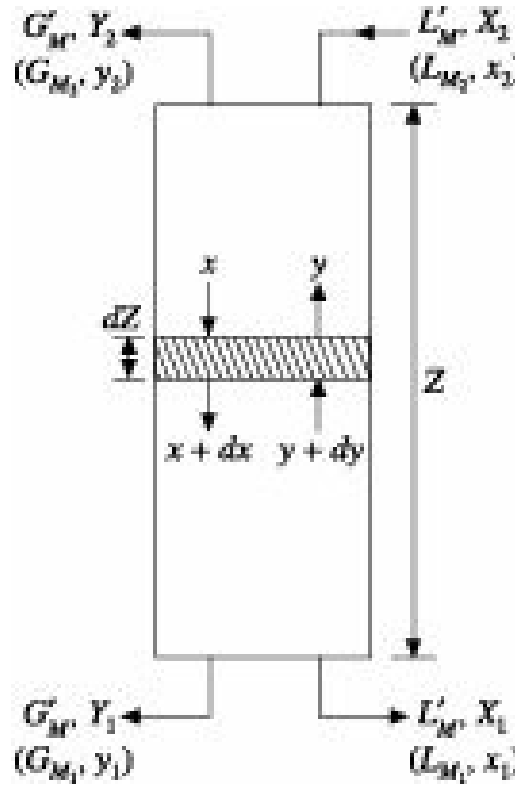


Figure 5.16 Flow diagram of a packed tower showing differential height ( $dZ$ ).

Considering the differential height  $dZ$  of a packed tower as shown in Figure 5.16, let  $dy$  be the change in gas composition and let  $(N_A a)$  be the point value of mass flux in mole/(unit time) (unit volume). A material balance for the absorbed component then becomes

$$-d(G_M y) = -G_M dy - y dG_M = N_A a dZ \quad (5.51)$$

Since for transfer of only one component,  $dG_M = -N_A a dZ$ , Eq. (5.51) may be written as

$$-G_M dy - y (-N_A a dZ) = N_A a dZ \quad (5.52)$$

Equation (5.52) may be rearranged as

$$dZ = -\frac{G_M dy}{N_A a(1-y)} \quad (5.53)$$

The required height of packing may be determined by integration of Eq. (5.53) over the tower after substituting for  $N_Aa$  from Eq. (3.19)

$$\int_1^2 \frac{dx}{Z} = \int_{y_2}^y \frac{G_M dy}{k_y a (1-y)(y-y_i)} \quad Z = (5.54)$$

Equation (5.54) is valid for those cases where the gas-phase resistance controls, i.e. where the gas is highly soluble in the solvent. With a slightly soluble gas, the corresponding equation for liquid-phase resistance controlling is

$$\int_1^2 \frac{dx}{Z} = \int_{x_2}^x \frac{L_M dx}{k_x a (1-x)(x_i-x)} \quad Z = (5.55)$$

Equations (5.54) to (5.55) may be integrated graphically by evaluating the constituent terms at a series of points on the operating line. Alternatively, the integration may be done numerically by a digital computer. The use of either of the above two equations requires the value of individual mass transfer coefficient which can be determined experimentally by the methods described in Chapter 6. However, the same may not be possible for some systems. In such situation values can be obtained from the literature. Figure 5.17 for instance depicts a relationship between the volumetric mass transfer coefficient and liquid flow rate while gas flow rate was kept constant for absorption of  $\text{CO}_2$  in  $\text{NaOH}$  using various packings.

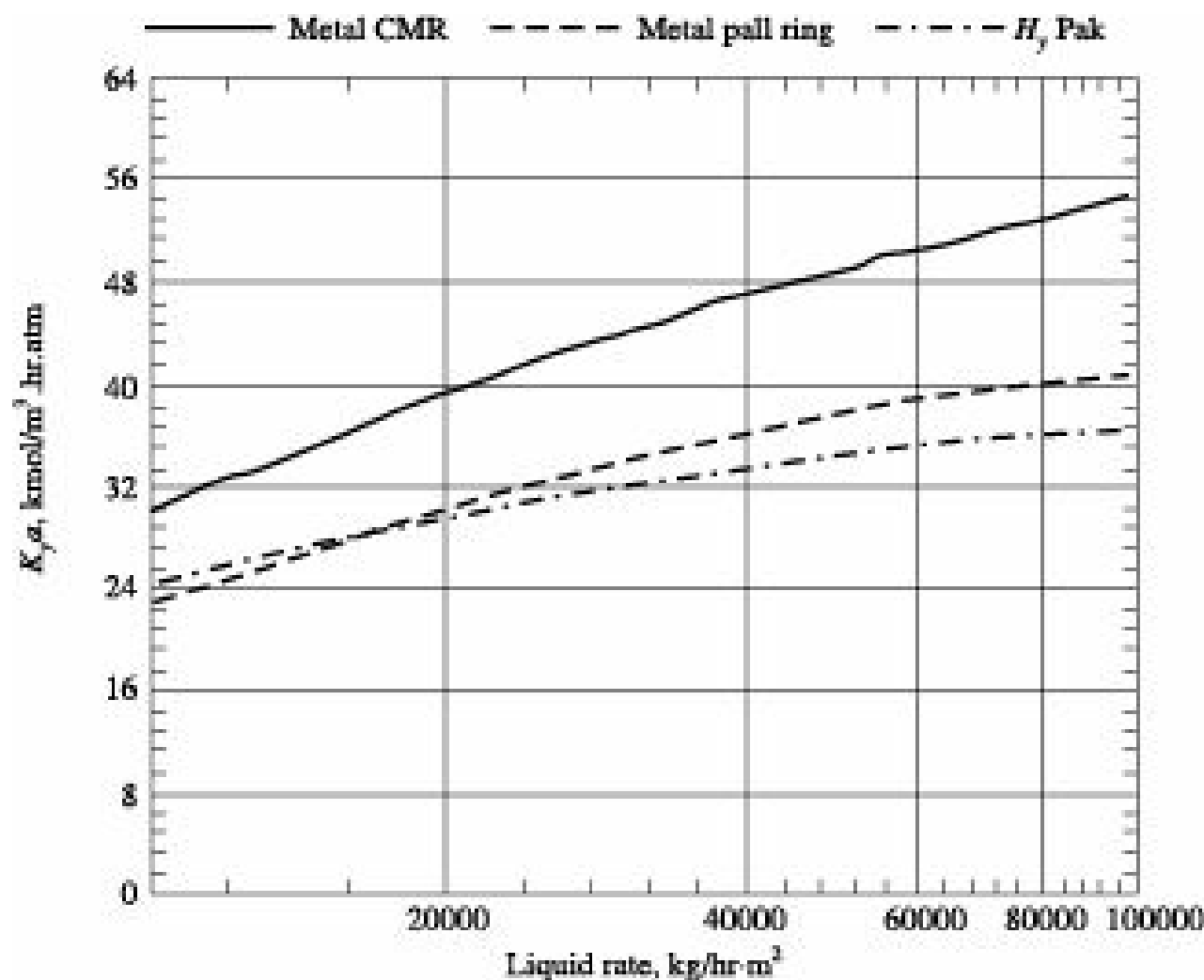


Figure 5.17 Volumetric mass transfer coefficient ( $K_ya$ ) for absorption of  $\text{CO}_2$  in  $\text{NaOH}$  solution with gas flow rate =  $1.22 \text{ kg}/\text{m}^2\text{s}$ .

Also, a number of empirical and semiempirical equations are available in the literature (Coulson et

al. 1991, Geankoplis, 2005). One such method (Bravo and Fair 1982) involves estimating the individual mass transfer coefficients and an effective interfacial area for mass transfer. The mass transfer coefficients in m/s established by these investigators are obtained from

$$\frac{0.119 a_p D_G \text{Re}_G^{0.7} \text{Sc}_G^{0.333}}{(a_p d_p)^2} k_y = (5.56)$$

and

$$k_x = 3.72 \times 10^{-5} \left( \frac{\mu_{Lg}}{\rho_L} \right)^{0.333} \left( \frac{\text{Re}_L a_p}{a_w} \right)^{0.667} \text{Sc}_L^{-0.5} (a_p d_p)^{0.4} \quad (5.57)$$

where,  $\frac{a_p}{a_w} =$

$$\left[ 1 - \exp \left\{ -1.45 \text{Re}_L^{0.1} \text{Fr}_L^{-0.05} \text{We}_L^{0.2} \left( \frac{\sigma_c}{\sigma} \right)^{0.75} \right\} \right]^{-1}$$

$$\text{Re}_G =$$

$$\text{We}_L = \frac{453.2 \rho_L L_M^2}{a_p \sigma}, \text{ Sc}_L = \frac{0.000672 \mu_L}{\rho_L D_L}, \quad \frac{1488 \rho_G G_M}{a_p \mu_G}, \quad \text{Re}_L = \frac{1488 \rho_L L_M}{a_p \mu_L}, \quad \text{Fr}_L = \frac{a_p L_M^2}{g}$$

where, subscripts *L* and *G* refer to the liquid-phase and vapour-phase, respectively,  
 $G_M$  and  $L_M$  are the superficial velocity of gas-phase and liquid-phase, respectively,  
 $a_p$  is the packing surface area,  $\text{m}^2/\text{m}^3$

$D$  represents the diffusivity,  $\text{m}^2/\text{s}$

$d_p$  means the packing diameter,  $\text{m}$

$a_w$  refers to the area of the wetted packing,  $\text{m}^2$

$\tau$  refers to the density,  $\text{kg}/\text{m}^3$

$\eta$  refers to the viscosity,  $\text{c.p}$

$\sigma$  represents the surface tension, dyne/cm and  $\sigma_c$  refers to the critical surface tension which is assumed to be 61 dynes/cm for ceramic packing, 75 dynes/cm for structured packing and 33 dynes/cm for PEB packing

Fr, We and Sc refer to Froude, Weber and Schmidt numbers, respectively.

Determination of the individual mass transfer coefficients permits evaluation of the effective area  $a$  for mass transfer using the relation

$$a = a_p \sigma^{0.5} (\text{Ca}_L \text{Re}_G)^{0.392} (\text{HTU})^{0.4} \quad (5.58)$$

where the dimensionless capillary number,  $\text{Ca}_L$  is obtained from

$$\frac{0.304 L_M \mu_L}{\sigma} \text{Ca}_L =$$

The mass transfer coefficients based on gas phase ( $k_y a$ ) and liquid phase ( $k_x a$ ) may also be approximately estimated from the following correlations (Semmelbaur 1967):

*Gas-film controlling:*

For  $100 < \text{Re}_G < 10,000$  and  $0.01 \text{ m} < d_p < 0.05 \text{ m}$

$$\text{Sh}_G = b \text{Re}_G^{0.59} \text{Sc}_G^{0.33} (5.59)$$

where,  $b = 0.69$  for Raschig rings and  $0.86$  for Berl saddles,  $d_p$  = packing size.

*Liquid-film controlling:*

For  $3 < \text{Re}_L < 3000$  and  $0.01 \text{ m} < d_p < 0.05 \text{ m}$

$$\text{Sh}_L = b' \text{Re}_L^{0.59} \text{Sc}_L^{0.50} (5.60)$$

where,  $b' = 0.32$  for Raschig rings and  $0.25$  for Berl saddles.

### **Method based on overall mass transfer coefficient**

It is often inconvenient to use single phase mass transfer coefficient because of the difficulty in measuring the interfacial concentration. As a result, overall coefficients are frequently used.

The following similar procedure as in previous section, i. e. by integration of Eq. (5.53) over the tower after substituting the expression for  $N_A a$  from Eq. (4.5), the equations for estimation of height of a tower can be developed in terms of overall gas-phase mass transfer coefficient and overall gas-phase driving force

$$Z = \int_{y_2}^y \frac{G_M dy}{K_y a (1-y)(y-y^*)} \quad (5.61)$$

Similar expression in terms of overall liquid-phase mass transfer coefficient and overall liquid-phase driving force, can be obtained as follows:

$$\text{and } Z = \int_{x_2}^x \frac{L_M dx}{K_x a (1-x)(x^*-x)} \quad (5.62)$$

Equation (5.61) is based on overall mass transfer coefficient and overall driving force, both in terms of gas-phase mole fraction of solute while in case of Eq. (5.62), both are in terms of liquid-phase mole fraction of solute.

For gas-film controlled processes, the following simple correlation may be used for estimation of overall mass transfer coefficient based on gas-phase concentration difference (Kowalke et al. 1925):

$$K_y a = a G'^{0.8} \quad (5.63)$$

where,

$K_y a$  is in  $\text{kmol}/\text{m}^3 \text{s}$  (unit partial pressure difference in  $\text{kN}/\text{m}^2$ )

$G'$  = mass velocity of gas,  $\text{kg}/\text{m}^2 \text{s}$

and  $a$  varies from  $0.00048$  for  $25 \text{ mm}$  spheres to  $0.001$  for  $6.4 \text{ mm}$  crushed stones.

### **Method based on height of a transfer unit**

Mass transfer data are not usually available in a form suitable for use in Eqs. (5.54), (5.55), (5.61) and (5.62). Some suitable method has to be developed to utilize these data.

Since for transfer of one component the term  $[G_M/(k_y a)(y_{BM})]$  is theoretically independent of concentration and total pressure (Sherwood and Pigford 1952), Eq. (5.54) may be multiplied and divided by  $y_{BM}$ , then we get

$$\int_{y_2}^{y_1} \frac{G_M}{k_y a y_{BM}} \times \frac{y_{BM} dy}{(1-y)(y-y_l)} = Z \quad (5.64)$$

$$\frac{(1-y) - (y-y_l)}{\ln \frac{(1-y)}{(y-y_l)}} \quad \text{where, } y_{BM} =$$

(5.65)

The left-hand term under the integral has the dimension of length (or height) and is designated as the Height of a Transfer Unit or HTU,  $H_t G$ .

$$H_t G = \frac{G_M}{k_y a y_{BM}} \quad (5.66)$$

As mentioned above,  $H_t G$  is independent of pressure and concentration. Mass transfer data are often reported in the form of  $H_t G$ . Unless the changes in flow rate or specific volume are large over the tower, an average value of  $H_t G$  may be used and it may be taken out of the integration sign, so that Eq. (5.64) becomes

$$\int_{y_2}^{y_1} \frac{y_{BM} dy}{(1-y)(y-y_l)} = Z = H_t G \quad (5.67)$$

The integral in Eq. (5.67) is called the Number of Transfer units of NTU, NtG.

$$N_t G = \int_{y_2}^{y_1} \left( \frac{y_{BM} dy}{(1-y)(y-y_l)} \right) \quad (5.68)$$

The tower height thus becomes the product of the  $H_t G$  and  $N_t G$ .

$$Z = H_t G \cdot N_t G \quad (5.69)$$

Similar equations can be developed by using liquid-phase mass transfer coefficient when the tower height becomes

$$Z = H_t L \cdot N_t L \quad (5.70)$$

The number of transfer units represents the difficulty encountered in the separation. A high degree of separation or a small available driving force requires large number of transfer units. The height of a transfer unit, on the other hand, represents inversely the relative ease with which the transfer can be achieved. As may be seen from Eq. (5.66), large mass transfer coefficient or large interfacial area per unit volume will give lower value of  $H_t G$  which means lower packing height for the same separation.

For dilute systems for which the equilibrium and operating lines are straight and parallel so that ( $y - y_i$ ) is approximately constant, Eq. (5.68) gives

$$N_t G \approx \frac{\int_{y_2}^{y_1} dy}{(y - y_i)_{av}} = \frac{(y_1 - y_2)}{(y - y_i)_{av}} \quad (5.71)$$

From Eq. (5.71), one transfer unit is equivalent to the height of packing over which the composition of the stream changes by an amount equal to the average driving force.

The following similar procedure as has been made in cases of individual phase coefficients in Eqs. (5.64) to (5.70), overall height of a transfer unit and overall number of transfer unit for gas-phase may be obtained as

$$H_{toG} = \frac{G_M}{K_p a y_{BM}} \quad (5.72)$$

$$\int_{y_2}^{y_1} \frac{y_{BM} dy}{(1-y)(y-y^*)} N_{toG} = (5.73)$$

$$Z = H_{toG} N_{toG} \quad (5.74)$$

In terms of overall mass transfer coefficients based on liquid phase, ‘height of an overall liquid-phase transfer unit’ and ‘number of overall liquid-phase transfer units’ are:

$$H_{toL} = \frac{L_M}{K_L a \alpha x_{BM}} \quad (5.75)$$

$$\int_{x_2}^{x_1} \left( \frac{x_{BM} dx}{(1-x)(x^*-x)} \right) N_{toL} = (5.76)$$

$$Z = H_{toL} \cdot N_{toL} \quad (5.77)$$

**Correlation for HTU:** A number of design procedures for evaluating HTU for packed columns are available in the literature. The values of HTU for certain types of packing for absorption of ammonia from air in water can be obtained from Figure 5.18.

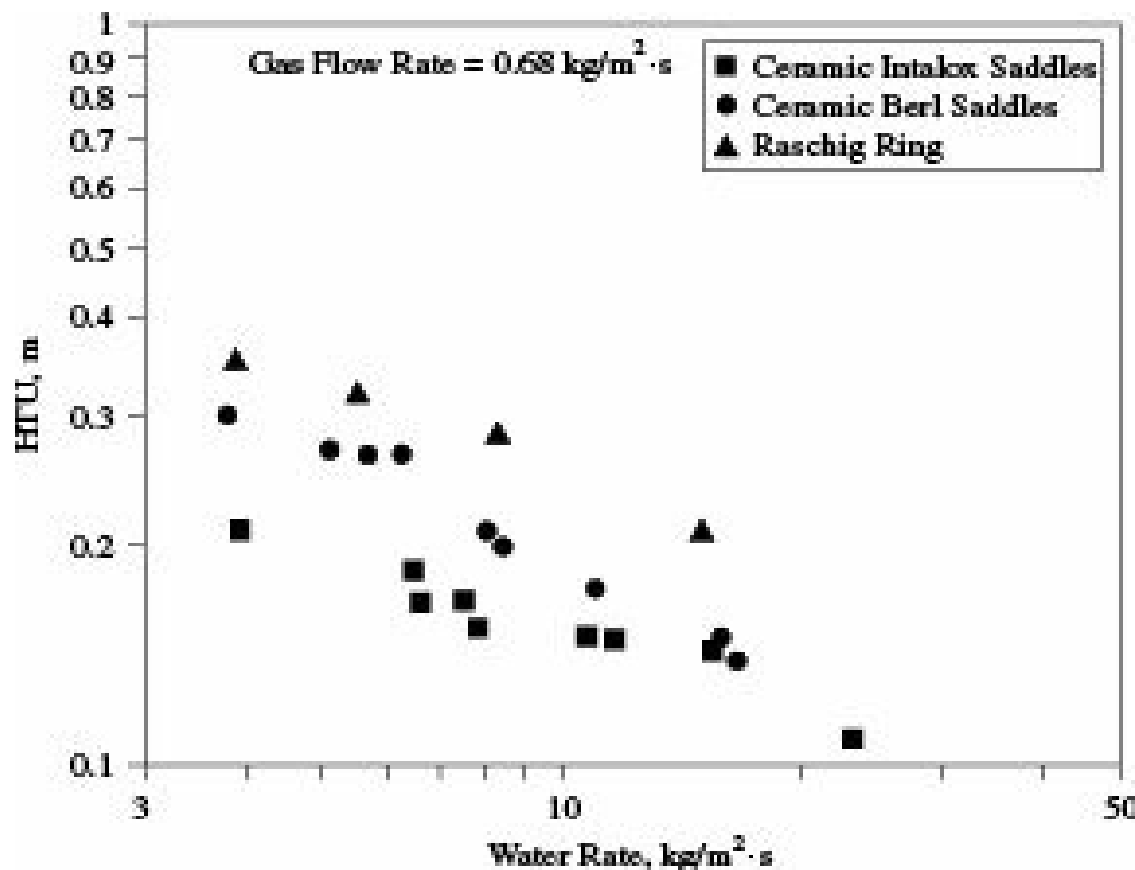


Figure 5.18 HTU of some packing for absorption of NH<sub>3</sub> from air by water.

Approximate range of values of HTU for packings of some common sizes are as follows:

Packing size, mm	HTU, m
25	0.30-0.60
38	0.50-0.75
50	0.60-1.00

A number of empirical and semiempirical correlations are also available in the literature (Fair and Bolles 1979, Geankoplis 2005).

## 5.4 Relation between Overall and Individual Phase Transfer Units

The relation between overall heights of transfer units and heights of individual phase transfer units may be established in a manner similar to that for overall and individual phase mass transfer coefficients.

By definition of heights of transfer units

$$\frac{(1-y)_M}{(1-y)_M^*} + \frac{mG_M}{L_M} H_{tL} \frac{(1-x)_M}{(1-y)_M^*} H_{tG} = H_{tG} \quad (5.78)$$

For gas-phase resistance controlling,  $y_i \approx y^*$  and we get

$$\frac{mG_M}{L_M} H_{tL} \frac{(1-x)_M}{(1-y)_M^*} H_{tG} = H_{tG} + (5.79)$$

$\frac{(1-x)_M}{(1-y)_M^*}$  For dilute solutions, may be taken as unity without any serious error and  $H_{tG}$  becomes

$$\frac{mG_M}{L_M} H_{tG} = H_{tG} + H_{tL} \quad (5.80)$$

Similarly, if the resistance to mass transfer is essentially in the liquid phase, we get

$$H_{tO}L = H_{tL} + \frac{L_M}{mG_M} H_{tG} \quad (5.81)$$

where,

$H_{tG}$  and  $H_{tL}$  = heights of transfer units based on gas phase and liquid phase coefficients, respectively

$H_{tO}G$  and  $H_{tO}L$  = overall heights of transfer units based on gas phase and liquid phase coefficients, respectively.

**EXAMPLE 5.4** (Determination of Packing Height by Using the Concept of Height and Number of Transfer Units): 800 kg/hr of an air-carbon tetrachloride mixture containing 5 mol%  $\text{CCl}_4$  is to be scrubbed in a counter-current packed tower to recover 90%  $\text{CCl}_4$ .

A nonvolatile  $\text{CCl}_4$ -free oil ( $M = 260$ ) will be used as solvent and the solvent rate will be 820 kmol/hr. The mass transfer coefficient  $K_y a$  has been estimated to be 25 kmol/(hr)( $\text{m}^3$ )(atm).

Determine the number of transfer units required and hence, the packed height of the tower.

The equilibrium relationship is given by  $y^* = 20x$ , where  $y^*$  and  $x$  are the mole fractions of  $\text{CCl}_4$  in gas and liquid respectively. The total pressure is 1 atm.

### Solution:

Molecular weight of entering gas =  $(0.05)(154) + (0.95)(28.92) = 35.17$ .

$$G_M = \frac{800}{35.17} = 22.75 \text{ kmol}/(\text{hr})(\text{m}^2), G'M = (22.75)(0.95) = 21.61 \text{ kmol}/(\text{hr})(\text{m}^2)$$

Solvent rate = 820 kmol/(hr)( $\text{m}^2$ ).

$$y_1 = 0.05, Y_1 = \frac{0.05}{(1 - 0.05)} = 0.0526, Y_2 = (0.10)(0.0526) = 0.00526 \approx y_2.$$

From material balance:

$$(820)(X_1 - 0) = (21.61)(0.0526 - 0.00526)$$

whence,

$$X_1 = 0.00125 \approx x_2.$$

Since both equilibrium and operating lines are straight,

$$N_{tO}G = \frac{Y_1 - Y_2}{\Delta y_{lm}}$$

$$\Delta y_1 = y_1 - y^*_1 = 0.05 - (20)(0.00125) = 0.025$$

$$\Delta y_2 = y_2 - y^*_2 = (0.00526 - 0) = 0.00526$$

$$Dylm = \frac{(0.025 - 0.00526)}{\ln(0.025/0.00526)} = 0.01266$$

$$N_{t0G} = \frac{(0.05 - 0.00526)}{0.01266} = 3.53$$

$$H_{t0G} = \frac{G_M}{K_y a P} = \frac{22.75}{(25.7)(1)} = 0.885 \text{ m}$$

Hence, packed height of the tower,  $Z = (H_{t0G})(N_{t0G}) = (0.885)(3.53) = 3.12 \text{ m}$ .

## Nomenclature

$A$  : absorption factor ( $= L'M/mG'M$ ), --

$C$  : number of components, used in phase rule

$F$  : degrees of freedom, used in phase rule

$G$  : molal/mass velocity of gas,  $M(\text{Mol})/\text{L}^2\text{q}$

$G'$  : molal/mass velocity of gas on solute-free basis,  $M(\text{Mol})/\text{L}^2\text{q}$

$G_M$  : average total molal flow rate of phase  $G$ , mol

$G'_M$  : average molal flow rate of phase  $G$  on solute-free basis, mol

$H_{tG}$  : height of a gas-phase transfer unit, L

$H_{tL}$  : height of a liquid-phase transfer unit, L

$H_{t0G}$  : overall height of a transfer unit based on gas-phase, L

$H_{t0L}$  : overall height of a transfer unit based on liquid-phase, L

$k_y, k_x$  : individual phase mass transfer coefficients in phases  $G$  and  $L$ , respectively

$K_y, K_x$  : overall mass transfer coefficients in terms of driving force based on phases  $G$  and  $L$ , respectively

$k_y a, k_x a$  : individual phase mass transfer coefficients on volumetric basis in phases  $G$  and  $L$ , respectively

$K_y a, K_x a$  : overall mass transfer coefficients on volumetric basis in terms of driving force based on phases  $G$  and  $L$ , respectively

$L$  : molal/mass velocity of liquid,  $M(\text{Mol})/\text{L}^2\text{q}$

$L'$  : molal/mass velocity of liquid on solute-free basis,  $M(\text{Mol})/\text{L}^2\text{q}$

$L_M$  : average total molal flow rate of phase  $L$ , mol

$L'_M$  : average molal flow rate of phase  $L$  on solute-free basis, mol

$m$  : slope of the equilibrium curve

$N$  : number of plate or stage counted from top

$N_A$  : molar mass flux per unit area of equipment,  $\text{mol}/\text{L}^2\text{q}$

$N_{tG}$  : number of gas-phase transfer units

$N_{tL}$  : number of liquid-phase transfer units

$N_{toG}$  : number of overall gas-phase transfer units

$N_{toL}$  : number of overall liquid-phase transfer units

$P$  : number of phases as used in phase rule

$x, y$  : mole fraction of a component in liquid and gas, respectively

$X, Y$  : mole ratio of a component in liquid and gas, respectively on solute-free basis

$Z$  : height of packed bed, L

### *Subscripts*

$A$  : component A

$B$  : component B

## **Numerical Problems**

**5.1 Rate of Flow of Solvent for Absorption of Sulphur Dioxide in a Packed Bed:** Sulphur dioxide is absorbed from air by water in a packed absorber with a diameter of 1 m. The  $\text{SO}_2$  content in the entering mixture is 7% (by volume). The absorption factor is 0.9. The water leaving the absorber contains 0.0072 kg of  $\text{SO}_2$ /kg of water. The overall mass transfer coefficient in the absorber,  $K_G = 0.005 \text{ kg of } \text{SO}_2/(\text{m}^2)(\text{s})$  ( $\text{kg of } \text{SO}_2/\text{kg of air}$ ). The packing is of ceramic rings 50 # 50 # 5 mm in size. The packing is completely wetted. The height of a transfer unit is 1.17 m. Determine the rate of flow of water in the absorber. [Ans: 30  $\text{m}^3/\text{hr}$ ]

**5.2 Mean Driving Force and Transfer Units for Benzene-Oil System:** Determine the mean driving force in units of  $Y$  (kmol of benzene per kmol of inert gas), and the total number of transfer units when benzene vapour is absorbed from a gas with oil. The initial concentration of the benzene in the gas is 4% (by volume), 80% of the benzene is absorbed. The concentration of the benzene in the oil leaving the absorber is 0.02 kmol of benzene per kmol of pure oil. The oil fed into the absorber contains no benzene. The equation of the equilibrium line in mole ratios is  $Y^* = 0.126X$ .

[Ans: Mean driving force: 0.02 kmol benzene/kmol inert gas, No. of transfer units: 1.66]

**5.3 Estimation of Flow Rate of Solvent and Mean Driving Force for  $\text{SO}_2\text{-H}_2\text{O}$  System:** Sulphur dioxide is absorbed by water from an inert gas (nitrogen) in a scrubber under atmospheric pressure. The initial content of the sulphur dioxide in the gas is 5% (by volume). The temperature of water is 20°C, and its flow rate is 20% greater than the minimum value. The amount of  $\text{SO}_2$  scrubbed from the gas is 90%. Determine the (i) flow rate of water needed to absorb 1000 kg/hr of  $\text{SO}_2$ , (ii) mean driving force of the process, and (iii) number of transfer units.

The equilibrium line may be assumed to be a straight line; the coordinates of two of its points are: (a) partial pressure of  $\text{SO}_2$  in the gaseous phase is 39 mm Hg, concentration of

$\text{SO}_2$  in liquid phase is 0.007 kg  $\text{SO}_2$ /kg water and (b) partial pressure of  $\text{SO}_2$  in the gaseous phase is 26 mm Hg, concentration of  $\text{SO}_2$  in liquid phase is 0.005 kg  $\text{SO}_2$ /kg water.

[Ans: (i) 175000 kg/hr, (ii) 5.67 mm Hg, (iii) 6.02]

**5.4 Determination of Compositions of Exit Streams Using Murphree Plate Efficiency:** Ammonia is required to be stripped at 1.1 atm pressure. One cube metre of water enters the equipment, and the ratio of the molar flow rates of air and water is 4. The inlet air and inlet water have 0.1 and 1.0 mol% of ammonia respectively. The Murphree plate efficiency for ammonia removal is 50% and the Henry's law constant for ammonia in water is  $2.574 \times 10^{-5}$  atm  $\text{m}^3/\text{mol}$ . Determine the compositions of the exit water and air, respectively.

[Ans: Exit water: 0.3 mol%, and Exit air: 0.275 mol%]

**5.5 Determination of Individual Transfer Units, Overall Transfer Coefficients and Murphree Point Efficiency:** Determination of efficiency is critical in plate column design. The gas and liquid rates are 0.1 and 0.25 kmol/s, respectively. The interfacial area for mass transfer is  $35 \text{ m}^2/\text{m}^3$  of froth on the plate. The residence time of both the liquid and gas in the froth zone is 3 s. The liquid-phase and gas-phase mass transfer coefficients are  $1 \times 10^{-2}$  m/s and  $2 \times 10^{-3}$  m/s, respectively. Calculate

- (i) liquid-phase transfer units,
- (ii) gas-phase transfer units,
- (iii) stripping factor, given that the slope of the equilibrium curve is 5.0.
- (iv) overall transfer coefficients,
- (v) Murphree point efficiency.

[Ans: (i) 0.714(ii) 1.43(iii) 2,(iv)  $K_Y = 10^{-3}$  m/s,  $K_X = 5 \times 10^{-3}$  m/s,(v)

50%]

**5.6 Number of Transfer Units by Graphical Construction and Integration Methods:** Ammonia is absorbed from a gas by water in equipment under atmospheric pressure. The initial ammonia content in the gas is 0.03 kmol/kmol of inert gas. The absorption factor is 90%. The water leaving the scrubber contains 0.02 kmol of ammonia per kmol of water. A constant temperature is maintained in the scrubber by removal of heat.

Data on the equilibrium concentrations of ammonia in water and gas at the prevailing temperature are as follows:

$X$ ,

kmol of ammonia

kmol of water

0

0.0050.0100.01250.0150.0200.023

$Y^*$ ,

kmol of ammonia

kmol of inert gas

Determine the required number of transfer units by graphical construction and graphical integration methods.

[Ans.  $5.83 \approx 6$ ]

**5.7 Determination of Number of Transfer Units and Height of Packing:** A scrubber with a diameter of 0.5 m is supplied with  $550 \text{ m}^3/\text{hr}$  of air at 760 mm Hg and  $20^\circ\text{C}$ , containing 2.8% (by volume) of ammonia which is absorbed by water under atmospheric pressure. Up to 95% ammonia is absorbed. The rate of flow of water is 40% higher than the minimum value. Determine (i) the rate of flow of water, (ii) the total number of transfer units, and (iii) the depth of packing layer of ceramic rings 50 # 50 # 5 mm in size. The overall mass transfer coefficient ( $K_y$ ) is  $0.001 \text{ kmol of ammonia/m}^2\text{s}$  ( $\text{kmol of ammonia/kmol of air}$ ). Use the equilibrium data given in Problem 5.6. Assume the coefficient of wetting of the packing to be 0.9.

[Ans: (i) 760 kg/hr (ii) 4.68 (iii) 1.93 m]

**5.8 Determination of Height of a Packed Bed Using HETP Value:** Ammonia from an air-ammonia mixture is absorbed by water at atmospheric pressure and at a temperature of  $20^\circ\text{C}$ . The initial content of ammonia in the gas mixture is 7% (by volume). The absorption factor is 90%. The rate of flow of the inert gas is  $10000 \text{ m}^3/\text{hr}$  under the operating conditions. Consider the equilibrium line to be straight; its equation in mass ratios is  $Y^* = 0.61X$ . The fictitious velocity of the gas in the absorber is 0.8 m/s. The excess absorbent coefficient is 1.3. Determine the height of the absorber packed with ceramic rings 50 # 50 # 5 mm in size, assuming that the height of the packing layer equivalent to a theoretical plate (HETP) equals 0.85 and considering the coefficient of packing wetting equals to 0.9.

[Ans: 5.1 m]

**5.9 Total Height of the Transfer Unit for Absorption of Carbon Dioxide in Water in a Packed Bed Using the Expressions for Individual Phase Transfer Units:** A scrubber with randomly packed ceramic rings 50 # 50 # 5 mm in size is used to absorb carbon dioxide with water from a gas under a pressure of 16 atm at a temperature of  $22^\circ\text{C}$ . The mass of the gas is 20.3 kg/kmol, the viscosity of the gas in the operating conditions is  $1.31 \times 10^{-5} \text{ Pa s}$ , the diffusion coefficient of carbon dioxide in the inert portion of the gas is  $1.7 \times 10^{-6} \text{ m}^2/\text{s}$ . The mean fictitious velocity of the gas in the scrubber is 0.041 m/s, the irrigation density (the fictitious velocity of the liquid) is  $0.064 \text{ m}^3/\text{m}^2\text{s}$ . Determine the total height of the transfer unit, assuming that the packing is completely wetted. The packing characteristics are: free volume in  $\text{m}^3$  of voids per  $\text{m}^3$  of packed volume, i.e. unit void area in a column section in  $\text{m}^2/\text{m}^2$  is  $0.785 \text{ m}^3/\text{m}^3$  and the unit surface area in  $\text{m}^2$  of dry packing per  $\text{m}^3$  of packed volume is  $87.5 \text{ m}^2/\text{m}^3$ . The diffusion coefficient of carbon dioxide in water at  $22^\circ\text{C}$  is  $1.87 \times 10^{-9} \text{ m}^2/\text{s}$ , and Henry's coefficient for carbon dioxide at  $22^\circ\text{C}$  is  $1.144 \times 10^6 \text{ mm Hg}$ . The following correlations may be used:

$$H_y \text{ (height of a transfer unit for the gas phase)} = 0.615 d_{\text{eq}} \text{ Re}_G^{0.345} \text{ Sc}_G^{0.67}$$

$H_x$  (height of a transfer unit for the liquid phase) =  $119 d \text{Re}_L^{0.25} \text{ Sc}_L^{0.5}$  (d is the thickness of the liquid film). [Ans: 0.88 m]

- 5.10** Determination of Height of a Packed Tower Using Expression for HTU: 95% of sulphur dioxide present in sulphur dioxide-air mixture containing 8% (mole basis) sulphur dioxide is recovered by fresh water in a packed absorption tower. Hourly rates of gas and water are 5000 kg and  $10^5$  kg, respectively. Calculate the height of the tower.

Data on the equilibrium data for sulphur dioxide-air-water system are as follows:

% (wt) SO<sub>2</sub> in solution 0.1 0.20.30.50.71.01.5

Partial pressure (mm Hg) 3.2 8.5 14.126395992

HTU may be calculated from

$$H_{\text{f},G} = 0.7 +$$

$$\frac{24.5 G_M}{L_M}$$

[Ans: 8.91 m]

- 5.11** Determination of LMCD, Overall Volumetric Mass Transfer Coefficient and Height of Transfer Units: An aqueous solution containing 1.5 kmol X/m<sup>3</sup> is fed at 36 ml/s to the top of packed column of height 1.60 m and crosssectional area of 0.0045 m<sup>2</sup>, and leaves at the bottom with 1.4 kmol/m<sup>3</sup>. An organic solvent, B, containing 0.006 kmol X/m<sup>3</sup> flows counter to the aqueous phase at 9 ml/s. The equilibrium relationship is

$$C_x, \text{organic} = 0.3 C_x, \text{aqueous}$$

Determine (i) the log-mean concentration difference for the transfer, (ii) the overall volumetric mass transfer coefficient based on the organic phase, and (iii) the height of transfer units.

The log-mean concentration difference, (DC)<sub>lm</sub> is expressed by the relation:

$$\frac{\Delta C_1 - \Delta C_2}{\ln(\Delta C_1 / \Delta C_2)} =$$

[Ans: (i) 0.162 kmol/m<sup>3</sup>, (ii)  $3.08 \times 10^{-3}$ /s (iii) 0.646 m]

- 5.12** Determination of Height of a Tower Analytically: Equilibrium relationship for the system heptane-oil-air is given by  $y = 2x$  where, y and x represent kg heptane/kg air and kg heptane/kg oil, respectively. Oil containing 0.005 kg heptane/kg oil is being used as solvent for reducing the heptane content of air from 0.10 to 0.02 kg heptane/kg air in a continuous counter-current packed bed absorber. Determine analytically the column height required to treat 1400 kg/hr.m<sup>2</sup> of empty tower crosssection of pure air containing heptane if the overall gas phase mass transfer coefficient is 320 kg/hr\$ m<sup>3</sup> per unit gradient of y. The oil rate employed is 3100 kg/hr m<sup>2</sup>.

[Ans: 25.7 m]

- 5.13** Determination of Height of a Tower Using HTU Value: An ammonia-air mixture containing 2% (by volume) ammonia is to be scrubbed using water at 20°C in a tower packed with 1.27

cm Raschig rings. The water and gas rates are  $1170 \text{ kg/hr} \cdot \text{m}^2$  each based on empty tower cross-section. Estimate the height of the tower required if 98% of the ammonia in the entering gas is to be absorbed. The tower operates at 1 atm pressure. The equilibrium relationship is given by the equation:

$$y^* = 0.746x$$

where,  $y$  = mole fraction of ammonia in air and  $x$  = mole fraction in solution with water. The height of transfer unit may be taken as equal to 2 m.

[Ans: 12.34 m]

**5.14 Calculation of Height of Packed Tower for CO<sub>2</sub>-water System Using HTU Value:** A packed tower is designed to recover 98% carbon dioxide from a gas mixture containing 10% CO<sub>2</sub> and 90% air using water as solvent. A relation  $y = 14x$  can be used for equilibrium conditions where  $y$  is kg CO<sub>2</sub>/kg dry air and  $x$  is kg CO<sub>2</sub>/kg water. The water to gas flow rate is kept 30% more than the minimum value. Calculate the height of the tower if the height of a transfer unit is 1 m.

[Ans: 11.29 m]

**5.15 Determination of Height of a Scrubber Using Log-mean Driving Force:** An ammonia-air mixture containing 2% ammonia at 25°C and 1 atm is to be scrubbed with water in a tower packed with 2.54 cm stoneware Raschig rings. The water and gas rates will be 1200 kg/hr.m<sup>2</sup> each. Water and gas are fed at the top and bottom, respectively. Assume that the tower operates isothermally at 25°C. At this temperature, the partial pressures of ammonia,  $p'_g$  over aqueous solution of ammonia are as follows:

$$p'_g, \text{ mm of Hg} \quad 12.018.231.750.0 \quad 69.5166.0$$

$$\text{Concentration, kg NH}_3/100 \quad \text{kg water} \quad 2.0 \quad 3.0 \quad 5.0$$

$$7.510.020.0$$

For the above packing  $k_{GA} = 62.39 \text{ kmol/hr} \cdot \text{m}^3 \text{ atm}$ . Using the logarithmic mean driving force, estimate the required height for the absorption of 98% of the ammonia in the entering gas.

[Ans: 4.13 m]

**5.16 Height of a Tower Using Correlation for Overall Transfer Unit:** It is desired to absorb 96% acetone from a 2% (mole) mixture of acetone and air in a continuous counter-current absorption tower using water at a rate of 43.3 kmol/hr. The water as solvent is introduced at the top of the tower and the gas mixture is blown into the bottom of the tower at 450 kg/hr. Find the height of the tower operating at 1 atm pressure and 300 K. The equilibrium relation is  $y = 2.5x$ , where  $y$  and  $x$  represent the mole fractions of acetone in air-acetone mixture and acetone-water solution, respectively. The following relationship and data are available:

$$H_{toG} = H_{tG} + H_{tL}$$

where,  $H_{tG} = 0.54 \text{ m}$  and  $H_{tL} = 0.32 \text{ m}$ .

[Ans: 9.34 m]

**5.17 Determination of Number of Transfer Unit and Height of Packing Required for Absorption of Hydrogen Sulphide in Triethanolamine Solution:** A counter-current packed tower is to reduce H<sub>2</sub>S content of a gaseous mixture from 0.03 to 0.0003 kmol per kmol of inert hydrocarbon gas by scrubbing with triethanolamine-water solution. The flow rate of the inert hydrocarbon gas will be 0.015 kmol/m<sup>2</sup> of tower cross-section. The tower will operate at 300 K and 1 atm pressure. The solution will enter the tower free of H<sub>2</sub>S and will leave it with 0.013 kmol H<sub>2</sub>S per kmol of solvent. The equilibrium relationship can be represented by  $Y^* = 2X$ , where  $X$  = kmol of H<sub>2</sub>S per kmol of solvent, and  $Y$  = kmol of H<sub>2</sub>S per kmol of inert gas. Calculate the (i) number of transfer units required, and (ii) height of packing to be provided. [Ans: (i) 20.77 (ii) 8.8 m]

## ***Short and Multiple Choice Questions***

1. How does phase rule help in the study of mass transfer?
2. What are the main differences between stage-wise and continuous contact mass transfer?
3. What do you mean by an equilibrium or an ideal stage?
4. What is stage efficiency? On which parameters does it depend?
5. In which units should flow rates and compositions be expressed so that the operating line is straight?
6. How does absorption factor affect the process of mass transfer?
7. When can algebraic method be used for determination of the number of stages during absorption of a gas?
8. Absorption factor is defined as
  - (a)  $\frac{\text{Slope of the equilibrium curve}}{\text{Slope of the operating line}}$
  - (b)  $\frac{\text{Slope of the operating line}}{\text{Slope of the equilibrium curve}}$
  - (c) (Slope of the operating line) # (Slope of the equilibrium curve)
  - (d) none of these
9. In an absorber, HETP does not vary with
  - (a) flow rate of liquid
  - (b) flow rate of gas
  - (c) type and size of packing
  - (d) none of these
10. With increase in solvent rate, the number of transfer units for a fixed degree of absorption from a fixed amount of gas
  - (a) increases
  - (b) decreases
  - (c) remains unchanged
  - (d) cannot be predicted
11. With increase in gas rate, the number of transfer units for a fixed degree of absorption by a

fixed amount of solvent

- (a) increases
- (b) decreases
- (c) decreases linearly
- (d) remains constant

12. The most economical range of absorption factor is

- (a) 0 to 0.5
- (b) 0 to 3
- (c) 1.25 to 2
- (d) 5 to 15

13. HETP is numerically equal to HTU only when operating line

- (a) lies below the equilibrium line
- (b) lies above the equilibrium line
- (c) is parallel to the equilibrium line
- (d) is far from the equilibrium line

14. When both the fluids flow cocurrently in an absorber, the slope of the operating line is

- (a) negative
- (b) positive
- (c) 1
- (d) uncertain

15. In an absorption operation, as the liquid flow rate is reduced for a given gas flow, the slope of the operating line

- (a) increases
- (b) decreases
- (c) remains constant
- (d) cannot be predicted

16. In gas absorption process, operating line lies

- (a) above the equilibrium curve
- (b) below the equilibrium curve
- (c) either above or below the equilibrium curve
- (d) partly above and partly below the equilibrium curve

17. For gas absorption from dilute solution under isothermal conditions

- (a) only equilibrium line is straight
- (b) only operating line is straight
- (c) both equilibrium and operating lines are straight
- (d) none of the these

18. The absorption factor can be increased by

- (a) increasing both gas and solvent flow rates
- (b) decreasing both gas and solvent flow rates
- (c) decreasing gas flow rate and increasing solvent flow rate
- (d) increasing gas flow rate and decreasing solvent flow rate

19. For absorption of a single component, the operating line is straight only when plotted in terms of

- (a) mole fraction units
- (b) partial pressure units
- (c) mole ratio units
- (d) none of these

20. For single component co-current absorption, the slope of the operating line when plotted in terms of mole ratio unit is

- (a) negative
- (b) zero
- (c) positive
- (d) infinity

#### *Answers to Multiple Choice Questions*

- 8. (b)
- 9. (d)
- 10. (c)
- 11. (a)
- 12. (c)
- 13. (c)
- 14. (a)
- 15. (c)
- 16. (a)
- 17. (b)
- 18. (c)
- 19. (c)
- 20. (a)

#### *References*

Bravo, J.L. and J.R. Fair, *Ind. Chem. Proc. Des. & Dev.*, **21**, 162 (1982).

Colburn, A.P., *Trans. AIChE*, **35**, 211 (1939).

Colburn, A.P., *Ind. Eng. Chem.*, **33**, 111 (1941).

Coulson, J.M., J.F. Richardson, J.R. Backhurst and J.H. Harker, *Chemical Engineering*, Vol. 2, Asian Books, New Delhi (2005).

Ellis, S.R.M., *Birmingham University Chem. Eng.*, **5**(1), 21 (1953).

Fair, J.R. and W.L. Bolles, *Inst. Chem. Eng. Symp. Ser.*, **56**(2), 3.3/35 (1979).

Frank, O., *Chem. Eng. Albany*, **84**, 111 (14th March, 1977).

Geankoplis, C.J., *Transport Processes and Separation Process Principles*, 4th ed., PHI Learning, New Delhi (2005).

Harrison, M.E. and J.J. France, *Chem. Eng.*, **96**(4), 121 (1989).

Kister, H. Z., *Distillation Design*, McGraw-Hill, New York (1992).

Kowalke, O.L., O.A. Hougen and K.M. Watson, *Bull. Univ. Wisconsin Eng. Sta. Ser.*, No. 68 (1925).

Kremser, A., *Natl. Petrol. News*, **22**, 42 (1930).

Murch, D.P., *Ind. Eng. Chem.*, **45**, 2616 (1953).

Peters, M.S. and K.D., Timmerhaus, *Plant Design and Economics for Chemical Engineers*, 4th ed., McGraw-Hill, New York (1991).

Semmelbaur, R., *Chem. Eng. Sci.*, **22**, 1237 (1967).

Sherwood, T.K. and R.L. Pigford, *Absorption and Extraction*, 2nd ed., McGraw-Hill, New York (1952).

Treybal, R.E., *Mass Transfer Operations*, 3rd ed., McGraw-Hill, Singapore (1985).



# 6

# Equipment for Gas–Liquid Contact

## 6.1 Introduction

Mass transfer operations of industrial importance involve transfer of material from one phase to another. The most widely used mode of transfer in the process industry is between gases/vapours and liquids as occurring in gas absorption, desorption, distillation, humidification, dehumidification and water cooling. Other methods include liquid-liquid operations as in liquid-liquid extraction, solid-gas operations as in drying and adsorption, and solid-liquid operations as in leaching, crystallization and adsorption. This chapter gives a brief discussion on the working principles, major characteristics and principal design aspects of some important pieces of equipments used for gas/vapour-liquid operations.

The primary requirements of gas-liquid equipment are capability of producing large interfacial area of contact and maximum possible turbulence in the fluids commensurate with cost. At the same time the pressure drop through the equipment and hence the power requirement should be as low as possible. One of the two phases, either the gas or the liquid is generally dispersed and the equipment are accordingly classified as gas dispersed and liquid dispersed depending upon the phase dispersed.

<i>Gas dispersed</i>	<i>Liquid dispersed</i>
Sparged vessels	Simulated Packed Towers
Agitated vessels	Wetted-wall towers
Plate columns:	String of discs
Bubble-cap columns	String of spheres
Sieve-plate columns	Packed towers
Valve-tray columns	Spray towers
	Venturi scrubbers
	Pulsed column

## 6.2 Gas Dispersed

Bubbling of gas through liquid is generally practised when the main resistance to mass transfer lies within the liquid phase. They are useful in dissolving gases of low solubility or for dissolving almost pure gases in liquids. Sparged vessels and agitated vessels are commonly used for bubbling gases through liquids.

### 6.2.1 Sparged Vessel

In its simplest form a sparged vessel consists of a tank holding the liquid in which the gas is introduced as small bubbles. For small tanks, an open tube located at the bottom serves the purpose of a sparger. For larger vessels, a horizontal pipe at the bottom of the tank with several orifices of 1.5 to 3 mm diameter disperses the gas into the liquid as fine bubbles. Sparging serves dual purposes, it makes better contact between the sparged gas and the liquid, and also provides gentle agitation.

## 6.2.2 Mechanically Agitated Device

An agitated vessel usually consists of a baffled tank provided with a turbine type stirrer and a ring shaped sparger equal to or slightly smaller than the impeller diameter. The sparger is usually located below the impeller and provided with holes varying from 3 to 6 mm in diameter. The number of holes is so adjusted as to provide a hole Reynold's number of not less than 10,000. The distance between the holes, i.e. pitch of the holes should be more than the bubble diameter. The depth of liquid is usually kept equal to the tank diameter with adequate free space at the top to allow for gas hold-up. If higher time of contact is desired, the liquid depth is increased while an additional impeller may be provided to redisperse the gas bubbles which otherwise tend to coalesce. The superficial gas velocity is normally kept within 0.10 m/s.

As in case of sparged tanks, the mass transfer resistance in agitated vessels also lies mostly in liquid phase. The mass transfer coefficient may be approximated by

$$Sh_L = 2.0 + 0.31 Ra^{1/3}$$

(6.1)

where

$$\frac{d_p^3 \cdot \Delta P \cdot g}{D_L \mu_L}$$

$Ra$  = Rayleigh number given by

$d_p$  being the bubble diameter.

Multi-stage counter-flow of gas and liquid may be achieved by arranging the tanks in cascade with the gas flowing from the top of one tank to the bottom of the next higher tank and the liquid flowing in the opposite direction.

## 6.2.3 Plate Column

Plate columns are widely used for distillation as well as for gas absorption/ desorption. These are vertical cylindrical towers in which liquid and gas or vapour are contacted counter-currently in stepwise manner on the plates or trays. The gas or vapour enters near the bottom, rises through the openings in the trays and then through the liquid pool on the trays in dispersed condition, thus coming into intimate contact with the liquid before leaving at the top. The liquid enters near the top, flows down from tray to tray through downcomers, crosses each tray, contacts the gas or vapour issuing from the openings on the trays and leaves at the bottom. The overall effect is multiple counter-current contact of liquid and gas or vapour while each tray provides cross flow of the two fluids. Depending on the requirement, configuration of cross flow trays may be of the three types, single pass, reverse flow, and multiple pass. However, the number of trays depends on the extent of mass transfer while the diameter of the tower depends on the quantity of liquid and gas or vapour to be handled, and in case of distillation, on the reflux ratio. Conditions leading to high mass transfer efficiencies cause operational difficulties. Each tray of the tower acts as a stage where the fluids are brought into intimate contact to permit diffusion of one or more component and then they are physically separated. In order to achieve high tray efficiency, there should be thorough mixing of the two fluids, interfacial surface of contact should be as large as possible and time of contact as long as possible. The pre-requisite for long exposure time is that the liquid pool on the tray should be as deep as possible.

When the gas rises slowly through the openings on the tray, bubble size is large and interfacial area of contact is relatively small, the liquid is quiescent and some of the liquid may pass without contact with the gas or vapour. If, on the other hand, the gas velocity is high, there is thorough agitation and foaming. For high plate efficiency, deep liquid pool and high gas velocity are required. These in turn lead to longer plate spacing resulting in taller tower and higher fixed cost. The pressure drop within the tower also increases leading to higher operating cost. High gas velocity may also lead to flooding and stoppage of operation. An intelligent compromise should therefore be made for which one should be aware about the constructional and operational aspects of the following hardwares.

**Tower shell:** Towers are generally made of cylindrical shells of metals and alloys although glass, glass-lined metal, impervious carbon, plastic or even wood are used for the purpose depending upon the specific requirements and corrosion conditions. Smaller diameter towers are provided with hand holes while larger ones are provided with manholes for cleaning and repairing.

**Tray and tray spacing:** Trays are usually made of sheet metal. Special alloys are used for corrosive fluids. Plate thickness depends on corrosion rate. The trays are stiffened and are fastened to the shell with allowance for thermal expansion to prevent their movement by surges of gases.

Tray spacing is decided from the convenience of construction, maintenance and cost and then checked that adequate provision has been made against flooding and entrainment. The spacing normally depends on the column diameter and operating conditions, and varies from 0.15 m to 1 m. However, tray spacing of 0.5 m is quite common for trays of 1 to 3 m diameter, the recommended range being 0.3 to 0.6 m. In the column employed in chemical process industries, tray spacing generally varies between 450 and 900 mm which help to avoid premature flooding as well as excessive entrainment. Lower tray spacing restricts allowable vapour velocity thereby promotes froth regime operation, however, may be used where tower height is a constraint. Standard tray spacing for large-diameter columns are generally either 0.46 or 0.61 m, but 0.3 and 0.91 m spacing are also used.

**Tower diameter:** Tower diameter should be sufficiently large to handle the liquid and gas or vapour at velocities within the range of satisfactory operation so as to ensure proper dispersion and mixing without excessive pressure drop, which may lead to flooding. Flooding may occur due to loading of liquid in the column caused by the high vapour or gas velocity in upward direction. During such counter-current flow of gas/vapour and liquid, the transfer of momentum takes place from gas/vapour phase to liquid phase. When the upward momentum exceeds the liquid weight, the flooding usually occurs. Detailed discussion on such flooding in the packed tower has been dealt within Section 6.3.2. However in plate columns for a specific liquid flow rate, a maximum vapour flow rate exists beyond which incipient column flooding occurs because of backup of liquid in the downcomer. This condition when sustained, leads to carryout of liquid with the overhead vapour leaving the column.

*Downcomer flooding* takes place when liquid backup is caused by downcomers of inadequate cross sectional area to carry the liquid flow but rarely occurs if the cross sectional area of downcomer is at least 10% of the total cross sectional area of the column and if tray spacing is at least 60 cm. Another design limit is *entrainment flooding* which is caused by excessive carry over of liquid by vapour entrainment to the tray above. This entrainment of liquid is due to carry up of suspended droplets by rising vapour or to throw up of liquid particles by vapour jets formed at tray perforations, valves, or bubble-cap slots. During passage of gas/vapour through the liquid, drops of various sizes are usually formed. The smaller sized drops do not tend to settle when their terminal velocities become less than

the gas/vapour velocity, thus resulting their carry over to the tray above. The large sized drops however will tend to fall back after travelling certain distance in upward direction. When such drops will not fall back, these will also be carried over to the next upper tray. The superficial gas velocity at flooding is given by

$$V_F = K \left( \frac{\sigma}{20} \right)^{0.2} \left( \frac{\rho_L - \rho_G}{\rho_G} \right)^{0.5}$$

(6.2)

where,

$V_F$  = net vapour velocity at flooding condition, i.e. volumetric flow rate of gas at flooding divided by the net tower cross section

$K$  = Souders and Brown factor at flooding condition in m/s may be obtained from Fair correlation presented in Figure 6.1 (adapted from Fair 1961) for different tray spacing

$\sigma$  = surface tension, dyne/cm

$\rho_L$  and  $\rho_G$  = densities of the liquid and vapour streams in the column respectively.

More discussions on calculation of flooding velocity in plate type column have been made elsewhere (Coulson et al. 1985, Lockett 1986, Humphrey and Keller 1997, Seader and Henley 2006).

A high vapour velocity is needed for high plate efficiencies, and the actual velocity ( $V_n$ ) will normally be between 70-90% of the flooding velocity. However for design, a value of 80 to 85% of the flooding velocity is usually used. The net column area,  $A_n$  is obtained from the relation

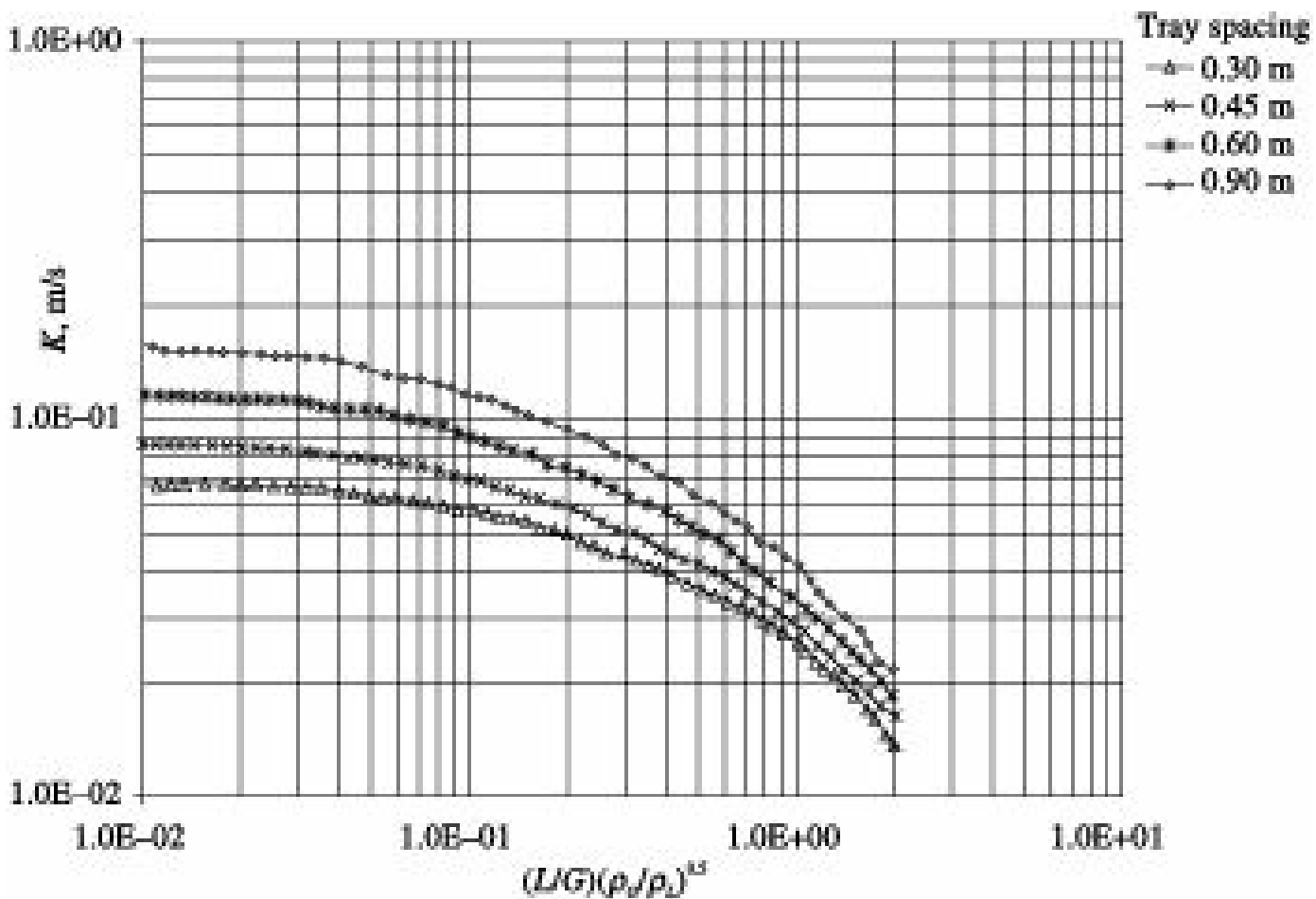
$$A_n = \frac{\text{Volumetric flow rate of vapour}}{\text{Actual vapour velocity, } V_n}$$

(6.3)

and  $A_C = A_n + A_d$

(6.4)

where  $A_C$  is the cross sectional area of the column and  $A_d$  is the downcomer area.



$L$  and  $G$  stand for liquid and vapour/gas flow rates respectively, kmol/s

Figure 6.1 Values of  $K$  for use in Eq. (6.2).

The column diameter,  $D$  is then calculated from the relation

$$D = \left( \frac{4A_c}{\pi} \right)^{0.5}$$

(6.5)

In actual practice the column diameter obtained using Eq. (6.5), is required to be rationalized.

### Downcomers

The liquid flows from a plate to the plate next below through downcomers or downspouts. A portion of the tower cross section, separated by a vertical plate, generally serves as the downcomer although circular pipes are also used. Sufficient residence time has to be allowed in the downcomer for releasing any gas or vapour that might be entrapped in the liquid. The bottom of the downcomer should be well submerged within the liquid on the next lower plate so as to prevent any gas or vapour escaping through it.

### Weir

Weirs are provided at the downcomer entrance to maintain the desired liquid pool on the plate. Extension of the downcomer plate usually acts as weir. The weir height required to maintain the volume of liquid on the plate, is an important parameter in determining the plate efficiency. A high weir will increase the plate efficiency but at the expense of a high pressure drop across the plate. For columns operating above atmospheric pressure weir heights should normally be between 40 and 90 mm; 40 to 50 mm being recommended. For vacuum operation lower weir heights are used to reduce

the pressure drop; 6 to 12 mm is generally recommended.

The three commonly used plate columns are bubble-cap columns, sieve-plate columns and valve-tray columns shown in Figure 6.2. Design procedures of these columns have been dealt with elsewhere (Smith 1963, Van Winkle 1967, Billet 1979, Coulson et al. 1985, Walas 1988, Ludwig 1997). When trays are designed properly, a stable operation is achieved wherein (i) vapour flows only through the perforations or open regions of the tray between the downcomers, (ii) liquid flows from tray to tray only by means of the downcomers, (iii) liquid neither weeps through the perforations of the tray nor is carried by the vapour as entrainment to the tray above, and (iv) vapour is neither carried down by the liquid in the downcomer to the tray below nor allowed to bubble up through the liquid in the downcomer.

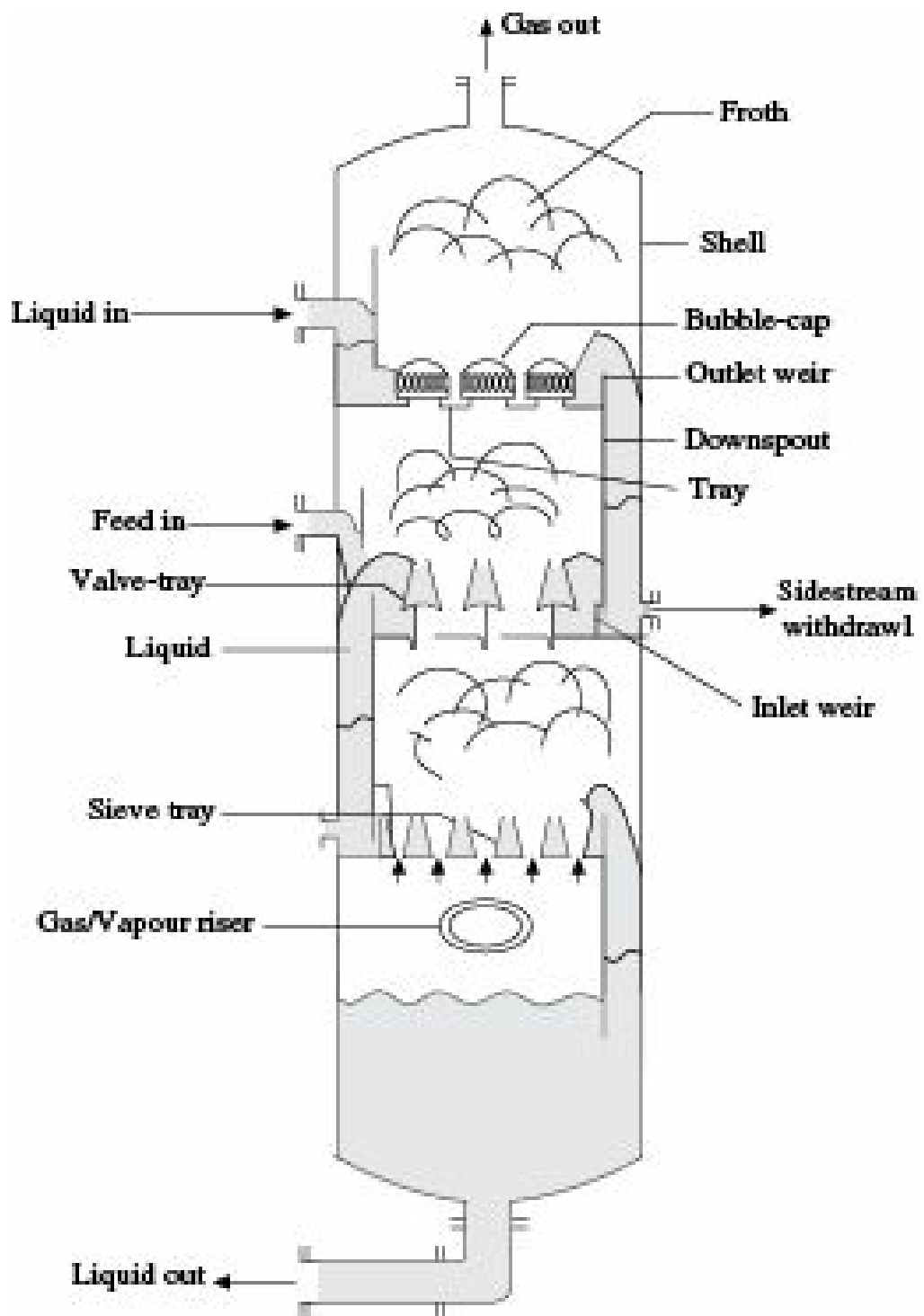


Figure 6.2 Three common types of plates used in column.

## Bubble-Cap Column

A schematic diagram of a typical bubble-cap column used in distillation operation is shown in Figure 6.3(a). The plates are provided with a number of short cylindrical vapour risers, covered by caps through which the gas or vapour bubbles, hence the name bubble-cap column. A typical configuration of bubble-cap tray has been shown in Figure 6.3(b) along with different types of caps which are in use. The gas or vapour from the next lower plate rises through the

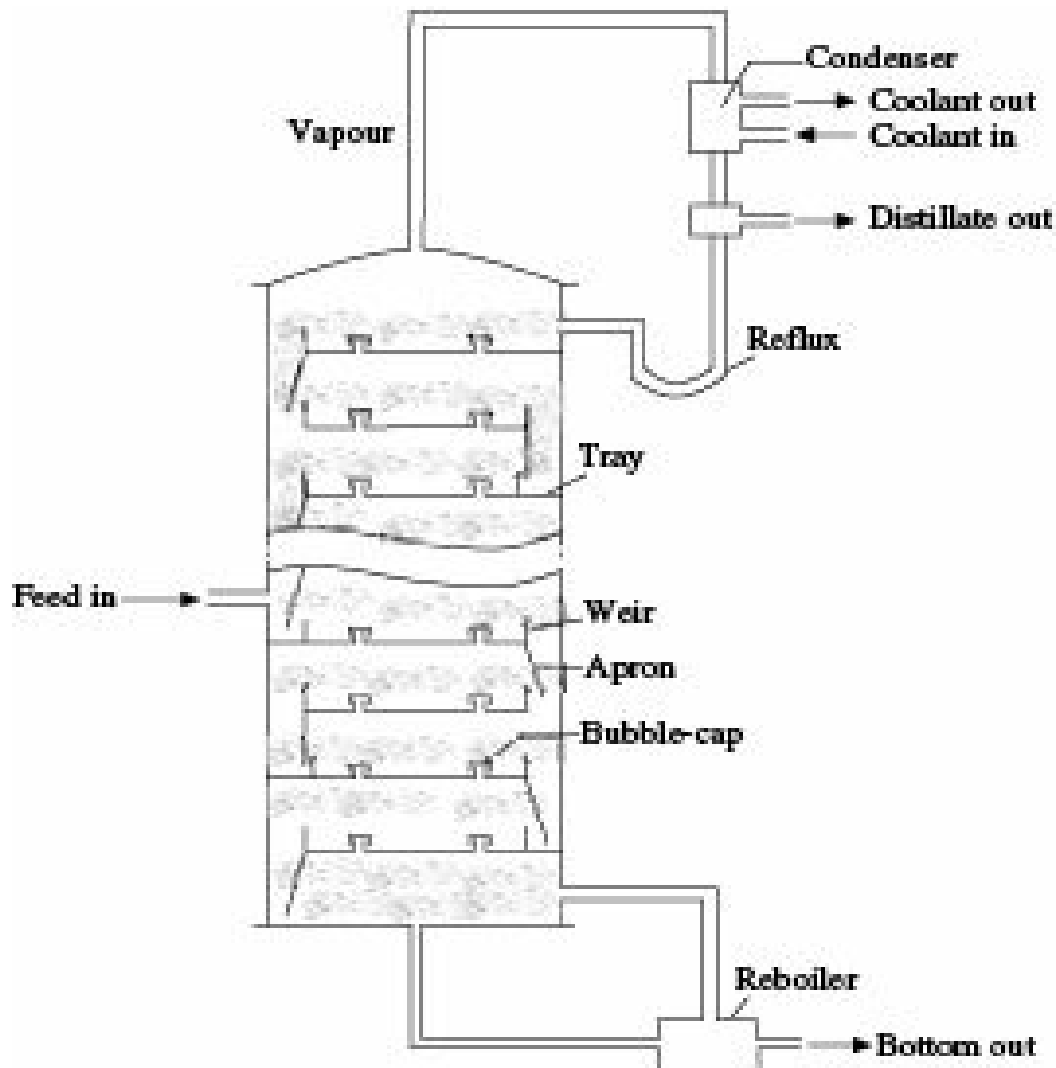
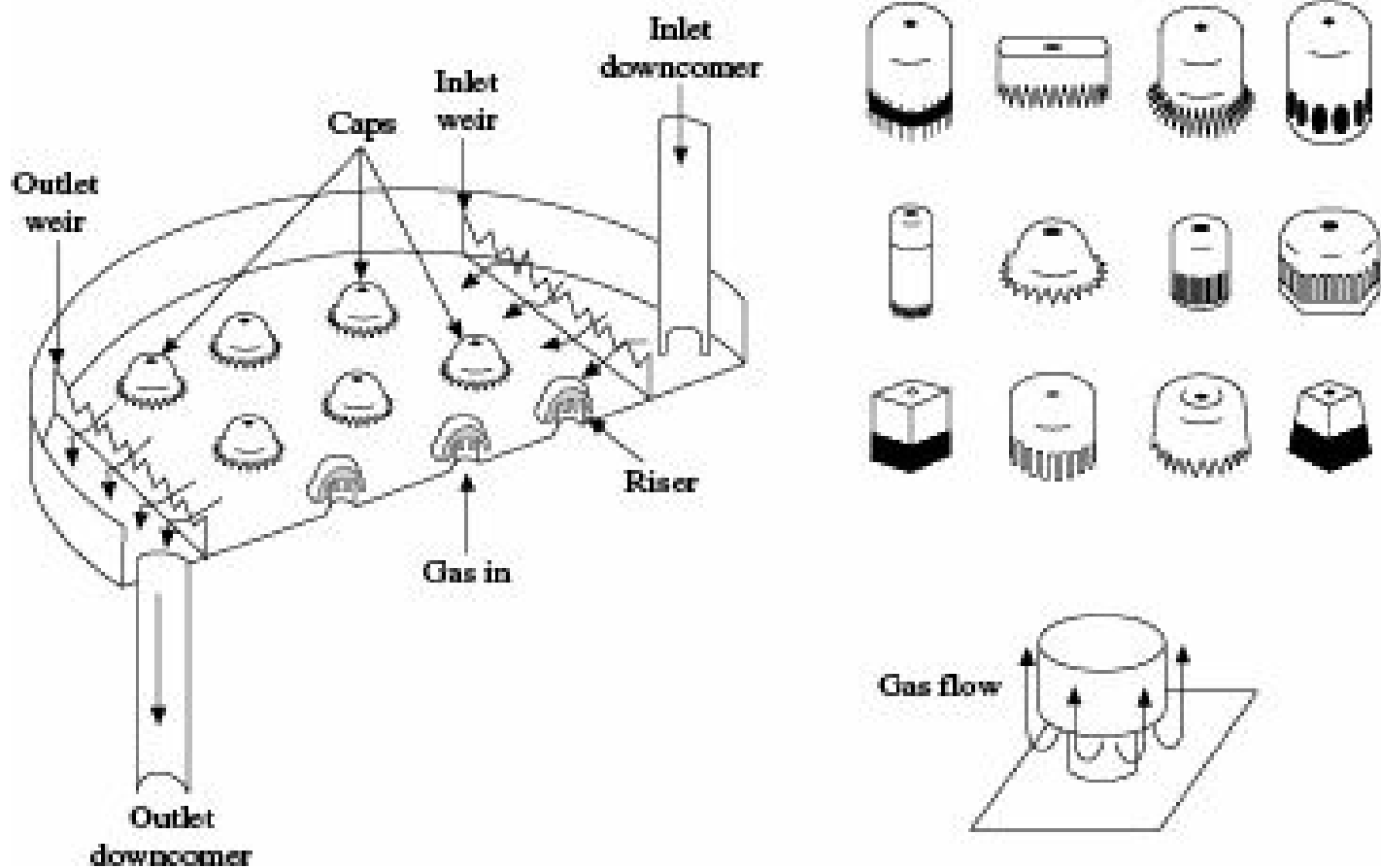


Figure 6.3(a) Schematic diagram of bubble-cap column.



**Figure 6.3(b)** Typical bubble-cap tray along with different types of caps.

vapour risers and then escapes into the liquid through slots cut in the rim or skirt of the caps. These slots being fully submerged in liquid on the plates, the gas is forced to bubble through the liquid in finely dispersed condition.

The liquid flows across each plate before passing on to the plate below through the downcomer. The flow pattern of vapour and liquid has been shown in Figure 6.3(c). Baffles are sometimes provided on the plates to ensure that liquid flows over all the caps. The gas or vapour rises through the bubble-caps in dispersed condition and produces a frothy mixture of liquid and gas providing large interfacial area for mass transfer.

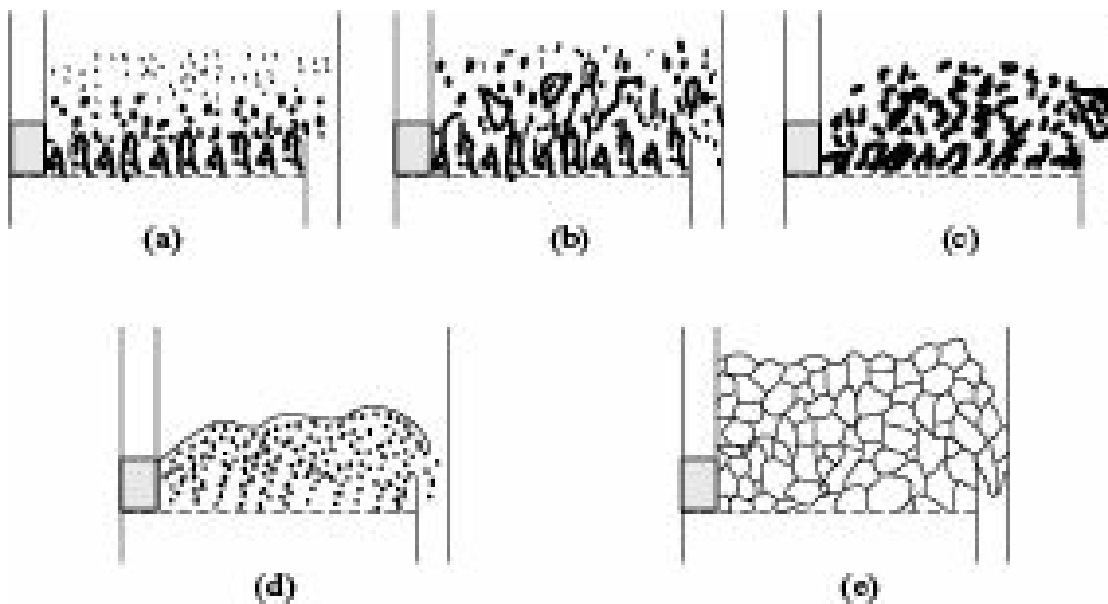


**Figure 6.3(c)** Flow pattern of vapour and liquid on a bubble-cap tray.

Because of their capacity to handle wide ranges of liquid and gas or vapour flow rates, bubble-cap

columns have been exclusively used in the industry for a pretty long time. At present however, they are seldom used in new installations in view of their high cost and availability of equally or even more efficient equipment at much lesser cost.

### Sieve-plate column

A section of a typical sieve-plate column is shown in Figure 6.4(a). Sieve plates are perforated plates usually made of stainless steel or other alloys and placed horizontally in the column. The gas or vapour from a plate rises through the perforations of the next upper plate and then bubbles through the liquid pool on the plate in finely subdivided state. Liquid flows across each tray when it comes in contact with the rising vapour or gas, then over an outlet weir, and finally into a downcomer which takes the liquid by gravity to the tray below as shown in Figure 6.4(b). A pool of liquid is retained on the plate by an outlet weir. The stated phenomena lead to form two-phase flow regime on the plate. As noticed by the practicing engineers, any one of the flow regimes shown in Figure 6.4(c) may prevail during operation.

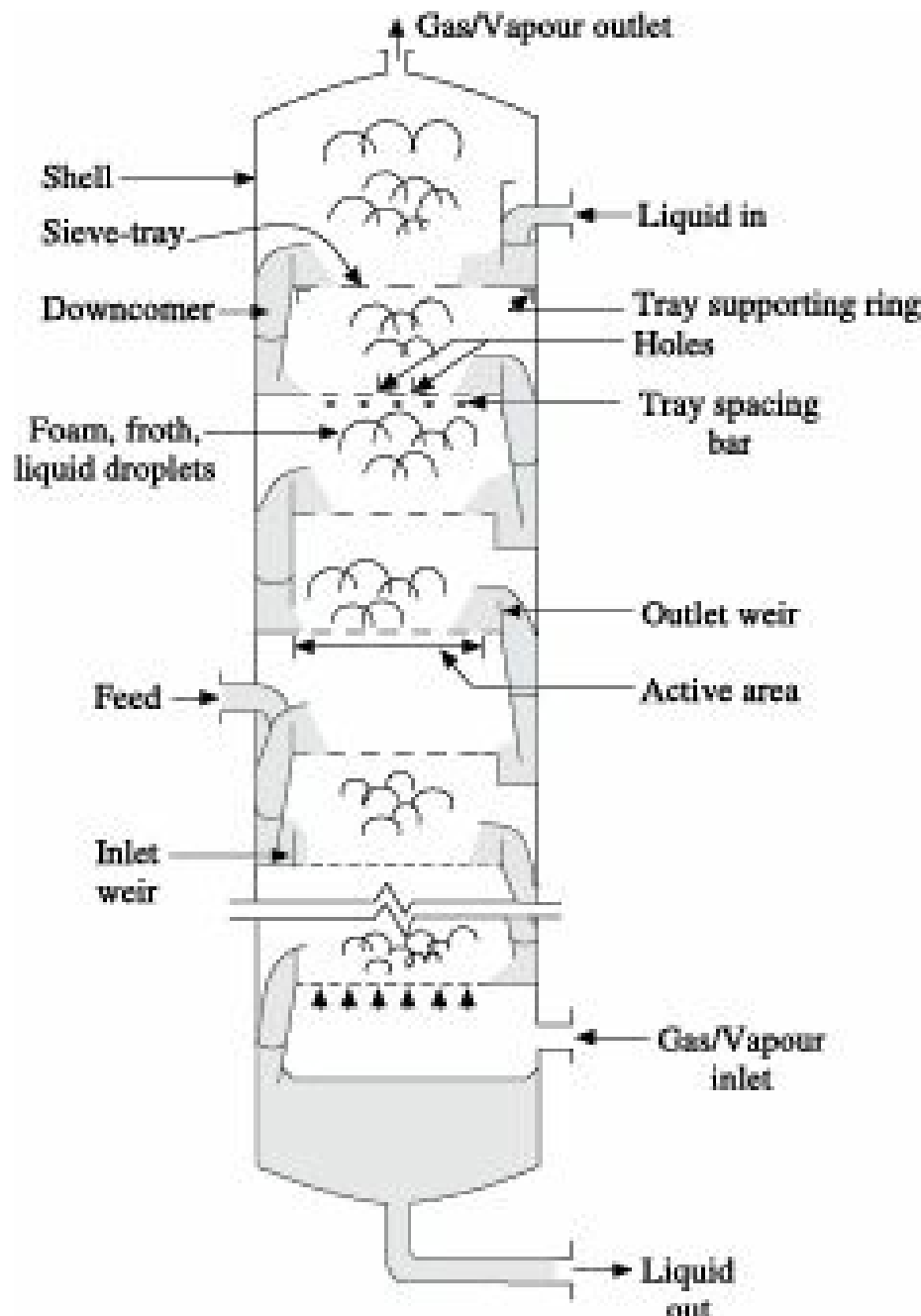


Figure 6.4(a) Schematic view of a typical sieve-plate column.

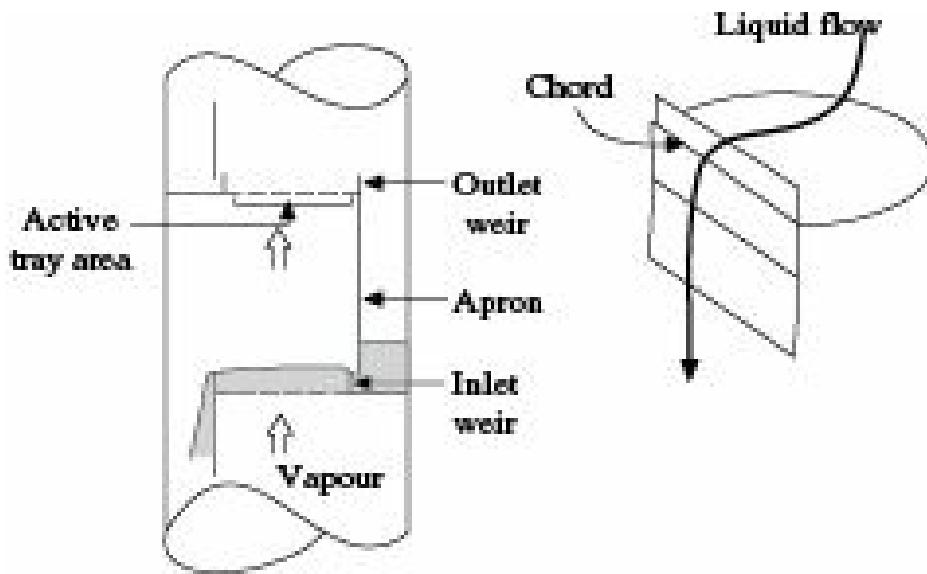


Figure 6.4(b) Downcomer operation over a plate.

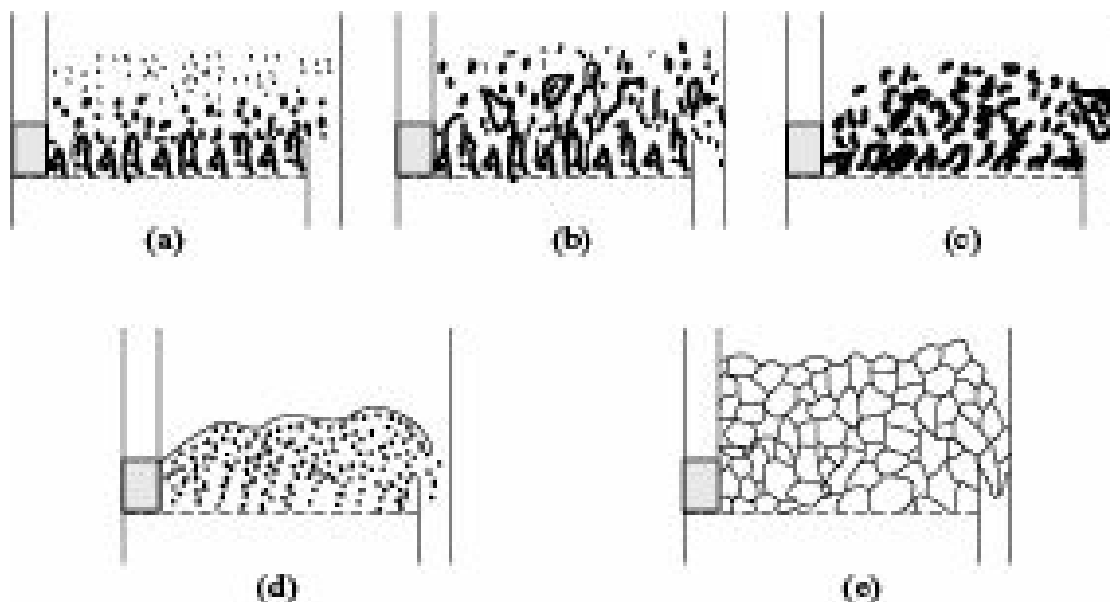


Figure 6.4(c) Two-phase flow regimes on sieve-plate: (a) Spray, (b) Foam, (c) Emulsion, (d) Bubble and (e) Cellular foam.

Downcomers are conduits having circular, segmental or rectangular cross sections which allow the liquid to flow from a tray to the next one located below. Figure 6.5 shows different types of downcomer used in plate type column. Circular downcomers (pipes) are sometimes used for small liquid flow rates. The straight, segmental vertical downcomer is the simplest in construction and less expensive than other types of downcomers, and is satisfactory for most purposes. The downcomer channel is formed by a flat plate, called an *apron*, which extends down from the outlet weir. The apron is usually vertical but may be sloped or inclined to increase the plate area available for perforation. Sometimes arc type configuration is also used. The area of a downcomer varies from 8 to 25% of the column area. In this area liquid and vapour cannot come in contact with each other. Such configuration reduces significantly the vapour handling capacity of a tray. When the downcomer is sloped from the top and truncated above the tray deck, available area for mass transfer will be somewhat higher. The sloped one providing maximum active area on the lower tray, enhances the vapour handling capacity. Also, adequate space becomes available on the top of the downcomer for the liquid and vapour to separate from each other. The downcomer extending downward from the bottom tray of a column should be sealed by a seal pan in order to restrict the flow of vapour through it. If more positive seal is required, an inlet weir can be fitted. The height of clear liquid in the

downcomer is always greater than the height of clear liquid on the tray because the pressure difference across the froth in the downcomer is equal to the total pressure drop across the tray from which liquid enters the downcomer, plus the height of clear liquid on the tray below to which the liquid flows, and the head loss for liquid flow under the downcomer apron.

The diameter of the perforation varies from 2.5 to 12 mm, 5 mm being the preferred size and they are drilled on triangular pitch of 2.5 to 5 times the hole diameter. It is to be noted that the small diameter of perforation will help in producing gas/vapour bubble of small diameter and a bubble with diameter less than or equal to 3 mm, will behave like a rigid sphere (Bond and Newton 1928, Hughes and Gilliland 1952, Davies 1960, Sherwood et al. 1975) thus preventing required mass transfer between gas and liquid phases. About 70 to 80% of plate surface is perforated. The perforated area is somewhat lower than the active area which is approximately the column area minus twice the downcomer area, due to the

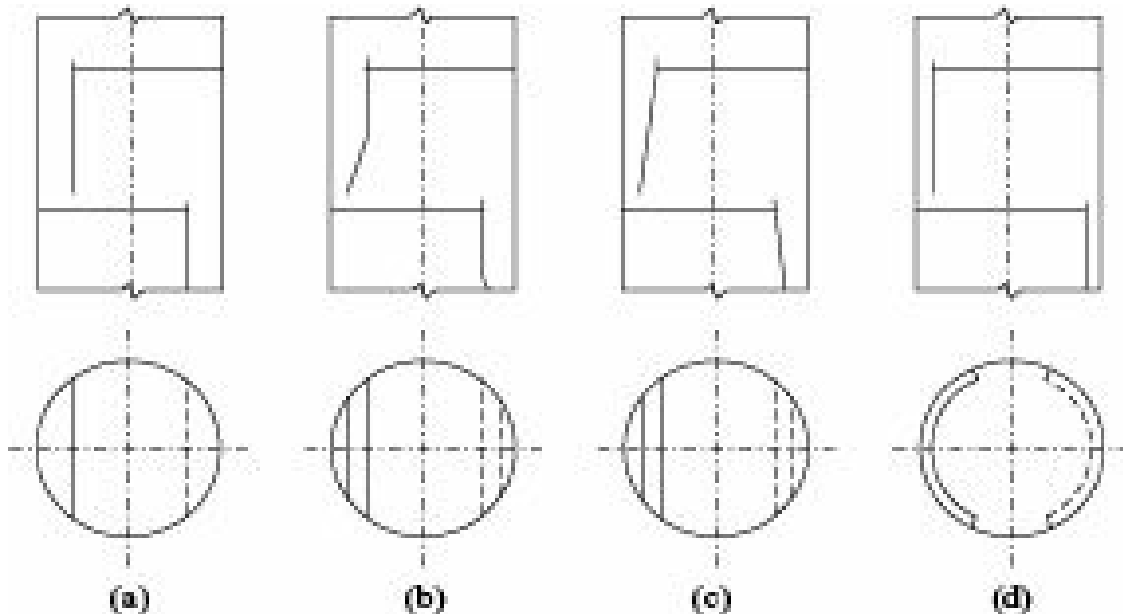
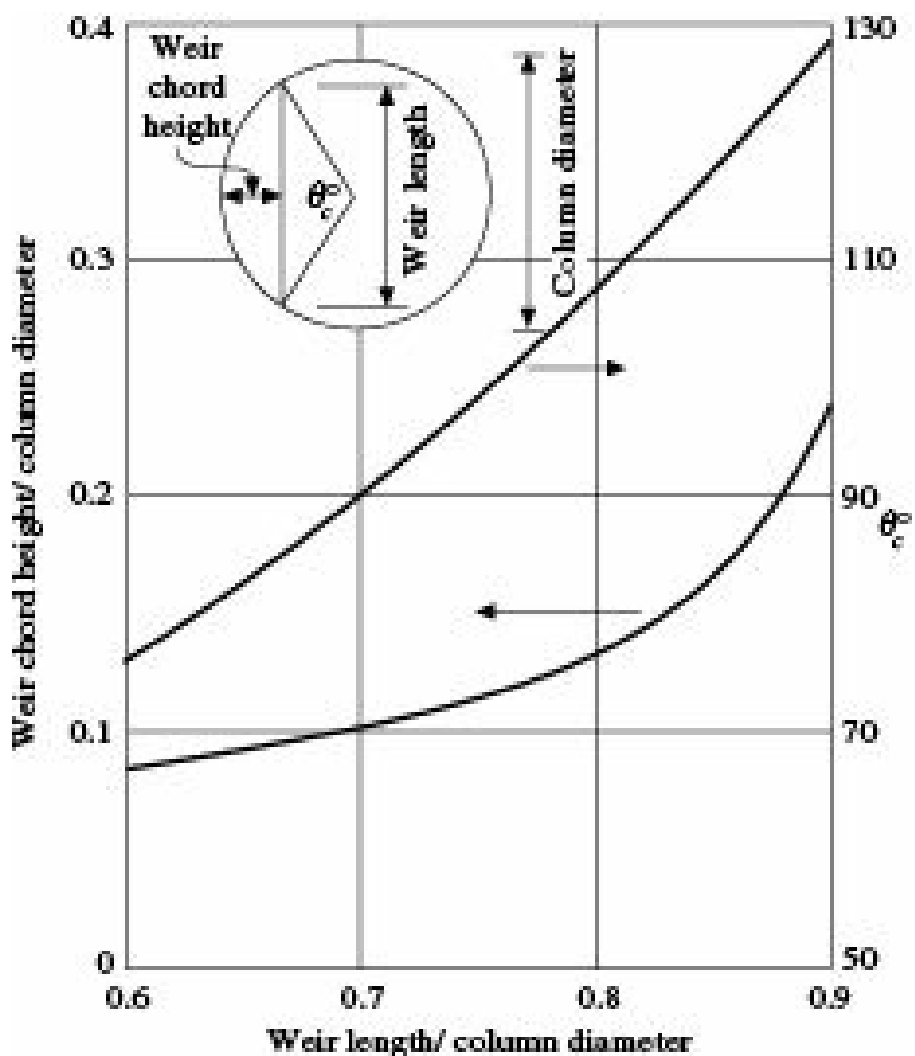


Figure 6.5 Different types of downcomers: (a) Segmental, (b) Sloped, (c) Inclined and (d) Arc.

following reasons: some spaces, called *calming zones*, on the plates just near the liquid inlet and near the overflow weir are left without perforations. This ensures minimum chances of gas or vapour escaping through the downcomer and also allows some degassing of the liquid before the same enters the downcomer. The area available for perforation may further be reduced by the obstructions caused by structural members, i.e. support rings, beams, etc. The perforated area can be calculated from the plate geometry. The relationship between the weir chord length, chord height and the angle subtended by the chord has been given in Figure 6.6 (Coulson et al. 1985).



**Figure 6.6** Relation between angle subtended by chord, chord height and chord length.

If the gas or vapour velocity through the holes falls below a certain minimum, liquid may not flow over the entire plate. Moreover, in such cases, liquid will drain through the holes. This phenomenon is known as *weeping*. As a result, gas-liquid contact on the plates will be seriously hampered. Weeping may be avoided by maintaining adequate velocity of gas or vapour through the holes.

For a tray to operate at high efficiency (i) weeping of liquid through the perforations of the tray must be small compared to flow over the outlet weir and into the downcomer, (ii) entrainment of liquid by the gas/vapour must not be excessive, and (iii) froth height in the downcomer must not approach tray spacing.

The gas-side pressure drop for flow of gas or vapour across each plate usually varies between 50-70 mm of water. This pressure drop is partly due to frictional loss for flow of gas or vapour through the holes, partly due to the liquid pool on the plate, and partly due to surface tension. In distillation, the required pressure drop is provided by the reboiler while in gas absorption, the same is provided by suitable blower.

### **Evaluation of height of column with Sieve tray**

The conversion of the equilibrium stages to actual stages requires the use of an overall tray efficiency. The most rigorous method begins with point efficiencies and then converts these efficiencies to an overall tray efficiency. Since this approach is not practicable for multi-component mixtures, a simple analytical expression developed by Lockett (1986) is recommended when no supporting experimental data are available:

$$E_O = 0.492 [n_L(a_{LK/HK})_{av}]^{-0.245} \quad (6.6)$$

where

$E_O$  = overall tray efficiency,

$(a_{LK/HK})_{av}$  = average relative volatility between the light and heavy keys, and

$n_L$  = viscosity of the feed (liquid) mixture.

Since the plate spacing was selected in a prior design step, all the information is now available to determine the height of the column exclusive of height required for phase disengagement and for housing of internal hardware.

Thus,

$$H_C = (N_{act} - 1)H_s + DH \quad (6.7)$$

where

$H_C$  = actual column height

$N_{act}$  = actual number of trays from the knowledge of overall tray efficiency and number of equilibrium stages.

$H_s$  = plate spacing, and

$DH$  = additional height required for column operation.

Detailed design of sieve-tray column has been dealt within literature (Coulson et al. 1985, Barniki and Davies 1989).

In recent years, a number of novel designs of sieve plate columns have been developed. A few important ones have been mentioned here.

Linde trays use slotted plates which not only reduce the hydraulic gradient in large plates but also eliminate stagnant areas in the liquid and approach plug flow conditions.

Counter-flow trays do not have any downcomer. Liquid and gas or vapour flow counter currently through the same openings.

Turbo-grids are sheet metals stamped with slotted openings to form the tray and so arranged that alternate trays have openings at right angles.

### Valve tray column

Valve trays are sieve trays with large, up to 40 mm diameter, variable openings for gas flow. The openings are covered with movable caps, which are lifted by the rising gas and act as variable orifices. As the gas flow increases, the valves are pushed up and provide larger space for gas flow. The valves are usually circular with dome shaped or flat caps. However, rectangular caps and caps with downward cones are also in use but they cannot always rotate as freely as the circular ones. The lifts of the caps are restricted by constructional features like special legs or spiral webs. Some caps have double lift system where the inner light caps are lifted at low gas load. As the gas flow rate increases and overcomes the weight and friction of the heavier caps, they also rise and make additional room for higher gas flow rates. Trays with such caps are known as *flexi* trays. *Ballast* trays have valves with flat caps.

A typical valve tray is shown in Figure 6.7(a). There are four main types of valve units. The V-1 type

is a general-purpose standard size unit suitable for all services. In these units, the legs are integral part of the valves and the units may be used for deck thickness up to 9.5 mm. The V-4 type incorporates a venturi shaped orifice, which substantially reduces the pressure drop across the unit. This low-pressure drop makes the V-4 type valve trays specially suitable for vacuum services.

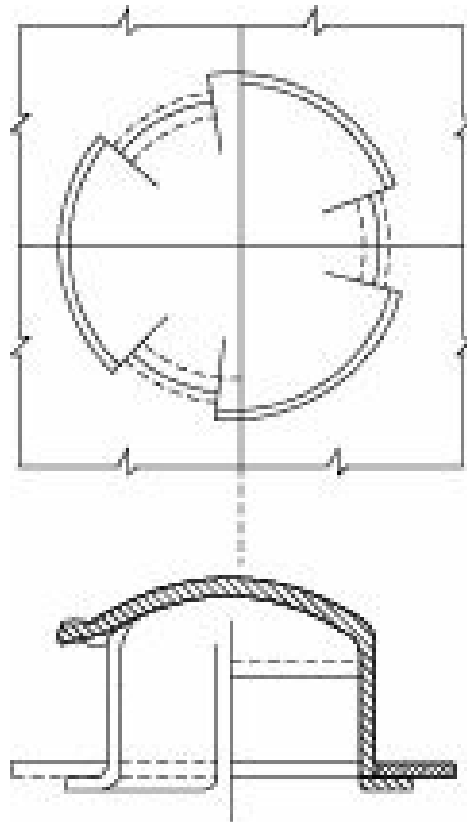


**Figure 6.7(a)** Schematic view of a typical valve.

Two kinds of valve and also a typical configuration of valve caps in a tray are shown in Figure 6.7(b). Valve trays can attain high turn-down ratio provided tray spacing is at least 0.60 m, the liquid is non-foaming, liquid loading is high and equal in all trays, vapour density is low and there is no restriction regarding pressure drop.

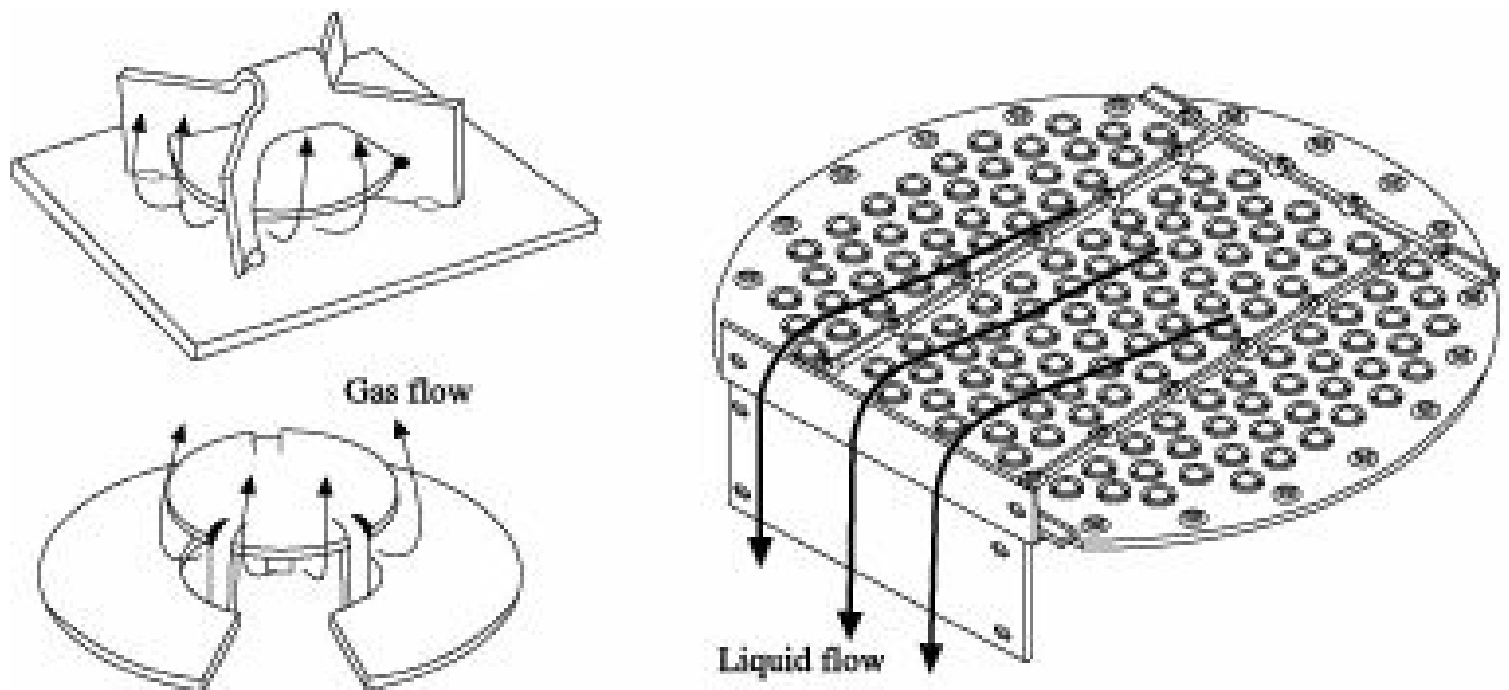


**Figure 6.7(b)** Valves and valve-caps configuration.

Valve trays can accommodate very large range of operating conditions and have higher capacity at reasonably low cost. The openings for gas flow being small at low gas velocities, chances of weeping are reduced. On the other hand, pressure drop even at high gas velocities, remain quite low due to increased openings.

The main reasons for valve trays becoming very popular in recent years are that among the three common types of trays, namely, bubble cap tray, sieve tray and valve tray, the latter is best in respect of capacity, turn-down and efficiency.

### **Selection of plate type column**

The factors need to be considered while comparing the performance of various plate columns are operating range, capacity, pressure drop, efficiency and cost. Table 6.1 gives a comparison of three types of tray on the basis of five different parameters.

**Table 6.1** Comparison of three trays

	<i>Sieve tray</i>	<i>Bubble tray</i>	<i>Valve tray</i>
Relative cost	1.0	1.2	2.0
Pressure drop	Lowest	Intermediate	Highest
Efficiency	Lowest	Highest	Highest
Vapour capacity	Highest	Highest	Lowest
Turndown ratio*	2.0	4.0	5.0

\* The ratio of the highest to the lowest flow rates is often referred to as the ‘turndown’ ratio.

Sieve plates are the cheapest and are satisfactory for most applications, valve trays will be useful where the specified turn-down ratio cannot be met with sieve plates, and bubble-caps are used where very low gas/vapour rates have to be handled and a positive liquid seal is essential at all flow rates. Sieve, valve and bubble-cap trays are examples of traditional cross-flow trays. The development of some trays over the last decades to provide improved performance has been significant. Descriptions of some of these trays including the Nye™, Max-Frac™, improved multiple-downcomer trays such as enhanced capacity multiple downcomer (ECMD) as well as the Ultra-Frac™, P-K™ and Trutna trays are available in the literature (Humphrey and Keller 1997). However, some newer trays like multiple-pass downcomer SUPERFRAC® trays and parallel flow multiple downcomer (PFMD) have been finding applications in industries.

#### **6.2.4 Plate Efficiencies**

The numbers of theoretical or equilibrium stages for a vapour-liquid separation process can be evaluated quite precisely when the equilibrium data are known. But in practice equilibrium is not attained completely on trays, and the height of packing equivalent to a theoretical stage is a highly variable quantity. In columns of large diameter ( $\geq 3$  m), significant concentration gradient exists along the path of liquid flow so that the amount of mass transfer may correspond to more than that calculated from the average terminal compositions. Mass transfer performance of packed towers is most conveniently expressed in terms of HETS (height equivalent to a theoretical stage), particularly when dealing with multicomponent mixtures to which the concept of HTU is difficult to apply. In addition to the geometrical configuration of the tray or packing, the main factors that affect their efficiencies are flow rates, viscosities, relative volatilities, surface tension, dispersion, submergence, and others that are combined in dimensionless groups.

The efficiency of mass transfer is expressed as the ratio of the actual change in mole fraction to the change that could occur if equilibrium were attained

$$\text{Efficiency, } E = \frac{\Delta y}{(\Delta y)^*} \quad \text{Figure 6.8 Concentration changes along plate } n. \quad (6.8)$$

Three kinds of efficiencies are usually found to be in use (i) Point efficiency or Murphree point efficiency,  $E_P$  (ii) Murphree efficiency or Murphree plate efficiency,  $E_M$  and (iii) Overall efficiency or Overall column efficiency,  $E_O$ .

A theoretical plate is defined as a plate in which the liquid and gas or vapour leaving the plate are in equilibrium in respect of the component being transferred. No real plate can achieve this because of the limited time of contact. Performance of a real plate is expressed in terms of Murphree plate efficiency defined as the ratio of actual enrichment on a plate to the theoretical enrichment that would occur if the system attains equilibrium.

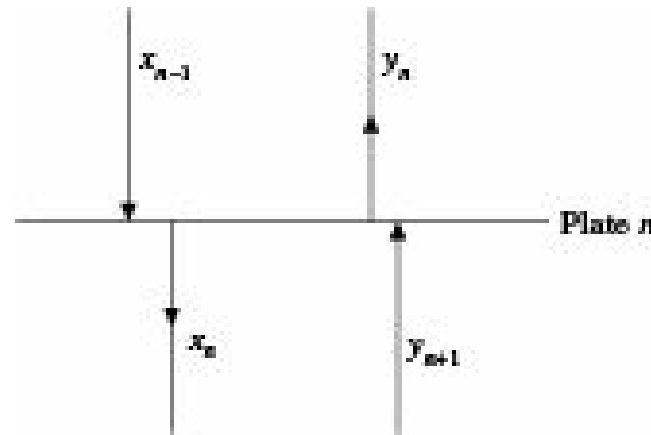


Figure 6.8 Concentration changes along plate  $n$ .

Referring to Figure 6.8, this may be expressed as

$$E_M = \frac{y_n - y_{n+1}}{y_n^* - y_{n+1}} \quad (6.9)$$

where,

$y_n$  = Average bulk concentration of solute in gas/vapour leaving the  $n$ th plate

$y_{n+1}$  = Average bulk concentration of solute in gas/vapour entering the  $n$ th plate

$y_n^*$  = Equilibrium solute concentration in gas/vapour leaving the  $n$ th plate corresponding to its average bulk concentration  $x_n$  in the liquid on the plate

Equation (6.9) represents the actual change in gas concentration on the  $n$ th plate as a fraction of the change that would have occurred if equilibrium were established.

Rewriting Eq. (5.59) for dilute systems when  $(1-y)$  may be assumed to be equal to unity, the number of overall transfer units between  $n$ th and  $(n+1)$ th plate is given by

$$N_{toG} = \int_{x_n}^{x_{n+1}} \frac{dy}{y - y^*} \quad (6.10)$$

On integrating and algebraic manipulation of Eq. (6.10), we have

$$\text{or } 1 - \exp(-N_t o_G) = \frac{y_n - y_{n+1}}{y_n^* - y_{n+1}^*} \quad (6.11)$$

Equating Eqs. (6.9) and (6.11), one can write

$$1 - E_M = \exp(-N_t o_G) \quad (6.12)$$

$$\text{or } -\ln(1 - E_M) = N_t o_G \quad (6.13)$$

$$\text{whence, } \frac{1}{-\ln(1 - E_M)} = \frac{1}{N_t o_G} \quad (6.14)$$

Comparing Eqs. (5.66), (5.67) and (5.71), we have

$$Z = H_t G \$ N_t G = H_t L \$ N_t L = H_t o_G \$ N_t o_G = H_t o_L \$ N_t o_L$$

$$\text{Hence, } \frac{1}{N_t o_G} = \frac{H_t o_G}{Z}$$

Substituting the expression for  $H_t o_G$  from Eq. (5.77) expressed as

$$H_t o_G = H_t G + \frac{mG_M}{L_M} H_t L$$

we have,

$$\frac{1}{N_t o_G} = \frac{H_t G}{Z} + \frac{mG_M}{L_M} \frac{H_t L}{Z} = \frac{1}{N_t G} + \frac{mG_M}{L_M} \frac{1}{N_t L}$$

Hence,

$$\frac{1}{-\ln(1 - E_M)} = \frac{1}{N_t o_G} = \frac{1}{N_t G} + \frac{mG_M}{L_M} \frac{1}{N_t L} \quad (6.15)$$

For large plates, Murphree plate efficiency which represents average performance of a plate is rather over simplification since it does not give any idea about performance of different parts of the plate, which may differ significantly. In such cases, point efficiency, defined by Eq. (6.9) may be used,

$$E_P = \frac{y_n - y_{n+1}}{y_n^* - y_{n+1}^*}$$

where, the concentrations are at a particular point on the plate.

Murphree plate efficiency may be correlated with Murphree point efficiency as

$$E_M = \frac{L_M}{mG_M} \left\{ \exp \left( E_P \frac{mG_M}{L_M} \right) - 1 \right\} \quad (6.16)$$

If the liquid on the plate is of uniform concentration every where due to complete mixing of the liquid,  $x = x_n$  for the liquid, and  $y^* = y$  will also be constant over the plate. In such situation, the Murphree plate efficiency and Murphree point efficiency become equal

$$E_M = E_p \quad (6.17)$$

The overall performance of a plate tower, in its simple form may be expressed in terms of overall plate efficiency,  $E_O$  as

$$E_O =$$

$$\frac{\text{No. of theoretical plates required}}{\text{No. of actual plates provided}}$$

An estimate of the overall plate efficiency although too much over simplification, is needed when the design method used gives an estimate of the number of ideal stages required for the separation. A relationship between the overall tray efficiency,  $E_O$  and Murphree plate efficiency,  $E_M$  is represented as follows:

$$E_O = \frac{\ln [1 + E_M ((mG_M/L_M) - 1)]}{\ln(mG_M/L_M)} \quad (6.18)$$

Because of concentration gradients along the tray, primarily in the liquid phase, the overall efficiency is different from point efficiency. Since the hydraulics of the tray usually cannot be known accurately, point and overall efficiencies are difficult to relate. Walas (1988) has shown selected values of efficiencies of some types of trays for various systems operating under different process conditions. Since the efficiency may vary with the position of individual tray and with the position of the tray in the tower, three kinds of efficiencies are not the same. In a situation if values of more than one type of efficiency are available, the lowest value of the efficiencies should be taken as the overall efficiency when required.

For estimation of tray efficiencies a number of simpler correlations/equations are available in literature (O'Connell 1946, Chu et al. 1951, AIChE 1958, Bakowski 1963, 1969, McFarland et al. 1972). A critical survey on the available correlations and or equations has been dealt by Vital et al. (1984). The relations proposed by Bakowski and McFarland et al. give a good fit to the experimental values while others give conservative values. However, the method of O'Connell is popular because of its simplicity. It expresses the efficiency in terms of the product of viscosity and relative volatility for fractionators, and the equivalent term  $HP/n$  for absorbers and strippers,  $H$  being the Henry's constant while  $P$  and  $n$  represent total pressure and viscosity, respectively. Nevertheless, the collected experimental data and the several correlations mentioned just give a background on the basis of which judicious decision can be made for solution of specific problems.

### 6.3 Liquid Dispersed

An important characteristic of liquid flow on tower packings is the mixing of the film which occurs as it flows over successive layers of the packing. This has the effect of reducing the average time of exposure of the surface, i or increasing the rate of surface renewal,  $s$  and therefore increases the transfer coefficient for the liquid film. However, in packed columns the area of the liquid film, i.e.

mass transfer area is a variable and cannot be measured with any degree of precision. These observations have triggered for an apparatus which would serve as a model for industrial packed towers so that experiments could be carried out on a small scale in the laboratory to provide data for the design of full scale equipment. Small packed towers are unsuitable for this purpose since they do not reproduce the type of flow and distribution which is characteristic of industrial packings as will be shown afterwards. A laboratory model which simulates a ‘point’ in the packed column may be used for generating data to be used in the design of regular packed towers. The simulated towers are the only mass transfer equipment in which the interfacial area of contact between the two phases can be measured precisely, as a result of which they are very useful for investigational purposes. But the relatively smaller surface area available for mass transfer has limited use in the industry. They are only used in cases where the rate of mass transfer is very fast and it may be necessary to keep the same under control.

### 6.3.1 Simulated Packed Tower

The following are the simulated packed towers used for predicting data to be used for scaling up and designing regular packed towers.

#### *Wetted-wall tower*

A wetted-wall tower (Figure 6.9) consists of a vertical pipe fitted with a liquid inlet section, a liquid outlet section and a calming section. The calming section sufficiently long enough is used to ensure that the gas flow has become steady and uniform before it enters the central zone (mass transfer zone). The liquid flows down in the form of thin film maintaining laminar flow along the inner wall and gas flows upwards through the central core, and the rate of mass transfer is calculated from the concentration of the gas and liquid entering and leaving the apparatus.

The gas film coefficient may be determined by measuring the rate of absorption of a highly soluble gas, but a more convenient method is to measure the rate of evaporation of a pure liquid in a gas stream since with this method the conditions can be adjusted so that there is no response due to diffusion in liquid. Liquid film coefficients are determined by measuring the rate of absorption or desorption of pure gases or gases of very low solubility. Wetted-wall towers have been employed in several investigations of the absorption of sparingly soluble gases, which are controlled by mass transfer in the liquid film. For instance, wetted-wall towers are used for absorption of hydrochloric acid gas which is accompanied by the evolution of large quantity of heat and the heat is removed by spraying water on the tower. In wetted-wall columns using transfer section of higher magnitude in length, the ripples which develop in the liquid film have a pronounced effect on the transfer coefficient (Vivian and Peaceman

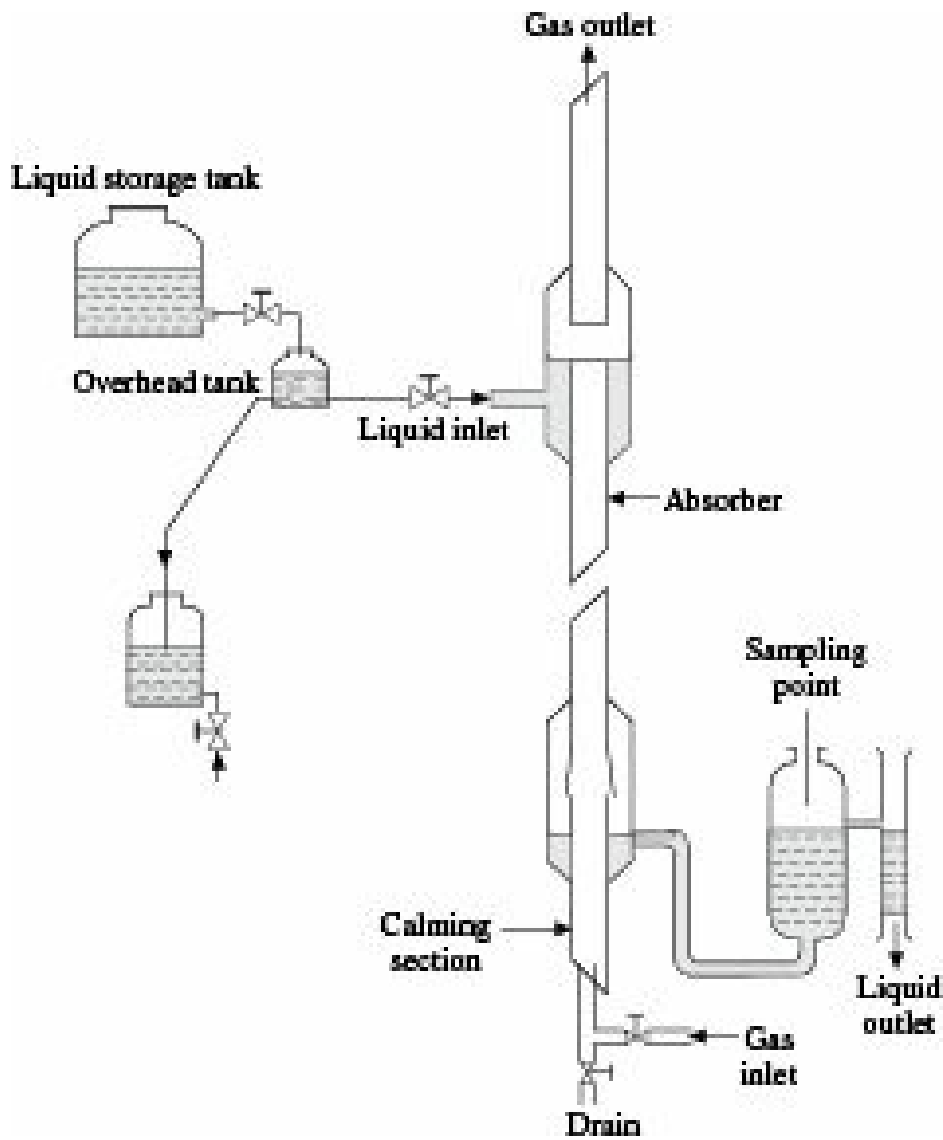


Figure 6.9 Wetted-wall tower.

1956). However, the surface ripples in water films can be suppressed by the addition of wetting agents which depress the surface tension by forming oriented molecular layers at the surface.

The wetted-wall column has been used in the study of mass transfer in distillation processes. In an adiabatic distillation column the molar rate of transfer of the more volatile component from the liquid to vapour phase is balanced by an equal molar transfer of less volatile component from the vapour to the liquid. The results correlated on the basis of the gas-film mass transfer coefficient, are in good agreement with the equation of Chilton and Colburn.

Wetted-wall towers are usually operated in counter-current fashion with liquid flowing down. But co-current flow is also used in some cases. Co-current flow with both the fluids moving upwards can achieve very high mass transfer rates. For instance, in a 15.8 mm diameter wetted-wall tube employing co-current up flow of air-ammonia mixture and water with water rate of 0.5 g/cm s and gas velocity of 52 m/s, the gas side mass transfer coefficient was found to be 19.5 cm/s (Sinha 1961), whereas for counter-current flow with similar equipment and liquid flow, the same seldom exceeds 1.5 cm/s.

The wetted-wall tower has provided valuable data for gas-film controlled processes but in liquid-film controlled processes, the mass transfer is strongly influenced by the rippling behaviour which varies with both the flow rate and height of the tower (Norman 1961). Consequently, it becomes difficult to relate the liquid film performance of wetted-wall and packed towers. However,

the wetted-wall column will remain as an excellent apparatus for carrying out such investigations due to its easy fabrication and maintenance.

### String-of-Discs Column

Stephens and Morris (1951) devised an apparatus which reproduces the mixing of the liquid and has been used in a number of studies of physical absorption and chemical reaction. The string-of-discs column as shown in Figure 6.10 (Guha and De 1981) consists of a glass tube of 2.5 cm diameter provided with gas inlet and outlet at the top and bottom, and a central vertical wire (dia 3 mm) made of stainless steel on which is threaded a row of discs on edge with every disc at right angles to its neighbours. The discs are made of metal or unglazed ceramic material of low porosity, the standard dimensions being 1.45 to 2.00 cm diameter and 0.44 to 0.50 cm thickness. The liquid is fed through a jet surrounding the supporting wire and spaced 4 to 5 cm above the top disc, and collected from the bottom disc by a 1 cm bore tube with an enlarged entry. This disc column reproduces the liquid mixing and redistribution which is characteristic of flow on tower packings. The investigations have shown that the mass transfer coefficient is independent of the height of the packing, which usually comprises of 20 to 50 discs.

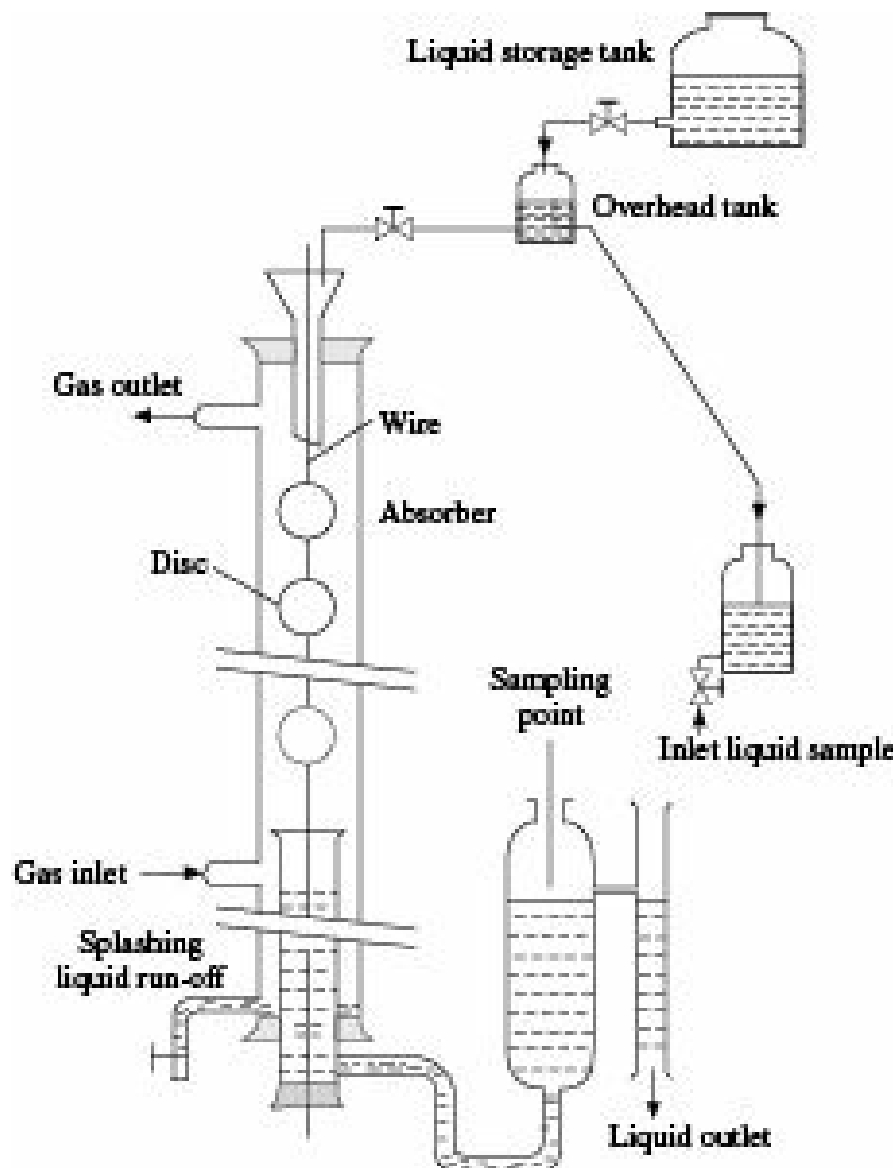


Figure 6.10 String-of-discs column.

Also, the experimental results on absorption of carbon dioxide in water at 20°C, the results have been correlated by the equation

$$k_L = 0.019 G^{0.7} \quad (6.19)$$

where  $k_L$  is the liquid-film mass transfer coefficient, cm/s and  $G$  is the water flow rate in g/s divided by the mean perimeter of the discs in cm for liquid flow. The investigations have shown the mass transfer coefficient to be independent of the gas flow rate for the systems (Guha and De 1981). However, in the gas-film controlled absorption system (ammonia-water), the mass transfer coefficient showed its dependency on the increase of gas flow rate relative to the liquid flow rate to the power 0.68.

### ***String-of-spheres column***

Another model for simulated packed towers comprises a string of spheres on a vertical wire or rod, with liquid fed to the top sphere and flowing down over each sphere in turn as shown in Figure 6.11 obeying the principle as in string-of-discs column.

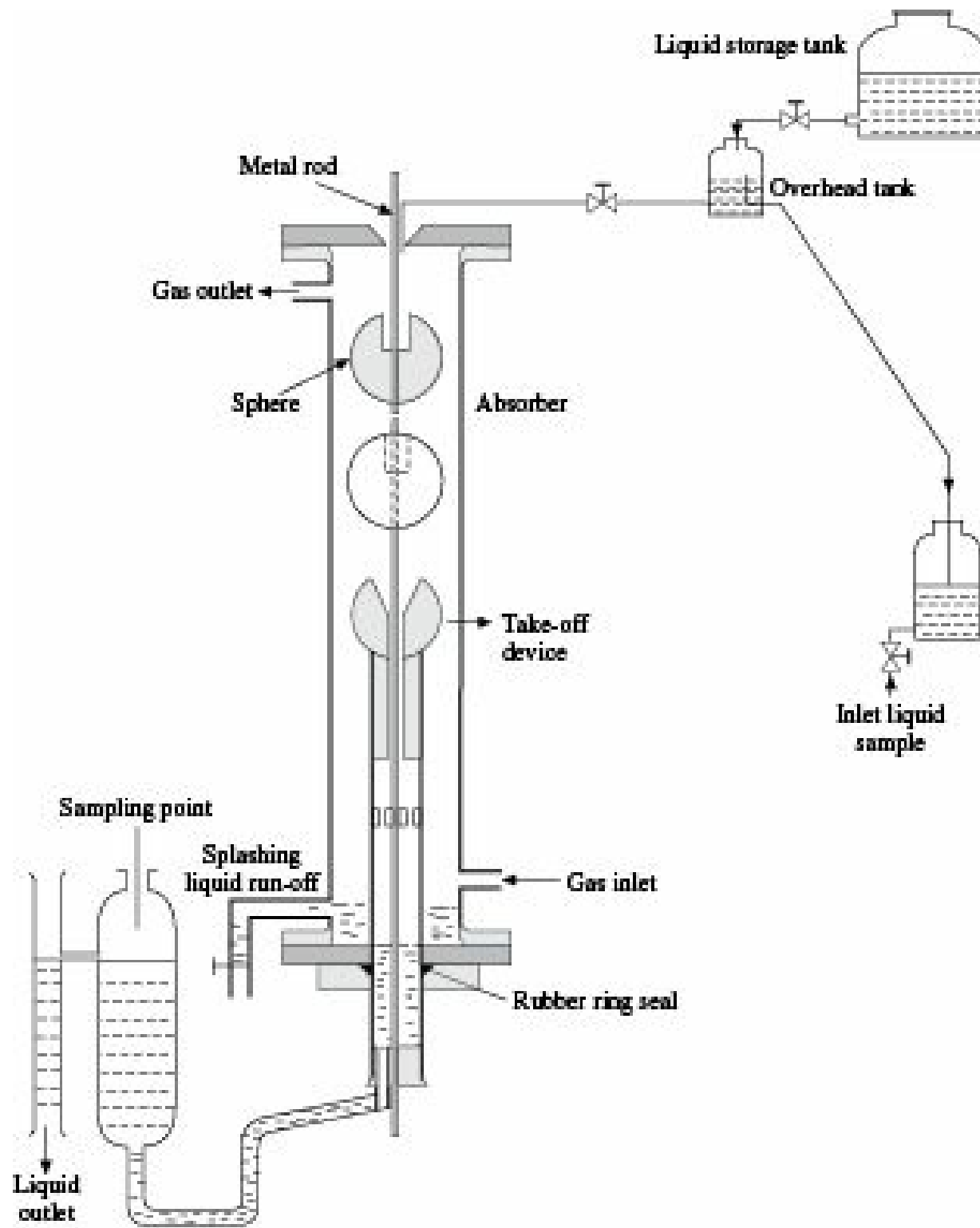


Figure 6.11 String-of-spheres column.

The column (Figure 6.11) consists of spheres, each of 3.5-4 cm in diameter with a cylindrical pool (1–1.25 cm diameter and 1.5-1.8 cm deep) at the top of each sphere. The spheres are supported on a rod of 3 mm diameter and the distance between two consecutive spheres can be kept in between 1.2-1.5 cm. The number of spheres exposed to the gas can be changed between 1 and 10 by removing some of the spheres and adjusting the position of the slidable take-off device.

When a liquid runs down a string-of-spheres column one might expect complete mixing at the junction between the spheres under certain conditions. Furthermore, there might be pools on the top of the spheres so that the mean residence time of liquid could be matched to that of an industrial column. The experimental findings by various workers show that the absorption is equal to that which would occur in a wetted-wall column of the same diameter and of height equal to 0.84 of the diameter (Lynn

et al. 1955). When a number of spheres are assembled in a column there is a loss in area due to the liquid meniscus which forms at the point of contact. If the flow is laminar and no mixing occurs at the junction between the spheres, the column is equivalent to a wetted-wall column of diameter equal to that of the spheres and of height equal to 0.795 times the height of the sphere column (Davidson et al. 1959). Alper and Danckwerts (1976) used one such column for simulation of a large packed column. Comparison of the experimental data with many gas-liquid systems in string-of-spheres and packed columns under the proper scaling conditions indicates that if the inlet compositions of the liquid and gas are same, the outlet compositions are likely to be closely the same. When a gas is absorbed in the sphere and packed columns, the total absorption rate in the latter can be predicted from the measurement of total absorption rate in the sphere column.

In order to simulate the packed column, the values of  $k_G$ ,  $k_L$ ,  $(aZ/\bar{u}_L)$ ,  $(\bar{u}_L/\bar{u}_G)$ ,  $(L_W Z/\bar{u}_L)$  in the laboratory absorber should be same as those in the full-scale packed column.  $k_G$  and  $k_L$  are the gas-side and liquid-side mass transfer coefficients respectively,  $a$  is the surface area per unit volume of laboratory column or the interfacial area per unit volume of packing,  $Z$  represents height of laboratory model or of packed column,  $\bar{u}_L$  and  $\bar{u}_G$  are the superficial velocities of liquid and gas in the columns, respectively and  $L_W$  represents the liquid hold-up. Furthermore, it is desirable to make the ‘scaling ratio’, defined as the ratio of heights of packed column and laboratory model, about 5-10 for convenience. This scaling ratio makes the value of the wetting rate ( $\bar{u}_L/a$ ) for the laboratory absorber small. This, in turn, makes the flow rate of gas in the model small as the ratio ( $\bar{u}_L/\bar{u}_G$ ) is fixed.

### 6.3.2 Packed Tower

Packed towers are frequently used in gas absorption/desorption and to a limited extent in distillation. Packed towers of low initial cost and low operating cost are commonly used for air-water contact like humidification, dehumidification and water cooling.

Packed towers are vertical towers filled with suitable packing and used for continuous contact of liquid and gas/vapour. Packed towers for absorption and distillation are usually cylindrical in cross section and are made of steel or other alloys depending upon the fluids handled. Towers for air-water contact, on the other hand, may not always be cylindrical and have walls made of asbestos, cement, concrete, reinforced plastic or red-wood.

A schematic diagram of a typical counter-current packed tower for gas absorption is shown in Figure 6.12 whereas Figure 6.13 depicts a packed column used for distillation operation. Various kinds of internals present in the tower are as follows:

- (i) Main column having inlet and outlet ports,
- (ii) Grid plate for support of packing and redistributor that can also serve as a sump for withdrawal of liquid from the tower,
- (iii) Gas and liquid distributors, as the case may be,
- (iv) Hold down plate to keep low density packing in place and to prevent fragile packing from disintegrating because of mechanical disturbances at the top of the packing.

Figure 6.12 shows that the liquid is pumped to the top, distributed over the packing through suitable distributors, trickles down through the packings thereby exposing large surface area to the gas and

leaves at the bottom. The gas, on the other hand, is introduced into the open space below the packing support near the bottom of the tower, flows upwards through the voids in and around the packing coming in intimate contact with the liquid and leaves at the top. This arrangement is for counter-current operation, which is mostly practiced with packed towers.

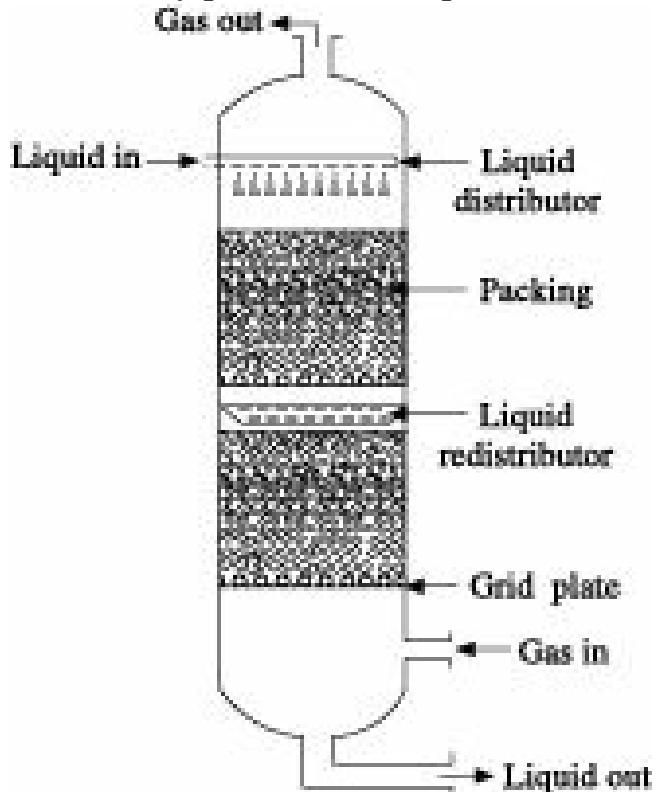


**Figure 6.12** Schematic diagram of a packed tower.

However, in case of distillation feed is introduced into the column at a point (generally at the middle along the height of the column) shown in Figure 6.13. Vapour going out through the port is passed through a condenser and a portion of the condensed liquid is fed back to the column (not shown in figure). Also, liquid at the bottom is passed through a reboiler (not shown in figure) while the vapour from the reboiler is sent back to the column. Thus, the liquid flowing in downward direction comes in intimate contact with the vapour moving in upward direction when the desired mass transfer takes place.

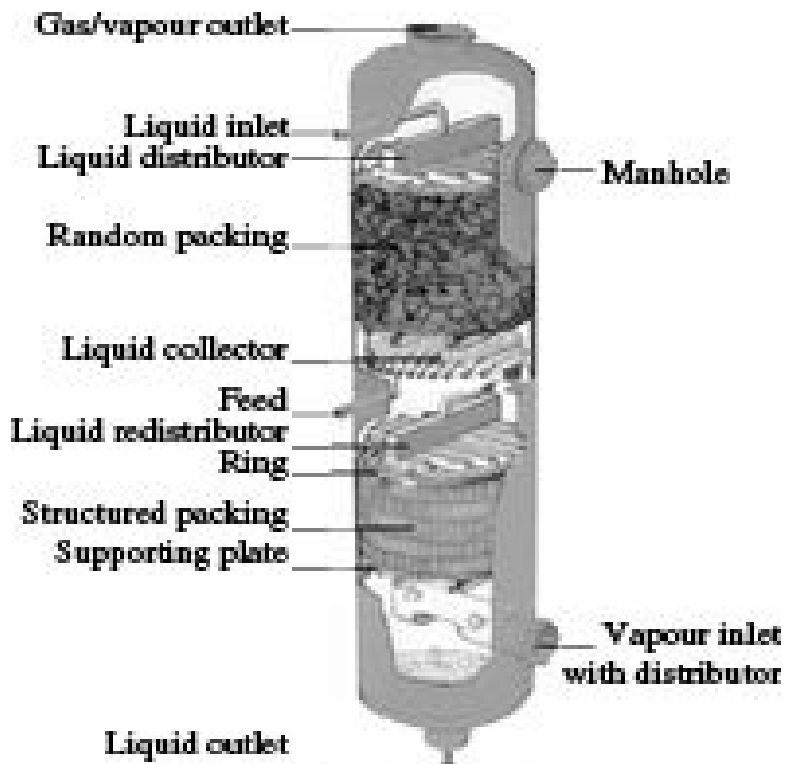


Figure 6.13 Packed tower with internals.

## Tower packing

Tower packings are manufactured in a wide variety of shapes, sizes, and materials of construction. The objectives of the packings are to provide large surface area, and large void space when packed in order to allow for efficient fluid flow characteristics.

In early days, broken rocks, coke, stoneware shapes, etc. were common packings. But they have been gradually replaced by manufactured packings. The shapes generally lead to manufacture packing in two broad categories, *random packing* and *structured packing*.

### **Random packings**

Random packings are small, hollow structures that are loaded in a nonuniform random arrangement, most often by dumping them into the tower. In order to prevent breakage of packings during dumping, the tower is first filled with water and then the packings are slowly dropped from the top. Random packings have been successfully used for more than 50 years as an inexpensive but very effective means to increase tower capacity and/or efficiency. This type of design allows higher specific surface area, but more often results in higher pressure drop. The newer random packings have thinner elements and therefore require less of the column volume than traditional packings. A variety of materials are available for random packings with both advantages and limitations. For example, stoneware is susceptible to attack by alkali and hydrofluoric acid. When metals are used, there is a concern for wettability of the surface and the possibility of high corrosion rates. Plastic packings are light weight, are easy to install, provide a low pressure drop per theoretical stage, are low-cost, and corrosion is not a problem. However, such packings can exhibit wettability problems and normally experience a temperature rise.

The following are random packings commonly used in commercial practice:

Raschig rings	Pall rings	Berl saddles
Lessing rings	Hypac	Intalox saddles
Partition rings	Tellerettes	Super intalox

Some common random packing are shown in Figure 6.14.

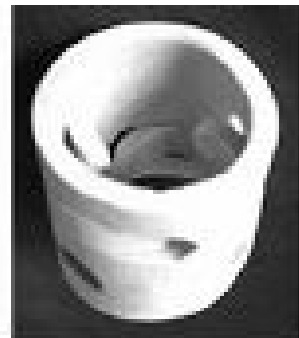
*Raschig rings*, the first ring type packing were first used in mass transfer equipment towards the end of 19th century. These are hollow cylinders with an aspect ratio, defined as the ratio of the height (or length) to the diameter, of 1:1 so that they adopt a random arrangement on dumping which assists the distribution of liquid over the packing. Available sizes range from 6 to 100 mm with void fraction varying from 80 to 98%. They are made of metals, plastics, porcelain and carbon depending upon the service requirement. Raschig rings because of their simplicity and early introduction have been investigated thoroughly and many data of their performances have been obtained, these data continue to be used today to a good extent in defining the lower limit of mass transfer efficiency that can be realized with the improved packings.



(a)



(b)



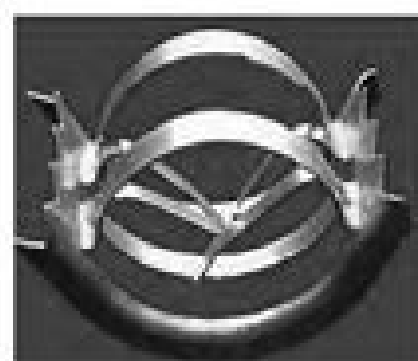
(c)



(d)



(e)



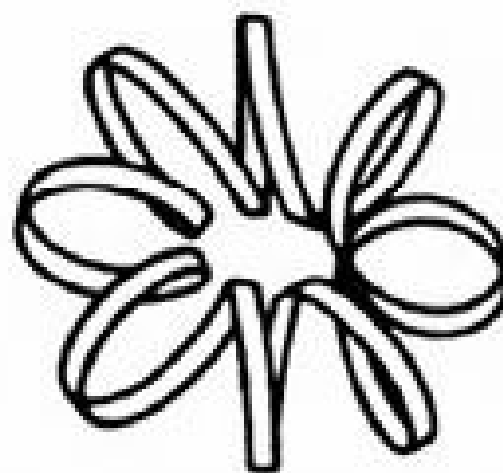
(f)



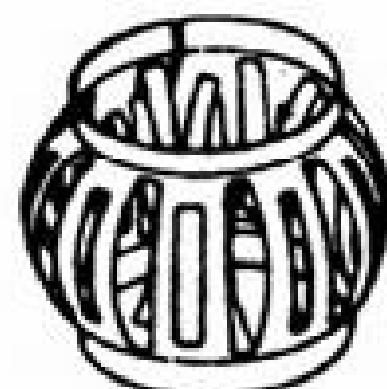
(g)



(h)



(i)



(j)

(a) Raschig ring, (b) Partition or lessing ring, (c) Ceramic Pall ring, (d) Plastic Pall ring, (e) Metal Intalox saddle, (f) IMTP packing (metal), (g) Ceramic Intalox saddle, (h) Ceramic Berl saddle, (i) Tellerette, and (j) Metal tripak.

**Figure 6.14** Some random packings.

*Lessing rings* and *partition rings* are similar in geometry to Raschig rings. Lessing ring contains a single cross-rib which provides strength and additional surface area for contacting. These are made of porcelain, stoneware, stainless steel, and other metals. Partition ring contains a double internal cross-rib and serves the following purposes:

- (i) It can act as conventional tower packing and also when stacked over a series of cross bar support grids,
- (ii) It can act as a support for dumped packing resting on it.

These are normally made of stoneware and porcelain with sizes varying from 75 to 150 mm. Larger sizes are always stacked. However, these packings have very limited use due to the introduction of packings with the newer designs.

*Cyclohelix spiral rings* are also similar to Raschig rings except there is a spiraling internal inside the cylinder. There may be single, double and triple spiral in such packing. The spiral helps in imparting swirling, spiraling turbulence to the gas to have good mixing with the liquid. This type of ring is almost always stacked rather than dumped to achieve maximum effectiveness of the spiral. Other packing designs feature openings in the walls of the ring with the resultant metal from the openings curved inward to partially simulate the cross-partition ring.

The *Pall ring*, an improvement to the Raschig ring, was introduced in the 1950s. The Pall ring used the same cylindrical dimensions employing two rows of punched and formed fingers protruding inward from the cylinder wall. Both packing elements are formed starting with a piece of metal of identical dimensions and surface area. The two rows of punched fingers causes a significant increase in performance. The capacity and efficiency have been improved and the pressure drop has been reduced. The slotted style ring utilizes its surface area much more efficiently than the tubular shape. They are economical as well. The slotted wall and internal projecting tongues lead to better wetting and distribution, and minimize flow of liquid towards the tower wall. All these factors along with low-pressure drop have made Pall rings superior to other packings and they are expected to supersede the use of other ring packings in future. Pall rings are made of stoneware, carbon, metals and plastics. Koch-Glitsch *Flexiring* packing offers a unique high strength with lower weight and improved mechanical strength. These are available in sizes ranging from 16-50 mm with void fraction varying from 93-98%. An improvement to the Flexiring is the *Hy-Pak*, introduced in the market in late 1960s maintaining 1:1 aspect ratio with the number of fingers doubled. It has corrugated walls and more intrusions than the standard designs. The mechanical strength has been enhanced through the introduction of circumferential stiffening ribs. The new geometry makes the ring, available in sizes from 30-90 mm with void fraction ranging from 97-98%, slightly larger and thus effectively provides with increased capacity, reduced pressure and same efficiency compared to those obtained using Flexiring. In 1971, *Cascade mini rings* was introduced in the market. Its improved design uses an aspect ratio of 1:3 (height of the cylinder is equal to 1/3 of its diameter). The packing elements preferentially orient themselves with the cylindrical axis tending towards vertical. This orientation provides better exposure of the interior and exterior surfaces of the rings to the liquid and gas/vapour, which helps towards more efficient use of packing surface and less restricted flow for the vapour resulting in enhanced capacity and reduced pressure drop compared to other pall rings. These are made of carbon steel, stainless steel, copper and some alloys and available in different sizes ranging

from 25-125 mm with void fraction varying from 97-98%. Nowadays *Beta ring*, an improved design of Cascade mini ring with an optimized aspect ratio, has been in use in mass transfer operations. This configuration made of carbon steel, stainless steel, copper, tantalum and other alloys, and available in sizes ranging from 19-50 mm with void fraction varying from 97-98%, has an additional row of fingers with alternate arrangement of short and long tabs resulting in significantly more drip points than most other random packings. The variation of the length of the internal tabs ensures high efficiency and optimal distribution, i.e. uninterrupted flow of gas and liquid. The additional drip points help in enhancing liquid film surface renewal thus causing more mass transfer. In addition, circumferential flanges added to the ring provide mechanical strength as well as enhanced liquid spreading characteristics. *Cascade M-Pak*, a latest packing developed by Glitsch (UK) is a significant improvement over slotted rings. It combines all technical advantages offered by Pall rings or Hy-Pak rings and in addition, because of its lower thickness, has the cost advantage ranging from 20-30% over the corresponding sizes of Hy-Pak and Pall rings. M-Pak rings have higher voidage as against other rings. These rings have a flanged cross section which considerably increases the stiffness value of the ring for diametrical compression when compared to the plain cross section of the Pall type rings. The improvised design provides effective mass transfer between the phases leading to more capacity while allowing free passage of the gas phase resulting in low-pressure drop. Also, liquid is not trapped between adjacent packings and thus increases the proportion of liquid surface being constantly renewed.

*Tellerette* packings and *Rosette type* packings are available in wide variety of plastic materials. These packings provide many more interstitial hold-up points than what can be obtained with other types of packings. These hold-up points and the use of non-wetting plastic materials create a dispersion/agglomeration cycle of the liquid, which results in constantly fresh liquid being exposed to the gas flow.

*Berl saddles* were the original type of saddle packing. Although the free gas space in saddles is less than that for rings, the greater surface and improved aerodynamic shape of the saddles increase their capacity and reduce the pressure drop. In recent years, intalox saddles and super intalox have largely replaced berl saddles, although they are still used in vacuum distillation and in cases where high contact efficiency is desired. Berl saddles are made of stoneware and porcelain, and are available in different sizes from 6 to 75 mm. However, in plastic construction they are made with a variety of holes and protrusions to enlarge the specific surface.

In *Intalox saddle*, the shape of the berl saddle has been modified so that adjacent elements do not block any active part of the wetting liquid. There is practically no stagnant pool of liquid and no entrapped gas bubbles in these packings. These factors, along with the smooth shape of intalox saddles ensure free flow of the liquid with minimum hold up and the gas is not subjected to violent changes in direction. Intalox saddles are available in ceramics and plastics.

*Intalox Metal Tower Packing* or IMTP is the first random packing designed especially for use in distillation columns. Its success and the advantages realized in distillation have been abundantly applied in absorption, stripping, extraction and direct contact heat transfer operations as well. Since its introduction in late 1970s, IMTP made of carbon steel, stainless steel, nickel and nickel alloys, aluminium, copper and copper alloys, titanium and zirconium has been successfully used in mass transfer equipment with diameters ranging from 0.15 to 12 m.

Subject to other constraints, the following figures, expressing packing size as fraction of tower

diameter, may be used for preliminary estimation of packing size:

$$\text{Raschig rings} < \frac{1}{30}, \text{ Saddles} < \frac{1}{15}, \text{ Pall rings} < \frac{1}{15} \text{ to } \frac{1}{10}.$$

Although packings are available in sizes varying from 6 to 100 mm, the following five sizes are most frequently used in gas-liquid separation: 13, 25, 38, 50 and 76 mm. On the basis of these sizes, the recommended values of packing size are:

Column diameter, m	Packing size, mm
< 0.30	< 25
0.30-0.90	25-38
> 0.90	50-76

For the same operation, smaller packings are usually more expensive per unit volume than larger ones. Up to packing size of 50 mm, the largest size of packing that is admissible for the column diameter should be used. But above 50 mm, the lower cost per cubic metre of packing does not usually compensate for the lower mass transfer efficiency.

In case of random packings, packing density is usually low near the tower wall. As a result, the liquid tends to flow towards the wall while the gas flows through the centre of the tower thereby causing channeling. Use of large packings in a smaller column leads to poor liquid distribution and causes channeling. In order to minimize channeling, the liquid is redistributed at intervals as indicated below:

Types of packing	Redistribution at interval of
Raschig ring	Every 6 m or every 2.5 to 3 times column diameter whichever is less
Pall ring	Every 6 m or every 5-10 times column diameter whichever is less
Saddle	Every 6 m or every 5-8 times column diameter whichever is less.

Recommended values of superficial gas/vapour velocity in the column and allowable gas side pressure drop for different types of packings are:

Type of packing	Gas velocity as percentage of Flooding velocity	Pressure drop, mm H <sub>2</sub> O/m of packing
Raschig ring	60%	40
Pall ring	80%	17
Saddle	90%	29

Smaller packings have higher mass transfer efficiencies compared to those provided by larger packings.

### **Structured packings**

Structured packing as in use at present are composed of:

- (i) Wire-mesh weavings,
- (ii) Corrugated sheet or crimped sheet, and
- (iii) Grid-type.

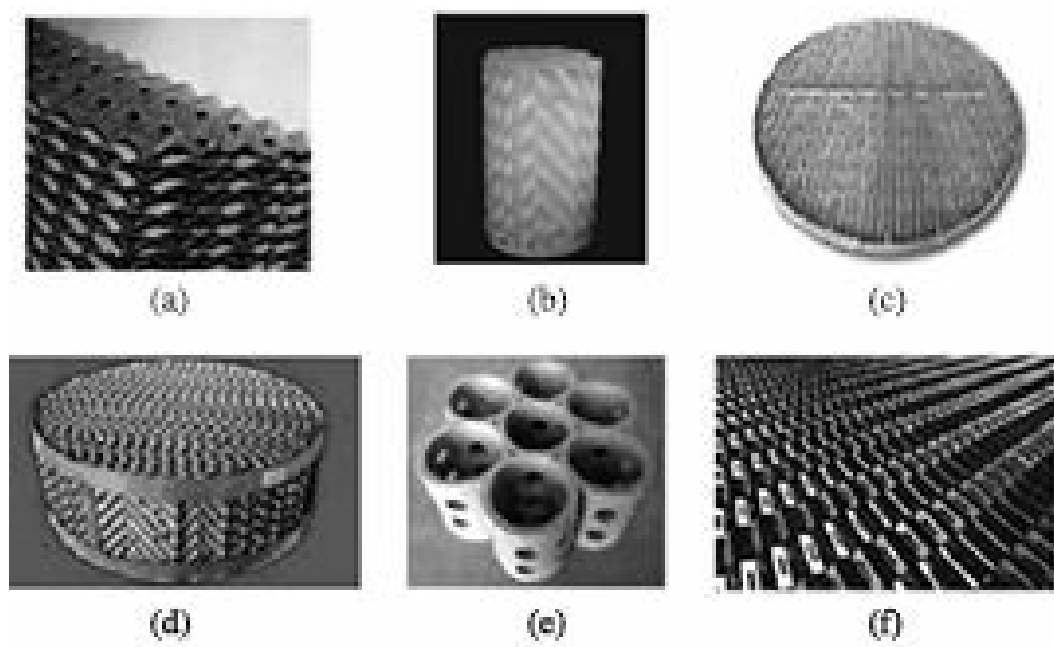
These types of packing have the advantage of low-pressure drop and better fluid flow characteristics but are relatively more costly.

Wooden grids are relatively less costly and are used where large void volumes are required. Structured packings are systematically stacked or laid out to provide uniform openings and surface area distribution throughout the tower packing area. These designs in some cases, provide less surface area but result in more uniform liquid distribution. This type of packing design is generally more costly to install due to the substantial extra labour involved or the higher cost of the packing itself. Structured packings may be layers of large rings or grids, but are most commonly made of

expanded metal or woven wire screen that are stacked in layers or as spiral windings. Several types of expanded metal packings are in use (Scofield 1950). Woven wire screen rolled into the cylinders provide large interfacial area combined with low pressure drop and are useful in vacuum distillation (Lubowicz and Reich 1971), their mass transfer efficiency is high when proper distribution of liquid over the cross section can be maintained.

Wood grid packings consist of beams of wood stacked with alternate layers perpendicular to each other. This type of packing provides lower packing efficiency. However, this design is extremely economical and may be considered where low performance is required and where the wood will not be affected by the working environment. Drip point grids are ceramic bricks with vertical holes similar in shape to cinder blocks. When stacked in equipment, they provide a large surface area and high void fraction, resulting in low-pressure drop. However, drip point grids are used occasionally in applications requiring particulate removal. Glitsch grids are having high open area with low-pressure drop, manufactured from stacked layers of perforated metal sheets which are cut to fit inside the tower. This packing design is frequently used in distillation columns where coking is a potential problem. It also finds use in some particulate scrubbing applications.

Structured packings are manufactured with geometric structure of relatively inexpensive metal or plastic corrugated sheets. Sheets are laid parallel to the flow with the corrugations running at a predetermined angle to the flow. Corrugations between adjacent layers of the sheet are reversed in direction, providing maximum mixing of the gas and liquid flow. The overall packing is manufactured in short length elements along the direction of flow. Some of the structured packing commonly used in equipment are shown in Figure 6.15.



(a) Metal intalox, (b) Plastic knitting, (c) Plastic grid, (d) Metal flexipac, (e) Ceramic micro-pores, and (f) Metal grid.

**Figure 6.15** Some structured packings.

These elements are stacked so that the direction of the corrugated sheets are at  $90^\circ$  to the previous pack as shown in Figure 6.13, creating complete mixing of the fluids over several elements. The packing occupies 60-70% of the column volume while the remaining space is used for flow distribution and phase disengagement. The depth of the corrugations can be varied. The higher capacity and lower-pressure drop are obtained with the deeper corrugations while shallower

corrugations provide higher contacting efficiency. Structured packings are available in sheet or gauge form. The characteristics of structured packings have been given in Table 5.1. These can provide higher mass transfer efficiencies than traditional tray columns for vacuum and low pressure applications. This enhanced efficiency causes the reduction of the size of the column required for a specific operation. The performance of structured packings remains unaffected even at gas flow rate as low as 10% of the design load. In case of absorption, another possible benefit of this packing is a reduction in the solvent/gas feed ratio that again permits the use of smaller equipment. However, structured packings have the following disadvantages: higher costs compared to conventional trays and difficulty in maintaining good liquid and vapour distribution throughout the column.

**Column internals:** In addition to the packings or trays as the case may be, the following are used as column internals:

Packings are placed on packing supports near the bottom of the column above the free space necessary for proper distribution of gas through the packings. In plate columns, trays are kept on some supports.

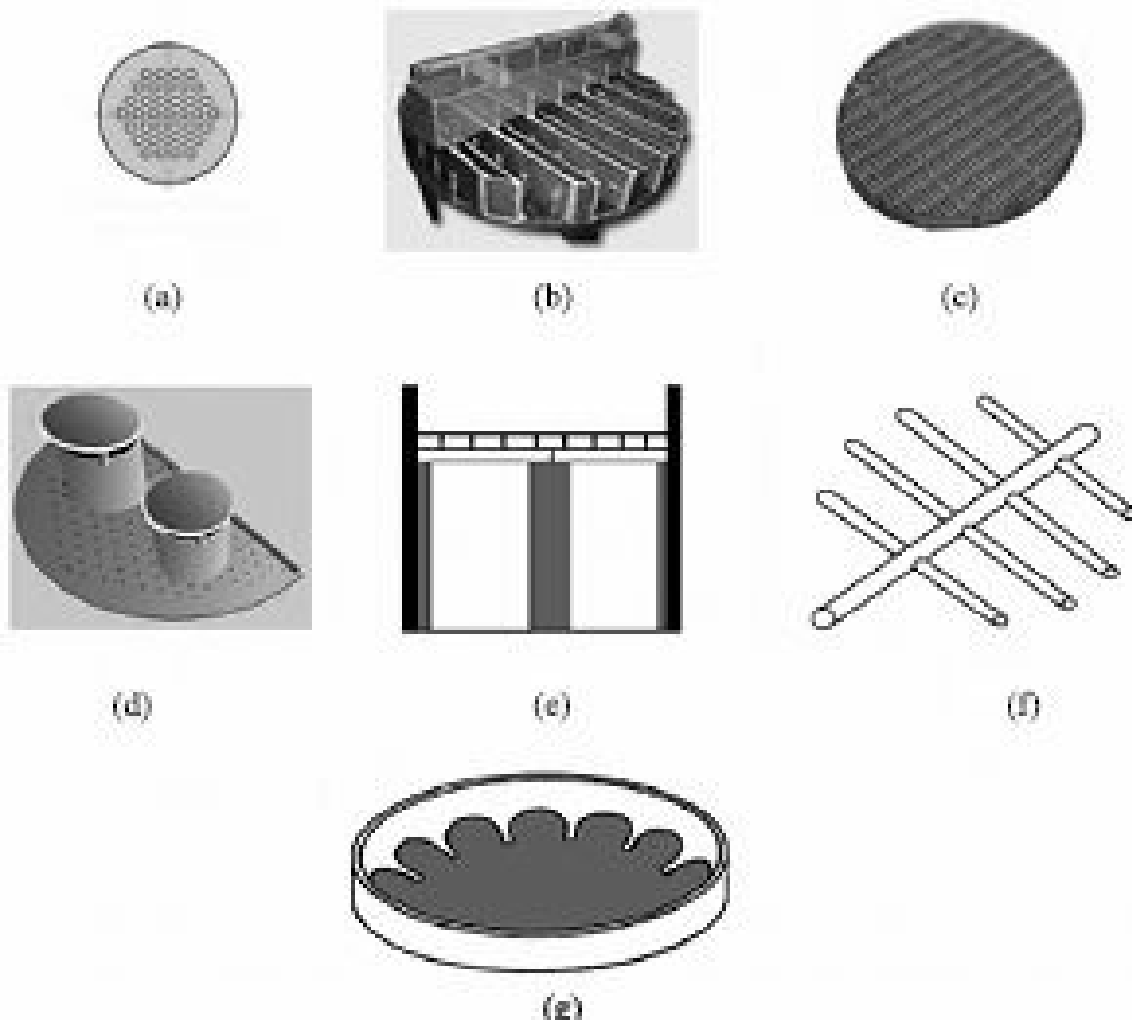
Mist eliminators are usually installed above the liquid inlet to minimize entrainment of liquid in outgoing gas, particularly at high gas velocities. About a metre of dry random packing is quite effective for the purpose. Alternatively, teflon or polyethylene wire mesh, about 100 mm thick may be used.

Liquid and gas distributors are to be properly designed and installed in the column in order to ensure uniform distribution of the phases, particularly in the equipment dealing with gas/vapour-liquid systems. Sometimes, redistributors are also used. Some of the internals used in mass transfer equipment are shown in Figure 6.16.

Since packings of individual manufacturers differ in detail, the manufacturer's pressure drop data are to be used.

The main requirements of a good tower packing are:

- (i) Chemical inertness towards the gas and liquid being handled.
- (ii) Low weight combined with sufficient mechanical strength to carry the combined weight of packings and liquid hold up.
- (iii) Large available surface per unit volume of packing to provide a high interfacial area between the gas and liquid.
- (iv) Large fractional void to allow desired fluid flow rates at reasonable pressure drops.
- (v) Uniform liquid distribution on the packing surface.
- (vi) Easy availability at reasonable cost.



(a) Perforated plate, (b) Trough distributor, (c) Hold down grid, (d) Orifice riser type distributor, (e) Cross partition ring, (f) Perforated piping distributor, and (g) Rosette distributor.

**Figure 6.16** Tower internals.

**Packed bed height:** Determination of the height of packing required in a column to achieve a specific separation involves use of either the height of a transfer unit (HTU) or the height equivalent to a theoretical plate (HETP) approach. To obtain the total height using the first approach requires one to determine the number of transfer units (NTU) to satisfy the relation

$$Z = (\text{HTU}) (\text{NTU})$$

Considering the contribution of both gas-phase and liquid-phase resistances, one may use Eq. (5.80) or Eq. (5.81) for determination of HTU. A number of design procedures for evaluating the HTU and HETP for packed columns have been described in Section 5.3.2.

### **Pressure drop in packings for counter-current flow–flooding**

Apart from general maintenance cost, the cost of forcing the gas through wet packings constitute the major operating cost of a counter-current packed tower. Typical pressure drop data for counter current flow of liquid and gas in packed towers are shown on logarithmic scales in Figure 6.17. For dry packings, a straight line with a slope of 1.8-2.0 is obtained indicating that the flow is turbulent. In wet packing, pressure drop at a fixed gas velocity increases with increase in liquid flow rate since the free area available for flow of gas is reduced. If, on the other hand, gas velocity is increased at a fixed liquid velocity, the pressure drop initially increases at a

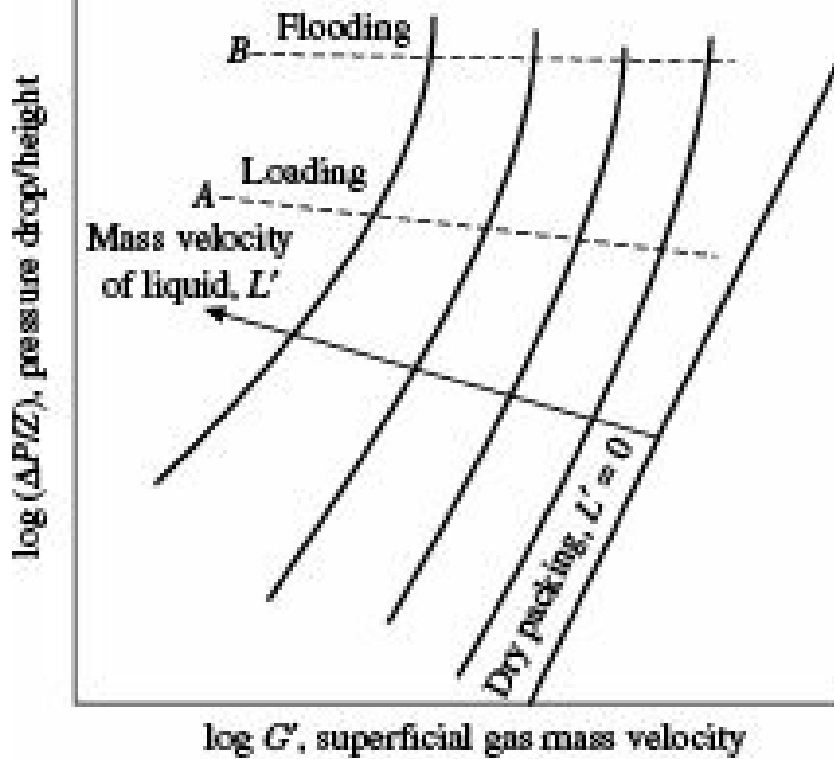


**Figure 6.17** Pressure drop for counter flow of gas and liquid in packed column.

constant rate but after a certain gas velocity (Point *A*) is reached, the steady conditions of the tower are disturbed and the liquid hold up starts increasing as indicated by the change in slope of the gas velocity-pressure drop curve. This is known as *loading point*. On further increasing the gas velocity, the point *B* is reached when the pressure drop increases abruptly, a liquid layer usually appears on the top of the packing and the liquid may fill up the tower so that the liquid phase becomes continuous. This point is known as the *flooding point* and the corresponding gas velocity is called *flooding velocity*. The region between the loading point and the flooding point is known as *loading region*; significant liquid entrainment is observed, liquid hold-up increases sharply, mass transfer efficiency decreases and the column operation becomes unstable. Although a packed column can operate in the loading region, most of the packed columns are designed to operate below the loading point, i.e. in the *preloading region*. Flooding velocity may therefore be defined as gas velocity at a given liquid velocity for which (i) gas pressure drop increases abruptly, or (ii) the tower is filled with the liquid which becomes the continuous phase, or (iii) a liquid layer appears at the top of the packing. Gas-side pressure drops in counter-current packed absorbers and strippers of the common type usually lie in the range of 200 to 440 N/m<sup>2</sup> per metre of packing.

Based on experimental studies using 54 different packing materials including structured packings, Billet and Schultes (1991) developed a dimensionless correlation for dry-gas pressure drop,  $DP_0$  as

$$\frac{\Delta P_0}{Z} = \varphi \frac{a_p}{\varepsilon^3} \frac{u_g^2 \rho_g}{2g_e} \frac{1}{K} \quad (6.20)$$

where,  $Z$  is the height of packed bed and  $K$  is the wall factor, an important parameter for columns with an inadequate ratio of effective packing diameter to inside column diameter, represented as

$$\frac{1}{K} = 1 + \frac{2}{3} \frac{1}{(1-\varepsilon)} \frac{D_p}{D} \quad (6.21)$$

The effective packing diameter  $D_p$  is determined from

$$D_p = 6 \frac{1 - \epsilon}{a_p} \quad (6.22)$$

and the dry-packing resistance coefficient  $\varphi$ , is given by the empirical equation

$$\varphi = C_h \frac{64}{Re_G} + \frac{1.8}{Re_G^{0.08}} \quad (6.23)$$

where,

$$Re_G = \frac{\bar{u}_G D_p \rho_G}{(1 - \epsilon) \mu_G K}$$

and  $C_h$  is a packing constant to be available from vendor or determined experimentally.

When the packed tower is irrigated, the liquid hold-up causes the pressure drop to increase. The experimental data are reasonably well correlated by

$$\frac{\Delta P}{\Delta P_0} = \left( \frac{\epsilon - L_w}{\epsilon} \right)^{1.5} \exp \left\{ \frac{Re_L}{200} \right\} \quad (6.24)$$

where,

$$Re_L = \frac{\bar{u}_L}{a_p t_L}$$

For operation in the preloading region, the liquid hold-up can be estimated by using Eq. (6.27) described later.

Flooding velocity plays an important role in the design of counter-current towers since a very important parameter, namely tower diameter is estimated from knowledge of flooding velocity.

It has been established that for several common packings and for wide ranges of liquid and gas velocities, the mass velocity of gas at flooding point is given by,

$$\frac{G'^2 (a_p / \epsilon^3) \mu_L^{0.2}}{g_c \rho_G \rho_L} = \frac{L'}{G'} \left( \frac{\rho_G}{\rho_L} \right)^{0.5} \quad (6.25)$$

where,

$G'$  and  $L'$  are mass velocities of gas and liquid respectively in  $\text{kg/m}^2 \text{ s}$

$\rho_G$  and  $\rho_L$  are densities of gas and liquid respectively in  $\text{kg/m}^3$

$\eta'_L$  is the viscosity of the solution in centipoises

$a_p$  is specific surface of packing in  $\text{m}^2/\text{m}^3$

$\epsilon$  is the fractional void, dimensionless

$g_c$  is the conversion factor,  $9.807 (\text{kg}_m/\text{kg}_f)\text{m/s}^2$

Since Eq. (6.25) is a semiempirical equation, the recommended units must be used while using the same.

The value of  $(L'/G')$  in the right-hand side of Eq. (6.25) is the same as the ratio of liquid ( $L$ ) and gas ( $G$ ) throughputs (kg/hr) which must be known before fixing the diameter. Flooding velocity is

$$\frac{L}{G} \left( \frac{\rho_G}{\rho_L} \right)^{0.5} \quad \frac{G^{0.2} (a_p / \varepsilon^3) \mu_L^{0.2}}{g_c \rho_G \rho_L}$$

determined from Eq. (6.25) by using a curve having  $\frac{L}{G} \left( \frac{\rho_G}{\rho_L} \right)^{0.5}$  as abscissa and  $\frac{G^{0.2} (a_p / \varepsilon^3) \mu_L^{0.2}}{g_c \rho_G \rho_L}$  as ordinate as shown in Figure 6.18.

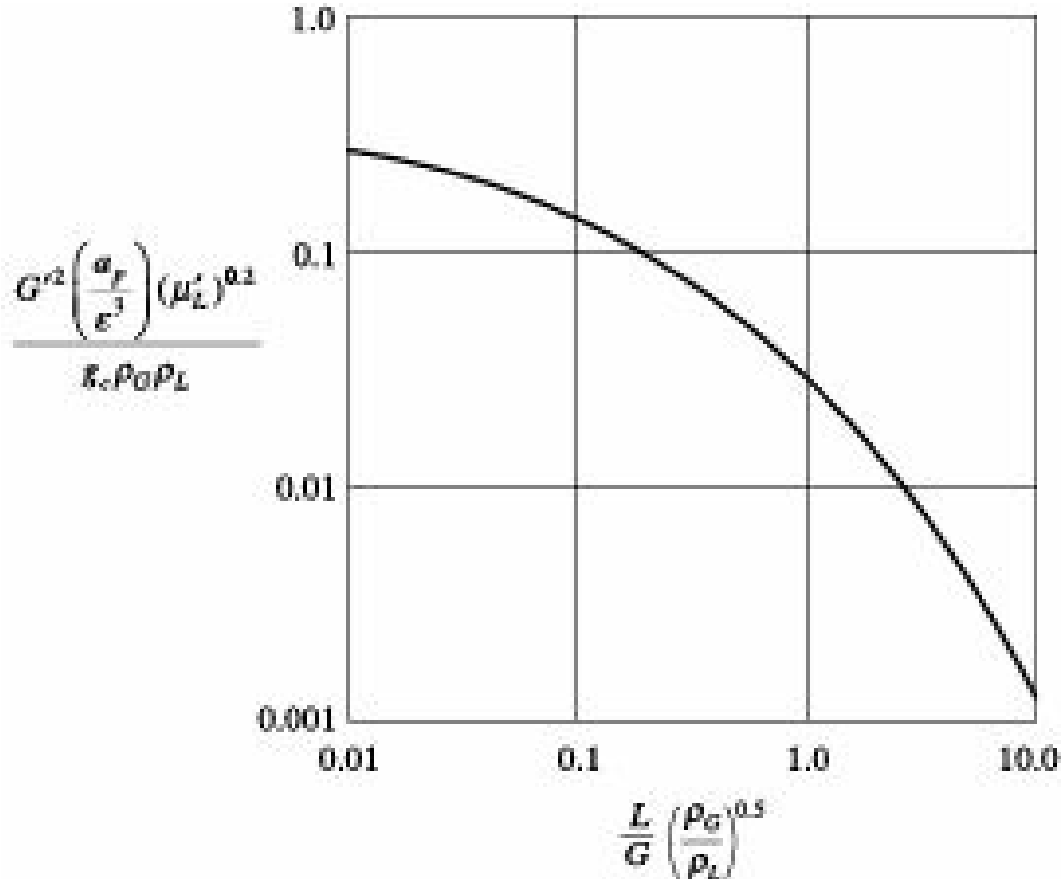


Figure 6.18 Flooding velocity estimation in counter-current packed tower.

### Evaluation of diameter of column with Random packings

In contrast to tray towers, performance in packed columns is strongly affected by both liquid and gas/vapour flow rates in the column. Not only is the flow limited, but also at high throughputs the gas flow impedes the liquid flow which can eventually lead to flooding of the column. Thus, packed columns also operate at a gas/vapour velocity which is 60-90% of that at flooding. A simplified shortcut method that has been the standard of the industries for several decades utilizes the generalized pressure drop correlation chart originally developed by Sherwood et al. (1938) and improved by several other investigators (Leva 1992). One version of this correlation chart, shown in Figure 6.17, permits the designer to estimate the cross sectional area of the column after selecting a recommended pressure drop per unit height of packing. Recommended pressure drops in packed columns for atmospheric and high-pressure separations range from 400 to 600 Pa/m, for vacuum operation between 4 and 50 Pa/m, and for absorption and stripping columns between 200 and 400 Pa/m. The cross sectional area of the tower is estimated by dividing the gas throughput by the operating gas mass velocity. The tower diameter,  $D$  is thereafter calculated using the relation:

$$D = \left( \frac{4 \times \text{Cross sectional area}}{\pi} \right)^{0.5} \quad (6.26)$$

## **Evaluation of diameter of column with Structured packings**

A procedure similar to that used for determining the diameter of a column with random packing may be used to obtain the diameter of the column with structured packing taking the suitable packing factor for the structured packing selected.

Another procedure (Kister and Gill 1991) involves calculating the pressure drop over a unit length of the column under flooding conditions. A correlation, similar in format to Figure 6.17 is used to determine flooding velocity in columns with structured packings. The operating velocity in the column is designated as a fraction of flooding velocity. The cross sectional area of the column is then obtained by dividing the volumetric flow rate of the vapour by the operating velocity. Column diameter is then obtained using the same procedure as described above.

**Liquid Hold-up:** The liquid hold-up is an important characteristic of packings owing to its relation to the wetted area, pressure drop and flooding characteristics. Reported literature shows the hold-up to be an exponential function of the liquid rate and to be independent of the gas velocity until the loading point is reached when the hold-up increases rapidly. It has also been reported that the hold-up depends primarily on the size of the packing. Static hold-up, measured as the weight of liquid retained when the column had drained to a constant weight, predominates on the smaller packings owing to the quantity of liquid held by the capillary forces at the points of contact of the packing. However, this liquid has only a small surface exposed to the gas and is not likely to be effective for absorption. Larger packings have fewer points of contact and the hold-up occurs mainly in the film flowing over the surface; this hold-up is equal to the product of the film thickness and the wetted area. For a fully wetted packing the hold-up depends only on the film thickness which is proportional to the cube root of the liquid flow rate. The amount of liquid hold-up in the packing is of interest when the liquid is unstable or when a desirable reaction is to be carried out in the tower. The specific liquid hold-up,  $L_W$  in the preloading region has been found from extensive experiments using a wide varieties of random and structured packings for a number of gas-liquid systems, to depend on packing characteristics and also on the viscosity, density and superficial velocity of liquid according to the dimensionless expression (Billet and Schultes 1995)

$$L_W = 12 \left( \frac{Fr_L}{Re_L} \right)^{1/3} \left\{ \frac{a_h}{a_p} \right\}^{2/3} \frac{\bar{u}_L^2 a_p}{g} \quad (6.27)$$

where,  $Fr_L = \frac{\bar{u}_L^2}{g}$

and the ratio of specific hydraulic area of packing,  $a_h$  to the specific surface area of packing,  $a_p$  is given by

$$\frac{a_h}{a_p} = C_h Re_L^{0.15} Fr_L^{0.1} \quad \text{for } Re_L < 5$$

and  $\frac{a_h}{a_p} = 0.85 C_h Re_L^{0.25} Fr_L^{0.1} \quad \text{for } Re_L \geq 5.$

Values of  $a_p$  and  $C_h$ , the packing constants vary with the type and size of packing, and are to be

collected from the vendors. Since the specific liquid hold-up is constant in the preloading region, neither the properties nor the velocity of the gas/vapour has been considered in Eq. (6.27).

### ***Choice between plate and packed towers***

The use of packings or plates in mass transfer equipment is governed by the operating requirements of the process and the costs of fabrication. The choice between the two can primarily be made considering advantages and disadvantages of each type. Some of the factors to be considered are stated as follows:

- Plate columns can be used for handling wide range of liquid and gas flow rates which packed column cannot handle.
- Provision can be made in plate columns to introduce or withdraw side streams, etc.
- If the liquid causes fouling or contains solid, it is easier to make provision for cleaning in a plate column. However, with small diameter columns it may be cheaper to use packing and replace the packing when it becomes fouled.
- Packed columns are not suitable for very low liquid flow rates.
- For corrosive liquids a packed column will usually be cheaper than the equivalent plate column.
- Packed columns are not suitable for handling foaming systems.
- Packed columns should always be considered when one requires a small diameter column (say less than 0.6 m), the capital cost of which is low. In such situation the plate column would be difficult to install and expensive. However, large diameter plates are always found to be cheaper than packings.
- Plate columns can be designed with more assurance than packed columns.
- It is easier to make provision for cooling in a plate column; coils can be installed on the plates.
- The efficiency of a plate, constant for a range of liquid and gas rates, can be predicted with more certainty than the equivalent term for packing as the same varies with the liquid and gas flow rates and also is very susceptible to maldistribution of liquid, particularly in the larger sizes. Distribution problems are not there in plate columns.
- The liquid hold-up is appreciably lower in a packed column than in a plate column; this is an important parameter when the inventory of toxic or flammable liquids needs to be kept as small as possible for safety reasons.
- The pressure drop per equilibrium stage (HETS) can be lower for packings than plates; and packing should be considered for columns operating under vacuum.
- The construction of packed towers is simple and it can easily be repaired or replaced.
- Packings are available in a variety of corrosion resistant materials whereas plates are available in only a limited range of corrosion resistant materials.

A designer, however must make a judicious selection based on performance and cost of the plate or packed columns. Also, one has to find out the suitability of the random packing or structured packing for the separation process under consideration. Typically, trays are favoured when the operating pressure and liquid flow rate are high, and when the column diameter is large. Random packings are more often recommended when the column diameter is small, corrosion and foaming are present, or batch operations are to be performed. Structured packings are considered for low pressure and vacuum operation. Moreover, they are often selected when low pressure drop across the column is

required or low hold-up is desired.

### 6.3.3 Spray Tower and Spray Chamber

A spray tower consists of an empty shell (chamber) into which the liquid is sprayed near the top by means of nozzles of various kinds; the droplets thus formed are then allowed to fall to the bottom of the tower or chamber through a stream of gas flowing upwards as shown in Figure 6.19. The use of sprays appears to offer an easy way of greatly increasing the surface area exposed to the gas, but the effectiveness of the method depends on the production of fine droplets. These are difficult to produce and suffer from the disadvantage that they are liable to entrainment by the gas even at low gas velocities. The surface area may also be reduced as a result of the coalescence of the droplets formed. As a consequence of these effects, the large increase in surface area expected may not be achieved, or if achieved may be accompanied by serious entrainment and internal circulation of the liquid so that true counter-current flow is not obtained. A single spray tower is not suitable for easy absorption duties. For difficult duties, a number of towers in series can be used.

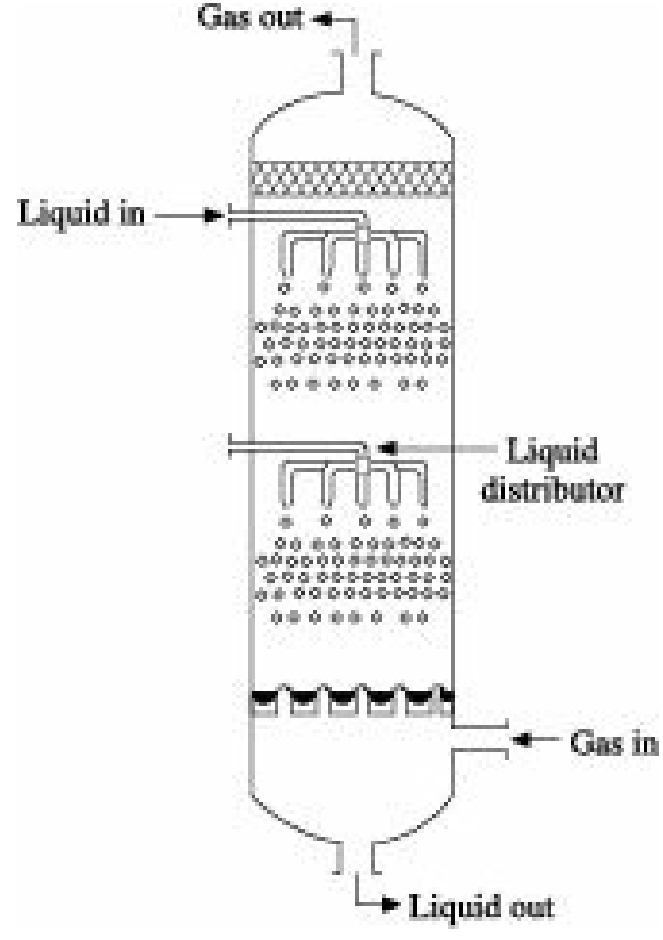


Figure 6.19 Spray tower.

For processes involving a gas of low solubility for which the main resistance to mass transfer lies in the liquid phase, it has generally been assumed that spray equipment would be unsuitable for mass transfer operations. Intense drop circulation may however, assist in making the process of absorption of slightly soluble gases quite feasible in such equipment. The rate of absorption of a gas by a liquid drop during the period of its formation and subsequent movement through the chamber has been investigated both theoretically and experimentally by a number of workers (Whitman et al. 1926, Hatta and Baba 1934, Johnson and Hamielec 1960, Zheleznyak 1967). The results show the absorption of gases by drops of various liquids falling freely to be 50-70 times greater than could be

explained by transient molecular diffusion in a sphere. Investigations (Vyarawalla 1970, De 1983) on the absorption of carbon dioxide by large drops of liquids like hydrated lime-slurry, water and 0.5N aqueous solution of sodium hydroxide in a spray absorber, showed that the maximum mass transfer was achieved only during the period of drop formation. The mass transfer rate was found to decrease progressively during the travel of drops through the column until steady-state was reached. This phenomenon of maximum mass transfer rate at the beginning is related to a high rate of circulation inside the liquid drop, initiated during drop formation. As the drop breaks away from the nozzle-tip, the progressive decrease in the rate of circulation and associated oscillation characteristics as well as the dampening forces acting on the surface of the drop cause a decrease in the rate of mass transfer. The flow may be counter-current as in vertical spray towers or co-current as in horizontal spray chambers. These equipment have the advantage of low gas side pressure drop. But liquid-side pressure drop is very high and entrainment of liquid by gas is also high.

Spray towers are not suitable for removing very fine particles, below  $10\text{ }\mu\text{m}$ . The collecting efficiency can be improved by the use of plates or packing but at the expense of a higher pressure drop. However, these equipment have certain specific advantages over plate and packed type absorbers such as simple mechanical construction, low pressure drop across the contacting section and the ability to handle suspensions of fairly large solid concentrations as found in hydrated lime-slurry.

#### 6.3.4 Venturi Scrubber

Venturi scrubbers and Orifice scrubbers are simple forms of wet scrubbers. Wet gas scrubbers use circulating liquid to contact the gas and absorb dust/acid vapours as the case may be, into the liquid stream. The amount of circulating liquid is a key process parameter for wet scrubbers. In wet scrubbing the dust is removed by counter-current washing with a liquid, usually water and the solids are removed as slurry. The principal mechanism involved is the impact or impingement of the dust particles and the droplets. Particle sizes down to 0.5 mm can be removed in suitably designed scrubbers. In addition to removing the solids, wet scrubbers can be used to simultaneously cool the gas and neutralize any corrosive constituents.

Packed tower wet scrubber (Figure 6.20), a vessel filled with some suitable packing, are considered to a certain degree an outdated technology although there are still many industrial operations that utilize them. One of the major applications of such scrubbers from an environmental standpoint is flue gas scrubbing. Many packaged designs are offered by vendors. Some of these designs are shown in Figure 6.21. Such scrubbers clean 97-100% of the sulphur dioxide and hydrochloric acid gases out of the flue gas and also a high percentage of dust (Cheremisinoff 2000). Wet gas scrubbers use circulating liquid to contact the flue gas and absorb the acid vapours into the liquid stream. The amount of circulating liquid is a key process parameter for wet scrubbers. Generally referred to in terms of  $L/G$  (liquid and gas ratio), the amount of circulating liquid must be enough to fully quench the gas and absorb adequate amount of acid vapours from the gas stream.

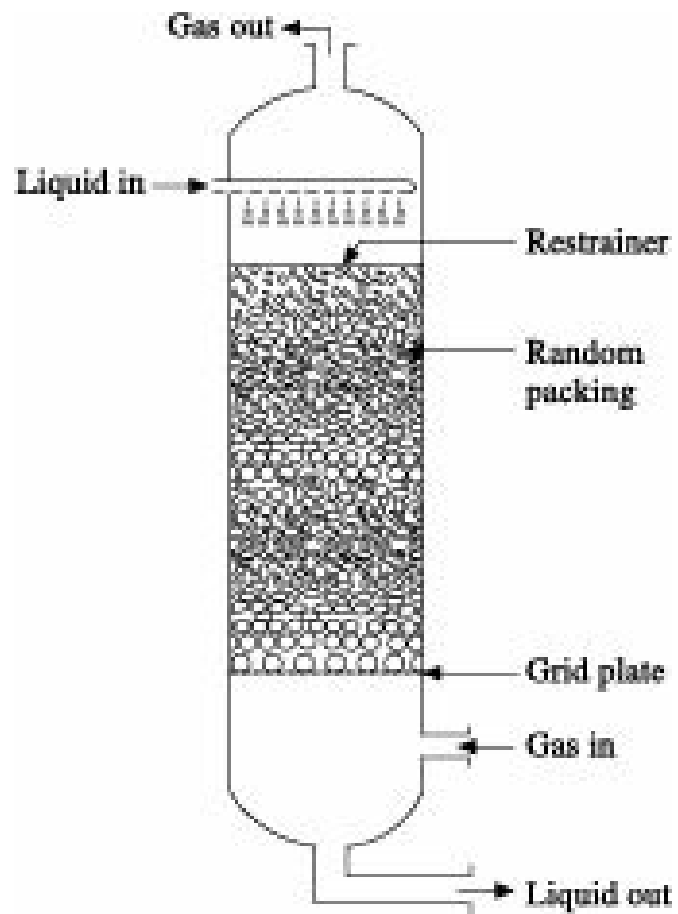


**Figure 6.20** Packed tower wet scrubber.

There are a number of different designs of wet gas scrubbers that are used for acid gas absorption. This will affect the total  $L/G$  ratio which will have a direct impact on power required for operation. In wet gas scrubbers, particulate matter (solid or liquid) requires energy to be imparted on the gas stream to capture the particulates by means of inertial impaction. This energy is usually measured in the form of gas-side pressure drop. The smaller the size of the particulate, the more energy (higher pressure drop) must be imparted to capture the particulate. It is imperative that the end users analyse initial cost not only for the scrubber itself, but also for all the auxiliary equipment required with the scrubber. These capital costs must be balanced against the operating cost of the unit and the impact the scrubber will have on the operating cost of other downstream equipment, in particular, the waste water treatment system. The trend in the use of gas scrubbers, particularly on small units, has shifted towards the use of non-packed columns.

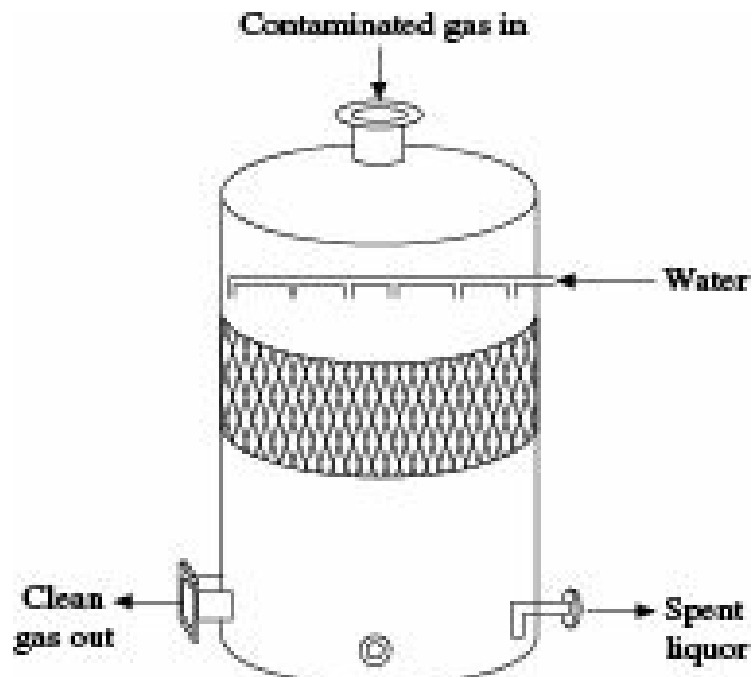


**Figure 6.21(a)** Sectional view of a co-current scrubber.

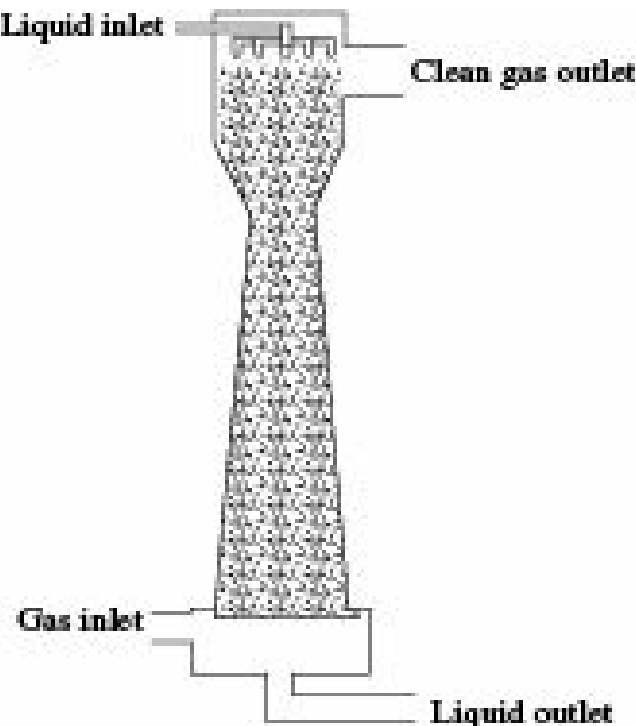


**Figure 6.21(b)** View of a counter-current wet scrubber..

Like spray towers, equipment that relies on the venturi/ejector principle are mainly used for removing particulate matter from gas streams. Also, there are some application areas of venturi scrubber in gas absorption, e.g. absorption of sulphur dioxide from furnace gas by slurries of lime, limestone or magnesia.

In such scrubbers as shown in Figure 6.22, the liquid is injected into the gas stream as it passes through the venturi or by admitting the gas to the liquid stream as it passes through the venturi. In the latter situation, the venturi also serves as a vacuum producing device and inspirates the gas into the venturi throat. The required interfacial contact is achieved by differences between the gas and liquid droplets, and by the turbulence created by the venturi. Venturi systems are able to achieve a high degree of gas-liquid mixing, but have the limitation of a relatively short contact time which generally leads to poor absorption efficiency. However, for gases with high solubilities and proper selection of

scrubbing liquid such scrubber can be an excellent device. Another disadvantage is the high pressure drop requiring high power for the operation. The materials of construction used for fabrication of such equipment are chemically inert, and are usually made from stainless steel, plastic, graphite or other suitable materials.

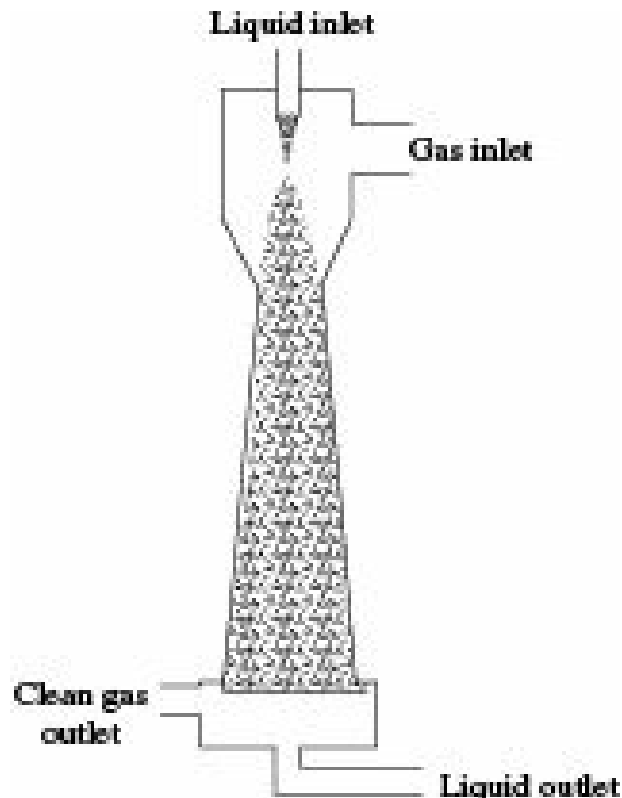


**Figure 6.22** Schematic view of a venturi scrubber.

A new technology developed by MECS, known as Dyna Wave Reverse Jet froth scrubber shown in Figure 6.23 uses only very few low pressure nozzles and minimum internals in the vessel. It can handle high solid concentrations and minimize the total effluent stream. A typical installation of the scrubber has been described elsewhere (Shukla 2006).

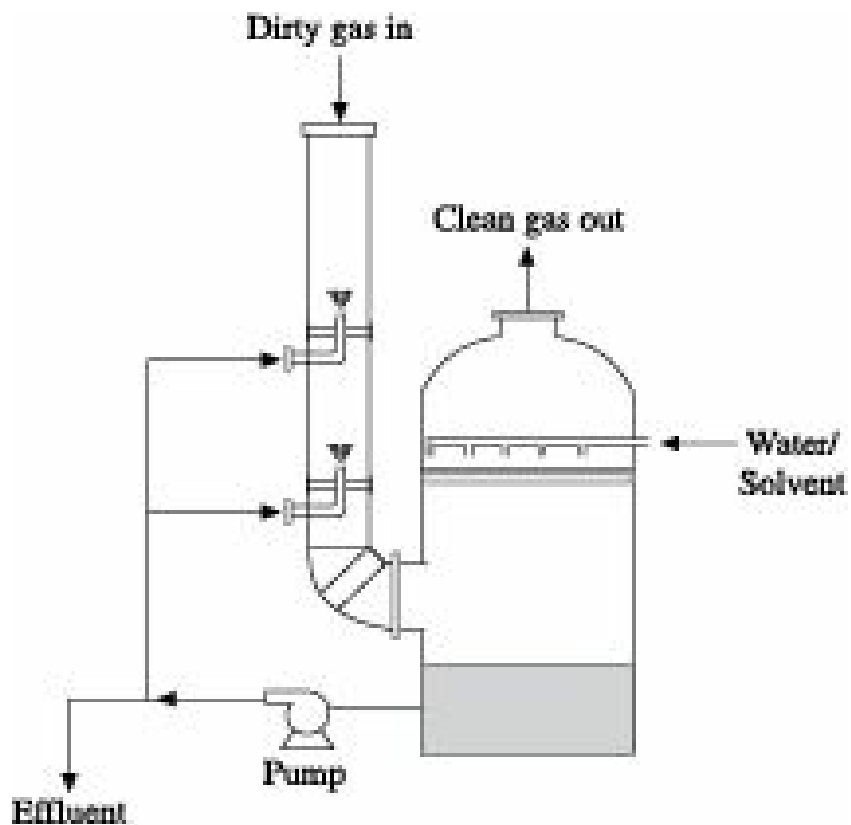


**Figure 6.23** Dyna wave froth scrubber.

### 6.3.5 Pulsed Column

Pulsating liquid-liquid extraction columns have been in use for a pretty long time in a large number of industrial processes. Many operations in chemical industries involve the contact of two phases of gas and liquid for mass transfer with and without chemical reaction. The rate of mass transfer in such processes is enhanced by providing pulsations in the continuous phase, thus indicating clearly that mass transfer has got direct bearing with the amplitude and frequency of pulsations under different flow conditions of the phases involved (Harbaum and Houghton 1962, Bretsznajder and Pasiuk 1964, Tudose 1964, Vyarawalla 1970, Sokolov et al. 1971, Baird and Garstang 1972, Gianetto and Sicardi 1972, 1975, Mollinear and Angelino 1977). Baird and Garstang used compressed air for pulsation while others used mechanical means for producing pulsation. The mechanical means used for the purpose (De 1983) is shown in Figure 6.24 for creating pulsations in the continuous phase.

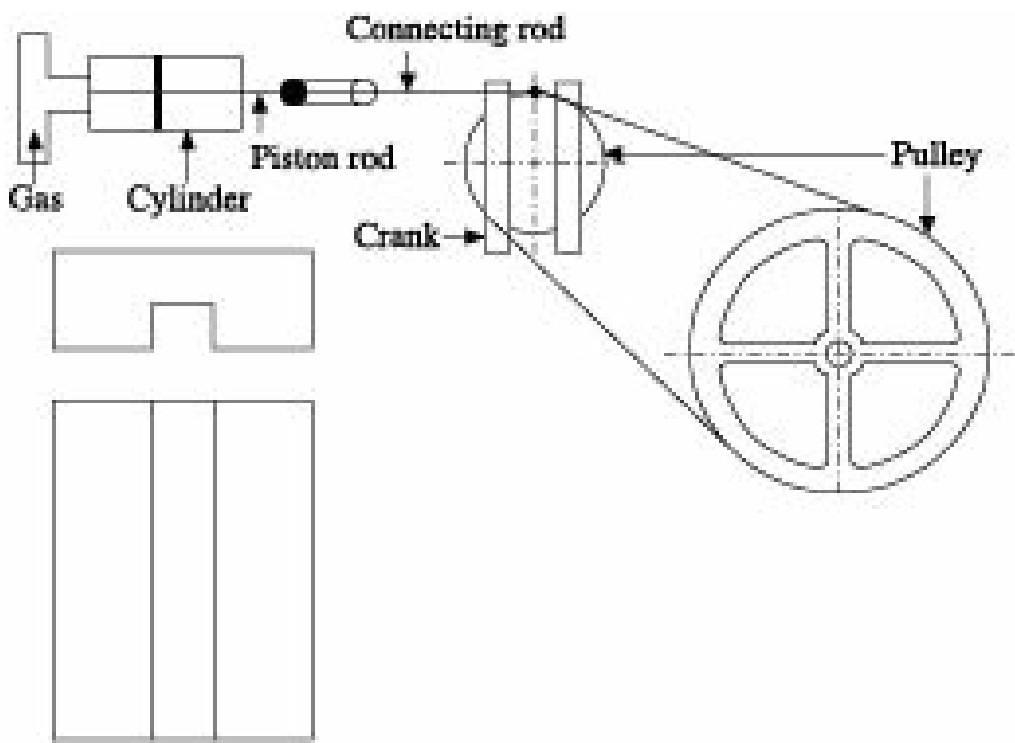


**Figure 6.24** A pulsating device.

The pulsating device consisting of a piston-cylinder system provides pulsations to the gases flowing in the column without any net flow from the reciprocating system. The piston is connected to a slotted member welded to the motor shaft through a connecting rod. Different slot lengths are taken so as to provide a wide range of strokes by the connecting rod in it. Rotation per minute of the motor shaft is changed by a duplex pulley-belt arrangement which is connected to speed governing motor. The speed of rotation of the larger pulley is measured by a tachometer. For each change in position of the connecting rod in the slotted member, the piston displacement is measured by a scale for estimation of the amplitude of pulsations. As the diameter of the column(s), i.e. the cross sectional area employed is different from that of the cylinder in the reciprocating system, the equivalent amplitudes of pulsations were evaluated taking into account the change in cross sectional areas. From the rotational speed of the larger wheel, the rotations per minute of the smaller wheel connected to the piston used for creation of pulsations, was measured and frequency of pulsations was measured there from. Stroboscopic technique was also used for the measurement of frequency of drop formation by synchronizing its frequency with that of the drop. There is an enhancement of mass transfer rate of about 200% (Guha and De 1983, 1985) during drop formation and in packed bed when pulsations are provided in the continuous gas phase. These observations indicate the pulsed column to be a viable option for enhanced mass transfer in gas-liquid operations.

### Nomenclature

$a$  : surface area per unit volume of laboratory column or the interfacial area per unit volume of packing,  $L^2/L^3$

$a_h$  : specific hydraulic area of packing,  $L^2/L^3$

$a_p$  : specific surface of packing,  $L^2/L^3$

$A_C$  : cross sectional area of the column,  $L^2$

- $A_d$  : downcomer area, L<sup>2</sup>  
 $A_n$  : net column area, L<sup>2</sup>  
 $C_h$  : packing constant  
 $d_p$  : bubble diameter, L  
 $D$  : column diameter, L  
 $D_L$  : depth of the liquid, L  
 $D_p$  : diameter of packing, L  
 $E$  : efficiency, —  
 $E_M$  : Murphree efficiency or murphree plate efficiency, —  
 $E_O$  : Overall efficiency or overall column efficiency, —  
 $E_P$  : Point efficiency or murphree point efficiency, —  
Fr : Froude number, —  
 $g$  : acceleration due to gravity, L/q<sup>2</sup>  
 $g_c$  : conversion factor, 9.807 (kg<sub>m</sub>/kg<sub>f</sub>)(m/s<sup>2</sup>).  
 $G$  : mass/molal flow rate of gas in the column, M/q  
 $G'$  : mass velocity of gas at flooding, M/L<sup>2</sup>q  
 $G_M$  : average total molal flow rate of phase G, Mol/L<sup>2</sup>q  
 $H_C$  : actual column height, L  
 $H_S$  : plate spacing, L  
 $\Delta H$  : additional height required for column operation, L  
 $H_{tG}$  : height of overall gas-phase transfer unit, L  
 $H_{tL}$  : height of a gas-phase transfer unit, L  
 $H_{tL}$  : height of a liquid-phase transfer unit, L  
HETP, HETS : height equivalent to a theoretical plate or stage, L  
HTU : height of a transfer unit, L  
 $k_L$  : liquid-film mass transfer coefficient, L/q  
 $k_G$  : gas-side mass transfer coefficient, M/L<sup>2</sup>q (mol frac.)  
 $K$  : Souders and Brown factor, L/q  
 $L$  : mass/molal flow rate of liquid in the column, M/q  
 $L_W$  : liquid hold-up, —  
 $L'$  : mass velocity of liquid at flooding, M/L<sup>2</sup>q  
 $L_M$  : average total molal flow rate of phase L, Mol/L<sup>2</sup>q  
 $m$  : slope of the equilibrium curve, —  
NTU : number of transfer unit, —  
 $N_{act}$  : actual number of trays, —  
 $N_{tG}$  : number of gas-phase transfer units, —

$N_{tL}$  : number of liquid-phase transfer units, —

$N_{toG}$  : number of overall gas-phase transfer units, —

$DP$  : pressure drop,  $F/L^2$

$DP_0$  : dry-gas pressure drop,  $F/L^2$

$Ra$  : Rayleigh number, —

$Re$  : Reynolds number, —

$Sh$  : Sherwood number, —

$\bar{u}$  : average/superficial velocity,  $L/q$

$V_F$  : net vapour velocity at flooding condition,  $L/q$

$y_n$  : average bulk concentration of solute in gas/vapour leaving the  $n$ th plate, mol.frac.

$y_{n+1}$  : average bulk concentration of solute in gas/vapour entering the  $n$ th plate, mol. frac.

$y_n^*$  : equilibrium solute concentration in gas/vapour leaving the  $n$ th plate corresponding to its average bulk concentration  $x_n$  in the liquid on the plate, mole fraction.

$Dy$  : change in mole fraction of a component, —

$(Dy)^*$  : change in mole fraction of a component at equilibrium, —

$Z$  : height of laboratory model or of packed bed, L

### *Greek Letters*

$\eta_L$  : viscosity of liquid, cp

$\eta_L'$  : viscosity of the solution, cp

$\sigma$  : surface tension of the fluid, dyne/cm

$\rho$  : density of liquid,  $M/L^3$

$\nu$  : kinematic viscosity,  $L^2/q$

$f$  : fractional void, —

$\{\}$  : dry-packing resistance coefficient (a modified friction factor)

$a$  : relative volatility

$G$  : water mass flow rate per unit mean perimeter of the discs,  $M/Lq$

### *Subscripts*

$LK$  : light key

$HK$  : heavy key

$G$  : gas phase

$L$  : liquid phase

## ***Numerical Problems***

**6.1** Estimation of Diameter of a Packed Scrubber for Hydrocarbon-Oil System: Absorption has been selected as the separation process to remove a hydrocarbon from a gas mixture by counter-current scrubbing with a lean oil. The column packed with 0.0254 m metal Pall rings, must handle a gas rate of 900 kg/hr and a liquid rate of 2700 kg/hr. A gas velocity equal to 70% of the maximum

allowable velocity at the given liquid and gas rates will be used. Densities of gas and liquid are 1.20 and 881 kg/m<sup>3</sup>, respectively. The viscosity of the oil is 20 cp. Estimate the required column diameter.

[Ans. 1.77 m]

- 6.2 Estimation of Diameter of a Bubble Column:** In designing a bubble-cap rectification column, the plate spacing was taken equal to 300 mm. Vapour flows through the column at a rate of 3200 m<sup>3</sup>/hr. The density of the vapour is 1.25 kg/m<sup>3</sup> and that of the liquid is 430 kg/m<sup>3</sup>. The rate of flow of vapour and the densities of the vapour and liquid are given at standard conditions. The pressure and mean temperature in the column are 1.2 atm (abs.) and -40°C, respectively. Determine the required diameter of the column.

The permissible optimum velocity of the vapour ( $v$ ) in a plate column is calculated by the equation:

$$v = C \left[ \frac{(\rho_l - \rho_v)}{\rho_v} \right]^{0.15}$$

where,  $C$  is the coefficient depending on the design of the plates, the distance between the plates, the operating pressures in the column, and the load on the column with respect to the liquid;  $\rho_l$  and  $\rho_v$  are the densities of the liquid and vapour, respectively in kg/m<sup>3</sup>. The value of  $C$  obtained from the nomograph is 0.0315.

[Ans: 1.275 m]

- 6.3 Estimation of Diameter of a Packed Rectification Column for Methyl Alcohol-Water System:** Determine the diameter of the rectifying section of a packed rectification column for separating a mixture of methyl alcohol and water under atmospheric pressure. The column is supplied with 1500 kg/hr of a feed consisting of 40% alcohol and 60% water. The concentration of the distillate (overhead product) is 97.5% alcohol. The bottom product contains 2% alcohol. All values are given in mole percentage. The reflux ratio is 1.48. Rings 25 # 25 # 3 mm in size are used as packing. The column operates in emulsifying conditions. Indirect steam is used for heating. The mean temperature in the top section of the column is maintained at 72°C.

The following is the equation for velocity of vapour ( $v$ ) in a packed rectification column operating under emulsifying conditions:

$$\log \left( \frac{v^2 \sigma \rho_v \mu_l^{0.16}}{g V_{\text{free}}^3 \rho_l} \right) = -0.125 - 1.75 \left( \frac{L}{G} \right)^{0.25} \left( \frac{\rho_v}{\rho_l} \right)^{0.125}$$

*Given data:*  $v = 204 \text{ m}^2/\text{m}^3$ ,  $V_{\text{free}} = 0.74 \text{ m}^3/\text{m}^3$ . The densities of the liquid and vapour of mean compositions are 840 kg/m<sup>3</sup> and 1.03 kg/m<sup>3</sup>, respectively. The viscosities of the liquid and vapour of mean compositions are  $0.5 \times 10^{-3}$  Pa s and  $1.11 \times 10^{-5}$  Pa s, respectively.  $L$  and  $G$  in kg/hr. [Ans: 0.61 m]

- 6.4 Calculation of Diameter of a Packed Column for SO<sub>2</sub>-H<sub>2</sub>O System:** Calculate the diameter of a packed tower used for absorption of sulphur dioxide as described in Problem 5.10. Given, the

flooding velocity =  $0.87 \text{ kg/m}^2 \text{ s}$  and the operating velocity = 66% of flooding velocity. [Ans: 1.75 m]

**6.5 Calculation of Residence Time in DownComer:** A distillation column has been proposed to be operated with following geometric and operational parameters:

Column diameter = 1454 mm, Tray spacing = 460 mm, Height of weir = 75 mm, Length of the weir = 910 mm, Liquid flow rate in rectification section = 5555 L/hr, and liquid flow rate in stripping section = 11110 L/hr. Calculate the residence time in the downcomers in the two sections. Is the residence time within safe limits?

[Ans: 32.88 s and 16.44 s in rectification and stripping sections, respectively considering the clearance = 25 mm. The time for both the sections are more than the minimum and hence within safe limits.]

**6.6 Estimation of Diameter of a Packed Tower for Absorption of Acetone by Water:** Find the diameter of the tower packed with 2.54 cm wet packed stoneware Raschig rings and operating at 50% of the flooding velocity for absorption of acetone from air-acetone mixture described in Problem 5.16.

Following data are available:

Density of acetone-air mixture =  $1.18 \text{ kg/m}^3$

Density of the solution and also of water =  $998.4 \text{ kg/m}^3$ , and Viscosity = 0.86 cp

Characteristic factor of the packing ( $a_p/f^3$ ) = 538

[Ans: 0.4 m]

**6.7 Estimation of Diameter of Counter-current Packed Tower for Liquid-Gas Contact:** 1000 L/s of a gas mixture at  $20^\circ\text{C}$  and 1 atm pressure, containing 8% (by volume) of a soluble gas  $A$  and the rest inert, is to be scrubbed with water in a counter-current packed tower to remove 90% of  $A$ . The tower is packed with 25 mm stoneware Raschig rings ( $a_p/f^3 = 538$ ). The molecular weight of  $A$  is 64 and that of inert is 30.

(i) Determine the minimum solvent rate; (ii) Assuming that the operating solvent rate is 20% in excess over the minimum and the operating velocity is 50% of that at flooding, estimate the tower diameter.

The following equilibrium data may be used:

$X: 0.001 \quad 0.002 \quad 0.003 \quad 0.004 \quad 0.005 \quad 0.006$

$Y: 0.024 \quad 0.055 \quad 0.090 \quad 0.129 \quad 0.170 \quad 0.212$

where,  $X$  = mol  $A$ /mol water and  $Y$  = mol  $A$ /mol inert gas.

Under the operating conditions, the flooding velocity is given by

$$\frac{G^2 (a_p/f^3) \mu_L^{0.2}}{g_c \rho_G \rho_L} = 0.03 \frac{L}{G} \left( \frac{\rho_G}{\rho_L} \right)^{0.5}$$

where viscosity is in cp and all other terms are in consistent units. The density and viscosity of the solution are  $1000 \text{ kg/m}^3$  and 1.02 cp, respectively.  $g_c$  may be taken as  $1.27 \times 10^8 \text{ m/hr}^{-2}$ .

[Ans: (i) 4067 kmol/hr, (ii) 33.48 cm]

**6.8** Estimation of Diameter of a Counter-Current Packed Tower for Absorption of Benzene in Kerosene: 35 cubic metre per minute of a benzene-nitrogen mixture at 25°C and 800 mm Hg pressure containing 6 mol% benzene, is to be scrubbed in a counter-current packed tower to remove 90% of benzene. Kerosene as solvent will be fed at a rate of 5450 kg/min. The tower will be packed with 25 mm stoneware Raschig rings ( $a_p/f^3 = 538$ ).

Assuming the operating gas velocity to be 50% of the flooding velocity, determine the tower diameter. For the operating condition involved,  $G'$  at flooding is given by

$$\frac{G'^2 (a_p/f^3) \mu_L^{0.2}}{g_c \rho_G \rho_L} = 0.415 \frac{L'}{G'} \left( \frac{\rho_G}{\rho_L} \right)^{0.5}$$

where the notations have their usual significances. The density and viscosity of the kerosene solution are 0.80 g/cm<sup>3</sup> and 2.3 cp, respectively. [Ans: 58.9 cm]

**6.9** Estimation of the Diameter of a Gas-Liquid Contactor Using the Correlation for Pressure Drop: A packed gas-liquid contactor uses ceramic Intalox saddles (38 mm) as packing material. The gas flow rate,  $G = 1.5$  kg/s and gas density,  $t_G = 1.5$  kg/m<sup>3</sup>. The liquid flow rate,  $L = 30$  kg/s and liquid density,  $t_L = 1000$  kg/m<sup>3</sup>. The column is designed for a pressure drop of 42 mm water. Norton's correlation for this pressure drop is

$$K = \frac{13.1 G^2 F_p (\mu_L / \rho_L)^{0.1}}{\rho_G (\rho_L - \rho_G)}$$

where  $K$  = flow coefficient;  $n_L$ , the liquid viscosity = 10<sup>-3</sup> Ns/m<sup>2</sup>;  $G'$  = gas flow rate per unit cross sectional area, kg/m<sup>2</sup> s;  $F_p$ , packing factor = 170 m<sup>-1</sup>.  $K$  is given by the equation:  $K = 0.62 - 0.5(m - 0.5)$  for  $0.5 \leq m \leq 1.0$ , where  $m = [(L/G)(t_G/t_L)]^{0.5}$ .

Calculate the diameter of the contactor. [Ans: 1.29 m]

### **Short and Multiple Choice Questions**

1. What are the primary requirements of a good gas-liquid mass transfer equipment?
2. How are equipment for gas-liquid contact classified?
3. Which are the three important types of plate columns?
4. What are the advantages of valve trays over other trays?
5. What are the requirements for high tray efficiency in a plate column and what are the associated problems?
6. Why is the use of bubble-cap columns declining in recent times?
7. What is weeping in sieve plate columns? How can weeping be avoided?
8. How is Murphree plate efficiency related with the number of overall transfer units?
9. What is the relation between Murphree plate efficiency and Murphree point efficiency when the liquid on the plate is of uniform concentration all through?

- 10.** Why is the wetted-wall tower generally used for investigational purposes?
- 11.** Name some common types of random packing stating their major characteristics.
- 12.** When is the redistribution of liquid necessary in packed towers? State the reason for such redistribution.
- 13.** What is flooding velocity in a counter-current packed tower? What role does it play in design of such towers? Can flooding occur in a co-current tower?
- 14.** A good tower packing should have
- (a) large active surface per unit volume
  - (b) high weight per unit volume
  - (c) low free cross section
  - (d) capacity to retain large amount of liquid
- 15.** A plate is called a theoretical plate when
- (a) the vapour and liquid leaving the plate are in equilibrium
  - (b) the vapour and liquid entering the plate are in equilibrium
  - (c) the vapour leaving the plate is in equilibrium with the liquid entering the plate
  - (d) the liquid leaving the plate is in equilibrium with the vapour entering the plate
- 16.** In a plate-type distillation column
- (a) the pressure increases gradually from bottom to top
  - (b) the pressure decreases gradually from bottom to top
  - (c) the pressure remains constant
  - (d) the temperature is highest at the top
- 17.** The overall plate efficiency of a plate column is the ratio of
- (a) number of theoretical plates to the number of actual plates required
  - (b) number of actual plates required to the number of theoretical plates
  - (c) number of actual plates required to the number of overall gas-phase transfer units
  - (d) none of these
- 18.** Very tall counter-current packed towers are divided into a number of beds in order to
- (a) reduce the total pressure drop
  - (b) reduce liquid hold-up
  - (c) avoid channelling
  - (d) none of these
- 19.** Channelling can be minimized in towers of moderate size by using the ratio of tower diameter to packing diameter as
- (a) more than 8:1 (b) more than 6:1
  - (c) less than 5:1 (d) less than 2:1
- 20.** Berl saddles made of carbon cannot be used
- (a) for alkalis (b) for sulphur dioxide
  - (c) for sulphuric acid (d) in oxidizing atmosphere
- 21.** In a counter-current packed tower, flooding results due to
- (a) high pressure drop (b) low pressure drop
  - (c) low velocity of the liquid (d) high temperature

**22.** Distillation columns are generally designed for reflux ratio between

- (a) 0.2 to 0.7 times  $R_m$  (b) 1.2 to 1.7 times  $R_m$
- (c) 2 to 5 times  $R_m$  (d) 4 to 10 times  $R_m$

where  $R_m$  is the minimum reflux ratio.

**23.** The minimum residence time for liquid in the downspout of a distillation column is

- (a) 8 s (b) 50 s (c) 80 s (d) 8 min

**24.** Diameters of perforation on a sieve plate vary between

- (a) 1.5 to 2 mm (b) 2.5 to 12 mm (c) 15 to 20 mm (d) 25 to 30 mm

**25.** In a counter-current packed tower using Raschig rings as packing, the pressure drop per metre of packing is

- (a) 10 mm H<sub>2</sub>O (b) 20 mm H<sub>2</sub>O (c) 40 mm H<sub>2</sub>O (d) 80 mm H<sub>2</sub>O

**26.** Murphree plate efficiency is represented by

$$(a) \frac{y_n - y_{n+1}}{y_n^* - y_{n+1}^*} \quad (b) \frac{y_n - y_{n+1}}{y_n^* - y_{n+1}}$$

$$(c) \frac{x_n - x_{n+1}}{x_n^* - x_{n+1}} \quad (d) \frac{x_n - x_{n+1}}{x_n^* - x_{n-1}}$$

**27.** When the liquid on a plate is in uniform concentration

- (a) Murphree plate efficiency > Point efficiency
- (b) Murphree plate efficiency < Point efficiency
- (c) Murphree plate efficiency = Point efficiency
- (d) none of these

**28.** Weeping in a distillation column

- (a) increases tray efficiency
- (b) results due to very high gas velocity
- (c) provides large interfacial area of contact
- (d) results due to very low gas velocity

*Answers to Multiple Choice Questions*

14. (a) 15. (a) 16. (b) 17. (a) 18. (c) 19. (c) 20. (d)

21. (a) 22. (b) 23. (d) 24. (b) 25. (c) 26. (b) 27. (c)

28. (d)

## **References**

AIChE Bubble-Tray Design Manual, *AIChE*, New York (1958).

Alper, E. and P.V. Danckwerts, *Chem. Eng. Sci.*, **31**, 599 (1976).

Baird, M.H.I. and J.H. Garstang, *Chem. Eng. Sci.*, **27**, 823 (1972).

Bakowski, S., *Brit. Chem. Eng.*, **8**, 384, 472 (1963); **14**, 945 (1969).

Barniki, S.D. and J.F. Davis, *Chem. Eng.*, 140 (Oct., 1989).

- Billet, R., *Distillation Engineering*, Chem. Pub. Co., New York (1979).
- Billet, R. and M. Schultes, *Packed Towers in Processing and Environmental Technology*, translated by J.W. Fullarton, VCH Publishers, New York (1995).
- Billet, R. and M. Schultes, *Chem. Eng. Technol.*, **14**, 89 (1991).
- Bond, W.N. and D.A. Newton, *Phil. Magazine*, **5**, 794 (1928).
- Bretsznajder, S. and W. Pasiuk, *Inter. Chem. Eng.*, **4**, 61 (1964).
- Cheremisinoff, N.S., *Handbook of Chemical Processing Equipment*, Butterworth-Heinemann, Boston (2000).
- Chu, J.C., J.R. Donovan, B.C. Bosewell and L.C. Furmeister, *J. Appl. Chem.*, **1**, 529 (1951).
- Coulson, J.M., J.F. Richardson and R.K. Sinnott, *Chemical Engineering*, **6**, (SI units) Design, Pergamon Press (1985).
- Davidson, J.F., E.J. Cullen, D. Hanson and D. Roberts, *Trans. Inst. Chem. Engrs.*, **37**, 122 (1959).
- Davies, J.T., *Trans. Inst. Chem. Engrs.*, **38**, 289 (1960).
- De, P., *Studies on Mass Transfer under Pulsations in Gas-Liquid Systems*, Doctoral Dissertation, IIT, Kharagpur, India (1983).
- Fair, J.R., *Petro/Chem. Engg.*, **33**(10), 45 (1961).
- Gianetto, A. and S. Sicardi, *Ing. Chim-Ital*, **8**, 173 (1972); **11**, 25, 31 (1975).
- Guha, D.K. and P. De, *Proc. 6th National Heat & Mass Trans. Conf.*, HMT-**41-81**, H-61 (1981).
- Guha, D.K. and P. De, *Proc. 7th National Heat & Mass Trans. Conf.*, HMT-**H10-31**, 483 (1983).
- Guha, D.K. and P. De, *Canad. J. Chem. Eng.*, **63**, 565 (1985).
- Harbaum, K.L. and G. Houghton, *J. Appl. Chem.*, **12**, 234 (1962).
- Hatta, S. and A. Baba, *J. Soc. Chem. Ind. (Japan)*, **37**, 162 (1934).
- Hughes, R.R. and E.R. Gilliland, *Chem. Eng. Prog.*, **48**, 497 (1952).
- Humphrey, J.L. and G.E. Keller, II, *Separation Process Technology*, McGraw-Hill, New York (1997).
- Johnson, A.I. and A.E. Hamielec, *AIChE J*, **6**, 145 (1960).
- Kister, H.Z. and D.R. Gill, *Chem. Eng. Prog.*, **87**(2), 32 (1991).
- Leva, M., *Chem. Eng. Prog.*, **88**(1), 65 (1992).
- Lockett, M.J., *Distillation Design Fundamentals*, Cambridge University Press, UK (1986).
- Lubowicz, R.E. and P. Reich, *Chem. Eng. Prog.*, **67**(3), 59 (1971).
- Ludwig, E.E., *Applied Process Design for Chemical and Petrochemical Plants*, **2**, 3rd ed., Gulf Pub., Houston, TX (1997).
- Lynn, S., J.R. Straatemeier and H. Kramers, *Chem. Eng. Sci.*, **4**, 49, 58, 63 (1955).
- McFarland, A., P.M. Sigmund and M. Van Winkle, *Hydro. Proc.*, **51**, 111 (Jul. 1972).
- Mollinar, J. and H. Angelino, *Int. J. Heat Mass Trans.*, **20**, 247 (1977).
- Norman, W.S., *Absorption, Distillation and Cooling Towers*, Longmans, The University Press, Aberdeen, Great Britain (1961).
- O'Connell, H.E., *Trans. Am. Inst. Chem. Eng.*, **42**, 741 (1946).

- Scofield, R.C., *Chem. Eng. Prog.*, **46**, 405 (1950).
- Seader, J.D. and E.J. Henley, *Separation Process Principles*, 2nd ed., John Wiley, New York (2006).
- Sherwood, T.K., G.H. Shipley and F.A.L. Holloway, *Ind. Eng. Chem.*, **30**, 765 (1938).
- Sherwood, T.K., R.L. Pigford and C.R. Wilke, *Mass Transfer*, Inter. Students Edition, 3rd ed., 224 (1975).
- Shukla, S., *Chem. Ind. Digest*, **XIX** (3), 60 (2006).
- Sinha, A.P., *Rate of mass transfer in presence of surface-active agents*, 12, Moscow Institute of Chem. Engg., Moscow (1961).
- Smith, B.D., *Design of Equilibrium Stage Processes*, McGraw-Hill, New York (1963).
- Sokolov, B.K. et al., *Sov. Chem. Ind.*, **10**, 699 (1971).
- Stephens, E.J. and G.A. Morris, *Chem. Eng. Prog.*, **47**, 232 (1951).
- Tudose, R.Z., *Inter. Chem. Eng.*, **4**, 219, 664 (1964).
- Van Winkle, M., *Distillation*, McGraw-Hill, New York (1967).
- Vital, T.J., S.S. Grossel and P.I. Olse, *Hydro. Proc.*, 55 (Oct.1984), 147 (Nov.1984), 75 (Dec.1984).
- Vivian, J.E. and D.W. Peaceman, *AIChE J*, **2**, 437 (1956).
- Vyarawalla, F., *Momentum and Mass Transfer Studies in a Gas-Liquid Spray Absorber-Pulsed and Unpulsed*, Ph.D. Thesis, IIT, Kharagpur, India (1970).
- Walas, S.M., *Chemical Process Equipment-Selection and Design*, Butterworths, USA (1988).
- Whitman, W.G., L. Long and W.Y. Wang, *Ind. Eng. Chem.*, **18**, 363 (1926).
- Zheleznyak, A.S., *J. Appl. Chem. (USSR)*, **40**, 834 (1967).

# 7

## Gas Absorption

### 7.1 Introduction

Gas absorption is a mass transfer operation in which a gas mixture is contacted with a liquid with the objective of preferentially dissolving one or more component(s) of the gas in the liquid and producing a solution of the dissolved gas(es) in the liquid. Thus, acetone may be recovered from an air-acetone mixture by bringing the gas into intimate contact with water in which acetone gets dissolved but air does not. Similarly, ammonia may be recovered from an air-ammonia stream by washing the mixture with water, benzene and toluene vapour are removed from coke oven gas by washing the gas with oil. In the examples given above, transfer is from gas phase to liquid phase. If the transfer is in the opposite direction, that is from liquid to gas, the operation is called *desorption* or *stripping*. Thus, when the benzene and toluene, as mentioned above, are removed from the absorption oil by passing steam through the solution, both benzene and toluene vapours pass on to the gas phase and are removed while the oil is reused. The basic principles of absorption and desorption or stripping are the same, the only difference being in the direction of mass transfer.

All the three examples of absorption of acetone, ammonia and benzene-toluene are physical processes since no chemical interaction is involved. However, during absorption of oxides of nitrogen in water to produce nitric acid or during absorption of carbon dioxide in a solution of sodium hydroxide, chemical reactions occur, the nature of which influences the process of absorption. Thus, absorption may be of two broad types: pure physical absorption and absorption accompanied by chemical reaction. Our discussions will mostly be limited to the physical absorption.

It may not be out of the way to sort out some major differences between absorption and distillation. These major differences are that in case of distillation vapour is produced in each stage by partial vaporisation of the liquid while in absorption the feed is a mixture of gases. In general, the ratio of liquid to gas flow rates is much higher in absorption than in distillation. In absorption diffusion is unidirectional while in distillation diffusion is both from liquid to gas and from gas to liquid.

### 7.2 Equilibrium Relations

Equilibrium relationship plays an important role in gas absorption as in other mass transfer operations. Equilibrium relations decide whether mass transfer will at all take place and if so, in which direction. During gas absorption for instance, gas molecules will diffuse into the liquid as long as the concentration of the gas in the liquid is less than the equilibrium value. If, on the other hand, the concentration of the gas in the liquid is higher than the equilibrium value, the gas will diffuse out of the liquid into the gas phase as in case of desorption. At any given temperature and concentration, each dissolved gas exerts a definite partial pressure. The degree, to which each gas is absorbed from a mixture of gases, depends upon the partial pressure of the concerned gas.

When certain amount of a gas and a relatively non-volatile liquid are allowed to remain in mutual contact for a sufficiently long time so that no more net transfer of a component *A* occurs between them, the system is said to be in equilibrium in respect of *A* and the resulting concentration of the dissolved gas *A* in the liquid is known as *gas solubility* at the prevailing temperature and pressure.

Figure 7.1 depicts the solubilities of ammonia in water, sulphur dioxide in water at 10°C and 20°C as well as that of hydrochloric acid gas in water at 10°C. It may be noted from the figure that for a highly soluble substance like hydrochloric acid gas, the equilibrium partial pressure at any given concentration and temperature is quite low while for a relatively insoluble gas like sulphur dioxide the same is high.

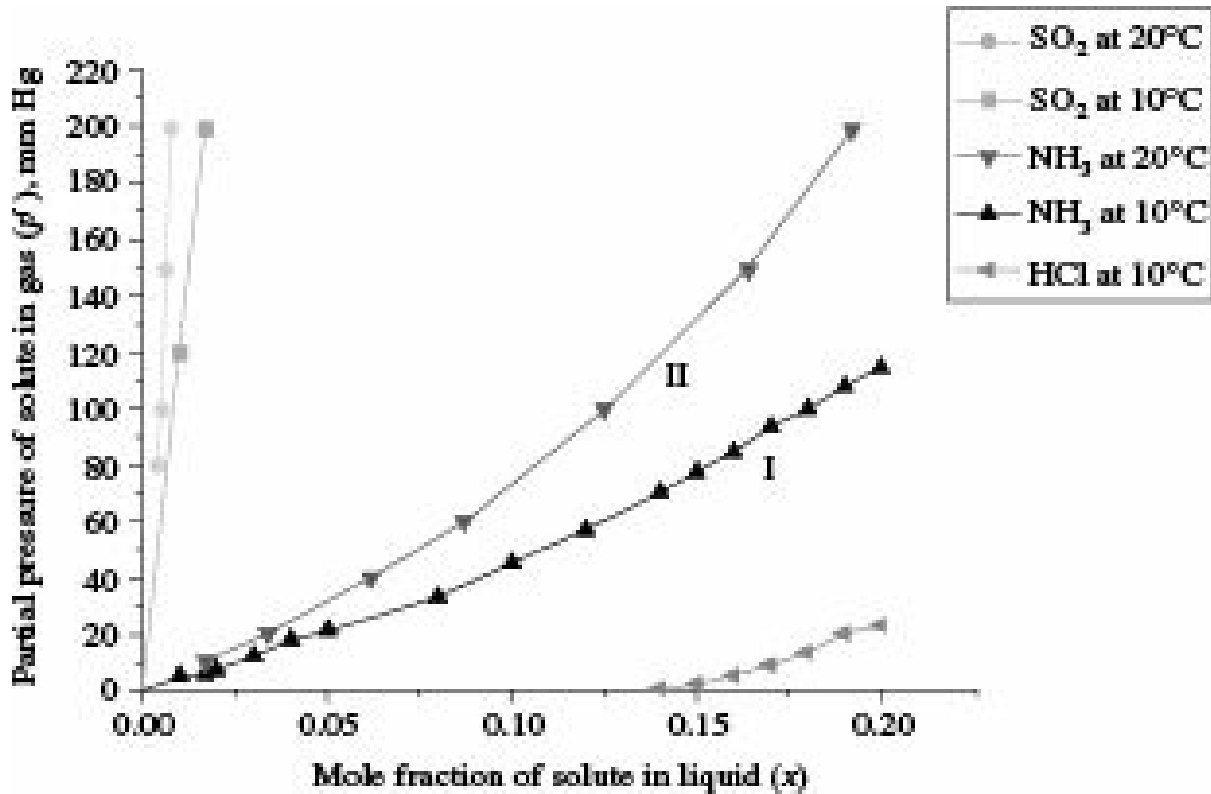


Figure 7.1 Solubility of gases in water.

Different pairs of gas and liquid exhibit different solubility curves which must ordinarily be determined experimentally.

The solubility of a gas is not substantially affected by the total pressure of the system up to a total pressure of about 500 kN/m<sup>2</sup>. Solubility of gas, however, decreases with increase in temperature as in case of ammonia and sulphur dioxide gases, i.e. shown in Figure 7.1. Thus for a concentration of 25 mass percent ammonia in water, the equilibrium partial pressure of ammonia is 30.3 kN/m<sup>2</sup> at 20°C and 46.9 kN/m<sup>2</sup> at 30°C. The solubility of a gas is generally affected by temperature according to Vant Hoff's law of mobile equilibrium (Treybal 1985).

If a mixture of gases is brought into contact with a liquid, the equilibrium solubility of each gas will not be affected by that of others provided the equilibrium is described in terms of the partial pressures of constituent gases. If all but one of the components of the gas mixture is substantially insoluble, its concentrations in the liquid will be so small that it will not be able to influence the solubility of the soluble components. For example, Curve I and II in Figure 7.1 describe the solubility of ammonia in water when the ammonia is diluted with air since air is almost insoluble in water, provided that the ordinate of the plot represents the partial pressure of ammonia in the mixture. The

above generalization is true in the case of several components being soluble only if the solute gases are indifferent to the nature of the liquid, which is possible only if the solution is ideal.

A solution is considered ideal when

- (i) the average intermolecular forces of attraction and repulsion do not change on mixing the constituents,
- (ii) the volume of the solution varies linearly with compositions,
- (iii) no heat is evolved or absorbed during mixing of the constituents, this criterion however does not include heat of condensation of the gas to the liquid state, and
- (iv) total vapour pressure of the solution varies linearly with composition expressed in mole fraction.

The molecules of the constituents of an ideal solution should be similar in size, structure and chemical nature.

In reality, no solution is ideal, actual mixtures only approach ideality as a limit. In practice, however, many solutions are so nearly ideal that they may be considered ideal for engineering purposes. Thus, solutions of benzene and toluene, ethyl- and propyl alcohol or of paraffin hydrocarbon gases in paraffin oils may be considered as ideal.

### 7.2.1 Raoult's Law

If a gas mixture in equilibrium with an ideal liquid solution follows the ideal gas laws, then it obeys the Raoult's law which states that the partial pressure  $p'_A$  of the solute gas  $A$  is equal to the product of its vapour pressure  $p_A$  at the same temperature and its mole fraction  $x_A$  in the solution.

$$p'_A = p_A x_A \quad (7.1)$$

The nature of the solvent liquid does not enter into consideration except establishing the ideality of the solution and it follows that the solubility of a particular gas in an ideal solution of any solvent is always the same.

Raoult's law does not hold good for nonideal solutions and Eq. (7.1) gives highly incorrect results.

In a binary system,

$$P = p'_A + p'_B = p_A x_A + p_B x_B \quad (7.2)$$

where,

$P$  = total pressure

$p'_A$  and  $p'_B$  = partial pressures of components  $A$  and  $B$ , respectively

$p_A$  and  $p_B$  = vapour pressures of components  $A$  and  $B$ , respectively

$x_A$  and  $x_B$  = mole fractions of components  $A$  and  $B$ , respectively in the solution

The composition of the vapour is given by

$$y_A = \frac{p'_A}{P} = \frac{p_A x_A}{P} \quad (7.3)$$

and

$$y_B = \frac{p'_B}{P} = \frac{p_B x_B}{P} \quad (7.4)$$

where,  $y_A$  and  $y_B$  are mole fractions of components  $A$  and  $B$ , respectively in the gas.

In a binary system,

$$y_A + y_B = 1 \quad (7.5)$$

### 7.2.2 Henry's Law

For moderately soluble gases with relatively little interaction between the gas and the liquid molecules, Henry's law as given below is often applicable

$$y_A = \frac{\frac{P_A}{P}}{\frac{P}{P}} = \frac{H_A x_A}{P} \quad (7.6)$$

where,  $H_A$  is Henry's law constant for component  $A$ .

Henry's law constant ( $H$ ) usually depends on temperature but is relatively independent of pressure at moderate levels. In solutions of inorganic salts,  $H$  depends on the ionic strength.

The value of  $H$  is different for different gases over a modest liquid concentration range. Failure to follow Henry's law over a wide concentration range may be due to chemical interaction with the liquid or electrolytic dissociation or non-ideality in the gas phase. Most gases follow Henry's law up to equilibrium pressure of about  $5 \times 10^5$  N/m<sup>2</sup> although, if the solubility is low as in the case of hydrogen-water, Henry's law holds good up to much higher pressure (Pray et al. 1952).

Solubilities are often expressed in terms of vapour-liquid equilibrium constants  $K$  or  $m$  defined by

$$y_A^* = K x_A \quad (7.7)$$

or,

$$y_A^* = m x_A \quad (7.8)$$

$K$  values are widely used to represent vapour-liquid equilibrium data for hydrocarbons in absorption and distillation.

When Eqs. (7.1) and (7.6) are applicable at constant temperature and pressure,  $K$  and  $m$  become constants and a plot of  $y^*$  vs.  $x$  for a given solute become linear from the origin. In many cases, the  $y^*-x$  plot may be drawn assuming linear relationship over small concentration ranges involved. For nonideal solutions or for non-isothermal operations,  $y^*-x$  plot may be curved and has to be determined experimentally.

In order to facilitate interpolation and extrapolation of experimental data an empirical method that gives linear relationship and is an extension of the reference substance plot on logarithmic scales, has been suggested (Othmer et al. 1944, 1959).

## 7.3 Nomenclature and Material Balance

Let us consider counter-current flow of a gas and a liquid through an absorption column as shown in Figure 7.2.

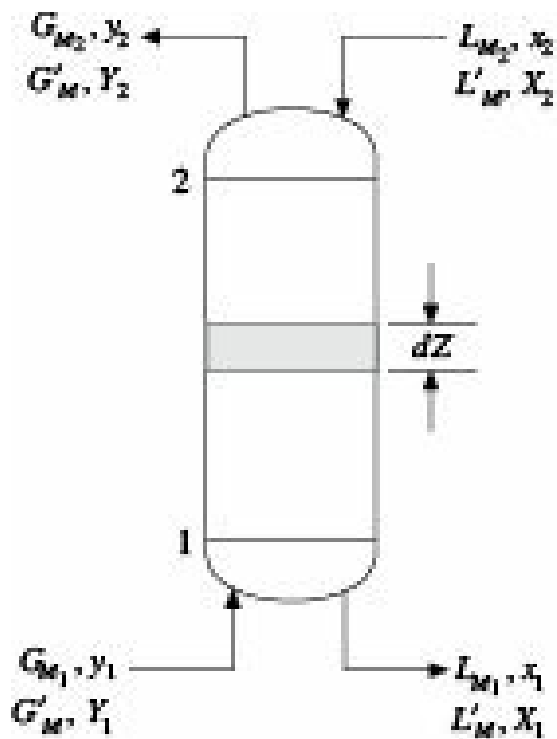


**Figure 7.2** Flow diagram of a counter-current absorption tower.

The total flow rates of gas and liquid are represented by  $G_M$  and  $L_M$ , respectively both being in moles/(unit time)(unit area). Since the gas entering at the bottom gradually loses its solute content as it moves up and the liquid picks up the solute as it flows down, both  $G_M$  and  $L_M$  change through the tower having their highest values at the bottom, called the *rich end* and lowest values at the top, called the *lean end*. These two ends are usually denoted by 1 and 2, respectively.  $G'_M$  and  $L'_M$  represent the flow rates of the inert carrier gas and pure solvent, respectively in same units. Both  $G'_M$  and  $L'_M$  remain unchanged during the process.

The mole fractions of solute in the gas and liquid are denoted by  $y$  and  $x$ , respectively. Since the total quantities of gas and liquid flowing through the tower are changing constantly, values of  $y$  and  $x$  cannot as such be used directly for stoichiometric computations.  $Y$  and  $X$  represent moles of solute per mole of solute-free carrier gas and pure solvent, respectively. Since the flow rates of inert carrier gas ( $G'_M$ ) and pure solvent ( $L'_M$ ) do not change during the process, values of  $Y$  and  $X$  can be directly used for computation of material balance.

Referring to Figure 7.2, the overall material balance is

$$G_{M1} + L_{M2} = G_{M2} + L_{M1} \quad (7.9)$$

and the solute balance is

$$L'_M(X_1 - X_2) = G'_M(Y_1 - Y_2) = G'_M \left( \frac{P'_1}{P - P'_1} - \frac{P'_2}{P - P'_2} \right) \quad (7.10)$$

Considering any intermediate point  $P$  within the tower where the compositions are  $Y$  and  $X$ , Eq. (7.10) assumes the form

$$L'_M(X_1 - X) = G'_M(Y_1 - Y) = G'_M \left( \frac{P'_1}{P - P'_1} - \frac{P}{P - P} \right) \quad (7.11)$$

Equation (7.11) is an equation of a straight line on  $Y-X$  co-ordinates, passing through the point  $(Y_1, X_1)$  and having a slope of  $(L'M/G'M)$ . This is the operating line and represents the actual compositions of gas and liquid at any point within the tower. If Eq. (7.11) is expressed in terms of total flow quantities  $G_M$  and  $L_M$ , and mole fractions  $y$  and  $x$ , the resulting operating line will still represent the compositions at any point within the tower but will be a curved line since the slope  $(L_M/G_M)$  varies throughout the tower.

In case of a lean gas, i.e. a gas having very low initial solute concentration, the variations in flow rates may be neglected and the material balance may be written in terms of average flow rates so that

$$G_M(y_1 - y) = L_M(x_1 - x) \quad (7.12)$$

Equation (7.12), an approximate equation of the operating line, is a straight line passing through the point  $(x_1, y_1)$  and having a slope  $(L_M/G_M)$ . It may be noted that Eq. (7.11) should be used for reliable design calculations. However, Eq. (7.12) may be used for lean gases for preliminary calculations.

For absorption to take place the concentration of solute in the gas phase must be higher than the equilibrium value and the operating line must therefore lie above the equilibrium line  $OE$  as shown in Figure 7.3(a). The distance between these two lines is a measure of the driving force available for mass transfer.

The vertical distance  $PQ$  is the driving force  $(y - y^*)$  in terms of the gas phase concentration and the horizontal distance  $PR$  is the driving force  $(x^* - x)$  in terms of liquid phase concentration. In case of desorption or stripping on the other hand, the transfer is from liquid to gas and the operating line  $A'B'$  lies below the equilibrium curve  $OE$  as shown in Figure 7.3(b), the vertical and horizontal distances between the equilibrium curve and the operating line still representing the driving force in terms of gas-phase and liquid-phase concentrations respectively.

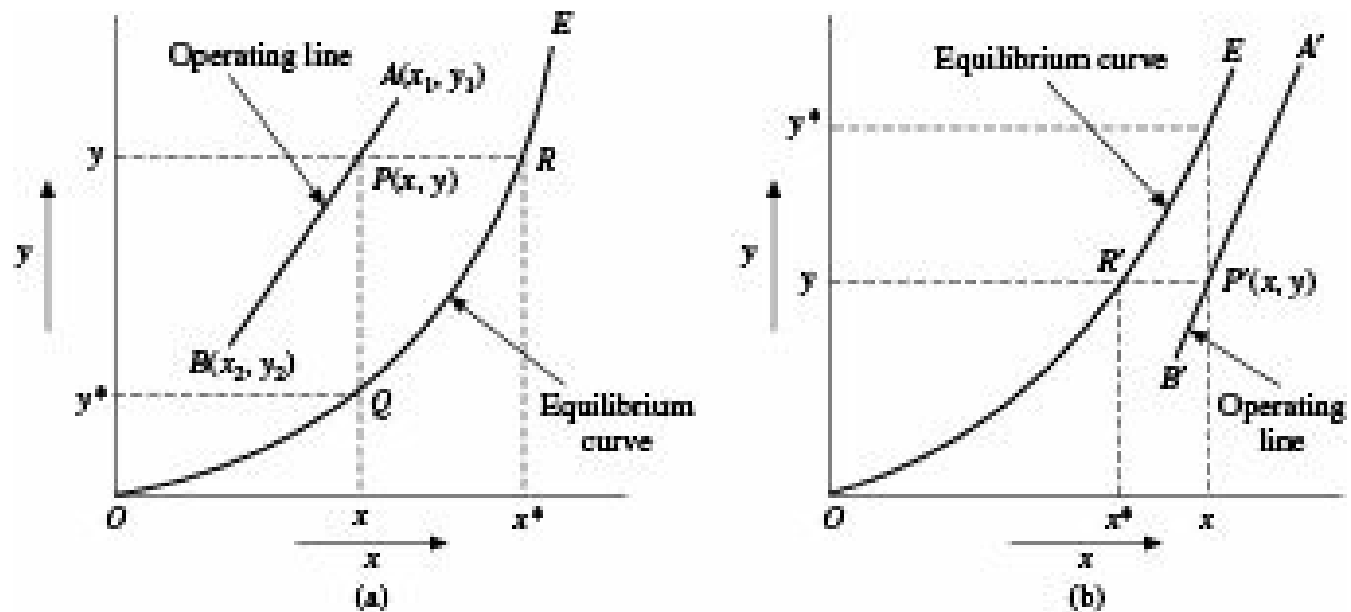


Figure 7.3 Location of operating line for (a) absorption and (b) desorption.

## 7.4 Selection of Solvent

A component to be removed from a gas mixture may be soluble in a number of solvents. The choice of the most suitable solvent has to be made on the basis of several considerations. There is hardly any solvent which will favourably fulfill all the requirements. Hence an intelligent compromise has to be

made to select the most suitable solvent for a given absorption operation. The following characteristics should be considered while selecting a solvent for gas absorption.

**Gas solubility:** It should be high to increase absorption, reduce the quantity of solvent requirement and hence the size of the equipment. If the chemical nature of the solvent is similar to that of the component to be absorbed, then solubility is generally high. Gas solubility is also very high if the solute enters into irreversible chemical reaction with the solute. However, if the solvent has to be recovered and reused, reaction, if any, must be reversible.

**Volatility:** The solvent should have low vapour pressure so as to make solvent loss along with the outgoing gas minimum. When a high volatile solvent has to be used because of high solubility of the gas to be removed, a second less volatile liquid is sometimes used to recover the high volatile solvent.

**Corrosiveness:** The solvent should not be corrosive to the materials of construction of the equipment and accessories and it should not normally require specialized or costly materials of construction.

**Viscosity:** The viscosity of the solvent should be low for higher absorption rate, higher flooding velocity, low pressure drop and better heat transfer characteristics.

**Cost and Availability:** The solvent should be cheap so that solvent loss does not seriously affect the cost of the process. Moreover, it should be easily available.

To the extent possible, the solvent should be nontoxic, nonflammable, chemically stable and of low freezing point.

## 7.5 Types of Equipment and Methods of Operation

Proper selection of equipment and method of operation are important since both have considerable effects on absorption. The principal types of equipment for gas absorption have been discussed in Chapter 6. Packed and plate towers are by far the most widely used equipment for the purpose. Packed towers are cheaper up to 0.5 m diameter. Their construction is simple; pressure drop and liquid hold-up are low.

Plate towers, on the other hand, are available in large sizes, can handle fouling liquids and can stand high liquid rate. These are particularly preferred when large numbers of theoretical plates or stages are required. Venturi scrubbers are useful in handling liquids with small suspended solids. Simulated packed towers, i.e. wetted-wall towers, string-of-discs columns and string-of-spheres columns are the only equipment in which the interfacial area of contact between gas and liquid can be precisely measured and hence, these are mostly used for investigational purposes but have very limited industrial use on account of their low performance. One of their industrial applications is in absorption of hydrochloric acid gas with water for production of hydrochloric acid solution, where removal of heat is more important than rate of absorption which is very fast.

So far in the discussion we have considered packed towers and plate towers as two different piece of equipments used in the industry for absorption or stripping. But the technological advancement in the design of gas-liquid contactors is changing dramatically to meet the requirement, i.e. to increase production performance of the process industry. Nowadays permutation and combination of the packings and trays in a tower are often found. There may be three types of arrangement as follows:

- (i) only packing of various geometries,
- (ii) only trays of different geometries, and

(iii) packings and trays (may be of same or different geometries) together. One such example is that three bed packed tower with Pall rings as packing material was being used in Rectisol absorption towers. The replacement of Pall rings as packing with high performance Cascade Mini Ring (CMR) packing of 1.25", 1.5" and 2" size in the top, middle and bottom beds (each of 5 m height) respectively in the column as shown in Figure 7.4, has increased the production of methanol by 1 metric ton per day (MTD) and also the tower throughput from 11000 to 12900 NM<sup>3</sup>/hr (Bhakta et al. 2006). They have also replaced the existing demister and liquid distributors by Otto York demister and Intalox high performance distributor, respectively.

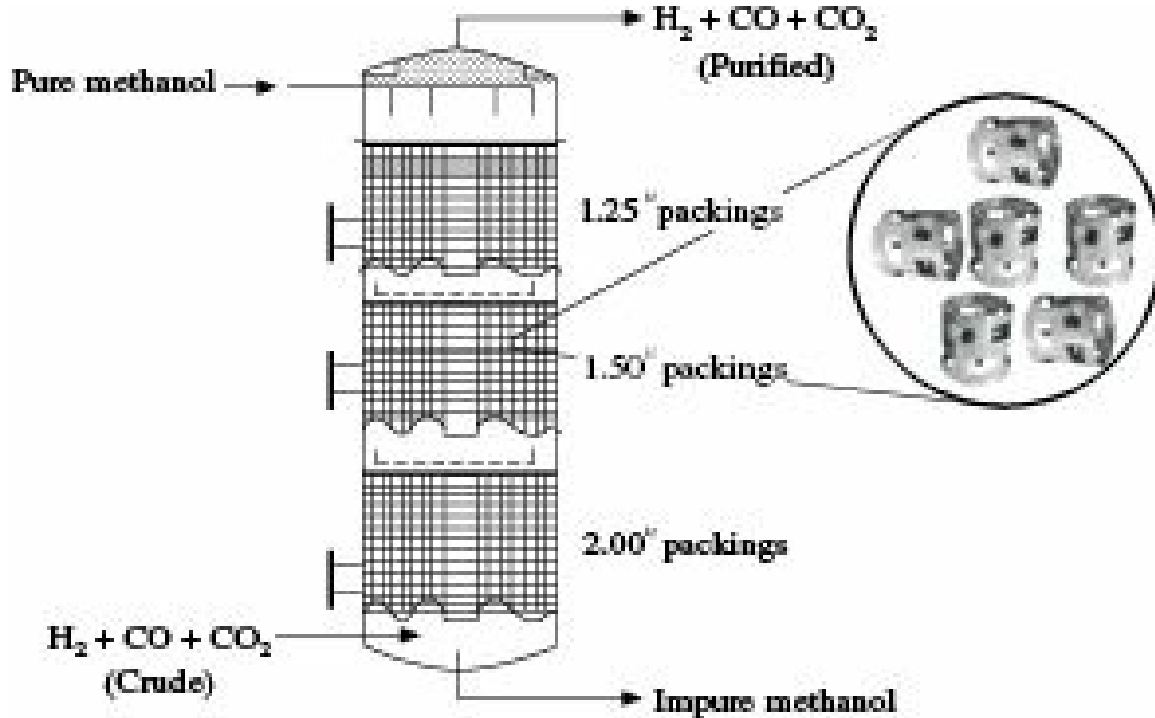


Figure 7.4 Methanol wash tower.

Another example, Pall rings and sieve trays are being used in a single column for treatment of the effluent from the reactor in formaldehyde plant. In the tower, Pall rings of two different materials of construction are used. Pall rings made of stainless steel are placed on the grid plate at the bottom of the column, plastic Pall rings are in the middle and sieve trays are on the top of the column. Such types of arrangement are preferred in a situation when a gas is being entered into the column at a very high temperature which the plastics cannot withstand. Trays are normally used to entrap the desired gas leaving the packings.

In the wake of stringent pollution control regulations, scrubbers have come a long way in effectively reducing industrial gaseous emissions. Different models of wet gas scrubbers described in Chapter 6, are available for cleaning the flue gas.

The packed tower is an efficient mass transfer device requiring relatively low  $L/G$  (liquid flow rate/gas flow rate) ratios. However, both the reagent and the resultant salts formed must be soluble, as otherwise the packed tower is susceptible to plugging. In addition, packed columns are not effective for removal of particulates from the gas stream since the gas-side pressure drop is typically very low. Spray towers generally have the highest  $L/G$  ratios for a particular application, but can use liquids with either suspended or dissolved solids. Spray towers can only operate at low pressure drop. These are therefore not very effective for the removal of particulate from the gas stream.

Venturi scrubbers are effective for particulate removal, but are not that good as a mass transfer

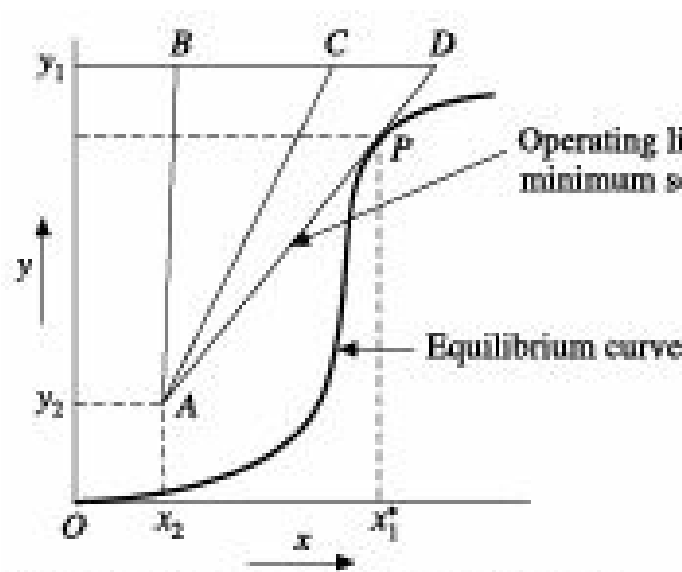
device.

Reverse Jet Froth scrubbing technology of MECS Dyna wave can handle a liquid with both dissolved and suspended solids. In addition,  $L/G$  ratios are modest, and the gas-side pressure drop can be varied. These allow this unit to handle both acid gas emissions and particulate with the same device. Gas absorption equipment are mostly operated in counter-current fashion because of the availability of higher average driving force. In case of co-current operation on the other hand, the effectiveness of a large portion of the equipment near the exit end become very low because of the low driving force available there.

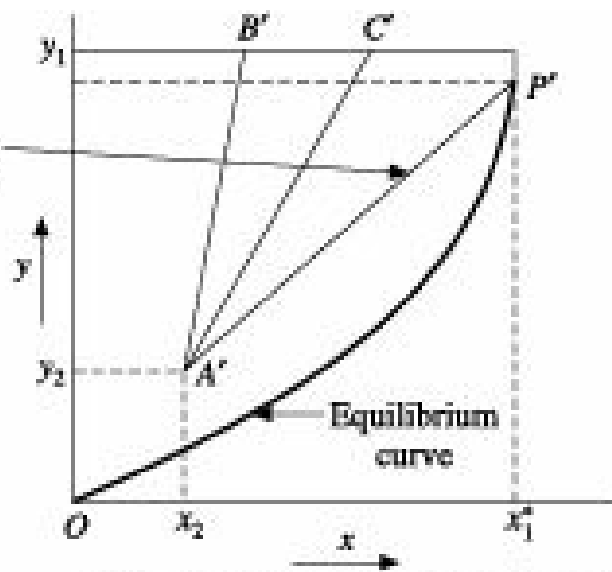
### 7.5.1 Minimum Solvent Rate–Actual Solvent Rate

In gas absorption the amount of gas to be handled, the entering and exit gas compositions, and the composition of the entering solvent are fixed by process requirements. The amount of solvent to be used has, on the other hand, to be fixed by the designer.

In Figure 7.5 the operating line must pass through the point  $A(x_2, y_2)$ , terminate at point  $B$  on the ordinate  $y_1$ , and have a slope  $(LM/GM)$ . As the amount of solvent is gradually decreased, the operating line rotates along the point  $A$  in the clockwise direction and the solute concentration in the exit solution increases till the line  $AD$  is tangent to the equilibrium curve at the point  $P$  as shown in Figure 7.5(a). Alternatively, if the equilibrium curve is concave upwards, as shown in Figure 7.5(b), till the operating line meets the equilibrium curve at point  $P'$  for  $y = y_1$ . The driving force for mass transfer at  $P$  or  $P'$  where the operating line touches the equilibrium curve is zero and infinite time of contact or infinitely long tower will be required to reach this point. This gives the condition for minimum solvent requirement. If the solvent rate is further reduced, the operating line will touch the equilibrium curve before the desired separation is achieved and it will not be possible to have the desired separation even with infinite time of contact or infinitely long tower. When minimum solvent rate is employed the exit liquor will be in equilibrium with the entering gas for the type of equilibrium curve shown in Figure 7.5(b) while for the type of equilibrium curve shown in Figure 7.5(a), equilibrium will be attained some where within the tower so that the remaining part of the tower will remain ineffective.



(a) Equilibrium curve concave downwards



(b) Equilibrium curve concave upwards

Figure 7.5 Graphical determination of minimum solvent rate.

For equilibrium curve concave upwards, the minimum solvent rate may be determined by rewriting Eq. (7.10) (for lean gas and low rate of absorption)

$$G'M(Y_1 - Y_2) = L'M, \min(X^*_1 - X_2) \quad (7.13)$$

where  $X^*_1$  is the equilibrium value corresponding to  $Y_1$ .

From Eq. (7.13),

$$\frac{G'M}{L'_{M,\min}} = \frac{X^*_1 - X_2}{Y_1 - Y_2} \quad (7.14)$$

Equation (7.14) may be employed for the type of equilibrium curve shown in Figure 7.5(a) by replacing  $X^*_1$  by the value of  $x$  corresponding to the point  $P$ , i.e. the point at which the operating line is tangent to the equilibrium curve.

The operating solvent rate is estimated from knowledge of the minimum solvent rate considering the value of solute to be absorbed, cost of solvent and other operating costs. Usually, but not always, the actual solvent rate is 20 to 40% higher than the minimum rate. As the solvent rate is increased, the average driving force increases thereby increasing the rate of mass transfer and reducing the required tower height. But the diameter of the tower has to be increased to accommodate higher liquid rate; cost of solvent as well as pumping cost increase resulting in higher operating cost.

When gas and liquid flow co-currently, the operating line has negative slope and there is no limit on the liquid-gas ratio.

## 7.5.2 Flooding–Tower Diameter

As discussed in Chapter 6, the liquid throughput is estimated from minimum liquid rate which in turn is determined from the given quantity of gas, its concentrations and concentration of initial solvent through material balance and equilibrium considerations. The linear velocities of gas and liquid, however, depend on the cross section of the tower. Further under given operating conditions, flooding velocity in a counter-current column is the gas velocity at which the downward flow of liquid is just stopped by the upward flow of gas and the tower is said to be flooded with the liquid. This corresponds to the minimum cross section of the tower. On further reducing the cross section, the column will cease to operate as a counter-current one. Flooding velocity is determined from Eq. (6.25) and Figure 6.18 by the method described in Chapter 6.

The actual cross section and hence diameter of the tower is worked out from a knowledge of the flooding velocity with adequate insurance against flooding during operation. The operating gas velocity normally lies between 50 and 90% of flooding velocity. After deciding on the operating gas velocity, the tower cross-section and hence tower diameter is determined by dividing the gas throughput [(kmol)/(s)] by the operating mass (molar) velocity of the gas ( $\text{kmol}/\text{s}\text{m}^2$ ). For given throughputs of gas and liquid, the smaller the tower diameter, the higher will be the gas velocity and hence the mass transfer coefficient. But the gas-side pressure drop will increase, residence time will decrease and chances of flooding will increase.

**EXAMPLE 7.1** (Estimation of minimum liquid rate, flooding velocity and tower diameter of a counter-current packed absorption column): 1.0  $\text{m}^3/\text{s}$  of a gas mixture at 20°C and  $1.013 \times 10^5 \text{ N/m}^2$  pressure containing 10% soluble gas  $A$  and the rest inert is to be scrubbed counter-currently with

water in a packed tower to remove 95% of *A*. The tower is packed with 25 mm stoneware Raschig rings ( $a_p/f^3 = 538$ ). Molecular weight of *A* is 64 and that of the inert is 30.

- (i) Determine the minimum liquid rate,
- (ii) for a liquid rate 20% in excess over the minimum and assuming the operating gas velocity to be 60% of that at flooding point, estimate the tower diameter.

*Given:*

The following equilibrium data may be used:

Mol <i>A</i> /mol water	: 0.001 0.002 0.003 0.004 0.005 0.006
Mol <i>A</i> /mol inert gas	: 0.024 0.055 0.090 0.129 0.170 0.212

The following relationship holds under the operating conditions:

$$\frac{(G'^2)(a_p/f^3)(\mu_L^{0.2})}{s_c \rho_G \rho_L} = 0.052 \frac{L'}{G'} \left( \frac{\rho_G}{\rho_L} \right)^{0.5}$$

where  $G'$  and  $L'$  are mass velocities in  $\text{kg/m}^2\text{s}$ ,  $\rho_G$  and  $\rho_L$  are densities in  $\text{kg/m}^3$  and the value of  $g_c$  is  $9.807 \text{ kg}_m \text{ s}^{-2}$ .

The density and viscosity of the solution may be taken as  $1.02 \text{ g/cm}^3$  and  $0.902 \text{ cp}$ , respectively.

**Solution:** Average molecular weight of the entering gas

$$= (0.10)(64) + (0.90)(30) = 33.4,$$

$$\text{Gas entering} = 1.0 \text{ m}^3/\text{s} = \frac{10 \times 273}{293} \times \frac{1}{22.4} = 0.0416 \text{ kmol/s}$$

$$= (0.0416)(33.4) = 1.39 \text{ kg/s}$$

$$\begin{aligned} \text{Amount of component } A \text{ absorbed} &= (0.0416)(0.10)(0.95)(64) \\ &= 0.253 \text{ kg/s} \end{aligned}$$

$$\rho_G = \left( \frac{1.39}{1.0} \right) = 1.39 \text{ kg/m}^3$$

$$y_1 = 0.10; Y_1 = \frac{0.10}{1 - 0.10} = 0.111 \text{ mol/mol of inert};$$

$$Y_2 = (0.05)(0.111) = 0.0055 = y_2, X_2 = 0.$$

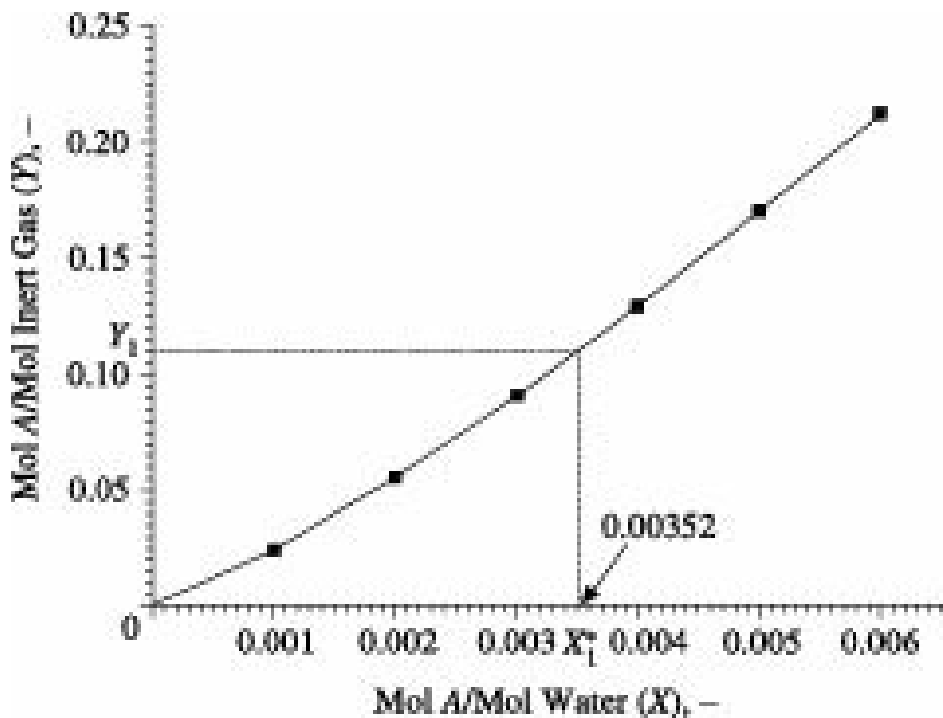


Figure 7.6 Example 7.1

From equilibrium diagram, Figure 7.6,  $X_1^* = 0.00352$ ,

$$\frac{L'}{G'} = \frac{Y - Y_2}{X_1^* - X_2} = \frac{(0.111 - 0.0055)}{(0.00352 - 0)} = 29.97$$

Minimum liquid rate,

$$L'_{\min} = (0.0416)(29.97)(18) = 22.443 \text{ kg/s Ans. (i)}$$

$$L'_{\text{op}} = (22.443)(1.20) = 26.93 \text{ kg/s}$$

$$\frac{L'}{G'} \left( \frac{\rho_G}{\rho_L} \right)^{0.5} = \frac{26.93}{1.39} \left( \frac{1.39}{1020} \right)^{0.5} = 0.715$$

From the given relation,

$$\frac{(G'^2)(a_p/\epsilon^2)(\mu_L^{0.02})}{g_c \rho_G \rho_L} = (0.052)(0.715) = 0.037$$

whence,

$$G'^2 = \frac{(0.037)(1.39)(1020)(9.807)}{(538)(0.902)^{0.2}} = 0.976$$

$$G' = (0.976)^{1/2} = 0.988 \text{ kg/(m}^2\text{s)}$$

and the operating gas mass velocity,

$$G'_{\text{op}} = (0.988)(0.60) = 0.5928 \text{ kg/(m}^2\text{s)}$$

$$\text{Tower cross section} = \frac{1.39}{0.5928} = 2.345 \text{ m}^2$$

whence, tower diameter =  $\frac{(4 \times 2.345)}{3.14}^{0.5} = 1.73 \text{ m}$  Ans (ii)

## 7.6 Stage-wise Contact–Number of Plates (Stages)

Single-stage and multistage cross-flow operations are seldom practised in gas absorption. Multistage counter-current operations are however common in gas absorption. Plate columns like bubble cap and sieve plate columns are generally used for the purpose. Plate columns are generally used for gas absorption when the load (amount of gas and liquid involved) is more than what can be handled by a packed tower of about one metre diameter or when there is chance of deposition of solids which would choke the packing. Plate towers are particularly useful when the required liquid rate is sufficiently high to flood a packed tower.

### 7.6.1 Graphical Method

A detailed discussion regarding counter-current multistage operation along with methods for determination of number of plates and evaluation of their performance by graphical method have been given in Chapter 5 [Eqs. (5.6) to (5.13) and Figures 5.8 and 5.9].

In order to determine the number of theoretical plates or equilibrium stages required for a given degree of absorption, equilibrium and operating lines are drawn on  $y$ - $x$  coordinates, the former from appropriate equilibrium relation for the system under the operating conditions and the latter by drawing a straight line through the points  $(x_0, y_1)$  and  $(x_N, y_{N+1})$  as shown in Figure 5.9. For concentrated gases which give rise to curved operating lines when concentrations are expressed in mole fraction, the operating line may be drawn in terms of molal stoichiometric ratios by plotting Eq. (5.9) in which case the equilibrium line should also be drawn in terms of mole ratios ( $X, Y$ ).

After locating the appropriate equilibrium and operating lines (Figure 5.9), the number of theoretical plates or stages may be determined by drawing a vertical line from the point  $(x_N, y_{N+1})$  to the equilibrium line and then moving horizontally to the left up to the operating line and so on till the point  $(x_0, y_1)$  is reached. Alternatively, steps may be drawn by starting at the point  $(x_0, y_1)$ , moving horizontally to the right up to the equilibrium line, then vertically up to the operating line and so on till the point  $(x_N, y_{N+1})$  is reached. The number of steps so drawn gives the number of theoretical plates or stages required to bring about the desired change.

### 7.6.2 Algebraic Method

If both equilibrium and operating lines are curved or even if any one of them is curved, the graphical method has to be followed for determination of the number of theoretical plates. But if both equilibrium and operating lines are straight then the graphical method can be avoided and algebraic method using Absorption factor ( $A$ ) can be used for the purpose as discussed in Chapter 5 [Eqs. (5.14) to (5.35)]. Equations (5.28) and (5.33) to (5.35) have been reproduced below:

$$\frac{Y_{N+1} - Y_1}{Y_{N+1} - mX_0} = \frac{A^{N+1} - A}{A^{N+1} - 1} \quad (5.28)$$

and

$$N = \frac{\ln \left[ \left( \frac{Y_{N+1} - mX_0}{Y_1 - mX_0} \right) \left( 1 - \frac{1}{A} \right) + \frac{1}{A} \right]}{\ln A} \quad (5.33)$$

where,  $A$  = Absorption factor ( $L'M/mG'M$ ).

When  $A = 1$ , Equation (5.28) becomes indeterminate. It may however be shown that for such condition,

$$\frac{Y_{N+1} - Y_1}{Y_{N+1} - mX_0} = \frac{N}{N+1} \quad (5.34)$$

whence,

$$N = \frac{Y_{N+1} - Y_1}{Y_1 - mX_0} \quad (5.35)$$

Equation (5.33) was suggested by Colburn (Colburn 1941). The relations represented by Eqs. (5.28) and (5.33) can also be used for concentrated solutions provided concentrations are expressed in terms of mole ratios and the equilibrium relation can be approximately represented in the form  $Y^* = mX$  (Coulson and Richardson 1998).

A high degree of absorption can be obtained either by using a large number of plates or by using a high absorption factor ( $L'M/mG'M$ ). Since  $m$  is fixed by the system, this means that ( $L'M/G'M$ ) must be large if high degree of absorption is desired. But this will lead to low solute content of the liquid leaving at the bottom. This may be partly avoided by recirculation of the liquid but in that case the advantage of counter-current operation will be largely lost. A value of 1.25 to 2 for ( $L'M/mG'M$ ) has been found to be most economical (Colburn 1939).

Similarly, for stripping operation the above equations may be represented as

$$\frac{X_0 - X_N}{X_0 - Y_{N+1}/m} = \frac{(1/A)^{N+1} - (1/A)}{(1/A)^{N+1} - 1} \quad (5.28a)$$

and

$$N = \frac{\ln \left[ \left( \frac{X_0 - Y_{N+1}/m}{X_N - Y_{N+1}/m} \right) (1 - A) + A \right]}{\ln (1/A)} \quad (5.33a)$$

where,  $1/A$  = Desorption factor ( $S$ ).

When  $A = 1$ , Equation (5.28a) becomes indeterminate. It may however be shown that for such condition,

$$\frac{X_0 - X_N}{X_0 - Y_{N+1}/m} = \frac{N}{N+1} \quad (5.34a)$$

whence,

$$N = \frac{X_0 - X_N}{X_N - Y_{N+1}/m} \quad (5.35a)$$

Souders and Brown (1932) have suggested that a graphical representation of the above equations as shown in Figure 7.7 for constant absorption or desorption factors, may be readily

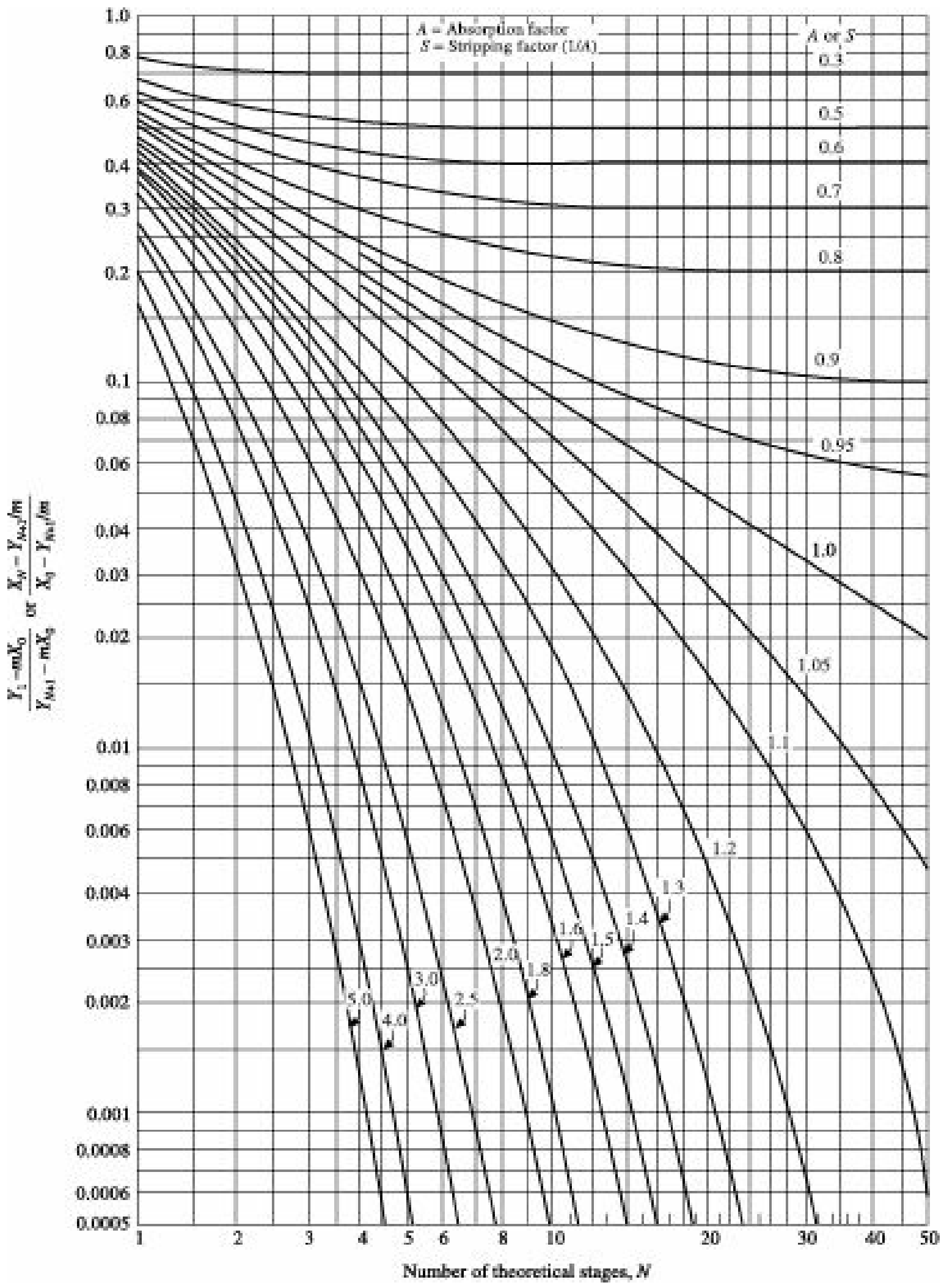


**Figure 7.7** Number of theoretical stages for counter-current absorption or desorption. [Hachmuth and Vance, *Chem. Eng. Prog.*, **48**, 523, 570, 617 (1952)].

used to find the number of plates for a given degree of absorption/desorption or the degree of absorption/desorption for a given number of plates.

## 7.7 Absorption of Concentrated Gases

In case of concentrated gases, the flow rates of gas and liquid through the column vary widely and their ratio changes appreciably as a result of which the operating line becomes curved. The equilibrium line may also become curved due to non-ideal solubility and temperature rise caused by heat of absorption. The graphical method can be applied rigorously to absorption of a concentrated component provided the design diagram takes into account the curvatures of these lines.

The algebraic method, developed for dilute gases may be used for concentrated gases by expressing the flow rates of gas and liquid in terms of solute-free carrier gas ( $G'$ ) and pure solvent ( $L'$ ) respectively and expressing solute concentrations in gas and liquid in terms of stoichiometric molal ratios ( $Y$  and  $X$ ) as in Eq. (5.28) provided the equilibrium relation can also be expressed in terms of molal stoichiometric ratios in the form  $Y^* = mX$ .

**EXAMPLE 7.2** (Determination of number of theoretical plates for a given gas absorption): An air-acetone mixture containing 6% acetone by volume is to be washed with water in a counter-current plate tower to recover 95% acetone. The air rate will be  $1400 \text{ m}^3$  of pure air per hour at standard conditions and the water rate will be  $3000 \text{ kg/hr}$ . The tower will operate at  $20^\circ\text{C}$  and  $1 \text{ atm}$  pressure. Under the operating condition, the equilibrium relation may be expressed as  $Y^* = 1.68X$ , where  $X$  and  $Y$  are moles of acetone per mole of acetone free water and air respectively.

Determine the number of theoretical plates required for the purpose.

**Solution:**

$$\text{The amount of acetone absorbed} = \frac{\frac{1400 \times 0.06 \times 0.95}{0.94 \times 22.4}}{3000} = 3.79 \text{ kmol/hr}$$

$$\text{The solvent (water) rate} = \frac{3000}{18} = 166.7 \text{ kmol/hr}$$

$$\text{The solvent enters the tower free of acetone, } X_2 = 0$$

$$\text{Concentration of acetone in the solution leaving the tower, } X_1 = \frac{3.79}{166.7} = 0.0227$$

$$\text{Concentration of acetone in the entering gas stream,}$$

$$Y_1 = \frac{0.06}{0.94} = 0.0638 \text{ kmol acetone/kmol air}$$

$$\text{Concentration of acetone in the gas stream leaving the tower,}$$

$$Y_2 = \frac{0.06 \times 0.05}{0.94} = 0.0032 \text{ kmol acetone/kmol air}$$

From the given equilibrium relation, it is evident that the equilibrium line passes through the origin and is straight.

Two other points on the equilibrium curve are

$X:$	0.030	0.060
$Y:$	0.050	0.101

The equilibrium line is plotted on the  $Y-X$  coordinates as shown in Figure 7.8.

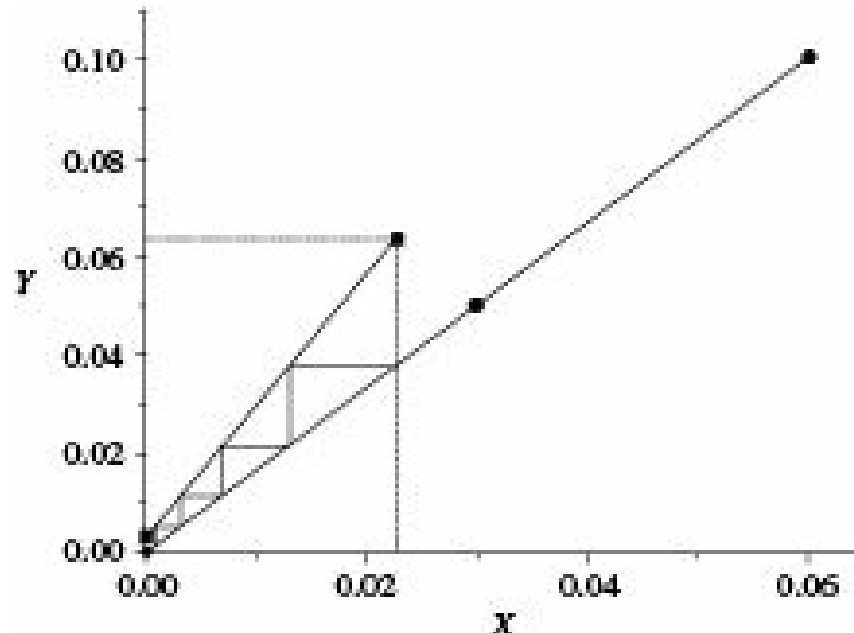


Figure 7.8 Example 7.2.

The operating line is drawn by joining the two points  $(0, 0.0032)$  and  $(0.0227, 0.0638)$  and steps are drawn between the equilibrium line and the operating line.

From Figure 7.8, number of theoretical plates = 4.6.

## 7.8 Estimation of Packing Height–Mass Transfer Rate Calculations

The basic equations for determining the height of packing for a given gas absorption in a counter-current packed tower, as developed in Chapter 5, has been reproduced as follows:

In terms of individual phase mass transfer coefficients:

$$Z = \int_{y_2}^{y_1} \frac{G_M dy}{k_y a (1-y)(y-y_1)} \quad (5.54)$$

and

$$Z = \int_{x_2}^{x_1} \frac{L_M dx}{k_x a (1-x)(x_1-x)} \quad (5.55)$$

In terms of overall mass transfer coefficients:

$$Z = \int_{y_2}^{y_1} \frac{G_M dy}{K_y a (1-y)(y-y^*)} \quad (5.61)$$

$$Z = \int_{x_2}^{x_1} \frac{L_M dx}{K_x a (1-x)(x^* - x)} \quad (5.62)$$

and

During high rates of absorption from rich gases, the mass velocities of both gas and liquid vary throughout the tower having their highest values at the bottom of the tower and lowest values at the top. Consequently, the mass transfer coefficients also vary throughout the tower being highest at the bottom and lowest at the top of the tower. These coefficients must therefore be kept within the integration sign for such absorption. If there exists any known relation between the mass transfer coefficient and the mass velocities of the respective fluids, the variation in the coefficient may be accounted for.

### 7.8.1 Absorption from Concentrated Gases

In case of absorption from concentrated gases, Eqs. (5.54), (5.55), (5.61) and (5.62) may be solved graphically provided values of relevant mass transfer coefficient at different points of the tower are known.

In order to solve Eq. (5.61) graphically for estimation of height of packing, the expression

$\frac{G_M}{K_x a (1-y)(y-y^*)}$  is plotted as ordinate against  $y$  as abscissa on  $y$ - $x$  coordinates as shown in Figure 7.9.

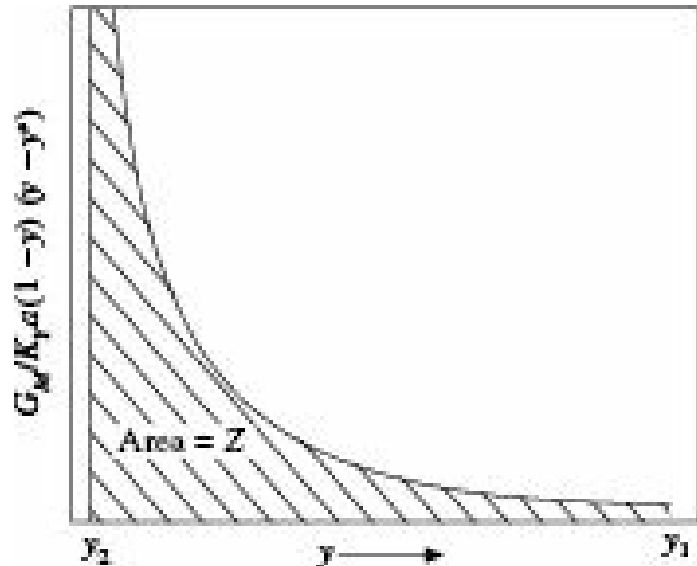


Figure 7.9 Estimation of packed height by graphical integration.

The area under the curve within the limits  $y = y_1$  and  $y = y_2$  gives the required height of packing. For

graphical solution of Eq. (5.62), the expression  $\frac{L_M}{K_x a (1-x)(x^* - x)}$  has to be plotted as ordinate against  $x$  as abscissa.

The area under the curve within the limits  $x = x_1$  and  $x = x_2$  gives the required height of packing for the given absorption. Similar procedure can also be followed for graphical solution of Eq. (5.54) and (5.55). It should however be remembered that the major drawback of employing individual phase mass transfer coefficients for estimation of the height of packing is that it is almost impossible to get

exact values of the interfacial concentration  $y_i$  and  $x_i$ .

### 7.8.2 Simplified Procedure for Lean Gases

If the solute content of the incoming gas as well as the rate of absorption are low, both mass velocity of the fluid and mass transfer coefficient may be assumed to be more or less constant and taken out of the integration sign. In such cases, the following simplifying assumptions may be made without any serious error:

- (i) The mole fractions of solute in gas ( $y$ ) and liquid ( $x$ ) being very small, both  $(1 - y)$  and  $(1 - x)$  may be assumed to be equal to unity,
- (ii) The mass transfer coefficients  $K_y a$  and  $K_x a$  may be assumed to be constant throughout the tower,
- (iii) Solute contents of gas and liquid being very low,

$$Y \approx y \approx p'/P \text{ and } X \approx x \approx c/t_M,$$

Also,  $G'_M \approx G_M$  and  $L'_M \approx L_M$ .

- (iv) Mean partial pressure of the inert carrier gas remains essentially constant and equal to the total pressure throughout the tower,  $p'BM \approx P$ .

With the above assumptions, Eq. (5.61) reduces to

$$\begin{aligned} Z &= \frac{G_M}{K_y a} \int_{y_2}^{y'} \frac{dy}{y - y^*} = \frac{G'_M}{K_y a} \int_{Y_2}^{Y'} \frac{dY}{Y - Y^*} \\ &= \frac{G_M}{K_G a P} \int_{P'_2}^{P'} \frac{dp'}{p' - p'^*} \end{aligned} \quad (7.15)$$

and Eq. (5.62) reduces to

$$\begin{aligned} Z &= \frac{L_M}{K_x a} \int_{x_2}^{x_1} \frac{dx}{x^* - x} = \frac{L'_M}{K_x a} \int_{X_2}^{X_1} \frac{dX}{X^* - X} \\ &= \frac{L_M}{K_L a \rho_M} \int_{x_2}^{x_1} \frac{dx}{x^* - x} \end{aligned} \quad (7.16)$$

**EXAMPLE 7.3** (Estimation of packed height of an absorption column for a liquid rate twice the minimum from given value of individual phase transfer coefficients): A counter-current packed tower is to be designed to recover 90% carbon tetrachloride from an air-CCl<sub>4</sub> mixture containing 5 mol% CCl<sub>4</sub>. The gas rate will be 800 kg/hr m<sup>2</sup> of tower cross section. A non-volatile CCl<sub>4</sub>-free organic oil of molecular weight 260 is to be used as solvent. The solvent rate should be twice the minimum. The tower will be operated at 30°C and 1 atm pressure.

Under the operating condition, the equilibrium relation is given by  $y^* = 20x$ , where  $y^*$  and  $x$  are mole fractions of CCl<sub>4</sub> in gas and liquid respectively.

If the gas and liquid phase mass transfer coefficients  $k_y a$  and  $k_x a$  are 60 and 900 kmol/(hr)(m<sup>3</sup>) (mol fraction) respectively, determine the packed height of the tower.

### Solution

The overall mass transfer coefficient is given by

$$K_y a = \frac{1}{\frac{1}{k_y a} + \frac{1}{k_x a}} = \frac{1}{\frac{1}{60} + \frac{20}{900}} = 25.71 \text{ kmol/(hr)(m}^3\text{)(mol fraction)}$$

Molecular weight of entering gas = 0.05 # 154 + 0.95 # 28.92 = 35.17

$$y_1 = 0.05, Y_1 = \frac{0.05}{1 - 0.05} = 0.0526,$$

$$Y_2 = (0.10)(0.0526) = 0.00526 \approx y_2,$$

$$G_M = \frac{800}{35.17} = 22.75 \text{ kmol/(hr)(m}^2\text{)},$$

$$G'_M = 22.75 \# 0.95 = 21.61 \text{ kmol/(hr)(m}^2\text{)}.$$

For minimum solvent rate, the exit liquor will be in equilibrium with the incoming gas.

Since  $y_1 = 0.05$ , we have  $0.05 = (20)(x_1 \text{ min})$ ,

whence,  $x_1 \text{ min} = 0.0025 \approx X_1 \text{ min}$

From material balance,

$$L_M \text{ min} (0.0025 - 0) = 21.61 (0.0526 - 0.00526)$$

$$\text{whence, } L_M \text{ min} = 409.2 \text{ kmol/(hr)(m}^2\text{)}$$

$$\text{Operating solvent rate} = 409.2 \# 2 = 818.4 \text{ kmol/(hr)(m}^2\text{)}.$$

Again, from material balance

$$818.4(X_1 - 0) = 21.61(0.0526 - 0.00526)$$

$$\text{whence, } X_1 = 0.00125,$$

$$\text{and } x_1 = \frac{0.00125}{(1 + 0.00125)} = 0.00125.$$

Since both equilibrium and operating lines are straight,

$$N_{t o G} = \frac{x_1 - y_1}{\Delta y_{lm}}$$

$$\Delta y_1 = y_1 - y_1^* = 0.05 - (20)(0.00125) = 0.025$$

$$\Delta y_2 = y_2 - y_2^* = 0.00526 - 0 = 0.00526$$

$$D_{ylm} = \frac{\frac{0.025 - 0.00526}{\ln(\frac{0.025}{0.00526})}}{\Delta y_{lm}} = 0.01266$$

$$N_{t0G} = \frac{\frac{y_1 - y_2}{\Delta y_{lm}}}{\frac{0.05 - 0.00526}{0.01266}} = 3.53$$

$$H_{t0G} = \frac{G_M}{K_y a} = \frac{22.75}{25.71} = 0.885 \text{ m}$$

Hence, height of packed bed  $Z = H_{t0G} \# N_{t0G}$   
 $= (0.885 \# 3.53) = 3.12 \text{ m}$

The different ways of evaluating the definite integral in Eqs. (7.15) and (7.16) give rise to the different methods for estimating packed height in a counter-current packed absorption column. These are as follows:

- Graphical method,
- Numerical method, where equilibrium relation is available in the form of equation,
- Method of NTU and HTU, which may be estimated both by numerical and graphical methods. When equilibrium relation is linear, NTU may be estimated by (i) use of log-mean average driving force and (ii) use of Colburn Eq. (5.33).

### Graphical method

In this method, the value of the definite integral in Eq. (7.15) is determined by graphical integration by plotting  $[1/(y - y^*)]$  as ordinate against  $y$  as abscissa. The area under the curve within the limits  $y_1$  and  $y_2$  gives the value of the definite integral which when multiplied by  $(G_M/K_y a)$  gives the required height of packing. Similar result may be obtained by plotting  $[1/(Y - Y^*)]$  against  $Y$  as shown in Figure 7.10 and then multiplying the area under the curve by  $(G'_M/K_y a)$  within the limits  $Y_1$  and  $Y_2$ . The height of packing can also be determined from Eq. (7.16) by following the same procedure.

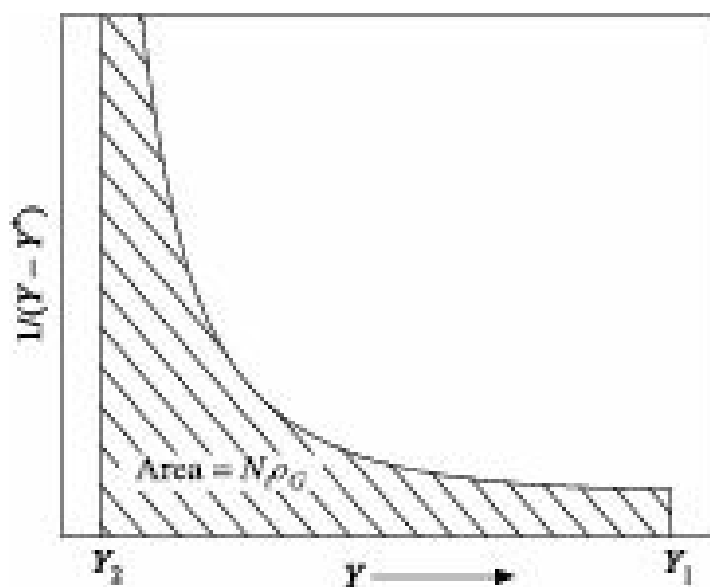


Figure 7.10 Determination of NTU by graphical integration.

### Numerical method

If the equilibrium relation between  $y$  and  $x$  can be expressed in the form of an equation, then Eq. (7.15) or (7.16) can be solved numerically to determine the packed height.

### **Method using the concept of transfer units**

A convenient method for estimation of tower height based on the concept of Number of Transfer Units (NTU) was originally proposed by Chilton and Colburn (1935). Because of its several advantages, this method is particularly suitable for quick and approximate estimation of packed height. The main advantages are as follows:

- (i) The method is simple, rapid and specially suitable for rough estimates.
- (ii) The mass transfer resistance of the packing is expressed in terms of a number having the dimension of length only.
- (iii) The procedure is parallel to that used in the design of plate towers.
- (iv) While  $K_y a$  varies along the tower due to variation in gas and liquid flow rates, the term  $(G_M/K_y a)$  used in this method remains more or less constant since both  $G_M$  and  $K_y a$  vary in the same direction. The same is true for  $(L_M/K_x a)$ .
- (v) While in the concept of theoretical stage or theoretical plate, equilibrium is assumed to reach in each stage or plate, in this method equilibrium is only assumed to approach.

The basic principle of this method is that determination of packed height involves evaluation of a definite integral like

$$\int_{y_2}^{y_1} \frac{dy}{(1-y)(y-y_0)}$$

or,

$$\int_{x_2}^{x_1} \frac{dx}{(1-x)(x-x_0)}$$

The above dimensionless quantity expresses the difficulty in mass transfer, in this case in gas absorption. Its value is higher; the larger is the desired change in gas composition or the smaller is the available driving force. This definite integral has been named Number of Transfer Units (NTU). NTU may be based on overall driving force as well as on individual phase driving forces. In the first case, it is denoted by  $N_{t0} G$  or  $N_{t0} L$  and in the second case by  $N_t G$  and  $N_t L$  depending upon the phase in terms of which the driving force is expressed. In terms of overall driving force based on gas phase, the expression for estimation of packed height has been presented in Eq. (5.61) as

$$Z = \frac{G_M}{K_y a} \int_{y_2}^{y_1} \frac{dy}{(1-y)(y-y_0)}$$

where,  $(G_M/K_y a)$  is called the Overall Height of a Transfer Unit and is denoted by  $H_{t0} G$ . HTU has the dimension of length and depends on type and size of packing as well as flow rates of gas and liquid. HTU may be expressed in terms of overall mass transfer coefficients ( $H_{t0} G$  or  $H_{t0} L$ ) as well as in terms of individual phase mass transfer coefficients ( $H_t G$  and  $H_t L$ ).

Number of Transfer units may also be represented in four different ways as follows:

- **Number of gas-phase transfer units**

$$N_{tG} = \int_{y_2}^{y_1} \frac{dy}{(1-y)(y-y)} \quad (7.17)$$

- **Number of liquid-phase transfer units**

$$N_{tL} = \int_{x_2}^{x_1} \frac{dx}{(1-x)(x-x)} \quad (7.18)$$

The number of overall transfer units based on overall driving force in terms of gas-phase concentration is:

$$N_{toG} = \int_{y_2}^{y_1} \frac{dy}{(1-y)(y-y^*)} \quad (7.19)$$

The number of overall transfer units based on overall driving force in terms of liquid-phase concentration is:

$$N_{toL} = \int_{x_2}^{x_1} \frac{dx}{(1-x)(x^*-x)} \quad (7.20)$$

The corresponding Height of a Transfer Unit (HTU) may be expressed as

- **Height of a gas-phase transfer unit**

$$H_{tG} = \frac{G_M}{k_y a} \quad (7.21)$$

- **Height of a liquid-phase transfer unit**

$$H_{tL} = \frac{L_M}{k_x a} \quad (7.22)$$

Overall height of a transfer unit based on overall mass transfer coefficient in terms of gas-phase concentration difference:

$$H_{toG} = \frac{G_M}{K_y a} \quad (7.23)$$

Overall height of a transfer unit based on overall mass transfer coefficient in terms of liquid-phase concentration difference:

$$H_{toL} = \frac{L_M}{K_x a} \quad (7.24)$$

It should be remembered that for estimation of packed height, both NTU and HTU must have the same suffix, which means these should be calculated on the same basis.

The overall volumetric mass transfer coefficients based on the gas phase ( $K_y a$ ) and on liquid phase ( $K_x a$ ) may be correlated with the individual volumetric-phase mass transfer coefficients ( $k_y a$  and  $k_x a$ ) by the relations similar to Eqs. (4.9) and (4.10), following the procedure described in Chapter 4 (Section 4.1).

$$\frac{1}{K_y a} = \frac{1}{k_y a} + \frac{m}{k_x a} \quad (7.25)$$

and

$$\frac{1}{K_x a} = \frac{1}{k_x a} + \frac{1}{m k_y a} \quad (7.26)$$

For low absorption from lean gases, the overall height of a transfer unit based on gas phase ( $H_{tG}$ ) and that based on liquid phase ( $H_{tL}$ ) can likewise be expressed in terms of individual phase HTU's by the Eqs. (5.80) and (5.81):

$$H_{tG} = H_{tG} + \frac{\frac{mG_M}{L_M}}{H_{tL}}$$

$$H_{tL} = H_{tL} + \frac{\frac{L_M}{mG_M}}{H_{tG}} = \frac{\frac{L_M}{mG_M}}{H_{tG}} H_{tG}$$

In the absence of experimental or otherwise reliable data, one may use the empirical or semiempirical correlations for evaluating volumetric mass transfer coefficients as discussed in Chapter 5.

**EXAMPLE 7.4** (Estimation of diameter and packed height of an absorption column): An air-acetone mixture, containing 5% acetone by volume, is to be scrubbed with water in a counter-current packed tower to recover 95% of the acetone. Air flow rate is  $1400 \text{ m}^3/\text{hr}$  at  $20^\circ\text{C}$  and  $1.013 \times 10^5 \text{ N/m}^2$ . The water rate will be  $3000 \text{ kg/hr}$ . The flooding velocity has been estimated to be  $1.56 \text{ m/s}$  and the operating gas velocity should be 40% of the flooding velocity. The operation will be carried out under a total pressure of  $1.013 \times 10^5 \text{ N/m}^2$ .

The interfacial area of the packing is  $204 \text{ m}^2/\text{m}^3$  and under the operating conditions the overall mass transfer coefficient  $K_y$  is  $0.40 \text{ kmol}/(\text{hr})(\text{m}^2)$  (mole fraction). The equilibrium relation is  $y^* = 1.68x$  where  $y^*$  and  $x$  are mole fractions of acetone in vapour and liquid respectively.

Estimate the diameter and packed height of the tower.

**Solution:** Mole fraction of acetone in entering gas,

$$y_1 = 0.05,$$

$$Y_1 = \frac{0.05}{1 - 0.05} = 0.0526 \text{ mol/mol of air.}$$

$$Y_2 = (0.0526)(0.05) = 0.00263 \text{ mol/mol of air} \approx y_2.$$

Air flow rate at  $20^\circ\text{C}$  and  $1.013 \times 10^5 \text{ N/m}^2 = 1400 \text{ m}^3/\text{hr}$

$$G_M = \frac{(1400)(273)}{(293)(22.4)} = 58.23 \text{ kmol/hr}$$

Gas flow rate at 20 °C and 1.013 # 10<sup>5</sup> N/m<sup>2</sup> = (1400)(1.05) = 1470 m<sup>3</sup>/hr  
 Gas flow rate at gas entrance,

$$G_{M1} = \frac{(1470)(273)}{(293)(22.4)} = 61.14 \text{ kmol/hr}$$

$$\text{Acetone entering} = (1400)(0.05) = 70 \text{ m}^3/\text{hr} \text{ at } 20 \text{ }^\circ\text{C} \text{ and } 1.013 \# 10^5 \text{ N/m}^2$$

$$= \frac{(70)(273)}{(293)(22.4)} = 2.91 \text{ kmol/hr}$$

$$\text{Acetone absorbed} = (2.91)(0.95) = 2.76 \text{ kmol/hr}$$

$$G_{M2} = (61.14 - 2.76) = 58.38 \text{ kmol/hr}$$

$$G_{M \text{ av}} = \frac{\underline{61.14 + 58.38}}{2} = 59.76 \text{ kmol/hr}$$

$$L_{M2} = \frac{\underline{3000}}{\underline{18}} = 166.67 \text{ kmol/hr at liquid inlet, } x_2 = 0$$

$$L_{M1} = (166.67 + 2.76) = 169.43 \text{ kmol/hr at liquid exit}$$

$$L_{M \text{ av}} = \frac{\underline{169.43 + 166.67}}{2} = 168.05 \text{ kmol/hr}$$

From material balance, 166.67 ( $X_1 - 0$ ) = 58.23(0.0526 - 0.00263)  
 whence,  $X_1 = 0.01746$ ,

$$x_1 = \frac{\underline{0.01746}}{\underline{1 + 0.01746}} = 0.01716$$

$$Dy_1 = 0.05 - (1.68)(0.01716) = 0.0212$$

$$Dy_2 = 0.00263$$

$$Dylm = \frac{\underline{0.0212 - 0.00263}}{\ln(\underline{0.0212/0.00263})} = 0.0089$$

Since both equilibrium and operating lines are straight

$$N_{tO}G = \frac{\underline{x_1 - y_2}}{\underline{\Delta y_{lm}}} = \frac{\underline{0.05 - 0.00263}}{\underline{0.0089}} = 5.32$$

$$H_{tO}G = \frac{\underline{59.76}}{\underline{(0.40)(204)}} = 0.732 \text{ m}$$

$$\text{Packing height, } Z = (0.732)(5.32) = 3.89 \text{ m}$$

$$\text{Operating gas velocity} = (1.56)(0.40) = 0.624 \text{ m/s}$$

$$\text{Tower cross section} = \frac{1470}{(0.624)(3600)} = 0.654 \text{ m}^2$$

$$\text{Hence, tower diameter} = \left( \frac{(0.654)(4)}{(3.14)} \right)^{0.5} = 0.913 \text{ m}$$

**EXAMPLE 7.5** (Determination of capacity coefficient for desorption of oxygen in a packed column):

Water saturated with oxygen was fed at the rate of  $7.5 \text{ kg/s m}^2$  into a tower packed with 1.5 m of 25 mm Raschig rings. Air containing 21% oxygen by volume was supplied to the tower at a rate of  $0.625 \text{ kg/s m}^2$ . The oxygen contents of the water entering and leaving the tower were 0.0029% and 0.0011% by weight, respectively. The tower was operated counter-currently at a temperature of  $25^\circ\text{C}$ . Calculate the overall capacity coefficient.

Henry's law may be assumed to be applicable, the value of Henry's constant being  $4.38 \times 10^4 \text{ atm/mole fraction}$ . Vapour pressure of water at  $25^\circ\text{C}$  is 24 mm Hg. Absorption is controlled by diffusion in liquid film.

**Solution:**

$$\text{Mole fraction of O}_2 \text{ in inlet water } (x_2) = \frac{(0.0029)/32}{(100/18)} = 1.631 \times 10^{-5}$$

$$\text{Mole fraction of O}_2 \text{ in exit water } (x_1) = \frac{(0.0011)/32}{(100/18)} = 0.619 \times 10^{-5}$$

$$\text{Mole fraction of O}_2 \text{ in inlet air } (y_1) = 0.21$$

$$L_M = 7.5 \text{ kg/s m}^2 = \frac{7.5}{18} = 0.4167 \text{ kmol/(s)(m}^2)$$

$$t_M = \frac{1000}{18} = 55.556 \text{ kmol/m}^3$$

$$G_M = 0.625 \text{ kg/s m}^2 = \frac{0.625}{28.92} = 0.0216 \text{ kmol/(s)(m}^2)$$

From material balance,

$$0.0216(y_2 - 0.21) = 0.4167(1.631 \times 10^{-5} - 0.619 \times 10^{-5})$$

whence,  $y_2 = 0.2102$  mole fraction.

$$x_1^* = \frac{0.21}{4.38 \times 10^4} = 0.4794 \times 10^{-5}$$

$$x_2^* = \frac{0.2102}{4.38 \times 10^4} = 0.4799 \times 10^{-5}$$

$$Dx_1 = (x_1 - x_1^*) = (0.619 \times 10^{-5} - 0.4794 \times 10^{-5}) = 0.1396 \times 10^{-5}$$

$$Dx_2 = (x_2 - x^*_2) = (1.631 \# 10^{-5} - 0.4799 \# 10^{-5}) = 1.1511 \# 10^{-5}$$

$$Dx_{lm} = \frac{\ln \left[ \frac{(1.1511 \times 10^{-5})}{(0.4799 \times 10^{-5})} \right]}{0.4794 \# 10^{-5}} = 0.4794 \# 10^{-5}$$

$$N_{tOL} = \frac{(x_l - x_2)}{\Delta x_{lm}} = \frac{(1.631 \times 10^{-5} - 0.4799 \times 10^{-5})}{0.4794 \times 10^{-5}} = 2.11$$

The process being controlled by diffusion in liquid, height of packing is given by

$$Z = \frac{L_M}{\rho_M K_L a} \int_{x_2}^{x_1} \frac{dx}{x_1^* - x}$$

$$\text{whence, } K_L a = \frac{L_M}{\rho_M Z} \# N_{tOL}$$

Substituting the values, we get

$$K_L a = \frac{0.4167}{(55.556)(1.5)} \# 2.11 = 1.055 \# 10^{-2}$$

Overall capacity coefficient,  $K_L a = 1.055 \# 10^{-2} \text{ kmol/(s)(m}^3\text{)(kmol/m}^3\text{)}$

### **Graphical Determination of NTU**

The number of transfer units for a given operation may also be determined graphically. Several methods have been proposed for graphical estimation of NTU. Amongst them, Baker's Method (Baker 1935) is simple and convenient.

Baker's Method for graphical solution of Number of Transfer Units is shown in Figure 7.11.  $OE$  is the equilibrium curve and  $AB$  is the operating line. A line  $MN$  is drawn vertically midway between the equilibrium and operating lines. Starting at  $A$ , a horizontal line  $AD$  is drawn such that  $AC = CD$ . From  $D$ , a vertical line  $DG$  is drawn to meet the operating line at  $G$ . From  $G$ , another horizontal line  $GK$  is drawn such that  $GH = HK$ . In this way, steps are drawn till the horizontal line  $y = y_1$  is reached. The number of steps thus drawn gives the number of transfer units. Construction of steps may be started either from the bottom or from the top.

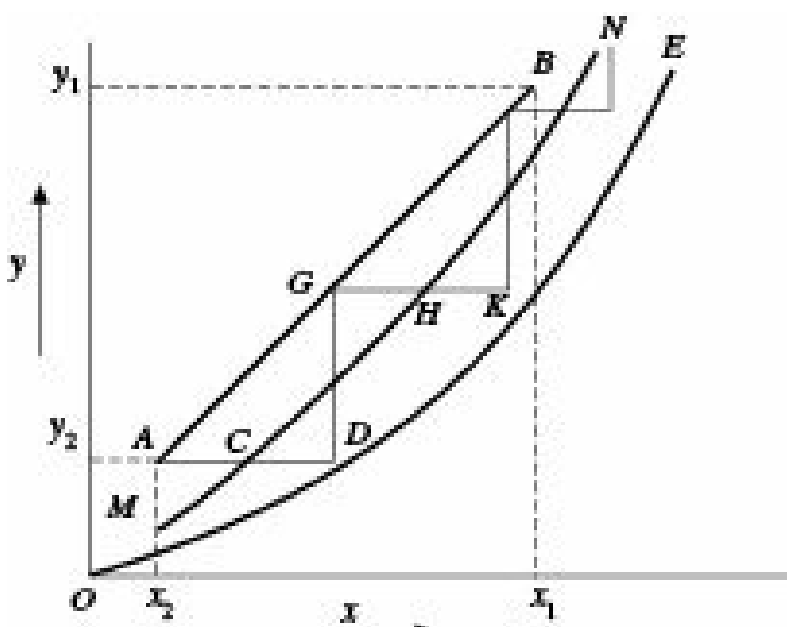


Figure 7.11 Graphical estimation of NTU.

### Determination of NTU when Equilibrium relation is Linear

**Use of Log-mean driving force:** For low absorption from lean gases, values of  $x$  and  $y$  are very small and  $(1 - y) \approx 1$ . Moreover in such cases, the operating line may be expressed in terms of average gas and liquid flow rates, and assumed to be linear without any serious error. If in addition, the equilibrium relation is also linear at least within the range of concentrations involved, then the driving force which is the difference between co-ordinates of operating and equilibrium lines, will also be linear and the number of transfer units may be estimated using the Eq. (7.19) rewritten as

$$N_{tOG} = \int_{y_2}^{y_1} \frac{dy}{y - y^*} = \frac{y_1 - y_2}{(y - y^*)_{lm}} \quad (7.27)$$

and the height of packing may be estimated from the simple relation

$$Z = \frac{G_M}{K_{y^*} a} \frac{y_1 - y_2}{(y - y^*)_{lm}} \quad (7.28)$$

where,  $(y - y^*)_{lm}$  is the logarithmic mean of the driving forces at the bottom and at the top of the packed section.

From Eq. (7.28), it may be seen that when the depth of packing is equal to one HTU and one transfer unit is available for mass transfer, the change in gas composition is equal to the average driving force.

**EXAMPLE 7.6** (To determine increase in packed height of an absorption column for higher recovery): A counter-current packed tower is being used for water scrubbing of an air-ammonia mixture containing 5 mol% NH<sub>3</sub>. The gas rate at the gas inlet is 1000 kg/hr m<sup>2</sup> and the water rate is 4000 kg/(hr)(m<sup>2</sup>). The tower operates at 35 °C and  $1.013 \times 10^5$  N/m<sup>2</sup> pressure. Under these conditions, 90% of the incoming ammonia is absorbed. Assuming all other operating conditions to remain unchanged, what should be the percent increase in tower height in order to absorb 98% NH<sub>3</sub>?

The equilibrium relation is given by  $y^* = 0.746x$ , where  $y$  and  $x$  are mole fractions of NH<sub>3</sub> in gas and liquid respectively. Variations in flow rates due to higher absorption may be neglected.

**Solution:**

$$\text{Molecular weight of entering gas} = (0.05)(17) + (0.95)(28.92) = 28.32$$

$$\text{Gas entering } (G_M) = \frac{\underline{1000}}{\underline{28.32}} = 35.31 \text{ kmol/hr}$$

$$\text{Air entering } (G'M) = (35.31)(0.95) = 33.54 \text{ kmol/hr}$$

$$\text{Water entering } (L'M) = \frac{\underline{4000}}{\underline{18}} = 222.22 \text{ kmol/hr}$$

**Case I: (90% absorption)**

$$y_1 = 0.05, Y_1 = \frac{\underline{0.05}}{\underline{1 - 0.05}} = 0.0526 \text{ mol/mol of air}$$

$$Y_2 = (0.10)(0.0526) = 0.00526, y_2 = \frac{\underline{0.00526}}{\underline{1 + 0.00526}} = 0.00523$$

From material balance,

$$G'M(Y_1 - Y_2) = L'M(X_1 - X_2)$$

Since  $X_2 = 0$ ,

$$X_1 = \frac{\underline{G'M(Y_1 - Y_2)}}{\underline{L'M}} = \frac{\underline{33.54(0.0526 - 0.00526)}}{\underline{222.22}} = 0.00715$$

and

$$x_1 = \frac{\underline{0.00715}}{\underline{1 + 0.00715}} = 0.00710$$

$$Dy_1 = (y_1 - y^*_1) = [0.05 - (0.746)(0.00710)] = 0.0447$$

$$Dy_2 = (y_2 - y^*_2) = (0.00523 - 0) = 0.00523$$

$$Dy_{lm} = \frac{\underline{(0.0447 - 0.00523)}}{\underline{\ln\left(\frac{0.0447}{0.00523}\right)}} = 0.0184$$

Since both equilibrium and operating lines are straight,

$$N_{t0G} = \frac{\underline{0.05 - 0.00523}}{\underline{0.0184}} = 2.433$$

$$Z_1 = 2.433H_{t0G}$$

**Case II: (98% absorption)**

$$y_1 = 0.05, Y_1 = 0.0526,$$

$$Y_2 = (0.02)(0.0526) = 0.00105 \approx y_2$$

$$X_1 = \frac{\underline{33.54(0.0526 - 0.00105)}}{\underline{222.22}} = 0.00778 \approx x_1$$

$$Dy_1 = y_1 - y^*_1 = 0.05 - (0.746)(0.00778) = 0.0442$$

$$Dy_2 = y_2 - y^*_2 = 0.00105 - 0 = 0.00105$$

$$Dylm = \frac{\underline{0.0442 - 0.00105}}{\ln(\frac{0.0442}{0.00105})} = 0.0115$$

$$N_{t0G} = \frac{\underline{(0.05 - 0.00105)}}{\underline{0.0115}} = 4.257$$

$$Z_2 = 4.257H_{t0G}$$

Hence, required percent increase in packed height

$$= \frac{\underline{Z_2 - Z_1}}{\underline{Z_1}} \# 100 = \frac{\underline{4.257H_{t0G} - 2.433H_{t0G}}}{\underline{2.433H_{t0G}}} \# 100 = 74.97\%$$

### ***Estimation of NTU by Colburn Equation***

In case of absorption from lean gases,  $(1 - y)$  becomes almost equal to unity and the number of transfer units may be estimated using Eq. (7.27).

Assuming both equilibrium and operating lines to be straight with slopes  $m$  and  $(L_M/G_M)$  respectively, Colburn (1939) developed the following algebraic expression for the integral in Eq. (7.27):

$$N_{t0G} = \frac{\ln \left[ \left( \frac{y_1 - mx_2}{y_2 - mx_2} \right) \left( 1 - \frac{1}{A} \right) + \frac{1}{A} \right]}{\left( 1 - \frac{1}{A} \right)}$$

(7.29)

$$\left( \frac{L_M}{mG_M} \right)$$

where,  $A$  is the Absorption factor =

Similar expression can be written for number of overall transfer units based on liquid-phase concentration difference ( $N_{t0L}$ ) in case of stripping operation

$$N_{t0L} = \frac{\ln \left[ \frac{x_2 - y_1/m}{x_1 - y_1/m} (1 - A) + A \right]}{1 - A}$$

(7.29a)

Equations (7.29) and (7.29a) may be used for calculation of number of overall transfer units based on gas-phase concentration difference and liquid-phase concentration difference, respectively. Alternatively, graphical method may be used for direct evaluation of  $N_{t0G}$  or  $N_{t0L}$  for calculated values of  $[(y_2 - mx_2)/(y_1 - mx_2)]$  or  $[(x_1 - y_1/m)/(x_2 - y_1/m)]$  and absorption factor or desorption factor, respectively (Treybal 1985).

## 7.9 Multicomponent Absorption

Some of the important industrial applications such as absorption of hydrocarbons in non-volatile hydrocarbon oils involve simultaneous absorption of a number of components from a gas mixture and are categorized as multicomponent absorption. In this section, we shall consider multicomponent absorption in counter-current plate columns.

The material balance of any one component in multicomponent absorption may be expressed as

$$G'(Y'_1 - Y') = L' (X'_1 - X') \quad (7.30)$$

or,

$$G'(Y - Y'_2) = L' (X - X'_2) \quad (7.31)$$

where,

$G'$  = moles of gas to be treated per unit time,

$L'$  = moles of solvent fed per unit time,

$X'$  = moles of one solute per mole of solute-free solvent,

$Y'$  = moles of one solute per mole of inert-gas to be treated,

Subscripts 1 and 2 represent the bottom and top of the column, respectively.

In Eqs. (7.30) and (7.31),  $X'$  and  $Y'$  are the concentrations of one component in the liquid and gas phases respectively flowing across any imaginary horizontal plane between any two plates of the column.

In terms of the above units, the equilibrium relation becomes

$$\frac{Y'}{\Sigma Y'} = \frac{KX'}{1 + \Sigma X'} \quad (7.32)$$

or,

$$Y' = KX' \frac{\Sigma Y'}{1 + \Sigma X'} \quad (7.33)$$

where,

$\Sigma Y'$  = sum of the values of  $Y'$  for the components present

$\Sigma X'$  = sum of the values of  $X'$  for the components present except the solvent

$$\frac{\Sigma Y'}{1 + \Sigma X'}$$

In the special case of absorption with large amount of solvent, the term  $\frac{\Sigma Y'}{1 + \Sigma X'}$  may be assumed to be unity and Eq. (7.33) becomes

$$Y' = KX' \quad (7.34)$$

The operation of a column treating a relatively lean gas may be represented by a plot of  $X'$  vs  $Y'$  on rectangular co-ordinates as shown in Figure 7.12 with straight equilibrium line for each component passing through the origin and having a slope of  $K$  for the component under the operating conditions. Each component will have its own straight operating line. These operating lines will be parallel to each other since each will have a slope of  $(L'/G')$ . The required value of  $(L'/G')$  has to be determined from the solubility of the least soluble component present in the gas which has to be removed completely.

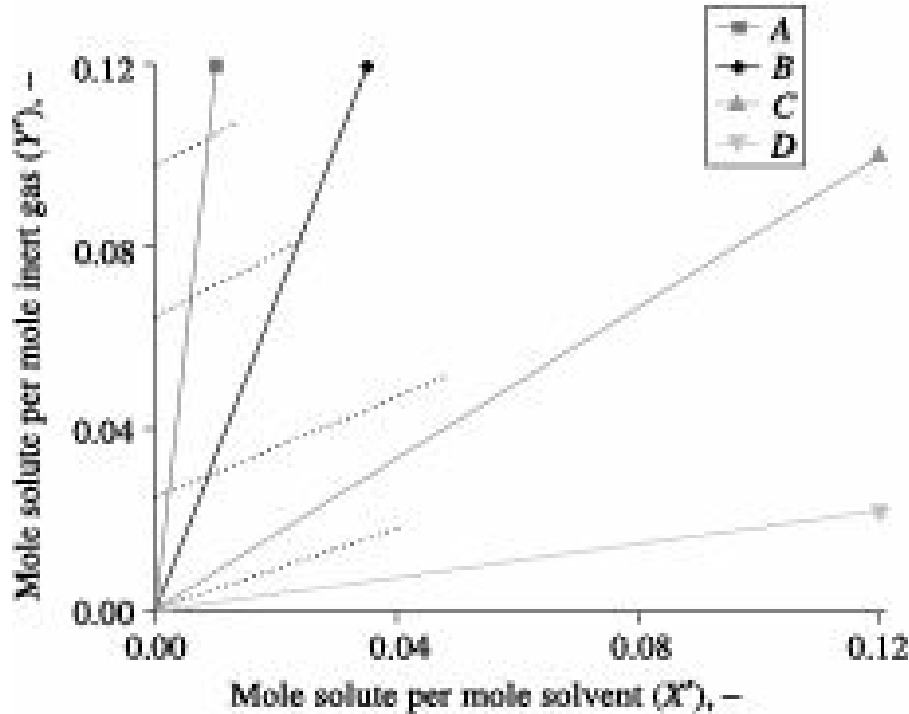


Figure 7.12 Graphical representation of multicomponent absorption from a lean gas.

Figure 7.12 shows the equilibrium and operating lines for four compounds  $A$ ,  $B$ ,  $C$  and  $D$  arranged in order of decreasing volatility. The solvent oil is assumed solute-free ( $X'_2 = 0$ ). The lower ends of the operating lines at their intersections with the ordinate indicate the composition of the treated gas with respect to each compound. The percentage absorption of each compound may be determined from the concentrations of the compound at the two ends of its operating line. Thus 50% of  $C$  is absorbed and the oil leaves with 0.05 mole of  $C$  per mole of solute-free solvent. The operating line for  $B$  is drawn parallel to that of  $C$  and is placed in such a way that the change in  $Y'$ , i.e.  $(Y'_1 - Y'_2)$  divided by the mean driving force (mean vertical distance between equilibrium and operating lines) is the same as that for  $C$ . In case of straight equilibrium and operating lines, the logarithmic mean of the vertical distances at the two ends of the operating line gives the mean driving force.

In multicomponent absorption, a *key component* is usually chosen on the basis of which rigorous calculations are made. The 'key component' is defined as the component absorbed in appreciable amount whose equilibrium curve is nearest to parallel to the operating line, i.e. a component for which the value of  $K$  is most nearly equal to  $(L'/G')$ . Generally, components more volatile than the key

component approach equilibrium with the liquid phase at the rich end of the column and components less volatile than the key component approach equilibrium near the top of the column which means that it is in equilibrium with the entering solvent. Thus components heavier than the key component are almost completely absorbed if the solvent enters the column as solute-free. Change in oil-gas ratio may change the key component.

Another method known as the theoretical plate method is similar to the one described above except the procedure for locating the operating lines. In this method, after locating the operating line of the key component, operating lines for other components are located to give the same number of theoretical plates as in the case of the key component.

### 7.9.1 Absorption of Concentrated Gases—Graphical Method

In absorption of concentrated multicomponent gases, the equilibrium lines become curved due to variation of the amount of solute carried by the solvent along the tower. The curvature depends on the fraction of gas absorbed and on the relative amounts of gas and liquid. For lean gases or for high solvent rate, the term  $SY/(1 + SX')$  in Eq. (7.33) was assumed to be unity without much error. But in case of rich gas or low solvent rate, this cannot be done. As a consequence, the equilibrium line has to be located from other considerations. When the solvent enters the column as solute-free, the equilibrium line may be located from the following two facts: (i) the slope of the equilibrium line at the origin is  $(K'SY_2)$  as obtained by differentiating Eq. (7.33), and (ii) a point on the equilibrium curve for conditions at the rich end of the column is determined by substituting  $Y_1$  or  $X'_1$ ,  $SY_1$  and  $SX'_1$  in Eq. (7.33).  $SY_1$  is unity by definition and  $SX'$  may be calculated if the total moles of all components absorbed are known. In many practical cases, however the curvature of the equilibrium lines are not serious and they may be located if the slope at the origin and the location at the rich end are known.

If the composition of the feed gas, gas and solvent rates, and the operating conditions are known, the performance of a column may be determined by following the steps:

**Step 1** From reliable sources, determine the value of  $K$  for each component for the operating conditions,

**Step 2** Calculate  $G'$  and  $L'$ ,

**Step 3** Make a rough estimate of the total absorption as moles per 100 moles of feed gas;

**Step 4** Based on the estimate of total absorption, calculate  $SX'$ . Also, calculate values of  $[L'(1 + SX')/KG']$ . Employ Kremser equation in molar stoichiometric units as represented by Eq. (5.28) as

$$\frac{Y_{N+1} - X}{Y_{N+1} - mX_0} = \frac{A^{N+1} - A}{A^{N+1} - 1}$$

with  $[L'(1 + SX')/KG']$  replacing  $A$  to get a second estimate of the absorption of the very volatile and nonvolatile components,

**Step 5** For the key component(s), construct a plot of  $Y$  vs  $X'$  and draw the equilibrium line through the origin with a slope of  $K'SY_2$ . Locate the point  $(X'_1, Y_1)$  from Eq. (7.33) and draw the equilibrium curve in the approximate position,

**Step 6** Locate the operating line for the key component with a slope of  $(L'/G')$  and in position above the equilibrium curve corresponding to the proper number of theoretical plates. From this line find out the value of  $Y_2$  for the key component and calculate the moles of that component absorbed,

**Step 7** Make a third estimate of the total absorption by adding the number of moles absorbed. If this differs appreciably from the value obtained in Step 4, repeat Steps 4, 5 and 6.

The number of theoretical plates required for a given performance of the column may be determined by minor modification of the above procedure and using Eq. (5.33) instead of Eq. (5.28) in Step 4.

### 7.9.2 Absorption of Lean Gases—Algebraic Method

In case of lean gas absorption with large amount of solvent, the equilibrium line may be represented by Eq. (7.34):

$$Y = KX'$$

The equilibrium line becomes straight and passes through the origin. If in addition, the operating lines are also straight, then the fraction of each component absorbed may be directly computed by algebraic method without locating the operating lines by trial and error. For this purpose Kremser equation in molal stoichiometric units, i.e. Eq. (5.28) may be used.

Alternatively, the number of plates required for a given separation may be determined by Eq. (5.33)

$$N = \frac{\ln \left\{ \left( \frac{Y_{M+1} - mX_0}{Y_1 - mX_0} \right) \left( 1 - \frac{1}{A} \right) + \frac{1}{A} \right\}}{\ln A}$$

where,  $A$  is Absorption factor  $(L'M/mG'M)$ .

### 7.10 Absorption with Chemical Reaction

Our discussions on gas absorption have so far been limited to physical absorption only. In some cases however, the solvent or some of its components may react chemically with the solute being absorbed to form unstable compounds. Such absorptions have two advantages, firstly the capacity of the solvent to dissolve the solute increases and secondly the partial pressure of the solute over the solution being negligible, the rate of absorption increases considerably due to increase in driving force. The compound so formed should be easily decomposable for ready recovery of the solute and reuse of the solvent. In the removal of carbon dioxide from lean gases, carbon dioxide is absorbed by sodium carbonate solution or by a solution of ethanolamine. In the first case,  $\text{CO}_2$  reacts with carbonate to form bicarbonate according to the equation:



On heating to boiling point, the bicarbonate decomposes releasing  $\text{CO}_2$  and is converted to carbonate which is reused for further absorption. In recent times,  $\text{CO}_2$  is absorbed by aqueous solution of diethanolamine or triethanolamine which combines with  $\text{CO}_2$  to form unstable carbonate



The carbonate decomposes on heating to about 50°C liberating CO<sub>2</sub>. Sodium carbonate is also used for absorption of H<sub>2</sub>S.

In any absorption involving chemical reaction, the reaction may be considered to be an additional resistance in series with the diffusional resistance. If the reaction is rapid, the resistance due to reaction becomes small compared to the diffusional resistance and the latter becomes the controlling factor for mass transfer. If, on the other hand, the reaction is slow, the resistance due to reaction is large compared to the diffusional resistance and the rate of absorption becomes almost equal to the reaction rate.

### 7.10.1 Rapid Reaction

In case of absorption with rapid chemical reaction, the reaction which occurs in the liquid film is limited to a narrow region parallel to the interface. Let us assume that a solute gas *A* is being absorbed from a gas mixture by a solution of *B* which reacts with *A* according to the equation:



As soon as the gas and liquid are placed in mutual contact, *A* gets dissolved in the solution and immediately reacts with *B* at the phase boundary. The product *AB*, assumed to be nonvolatile, starts diffusing towards the main bulk of the liquid. As the component *B* near the phase boundary is consumed, *B* will diffuse from the bulk of the liquid towards the interface. Due to depletion of *B* at the interface, solute *A* will diffuse through the liquid film to meet the incoming *B*. As a result, the zone of reaction moves away from the interface into the liquid film taking up a position such that the rate of diffusion of *A* from the gas phase and that of *B* from the bulk of the liquid are equal. The process stabilizes within a very short time. The conditions within the gas phase are similar to those for physical absorption, but in the liquid phase there is a liquid film followed by a reaction zone.

A diagrammatic sketch of the resulting concentration profiles has been shown in Figure 7.13 where *TT'* is the equilibrium position of the reaction zone. *A* diffuses through the gas film due to the potential difference (*p<sub>G - *p<sub>i</sub>*) and then diffuses to the reaction zone through the liquid film due to the driving force *c<sub>i</sub>*. *B* diffuses from the bulk of the liquid to the reaction zone under the influence of the driving force *q*. The reaction product *AB* diffuses towards the bulk of the liquid under the influence of the driving force (*m* - *n*).</sub>*

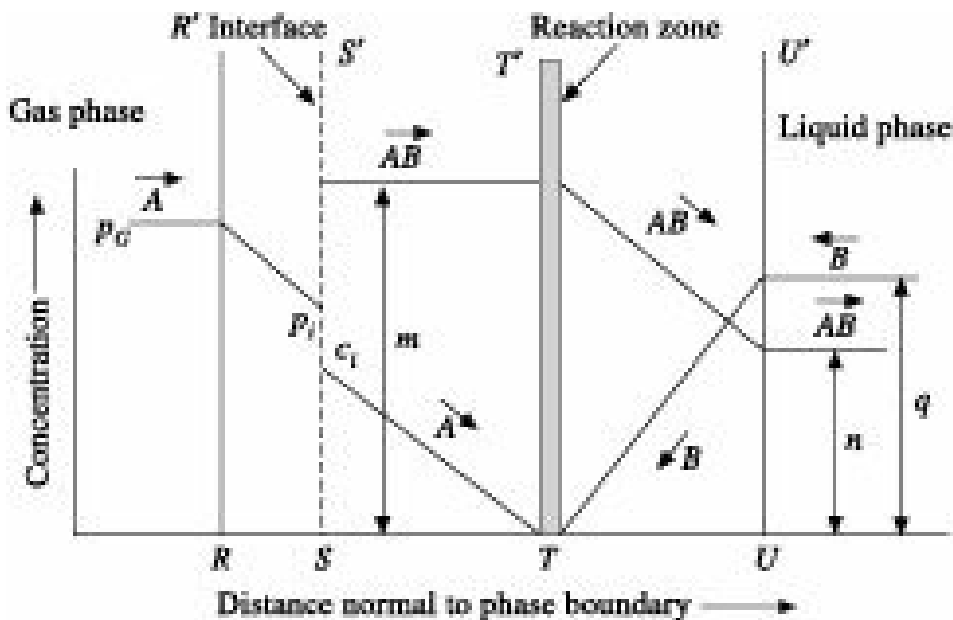


**Figure 7.13** Concentration profile for absorption with rapid chemical reaction.

Applying the basic diffusion equation to diffusion of  $A$  through gas and liquid films, and diffusion of  $B$  and  $AB$  through the liquid film and rearranging, Sherwood and Pigford (1952) obtained the following equation for the overall rate of mass transfer:

$$N_A = \frac{H p_G + (D_B/D_A) q}{H/K_G + X_L/D_A} \quad (7.38)$$

Equation (7.38) states that the rate of absorption is directly proportional to the overall driving force expressed by the sum of the two terms of the numerator and inversely proportional to the overall resistance represented by the denominator. The first term of the denominator represents the resistance of the gas film while the second term represents the combined resistance of the liquid film. This equation also indicates that for constant gas composition and constant film conditions, the rate of diffusion is a linear function of the residual concentration of  $B$  in the liquid.

It has further been shown that

$$p_i = \frac{k_G p_G - D_B q / x_L}{k_G + H D_A / x_L} > 0 \quad (7.39)$$

$$\text{whence, } q < \frac{x_L k_G p_G}{D_B} \quad (7.40)$$

which is a necessary condition for application of Eq. (7.38). When  $q > \frac{x_L k_G p_G}{D_B}$ ,  $p_i$  approaches zero and absorption takes place at a constant rate of

$$N_A = k_G p_G \quad (7.41)$$

## 7.10.2 Slow Reaction

If the reaction is slow, the diffusing components do not react within a well defined plane or a narrow region, but continue to react as they diffuse into the liquid. The concentration profile is somewhat

similar to that shown in Figure 7.14.

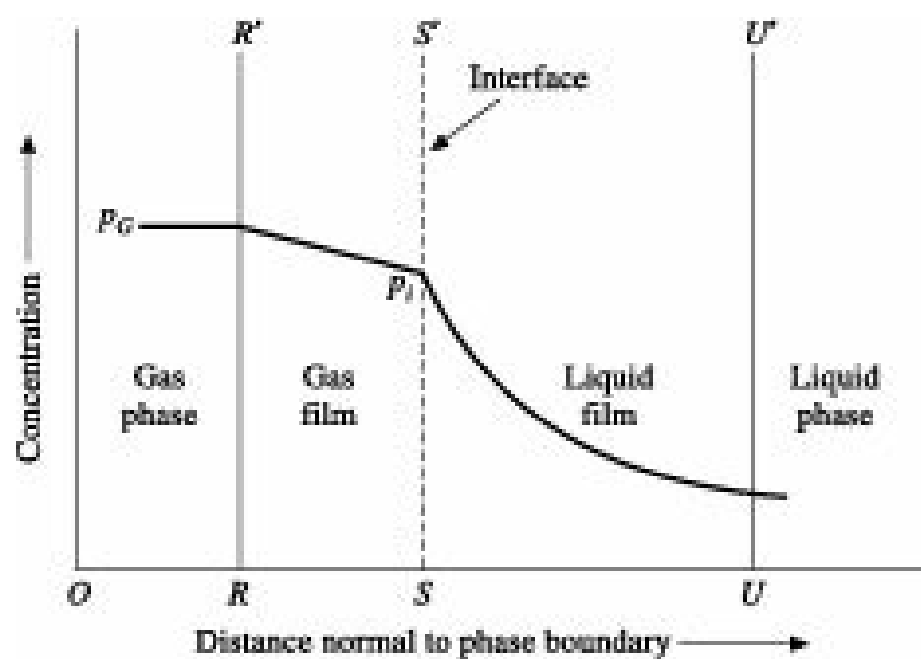


Figure 7.14 Concentration profile for absorption with slow chemical reaction.

The solute  $A$  diffuses through the gas film under the influence of the driving force ( $p_G - p_i$ ) as before. After crossing the interface, it starts diffusing through the liquid film towards the main body of the liquid but simultaneously reacts with  $B$ . Since the diffusing component is being depleted as it diffuses into the liquid, the concentration profile is concave upwards. Assuming the reaction to be first order and equating the difference in diffusion rates in and out of a differential element  $dx$  of the liquid film with the disappearance of  $A$  due to chemical reaction, Sherwood and Pigford (1952) had suggested the following equation based on the analysis of Hatta (1932):

$$c = \frac{c_L \sinh(a_0 x) + c_i \sinh[a_0(x_L - x)]}{\sinh(a_0 x_L)} \quad (7.42)$$

When  $c_L = 0$ , Eq. (7.42) reduces to

$$c = \frac{\sinh[a_0(x_L - x)]}{\sinh(a_0 x_L)} c_i \quad (7.43)$$

For the special case where the concentration of  $A$  in the bulk of the liquid is low,

$$N_A = \frac{b D_A (c_i - c_L)}{x_L} \quad (7.44)$$

$$\text{where, } b = \frac{a_0 x_L}{\tanh(a_0 x_L)} \quad (7.45)$$

The equation for overall resistance then becomes

$$\frac{1}{K_L} = \frac{x_L}{b D_A} + \frac{H}{k_G} \quad (7.46)$$

and the rate of diffusion is given by

$$N_A = \frac{\frac{c^* - c_L}{x_L} + \frac{H}{k_G}}{bD_A} \quad (7.47)$$

## 7.11 Reactive Absorption and Stripping

In the present scenario, reengineering of chemical process industries requires to be looked into carefully for process intensification which is defined as ‘any chemical engineering development that leads to a substantially smaller, cleaner and more energy efficient technology’ (Stankiewicz and Moulijn 2004). Reactive separation which can be viewed as integration of reaction and separation in a single step in single equipment may be considered to be a viable option. This would aim at smaller inventory, more compact plant and better energy management when the reaction and separation would not influence each other. However, such separations can also be beneficial when the reaction and separation influence each other. This may be attributed to the reason that a shift of reaction beyond equilibrium occurs leading to more product formation and *in situ* separation causing enhancement of separation efficiency by the chemical reaction. As a whole, such operation helps in enhancing the conversion in equilibrium limited reactions by shifting the equilibrium, preventing undesirable product formation thereby improving selectivity and increasing reaction rates for product inhibited reactions. This process would be discussed in respective chapters of phase separations. The present discussion is confined to reactive absorption/stripping.

In reactive absorption, reactions occur simultaneously with component transport and absorptive separation. This process is characterized by selective solubility of gas(es) in a liquid combined with chemical reactions. This can be achieved at a lower pressure compared to physical absorption process. The involvement of chemical reaction helps in shifting the equilibrium resulting in enhancement of solubility of the absorbed components. These processes are predominantly used for production of sulphuric acid and nitric acid and the removal of component gases and liquid streams. Some of the examples of reactive absorption are in chemical synthesis such as manufacture of sulphuric acid, preparation of formaldehyde, in coke oven gas purification by washing with amine solutions, in water removal from natural gas, in removal of  $\text{NO}_x$  from a gas stream by weak nitric acid solution, etc. The advantages of the process are increase in driving force for mass transfer caused by reaction in the liquid phase which reduces the equilibrium partial pressure of the solute over the solution, higher mass transfer coefficient due to higher interfacial area in stagnant regions, and a favourable equilibrium relationship for chemical absorption compared to physical absorption. The process has got also some limitations caused due to reaction stoichiometry in a region of low gas phase concentration, heat of reaction in exothermic reactions for solvent selection and regeneration. Reactive stripping used in production of bisphenol *A* promotes the condensation reaction by removing water formed by stripping it from the reaction zone using an inert gas leading to high phenol conversion. The process in monolithic reactors has been studied for esterification of octanol with hexanoic acid (Mueller et al. 2007).

## Nomenclature

*A* : Absorption factor, ( $L_M/mG_M$ ), —

$a$  : specific interfacial area of packings,  $\text{L}^2/\text{L}^3$

$c$  : concentration in liquid,  $\text{mol}/\text{L}^3$

$D$  : diffusivity,  $\text{L}^2/\text{q}$

$G_M$  : total gas flow rate,  $\text{mol}/\text{q}$ ,  $\text{mol}/\text{L}^2\text{q}$

$G'_M$  : flow rate of solute-free carrier gas,  $\text{mol}/\text{q}$ ,  $\text{mol}/\text{L}^2\text{q}$

$H$  : Henry's law constant

$H_tG, H_tL$  : height of gas-phase and liquid-phase transfer unit respectively,  $\text{L}$

$H_{toG}, H_{toL}$  : height of overall transfer unit based on concentration difference in terms of gas-phase and liquid-phase respectively,  $\text{L}$

$K$  : equilibrium constant,  $y^*/x$ , —

$K_x, K_y$  : overall mass transfer coefficient based on concentration difference in terms of liquid-phase and gas-phase respectively,  $\text{mol}/(\text{L}^2)(\text{q})(\text{mol fraction})$

$k_x, k_y$  : individual liquid-phase and gas-phase mass transfer coefficient respectively,  $\text{mol}/(\text{L}^2)(\text{q})(\text{mol fraction})$

$K_{Ga}$  : gas-phase volumetric mass transfer coefficient,  $\text{mol}/(\text{L}^3)(\text{q})(\text{mol}/\text{L}^3)$

$K_{La}$  : liquid-phase volumetric mass transfer coefficient,  $\text{mol}/(\text{L}^3)(\text{q})(\text{mol}/\text{L}^3)$

$L_M$  : total liquid flow rate,  $\text{mol}/\text{q}$ ,  $\text{mol}/\text{L}^2\text{q}$

$L'_M$  : flow rate of solute-free liquid,  $\text{mol}/\text{q}$ ,  $\text{mol}/\text{L}^2\text{q}$

$m$  : equilibrium constant,  $y^*/x$ , —

$N_tG, N_tL$  : number of gas-phase and liquid-phase transfer unit respectively, —

$N_{toG}, N_{toL}$  : number of overall transfer unit based on concentration difference in terms of gas-phase and liquid-phase respectively, —

$P$  : total pressure,  $\text{F}/\text{L}^2$

$p$  : vapour pressure,  $\text{F}/\text{L}^2$

$p'$  : partial pressure,  $\text{F}/\text{L}^2$

$q$  : driving force for diffusion of a component through liquid film to reaction zone

$X$  : mole ratio of solute to solute-free liquid

$x$  : mole fraction of solute in liquid

$Y$  : mole ratio of solute to solute-free gas

$y$  : mole fraction of solute in gas

$Z$  : height of packing in column,  $\text{L}$

$a, b, b'$  : constants

$t$  : density of liquid,  $\text{M}/\text{L}^3$

## Suffixes

A, B : refer to component A and B, respectively

1, 2 : refer to location 1 and 2, respectively

## Numerical Problems

**7.1** Estimation of Minimum Flow Rate of Liquid Absorbent Used for Separation of Butane and Propane from a Gas Mixture; Solubilities of Propane and Butane are to be Calculated Using Raoult's Law: Determine the minimum rate of flow of a liquid absorbent (molecular weight 224) needed to completely extract propane and butane from 1000 m<sup>3</sup>/hr of a gas mixture which contains 15% and 10% by volume of the two gases, respectively. The temperature in the absorber is 30 °C, and the total pressure is 294 kPa. The solubilities of butane and propane in the absorbent are characterized by Raoult's law. The saturated vapour pressures of propane and butane at 30°C are 981 and 265 kPa, respectively.

(Hints: the minimum rates of flow of absorbent required for absorption of propane and butane are to be found out separately, and the maximum of the two values thus obtained will be the minimum flow rate of absorbent.)

[Ans. 142 kmol/hr or 31800 kg/hr]

**7.2** Determination of the Rate of Solvent Required for Absorption of Benzene from a Coal Gas: A gas absorber has to be designed to handle 900 m<sup>3</sup>/hr of coal gas containing 2% benzene (by volume). Coal gas enters the absorber at a temperature of 300 K containing 0.005 mole fraction of benzene and has an average molecular weight of 260. Calculate the circulation rate of solvent per second if the column is to be operated at 1.5 times the minimum value.

The equilibrium relationship is given as

$$\frac{Y}{1+Y} = 0.125 \frac{X}{1+X}$$

where, Y and X are the mole ratios of benzene to dry gas and to solvent, respectively.

[Ans: 0.43 kg/s]

**7.3** Estimation of Concentration of NH<sub>3</sub> in Exit Liquid and Number of Stages Required for Scrubbing of NH<sub>3</sub> by Water: A counter-current plate absorber is to be installed for scrubbing of an air-ammonia mixture containing 5% ammonia by volume. The scrubber is fed with water containing 0.002 mole ammonia per mole of water. The scrubbing water flows at a rate of 1.0 mole water per mole of air. It is necessary to absorb 85% of the ammonia present in the gas by operating the absorption at 20°C.

$$K = 0.80 \frac{\text{mol NH}_3/\text{mol air}}{\text{mol NH}_3/\text{mol water}}$$

Calculate the (i) concentration of NH<sub>3</sub> in the outgoing liquid, and (ii) number of stages necessary for the operation. [Ans. (i) 0.0471 mol NH<sub>3</sub>/mol water, (ii) 3.98]

**7.4** Determination of Minimum Flow Rate of Steam and the Number of Theoretical Stages Required for Removal of Impurity from Cream Using Steam: A counter-current multistage stripper is used

to remove an impurity from a cream using pure steam. 100 kg/hr of liquid cream containing 20 parts per millions (ppm) by weight of impurity is fed to the stripper. It is desired to reduce the concentration of impurity in the cream to 1 ppm. Assume that the liquid cream does not evaporate and steam does not condense. The equilibrium relation is  $y = 10x$ , where  $y$  and  $x$  are the ppm of impurity in steam and cream, respectively.

(i) Determine the minimum flow rate of steam required

(ii) If the rate of steam input to the stripper is 1.5 times the minimum, determine the required integral number of theoretical stages

[Ans. (i) 14.25 kg/hr, (ii) 6]

**7.5 Determination of Minimum Liquid Rate and Number of Overall Gas-Phase Transfer Units in a Packed Tower:** Carbon dioxide coming out from a fermenter contains 0.02 mol fraction of ethanol which has to be reduced to 0.0002 mol fraction by scrubbing with water in a counter-current packed tower. The gas flow rate is 230 kmol/hr and may be assumed constant throughout the tower. The equilibrium mole fraction of ethanol in the gas phase,  $y^*$  is related to that in liquid,  $x$  as

$$y^* = 1.08x$$

Determine the (i) minimum liquid rate needed, and (ii) number of overall gas-side transfer units needed at 1.5 times the minimum liquid rate. The liquid may be assumed to be free from ethanol.

[Ans. (i) 261.12 kmol/hr, (ii) 5]

**7.6 Estimation of Height of Packing for Absorption of a Gas, Values of Individual Phase Mass Transfer Coefficients Being Given:** A counter-current packed tower is to be designed to recover 90% carbon tetrachloride from 800 kg/hr of an air-CCl<sub>4</sub> mixture containing 5 mol% CCl<sub>4</sub>. A nonvolatile CCl<sub>4</sub>-free organic oil (molecular weight = 260) is to be used as solvent and the solvent rate shall be twice the maximum. The tower will be operated at 30°C and 1 atm pressure. The equilibrium relation under the operating conditions is given by  $y^* = 20x$ , where  $y$  and  $x$  are mole fractions of CCl<sub>4</sub> in gas and liquid, respectively.

If the mass transfer coefficients  $k_x a$  and  $k_y a$  are 900 and 60 kmol/(hr)(m<sup>3</sup>)(mol fraction) respectively, determine the height of packing to be provided.

[Ans: 3.64 m]

**7.7 Estimation of Required Packing Height for Absorption of a Gas in a Counter-Current Packed Tower, the Value of the Overall Mass Transfer Coefficient Being Given:** An air-ammonia mixture containing 8 mol% NH<sub>3</sub> is to be scrubbed with water in a counter-current packed tower to remove 95% NH<sub>3</sub>. The gas rate at the inlet will be 3000 kg/hr m<sup>2</sup> and the water rate will be 2500 kg/hr m<sup>2</sup>. The tower will operate at 30°C and 1 atm pressure. The overall mass transfer coefficient is expected to be 70 kmol/hr m<sup>3</sup> atm. Equilibrium relation may be assumed to be  $y^* = 0.746x$ , where  $x$  and  $y$  are mole fractions of NH<sub>3</sub> in liquid and gas respectively. Estimate the required packed height of the tower. [Ans: 7.4 m]

**7.8 Determination of Height and Diameter of a Packed Tower used for Scrubbing of Acetone by Water, Overall Mass Transfer Coefficient Value Being Given:** A scrubber for absorbing acetone

vapour from air is irrigated with water at a rate of 3000 kg/hr. The mean temperature in the scrubber is 25°C. A mixture of air with acetone vapour containing 6% by volume of acetone is passed through the scrubber at 1 atm pressure. This mixture contains 1400 m<sup>3</sup>/hr of pure air. The scrubber absorbs 98% of the acetone. The equation for the equilibrium line is

$$Y^* = 1.68X$$

where  $X$  and  $Y^*$  are expressed in kmol of acetone per kmol of the second component.

Find the diameter and height of a scrubber packed with ceramic rings 25 # 25 # 3 mm in size (unit surface area and free volume of the packing are 204 m<sup>2</sup>/m<sup>3</sup> and 0.74 m<sup>3</sup>/m<sup>3</sup>, respectively). Assume that the velocity of the gas is 75% of the flooding velocity.

The overall coefficient of mass transfer is 0.4 kmol of acetone/[(m<sup>2</sup>) (hr) (kmol of acetone/kmol of air)]. Assume that the packing is wetted completely.

[Ans: Diameter: 0.675 m, Height: 16.8 m]

**7.9 Determination of Height of Packing and Diameter of the Square Packed Tower for Absorption of Sulphur Dioxide in Dilute Alkaline Solution using the Expression for Mass Transfer Coefficient:** 5000 m<sup>3</sup>/hr of air containing 1% of sulphur dioxide by volume is scrubbed at 20°C in order to reduce the concentration of sulphur dioxide to 0.01% before it is discharged to the atmosphere. A square tower packed with wood grids is to be used, and sulphur dioxide will be absorbed by circulating a dilute alkaline solution through the scrubber. It may be assumed that the absorption is gas-film controlled and the partial pressure of sulphur dioxide in equilibrium with the solution is zero. The surface of the packing per unit volume is 98 m<sup>2</sup>/m<sup>3</sup>. It may also be assumed that the coefficient,  $K_G$  in kmol/hr m<sup>2</sup> atm is given by the equation

$$K_G = 0.002G^{0.8}, G \text{ being the mass velocity of air in kg/m}^2 \text{ hr.}$$

Calculate the size of the tower and the height of packing used.

[Ans: Size of the tower: 0.745 m each side, Height of packing: 5.19 m]

**7.10 Estimation Of Minimum Water Flow Rate And Height of the Square Packed Tower for Absorption of Ammonia Using the Values of Diffusivities:** 5000 m<sup>3</sup>/hr air containing 2% ammonia is to be scrubbed using the tower as in Problem 7.9. The absorbing liquid water is available at 20 °C, and 98% of the ammonia is to be removed from the air. The equilibrium partial pressure of ammonia in dilute solutions at 20 °C is given by  $p = 0.76x$ ,  $x$  being the mole fraction of ammonia in solution. Following expression may be used:

$$(K_G)_{\text{NH}_3} = (K_G)_{\text{SO}_2} \left[ \frac{D_{\text{NH}_3-\text{air}}}{D_{\text{SO}_2-\text{air}}} \right]^{2/3}$$

Calculate the (i) theoretical minimum rate of water to be used, and (ii) height of packing when the water flow rate is 1.5 times the minimum.

[Ans: (i) 270.51 kmol/m<sup>2</sup> hr, (ii) 7.19 m]

**7.11 Estimation of Minimum Water Flow Rate, the Number of Transfer Units, and Height of Packed Bed for Absorption of Ammonia:** 1000 m<sup>3</sup>/hr m<sup>2</sup> of an air-ammonia mixture at standard

conditions, containing 6% NH<sub>3</sub> by volume is to be scrubbed with water in a counter-current packed tower to remove 98% NH<sub>3</sub>. The temperature will be kept constant at 20 °C and the pressure at 1 atm. The equilibrium relation is given by  $y^* = 0.746x$ , where  $x$  and  $y$  represent mole fractions of ammonia in water and air, respectively. The overall mass transfer coefficient has been estimated to be 70 kmol/hr m<sup>3</sup> atm. Calculate the minimum flow rate of water required for the operation. Also, find out the number of transfer units and height of the packed bed assuming the operation to be carried out with water flow rate 1.6 times the minimum.

[Ans: Minimum water flow rate: 587.5 kg/hr m<sup>2</sup>, No. of transfer unit: 7.516, Height of the packed bed: 4.8 m]

**7.12 Use of Expression for Overall Volumetric Mass Transfer Coefficient to Determine the Height of Packing for Chlorine-Caustic Soda Solution System:** A gas mixture containing 50% chlorine and 50% of air is to be treated with caustic soda solution to remove 99.5% of the chlorine. The gas flow rate measured at 15°C and 1 atm pressure is 113.3 m<sup>3</sup>/hr. The absorption will be carried out in a tower of 0.3 m diameter. It is assumed that the overall volumetric mass transfer coefficient,  $K_G a$  in kmol/hr m<sup>3</sup> atm varies in proportion to the drift factor as

$$K_G a = 0.12 \frac{P}{P'_{BM}} G^{0.8}$$

where,  $G$  is the mass velocity in kg/m<sup>2</sup> hr and  $p'_{BM}$  is the logarithmic-mean of the partial pressure of air in the gas ( $p_B$ ) and at the interface.

Calculate the height of the packing. [Ans: 1.1 m]

**7.13 Determination of Height of Packing Using Number of Transfer Units Obtained Analytically:** Using the data of Problem 7.10, calculate the number of transfer units analytically and the height of packing.

[Ans: No. of transfer unit: 4.91 ≈ 5, Height of packing: 1.25 m]

**7.14 Calculation of Height of Packing Using Individual Film Transfer Units:** Sulphur dioxide is manufactured by the combustion of sulphur in air, the burner gas is cooled and the sulphur dioxide is extracted by absorption in water. Pure sulphur dioxide is recovered by heating the solution and stripping with steam.

The burner gas contains 8% SO<sub>2</sub>, and 98% of it is to be recovered by absorption at 15 °C, and 1 atm pressure in a packed tower. The heights of the gas and liquid film transfer units are  $H_tG = 0.6$  m and  $H_tL = 0.6$  m. Calculate the height of packing for the following cases:

- (i) aqueous solution 70% saturated with SO<sub>2</sub>
- (ii) aqueous solution 90% saturated with SO<sub>2</sub>.

At 15°C, the equilibrium data for SO<sub>2</sub>-water system are as follows:

$x \# 10^3$  0.056 0.14 0.28 0.422 0.566 0.845 1.4 1.96 2.8 4.22 7.0

$y \# 10^3$  0.40 1.1 2.9 5.0 7.5 13.2 25.0 36.8 57.9 93.4 167.0

[Ans: (i) 6.19 m, (ii) 11.03 m]

**7.15 Estimation of Diameter and Height of a Plate Absorber for NH<sub>3</sub>-Water System:** Determine the diameter and height of a plate absorber for absorbing ammonia with water from an air-ammonia mixture at 1 atm pressure and a temperature of 20°C. The initial content of ammonia in the gas mixture is 7% (by volume). The absorption factor is 90%. The rate of flow of the inert gas (air) is 10,000 m<sup>3</sup>/hr under the operating conditions. Consider the equilibrium line to be straight, its equation in mass ratios is  $Y^* = 0.61X$ . The fictitious velocity of the gas in the absorber is 0.8 m/s. The distance between the plates is 0.6 m. The mean efficiency of the plates is 0.62. The excess absorbent coefficient (ratio of the actual and minimum flow rates of the absorbent) is 1.3.

[Ans: diameter = 2.15 m, height of the plate absorber = 5.4 m]

**7.16 Determination of Diameter of the Absorber and Concentration of Benzene in the Exit Liquid:** Benzene is absorbed at a rate of 300 kg/hr from a vapour-gas mixture in an absorber under 1 atm pressure at a temperature of 20°C. The initial content of the benzene vapour in the mixture is 4% (by volume). The absorption factor is 0.85. The liquid absorbent fed into the absorber after regeneration, contains 0.0015 kmol of benzene per kmol of absorbent. The fictitious velocity of the gas in the absorber is 0.9 m/s. The equation for the equilibrium line is  $Y^* = 0.2X$ , where  $Y^*$  and  $X$  are expressed in kmol of benzene/kmol of inert gas and kmol of benzene/kmol of absorbent, respectively. The actual liquid flow rate is 1.4 times the minimum liquid flow rate. Determine the diameter of the absorber and the concentration of benzene in the absorbent leaving the absorber.

[Ans: 1.03 m, 0.149 kmol of benzene/kmol of absorbent]

**7.17 Estimation of Rate of Flow of Water and Height of Packing for Absorption of Methyl Alcohol, the Value of Overall Mass Transfer Coefficient Being Given:** A packed absorber is used to absorb the vapour of methyl alcohol with water from a gas under 1 atm pressure and at a mean temperature of 27 °C. The content of the methyl alcohol in the gas fed into the scrubber is 100 g/m<sup>3</sup> of the inert gas (taking the volume of the gas in operating conditions). At the outlet from the scrubber, the water has a concentration of 67% of the maximum possible one, i.e. of the equilibrium one with the incoming gas. The equation of solubility of methyl alcohol in water in mole ratios is  $Y^* = 1.15X$ . The fraction of the initial amount of the alcohol absorbed by the water is 98%. The overall mass transfer coefficient,  $K_x = 0.5 \text{ kmol of alcohol}/(\text{m}^2)(\text{hr})$  (kmol of alcohol/kmol of water). The rate of flow of inert gas is 1200 m<sup>3</sup>/hr under the operating conditions. The absorber is filled with ceramic ring packing having a unit surface area of 190 m<sup>2</sup>/m<sup>3</sup>. The coefficient of wetting of the packing is 0.87. The fictitious velocity of the gas in the absorber is 0.4 m/s. Determine the rate of flow of water and the required height of the packing.

[Ans: 1475 kg/hr, 7.2 m]

**7.18 Estimation of the Mass Flow Rate of the Absorbent, Diameter of the Tower and Height of Packing using the Value of HTU, and Height of the Absorber When it is Plate Type:** An absorber for removing benzene vapour from a vapour and gas mixture is irrigated with absorbing oil having a mass of 260. The mean pressure in the absorber is 800 mm Hg, and the temperature is 40 °C. The rate of flow of the vapour-gas mixture is 3600 m<sup>3</sup>/hr under the operating conditions. The concentration of benzene in the gas mixture at the inlet to the absorber is 2% (by volume), and 95% of the benzene is absorbed. The benzene content in the absorbing oil entering the absorber

after regeneration is 0.2 mol%. The rate of flow of the absorbing oil is 1.5 times higher than the minimum value. To calculate the equilibrium compositions, assume that the solubility of benzene in the oil is determined by Raoult's law. Consider that the equilibrium relationship  $Y^* = f(X)$  is linear at benzene concentrations in the liquid up to  $X = 0.1$  kmol per kmol of oil. Determine (i) the rate of flow of the absorbing oil in kg/hr, (ii) the concentration of benzene in the absorbing oil leaving the absorber, (iii) the diameter and height of an absorber if it is a packed bed, for a fictitious velocity of the gas in it of 0.5 m/s and a transfer unit height (HTU) of 0.9 m, and (iv) the height of the absorber if it is a plate type, for a mean plate efficiency of 0.67 and a plate spacing of 0.4 m.

[Ans: (i)  $12.3 \times 10^3$  kg/hr, (ii) 0.0611 kmol benzene/kmol oil, (iii) Diameter = 1.59 m and Height of packing = 7.02 m, (iv) 4.0 m]

**7.19 Estimation of Percentage Increase in Tower Height if the Extent of Absorption of a Gas be Higher in a Counter-Current Packed Column:** 1000 m<sup>3</sup>/hr of an air-benzene mixture at 26.6 °C and 1 atm pressure, containing 6 mol% benzene vapour, is being scrubbed with 1500 kg/hr of a benzene-free hydrocarbon oil (molecular weight = 260) in a packed tower. Under the operating conditions, 90% of the incoming benzene is absorbed.

Assuming all the operating conditions to remain unchanged, how much taller the tower should be to absorb 98% benzene?

Raoult's law holds good for the system. The vapour pressure of benzene at 26.6°C is 100 mm Hg.

[Ans: 124.5%]

### ***Short and Multiple Choice Questions***

1. How are the solute contents of incoming gas and outgoing liquor related in a counter-current absorption tower when operated at minimum solvent rate?
2. What is flooding velocity? What role does it play in the design of counter-current absorption towers? How would you determine the tower diameter during such absorption?
3. How is the chance of flooding in a counter-current absorption column affected by increasing gas pressure drop?
4. Why should a good solvent for gas absorption have low vapour pressure and low viscosity?
5. What will happen if absorption factor in an absorption operation is less than unity?
6. How should the ratio ( $L/G$ ) in a counter-current absorption operation be changed in order to increase absorption factor?
7. What is the most economical range of absorption factor?
8. What are NTU and HTU? What are their major advantages?
9. Under which conditions logarithmic mean driving force may be used for estimation of NTU?
10. Why is the ratio ( $G_M/K_y a$ ) more reliable than either  $G_M$  or  $K_y a$ ?
11. In an absorber, both equilibrium and operating lines may be straight for
  - (a) concentrated solution and nonisothermal operation
  - (b) dilute solution and nonisothermal operation
  - (c) concentrated solution and isothermal operation

(d) dilute solution and isothermal operation

**12.** Absorption factor is defined as

- |     |   |     |   |
|-----|---|-----|---|
| (a) | $\frac{\text{slope of equilibrium line}}{\text{slope of operating line}}$ | (b) | $\frac{\text{slope of operating line}}{\text{slope of equilibrium line}}$ |
|-----|---|-----|---|

- (c) (slope of operating line) # (slope of equilibrium line)  
(d) (slope of operating line) - (slope of equilibrium line)

**13.** Minimum liquid rate to be used in a counter-current absorption tower corresponds to an operating line

- (a) having a slope of unity  
(b) having a slope of 0.1  
(c) tangential to the equilibrium curve  
(d) none of these

**14.** Slope of the operating line for an absorber is given by

- (a)  $L'/G'$  (b)  $G'/L'$  (c) always  $< 1$  (d) none of these

where,  $G'$  = insoluble gas in the gas stream, and  $L'$  = nonvolatile solvent in the liquid stream.

**15.** Operating gas velocity in a counter-current packed absorption tower as compared with flooding velocity is nearly

- (a) half (b) twice (c) equal to (d) more than

**16.** In a co-current packed absorption tower, the slope of the operating line is

- (a) negative (b) positive (c) unity (d) uncertain

**17.** Very tall packed towers are divided into a number of beds in order to

- (a) reduce the overall pressure drop  
(b) avoid channeling  
(c) reduce liquid hold-up  
(d) all these

**18.** Absorption accompanied by heat evolution results in

- (a) increase in capacity of the absorber  
(b) increase in equilibrium solubility  
(c) decrease in equilibrium solubility  
(d) none of these

**19.** Co-current absorbers are usually used when the gas to be dissolved in the liquid is

- (a) sparingly soluble (b) highly soluble  
(c) a pure substance (d) none of these

**20.** In a counter-current packed absorption column, flooding results in

- (a) low efficiency (b) high efficiency  
(c) high gas velocity (d) none of these

**21.** In a counter-current packed absorption column, as the liquid flow rate is reduced for a given gas flow, the slope of the operating line

- (a) remains constant (b) increases  
(c) decreases (d) cannot be predicted

**22.** In an absorption tower, overall HTU's ( $H_{t0G}$  and  $H_{t0L}$ ) are constant for

- (a) constant slope of equilibrium curve
- (b) constant molal velocities of gas and liquid based on total tower cross section
- (c) constant individual mass transfer co-efficients ( $k_x, k_y$ )
- (d) all of these

**23.** For absorption of highly soluble gases

- (a) the slope of the equilibrium curve is large
- (b) at equilibrium, a low gas concentration corresponds to a high liquid concentration
- (c) gas phase resistance is said to control
- (d) all of these

**24.** Low viscosity of solvent is preferred for gas absorption because of

- (a) rapid absorption rate (b) improved flow characteristics
- (c) low pressure drop on pumping (d) all of these

**25.** In a gas absorber, HETP does not vary with

- (a) liquid flow rate (b) gas flow rate
- (c) type and size of packing (d) none of these

**26.** For absorbing a sparingly soluble gas in a liquid, the

- (a) gas-side coefficient should be increased
- (b) liquid-side coefficient should be increased
- (c) gas-side coefficient should be decreased
- (d) liquid-side coefficient should be decreased

**27.** Desirable value of absorption factor in a gas absorber is

- (a) 1 (b) < 1 (c) > 1 (d) 0.5

**28.** The overall mass transfer coefficient for absorption of  $\text{SO}_2$  from air with dilute sodium hydroxide solution can be substantially increased by

- (a) increasing the gas film coefficient
- (b) increasing the liquid film coefficient
- (c) increasing the total pressure
- (d) decreasing the total pressure

**29.** With increase in solvent rate in gas absorption, the number of transfer units for a fixed degree of absorption

- (a) increases (b) decreases
- (c) decreases linearly (d) remains unaffected

**30.** Stripping factor is defined as

- (a) the ratio of the slope of the operating line to that of the equilibrium line
- (b) the ratio of the slope of the equilibrium line to that of the operating line
- (c) the product of the slopes of the operating and equilibrium lines

*Answers to Multiple Choice Questions*

- 11. (d) 12. (b) 13. (c) 14. (a) 15. (a) 16. (a)
- 17. (b) 18. (c) 19. (c) 20. (c) 21. (c) 22. (c)
- 23. (d) 24. (d) 25. (d) 26. (b) 27. (c) 28. (a)

29. (b) 30. (b)

## References

- Baker, T.C., *Ind. Eng. Chem.*, **27**, 977 (1935).
- Bhakta, C.D., A.I. Shaikh and Y.N. Patel, *Chem. Eng. Digest*, **XIX**(3), 67 (2006).
- Chilton, T.H. and A.P. Colburn, *Ind. Eng. Chem.*, **27**, 235 (1935).
- Colburn, A.P., *Trans. AIChE.*, **35**, 211 (1939).
- Colburn, A.P., *Ind. Eng. Chem.*, **33**, 111 (1941).
- Coulson, J.M. and J.F. Richardson, *Chemical Engineering*, vol. 2, 4th ed., Butterworth Heinemann, Oxford (1991), Asian Ed. (1998).
- Hatta, S., *Tech. Rep.*, Tohoku Imp. Univ., **10**, 119 (1932).
- Mueller, I., T.J.C. Schildhauer, A. Madrane, F. Kapteijn, J.A. Moulijn and E.Y. Kenig, *Ind. Eng. Chem. Res.*, **46**, 4149 (2007).
- Othmer, D.P., R.C. Kollman and R.E. White, *Ind. Eng. Chem.*, **36**, 963 (1944); **51**, 89 (1959).
- Pray, H.A., C.C. Schweickert and B.H. Minnich, *Ind. Eng. Chem.*, **44**, 1146 (1952).
- Sherwood, T.K. and R.L. Pigford, *Absorption and Extraction*, 2nd ed., McGraw-Hill, New York (1952).
- Souders, M. and G.G. Brown, *Ind. Eng. Chem.*, **24**, 519 (1932).
- Stankiewicz, J. and J.A. Moulijn, *Re-engineering the Chemical Process Plant Process Intensification*, CRC Press (2004).
- Treybal, R.E., *Mass Transfer Operations*, 3rd ed., McGraw-Hill, Singapore (1985).



# 8

# Distillation

## 8.1 Introduction

Distillation is a unit operation in which vaporisation of a liquid mixture yields a vapour phase containing more than one component and it is desired to recover one or more of them in nearly pure state. Separation by distillation primarily depends on the difference in volatilities of the components to be separated. The basic requirement of distillation is that the composition of the vapour should be different from that of the liquid with which it is in equilibrium. In distillation, except some special types like azeotropic, extractive or steam distillation, no foreign substance is added to the mixture to cause separation as a result of which the separated components are obtained in relatively pure form. Although distillation appears to be similar to evaporation, these two operations are basically different. For instance, in evaporation the vapour contains only one component while in distillation the same contains at least two components. In evaporation, a volatile component is separated from a nonvolatile one while in distillation all the components are volatile but their volatilities are different. The concentration of glycerine from dilute aqueous solution provides an excellent example of the difference between these two operations. During concentration of glycerine from dilute solution, up to 80% glycerine, a single component, namely, water is present in the vapour phase and the operation is therefore evaporation. Beyond 80% glycerine, the operation is distillation since both water and glycerine appear in the vapour phase.

Since separation of the components of a liquid mixture by distillation largely depends on vapour-liquid equilibrium, i.e. distribution of the components between the liquid and the vapour streams at equilibrium, we shall briefly recapitulate the relevant vapour-liquid equilibrium relations.

## 8.2 Vapour–Liquid Equilibrium

Boiling point diagrams provide primary data for vapour-liquid equilibrium. Only in a very few cases, reliable vapour-liquid equilibrium data are available in the literature for the exact operating conditions under which commercial distillation has to be carried out. Boiling point diagrams are, therefore, mostly constructed from experimental data. The basic principle involved in measurement of vapour-liquid equilibrium data is continuous vaporisation of a liquid mixture containing the components in a boiling flask or still, condensing all the vapour generated and recycling the condensate to the boiling flask or still till there is no further change in composition on continuing heating. Samples are then drawn from the still and the condensate receiver, and analysed to give the composition of the liquid ( $x$ ) in equilibrium with that of the vapour ( $y^*$ ). This gives one set of data. Several such data points are collected by repeating the experiment with different liquid compositions. Several types of experimental set-up have been used for measuring vapour-liquid equilibrium data. A simple experimental set-up using the ‘Othmer Still’ for vaporising the liquid mixture, has been widely

used for a pretty long period. It works according to the principle described above. Establishment of equilibrium is confirmed by the constant reading of the thermometer measuring the temperature of the boiling liquid. The main drawbacks of this method are chances of overheating which may lead to error in determining the boiling point and heat loss due to condensation before entering the condenser. Various modifications of the Othmer still method have been proposed from time to time. Amongst these, the modified Gillespie method (Yuan et al. 1963) gives fairly accurate results and is almost free from the above drawbacks. In this method, the liquid mixture is taken in a still, which is provided with an internal heating coil within a glass sheath. The vapour-liquid mixture generated here enters an equilibrium chamber where the liquid and vapour phases get separated and attain equilibrium. The liquid then flows to the liquid receiver and the vapour flows to the condenser from where it is collected.

Vapour-liquid equilibrium data may be represented both at constant pressure and constant temperature.

### 8.2.1 Vapour–Liquid Equilibrium at Constant Pressure

Figure 8.1 shows the vapour-liquid equilibrium diagram ( $T$ - $x$ - $y$ ) for a binary mixture of compounds  $A$  and  $B$ ,  $A$  being more volatile. In this diagram, commonly known as the boiling

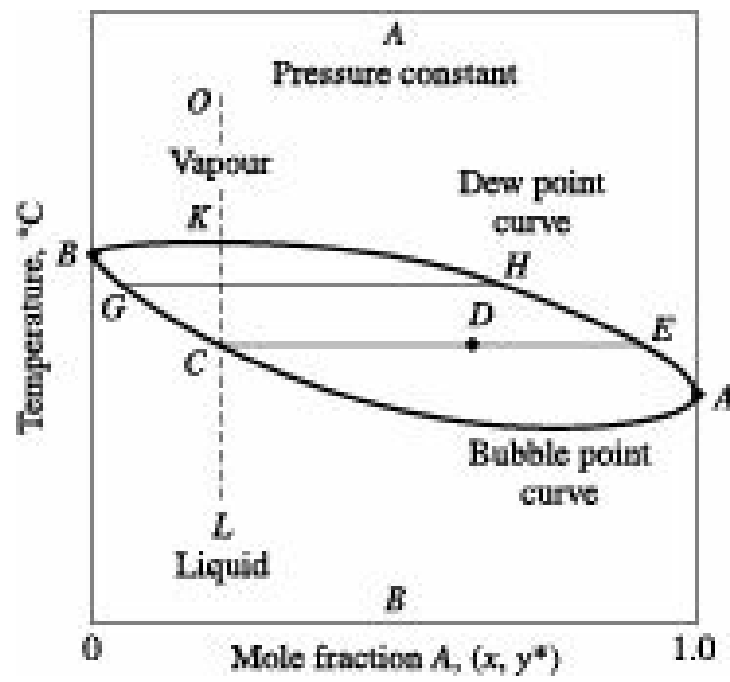


Figure 8.1 Boiling point diagram at constant pressure.

point diagram, mole fractions of  $A$  and  $B$  are plotted along the abscissa and temperature is plotted along the ordinate. The lower curve joining the two boiling points is obtained by plotting the boiling temperature against liquid composition ( $x$ ) and is known as the bubble point curve. The upper curve, obtained by plotting temperature against equilibrium vapour composition ( $y^*$ ) is the dew point curve. The region above the dew point curve consists of only vapour while the region below the bubble point curve consists of only liquid. The region enclosed by these two curves is two-phase region. Liquid and vapour mixtures at equilibrium being at the same temperature and pressure throughout, the tie lines are horizontal.  $CE$  is a tie line joining equilibrium mixtures at  $C$  and  $E$ . There are infinite numbers of such tie lines. The point  $C$  on the lower curve is a saturated liquid, while the point  $E$  on the upper curve is a saturated vapour. A point such as  $D$  represents a two-phase mixture; the relative

amount of the two may be determined by the inverse arm rule as below:

$$\frac{\text{Moles of } C}{\text{Moles of } E} = \frac{DE}{CD}$$

Let us consider a solution at  $L$  in a closed container which can be kept at a constant pressure with the help of a piston. If the solution, assumed to be entirely liquid at the beginning is heated, the first bubble of vapour forms at  $C$  having the composition  $E$  richer in the more volatile component. Hence the lower curve has been termed the bubble point curve. The last drop vaporises at  $K$ . From  $K$  to  $O$ , the vapour is being superheated.

It may be noted that the mixture has been vaporised over a range of temperature between the bubble point and dew point curves, and not at a definite temperature. If the mixture at  $O$  is cooled, the entire process is reversed. Condensation starts at  $K$  on the upper curve which is therefore termed the dew point curve.

Boiling point diagrams as such are not used in distillation calculations. But equilibrium distribution ( $x$  vs  $y^*$ ) curves as shown in Figure 8.2 are generally used for the purpose. Equilibrium curves may be drawn from boiling point diagrams by drawing several tie lines between the bubble point curve and the dew point curve of the boiling point diagram and noting the values of  $x$  and  $y^*$  which are equilibrium values.

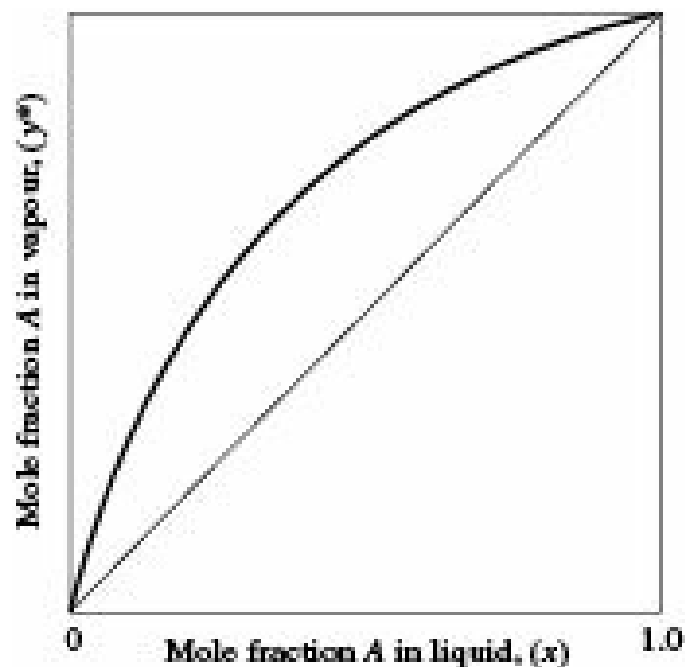
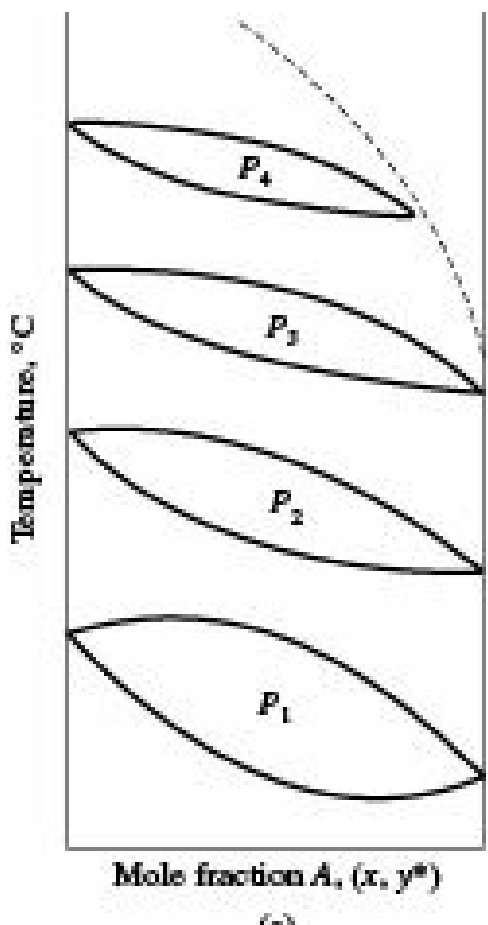
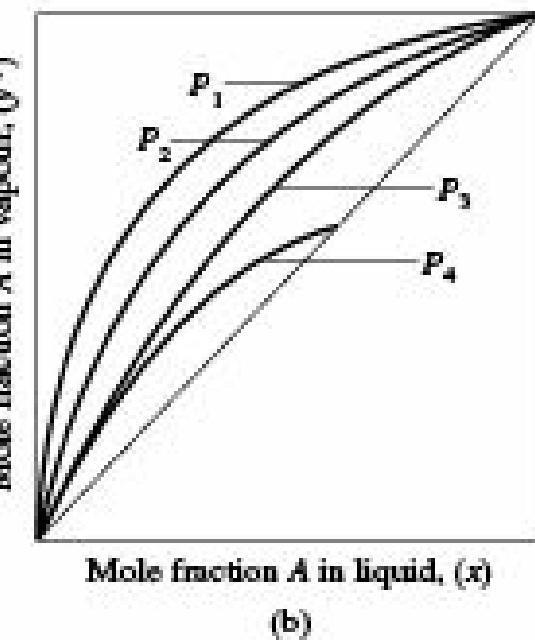


Figure 8.2 Vapour-liquid equilibrium curve.

As the total pressure is increased, the looped curves of Figure 8.1 move to higher temperatures and become closer to each other as may be seen from Figure 8.3(a). This may also be noted from the  $y$ - $x$  diagram shown in Figure 8.3(b).



(a)



(b)

Figure 8.3 Vapour-liquid equilibria at higher pressure.

### 8.2.2 Vapour–Liquid Equilibrium at Constant Temperature

A typical constant temperature vapour-liquid equilibrium curve is shown in Figure 8.4.

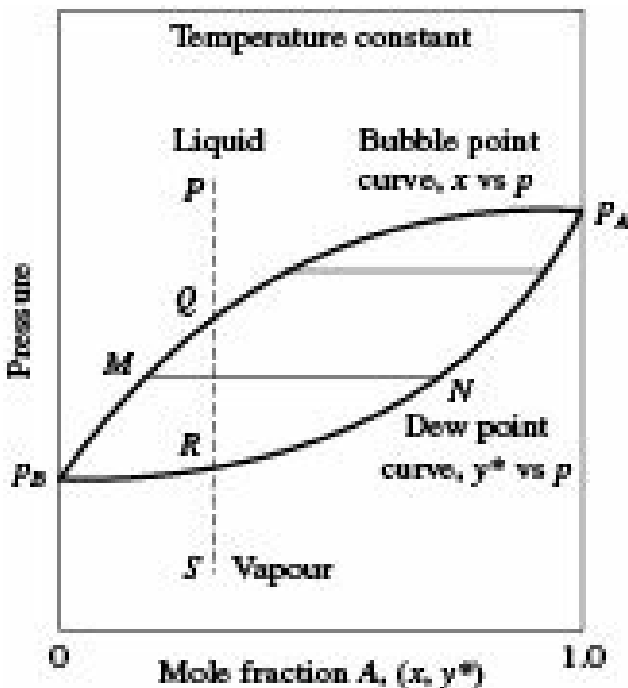


Figure 8.4 Vapour-liquid equilibria at constant temperature.

As in case of constant pressure equilibrium, the bubble point curve and the dew point curve extend from the vapour pressure of pure  $B$  to that of pure  $A$ , but interchange their positions. As before, there are infinite numbers of horizontal tie lines such as  $MN$  which join an equilibrium vapour composition as at  $N$  to its corresponding liquid composition at  $M$ . A solution in a closed container at  $P$  is entirely

liquid and if the pressure is reduced at constant temperature, the first bubble is found at *Q*, complete vaporisation occurs at *R* and further reduction in pressure results in superheated vapour at *S*.

### 8.2.3 Raoult's Law

Raoult's law applies to ideal solutions in which the components are chemically similar and their molecules do not interact mutually. The criteria of ideal solutions have been discussed in Section 7.2. Benzene-toluene mixture obey Raoult's law whereas alcohol-water mixture do not.

Raoult's law states that at constant temperature the partial pressure of a component in solution is equal to its mole fraction in the liquid multiplied by the vapour pressure of the pure component at that temperature.

According to this law,

$$p'_A = p_A x_A \quad (8.1)$$

and for a binary system,

$$p'_B = p_B x_B = p_B (1 - x_A) \quad (8.2)$$

If the vapour phase obeys ideal gas law

$$P = p'_A + p'_B = p_A x_A + p_B (1 - x_A) \quad (8.3)$$

where,

$P$  = total pressure

$p_A$  and  $p_B$  = vapour pressures of components *A* and *B*, respectively

$p'_A$  and  $p'_B$  = partial pressures of components *A* and *B*, respectively.

### Relative volatility

For a vapour phase in equilibrium with a liquid phase, relative volatility is defined as

$$\alpha_{AB} = \frac{y_A/x_A}{y_B/x_B} \quad (8.4)$$

where,

$\alpha_{AB}$  is the relative volatility of *A* with respect to *B*.

For a binary system,  $x_B = (1 - x_A)$  and  $y_B = (1 - y_A)$ .

Therefore, Eq. (8.4) may be rewritten, by dropping the suffixes, as

$$\alpha_{AB} = \frac{y^*/(1 - y^*)}{x/(1 - x)} \quad (8.5)$$

By rearranging Eq. (8.5), we get

$$y^* = \frac{\alpha_{AB} \cdot x}{1 + (\alpha_{AB} - 1)x} \quad (8.6)$$

Equation (8.6) is useful in constructing equilibrium curve from a knowledge of relative volatility of the concerned components.

### 8.2.4 Positive Deviation from Ideality

A mixture whose total pressure is higher than that computed from Raoult's law [Eq. (8.1)] is said to have positive deviation from Raoult's law. In such a case, the partial pressure of each component is larger than the ideal value as shown in Figure 8.5. The ratio of the actual equilibrium partial pressure ( $p'^*$ ) of the component to the ideal value ( $p'x$ ) is the activity coefficient of the pure substance,  $c = (p'^*/p'x)$ .  $c$  being greater than unity in these cases and  $\log c$  being positive, the deviation is called positive deviation.

It may be noted from Figure 8.5 that as the mole fraction of the component approaches unity, its partial pressure approaches ideality tangentially. In other words, Raoult's law is nearly applicable to the substances present in high concentration. This is true for all substances except where association in the vapour or electrolytic dissociation in the liquid occurs.

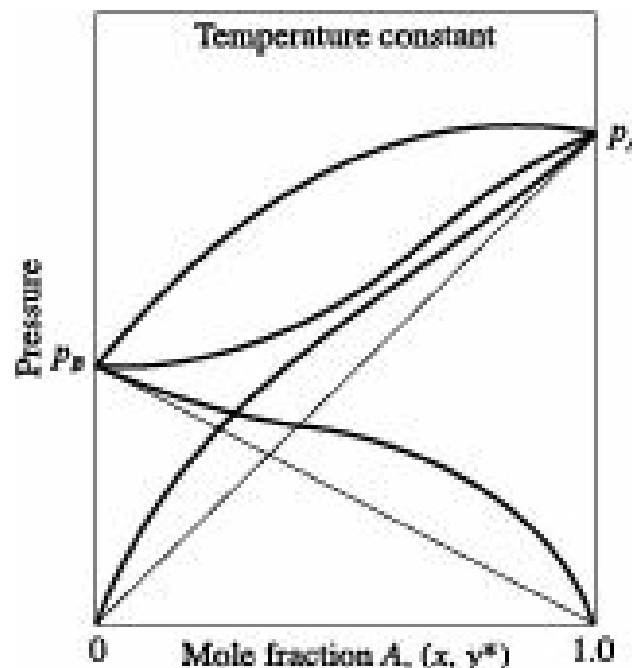


Figure 8.5 Positive deviation from ideality.

### **Minimum boiling mixture**

When positive deviation from ideality is very large and the vapour pressures of the two components are close to each other, then the total pressure curve at constant temperature may pass through a maximum. Such a mixture is called a *constant boiling mixture* or an *azeotrope*.

The situation becomes much more clear from a study of the vapour-liquid equilibrium curve at constant pressure as shown in Figure 8.6 where the bubble point curve and the dew point curve become tangent at a point  $M$  which represents the minimum boiling temperature. Figure 8.7 further shows that at the point  $M$  the equilibrium curve intersects the diagonal. At this point, the liquid and vapour compositions become the same and they cannot further be separated by ordinary distillation.

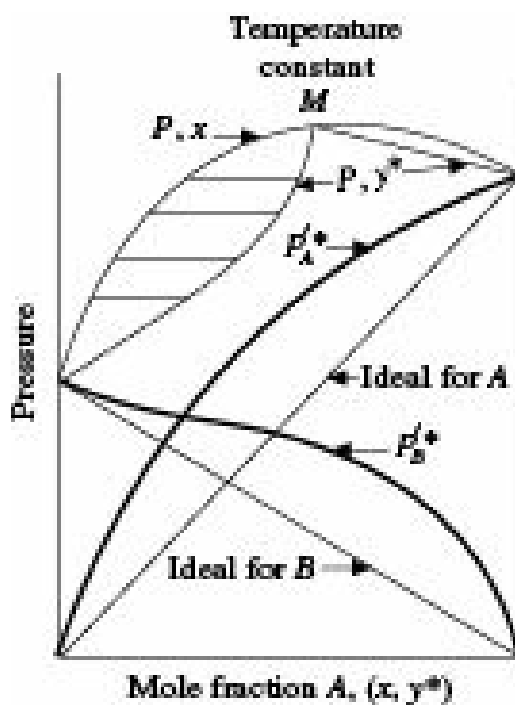


Figure 8.6 Minimum boiling azeotrope at constant temperature.

Azeotropic mixtures of this type are very common and a large number of such mixtures have been recorded (Horsley 1973). A most important example of this category is ethanol-water azeotrope which at 1 atm pressure occurs at 89.4 mol% ethanol at 78.2°C. This mixture is commonly known as *rectified spirit*. Higher concentrations of ethanol can be obtained by azeotropic distillation. The system carbon disulphide-acetone is another example of minimum boiling azeotrope.

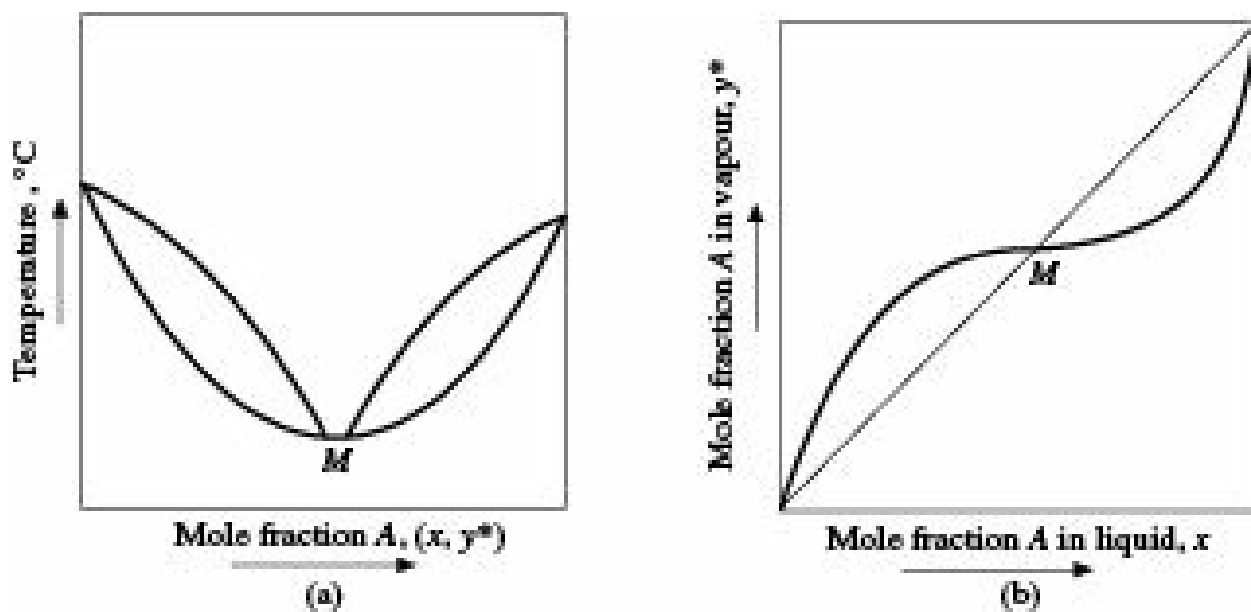


Figure 8.7 Minimum boiling azeotrope at constant pressure: (a) Boiling point diagram, (b) Equilibrium distribution curve.

### 8.2.5 Negative Deviation from Ideality

If the total pressure of a vapour-liquid system at equilibrium is less than that predicted by Raoult's law, the system is said to have negative deviation from Raoult's law. Such a situation at constant temperature is shown in Figure 8.8.

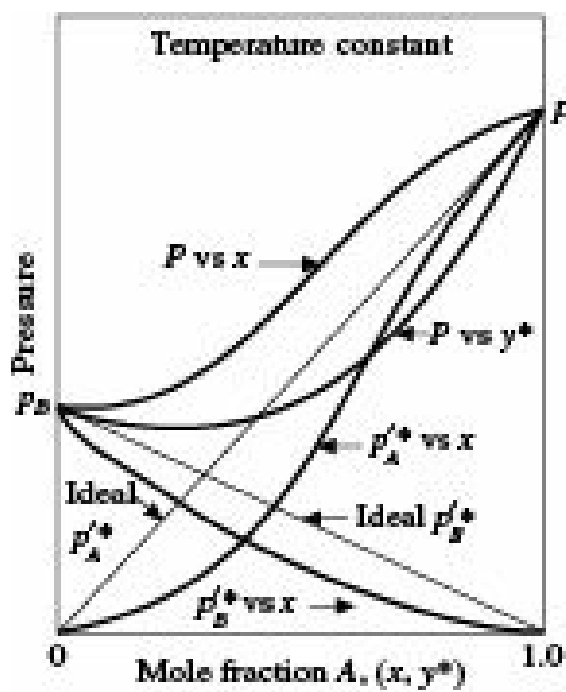


Figure 8.8 Negative deviation from ideality.

As in case of positive deviation from Raoult's law, in this case also the partial pressures of the solutes in the solution approach ideality as their mole fractions in the solution approach unity subject to the conditions of absence of association in vapour and electrolytic dissociation in liquid.

### Maximum boiling mixture

When the deviation from ideality is very large and the vapour pressures of the components are close to each other, the curve for total pressure against composition may pass through a minimum. This condition leads to a maximum in the boiling temperature as is evident from Figures 8.9(a) and 8.9(b). The equilibrium vapour is leaner in the more volatile component for liquid having solute concentration less than the azeotropic concentration. On the other hand, the equilibrium vapour will be richer in the more volatile component when its concentration in the liquid is higher than the azeotropic concentration. The system acetone-chloroform is an example of maximum boiling azeotrope.

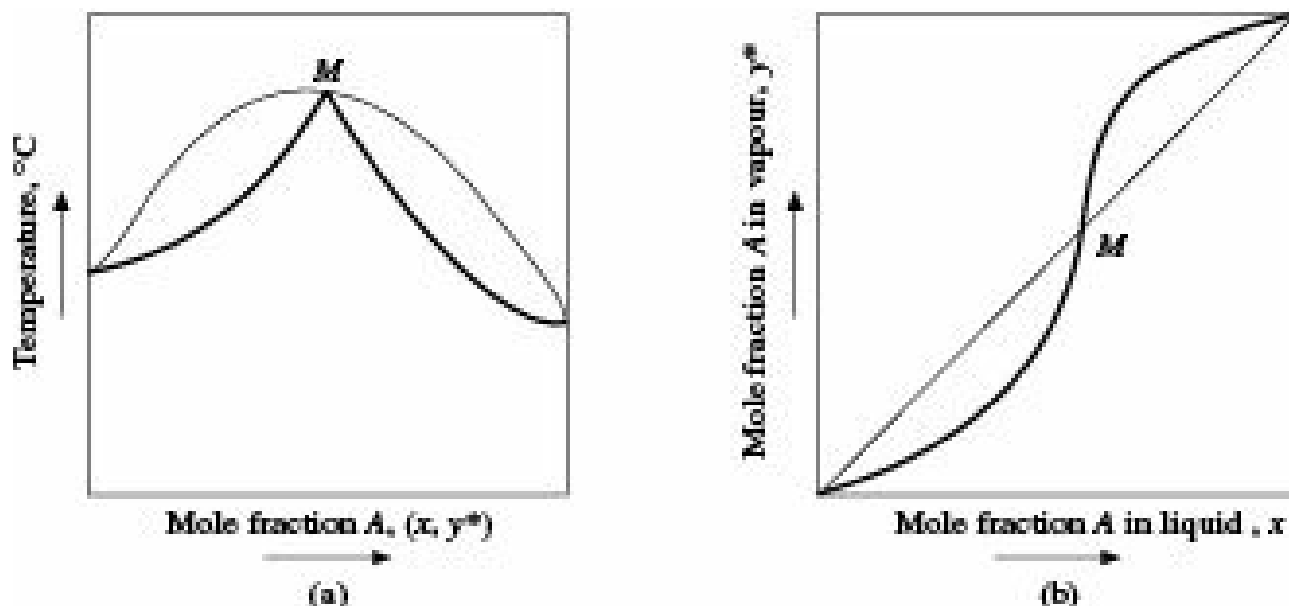


Figure 8.9 Maximum boiling azeotrope at constant pressure: (a) Boiling point diagram, (b) Equilibrium distribution curve.

Maximum boiling azeotropes are less common than the minimum boiling ones. A very well known

example of maximum boiling azeotrope is hydrochloric acid-water (11.1% HCl at 110°C and 1 atmosphere pressure).

Substances, which have minimum or maximum boiling points, are called *constant boiling mixtures* or *azeotropes*. These cannot be separated by ordinary methods of distillation beyond the compositions at which azeotropes are formed since at these points the liquid and vapour compositions become identical. Although very minor adjustment can be made by changing the total pressure, these substances are usually separated by azeotropic or extractive distillation in which a third component is added to break the azeotrope.

### 8.3 Prediction of Equilibrium Data

Experimental values of vapour-liquid equilibrium data, wherever available, should be used for design and other calculations since they are quite reliable. Where such data are not available, vapour liquid equilibrium may be predicted by using one of the following equations as applicable:

For systems that obey both Raoult's law and ideal gas law, equilibrium data may be predicted from Eqs. (8.1) to (8.3). Equation (8.3) indicates that the total pressure is linear function of liquid composition. The relation between  $x$  and  $y$  for a binary system may be expressed as

$$y_A^* = \frac{P_A'}{P} = \frac{P_A x_A}{P} \quad (8.7a)$$

and

$$y_B^* = \frac{P_B'}{P} = \frac{P_B(1 - x_A)}{P} = (1 - y_A) \quad (8.7b)$$

Values of vapour pressures for use in Eqs. (8.1) to (8.3) for calculation of equilibrium vapour composition as well as bubble point and dew point data, if not available in the literature, may be calculated from Antoine equation as given below:

$$\ln p_A = A' - \frac{B'}{C' + T} \quad (8.8)$$

where,

$p_A$  = vapour pressure of component  $A$  in mm Hg,

$T$  = temperature in °C,

$A'$ ,  $B'$ ,  $C'$  = Antoine constants.

The values of the constants  $A'$ ,  $B'$ ,  $C'$  for a few common substances are given in Table 8.1.

**Table 8.1** Constants for the Antoine Equation (vapour pressure relation)

Substances	BP, °C	$A'$	$B'$	$C'$
Acetaldehyde	20.5	16.6006	2532.41	234
Acetic acid	118	18.47233	4457.83	258.46
Acetone	56.2	16.39112	2787.50	229.67
Ammonia	-33.4	17.51202	2363.24	250.54
Aniline	184.5	16.67784	3858.22	200
Benzene	80	15.9037	2789.01	220.79
<i>n</i> -Butanol	117.6	17.62995	3367.12	188.7
Butyl acetate	126	16.4145	3293.66	210.75

Carbon disulphide	46	15.77889	2585.12	236.46
Carbon tetrachloride	76.5	15.8434	2790.78	226.46
Chlorobenzene	131.5	16.4	3485.35	224.87
Chloroform	61.2	16.017	2696.25	226.24
Cyclohexane	80.5	15.7794	2778.00	223.14
Cyclopentane	49.2	15.8602	2589.20	231.36
Diethyl ether	34.5	16.5414	2847.72	253
Ethanol	78.3	18.68233	3667.70	226.1
Ethyl acetate	77	16.35578	2866.60	217.9
Ethylamine	16.5	7.3862	1137.30	235.85
Formic acid	100.5	15.9938	2982.45	218
Furfural	162	15.14517	2760.09	162.8
<i>n</i> -Heptane	98.5	15.877	2911.32	226.65
<i>n</i> -Hexane	69	15.9155	2738.42	226.2
Methanol	64.5	18.61042	3392.57	230
Methyl acetate	57	16.58646	2839.21	228
Nitrobenzene	131.5	16.42172	3485.35	224.84
Nitrogen	-195.8	15.3673	648.59	270.02
Oxygen	-183	15.06244	674.59	263.07
<i>n</i> -Pentane	36	15.8365	2477.07	233.21
Phenol	180	15.9614	3183.67	159.5
Propane	-42	15.7277	1872.82	250
Pyridine	115	16.1520	3124.45	212.66
Styrene	135	15.94618	3270.26	206
Toluene	110.6	16.00531	3090.78	219.14
<i>o</i> -Xylene	134.5	7.00154	1476.393	213.872
<i>p</i> -Xylene	129.2	6.99052	1453.430	215.307
Water	100	18.5882	3984.92	233.43

For systems that obey Raoult's law but do not obey ideal gas law, Raoult's law may be expressed in terms of fugacity

$$f_A = f_A^0 x_A \quad (8.9)$$

where

$f_A^0$  = fugacity of the pure component *A*

$f_A$  = partial molal fugacity of component *A*.

whence,

$$x_A = \frac{f_A}{f} = a_A \quad (8.10)$$

$$x_B = \frac{f_B}{f} = a_B \quad (8.11)$$

where, *a* is the activity. The ratio (*a/x*) is the activity coefficient (*c*).

For ideal gases:

$$c_A = c_B = 1.$$

Vapour-liquid equilibrium data for non-ideal mixtures may be predicted by Gibbs-Duhem equation:

$$\left( \frac{\partial \ln f_A}{\partial x_A} \right)_{T,P} = x_B \left( \frac{\partial \ln f_B}{\partial x_B} \right)_{T,P} \quad (8.12)$$

An integrated form of Eq. (8.12), known as *van Laar equation* is useful in determining the activity coefficient for prediction of equilibrium data.

$$\log c_A = \frac{A_{AB}}{(1 + A_{AB}x_A/A_{BA}x_B)^2} \quad (8.13)$$

$$\log c_B = \frac{A_{BA}}{(1 + A_{BA}x_B/A_{AB}x_A)^2} \quad (8.14)$$

$$A_{AB} = \log c_A \left( 1 + \frac{x_B \log \gamma_B}{x_A \log \gamma_A} \right)^2 \quad (8.15)$$

$$A_{BA} = \log c_B \left( 1 + \frac{x_A \log \gamma_A}{x_B \log \gamma_B} \right)^2 \quad (8.16)$$

$$c_A = \frac{a_A}{x_A} = \frac{p_A^r}{p_A x_A} = \frac{y_A P}{p_A x_A}; c_B = \frac{a_B}{x_B} = \frac{p_B^r}{p_B x_B} \quad (8.17)$$

Also,

$$c_A = \frac{a_A}{x_A} = \frac{f_A}{f_A^0 x_A}; c_B = \frac{a_B}{x_B} = \frac{f_B}{f_B^0 x_B} \quad (8.18)$$

van Laar equations are useful in smoothing of isothermal data with constants applicable to the particular temperature. But these equations often cannot give proper picture of the temperature dependence of the activity coefficient.

Several equations have been proposed by different authors, which give better results. One such equation is Wilson equation which is given as follows:

$$\ln c_i = 1 - \ln \left( \sum_{j=1}^{\infty} x_j L_{ij} \right) - \sum_{k=1}^{\infty} \left( \frac{x_k L_{ki}}{\sum_{j=1}^{\infty} x_j L_{kj}} \right) \quad (8.19)$$

where

$L_{ij}$  is the Wilson's parameter for the  $ij$  pair.

$L_{ii} = 1$  and  $L_{ij} \neq L_{ji}$ . These are adjustable binary parameters to be determined by fitting of

experimental binary vapour-liquid equilibrium data.

Another theoretically sound model based on statistical mechanics is the Universal Quasi Chemical Model (UNIQUAC). It can predict vapour-liquid equilibria of non-ideal mixtures, but contains adjustable parameters to be estimated by experimental data fitting. The Uniquac Functional-group Activity Coefficient (UNIFAC) method that uses the group contribution is an improvement of the UNIQUAC method (Prausnitz et al. 1999).

**EXAMPLE 8.1** (Composition of the vapour phase in equilibrium with a binary liquid mixture): Determine the composition of the vapour phase in equilibrium at 50°C with a liquid consisting of a mixture of hexane and water. Hexane and water may be assumed to be completely immiscible.

At 50 °C, the saturated vapour pressure of hexane is 400 mm Hg and that of water is 92.5 mm Hg.

**Solution:** Let us call hexane as *A* and water as *B*.

Since hexane and water have been assumed to be completely immiscible, the partial pressure of each component may be taken as equal to respective saturated vapour pressure.

The total pressure of the vapour mixture may, therefore, be calculated from Eq. (8.3) as

$$P = p'_A + p'_B = p_A + p_B = 400 + 92.5 = 492.5 \text{ mm Hg}$$

The equilibrium mole fraction of hexane in the vapour phase is calculated from Eq. (8.7).

$$y_A^* = \frac{p'_A}{P} = \frac{400}{492.5} = 0.812$$

and the mole fraction of water in the vapour phase is

$$y_B^* = (1 - y_A) = (1 - 0.812) = 0.188$$

Equilibrium vapour composition is

0.812 mole fraction hexane and 0.188 mole fraction water.

**EXAMPLE 8.2** (Composition of the vapour phase in equilibrium with a liquid mixture of given composition and the composition of liquid mixture that will boil at a given temperature): Calculate the composition of the vapour phase in equilibrium at 60°C with a liquid mixture consisting of 40 mol% benzene and 60 mol% toluene. Also, determine the composition of a mixture of benzene and toluene that will boil at a temperature of 90°C under a pressure of 760 mm Hg.

Liquid mixtures of benzene and toluene obey Raoult's Law.

The saturated vapour pressures of benzene and toluene at 60°C are 385 mm Hg and 140 mm Hg, respectively. At 90°C, these values are 1013 and 408 mm Hg, respectively.

**Solution:** Let us call benzene as *A* and toluene as *B*.

The partial pressures of benzene and toluene are

$$p'_A = (385 \# 0.40) = 154 \text{ mm Hg}$$

$$p'_B = (140 \# 0.60) = 84 \text{ mm Hg}$$

The total pressure becomes  $(154 + 84) = 238 \text{ mm Hg}$ .

The mole fractions of benzene and toluene in the vapour are calculated from Eq. (8.7):

$$y_A^* = \frac{P'_A}{P} = \frac{154}{238} = 0.648 \text{ mole fraction}$$

$$y_B^* = \frac{P'_B}{P} = \frac{84}{238} = 0.352 \text{ mole fraction}$$

The mixture will boil when the total pressure is 760 mm Hg.

From Eq. (8.3), we have

$$760 = 1013x_A + 408(1 - x_A)$$

whence,

$$x_A = 0.583 \text{ and}$$

$$x_B = (1 - 0.583) = 0.417$$

The composition of the liquid that will boil at 90 °C is

benzene 58.3% and toluene 41.7%

## 8.4 Multicomponent Equilibria

Graphical treatment of non-ideal equilibria for three component systems can be carried out in triangular co-ordinates. But treatment of systems having more than three components is quite complicated. Fortunately many of the multicomponent systems of industrial importance can be considered to be nearly ideal in the liquid phase for practical purposes. This is particularly true for hydrocarbons of the same homologous series. In such cases, Raoult's law or its equivalent in terms of fugacity can be used for calculating equilibrium relations from the properties of the pure components. It should, however, be kept in mind that prediction of detailed equilibrium relations of a multicomponent system by considering properties of pure components or from a knowledge of their binary compounds may often be unreliable. Formation of binary or ternary azeotropes is one such area that may lead to erroneous results and needs special consideration.

Equilibrium data for multicomponent systems are generally expressed in terms of distribution coefficient  $K$ . Thus for a component  $J$

$$K_J = \frac{y_J^*}{x_J} \quad (8.20)$$

$K_J$  generally depends on the temperature, pressure and composition of the mixture.

The relative volatility of component  $I$  with respect to component  $J$  is given by

$$\alpha_{IJ} = \frac{y_I^*/x_I}{y_J^*/x_J} = \frac{K_I}{K_J} \quad (8.21)$$

For ideal solutions at moderate pressure,  $K_J$  is independent of composition and depends only on the total pressure and the temperature. It depends on temperature since temperature affects the vapour pressure.

$$K_J = \frac{P_J}{P} \quad (8.22)$$

$$a_{IJ} = \frac{P_I}{P_J} \quad (8.23)$$

### Bubble point

For the bubble point vapour

$$S y_I^* = 1.0$$

or,

$$K_A x_A + K_B x_B + K_C x_C + \dots = 1.0 \quad (8.24)$$

Taking  $J$  as a reference substance,

$$\frac{K_A x_A}{K_J} + \frac{K_B x_B}{K_J} + \frac{K_C x_C}{K_J} = S a_{IJ} x_I = \frac{1}{K_J} \quad (8.25)$$

The equilibrium bubble point vapour composition is given by

$$y_I = \frac{\alpha_{IJ} x_I}{\sum \alpha_{IJ} x_I} \quad (8.26)$$

The liquid composition and the total pressure having been fixed, the temperature is estimated by trial to satisfy Eq. (8.25).

### Dew point

Proceeding in the same way as above, the dew point liquid composition is found to be

$$x_I = \frac{y_I / \alpha_{IJ}}{\sum (y_I / \alpha_{IJ})} \quad (8.27)$$

On the basis of the above discussion, the method of computation of vapour-liquid equilibria is summarized below:

**Step 1** As a first estimate of the bubble point, a temperature is chosen and values of  $K$  for the assumed temperature and given pressure are taken from a reliable source.

**Step 2** A reference component ( $J$ ) is chosen and the relative volatilities ( $a_{CI} C_J$ ),  $S(a_{IJ} C_J x_I)$ , and  $K$  are calculated and tabulated against each composition.

**Step 3** The corresponding temperatures are noted from De Priester nomograph (De Priester, 1953).

**Step 4** The calculations are repeated for these temperatures and  $K C_J$  estimated. These are bubble point temperatures.

**Step 5** The corresponding bubble point vapour compositions ( $y_I$ ) are calculated from Eq. (8.26).

**Step 6** In a similar way as above, the dew point temperatures and corresponding dew point compositions ( $x_I$ ) are calculated from Eq. (8.27).

**Step 7** The bubble point and dew point curves are drawn with the compositions determined in Steps 5 and 6.

## 8.5 Methods of Distillation

Distillation operations are carried out both in single-stage and multistage units.

### 8.5.1 Single-Stage Distillation

#### *Equilibrium distillation or flash vaporisation*

In single-stage operation a liquid mixture is partially vaporised; the vapour and the residual liquid are kept in mutual contact so that they attain equilibrium and then these are separated. The operation may be batch type or continuous.

A schematic diagram of a continuous flash vaporisation unit is shown in Figure 8.10. The liquid feed is heated to the desired temperature under pressure in a preheater. The hot liquid is passed through a throttle and enters into a flash drum where flash vaporisation under reduced pressure occurs. The flash drum also acts as separator for the vapour-liquid mixture. The vapour leaves at the top and is condensed in the condenser. The liquid is collected from the bottom. The flash drum is provided with baffle plates to reduce entrainment of liquid with the outgoing vapour.

Binary flash vaporisation problems can be solved graphically using enthalpy-composition or vapour-liquid equilibrium data. In terms of the notations used in Figure 8.10, the material and enthalpy balance equations may be written as:

$$F = D + W \quad (8.28)$$

$$Fx_F = Dy_D + Wx_W \quad (8.29)$$

$$Fh_F + Q = DH_D + Wh_W \quad (8.30)$$

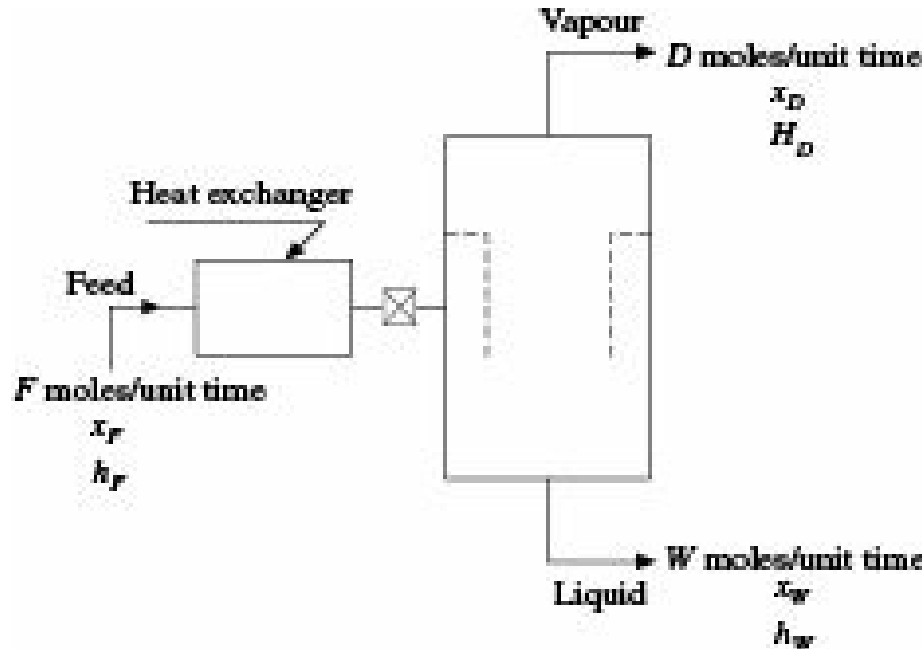


Figure 8.10 Schematic diagram of a continuous flash vapouriser.

From Eqs. (8.28) and (8.29), we have

$$-\frac{W}{D} = \frac{y_D - x_F}{x_W - x_F} \quad (8.31)$$

and from Eqs. (8.28) and (8.30), we get

$$\frac{W}{D} = \frac{H_D - (h_F + Q/F)}{h_W - (h_F + Q/F)} \quad (8.32)$$

Equation (8.32) represents a straight line on the enthalpy-composition diagram [Figure 8.11(a)] passing through the points  $(H_D, y_D)$ ,  $(h_W, x_W)$  and  $(h_F + Q/F, x_F)$  being represented by  $D$  the distillate,  $W$  the bottom product and  $F$  the preheated feed. On the distribution curve [Figure 8.11(b)], the points  $F$  and  $M$  represent the preheated feed and the effluent streams.

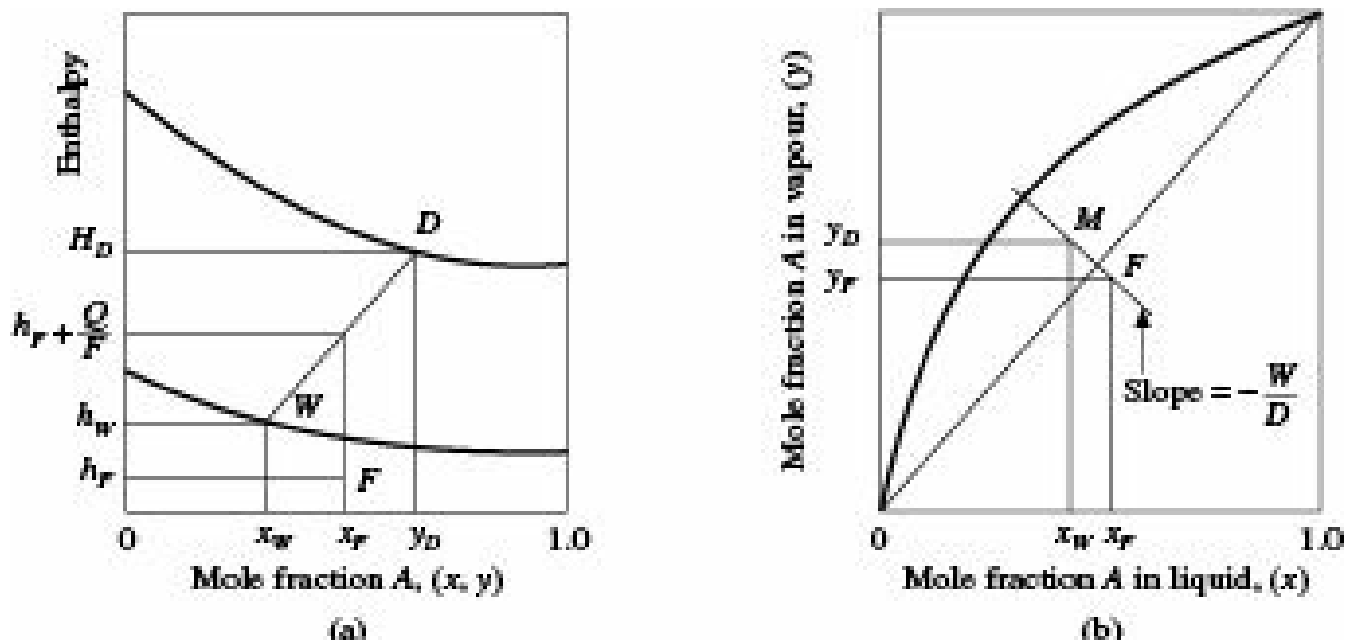


Figure 8.11 Graphical representation of flash vaporisation. (a) On enthalpy-composition diagram, (b) On  $y$ - $x$  distribution coordinates.

### Partial condensation

When the feed is a vapour, separation is effected by removal of heat in the heat exchanger. All the above equations are applicable except that  $Q$  becomes negative. On the enthalpy-composition diagram, the point  $F$  then becomes saturated or superheated vapour.

Equilibrium distillation is not much in use in binary systems. It is however used in multicomponent systems, particularly in the petroleum industry.

### Multicomponent system—ideal solution

For a multicomponent mixture leaving an equilibrium stage, the equilibrium relation for any component  $J$  becomes

$$y^*_{JD} = K_J x_{JW} \quad (8.33)$$

Equations (8.31) and (8.32) also apply to each of the components and when combined with Eq. (8.33) for any component  $J$  for an equilibrium stage yields

$$\frac{W}{D} = \frac{K_J x_{JW} - x_{JF}}{x_{JF} - x_{JW}} = \frac{y^*_{JD} - x_{JF}}{x_{JF} - (y^*_{JD}/K_J)} \quad (8.34)$$

The following equations useful for equilibrium vaporisation and condensation may be obtained from Eq. (8.34):

For equilibrium vaporisation

$$y^*_{JD} = \frac{x_{JF} [(W/D) + 1]}{1 + (W/D K_J)} \quad (8.35)$$

and for condensation

$$S y^* D = 1.0 \quad (8.36)$$

$$x JW = \frac{x_F [(W/D) + 1]}{K_J + (W/D)} \quad (8.37)$$

and

$$S x W = 1.0 \quad (8.38)$$

Thus, Eq. (8.35) can be used for each of the components with appropriate values of  $K$  and  $x_F$ . The sum of the values of  $y^* D$  so calculated must be 1.0 if correct conditions of  $(W/D)$ , temperature and pressure have been chosen. Otherwise a new set of assumptions have to be made. A similar treatment has to be made for Eq. (8.37).

**EXAMPLE 8.3** (Flash Vaporisation): A liquid mixture containing 40 mol% *n*-heptane and 60 mol% *n*-octane at 30°C is continuously flash vaporised at 1 atm pressure. If the operation is continued till 50 mol% of the mixture is vaporised, determine the compositions of the distillate and the residue. The following equilibrium data may be used:

$x$	0	0.157	0.312	0.487	0.655	1.0
$y^*$	0	0.279	0.492	0.674	0.810	1.0

where

$x$  = mole fraction of *n*-heptane in liquid, and

$y^*$  = mole fraction of *n*-heptane in vapour in equilibrium with  $x$ .

**Solution:** Basis:  $F = 100$  mole feed,  $x_F = 0.40$  mole fraction.

$$D = 50 \text{ moles}, W = (100 - 50) = 50 \text{ moles}, -(W/D) = -(50/50) = -1.$$

The equilibrium data are plotted in Figure 8.12.

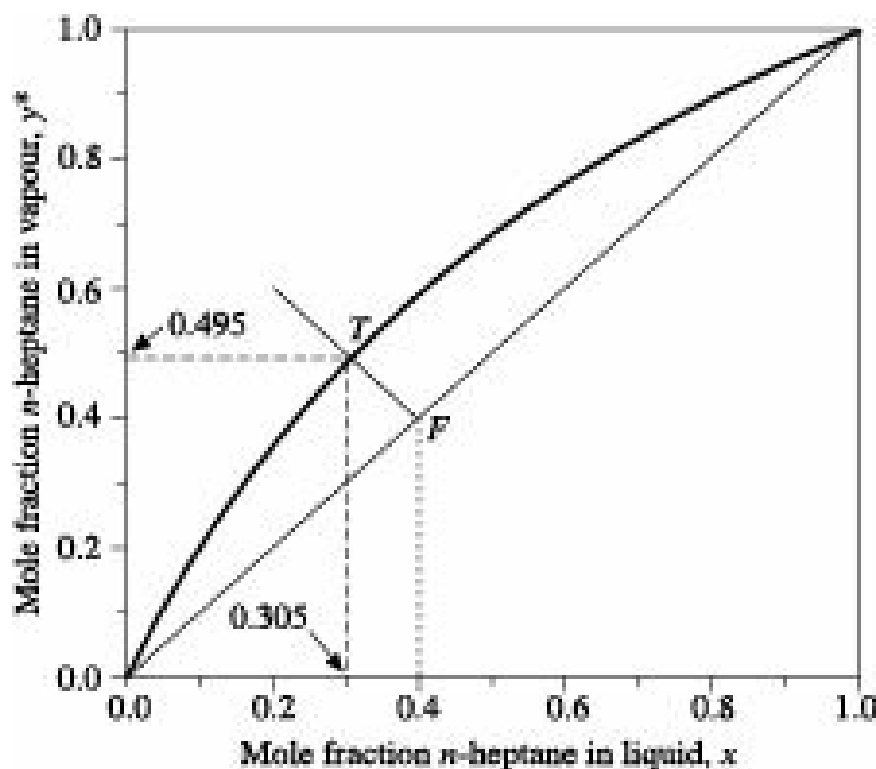


**Figure 8.12** Example 8.3.

Point  $F$  represents the feed composition. The operating line is drawn from point  $F$  with a slope of (-1) to intersect the equilibrium curve at  $T$ , where  $y^* D = 0.495$  mole fraction  $n$ -heptane and  $x_W = 0.305$  mole fraction  $n$ -heptane.

Vapour composition: 49.5%  $n$ -heptane and 50.5%  $n$ -octane;

Liquid composition: 30.5%  $n$ -heptane and 69.5%  $n$ -octane.

### Simple or differential distillation

In simple or differential distillation, a liquid is subjected to infinite number of successive flash vaporisation but only an infinitesimal amount of liquid is vaporised each time.

A commercial differential distillation unit consists of a kettle or still provided with some heating device like steam coil or steam jacket. It is also provided with a suitable condenser and receiver(s).

Batch of liquid is taken in the still and boiled. The vapours are removed as soon as they are formed and condensed so that the bulk liquid and bulk vapour cannot attain equilibrium. The condensate is collected in receiver(s) connected to a vacuum pump. The equipment is essentially a large-scale replica of the ordinary laboratory distillation flask. The first portion of the distillate is the richest in the more volatile component and as distillation proceeds, the distillate becomes leaner in more volatile component. The distillate can therefore be collected in different batches called cuts to give a series of products of different purities.

In differential distillation, the vapour produced at any time is in equilibrium with the liquid from which it is produced, but its composition changes continuously since the liquid with which it is in equilibrium is constantly changing in composition. Therefore, mathematical treatment of such distillation has to be differential.

At any time during distillation, let there be  $L$  moles of liquid having  $x$  mole fraction of the more volatile component  $A$ , and let an amount  $dD$  moles of vapour having  $y^*$  mole fraction of  $A$  in equilibrium with the liquid be vaporised.

The material balance equations in differential form may be written as:

$$\text{Overall material balance: } -dL = dD \quad (8.39)$$

$$\text{Component } A \text{ balance: } -d(Lx) = y^* dD \quad (8.40)$$

From Eq. (8.40), we get

$$-Ldx - x dL = y^* dD \quad (8.41)$$

Substituting for  $dD$  from Eq. (8.39) and rearranging, we obtain

$$dL(y^* - x) = Ldx$$

or,

$$\frac{dx}{L} = \frac{dy^*}{y^* - x} \quad (8.42)$$

If distillation starts with  $F$  moles of liquid of composition  $x_F$  and continues till  $W$  moles of liquid with composition  $x_W$  are left in the still, Eq. (8.42) may be integrated to give

$$\int_F^W \frac{dL}{L} = \int_{x_F}^{x_W} \frac{dx}{y^* - x}$$

or,

$$\ln \frac{F}{W} = \int_{x_F}^{x_W} \frac{dx}{y^* - x} \quad (8.43)$$

Equation (8.43) is also known as *Rayleigh equation* after Lord Rayleigh who first derived it. If vapour-liquid equilibrium data are available, Eq. (8.43) can be solved graphically by plotting  $[1/(y^* - x)]$  as ordinate against  $x$  as abscissa and finding the area under the curve between the limits  $x_W$  and  $x_F$ .

If the relation between  $x$  and  $y^*$  is available in the form of an algebraic equation, analytical integration is possible. For example, if the relative volatility  $\alpha$  of  $A$  is constant, as in case of ideal solutions, we have

$$\begin{aligned} \ln \frac{F}{W} &= \int_{x_W}^{x_F} \frac{dx}{\frac{\alpha x}{1 + (\alpha - 1)x} - x} \\ &= \frac{1}{\alpha - 1} \ln \frac{x_F(1 - x_W)}{x_W(1 - x_F)} + \ln \frac{1 - x_W}{1 - x_F} \end{aligned} \quad (8.44)$$

Equation (8.44) can be expressed in a more convenient form as

$$\ln \frac{Fx_F}{Wx_W} = \alpha \ln \frac{F(1 - x_F)}{W(1 - x_W)} \quad (8.45)$$

The average composition of the collected distillate can be determined from material balance. Batch distillation is one of the oldest methods for distilling liquid mixtures. This is the most common, simple and least capital intensive method for distilling binary as well as multicomponent mixtures. Such system can also be used to develop or scale-up commercial level continuous distillation equipment. However, proper attention need to be given to certain aspects while operating or designing the batch distillation column:

Hold-up in column packing and internals affect the yield of pure cut. Because of the hold-up in the column it becomes necessary to allow some losses of pure product. To reduce the hold-up in the column, it is necessary that volume of batch distillation column should be minimum. If capacity of the column required is very large, it is better to switch over to continuous operation. Structured packings offer lower hold-up. Structured packings also help to reduce the size of the column, i.e. hold-up associated with it. If structured packing are not suitable, random packings should be used. In any case, trays should be avoided.

For a fixed size of distillation column having size and type of packing already fixed up, the vapour load that a column can handle is fixed depending upon the operating pressure of the column. At higher operating pressures the vapour densities are higher and at lower operating pressures like vacuum the

densities are lower.

In batch distillation column, different cuts are required to be distilled at different reflux ratios. Reflux ratio at start of a cut can be low, and at the end of a cut it may be very high in order to maintain top product purity. This results in the design of liquid distributor for column becoming complex, because the distributor has to handle a very wide range of liquid loads to take care of high to low reflux conditions for a given cut. This problem becomes more and more complex if the column is to be operated at different pressures. To overcome such problem a designer should ensure that packing should be irrigated all across the column cross section for all liquid load conditions. This can be taken care of by designing an efficient liquid distributor.

Because of excessively high reflux ratio requirement at the end of a batch distillation cut of a given isomer, it is no longer economical to operate a batch distillation column for separation of close boiling isomers. This results in poor recovery of valuable isomers. In such situation one should opt for continuous distillation. Batch distillation should be used for only final fine-tuning of an important isomer in the mixture.

### Multicomponent systems—ideal solutions

For ideal solutions of multicomponent systems, Eq. (8.45) can be applied to any two components. Generally, the component on which the relative volatilities of other components are to be based is chosen for application of Eq. (8.45), so that the equation is applied once for each of the other components. Thus for component  $J$  with relative volatility based on component  $C$ , we have

$$\log \frac{Fx_{JF}}{Wx_{JW}} = \alpha_{JC} \log \frac{Fx_{CF}}{Wx_{CW}} \quad (8.46)$$

and

$$Sx_W = 1.0 \quad (8.47)$$

where

$x_{JF}$  = mole fraction of  $J$  in the feed, and

$x_{JW}$  = mole fraction of  $J$  in the residue.

**EXAMPLE 8.4** (Calculation of the percent distilled off in differential distillation): An aqueous solution of  $A$  containing 70 mol%  $A$  and 30 mol% water is subjected to differential distillation. What percentage of the original solution must be distilled off in order to reduce the concentration of  $A$  in the residue to 20 mol%?

The relative volatility of  $A$  with respect to water is 2.15.

**Solution:** Relative volatility,  $\alpha_{AB} = 2.15$

$$y^* = \frac{\alpha x}{1 + (\alpha - 1)x} = \frac{2.15x}{1 + 1.15x}$$

From the above relation,  $y^*$ - $x$  data and value of  $[1/(y^* - x)]$  are calculated as under:

$x:$	0.10	0.20	0.30	0.40	0.50	0.60	0.70
$y^*:$	0.19	0.35	0.48	0.59	0.68	0.76	0.83

$$[1/(y^* - x)] = 11.11 \quad 6.67 \quad 5.56 \quad 5.26 \quad 5.56 \quad 6.25 \quad 7.69$$

$1/(y^* - x)$  is plotted as ordinate against  $x$  as abscissa in Figure 8.13 and the area under the curve between the limits  $x = 0.70$  and  $x = 0.20$  is measured.

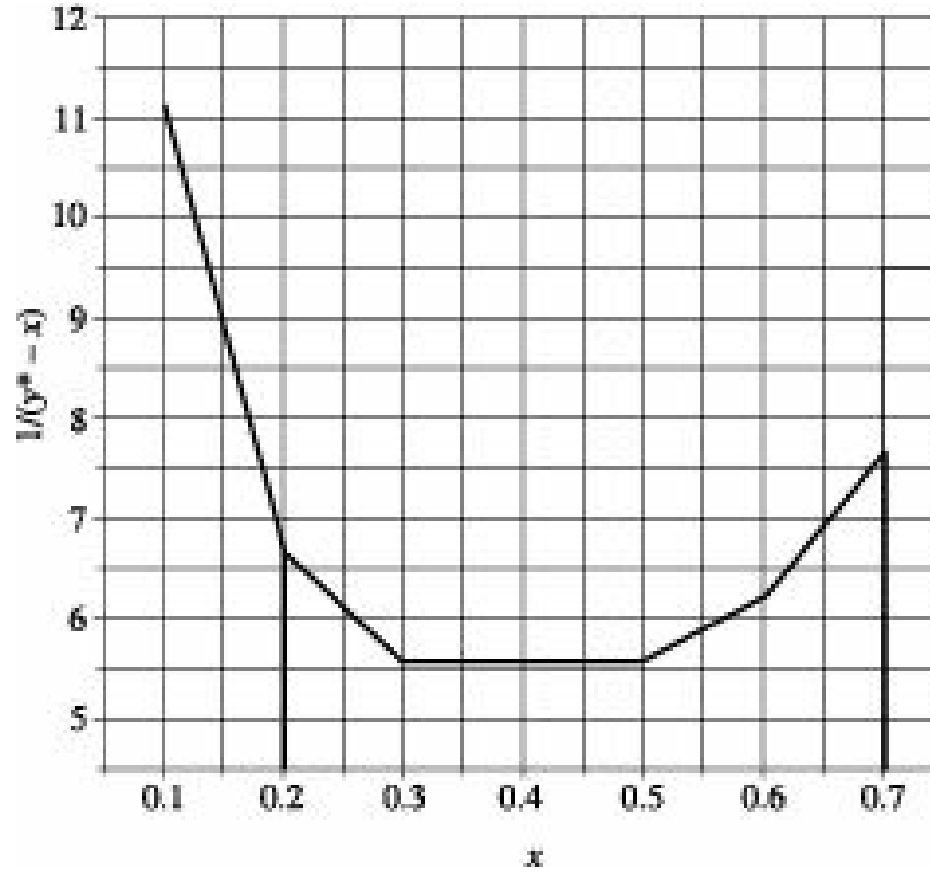


Figure 8.13 Example 8.4.

Area under the curve = 3.01 units.

Basis: 100 moles of original solution.

From Rayleigh Eq. (8.43),

$$\int_{0.20}^{0.70} \frac{dx}{y^* - x} = \ln \frac{100}{W} = 3.01$$

whence,

$$W = 4.93 \text{ moles.}$$

Percent to be distilled off =  $(100 - 4.93) = 95.07 \text{ mol\%}$ .

Alternatively, Eq. (8.45) may be used:

$$\log \frac{\frac{F \cdot x_F}{W \cdot x_W}}{a} = \log \frac{F(1 - x_F)}{W(1 - x_W)}$$

Substituting the values, we get

$$\log \left( \frac{(100)(0.70)}{(W)(0.20)} \right) = 2.15 \log \frac{(100)(0.30)}{(W)(0.80)}$$

Solving,  $W = 5.37 \text{ moles}$ ,

Percent distilled off =  $(100 - 5.37) = 94.63 \text{ mol\%}$ .

**EXAMPLE 8.5** (Calculation of the compositions of the distillate and residue in batch distillation): A solution of 25 mol% acetic acid in water was distilled at atmospheric pressure until 60 mol% of the liquid was distilled. Compute the compositions of the distillate and the residue.

**Equilibrium Data:**

$x:$	0.07	0.15	0.27	0.50	0.62	0.72	0.82	0.90	1.00
$y^*:$	0.05	0.11	0.20	0.38	0.49	0.60	0.73	0.84	1.00

where  $x$  and  $y^*$  are mole fractions of acetic acid in liquid and vapour, respectively.

**Solution:** Since water is more volatile than acetic acid, equilibrium data are expressed in terms of mole fractions of water and corresponding values of  $[1/(y^* - x)]$  calculated are as under:

$x:$	0.93	0.85	0.73	0.50	0.38	0.28	0.18	0.10
$y^*:$	0.95	0.89	0.80	0.62	0.51	0.40	0.27	0.16
$[1/(y^* - x)]:$	50.00	25.00	14.29	8.33	7.69	8.33	11.11	16.67

Let  $x_1$  be the mole fraction of water in the residue.

Then from Rayleigh equation, we get

$$\int_{x_1}^{0.75} \frac{dx}{y^* - x} = \ln \frac{100}{40} = 0.916$$

$[1/(y^* - x)]$  is plotted as ordinate against  $x$  as abscissa in Figure 8.14.

$x_1$  is located by trial and error so that the area under the curve is 0.916.

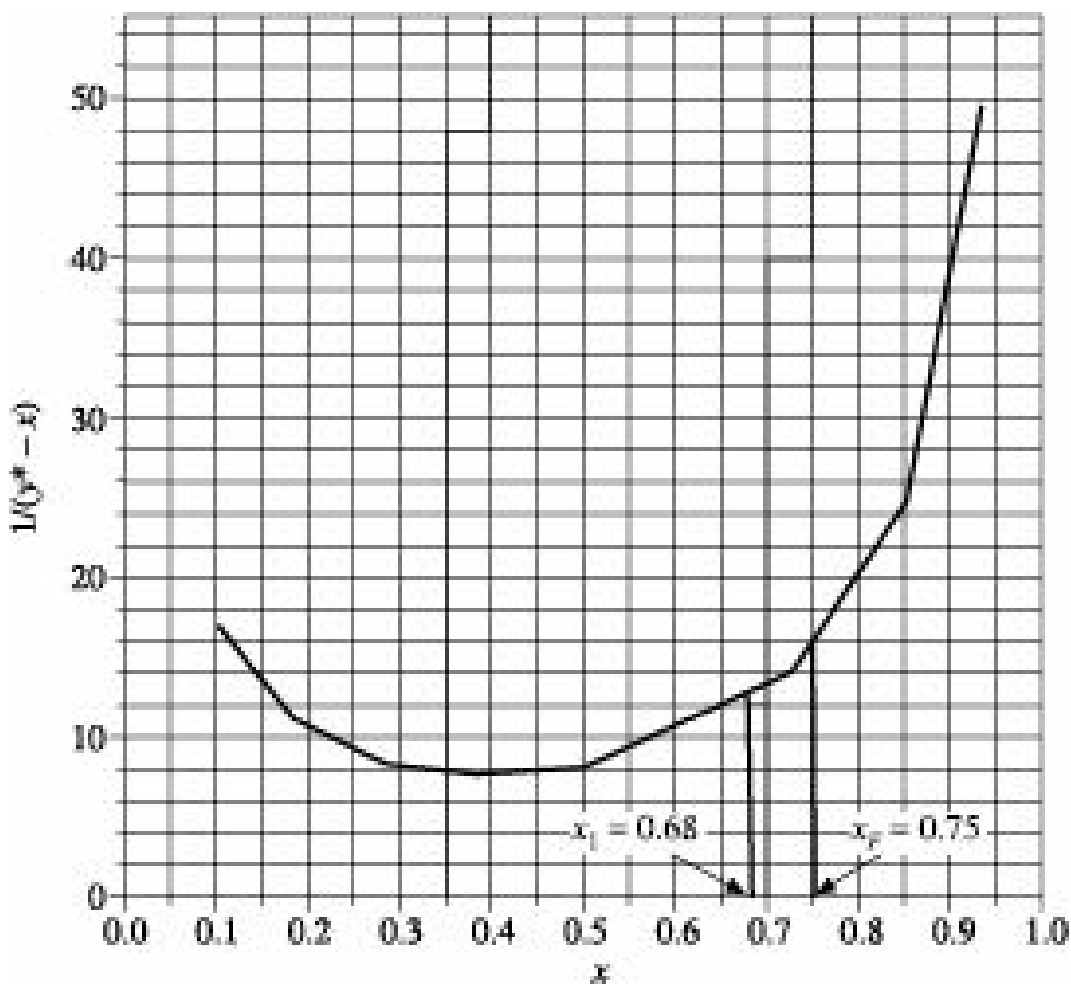


Figure 8.14 Example 8.5.

By trial and error:  $x_1 = 0.68$

The area under the curve  $[1/(y^* - x)]$  vs  $x$  between  $x_F = 0.75$  and  $x_1 = 0.68$  is found to be 0.915 units which agrees well with the calculated value.

Composition of Residue: 68 mol% water,  
and  $(100 - 68) = 32$  mol% acetic acid.

Moles of water in residue =  $(40 \# 0.68) = 27.2$  mol

Moles of water in vapour =  $(75 - 27.2) = 47.8$  mol

Moles of acetic acid in residue =  $(40 \# 0.32) = 12.8$  mol

Moles of acetic acid in vapour =  $(25 - 12.8) = 12.2$  mol

Composition of distillate:

$$\text{Mol\% of water} = \frac{47.8}{60} \# 100 = 79.67\%$$

$$\text{Mol\% of acetic acid} = \frac{12.2}{60} \# 100 = 20.33\%$$

### **Steam distillation**

If the two components of a binary liquid mixture are immiscible, the mixture exerts a total vapour pressure which is equal to the sum of the vapour pressures of the components at the prevailing temperature, and the mixture boils at temperature which is lower than the boiling points of either component. This principle is the basis of steam distillation.

In steam distillation, live steam is introduced into a liquid containing a component  $A$ , having low

volatility and low solubility with water, along with nonvolatile substance(s). On passing live steam, component *A* volatilizes and is carried away with the steam leaving behind the nonvolatile impurities present. The feed is taken in a still with provision of sparging live steam at the bottom. The vaporised component *A* along with steam passes on to a condenser near the upper end of the still. The mixture then flows into a separator where component *A* and water form two layers, and are removed separately. In addition to open steam, steam coils are provided to supply the heat required to vaporise the mixture and to make up for the loss of heat from the still.

Let *P* be the total pressure in the still, and *p<sub>A</sub>* and *p<sub>W</sub>* be the vapour pressures of component *A* and water respectively at the operating temperature, then

$$P = p_A + p_W \text{ or } p_W = P - p_A \quad (8.48)$$

If *n<sub>A</sub>* moles of component *A* is vaporised by using *n<sub>W</sub>* moles of steam, and if the system operates at equilibrium, we have

$$\frac{n_A}{n_W} = \frac{p_A}{p_W} = \frac{p_A}{P - p_A} \quad (8.49)$$

or,

$$n_A = n_W \frac{p_A}{p_W} = n_W \frac{p_A}{P - p_A} \quad (8.50)$$

However, if the system does not operate at equilibrium the partial pressure of component *A* will be less than its vapour pressure. This is taken into account by using a factor known as vaporisation efficiency (*E*), so that Eq. (8.50) becomes

$$n_A = n_W \frac{\frac{E p_A}{p_W}}{P - E p_W} = n_W \frac{E p_W}{P - E p_W} \quad (8.51)$$

The amount of steam required to produce a given amount of *A* can also be estimated from Eq. (8.51).

**EXAMPLE 8.6** (Estimation of time required in steam distillation): An essential oil (Mol.wt. = 170) containing a small amount of nonvolatile impurity is to be purified by steam distillation. An experimental distillation still is charged with 1 kg of the impure essential oil. Saturated steam at 108 °C is passed through the still at a rate of 30 kg/ hr.

Assuming that the essential oil is immiscible with water and neglecting condensation of steam, estimate the time required for the distillation. The vaporisation efficiency may be taken as 80%.

At 108 °C, the vapour pressure of the essential oil is 6.5 mm Hg and that of water is 1000.6 mm Hg.

**Solution:**

Moles of the essential oil in the initial mixture = (1/170) = 5.88 # 10<sup>-3</sup> kmol.

From Eq. (8.51), we have

$$n_W = n_A \frac{p_W}{E p_A} = (5.88 \# 10^{-3}) \frac{1000.6}{(0.80)(6.5)}$$

$$= 1.137 \text{ kmol steam} = (1.137 \# 18) = 13.52 \text{ kg steam}$$

$$\text{Time required} = \frac{30}{30} \# 60 = 27.04 \text{ min}$$

### 8.5.2 Continuous Multistage Distillation—Binary Systems

Continuous multistage distillation, also called *rectification* or *fractionation*, is one of the most frequently used separation processes in chemical and allied industries. With a few exceptions, rectification can separate a binary solution into its components in any state of purity desired.

A schematic diagram of a rectification column is shown in Figure 8.15. The rectification column consists of a tall vertical column provided with plates which may be of different types and designs (Sections 6.2.3 and 6.2.4). The major accessories include a reboiler at the bottom, a condenser and reflux regulator near the top, arrangement for introduction of feed, etc. The feed is introduced on a plate somewhere near the middle of the column. The section above the feed plate is called the *absorption* or *enriching* or *rectifying* section. The vapour rising in this section is stripped of part of its content of the less volatile component by the liquid obtained by condensing the vapour leaving at the top. The liquid so returned is called the *reflux*. The portion withdrawn from the top of the column is called the *distillate*. The distillate may be liquid or vapour or a mixture of the two, but the reflux is always liquid. The section below the feed plate is called the *stripping* or *exhausting* section. The liquid in this section is stripped of a part of the more volatile content by the vapour produced in the reboiler. The liquid withdrawn from the bottom is the *residue* or *bottoms*. Inside the column the liquid and vapour are always at their bubble points and dew points respectively so that the highest temperature is at the lower end of the column and the lowest temperature is at the top. The plates are numbered starting from the top, the top most plate being plate 1. Liquid and vapour leaving any plate is designated by the respective plate number. Thus,  $L_n$  means the liquid leaving plate  $n$ .

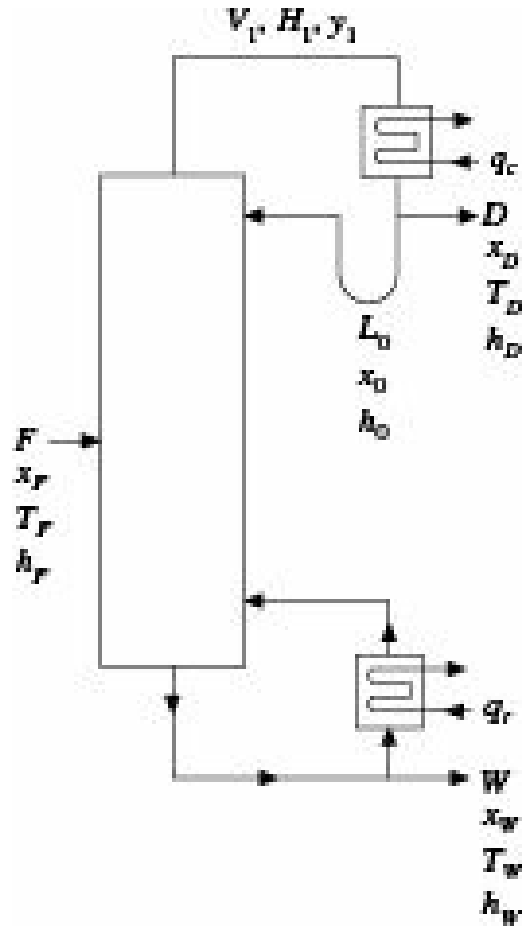


**Figure 8.15** Rectification column-flow diagram.

Reflux plays a very important role in rectification practice. Reflux is a part of the condensed overhead product which is returned to the column near its top and allowed to come in intimate contact with the vapour rising from below so that mass transfer can take place between them. The less volatile component passes from the vapour to the liquid and by utilizing the heat released by it, the more volatile component passes from the liquid to the rising vapour. In this way the vapour becomes more and more enriched in the more volatile component while the liquid becomes more and more concentrated in the less volatile component. As a result, the concentration of the more volatile component in the distillate may be several times higher than the equilibrium value corresponding to the concentration in the liquid leaving at the bottom.

As reflux is increased, the number of plates required for a given separation and hence the tower height decrease and capital expenditure decreases despite marginal increase in tower diameter. But operating cost increases due to high pumping cost and large heat requirements. The tower cross section, on the other hand, depends on the amount of liquid and vapour to be handled.

### 8.5.3 Rectification—Methods of Calculation

#### *Material and Heat Balance*

In distillation practice, major design calculations include determination of number of plates or height of packing and diameter.

In Figure 8.15,  $F$  is the feed,  $D$  is the distillate and  $W$  is the bottom product, all in mass per unit time.  $x_F, x_D, x_W$  are the compositions;  $T_F, T_D, T_W$  are the temperatures and  $h_F, h_D, h_W$  are the enthalpies of the feed, distillate and bottom product, respectively.

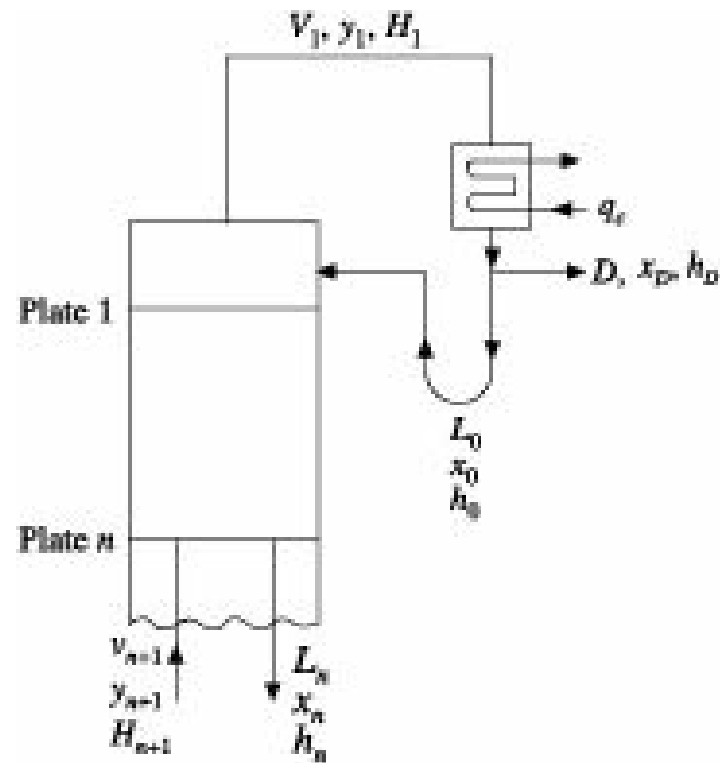


**Figure 8.17** Section above feed plate.

From material balance around the column under steady conditions:

$$F = D + W \quad (8.52)$$

$$Fx_F = Dx_D + Wx_W \quad (8.53)$$

Solving,

$$D = \frac{F(x_F - x_W)}{x_D - x_W} \quad (8.54)$$

and

$$W = \frac{F(x_D - x_F)}{x_D - x_W} \quad (8.55)$$

From energy balance, assuming no heat loss,

$$Fh_F + q_r = Dh_D + Wh_W + q_c \quad (8.56)$$

where  $q_r$  is the heat added in the reboiler and  $q_c$  is the heat removed from the condenser.

Equation (8.56) states that if heat input to the reboiler is fixed, then heat to be removed from the condenser also gets fixed. Similarly, if  $q_c$  is fixed,  $q_r$  gets fixed. Therefore, one of them should be fixed before any calculations are made.

Writing the material and energy balance for the condenser alone:

$$V_1 = L_0 + D \quad (8.57)$$

$$V_1y_1 = L_0x_0 + Dx_D \quad (8.58)$$

$$V_1H_1 = L_0h_0 + Dh_D + q_c \quad (8.59)$$

where  $h$  and  $H$  represent the enthalpies of saturated liquid and vapour, respectively.

In case of a total condenser,  $y_1 = x_0 = x_D$  and  $h_0 = h_D$ .

Solving Eq. (8.59) for  $q_c$  and substituting for  $V_1$  from Eq. (8.57), we get

$$q_c = (L_0 + D)H_1 - (L_0 + D)h_D = (L_0 + D)(H_1 - h_D)$$

or,

$$\frac{q_c}{D} = \left( \frac{L_0}{D} + 1 \right) (H_1 - h_D) \quad (8.60)$$

$(L_0/D)$  is called the reflux ratio and is denoted by  $R$ . From Eq. (8.60), it may be seen that fixing  $(L_0/D)$  means fixing  $q_c$ .

#### 8.5.4 Determination of Number of Theoretical Plates

A theoretical plate is defined as a plate in which the vapour leaving the plate and passing on to the plate above is in equilibrium with the liquid leaving the plate and passing on to the plate below. A theoretical plate is similar in performance to an equilibrium stage.

Although several methods are available for determination of the number of theoretical plates in a plate column, only the following four methods will be discussed here.

- Plate-to-plate rigorous calculation

- Graphical solution on enthalpy composition diagram: Ponchon-Savarit method
- McCabe Thiele method,
- Fenske-Underwood method

### **Plate-to-plate rigorous calculation**

This method does not make any simplifying assumption except using the concept of theoretical plate. As a result, it is a very reliable method for calculation of number of theoretical plates in distillation and provides solutions much more accurate than the approximate methods based on a variety of simplifying assumptions. But it involves solution of a large number of complex simultaneous equations. With the advent of high speed computers, these calculations have become rather easy and this method is recommended for any detailed design calculation.

In this method computations are started from known terminal conditions, which may be either end of the column. Thus, starting from the top

Overall material balance around plate 1 as shown in Figure 8.16:

$$L_0 + V_2 = L_1 + V_1 \quad (8.61)$$

Component A balance:

$$L_0 x_0 + V_2 y_2 = L_1 x_1 + V_1 y_1 \quad (8.62)$$

Enthalpy Balance:

$$L_0 h_0 + V_2 H_2 = L_1 h_1 + V_1 H_1 \quad (8.63)$$

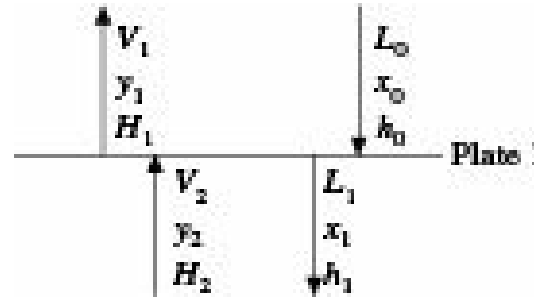


**Figure 8.16** Material balance around plate 1.

Here  $L_0, x_0, h_0, V_1, y_1, H_1$  being terminal conditions are known. There still remain six unknowns with three equations available. Hence some more information about the variables must be provided for their solution. From the concept of theoretical plate,  $x_1$  and  $y_1$  are equilibrium values. Hence  $x_1$  gets fixed if  $y_1$  is fixed. Moreover  $h_1$  being enthalpy of saturated liquid, its value is also fixed as soon as  $x_1$  is fixed. Also  $V_2$  being saturated vapour, its enthalpy  $H_2$  is fixed by its composition. The number of independent variables thus reduces to three, namely  $L_1, V_2$  and  $y_2$  so that Eqs. (8.61) to (8.63) may be solved simultaneously.

The known values of  $L_1, x_1, h_1$  and  $V_2, y_2, H_2$  are next used to find the values of  $L_2, x_2, h_2$  and  $V_3, y_3, H_3$  of the streams leaving and entering plate 2. Computations are continued in this fashion till the composition of the bottom product is reached and the number of steps involved gives the number of theoretical plates required.

### **Ponchon-Savarit method**

In Ponchon-Savarit method, the number of theoretical plates is determined graphically on the enthalpy-composition diagram by the application of the principles of graphical addition and

subtraction. The procedure has been developed separately for the sections above and below the feed plate.

### • Section above the Feed Plate

The section above the feed plate is shown in Figure 8.17.

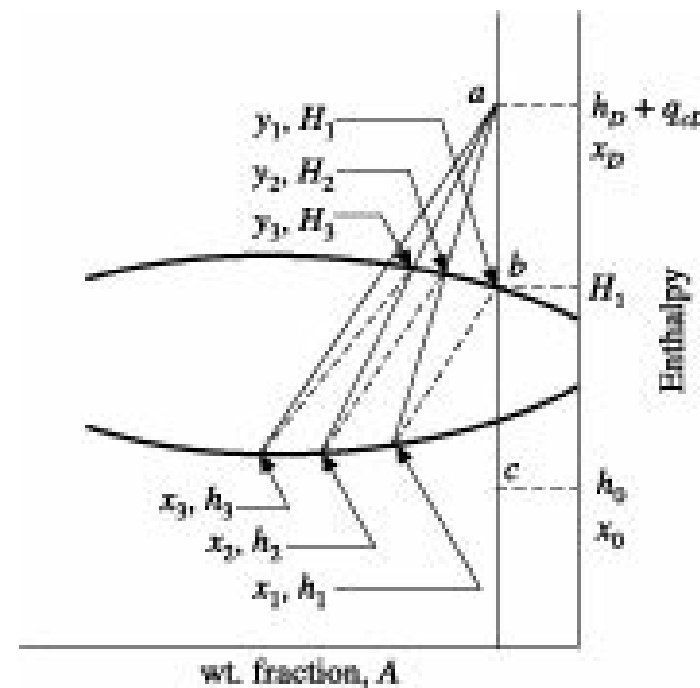


**Figure 8.18** Graphical solution for section above feed plate.

For this section, the material and energy balance equations may be written as

$$V_{n+1} - L_n = D \quad (8.64)$$

$$V_{n+1} y_{n+1} - L_n x_n = D x_D \quad (8.65)$$

$$V_{n+1} H_{n+1} - L_n h_n = D h_D + q_c \quad (8.66)$$

where plate  $n$  is any plate above the feed plate and plate  $(n + 1)$  is the plate next below.

$$\frac{q_c}{D}$$

Defining  $q_{cD} = \frac{q_c}{D}$  and substituting in Eq. (8.66), we get

$$V_{n+1} H_{n+1} - L_n h_n = D(h_D + q_{cD}) \quad (8.67)$$

From Eqs. (8.65) and (8.67), it may be concluded that the points  $(y_{n+1}, H_{n+1})$ ,  $(x_n, h_n)$  and  $(x_D, h_D + q_{cD})$  must lie on a straight line. From material and energy balance around the condenser, it has been shown in Eq. (8.60) that  $q_{cD}$  can be calculated using the reflux ratio ( $L_0/D$ ). The point  $(x_D, h_D + q_{cD})$  may, therefore, be located by calculation.

Since Eqs. (8.64) to (8.66) are valid for any plate above the feed plate, they hold good for the case  $n = 0$ , i.e. when  $y_{n+1} = y_1$ ,  $H_{n+1} = H_1$  and  $x_n = x_0$ . Therefore, the points  $(y_1, H_1)$ ,  $(x_0, h_0)$  and  $(x_D, h_D + q_{cD})$  must also lie on a straight line. However, the reflux may not always return at the temperature of the top plate due to sub-cooling and the point  $(x_0, h_0)$  may sometimes lie below the saturated liquid line.

If Eqs. (8.64) to (8.66) are rewritten for the case  $n = 0$ , they may be solved simultaneously to give

$$\frac{L_0}{D} = \frac{(h_D + q_{cD}) - H_1}{H_1 - h_0} \quad (8.68)$$

From Eq. (8.68), it is evident that the ratio of the distances  $ab$  and  $bc$  as shown in Figure 8.18 is equal to  $(L_0/D)$ ,

$$\frac{L_0}{D} = \frac{\overline{ab}}{\overline{bc}}$$

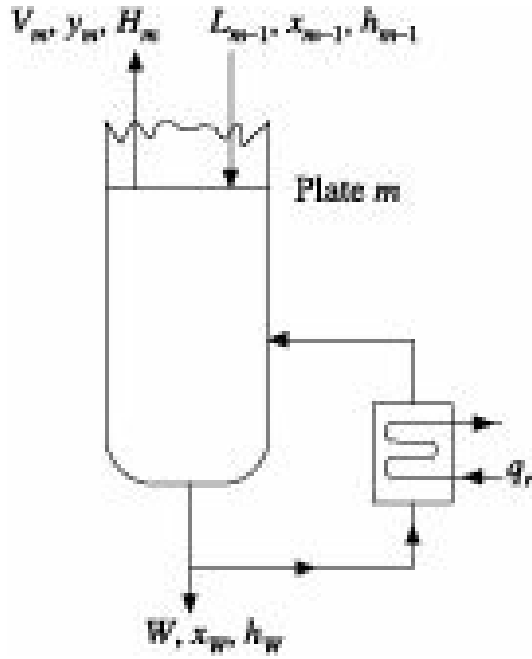


Figure 8.19 Section below feed plate.

Since the point  $(x_0, h_0)$  is fixed and the point  $(y_1, H_1)$  must lie on the saturated vapour line, the point  $(x_D, h_D + q_{cD})$  may also be located graphically from knowledge of the reflux ratio  $(L_0/D)$ . The points  $(x_1, h_1)$  and  $(y_1, H_1)$  are connected by tie line. Hence, once the point  $(y_1, H_1)$  is located,  $(x_1, h_1)$  may be located from knowledge of the equilibrium relation.

For  $n = 1$ , the points  $(y_2, H_2)$ ,  $(x_1, h_1)$  and  $(x_D, h_D + q_{cD})$  must lie on a straight line. Therefore, a straight line joining  $(x_1, h_1)$  and  $(x_D, h_D + q_{cD})$  will provide  $(y_2, H_2)$  at its point of intersection with the saturated vapour line. In this way the compositions and enthalpies of all the streams are determined till the feed plate is reached.

### • Section below the feed plate

The material and energy balance equations for the section below the feed plate may be written as  
 $L_{m-1} - V_m = W \quad (8.69)$

$$L_{m-1} x_{m-1} - V_m y_m = W x_W \quad (8.70)$$

$$L_{m-1} h_{m-1} - V_m H_m = W h_W - q_r \quad (8.71)$$

where plate  $m$  is any plate below the feed plate as shown in Figure 8.19.

As before, defining  $q_rW = q_r/W$ , Eq. (8.71) may be written as

$$L_{m-1} h_{m-1} - V_m H_m = W(h_W - q_rW) \quad (8.72)$$

From Eqs. (8.70) and (8.72), it is evident that the points  $(x_{m-1}, h_{m-1})$ ,  $(y_m, H_m)$  and  $(x_W, h_W - q_rW)$

lie on a straight line.

The point  $(x_W, h_W - q_rW)$  may be located from overall material and energy balance Eqs. (8.52), (8.53) and (8.56). Substituting  $Dq_cD$  for  $q_c$  and  $Wq_rW$  for  $q_r$ , and rearranging,

$$Fh_F = D(h_D + q_cD) + W(h_W - q_rW) \quad (8.73)$$

From Eqs. (8.53) and (8.73), it is evident that the points  $(x_F, h_F)$ ,  $(x_D, h_D + q_cD)$  and  $(x_W, h_W - q_rW)$  must lie on a straight line. The first two points are known and a line through them intersects the vertical line  $x = x_W$  at the desired point.

On the basis of the above analysis, the steps involved in determination of the number of theoretical plates for rectification by Ponchon-Savarit method have been summarised below and shown in Figure 8.20.

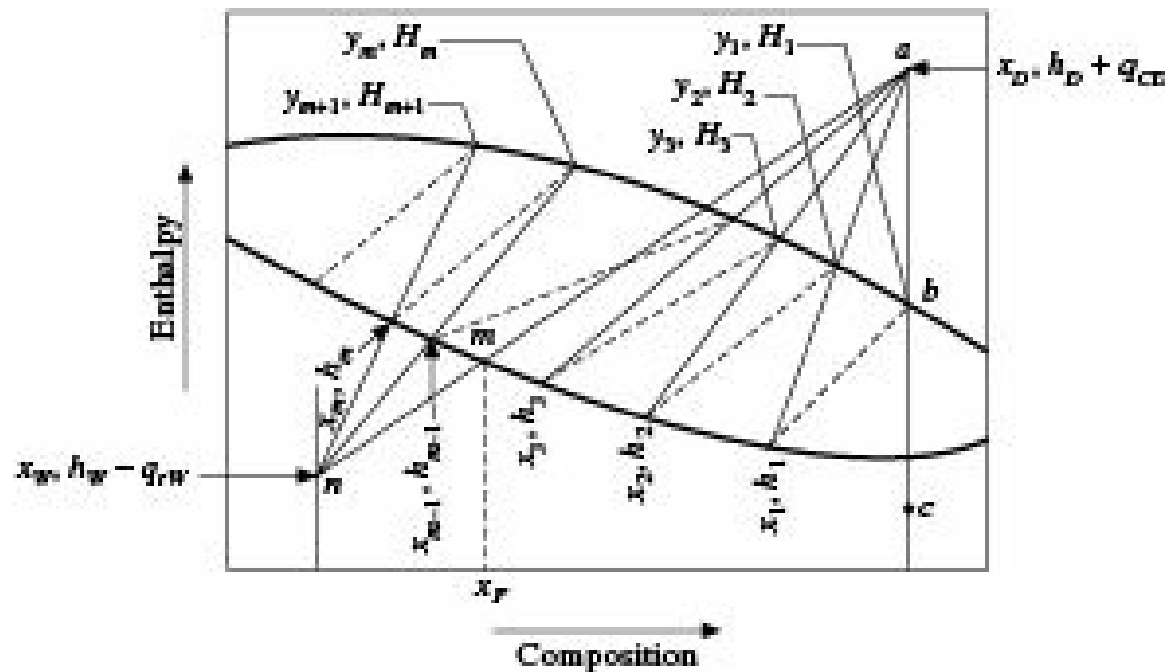


Figure 8.20 Graphical solution on enthalpy-composition diagram.

1. The saturated vapour and saturated liquid curves are drawn on enthalpy-composition co-ordinates. The points  $x_D$ ,  $x_F$  and  $x_W$  are located on the abscissa and vertical lines are drawn through them.
2. The point  $(x_D, h_D + q_cD)$  is next located. The value of  $(h_D + q_cD)$  can be directly calculated if the necessary enthalpy data are available. Alternatively, the point  $a$  can be located from the relation  $\frac{ab}{bc} = L_0/D$ , where the point  $c$  represents the enthalpy of the reflux.
3. The point of intersection of the vertical line  $x = x_F$  and the saturated liquid line is denoted by  $m$ . Points  $a$  and  $m$  are joined and extended to meet the vertical line  $x = x_W$  at the point  $(x_W, h_W - q_rW)$ .
4. From  $y-x$  data, a tie line is drawn from the point  $b$  to meet the saturated liquid line at  $(x_1, h_1)$ .
5. The point  $(x_D, h_D + q_cD)$  and  $(x_1, h_1)$  are joined and the line intersects the saturated vapour line at  $(y_2, H_2)$ . A tie line through  $(y_2, H_2)$  gives  $(x_2, h_2)$  and so on.
6. As soon as the line  $x = x_F$  is crossed the point  $(x_W, h_W - q_rW)$  denoted by  $n$  is joined with  $(x_{m-1}, h_{m-1})$  to give  $(y_m, H_m)$ . A tie line through  $(y_m, H_m)$  gives  $(x_m, h_m)$ . This procedure is repeated

till the vertical line  $x = x_W$  is reached. The number of tie lines gives the number of theoretical plates required for the given separation. Feed should be introduced on the plate for which the tie line crosses the vertical line  $x = x_F$ . Feed may be introduced on a different plate, but in that case the number of theoretical plates required will be more.

### • Minimum Number of Theoretical Plates

From Eq. (8.60) it may be seen that as the reflux ratio ( $L_0/D$ ) is increased,  $q_{cD}$  and hence  $(h_D + q_{cD})$  increases. For total reflux ( $L_0/D$ ) is infinity, consequently  $(h_D + q_{cD})$  also becomes infinity. The point  $a$  moves to infinity and the operating lines become vertical. This sets the condition for minimum number of theoretical plates, which corresponds to total reflux. For determination of minimum number of theoretical plates, it is not necessary to locate the points  $(x_D, h_D + q_{cD})$  or  $(x_W, h_W - q_{rW})$ . Vertical operating lines are drawn from the lower ends of the tie lines and the number of tie lines gives the minimum number of theoretical plates.

### • Minimum Reflux

If at any section of a distillation column a tie line touches or crosses an operating line, equilibrium will be established there and infinite number of plates will be required for the section. Hence slopes of operating lines must always be greater than the slopes of the corresponding tie lines. This sets the condition for minimum reflux. For the section above the feed plate that tie line which gives the highest value of  $(h_D + q_{cD})$  and for the section below the feed plate that tie line which gives the lowest value of  $(h_W - q_{rW})$ , sets the condition for minimum reflux.

In order to determine the minimum reflux in the section above the feed plate, the vertical line  $x = x_D$  is drawn and a number of tie lines are drawn at random. The highest point of intersection of any tie line with the vertical line  $x = x_D$  is denoted by  $a'$  and then the minimum reflux is determined from the relation

$$\left(\frac{L_0}{D}\right)_{\min} = \frac{a'b}{bc}$$

### **McCabe-Thiele method**

If the saturated vapour and saturated liquid lines on the enthalpy-composition diagram are straight and parallel, then a simpler method known as McCabe-Thiele method may be developed. This may happen if the enthalpies and latent heats of vaporisation of both the components are same. Since molal enthalpies of many systems are very close, this method gives fairly reliable results if all quantities are expressed in terms of moles and all compositions are expressed in mole fraction.

McCabe-Thiele method is very simple and permits quick estimation of the number of theoretical plates on  $y-x$  diagram.

In Figure 8.21, the enthalpy-composition lines are straight and parallel.

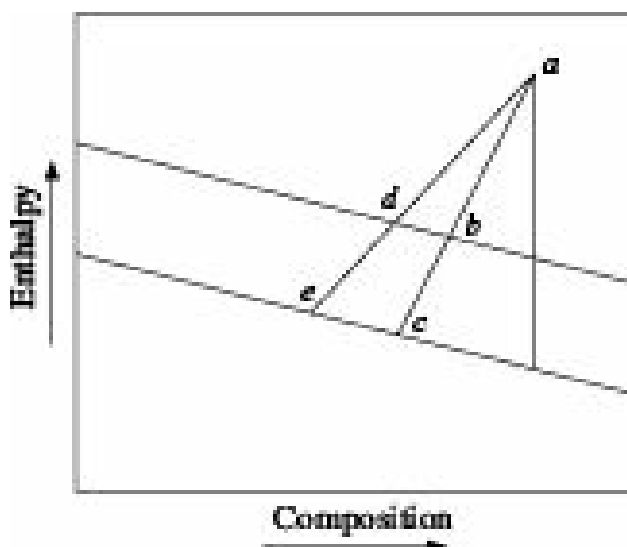


**Figure 8.21** Straight and parallel enthalpy-composition lines.

Therefore, the triangles  $abd$  and  $ace$  are similar, and

$$\frac{\overline{ab}}{\overline{ac}} = \frac{\overline{ad}}{\overline{ae}} \text{ or } \frac{L_1}{V_2} = \frac{L_2}{V_3}$$

We may therefore write,

$$\frac{L_1}{V_2} = \frac{L_2}{V_3} = \dots = \frac{L_{n-1}}{V_n} = \frac{L_n}{V_{n+1}} = K(\text{say})$$

$$\text{or, } L_{n-1} = KV_n, L_n = KV_{n+1} \quad (8.74)$$

By a material balance around plate  $n$ , (Figure 8.22)

$$L_{n-1} + V_{n+1} = L_n + V_n \quad (8.75)$$

$$\text{or, } KV_n + V_{n+1} = KV_{n+1} + V_n \quad (8.76)$$

$$\text{or, } V_n(K - 1) = V_{n+1}(K - 1)$$

$$\text{whence, } V_n = V_{n+1} \text{ and } L_n = L_{n+1} \quad (8.77)$$

The above statement can be generalised by writing

$$V_1 = V_2 = V_3 = \dots = V_{n+1} \quad (8.78)$$

$$\text{and } L_1 = L_2 = L_3 = \dots = L_n \quad (8.79)$$

Similarly, for the section below the feed plate

$$V_m = V_{m+1} = V_{m+2} \quad (8.80)$$

$$\text{and } L_{m-1} = L_m = L_{m+1} \quad (8.81)$$

$$\frac{L_0}{V_1} = \frac{L_1}{V_2}$$

If the reflux is not much sub-cooled, then

From Eqs. (8.78) to (8.81), it is evident that the amounts of vapour rising from each plate are equal separately for the sections above and below the feed plate.

Also, the liquids flowing down each plate are equal separately for the two sections. These are known

a s *constant molal vaporisation* and *constant molal overflow*, and are the basic assumptions of McCabe-Thiele Method.

### • Section above the feed plate

Overall material balance and more volatile component balance for the section above the feed plate, shown in Figure 8.22, are

$$V_{n+1} = L_n + D \quad (8.82)$$

$$V_{n+1}y_{n+1} = L_nx_n + DxD \quad (8.83)$$

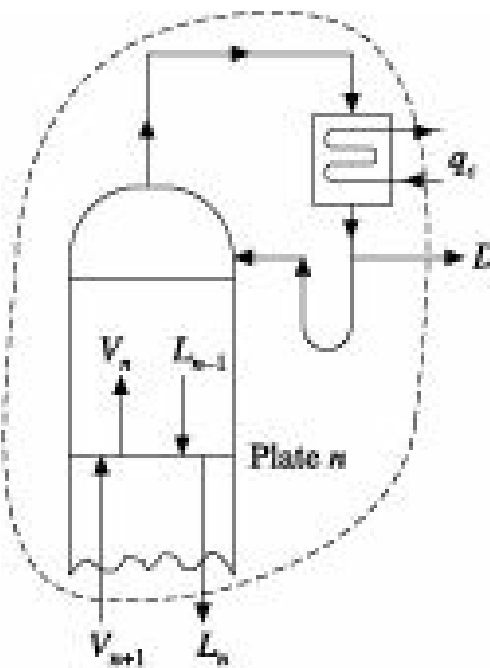


Figure 8.22 Section above feed plate.

Since the vapour and liquid streams leaving each plate are constant in amount in molal units, the subscripts of  $V$  and  $L$  may be dropped.

Eliminating  $V$  from Eq. (8.83), we obtain

$$y_{n+1} = \frac{L}{L+D} x_n + \frac{D}{L+D} x_D$$

Denoting the reflux ratio ( $L/D$ ) by  $R$ , the above equation becomes

$$y_{n+1} = \frac{R}{R+1} x_n + \frac{x_D}{R+1} \quad (8.84)$$

Equation (8.84) is the equation of the operating line for the section above the feed plate. It is an

equation representing a straight line having a slope of  $\frac{R}{R+1}$ , an intercept of  $\frac{x_D}{R+1}$  and passing through the point  $x = x_D, y = x_D$ .

### • Section below the feed plate

For this section, the operating line becomes

$$y_m = \frac{\bar{L}}{\bar{L}-W} x_{m-1} - \frac{Wx_W}{\bar{L}-W} \quad (8.85)$$

where,  $\bar{L}$  is the molal flow rate of liquid below the feed plate. Since  $\bar{L}$  is different from  $L$  and it is very difficult to estimate  $\bar{L}$ , the lower operating line is located from a knowledge of its point of intersection with the upper operating line. The lower operating line passes through the point  $x = x_W$ ,  $y = x_W$ .

The locus of the points of intersection of the two operating lines can be represented by the equation

$$y = \frac{q}{q-1}x - \frac{x_F}{q-1} \quad (8.86)$$

where,  $q$ , the fraction of liquid in a mixture of liquid and vapour, is represented by

$$q = \frac{\bar{L} - L}{F}.$$

Equation (8.86) can be derived in the following way:

Let us consider the equations relating to material balance for sections above and below feed plates as

$$V_n y_n - L_{n-1} x_{n-1} = D x_D \quad (i)$$

$$L_{m-1} x_{m-1} - V_m y_m = W x_W \quad (ii)$$

As stated earlier, the upper and lower operating lines will intersect at a point. If the point of intersection be denoted by  $(y_p, x_p)$ , above Eqs. (i) and (ii) can be written as

$$V_n y_p - L_{n-1} x_p = D x_D \quad (iii)$$

$$L_{m-1} x_p - V_m y_p = W x_W \quad (iv)$$

Considering the assumptions of constant molar heat of vaporisation as well as of no heat of mixing and of no heat losses, one can have constant molar reflux as well as constant molar vapour flow in any section of the column, i.e.  $L_{m-1} = L_m$  and  $V_n = V_{n-1}$ . Hence, Eqs. (iii) and (iv) can be rewritten respectively as

$$V_n y_p = L_n x_p + D x_D \quad (v)$$

$$V_m y_p = L_m x_p - W x_W \quad (vi)$$

Subtracting Eq. (v) from Eq. (vi), one can have

$$y_p (V_m - V_n) = x_p (L_m - L_n) - (D x_D + W x_W) \quad (vii)$$

The material balance over feed plate gives rise to

$$F + V_m + L_{n-1} = L_{m-1} + V_n \quad (viii)$$

or,

$$V_m - V_n = L_{m-1} - L_{n-1} - F = L_m - L_n - F \quad (ix)$$

As the contribution of the feed stream to the internal flow of liquid is  $qF$  and the contribution of the feed stream to the internal flow of vapour is  $F(1 - q)$ , the total flow rate of reflux in the section below the feed plate and the total flow rate of vapour in the upper section of the feed plate can be represented respectively by

$$L_m^{(\bar{L})} = L_n(L) + qF \text{ or } L_m^{(\bar{L})} - L_n(L) = qF$$

and

$$V_m(\bar{V}) - V_n(V) = qF - F = F(q - 1).$$

Hence, Eq. (vii) can be rewritten as

$$y_p F(q - 1) = x_p qF - (Dx_D + Wx_W) = x_p qF - FxF \quad (\text{x})$$

$$y_p = \frac{q}{q-1} x_p - \frac{x_F}{q-1} \quad (\text{xi})$$

When  $x_p = x_F$ ,  $y_p$  becomes equal to  $x_F$  indicating that the point of intersection of the upper and lower operating lines lies on the straight line of slope  $q/(q - 1)$  and passes through the point  $(x_F, x_F)$ .

Deleting the subscripts of the above equation, we have derived Eq. (8.86)

$$y = \frac{q}{q-1} x - \frac{x_F}{q-1}$$

Alternatively,

If the feed is a mixture of liquid and vapour,  $q$  is the fraction that is liquid. Let the concentration of the more volatile component in the feed is  $x_F$ . Such a feed may be produced by an equilibrium flash operation, so  $q = 1 - f$ , where  $f$  is the fraction of the original stream vaporised in the flash (as in Figure 8.10). Then  $(1 - f)$  is the fraction of feed that leaves continuously as liquid. Let  $y_D (=x_D)$  and  $x_W$  be the concentrations of the vapour and liquid, respectively. By a material balance of the more volatile component based on 1 mol of feed assuming all of that component in the feed must leave in the two exit streams,

$$x_F = fy_D + (1 - f)x_W$$

Replacing  $y_D$  and  $x_W$  by  $y$  and  $x$  respectively, one can write

$$y = -\frac{1-f}{f} x + \frac{x_F}{f}$$

or,

$$y = \frac{q}{q-1} x - \frac{x_F}{q-1}$$

Above derived Eq. (8.86) is called the  $q$ -line. It is an equation of a straight line having a slope of  $\frac{q}{q-1}$  and intersecting the line  $y = x$  at the point  $(x = x_F, y = x_F)$ .

The value of  $q$ , defined as the ratio of the amount of heat required for vaporisation of 1 mol of feed and the molar latent heat of the vapour, can be estimated using the following equation obtained by making enthalpy balance over the feed plate as shown in Figure 8.23:

$$q = \frac{H_f - h_F}{H_f - h_f} \quad (8.87)$$

where

$h_F$  = enthalpy of feed

$H_f$  = enthalpy of vapour leaving feed plate

$h_f$  = enthalpy of liquid leaving feed plate

The natures of the  $q$ -line for different conditions of feed, as shown in Figure 8.24, are:

- (a) When feed is liquid below its boiling point:  $h_F < h_f$ ,  $q = (+)$ ve  $> 1$ , slope of  $q$ -line is positive and greater than 1 ( $PA$ ).
- (b) When feed is liquid at its boiling point:  $h_F = h_f$ ,  $q = 1$ , slope of  $q$ -line is infinity, the line is vertical ( $PB$ ).
- (c) Feed is mixture of liquid and vapour:  $h_f < h_F < H_f$ ,  $q = (+)$  ve between 0 and 1, slope of  $q$ -line is negative ( $PC$ );
- (d) Feed is saturated vapour:  $h_F = H_f$ ,  $q = 0$ , slope of  $q$ -line is zero and the line is horizontal ( $PD$ );
- (e) Feed is superheated vapour:  $h_F > H_f$ ,  $q = (-)$ ve, slope of  $q$ -line is positive and lower than 1 ( $PE$ ).

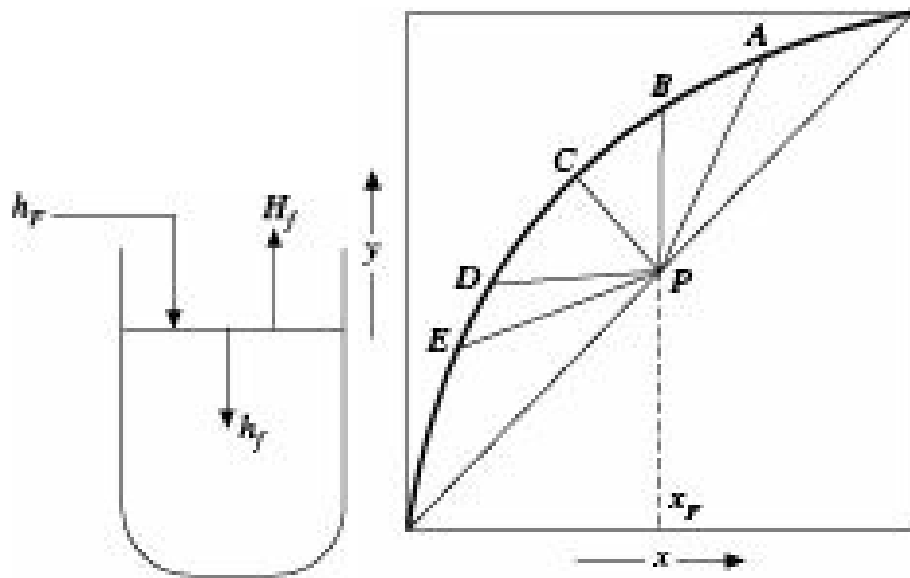


Figure 8.23 Section below feed plate. Figure 8.24 Location of  $q$ -line for different conditions

of feed.

When the feed is liquid at its boiling point,  $q$ -line is vertical and when the feed is saturated vapour, the  $q$ -line becomes horizontal as shown above and can therefore be located without any calculation.

### Summary of McCabe-Thiele method

Summary of steps involved in estimation of number of theoretical plates by McCabe-Thiele method is given below:

**Step 1** Equilibrium curve on molal basis and the diagonal ( $y = x$ ) are drawn on  $y$ - $x$  co-ordinates as shown in Figure 8.25

**Step 2**  $q$  is calculated from Eq. (8.87), and  $q$ -line from Eq. (8.86) by drawing a line of slope  $\frac{q}{q-1}$  through the point ( $x = x_F$ ,  $y = x_F$ ). If feed is liquid at its boiling point,  $q$ -line is vertical and if the feed is saturated vapour,  $q$ -line is horizontal.

**Step 3** Upper operating line is located by joining the points ( $x = x_D$ ,  $y = x_D$ ) and  $\left(0, \frac{x_D}{R+1}\right)$

**Step 4** Lower operating line is drawn by joining the points ( $x = x_W$ ,  $y = x_W$ ) with the point of intersection of the upper operating line and the  $q$ -line.

**Step 5** Starting at the point ( $x = x_D$ ,  $y = x_D$ ) horizontal and vertical steps are drawn between the equilibrium curve and the respective operating lines till the vertical line through  $x = x_W$  is reached as shown in Figure 8.25.

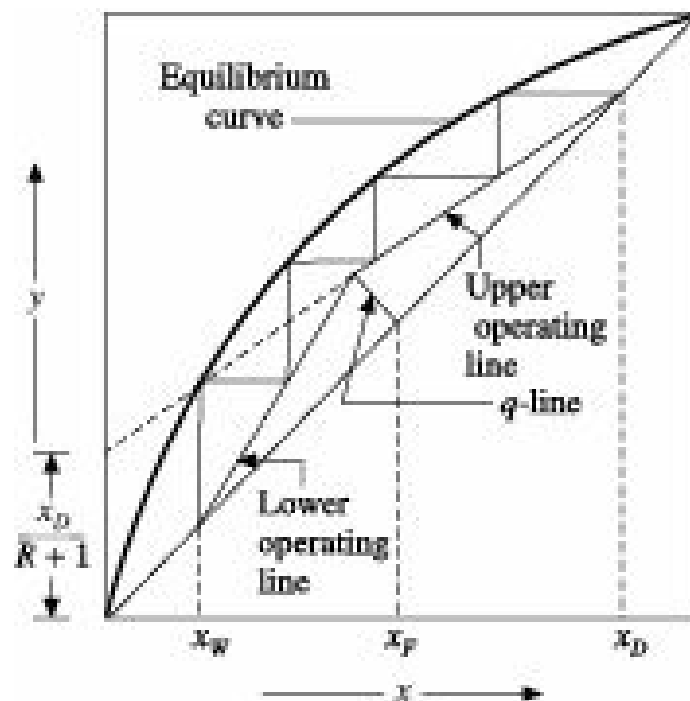


Figure 8.25 Graphical solution by McCabe– Thiele method.

The number of steps so drawn gives the number of theoretical plates or stages required for the given separation. Feed should be introduced on the plate for which the horizontal line of the step is intersected by the  $q$ -line.

In fact, introduction of feed demarcates the enriching and stripping sections of the column. It also changes the operating line for the enriching section to that for the stripping section.

Sometimes, feed is being introduced into the column in more than one location for having the same distillate and bottom product as in case of the feed in a single column. In such situation, the operating lines will be drawn in the same fashion as in case of a single feed. However, the number of operating lines will be number of feed location plus one.

#### • Minimum Number of Theoretical Plates

As the reflux ratio increases, the value of the intercept  $x_D/(R + 1)$  decreases. Finally, for total reflux the intercept becomes zero, and both upper and lower operating lines coincide with the diagonal. This gives the condition for minimum number of theoretical plates, which occur at total reflux and may be obtained by drawing steps between the equilibrium curve and the diagonal.

#### • Minimum Reflux

When the reflux in the column becomes less than the total, the requirement of number of plates in the column becomes more than that required for the operation at total reflux condition, and the requirement increases with decrease in reflux ratio. On gradual decrease in reflux ratio, a point will ultimately be reached when the requirement of the number of plates will be maximum. This is known as minimum reflux ratio. In such situation, the number of theoretical plates or stages required for the

desired separation will be infinite. In fact when the reflux is reduced, the value of  $x_D/(R + 1)$  gets increased. The highest possible value of  $x_D/(R + 1)$  corresponds to the location of the upper operating line when it passes through the point of intersection of the equilibrium curve and the  $q$ -line. This sets the condition for minimum reflux since on further reduction in reflux, the upper operating line will have to cross the equilibrium curve which is impossible.

If  $x'$  and  $y'$  are the co-ordinates of the point of intersection of the equilibrium curve and the  $q$ -line, then

$$\frac{R_{\min}}{R_{\min} + 1} = \frac{x_D - y'}{x_D - x'}$$

$$R_{\min} = \frac{x_D - y'}{y' - x'} \quad (8.88)$$

**EXAMPLE 8.7** (Minimum reflux ratio and minimum number of theoretical plates in rectification): Pentane has a relative volatility of 3.15 with respect to hexane. A rectification column is fed with an equimolal mixture of pentane and hexane. The feed is 50% vaporised. The top product should contain 90 mol% pentane and the bottom product should contain 90 mol% hexane.

Determine the minimum reflux ratio and the minimum number of theoretical plates for the operation.

**Solution:** Relative volatility,  $\alpha = 3.15$

$$y^* = \frac{\alpha x}{1 + (\alpha - 1)x} = \frac{3.15x}{1 + 2.15x}$$

From the above equation, equilibrium values for the system are calculated as under:

$x:$	0	0.10	0.20	0.40	0.60	0.80	1.00
$y^*:$	0	0.259	0.440	0.677	0.825	0.926	1.00

where  $x$  and  $y^*$  are mole fractions of pentane in liquid and vapour, respectively.

The equilibrium curve is drawn as in Figure 8.26 on the basis of the above data, and the diagonal is located.

Given:  $x_F = 0.50$ ,  $x_D = 0.90$ ,  $x_W = 0.10$  mole fraction.

$q$ -line is  $45^\circ$  inclined, since for saturated liquid the same is vertical and for saturated vapour it is horizontal.

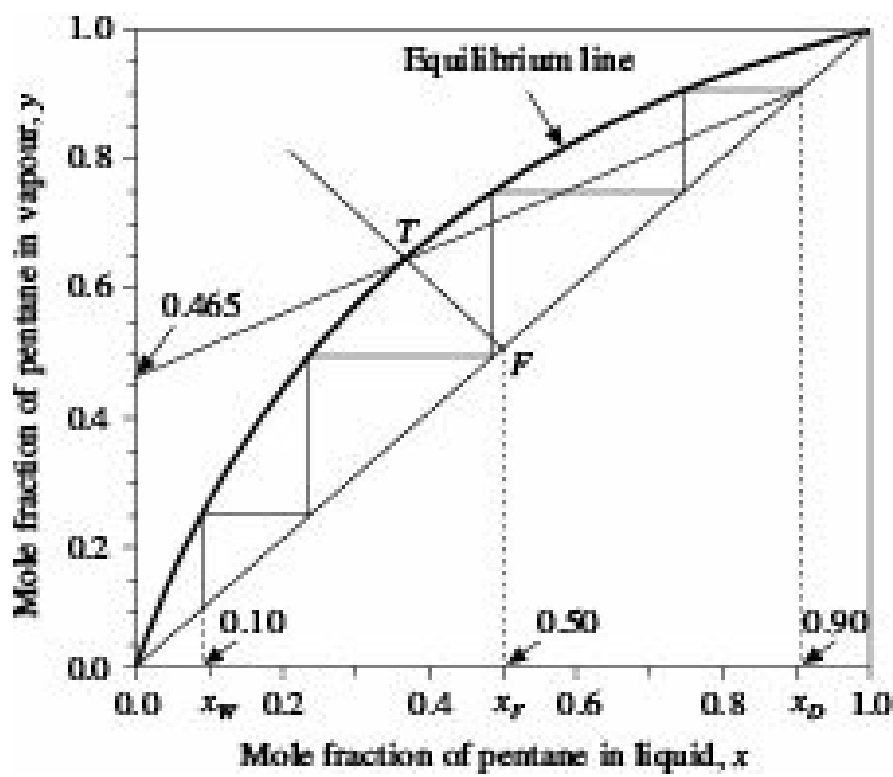


Figure 8.26 Example 8.7.

The upper operating line for minimum reflux is drawn through the point ( $x = x_D$ ,  $y = x_D$ ), and the point of intersection of the equilibrium curve and the  $q$ -line.

From the Figure 8.26, intercept of the upper operating line for minimum reflux = 0.465

$$\frac{x_D}{R_{\min} + 1} = \frac{0.90}{R_{\min} + 1} = 0.465$$

whence,  $R_{\min} = 0.935$ , i.e. minimum reflux = 0.935

By drawing steps between the equilibrium curve and the diagonal (since the diagonal and operating lines coincide at total reflux condition) from  $x_D = 0.90$  till it crosses the value of  $x = x_W = 0.10$ , the minimum number of theoretical plates was found to be 4.

### Fenske–Underwood Equation

If the relative volatilities of the components are more or less constant and use of average value is justified, then a simple analytical expression known as Fenske-Underwood equation (Fenske 1931, Underwood 1932) can be developed for the minimum number of theoretical plates or stages, which correspond to the condition of total reflux.

In Eq. (8.5), relative volatility has been defined as

$$a = \frac{\frac{y^*}{1-y^*}}{\frac{x}{1-x}}$$

Applying this equation to the bottom product, we get

$$\frac{y_W}{1-y_W} = \alpha_W \frac{x_W}{1-x} \quad (8.89)$$

where  $a_W$  is the relative volatility at the reboiler. At total reflux, the operating line and the diagonal coincide so that  $y_W = x_{N_m}$ ,

$$\text{whence, } \frac{x_N}{1-x_N} = a_W \frac{x_W}{1-x_W} \quad (8.90)$$

Similarly, for the bottom plate of the column

$$\frac{y_N}{1-y_N} = \alpha_{N_m} \frac{x_N}{1-x_N} = \alpha_{N_m} \alpha_W \frac{x_W}{1-x_W} \quad (8.91)$$

This procedure may be continued along the column up to the top plate, when

$$\frac{y_1}{1-y_1} = \frac{x_D}{1-x_D} = a_1 a_2 \dots \alpha_{N_m} \alpha_W \frac{x_W}{1-x_W} \quad (8.92)$$

If some average relative volatility  $a_{av}$  may be used, then

$$\frac{x_D}{1-x_D} = a_{av}^{N_m+1} \frac{x_W}{1-x_W} \quad (8.93)$$

or,

$$N_m + 1 = \frac{\log \left[ \left( \frac{x_D}{1-x_D} \right) \left( \frac{1-x_W}{x_W} \right) \right]}{\log a_{av}} \quad (8.94)$$

Thus if  $x_D$ ,  $x_W$  and  $a_{av}$  are known, then the minimum number of theoretical plates ( $N_m$ ) may be determined from the simple analytical expression presented in Eq. (8.94). If the value of the relative volatility changes appreciably in between top and bottom of the distillation column, a geometric mean of the extreme values can be considered as a wise choice.

### • Optimum Reflux

Any reflux ratio between minimum and infinity may be used for a given separation. As the reflux ratio increases from the minimum, the number of plates required for a particular separation decreases dramatically initially and then slowly till the requirement becomes minimum at total reflux. With the increase in reflux ratio the column diameter increases resulting the increase of plate area required,

and such increase becomes more rapid than the decrease in number of plates up to certain values of liquid and vapour flow rates. The fixed cost incurred due to column and plates, therefore, initially decreases followed by its increase with reflux ratio. The operating cost for supplying heat to the reboiler and withdrawing the same at the condenser increases with increase in reflux ratio. As a result, the total cost for operation comprising fixed and operating costs, initially decreases, attains a minimum and thereafter increases with the increase in reflux ratio. The reflux ratio corresponding to the least cost is known as the *optimum reflux ratio* for economical operation of the tower. However, the column in process industries is operated at reflux ratio higher than the optimum, generally in a range of 1.2 to 2.0 times the minimum reflux ratio; the total cost does not change appreciably and better operational flexibility is obtained.

The design of a distillation column largely depends on the reflux ratio. For instance, at minimum reflux, a column requires infinite number of plates and the fixed cost becomes infinite. But the operating costs for reboiler, condenser, and reflux pump, etc. are minimum.

As the reflux ratio is increased, the number of trays decreases but the column diameter increases due to larger quantities of recirculated liquid and vapour per unit of product. The reboiler, condenser and reflux pump must also be larger. The fixed cost therefore passes through a minimum and rises again to infinity for total reflux. The operating cost consisting of heating and cooling, pumping cost as well as general maintenance charges, increases almost directly with reflux ratio as shown in Figure 8.27. The total cost which consists of fixed and operating costs must therefore pass through a minimum and the corresponding reflux is the optimum reflux. Generally, but not always, the optimum reflux would be 20 to 50% higher than the minimum reflux.

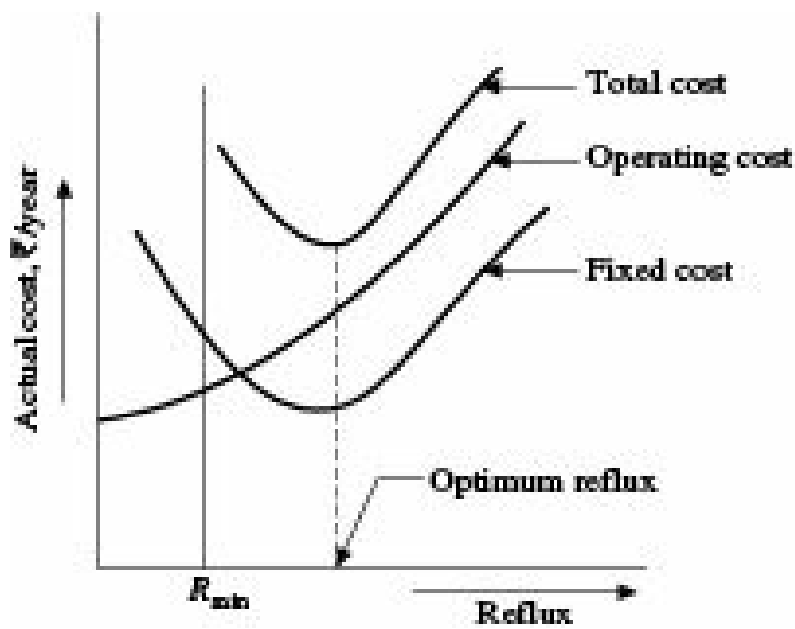


Figure 8.27 Determination of optimum reflux.

## 8.6 Use of Open Steam

When an aqueous solution of a more volatile nonaqueous substance is fractionated, the nonaqueous substance being more volatile is collected as distillate and water leaves at the bottom as residue. In such cases, the heat required can be provided by introducing open steam directly to the bottom of the tower and the reboiler can be eliminated. For a given distillate composition and reflux ratio, the number of plates required may be slightly more, but the additional cost involved will be more than compensated by savings in cost of the reboiler and its maintenance.

The enriching section of the column remains unaffected by the use of open steam and hence, the operating line in this section remains unchanged. But the operating line in the stripping section changes. The material balance equation for the more volatile component in the stripping section becomes,

$$\bar{L}x_m + \bar{G}(0) = \bar{G}y_{m+1} + Wx_W \quad (8.95)$$

Since there is no reboiler,

$$\bar{L} = W, \text{ and } \bar{L}x_m = \bar{G}y_{m+1} + \bar{L}x_W$$

$$\frac{\bar{L}}{\bar{G}} = \frac{y_{m+1}}{x_m - x_W} \quad (8.96)$$

or,

Equation (8.96) provides the slope of the lower operating line.

Open steam can also be used when there is chance of partial condensation of the vapour in the upper part of the column.

## 8.7 Side Stream

Sometimes products of intermediate composition are required to be withdrawn from different locations (intermediate plates) along the height of the column. These are termed as side streams. Such phenomena are very frequently encountered in distillation of petroleum crude. Side streams are rarely used in binary distillation.

## 8.8 Plate Efficiency

No actual plate can operate as a theoretical plate, so that the vapour leaving any actual plate is weaker in more volatile components than the vapour in equilibrium with the liquid on the plate. This calls for a larger number of actual plates than theoretical plates for a given separation. The performance of a plate is judged by its efficiency, which is a measure of the degree of perfectness attained by a plate or a group of plates.

There are three types of plate efficiencies used in practice:

### *Overall plate efficiency*

Overall plate efficiency is defined as hundred times the ratio of number of theoretical plates to that of actual plates required for a stipulated separation:

$$E_O = \frac{\text{No. of theoretical plates}}{\text{No. of actual plates}} \times 100 \quad (8.97)$$

where,  $E_O$  is the overall efficiency.

The concept of overall plate efficiency is too much over simplification since it does not distinguish between the performances of different plates.

### *Murphree plate efficiency*

Referring to Figure 8.28, the Murphree plate efficiency for any plate  $n$  is defined as

$$E_M = \frac{\frac{y_n - y_{n+1}}{y_n^* - y_{n+1}}}{\frac{y_n^* - y_{n+1}}{\text{Theoretical enrichment}}} \times 100 = \frac{\text{Actual enrichment}}{\text{Theoretical enrichment}} \times 100 \quad (8.98)$$

where  $y_n^*$  is the equilibrium value corresponding to  $x_n$ .

Murphree plate efficiency gives the performance of a single plate and is much more reliable than overall efficiency. However, in case of very large diameter plates, efficiency may not be the same all over the plate due to non-uniform distribution of liquid and vapour. In such cases Murphree point efficiency which is the efficiency of a single point on a plate, may be used. Detailed discussions on plate efficiency has been made in Chapter 6.

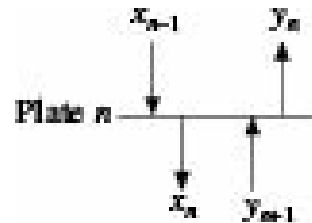


Figure 8.28 Composition of streams around Plate  $n$ .

**EXAMPLE 8.8** (Determination of number of plates using overall efficiency): A continuous rectification column with a reboiler and a total condenser is to be designed to separate a solution of *n*-heptane and octane having 70 mol% *n*-heptane. The overhead and bottom products should contain 95 and 5 mol% *n*-heptane, respectively. The feed will be liquid at its boiling point and the reflux ratio will be 1.80 times the minimum reflux. The column is to operate at a pressure of 101.33 kN/m<sup>2</sup>.

- (a) Assuming the overall plate efficiency to be 70%, determine the number of plates to be provided in the column.

Equilibrium data for the system are as under:

$x$ :	0	0.13	0.22	0.32	0.46	0.57	0.69	0.82	0.92	1.00
$y^*$ :	0	0.24	0.37	0.50	0.65	0.74	0.83	0.91	0.96	1.00

where  $x$  and  $y^*$  are mole fractions of *n*-heptane in liquid and vapour, respectively.

- (b) If an identical tower but having 16 plates is employed for the above separation with the same operating conditions, what will be the overall plate efficiency of the column?

**Solution:** The equilibrium curve is drawn in Figure 8.29 from the given equilibrium data. The diagonal is also drawn.

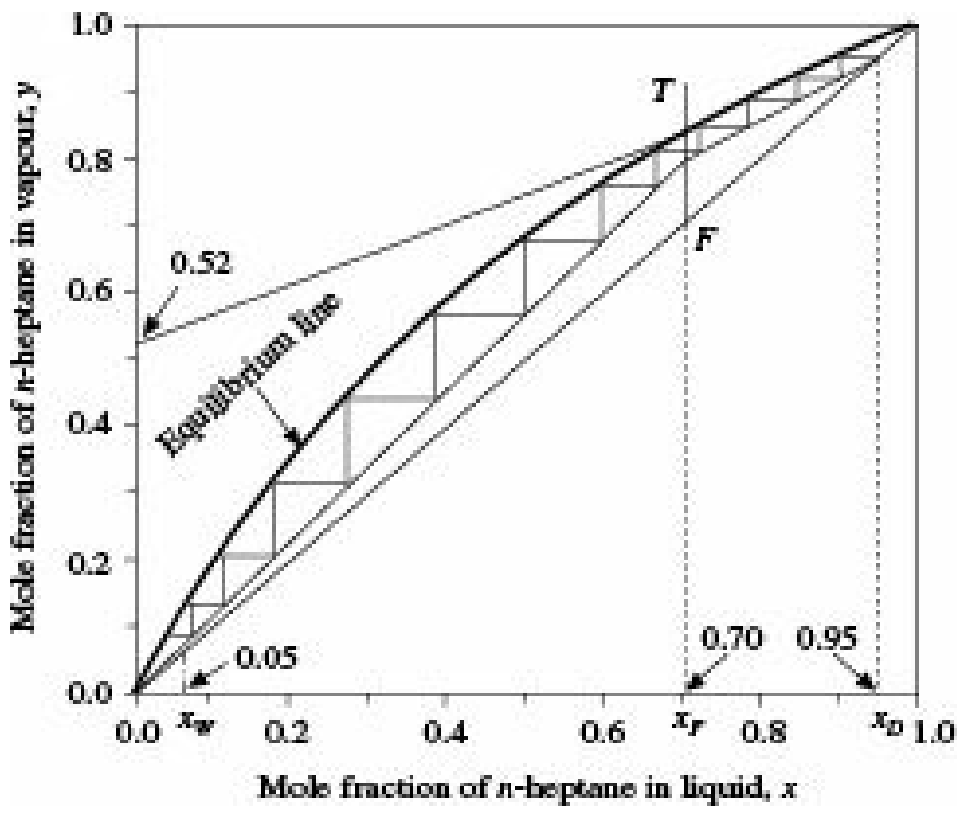


Figure 8.29 Example 8.8.

Given:  $x_F = 0.70$ ,  $x_D = 0.95$ ,  $x_W = 0.05$  mol fraction.

The  $q$ -line is vertical since feed is saturated liquid.

For minimum reflux, the upper operating line is drawn to pass through the point ( $x = 0.95$ ,  $y = 0.95$ ) and the point of intersection of the equilibrium curve and the  $q$ -line.

From the figure, intercept for upper operating line = 0.52.

$$\frac{x_D}{R_{\min} + 1} = \frac{0.95}{R_{\min} + 1} = 0.52$$

whence,  $R_{\min} = 0.83$

$$R_{\text{op}} = (1.80 \# 0.83) = 1.494,$$

$$\frac{0.95}{R_{\text{op}} + 1} = \frac{0.95}{1.494 + 1} = 0.38$$

The operating lines are located and steps are drawn between equilibrium curve and respective operating line.

(a) From the curve, number of theoretical plates = 12.4

$$\text{Number of actual plates} = \frac{\frac{12.4 - 1}{0.70}}{16} = 16.29 \approx 17$$

When 16 plates are provided ,

$$E = \frac{\frac{(12.4 - 1) \times 100}{16}}{16} = 71.25\%$$

## 8.9 Continuous Differential Contact Distillation—Packed Tower

In distillation practice packed towers are sometimes preferred to plate towers, particularly where

pressure drop must be low as in low pressure distillation or where liquid hold-up must be small as in distillation of heat sensitive materials requiring minimum exposure to high temperature. Figure 8.30 shows a schematic diagram of a packed fractionating column. The column is provided with a reboiler at the bottom, a condenser at the top with a reflux regulator for regulating the reflux rate, and a device for introducing the feed. The feed is generally introduced into a short unpacked section at the feed entry with adequate provision of distributing the feed over the top of the exhausting section.

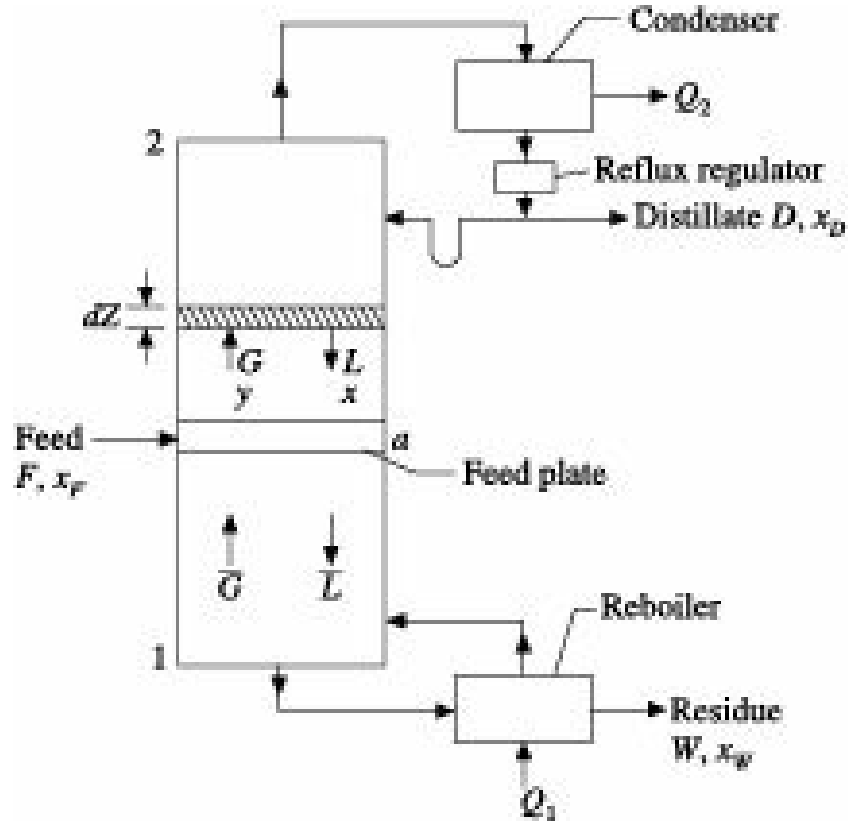


**Figure 8.30** Packed fractionating column.

The operating diagram shown in Figure 8.31 is drawn in a manner similar to that for plate towers. Calculations may be made on enthalpy-composition diagram by the Ponchon-Savarit method or by the McCabe-Thiele method if the simplifying assumptions of this method are applicable. Graphical solution is similar to that for plate towers except that the tray numbers are not required. The operating lines now represent the bulk liquid composition ( $x$ ) and bulk vapour composition ( $y$ ) prevailing in each horizontal section of the tower. As in case of plate towers the change in operating line from enriching section to exhausting section is done at the point where the feed actually enters.

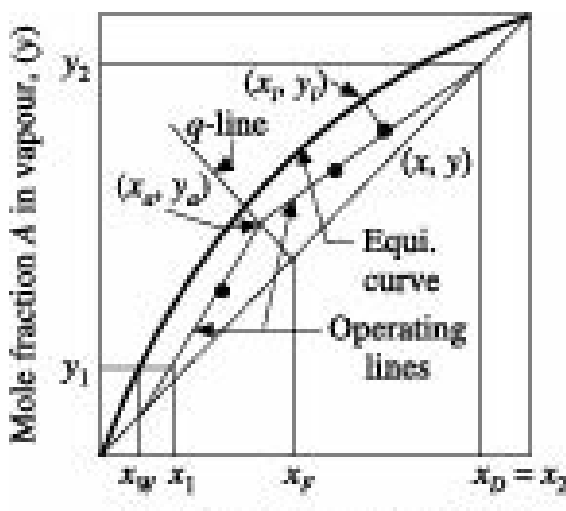


Figure 8.31 Operating diagram for fractionation in packed column.

In packed towers, rates of flow are based on unit tower cross section. Accordingly, in the differential volume  $dZ$  the interfacial area is  $(a \cdot dZ)$  where  $a$  is the specific area of the packing ( $L^2/L^3$ ). The amount of component  $A$  in the vapour passing through the differential section is  $(Gy)$  and the rate of mass transfer is  $d(Gy)$ . Since  $G$  and  $L$  are more or less constant in equimolar counter-diffusion,  $N_A = -N_B$  and the mass transfer flux is

$$N_A = \frac{d(Gy)}{a \cdot dZ} = k_y(y_i - y)$$

$$= \frac{d(Lx)}{a \cdot dZ} = k_x(x - x_i) \quad (8.99)$$

$$Z = \int_0^{z_e} dz = \int_{(Gy)_e}^{(Gy)_2} \frac{d(Gy)}{k_y a (y - y)}$$

Therefore,

$$= (Lx)_2 \int_{(Lx)_e}^{(Lx)_2} \frac{d(Lx)}{k_x a (x - x_i)} \quad (8.100)$$

A similar expression with appropriate integration limits can be used for the stripping section. For any point  $(x, y)$  on the operating line, the corresponding point  $(x_i, y_i)$  on the equilibrium curve may be obtained at the intersection of a line of slope  $(-k_x a/k_y a)$  drawn from the point  $(x, y)$  as shown in Figure 8.31.

If the simplifying assumptions are applicable, both  $G$  and  $L$  within any section of the tower can be assumed to be constant and the heights of transfer units

$$H_t G = \frac{G}{k_y a} \text{ and } H_t L = \frac{L}{k_x a}$$

become more or less constant or else their average values can be used so that Eq. (8.100) can be written as

$$Z = H_t G \int_{x_a}^{x_2} \frac{dy}{y^* - y} = H_t G \cdot N_t G \quad (8.101)$$

$$= H_t L \int_{x_a}^{x_2} \frac{dx}{x - x^*} = H_t L \cdot N_t L \quad (8.102)$$

with similar expression for the stripping section, where  $x_a$  and  $y_a$  are the co-ordinates of the operating line intersection.

Ordinarily, the equilibrium curve will not be straight since its slope changes throughout the tower. However, if the equilibrium line may be taken as straight, at least within the range of concentration involved, overall transfer units can be used.

$$Z = H_t o G \int_{x_a}^{x_2} \frac{dy}{y^* - y} = H_t o G \cdot N_t o G \quad (8.103)$$

$$Z = H_t o L \int_{x_a}^{x_2} \frac{dx}{x - x^*} = H_t o L \cdot N_t o L \quad (8.104)$$

$$H_t o G = \frac{G}{K_y a}, H_t o L = \frac{L}{K_x a} \quad (8.105)$$

## 8.10 Multicomponent Distillation

Many industrial distillation operations involve more than two components. The principles of calculation in multicomponent distillation are basically the same as those for binary systems. However, the presence of several components and the absence of reliable vapour-liquid equilibrium data make the calculations for multicomponent distillation much more complex. Since mathematical treatment of multicomponent systems requires extensive trial and error calculations, high speed computers are often indispensable for such calculations.

A single fractionator cannot separate more than one component in reasonably pure state from a multicomponent solution. Therefore, ( $N - 1$ ) fractionators are required for complete separation of a multicomponent solution having  $N$  components.

### **Key component**

The term key component is very common in multicomponent distillation. Calculations in multicomponent distillation are usefully based on key components. The two components in the feed whose concentrations are specified in the distillate and in the bottom product, are called the *key components*. The more volatile of the two key components that concentrate in the distillate is called the *light key*, the less volatile one is called the *heavy key*. All other components which distribute themselves between the distillate and the bottoms are non-keys.

Before proceeding to calculate the number of theoretical plates it is necessary to determine the top and bottom compositions as well as the operating conditions like temperature and pressure. As a first approximation, the top and bottom compositions are estimated from the desired concentrations or

recoveries of the key components. The top temperature is usually determined from the temperature of the available coolant. The bubble point of the condensate has to be so adjusted that a temperature difference of 5-10°C is available in the condenser. The condenser pressure can now be estimated and assuming a reasonable pressure drop in the column including the condenser, the reboiler pressure may be estimated. Once the trial compositions and operating conditions at the two ends of the column are fixed, the number of theoretical plates can be determined by using one of the exact methods.

## 8.11 Methods of Calculation

Several authors have proposed different methods for calculations involved in multicomponent distillation. These methods are broadly classified as approximate methods and exact methods.

### 8.11.1 Approximate Methods

#### Fenske Equation

Fenske Eq. (8.94) for minimum number of plates for distillation of a binary mixture under total reflux can be extended to the key components of multicomponent mixtures to determine the minimum number of plates,

$$N_m = \frac{\log \left( \frac{(x_{lkD} D)}{(k_{hkD} D)} \frac{(x_{hkW} W)}{(x_{lkW} W)} \right)}{\log (\alpha_{lk})_{av}} \quad (8.106)$$

where

$N_m$  = minimum number of plates

$x_{lkD}$  and  $x_{lkW}$  = mole fraction of light key in the distillate and the bottom respectively

$x_{hkD}$  and  $x_{hkW}$  = mole fraction of heavy key in the distillate and bottom respectively

$(\alpha_{lk})_{av}$  = geometric mean of the relative volatility of the *LK* (light key) component,  $a_{lkD}$  with respect to the *HK* (heavy key) component,  $a_{lkW}$  being expressed as  $(\alpha_{lk})_{av} = (a_{lkD} a_{lkW})^{0.5}$

Equation (8.106) can then be used to determine the distribution of other components under total reflux

$$\frac{x_{J,D} D}{x_{J,W} W} = (\alpha_{J,av})^{N_m+1} \frac{x_{hkD} D}{x_{hkW} W} \quad (8.107)$$

Having calculated  $N_m$  and  $R_m$ , the number of plates at any reflux ratio  $R$  may be determined by one of the several equations available. The result of such an estimate can act as the starting point of an exact method.

#### Underwood Equation for minimum reflux

Starting with separate mass balance equations for the enriching and stripping sections, Underwood obtained the following equations for the two sections:

For the enriching section,

$$G_{min} = \frac{\sum \frac{\alpha_J D x_{JD}}{L_{min}}}{\alpha_J - \frac{L_{min}}{G_{min} K_{hk}}} \quad (8.108)$$

where  $G$  and  $L$  are the vapour and liquid rates, respectively in the enriching section. For the stripping section,

$$-\bar{G}_{\min} = \frac{\sum \frac{\alpha_I w x_{Iw}}{\alpha_I - \frac{L_{\min}}{G_{\min} K_{hk}}}}{\alpha_I - \frac{L_{\min}}{G_{\min} K_{hk}}} \quad (8.109)$$

where  $\bar{G}$  and  $\bar{L}$  are the vapour and liquid rates, respectively in the stripping section. Further assuming (i) constant relative volatility (by taking the geometric mean of the relative volatilities at the top and at the bottom if they are not equal)

$$\text{and } (ii) \frac{L_{\min}}{G_{\min} K_{hk}} = \frac{L_{\min}}{G_{\min} K_{lk}}$$

the value of this ratio in (ii) lies between the values of the light key and heavy key components, usually of magnitude 1.

Underwood suggested the following equations:

$$1 - q = \frac{\sum \frac{\alpha_I x_{IF}}{\alpha_I - \frac{L_{\min}}{G_{\min} K_{hk}}}}{\alpha_I - \frac{L_{\min}}{G_{\min} K_{hk}}} \quad (8.110a)$$

$$R_{\min} + 1 = \frac{\sum \frac{\alpha_I x_{JD}}{\alpha_I - \frac{L_{\min}}{G_{\min} K_{hk}}}}{\alpha_I - \frac{L_{\min}}{G_{\min} K_{hk}}} \quad (8.110b)$$

where,  $q$  is the fraction of liquid in the feed and  $x_{IF}$  is the mole fraction of component  $I$  in the feed.

Equation (8.108) is known as *Underwood equation*. This equation along with Eq. (8.106) allows to calculate the minimum vapour rate ( $G_{\min}$ ), the minimum liquid rate ( $L_{\min}$ ) and hence the minimum reflux ratio ( $R_{\min}$ ). This is well known short-cut method for calculating minimum reflux ratio. When distributed components appear between the key components, modified methods (Smith 1963, Van Winkle 1967) may be used.

### **Gilliland Equation**

By making plate to plate calculations to determine the number of theoretical plates including the reboiler required for the distillation of a number of multicomponent mixtures, Gilliland (1940) correlated the same with the reflux ratio, the minimum reflux ratio and the minimum number of plates at total reflux. He presented his correlations in graphical form. His correlation was later expressed by the following empirical equation (Seader and Henley 2006):

$$Y = 1 - \exp \left\{ \left( \frac{1 + 54.4X}{11 + 117.2X} \right) \left( \frac{X - 1}{X^{0.5}} \right) \right\} \quad (8.111)$$

where,

$$X = \frac{R - R_{\min}}{R + 1} \quad \text{and} \quad Y = \frac{N - N_{\max}}{N + 1}.$$

## 8.11.2 Exact Methods

The two well known exact methods are—the Thiele-Geddes method and the Lewis-Matheson method.

### ***The Thiele-Geddes method***

In multicomponent distillation, the Thiele-Geddes (1933) method can predict the resulting products fairly accurately thus acting as a check for all earlier calculations. In order to use this method, the number of plates, location of the feed plate, temperatures and vapour-liquid ratios should be known either through an appropriate approximate method or by reasonable assumptions. The discussion presented below is based on Edmister's (Edmister 1957) modification of the original Thiele-Geddes method. All the undermentioned equations are separately applicable to each component.

The enriching and stripping sections have been treated separately.

**The Enriching section:** Starting with the mass balance equation at the condenser, the authors obtained the following equations:

For any plate in the enriching section,

$$\frac{\frac{G_n y_n}{Dx_D}}{Dx_D} = \frac{\frac{A_{n-1} G_{n-1} y_{n-1}}{Dx_D}}{Dx_D} + 1 \\ = A_0 A_1 A_2 \dots A_{n-1} + A_1 A_2 \dots A_{n-1} + \dots + A_{n-1} + 1 \quad (8.112)$$

and for the feed plate,<sup>f</sup>

$$\frac{\frac{G_f y_f}{Dx_D}}{Dx_D} = A_0 A_1 A_2 \dots A_{f-1} + A_1 A_2 \dots A_{f-1} + 1 \quad (8.113)$$

where,  $A_0 = R$  for a total condenser and  $A_0 = (R/K_0)$  for a partial condenser.  $A_1, A_2$ , etc. are absorption factors.

**The stripping section:** For the stripping section, they obtained the following equations:

For any plate in the stripping section,

$$\frac{\frac{L_m x_m}{Wx_W}}{Wx_W} = \frac{\frac{S_{m+1} L_{m+1} x_{m+1}}{Wx_W}}{Wx_W} + 1 \\ = S_{m+1} \dots S_{NP-1} S_{NP} S_W + S_{m+1} \dots S_{NP-1} S_{NP} \\ + S_{m+1} \dots S_{NP-1} + \dots + S_{m+1} + 1 \quad (8.114)$$

and for the feed plate,

$$\frac{\frac{L_f x_f}{Wx_W}}{Wx_W} = S_{f+1} \dots S_{NP} S_W + S_{f+1} \dots S_{NP} + \dots + S_{f+1} + 1 \quad (8.115)$$

where,  $S$  is the stripping factor and  $S_W$  is the reboiler stripping factor.

Edmister suggested short cut methods in terms of effective absorption and stripping factors for use in Eqs. (8.113) and (8.114).

$$A_f = \frac{L_f}{G_f K_f} = \frac{L_f x_f}{G_f y_f} \quad (8.116)$$

$$\frac{Wx_W}{Dx_D} = \frac{\frac{L_f x_f}{G_f y_f}}{\frac{L_f x_f}{Wx_W}} = A_f \frac{\frac{G_f y_f}{Dx_D}}{\frac{L_f x_f}{Wx_W}} \quad (8.117)$$

and

$$\text{Since, } Fx_F = Wx_W + Dx_D \quad (8.118)$$

$$Dx_D = \frac{Fx_F}{(Wx_W/Dx_D) + 1} \quad (8.119)$$

$(Wx_W/Dx_D)$  for each component can be calculated from Eqs. (8.113), (8.115) and (8.117). Equation (8.119) then gives  $(Dx_D)$ , and Eq. (8.118) provides  $(Wx_W)$ .

If the values of  $A$  and  $S$  (or  $[L/G]$  and temperatures) are correct, the products thus computed will be consistent with the number of plates, feed plate location and reflux ratio used. These may be checked by using Eq. (8.112) for the enriching section and Eq. (8.114) for the stripping section.

To check a plate  $n$  in the enriching section,

$$\frac{G_n y_n}{Dx_D} \frac{Dx_D}{G_n} = y_n \quad (8.120)$$

If  $Sy_{J,n} = 1$ , the temperature is satisfactory. If not, a new temperature has to be obtained by adjusting the  $y$ 's proportionally until they add to unity and computing the corresponding dew point.

The following equation may be used to check a plate  $m$  in the stripping section,

$$\frac{Lx_m}{Wx_W} \cdot \frac{Wx_W}{L_m} = x_m \quad (8.121)$$

If  $Sx_{J,m} = 1$ , the temperature is correct; otherwise the values of  $x$  are to be adjusted till they add to unity and the bubble point computed.

The optimum feed plate location is decided by trial, changing the location and noting which location requires the smallest number of plates for the desired products.

### ***The Lewis–Matheson method***

The stage-by-stage, equation-by-equation calculation method was developed by Lewis–Matheson (1932). It is also an equation tearing procedure used for solving simple fractionators with one feed and two products. It was formulated to determine stage requirements for the separation of two key components, a reflux ratio and a feed-stage location. Both outer and inner iterations are required. The outer loop tear variables are the mole fractions or flow rates of nonkey components in the products. The inner loop tear variables are the interstage vapour (or liquid) flow rates. The method was widely used for hand calculations (Stichlmair 1988), but it also proved often to be numerically unstable when implemented on a digital computer.

## 8.12 Distillation Equipment and Energy Conservation Practices

Distillation is the still most widely used operation for separating large multicomponent streams to high purity products. Developments are going on further to reduce capital cost, save energy and improve operating flexibility. The specific goals are:

- (i) minimize the height of column per theoretical stage
- (ii) minimize pressure drop per theoretical stage and
- (iii) maximize operational range, i.e. turn down or turn up ratio.

A distillation column use either trays or packings. Mechanisms of mass transfer in two cases differ. But both are designed to approach equilibrium through the generation of large interfacial area. In trays, interfacial area results from passage of vapour through perforations in trays, whereas in packings interfacial area is created by spreading of liquid on the packing surface. When any problem develops that does not allow the vapour and liquid to come in contact with each other or which keep the vapour and liquid from separating, will affect the performance of the column. Some examples include corroded devices, plugged or fouled valves, and thrash in downcomers, pinched downcomers, excessive rates and mechanical damage such as displaced distributors or packed beds. A fouled distributor will cause maldistribution of liquid. Design error, both processes and mechanical, may be the cause of the problem. Process design errors include faulty vapour-liquid equilibrium data and assumed tray efficiencies as well as feed composition or the presence of undesired components. Mechanical errors such as improperly designed trays or packings are much easier to detect. These problems should be identified during the process design and during the preconstruction design review.

In a tray column, liquid flows down the column through downcomers and then across the tray deck, while vapour flows upward through the liquid inventory on the tray. In cross-flow trays commonly used, direction of flow of liquid on one tray reverses when it reaches the tray below. However, in parallel-flow trays, direction of liquid movement is the same in all trays. Parallel-flow trays are more expensive but can provide 10% or more efficiency. Performance of tray depends on types of tray deck and tray efficiency changes with column throughput. In stable operation shown in Figure 8.32, there is gradual increase in efficiency as vapour velocity through holes and liquid height rise with throughput. Exchange of momentum created by vapour with that liquid on the tray resulting in bubbles is the critical element in mass transfer rate. On either side of the stable region, performance drops off. A number of correlations are available on tray efficiency and pressure drop with hole diameter, liquid height, vapour velocity and physical properties for sieve trays. But no generalised correlations are available that can be applied to all types of tray design.

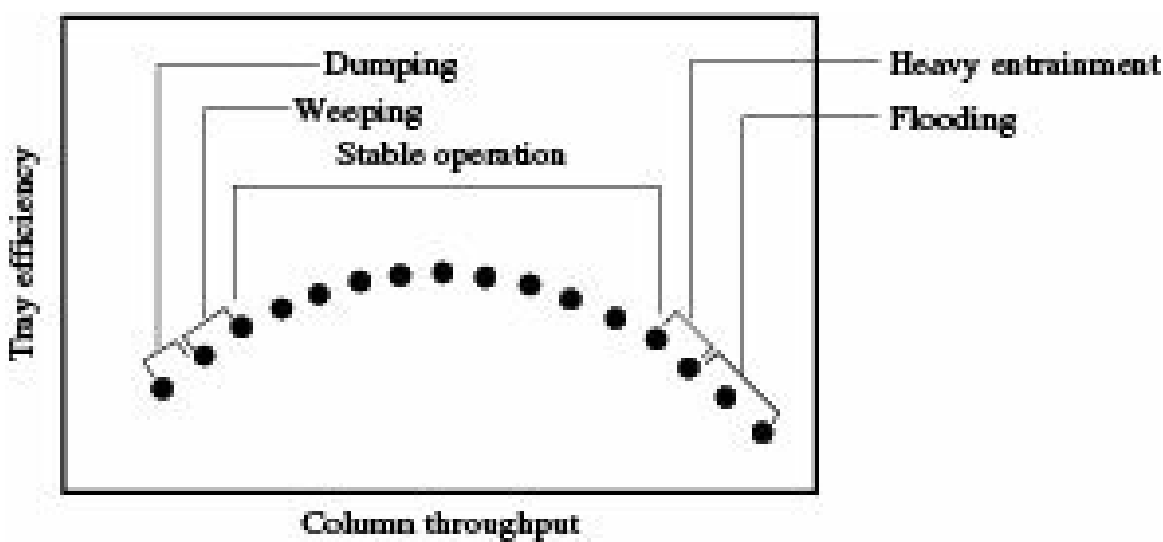


**Figure 8.32** Tray efficiency vs. column throughput.

Trays with small fixed valves can give slightly smaller tray efficiency and higher pressure drop than sieve trays but give higher operating range. In floating valve trays, minimum flow area varies with vapour throughput. These have higher operating range, about a factor of 3, with lower pressure drop than sieve trays. But its cost is higher.

In divided wall column (DWC) technology, the separation of a ternary mixture is conveniently achieved by using two columns in series as shown in Figure 8.33. DWC offers better separation technique and being a single column configuration is more energy efficient than conventional arrangements.

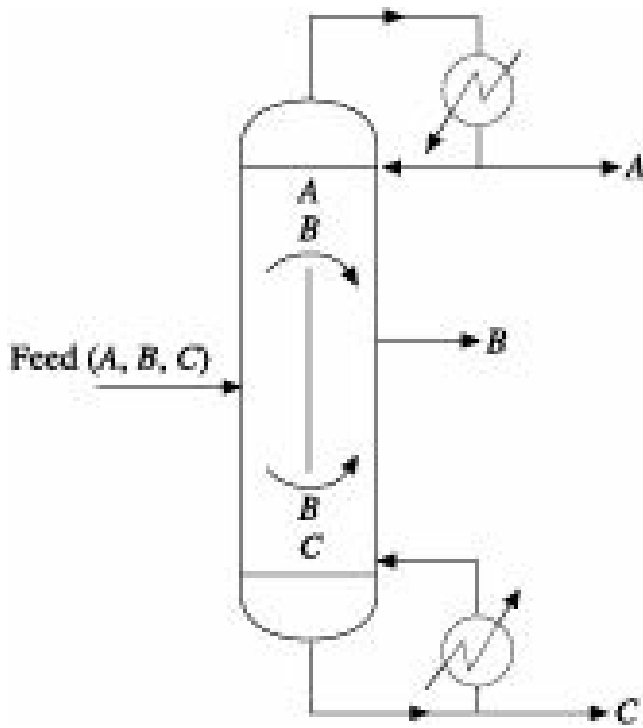


**Figure 8.33** DWC configuration for separation of ternary mixture.

The overall energy requirements of the column can be reduced significantly by using a heat pump for integrating the functions of the reboiler and condenser in a distillation column. In this technology shown in Figure 8.34, the heat input to the reboiler is accomplished by the heat liberated by condensing refrigerant and the condensed refrigerant leaving the reboiler as liquid evaporates in the overhead condenser thereby removing heat from the overhead vapour. Heat pump finds extensive applications in the following two situations: (i) whenever chilled water or direct refrigerant is

required for condensation, and (ii) columns using high pressure steam in the reboiler with no heat recovery at the condenser.

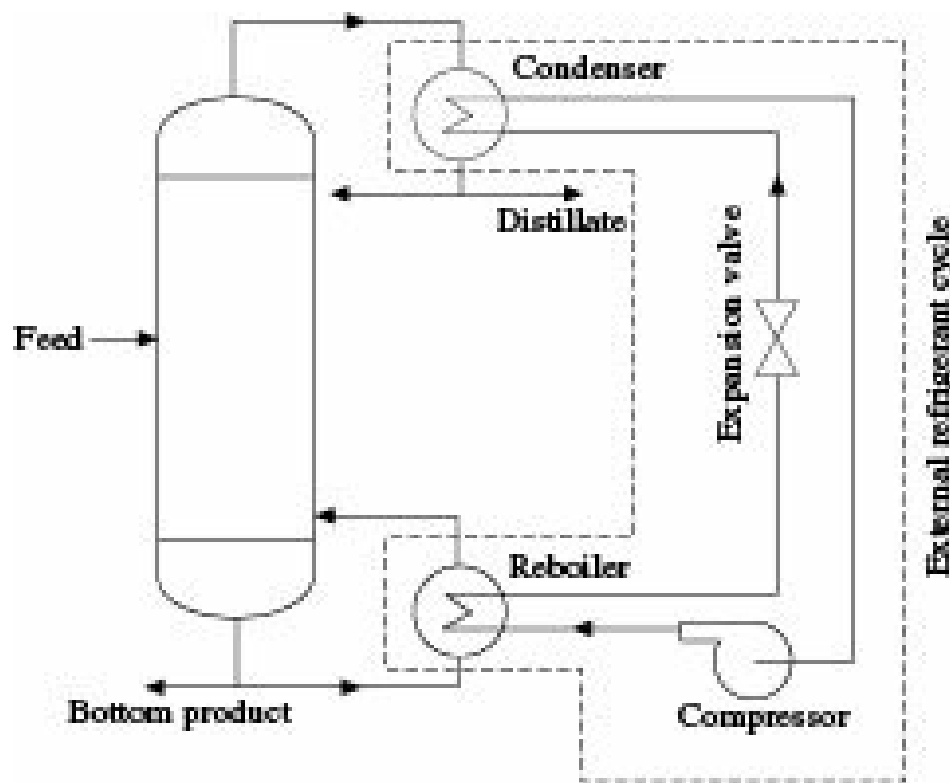


Figure 8.34 Heat pump with refrigerant.

The vapour recompression is another technology used in energy conservation in distillation operations. In this technology, the overhead vapour of the column is compressed and condensed thereby using the heat liberated by condensation to reboil the bottom liquid. No external heat transfer fluid like refrigerant in heat pump is required for vapour recompression operation. A conventional column with steam heating and water cooling use about ten times the heat load required in a column running with vapour recompression.

Another way of conserving energy is the two stage condensation shown in Figure 8.35.

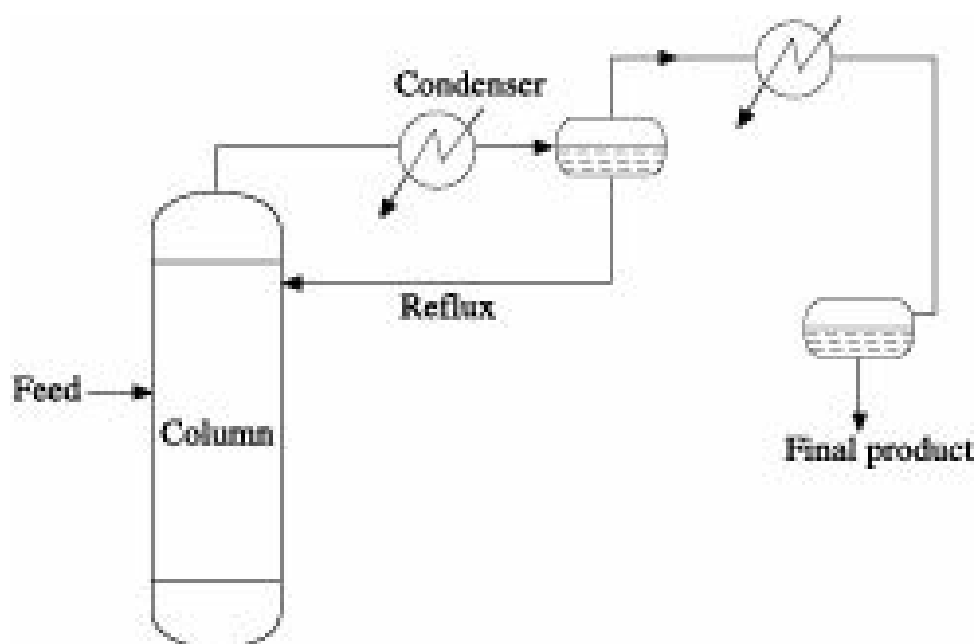


Figure 8.35 Two stage condensation.

The first stage condenses part of the overhead vapour to provide reflux and the second stage

condenses the rest to yield the top product. This has found to be economical provided the overhead vapour must be a multicomponent mixture having a reasonable temperature spread between its dew point and bubble point, and the temperature at the top of the column must be high enough to be in useful range of heat recovery.

Use of intermediate reboilers and condensers shown in Figure 8.36 can reduce the energy cost of a distillation column significantly. However, change in column design with respect

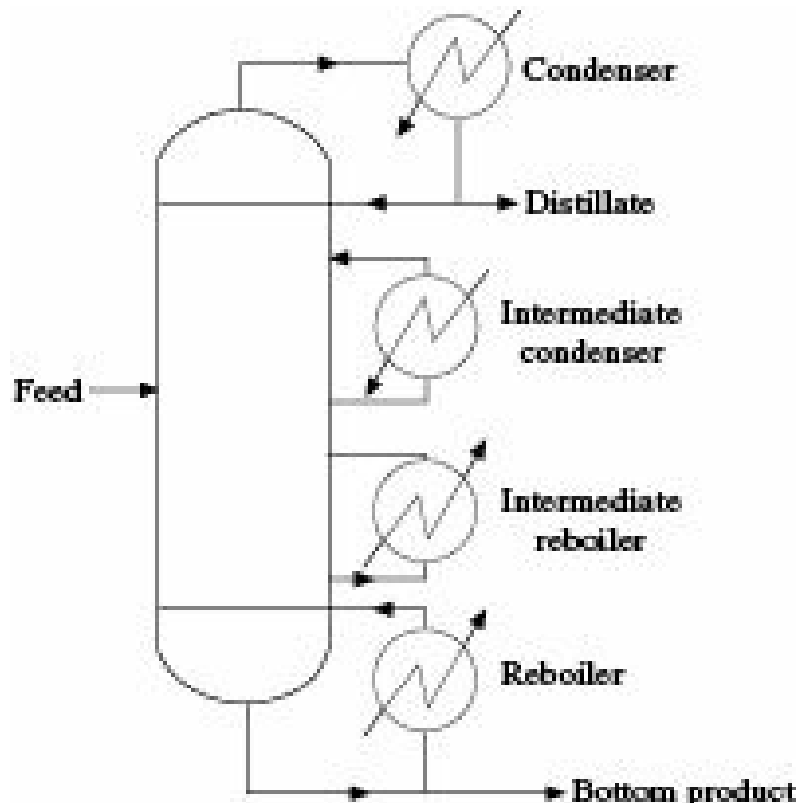
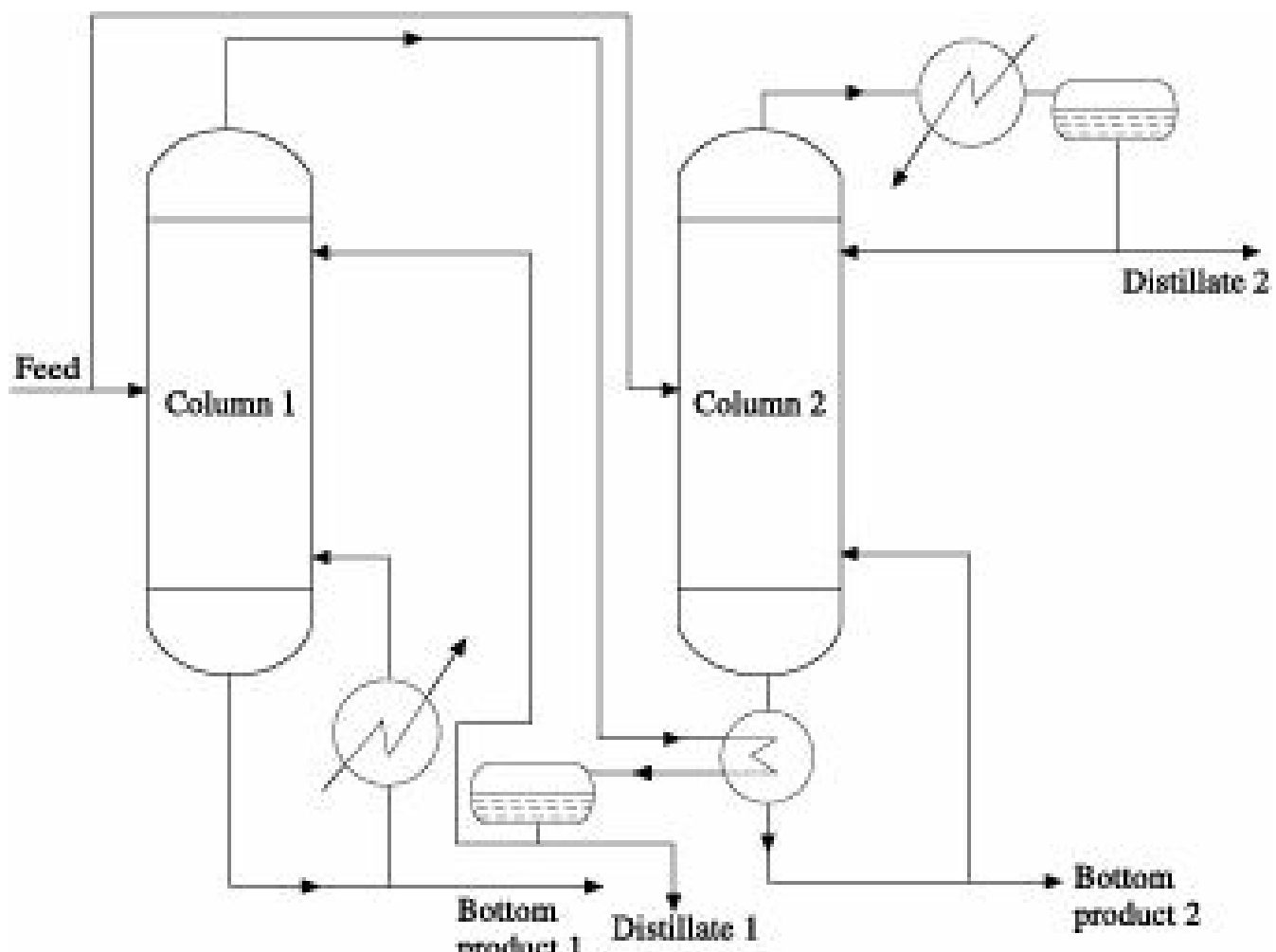


Figure 8.36 Intermediate reboiler and condenser.

to the followings needs consideration: (i) the number of trays in the column increases by use of multicondensers and multireboilers in rectification and stripping sections, respectively, (ii) there exists potential for reducing diameter of the column above the intermediate condensers and below intermediate reboilers.

Split tower arrangement shown in Figure 8.37 can save the energy requirement almost half. In this process the feed is split into two equivalent streams followed by distillation in two smaller columns operating at different pressures. The condenser duty of the high pressure column shall match the required reboiler duty of the low pressure column.



**Figure 8.37** Split tower arrangement.

Multiple effect heat cascading is another technology for energy conservation in distillation columns. In this technology, the condensing overhead vapours of one distillation column is used to provide the reboiler duty of another column where the condensing temperature is higher than the reboiling temperature. The heat savings by use of heat cascading are obvious as each reboiler run by the overhead vapours of another column removes that much of an external heat input.

## 8.13 Distillation of Constant Boiling Mixtures

Binary mixtures having very low relative volatility can be separated by ordinary rectification but only with very large number of plates and very high reflux ratio requiring large tower diameter and high operating cost. Substances forming constant boiling mixtures or azeotropes, on the other hand, cannot be separated by ordinary methods of distillation since the compositions of liquid and vapour become same at the point where azeotrope is formed. In such cases, a third component is added to the binary mixture to make the separation readily possible. The added component is so chosen that it can be easily separated from the distillate or the residue as the case may be. Two types of such distillation are used in practice. When the added substance combines with the low boiling component and is recovered from the distillate, the operation is called *azeotropic distillation*. When, on the other hand, the third component combines with the high boiling component and is recovered from the residue, the operation is *extractive distillation*.

### 8.13.1 Azeotropic Distillation

In azeotropic distillation, the added substance called the *entrainer* combines with one of the original constituent to form a new low-boiling azeotrope whose volatility is such that it can be easily separated from the other constituent.

Proper choice of entrainer is very important in azeotropic distillation. Some desirable properties of a good entrainer are:

- The entrainer should form a highly volatile azeotrope with one of the constituents of the original mixture to ensure easy separation and minimize entrainer loss with the residue.
- It should preferably combine with the constituent present in lesser quantity so that both entrainer requirement and heat requirement are minimum.
- The entrainer should be easily recoverable from the constituent with which it vaporises.
- It should be inactive towards the solution to be separated, chemically stable, noncorrosive, nontoxic, cheap and easily available.
- Latent heat of vaporisation, freezing point and viscosity of the entrainer should be low.

The production of absolute alcohol (100% ethanol) from its dilute aqueous solution is an example of azeotropic distillation. Dilute aqueous solution of ethanol can be concentrated by ordinary rectification only up to 89.4 mol% ethanol, commonly known as rectified spirit, because a minimum boiling azeotrope is formed at this concentration. However, if sufficient benzene is added to the mixture, a low boiling azeotrope containing benzene, water and ethanol is formed which readily separates from ethanol, and is collected as the top product while pure ethanol is collected as the bottom product. The heteroazeotrope at the top on condensation separates into two layers; the upper layer rich in benzene is returned to the column as entrainer along with make-up benzene and the lower layer rich in water is further treated in a small column to recover as much benzene as possible for use as entrainer.

A flow diagram for production of absolute alcohol from water-ethanol azeotrope is shown in Figure 8.38.

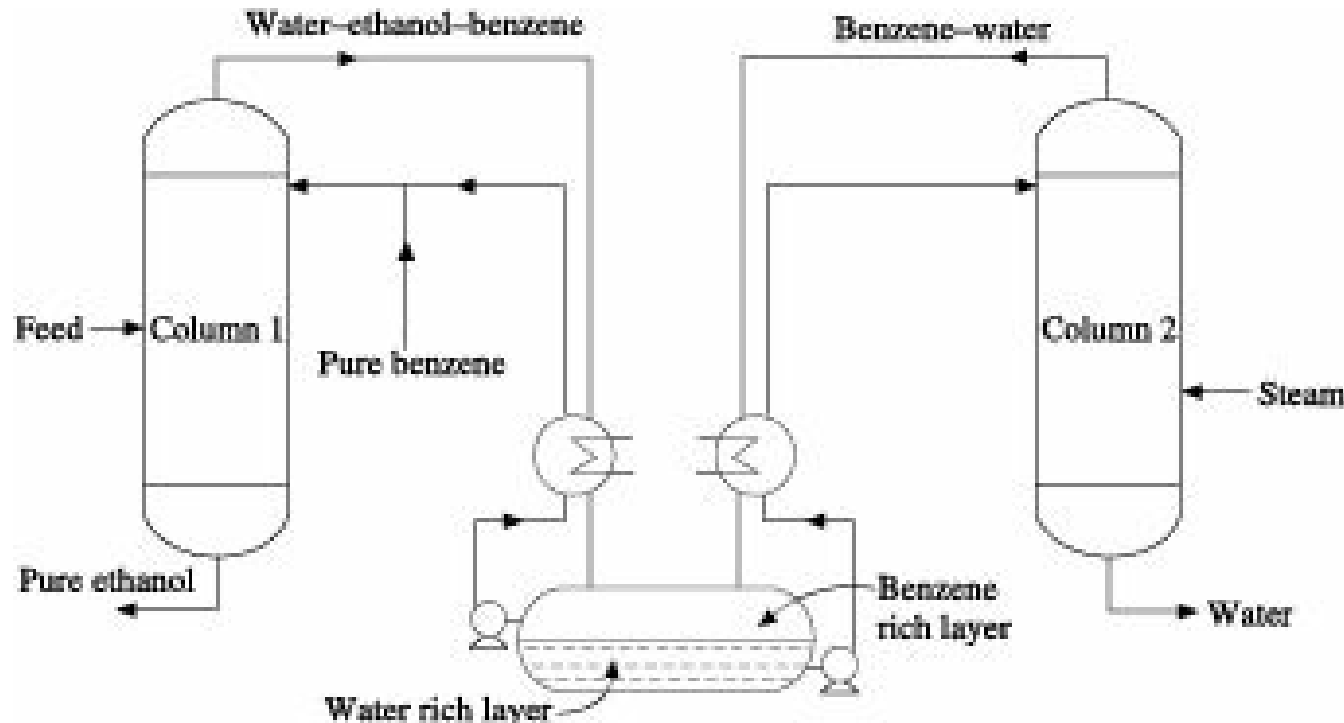


Figure 8.38 Azeotropic distillation of water-ethanol solution.

When a binary azeotrope disappears at some pressure or changes composition by 5 mol% or more

over a moderate range of pressure, consideration has to be given to using two distillation columns operating in series at different pressures without adding any solvent. This process is known as *pressure swing distillation*. Sometimes it is also called *two-columns distillation*. The method was applied by Lewis (1928) for separations of minimum boiling azeotrope of tetrahydrofuran water and the maximum boiling azeotropes of hydrochloric acid water and formic acid water. This method can be applied for the separation of less common maximum boiling azeotropes where both products are withdrawn as distillates rather than as bottoms. For all pressure swing distillation sequences, the recycle ratio is an important factor in the design and depends on the difference in azeotropic composition for the column pressures.

### 8.13.2 Extractive Distillation

In extractive distillation, the third component known as the *solvent* is added to change the relative volatility of the constituents to be separated. The solvent itself is however of low volatility and in contrast to azeotropic distillation, remains mostly with the bottom product without being appreciably vaporised.

The following are requirements of a satisfactory solvent:

- The solvent should be able to change the vapour-liquid equilibrium of the original solution so that its constituents may be easily separated with relatively small amount of solvent.
- It should be capable to dissolve the components of the original mixture.
- The solvent should preferably be nonvolatile or at least of low volatility under the conditions of operation in order to minimize solvent loss with the distillate.
- The solvent should be easily separable from the constituents of the original mixture.
- Other properties like chemical stability, noncorrosiveness, nontoxicity, low freezing point, low viscosity, cheapness and easy availability should also be considered.

An azeotrope of toluene and iso-octane may be separated by extractive distillation using phenol as the solvent. If sufficient amount of phenol is added to combine with all the toluene present, the iso-octane is liberated and is easily distilled off requiring only a few plates in the main column. The bottom product containing toluene and phenol is sent to a second smaller column to recover phenol which is sent back to the main column as solvent along with make-up phenol as required.

### 8.14 Molecular Distillation

Many organic substances, on being heated, decompose before their normal boiling points are reached. These cannot, therefore, be separated by ordinary distillation unless the pressure is kept extremely low and the time of contact is drastically reduced.

In distillation of many natural products like separation of vitamins from animal or fish oils as well as separation of industrial products such as plasticizers, the temperature of distillation cannot exceed 200-300°C at which the vapour pressures of the substances seldom exceed a few millimetres of mercury. Commercial distillation equipment cannot be used for these purposes because of the lower limits of the operating pressures and also the long time of exposure caused by high hold-up. Molecular distillation which is conducted at absolute pressures of 0.003 to 0.03 mm Hg is suitable for heat-sensitive materials mentioned above and also to purify small amount of compound.

As predicted by Langmuir, the rate of evaporation from a liquid surface is quite high. But in practice,

the rate is very much reduced since a large fraction of the evaporated molecules return to the liquid surface after mutual collision in the vapour space above the liquid.

The process of molecular or short-path distillation is carried out under moderate to ultra vacuum (from 0.4 to 4 N/m<sup>2</sup>) when fluids remain in the free molecular flow regime, i.e. the mean free path of molecules is comparable to the size of the equipment. As a result, both the operating temperature and time required for separation of the components are highly reduced. In molecular distillation the mean free path of the light molecules helps to accumulate the same on the condensation zone whereby the heavy molecules remain preferably on the heating zone due to heating effect. In the operation, conditions are created to keep mutual collision of evaporated molecules at its minimum. Firstly, ultra vacuum is maintained in the vapour space so that the mean free path of the vaporising components considerably increase being of the order of 1 cm. Secondly, attempts are made to place the condensing surface within a few centimetres from the evaporating surface so that a large fraction of the evaporated molecules reach the condensing surface before undergoing mutual collision and striking back on the evaporating surface. This is a secondary purification step for producing a lighter coloured and more stable product by the process of elimination of undesirable constituents of high molecular weight present in the liquid extract which was earlier recovered by the primary process of steam distillation or solvent extraction. In this process a heavy and a light solvent are combined with the extract to be purified and then the mixture is passed through an evaporator as shown in Figure 8.39. The more volatile components are collected with a light solvent on the finger in the middle of the evaporator and then recovered as the first distillate fraction in receiver 2. The remaining constituents are condensed on the walls of the first evaporator and collected in two other receivers following its passage into a second evaporator. As before, second distillate fraction is collected in the middle of the evaporator. The residues and heavy solvent are condensed and collected in the residue tank.

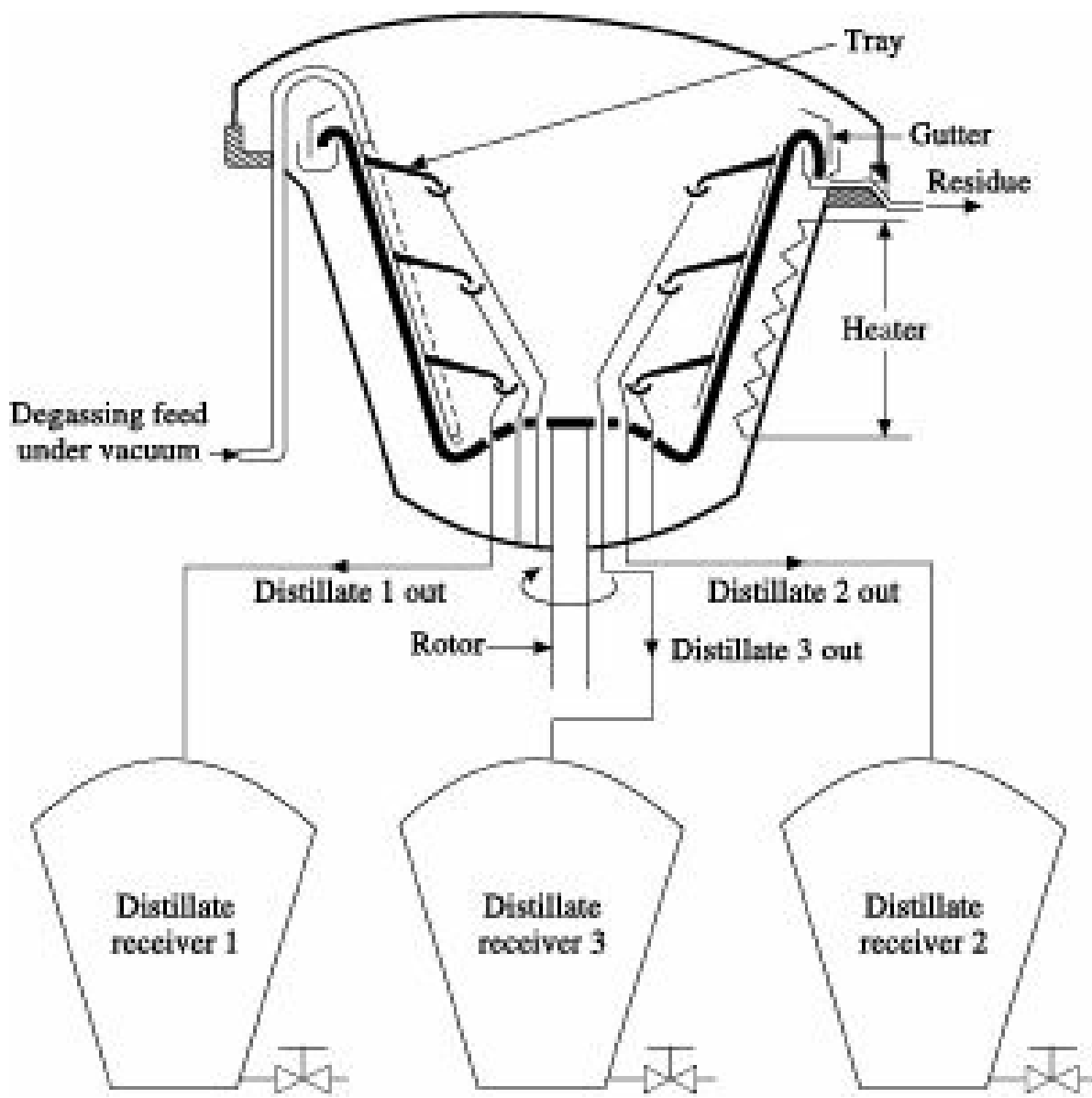


Figure 8.39 Molecular distillation unit.

## 8.15 Fractional Distillation

Fractional distillation is the process used to efficiently extract or distill products that are a mixture of chemicals. It is practically accomplished in a fractionating tower designed specifically for rectifying petroleum products from crude oil by creating a temperature gradient along the height of the tower or stack. In the stack, crude oil is pumped into a boiler and heated. Cascading action increases the surface area of the liquid to aid in rapid evaporation. Condensate trays or plates extend up the height of the tower along the temperature gradient. Highly volatile chemicals condense farthest up the stack and are extracted from the tower via a network of pipelines. The less volatile chemicals condense lower in the stack at higher temperatures. By putting together a system of multiple fractionating towers operating at different temperatures, it is possible to extract individual compounds from the crude oil mixture. For example, in the first stage crude oil may be added to the main stack and heated. At a certain height in the stack, a plate is present that gasoline condenses on. The gasoline condensate can then be piped in two pathways—(i) raw gasoline to another refinery to be modified by additives for use in internal combustion engines, and (ii) raw gasoline into another stack. In the second pathway, the second stack can be operated at a temperature and with specific plates that can rectify the individual chemical compound constituents of the gasoline such as benzene, toluene, ethyl benzene

and xylenes with a trace amount of naphthene and paraffinic hydrocarbons through evaporation and condensation. This process can be used for any of the general fractions of crude oil to further rectify the constituent compounds. Crude oil can generally be grouped into fractions as follows:

Natural gas—the lightest, most volatile petroleum fractions such as propane, pentane, etc.

Gasolines—higher distillates used for automotive fuel

Middle distillates—lower volatility distillates including diesel oil, kerosene, jet fuels and lighter fuel oils

Heavier fuel oils and lubricating oils—low volatility distillates, e.g. motor oil

Asphalts and tars—lowest volatility and generally a smelly, sticky mass filled with impurities.

## 8.16 Cryogenic Distillation

Cryogenic distillation is also a separation process carried out under sub-atmospheric temperature, e.g. at a temperature close to -170 °C when air starts to liquefy. Before separation can occur, there are specific operating conditions that must be achieved. Distillation involves two phases—gas and liquid. Air must be cold for this to happen. Distillation of air is actually not that different from distillation of alcohol from water. Air separation in cryogenic distillation begins when air from the atmosphere is compressed to about 10 atm. Hydrocarbons, water and carbon dioxide that freeze later in the process are removed from the compressed air through molecular sieves in the temperature swing adsorber bed. Compressed, dry air is cooled to cryogenic temperatures (about 100 K) by cold process fluids in a series of heat exchangers. Air is cooled to this temperature until it becomes a boiling liquid. Nitrogen boils off faster than argon and oxygen, and the vapour produced is mostly nitrogen. The cold air is separated into an oxygen rich bottom stream and nitrogen rich top stream in the distillation tower. The oxygen rich waste stream is flashed through a valve to cool it further and is used to condense nitrogen coming off the top of the column. The oxygen-rich waste stream is then used to cool incoming air. The waste stream is expanded through a turbine generating electricity to run the compressor. After being used again to cool incoming air, the expanded waste is either purged to the atmosphere or used to regenerate the adsorber bed. Nitrogen is taken out of the distillation column and partially condensed. The liquid flows back into the column and the vapour is drawn off as product. Cold product nitrogen is used to cool incoming air before exiting the process, air is ultimately cooled to 100 K by compression and expansion. To recycle energy, product and waste stream are used to cool entering air. Energy is further recycled by expanding the waste oxygen stream and using the electricity to run the compressor.

For 99% pure nitrogen, the distillation tower contains about 25 trays. Starting up for a cryogenic distillation process is a complex task that requires careful monitoring. Cryogenics can produce large quantities of high purity nitrogen.

Cryogenic argon recovery and purification system contain three columns. The crude argon column can be even bigger in size than the main double column of air separation unit. Typically for 55 TPD production plant, the crude argon column can be as high as 30 m with about 100 distillation stages. The pure argon column is relatively smaller in size and can have 35-40 stages. The nitrogen stripper column is very small in size. All three columns are utilized to achieve the desired argon product.

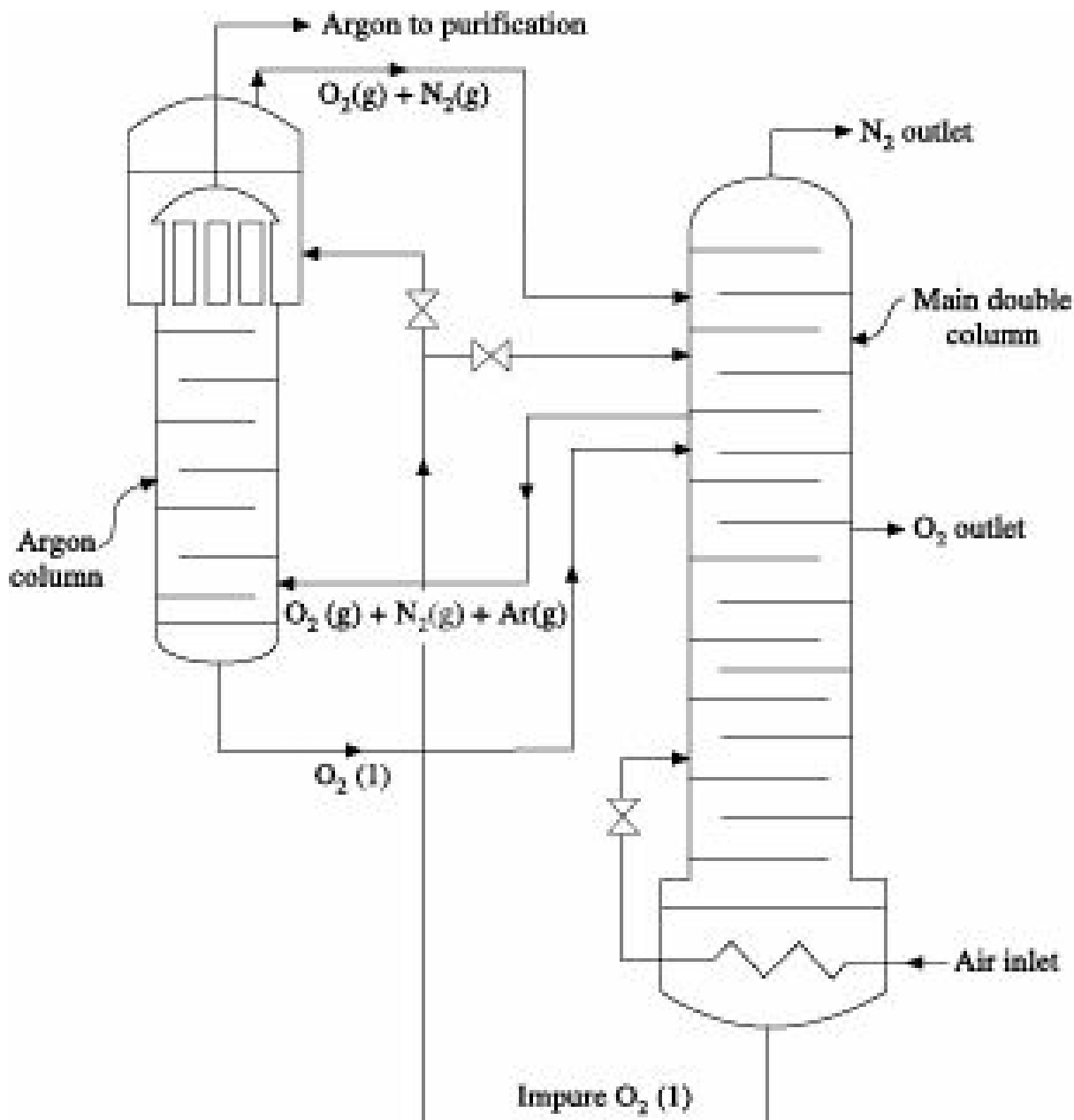


**Figure 8.40** Argon recovery subsystem.

Figure 8.40 shows that the argon rich stream from the upper column of main double column of air separation unit is fed into the lower crude argon column as feed. In the lower argon column, as vapour rises the oxygen content gets reduced. The crude argon vapour leaving the top of the lower argon column is introduced at the base of the upper argon column (not shown in Figure 8.40) where the oxygen content is further reduced until a virtually oxygen free argon stream is obtained. The overhead vapour is then flown into the argon condenser where the argon rich vapour condenses to provide reflux. The reflux stream for the lower argon column is transferred from the pump of this column through argon reflux pump. Oxygen free argon is withdrawn from the top of the pure argon column and passed to the nitrogen stripper column. Pure liquid argon is withdrawn from the bottom of the nitrogen removal column and sent to the storage. A small purge is taken from the top to remove the nitrogen enriched vapour. Refrigeration for reflux to the nitrogen stripper column is provided by an intermediate stream drawn from the lower column of air separation unit.

Another industrial installation is Demethanizer column which operates at about  $-107^{\circ}\text{C}$  and fractionates the condensed hydrocarbons to reduce the methane content in the bottom product with recovery of more than 90% ethane. The column contains more than one bed with packings of different geometries and also valve trays.

Cryogenic processes in general have very large capital cost, mostly due to the costs of compressors and turbines. This separation requires the use of not only the compressors and turbines but also numerous heat exchangers, insulators and distillation column(s), all of which add to the high costs of the process.

## 8.17 Reactive Distillation

*Reactive distillation*, combination of reaction and distillation processes in a single column, is a relatively new inclusion in the field of chemical engineering operations. This is a hybrid or combo operation and involves using reaction vessel as the still. The method adds a separating agent to react selectively and reversibly with one or more of the constituents of the feed. The reaction product is subsequently distilled from the nonreacting components. The reaction is then reversed to recover the separating agent and the other reacting components. It is a case where a chemical reaction and multistage distillation are conducted simultaneously in the same apparatus to produce other chemicals. The combined operation sometimes referred to as *catalytic distillation*, if a catalyst is used. This is specially suited to chemical reactions limited by equilibrium constraints since one or more of the products of the reaction are continuously separated from the reactants (Seader and Henley 2006). Though its first application dates back to Solvay process for soda manufacture, its recognition came nearly a century later (Easmin 2007). 150 such operations were in commercial practice in 2006. The major commercial reactive distillation processes are used for production of ethers like MTBE from isobutene and methanol, TAME from isoamylene and methanol, ETBE from isobutene and ethanol, etc.; esters like Methyl/Ethyl acetate, fatty acid ester, etc.; olefins like Isobutylene, Butene-1, etc.; Cumene by alkylation of propylene and benzene; Monosilane by dismutation of trichlorosilane; 4-nitro chlorobenzene by nitration of chlorobenzene and nitric acid; Bisphenol-A by condensation of phenol and acetone. The method is also used for hydroprocessing like hydrogenation of aromatics, hydro-desulfurisation; transesterification like production of Diethyl carbonate; hydration like manufacturing of Ethylene glycol from ethylene oxide; for hydrolysis of Methyl acetate. A comparison of the conventional process and the reactive distillation process depicted in Figure 8.41 (Stankiewicz 2003) for production of methyl acetate by acid-catalyzed esterification reaction of acetic acid and methanol shows that 28 nos. of major pieces of equipment used in conventional process has been reduced to only 3 in reactive distillation process representing the entire plant and costs one-fifth of the energy (Krishna 2002).

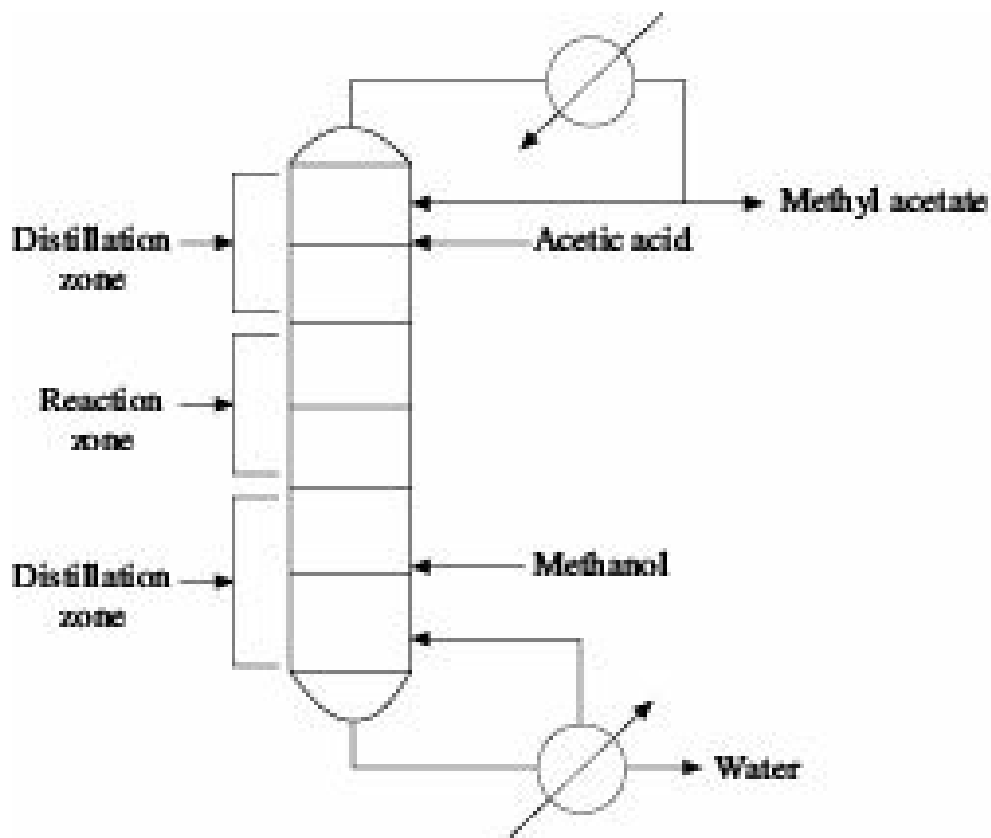


**Figure 8.41** Reactive distillation.

The reactive distillation process should be considered as an alternative to the use of separate reactor and distillation tower whenever the following hold:

- The chemical reaction occurs in liquid phase in the presence or absence of a catalyst;
- Feasible temperature and pressure for the reaction and distillation are the same, i.e. the reaction rate and the distillation rate are of the same order of magnitude;
- The reaction is equilibrium limited such that if one or more of the products formed can be removed, the reaction can be driven to completion. Thus, a large excess of a reactant is not necessary to achieve high conversion. This is particularly advantageous when recovery of the excess reagent is difficult because of azeotrope formation.

This technology helps in process intensification, effective heat utilization, reduction of capital and operating costs, increased reliability, averting hot spots and run-away in process, effective handling of the process when reaction products form azeotrope(s), better heat economy, etc. However, reactive distillation in general is not attractive for supercritical conditions, for gas phase reactions, and for reactions that take place at high temperatures and pressures, and/or that involve solid reactants or products.

Reactive distillation with divided wall column (RDWC), the new configuration, shows a tremendous potentiality in commercial sector due to higher thermodynamic efficiency caused by reduced remixing effects and reduced number of equipment, more number of products from a single column thus minimizing capital cost, lower energy consumption causing reduction in operating cost compared to that in conventional column along with high purity products from a single column.

Careful consideration must be given to the configuration of the distillation column when employing reactive distillation. Important factors are feed entry and product removal stages, the possible need for intercooler and interheaters when heat of reaction is appreciable, and the method for obtaining required residence time for the liquid phase. Feasibility and efficiency of a particular reactive

distillation process depend on liquid residence time, separation efficiency, liquid hold-up and pressure drop. The limitations of reactive distillation are narrow feasible region in the pressure-temperature domain for simultaneous reaction and distillation, proper boiling point sequence and difficulties in providing adequate residence time. Harmsen (2007) has provided an excellent review of research, scale-up, design, operation and commercial applications of reactive distillation showing it to be a front-runner of industrial process intensification.

## Nomenclature

$a$  : activity

$A$  : more volatile component of a binary mixture, absorption factor ( $\text{L}/\text{mG}$ ), —

$B$  : less volatile component of a binary mixture.

$D$  : distillate rate,  $\text{mol}/\text{q}$  for plate towers,  $\text{mol}/\text{L}^2\text{q}$  for packed towers.

$E_O$  : overall plate efficiency, fractional.

$E_M$  : Murphree plate efficiency, fractional.

$F$  : feed rate,  $\text{mol}/\text{q}$  for plate towers,  $\text{mol}/\text{L}^2\text{q}$  for packed towers.

$f_A$  : partial molal fugacity of component  $A$ ,  $\text{F}/\text{L}^2$

$f_A^0$  : fugacity of pure component  $A$ ,  $\text{F}/\text{L}^2$

$G, \bar{G}$  : vapour rate in enriching section and stripping section, respectively,  $\text{mol}/\text{q}$  for plate towers,  $\text{mol}/\text{L}^2\text{q}$  for packed towers.

$H$  : enthalpy of saturated vapour,  $\text{FL}/\text{mole}$

$H_tG, H_tL$  : height of gas phase and liquid phase transfer unit, respectively,  $\text{L}$ .

$H_{toG}, H_{toL}$  : height of overall transfer unit based on gas phase and liquid phase, respectively,  $L$ .

$h$  : enthalpy of saturated liquid,  $\text{FL}/\text{mole}$

$I, J$  : components  $I, J$

$K$  : equilibrium distribution coefficient,  $y^*/x$ , —

$k_x, k_y$  : liquid phase and gas phase mass transfer coefficient respectively,  $\text{mol}/\text{L}^2\text{q}$  (mole fraction).

$K_x, K_y$  : overall mass transfer coefficient based on liquid phase and gas phase respectively,  $\text{mol}/\text{L}^2\text{q}$  (mole fraction).

$L, \bar{L}$  : liquid rate in enriching and stripping section, respectively,  $\text{mol}/\text{q}$  for plate towers,  $\text{mol}/\text{L}^2\text{q}$  for packed towers.

$m$  : equilibrium distribution coefficient,  $y^*/x$ , —

$N_m$  : minimum number of plates.

$N_p$  : number of theoretical plates.

$N_tG, N_tL$  : number of gas phase and liquid phase transfer unit respectively.

$N_{toG}, N_{toL}$  : number of overall transfer unit based on gas phase and liquid phase respectively.

$P$  : total pressure,  $\text{F}/\text{L}^2$

$p$  : vapour pressure, F/L<sup>2</sup>

$p'$  : partial pressure, F/L<sup>2</sup>

$q$  : fraction of liquid in feed.

$q_C$  : heat removed in the condenser, FL/q for plate tower, FL/L<sup>2</sup>q for packed tower.

$q_r$  : heat added at the reboiler, FL/q for plate tower, FL/L<sup>2</sup>q for packed tower.

$R$  : reflux ratio, mol/mol

$R_m$  : minimum reflux ratio, mol/mol.

$S$  : stripping factor, mG/L, —

$V$  : vapour velocity, L/q

$W$  : residue rate, mol/q for plate tower, mol/L<sup>2</sup>q for packed tower.

$x, y$  : concentration of  $A$  in liquid and vapour, respectively, mol fraction.

$x^*, y^*$  :  $x$  and  $y$  in equilibrium with  $y$  and  $x$ , respectively, mol fraction.

$Z$  : height of packing, L.

### Greek Letters

$\alpha$  : relative volatility, —

$c$  : activity coefficient, —

$m$  : molar latent heat of vaporisation, FL/mol.

$t$  : density, M/L<sup>3</sup>

$L$  : Wilson parameter.

## Numerical Problems

**8.1** Estimation of the Equilibrium Composition of a Binary System and also the Composition of a Binary Mixture at Specified Conditions: Calculate the composition of the equilibrium vapour phase at 60°C for a liquid mixture consisting of 40 mol% benzene and 60 mol% toluene considering that the given mixture is characterized by Raoult's law. Also, find the composition of a liquid mixture of benzene and toluene that boils at 90 °C under a pressure of 760 mm Hg.

Given, the saturated vapour pressures of benzene at 60°C and 90 °C are 385 and 1013 mm Hg, respectively whereas those of toluene at the respective temperatures are 140 and 408 mm Hg.

[Ans: Composition of the equilibrium vapour phase: 64.8 mol% benzene and 35.2 mol% toluene; Composition of the liquid mixture: 58.3 mol% benzene and 41.7 mol% toluene.]

**8.2** Calculation of Equilibrium Phase Compositions and Construction of  $T$ - $x$ - $y$  Diagram: Calculate the equilibrium phase compositions and construct equilibrium diagrams in the coordinates  $T$  against  $x$  and  $y$ , and  $y^*$  against  $x$  for a benzene-toluene mixture under atmospheric pressure, considering that the mixture is characterized by Raoult's law.

Using the diagram of  $t$  against  $x$  and  $y$  as drawn, determine the composition of the equilibrium vapour and the boiling point for a liquid containing 55 mol% benzene and 45 mol% toluene.

[Ans:

Temperature, $T^{\circ}\text{C}$	80	84	88	92	96	100	104	108	110
$x$ , mole fraction of benzene in liquid	1.0	0.823	0.659	0.508	0.376	0.256	0.155	0.058	0
$y^*$ , mole fraction of benzene in vapour	1.0	0.922	0.830	0.720	0.596	0.453	0.304	0.128	0

Construct the diagrams as directed and find out the following:

Boiling point:  $91^{\circ}\text{C}$ ; Composition: 75 mol% benzene and 25 mol% toluene.]

**8.3 Calculation of Vapour-liquid Equilibrium data, Construction of Equilibrium Diagram, and Computation of Relative Volatility:** Solutions of methanol and ethanol are substantially ideal. Compute the vapour-liquid equilibrium data for this system at 1 atm pressure, and plot  $x$ - $y^*$  and  $T$ - $x$ - $y$  diagrams. Compute also the relative volatilities and its average value. The vapour pressure temperature ( $T$  in  $^{\circ}\text{C}$ ) relationships are

$$\log P_{\text{MeOH}}, \text{mm Hg} = 7.84863 - \frac{1473.11}{230 + T}$$

$$\log P_{\text{EtOH}}, \text{mm Hg} = 8.04494 - \frac{1554.3}{222.65 + T}$$

Ans:

$T, ^{\circ}\text{C}$	$x_A$	$y_A$	$P_A$	$P_B$	$\alpha$	$\alpha_{av}$
64.75	1.0	1.0	760	433	1.755	
68.00	0.724	0.819	860	498	1.727	
72.00	0.415	0.548	1002	588	1.704	1.704
76.00	0.143	0.219	1160	698	1.670	
78.33	0	0	1262	760	1.661	

**8.4 Use of the Rule of Linearity and Construction of Equilibrium Curve:** Construct the equilibrium curve for a mixture of carbon tetrachloride and sulphur dichloride at a pressure of 760 mm Hg.

Given: the saturated vapour pressures ( $p$ ) of  $\text{CCl}_4$  for different temperatures are:

$T, ^{\circ}\text{C}$	40	50	60	70	75	80
$p, \text{mm Hg}$	214	315	439	621	715	843

Also given the boiling points of  $\text{SCl}_2$  at 760 and 400 mm Hg pressures are  $59^{\circ}\text{C}$  and  $41^{\circ}\text{C}$ , respectively.

[Hints: Use the rule of linearity to find the saturated vapour pressures of  $\text{SCl}_2$  at different temperatures, taking water as standard liquid whose boiling points at different pressures are available in literature]

**8.5 Flash Vaporisation of a Binary Mixture and Computation of Equilibrium Composition:** A liquid mixture containing 50 mol% heptane and 50 mol% octane is to be continuously flash vaporised at 1 atm pressure to vaporise 60 mol% of the feed. What will be the composition of the vapour and liquid in the separator for an equilibrium stage?

Data:

Temperature, °C	98.5	105	110	115	120	125.5
Vapour pressure of heptane, mm Hg	760	940	1050	1200	1350	1540
Vapour pressure of octane, mm Hg	333	417	484	561	650	760

[Ans:

$x_A$	1.0	0.656	0.488	0.311	0.157
$y_A$	1.0	0.812	0.674	0.491	0.279

where, subscript A refers to heptane ]

**8.6 Distillation of a Binary Mixture in Order to find out the Percentage of the Mixture Distilled and the Composition of the Distillate:** A binary mixture of benzene and toluene containing 40 mol% benzene is to be distilled at atmospheric pressure to recover 95% of the benzene. Estimate the molal percentage of the mixture which should be distilled, and the composition of the distillate obtained if the distillation is carried out by (i) simple equilibrium distillation and (ii) differential distillation collecting all the distillates together. The average relative volatility of benzene to toluene in the temperature range involved is 2.5.

[Ans: (i) Molal% of mixture = 90.5, Distillate contains 42 mol% benzene and 58 mol% toluene (ii) Molal% of mixture = 80.6, Distillate contains 47 mol% benzene and 53 mol% toluene]

**8.7 Simple Batch Distillation of Acetic Acid from Aqueous Solution to Find out the Percentage of the Solution Distilled Using Vapour-liquid Equilibrium Data:** An aqueous solution of acetic acid containing 20 mol% acetic acid is subjected to differential distillation at atmospheric pressure. What percentage of the original solution must be distilled off to raise the concentration of acetic acid in the residue to 35 mol%?

The following equilibrium data may be used where  $x$  and  $y$  are mole fractions of water in liquid and vapour respectively:

$x:$	0	0.10	0.18	0.28	0.38	0.50	0.78	0.85	0.93
$y:$	0	0.20	0.27	0.40	0.51	0.62	0.80	0.89	0.95

[Ans: 88.815%]

**8.8 Simple Batch Distillation of Ethyl Alcohol-water Mixture to Determine the Composition of Overhead Product, and also the Amounts of Top and Bottom Products:** A simple batch still is used to distill 1000 kg of a mixture containing 60 mass% ethyl alcohol and 40 mass% of water. After distillation, the bottom product contains 5 mass% of alcohol. Determine the composition of overhead product, its mass and mass of bottom product. The data on the equilibrium composition are given below, where  $x$  and  $y$  stand for weight% of ethyl alcohol in the liquid and in equilibrium vapour respectively:

$x:$	5	10	20	30	40	50	60
$y:$	36	51.6	65.5	71	74	76.7	78.9

[Ans: Composition: alcohol = 590.39 kg (wt.% = 73.09), water = 217.33 kg (wt.% = 26.91), Masses of distillate and bottom product are 807.72 kg and 192.28 kg, respectively]

**8.9 Estimation of the Mole Fraction of Benzene Obtained in the Receiver on Completion of its Separation from Toluene in a Batch Still:** A benzene-toluene mixture consists of 40 mol benzene and 60 mol toluene. It is desired to reduce the residual benzene concentration in a batch distillation column down to 10%. What is the mole fraction of benzene in the receiver after the batch separation has been completed? Assume that the relative volatility of the benzene-toluene

mixture remains constant at 2.90 throughout the separation process; vapour rate is considered to be constant, and column hold-up is negligible.

[Ans. 0.24 mole fraction of benzene]

**8.10 Simple Batch Distillation of an Aqueous Solution of Component *A* to Determine the Percentage of the Original Mixture Distilled off Using Relative Volatility Data:** An aqueous solution of *A* containing 60 mol% of *A* and the rest water is subjected to differential distillation. What percentage of the original mixture must be distilled off in order to reduce the concentration of *A* in the residue to 20 mol%? The relative volatility of *A* with respect to water is 2.15. [Ans: 89.47%]

**8.11 Differential Distillation of Benzene-Toluene Mixture to Determine the Amount of Mixture Distilled off Using Relative Volatility Data:** 100 mol/hr of benzene (*A*) and toluene (*B*) mixture containing 50 mol% of benzene is subjected to differential distillation at atmospheric pressure till the composition of the benzene in the residue is 33%. Calculate the total moles of the mixture distilled. Average relative volatility is 2.16. [Ans: 60.94 mol/hr]

**8.12 Calculation of the Amount of Ethanol Left in the Still, Recovered in the Distillate, and its Fraction in the Distillate:** Ethanol is recovered from an ethanol-water mixture by differential distillation at atmospheric pressure. The mole fraction of ethanol in the still is reduced from  $x_0 = 0.2$  to  $x = 0.015$ . (i) Calculate the number of kmol left in the still per kmol of initial charge, (ii) what percentage of ethanol in the initial mixture is recovered in the distillate? and (iii) what is the fraction of ethanol in the distillate?

*V-L* data for ethanol-water mixture:

<i>x</i> :	0.01	0.02	0.04	0.08	0.12	0.16	0.20
$(y^* - x)$ :	0.10	0.16	0.23	0.31	0.34	0.34	0.325

[Ans : (i) 0.4953 (ii) 96.29% (iii) 0.3816]

**8.13 Estimation of Reflux Ratio and Vapour Rate in the Stripping Section:** A continuous rectification column is used to separate a binary mixture of *A* and *B*. Distillate is produced at 100 kmol/hr containing 98 mol% of *A*. The mole of *A* in liquid and in the vapour, *x* and *y*, respectively from two adjacent ideal plates in the enriching section are as follows:

<i>x</i>	<i>y</i>
0.65	0.62
0.56	0.78

If the latent heat of vaporisation is same for all mixtures and if the feed is a saturated liquid, calculate

(i) reflux ratio (ii) vapour rate in the stripping section in kmol/hr. [Ans: (i) 1.99 (ii) 296.65 kmol/hr]

**8.14 Estimation of Operating Reflux Ratio and the Relative Flow Rates of Feed and Bottom Products per kmol of Overhead Product:** A mixture of ethyl alcohol and water containing 25 mol% alcohol is distilled in a continuous rectification column under atmospheric pressure. The required concentration of the overhead product is 80 mol%, and the permissible alcohol content in the bottom product is not more than 0.1 mol%. The still of the column is supplied with direct steam. Determine the operating reflux ratio, *R* and the relative molar rates of flow of the feed and the bottom product per kmol of overhead product. The operating reflux ratio may be calculated using the expression  $R = 1.3R_m + 0.3$ .

[Ans: 1.77, Relative molar rates of feed and bottom products are 3.21 and 4.98, respectively]

**8.15** Determination of the Number of Plates in a Batch Rectification Column and also the Ratio of Minimum Refluxes at the End and Beginning of Operation: A batch plate rectification column is used to fractionate a liquid mixture of carbon tetrachloride and sulphur dichloride containing 50 mol% of  $\text{SCl}_2$  under atmospheric pressure. The operation is carried out maintaining a reflux ratio of 7.8. The overhead product is to contain 90 mol% and the bottom product after fractionation 15 mol% of  $\text{SCl}_2$ .

Using the equilibrium data for the mixture obtained in Problem 8.4, determine the number of plates required assuming the plate efficiency to be 58%. Also, determine the ratio of the minimum reflux ratios at the end and the beginning of the operation.

[Ans: 19 plates, 3.5]

**8.16** Determination of the Required Number of Plates in a Batch Rectification Column for Separation of a Given Mixture: Determine the required number of plates in a batch rectification column for fractionating a mixture of chloroform and benzene under atmospheric pressure. The feed contains 38 mol% chloroform, the overhead product should contain 97 mol%, and the bottom product 10 mol% chloroform. The reflux ratio is maintained at 2. The number of plates corresponding to one stage of the change in concentration is 1.4.

The equilibrium data at atmospheric pressure are given as

$T, ^\circ\text{C}$	Mole% of chloroform in liquid	Mole% of chloroform in vapour
80.6	0	0
79.8	8	10
79.0	15	20
78.2	22	30
77.3	29	40
76.4	36	50
75.3	44	60
74.0	54	70
71.9	66	80
68.9	79	90
61.4	100	100

[Ans: 17]

**8.17** Steam Distillation of Stearic Acid, Weight of Acid Distilled per kg of Steam as a Function of Total Pressure: Stearic acid ( $\text{C}_{17}\text{H}_{35}\text{COOH}$ ) is to be distilled using steam at  $200^\circ\text{C}$  in a direct fired still, heat jacketed to prevent condensation. Steam is introduced into the molten acid in small bubbles and the vapour leaving the still has a partial pressure of acid equal to 70% of the vapour pressure of pure stearic acid at  $200^\circ\text{C}$ . Plot the kg of acid distilled per kg of steam added as function of the total pressure which ranges from 100 down to 20 mm of Hg absolute. At  $200^\circ\text{C}$ , the vapour pressure of stearic acid is 3 mm of Hg.

[Ans:

Total pressure, mm Hg: 100 80 60 40 20

$$\frac{\text{kg stearic acid}}{\text{kg steam}} : 0.338 \ 0.425 \ 0.572 \ 0.874 \ 1.851 ]$$

**8.18** Determination of Minimum Amount of Steam for a Steam Distillation Operation: A mixture of two high boiling liquids  $A$  and  $B$  is to be separated from a small amount of nonvolatile carbonaceous material by steam distillation at  $100^\circ\text{C}$  under a total pressure of 150 mm Hg. The

organic acid mixture contains 70 mol% of *A* and 30 mol% of *B* in the liquid phase. At 100°C, the vapour pressure of pure *A* is 20 mm Hg and that of pure *B* is 8 mm Hg. It may be assumed that the mixture of *A* and *B* obeys Raoult's law for both the components.

If no condensation of steam takes place within the still, what is the minimum amount of steam required in gmol per gmol of the organic mixture of *A* and *B* distilled?

[Ans: 8.146 gmol]

**8.19 Estimation of the Consumption of Heating Steam for Distillation of Ethyl Alcohol-Water Mixture:** Find the consumption of heating steam available at 2 atm absolute pressure for the distillation process stated in Problem 8.8. The feed is supplied to the still at the temperature of the beginning of boiling. Assume that the losses of heat to the surroundings are 10% of the usefully consumed amount of heat. It has been found from the diagram of *T* against *x* and *y* that the temperature of the beginning of distillation when the boiling mixture contains 60 mass% of alcohol, is 81°C, and the temperature of the end of distillation when the boiling mixture contains 5 mass% of alcohol, is 94.9°C. The moisture content of the heating steam is 5%.

[Ans: 535 kg]

**8.20 Calculation of Number of Plates in a Rectification Column for Methyl Alcohol-Water System:** Determine the number of plates in a continuous rectification column for separating a mixture of methyl alcohol and water under atmospheric pressure. The content of the methyl alcohol in the feed is 31.5 mol%. It is required to obtain an overhead product containing 97.5 mol% of the alcohol; the bottom product may contain up to 1.1 mol% of the alcohol. The reflux ratio for the operation is maintained at 1.48. The number of plate equivalent to one stage of the change in the concentration is 1.7. The column is heated with indirect steam.

The equilibrium data for the system are given:

Temperature, *T*°C 100.0 96.4 93.5 91.2 87.7 81.7 78.0 75.3 73.1 71.2 69.3 67.5 66.0 64.5

Mol% of Methyl alcohol

in liquid 0 2.0 4.0 6.0 10.0 20.0 30.0 40.0 50.0 60.0 70.0 80.0 90.0 100

Mol% of Methyl alcohol

in vapour 0 13.4 23.0 30.4 41.8 57.9 66.5 72.9 77.9 82.5 87.0 91.5 95.8 100

[Ans: 12 plates for the top and 7 plates for the bottom of the column, altogether 19 plates]

**8.21 Estimation of Steam Requirement and Number of Plates:** 1 kg/s of an aqueous solution containing 15% by weight of methyl alcohol is to be distilled to recover 95% of the alcohol at a concentration of 92% by weight. The reflux ratio is to be twice the minimum value. Calculate the (i) steam requirement and (ii) number of theoretical plates.

[Ans: (i) 0.38 kg/s (ii) 8 plates]

**8.22 Use of Three Different Relative Volatilities to Calculate the Number of Plates Required for Separation of a Binary Mixture:** Calculate the number of theoretical plates required in a continuous column used to separate a binary mixture containing 70 mol% of the more volatile component into an overhead product of 98% purity and a bottom product of 97% purity when the reflux ratio is 1.5 times the minimum value. The calculations are to be performed for three different relative volatilities, viz., 1.4, 2.0 and 4.0.

[Ans: 37, 19 and 10 plates]

**8.23 Estimation of Number of Plates for Separation of Benzene-toluene Mixture:** A continuous fractionating column is to be designed to separate a mixture containing 50 mol% each of benzene

and toluene into top product containing 95 mol% benzene and a bottom product containing 97 mol% toluene. The column will be equipped with a reboiler and a total condenser, and will operate at 1 atm pressure. The feed will be liquid at its boiling point. How many plates will be required in the column if the reflux ratio used is thrice the minimum and the overall plate efficiency is 70%?

The following equilibrium data may be used where  $x$  and  $y$  represent mole fraction of benzene in liquid and vapour respectively:

$x:$	0.013	0.075	0.141	0.211	0.281	0.370	0.459	0.555	0.659	0.773
$y:$	0.031	0.161	0.281	0.393	0.496	0.591	0.678	0.757	0.831	0.897

[Ans: 13]

**8.24 Calculation of Number of Actual Trays Required in a Valve-Tray Tower for Separation of Benzene-Toluene Mixture:** A valve-tray tower has been designed to separate a mixture of 60 mol% benzene and 40 mol% toluene into an overhead product containing 96 mol% benzene and a bottom product containing 25 mol% benzene. Calculations have shown that 6.1 theoretical stages will be required to obtain the desired separation conducted essentially at atmospheric pressure. The temperature at the top of the column is 82.8°C while at the bottom of the column it is 100.5°C. Assuming the reboiler acts as one theoretical stage, estimate the number of actual trays required. To simplify the calculation, assume that mixtures of benzene and toluene may be considered as ideal. At an average temperature of 91.6°C, the vapour pressure of pure benzene is 1070 mm Hg, and the vapour pressure of pure toluene is 429 mm Hg.

[Ans: 5.7  $\approx$  8]

**8.25 Calculation of Number of Plates Using Relative Volatility, and also the Diameter and Height of a Bubble-cap Distillation Column:** A mixture of benzene and toluene containing 50 mol% benzene is to be separated in a bubble-cap distillation column giving distillate having 90 mol% benzene and bottom with 90 mol% toluene. The feed enters column at its boiling point at a rate of 10 tonne/day. The relative volatility between benzene and toluene may be taken as 2.28 and the operating reflux to be 1.5 times the minimum. If the overall plate efficiency is 0.75, calculate the number of plates required. Also, estimate the diameter and height of the column.

The superficial vapour velocity,  $v$  for a plate spacing of 450 mm and liquid seal of 25 mm, may be calculated using the relation

$$v = K \left[ \frac{(\rho_L - \rho_G)}{\rho_G} \right]^{0.5}$$

where

$$\rho_L = 0.879 \text{ g/mL of benzene and } 0.866 \text{ g/mL of toluene}$$

$$\rho_G = 5 \text{ g/mL.}$$

[Ans: 13 plates, 35 cm diameter and 6.3 m height]

**8.26 Calculation of the Amounts of Top and Bottom Products, Number of Trays Required Indicating the Location of Feed Point, and the Number of Trays at Total Reflux Condition:** A saturated liquid feed at 200 mol/hr at the boiling point containing 44 mol% heptane and 56 mol% ethylbenzene is to be fractionated at 101.32 kPa pressure to give a distillate containing 98% heptane and a bottom

product containing 1% heptane. A reflux ratio of 2.3 is to be used. Calculate (i) the amount of distillate and the bottom products in mol/hr (ii) the number of trays to be used, indicating the feed point location (iii) the number of trays required if the operation is carried out at total reflux condition.

Equilibrium data at 101.32 kPa pressure for heptane  $x_H$  and  $y_H$  in mole fraction:

$x_H$	0	0.08	0.25	0.485	0.79	1.0
$y_H$	0	0.23	0.514	0.73	0.904	1.0

[Ans: (i) 88.66 mol/hr and 111.34 mol/hr (ii) No. of trays: 12, Feed plate: 7th tray (iii) 8]

**8.27 Estimation of Overall Plate Efficiency of a Continuous Rectification Column:** A continuous plate type rectification column with 12 plates has to separate a mixture of 30 mol% carbon disulphide and 70 mol% carbon tetrachloride into product streams of 95 mol%  $CS_2$  and 95 mol%  $CCl_4$  respectively. A reflux ratio of 1.5 times the minimum will be used. The column will operate at 1 atm. Feed will enter as saturated vapour. Estimate the overall plate efficiency of the column.

Equilibrium data are as under where  $x$  and  $y$  represent fractions of  $CS_2$  in liquid and vapour respectively:

$x$ :	0.03	0.11	0.26	0.53	0.66	0.76	0.86
$y$ :	0.08	0.27	0.50	0.75	0.83	0.88	0.93

[Ans: 68.33%]

**8.28 Estimation of the Number of Plates Considering the Overall Plate Efficiency same as that of the Separate Plates, and by Graphical Construction Considering the Murphree Efficiency:** A plate type rectification column fed with a liquid mixture containing 51.5 mol% of a low boiler (low boiling component) is to be used to obtain an overhead product with a concentration of 97.5 mol%. According to experimental data, the Murphree efficiency of a plate of the adopted design for the given mixture within a concentration range from 50 to 100 mol% does not virtually depend on the composition of the liquid and for the given vapour velocity equals 0.5 (same for all the plates). Determine the number of plates needed in the upper section of the column in two ways: (i) through the number of stages of the change in concentration considering that the overall plate efficiency is the same as that of the separate plates and (ii) by direct graphical construction of the number of actual plates taking into account the Murphree efficiency to be 0.5 (the method of kinetic curve).

[Ans: (i) 4 (ii) 6]

**8.29 Calculation of Composition of the Vapour Across a Plate using Murphree Efficiency:** A liquid containing 65 mol % of the low boiler (low boiling component) is on one of the plates of the top section of a rectification column. The latter operates with a reflux ratio of 2.5. The overhead product contains 98% of low boiler. Determine the compositions of the vapour entering the given plate and leaving it if the Murphree efficiency of the plate is 0.75, the mixture obeys Raoult's law and the relative volatility is 2.5. The liquid on the plate mixes completely.

[Ans: 74.4 mol%; 80.3 mol%]

**8.30 Number of Plates Required for a Continuous Rectification and the Location of the Feed Plate:** An equimolal mixture of heptane and ethyl benzene is to be rectified in a plate column. The overhead and bottom products should be 95 mol% pure. The feed will enter as liquid at its boiling point

and the reflux will be 2.5 times the minimum. The overall plate efficiency is 70%. How many plates must be provided and on which plate the feed should be introduced?

The following vapour-liquid equilibrium data are applicable where  $x$  and  $y$  are mole fractions of heptane in liquid and vapour, respectively:

$x:$	0.08	0.185	0.251	0.335	0.487	0.651	0.788	0.914
$y:$	0.233	0.428	0.514	0.608	0.729	0.834	0.904	0.963

[Ans: 10 plates, feed plate: 5th theoretical (6th actual) plate]

**8.31 Number of Plates to be Provided for a Rectification Operation at a Total Reflux:** A laboratory rectification column is operated at atmospheric pressure and at total reflux with a benzene-chlorobenzene system. Samples of liquid from the condenser and reboiler analyse 95 mol% benzene and 98 mol% chlorobenzene, respectively. Assuming a perfect reboiler, a total condenser, constant molal overflow and no heat loss from the column, calculate the actual number of plates in the column. The overall plate efficiency is 70%. The relative volatility of benzene to chlorobenzene is 4.13. [Ans: 5]

**8.32 Computation of Height and Diameter of Column Used for Distillation of Methanol-Water Mixture:** A plant with an annual throughput of 0.06 million tonnes (365 days basis) requires a distillation column to separate an equimolar mixtures of methanol and water available at its boiling point. Compute (i) the number of actual plates, (ii) the height of the column, and (iii) the diameter of the column.

*Given:*

Overhead product = 91.4 mol% methanol, Residue = 1.5 mol% methanol, Average liquid density = 870 kg/m<sup>3</sup>, Vapour density (top) = 2.8 kg/m<sup>3</sup>, Vapour density (bottom) = 3.1 kg/m<sup>3</sup>, Average liquid viscosity =  $0.3 \times 10^{-3}$  kg/(m)(s), Column temperature (top) = 340.06 K, Column temperature (bottom) = 372.6 K, Tray spacing = 60 cm, and Tray efficiency = 49%.

Vapour velocity ( $v$ ) in the column can be calculated using the Brown-Souders equation:

$$v = C \left( \frac{\rho_G - \rho_L}{\rho_G} \right)^{0.5}$$

where,  $C = 0.0428$ ,  $\rho_G$  and  $\rho_L$  are the densities of vapour and liquid, respectively.

Vapour-liquid equilibrium data for methanol-water system are as follows:

$x:$	0.0	0.10	0.20	0.30	0.40	0.50	0.60	0.70	0.80	0.90	1.0
$y:$	0.0	0.42	0.57	0.66	0.73	0.78	0.83	0.87	0.92	0.96	1.0

[Ans: (i) 13 (ii) 8.4 m (iii) top: 1.825 m and bottom: 1.958 m]

**8.33 Amounts of Top and Bottom Products, and also the Amount of Steam Condensing in the Reflux Condenser:** A continuous distillation column is fed with 1000 kmol/hr of a mixture containing 30 mol% of pentane and 70 mol% of hexane. The overhead product contains 95 mol% of pentane, the bottom product 90 mol% of hexane. Determine the amount of the overhead and bottom products, and also the amount of steam condensing in the reflux condenser if the slope of the operating line of the rectifying section of the column equals 0.75.

[Ans: Overhead: 17150 kg/hr, Bottom: 64700 kg/hr, Steam condensed: 68400 kg/hr]

**8.34 Determination of Number of Stages and Also the Requirement of Heating Steam in the Reboiler:**

A continuous rectification column produces 200 kg/hr of acetic acid with a concentration of 70 mol%. The column processes a mixture of acetic acid and water, which is fed into the column at its boiling point. The content of the acetic acid in the feed is 31 mol%. The overhead product is water containing 8 mol% of acetic acid. The column operates at atmospheric pressure. Determine the number of stages of the change in concentration with a reflux ratio of 4. Also, determine the consumption of heating steam in the reboiler of the column operating at 4 atm pressure (abs.) if the steam has a moisture content of 5%. The heat losses are 4% of the usefully spent heat. The data on the equilibrium compositions are given below:

$T, {}^{\circ}\text{C}$  Mol% of water in liquid Mole% of water in vapour

118.1	0 0
115.4	5 9.2
113.8	10 16.7
110.1	20 30.2
107.5	30 42.5
105.8	40 53.0
104.4	50 62.6
103.2	60 71.6
102.1	70 79.5
101.3	80 86.4
100.6	90 93.0
100.0	100 100.0

[Ans: 9720 kg/hr]

### 8.35 Determination of the Heating Surface Area in the Reboiler and Consumption of Heating Steam:

The equations of the operating lines of a rectification column for separating a mixture of benzene and toluene under atmospheric pressure are:

$$y = 0.723x + 0.263$$

$$y = 1.25x - 0.0188$$

The column is fed with 75 kmol/hr of the mixture at its boiling point. The heating steam in the column reboiler has a gauge pressure of 3 atm. Determine the required heating surface area in the reboiler and the consumption of heating steam having a moisture content of 5%. The overall heat transfer coefficient for the system is  $580 \text{ W}/(\text{m}^2)(\text{K})$ . Disregard the heat losses. Assume that the boiling point of the liquid in the reboiler equals that for pure toluene. [Ans:  $59.2 \text{ m}^2$ , 2170 kg/hr]

### 8.36 Calculation of the Amount of Top and Bottom Products, Reboiler and Condenser Duties, and Requirement of Steam and Cooling Water: A continuous fractionating column operating at a pressure of 1 bar is used to separate 1000 kg/hr of a solution containing 10% acetone and 90% water at $35 {}^{\circ}\text{C}$ , into an overhead product containing 99% acetone and 1% water at $25 {}^{\circ}\text{C}$ and a bottom product containing less than 100 ppm acetone at $100 {}^{\circ}\text{C}$ . All compositions are by weight.

The operation is supposed to be carried out at a reflux ratio of 10.

- (i) Calculate the amount of top and bottom products.
- (ii) Calculate the reboiler and condenser duties assuming the rise in temperature of cooling water used in the condenser is limited to  $30 {}^{\circ}\text{C}$ . Boiling point of the solution containing 99% acetone is  $56.5 {}^{\circ}\text{C}$ . The latent heats of acetone and water at  $56.5 {}^{\circ}\text{C}$  are 620 kJ/kg and 2500 kJ/kg, respectively. The mean heat capacity of acetone in the temperature range of 25 to  $35 {}^{\circ}\text{C}$  and that of water in the temperature range of 25 to  $100 {}^{\circ}\text{C}$  are 2.2 kJ/kg K and 4.2 kJ/kg K, respectively.
- (iii) Estimate the rates of steam and cooling water required for the operation.

Dry saturated steam is available at 25 psig ( $276 \text{ kN/m}^2$ ) giving latent heat of  $2730 \text{ kJ/kg}$ .

[Ans: (i) Top: 101 kg/hr and Bottom: 899 kg/hr (ii) Reboiler: 1029884 kJ/hr and Condenser: 786699 kJ/hr (iii) Steam rate: 377.3 kg/hr and Water rate: 6244 kg/hr]

**8.37 Number of Theoretical Stages, Feed Plate Location, Heat Load in Reboiler and Condenser:** A fractionating column operating at 1 atm pressure is applied at the optimum location with a saturated liquid feed containing 40 mol% ethanol and 60 mol% water. The column produces a saturated overhead product containing 80 mol% ethanol and a saturated liquid bottom product containing 20 mol% ethanol. The reflux is 2.0. Determine (i) the number of theoretical stages required for the desired separation, (ii) the optimum feed plate location assuming 100% plate efficiency, (iii) the heat load in reboiler in kcal/kmol of bottom product, and (iv) the heat load in the condenser in kcal/kmol of overhead product.

The relative volatility of the system may be assumed to be 2.2.

[Ans (i) 6 stages (ii) 3rd from the top (iii) 117861 kcal/kmol (iv) 57486 kcal/kmol]

**8.38 Construction of  $H-x$  Diagram for  $\text{CH}_4\text{-N}_2$  System at Elevated Pressure:** Construct a diagram of  $H$  against  $x$  in the saturation region for a mixture of  $\text{CH}_4$  and  $\text{N}_2$  at 10 atmospheric absolute pressure. The enthalpies ( $H$ ) of the pure components per kmol of vapour and liquid (kJ/kmol) within the limits of the temperatures at which the system  $\text{CH}_4\text{-N}_2$  exists at the prevailing pressure, are

$T, \text{ K}$	Vapour		Liquid	
	$H_{\text{CH}_4}$	$H_{\text{N}_2}$	$H_{\text{CH}_4}$	$H_{\text{N}_2}$
170	11100	9420	4690	—
160	10700	9100	3930	—
150	10270	8800	3310	—
145	—	8640	3040	—
140	—	8480	2820	—
135	—	8330	2550	—
130	—	8160	2310	—
125	—	7990	2050	—
120	—	7810	1830	—
115	—	7630	1580	3460
110	—	7420	1360	3160
105	—	7210	—	2890
100	—	—	—	2610

**8.39 Calculation of Minimum Reflux Ratio, Number of Stages Required, Amounts of Heat Supplied in the Condenser and Reboiler Using Enthalpy-Concentration Diagram:** A mixture consisting of 30 mol% of  $\text{CH}_4$  and 70 mol% of  $\text{N}_2$  is fed into a continuous rectification column. The feed is supplied at a rate of  $1000 \text{ m}^3/\text{hr}$  in the vapour state at 10 atm absolute pressure and at saturation temperature. As a result of fractionation, gaseous products are obtained in the column: a methane fraction containing 3% of  $\text{N}_2$  and nitrogen fraction containing 5% of  $\text{CH}_4$ .

Using the equilibrium diagram of the system  $\text{CH}_4 - \text{N}_2$  for 10 atm in the co-ordinates  $H-x$  constructed in Problem 8.38, determine (i) the amounts of the fractions obtained, (ii) the minimum reflux

ratio, (iii) the number of stages of the change in concentration for an excess reflux coefficient of 1.25, (iv) the amount of heat supplied in the reflux condenser of the column, and (v) the amount of heat supplied in the still (if the methane fraction is withdrawn from the column still in the liquid state).

[Ans: (i) Volumetric flow rate of methane fraction:  $272 \text{ m}^3/\text{hr}$  and that of nitrogen fraction is  $728 \text{ m}^3/\text{hr}$  (ii) 0.518 (iii) 2 stages in rectifying section and 4 stages in stripping section (iv) 44200 W (v) 17300 W]

**8.40** Estimation of Number of Actual Plates, Quantity of Steam Required, Height and Diameter of the Column: A feed mixture containing 44 mol% benzene and rest toluene is fed to a continuous fractionating column at the rate of 9 tonnes/hr to yield an overhead product of 97.4 mol% benzene and a bottom product of 23 mol% benzene. A reflux ratio of 3.5 is to be used. The molar latent heat of benzene and toluene may be taken as 30 MJ/kmol. The feed is liquid at 295 K and has a boiling point of 370.4 K. Calculate (i) the number of actual plates assuming plate efficiency of 50%, (ii) the quantity of steam at  $240 \text{ kN/m}^2$  required in the reboiler, (iii) the column height for a plate spacing of 450 mm, and (iv) the column diameter if it operates at atmospheric pressure and vapour velocity of 60 cm/s.

*Given:*

Specific heat of feed is  $1.84 \text{ kJ/kg K}$ , and Vapour flow in the stripping section is 2.48 mol/mol of feed.

Equilibrium data for benzene-toluene system:

x: 0.10 0.20 0.30 0.40 0.50 0.60 0.70 0.80 0.90 1.00

y: 0.22 0.38 0.51 0.63 0.70 0.78 0.85 0.90 0.96 1.00

where, x and y are the mole fractions of benzene in liquid and vapour, respectively.

[Ans: (i) 20 (ii) 3547 kg/hr (iii) 9.45 m (iv) top: 1.87 m and bottom: 2.19 m]

### ***Short and Multiple Choice Questions***

1. Between Raoult's law and Henry's law, which one is better applicable to solvent?
2. What do you mean by positive and negative deviations from Raoult's law?
3. How does heat load of a condenser attached to a distillation column change with increase in reflux ratio?
4. What is the value of reflux ratio at total reflux?
5. Show that in a distillation column, if the heat input to the reboiler is fixed, the heat load of the condenser also gets fixed.
6. For what value of reflux ratio, the upper and lower operating lines in McCabe-Thiele method coincide with the diagonal?
7. What should be the nature of volatility of solvents for use in extractive distillation?
8. How does entrainers added in azeotropic distillation affect separation?
9. Under what range of pressure is molecular distillation usually carried out?
10. Under which condition are Murphree plate efficiency and Point efficiency equal?
11. In order to separate the components of a binary mixture, the relative volatility should be

- (a) less than unity (b) equal to unity  
 (c) greater than unity (d) greater than zero.

**12.** Relative volatility of a binary system

- (a) decreases with increase in pressure  
 (b) increases with increase in pressure  
 (c) increases with increase in temperature at constant pressure  
 (d) is independent of temperature and pressure

**13.** Flash distillation is suitable for separating components which

- (a) boil at very close temperatures  
 (b) boil at widely different temperatures  
 (c) form minimum boiling azeotrope  
 (d) form maximum boiling azeotrope

**14.** In a distillation operation, the heat removed in the condenser

- (a) increases with increase in reflux ratio  
 (b) decreases with increase in reflux ratio  
 (c) remains unaltered with change in reflux ratio

**15.** Murphree plate efficiency ( $E_M$ ) is defined as

$$(a) E_M = \frac{y_n - y_{n+1}}{y^* - y_{n+1}} \quad (b) E_M = \frac{y_n - y_{n+1}}{y_n - y^*}$$

$$(c) E_M = \frac{x_n - x_{n+1}}{x^* - x_{n+1}} \quad (d) E_M = \frac{y_n - y_{n-1}}{y^* - y_{n-1}}$$

**16.** Continuous rectification to get nearly pure products from a binary mixture having low relative volatility will require

- (a) low reflux ratio (b) high reflux ratio  
 (c) less number of plates (d) small column cross section

**17.** Minimum number of theoretical plates is required in a fractionating column when the reflux ratio is

- (a) the minimum reflux ratio (b) the optimum reflux ratio  
 (c) zero (d) infinity

**18.** In an azeotropic mixture, the equilibrium vapour composition as compared with the liquid composition, is

- (a) more (b) same (c) less (d) uncertain

**19.** The system which does not form an azeotrope at 1 atm, is

- (a) Ethanol-Water (b) Benzene-Toluene  
 (c) Hydrochloric acid-Water (d) Acetone-Chloroform.

**20.** If reflux in a distillation column is 100 mol/hr and the overhead product rate is 50 mol/hr, the reflux ratio is

- (a) 0.5 (b) 2 (c) 50 (d) 150

**21.** Solvent used in extractive distillation

- (a) alters the relative volatility of the original components
  - (b) is of low volatility
  - (c) must not form any azeotrope with the original substance
  - (d) all the above
- 22.** For a given separation in a distillation column, the minimum number of theoretical plates corresponds to
- (a) minimum reflux ratio (b) optimum reflux ratio
  - (c) total reflux (d) zero reflux ratio
- 23.** An example of maximum boiling azeotrope at 1 atmosphere is
- (a) Ethanol-Water (b) Carbon disulphide-Acetone;
  - (c) Benzene-Ethanol (d) Acetone-Chloroform
- 24.** Fenske equation determines
- (a) maximum number of theoretical plates
  - (b) height of the distillation column
  - (c) minimum number of theoretical plates
  - (d) optimum reflux ratio
- 25.** The dew point of a saturated gas phase is equal to
- (a) 0 °C (b) 20 °C
  - (c) gas temperature (d) bubble temperature
- 26.** If an azeotropic mixture of two liquids has a boiling point higher than that of either of them, the mixture shows
- (a) negative deviation from Raoult's law
  - (b) positive deviation from Raoult's law
  - (c) no deviation from Raoult's law
  - (d) none of the above
- 27.** Steam distillation is used to separate
- (a) azeotropes
  - (b) high boiling substances from nonvolatile impurities
  - (c) heat-sensitive materials
  - (d) mixtures of low relative volatility
- 28.** When the liquid on a plate of a distillation column is of uniform concentration
- (a) Murphree plate efficiency > Point efficiency
  - (b) Murphree plate efficiency < Point efficiency
  - (c) Murphree plate efficiency = Point efficiency
  - (d) none of the above
- 29.** Weeping in a distillation column
- (a) increases plate efficiency
  - (b) provides large interfacial surface for mass transfer
  - (c) results due to very high gas velocity
  - (d) results due to very low gas velocity
- 30.** The slope of the operating line for the rectifying section of a distillation column is
- (a) 0 (b) < 1 (c) > 1 (d)  $\infty$

## *Answers to Multiple Choice Questions*

- 11. (c) 12. (a) 13. (b) 14. (a) 15. (a) 16. (b)
- 17. (d) 18. (b) 19. (b) 20. (b) 21. (b) 22. (c)
- 23. (d) 24. (c) 25. (c) 26. (a) 27. (b) 28. (c)
- 29. (d) 30. (c)

## *References*

- Easmin, F., S. Dutta, P. Ray and R. Paul, *Ind. Chem. Engr.*, **49**, 492 (2007).
- Edmister, W.C., *AICHE J.*, **3**, 165 (1957).
- Fenske, E.D., *Ind. Eng. Chem.*, **25**, 482 (1931).
- Gilliland, E.R., *Ind. Eng. Chem.*, **32**, 1220 (1940).
- Harmsen, G.J., *Chem. Eng. Prog.*, **46**, 774 (2007).
- Horsley, L.H., “Azeotropic Data III”, *Adv. Chem. Ser.*, **116** (1973).
- Krishna, R., *Chem. Eng. Sci.*, **57**, 1491 (2002).
- Lewis, W.K., US Patent 1676700 (1928).
- Lewis, W.K. and G.L. Matheson, *Ind. Eng. Chem.*, **24**, 494 (1932).
- Prausnitz, J.M., R.N. Lichtenthaler and E.G. de Azevedo, *Molecular Thermodynamics of Fluid Phase Equilibria*, 3rd ed., Prentice Hall, Englewood Cliffs, N.J. (1999).
- Seader, J.D. and E.J. Henley, *Separation Process Principles*, 2nd ed., John Wiley, New York (2006).
- Smith, B.D., *Design of Equilibrium Stage Processes*, McGraw-Hill, New York (1963).
- Stankiewicz, A., *Chem. Eng. Proc.*, **42**(3), 137 (2003).
- Stichlmair, J., “Distillation and Rectification” in *Ullmann’s Encyclopedia of Industrial Chemistry*, 5th ed., VCH Verlagsgesellschaft Weinheim, **B3**, 4-1 (1988).
- Thiele, E.W. and R.L. Geddes, *Ind. Eng. Chem.*, **25**, 289 (1933).
- Underwood, A.J.V., *Trans. Inst. Chem. Engrs.*, London, **10**, 112 (1932) .
- Van Winkle, M., *Distillation*, McGraw-Hill, New York (1967).
- Yuan, K.S., J.C.K. Ho, A.K. Keshpande and B.C. -Y. Lu, “Vapour-Liquid Equilibria”, *J. Chem. Eng. Data*, **8**, 549 (Oct. 1963).





# 9

# Humidification Operations

## 9.1 Introduction

Humidification operations involve simultaneous transfer of heat and mass between a gas and a liquid when the gas is brought into contact with a liquid in which it is insoluble. Humidification is a general term and includes humidification, dehumidification and cooling of gases as well as cooling of liquids. Although humidification and dehumidification operations may occur between any gas and liquid in which the gas is insoluble, an air-water system is so frequently encountered in practice that the terms humidification and air-water contact have become almost synonymous and unless otherwise mentioned, humidification operations mean air-water contact.

The air-water contact is practiced in four major areas as follows:

- *Humidification*: It is used for producing air of specific moisture content as required for some processes like drying of certain solids under controlled conditions.
- *Dehumidification*: This is commonly used in air conditioning. Moist warm air is dehumidified by contacting with water at a lower temperature.
- *Water cooling*: Warm water from coolers and condensers is cooled by air-water contact before reuse. Water cooling is the most widely used process involving air-water contact.
- *Gas cooling*: A hot air stream can be cooled by bringing it in contact with water.

If a gas is brought into contact with a liquid in which it is insoluble, the liquid will continue to evaporate till the partial pressure of the vaporised liquid in the vapour-gas mixture reaches its vapour pressure at the prevailing temperature. If the gas is totally insoluble in the liquid, its partial pressure in the vapour-gas mixture depends only on the liquid and the temperature, being independent of the nature of the gas and the total pressure except at very high pressure. However, the absolute humidity depends on the nature of the liquid and the molal absolute humidity depends on the total pressure.

When the partial pressure of the vapour in the vapour-gas mixture is equal to the vapour pressure of the liquid at that temperature, the vapour-gas mixture contains maximum possible vapour at that temperature and is said to be saturated. If, on the other hand, the partial pressure of the vapour in the vapour-gas mixture is less than the equilibrium vapour pressure of the liquid at that temperature, the mixture is said to be *unsaturated* and there is scope for further vaporisation.

All humidification, dehumidification and allied operations involve simultaneous heat and mass transfer.

## 9.2 Terminologies Commonly Used

### *Dry-Bulb temperature*

The temperature of a vapour-gas mixture as recorded by immersing the bulb of a thermometer in the

mixture is called *dry-bulb temperature* (DBT).

### Absolute humidity

The weight of vapour per unit weight of bone-dry gas in any consistent unit is called *absolute humidity* ( $Y$ ).

### Molal absolute humidity

Moles of vapour per mole of vapour-free gas is called *molal absolute humidity* ( $Y_m$ ).

Applying Dalton's law of partial pressure to the system, we get

$$CY_m = \frac{n_A}{1} = \frac{P'_A}{P - P'_A} \quad (9.1)$$

where

$n_A$  = moles of vapour in the vapour-gas mixture, the moles of gas being unity

$P'_A$  = partial pressure of vapour and  $P$  the total pressure

From the definitions of absolute humidity and molal absolute humidity,

$$Y = Y_m \# \frac{M_A}{M_B} \quad (9.2)$$

where  $M_A$  and  $M_B$  are the molecular weights of the vapour and the gas, respectively.

In case of an air-water system, since the molecular weights of air and water are 28.97 and 18.02, respectively

$$Y = \left( \frac{18.02}{28.97} \right) \$ Y_m = 0.622 Y_m = 0.622 \left( \frac{P'_A}{P - P'_A} \right) \quad (9.3)$$

### Saturation humidity

When the partial pressure of the vapour in the vapour-gas mixture is equal to the vapour pressure of the pure liquid at the dry-bulb temperature of the gas, the gas is fully saturated and the corresponding humidity is known as *saturation humidity* ( $Y_S$ ).

For air-water systems,

$$Y_S = 0.622 \left( \frac{P_A}{P - P_A} \right) \quad (9.4)$$

where,  $P_A$  is vapour pressure of water at dry-bulb temperature of the mixture. Vapour in a saturated gas is in equilibrium with the liquid at gas temperature with which it is in contact.

### Percentage humidity

*Percentage humidity* is the ratio of actual absolute humidity to the saturation humidity.

$$\text{Percentage humidity} = \frac{Y}{Y_S} \times 100 = \left( \frac{P'_A}{P_A} \times \frac{P - P_A}{P - P'_A} \right) \times 100 \quad (9.5)$$

Percentage humidity is also known as *percentage absolute humidity* or *percentage saturation*.

### **Relative humidity**

*Relative humidity* (RH) is defined as the ratio of partial pressure of vapour actually present in the gas to the vapour pressure of the liquid at the dry-bulb temperature of the gas,

$$RH = \frac{P_A'}{P_A} \times 100\% \quad (9.6)$$

Relative humidity is also known as *percentage relative humidity* or *relative saturation*.

### **Humid volume**

The volume occupied by unit mass of dry gas and the volume of vapour contained by it at that condition in consistent units is termed *humid volume* ( $y_H$ ) of the vapour-gas mixture,

$$y_H = \left( \frac{Y}{M_A} + \frac{1}{M_B} \right) \times 22.414 \times \left( \frac{t_G + 273}{273} \right) \times \frac{1}{P} \quad (9.7)$$

where  $y_H$  is the humid volume in  $\text{m}^3/\text{kg}$ ,  $t_G$  is the dry-bulb temperature of the gas in  $^\circ\text{C}$  and  $P$  is the total pressure in atmosphere.

### **Humid heat**

*Humid heat* ( $C_S$ ) is defined as sum of the specific heat of the dry gas and the specific heat of the vapour contained by the gas multiplied by the absolute humidity,

$$C_S = C_B + Y C_A \quad (9.8)$$

where  $C_A$  and  $C_B$  are the specific heats of the vapour and the dry gas, respectively.

In *air-water system*, at ordinary temperature and pressure, the heat capacities of dry air and water vapour being approximately 1.005 and 1.88  $\text{kJ/kg K}$ , respectively the humid heat of moist air may be expressed as

$$C_B = 1.005 + 1.88Y \text{ kJ/kg dry air K} \quad (9.9)$$

### **Dew point**

*Dew point* (DP) is defined as the temperature at which a vapour-gas mixture becomes saturated when cooled at constant pressure in the absence of the liquid. In other words, at dew point the partial pressure of the vapour in the mixture becomes equal to the vapour pressure of the liquid.

Dew point is always lower than the dry-bulb temperature of the gas except at saturation when both become equal.

### **Enthalpy**

The *enthalpy* ( $H$ ) of a vapour-gas mixture is the sum of the enthalpies of the dry gas and of the vapour contained in it. The enthalpy of a vapour-gas mixture per unit weight of the dry gas is given by

$$H = C_B(t_G - t_0) + Y[C_A(t_G - t_0) + m_0] = C_S(t_G - t_0) + Ym_0 \quad (9.10)$$

**EXAMPLE 9.1** (Psychrometric properties of moist air): A certain air has a dry-bulb temperature of  $30^\circ\text{C}$  and a dew point of  $20^\circ\text{C}$ . The total pressure is 760 mm Hg. Calculate

- (a) molal humidity ( $Y_m$ )
- (b) absolute humidity ( $Y$ )
- (c) percentage relative humidity
- (d) percentage saturation
- (e) humid volume
- (f) humid heat

*Given:* Vapour pressures of water at 20 °C and 30 °C are 17.535 mm Hg and 31.824 mm Hg, respectively.

**Solution:**

$$\begin{aligned}\text{Partial pressure of water in air} &= \text{Vapour pressure of water at dew point} \\ &= 17.535 \text{ mm Hg.}\end{aligned}$$

(a) From Eq. (9.1), we have

$$Y_m = \frac{\frac{P'_A}{P - P'_A}}{\frac{17.535}{760 - 17.535}} = 0.0236 \text{ mol H}_2\text{O/mol dry gas}$$

(b) From Eq. (9.3), we get

$$Y = 0.622 Y_m = (0.622 \# 0.0236) = 0.0147 \text{ kg H}_2\text{O/kg dry air}$$

(c) From Eq. (9.6), vapour pressure of water at saturation, i.e., at 30 °C = 31.824 mm Hg

$$\text{Percentage relative humidity} = \frac{\frac{P'_A}{P_A}}{\frac{17.535}{31.824}} \# 100 = \frac{17.535}{31.824} \# 100 = 55.10\%$$

(d) From Eq. (9.5), we obtain

$$\begin{aligned}\text{Percentage saturation} &= \left( \frac{P'_A}{P_A} \times \frac{P - P'_A}{P - P'_A} \right) \# 100 = \left( \frac{17.535}{31.824} \times \frac{760 - 31.824}{760 - 17.535} \right) \# 100 \\ &= 54.04\%\end{aligned}$$

(e) From Eq. (9.7), we get

$$\begin{aligned}\text{Humid volume (y}_H\text{)} &= \left( \frac{Y}{M_A} + \frac{1}{M_B} \right) \# 22.414 \# \left( \frac{t_G + 273}{273} \right) \times \frac{1}{P} \\ &= \left( \frac{0.0147}{18.02} + \frac{1}{28.97} \right) \times 22.414 \times \left( \frac{30 + 273}{273} \right) \times \frac{1}{1} \\ &= 0.8787 \text{ m}^3/\text{kg dry gas}\end{aligned}$$

(f) From Eq. (9.9), we get

$$\begin{aligned}\text{Humid heat (C}_S\text{)} &= 1.005 + 1.88 \# 0.0147 \\ &= 1.033 \text{ kcal/kg dry air. } ^\circ\text{C.}\end{aligned}$$

### 9.3 Adiabatic Saturation Temperature

For any vapour-gas mixture, there is a temperature known as *adiabatic saturation* temperature ( $t_{as}$ ) such that if contacted adiabatically with a liquid at this temperature, the gas will be humidified and cooled since the latent heat of vaporisation required by the liquid will have to be supplied by the gas. If sufficient time is allowed the gas will be saturated, otherwise its temperature and humidity will lie somewhere on the adiabatic saturation curve of the initial gas.

### Air-water system

Let us consider a humidification chamber in which water is continuously sprayed and then collected at the bottom of the chamber from where it is pumped out and recirculated. The chamber is thoroughly insulated. A small quantity of water at the temperature  $t_{as}$  of the water in the chamber is continuously introduced to compensate for the water loss due to vaporisation.

An air stream is continuously introduced into the chamber and comes in intimate contact with the water spray. The air stream attains thermal equilibrium with the water at temperature  $t_{as}$  and also gets saturated with water at this temperature. The temperature  $t_{as}$  is called the *adiabatic saturation temperature*. Let  $Y_{as}$  be the humidity of the saturated exit air.

Choosing  $t_{as}$  as the reference temperature,

$$\text{Enthalpy of the inlet air: } C_S(t_G - t_{as}) + m_{as}Y, \text{ kJ/kg dry air} \quad (9.11)$$

$$\text{Enthalpy of the exit air: } C_S(t_{as} - t_{as}) + m_{as}Y_{as} = m_{as}Y_{as} \quad (9.12)$$

The enthalpy of water does not change since its temperature remains constant. There being no heat exchange with the surroundings, the enthalpy of the air also remains constant. Therefore, at steady-state

$$C_S(t_G - t_{as}) + m_{as}Y = m_{as}Y_{as} \quad (9.13)$$

or,

$$t_G - t_{as} = (Y_{as} - Y) \frac{\lambda_{as}}{C_S} \quad (9.14)$$

Equation (9.14) may be used to make a plot of  $t_G$  vs  $Y$  for a given set of values of  $t_{as}$  and  $m_{as}$ . Such a plot is known as *adiabatic saturation curve*. An adiabatic saturation curve terminates on the 100% saturation curve of the psychrometric chart shown in Figure 9.2. Since the humid heat  $C_S$  contains the term  $Y_1$ , the curve is not straight but slightly concave upward. The adiabatic saturation curve is the constant enthalpy locus of the point  $(t_G, Y)$  on the  $(t-Y)$  plane. The point  $(t_{as}, Y_{as})$  lies on the 100% humidity curve.

## 9.4 Wet-Bulb Temperature

*Wet-Bulb Temperature* is the steady-state temperature attained by a small amount of liquid evaporating into a large amount of unsaturated vapour-gas mixture.

When a small drop of liquid is brought into contact with a moving stream of vapour-gas mixture whose dew point is lower than the temperature of the liquid, the vapour pressure of the liquid at its surface becomes higher than the partial pressure of the vapour in the bulk of the gas. As a result, the

liquid evaporates and diffuses into the gas. The required latent heat is initially drawn from the liquid and the temperature of the liquid starts going down. Finally, a dynamic equilibrium is established so that the sensible heat transferred from the gas to the liquid is equal to the latent heat required to maintain the evaporation of the liquid. This steady-state temperature is called the *wet-bulb temperature* (WBT).

Wet-bulb temperature is an important psychrometric property of air-water system. It is measured by a wet-bulb thermometer. In a wet-bulb thermometer, a wet wick covers the bulb of the thermometer, the other end of the wick is dipped into a water pot. The wick remains wet by capillary action. The thermometer is placed in a moving stream of unsaturated air-water vapour mixture whose wet-bulb temperature has to be measured. The temperature indicated by the wet-bulb thermometer is the wet-bulb temperature. Wet-bulb temperature mainly depends on the dry-bulb temperature of the air and its humidity. However, the air velocity and the shape of the thermometer bulb have some effects on the measurement of wet-bulb temperature. It has been reported that for air velocity above 30 km/hr wet-bulb temperature depends only on the dry-bulb temperature of the air and its humidity. In order to keep the air velocity above 30 km/hr, the ‘sling thermometer’ is often used. In a sling thermometer, the wet-bulb thermometer is fixed on a panel which can swing rapidly to maintain the relative air velocity above 30 km/hr.

Wet-bulb temperature is lower than the dry-bulb temperature of the air-water vapour mixture except at 100% saturation when both the temperatures are same.

Let us consider a drop of water surrounded by a moving stream of large quantity of unsaturated air-water vapour as stated above and shown in Figure 9.1.

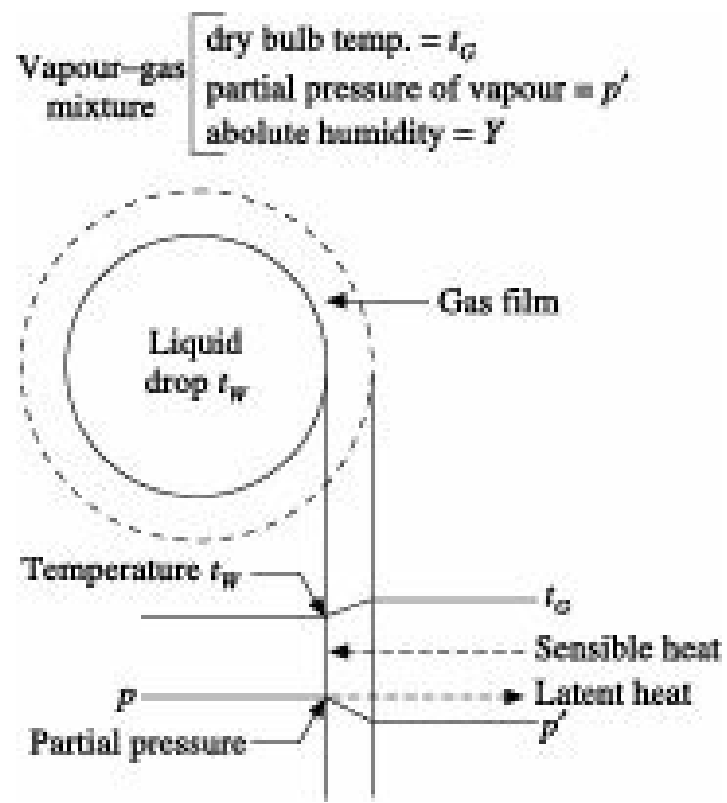


Figure 9.1 Wet-bulb temperature.

Under steady-state conditions, the sensible heat  $q_1$  transferred from air to water drop is

$$q_1 = h_G (t_G - t_W) \quad (9.15)$$

where

$t_G$  = DBT of the air

$t_W$  = WBT

$h_G$  = heat transfer coefficient of the air-film

The number of moles of water evaporated is

$$N_A = k_G (p'W - p'A) \quad (9.16)$$

Since the sensible heat transferred from air to water is fully utilized as latent heat of vaporisation of water, we have

$$h_G(t_G - t_W) = m_W M_A k_G (p'W - p'A) = m_W k_y (Y_W - Y) \quad (9.17)$$

From Eq. (9.17), we get

$$t_G - t_W = \frac{\lambda_w (Y_W - Y)}{h_G/k_y} \quad (9.18)$$

where,

$k_G$  and  $k_y$  = mass transfer coefficient of water vapour per unit partial pressure/mole fraction driving force respectively,  $\text{kg}/(\text{m}^2)(\text{hr})$  (driving force),

$m_W$  = latent heat of vaporisation of water at WBT

$Y$  = humidity of ambient air

$Y_W$  = saturation humidity of air at WBT.

Equation (9.18) is the expression for WBT. The quantity ( $t_G - t_W$ ) is known as *wet-bulb depression*. This equation can be used to determine the wet-bulb temperature provided  $h_G$  and  $k_y$  are known. Experimental data indicate that for air-water system under moderate conditions, the ratio ( $h_G/k_y$ ) is approximately equal to 0.227  $\text{kcal}/(\text{kg})(^\circ\text{C})$  which is equal to the humid heat ( $C_S$ ) of air at moderate humidities. This leads to a very interesting correlation known as Lewis relation after W.K. Lewis.

$$\frac{h_G}{k_y} = C_S \text{ or } \frac{h_G}{k_y C_S} = 1 \quad (9.19)$$

Combining Eqs. (9.18) and (9.19), we get

$$t_G - t_W = \frac{\lambda_w (Y_W - Y)}{C_S} \quad (9.20)$$

Comparing Eqs. (9.14) and (9.20) it is found that

$$t_{as} = t_W$$

Thus, the adiabatic saturation temperature and wet-bulb temperature of an air-water system are almost equal. This is however, not true for other systems.

Henry and Epstein (1970) conducted several experiments on flow of gases past cylinders, such as wet-bulb thermometers, and past single spheres. They correlated their results with 18 vapour-gas mixtures by the relation

$$\text{Psychrometric ratio} = \frac{k_G}{k_y C_S} = \left( \frac{\text{Sc}}{\text{Pr}} \right)^{0.567} = \text{Le}^{0.567} \quad (9.21)$$

For dilute mixtures of vapour and air where  $C_S = C_B$ , and taking Pr for air as 0.707 Eq. (9.21) becomes

$$\frac{k_G}{k_y} = 1223 (\text{Sc})^{0.567} \text{ J/(kg)(K)} \quad (9.22)$$

As stated earlier, humidification and associated operations in practice mostly involve air-water contact. Different types of tables and charts have, therefore, been prepared representing various *psychrometric* properties of air-water systems. The psychrometric chart or humidity chart is one such representation which is widely used for determining and correlating different psychrometric properties of air-water mixtures.

### **The psychrometric chart**

A psychrometric chart for air-water vapour at 1 atm pressure is shown in Figure 9.2.

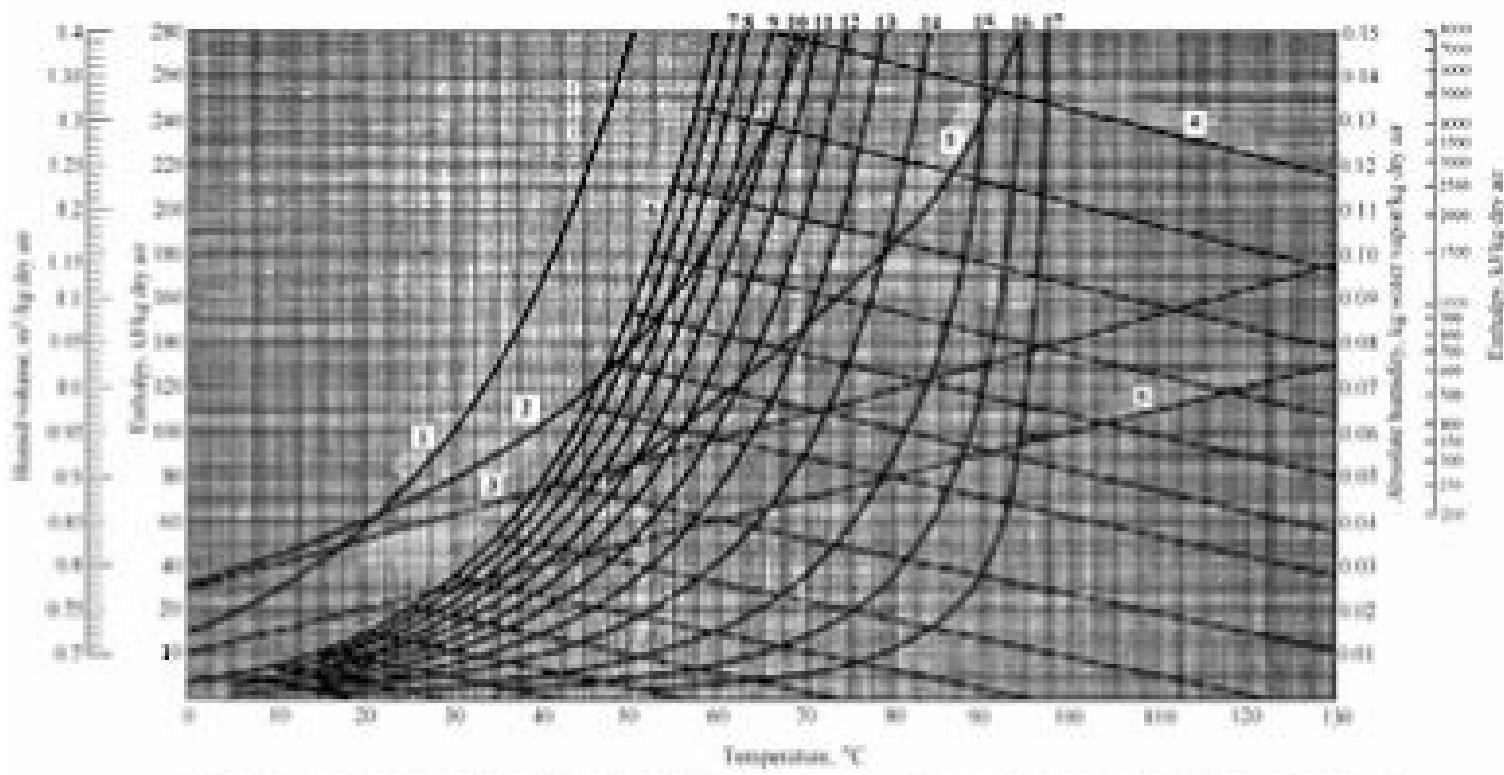


**Figure 9.2** Psychrometric chart for air-water vapour, at 1 std atm pressure in SI unit.

In this chart, temperature is plotted along the abscissa. All the four relevant temperatures, namely, dry-bulb temperature, wet-bulb temperature, adiabatic saturation temperature (which is the same as wet-bulb temperature for an air-water system) and dew point can be read from the abscissa. The ordinate represents the absolute humidity, percentage humidity, specific volume of dry air, humid volume of saturated air, enthalpy of dry air and enthalpy of saturated air. These properties are all interrelated so that if any two of them are known, the rest can be determined from the chart. Adiabatic saturation curves are plotted on this chart according to Eq. (9.14). Psychrometric charts may be drawn for any other systems.

The method of using the psychrometric chart has been explained in Example 9.2.

**EXAMPLE 9.2** (Use of psychrometric chart): An air-water vapour mixture has a dry-bulb temperature of 50°C and a wet-bulb temperature of 32.4°C. Using the psychrometric chart, determine the psychrometric properties of the mixture.

**Solution:** A schematic diagram of the relevant portion of the psychrometric chart is shown in Figure 9.3.

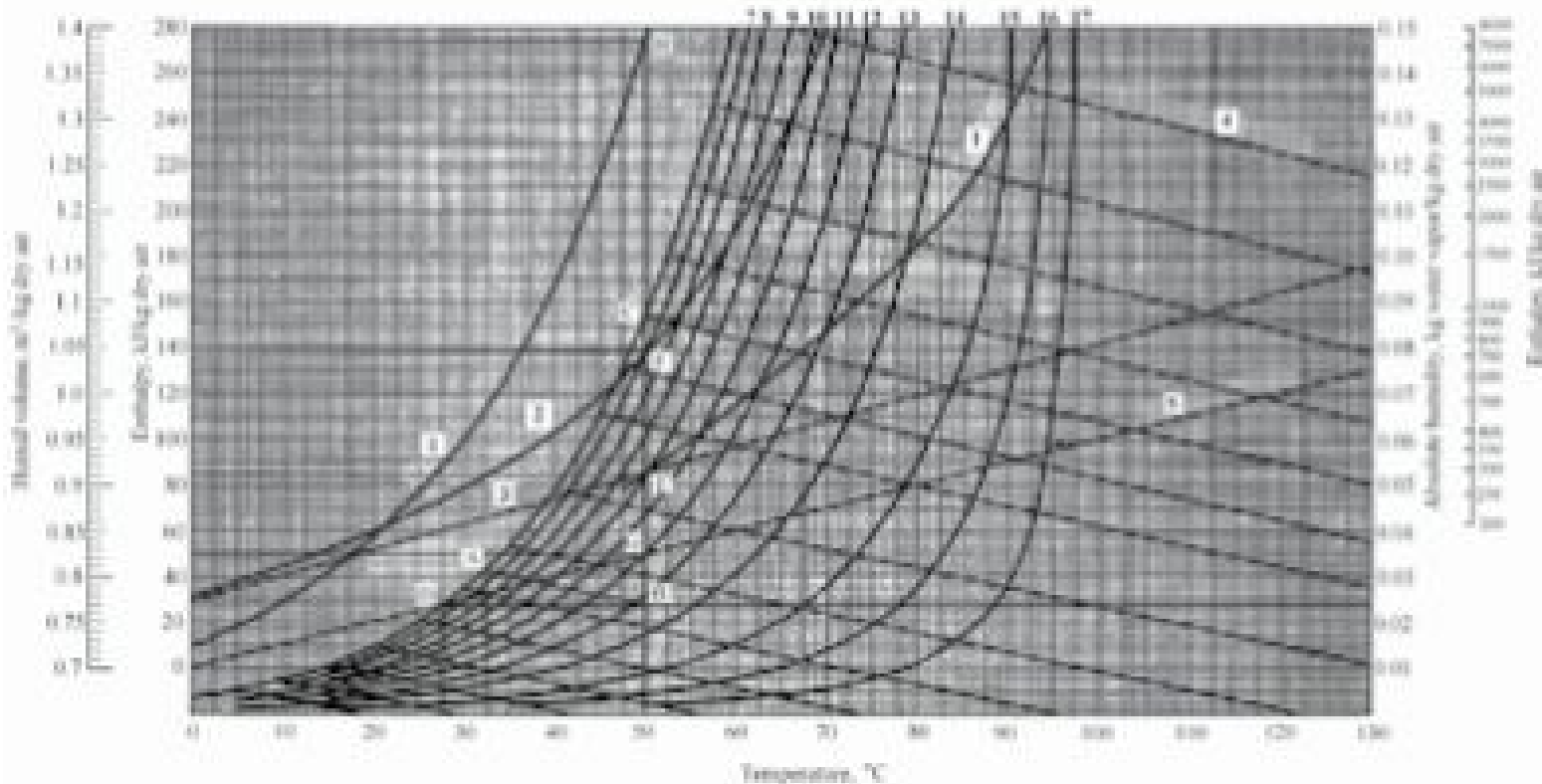


**Figure 9.3** Example 9.2.

(a) *Absolute humidity*: A vertical line is drawn from the given wet-bulb temperature (32.4°C) to meet the 100% humidity line at point A. From A, a line is drawn parallel to the nearest adiabatic saturation curve which meets the vertical from the dry-bulb temperature of the air (50°C) at point B. A horizontal line from B shows the absolute humidity ( $Y$ ) of the air as 0.024 kg water/kg dry air. B indicates the position of the air-water vapour mixture on the psychrometric chart.

(b) *Molar humidity*: From Eq. (9.3), the molar humidity is

$$Y_m = \frac{Y}{0.622} = \frac{0.024}{0.622} = 0.0386 \text{ kmol water/ kmol dry air.}$$

(c) *Percentage humidity*: By vertical interpolation between adjacent curves of constant percentage humidity, the air-water vapour mixture has a percentage humidity of 27.8%. Alternatively, the saturated humidity (corresponding to point C) of the air at 50°C is 0.086, so that the percentage humidity of the air at B is

$$\frac{0.024}{0.086} \# 100 = 27.91\%.$$

(d) The *partial pressure* of water vapour in the air is

$$p'_A = \frac{Y_m P}{1 + Y_m} = \frac{(0.0386)(1.0133 \times 10^5)}{1.0386} = 3765.97 \text{ N/m}^2$$

(e) *Relative humidity*:

The vapour pressure of water at 50 °C = 92.51 mm Hg = (92.51) (133.3)  
 $= 12331.6 \text{ N/m}^2$

$$\text{Relative humidity} = \frac{P'_A}{P_A} \# 100 = \frac{(3765.97)(100)}{12331.6} = 30.54\%.$$

(f) *Dew point*: A horizontal line is drawn from point *B* to meet the saturation curve at point *D*. The temperature corresponding to point *D* is the dew point. Its value is 27.5°C.

(g) *Humid volume*: Specific volume of dry air is first determined by drawing a vertical line from the point *B* up to the curve for specific volume of dry air (Point *E*) and its value is determined from the left-hand scale as 0.91 m<sup>3</sup>/kg dry air. The humid volume of the saturated air as read from the curve (corresponding to Point *F*) is 1.045 m<sup>3</sup>/kg. The humid volume of the sample air is obtained by interpolation for 27.8% humidity,

$$y_H = 0.91 + (1.045 - 0.91)(0.278) = 0.95 \text{ m}^3/\text{kg dry air.}$$

(h) *Humid heat*: The humidity of the air is 0.024 kg water/kg dry air.

From Eq. (9.9), the humid heat of moist air is

$$C_B = 1.005 + (1.88)(0.024) = 1.05 \text{ kJ/kg dry air. K}$$

(i) *Enthalpy*: At 50°C, the enthalpy of dry air (corresponding to Point *G*) is 50 kJ/kg dry air and that of saturated air (corresponding to Point *H*) is 274 kJ/kg dry air.

Interpolating for 27.8% humidity,

$$H = (274 - 50) \# 0.278 = 62.27 \text{ kJ/kg dry air.}$$

**EXAMPLE 9.3** (Production of air of a given relative humidity): It is desired to maintain 75% relative humidity in the packaging unit of a plant. For this purpose, fresh air at 42°C dry-bulb and 25 °C wet-bulb temperatures is introduced into a spray chamber where the RH is raised to 95%. This air is then heated by steam coils to attain 75% RH. Calculate

(a) amount of moisture added to the air in the spray chamber

(b) dry-bulb and wet-bulb temperatures of the exit air

(c) heating load on steam coil per kg dry air and

(d) steam consumption in kg/hr if the fresh air rate is 2000 m<sup>3</sup>/hr and steam is available at 2.0 kgf/cm<sup>2</sup> g pressure

**Solution:**

(a) From psychrometric chart, absolute humidity of initial air at 42°C dry-bulb and 25°C wet-bulb temperatures:

$$Y_1 = 0.0118 \text{ kg/kg dry air}$$

By following the adiabatic saturation curve through this point up to 95% RH:

$$Y_2 = 0.0185 \text{ kg/kg dry air}$$

Moisture added to air in spray chamber

$$\begin{aligned} &= (0.0185 - 0.0118) = 0.0067 \text{ kg/kg dry air} \\ &= 6.7 \text{ g/kg dry air} \end{aligned}$$

- (b) During heating, the absolute humidity remains constant and hence the air follows the horizontal line up to 75% RH. For this air,

dry-bulb temperature = 28.0 °C, wet-bulb temperature = 24.8 °C

- (c) From Eq. (9.9), humid heat of air at  $Y_2 = 0.0185 \text{ kg H}_2\text{O/kg dry air}$ ,

$$C_S = 1.005 + 1.88 \# 0.0185 = 1.043 \text{ kcal/kg dry air } ^\circ\text{C}$$

Temperature rise during heating =  $(28.0 - 25.5) = 2.5 \text{ } ^\circ\text{C}$

Heating load on steam coils =  $(0.249 \# 2.5) = 0.623 \text{ kcal/kg dry air}$

- (d) Humid volume of entering air =  $0.906 \text{ m}^3/\text{kg dry air}$

$$\text{Mass flow rate of air} = \frac{2000}{0.906} = 2207.5 \text{ kg dry air/hr}$$

$$\text{Total heat load on steam coils} = 2207.5 \# 0.623 = 1375.27 \text{ kcal/hr}$$

$$\text{Latent heat of steam at } 3.033 \text{ kgf/cm}^2\text{a, } m = 517.04 \text{ kcal/kg}$$

$$\text{Steam consumption} = \frac{1375.27}{517.04} = 2.66 \text{ kg/hr}$$

## 9.5 Operation Involving Gas–Liquid Contact

Humidification and associated operations apparently seem to be quite simple since mass transfer occurs only in the gas phase. But in practice, they are complex due to large heat effects caused by phase change.

Humidification operations are broadly classified into adiabatic and non-adiabatic operations. Some important adiabatic operations are as follows:

- (a) Cooling of a liquid by a gas such as water cooling involving both sensible and latent heat transfer,
- (b) Humidifying a gas such as in control of humidity of air for drying,
- (c) Cooling a hot gas by direct contact with a liquid is very effective provided the presence of some of the vapour of the liquid is not objectionable,
- (d) Dehumidifying a gas by contact of the warm vapour-gas mixture with a cold liquid when some of the vapour condenses. Used in air-conditioning, recovery of solvent vapour from gases, etc.

Non-adiabatic operations include:

- (a) Evaporative cooling,
- (b) Dehumidifying a gas by contact with refrigerated pipes.

### 9.5.1 General Equations

Considering counter-current contact of gas and liquid as shown in Figure 9.4, the overall material balance is given by

$$L'2 + G'SY_1 = L'1 + G'SY_2 \quad (9.23)$$

or,  $L'2 - L'1 = G'S(Y_2 - Y_1)$

and enthalpy balance is:

$$L'2h'2 + G'SH_1 + Q = L'1h'1 + G'SH_2 \quad (9.24)$$

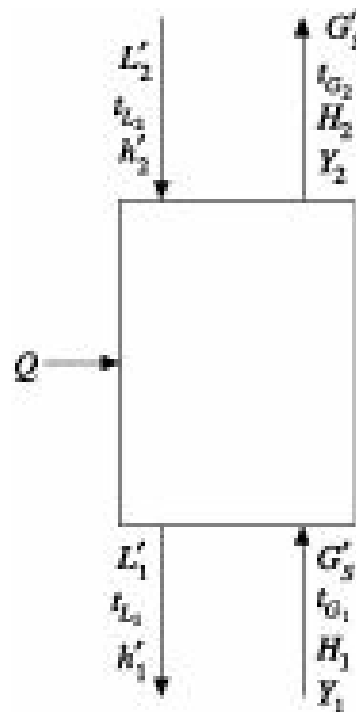


Figure 9.4 Flow diagram of counter-current gas–liquid contact.

### Adiabatic gas–liquid contact:

For adiabatic operations:  $Q = 0$

Referring to Figure 9.5,

$$\text{Material Balance: } dL' = G'S . dY \quad (9.25)$$

$$\text{Interfacial Area: } ds = a . dZ$$

where  $a$  is the specific interfacial area per unit volume of packed bed and  $dZ$  is differential height being equal to volume per unit cross section.

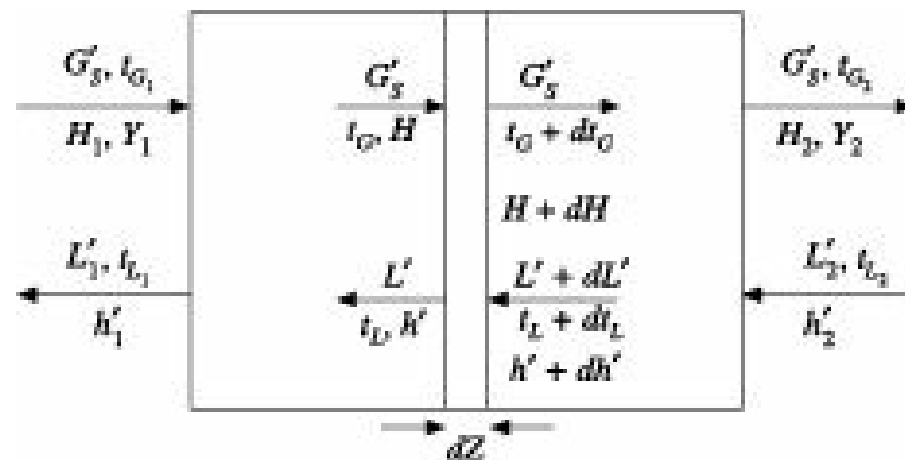


Figure 9.5 Adiabatic gas–liquid contact.

## 9.5.2 Enthalpy Balance

$$d(L'h') = G'SdH \quad (9.26)$$

Since  $L'2 \approx L'1 \approx L'$ , Eq. (9.26) becomes

$$L'C_{AL}dt_L = G'S dH \quad (9.27)$$

Substituting the expression for H from Eq. (9.10), we get

$$G'S dH = G'S d [C_S(t_G - t_0) + Ym_0]$$

or,

$$G'S dH = G'S C_S dt_G + G'S m_0 dY \quad (9.28)$$

The first term of the right-hand side in the Eq. (9.28) represents sensible heat transfer while the second term represents latent heat transfer. Their rates may be expressed as under:

Rates of sensible heat transfer:

$$\text{Liquid film: } L'C_{AL} dt_L = h_L a (t_L - t_i)dZ \quad (9.29)$$

$$\text{Gas film: } G'S C_S dt_G = h_G a (t_i - t_G)dZ \quad (9.30)$$

Rate of mass transfer:

$$G'SdY = k_y a(Y_i - Y)dZ \quad (9.31)$$

The above equations form the basis for developing design equations for adiabatic humidification operations and may be used where appropriate simplified equations are not available.

## 9.6 Water Cooling

Huge quantity of water is required for cooling purposes in chemical, metallurgical and allied industries. The largest users of cooling water are the power plants which use water for condensing huge quantity of low pressure steam from turbines. Since the water used for cooling purposes involves pumping and treatment costs, nobody can afford to throw away the water after single use. Moreover, disposal of hot water into water resources such as rivers, lakes, etc. often causes serious problems by leading to thermal imbalance and adversely affecting aquatic life. In order to conserve water, the warm water coming out from coolers and condensers is cooled and reused. Cooling of water is done by direct contact with unsaturated air in cooling towers. Warm water is fed at the top of the cooling tower and air is drawn at the bottom or through the side walls. This makes water cooling a very widely used gas-liquid operation.

Since enthalpy difference is a significant driving force in this case, design equations are developed on the basis of enthalpy difference. From Eq. (9.27),

$$L'C_{AL} \int_{t_1}^{t_2} dt_L = G'S \int_{H_1}^{H_2} dH \quad (9.32)$$

Integrating both sides, we obtain

$$L'C_{AL}(t_{L2} - t_{L1}) = G'S(H_2 - H_1) \quad (9.33)$$

Expressing the two terms of the right-hand side of Eq. (9.28) in terms of Eqs. (9.30) and (9.31),

respectively

$$G'SdH = h_G a(t_i - t_G) dZ + k_y a(Y_i - Y) m_0 dZ \quad (9.34)$$

Assuming  $\frac{h_G a}{k_y a C_S} = r$ , Eq. (9.34) becomes

$$G'SdH = k_y a[(C_S r t_i + m_0 Y_i) - (C_S r t_G + m_0 Y)] dZ \quad (9.35)$$

In the special case, where  $r = 1$  which is true for air-water systems (Mickley 1949),

$$G'SdH = k_y a(H_i - H) dZ \quad (9.36)$$

Replacing the enthalpy driving force within the gas phase by an overall driving force ( $H^* - H$ ) representing the enthalpy difference for the bulk phases and using an overall coefficient  $K_y a$ , Eq. (9.36) can be expressed as

$$G'SdH = K_y a(H^* - H) dZ \quad (9.37)$$

$$\int_{H_1}^{H_2} \frac{dH}{H^* - H} = \frac{K_y a}{G'_S} \int_0^Z dZ = \frac{K_y a Z}{G'_S}$$

whence,

$$\text{or, } Z = \frac{G'_S}{K_y a} \int_{H_1}^{H_2} \frac{dH}{H^* - H} = H_{toG} \cdot N_{toG} \quad (9.38)$$

where  $H_{toG}$  and  $N_{toG}$  are overall height and number of transfer units, respectively.

Since  $G'SdH = L' C_{AL} dt_L$ , [Eq. (9.27)] and for water  $C_{AL} \approx 1$ , Eq. (9.38) may also be written as

$$Z = \frac{L'}{K_y a} \int_{t_{L_1}}^{t_{L_2}} \frac{dt_L}{H^* - H} \quad (9.39)$$

The use of overall driving force is justified only if the equilibrium curve representing enthalpy of saturated gas as a function of liquid temperature is straight, at least over the range of enthalpies involved. This may, however, be used as an approximation for slightly curved equilibrium relation without serious error. Further, in case of linear equilibrium relation,

$$N_{toG} = \frac{t_{L_1} - t_{L_2}}{(H^* - H)_{av}} \quad (9.40)$$

The value of  $N_{toG}$  may be estimated from Eq. (9.39) through graphical integration by plotting  $[1/(H^* - H)]$  as ordinate against  $t_L$  as abscissa and finding out the area under the curve between the limits  $t_{L_1}$  and  $t_{L_2}$ . Alternatively, for linear equilibrium relationship, the estimation may be made from Eq. (9.40) by determining the enthalpies at the two ends of the equipment.

The equilibrium and operating lines for water cooling are shown in Figure 9.6. The operating line will lie below the equilibrium curve since the enthalpy of entering air must be less than the saturation

enthalpy  $H^*$  for air at temperature  $t_{L1}$ . Enthalpy for an air-water system being a function of wet-bulb temperature only, the wet-bulb temperature of the entering air must be below the liquid temperature  $t_{L1}$ , but the dry-bulb temperature need not be so. That is why it is possible to cool water to a temperature below the dry-bulb temperature of the entering air. The difference between the temperature of the exit liquid and the wet-bulb temperature of the entering air, ( $t_{L1} - t_{W1}$ ), is called the *wet-bulb temperature approach* and is a measure of the driving force available at the lower end of the cooling tower. This is usually kept between 2.5 to 5 °C in the design of cooling towers.

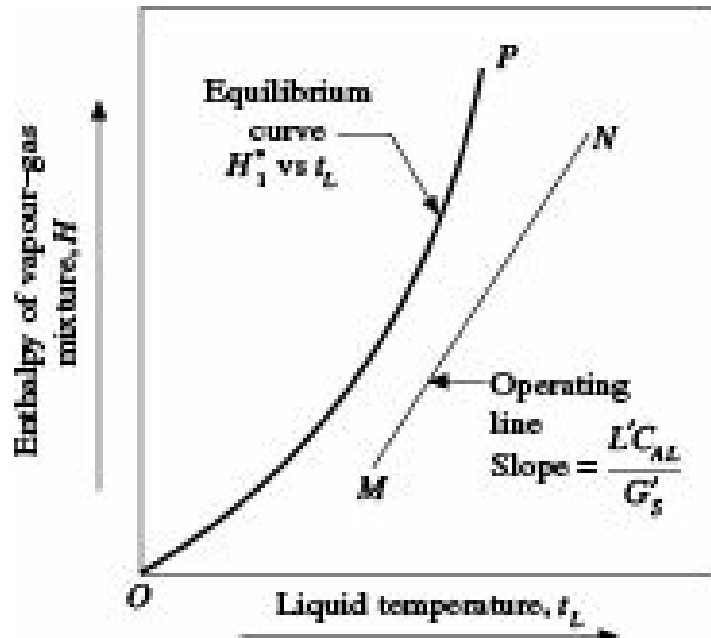


Figure 9.6 Equilibrium curve and operating line for water cooling.

As in case of gas absorption, the highest slope of the operating line for which it touches the equilibrium curve at the point  $(t_{L1}, H_1^*)$  or earlier, marks the condition for minimum gas rate possible.

**EXAMPLE 9.4** (Design of an induced draft cooling tower): An induced draft counter-current cooling tower is to be designed to cool 20 kg/s water from 45 °C to 29 °C. The design wet-bulb temperature of the entering air is to be 24 °C having an enthalpy of 72 kJ/kg dry air. It has been decided to use 30% excess air over the minimum air rate. Make-up water is available at 10 °C.

For the packing to be used,  $k_y a$  is expected to be 1.25 kg/(m<sup>3</sup>)(s)(DY) provided the minimum liquid and gas rates are 2.5 and 2.2 kg/(m<sup>2</sup>)(s), respectively.

Estimate the diameter and packed height of the tower.

Equilibrium Data:

$t_L, ^\circ\text{C}$	29	33	35	39	43	45	47.5
$H^*, \text{kJ/kg dry air}$	100	117	130	159	196	216	244

**Solution:** The equilibrium curve is drawn by plotting saturated air enthalpy ( $H^*$ ) against liquid temperature ( $t_L$ ) as shown in Figure 9.7.

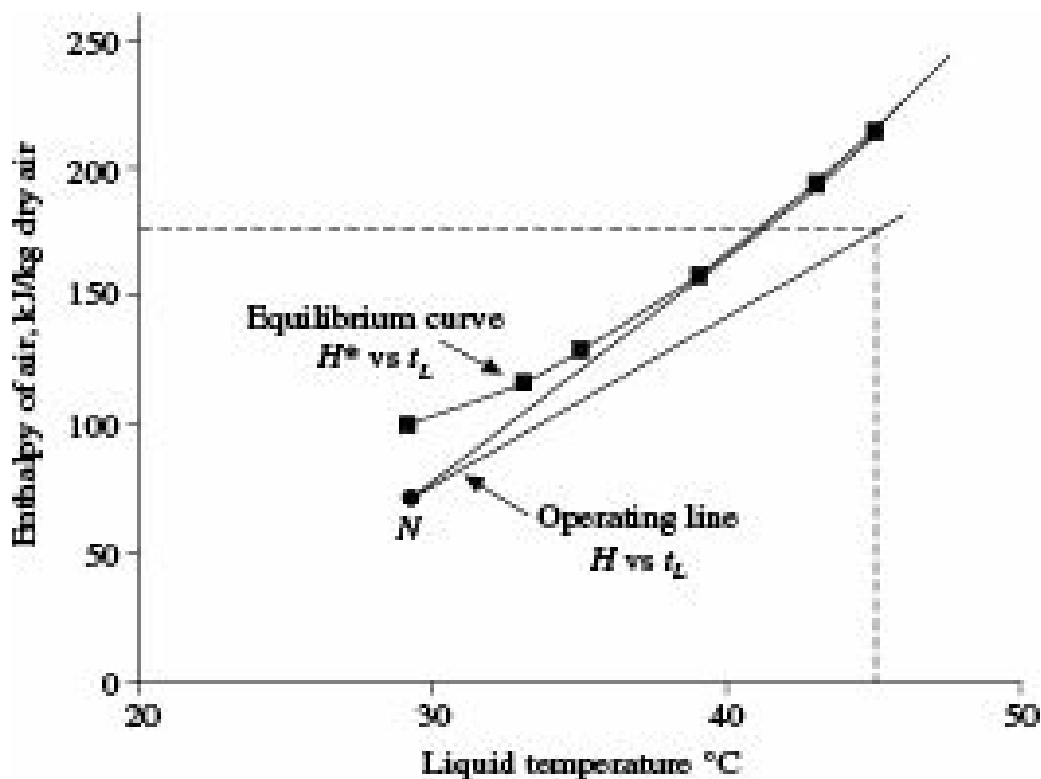


Figure 9.7 Example 9.4.

The operating line shall pass through the point  $N(t_{L1} = 29^\circ\text{C}, H = 72 \text{ kJ})$ . For minimum air rate, the operating line from  $N$  touches the equilibrium curve at  $t_{L2} = 45^\circ\text{C}$  or earlier. In this case, the operating line becomes tangent to the equilibrium curve at  $t_L = 39^\circ\text{C}$ .

From Eq. (9.33), for minimum liquid rate

$$\frac{LC_{AL}}{(G'_S)_{\min}} = \frac{(20)(4187)}{(G'_S)_{\min}} = \frac{H_2 - H_1}{t_{L2} - t_{L1}}$$

or,

$$\frac{(20)(4187)}{(G'_S)_{\min}} = \frac{209500 - 72000}{45 - 29}$$

whence  $(G'_S)_{\min} = 9.74 \text{ kg dry air/s}$ .

With 30% excess air,  $G'_S = (1.30)(9.74) = 12.66 \text{ kg. dry air/s}$ .

Slope of operating line:

$$\frac{H_2 - 72000}{45 - 29} = \frac{(20)(4187)}{12.66}$$

whence,  $H_2 = 177.832 \text{ kJ/kg dry air}$ .

For a liquid rate ( $L'$ ) of at least  $2.5 \text{ kg}/(\text{m}^2 \text{ s})$ ,

$$\text{cross section} = \frac{L'}{L} = \frac{20}{2.5} = 8 \text{ m}^2$$

For a gas rate ( $G'$ ) of at least  $2.2 \text{ kg}/(\text{m}^2 \text{ s})$ ,

$$\text{cross section} = \frac{G}{G'} = \frac{12.66}{2.2} = 5.75 \text{ m}^2$$

The lower value should be used so that  $k_y a = 1.25$

$$\text{Tower diameter} = \left( \frac{5.75 \times 4}{3.14} \right)^{0.5} = 2.70 \text{ m}$$

The values of  $[1/(H^* - H)]$  at different values of  $t_L$  are tabulated below:

$t_L, ^\circ\text{C}$	$H^*, \text{kJ/kg}$	$H, \text{kJ/kg}$	$[1/(H^* - H)], \text{kg/kJ}$	$[1/(H^* - H)], \text{kg/J}$
29	100	72	$3.57 \times 10^{-2}$	$3.57 \times 10^{-5}$
33	117	96	$4.76 \times 10^{-2}$	$4.76 \times 10^{-5}$
35	130	112	$5.55 \times 10^{-2}$	$5.55 \times 10^{-5}$
39	159	138	$4.76 \times 10^{-2}$	$4.76 \times 10^{-5}$
43	196	164	$3.13 \times 10^{-2}$	$3.13 \times 10^{-5}$
45	216	178	$2.63 \times 10^{-2}$	$2.63 \times 10^{-5}$

$[1/(H^* - H)]$  is plotted against  $H$  in Figure 9.8 and the area under the curve is measured between  $H_1 = 72 \text{ kJ}$  and  $H_2 = 178 \text{ kJ}$ .

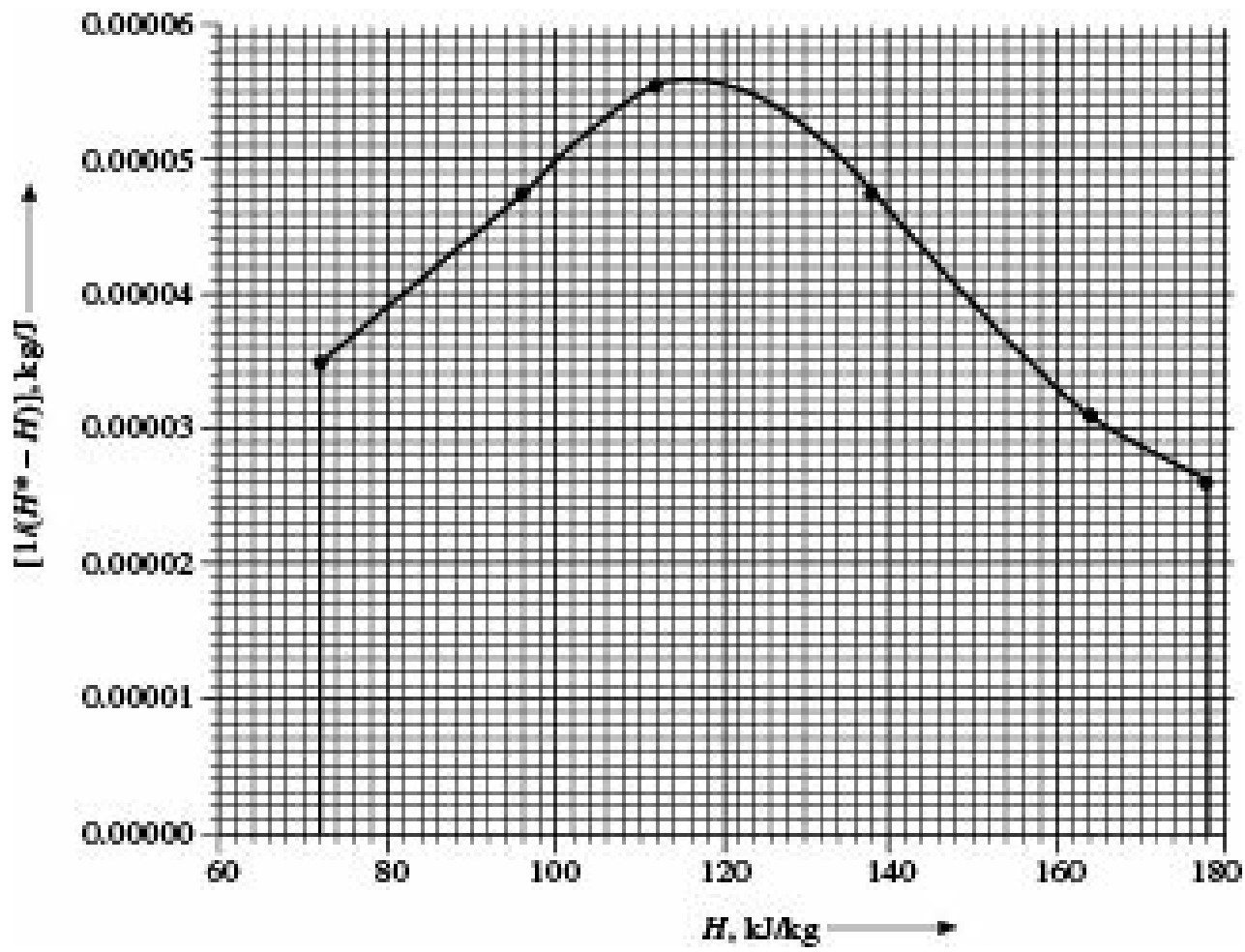


Figure 9.8 Example 9.4.

Area under the curve = 4.58 units

$$\text{Therefore, } 4.58 = \frac{k_y a Z}{G'} = \frac{(1.25)(Z)}{2.2} \text{ whence, } Z = 8.06 \text{ m.}$$

## 9.7 Adiabatic Humidification—Cooling

If the exit liquid from a humidifier is constantly recirculated without addition or removal of heat, the liquid will attain the adiabatic-saturation (as) temperature of the inlet air. The gas will be cooled and humidified along the adiabatic-saturation curve that passes through the inlet gas condition. Depending upon the intensity and time of contact, the gas will approach equilibrium with the liquid or its adiabatic-saturation conditions. The make-up water should also enter at the adiabatic-saturation temperature, but its quantity is so small that minor deviation in make-up water temperature has negligible effect.

Since the enthalpy of a gas is a function only of its adiabatic-saturation temperature which remains constant throughout the operation and the enthalpy of the liquid is also constant because its temperature remains constant, the operating line for such an operation on the enthalpy-temperature diagram becomes only a point. This type of diagram cannot, therefore, be used for design calculations. Temperature and humidity changes can, however, be used as the basis of design.

If mass transfer in the gas phase is used as the basis of design, the rate equation may be written as

$$G'SdY = k_y a(Y_{as} - Y)dZ \quad (9.41)$$

$$\int_{Y_1}^{Y_{as}} \frac{dY}{Y_{as} - Y} = \frac{k_y a}{G'_s} \int_0^Z dZ \quad (9.42)$$

or,

$$\ln \frac{Y_{as} - Y_1}{Y_{as} - Y_2} = \frac{k_y a Z}{G'_s} \quad (9.43)$$

Equation (9.43) can be solved directly for height of packing. Alternatively, it can be rearranged as

$$G'S(Y_2 - Y_1) = \frac{k_y a Z [(Y_{as} - Y_1) - (Y_{as} - Y_2)]}{\ln [(Y_{as} - Y_1)/(Y_{as} - Y_2)]}$$

$$= k_y a Z (DY)_{lm} \quad (9.44)$$

where  $(DY)_{lm}$  is the log-mean average of the humidity difference driving forces at the two ends of the equipment.

From Eqs. (9.43) and (9.44), we have

$$N_t G = \frac{Y_2 - Y_1}{(DY)_{lm}} = \ln \frac{Y_{as} - Y_1}{Y_{as} - Y_2} \quad (9.45)$$

and

$$H_t G = \frac{G'_s}{k_y a} \quad (9.46)$$

$$Z = H_t G \$ N_t G \quad (9.47)$$

where,  $H_t G$  is the height of a gas-phase transfer unit and  $N_t G$  is the corresponding number of transfer units.

Heat transfer can also be used for design calculations by using the following equation, which is similar to Eq. (9.44):

$$G' S C_{S1} (t_{G1} - t_{G2}) = \frac{h_G a Z [(t_{G1} - t_{\text{as}}) - (t_{G2} - t_{\text{as}})]}{\ln [(t_{G1} - t_{\text{as}})/ (t_{G2} - t_{\text{as}})]}$$

$$= h_G a Z (\Delta t)_{\text{lm}} \quad (9.48)$$

whence,

$$N_t G = \frac{t_{G1} - t_{G2}}{(\Delta t)_{\text{lm}}} \quad (9.49)$$

and

$$H_t G = \frac{G' S C_{S1}}{h_G a} \quad (9.50)$$

The Murphree gas-phase stage efficiency for such operations can be expressed as

$$E_{MG} = \frac{\frac{Y_2 - Y_1}{Y_{\text{as}} - Y_1}}{1 - \frac{Y_{\text{as}} - Y_1}{Y_{\text{as}} - Y_2}} = 1 - \exp (-k_y a Z / G' S)$$

$$= 1 - \exp (-N_t G) \quad (9.51)$$

Alternatively, in terms of temperature difference,

$$E'_{MG} = \frac{\frac{t_{G1} - t_{G2}}{t_{G1} - t_{\text{as}}}}{1 - \frac{t_{G2} - t_{\text{as}}}{t_{G1} - t_{\text{as}}}} = 1 - \exp (h_G a Z / G' S C_{S1})$$

$$= 1 - \exp (N_t G) \quad (9.52)$$

If one knows the tower characteristics,  $H_t G$  or  $H_t L$  at ambient condition, one can predict tower performance at another set of conditions prevailing during testing or operation of the tower. The tower characteristic is determined by integration-graphically or numerically (Perry et al. 1997). The correlations for mass transfer coefficients for standard packings discussed in Chapter 6, are also used for designing cooling towers. Additional data on Berl Saddles (Hensel and Treybal 1952) and on Intalox saddles and Pall rings (Nemunaitis and Eckert 1975) are available in the literature. Data on some special types of fittings for water coolers are also available in the literature (McKelvey and Brooke 1959).

## 9.8 Cooling Range and Approach

While selecting or designing a cooling tower, it is of primary importance that a reasonably accurate heat load determination is made. All else being equal, the size and cost of a cooling tower is proportional to heat load. The heat load of a cooling tower is determined by the flow rate of water being circulated through the process multiplied by the number of degree centigrade by which the process raises the circulating water temperature, according to the relation

$$\text{Heat load} = L \# C_p L \# R \quad (9.53)$$

where

$L$  = mass flow rate of liquid, kg/s

$CpL$  = specific heat of liquid, kcal/(kg)(°C)

$R$  = difference between hot water temperature entering the tower and cold water temperature leaving the tower, °C.

The difference between the temperatures of the entering warm water and leaving cold water in a cooling tower is called the *cooling range* or simply the *range*,  $R$ . The difference between the temperatures of the leaving cold water and the wet-bulb temperature of the entering air is called the *temperature approach*. Given two towers of equal efficiency, operating with proportionate air rate and fill configuration, the larger tower will deliver colder water. On the other hand, a large tower of average efficiency will deliver cold water at an approach no closer than a somewhat small tower having better efficiency, i.e. better fill and water distribution. The effect of chosen approach on tower size at fixed heat load, water flow rate and wet-bulb temperature is remarkable as shown in Figure 9.9.

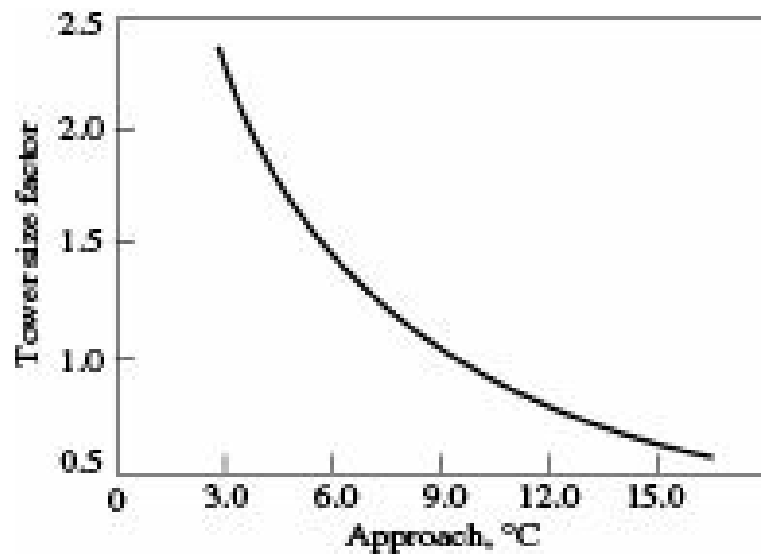


Figure 9.9 Chosen approach vs tower size at design heat load, LPM and wet-bulb temperature.

The tower size increases rapidly when the specified approach is less than about 9 °C and move asymptotically towards infinity when approach desired is much less below 3 °C, indicating that the lower is the desired approach, the higher will be the height of the tower. Therefore, a cooling tower manufacturer will not usually guarantee any approach below 3 °C.

**EXAMPLE 9.5** (Adiabatic humidification and cooling of air): Air has to be humidified and cooled adiabatically in a horizontal spray chamber with recirculated water. The active part of the chamber is 1 m # 2 m # 1.5 m long. Under the operating conditions, the coefficient of heat transfer is expected to be 1300 kcal/(hr)(m<sup>2</sup>)(°C). 200 m<sup>3</sup>/min of air at 60 °C and 1 atm pressure with a humidity of 0.018 kg water/kg dry air is to be blown through the spray chamber. Calculate the following:

- the temperature and humidity of the exit air
- make-up water to be supplied, windage and blow down are neglected
- the expected gas-phase mass transfer coefficient,  $k_y a$
- the temperature and humidity of the exit air if an identical spray chamber is added in series with the existing one.

**Solution:**

From psychrometric chart, % humidity of entering air = 12%

Humid volume of entering air =  $0.97 \text{ m}^3/\text{kg dry air}$

$$G'S = \frac{(200)(60)}{(0.97)(2)} = 6185.6 \text{ kg dry air/(hr)(m}^2)$$

Humid heat of initial air,  $C_{S1} = 0.24 + 0.46 \# 0.018 = 0.248 \text{ kcal/kg } ^\circ\text{C}$

$Z = 1.5 \text{ m}$ . From psychrometric chart,  $t_{as} = 31.6^\circ\text{C}$

(a) From Eq. (9.48),

$$\ln \frac{t_{G_1} - t_{as}}{t_{G_2} - t_{as}} = \frac{h_G a Z}{G'_S C_{S1}}$$

Substituting the values, we get

$$\ln \frac{60 - 31.6}{t_{G_2} - 31.6} = \frac{(1300)(1.5)}{(6185.6)(0.248)} = 1.271$$

$$\text{whence, } \frac{60 - 31.6}{t_{G_2} - 31.6} = e^{1.271} \text{ and } t_{G_2} = 39.57^\circ\text{C}$$

From psychrometric chart,  $Y_2 = 0.027 \text{ kg moisture/kg dry air}$

(b) Make-up water needed =  $(0.027 - 0.018)(6185.6 \# 2) = 111.34 \text{ kg/hr}$

(c) From psychrometric chart,  $Y_{as}$  for the entering air =  $0.0305 \text{ kg water/kg dry air}$

From Eq. (9.45),

$$\ln \frac{(0.0305 - 0.018)}{(0.0305 - 0.027)} = \frac{(k_y a)(1.5)}{6185.6}$$

$$\text{whence, } k_y a = 5249.5 \text{ kg/(m}^3\text{)(hr)(DY)}$$

$$\frac{h_G a}{C_S} = \frac{1300}{0.248}$$

Alternatively, from Lewis relation,  $k_y a =$

$$= 5241.9 \text{ kg/(m}^3\text{)(hr)(}\Delta Y\text{)}$$

(d) In this case  $Z = 1.5 \# 2 = 3 \text{ m}$ , other things remain unchanged.

$$\text{Therefore, } \ln \frac{60 - 31.6}{t_{G_2} - 31.6} = \frac{(1300)(3)}{(6185.6)(0.248)} = 2.54$$

$$\text{whence, } t'_{G_2} = 33.84^\circ\text{C}$$

$$\text{and } Y_2' = 0.029 \text{ kg moisture/kg dry air.}$$

## 9.9 Nonadiabatic Operations: Evaporative Cooling

In evaporative cooling, a fluid is cooled while flowing through tubes. Water is made to flow in thin films or as spray outside the tubes and air is blown past the water to remove the heat extracted from the tube side fluid. Since the water film or spray is evaporated into the air stream, the rate of heat transfer from water to air becomes very high. Since the water is recirculated from bottom to top of the heat exchanger, the terminal temperatures remain very close to each other. Although the water temperature does not remain constant within the equipment, it does not vary greatly from the terminal values. Detailed information in this regard has been given elsewhere (Treybal 1985).

## 9.10 Equipment for Air–Water Contact

Process plants, power stations as well as air conditioners and chillers generate huge amount of heat. This heat has to be dissipated continuously if the processes or machines are to be operated efficiently. In the past, this heat used to be transferred to flowing cool water such as a river and finally to the atmosphere through evaporation. To save consumption of fresh cooling water, cooling towers are installed where hot water from the process or machines is cooled by evaporation through intimate contact with a stream of air. Water thus cooled is recirculated to the condensers and other heat exchangers in the plant. A fraction of the circulating water is purged to prevent build up of contaminants beyond tolerance level. The function of the cooling tower is to dissipate waste heat which is always produced when we generate or utilize energy. More efficient a system or a machine is, less is the waste heat produced and smaller is the cooling tower capacity required. In other words, huge cooling towers in power plants, petroleum refineries or fertilizer plants show industries effort towards conserving water. But at the same time their big sizes symbolize the level of inefficiency in the current methods of energy utilization. Water cooling is by far the most important and widely used air-water contact operation. Our present discussion will therefore be limited to water cooling.

The following terms are commonly used in cooling tower industry and their definitions should be known while discussing operation of cooling towers:

*Air rate*—mass flow rate of dry air per unit cross sectional area in the tower's heat transfer region,  $M/L^2\square$ , or mass flow rate of dry air,  $M/\square$ .

*Air travel*—distance which the air travels in its passage through the fills.

*Blow down*—water discharged from the system to control concentration of salts and other impurities in the circulating water, percent circulating water rate.

*Drift*—water lost from tower as entrained liquid water droplets in the exhaust air stream, % circulating water rate.

*Fan cylinder*—cylindrical or venturi structure in which a propeller fan operates.

*Length*—for cross-flow towers length is perpendicular to the direction of air flow through the fill while for counter-flow towers length is parallel to the long dimension of a multicell tower,  $m$ .

*Make-up*—water added to circulating water to replace water lost, % circulating water.

*Plenum chamber*—the enclosed space between the drift eliminator and fan in induced draft towers.

*Pumping head*—static lift from elevation of the cold water basin curb to the centre line elevation of distribution system plus pressure necessary at that point to effect water distribution,  $m$  of water.

*Water rate*—mass flow rate of water per unit fill plan area,  $M/L^2\square$ , or mass flow rate of water,  $M/\square$ .

Most of the equipment for gas-liquid contact particularly packed and plate towers, described in Chapter 6, can be used for air-water contact as in humidification, dehumidification and water cooling. However, in view of the fact that both air and water are low cost materials and since large volumes of both have to be handled, equipment of low initial cost and low operating cost are preferred. Red wood which can stand continuous exposure to water for a very long time, has been traditionally used for making tower body and internal packings. The wood is, generally, impregnated with fungicides such as coal tar, creosote, pentachlorophenol, etc. The present trend, however, is towards use of reinforced concrete for tower body and fibre reinforced polymers (FRP) for tower body and internals.

Industrial cooling towers are designed and fabricated in several types and sizes. Knowledge of the applications and advantages of various types is essential for clear understanding of the principles of its design and operation. Cooling towers are usually classified into three groups according to the nature of air draft employed:

- (i) atmospheric towers,
- (ii) natural draft towers and
- (iii) mechanical draft towers.

Mechanical draft towers are further subdivided into forced draft and induced draft towers. According to another system of classification, the towers are divided into two groups, namely (a) cross-flow towers and (b) counter-flow towers according to the flow pattern of air through the tower.

### ***Atmospheric towers***

An atmospheric tower, shown in Figure 9.10, consists of a rectangular tower with a water trough at the bottom. Two opposite walls of the tower are provided with louvers for entry of air. The tower is packed with suitable tower fills (see Section 9.11). Atmospheric air enters the tower by virtue of its own velocity and comes in contact with water which flows from above as shower. These types of cooling towers are cheap but inefficient. Their performance largely depends on the velocity and direction of the wind.

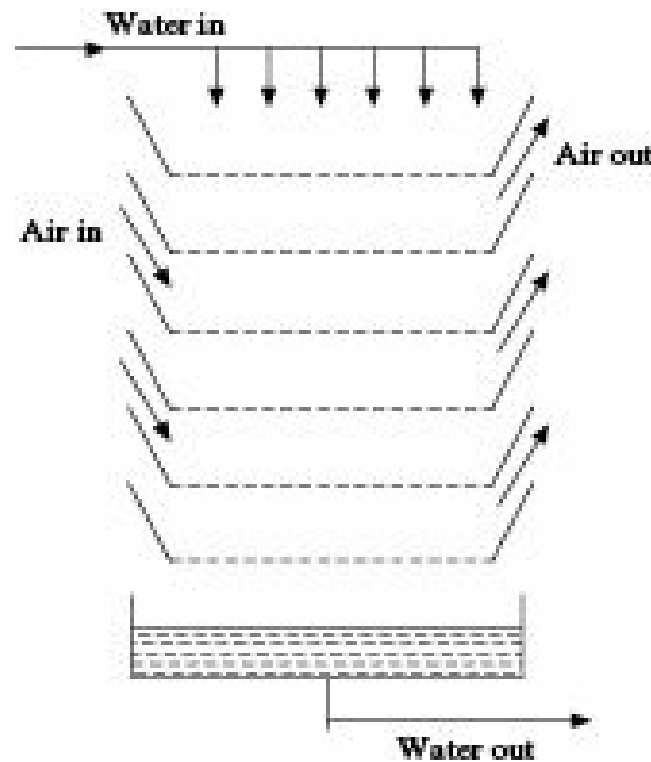


**Figure 9.10** Atmospheric cooling tower.

### Natural draft towers

A natural draft cooling tower shown in Figure 9.11, has a large concrete shell of hyperbolic shape. The advantage of hyperbolic shape is that the compound curvature allows use of a relatively thin shell of reinforced concrete. A small part of the tower near the bottom is filled with high void packing consisting of inclined wooden or PVC batters, 25 mm # 50 mm cross section fitted into slots along the supporting frames. Warm water from the distributor falls on the packing in the form of fine drops and then slips from one battern to the next below thus providing large surface for air-water contact. Cooling occurs by evaporation of a part of water. Air flow through these towers is produced by the density difference between the heated, humid air inside the stack and relatively cool ambient air outside the tower. Natural draft is affected by decrease in density of the air due to rise in temperature and humidity of the air as well as wind velocity at the bottom of the tower.

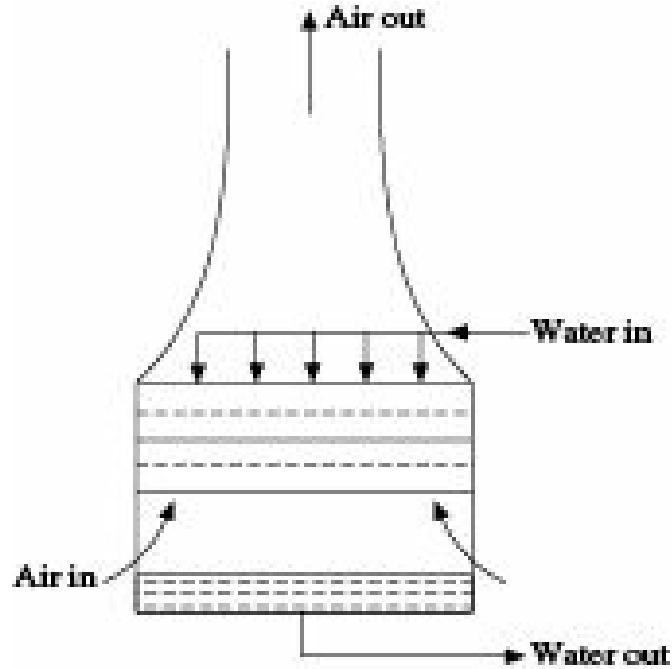


**Figure 9.11** Natural draft cooling tower.

Natural draft cooling towers may be very large, up to 100 m in diameter and up to 200 m high. For very high hot water load ( $1000 \text{ m}^3/\text{min}$  or more) natural draft cooling towers are often selected. These are generally used in power plants which require huge quantity of cooling water. Although these towers cost more than the mechanical draft towers, still are used when large unified heat load exists, e.g. in thermal power plants. Savings in power used by fan and the maintenance cost justify higher investment if the amortization period is sufficiently long. Sometimes fan-assisted natural draft towers are selected to minimize the power required for air movement, with the least possible stack cost. Relatively short stacks in these hybrid towers prevent low-level discharge of humid exit air and can operate without running the fan, except at the time of peak loads.

### Mechanical draft towers

Mechanical draft cooling towers are now preferred in process industries because of their compact design and high performance. These cooling towers use blowers or fans for moving the air through the towers. A number of chambers or cells, each equipped with a fan, are constructed in cellular fashion, when required to accomplish specified thermal load. The cells are normally put in rectilinear fashion

or in a round configuration. In round mechanical draft towers, the fans are positioned around the centre of the tower. Round shaped multicell towers require less site area and piping than those required by multiple rectilinear towers of large capacities.

Mechanical draft towers use either single or multiple fans to provide flow of air through the tower, the rate of which is known. Thus, these towers are less affected by variation in ambient conditions and have greater stability in performance. The fans can be provided with the means of regulating air flow to compensate for changing thermal load or atmospheric conditions. Mechanical draft cooling towers may be of two types—a forced draft cooling tower and an induced draft cooling tower.

A *forced draft* cooling tower usually equipped with one or more centrifugal blower(s) at the bottom to push air into the tower, is shown in Figure 9.12. These blowers have the advantage of being able to operate against high static pressure associated with duct work. Air and water flow counter-currently in this type of towers, a part of the velocity head of the air imparted by the blower(s) is converted to pressure head thereby making the towers more energy efficient than the induced draft towers. Also, the blower(s) being firmly secured on the foundation vibration is much less. The disadvantages are as follows:

- (i) the flow of air may not be uniform,
- (ii) some of the warm and humid air may flow back into the tower and adversely affect the performance of the tower and
- (iii) these are very much susceptible to recirculation because of high entrance velocity and low exit velocity of air.

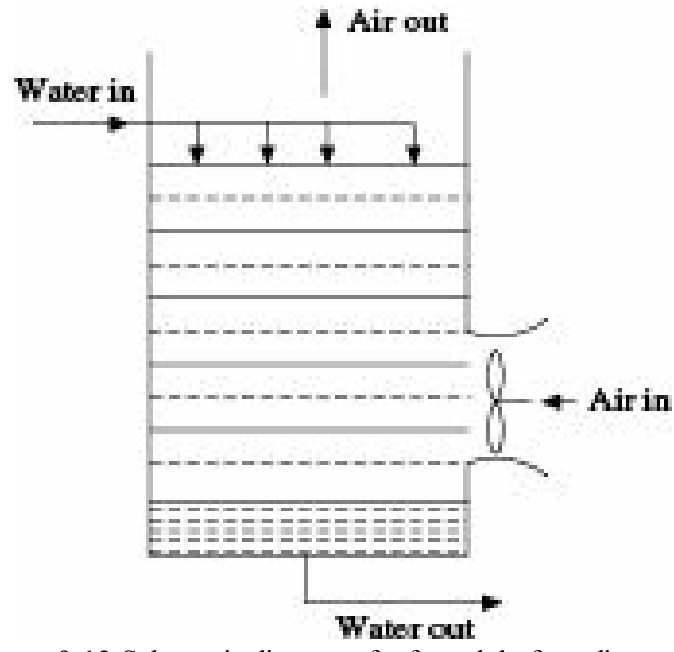
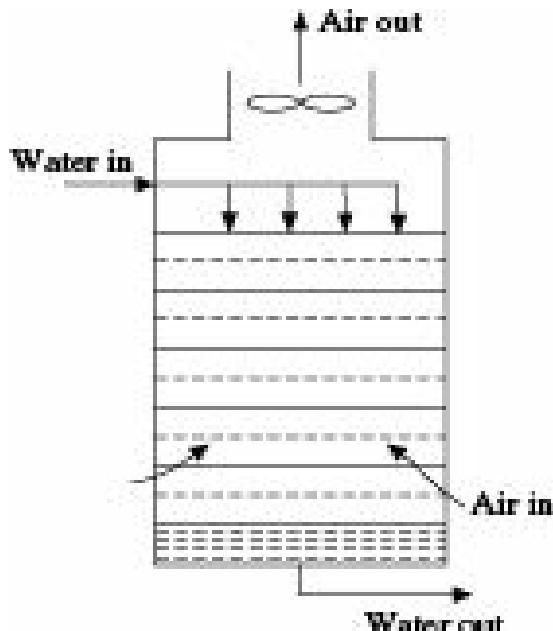


Figure 9.12 Schematic diagram of a forced draft cooling tower.

An *induced draft* cooling tower has one or more fan(s) located at the top, i.e. in the exit air stream which sucks fresh air through the air inlet at the bottom. Based on the relative flow relationship between air and water, induced draft cooling towers may be characterized as: counter-flow tower and cross-flow tower.

In a counter-flow induced draft cooling tower shown in Figure 9.13, air flows vertically counter-current to the downward flow of water. The major advantage of this arrangement is that the relatively dry air comes in contact with the coldest water at the bottom while the humid air comes in contact with the warm water at the top. This provides maximum advantage of driving force for both

heat and mass transfer. Counter-flow towers usually use high pressure water spray systems and utilize more fan power than the corresponding cross-flow towers, if these are of relatively small capacities. In large towers, however, use of low pressure water systems and availability of generous air intake areas tend to reverse the situation. The enclosed nature of counter-flow towers restricts exposure of the circulating water to sunlight and retards the growth of algae. But power loss is more due to the restricted area available for air flow and unlike the forced draft tower; the velocity head of the air is lost.



**Figure 9.13** Schematic diagram of a counter-current induced draft cooling tower.

The cross-flow induced draft cooling tower shown in Figure 9.14 provides horizontal air flow through the packings or fills. The air flows cross-current to the water which flows vertically downwards. Louvers are provided all along the walls of the tower through which air moves in. Cross-flow towers can be classified by the number of packing or fill banks and air inlets that are served by each fan. In double-flow tower, the fan induces air flow through two air inlets and across two banks of fill. A single flow tower has only one air inlet and one fill bank, the remaining three sides being enclosed. Such towers are used where an unrestricted path to the tower is available from only one direction. For the same air flow rate these types of towers require less power than the power required by counter-flow towers.

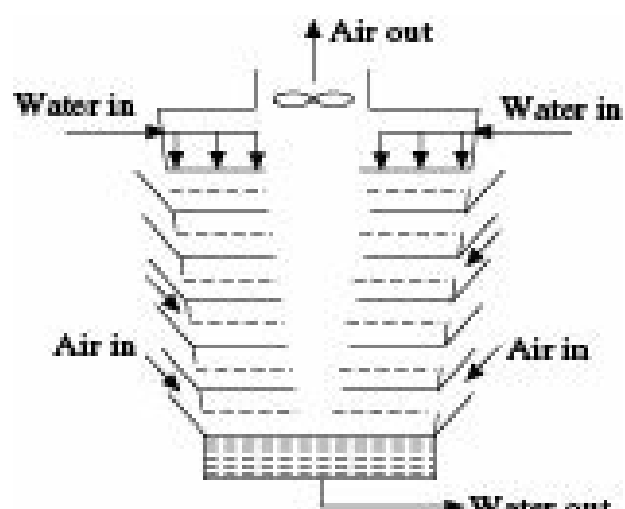


**Figure 9.14** Schematic diagram of a cross flow induced draft cooling tower.

These towers have air discharge velocity of 3-4 times higher than the air entrance velocity (approx. 7-8 km/hr). There is, therefore, little tendency for a reduced pressure zone created at the air inlet; pressure drop usually remains below 25 mm of water. These towers are accepted worldwide by the process industries for relatively small ( $0.1 \text{ m}^3/\text{min}$  water load) as well as large capacity ( $2000 \text{ m}^3/\text{min}$  water load) installations.

### **Cooling tower for water conservation**

In regions where water is so scarce that evaporative losses have to be minimized, a water conservation type of cooling tower is chosen (Figure 9.15).

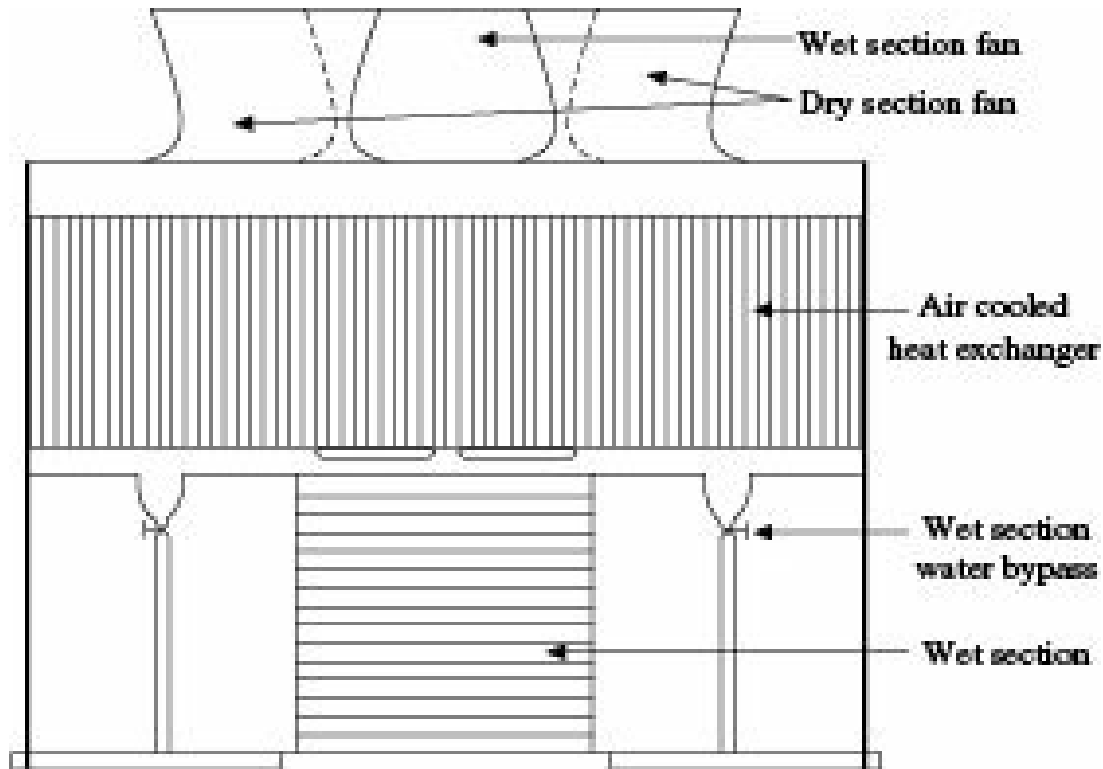


**Figure 9.15** Sectional view of cooling tower with dry and wet sections.

In such tower, hot water entering the tower flows first through a section containing finned tube heat exchanger where its temperature is reduced to the minimum level permitted by the dry-bulb temperature of air flowing outside the coils. When further cooling is necessary, flow is directed to the wet section of the tower where evaporative cooling removes the remaining portion of the heat load. Because of reduced evaporation there is a proportional reduction in drift and blow down losses. When only the dry section of tower is utilized, the cold water temperature attainable might be 10 to 15°C higher than what can be expected from a normal evaporative type cooling tower.

### **Spray chamber**

Spray chambers are frequently used for adiabatic humidification—cooling of air with recirculated water as in air conditioning. Spray chambers are essentially horizontal spray tower. A schematic diagram of the arrangements in a typical spray chamber is shown in Figure 9.16.

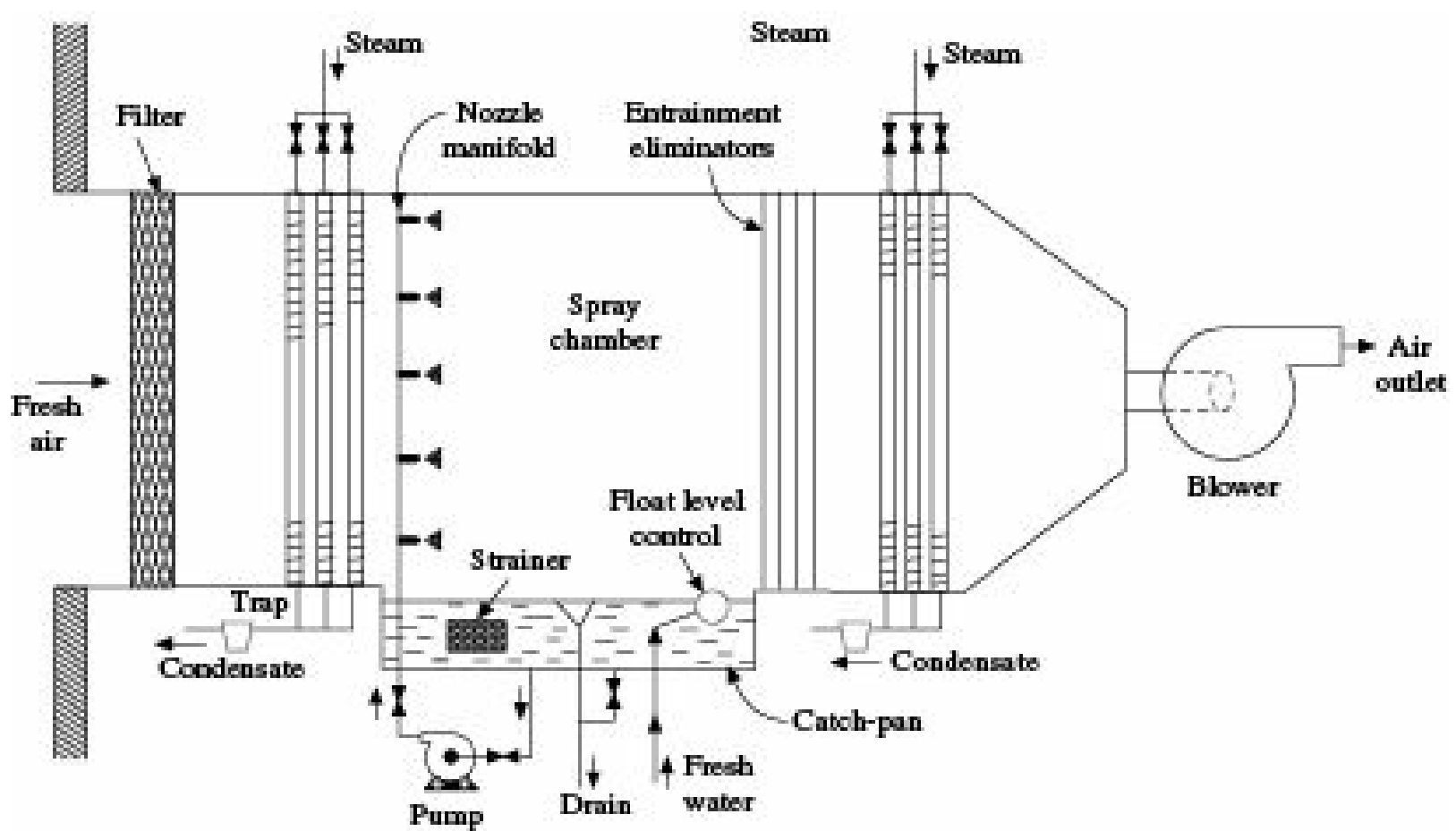


Figure 9.16 Sectional view of spray chamber assembly.

## 9.11 Some Important Accessories and Operational Features of Cooling Towers

### 9.11.1 Accessories

The essential components of cooling towers have been discussed here.

**Tower fills or packings:** Cooling towers produce the cooling effect primarily from evaporation of water that takes place when hot water is brought into contact with air. Greater the contact surface and contact time, higher is the transfer of heat from water to air. A well designed and good tower fill increases the contact surface and contact time coupled with low resistance to air flow, thus enhancing the efficiency of a tower to a high level. Tower fills used in water coolers are of two types—splash type and film type. *Splash type fills* consist of staggered rows of splash bars made of treated wood, extruded PVC, injection mouldings of polypropylene or FRP. The plastic resins used are compounded with fillers, fire retardant, etc. to impart to them the required properties. The sizes of the fill usually vary approximately from 12.5 to 25 mm thick, 75 to 100 mm wide, and 120 to 180 mm long. Splash type fills break up the water and interrupt its vertical progress by causing it to cascade through successive offset levels of parallel splash bars. These are known for low air pressure loss and lower susceptibility to clogging. *Film type fills* consist of vertical corrugated sheets arranged with a spacing of 18 to 25 mm. PVC is commonly used for making these fills because it is inert and can be easily moulded to any shape. The sheets are joined to make rectangular units. The warm water is distributed on the fills as thin film which enhances cooling.

**Louvers:** These are used to provide uniform air entry into the tower and at the same time prevent splashing out of water. They are inclined blade type assemblies fitted at the air inlet. Cross-flow towers are always provided with louvers. Louvers are mostly made of fibre-reinforced polyester

(FRP). Treated wood is also used in louvers.

**Drift eliminators:** Water droplets carried over by the outgoing air are called *drifts*. It causes loss of cooling water and at the same time is a source of nuisance for the locality. Drift eliminators are usually made of a few layers of slats placed in the frames above the water distributor. Honeycomb type drift eliminators made of PVC, are also in use.

**Fans and blowers:** Propeller type fans are usually employed in cooling towers although centrifugal fans are not uncommon in smaller units. Cooling tower fans are required to handle large volumes of air and their diameters may be as large as 10 m. Fan rpm usually varies between 150 and 400. The fan blades, of most of the cooling towers, are designed with airfoil section which contributes to the efficiency of the fan. The face of the blades moving towards the air stream is flat while the opposite side is convex. Uniform discharge velocity across the face of the fan is desirable for high efficiency because power increases as the cube of the velocity. A blade of constant pitch will discharge air at high velocity at the tip. Therefore, normally the pitch angle is increased inwards and the width is also increased. Such cooling tower fan blades are said to have twist and tapered to give increasing pitch and more blade area towards the hub of the fan. FRP is the common material of construction for fan blades.

A fan performs work by overcoming static pressure and imparting velocity to the air. In SI unit 1 kg m equals to 9.8 J and 1 cm water gauge equals to 10 kg/m<sup>2</sup>.

$$\text{Air power } (P) = \frac{\text{m}^3}{\text{s}} \frac{\text{kg}}{\text{m}^2} \# 9.8 \text{ W} \quad (9.54)$$

Air power divided by input power is efficiency. The following fan laws are used to adjust deviations from base conditions of fan curve assuming constant efficiency:

$Q$ , the volumetric flow rate varies as fan speed with air density constant,

Power varies as the cube of fan speed,

$Q$  varies as fan diameter squared with tip speed constant, and

Static pressure varies as  $(Q_1/Q_2)^2$ .

Tip speed of fan blades should not exceed 5 m/s mainly to minimize noise. Power for the cooling tower fan is estimated from cooling tower fan curves provided by the manufacturers.

The fan in a cooling tower is often placed in velocity recovery stack in which an expanding flow nozzle discharges air to the atmosphere at a lower velocity. This effectively converts velocity pressure to static pressure resulting in a significant increase in air velocity over what could be accomplished with a straight stack at the same fan power. Air leaving the fan continuously moves from lower to a higher pressure and enters the atmosphere at ambient pressure. Pressure decreases downward towards the fan as the velocity increases due to decreasing diameter of the stack. The stack wall diverges at an angle of 15 to 17 degrees. About 75% of the velocity head is recovered in a well designed stack.

**Water distributor:** Spray type water distributors are common in counter-flow towers while open distribution decks are common in cross-flow towers.

## 9.11.2 Operational Features

To operate a cooling tower with good water and energy management, one should take into account the limitations of the various components in the cooling tower. Some of the points are considered here.

**Variation in wet-bulb temperature:** The primary basis for design of a cooling tower is the wet-bulb temperature of the air entering the tower and the heat load during operation. The wet-bulb temperature varies almost daily, the highest being in the summer. There is almost linear relationship between the wet-bulb temperature and cold water temperature in a given cooling tower, the other factors, e.g. water and air flow rates being the same. If the actual wet-bulb temperature is higher than the design wet-bulb temperature, warmer than desired average cold water temperature will result. If the ambient wet-bulb temperature is lower than expected, then cold water temperature will be lower than what is required. In actual practice, the heat load dissipation is accomplished with continuously changing ambient wet-bulb temperature and varying water flow rate.

**Variation in water loading:** The heat load determines the temperature rise in the external circuit and cooling tower comes to equilibrium when the cooling range equals the temperature rise. At constant wet-bulb temperature, air load and range, decrease in water loading will result in closer approach, i.e. colder water. The water loading vs approach curve under these constant conditions does not deviate much from a straight line. If a tower operating at the design water loading has an approach of 6°C, an increase in water rate by 20% will result in 20% higher approach, i.e. about 7.2°C. On the other hand, an approach of 4.8°C is desired; the water rate has to be decreased by 20% keeping the other conditions constant. With increase in wet-bulb temperature, the enthalpy driving force in a tower operating with same liquid and air flow rates would be increased throughout the tower. As a general rule, for normal operating conditions, the rate of change in the cold water temperature is about half the rate of change in wet-bulb temperature. The approach decreases with an increase in wet-bulb temperature and increases as the wet-bulb temperature decreases.

**Distribution of hot water:** Hot water should be divided equally among the cells of a multicell cooling tower or between two similar cooling towers. Any uneven loading results in poor performance of the tower.

**Variation in available coefficient:** Available coefficient of a cooling tower at given conditions depends on the effectiveness of the fill. More effective the fill is, higher is the available coefficient enabling the tower to operate with less driving force and the air operating line moves horizontally closer to the saturation curve. The required coefficient is a measure of degree of difficulty of a cooling task. A long cooling range and close approach have a high required coefficient. A short cooling range and long approach have easy performance task and have low required coefficient. As the water loading is decreased to obtain a close approach, the driving force increases at the hot end. Easy performance allows water loading to be increased, thus increasing the driving force at the hot end and decreasing it at the cold end.

**Variation of heat load:** An increase in heat load will increase the range accompanied by increase in approach. Equilibrium will be established in the cooling water circuit with higher hot water temperature, range and approach. With increase in cooling range, the air operating line moves to the right and the driving force increases much more rapidly at the hot end. With normal operating limits, increase in approach is generally about half of the increase in range. Heat removed from the water is added to the air. So, the tower should be operated to obtain the highest attainable outgoing wet-bulb temperature. If a portion of hot water is bypassed, the ratio of liquid and gas decreases, and the

enthalpy of the leaving air decreases. Thus, any amount of bypassing reduces the outgoing wet-bulb temperature and less heat is removed from water.

**Maintaining water quality:** Cooling towers are excellent air washers. The quality of water being circulated reflects the quality of air contacting it in the tower. At the same time the air exits the cooling tower much cleaner than its entering state. Make-up water supply also brings in impurity as total dissolved solids (TDS). The process of evaporation in the tower causes incoming contaminant level to concentrate. High TDS level in circulating cooling water will cause corrosion or scaling not only in the heat exchangers but also in the cooling tower itself. To control TDS, a portion of the circulating water flow is continuously replaced with relatively pure make-up water. The continuous purge of a portion of circulating water with its TDS burden is called *blow down*. To minimize scaling, corrosion and algae formation, chemicals and biocides are added to the circuit.

The level to which contaminants can concentrate in the circulating water can be estimated using appropriate relation. The needed blow down would be higher because of the effects of air-borne contaminants. Once the approximate level of blow down has been determined, the circulating cooling water quality must be regularly maintained and adjustment be made to prevent corrosion or scale formation.

Calcium carbonate is the main scale forming compound and is formed by decomposition of calcium bicarbonate. Two indices are used to assess the carbonate stability or corrosion property of cooling water: saturation index calculated by Langelier equation and stability index estimated by Ryznar equation. These index values are calculated using the equation and relevant data available in literature (IS code 1999). These indices are used to arrive at a calculated method of treatment. In general, an increase in dissolved solids particularly chloride ion concentration increases the corrosion potential. Corrosion inhibitors are often added to minimize corrosion. Common corrosion inhibitors are chromates (anodic), zinc (cathodic), and ortho- and poly-phosphates. Polymeric dispersing agents and organo-phosphorous compounds are commonly used as scale inhibitors. Slime and algae may grow in cooling towers and affect their cooling efficiencies. Chlorine and chlorine containing compounds are effective biocides. Proprietary non-oxidizing biocides, e.g. quaternary amines also play an important role in the control of biofouling.

## Nomenclature

$a$  : specific interfacial area,  $\text{L}^2/\text{L}^3$

$c$  : molar density,  $\text{mol}/\text{m}^3$

$C$  : heat capacity of gas or vapour,  $\text{FL}/\text{MT}$

$C_S$  : humid heat of vapour-gas mixture,  $\text{FL}/\text{MT}$

$E_{MG}$  : Murphree gas-phase stage efficiency, fraction

$G$  : mass flow rate of gas,  $\text{M}/\square$

$G'$  : molar or mass velocity of gas,  $\text{mol}/\text{L}^2\square, \text{M}/\text{L}^2\square$

$h$  : convective heat transfer coefficient,  $\text{FL}/\text{L}^2\text{T}\square$

$h'$  : enthalpy of liquid,  $\text{FL}/\text{M}$

$H$  : enthalpy of vapour-gas mixture per unit mass of dry gas, FL/M

$H^*$  : enthalpy of saturated air at bulk water temperature, FL/M

$H_tG$  : height of a gas-phase transfer unit, L

$H_{toG}$  : overall height of a transfer unit based on gas-phase driving force, L

$k_G$  : gas-phase mass transfer coefficient, mol/L<sup>2</sup> (F/L<sup>2</sup>)

$k_y$  : gas-phase mass transfer coefficient, mol/L<sup>2</sup> (mol/mol)

$K_x$  : overall mass transfer coefficient based on liquid-phase, mol/ L<sup>2</sup> (mol/mol)

$K_y$  : overall mass transfer coefficient based on gas-phase, mol/ L<sup>2</sup> (mol/mol)

$L$  : mass flow rate of liquid, M/□

$L'$  : molar or mass velocity of liquid, mol/L<sup>2</sup>, M/ L<sup>2</sup>

$N$  : mass transfer flux, mol/L<sup>2</sup>

$N_tG$  : number of gas-phase transfer unit, —

$N_{toG}$  : number of overall transfer units based on gas-phase driving force, —

$p$  : vapour pressure, F/L<sup>2</sup>

$p'$  : partial pressure, F/L<sup>2</sup>

$P$  : total pressure, F/L<sup>2</sup>

$s$  : interfacial surface, L<sup>2</sup>

$t$  : temperature, T

$t_W$  : wet-bulb temperature, T

$v$  : molal specific volume, L<sup>3</sup>/mol

$y_H$  : humid volume, L<sup>3</sup>/M

$Y$  : absolute humidity, mass vapour/mass of dry gas, M/M

$Y_m$  : molal humidity, mole vapour/mol dry gas, mol/mol

$Z$  : height or length of active part of equipment, L

### *Greek Letters*

$m$  : latent heat of vaporisation, FL/M

$n$  : viscosity, M/L<sup>2</sup>

$\rho$  : density, M/L<sup>3</sup>

### *Subscripts*

as : adiabatic saturation

*A* : substance *A*, the vapour

*B* : substance *B*, the gas

*G* : pertaining to the gas

*L* : pertaining to the liquid

*s* : saturation

*W* : wet-bulb temperature

1,2 : refer to position ( for enthalpy change 1 and 2 refer to the entering and leaving positions respectively, and for temperature change 1 and 2 refer to the positions of cold water out and hot water in respectively).

## Numerical Problems

**9.1** Determination of Enthalpy and Moisture Content of Air Leaving the Heater: Air having a temperature of 24 °C and a relative humidity of 0.7 is heated in an air heater to 90 °C. Find the enthalpy and moisture content of the air leaving the heater.

[Ans: 126 kJ/kg of dry air; 0.013 kg/kg of dry air]

**9.2** Partial Pressure of Water Vapour, Density and Moisture Content of Air: Find the partial pressure of water vapour, and the density and moisture content of air if its temperature is 60 °C, its absolute pressure is 380 mm Hg, and the relative humidity is 0.4.

[Ans: 59.8 mm Hg; 0.5 kg/m<sup>3</sup>; 0.116 kg/kg of dry air]

**9.3** Determination of Some Psychrometric Properties of Unsaturated Air-water Vapour Mixture Without the Psychrometric Chart: The dry-bulb temperature of an unsaturated sample of air is 30°C and its percent saturation is 50% at a pressure of 101.3 kN/m<sup>2</sup>.

Without using humidity chart, calculate the following properties of the air sample:

- (i) Humidity
- (ii) Relative saturation
- (iii) Humid volume.

The vapour pressure ( $p_A$ ) data for water are as under:

$T, ^\circ\text{C} :$	6.7	17.2	23.8	28.6	32.6	35.9	38.7	41.2
$p_A, \text{kN/m}^2 :$	0.98	1.96	2.94	3.92	4.90	5.88	6.86	7.85

[Ans: (i) 0.0136 kg water/kg dry air (ii) 51.06% (iii) 0.8775 m<sup>3</sup>/kg dry air]

**9.4** Determination of Some Psychrometric Properties of Air: Find the moisture content, enthalpy, wet-bulb temperature and dew point for the air at a temperature of 50°C and a relative humidity of 0.7.

[Ans: 0.06 kg/kg dry air; 209 kJ/kg dry air; 43°C; 42°C]

**9.5** Determination of Some Psychrometric Properties of Air from the Given Dry and Wet-bulb Temperatures): The dry-bulb and wet-bulb temperatures of air are 50 and 30°C, respectively. Find (i) the moisture content of air, (ii) enthalpy of air, (iii) dew point of the air, (iv) relative humidity of air, and (v) partial pressure of water vapour in the air at the dry-bulb temperature.

[Ans: (i) 0.02 kg/kg dry air (ii) 105 kJ/kg air (iii) 24°C (iv) 0.25 (v) 23 mm Hg]

**9.6** Estimation of Psychrometric Properties of Air being used in a Dryer as Drying medium: The air

supply to a drier has a dry-bulb temperature of 23 °C and a wet-bulb temperature of 16°C. It is heated to 85°C by heating coils and introduced into the drier. In the drier, it cools along the adiabatic cooling line and leaves the drier fully saturated.

- (i) What is the humidity of the initial air?
- (ii) What is the dew point of the initial air?
- (iii) How much heat is needed to heat 100 m<sup>3</sup> air to 85°C?

[Ans: (i) 0.0075 kg water/kg dry air (ii) 8.8°C (iii) 7442 kJ]

**9.7 Estimation of Air Temperature using the Value of Psychrometric Ratio:** Air at 1 atm is blown past the bulb of a mercury thermometer. The bulb is covered with a wick. The wick is immersed in an organic solvent (molecular weight = 58). The reading of the thermometer is 7.6 °C. At this temperature, the vapour pressure of the liquid is 5 kPa. Find the air temperature given that the ratio of the heat transfer coefficient to the mass transfer coefficient (psychrometric ratio) is 2 kJ/(kg)(K) and the latent heat of vaporisation of the liquid is 360 kJ/kg. Assume that the air which is blown is free from the organic vapour.

**Ans: 30 °C.**

**9.8 Calculation of the Temperatures on Each Set of Shelves, Rate of Water Removed from the Dryer, and the Temperature of the Inlet Air if the Operation be Carried out in Single Stage:** Air containing 0.05 kg water vapour per kg of dry air is heated to 325 K in a dryer and then passed to the lower shelves. It leaves these shelves at 60% relative humidity and is reheated to 325 K and passed over another set of shelves, again leaving at 60% relative humidity. In all there are four sets of shelves, after which the air leaves the dryer. On the assumption that the material on each shelf has reached the wet-bulb temperature and that heat losses from the dryer can be neglected, determine (i) the temperature of the material on each set of shelves; (ii) the amount of water removed in kg/s if 5 m<sup>3</sup>/s moist air leaves the dryer; (iii) the temperature to which the inlet air would have to be heated to carry out the drying in single stage.

[Ans: (i) Shelf-1: 25 °C, Shelf-2: 32.5 °C, Shelf-3: 35.5 °C, Shelf-4: 38 °C(ii) 0.172 kg/s (iii) 380 K]

**9.9 Adiabatic Humidification and Cooling of Air in Horizontal Spray Chamber:** A horizontal spray chamber with recirculated water is to be used for the adiabatic humidification and cooling of air. The effective part of the chamber is 1.5 m long and has a cross-section of 1.9 m<sup>2</sup>. The coefficient of heat transfer is 1300 kcal/(m<sup>3</sup>)(hr)(°C). 210 m<sup>3</sup>/min of air at 60 °C with a humidity of 0.0170 kg water/kg dry air is to be blown through the spray chamber. What will be the exit temperature and humidity of the air?

[Ans: 40 °C, 0.025 kg water/kg dry air]

**9.10 Determination of Temperatures of Preheater, Spray Chamber and Reheater, and also the Requirements of Heat for Pre- and Reheating:** Fresh air at 21.2°C in which partial pressure of water vapour is 0.0118 atmosphere, is blown at the rate of 214 m<sup>3</sup>/hr first through a preheated and then adiabatically saturated spray chamber to 100% saturation and again reheated. This reheated air has a humidity of 0.024 kg water vapour per kg dry air. It is assumed that the fresh air and the air leaving the reheat have the same percentage of humidity. Determine (i) the temperatures of preheater, spray chamber and reheat; (ii) heat requirements for preheating and

reheating

[Ans: (i) 65 °C, 28 °C, 41 °C (ii) 2702.35 kcal/hr and 828.5 kcal/hr]

**9.11 Estimation of Number of Transfer Units in a Horizontal Spray Chamber:** 350 m<sup>3</sup>/min of air at 70 °C and 1 atm pressure having a wet-bulb temperature of 30 °C is to be adiabatically humidified and cooled in a horizontal spray chamber using recirculated water. The chamber is 1.5 m wide, 1.5 m high and 2.0 m long. The coefficient of heat transfer has been estimated to be 1200 kcal/(m<sup>3</sup>)(hr)(°C). The specific volume and specific heat of the entering air are 0.85 m<sup>3</sup>/kg and 0.248 kcal/(kg.)(°C), respectively.

- Determine the temperature and humidity of the exit air, and
- Estimate the number of transfer units.

[Ans: (i) 46.5 °C, 0.021, (ii) 0.93]

**9.12 Determination of Minimum air Requirement, Diameter and Height of Packed Bed in a Counter-Current Cooling Tower:** A counter-current cooling tower is to be designed to cool 2000 kg/min of water from 50 °C to 30 °C. Air is available at 30 °C dry-bulb and 24 °C wet-bulb temperatures. 30% excess air will be used. Make-up water will enter at 15°C. The value of the mass transfer coefficient is expected to be 2500 kg/(hr)(m<sup>3</sup>)(DY) provided the minimum liquid and gas rates are 12000 and 10000 kg/(hr)(m<sup>2</sup>), respectively.

- Estimate the minimum air requirement
- Determine the diameter and packed height of the tower

The following data may be used. Here  $T$  indicates the liquid temperature in °C and  $H$  is the enthalpy of saturated air in kcal/kg dry air:

$T:$	25	30	35	40	45	50	55
$H:$	19.1	23.9	31.8	40.4	51.3	63.1	82.3

[Ans: (i) 873 kg dry air/min. (ii) 2.95 m; 4.17 m]

### **Short and Multiple Choice Questions**

- What are humid volume and humid heat?
- How does the dew point of an unsaturated air-water vapour mixture change with increase in absolute humidity?
- What is the dew point of a saturated air-water vapour mixture at 60 °C?
- What is wet-bulb temperature?
- Under which conditions dry-bulb and wet-bulb temperatures of a vapour-gas mixture become the same?
- What is adiabatic saturation temperature? What is the nature of adiabatic saturation lines for air-water system?
- Show that for air-water system, wet-bulb temperature and adiabatic saturation temperature are equal.
- Which dimensionless number indicates the ratio of rates of heat transfer and mass transfer in a cooling tower?

- 9.** What do you mean by wet-bulb temperature approach in a cooling tower?
- 10.** Can a cooling tower cool water below the dry-bulb temperature of the entering air?
- 11.** Psychrometric ratio is defined as
- (a)  $\frac{k_G}{k_F}$  (b)  $\frac{k_F}{k_G}$  (c)  $\frac{k_G}{k_F C_S}$  (d)  $\frac{Sc}{Pr}$
- 12.** Lewis number is the ratio of  
(a) thermal diffusivity to mass diffusivity  
(b) mass diffusivity to thermal diffusivity  
(c) mass diffusivity to momentum diffusivity  
(d) momentum diffusivity to thermal diffusivity
- 13.** In a saturated gas, the  
(a) vapour is in equilibrium with the liquid at the gas temperature  
(b) vapour is in equilibrium with the liquid at room temperature  
(c) partial pressure of vapour equals the vapour pressure of the liquid at room temperature  
(d) none of the above
- 14.** The dew point of an unsaturated mixture of water vapour and air at constant temperature and pressure  
(a) does not change with change in absolute humidity  
(b) increases with increase in absolute humidity  
(c) decreases with increase in absolute humidity  
(d) decreases linearly with increase in absolute humidity
- 15.** The steady-state temperature attained by a small amount of liquid evaporating into a large amount of unsaturated vapour-gas mixture is called  
(a) dry-bulb temperature (b) adiabatic saturation temperature  
(c) wet-bulb temperature (d) dew point.
- 16.** For pure air at atmospheric condition, Lewis number is  
(a) 1 (b) 1 (c)  $\approx 1$  (d) 0.5
- 17.** The cooling effect in a cooling tower can be increased by  
(a) increasing the air velocity  
(b) lowering the barometric pressure  
(c) reducing the humidity of the entering air  
(d) all of these
- 18.** A mixture of 10% benzene vapour in air at 25 °C and 750 mm Hg pressure has a dew point of 20 °C. Its dew point at 30 °C and 700 mm Hg pressure will be around  
(a) 22.7 °C (b) 20 °C (c) 27.5 °C (d) 18.7 °C.
- 19.** Under the same conditions of temperature and pressure  
(a) 1 m<sup>3</sup> of dry air is lighter than 1 m<sup>3</sup> of humid air  
(b) 1 m<sup>3</sup> of dry air is heavier than 1 m<sup>3</sup> of humid air  
(c) both 1 m<sup>3</sup> of dry air and 1 m<sup>3</sup> of humid air have the same weight  
(d) none of these

- 20.** Ratio of the partial pressure of the vapour to the vapour pressure of the liquid is known as  
(a) humidity      (b) saturated humidity      (c) relative humidity      (d) none of these
- 21.** Humid volume is the total volume of unit mass of vapour free gas plus  
(a) whatever vapour it may contain at 1 atm pressure  
(b) whatever vapour it may contain at 1 atm pressure and at gas temperature  
(c) whatever vapour it may contain at 1 atm pressure and at room temperature  
(d) none of these
- 22.** The dew point of a saturated gas phase at 25°C is  
(a) 0 °C      (b) 20 °C      (c) 25 °C      (d) none of these
- 23.** Which of the following remains constant during evaporative cooling with recirculated water?  
(a) relative humidity      (b) wet-bulb temperature  
(c) partial pressure of vapour      (d) none of these
- 24.** Relative saturation is  
(a) lower than percentage saturation  
(b) equal to percentage saturation  
(c) higher than percentage saturation  
(d) there is no relation between them
- 25.** Unsaturated air with dry-bulb temperature of 35 °C and wet-bulb temperature of 25 °C is passed through a water spray chamber maintained at 35 °C. The air will be  
(a) cooled      (b) humidified  
(c) dehumidified      (d) cooled and humidified
- 26.** To measure wet-bulb temperature with precision  
(a) the wick must be completely wet  
(b) the velocity of the gas should be large  
(c) the make-up liquid if supplied to the bulb, should be at the wet-bulb temperature  
(d) all of these
- 27.** The adiabatic saturation curve for a vapour-gas mixture is  
(a) straight line      (b) slightly concave upward  
(c) slightly concave downward      (d) none of these
- 28.** The dry-bulb and wet-bulb temperatures of a vapour-gas mixture are 30 °C and 25 °C, respectively. If the mixture is heated to 45°C at constant pressure, its wet-bulb temperature will be  
(a) 25 °C      (b) > 25 °C      (c) < 25 °C      (d) -25 °C.
- 29.** The relative humidity of air can decrease inspite of an increase in the absolute humidity when the  
(a) pressure rises      (b) temperature rises  
(c) pressure falls      (d) temperature falls
- 30.** In the operation of cooling towers, the term “cooling range” refers to the difference in the temperature of  
(a) cold water leaving the tower and the wet-bulb temperature of the surrounding air  
(b) warm water entering the tower and the wet-bulb temperature of the surrounding air  
(c) warm water entering the tower and the cold water leaving the tower

(d) none of these

### *Answers to Multiple Choice Questions*

- |         |         |         |         |         |         |
|---------|---------|---------|---------|---------|---------|
| 11. (a) | 12. (a) | 13. (a) | 14. (b) | 15. (c) | 16. (c) |
| 17. (d) | 18. (d) | 19. (b) | 20. (c) | 21. (a) | 22. (c) |
| 23. (b) | 24. (a) | 25. (b) | 26. (d) | 27. (b) | 28. (b) |
| 29. (b) | 30. (c) |         |         |         |         |

### ***References***

Henry, H.C. and N. Epstein, *Canad. J. Chem. Eng.*, **48**, 595, 602,609 (1970).

Hensel, S.L. and R.E. Treybal, *Chem. Eng. Prog.*, **48**, 362 (1952).

Indian Standard Code, IS 8188 (1999).

McKelvey, K.K. and M. Brooke, *The Industrial Cooling Tower*, Von Nostrand, Princeton, N.J. (1959).

Mickley, H.S., *Chem. Eng. Prog.*, **45**, 739 (1949).

Nemunaitis, R.R. and J.S. Eckert, *Chem. Eng. Prog.*, **71**(8), 60 (1975) .

Perry, R.H., D.W. Green and J.O. Malony (Eds.), *Perry's Chemical Engineers' Handbook*, 7th ed., McGraw Hill (1997).

Treybal, R.E., *Mass Transfer Operations*, 3rd ed., McGraw Hill, Singapore (1985).



# 10

## Liquid–Liquid Extraction

### 10.1 Introduction

The term extraction generally includes those operations in which one or more soluble constituents, present either as solid or as liquid, are removed from a solid or a liquid by the use of a solvent. Extraction operations are broadly classified into two major groups:

Liquid-liquid extraction or simply liquid extraction which involves the extraction of one or more constituents from a liquid.

Leaching or lixiviation, which involves extraction of one or more soluble constituents from a solid.

In this chapter we will restrict our discussion only to liquid-liquid extraction. Leaching has been dealt within Chapter 11.

Separation of two or more components of a liquid solution is a very common problem in chemical engineering practice. The conventional methods for such separation are evaporation, distillation, crystallization, etc. which utilize the differences in volatilities or solubilities of the components. It is also possible to accomplish the desired separation by treating the solution with a second liquid, the solvent, which selectively dissolves one or more components of the original solution. The initial solution and the solvent added must not be completely miscible since the two liquid phases formed after mixing are separated by mechanical means based on the density difference.

Liquid-liquid extraction was developed during the second world war mainly for separation of radioactive substances. But today, it has a number of important uses. Some of the important fields of application of liquid-liquid extraction are as follows:

- (a) The separation of substances differing in chemical nature but having close volatilities. Thus, aromatic and paraffinic hydrocarbons having very close volatilities cannot be easily separated by distillation. But they can be readily separated by liquid extraction for which a number of solvents are available.
- (b) Where the substances to be separated are heat-sensitive and decompose even before reaching their ordinary temperatures of distillation. Many pharmaceutical products such as penicillin, streptomycin, etc. are produced in complex mixtures and being very heat sensitive, are separated from other by-products by liquid extraction.
- (c) Where other methods of separation such as distillation, crystallization, etc. are quite possible but extraction is more economical. Thus, concentration of acetic acid from dilute aqueous solution by evaporation of water is possible but extraction of the acid with isopropyl ether is much more economical. Extraction may also be more economical than high vacuum distillation.
- (d) Extraction can also be gainfully used for separations which otherwise involve costly chemical methods. For instance, separation of uranium-vanadium or tungsten-molybdenum is more

economical by liquid extraction.

Some examples of specific applications of liquid-liquid extraction are (Cusack and Glatz 1996):

- Separation of BTX (benzene, toluene and xylene) from petroleum fractions
- Lube oil extraction
- Extraction of caprolactum from lactum oil
- Extraction of phenol from aqueous wastes
- Extraction of copper
- Refining of fats and oils (removal of mono- and di-glycerides from triglycerides).

In addition to the above, liquid-liquid extraction is used in several food, pharmaceutical, metallurgical, environmental and organic chemical industries.

Our present discussion will be limited to extraction of a single solute.

## 10.2 Terminologies Used

In extraction operations, the solution from which extraction is to be made is called the *feed* and the liquid used for extraction is the *solvent*. The solvent-rich product is called the *extract* while the residual liquid from which most solute has been removed is the *raffinate*.

*A* is the initial carrier liquid, *B* is the pure solvent added, *C* is the distributed solute and *S* is the quantity of contaminated solvent added, all expressed in mass for batch operations and in mass per unit time for continuous operations.

*E* represents the extract phase and *R* represents raffinate phase, *E'* and *R'* being extract and raffinate on solvent-free basis, all expressed in mass for batch operations and mass per unit time for continuous operations.

The compositions of the raffinate and extract are represented by the following notations:

$x$  = mass fraction of solute *C* in raffinate (*A*-rich) phase,

$y$  = mass fraction of solute *C* in extract (*B*-rich) phase,

$x' = \text{mass of solute per unit mass of solute free raffinate, } [x / (1 - x)]$

$y' = \text{mass of solute per unit mass of solute free extract, } [y / (1 - y)]$

$X = \text{mass fraction of solute in raffinate on } S\text{-free basis, } [C / (A + C)]$

$Y = \text{mass fraction of solute in extract on } S\text{-free basis, } [C / (A + C)]$

## 10.3 Extraction Equilibrium

As in all mass transfer operations, equilibrium relations are of prime importance in liquid extraction. Equilibrium relations in extraction can be represented in different ways.

In case of two immiscible liquids, the equilibrium distribution of a third component in each of the two phases are often related by the so called distribution law,  $y = mx$ . For several systems *m* varies with concentration of solute in one of the phases.

If the solute is associated in any one phase forming double or triple molecules, the equilibrium and mass action laws are combined together to give the equilibrium relation. Thus for triple molecules formed in the extract phase,

$$y_3 = k'y_1^3 \quad (10.1)$$

where  $y_3$  is the concentration of triple molecules.

The total concentration  $y_T$  is then given by

$$y_T = y_1 + 3y_3 = y_1 + 3k'y_1^3 \quad (10.2)$$

Assuming the distribution law for single molecules

$$y_T = mx + 3k'(mx)^3 = (m + 3k'm^3x^2)x \quad (10.3)$$

### 10.3.1 Ternary Equilibrium

The majority of cases in liquid-liquid extraction involve two phases, which are partially miscible, and it is necessary to have their mutual solubility data as well as information regarding distribution of the solute between them at equilibrium. Necessary data are best represented by triangular diagrams, which are extensively used for graphical representation of ternary equilibrium. Triangular diagrams are of two types—equilateral triangle and right-angled triangle on rectangular co-ordinates.

In an equilateral triangle, shown in Figure 10.1, the sum of the three perpendicular distances from any point within the triangle to the three sides is constant and equal to the altitude of the triangle. The perpendicular distances from any point within the triangle to the three sides may, therefore, be chosen to represent the percentages or fractions of the three components of a ternary system so that their sum is constant which then represents 100% composition. In Figure 10.1 the three apexes  $A$ ,  $B$  and  $C$  represent 100%  $A$ , 100%  $B$  and 100%  $C$  respectively. Considering any point within the triangle, the perpendicular distances to the three sides  $BC$ ,  $CA$  and  $AB$  represent the percentages of  $A$ ,  $B$  and  $C$ , respectively which can be read on the diagram from the lines parallel to  $BC$ ,  $CA$  and  $AB$ , respectively.

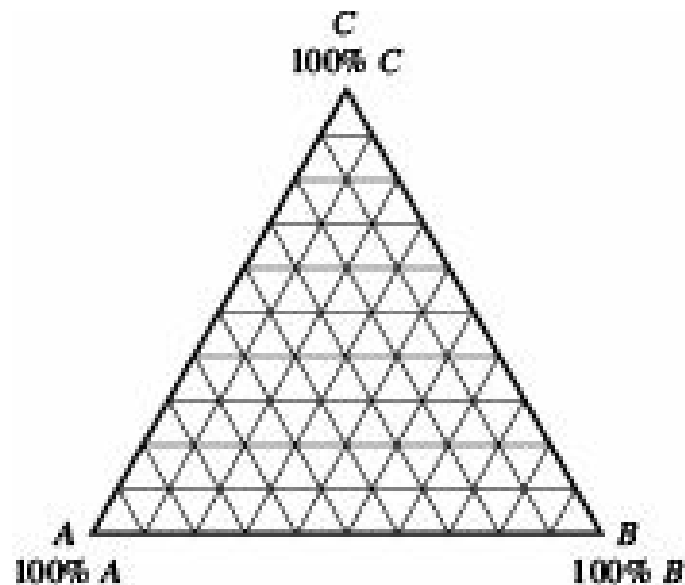


Figure 10.1 Equilateral triangular co-ordinates.

In a ternary system, if the percent compositions or weight fractions of two components are fixed, the composition of the third component automatically gets fixed. This principle is utilized in representing ternary compositions on right triangle. The advantage of this method is that a right triangle can be easily constructed on rectangular co-ordinates and plotting and reading of data are much easier.

In Figure 10.2, point  $A$  represents 100%  $A$  and point  $C$  represents 100%  $C$ . Once the percentage of  $A$  and  $C$  have been found out from the diagram, that of  $B$  can be determined from the relation  $B = 100 - (A + C)$ . Alternatively, the perpendicular from the point  $O$  to the side  $AC$  may be made to represent

100% *B* so that the percentage of *B* can be read from the diagram.

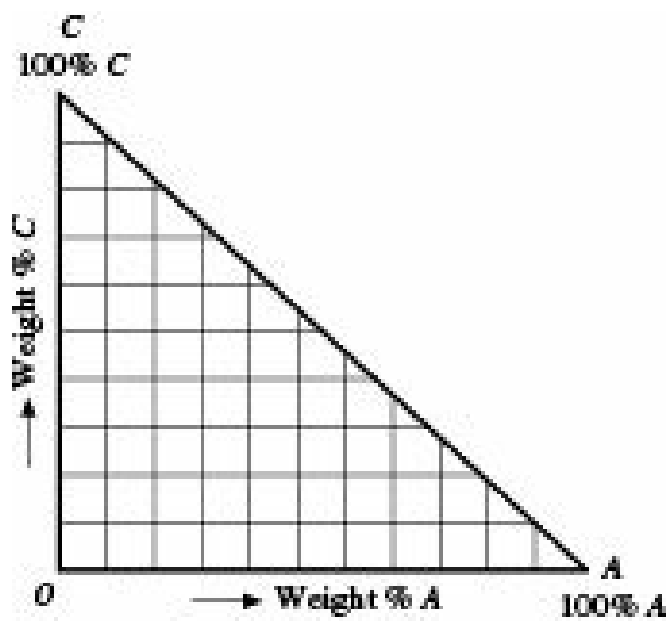


Figure 10.2 Right-angled triangle on rect-angular co-ordinates.

Ternary liquid equilibrium systems may be of different types. Only two of them, which are commonly encountered in practice, have been discussed here.

### 10.3.2 System of 3 Liquids, One Pair Partially Miscible

This system is most frequently encountered in practice.

The equilibrium system is shown in triangular diagram in Figure 10.3. Liquids *B-C* and *C-A* are completely miscible. But *A* and *B* are miscible with each other only to a limited extent giving rise to two saturated solutions at *K* (*A*-rich) and *L* (*B*-rich). A binary mixture at *J* anywhere between *K* and *L* will separate into two immiscible liquid phases of compositions *K* and *L*. Curve *KRPEL* is the bimodal solubility curve which shows the change in solubilities of *A*-rich and *B*-rich phases upon addition of *C*. Any mixture outside this curve is single phase homogeneous liquid and hence unsuitable for extraction. Any mixture such as *M* within this curve will split into two saturated liquid phases *R* and *E*. The line *RE* is a tie line passing through *M*. There may be infinite number of such tie lines.

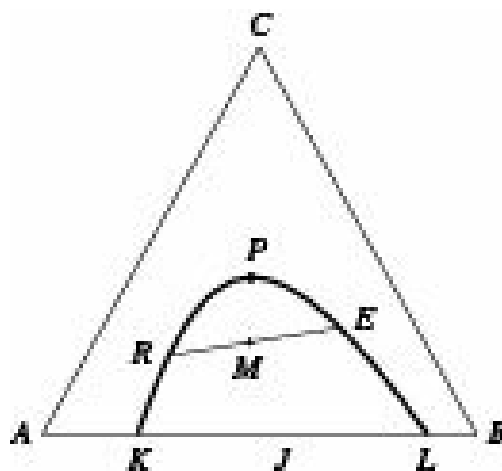


Figure 10.3 System of 3 liquids, one pair partially miscible.

Typical examples of this system are Water (*A*)-Chloroform (*B*)-Acetone (*C*) and Benzene (*A*)-Water (*B*)-Acetic acid (*C*). This type of systems are known as Type-I systems.

The tie lines are rarely found to be parallel rather their slopes change slowly in one direction. However, in some systems the direction of the slope of tie lines change with one tie line remaining horizontal. Such systems are known as *Solutropic systems*. Point *P* where the *A*-rich and *B*-rich solubility curves converge is known as the *plait point* which may be at the maximum value of *C* on the solubility curve. Generally, ternary mixtures having two liquid phases between which one is distributed in an apparent ratio varying with concentration from less than one to more than one, are defined as *solutropes*. The term is analogous to azeotrope. Relatively few ternary systems exhibiting a reversal in selectivity, defined as *solutropy*, are found to be normal or regular solution compared to the majority of systems having one pair of immiscible components. In triangular diagram of such systems, e.g. Glycerol-water-solvent mixtures, a turning is shown by a reversal of the slope of the tie lines indicating reversal in selectivity of a solvent for distributed components. A particular component exists for which the solvent is non-selective.

### 10.3.3 System of 3 Liquids, Two Pairs Partially Miscible

As shown in Figure 10.4, liquids *A* and *C* are completely miscible while *A-B* and *B-C* have only limited miscibility. Compositions *H* and *J* on the base *AB* represent the mutual solubility of *A* and *B*. Similarly, compositions *K* and *L* on the base *BC* represent the mutual solubility of *B* and *C*. Curves *HRK* (*A*-rich) and *JEL* (*B*-rich) are the ternary solubility curves.

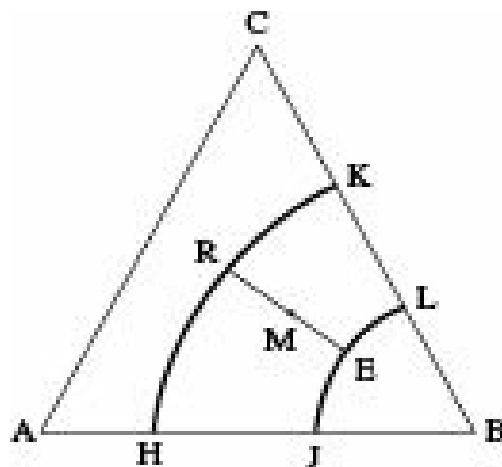


**Figure 10.4** System of 3 liquids, two pairs partially miscible.

Any composition *M* within the region *HKLJ* automatically splits into two saturated layers of equilibrium compositions *R* and *E* at the two extremities of the tie line *RE*. Any composition outside this region will form a single phase homogeneous solution and hence will be unsuitable for extraction. A typical example of this system is chlorobenzene (*A*)-water (*B*)-methyl ethyl ketone (*C*). This type of systems is known as Type-II systems.

Temperature has a strong effect on liquid-liquid equilibria. In general, the solubility of a pair of liquids increases with temperature. In case of Type-I systems, the mutual solubility of the initial carrier (*A*) and solvent (*B*) increases with increase in temperature till the critical solution temperature is reached above where *A* and *B* are completely miscible. Extraction with Type-I systems must, therefore, be carried out below the critical solution temperature.

With increase in temperature of Type-II systems, the mutual solubility of the solvent (*B*)-solute (*C*) pair increases at a rate faster than that of the carrier (*A*)-solvent (*B*) pair. At the critical solution temperature of the solvent (*B*)-solute (*C*) pair, this pair becomes completely miscible and consequently, the Type-II system behaves as Type-I system.

### 10.3.4 Liquid-Liquid Equilibria on Solvent-Free Coordinates

A rectangular co-ordinate system where all the quantities are expressed on solvent-free basis is sometimes used in liquid-liquid extraction. In this system, the mass ratios  $X$  and  $Y$  of the solute in the

two liquid phases are plotted against the corresponding mass ratios of the solvent  $\left(\frac{B}{A+C}\right)$  in the respective phases, all on solvent-free basis, where,

$$X = \frac{C}{A+C} \text{ in the raffinate phase, and}$$

$$Y = \frac{C}{A+C} \text{ in the extract phase.}$$

Such a plot is known as *Janecke diagram*.

## 10.4 Selection of Solvent

A number of solvents are usually available for an extraction operation. No solvent, however, possesses all the desirable qualities of a good solvent. An intelligent compromise should, therefore, be made. The following properties are to be considered during selection of a suitable solvent for a given extraction operation.

**Selectivity (b):** The solvent should dissolve maximum amount of solute ( $C$ ) and minimum amount of initial carrier liquid ( $A$ ), if at all. If the solubilities of  $C$  and  $A$  in the solvent are proportional to their initial concentrations, then there would be no separation. The effectiveness of a solvent in separating the components of a solution is measured by selectivity (b), which is defined as the ratio of solute to initial carrier liquid in the extract to that in the raffinate.

$$\begin{aligned} \text{Selectivity } (\beta) &= \frac{(\text{wt. fraction } C \text{ in extract}) / (\text{wt. fraction } A \text{ in extract})}{(\text{wt. fraction } C \text{ in raffinate}) / (\text{wt. fraction } A \text{ in raffinate})} \\ &= \frac{y \text{ (wt. fraction } A \text{ in } R)}{x \text{ (wt. fraction } A \text{ in } E)} \end{aligned} \quad (10.4)$$

For effective extraction, selectivity should be greater than unity, the higher its value the better. Selectivity is analogous to relative volatility.

**Distribution coefficient ( $y^*/x$ ):** It is the ratio of concentration of solute in extract to that in raffinate at equilibrium. Distribution coefficient need not be greater than unity, but the higher its value the better, since that will reduce solvent requirement.

**Insolubility of Solvents:** The more insoluble is the added solvent ( $S$ ) with the initial carrier liquid ( $A$ ) the better since that will reduce solvent requirement as well as cost of solvent recovery.

**Density Difference:** On completion of mixing to allow for mass transfer, the extract and raffinate phases are separated by settling which take advantage of their density difference. Hence the higher the density difference between the phases the better.

**Interfacial Tension:** Higher interfacial tension makes dispersion difficult but helps in coalescence of

the dispersed phase. Since dispersion can be enhanced by manipulating the flow conditions or by mechanical agitation while coalescence has to occur all by itself, higher interfacial tension is preferred.

**Recoverability:** The added solvent should be easily recoverable for reuse. Since recovery of solvent is most frequently done by distillation, that substance in the extract, either the solute or the solvent, which is present in lesser quantity, should preferably be more volatile, their relative volatility should be high and they should not form any azeotrope.

**Viscosity, vapour pressure and freezing point:** All these should be low. Low viscosity makes handling of solvent easier and keeps the pressure drop low. Low vapour pressure reduces solvent loss by vaporisation during handling and extraction. Freezing point is important in cold countries where low freezing point may prevent solidification of solvent in pipe lines.

In addition to the above, the solvent should be stable and should not react with the materials of construction of the equipment or other components of the system. It should be nontoxic, nonflammable, cheap and easily available.

## 10.5 Methods of Extraction

Four major steps are involved in liquid extraction:

- Bringing the solution and the solvent into intimate contact
- Separating the extract and raffinate phases
- Removing the solute from the extract phase
- Recovering the solvent from both the phases, usually by distillation, for reuse

Extraction methods are broadly classified into two groups, stage-wise contact and continuous differential contact.

### 10.5.1 Stage-wise Contact

As discussed in Chapter 5 (Section 5.2), a stage consists of devices for thoroughly mixing the solution to be treated with the added solvent so that mass transfer can take place between them and then separating the two phases formed. The raffinate may be treated with fresh solvent for further extraction of solute. Stage-wise extraction may be of three major types:

- Single-stage extraction
- Multistage cross-current extraction
- Multistage counter-current extraction

Our discussion of stage-wise extraction will be further subdivided into two categories:

- (i) where the initial carrier liquid and the added solvent are completely immiscible, and
- (ii) where the two solvents are partially miscible.

It should be noted that extraction is not possible if the two solvents are completely miscible.

#### ***Extraction with immiscible solvents***

If the initial carrier liquid and the added solvent are completely immiscible, then stage calculations become quite simple and can be followed on ordinary rectangular co-ordinates by plotting equilibrium concentrations  $x'$  and  $y^*$  for constructing the equilibrium curve and plotting  $x'$  and  $y'$  for

the operating line. The initial carrier liquid *A* and the added solvent *B* being completely immiscible, the raffinate from each stage always contains *A* unit initial carrier liquid and the extract always contains *B* unit solvent.

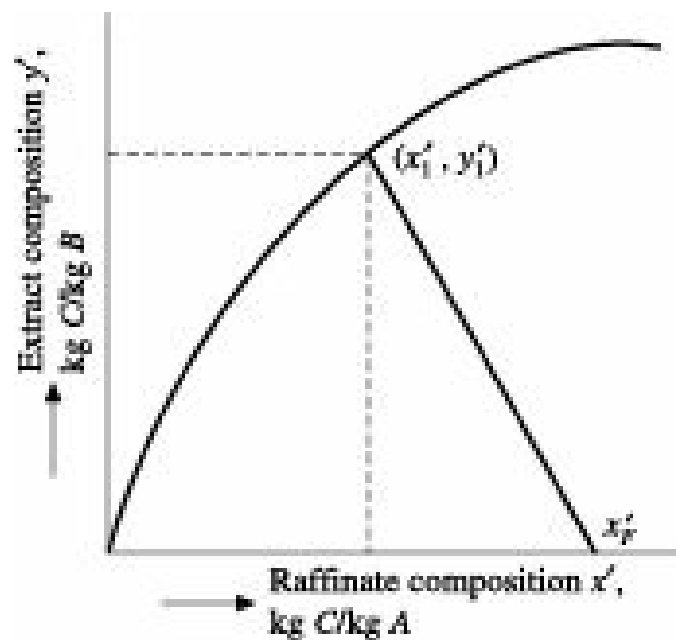
### • Single-stage Extraction

Figure 10.5 shows a schematic flow diagram of a single-stage extraction unit which may be either batch or continuous.



**Figure 10.5** Schematic flow diagram of single-stage extraction.

For batch operation, *F* kg feed containing  $x'_F$  mass fraction solute *C* and *S* kg solvent containing  $y'_S$  mass fraction solute *C* are introduced into stage 1 where the liquids are thoroughly mixed. After the stipulated mass transfer has taken place, the mixture is allowed to settle and *E* kg extract of composition  $y'_1$  and *R* kg raffinate of composition  $x'_1$  are withdrawn. *E'* and *R'* are the amounts of extract and raffinate on *B*-free basis after removal of solvent from the respective streams. In case of continuous operation, all the quantities *F*, *S*, *E* and *R* are expressed in mass per unit time. The operation is represented graphically on rectangular  $y'-x'$  co-ordinates in Figure 10.6.



**Figure 10.6** Graphical representation of single stage extraction.

A solute balance around the stage provides

$$Ax'_F + Sy'_S = Ax'_1 + Sy'_1 \quad (10.5)$$

or,

$$-\frac{A}{S} = \frac{y'_S - y'_1}{x'_F - x'_1} \quad (10.6)$$

where  $x'$  and  $y'$  are mass fractions of solute in raffinate and extract, respectively on solute free basis. Equation (10.6) is the equation to the operating line which passes through the point  $x'_F, y'_S$  and has a

slope of  $[-(A/S)]$ . The operating line is drawn accordingly and its point of intersection with the equilibrium curve gives the compositions of the extract and raffinate phases. If the equilibrium relationship is linear, then graphical construction may be avoided and the composition of the raffinate may be determined by simple algebraic method as suggested by Laddha and Degaleesan (1976). From Eq. (10.5), assuming  $y_S$  to be zero,

$$x_1' = \frac{Ax_F'}{A + mS} \quad (10.7)$$

$$\text{and } y_1' = \frac{A(x_F' - x_1')}{S} \quad (10.8)$$

where,  $m = y'/x'$ .

**EXAMPLE 10.1** (Single-stage extraction with immiscible solvent): 100 kg of a water-dioxane solution containing 20% dioxane is being extracted with 80 kg benzene at 25°C in a single-stage extraction unit.

Water and benzene are essentially insoluble. The equilibrium distribution of dioxane between water and benzene at 25 °C are as follows:

wt.% dioxane in water ( $100x'$ ) : 5.1 18.9 25.2

wt.% dioxane in benzene ( $100y'$ ) : 5.2 22.5 32.0

Determine the percentage of dioxane extracted.

**Solution:**

$$x_F = 0.20, x_F' = \frac{0.20}{(1 - 0.20)} = 0.250 \text{ kg dioxane/kg water.}$$

Amount of water in initial solution:  $A = 100 (1 - 0.20) = 80 \text{ kg}$

$$\text{Solvent added: } S = 80 \text{ kg, } -\left(\frac{A}{S}\right) = -\left(\frac{80}{80}\right) = -1.$$

The given equilibrium data are plotted on  $y'-x'$  diagram as shown in Figure 10.7.

**Figure 10.7** Example 10.1.

The point  $F(0.25, 0)$  representing the feed is located on the abscissa. The operating line is drawn from  $F$  with a slope of  $(-1)$ . The operating line meets the equilibrium line at the point  $P$ .

From Figure 10.7,  $x' = 0.116 \text{ kg dioxane/kg water}$ .

Hence, Dioxane extracted =  $(0.250 - 0.116) = 0.134 \text{ kg dioxane/kg water}$ .

$$\text{Percentage of dioxane extracted} = \frac{0.134}{0.250} \# 100 = 53.6\%$$

### • Multistage Cross-current Extraction

A schematic flow diagram of a multistage cross-current extraction unit is presented in Figure 10.8. This is an extension of single-stage extraction where the raffinate from each stage is being treated with fresh solvent in the following stage.

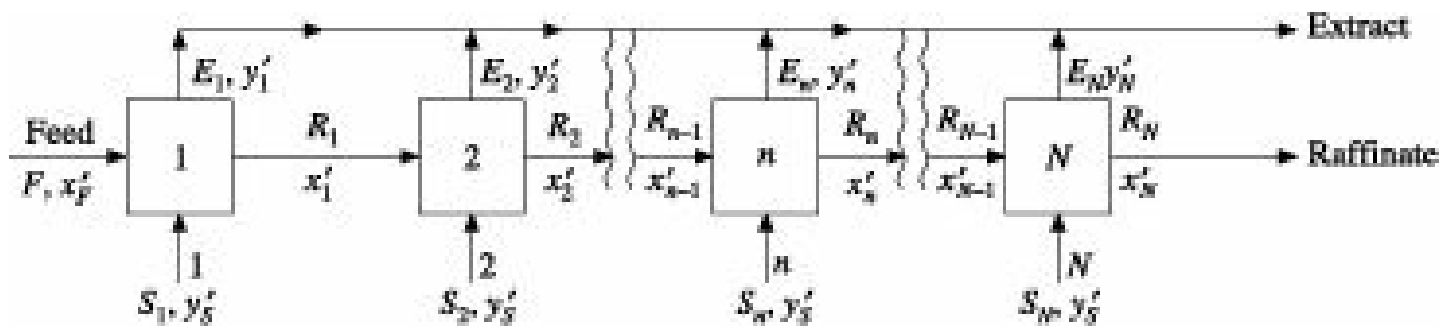


**Figure 10.8** Schematic flow diagram of multistage cross-current extraction.

Equations (10.5) and (10.6) apply to the first stage as before. A solute balance for any stage  $n$  may be written as

$$Ax'_{n-1} + S_n y'_S = Ax'_n + S_n y'_n \quad (10.9)$$

Equation (10.9) is the operating line for the  $n$ th stage having a slope of  $[-(A/S_n)]$  and passing through the points  $(x'_{n-1}, y'_S)$  and  $(x'_n, y'_n)$ . The graphical construction is shown in Figure 10.9.

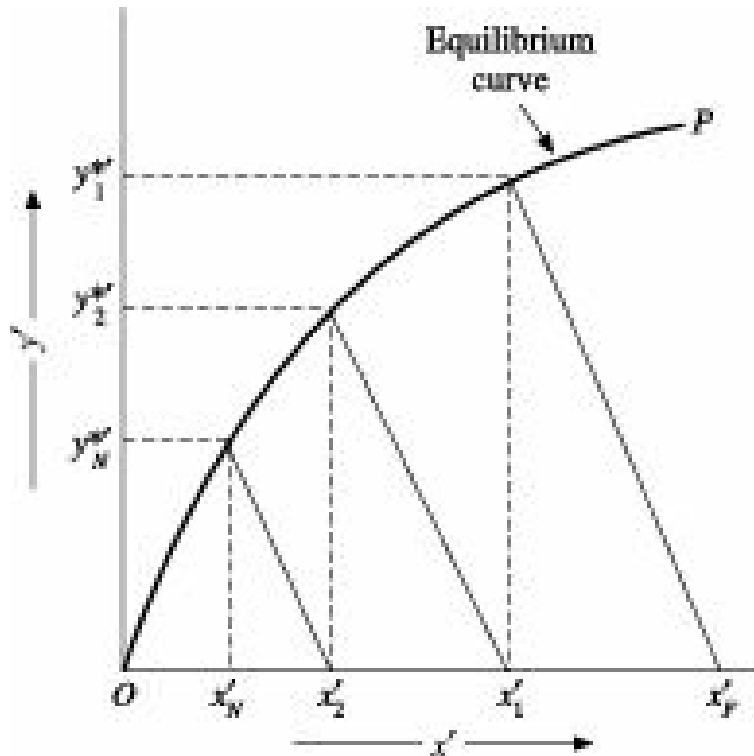


**Figure 10.9** Graphical representation of multistage cross-current extraction.

The equilibrium curve ( $OP$ ) is drawn from  $x'$  vs  $y^*$  data. The operating line for the first stage is obtained by drawing a straight line of slope  $[-(A/S_1)]$  through the point  $(x'_F, y'_S)$ . Operating line for any other stage  $n$  is drawn through the point  $(x'_{n-1}, y'_S)$  with a slope  $[-(A/S_n)]$ . The point of intersection of any operating line with the equilibrium curve gives the concentrations of extract and raffinate from that stage.

**EXAMPLE 10.2** (Single-stage and multistage cross-current extraction): 100 kg of an aqueous solution of acetone, containing 10% acetone by weight is to be extracted using monochlorobenzene (MCB) as solvent. Water and monochlorobenzene are immiscible within the range of concentration involved. Determine

- percentage extraction of acetone if the extraction is carried out in a single-stage with 150 kg

monochlorobenzene.

- (ii) percentage extraction of acetone if the extraction is carried out in three stages using 50 kg of monochlorobenzene in each stage.

Equilibrium data are as follows:

kg acetone/kg water	:	0	0.030	0.074	0.16	0.21
kg acetone/kg monochlorobenzene	:	0	0.029	0.070	0.156	0.24

**Solution:**

Given:  $F = 100 \text{ kg}$   $x_F = 0.10$ .

$$x'_F = 0.10 / (1 - 0.10) = 0.1111 \text{ kg acetone/kg water},$$

- (i) Using single-stage,

$$A = 100 (1 - 0.10) = 90 \text{ kg}, S = 150 \text{ kg}$$

$$\left( \frac{A}{S} \right) = \left( \frac{90}{150} \right) = -0.60$$

$x'_F = 0.1111$  is located on the abscissa, and the operating line with a slope of (-0.60) is drawn from  $x'_F$  in the Figure 10.10.

From the Figure,  $x_1 = 0.0428$

$$\text{Acetone extracted} = 90(0.1111 - 0.0428) = 6.15 \text{ kg}$$

$$\text{Percentage extraction} = \left( \frac{6.15}{10} \right) \square 100 = 61.5 \%$$

- (ii) Using three-stages,

$$A = 90 \text{ kg}, S = 50 \text{ kg}, \left( \frac{A}{S} \right) = \left( \frac{90}{50} \right) = -1.80$$

Starting from  $x'_F = 0.1111$ , three operating lines with slope of (-1.80) are drawn (Figure 10.10).

From Figure 10.10,  $x'_3 = 0.03098$

$$\text{Acetone extracted} = 90 (0.1111 - 0.03098) = 7.21 \text{ kg.}$$

$$\text{Percentage extraction} = \left( \frac{7.21}{10} \right) \square 100 = 72.1\%$$

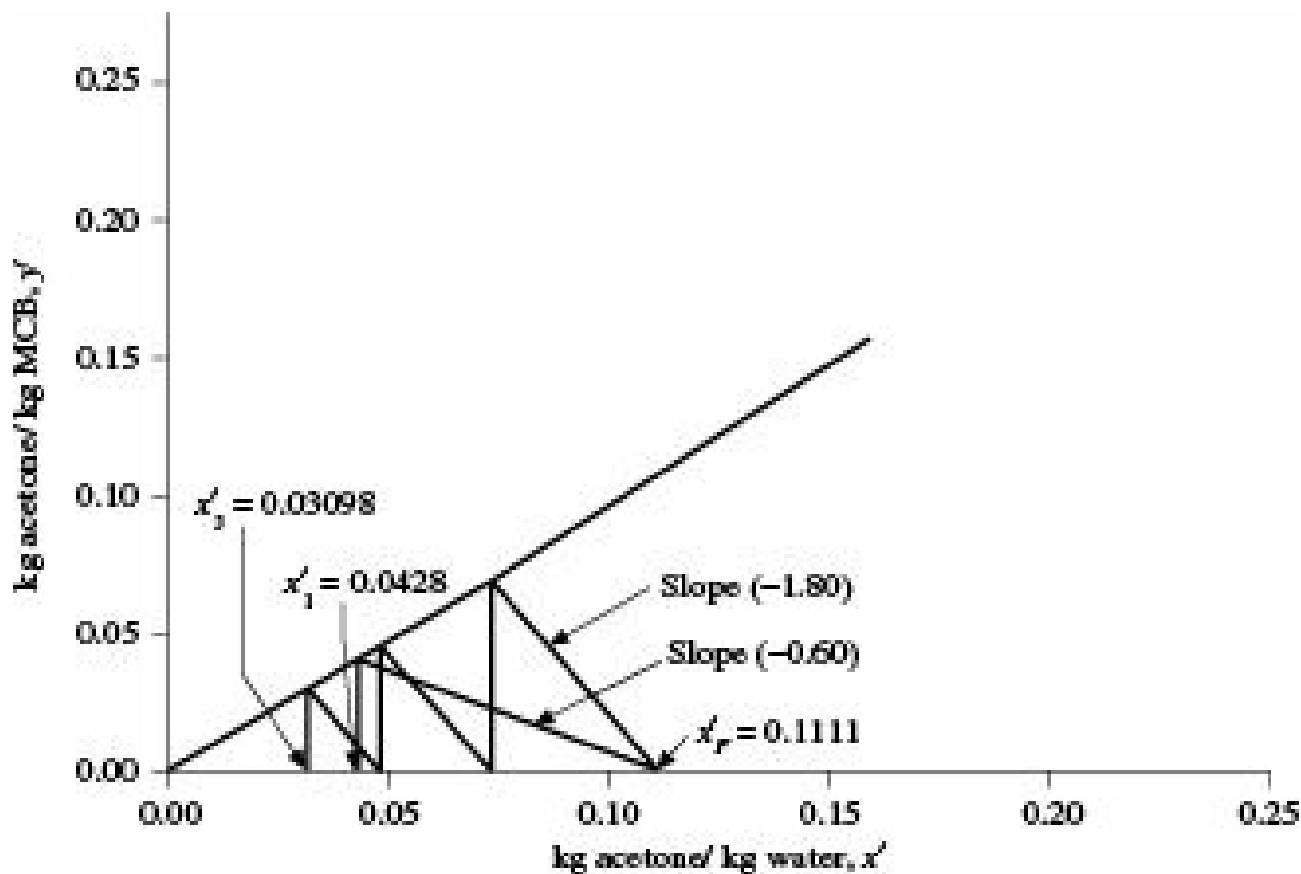


Figure 10.10 Example 10.2.

### • Multistage counter-current extraction

Figure 10.11 shows a schematic flow diagram of continuous counter-current multistage extraction which may be carried out either in a cascade of separate extraction units including separators or in a single equipment like a plate tower. Feed and solvent are introduced at the two opposite ends of the unit. The extract and raffinate phases flow in opposite directions and produce two product streams, the final extract  $E_1$  and the final raffinate  $R_N$ . This method is more economical than the previous methods since for a desired degree of separation, it requires lesser number of stages for a given amount of solvent or lesser solvent for a given number of stages.

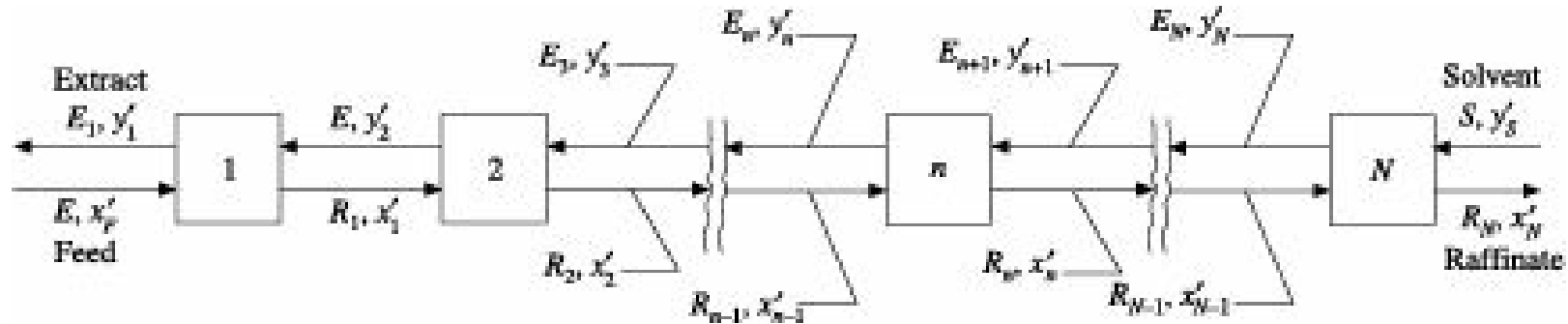


Figure 10.11 Schematic flow diagram of counter-current multistage extraction.

The material balance for the solute over the entire operation may be written as

$$Ax'_F + Sy'_S = Ax'_N + Sy'_1 \quad (10.10)$$

$$\text{whence, } \frac{A}{S} = \frac{y'_1 - y'_S}{x'_F - x'_N} \quad (10.11)$$

Equation (10.11) is the equation to the operating line which gives the actual solute concentrations in

the two phases at any point within the equipment. As is evident, this is an equation to a straight line having a slope of ( $A/S$ ) and passing through the points  $(x'_F, y'_1)$  and  $(x'_N, y'_S)$  at its two extremities. It should be noted that for pure solvent  $y'_S = 0$ .

The method of graphical computation for number of theoretical stages in continuous counter-current multistage extraction is shown in Figure 10.12. Equilibrium curve is plotted on rectangular co-ordinates from  $(x', y'^*)$  data. The operating line is drawn through any of the points  $(x'_F, y'_1)$  or  $(x'_N, y'_S)$  having a slope of  $(A/S)$ .

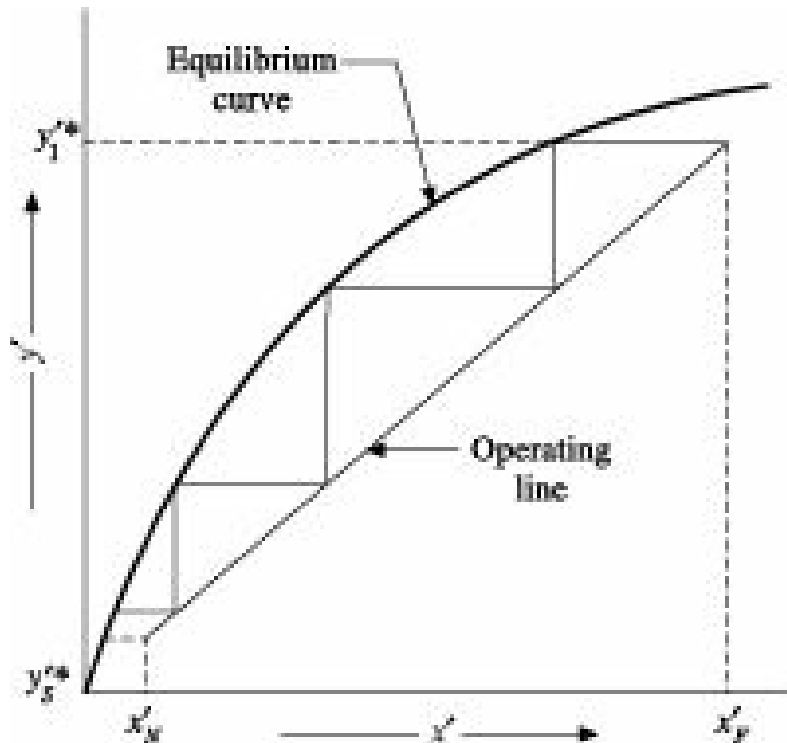


**Figure 10.12** Graphical representation of continuous counter-current multistage extraction.

Starting from either end of the operating line, steps are drawn between the equilibrium curve and the operating line till the other end of the operating line is reached. The number of steps gives the number of theoretical stages or theoretical plates required for the given separation.

For the special case where the equilibrium relationship is linear, i.e.  $y'^*/x' = m'$ , the following equation may be used for estimation of  $x'_N$  and graphical solution may be avoided:

$$\frac{x'_F - x'_N}{x'_F - y'_S/m'} = \frac{(m'B/A)^{N+1} - (m'B/A)}{(m'B/A)^{N+1} - 1} \quad (10.12)$$

where  $(m'B/A)$  is the extraction factor and ' $N$ ' is the number of theoretical stages.

**EXAMPLE 10.3** (Counter-current multistage extraction-immiscible solvents): 1000 kg/hr of a solution of  $C$  in  $A$  containing 20%  $C$  by weight is to be counter-currently extracted with 400 kg/hr of solvent  $B$ .  $A$  and  $B$  are mutually insoluble.

The equilibrium distribution of component  $C$  between  $A$  and  $B$  are as follows:

wt. of $C$ /wt. of $A$ :	0.05	0.20	0.30	0.45	0.50	0.54
wt. of $C$ /wt. of $B$ :	0.25	0.40	0.50	0.65	0.70	0.74

How many theoretical stages will be required to reduce the concentration of  $C$  in  $A$  to 5%?

**Solution:**

$$F = 1000 \text{ kg/hr}, A = 1000(1 - 0.20) = 800 \text{ kg}$$

$$x_F = 0.20, x'_F = 0.20/(1 - 0.20) = 0.25$$

$$x_N = 0.05, x'_N = 0.05/(1 - 0.05) = 0.0526$$

$$S = 400 \text{ kg/hr}, (A/S) = (800/400) = 2.0$$

As shown in Figure 10.13, the equilibrium line is drawn from the given data.

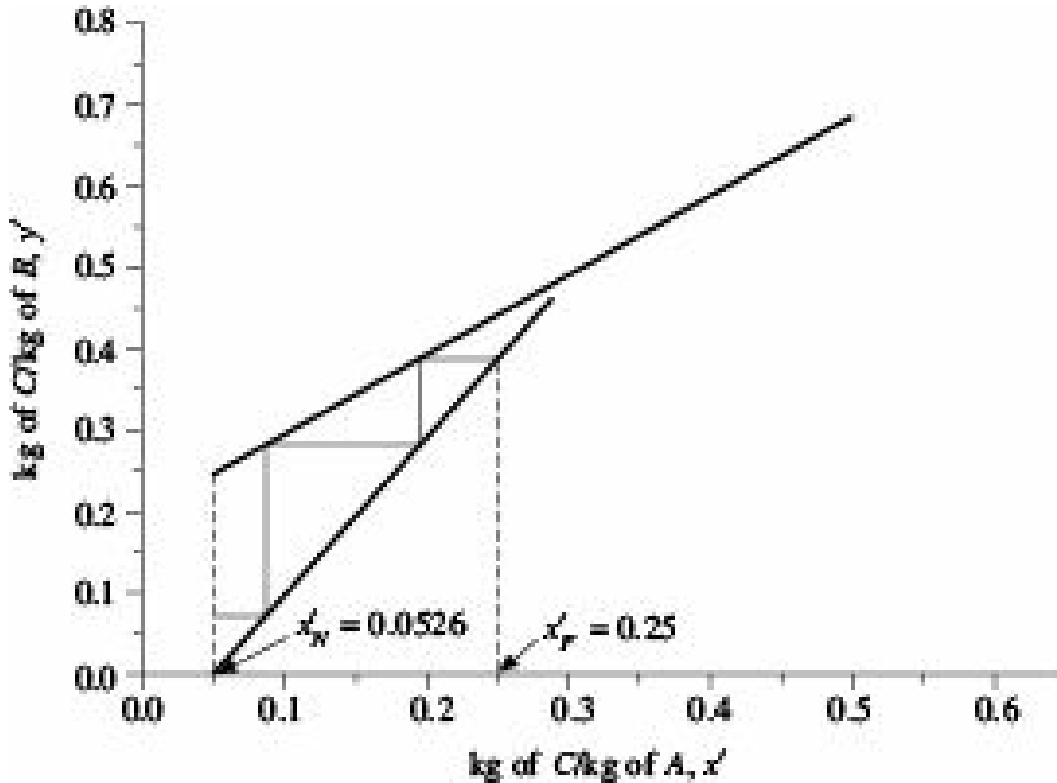


**Figure 10.13** Solution to Example 10.3.

The operating line is drawn through the point  $(0.0526, 0)$  with a slope of 2.0.

By drawing steps between equilibrium and operating lines, the number of ideal stages required is found to be 2.50.

### ***Extraction with partially miscible solvents***

In solving problems on extraction with partially miscible solvents, data on mutual solubility of the initial carrier liquid and the added solvent as well as on equilibrium distribution of one or more solute between them are required. Such problems may be solved on triangular diagrams, right-angled triangles on rectangular co-ordinates or solvent free co-ordinates. In case of extraction with partially miscible solvents, concentrations are expressed in terms of mass fractions.

#### **• Single-stage Extraction**

The flow diagram of Figure 10.5 and the operational procedure for extraction with immiscible solvents are also applicable for extraction with partially miscible solvents. After adding the solvent to the feed, the mixture is thoroughly mixed and allowed to settle when it separates into two immiscible equilibrium phases, extract  $E_1$  and raffinate  $R_1$ .

Overall material balance for the entire unit is

$$F + S = M_1 = E_1 + R_1 \quad (10.13)$$

The operation is graphically represented on triangular co-ordinates in Figure 10.14. The following

steps may be followed for graphical determination of the number of theoretical stages.

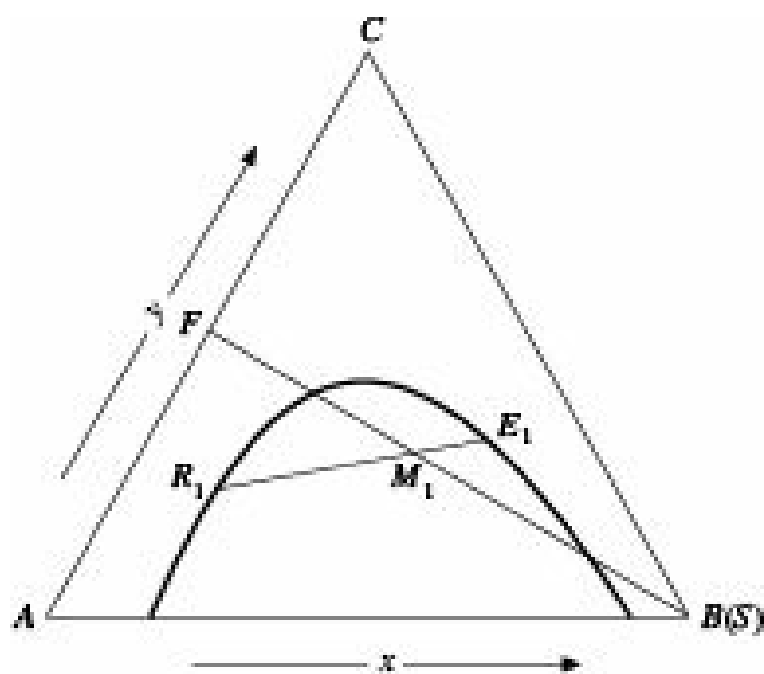


**Figure 10.14** Graphical representation of single stage extraction with partially miscible solvent.

After drawing the binodal solubility curve along with a few tie lines, the points  $F$  and  $S$  are located, the former from a knowledge of  $x_F$  and the latter from a knowledge of  $y_S$ . If the solvent is pure,  $y_S = 0$  and the point  $S$  coincides with the apex  $B$  as shown in the above figure.  $F$  and  $B$  are joined and the point  $M_1$  representing the mixture is located on the line  $FB$  from a knowledge of its solute content ( $x_{M_1}$ ) through the following equations:

$$F x_F + S y_S = M_1 x_{M_1} \quad (10.14)$$

or,

$$x_{M_1} = \frac{\frac{F x_F + S y_S}{M_1}}{F + S} \quad (10.15)$$

The point  $M_1$  can also be located by the inverse arm rule, but it is more convenient to locate  $M_1$  from its solute content.

The amount of solvent to be added for a given location of  $M_1$  to provide a predetermined value of  $y_1$  or  $x_1$  can be computed from the following equation:

$$S = \frac{\frac{F(x_F - x_{M_1})}{x_{M_1} - y_S}}{y_1 - x_1} \quad (10.16)$$

The amount of extract and raffinate can be computed from solute balance as under:

$$E_1 y_1 + R_1 x_1 = M_1 x_{M_1} \quad (10.17)$$

$$whence, \quad E_1 = \frac{\frac{M_1(x_{M_1} - x_1)}{y_1 - x_1}}{y_1 - x_1} \quad (10.18)$$

From Eq. (10.13), we get

$$R_1 = M_1 - E_1 = F + S - E_1 \quad (10.19)$$

The removal of solvent from  $E_1$  and  $R_1$  provides solvent-free extract  $E'$  and raffinate  $R'$  on the base  $AC$

$$F = E' + R' \quad (10.20)$$

$$Fx_F = E'y'E + R'x'R \quad (10.21)$$

$$\text{whence, } E' = \frac{F(x_F - x'_R)}{y_E - y'_R} \quad (10.22)$$

Once  $E'$  is known,  $R'$  may be determined from Eq. (10.20).

If the solvent is pure,  $y_S = 0$  and the line from  $F$  extends up to the apex  $B$ . In that case,  $y_S$  and terms containing  $y_S$  disappear from Eqs. (10.14) to (10.16) and  $S$  may be replaced by  $B$ .

### • Multistage Cross-current Extraction

The flow diagram of Figure 10.8 is valid for extraction with partially miscible solvents since the operational procedure is the same except that concentrations are expressed in mole fraction. The operation may be both batch and continuous. This being an extension of single-stage extraction where the raffinate from each stage is treated with fresh solvent in the next stage, Eqs. (10.13) to (10.22) apply to the first stage as before. For any other stage  $n$ , the total material balance equation becomes

$$R_{n-1} + S_n = M_n = E_n + R_n \quad (10.23)$$

A solute  $C$  balance gives

$$R_{n-1}x_{n-1} + S_n y_n = M_n x_{M_n} = E_n y_n + R_n x_n \quad (10.24)$$

$$\text{whence, } x_{M_n} = \frac{R_{n-1}x_{n-1} + S_n y_n}{M_n} = \frac{R_{n-1}x_{n-1}S_n y_n}{R_{n-1} + S_n} \quad (10.25)$$

Similarly, Equations for  $S_n$  and  $E_n$  can be written and solved. Point  $M_n$  is located on the line  $R_{n-1} S_n$  and a tie line through  $M_n$  provides  $E_n$  and  $R_n$ .

The graphical solution for multistage cross-current extraction with partially miscible solvents is shown in Figure 10.15 on triangular co-ordinates.

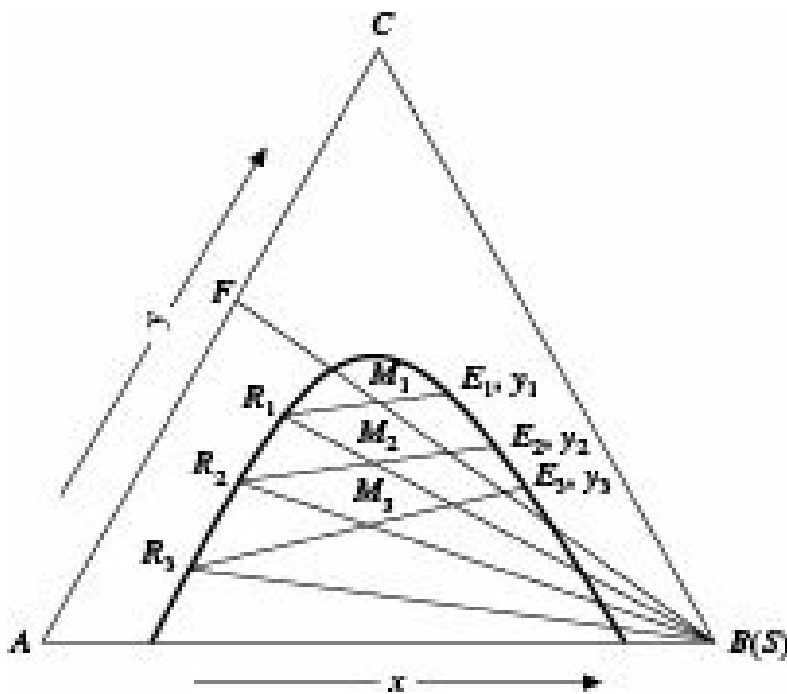


**Figure 10.15** Graphical representation of multistage cross-current extraction with partially miscible solvent.

The points  $F$ ,  $S$  and  $M_1$  are located as in case of single-stage extraction.  $A$  tie line through  $M_1$  provides  $R_1$  and  $E_1$ . Since  $R_1$ ,  $R_2$  and  $R_3$  act as feed to the respective next stages, they are successively joined with  $S$  or  $B$  as the case may be. The points  $M_2$  and  $M_3$  are located on the lines  $SR_1$ ,  $SR_2$ , ... from Eq. (10.25). Tie lines through  $M_2$ ,  $M_3$ , ... give  $E_2R_2$ ,  $E_3R_3$ , ... respectively at the two sides of the binodal solubility curve.

The extracts may be withdrawn separately from each stage. Alternatively they may be combined to produce a composite extract  $E$ .

**EXAMPLE 10.4** (Multistage cross-current extraction with partially miscible solvent): 250 kg of an aqueous solution of pyridine containing 50% pyridine by weight is extracted twice using 200 kg chlorobenzene each time.

- What will be the concentration of pyridine in the raffinate?
- Estimate the percentage extraction of pyridine.

The mutual solubility of water-chlorobenzene and the equilibrium distribution of pyridine between them are as under:

Pyridine	Chlorobenzene	Water	Pyridine	Chlorobenzene	Water
0	99.95	0.05	0	0.08	99.92
11.05	88.28	0.67	5.02	0.16	94.82
18.95	79.90	1.15	11.05	0.24	88.71
24.10	74.28	1.26	18.90	0.38	80.72
28.60	69.15	2.25	25.50	0.58	73.92
31.55	65.58	2.87	36.10	1.85	62.05
35.05	61.00	3.95	44.95	4.18	50.87
40.60	53.00	6.40	53.20	8.90	37.90
49.00	37.80	13.20	49.00	37.80	13.20

All compositions are in weight percent.

**Solution:****1st Stage:**

From the given data, the mutual solubility curve is drawn on a right angled triangle on rectangular co-ordinates as shown in Figure 10.16. The feed point is located on the *AC*-base for  $x_F = 0.50$ . Points *B* and *F* are joined and mixture point  $M_1$  is located from a knowledge of  $x_{M_1}$ .

$$x_{M_1} = \frac{Fx_F}{F+B} = \frac{(250)(0.5)}{250+200} = 0.278;$$

$$M_1 = 250 + 200 = 450 \text{ kg}$$

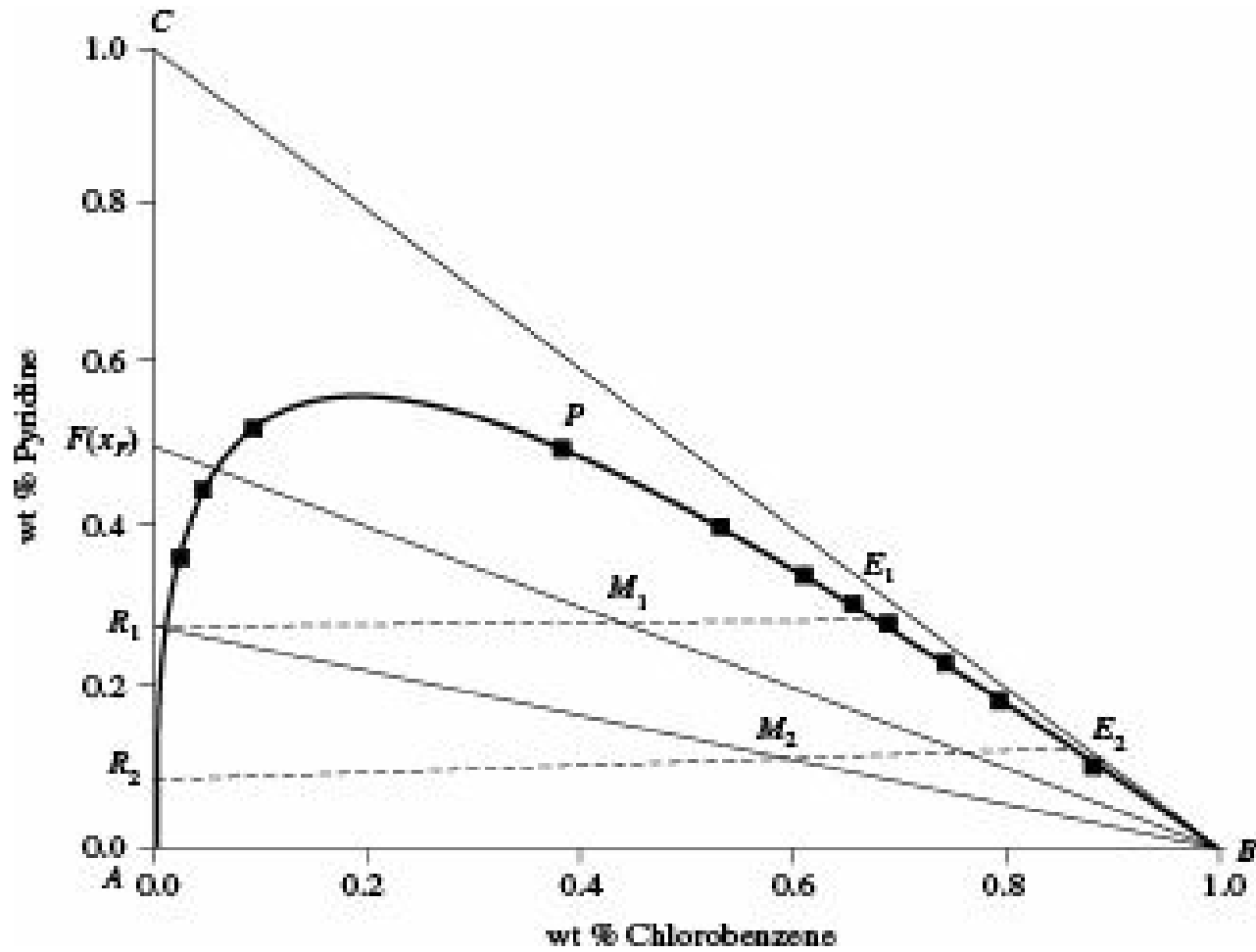


**Figure 10.16** Solution to Example 10.4.

A tie line through  $M_1$  gives  $E_1$  and  $R_1$ .

From above figure,  $x_1 = 0.265$  and  $y_1 = 0.285$ .

Hence, from Eq. (10.18)

$$E_1 = \frac{\frac{M_1(x_{M_1} - x_1)}{y_1 - x_1}}{\frac{(450)(0.278 - 0.265)}{0.285 - 0.265}} = 292.5 \text{ kg}$$

$$R_1 = 450 - 292.5 = 157.5 \text{ kg}$$

**2nd Stage:**

$$x_{M2} = \frac{R_1 x_1}{R_1 + B} = \frac{(157.5)(0.265)}{157.5 + 200} = 0.117$$

A tie line through  $M_2$  gives  $E_2$  and  $R_2$ .

From Figure 10.16,  $x_2 = 0.072$  and  $y_2 = 0.120$ .

$$M_2 = 157.5 + 200 = 357.5 \text{ kg}$$

$$E_2 = \frac{\frac{M_2(x_{M_2} - x_2)}{y_2 - x_2}}{0.120 - 0.072} = 335.15 \text{ kg}$$

(i) Concentration of pyridine in final raffinate =  $0.072 \# 100 = 7.2\%$

(ii) Pyridine originally present =  $(250)(0.50) = 125 \text{ kg}$

$$\text{Pyridine in composite extract} = E_1 y_1 + E_2 y_2$$

$$= (292.5)(0.285) + (335.15)(0.120) = 123.58 \text{ kg}$$

123.58

$$\text{Percentage of extraction} = \frac{123.58}{125} \# 100 = 98.86\%$$

#### • Continuous Counter-current Multistage Extraction

The schematic flow diagram of Figure 10.11 also represents the operation of counter-current multistage extraction with partially miscible solvents, which is similar to that for extraction with immiscible solvents. The feed and the solvent are introduced at the two opposite ends of the equipment as before. The extract and raffinate phases flow counter currently and are collected from two ends.

Graphical construction of stages for continuous counter-current multistage extraction is shown on triangular co-ordinates in Figure 10.17. Construction on right triangle or solvent-free co-ordinates are similar.

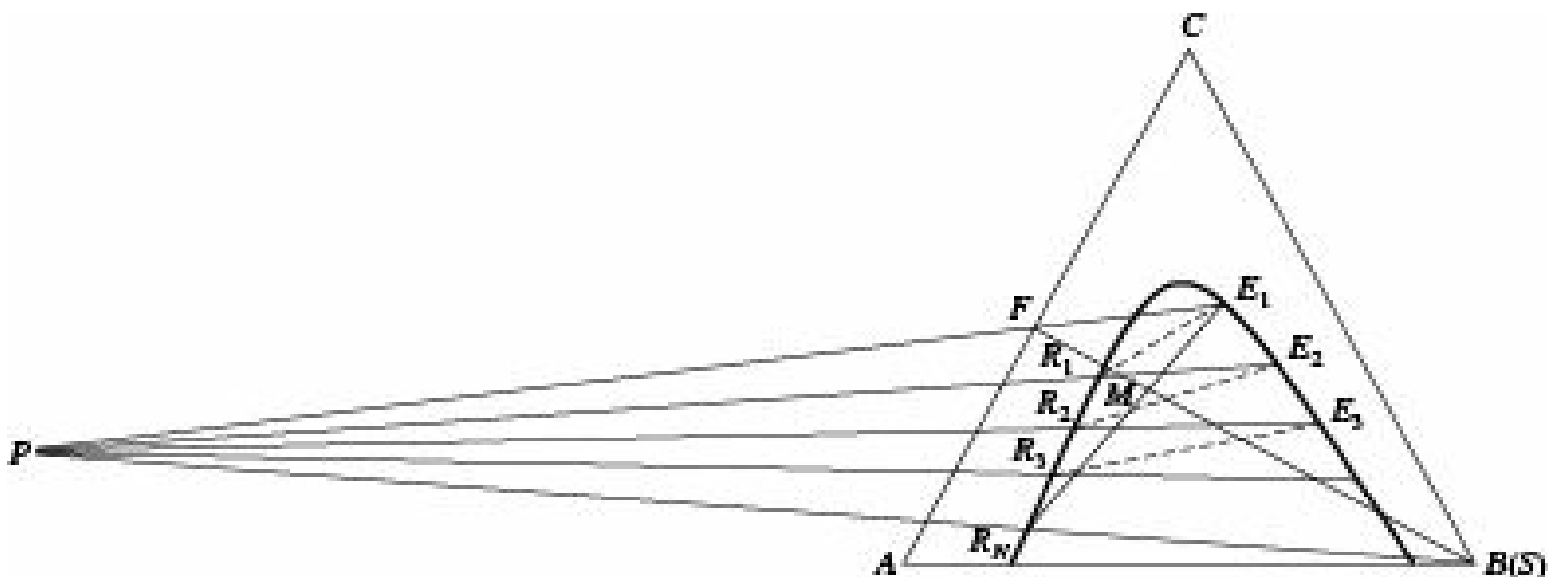


Figure 10.17 Graphical solution for continuous counter-current multistage extraction with partially miscible solvent.

An overall material balance for the entire plant is

$$F + S = M = E_1 + R_N \quad (10.26)$$

Points  $F$  and  $S$  or  $B$  are joined, and the mixture  $M$  is located on this line by a component  $C$  balance

$$Fx_F + Sy_S = Mx_M = E_1y_1 + R_Nx_N \quad (10.27)$$

$$\frac{Fx_F + Sy_S}{F + S}$$

whence,  $x_M = \frac{F + S}{F + S} (Fx_F + Sy_S)/(F + S) \quad (10.28)$

It is evident from Eq. (10.26) that the point  $M$  must lie on the straight line  $E_1R_N$ . Hence, if the composition of either the final extract or the final raffinate is known, the other can be located by joining the given composition with  $M$  and extending up to the other side of the mutual solubility curve. Rearranging Eq. (10.26), we get

$$R_N - S = F - E_1 = D \quad (10.29)$$

where  $D$  is the difference between flow quantities or the net outward flow at the last stage. From Eq. (10.29), it may be further concluded that the extended lines  $E_1F$  and  $SR_N$  must meet at a point. This point is denoted by  $D$ . Depending on the amounts of  $F$ ,  $E_1$ ,  $R_N$  and  $S$ , the two lines may intersect on either side of the triangle  $ABC$ .

A total material balance from any stage  $n$  to the last stage  $N$  is

$$R_{n-1} + S = E_n + R_N \quad (10.30)$$

or,

$$R_N - S = R_{n-1} - E_n = D \quad (10.31)$$

Equation (10.30) leads to the conclusion that the difference in flow rates between any two adjacent stages is constant and equal to  $D$ . Any line  $E_NR_{N-1}$  when extended must therefore pass through the point  $D$ .

The graphical construction for determination of number of stages is based on the above principle and consists of the following major steps.

The point  $F$  is located on the base  $AC$  from knowledge of  $x_F$  and the point  $S$  is located from knowledge of  $y_S$ . For  $y_S = 0$ ,  $S$  will coincide with the apex  $B$ .

$F$  and  $S$  are joined and the point  $M$  is located on the line  $FS$  from a knowledge of  $x_M$  from Eq. (10.28).  $R_N$  and  $M$  are joined and extended to get  $E_1$ . Alternatively,  $E_1$  and  $M$  may be joined and extended to get  $R_N$ .

$E_1F$  and  $SR_N$  are joined and extended to meet at  $D$ .

A tie line through  $E_1$  gives  $R_1$ , the line  $DR_1$  when extended gives  $E_2$ , a tie line through  $E_2$  gives  $R_2$  and so on.

This procedure is followed till the point  $R_N$  is reached.

The number of tie lines connecting  $E_nR_n$  gives the number of stages required for the extraction. It may be noted that one additional data, either  $x_N$  or  $y_1$  must be available for determination of number of stages in continuous counter-current multistage extraction.

Points  $E'$  and  $R'$  representing solvent-free extract and raffinate respectively are located by extending the lines from  $S$  through  $E_1$  and  $R_N$  respectively to the base  $AC$ .

On increasing the amount of solvent, point  $M$  becomes closer to  $S$  and point  $D$  moves to further left. If

the solvent rate is such that the lines  $E_1F$  and  $SR_N$  become parallel, the point  $D$  moves to infinity. As a result, the line  $E_{n+1}R_N$  becomes parallel to both  $E_1F$  and  $SR_N$ . Further increase in solvent rate makes the point  $D$  move to the right of  $B$ , approaching  $B$  with increase in solvent rate.

**EXAMPLE 10.5** (Counter-current multistage extraction with partially miscible solvent): 1000 kg/hr of a 50% pyridine-50% water solution is to be continuously and counter-currently extracted with chlorobenzene to reduce the pyridine concentration to 2%. All compositions are expressed as weight percent.

- Determine the minimum solvent rate required;
  - How many theoretical stages will be required if 1000 kg of solvent is used per hour?
- The equilibrium data of Example 10.4 may be used.

**Solution:** From the given data, the mutual solubility curve is drawn on a right-angled triangle on rectangular co-ordinates as shown in Figure 10.18. The feed point  $F$  is located on the base  $AC$  for  $x_F = 0.50$ . The final raffinate  $R_N$  is located on  $AC$  from a knowledge of  $x_N = 0.02$ .  $R_N$  and  $B$  are joined and extended.

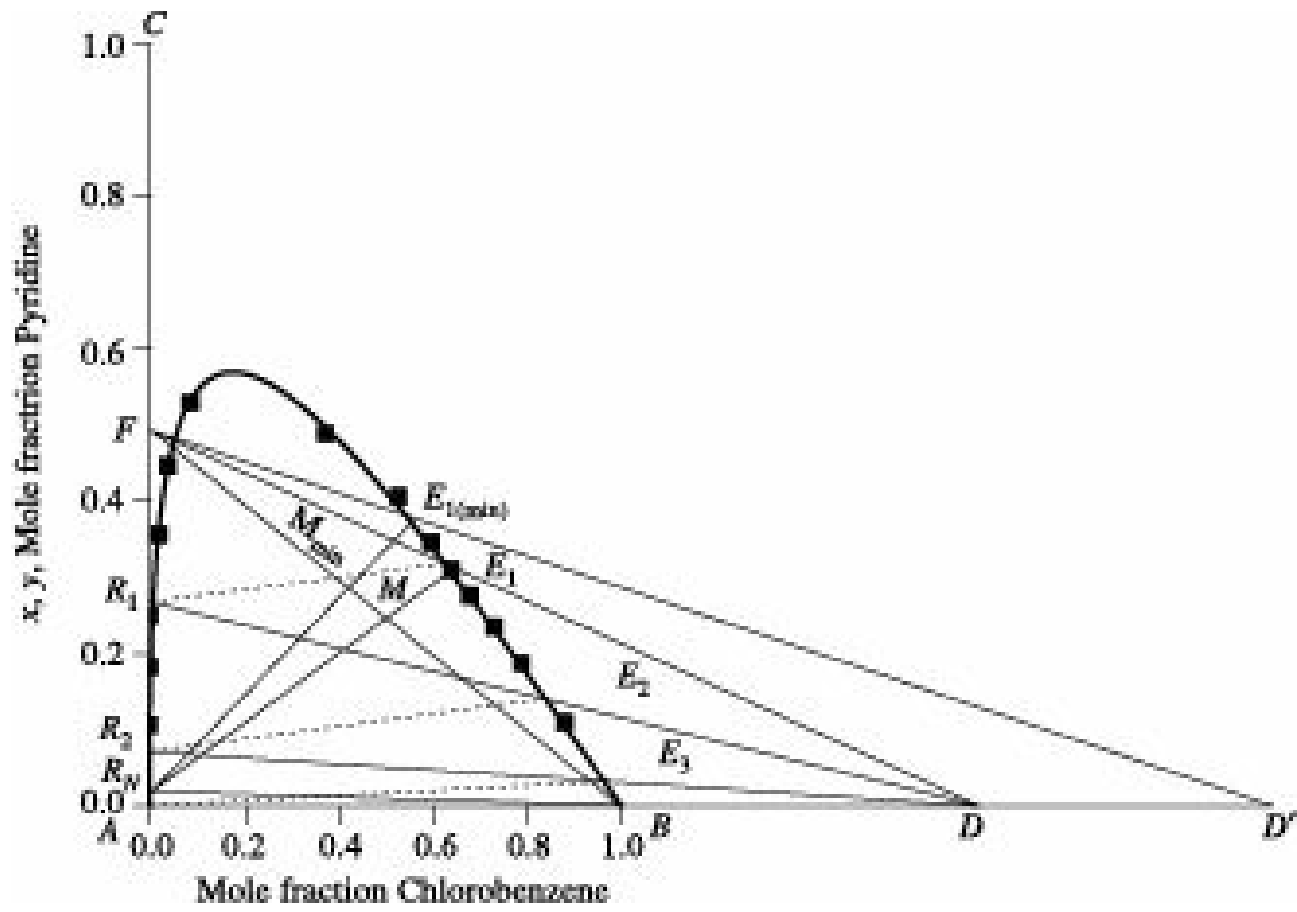


Figure 10.18 Example 10.5.

- A few tie lines around  $F$  are drawn and extended to meet  $R_NB$  extended. In this case, they meet to the right of  $B$ , hence the tie line that meets  $R_NB$  at the nearest point, gives the condition for minimum solvent.  $E_1(\min)$ , the extract corresponding to minimum solvent is located on the base  $BC$ .  $R_N$  and  $E_1(\min)$  are joined. The line intersects  $FB$  at  $M_{\min}$ .

From Figure 10.18,  $x_{M(\min)} = 0.285$

$$\text{From the relation } \frac{Fx_F}{F + B_{\min}} = x_M \text{ (min)}, \quad \frac{(1000)0.50}{1000 + B_{\min}} = 0.285$$

whence,  $B_{\min} = 754.4 \text{ kg/hr}$

$$\frac{(1000)(0.50)}{1000 + 1000}$$

$$(b) \text{ In this case, } B = 1000 \text{ kg/hr}, x_M = \frac{(1000)(0.50)}{1000 + 1000} = 0.25$$

$x_M$  is located on  $FB$ .  $R_N$  and  $M$  are joined and extended to the other side of the mutual solubility curve to get  $E_1$ .  $FE_1$  and  $R_NB$  are extended to meet at  $D$ . A tie line through  $E_1$  gives  $R_1$ .  $R_1$  and  $D$  are joined to get  $E_2$ . A tie line through  $E_2$  gives  $R_2$  and so on. This procedure is continued till  $R_N$  is reached.

From the Figure 10.18, the number of theoretical stages required = 3.

### **Minimum solvent rate**

The lines from  $D$  are the operating lines while the tie lines represent equilibrium relation. If the two coincide at any point within the equipment, the available driving force at that point becomes zero and infinite numbers of stages are required for any mass transfer to take place. This marks the condition for minimum solvent rate. Minimum solvent requirement may be determined by drawing several tie lines passing through the point  $F$  and below and extending them up to the line  $BR_N$ . That tie line, which meets  $BR_N$  at the farthest point if on the left and at the nearest point if on the right, gives the condition for minimum solvent. For any finite number of stages, the point  $D$  should be nearer to  $B$  than the farthest point of intersection of a tie line with  $BR_N$  if on the left and away from the point of intersection if on the right. The tie line, which passes through  $F$  usually, gives the condition for minimum solvent. For any extraction operation, the solvent rate should be higher than the minimum, the more so, the less will be the number of stages required.

In case the number of stages required is very large, computations on triangular diagram become difficult due to overcrowding of lines. In such cases, after location of the point  $D$  on a triangular diagram, few straight lines are drawn at random to meet the two branches of the mutual solubility curve at  $x_n$  and  $y_{n+1}$ . The operating line is then drawn on rectangular  $y$ - $x$  diagram by plotting the obtained values of  $x_n$  and  $y_{n+1}$ . The equilibrium curve  $y^*$  vs  $x$  is drawn on the same co-ordinates and steps are drawn between the equilibrium and operating lines. The number of steps gives the required number of stages.

### **Continuous counter-current multistage extraction with reflux**

Use of reflux at the extract end of a counter-current multistage extraction cascade can produce an extract with much higher solute content than in operations without reflux as in the rectifying section of a distillation unit. In such case, the feed is introduced some where within the cascade. The concentration of solute in the extract increases in the extract enriching section by counter-current contact with the raffinate rich in solute content. Part of the final extract is withdrawn as product and the remaining part is returned to the unit as reflux. Use of reflux at the raffinate end is not generally practised.

### **Stage efficiency**

In case of extraction, the performance of individual stages can be expressed in terms of approach to equilibrium actually achieved by the extract and raffinate phases.

As in case of gas-liquid contact, the Murphree stage efficiency can be expressed in terms of extract composition and raffinate composition as shown below:

In terms of extract composition,

$$E_{ME} = \frac{(y_m - y_{m+1})}{(y_m^* - y_{m+1})} \# 100 \quad (10.32)$$

In terms of raffinate composition,

$$E_{ME} = \frac{(x_{m-1} - x_m)}{(x_{m-1}^* - x_m^*)} \# 100 \quad (10.33)$$

where,  $x_m$  and  $y_m$  are the actual average effluent compositions, and  $y_{m+1}$  and  $x_{m-1}$  are the actual average compositions of the streams entering the stage.

Any consistent units may be used for expressing the values of  $x$  and  $y$ . The overall stage efficiency  $E_O$  can be defined as the ratio of the number of theoretical stages to the number of actual stages for a given change in concentration.

### Fractional extraction

If a solution contains two solutes both of which are soluble in a particular solvent then they can be extracted from the solution by using the solvent. But it is not possible to achieve high degree of separation by this method unless the distribution coefficients of the two solutes are widely different. Separation to any extent can, however, be made by the technique of fractional extraction provided the distribution coefficients are different.

A simple flow sheet for fractional extraction is shown in Figure 10.19. The feed having two solutes  $B$  and  $C$  is introduced into a counter-current cascade where two immiscible or partly miscible solvents  $A$  and  $D$  flow counter currently. At the feed stage, both the solutes distribute themselves between the solvents with solute  $B$  favouring solvent  $A$  and solute  $C$  favouring solvent  $D$ . In the stages ( $f' - 1$ ) to  $1'$  to the left of the feed stage, solvent  $A$  preferentially extracts solute  $B$  from solvent  $D$  so that solvent  $D$  becomes richer in  $C$ . In the stages ( $f - 1$ ) to  $1$  to the right of the feed stage, solvent  $D$  preferentially extracts solute  $C$  from solvent  $A$  so that  $A$  becomes richer in  $B$ .

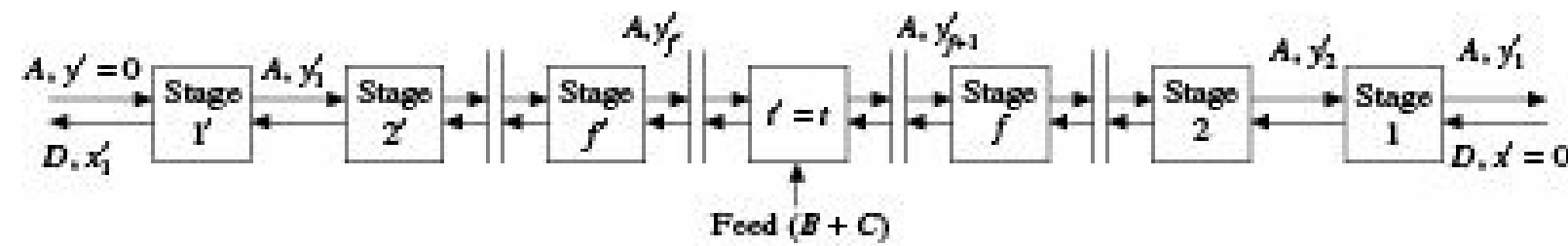


Figure 10.19 Flow diagram of fractional extraction.

### 10.5.2 Continuous Differential Contact

In continuous differential contact equipment like packed towers, the change in solute concentration in both the phases along the height of the tower is differential as shown in Figure 10.20. The tower height is therefore expressed in terms of transfer units instead of stages.

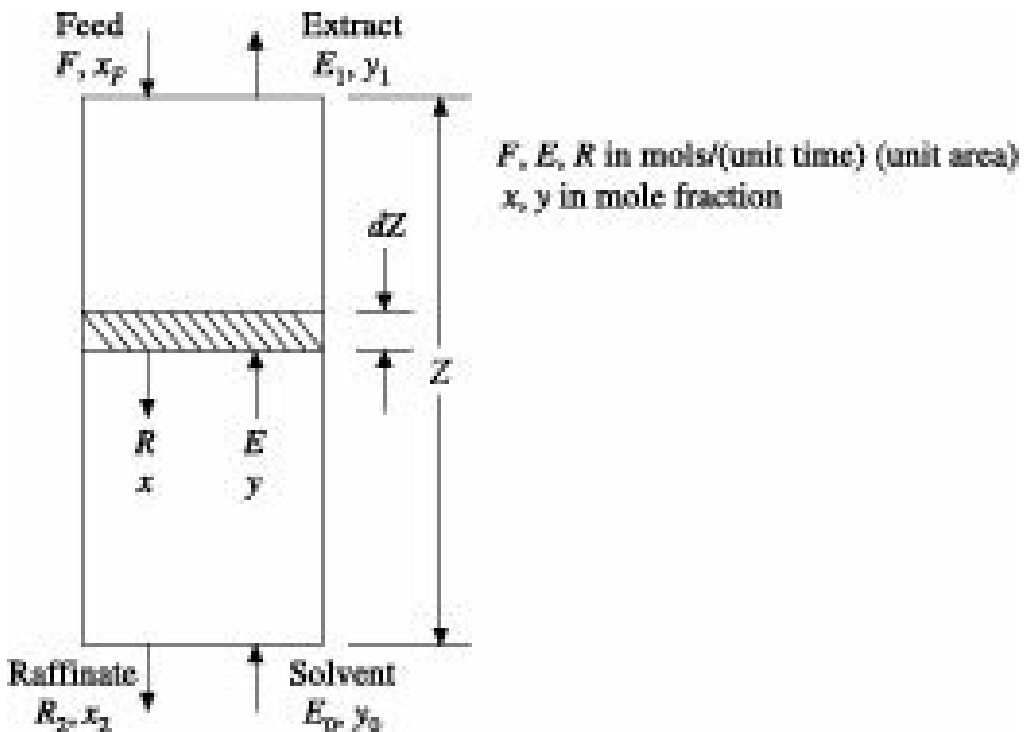


Figure 10.20 Continuous contact extraction.

The relevant equations have been developed by analogy with corresponding equations for gas absorption. Hence flow quantities are expressed in moles per unit time per unit area and compositions in mole fractions. The number and height of transfer units based on overall driving force are

### **Principal resistance in raffinate phase**

$$N_{tOR} = \frac{\int_{x_2}^{x_1} \frac{(1-x)}{K_R a} dx}{(1-x)(x-x^*)} \quad (10.34)$$

$$H_{tOR} = \frac{R}{K_R a (1-x)_{lm}} \quad (10.35)$$

and

$$Z = H_{tOR} \# N_{tOR} \quad (10.36)$$

where,

$N_{tOR}$  = number of transfer units based on overall driving force in raffinate phase

$H_{tOR}$  = height of transfer unit based on overall driving force in raffinate phase, m

$K_R a$  = overall mass transfer coefficient based on overall driving force in terms of raffinate phase, kmol/(hr)(m<sup>3</sup>)(mole fraction)

$Z$  = Height of tower, m

$R$  = Raffinate flow rate, kmol/(hr)(m<sup>2</sup>)

The quantity  $(1 - x)_{lm}$  is the log-mean average of the nonsolute concentrations at the two ends of the tower. In moderately dilute solutions, arithmetic average may be used so that

$$N_{t0R} = \frac{\int_{x_2}^{x_1} \frac{dx}{x - x^*} + \frac{1}{2} \ln \frac{1-x_2}{1-x_1}}{(x - x^*)_{lm}} \quad (10.37)$$

For very dilute solutions, the second term of Eq. (10.37) may be neglected which reduces the equation to the form

$$N_{t0R} = \frac{x_1 - x_2}{(x - x^*)_{lm}} \quad (10.38)$$

### **Principal resistance in extract phase**

$$N_{t0E} = \frac{\int_{y_2}^{y_1} \frac{(1-y)_{lm} dy}{(1-y)(y^* - y)}}{(1-y)_{lm}} \quad (10.39)$$

$$H_{t0E} = \frac{E}{K_E a (1-y)_{lm}} \quad (10.40)$$

and

$$Z = H_{t0E} \# N_{t0E} \quad (10.41)$$

where,

$N_{t0E}$  = number of transfer units based on overall driving force in extract phase

$H_{t0E}$  = height of transfer unit based on overall driving force in extract phase, m

$K_E a$  = overall mass transfer coefficient based on overall driving force in extract phase, kmol/(hr)  
( $m^3$ )(mole fraction)

$E$  = extract flow rate, kmol/(hr)( $m^2$ )

For moderately dilute solutions,

$$N_{t0E} = \frac{\int_{y_2}^{y_1} \frac{dy}{y^* - y} + \frac{1}{2} \ln \frac{1-y_1}{1-y_2}}{(y^* - y)_{lm}} \quad (10.42)$$

and for very dilute solutions,

$$N_{t0E} = \frac{y_1 - y_2}{(y^* - y)_{lm}} \quad (10.43)$$

Since rates of mass transfer in liquid extraction depend on several complex factors, data on mass transfer coefficient are very scanty and the above equations are only of limited use till now.

**EXAMPLE 10.6** (Continuous differential contact extraction): An aqueous solution of acetic acid containing 0.70 kmol/m<sup>3</sup> acetic acid is being extracted with benzene in a counter-current packed tower to reduce the acid content of the aqueous phase to 0.69 kmol/m<sup>3</sup>. The tower is 8.0 cm in diameter and 1.5 m long. The flow rate of benzene is 6.0 cm<sup>3</sup>/s. The benzene stream enters the tower

at its bottom with an acid content of  $0.002 \text{ kmol/m}^3$  and leaves with an acid content of  $0.012 \text{ kmol/m}^3$ .

The equilibrium relationship is given by  $y^* = 0.0247x$ , where  $x$  and  $y^*$  are the concentrations of acetic acid in water and benzene phases, respectively.

Determine the overall mass transfer coefficient and the height of the transfer unit based on the extract phase.

### Solution:

Given: diameter of the tower = 8.0 cm

$$\frac{\pi(8)^2}{4 \times 10^4}$$

Therefore, cross section of the tower =  $\frac{\pi(8)^2}{4 \times 10^4} = 0.0050 \text{ m}^2$

Volume of the tower =  $0.0050 \# 1.5 = 0.0075 \text{ m}^3$

### Aqueous Phase

Acid concentration in incoming stream,  $x_F(x_1) = 0.70 \text{ kmol/m}^3$

Acid concentration in exit stream ( $x_2$ ) =  $0.69 \text{ kmol/m}^3$

### Benzene Phase

Acid concentration in incoming stream,  $y_0(y_2) = 0.002 \text{ kmol/m}^3$

Acid concentration in exit stream ( $y_1$ ) =  $0.012 \text{ kmol/m}^3$

Flow rate of benzene phase =  $6.0 \text{ cm}^3/\text{s}$

$$= (6.0 \# 10^{-6})/(0.0050) = 1.20 \# 10^{-3} \text{ m}^3/(\text{m}^2)(\text{s})$$

Acid transferred to the benzene phase =  $6.0 \# 10^{-6} (0.012 - 0.002)$   
=  $6.0 \# 10^{-8} \text{ kmol/s}$

The equilibrium relation is  $y^*/x = 0.0247$

$$y^*_2 = 0.0247 \# 0.69 = 0.01704$$

$$y^*_1 = 0.0247 \# 0.70 = 0.01729$$

Driving force at the bottom of the tower ( $\Delta C_1$ ) =  $0.01704 - 0.002 = 0.01504$

Driving force at the top of the tower ( $\Delta C_2$ ) =  $0.01729 - 0.012 = 0.00529$

$$\text{Log-mean average driving force} = \frac{(0.01504 - 0.00529)}{\ln(0.01504/0.00529)} = 0.00935$$

From definition of mass transfer coefficient, overall mass transfer coefficient based on extract phase is

$$K_E = \frac{\text{Moles acid transferred}}{(\text{Volume of packing})(\Delta C_{lm})}$$

$$= \frac{6.0 \times 10^{-8}}{(0.0075)(0.00935)} = 8.56 \times 10^{-4} \text{ kmol/(s)(m}^3\text{)(kmol/m}^3\text{)}$$

and Height of a transfer unit based on extract phase

$$H_{tOE} = \frac{E}{K_E} = \frac{1.20 \times 10^{-3}}{8.56 \times 10^{-4}} = 1.40 \text{ m}$$

## 10.6 Extraction by Supercritical Fluids

In recent years, supercritical fluids have emerged as very powerful tools for extraction of solutes both from liquids and solids. First commercialized in Germany during the nineteen seventies for removal of caffeine from coffee, supercritical fluids, particularly water-carbon dioxide solution have found extensive applications in process industries not only for extraction but also in such areas as supercritical fluid chromatography, supercritical fluid reactions and supercritical fluid processing. A supercritical fluid is any fluid whose temperature and pressure are above its critical point as shown in Figure 10.21. It exhibits physico-chemical properties intermediate between those of liquids and gases. Its relatively high density increases its dissolving power while relatively low viscosity and high diffusivity compared to those of liquid solvents permit rapid penetration and better phase separation (Wang et al. 1995). These properties result in higher rates of mass transfer in supercritical fluids than in conventional liquid solvents. This technique provides higher yields, better product quality and is useful in recovering high value and low volume products from dilute systems typical in chemical, pharmaceutical and biotechnological processes. Moreover, supercritical fluid extraction can be operated over a wide range which facilitates manufacture of tailor-made end products.

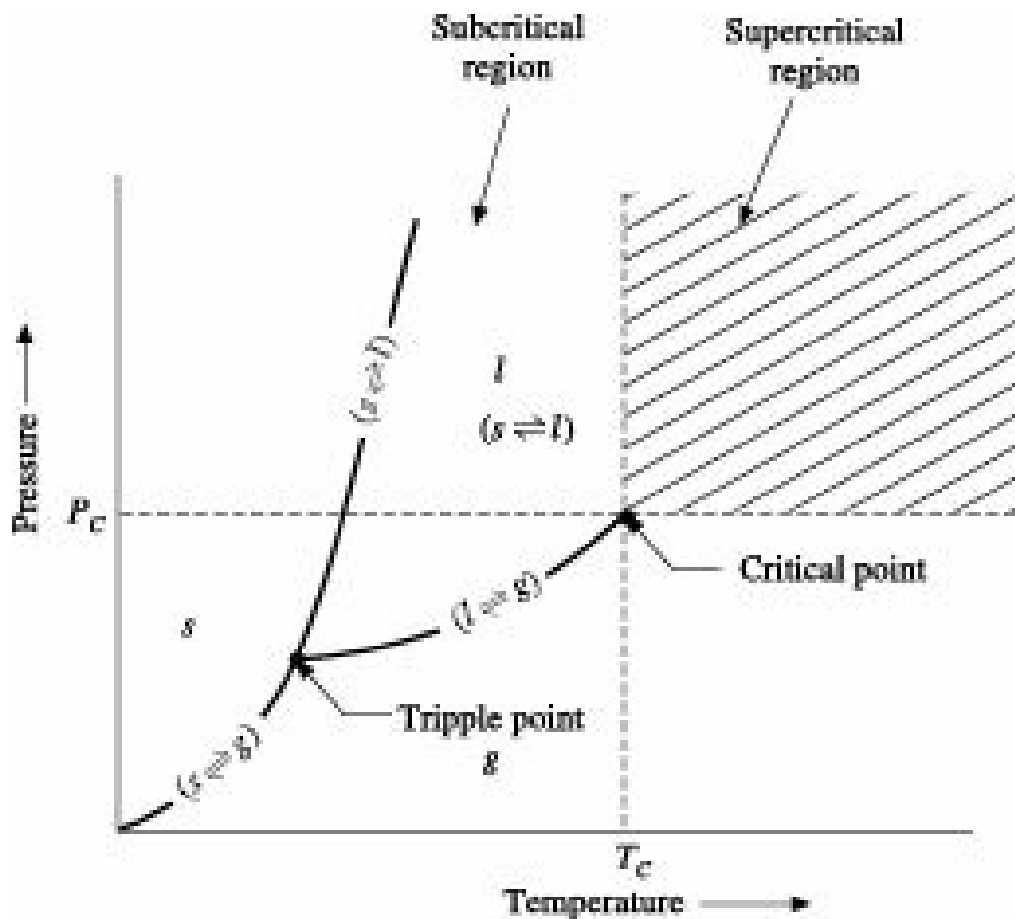


Figure 10.21 P-T Phase diagram.

The effectiveness of supercritical fluid extraction can be attributed to four major factors (Bulley and Fattori 1984):

- increase in selectivity as critical pressure is approached
- wide variation in solubility depending upon density of solvent, consequently on its temperature and pressure
- variation in solubility with molecular weight of solute for similar molecular structures
- high solubility of nonvolatile hydrophobic materials

The main criteria to be considered during selection of a solvent for supercritical fluid extraction are the capacity of the solvent to dissolve the desired solute from the mixture. The solvent should have low boiling point for ease of recovery and moderate critical pressure. In addition, it should be inert, nontoxic, noncarcinogenic, nonflammable, cheap and easily available. Carbon dioxide in water is the most commonly used supercritical fluid for extraction since it fulfils all the above criteria.

A simple supercritical fluid extraction system consists of four basic units, a solvent compressor or pump, an extractor, a temperature/pressure control system and a separator or an absorber. The schematic diagram of a common system is shown in Figure 10.22. It is very difficult to operate a system very near the critical point. However, in order to take advantage of the desirable properties, the operating range should normally be within  $T_R = 1.01$  to  $1.10$  and  $P_R = 1.01$  to  $1.50$  (Brennecke and Eckert 1989).

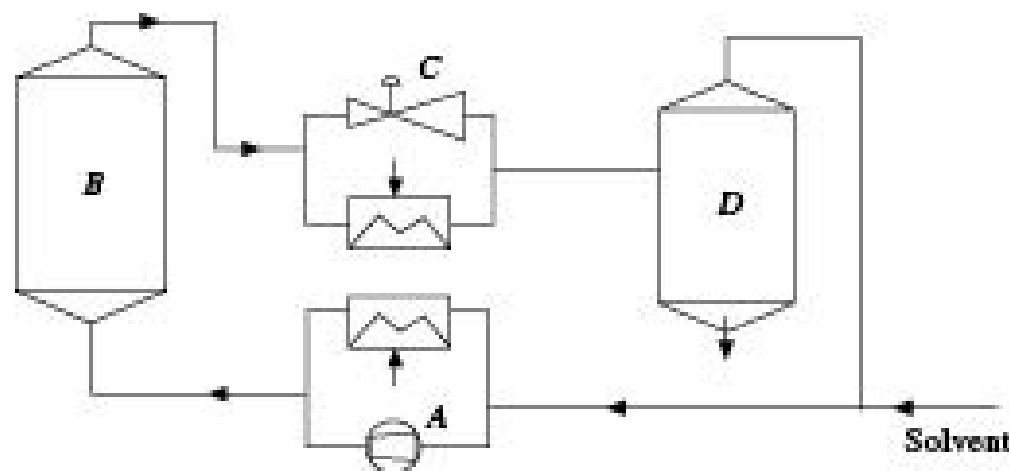


**Figure 10.22** Super critical extraction equipment. *A*: Solvent compressor/pump, *B*-Extractor, *C*: Temperature/pressure control system, *D*: Separator.

Till now supercritical fluid extraction is mostly used in food, petroleum, and flavour and fragrance industries. In food industry, supercritical carbon dioxide has become the common solvent for decaffination of coffee. The concentration of caffeine can be reduced to 0.02% by this solvent. It has readily replaced the conventional solvent methylene chloride since energy effective roasting can be avoided and, unlike methylene chloride, carbon dioxide is noncarcinogenic. Moreover, 100% solvent removal is possible in supercritical extraction. Carbon dioxide has also replaced conventional toxic solvents in decaffination of tea leaves. For dairy and confectionery products, carbon dioxide extracts are preferred in the formulation of high quality natural flavours. For use in soft drinks, carbon dioxide extracts like ginger offers both pungency and flavour in the most stable form and can be used in bottled syrup. It is fact that carbon dioxide extracted orange peel oils have fewer terpenes (limonene) and more aldehydes (citrals) as compared to the cold pressed oils. Supercritical carbon dioxide is fast replacing conventional solvents like hexane in extraction of oil from different seeds. Other areas

of its application include separation and fractionation of fish oil compounds, extraction of fat and cholesterol from egg and meat, refining and fractionation of cod liver oil, deodorisation of vegetable and animal oils, in recovery of aroma from certain fruits and flowers and in oil recovery from several vegetables and fruits.

In petroleum industry, the ROSE (Residuum Oil Supercritical Extraction) process employs supercritical pentane in lieu of propane for fractionation of crude residuum into asphaltenes, resins and oils.

In flavour and fragrance industry, the use of supercritical carbon dioxide ( $\text{SCCO}_2$ ) as solvent has made a dramatic change. Most of the drawbacks encountered in the conventional processes are circumvented by using  $\text{SCCO}_2$  as the extractant. The advantages of this method include (Mukhopadhyay 2000):

- No residual toxic solvents and significantly reduced pesticides
- No thermal degradation because of near-ambient operating temperature and inert environment of  $\text{CO}_2$
- Energy savings in solvent regeneration
- Faster extraction and high recovery of extracts
- Nonflammable solvent with no environmental hazard
- Better shelf life due to co-extraction of antioxidants and elimination of dissolved oxygen
- High purity and tailor-made specifications of the product due to easy manipulation of selectivity of separation
- Generally regarded as safe and noncombustible
- A wide spectrum of physical properties can be obtained in a single solvent by small variations of process parameters such as pressure, temperature or an entrainer making it a flexible, versatile and multiproduct solvent

Out of all available and allowable volatile solvents for extraction, supercritical carbon dioxide brings out the most natural smell and taste in the extracts, bearing the closest resemblance to the original material.

Some of the difficulties with supercritical fluid extraction are that they are mostly batch operations, initial costs are high, operating pressures are pretty high and very often necessary equilibrium data are not available. The high cost of supercritical extraction equipment is often offset by more complete extraction and the possibility of fractionation of the extract to a number of products. However, none of these difficulties are insurmountable and constant efforts are on to overcome them.

## 10.7 Equipment for Liquid–Liquid Extraction

Liquid-liquid extraction involves a number of steps which include bringing two immiscible or partially miscible liquid phases into intimate contact; creating conditions for effective mass transfer to take place between them; separation of the two liquid phases; recovery of the solute from the extract; and recovery of solvent from both the phases. The recovered solvent, with the exception of water, is reused for further extraction.

If one of the liquids is water and the other is organic, one of the two liquids gets distributed in the form of drops in the continuum of the other liquid. When the aqueous phase forms the continuous

phase, the dispersion is termed organic in aqueous dispersion. On the other hand, when the organic liquid becomes the continuous the dispersion is known as aqueous in organic dispersion. In such dispersions, it is not always easy to predict which of the liquids would be considered as dispersed phase under the situation. Many factors like the physical properties of the two liquids and different operating parameters of the equipment influence the same. This change could be from organic to aqueous or aqueous to organic phase. This abrupt catastrophic change of dispersion structure is termed *phase inversion*. This does not happen in case of organic-organic liquids.

Dispersing one liquid into another liquid is much more difficult than dispersing a gas in a liquid as encountered in gas liquid operations. In case of gas-liquid contact, large difference in densities of the two fluids and low viscosity of the gas leads to high bubble rise velocity, enhanced turbulence and rapid bubble breakage resulting in large interfacial area of contact and thorough mixing of the phases. But due to the small differences in densities of liquids, the rising velocity of the drops of one liquid through another liquid is much lower and turbulence created is also very low. In comparison to gas-liquid systems, much higher energy is required for dispersing one liquid in another liquid. Moreover, unlike gas-liquid system, very low density difference and low interfacial tension in liquid-liquid systems make it much more difficult to separate liquid-liquid dispersions into two clear liquid phases.

In most industrial liquid-liquid extractions, dispersion of one liquid phase into another liquid phase and subsequent phase separation are accomplished by taking advantage of the differential effects of either gravity or mechanical agitation or centrifugal force on the two phases having different densities.

Because of the wide diversity of applications utilizing liquid-liquid extraction, a wide variety of separation devices have been developed. Some equipment is similar to that used for distillation, absorption and stripping. However, such devices can be inefficient unless the liquid viscosities are low and the differences in phase densities are high.

Liquid-liquid extractors are of two broad categories:

- Stage-wise contactors in which the equipment consists of a single or a series of physical stages in which the phases are mixed and separated,
- Differential contactors in which the phases are continuously brought into contact and phase separation takes place only near the exit of the equipment.

A classification of extractors in line with the classification suggested by Coulson and Richardson (1991) is given in Table 10.1.

**Table 10.1** Classification of extractors

Counter-current flow produced by	Phase dispersed by	Stage-wise contact	Differential contact
Gravity	Mechanical Agitation	Mixer-Setter, Scheibel extractor	Rotating disc contactor
	Pulsation	Pulsed sieve	Pulsed packed column
	Gravity	Plate column Perforated plate column	Pulsating plate column Spray column Packed column
Centrifugal force	Centrifugal force	Rebatel extractor	Podbielniak extractor, DeLaval.

Important characteristics of some common extractors are given in Table 10.2 (Wankat 1988; Henley and Seader 1998).

Pulsed, Rotary agitated and Reciprocating columns belong to the class “Continuous counter-flow contactors with mechanical agitation”. This type of equipment have the advantages of incurring medium capital cost, good dispersion between liquids, capability of many stages and easy scale-up. However, limitations of this class of equipment are: limited capacity with small density differences, flow rate restrictions, inadequate for emulsifying systems. With such an array of extraction equipment available, the design engineer will need to consider the advantages and limitations associated with each class of equipment. Reissinger and Schröeter (1984) have compared a number of industrial column-type extractors for maximum liquid capacity and maximum column design. The comparison has been given in Table 10.3. Liquid capacities per unit cross sectional area are highest with the Karr extractor and lowest with the Graesser extractor.

**Table 10.2** Characteristics of some common extractors

<i>Extractor class</i>	<i>Extractor type</i>	<i>Important characteristics</i>
Mixer-Settler	Agitated vessels	Good contacting, high stage efficiency, capability of many stages, handles wide phase ratios and liquids with high viscosity, flexible, reliable, good scale-up. However, incurs high capital and operating costs, large liquid hold-up, may require interstage pumping and storage.
	Static mixers	
Unagitated columns	Plate, packed and spray columns	Low capital cost, low operating/maintenance cost, simple construction, handles corrosive materials. However, can exhibit low efficiency, limited capacity with small density differences, flow rate restrictions, poor scale-up.
Pulsed columns	Perforated plate, packed columns	Low HETS, high mass transfer coefficient, no internal moving parts.
Rotary agitated columns	RDC, Oldshue-Rushton, Scheibel, Asymmetric Rotating Disk (ARD), Kuhni extractor	Moderate to high capacity, reasonable HETS, accommodates many theoretical stages, moderate cost, low cost of operation and maintenance.
Reciprocating plate	Karr column, Graesser extractor	High loading, low HETS, high versatility and flexibility, simple construction, handles liquids with suspended solids.
Centrifugal	Podbielnik extractor	Short contact time, low hold-up volume, small solvent requirement, suitable for unstable materials, small size (limited space requirements), easily handles emulsifiable and small density difference systems. However, incurs high capital, operating and maintenance costs; limited number of stages per unit.

**Table 10.3** Maximum loading and diameter of commercial column-type extractors

<i>Commercial column type</i>	<i>Approx. maximum liquid loading, m<sup>3</sup>/(m<sup>2</sup>)(hr)</i>	<i>Maximum column diameter, m</i>
Lurgi (a type of Mixer-Settlers)	30	8.0
Pulsed packed	40	3.0
Pulsed sieve tray	60	3.0
Scheibel	40	3.0
RDC	40	8.0
ARD	25	5.0
Kuhni	50	3.0
Karr	100	1.5
Graesser	< 10	7.0

## 10.7.1 Phase Dispersion by Mechanical Agitation

In case of liquid–liquid extraction, the density difference is very small and as such equipment like perforated plate, spray and packed towers, which depend entirely on density difference have poor

mass transfer characteristics, particularly for systems having high interfacial tensions. As a result, a number of extraction equipment have been developed which make use of mechanical agitation to effect dispersion and thereby achieve enhanced mass transfer rates. At the same time, baffles are provided to reduce axial mixing caused by such agitation.

### **Stage-wise contact**

#### **• The Mixer-Settler**

A single-stage mixer-settler consists of a simple mixer for contacting the two liquids and a settler for separating the two phases after the desired mass transfer has taken place. In batch operation the same tank may act both as mixer and settler with the agitator stopped after mixing. Mixers may be of two types: agitated vessels and flow mixer.

An agitated vessel is a vertical cylindrical tank provided with a flat-blade turbine type impeller located centrally near the middle of the tank or near the liquid inlet at the bottom. The tank may be opened or covered. The tank is usually provided with four baffles to create intense turbulence and prevent vortex formation. Both the liquid streams enter the mixer near the bottom. One liquid is dispersed in the form of fine droplets in the other liquid and the resulting emulsion leaves the tank near its top. The liquids are kept in the tank for sufficient time known as *holding time*, so that the stipulated mass transfer can take place.

Different types of impellers, namely, turbine type, propeller type or paddle type are used in mixers. Some common types of impellers are shown in Figure 10.23. The ratio of the impeller diameter to the tank diameter usually lies within the range 0.25-0.33.

In the mixer, the two liquids form a mixture consisting of droplets of one liquid dispersed in a continuum of the other. The liquid flowing at lower rate is usually dispersed. In batch operation, the liquid in which the impeller is submerged when at rest is generally the continuous phase. For continuous operation, the vessel is first filled with the liquid intended to be continuous and, with agitation in progress; both the liquids are introduced in the desired ratio. The volume fraction of the dispersed phase hardly exceeds 0.6 to 0.7. Any attempt to increase this ratio generally results in inversion of dispersion, i.e. the continuous phase becomes dispersed (Quinn and Sigloch 1963, Yeh et al. 1964).

#### **• Flow Mixers**

Flow mixers are devices such as orifices or nozzles of very small volume placed in the pipe line through which the two liquids are pumped co-currently. A part of the pressure drop is utilized in dispersing the liquid, which then flows to a settler. Flow mixers are used only for continuous operations and have limited application because of their poor performance due to short duration of dispersion and short time of contact.

#### **• The Settler**

A settling tank shown in Figure 10.24 is a horizontal vessel having horizontal baffles. The length to diameter ratio is usually 4:1.

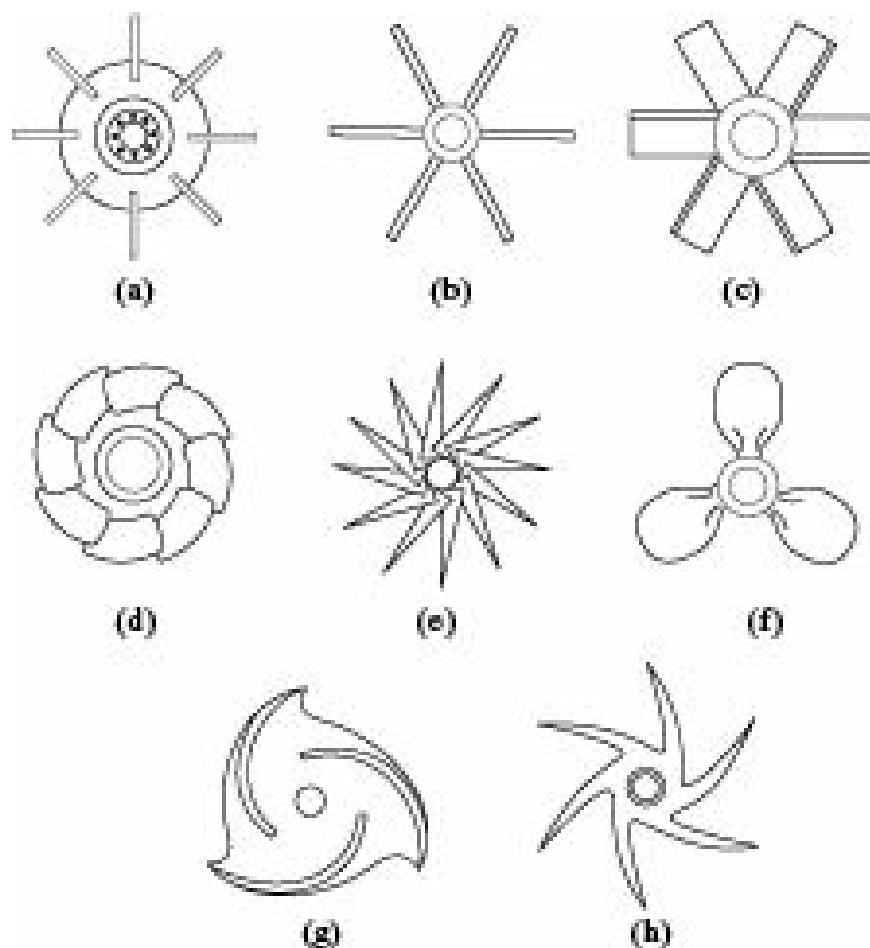


**Figure 10.23** Some impellers: (a) Flat-blade turbine, (b) Flat-blade paddle, (c) Pitch-blade turbine, (d) Semi-axial type impeller, (e) Centrifugal compressor impeller, (f) Maxine-type impeller, (g) 3-passage non-clogging cylindrical vanes type impeller, (h) Centrifugal turbine.

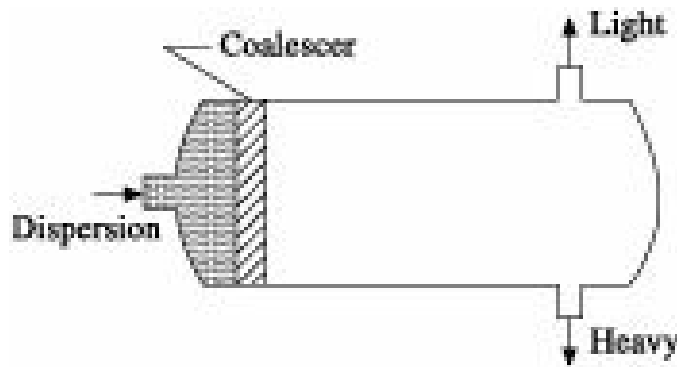


**Figure 10.24** Schematic diagram of a horizontal settler.

Settling aids are sometimes used to increase the separating efficiency and to reduce the holding time and the settler volume. Tower packing, wire-mesh packing or oblique plate nests are generally used as settling aids. The impinging drops stick to the settling aids and then coalesce to form bigger drops that help the dispersed phase to separate out of the dispersion. A higher interfacial tension between the liquids increases coalescence rate.

In the absence of reliable data, design methods for settler dimensions are still empirical and arbitrary. However, the following important factors should be kept in mind while designing settlers:

- (i) provision of sufficient residence time based on laboratory tests
- (ii) estimation of the rate of flow to produce a sufficient dispersion band thickness, and
- (iii) calculation of the time of settling of individual drops through clear liquid above and below the dispersion band.

In the absence of any reliable data, a preliminary estimate of settler diameter for a length-diameter ratio of 4, can be made from the following empirical relation (Treybal 1985):

$$DS = 8.4(q_c + q_d)^{0.5} \quad (10.44)$$

where,

$DS$  = settler diameter, m

$q_c$  and  $q_d$  = volumetric flow rates of the continuous and dispersed phases respectively,  $\text{m}^3/\text{s}$ .

The advantages of the mixer-settlers are:

- High stage efficiency
- Operational flexibility
- Ability to handle varying flow rates and phase ratios
- Can handle viscous liquids and liquids with suspended solids.

The disadvantages are

- High piping and pumping cost
- Requires larger space,
- Higher solvent cost as some solvent is retained in the settling tank

#### • Multistage Units

A number of mixer-settlers arranged in series constitute a *multistage extraction cascade*, each stage having at least one mixer and one settler. They may be operated as cross-flow extractors where the raffinate from a stage is treated with fresh solvent in the next stage and the combined extract is withdrawn. Alternatively, they may be operated as counter-current multistage extraction unit as shown in Figure 10.25.

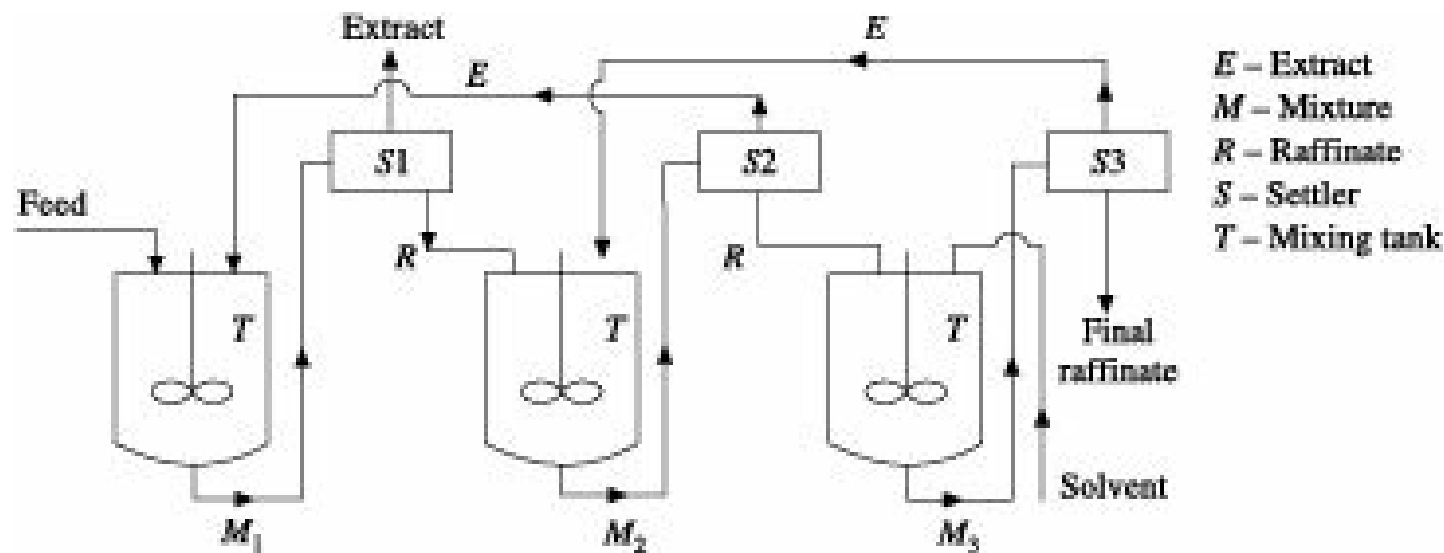


Figure 10.25 Mixer-settler extraction system.

The liquid is generally pumped from, one stage to another although gravity flow can also be arranged if sufficient head space is available. Many innovations have been made to reduce the interconnecting pipelines. In one such design, the mixing tanks are placed within large settling tanks. Heavy liquid flows by gravity, light liquid by air-lift and the separated light liquid is recycled by overflow.

### • Scheibel extractor

The *Scheibel extractor* (Scheibel 1966) shown in Figure 10.26, is an example of mechanically agitated extraction tower in which mechanical energy provided by turbine or other types of agitators mounted on a central shaft and operating in alternate chambers cause thorough mixing of the two liquids. The remaining chambers with knit wire mesh packing act as settlers where the two phases are separated by density difference. Thus, mixing and settling take place in alternate chambers while the two liquids move counter-currently. Scheibel extractors are the oldest column extractor with mechanical agitation.

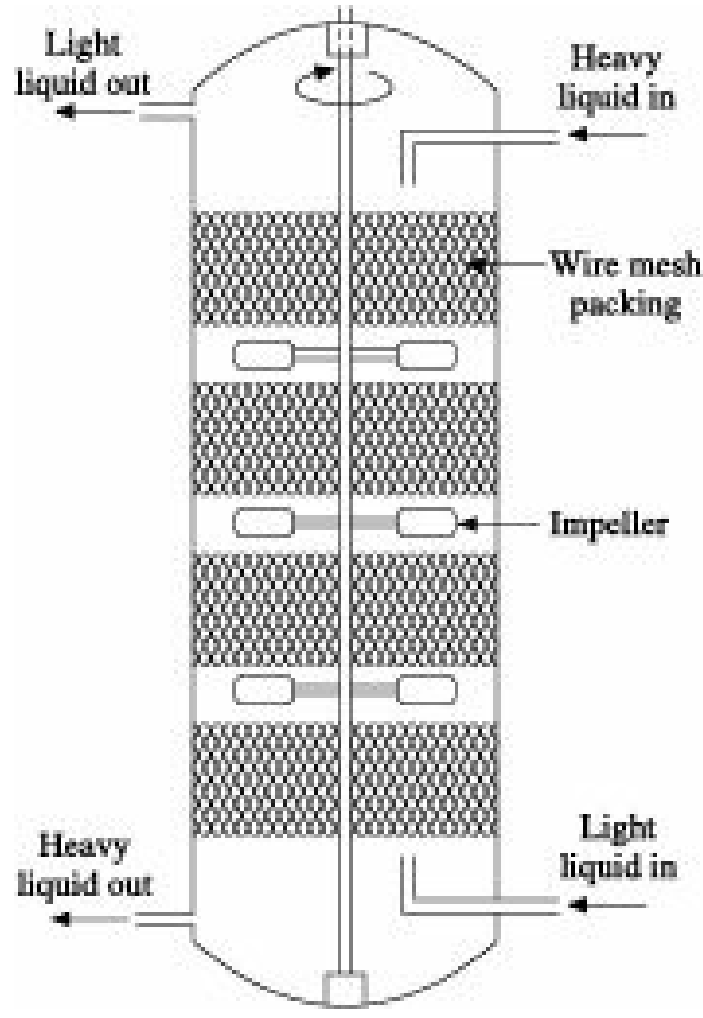


Figure 10.26 Scheibel extractor.

In recent designs, the wire mesh packings are done away with and the turbine impellers are surrounded by doughnut type baffles, supported on vertical tie-rods, which reduce the effect of axial mixing. Some more informations on the design parameters of the extractor are available in the literature (Bonnet and Jeffreys 1985). Two such units have been described below.

### • Oldshue-Rushton column

The *Oldshue-Rushton column*, shown in Figure 10.27, is a modification of the Scheibel extraction column in which the wire-mesh packings are not there. Annular partition discs are used as before but they have smaller inner diameter and are perforated. Vertical baffles are placed along the inner wall

of the column. Larger diameter columns are now in use.

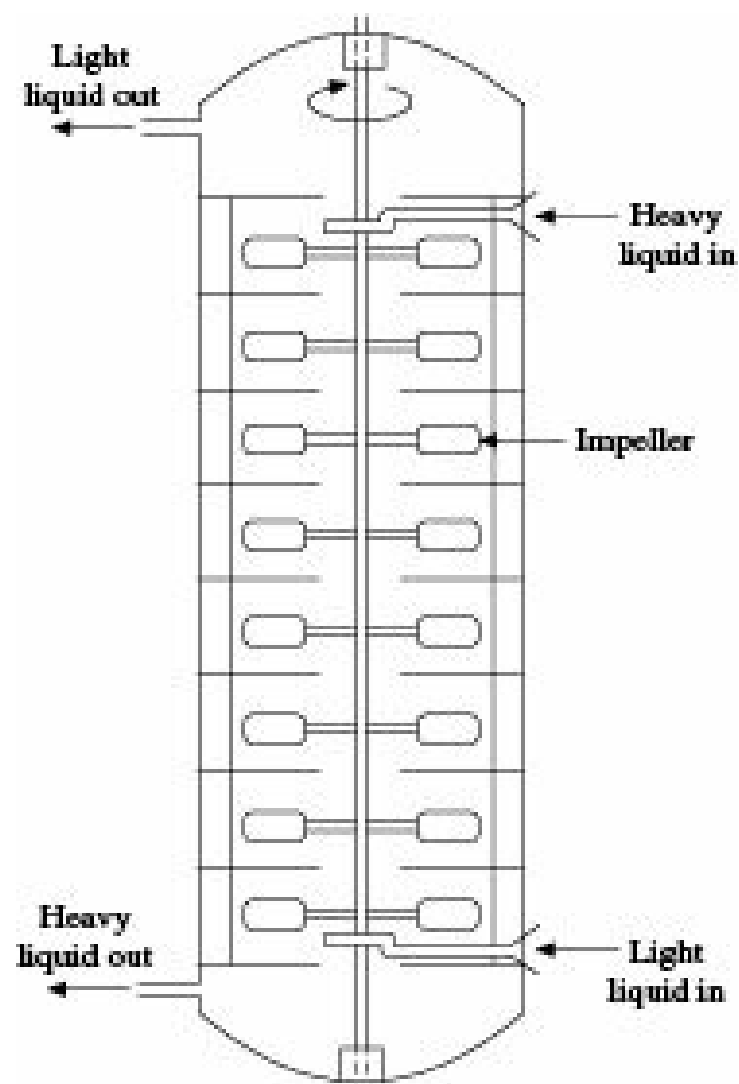


Figure 10.27 Oldshue–Rushton extractor.

#### • Kuhni extractor

The *Kuhni extractor* is another modification of the Scheibel extractor also without any packing. A baffled turbine impeller agitates the liquid in each compartment. Perforated plate stators separate the compartments. The column can provide up to ten theoretical stages per metre. A schematic diagram of the Kuhni extractor is shown in Figure 10.28.

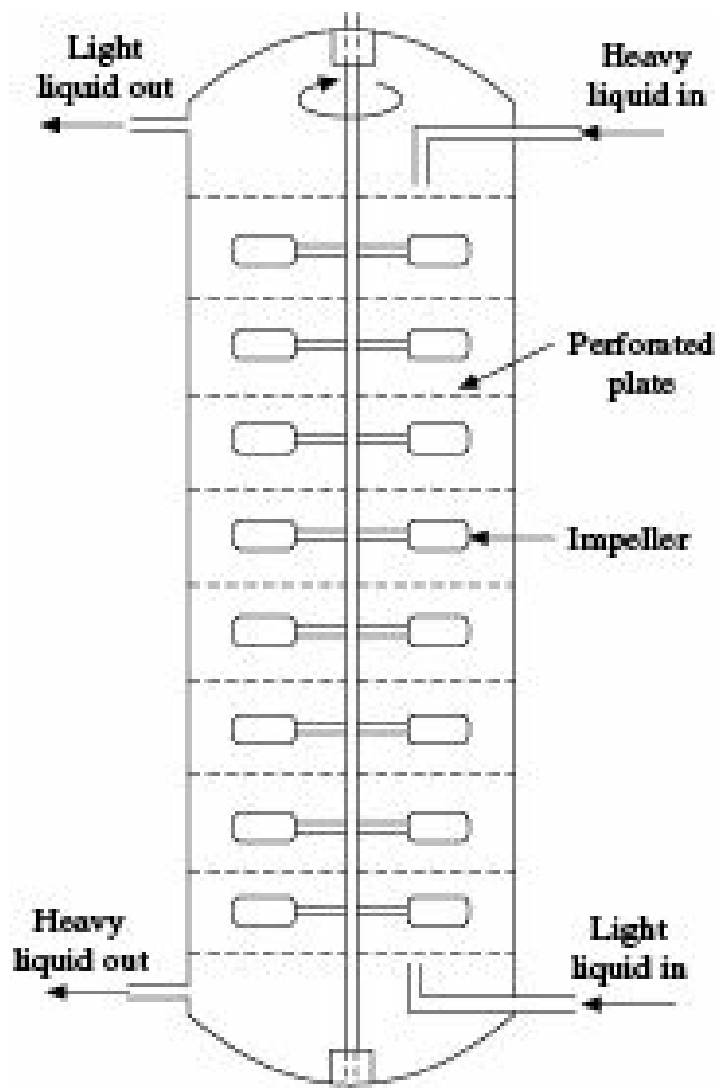


Figure 10.28 Kuhni extractor.

### Differential Contact

- **Rotating Disc Contactor (RDC)**

The *rotating disc contactor* is one of the best agitated column extractor and is widely used in chemical and allied industries. As shown in Figure 10.29(a), horizontal discs mounted on a central vertical shaft provide power required for mixing the two liquids. A set of annular discs having inner diameter slightly bigger than the rotating discs, is also mounted on the shaft. The column has considerable flexibility of operation and can handle liquids having suspended solids. However, this is not suitable for viscous liquids. Considerable back mixing occurs in the rotating disc contactor. The number of theoretical stages is also low; 0.5 to 1 theoretical stage can be achieved per metre height.

Figure 10.29(b) shows the configuration of an asymmetric Rotating (ARD) Disc contactor, slight modification of DC.

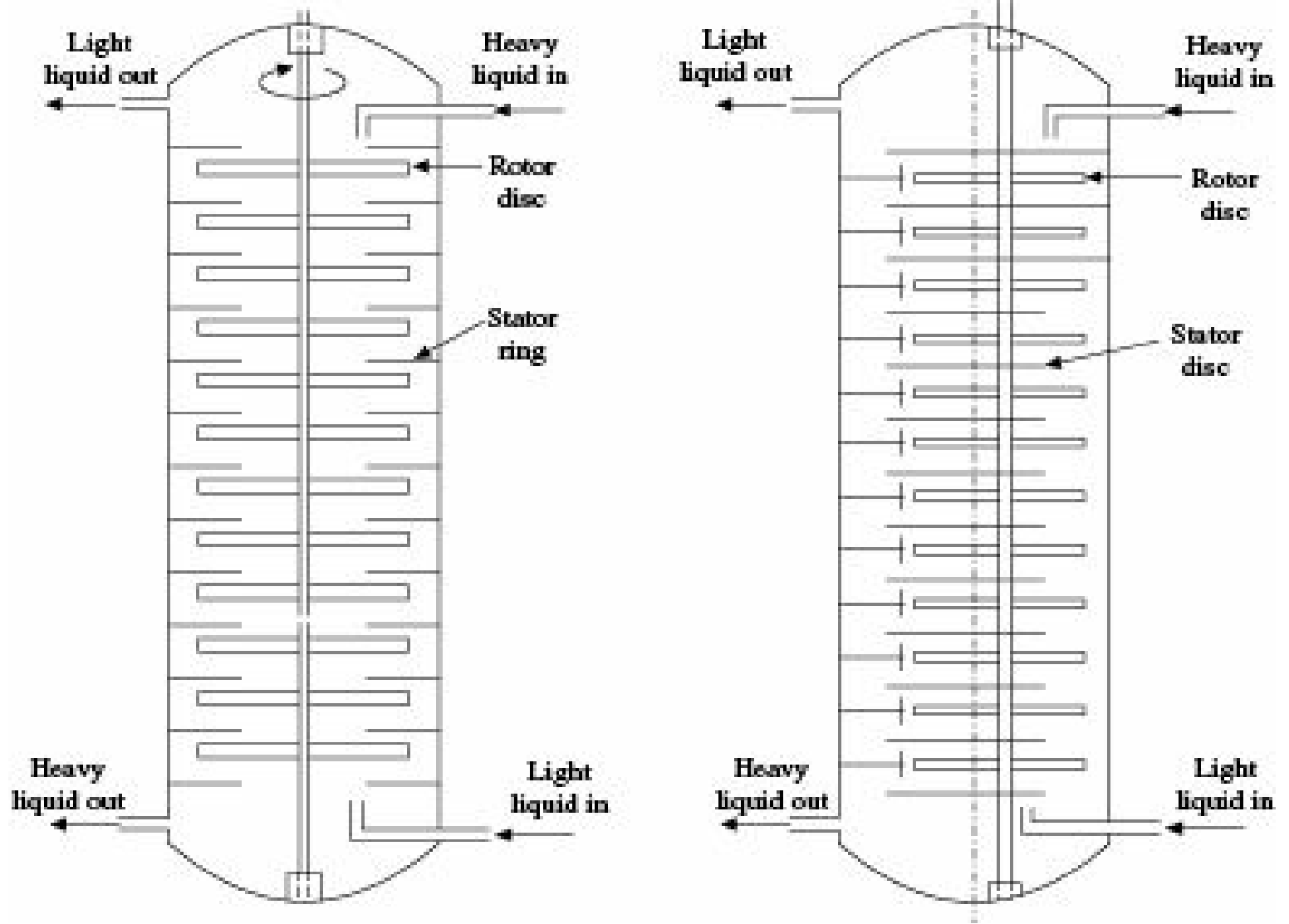


**Figure 10.29** (a) Rotating disc contractor, (b) Asymmetric rotating disc contactor.

The column consists of a vertical rotating shaft placed asymmetrically and the horizontal discs are mounted on it. Stators are also provided in the column. In the contactor, the mixing and transport zones are separated by a vertically placed baffle due to which the back mixing during the operation gets reduced. This extractor is being used for a pretty long time in process industries.

### 10.7.2 Phase Dispersion by Gravity

#### *Stage-wise contact*

- **Perforated Plate Tower**

The *perforated plate towers* accommodate a number of stages within a single piece of equipment. They usually operate with light liquid dispersed although heavy liquid may also be dispersed. A simple perforated plate tower is shown in Figure 10.30. The general arrangements are more or less similar to those in a sieve plate towers for gas-liquid operations except that weirs are dispensed with. As shown in figure, the light liquid, while rising through the perforations on a plate, is dispersed into fine droplets which then rise through a layer of heavy liquid on the plate and collect below the next upper plate as coalesced layer. The heavy liquid flows across each plate through the rising droplets of the light liquid and passes to the plate below through down comers. Almost all extraction takes place in the mixing zone above the perforations.

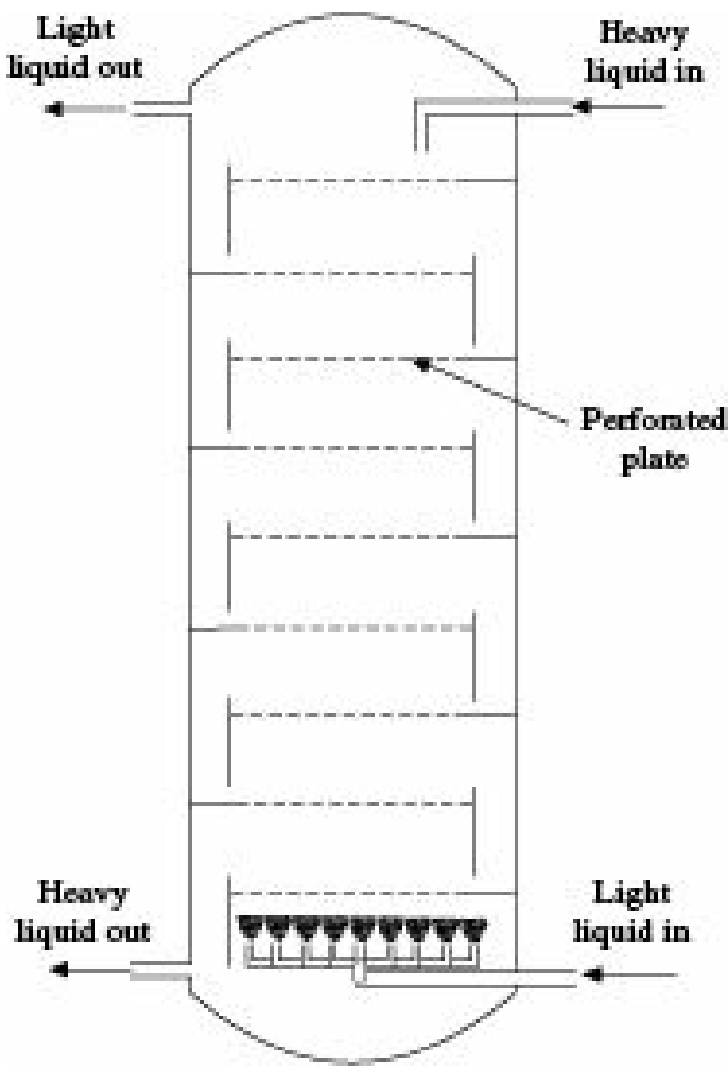


**Figure 10.30** Perforated plate/Sieve-tray extractor.

If heavy liquid is dispersed, it flows through the plates and is dispersed into droplets by the perforations on the plates. The light liquid which acts as the continuous phase, rises through the spouts.

Perforation diameter usually varies from 1.5 to 4.5 mm drilled at distances of 12 to 20 mm. Plate spacing is in the range of 150 to 600 mm. Perforated plate towers are very effective in terms of liquid handling capacity and efficiency.

### **Differential contact**

- **Spray Tower**

The *spray towers* are the simplest type of continuous-contact equipment. A spray tower consists of an empty tower with provisions of introducing and removing the two liquids at the two ends. These are inexpensive, have high flow capacities and are easy to clean. But their performance is poor because of high axial mixing. Horizontal baffles have been used to reduce the effect of axial mixing, but the results are not encouraging. Spray towers may operate with any of the light or heavy liquid dispersed. In case of light liquid dispersed, as shown in Figure 10.31, the tower is filled with the heavy liquid and then the light liquid is sprayed through the nozzles near the bottom, which rises through the heavy liquid as fine droplets and coalesce at the top. In case of heavy liquid dispersed, the tower is first filled with the light liquid and then the heavy liquid is sprayed from the top, which drops through the light liquid and then coalesces at the bottom.

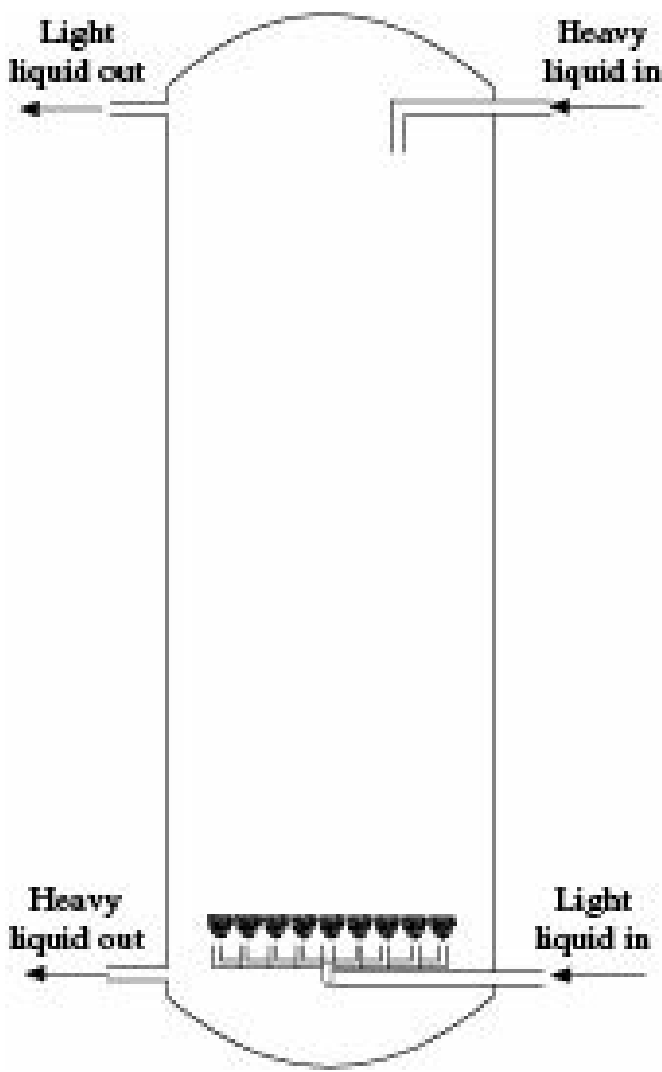


**Figure 10.31 Spray tower extractor.**

### • Packed Tower

The *packed towers* for liquid-liquid operations are similar to those used in gas-liquid operations. The packings reduce axial mixing and help dispersion of the desired phase thereby increasing the mass transfer efficiency.

A packed tower, arranged for light liquid dispersion is first filled with the heavy liquid, which largely occupies the void spaces between the packings. The remaining void space is then filled with droplets of the dispersed light liquid, which rise through the heavy liquid phase and coalesce into a continuous phase at the top. In order to maintain the interface between the two liquids above the heavy liquid inlet, the pressure in the tower at the bottom must be balanced by a corresponding pressure in the bottom outlet pipe by a set of control valves. The dispersed phase should not preferentially wet the packings since then the interface will be smaller. Packing size should not be larger than one-eighth of the tower diameter. Mass transfer rates in packed towers are poor. However, this type of equipment is being used in process industries to a good extent. For example, such column operating under counter-current fashion may be used for removal of aromatics particularly naphthenes from the naphtha crude before it is fed to the naphtha cracker. The objective of reducing naphthene load in the extract recycle column (ERC) may be achieved, and production of pure BTX from off-spec naphtha may be a viable option..

### 10.7.3 Phase Dispersion by Pulsation

In *pulsed columns*, both mixing and separation of phases are achieved by mechanical pulsations from

outside.

### Stage-wise contact

- **Perforated Plate Pulsed Column**

In these columns, the perforated plates without downspouts are so drilled (about 1 mm) that liquids will not ordinarily flow through them. The pulsations generated by a reciprocating device alternately forces light and heavy liquids through the perforations. Pulse amplitude varies from 5 to 25 mm and the frequency lies between 30 to 200 per minute. Pulsations may similarly be introduced in towers filled with ordinary packings. The pulsations largely improve dispersion and contact. A perforated plate pulsed column is shown in Figure 10.32.

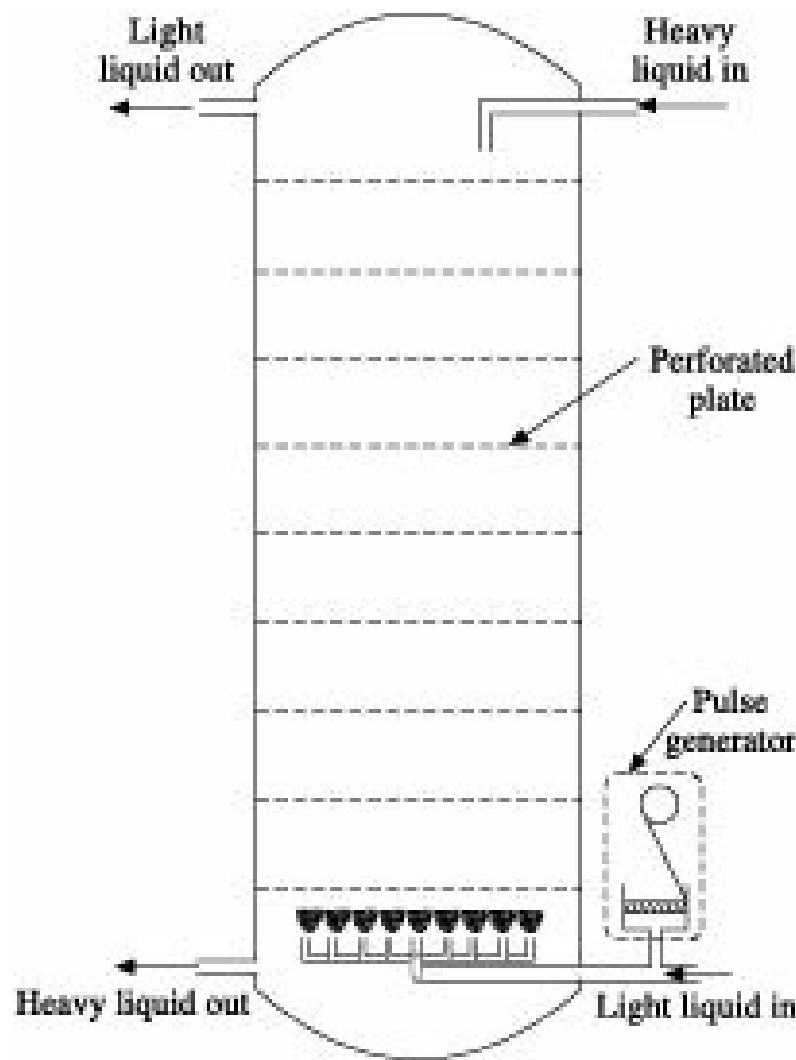


Figure 10.32 Pulsed extraction column.

Pulsed columns are very effective in small sizes and because of the absence of any moving parts within the column, are widely used in processing radioactive solutions.

### Differential contact

- Differential contact pulsed column is the packed tower as described in Section 10.7.2, provided with pulsations by mechanical means in either of the phases.

#### 10.7.4 Phase Dispersion by Reciprocating Action

The reciprocating plate extraction column with pulsating internals developed by Karr (Prochazka et al 1970, 1971) and commercialized under the trademark of vibrating-plate extractor (VPE), is shown in

Figure 10.33.

There are two modifications of VPE: (i) the column with uniform motion of plates, and (ii) column with counter-motion of plates. In Figure 10.33, the shell of the column is provided with settling sections at each end. According to the choice of the phase being dispersed, either section may be equipped with an interface control.

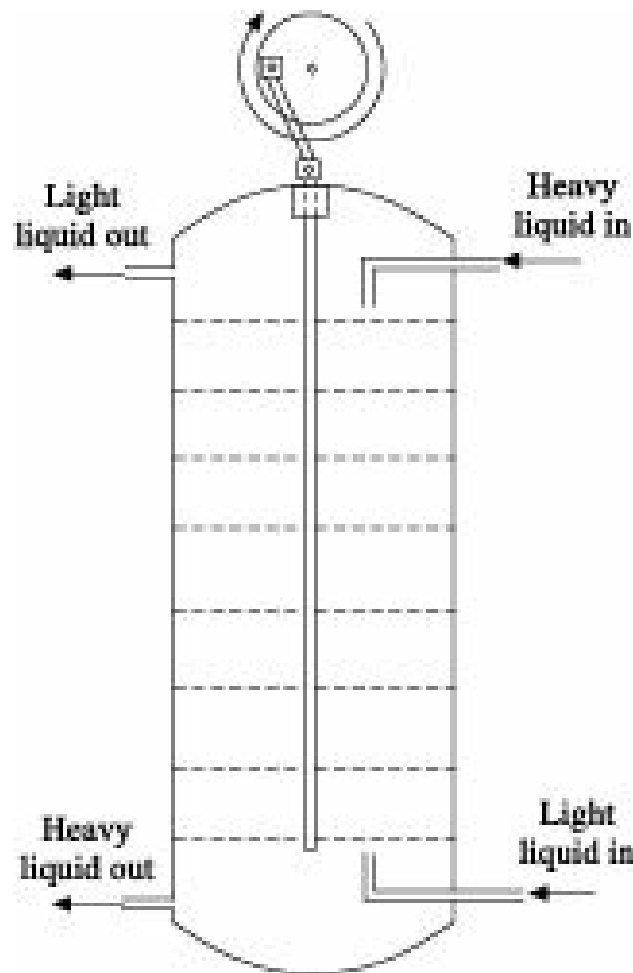


Figure 10.33 Vibrating plate/Reciprocating plate extractor.

A stack of perforated plates is located in the shell, fastened to a rod connected to an eccentric that imparts to the whole stack a vertical harmonic motion; the amplitude and frequency of which are the important controlling variables. The plates are provided with a number of small circular holes for the dispersed phase and with one or more large openings for the continuous phase. These openings may either be circular or of various forms suitable from the point of view of plate design. In columns of smaller diameter, the passages for continuous phase of neighbouring plates are placed on opposite sides of the column axis, so that a cross-flow of phases between the plates can occur. On large plates, the distribution of passages is such that several parallel sections with a cross-flow of phases are created. This type of reciprocating plate displays several adorable properties. The separation of passages for continuous and dispersed phase ensures high throughputs of dispersed phase even in case of high flow rate of the continuous phase. It also permits the maintenance of a stable mixer-settler regime over a wide range of amplitude and frequency. In this regime a pattern with one dispersed phase can be ensured during the entire period of reciprocating motion because the passages for the continuous phase suppress the dispersion of continuous phase into the layer of dispersed phase on the plate. In the small perforations the drops are formed or reshaped by a mechanism similar to that of periodic outflow from a nozzle. Splitting of the coalescence if formed, under the conditions does not

require high velocity. Naturally the VPE operates at relatively low amplitudes and frequencies. This implies low mechanical stress and energy consumption.

### 10.7.5 Phase Dispersion by Centrifugal Force

In *centrifugal extractors*, dispersion and separation of phases are appreciably accelerated by centrifugal force. In the Podbielniak extractor shown in Figure 10.34, a perforated spiral ribbon inside a heavy metal casing is wound about a hollow horizontal shaft through which the two liquids enter and leave. The light liquid is pumped to the outside of the spiral at a pressure of  $3-12 \text{ } \# 10^5 \text{ N/m}^2$  to overcome the centrifugal force generated by the shaft moving at 1800 to 5000 revolutions per minute. The heavy liquid is pumped at the centre. The two liquids flow counter-currently, heavy liquid outward and light liquid inward.

Such extractors are also available with co-current flow of light and heavy liquids.

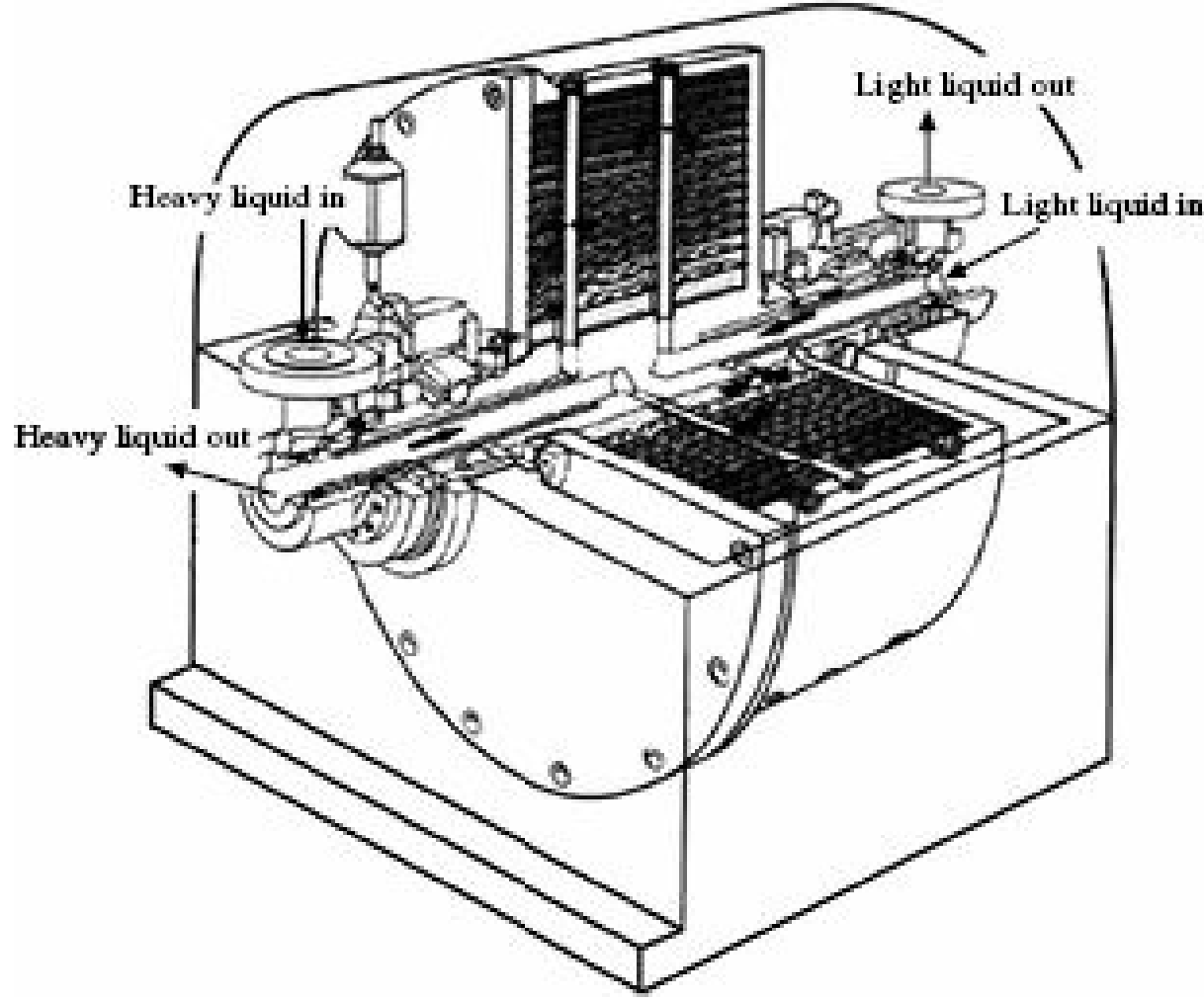


Figure 10.34 Podbielniak extractor.

These extractors provide large number of theoretical stages within a limited space and are particularly useful for liquids having very close densities and requiring short residence time. They are particularly useful in extraction of vitamins and antibiotics.

## 10.8 Estimation of Some Important Parameters in Agitated Liquid Dispersions

Although large number of bench scale and pilot plant studies have been made on the characteristics of agitated liquid dispersions, the results are hardly applicable beyond the systems and range of variables studied and it has not been possible to develop generalized correlations for the design of

commercial extractors. The following correlations can however be used for mixer type extractors using flat-blade turbine type impellers.

**Drop Size:** As a result of frequent breakage and coalescence of drops, an agitated liquid-liquid dispersion contains a wide range of drop size distribution (Godfrey and Slater 1994). Several mean values of drop size have been defined of which the volume to surface diameter  $d_{32}$  called the *Sauter-mean diameter*, is widely used

$$d_{32} = \frac{\sum_{i=1}^k d_i^3}{\sum_{i=1}^k d_i^2} \quad (10.45)$$

Lewis et al. (1951) showed that the Sauter-mean drop diameter attained in a packed tower can be well represented by the following expression:

$$d_{32} = 0.92 \left( \frac{\sigma}{\Delta \rho g} \right)^{0.50} \left( \frac{u_t \epsilon \varphi}{V_d} \right) \quad (10.46)$$

Since the drop size in the Karr column are not uniform, the Sauter-mean diameter is used as the single measure of drop diameter by the expression (Godfrey and Slater 1994):

$$d_{32} = 0.36 v^{0.6} t_d^{-0.2} P_m^{-0.4} \quad (10.47)$$

when  $P_m$ , the mechanical power dissipation per unit volume of the mixed phases, can be calculated using the expression

$$P_m = \frac{16 N^2 \rho_d}{3H} \frac{1 - \epsilon^2}{\epsilon^2 C_0^2} (\Omega f)^3$$

where,  $C_0 = 0.6$ .

This equation is valid for high agitation levels and when there is no mass transfer.

In spray columns using multinozzle distributors, the following correlation can be used for prediction of Sauter-mean drop diameter:

$$\frac{d_{32}}{D_N} = Eö^{-0.35} \left[ 0.80 + \exp \left( -2.73 \times 10^{-2} \frac{We_N}{Eö} \right) \right] \quad (10.48)$$

where,

$Eö$  = nozzle Eötvös number ( $= D_N^2 D_{tg}/v$ )

$D_N$  = nozzle diameter, m

$We_N$  = nozzle Weber number ( $= t_d D_N V_N^2/v$ )

$V_N$  = nozzle velocity, m/s

The Sauter-mean diameter data from the nonmass transfer and the mass transfer experiments in a Scheibel extractor were correlated by regression (Bonnet 1982). The results obtained from the

nonmass transfer runs confirmed that drop size is independent of compartment number. This may be due to the fact that coalescence and redispersion conditions exist in each stage. The preferred correlation is

$$d_{32} = 5.719 \# 10^{-5} \square 10^{(1 + 1.397 \{ \}) P_m - 0.708} \quad (10.49)$$

Hold-up was found to be a significant variable.

For the drop diameter data resulting from experiments, the best correlations are:

(i) Mass transfer direction; dispersed to continuous phase

$$d_{32} = 1.240 \# 10^{-4} \square 10^{(1 + 3.417 \{ \}) P_m - 0.277} \quad (10.50)$$

(ii) Mass transfer direction; continuous to dispersed phase

$$d_{32} = (1.763 \# 16.117 \{ \}) (We)^{-0.907} \quad (10.51)$$

$$\frac{17.6 N_l^3 D_l^5 \rho_c}{\pi D_e^2 H_M \rho_d}$$

where  $P_m$ , average energy dispersion per unit mass =

$$\frac{N_l^2 D_l^3 \rho_c}{\sigma}$$

the vessel Weber number (We) =

$$d_{32} = C \left( \frac{\sigma}{\Delta \rho g} \right)^{0.5} \quad (10.52)$$

where, the constant  $C$  is a function of the column geometry and mass transfer and may also depend on the liquid-liquid system. Chang-Kakoti et al. (1985) found  $C = 1.3$  for butanol (dispersed)-water (continuous) system in a Rotating disc column, Logsdail and Slater (1983) suggested a value of 0.92 for pulsed perforated plate column.

### **Minimum impeller speed**

Depending upon the properties of the two liquids and the fractional hold-up of the dispersed phase, a minimum impeller speed  $N_{im}$  has to be maintained to have a stable dispersion. The following correlation (Skelland and Ramsey 1987) may be used for estimating the minimum impeller speed:

$$(Fr_m)_{min} = 1.03 \left( \frac{D_t}{D_l} \right)^{2.76} (\{ )^{0.106} (Ga \square Bo)^{-0.084} \quad (10.53)$$

where,

$$\text{Froude number of the mixture } (Fr_m) = \frac{D_t N_l \rho_m}{g \Delta \rho},$$

$D_t$  = tube diameter, m

$D_i$  = impeller diameter, m

$$\text{Galileo number (Ga)} = \frac{\frac{D_i^3 \rho_m g \Delta \rho}{\mu_m^2}}{\mu_m^2}$$

$$\text{Bodenstein number (Bo)} = \frac{\frac{D_i^3 g \Delta \rho}{\mu_m^2}}{\mu_m^2}$$

The density and viscosity of the two-phase dispersion is given by Godfrey and Slater (1994):

$$t_m = \{ + (1 - \{) t_c, \text{ and } n_m = \left( \frac{1 + 1.5 \mu_d \varphi}{\mu_c + \mu_d} \right) \quad (10.54)$$

### **Impeller power requirement**

The power required by the impeller under a given set of conditions can be expressed in terms of the dimensionless group known as Power number (Po) as a function of impeller Reynold's number ( $Re_i$ ).

If the Reynold's number of a turbine type impeller in a baffled vessel is above 10,000, the Power number asymptotically approaches a value of 5.7 (Godfrey and Slater 1994).

Thus if  $Re_i > 10,000$

$$Po = \frac{P}{N_i^3 D_i^5 \rho_m} = 5.7 \quad (10.55)$$

where  $P$  is power input to the impeller in kW.

The power input can be calculated from Eq. (10.55).

### **Mass transfer coefficient**

Assuming the drops to be rigid, (a drop can be considered rigid if its diameter is less than 3 mm and the interfacial tension is more than 15 dyne/cm) the dispersed phase mass transfer coefficient can be approximately calculated from the following relation (Treybal 1963):

$$(Sh_d) = \frac{k_d d_{32}}{D_d} = 6.6 \quad (10.56)$$

where,

$Sh_d$  = dispersed phase Sherwood number and

$D_d$  = diffusivity of the solute in the dispersed phase

If the distribution of solute in the two phases is linear, the overall mass transfer coefficient is given by

$$\frac{1}{K_{od}} = \frac{1}{k_d} + \frac{m'}{k_c} \quad (10.57)$$

where,

$K_{od}$  = overall mass transfer coefficient based on dispersed phase concentration difference

$k_c$  and  $k_d$  = mass transfer coefficients of the continuous and dispersed phases, respectively

$m'$  = solute partition coefficient

## 10.9 Reactive Extraction

Reactive extraction is another reactive separation process mentioned in Chapter 7. This process can primarily be applied in multireaction systems for improvement in yields and selectivities to the desired products. Various aspects of reactive extraction, i.e. the combination of reaction with liquid-liquid extraction have been described elsewhere (Bart 2001) along with its several applications. Bora et al. (2008) have explored the reactive extraction in liquid membrane separation and purification of antibiotics. Such hybrid separations are gaining importance day by day. Such process can also be used for the separation of waste byproducts that are difficult to separate using conventional methods. Reactive extraction makes use of specific chemical reactions in order to promote or achieve a separation task, mostly using commercially available liquid ion exchangers. Methyl trioctyl ammonium chloride is the commonly used ionic liquid. The characteristic of reactive solvent system is that the organic phase consists of a mixture of liquid ion exchangers and a diluent. The transfer of solute from one phase to another is enhanced by using reactive compounds dissolved in the solvent phase (Rani 2008).

Reactive extraction process has found wide spread applications in bioprocesses like enzymatic hydrolysis of the potassium salt of Penicillin-G into phenyl acetic acid and potassium salt of 6-amino penicillanic acid (6-APA). During the process, the pH of the reaction mixture falls due to the accumulation of phenyl acetic acid thus lowering the stability of the enzyme used. The phenyl acetic acid is extracted by a long chain tertiary amine which is the dispersed phase as liquid ion exchanger. Simulation, modelling and experimental validation of reactive extraction in a fat splitting process have been done using a commercial simulation software (Pradhan 2007). Steensma et al. (2007) carried out similar work during reactive extraction for chiral separation of amines, amino acids and amino alcohols. It is established that reactive extraction columns can be very efficient equipment for continuous reaction and liquid-liquid separations.

### Nomenclature

*A* : initial solvent, M, M/q

*B* : pure solvent, M, M/q

*Bo* : Bodenstein number, -

*C* : distributed solute, M, M/q

*d<sub>32</sub>* : Sauter mean drop diameter, L

*D<sub>c</sub>* : column diameter, L

*D<sub>i</sub>* : impeller diameter, L

*D<sub>S</sub>* : settler diameter, L

*D<sub>t</sub>* : tube diameter, L

*D<sub>N</sub>* : nozzle diameter, L

*E* : extract phase, M, M/q

*E'* : solvent free extract phase, M, M/q

*E<sub>ME</sub>* : Murphree plate efficiency, dimensionless

*E<sub>ö</sub>* : Nozzle Eötvös number, dimensionless

*f* : frequency

*Fr<sub>m</sub>* : Froude number of the mixture, -

*g* : acceleration due to gravity, L/q<sup>2</sup>

*Ga* : Galileo number, -

*H* : plate spacing, L

*H<sub>M</sub>* : height of a mixing compartment in a Scheibel stage, L

*H<sub>tOE</sub>* : overall height of a transfer unit based on extract phase, L

*H<sub>tOR</sub>* : overall height of a transfer unit based on raffinate phase, L

HETS : height equivalent to a theoretical stage, L

*k* : individual mass transfer coefficient, L/q

*K<sub>Ea</sub>, K<sub>Ra</sub>* : overall mass transfer coefficient based on overall driving force in terms of extract and raffinate phases, respectively,

*m* : slope of equilibrium line, y\*/x

*N* : number of theoretical stages, -

*N<sub>i</sub>* : impeller speed, rpm

*N<sub>tOE</sub>* : number of transfer units based on extract phase, -

*N<sub>tOR</sub>* : number of transfer units based on raffinate phase, -

*P* : power input, kW

*Po* : Power number, -

*P<sub>m</sub>* : specific power dissipation

*q* : volumetric flow rate of phases, L<sup>3</sup>/q

*R* : raffinate phase, M, M/q

*Re<sub>i</sub>* : impeller Reynold's number, -

*R'* : solvent-free raffinate phase, M, M/q

*S* : contaminated solvent, M, M/q

*u<sub>t</sub>* : terminal velocity of a falling drop, L/q

*V* : volumetric flow rate per unit area, L/q

*V<sub>N</sub>* : nozzle velocity, L/q

We : vessel Weber number, dimensionless

We<sub>N</sub> : nozzle Weber numer, dimensionless

*x* : mass fraction solute in raffinate, —

*x'* : mass of solute per unit mass of solute-free raffinate, *x*/(1 - *x*)

*X* : mass fraction solute in raffinate on S-free basis, —

*y* : mass fraction solute in extract, —

*y'* : mass of solute per unit mass of solute-free extract, *y*/(1 - *y*)

*Y* : mass fraction solute in extract on S-free basis, —

*Z* : height of a tower, L

## *Greek Letters*

b : selectivity

{ : fractional hold-up of dispersed phase, -

t : density, M/L<sup>3</sup>

Dt : density difference between the phases, M/L<sup>3</sup>

v : interfacial tension, M/q<sup>2</sup>

i : time

f : voidage of packing, -

$\Omega$  : amplitude

n : viscosity, M/Lq

## *Subscripts*

c : continuous phase

d : dispersed phase

E : extract

F : feed

i : 1, 2, 3, . . .

m : mixture

n : stage

R : raffinate

S : settler

1, 2, . . . : stage number

## **Numerical Problems**

**10.1 Extent of Solute Extraction, and Concentration of Solute in Extract and Raffinate Phases for Stage-wise Extraction with Immiscible Solvent:** An acetaldehyde-toluene solution containing 6% acetaldehyde by weight is being treated with water in a three-stage cross-current extraction battery to remove acetaldehyde. Water and toluene are completely immiscible and the equilibrium distribution of acetaldehyde between them is given by the relation:

$$Y^* = 2.2X$$

where,  $Y^*$  = kg acetaldehyde per kg water and  $X$  = kg acetaldehyde per kg toluene.

- (i) If 60 kg water is used in each stage per 100 kg feed, calculate the percentage of acetaldehyde extracted and the final concentrations of the extract and raffinate phases.
- (ii) What will be the percentage of acetaldehyde extracted and the concentrations of the extract and raffinate phases if 100 kg feed is extracted once with 180 kg water?

[Ans: (i) Percent extraction: 95.85%, Final concentrations of acetaldehyde: 3.175% in extract and 0.30% in raffinate (ii) Percent extraction: 88.98%, Concentrations of acetaldehyde: 2.96% in extract and 0.71% in raffinate]

**10.2 Estimation of Required Flow Rate of the Organic Phase in the Extraction Unit:** Streptomycin is extracted from the fermentation broth using an organic solvent in a counter-current staged

extraction unit. The distribution coefficient ( $K_D$ ) of streptomycin at pH = 4 is  $K_D = (Y_i/X_i) = 40$ , and the flow rate of aqueous phase ( $H$ ) is 150 L/min. If only five extraction units are available to reduce the streptomycin concentration from 10 g/L in the aqueous phase to 0.2 g/L, determine the required flow rate of the organic phase ( $L$ ) in the extraction unit.

*Given:* The extraction factor,  $E (= K_DL/H)$  equals to 2.0 for a degree of extraction ( $X_n/X_0$ ) of 0.2 using 5 stages in counter-current extraction.

[Ans: 7.5 L/min]

**10.3 Estimation of Mass Fraction of Penicillin in Raffinate and Extract Phases:** A fermentation broth containing 2.5 g/L penicillin is passed through an extractor. The feed flow rate is 7 m<sup>3</sup>/day and Butyl acetate at pH 2.8 is used as solvent for extraction of penicillin from the broth. The partition coefficient of penicillin between the extract and raffinate phases at pH 2.8 is 38. Density of aqueous phase, i.e. broth is 997 kg/m<sup>3</sup> and that of butyl acetate is 882 kg/m<sup>3</sup>. Considering 95% extraction of penicillin and the flow rate of solvent 1.5 times the minimum, find the mass fraction of penicillin in the raffinate and extract phases. [Ans: 1.25 # 10<sup>-4</sup>, 0.077]

**10.4 Estimation of Water Content and Chlorobenzene Content in Aqueous Layer, Composition of Chlorobenzene Layer, and the Amount of Acetone Causing the Aqueous Layer to Stop Stratifying:** Determine (i) the content of water and chlorobenzene in an aqueous layer with an acetone concentration of 45 mass%, (ii) the composition of a chlorobenzene layer in equilibrium with it, and (iii) the amount of acetone whose addition will cause a mixture of 0.11 kg of chlorobenzene and 0.09 kg of water to stop stratifying.

The equilibrium compositions of coexisting phases (in mass%) are follows as

Aqueous phase			Chlorobenzene phase		
water	acetone	chlorobenzene	water	acetone	chlorobenzene
99.89	0	0.11	0.18	0	99.82
89.79	10	0.21	0.49	10.79	88.72
79.69	20	0.31	0.79	22.23	76.98
69.42	30	0.58	1.72	37.48	60.80
58.64	40	1.36	3.05	49.44	47.51
46.28	50	3.72	7.24	59.19	33.57
27.41	60	12.59	22.85	61.07	15.08
25.66	60.58	13.76	25.66	60.58	13.76

[Ans: (i) Water: 52.8% (mass), chlorobenzene: 2.2% (mass) (ii) Acetone: 54.9%, water: 4.3% and chlorobenzene: 40.8% (all by mass) (iii) 0.325 kg]

**10.5 Computation of the Amount of Solvent Required per 100 kg of Feed in Single Stage, Yield and Composition of the Extract Phase:** Acetone is extracted with chlorobenzene from a 50% aqueous solution. The raffinate should contain not over 2 mass% of acetone. Using the diagram constructed in Problem 10.4, determine the amount of solvent needed for processing 100 kg of the feed if extraction (cross-current) is conducted in one stage. Also, determine the yield of the raffinate, and the yield and composition of the extract-product.

[Ans: Amount of solvent: 1630 kg Yield of raffinate: 48 kg Yield of extract -product: 52 kg, Composition of extract-product: Acetone = 95.5% (mass) and water = 4.5% (mass)]

**10.6 Determination of the Amount of Solvent, Yield and Composition of Product, and Number of Extraction Stages:** Determine (i) the required amount of solvent, (ii) the compositions and yields

of the products, and (iii) the number of extraction (cross-current) stages for the conditions of the preceding problem if fresh solvent in an amount equal to the mass of the mixture being processed is used for extraction in each stage.

[Ans: (i) 270.8 kg (ii) 96% of acetone (mass), 51 kg yield (iii) 4]

**10.7 Estimation of Yield and Composition of Products, and the Number of Stages in Counter-Current Extraction:** Determine the composition and yield of products, and also the number of theoretical extraction stages for the conditions stated in Problem 10.5 if counter-current extraction is used with a flow ratio of 1:1.

[Ans: 97.5 mass % of acetone and 2.5 mass % of water, 50.5 kg yield and 4 stages]

*Make a comparison of the results obtained in Problems 10.5-10.7.*

**[Results:** Counter-current extraction is advantageous for the given case due to lowest consumption of solvent, higher purity of extract, etc.]

**10.8 Estimation of Solvent Requirement and Number of Ideal Stages for An Extraction Operation with Immiscible Solvent:** 1000 kg/hr of an aqueous solution of uranyl nitrate containing 5% uranyl nitrate is to be extracted counter-currently using tributyl phosphate as solvent to recover 90% uranyl nitrate. Water and tributyl phosphate are immiscible.

(i) Estimate the minimum solvent rate

(ii) Determine the number of ideal stages required if the solvent rate is twice the minimum

*Equilibrium Data:*

kg uranyl nitrate/kg water:	0.01	0.03	0.06
kg uranyl nitrate/kg tributyl phosphate:	0.055	0.165	0.33

[Ans: (i) 186.1 kg/hr (ii) 2.9]

**10.9 Calculation of Minimum Solvent Rate and the Number of Theoretical Stages:** Hexadecane containing 35% 1,3,5-trimethylbenzene is being passed through a Schiebel extractor. The feed flow rate is 2283 kg/hr and N-methyl-2-pyrrolidone (NMP) is used as solvent in the operation. It is proposed to bring down the aromatics content to less than 5%. Calculate (i) the minimum solvent rate, and (ii) the number of theoretical stages required if the operation is carried out with solvent rate 1.5 times the minimum.

Equilibrium data for Hexadecane–1,3,5-trimethylbenzene–NMP are as follows:

Hexadecane rich phase			NMP rich phase		
Hexadecane	1,3,5-trimethyl- benzene	NMP	Hexadecane	1,3,5-trimethyl- benzene	NMP
0.8769	0	0.1231	0.008	0	0.992
0.8005	0.0482	0.1513	0.0112	0.0167	0.9721
0.6915	0.1094	0.1991	0.0137	0.0497	0.9366
0.5518	0.2262	0.2220	0.016	0.0925	0.8915
0.4557	0.2831	0.2612	0.0191	0.1281	0.8528
0.3437	0.3296	0.3267	0.0203	0.1553	0.8244
0.305	0.3401	0.3549	0.0256	0.1801	0.7943
0.275	0.3502	0.3748	0.033	0.2102	0.7568

[Ans: (i) 4566 kg/hr (ii) 4 stages]

**10.10 Determination of Minimum Solvent Rate for a Counter-Current Extraction Operation with Immiscible Solvent and also the Number of Ideal Stages for a Specified Solvent Rate:** 500 kg/hr of an aqueous solution of dioxane containing 30% dioxane is to be continuously and counter-currently extracted with benzene at 25 °C to remove 80% dioxane. Determine the

minimum solvent requirement and the number of theoretical stages if the solvent rate is 1.5 times the minimum. Water and benzene are essentially immiscible.

At 25 °C, the equilibrium distribution of dioxane between water and benzene are as follows:

wt.% dioxane in water:	5.1	18.9	25.2
wt.% dioxane in benzene:	5.2	22.5	32.0

[Ans: 239.9 kg/hr; 3 stages]

**10.11** Estimation of the Number of Stages Required for Extraction of Dioxane Using Benzene Containing Dioxane, as Solvent: Using the equilibrium data of dioxane between benzene and water as given in Problem 10.10, find (i) the minimum amount of solvent needed per 100 kg of the feed, and (ii) the required number of theoretical stages assuming that the amount of solvent used is 1.5 times higher than the minimum for the following conditions: feed is an aqueous solution containing 25% dioxane, benzene used as solvent contains 0.5% dioxane, and the raffinate product contains 2% dioxane. Neglect the miscibility of water and benzene.

[Ans: (i) 99 kg (ii) 8 stages]

**10.12** Estimation of Solvent Rate and the Number of Theoretical Stages Required for Extraction of Acetic Acid using Diethylether as Solvent: Acetic acid is extracted from its 20% (mass) aqueous solution in a counter-current extractor with diethylether as solvent. Determine the (i) amount of solvent needed for 1000 kg/hr of the feed and (ii) number of theoretical extraction stages if the extract-product is to contain 60% (mass) and the raffinate-product not more than 2% (mass) of the acid. The following equilibrium data may be used:

Water	Water layer			Ether layer		
	Acetic acid	Diethylether	Water	Acetic acid	Diethylether	
93.3	0	6.7	2.3	0	97.7	
88.0	5.1	6.9	3.6	3.8	92.6	
84.0	8.8	7.2	5.0	7.3	87.7	
78.2	13.8	8.0	7.2	12.5	80.3	
72.1	18.4	9.5	10.4	18.1	71.5	
65.0	23.1	11.9	15.1	23.6	61.3	
55.7	27.9	16.4	23.6	28.7	47.7	

[Ans: (i) 1334 kg/hr (ii) 4]

**10.13** Number of Stages in a Counter-Current Extractor for Extraction of Phenol from Sewage Water Using Benzene as Solvent: A continuous counter-current extractor is used to treat phenol sewage water with pure benzene for purification of the water and the extraction of the phenol. Determine the required amount of solvent and the number of theoretical stages if 10 m<sup>3</sup> of sewage water is processed per hour. The initial and final contents of the phenol in the water are 8 and 0.5 kg/m<sup>3</sup>, respectively, the final phenol content in the benzene is 25 kg/m<sup>3</sup> and the temperature of the liquids is 25°C. The equilibrium data collected from International Critical Tables are as follows:

Content of phenol in water, g-eq/dm <sup>3</sup> :	0.0272	0.1013	0.3660
Equilibrium content of phenol in benzene, g-eq/dm <sup>3</sup> :	0.062	0.279	2.978

[Ans: 0.73 kg/s, 7 stages]

**10.14** Extraction Of Benzoic acid using Benzene as Solvent to Determine the Number of Stages Required and also the Compositions of the Extract: Benzoic acid is extracted from an aqueous solution containing 1.5 kg/m<sup>3</sup> of water by consecutive washing with benzene containing 0.2 kg of

benzoic acid per  $\text{m}^3$  of benzene with a ratio of the volumes of the water and benzene equals to 4. Determine how many stages are needed if the benzene content in the raffinate-product is 0.2  $\text{kg}/\text{m}^3$ . Also, determine the compositions of the extracts obtained. The equilibrium data at the operating temperature are:

Concentration of benzoic acid in water, $\text{kg}/\text{m}^3$ :	0.104	0.456	0.707	1.32	1.56
Concentration of benzoic acid in benzene, $\text{kg}/\text{m}^3$ :	0.182	2.45	6.12	18.2	24.5

[Ans: 3 stages, Compositions of the extracts: 4  $\text{g}/\text{dm}^3$ , 1.2  $\text{g}/\text{dm}^3$ , 0.6  $\text{g}/\text{dm}^3$ ]

**10.15 Estimation of Theoretical Stages for a Given Extent of Extraction with Immiscible Solvent:** 1000 kg/hr of a solution of  $C$  in  $A$  containing 20%  $C$  (by weight) is to be counter-currently extracted with 400 kg/hr of solvent  $B$ .  $A$  and  $B$  are mutually insoluble.

The equilibrium distribution of component  $C$  between  $A$  and  $B$  are as follows:

wt. of $C$ /wt. of $A$ : 0.05 0.20 0.30 0.45 0.50 0.54
wt. of $C$ /wt. of $B$ : 0.25 0.40 0.50 0.65 0.70 0.74

How many theoretical stages will be required to reduce the concentration of  $C$  in  $A$  to 5%? [Ans: 2.85]

**10.16 Determination of Quantity of Chloroform used in Each Stage and Mole Fraction Of Acetone in Final Product in a Cross-Current Extraction:** It is desired to extract acetone from a feed containing acetone and water, using chloroform as the solvent in two cross-current extraction stages. Assume that water and chloroform are immiscible. The following data are given for the process:

- (i) the feed is an equimolar mixture of acetone and water
- (ii) the quantities of chloroform used in two stages are equal
- (iii) 60 mol% of the acetone in the feed is extracted in stage 1
- (iv) The extract and raffinate phases from each stage are in equilibrium. The equilibrium relationship for the distribution of acetone is given by

$$\frac{\text{Moles of acetone in water rich phase}}{\text{Moles of water in water rich phase}}$$

$$= 2 \times \frac{\text{Moles of acetone in chloroform rich phase}}{\text{Moles of chloroform in chloroform rich phase}}$$

- (a) Determine the quantity of chloroform used in each stage per mole of feed
- (b) Determine the mole fraction of acetone in final product stream.

[Ans. (i) 0.667 (ii) 19.35% ]

**10.17 Cross-current Extraction for Separation of Acetic Acid using Diethylether as Solvent:** Acetic acid is extracted from its 15% (mass) aqueous solution at 25°C. The mass of the initial mixture is

1200 kg. Determine the compositions and amounts of the final products after distillation of the solvent if cross-current extraction with pure diethylether is used. The process is carried out in two stages with a ratio of the mass of the solvent to that of the feed equal to 1.5. The equilibrium data given in Problem 10.12 may be used.

[Ans: Extract: 1940 kg, 180 kg, 55% (mass), 1735 kg, 99 kg, 35% (mass)  
Raffinate: 915 kg, 850 kg, 4% (mass)]

**10.18 Extent of Extraction in Multistage Extraction with Immiscible Solvent:** Nicotine in an aqueous solution containing 1.5% nicotine is to be extracted with kerosene at 20°C. Water and kerosene are mutually insoluble.

Determine the percentage extraction of nicotine if 100 kg of the feed solution is extracted in three ideal stages using 50 kg kerosene in each stage.

The following equilibrium data may be used where  $x' = \text{kg nicotine/kg water}$ , and  $y' = \text{kg nicotine/kg kerosene}$ :

$x'$ :	0.001011	0.00246	0.00502	0.00751	0.00998	0.0204
$y'$ :	0.000807	0.00196	0.00456	0.00686	0.00913	0.0187

[Ans: 68.8%]

**10.19 Determination of Height of a Continuous-Contact Extractor:** A continuous-contact extraction column is used to extract a solute from an aqueous stream using a solvent. Each of the aqueous streams, i.e. the feed and the solvent enters the column at a flow rate 100 kg/hr, and the solvent is free from solute whereas the feed contains 10% solute. The distribution coefficient ( $y/x$ ) is 1.0, where  $x$  and  $y$  are the mass fractions of solute in extract and raffinate phases, respectively. The extract phase and the raffinate phases contain 9% and 1% solute, respectively. Assuming the phase flow rates are constant, find the height of the column.

[Ans. 18 m]

**10.20 Determination of Number of Stages in an Extractor with Reflux:** Methylcyclohexane is extracted with aniline from its 40% solution in heptane at 25°C in an extractor with reflux of part of the extract and raffinate. The extract contains 98% (mass) and the raffinate 1% (mass) of methylcyclohexane (excluding the solvent). The ratio of the amounts of reflux of the extract and the extract-product is 1.615 times greater than the minimum value. Determine the number of extraction stages required for treatment of 100 kg of feed per hour.

The data on the equilibrium compositions of the coexisting phases (in mass ratio) are given below:

Raffinate layer		Extract layer		Raffinate layer		Extract layer	
$X$	$z$	$Y$	$Z$	$X$	$z$	$Y$	$Z$
0	0.064	0	15.7	0.610	0.087	0.770	6.58
0.085	0.064	0.150	13.8	0.730	0.099	0.870	5.67
0.216	0.070	0.365	11.2	0.810	0.105	0.920	5.10
0.445	0.078	0.623	8.2	0.885	0.117	0.960	4.80
0.525	0.079	0.700	7.33	1.0	0.124	1.0	4.70

[Ans: 18 stages]

**10.21 Determination of Number of Stages and Location of Feed Plate in a Counter-current Extractor:** A continuous counter-current extractor is used to extract styrene from its 38% solution in ethylbenzene with diethyleneglycol. The capacity of the extractor with respect to the feed is 100 kg/hr. Since conventional counter-current extraction cannot provide the required purity of

separation, extraction with partial extract and raffinate refluxes is employed. The extract and raffinate products contain 95 and 3% (mass) of styrene, respectively. Determine the required number of theoretical stages assuming that the extract reflux is 1.5 higher than the minimum amount. Also, find out the location of feed plate.

[Ans: 23 stages, 12th stage from the top]

### **Short and Multiple Choice Questions**

1. Which parts of an equilateral triangular diagram representing ternary liquid equilibrium represent binary equilibrium?
2. Give an example of Type-I ternary liquid system.
3. How does the mutual solubility of the initial solvent and the added solvent in extraction change with temperature?
4. Why should extraction with partially miscible solvents be limited within the bimodal solubility curve?
5. Why should a good solvent for liquid extraction have low viscosity and low latent heat of vaporisation?
6. What will happen if selectivity of solvent in liquid extraction is unity?
7. What are the major steps involved in liquid extraction?
8. How do you express the number of overall transfer units for the raffinate phase during extraction from a very dilute solution?
9. What are the advantages of extraction with supercritical fluids?
10. What are the basic units required in a simple supercritical fluid extraction system?
11. In liquid-liquid extraction, if the selectivity is unity, then
  - (a) separation of the constituents is most effective
  - (b) no separation is possible
  - (c) amount of solvent requirement is minimum
  - (d) solvent flow rate should be very high
12. In liquid-liquid extraction, as the temperature increases, the area covered by the binodal curve
  - (a) decreases
  - (b) increases
  - (c) remains unchanged
  - (d) none of these
13. Operating pressure for liquid extraction should be
  - (a) sufficiently high to maintain completely condensed system
  - (b) below the vapour pressures of all the components
  - (c) equal to the vapour pressure of the most volatile component
  - (d) equal to the vapour pressure of the least volatile component
14. During distribution of a solute between two partially miscible solvents, the selectivity at the plait point is
  - (a) zero
  - (b) 1.0
  - (c) less than zero
  - (d) very large
15. The mutual solubility of two liquids
  - (a) increases with increase in temperature
  - (b) decreases with increase in temperature
  - (c) does not change with change in temperature

(d) decreases linearly with increase in temperature

16. For solvent economy in liquid extraction, the distribution coefficient must be

(a) less than one      (b) equal to one

(c) greater than one      (d) as large as possible

17. Which of the following operations is more economical for concentration of acetic acid from very dilute aqueous solution?

(a) evaporation

(b) solvent extraction

(c) atmospheric distillation

(d) drying

18. Which of the following changes causes a Type-II liquid-liquid system to become a Type-I system?

(a) an increase in temperature

(b) a decrease in temperature

(c) an increase in pressure

(d) a decrease in pressure

19. Heat sensitive material with very high latent heat of vaporisation may be economically separated by

(a) distillation (b) evaporation

(c) liquid extraction (d) absorption

20. In ternary liquid equilibria, the apex of the equilateral triangular diagram represents

(a) a pure component (b) a binary mixture

(c) a ternary mixture (d) an insoluble binary system

21. Three solvents have been chosen for the extraction of a solute from an aqueous solution. All other factors remaining identical, the interfacial tensions for the solvents are as under

(a) 0.002 N/m      (b) 0.02 N/m      (c) 0.06 N/m

which solvent is most suitable?

22. The temperature of a supercritical fluid should be above its

(a) freezing point      (b) boiling point

(c) critical point      (d) none of these

23. For fractionation of crude residum, the ROSE process employs supercritical

(a) propane      (b) butane

(c) pentane      (d) hexane

24. Selectivity of a solvent for extraction operation

(a) is analogous to relative volatility in distillation practice

(b) must be less than unity

(c) is 0.5 at the plait point

(d) none of these

25. The number of stages required for a given amount of extraction with a given amount of solvent in continuous cross-current multistage extraction is

(a) equal to the number of stages required in continuous counter-current multistage extraction

(b) more than the number of stages required in continuous counter-current multistage extraction

(c) less than the number of stages required in continuous counter-current multistage extraction

26. As axial mixing increases in a counter-current extractor, the extraction efficiency  
(a) increases  
(b) decreases  
(c) remains unchanged
27. Radioactive nuclear wastes are treated in  
(a) mixer-settler extractor  
(b) rotating disc contactor  
(c) pulsed extractor
28. Which of the following is most suitable for extraction from a system having very low density difference?  
(a) mixer-settler extractor  
(b) centrifugal extractor  
(c) pulsed extraction column  
(d) packed extraction column

*Answers to Multiple Choice Questions*

11. (b)    12. (a)    13. (c, a)    14. (b)    15. (c)    16. (d)    17. (b)  
18. (a)    19. (c)    20. (a)    21. (c)    22. (c)    23. (c)    24. (a)  
25. (b)    26. (b)    27. (d, c)    28. (b)

**References**

- Bart, H.J., *Reactive Extraction*, Springer, Berlin (2001).
- Bonnet, J.C., *Hydrodynamics and Mass Transfer studies in a Scheibel Extractor*, Ph.D. Thesis, Univ. of Aston, Birmingham, London (1982).
- Bonnet, J.C. and G.V. Jeffreys, *AIChE J.*, **3** (5), 788 (1985).
- Bora, M.M., S. Borthakur, P.G. Rao and N.N. Dutta, *Chem. Eng. Process*, **47**, 1 (2008).
- Brennecke, J.F. and C.K. Eckert, *AIChE J.*, **35**, 1409 (1989).
- Bulley, N.R. and M. Fattori, *J. Am. Oil Chem. Soc.*, **61**(8), 1362 (1984).
- Chang-Kakoti, D.K., W-Y. Fei, J.C. Godfrey and M.J. Slater, *J. Sep. Process Tech.*, **6**, 40 (1985).
- Coulson, J.M. and J.F. Richardson, *Chemical Engineering*, vol. 2, 4th ed., Butterworth, Oxford (1991).
- Cusack, R.W. and D.J. Glatz, *Chem. Eng.*, 91, July (1996).
- Godfrey, J.C. and M.J. Slater, *Liquid-liquid Extraction Equipment*, John Wiley; New York (1994).
- Henley, E.J. and J.D. Seader, *Separation Process Principles*, John-Wiley, New York (1998).
- Laddha, G.S. and T.E. Degaleesan, *Transport Phenomena in Liquid Extraction*, Tata McGraw-Hill, New Delhi (1976).
- Lewis, J.B., I. Jones and H.R.C. Pratt, *Trans. Inst. Chem. Eng.*, **29**, 126(1951).
- Logsdail, D.H. and M.J. Slater, in *Handbook of Solvent Extraction*, Lo, T.C., M.H.I. Baird and C. Hanson (Eds.), Wiley, New York (1983).
- Mukhopadhyay, M., *Natural Extracts using Supercritical Carbon dioxide*, CRC Press, New York (2000).

- Pradhan, G., *Chem. Ind. Digest*, **XX** (2), 73 (2007).
- Prochazka, J., J. Landau and F. Souhrada, US Patents 3488037 (1970), 3583856 (1971).
- Rani, K.Y., *Chem. Ind. Digest*, **XXI** (3), 78 (2008).
- Quinn, J.A. and D.B. Sigloch, *Canad. J. Chem. Eng.*, **41**, 15 (1963).
- Reissinger, K.H. and J. Schröeter, in *Encyclopedia of Chemical Processing and Design*, vol. 21, J.J. McKetta (Ed.), Marcel Dekker, Inc., New York (1984).
- Scheibel, E.G., *Chem. Eng. Prog.*, **62**(9), 76 (1966).
- Skelland, A.H.P. and G.G. Ramsey, *Ind. Eng. Chem. Res.*, **26**, 77 (1987).
- Steensma, M., N.J.M. Kuipers, A.B. de Haan and G. Kwant, *Chem. Eng. Sci.*, **62**, 1395 (2007).
- Treybal, R.E., *Liquid Extraction*, 2nd ed., McGraw Hill, New York (1963).
- Treybal, R.E., *Mass Transfer Operations*, 3rd ed., McGraw Hill, Singapore (1985).
- Wang, J.H., S.J. Pork, M.D. Dea and V. Houton, *Ind. Eng. Chem., Pro. Res. Des. and Dev.*, **34**(4), 1280 (1995).
- Wankat, P.C., *Equilibrium Staged Separation*, Elsevier, New York (1988).
- Yeh, J.C., F.H. Haynes and R.A. Moses, *AIChE J.*, **10**, 260 (1964).

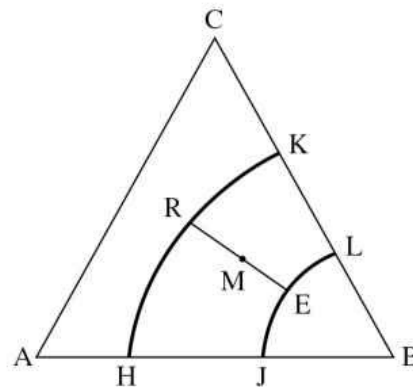


**Figure 10.4** System of 3 liquids, two pairs partially miscible.

Any composition  $M$  within the region  $HKLJ$  automatically splits into two saturated layers of equilibrium compositions  $R$  and  $E$  at the two extremities of the tie line  $RE$ . Any composition outside this region will form a single phase homogeneous solution and hence will be unsuitable for extraction.

A typical example of this system is chlorobenzene ( $A$ )–water ( $B$ )–methyl ethyl ketone ( $C$ ). This type of systems is known as Type-II systems.

Temperature has a strong effect on liquid–liquid equilibria. In general, the solubility of a pair of liquids increases with temperature. In case of Type-I systems, the mutual solubility of the initial carrier ( $A$ ) and solvent ( $B$ ) increases with increase in temperature till the critical solution temperature is reached above where  $A$  and  $B$  are completely miscible. Extraction with Type-I systems must, therefore, be carried out below the critical solution temperature.

With increase in temperature of Type-II systems, the mutual solubility of the solvent ( $B$ )–solute ( $C$ ) pair increases at a rate faster than that of the carrier ( $A$ )–solvent ( $B$ ) pair. At the critical solution temperature of the solvent ( $B$ )–solute ( $C$ ) pair, this pair becomes completely miscible and consequently, the Type-II system behaves as Type-I system.

#### 10.3.4 Liquid–Liquid Equilibria on Solvent-Free Coordinates

A rectangular co-ordinate system where all the quantities are expressed on solvent-free basis is sometimes used in liquid–liquid extraction. In this system, the mass ratios  $X$  and  $Y$  of the solute in the two liquid phases are plotted against the corresponding mass ratios of the solvent  $\left(\frac{B}{A+C}\right)$  in the respective phases, all on solvent-free basis, where,

$$X = \frac{C}{A+C} \text{ in the raffinate phase, and}$$

$$Y = \frac{C}{A+C} \text{ in the extract phase.}$$

Such a plot is known as *Janecke diagram*.

#### 10.4 Selection of Solvent



# Leaching

## 11.1 Introduction

*Leaching* is a unit operation in which a liquid solvent preferentially dissolves one or more constituents of a solid mixture with the object of separating them from the insoluble ones. Leaching is also known as *solid-liquid extraction*, *lixiviation* or *decoction*, the last term being used when the solvent is at its boiling point. Leaching has extensive application in metallurgical industries. For instance, copper compounds are removed from copper ores by sulphuric acid or an ammoniacal solution, uranium compounds get separated from the uranium ore on treatment with acid/alkali solution and gold is separated from its ores by leaching with sodium cyanide or other appropriate solvents. Leaching is also used for removal of sugar from sugar beat, tannin from tree barks, for removal of oil from oil seeds and fish oil from fish.

## 11.2 Classification

Rickles (1965) classified commercial solid-liquid extraction into the following four categories.

### ***Diffusional extraction***

In this category almost the entire resistance to mass transfer is in the solid phase. Extraction of sugar from sugar beat with warm water is an example. In this type of extraction, the rate of extraction depends on the thickness of the solid material, the effective diffusivities of the solute in the solid and the concentration of the extracted solute in the extract solution.

### ***Washing extraction***

When the particle size of the solid is very small, the diffusional resistance of the solid phase becomes negligible and extraction virtually becomes washing the solid with the solvent. Example of this category is extraction of oil from flakes of oil seeds.

### ***Leaching***

In this category one or more constituents are dissolved by chemical reaction. An acid, an alkali or a complex chemical solution is generally used as solvent. The extraction of copper or gold using appropriate solvents come under this category.

### ***Chemical extraction***

This is similar to leaching but usually refers to solids of organic nature such as gelatin.

A novel method (Ciminelli et al. 2001) employs microbes instead of chemical agents for dissolving ores, particularly the low grade ones at near ambient conditions. Bacterial species such as *Thiobacillus ferroxidans* and *T. thermophile* species convert the ores, particularly the sulphides into soluble sulphates. The process is slow but nonpolluting since no sulphur dioxide is produced. This

process is used for extraction of copper from its ore.

### 11.3 Terminologies Used

The following nomenclatures have been used in this chapter:

$A$  = insoluble carrier solid

$B$  = pure solvent

$C$  = soluble solute

Since insoluble solids remain unchanged during the process, all concentrations have been expressed on insoluble solid-free basis.

$S$  = concentration of insoluble solid  $A$  in any liquid or slurry on  $A$ -free basis,  $\frac{\text{wt. } A}{\text{wt. } (B + C)}$

$x$  = weight fraction of solute  $C$  in solid or slurry on  $A$ -free basis,  $\frac{\text{wt. } C}{\text{wt. } (B + C)}$

$x$  includes all solute  $C$  present in the slurry either dissolved or suspended or adsorbed.

$y$  = weight fraction of solute  $C$  in solvent or effluent solution from a stage on  $A$ -free basis,

$\frac{\text{wt. } C}{\text{wt. } (B + C)}$

For dry solid before adding solvent,  $x = 1$  and for pure solvent  $S = 0$ ,  $y = 0$ .

### 11.4 Solid–Liquid Equilibria

Under a given set of operating conditions, the number of stages required to leach a certain amount of solute from a solid or the extent of leaching with a given number of stages can be most conveniently determined by graphical methods. Calculations may be made on triangular co-ordinates as in case of liquid-liquid extraction. However, on account of too much congestion of lines in one corner of triangular diagrams, it is convenient to use rectangular co-ordinates.

The method of plotting different data on rectangular co-ordinate is shown in Figure 11.1. In the simple case of a mixture of insoluble solids in contact with a solution in which all the solute has been dissolved, the mixture is represented by the point  $M_1$ . The concentration of solute  $C$  in the mixture is  $x_{M_1}$  and the insoluble solid to solution ratio is  $S_{M_1}$ . If the mixture is now allowed to settle and the solid is nonadsorbent, the clear solution will be represented by the point  $E_1$  and the settled sludge by the point  $R_1$ . Since the composition of the solution retained by the sludge is the same as that of the clear solution withdrawn,  $y = x^*$  and the tie line  $E_1R_1$  is vertical. The value of  $S_{R_1}$  will depend upon the time of settling. There will be some highest value of  $S_{R_1}$  for the ultimate settled height of the sludge. If less time is allowed for settling, the sludge will contain more of the solution and the point  $R_1$  will shift to  $R_2$ . Similarly, if the withdrawn liquid contains some  $A$ , either suspended or dissolved, the point  $E_1$  will shift to  $E_2$ .

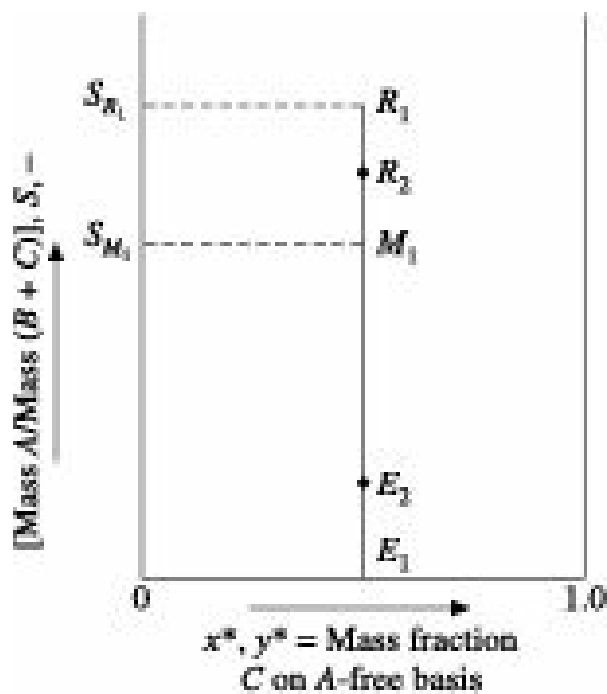


**Figure 11.1** Graphical representation of concentration in leaching.

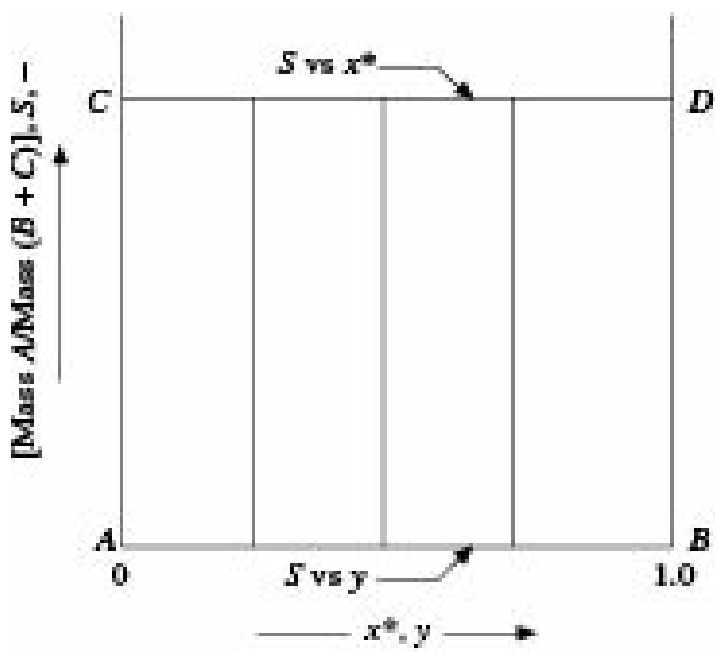
The underlying principle of computation for the number of stages or extent of leaching in a leaching operation is basically the same as that for liquid-liquid extraction. But the concept of theoretical stage or ideal stage is not justified in this case because of the following reasons:

- (i) the solute may not be completely dissolved due to inadequate contact,
- (ii) solid-liquid mechanical separation is seldom perfect and the solids leaving a stage will always retain some solution and
- (iii) some solute may be adsorbed by the solids.

In view of the above, it is almost impossible to get reproducible equilibrium data for leaching operations. Practical equilibrium data, which take care of stage efficiency, are therefore commonly used. These data are collected under the same operating conditions in which the actual plant is expected to operate.

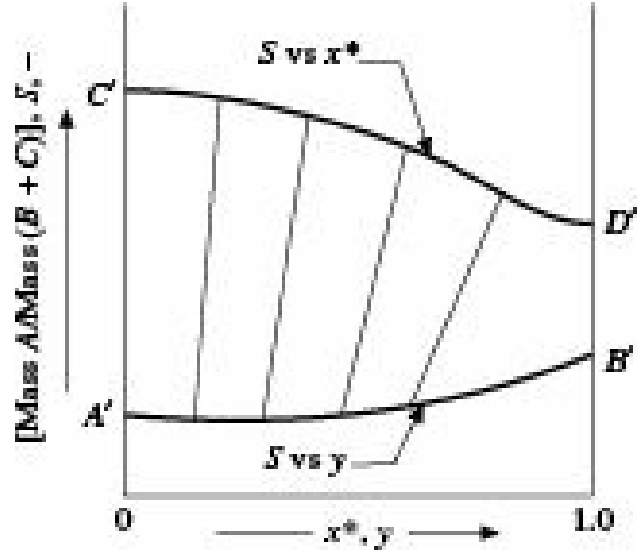
Some typical equilibrium curves usually encountered in practice are shown in Figures 11.2 to 11.4.

Figure 11.2 represents equilibrium relation where  $C$  is infinitely soluble in  $B$  so that  $x$  and  $y$  may have any value between 0 and 1.0. No adsorption of solute by the solid takes place. As a result, the withdrawn solution and the solution retained by the sludge have the same composition and the tie lines are vertical. The line  $CD$  is horizontal as the solids settle equally at all solute concentrations. The curve  $S$  vs.  $y$  coincides with the abscissa indicating that the solution does not contain any solid.



**Figure 11.2** Equilibrium diagram: C infinitely soluble in B, no adsorption of solute.

In the equilibrium relation shown in Figure 11.3, C is infinitely soluble in the solvent B so that  $x$  and  $y$  may have any value between 0 and 1 as before. The curve  $A'B'$  representing the composition of the withdrawn solution lies above  $S = 0$  since the solution contains some solid A, either dissolved or suspended due to imperfect settling. The tie lines are inclined indicating that the solute contents of the withdrawn solution and the solution retained by the sludge are different which may be due to insufficient time of contact or adsorption of solute by the solid or partial solubility of solute in the solvent with unequal distribution between liquid and solid phases.



**Figure 11.3** Equilibrium diagram: C infinitely soluble in B, solution contains some A.

In the type of equilibrium shown in Figure 11.4, solute C has a limited solubility in solvent B as shown by the curve  $C''D''$ . The tie lines to the right of  $y_S$  converge at  $y_S$ , which mean that the maximum solute concentration in the withdrawn solution cannot be higher than  $y_S$ . Any mixture to the right of  $y_S$  will give a clear saturated solution P and slurry Q depending on the position of M. The tie lines to the left of  $y_S$  are vertical since the solid does not adsorb any solute.

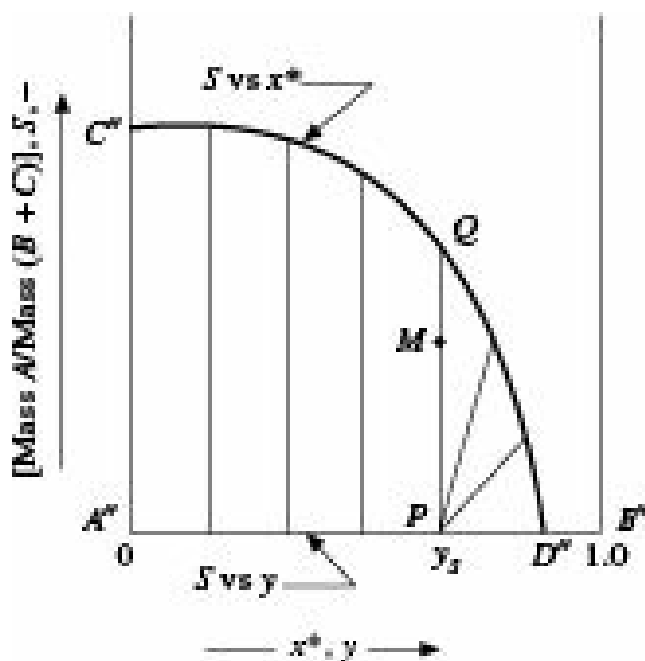


Figure 11.4 Equilibrium diagram: Limited solubility of  $C$  in  $B$ , no adsorption of solute.

## 11.5 Leaching Operation

As in case of liquid-liquid extraction, leaching operation consists of four distinct steps. These are:

- (i) thorough mixing of the solid with the selected solvent with vigorous agitation so that maximum possible mass transfer can take place between them,
- (ii) separation of the extract solution from the leached solids,
- (iii) separation of the solvent and associated solid if any, from the extract phase and
- (iv) recovery of solvent from the leached solids.

The success of the leaching operation have direct bearing with the following aspects:

### ***Pre-treatment of the solid***

The rate of extraction largely depends upon the nature and characteristics of the solute-bearing solid. If the solute is distributed within an insoluble matrix of the carrier solid, it gradually dissolves and diffuses out leaving a porous structure. Sometimes, a large portion of the solute may be adsorbed by the carrier solid. In any case, the rate of extraction becomes faster if the size of the carrier solid is smaller so that a relatively large surface of the solid is exposed to the action of the solvent. For compact solids like mineral bearing ores, size range of 60 to 100 mesh is quite common. Plants, vegetables and animal bodies are not crushed since that may rupture the cell walls and some undesirable materials may pass on to the extract phase. They are sliced into thin pieces or flaked so that the solute to be leached is exposed to the action of the solvent.

### ***Solvent***

No single solvent posses all the qualities of a good solvent for leaching. An intelligent compromise should therefore be made while selecting a solvent. The target solute should have high solubility in the solvent. At the same time, the solvent should not dissolve any undesirable material. The solvent should have low viscosity, low boiling point. It should preferably be nontoxic, nonflammable, cheap and easily available.

### ***Temperature***

Temperature is an important parameter in leaching. Temperature of leaching should be as high as possible since at high temperature the solute is more soluble, the concentration of solute in the leach solution is more, the diffusivity of the solute through the solid is higher and the viscosity of the solution is lower, all of which contribute to higher leaching efficiency. However, at higher temperature solvent loss may be more and some undesirable materials may be extracted.

## **Agitation**

Agitation increases the rate of leaching by increasing the mass transfer coefficient. At the same time, vigorous stirring may disintegrate the solid causing subsequent settling problem. However, the effect of agitation is not so pronounced if the controlling resistance to mass transfers lies in the solid phase.

## **11.6 Methods of Calculation**

### **11.6.1 Single Stage Leaching**

Figure 11.5 represents a flow diagram of single stage leaching which consists of thoroughly mixing the solids to be leached with the solvent, allowing the mixture to settle and then withdrawing the clear solution.

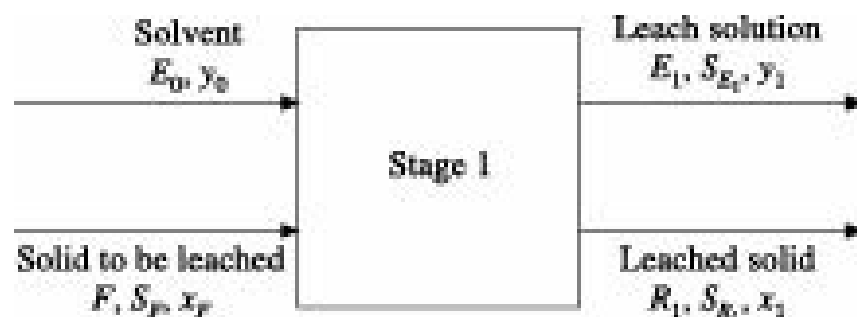


Figure 11.5 Flow diagram of single stage leaching.

The operation has been represented graphically in Figure 11.6.

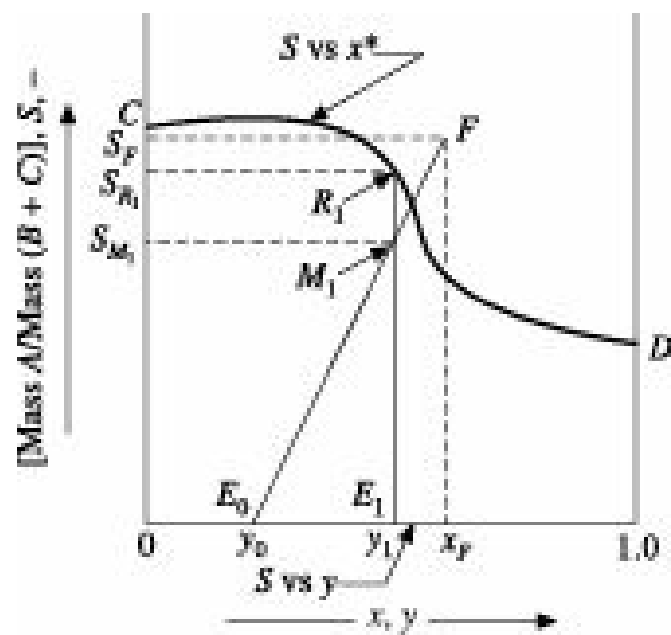


Figure 11.6 Graphical representation of single stage leaching.

The steps to be followed in graphical solution are as under:

- The equilibrium curve  $CD$  is drawn from appropriate equilibrium data.
- Point  $F(x_F, y_F)$  representing the feed and point  $E_0 (0, y_0)$  the solvent respectively are located from

given data and these two points are joined.

- Point  $M_1$  representing the overall mixture is then located on the line  $E_0F$  from knowledge of  $x_{M1}$  or  $S_{M1}$ . The composition of the mixture  $M_1$  can be calculated from solute balance:

$$Fx_F + E_0y_0 = E_1y_1 + R_1x_1 = M_1x_{M1} \quad (11.1)$$

$$\frac{Fx_F + E_0y_0}{M_1} = \frac{Fx_F + E_0y_0}{F + E_0}$$

whence,  $x_{M1} =$  (11.2)

From definition of  $S$ , assuming  $A$  is insoluble in the solvent and the leach solution does not contain any  $A$ ,

$$FS_F = M_1S_{M1} = R_1S_{R1} \quad (11.3)$$

whence,  $S_{M1} =$  (11.4)

$$\frac{FS_F}{M_1} = \frac{FS_F}{F + E_0}$$

The tie-line through  $M_1$  is drawn and points  $E_1$  and  $R_1$  representing the leach solution and the leached solids, respectively are located at the point of intersection of the tie-line with the  $S$  vs  $y$  and  $S$  vs  $x$  curves, respectively. Their compositions  $y_1$  and  $x_1$  can be directly read from the diagram.

The weight of the leached solids  $R_1$  can be calculated from Eq. (11.3):

$$R_1 = \frac{FS_F}{S_{R1}} \quad (11.5)$$

The weight of the leach solution  $E_1$  may be calculated from solution balance:

$$F + E_0 = E_1 + R_1 = M_1 \quad (11.6)$$

whence,  $E_1 = F + E_0 - R_1 \quad (11.7)$

## 11.6.2 Multistage Cross-current Leaching

Additional solute can be extracted by treating the leached solids from stage 1 with fresh batch of solvent as shown in Figure 11.7 for a 3-stage cross-current leaching unit. The calculations for subsequent stages are similar to those for the first stage with the leached solids from any stage becoming the feed for the next stage.

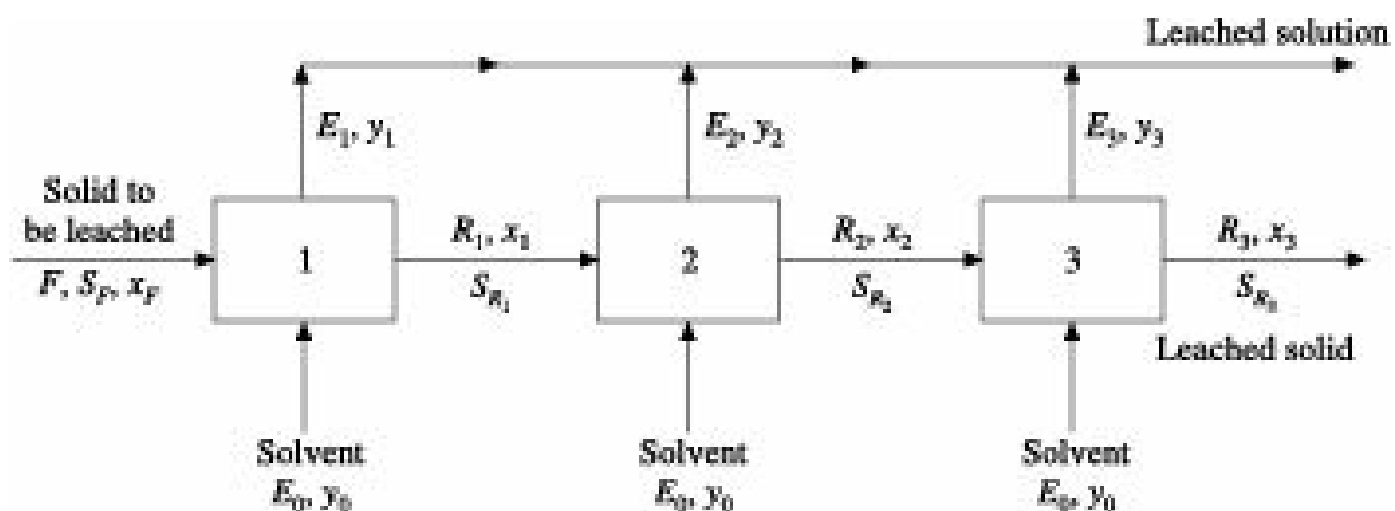


Figure 11.7 Flow diagram of multistage cross-current leaching.

To continue the calculations,  $E_0R_1$  is joined and  $M_2$  is located on this line from knowledge of  $x_{M_2}$  or  $S_{M_2}$ .

A tie line through  $M_2$  gives  $E_2$  and  $R_2$ . This procedure is continued till the desired composition or number of stages is reached.

The graphical method of solution is shown in Figure 11.8.

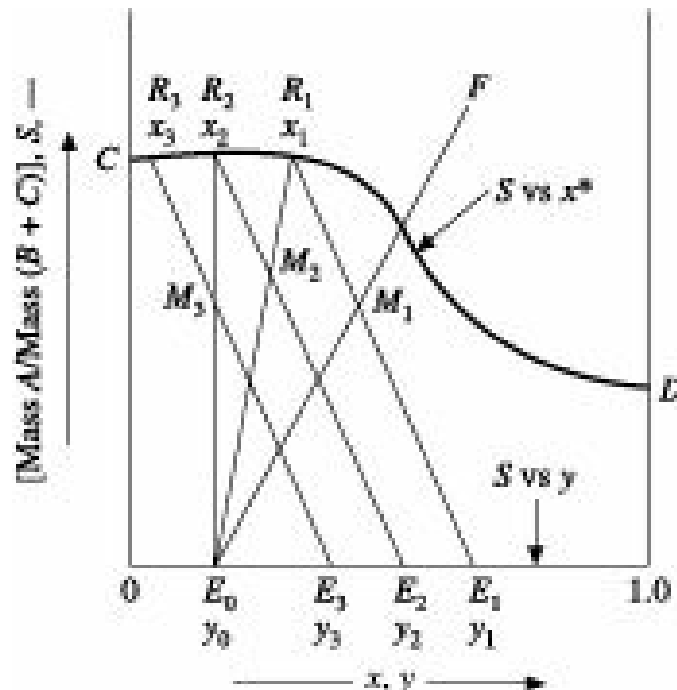


Figure 11.8 Graphical representation of multistage cross-current leaching.

### 11.6.3 Multistage Counter-current Leaching

A flow diagram for multistage counter-current leaching has been shown in Figure 11.9. It is assumed that solid  $A$  is insoluble and is not lost in the leach solution.

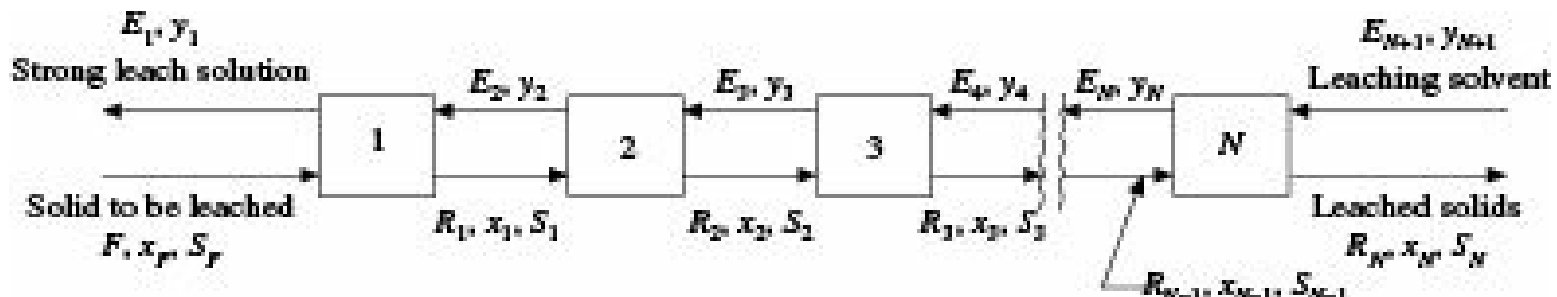


Figure 11.9 Flow diagram for multi-stage counter-current leaching.

A material balance for the entire unit is

$$F + E_{N+1} = E_1 + R_N = M \quad (11.8)$$

A solute balance provides

$$Fx_F + E_{N+1} y_{N+1} = E_1 y_1 + R_N x_N = M x_M \quad (11.9)$$

From Eqs. (11.8) and (11.9), we obtain

$$\frac{Fx_F + E_{N+1} y_{N+1}}{F + E_{N+1}} x_M = \quad (11.10)$$

$\frac{Fx_F + E_{N+1} y_{N+1}}{F + E_{N+1}}$  By analogy with Eq. (11.4), we get

$$\frac{FS_F}{F + E_{N+1}} S_M = \quad (11.11)$$

Equation (11.8) can be rearranged as

$$F - E_1 = R_N - E_{N+1} = P \text{ (say)} \quad (11.12)$$

where  $P$  is the difference point.

From Eq. (11.12), it may be concluded that the lines  $FE_1$  and  $(R_N E_{N+1})$ , when extended, must meet at the point  $P$ .

A material balance about any  $m$  stages gives,

$$F - E_1 = R_m - E_{m+1} = P \quad (11.13)$$

From Eq. (11.13), it may be further concluded that any line  $R_m E_{m+1}$ , when extended must also meet the line  $FE_1$  at the point  $P$ .

On the basis of the above equations, the following steps are suggested for graphical solution of number of stages or extent of leaching in multistage counter-current leaching as shown in Figure 11.10:

*Step 1* The equilibrium curve  $CD$  and the tie lines are drawn from the given data.

*Step 2* The points  $F(x_F, S_F)$  and  $E_{N+1} (0, y_{N+1})$  are located and joined.

*Step 3* The point  $M$  representing the  $A$ -free mixture is located on the line  $FE_{N+1}$  from a knowledge of  $x_M$  vide Eq. (11.10) or  $S_M$  vide Eq. (11.11).

*Step 4* The point  $E_1$  or  $R_N$  whichever is given is located from a knowledge of  $y_1$  or  $x_N$ .

*Step 5* If  $E_1$  is given,  $E_1$  and  $M$  are joined and extended upto the curve  $S$  vs  $x^*$  to get  $R_N$ . If on the other hand  $R_N$  is given,  $R_N$  and  $M$  are joined and extended upto  $S$  vs  $y$  curve to get  $E_1$ .

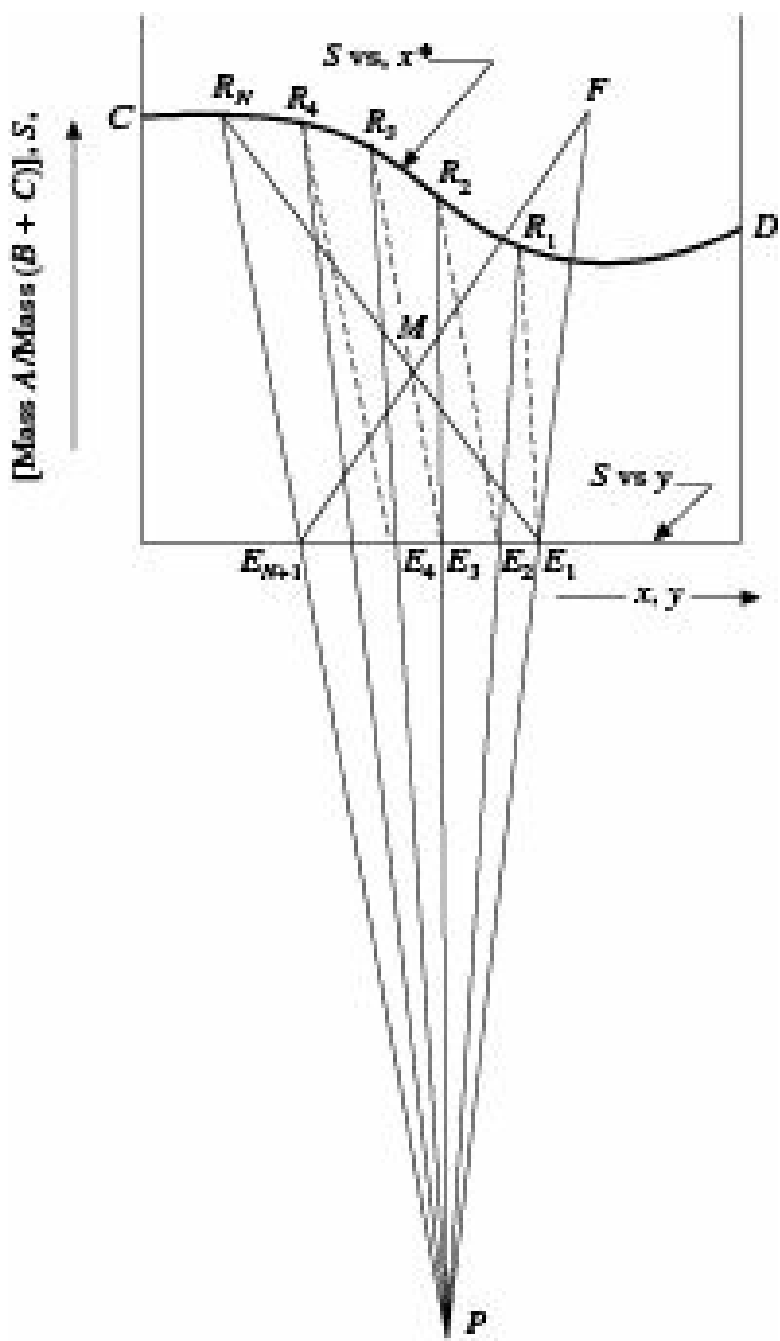


**Figure 11.10** Graphical representation of multistage counter-current leaching.

**Step 6** The points  $R_N$  and  $E_{N+1}$  are joined and extended to meet  $FE_1$  extended at the point  $P$ .

**Step 7** A tie line through  $E_1$  gives  $R_1$ .

**Step 8** The points  $P$  and  $R_1$  are joined to get  $E_2$  on the  $S$  vs  $y$  line. A tie-line through  $E_2$  gives  $R_2$ .  $PR_2$  are joined to get  $E_3$  and so on.

**Step 9** Construction is continued in this fashion till a tie-line touches or crosses the point  $R_N$ .

**Step 10** The quantities  $R_N$  and  $E_1$  may be calculated by solving Eqs. (11.8) and (11.9), respectively.

It should be noted that since practical stages are used in case of leaching the number of stages should be integral.

**EXAMPLE 11.1** (Determination of the amount of wash water and the number of units required in multistage counter-current washing): 1000 kg/hr of a reaction product from an alum reactor, containing 49.28%  $\text{Al}_2(\text{SO}_4)_3$ , 14.70% insolubles and the rest water has to be washed with water in

multistage counter-current leaching units to remove the insolubles.

The strong solution is to contain 22%  $\text{Al}_2(\text{SO}_4)_3$ . Not more than 2% of the  $\text{Al}_2(\text{SO}_4)_3$  should be lost in the washed mud. The underflow from each thickener should contain 4.0 kilograms of liquid per kilogram of solid. Equilibrium is ensured between overflow and underflow leaving each unit. Determine the amount of wash water required per hour and the number of units to be provided.

**Solution:** 1000 kg/hr reaction mass contains:

492.8 kg/hr  $\text{Al}_2(\text{SO}_4)_3$ , 147.0 kg/hr insolubles and 360.2 kg/hr water.

**Feed:**  $F = C + B = 492.8 + 360.2 = 853.0 \text{ kg/hr}$

$$x_F = \frac{C}{C+B} = \frac{492.8}{853.0} = 0.578, S_F = \frac{147.0}{853.0} = 0.172$$

**Solvent:**  $y_{N+1} = 0, S_{N+1} = 0, E_{N+1} = ?$

**Underflow:**

Total underflow ( $R_N$ ) =  $(147.0 \# 5) = 735.0 \text{ kg/hr}$

Liquid in underflow =  $(735.0 \# 0.8) = 588.0 \text{ kg/hr}$

$\text{Al}_2(\text{SO}_4)_3$  in underflow =  $(492.8 \# 0.02) = 9.856 \text{ kg/hr}$

Water in underflow =  $(588.0 - 9.856) = 578.14 \text{ kg/hr}$

$$x_N = \frac{9.856}{588.0} = 0.0168, S_N = \frac{147.0}{588.0} = 0.25$$

**Strong solution:**

$\text{Al}_2(\text{SO}_4)_3$  present =  $492.8 - 9.856 = 482.94 \text{ kg/hr}$

$y_1 = 0.22, S_1 = 0$

$$E_1 = \left( \frac{482.94}{0.22} \right) = 2195.2 \text{ kg/hr}$$

As shown in Figure 11.11, points  $F$ ,  $E_{N+1}$ ,  $E_1$  and  $R_N$  are located from knowledge of  $(x_F, S_F)$ ,  $(y_{N+1}, S_{N+1})$ ,  $(y_1, S_1)$  and  $(x_N, S_N)$ , respectively.  $(E_1, R_N)$  and  $(F, E_{N+1})$  are joined. They intersect at  $M(x_M)$ .

From Figure 11.11,  $x_M = 0.175$

$$\frac{Fx_F + E_{N+1}y_{N+1}}{F + E_{N+1}} \quad \text{From Eq. (11.10):} \quad x_M =$$

$$\text{or,} \quad 0.175 = \frac{(853.0)(0.578)}{853.0 + E_{N+1}}$$

whence,

$$E_{N+1} = 1964.3 \text{ kg/hr}$$

Wash water to be added = 1964.3 kg/hr

From Figure 11.11, Number of units required = 3

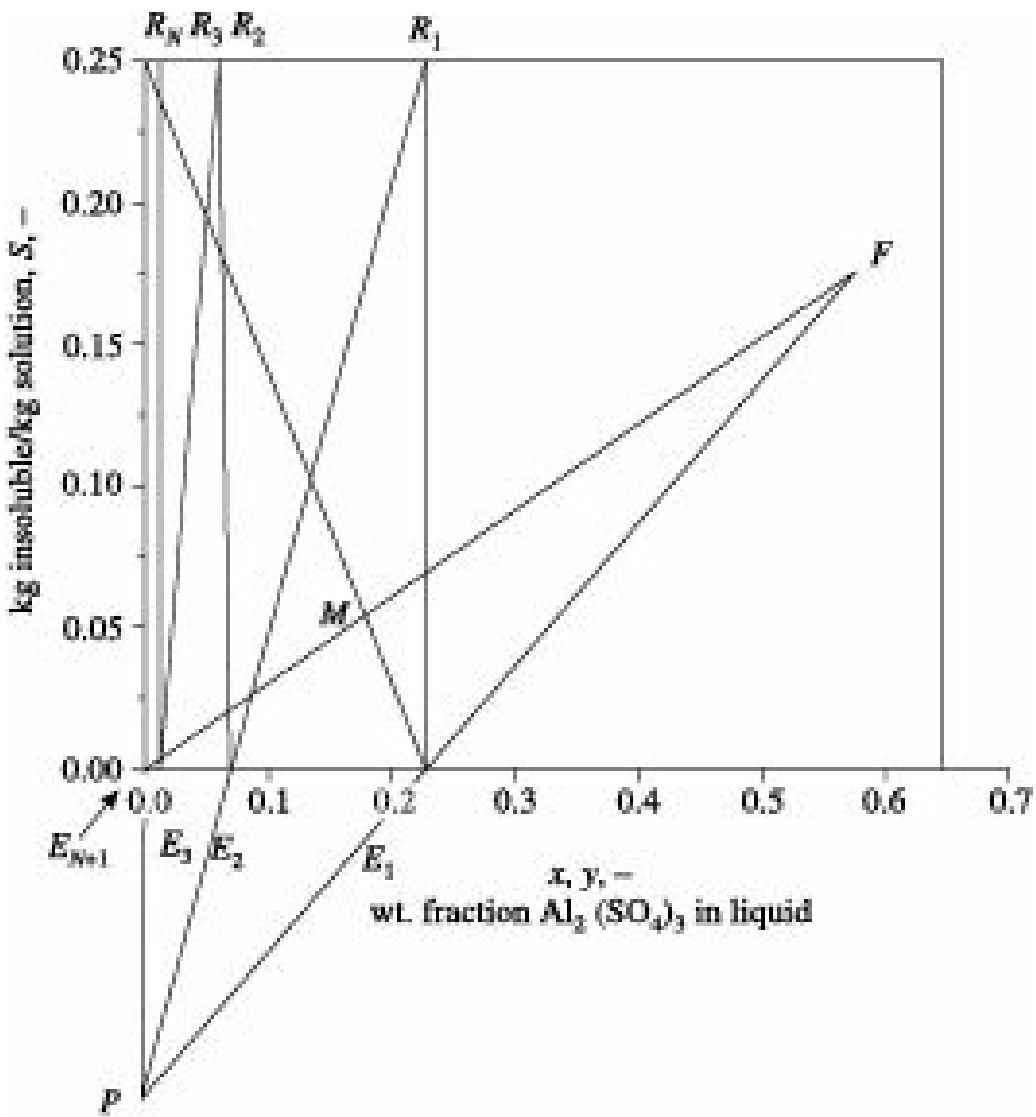


Figure 11.11 Solution to Example 11.1.

#### 11.6.4 Algebraic Method

In the special case of constant underflow or constant value of  $S$  for all sludges and constant  $y/x^*$ , the number of stages ( $N$ ) can be determined directly by algebraic method.

Using an appropriate form of Kremser Eq. (Souders and Brown 1932) as under:

$$\frac{x_F - x_N}{x_F - (y_{N+1}/m)} = \frac{(mE/R)^{N+1} - (mE/R)}{(mE/R)^{N+1} - 1} \quad (11.14)$$

$$N = \frac{\log\left(\frac{(x_F - (y_{N+1}/m))}{(x_N - (y_{N+1}/m))}\{1 - R/mE\} + (R/mE)\right)}{\log(mE/R)} \quad (11.15)$$

**EXAMPLE 11.2** (Determination of the quantity and composition of the discharged solids, amount of solvent required and the number of stages to be used): 100 kg/hr of fresh fish liver containing 25% oil has to be extracted with ethyl ether in a continuous counter-current leaching unit. 95% of the oil has to be extracted and the strong solution should contain 0.70 mass fraction oil.

Determine

- (i) the quantity and composition of the discharged solids

(ii) kilograms of oil-free ether required per hour

(iii) number of stages required

Laboratory experiments have furnished the following equilibrium data:

$y:$	0.10	0.20	0.30	0.40	0.50	0.65	0.70	0.70
$S:$	4.13	3.50	2.95	2.47	2.04	1.67	1.49	1.31

where,  $y = \text{kg oil/kg solution}$  and  $S = \text{kg oil-free liver/kg solution}$ .

**Solution:** Basis: 1 hour.

**Feed:**  $F = 25 \text{ kg oil}$ ,  $A = 75 \text{ kg insoluble}$ ,  $x_F = 1.0$ ,

$$S_F = (75/25) = 3.0.$$

**Solvent:**  $y_{N+1} = 0$ ,  $S_{N+1} = 0$ , Fresh Solvent  $E_{N+1} = ?$

**Leached Solids:**

$$\text{Oil extracted} = (25 \# 0.95) = 23.75 \text{ kg}$$

$$\text{Oil left un-extracted} = (25 - 23.75) = 1.25 \text{ kg}$$

$$\text{kg oil/kg insoluble liver} = \left(\frac{1.25}{75}\right) = 0.01667$$

The given equilibrium data are rearranged as under:

kg oil/kg solution	kg liver/kg solution	kg oil/kg liver
0.10	4.13	0.0242
0.20	3.50	0.0571
0.30	2.95	0.1017
0.40	2.47	0.1619
0.50	2.04	0.2451

By extrapolation of the above data, it is found that for kg. oil/kg. liver = 0.01667,  $S_N = 4.40$ .

$$\text{Solution retained by the leached solids} = \left(\frac{75}{4.40}\right) = 17.05 \text{ kg}$$

$$\text{Amount of oil retained} = 1.25 \text{ kg}$$

$$\text{Amount of ether retained} = (17.05 - 1.25) = 15.8 \text{ kg}$$

$$x_N = \left(\frac{1.25}{17.05}\right) = 0.0733.$$

(i) Amount of discharged solids =  $(75 + 1.25 + 15.8) = 92.05 \text{ kg}$

Composition of the discharged solids:

$$\frac{75}{92.05} \text{ Liver} = \# 100 = 81.48\%$$

$$\text{Oil} = \frac{1.25}{92.05} \# 100 = 1.36\%$$

$$\text{Ether} = \frac{15.8}{92.05} \# 100 = 17.16\%$$

(ii) Amount of oil in feed = 25 kg

$$\text{Amount of oil in leached solids} = 1.25 \text{ kg}$$

$$\text{Amount of oil in strong solution} = (25 - 1.25) = 23.75 \text{ kg}$$

The strong solution contains 0.70 mass fraction oil.

$$\text{Therefore, amount of strong solution} = \frac{(23.75)}{0.70} = 33.93 \text{ kg}$$

$$\text{Amount of solvent in strong solution} = (33.93 - 23.75) = 10.18 \text{ kg}$$

$$\text{Amount of solvent in sludge} = 15.8 \text{ kg}$$

$$\text{Therefore, solvent added} = (10.18 + 15.8) = 25.98 \text{ kg/hr}$$

(iii) From Figure 11.12, number of stages required = 7.

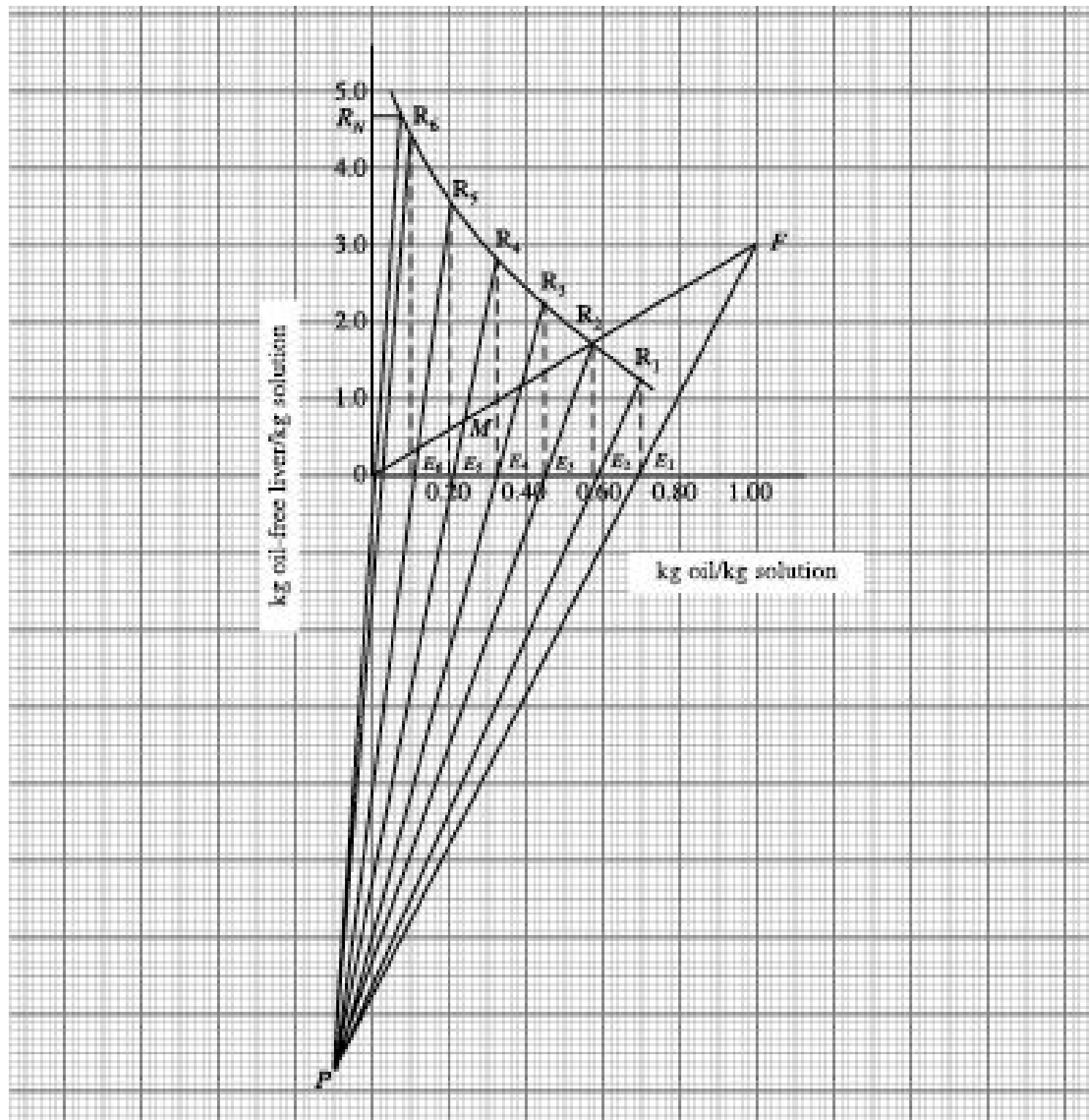


Figure 11.12 Solution to Example 11.2.

## 11.7 Leaching Equipment

In view of the difficulty in moving solids, particularly the coarse ones, leaching operations are often carried out in unsteady state. Accordingly, leaching equipment are broadly classified into unsteady state and steady state. Unsteady state equipment may be of batch type and semi-batch type. In batch type, predetermined quantities of solid and liquid are contacted for a specified period of time and then separated. In semi-batch type, a stream of flowing liquid is contacted with a stationary batch of solid. The most commonly used equipment for unsteady state leaching are—percolation tanks, agitated vessels and pachuca tanks. In steady state equipment on the other hand, solids and liquids are contacted while moving through equipment either in stage-wise or in continuous counter-current fashion.

### 11.7.1 Unsteady-State Equipment

#### ***Percolation tank***

Percolation tanks are simple and inexpensive equipment and can handle solids of intermediate size ranges. Depending upon the nature of solid and solvent to be handled, these tanks are made of wood, reinforced concrete or metal and if required, may be lined with lead or bitumen. Small tanks are usually made of wood provided the wood is not chemically attacked by the leach solution. The solids to be treated are placed on a false bottom which in the simplest case is made of gratings of wooden strips arranged parallel to each other and placed sufficiently close to support the solid but allow the solution to pass freely. For supporting fine particles, the wooden grating may be covered by coconut matting and canvas filter cloth.

Small tanks are usually made of metal with perforated metal bottom upon which a filter cloth is placed. These are mostly used for leaching pharmaceutical products from plants. Very large percolation tanks with over  $8000\text{ m}^3$  volume for treating copper ores have been made of reinforced concrete and lined with lead or bituminous mastic.

Tanks should be filled with solids of uniform size as far as possible in order to get maximum voids and pressure drop is least.

The percolation tank may be operated in different ways. In one case, after filling the tank with the solids to be treated, a batch of solvent sufficient to immerse the solid is completely introduced in the tank by pumping. The solid and the solvent are then allowed to remain in mutual contact for the predetermined length of time. During the period, the liquid may be withdrawn from the bottom and recirculated with the help of a pump. The liquid is then drained through the false bottom of the tank. The entire operation represents a single stage. The extract solution adhering to the solid may be removed by washing with fresh solvent. In spray percolation, on the other hand, the liquid is distributed at the top by spraying and trickles down the solid bed. A common problem with spray, percolation is the chance of channeling.

#### ***The Shank's system***

Leaching in percolation tanks results in weak solution of the solute. Much stronger solution can be obtained if the final solution before withdrawal is in contact with the fresh solid, and fresh solvent is added to the solid from which most of the solute has been leached. Instead of physically moving the solid from tank to tank, this is achieved by introducing the liquid to the different tanks in sequence in a system known as Shank's system, shown in Figure 11.13.

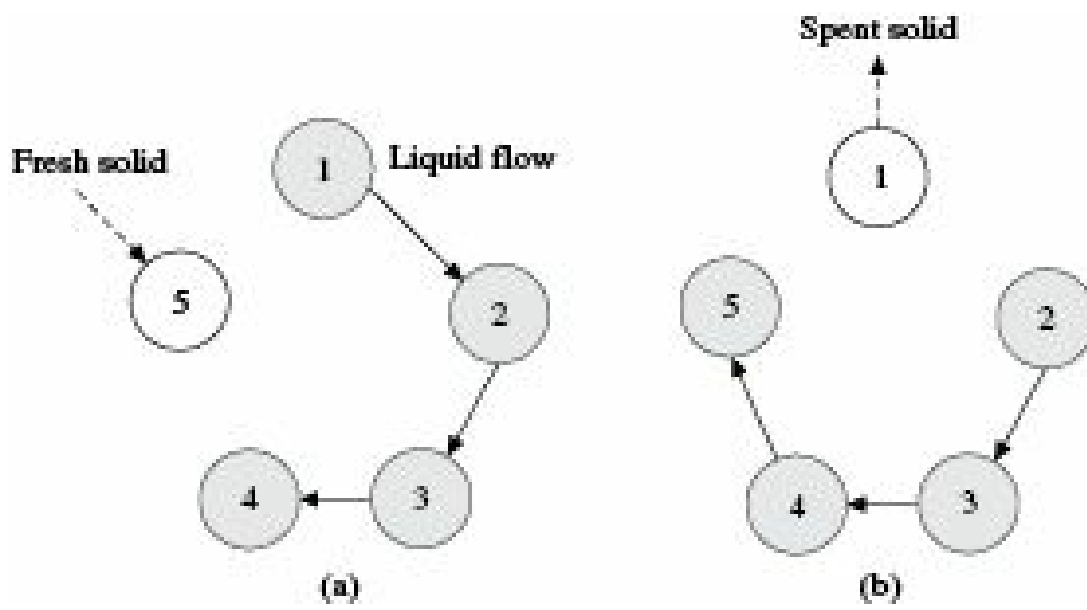


Figure 11.13 Shank's system.

Figure 11.13(a) depicts that at any instant, tank 5 is empty, others are filled with the solid, tank 4 most recently and tank 1 for the longest time. Tanks 1 to 4 are also filled with the leached liquid. The most concentrated solution is in tank 4 since it is in contact with the freshet solid. Fresh solvent is just added to tank 1.

Concentrated solution is withdrawn from tank 4. Liquid is transferred from tank 3 to 4, 2 to 3 and from 1 to 2. Fresh solid is added to tank 5 as shown in Figure 11.13(a).

Then the spent solid is discharged from tank 1 as shown in Figure 11.13(b). The liquid from tank 4 is transferred to tank 5, from 3 to 4 and from 2 to 3. Fresh solvent is added to tank 2. The conditions are now the same as during the start except that tank 1 has assumed the conditions of tank 5.

The system can be operated with any number of tanks and up to 16 tanks are in use. The tanks are also placed in a row called an *extraction battery* so that any number of tanks may be added or removed as per the requirement. The tanks can be arranged in cascade so that liquid can flow from one tank to the other by gravity with minimum use of pumping.

When the pressure drop for flow of liquid through the bed is too high for gravity flow, closed vessels called *diffusers* are used and the liquid is pumped through the bed of solids.

### ***Agitated vessels***

The slow and incomplete leaching in fixed beds with chances of channeling can be avoided by stirring the solid and the liquid in the leaching tank.

For coarse solids, agitated vessels may be closed vertical cylindrical vessels provided with paddles or stirrers on vertical shafts and false bottoms for drainage of leach solution at the end of leaching as shown in Figure 11.14. In other cases, the vessels are horizontal with stirrers mounted on horizontal shaft.

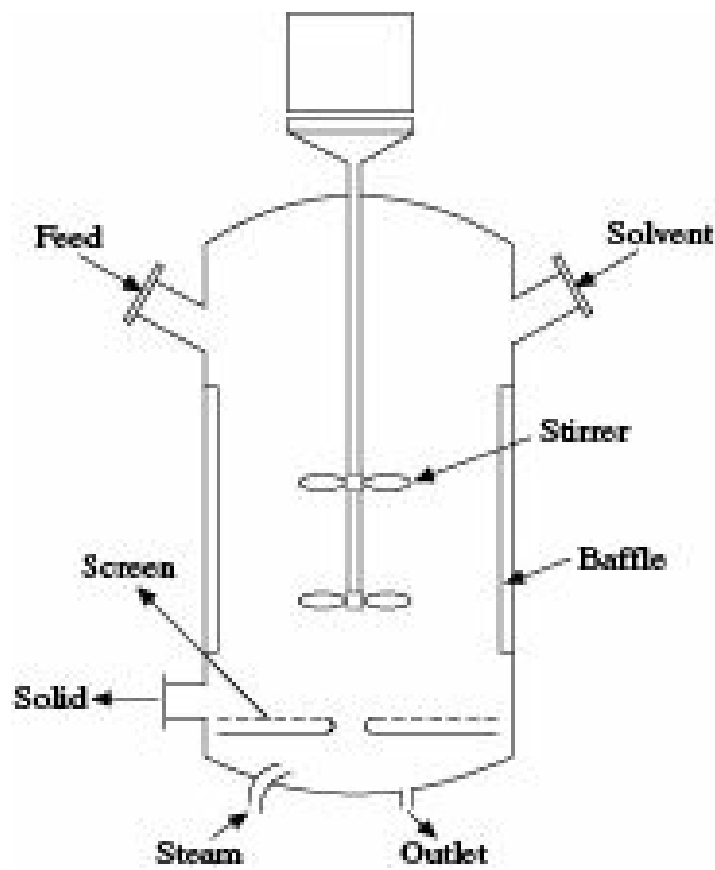


Figure 11.14 Agitated vessel.

### **Pachuca tanks**

*Pachuca tanks* are simple type of agitated vessels used for leaching finely divided solids which can be kept suspended in the leach solution by agitation. They are made of wood, metal or concrete and may have some inert lining. Agitation is done by mechanical agitators and/or air lift. The bubbles of air rising through the central tube cause upward flow of liquid and suspended solid which ultimately causes vertical circulation of the slurry (Lamont 1958). Standard mechanical agitators with turbine type impellers help in thorough mixing and also to keep the solids in suspension. On completion of leaching, agitation is stopped and the solids are allowed to settle either in the same vessel or in a separate one and the clear liquid from the top is removed by siphoning or otherwise. If necessary, several such tanks may be used with counter-current flow. A Pachuca tank is shown schematically in Figure 11.15. They find frequent use in metallurgical industries.

### **11.7.2 Steady-State Equipment**

Equipment for steady-state operation may be further grouped as stage-wise and continuous contact equipment. Several stage-wise equipment may also be arranged in multiple units to produce multistage effect. Continuous contact equipment usually provide several stages within a single equipment. The working principles of some commonly used steady-state equipment have been briefly discussed below.

#### ***Agitated vessel***

These are similar in design to the agitated vessels for batch operation but having arrangements for continuous flow of liquid and solid into and out of the tanks. Vessels with turbine type agitators are generally used.

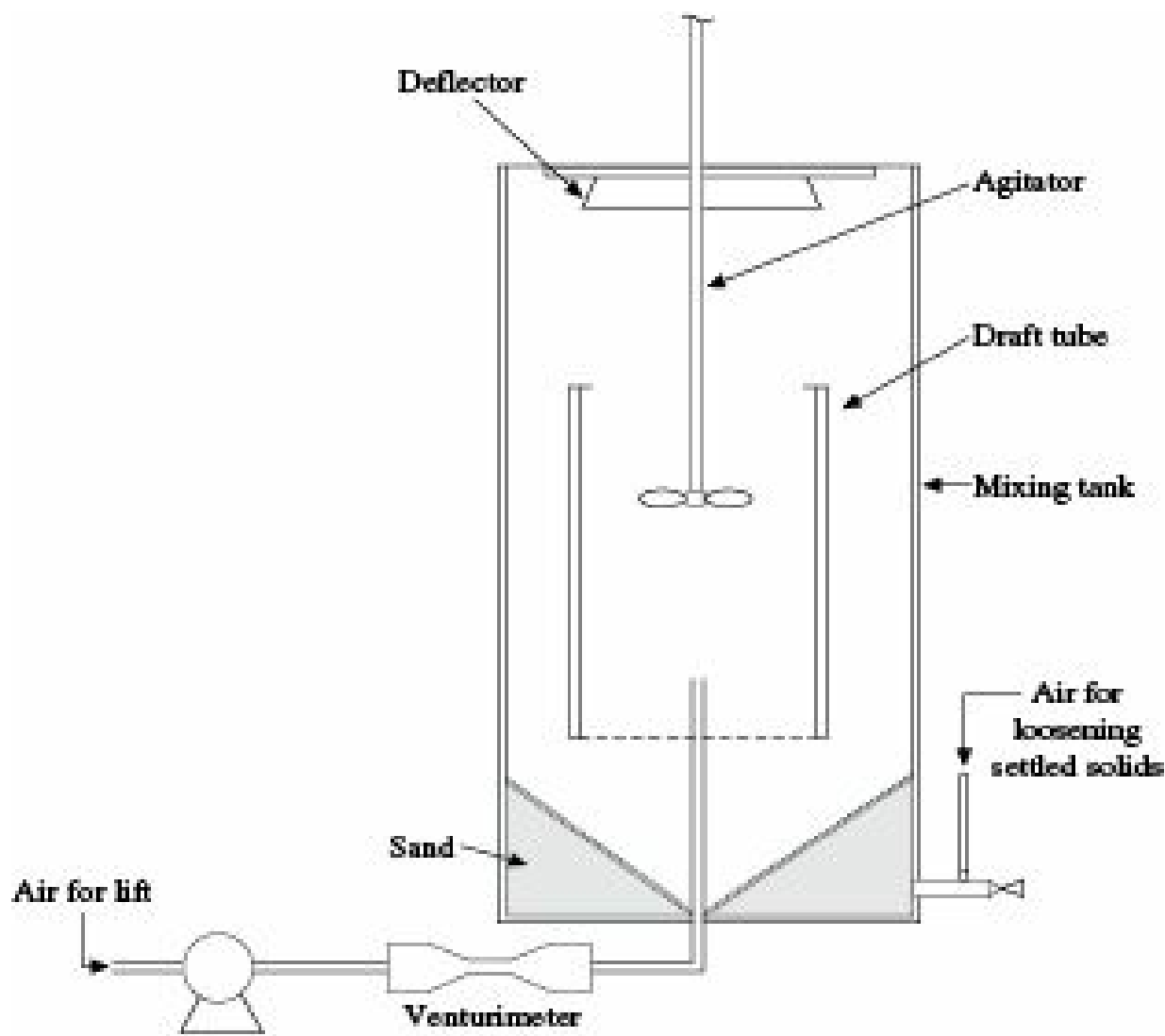


Figure 11.15 Pachuca tank.

The *Dorr Agitator* is also widely used in metallurgical and chemical industries for continuous leaching and washing of fine solids. It utilizes both air-lift and mechanical raking of settled solids. The central hollow shaft which acts as air-lift, rotates slowly and the arms attached to its bottom push the settled solids towards the centre of the tank bottom from where they are air lifted through the shaft and are then distributed by the launders at the top.

### **Thickeners—C.C.D. Units**

*Thickeners* are used to separate slurry of fine solids into clear liquid and a thickened sludge. These are frequently used to wash leached solids and chemical precipitates.

The slurry to be thickened is fed to the tank through the feed well at the top centre taking care to avoid its mixing with the clear liquid at the top. The diameter to height ratio of the tank is so adjusted that by the time the liquid from the centre reaches the periphery, the smallest or lightest solid to be removed, reaches the bottom. The settled sludge is pushed by the slowly rotating rakes to the central discharge cone from where they are removed by diaphragm pump. The clear liquid overflows to the launder at the upper periphery of the tank. The Dorr Thickeners vary widely in size, the diameter ranging from 2 to 180 m for handling granular as well as flocculant solids (Treybal 1985).

*Counter-current decantation units* consist of a cascade of thickeners for continuous counter-current washing of solids to free them from adhering solute. They are also used for washing solids formed by chemical reaction. In the simple arrangement shown in Figure 11.16, the solids to be leached and the solution from the second thicker are sent to the first agitator and then to the second agitator. The

strong solution produced there is decanted off from the solids in the first thickener. The sludge from the first thickener moves to the second thickener and then to the third thickener. The leached or washed solids are withdrawn from the third thickener to which fresh solvent is added. The solution moves counter-currently to the first thickener from where the strong solution is withdrawn.

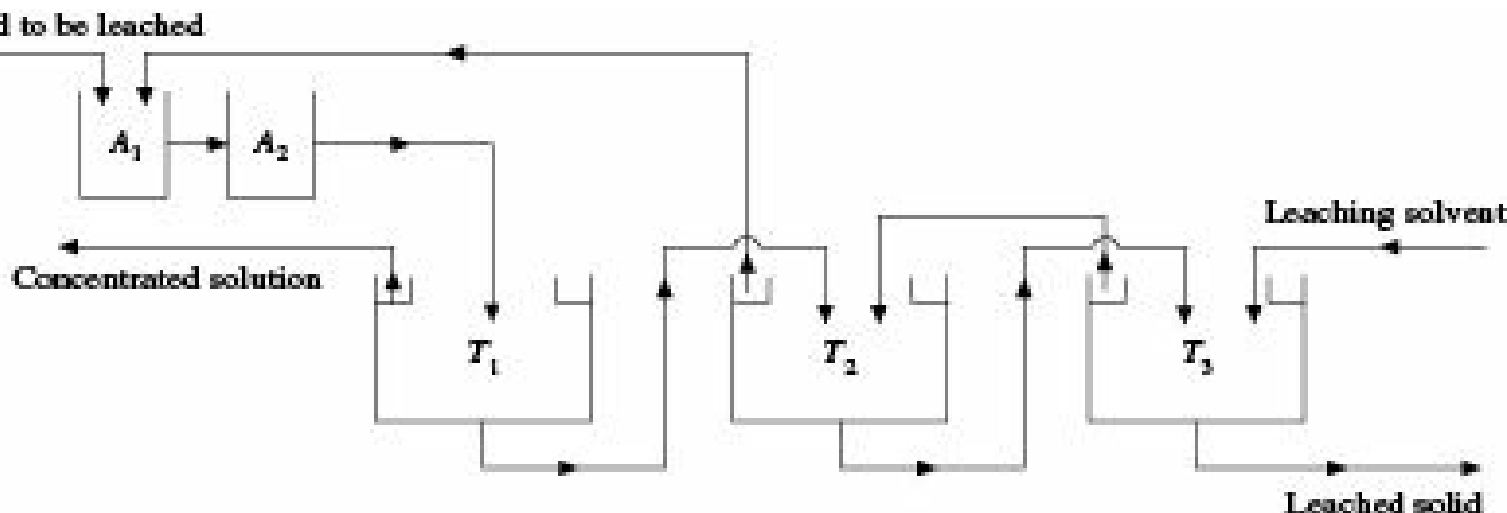


**Figure 11.16** Flow diagram of C.C.D. Unit.  $A$  is the agitator and  $T$  is the thickner.

### ***Rotocel***

A *Rotocel* shown in Figure 11.17 is a modification of the Shank's system and consists of a circular rotor with a number of cells usually 15 to 18, each having a hinged screen bottom for supporting the solids. The rotor rotates above a stationary compartmented tank. The feeding and discharging devices are at fixed points. When a cell comes under the feeder, it is filled with pretreated solids to be leached. The rotor then passes under a series of sprays from which solvent is periodically sprayed on the solids. The speed of the rotor is so adjusted that leaching or washing is complete within one revolution when the leached solids are automatically dumped into one of the lower stationary compartments from where they are removed. The solvent or solution percolates through the solids and the supporting screen into the corresponding compartment of the lower tank from where it is pumped into the appropriate spray (Anderson and McCubbin 1954).

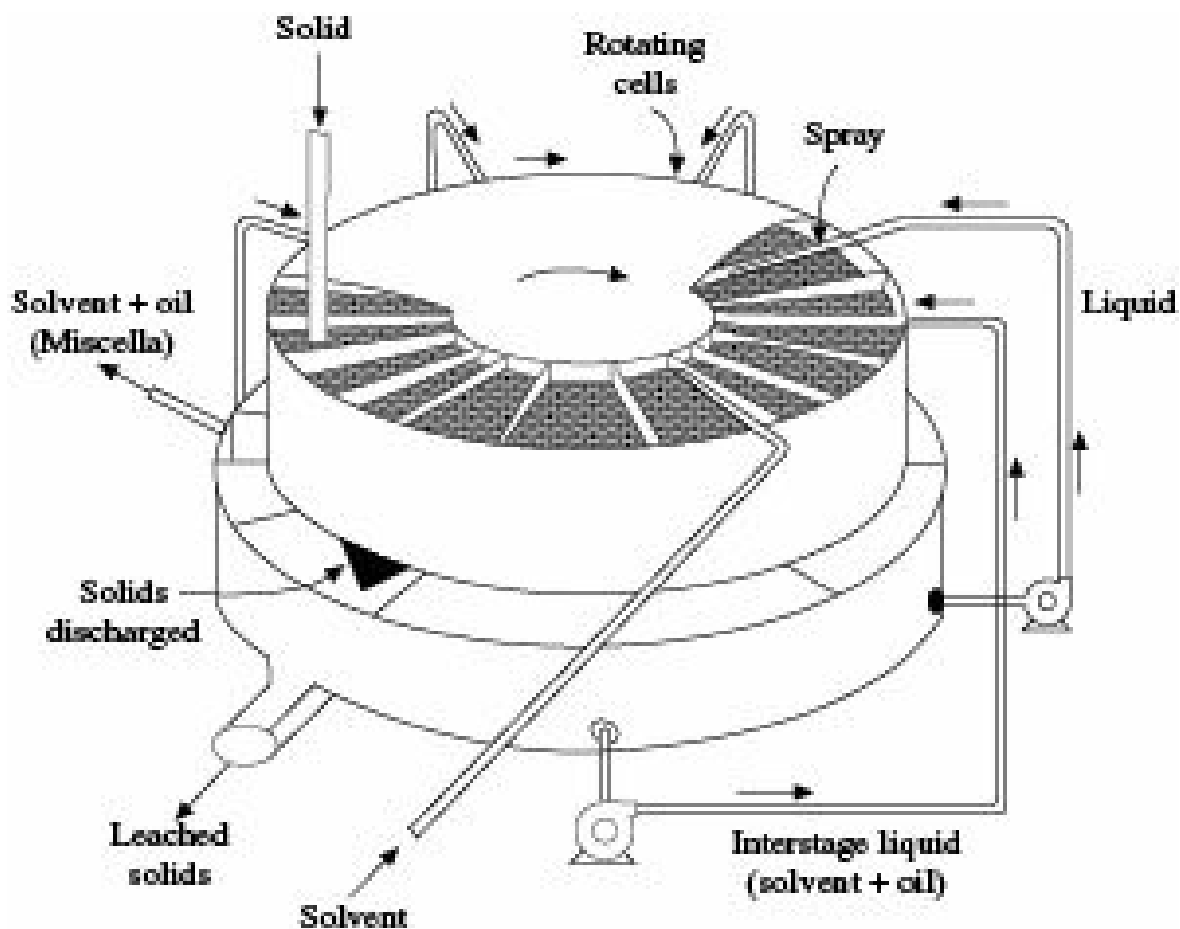


Figure 11.17 Rotocel extractor.

Leaching in a Rotocel is counter-current and the strongest solution is withdrawn from the freshest solids.

Rotocels are used for extraction of oils from seeds, for extraction of sugar from sugar beat and for removal of the soluble materials from leaves, bark, etc.

### Hilderbrandt extractor

The *Hilderbrandt extractor* consists of a U-shaped screw conveyor with three separate screws one each in the vertical sections and one in the horizontal section. The screws turn at different speeds to give considerable compaction of the solids in the horizontal section. The screws are perforated so that the solvent can pass through them. Solids are fed to one leg of the U and fresh solvent to the other so that counter-current flow occurs. The rich extract solution is withdrawn from near the top of the left leg and the leached solids are taken out from the other leg. A schematic diagram of Hilderbrandt extractor is shown in Figure 11.18.

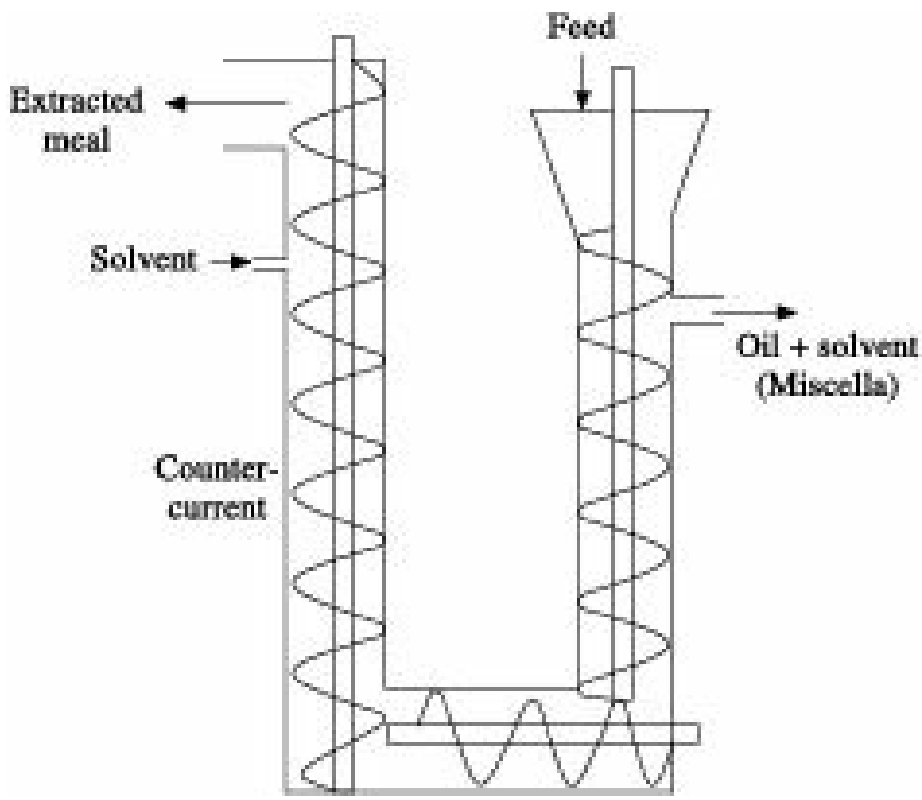


**Figure 11.18** Hilderbrandt extractor.

### **Bollman extractor**

A schematic diagram of a *Bollman extractor* is shown in Figure 11.19. The unit consists of a bucket elevator enclosed in a vapour tight casing. The lower horizontal part of the casing is divided into two chambers by a partition wall.

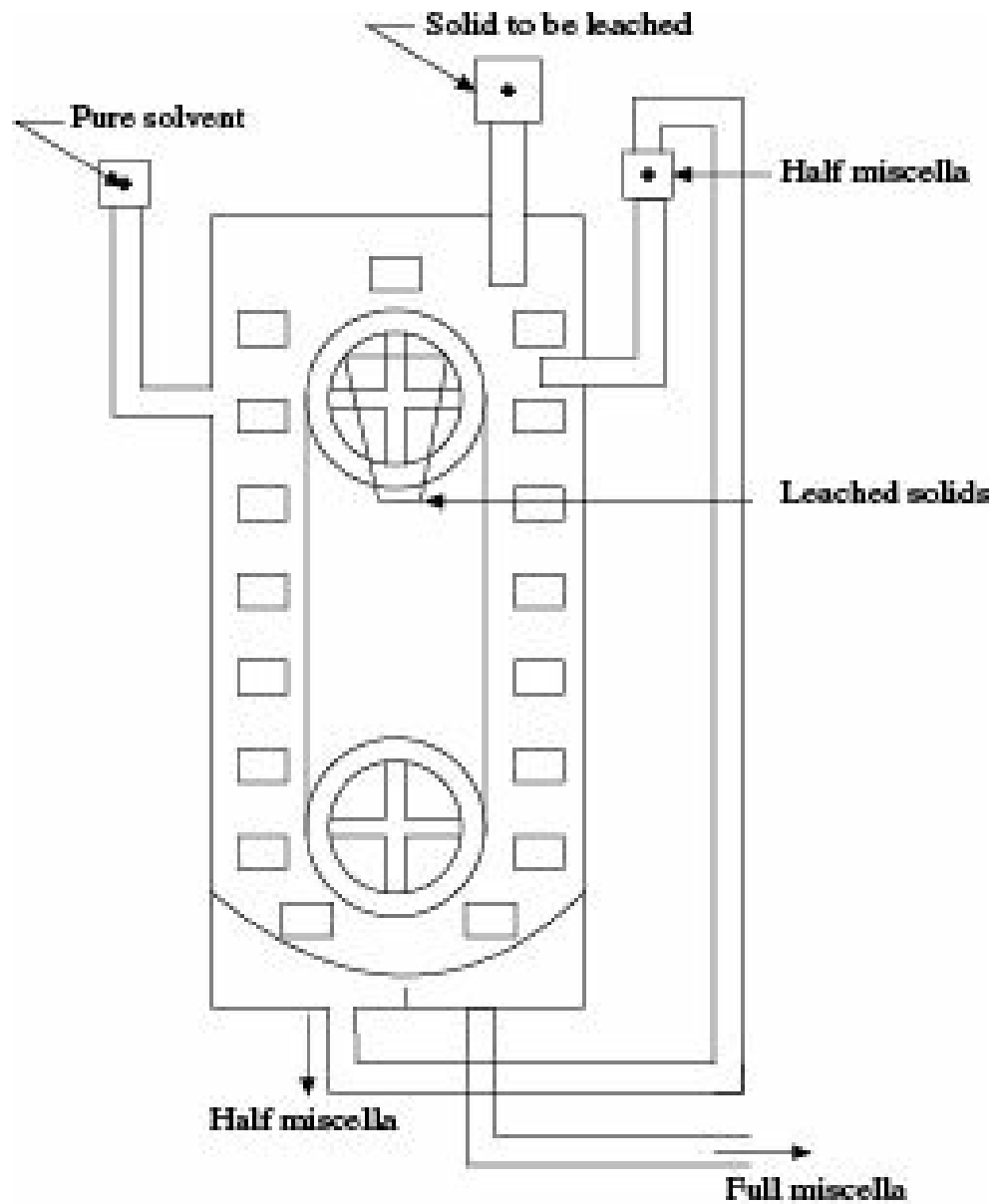


**Figure 11.19** Bollman extractor.

The buckets are usually 0.5 to 0.7 m deep and are provided with perforated bottoms (Schwartzberg 1980). A Bollman extractor may be 13 to 20 m high and can handle up to 50 tonnes of seeds per hour. The buckets are loaded with flaky solids like soyabeans at the top right corner and appropriate amount of partially used solvent with some extracted oil, called half-miscella is added along with the solids. As the solids and the solvent flow down co-currently, the solvent extracts more oil and full miscella or strong solution is pumped out from the right sump. As the buckets loaded with partially extracted solids move upward through the left leg, pure solvent fed at the top of the left leg, flow counter-currently through the solids and extract more oil. Fully extracted solids are collected from the buckets through a hopper at the top of the left leg. Half-miscella is collected from the bottom of the left leg and sent to the top of the right leg. Since there is no agitation, the solution is relatively clear.

### Bonotto extractor

The Bonotto extractor consists of a vertical column divided into a number of compartments by horizontal plates, each plate having a slot. Each plate also has a scraper. The scrapers are fixed to an axial shaft running through the column.

The solids, introduced at the top, move down from plate to plate by the action of the scrapers. The solvent is introduced at the bottom, flows upwards through the beds of solid on the plates and leave

near the top. A small portion of the column near the top is slightly enlarged to decrease the velocity of the extract solution in order to reduce entrainment of fine solids along with the liquid.

A schematic diagram of a Bonotto extractor is shown in Figure 11.20.

### Kennedy extractor

The Kennedy extractor (Scofield 1951) shown in Figure 11.21, is a stage-wise extractor used for extraction of oil from oil-seeds and other chemical leaching.

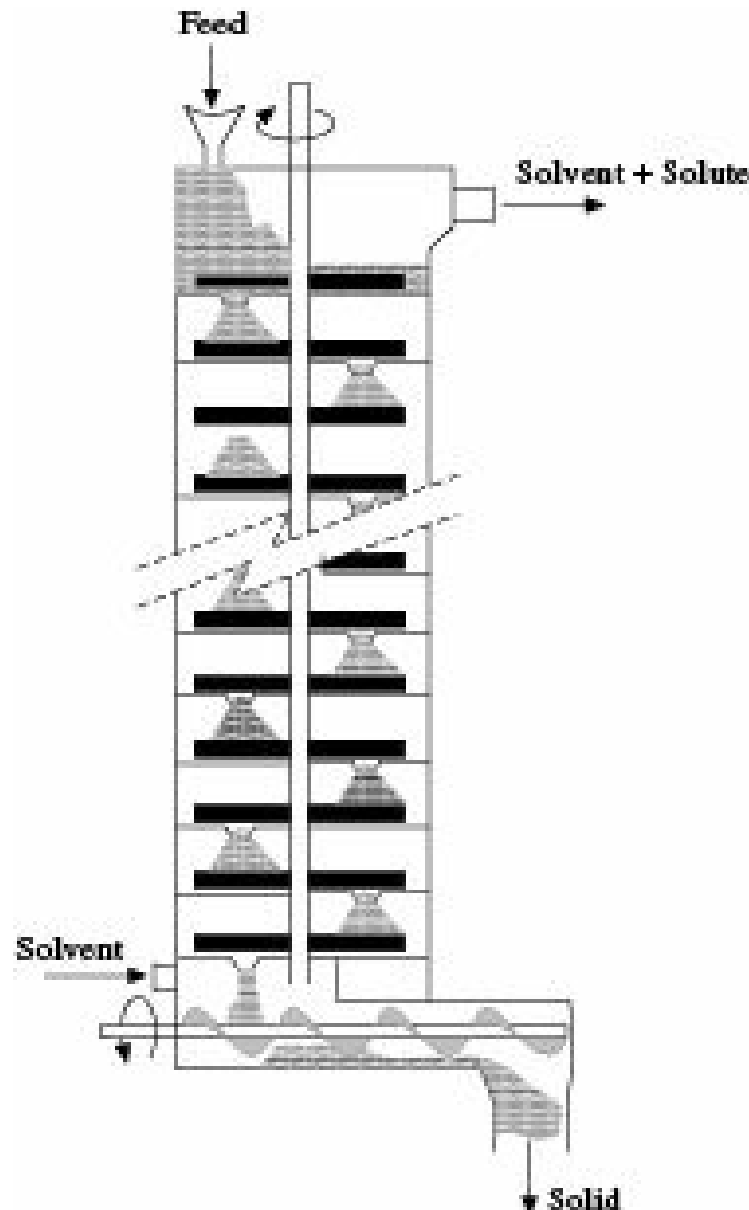


**Figure 11.20** Bonotto extractor

In this type of extractor, the solids are leached in a series of tubs arranged in a cascade and are pushed from one tub to the next higher one by paddles while the solvent flows counter-currently. Perforations in the paddles facilitate drainage of solids between stages and the solids are scraped from each paddle. The number of tubs in a cascade can be changed according to the requirement.

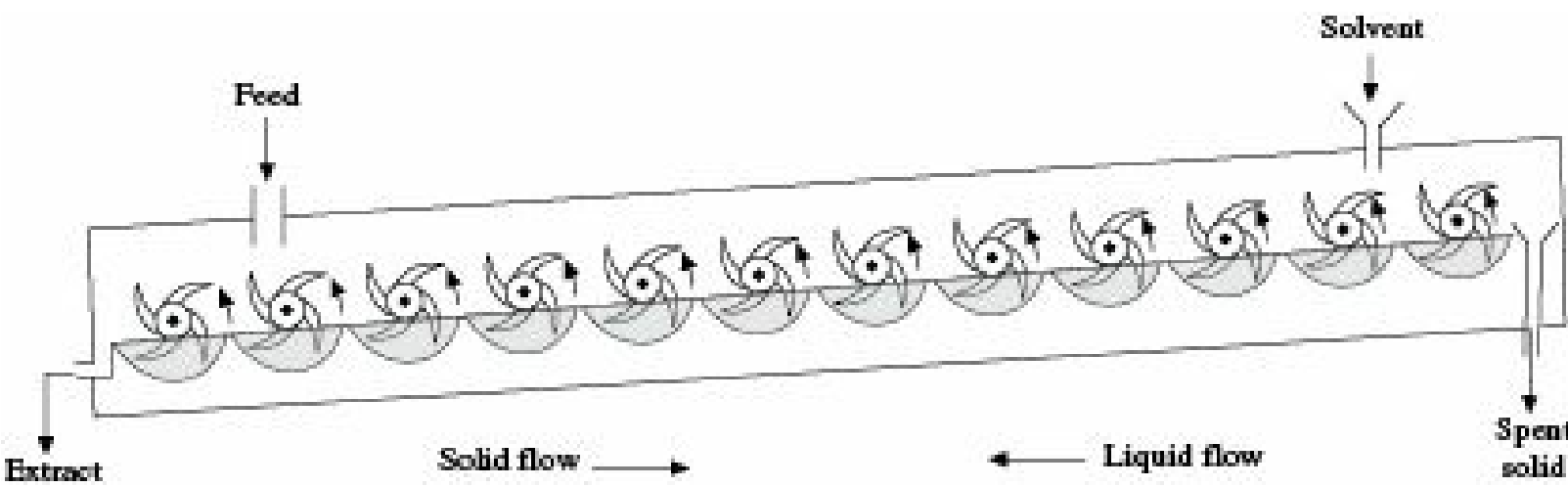


Figure 11.21 Kennedy extractor.

## Nomenclature

$A$  : insoluble carrier solid, M (batch),  $M/L^2\square$  (continuous)

$B$  : pure leaching solvent, M (batch),  $M/L^2\square$  (continuous)

$c$  : solid concentration in slurry,  $M/L^3$

$C$  : soluble solute

$E$  : solvent and solute associated with the leached solids, M (batch),  $M/L^2\square$  (continuous)

$F$  : solute and solvent in solids to be leached, M (batch),  $M/L^2\square$  (continuous)

$m$  : slope of the equilibrium curve,  $dx^*/dy$

$M$  : solvent and solute content of a slurry or mixture, M or  $M/L^2\square$

$N$  : number of stages

$P$  : difference point defined by Eq. (11.13)

$R$  : leached solids, M or  $M/L^2\square$

$S$  : concentration of insoluble  $A$  in any slurry or mixture

$x$  : weight fraction of solute  $C$  in solid or slurry on A-free basis

$y$  : weight fraction of solute  $C$  in solvent or effluent on A-free basis

## Subscripts

$F$  : feed, solids to be leached

$s$  : saturated

1, 2, etc. Stage 1, Stage 2, etc.

## Numerical Problems

### 11.1 Determination of the Amount of NaOH, % of Extraction of NaOH, and the Content of NaOH in

Feed: A vertical settling tank with a conical bottom contains sediment and  $7\text{ m}^3$  of a solution in which 2 tonnes of NaOH are dissolved. After settling, the transparent part is poured out in an amount of  $6\text{ m}^3$ , pure water is added to the settling tank, and the suspension is agitated. After repeated settling,  $6\text{ m}^3$  of the clean solution are again poured out. Three solutions poured out

from the settling tank are mixed and fed for evaporation. Determine (i) the amount of NaOH remaining in the sediment (slurry), (ii) the percent of extraction of NaOH, and (iii) the content in percent of the NaOH in the solution fed for evaporation.

[Ans: (i) 5.8 kg, (ii) 99.7%, (iii) 10%]

**11.2 Estimation of Number of Stages:** Determine the number of extraction stages in the conditions stated in Problem 11.1 if the extraction factor of the NaOH equals 0.98.

[Ans: 2 stages]

**11.3 Estimation of Number of Stages in Counter-Current Battery for Extraction of Copper:** To extract copper, pyrite cinders are subjected to chlorinating roasting with sodium chloride. The copper is contained in the roasted material in the form of cupric chloride ( $CuCl_2$ ) whose content is 11%. The roasted product is leached in a counter-current battery using acidified water obtained as a result of washing the flue gases. The inert solid material retains 2 kg of water per kg. of solid. Equilibrium is reached in each stage. How many stages are needed in the battery to produce a solution containing 12% (mass) of  $CuCl_2$  and extract 98% of the copper from the roasted product? [Ans: 11 stages]

**11.4 Estimation of the Number of Stages in the Extraction with Changed Value of  $CuCl_2$  in Extract and also Extraction Factor:** Determine the number of stages required in the conditions as in Problem 11.3 if the content of  $CuCl_2$  in the extract equals 9% (mass), and the extraction factor of the copper is 92%.

[Ans: 6 stages]

**11.5 Determination of the Amount of Water Required as Solvent and also the Number of Stages in a Counter-Current Battery for Extraction of Sodium Hydroxide:** A counter-current extraction battery is used to extract sodium hydroxide from the products of the reaction



The feed contains water in an amount equal to half the mass of the sediment ( $CaCO_3$ ). The battery extracts 95% of the NaOH, and a 15% solution is obtained. How much water should be fed to the battery as solvent and how many stages should the battery have? It is known from experimental data that the sediment retains the solution in the following amounts depending on the NaOH content in it:

Content of NaOH, % (mass):	0	5	10	15	20
Solution retained per kg of sediment, kg:	1.39	1.72	2.04	2.70	3.85.

[Ans: 565 kg, 3 stages]

**11.6 Processing of Barium Sulphide in a Five-Stage Counter-Current Battery: loss of  $Na_2S$ , Amount of Water Required as Solvent and Concentrations in Each Thickener:** A plant processes 10 tonnes of barium sulphide a day with the corresponding amount of soda and 35 tonnes of water to produce barium carbonate and a solution of sodium sulphide. A five-stage counter-current battery is used. During the process, the barium carbonate sediment retains double (by mass) its own mass of water. The processing results in a 10% solution of sodium sulphide. It is desired to achieve 98% of sodium sulphide extraction. Determine (i) the loss of sodium sulphide in the residue, (ii)

the amount of water that must be added as solvent, and (iii) the concentrations in each thickener.

[Ans: (i) 0.1 tonne or 2% (ii) 28.8 tonne (iii) I-10%, II-7.9%, III-6.1%, IV-4.7%, V-3.6%]

**11.7 Extraction of Oil from Sunflower Seeds using Benzene as Solvent:** Amount of Extract and of Solution Retained by the Solid along with Their Oil Contents, and also the Number of Stages: An oil-extracting plant processes 1 tonne/hr of meal (crushed and partially degreased sunflower seeds) containing 28% of oil and 2.5% of benzene. The solvent is the regenerated benzene containing 1.5% of oil and fed in an amount of 50% of the mass of the meal. Experiments show that the amount of solution retained by the solid phase depends on the oil content in it:

Oil content, kg/kg of solution	Solution retained, kg/kg of solid	Oil content, kg/kg of solution	Solution retained, kg/kg of solid
0.0	0.500	0.4	0.550
0.1	0.505	0.5	0.571
0.2	0.515	0.6	0.595
0.3	0.530	0.7	0.620

The solid residue after extraction contains 5% of oil. Determine (i) the amount of extract and its oil content, (ii) the amount of solution retained by the soild phase (meal cake) and the oil content in it, and (iii) the number of leaching stages.

[Ans: (i) 483 kg/hr, 50.4% (ii) 322 kg/hr, 11.7% (iii) 7 stages]

**11.8 Determination of the Amount of Oil in the Vegetable Oil Seeds after Leaching with Organic Solvent:** Vegetable oil seeds containing 100 g insoluble solid and 10 g oil are contacted with 200 g of organic solvent in a single-stage leaching operation. The solvent is fresh. Determine the amount of oil left in the oil seeds after leaching. The equilibrium data can be expressed as  $N = -4y + 8$

where

$$N = [(g \text{ insoluble})/(g \text{ solvent} + g \text{ oil})]$$

$$y = [(g \text{ oil})/(g \text{ solvent} + g \text{ oil})] \text{ in the seed phase, and}$$

$$x = [(g \text{ oil})/(g \text{ solvent} + g \text{ oil})] \text{ in the solvent phase.}$$

The tie line data are:

y:	0.26	0.28	0.31	0.34
x:	0.02	0.04	0.06	0.08

[Ans: 3.9 g]

**11.9 Estimation of the Number of Stages in a Continuous Counter-current Extraction Battery using Overall Efficiency:** 60 tonnes/day of oil sand (25 mass% oil and 75 mass% sand) is to be extracted with tonnes per day of naphtha in a continuous counter-current extraction battery. The final extract from the battery is to contain 40 mass% oil and 60 mass% naphtha, and the underflow from each unit is expected to consist of 35 mass% solution and 65 mass% sand if the overall efficiency of the battery is 50%. How many stages will be required?

[Ans: 5 stages]

### **Short and Multiple Choice Questions**

1. What is decoction? Give two examples.
2. Why practical equilibrium data are used in leaching?
3. Why triangular diagrams are not generally used in graphical solution of leaching problems?

- 4.** What will be the nature of equilibrium curve in leaching if the solute has a limited solubility in the solvent?
- 5.** Name three factors on which rate of leaching depend.
- 6.** What are the reasons of carrying out leaching operations at elevated temperatures?
- 7.** State briefly the steps to be followed in graphical solution for single stage leaching.
- 8.** What are the steps to be followed in graphical solution for number of stages in continuous counter-current leaching?
- 9.** The Bollman extractor  
(a) is a static bed leaching equipment  
(b) is a centrifugal extractor  
(c) is used for extraction of oil from oil seeds  
(d) employs only counter-current leaching
- 10.** Rate of leaching increases with increasing  
(a) temperature (b) pressure  
(c) viscosity of solvent (d) size of the solid
- 11.** Other conditions remaining the same, if the fractional retention of solution in the underflow increases then the number of ideal stages required for a counter-current washing operation  
(a) increases  
(b) decreases  
(c) remains the same  
(d) cannot be determined
- 12.** Which of the following operations does not involve leaching?  
(a) dissolving gold from its ores  
(b) dissolving sugar from sugar beat  
(c) removing nicotine from its aqueous solution by kerosene  
(d) dissolving pharmaceutical products from bark
- 13.** Which of the following factors does not affect stage efficiency in a leaching operation?  
(a) time of contact between the solid and the solvent  
(b) rate of diffusion of the solute from solid to liquid  
(c) size of the solid  
(d) vapour pressure of the solution
- 14.** Leaching of sugar from sugar beat is done by  
(a) dilute sulphuric acid  
(b) hot water  
(c) lime water  
(d) hexane
- 15.** Which solvent will you recommend for the extraction of  
(a) copper from roasted copper ore  
(b) gold from its ore  
(c) oil from peanut cake  
(d) coffee from roasted coffee beans

- 16.** Higher temperature increases the rate of extraction in solid-liquid system due to  
(a) increased liquid viscosity and decreased diffusivity  
(b) increased liquid viscosity and increased diffusivity  
(c) decreased liquid viscosity and decreased diffusivity  
(d) decreased liquid viscosity and increased diffusivity

- 17.** If the solute concentrations on solid-free basis in the overflow and underflow are equal, the tie lines are  
(a) vertical      (b) inclined  
(c) horizontal      (d) of varying slopes

- 18.** Which equipment will you recommend for the extraction of  
(a) oil from oil-seed  
(b) sugar from sugar beat  
(c) pharmaceutical from plant leaves  
(d) copper from roasted copper ore

*Answers to Multiple Choice Questions*

9. (c)      10. (a)      11. (a)      12. (c)      13. (d)      14. (b)      15. (a)  
16. (d)      17. (a)

**References**

- Anderson, E.T. and K. McCubbin, *J. Am. Oil Chem. Soc.*, **31**, 475 (1954).  
Ciminelli, V.S.T., O. Garcia Jr., M.C. Teixeira, R.P. de Carvalho and P.F. Pimentel, *Biohydrometallurgy—Fundamentals, Technology and Sustainable Development*, Part A, Elsevier (2001).  
Lamont, A.G.W., *Canad. J. Chem. Eng.*, **36**, 153 (1958).  
Rickles, R.N., *Chem. Eng.*, March **15**, 157 (1965).  
Schwartzberg, H.G., *Chem. Eng. Prog.*, 67 (April 1980).  
Scofield, E.P., *Chem. Eng.*, **58(1)**, 127 (1951).  
Souders, M. and G.C. Brown, *Ind. Eng. Chem.*, **24**, 519 (1932).  
Treybal, R.E., *Mass Transfer Operations*, 3rd ed., McGraw Hill, Singapore (1985).

# 12

## Drying

### 12.1 Introduction

Drying may be defined as removal of a liquid from a wet solid or suspension or solution by vaporisation into a gas to get a relatively liquid-free substance. Drying is frequently practiced in many industrial operations, particularly in the chemical industry. For instance, sugar crystals are dried before packaging, soaps are dried before marketing, and the drying of leather under controlled conditions is an important step in the leather processing. During drying the material to be dried is brought into contact with a hot gas in which the partial pressure of the liquid is less than the equilibrium value corresponding to the liquid in the material to be dried. The hot gas serves dual purpose: on one hand it provides the energy required for the drying and, on the other hand, it carries away the evaporated liquid.

Drying may be carried out under different conditions depending upon the requirement of the situation. Thus, heat sensitive materials are dried under vacuum, direct contact of the material to be dried, and the hot gases are to be avoided if there are chances of over heating or contamination.

Drying does not include the removal of moisture by mechanical means such as filtration, centrifuging, etc. or by boiling a solution in the absence of a gas. In most cases generally encountered in practice, the liquid is water and the gas is air. Our discussion will therefore be limited to this combination.

### 12.2 Drying Equilibria

Driving force in drying generally being the difference in vapour pressure exerted by moisture present in the material to be dried and the partial pressure of moisture in the surrounding air, equilibrium relations are usually expressed in terms of these two quantities.

Moisture present in a wet solid exerts a vapour pressure which depends on the moisture, the temperature and the nature of the solid. If a solid is exposed to air containing moisture, the solid will be dried by loosing moisture if the partial pressure of moisture in the air is less than the vapour pressure exerted by the moisture in the solid. If on the other hand, the partial pressure of moisture in the air is higher, the solid will absorb moisture from the air. When the vapour pressure exerted by the moisture in the solid is the same as the partial pressure of moisture in the surrounding air, there will be no net transfer of moisture and the solid will have equilibrium moisture content. Drying can theoretically proceed only up to the equilibrium moisture content.

Equilibrium data for drying are usually expressed in the form of moisture content of the solid as a function of relative saturation or relative humidity ( $p'/p$ ) of the surrounding air. Equilibrium moisture contents of a few solids have been shown in Figure 12.1.

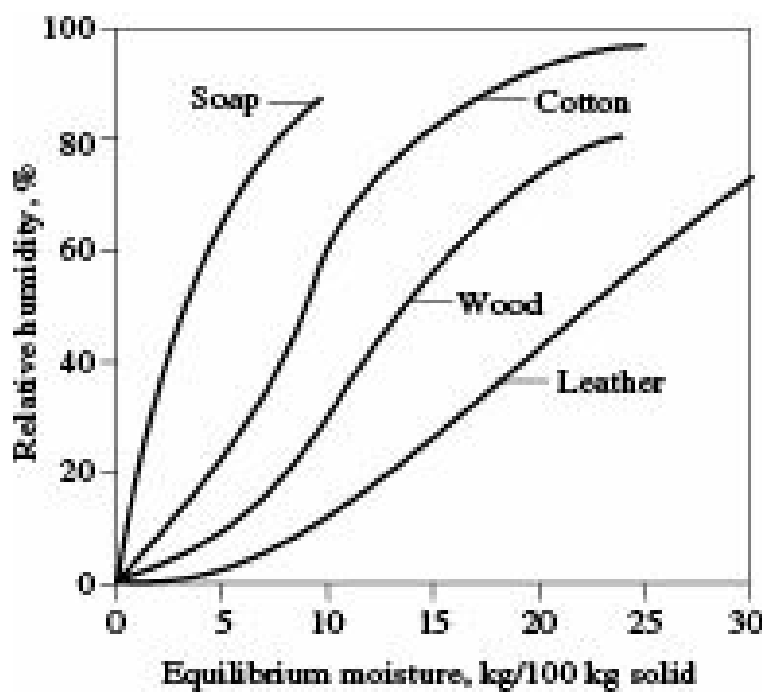


**Figure 12.1** Equilibrium moisture content of solids as function of relative humidity.

Several solids exhibit hysteresis. Their equilibrium moisture characteristics vary depending upon whether equilibrium is reached by condensation or by evaporation of moisture (Figure 12.2).

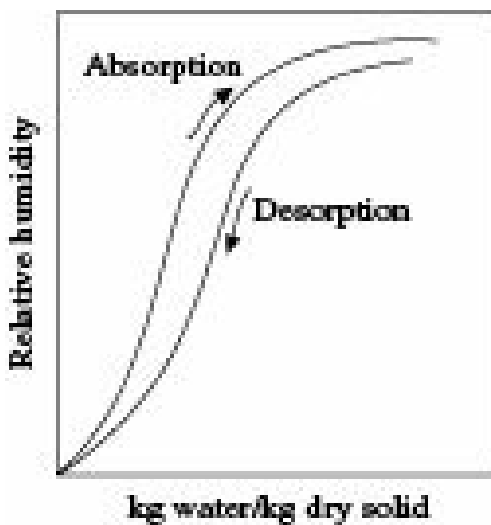


**Figure 12.2** Equilibrium moisture content of a solid exhibiting hysteresis.

Solids which are soluble in moisture, show insignificant equilibrium moisture content when exposed to air having partial pressure of moisture less than the vapour pressure of the saturated solution of the solid. If, on the other hand, the partial pressure of moisture in air is higher than the vapour pressure of a saturated solution of the solid, the solid will absorb sufficient moisture to get dissolved, a phenomenon known as *deliquescence*.

## 12.3 Some Important Terminologies

**Bone-dry solid:** A solid without any moisture in it is called *bone-dry* solid. This is an ideal situation since as soon as a bone-dry solid is brought into contact with humid air, it absorbs moisture till equilibrium is established.

**Moisture content on dry basis:** Moisture content is generally expressed as weight fraction or weight percent. Moisture content on dry basis is defined as kg moisture per kg dry solid ( $X$ ). Percentage moisture on dry basis is  $100X$ .

**Moisture content on wet basis:** Moisture content on wet basis is the amount of moisture per unit amount of wet solid,  $[(\text{kg moisture})/(\text{kg dry solid} + \text{kg moisture})] = [X/(1 + X)]$ , where  $X$  is the moisture content on dry basis. Unless otherwise stated, moisture content means on wet basis and is expressed in percentage.

**Equilibrium moisture content( $X^*$ ):** This is the moisture content of a substance in equilibrium with a given partial pressure of moisture in the surrounding air. It, therefore, depends on the condition of the surrounding air.

**Free moisture:** This is the moisture present in a substance in excess of the equilibrium moisture content,  $(X - X^*)$ . Only free moisture can be removed during drying under a given set of operating conditions.

**Critical moisture:** This is the moisture content of a substance at which drying rate changes from constant rate to falling rate (Section 12.5).

**Bound moisture:** The moisture contained by a substance, which exerts an equilibrium vapour pressure less than the vapour pressure of pure water at that temperature is called *bound moisture*.

**Unbound moisture:** The moisture contained by a substance that exerts an equilibrium vapour pressure equal to that of pure water at that temperature is known as *unbound moisture*.

The distinction between bound and unbound moisture is shown in Figure 12.3.

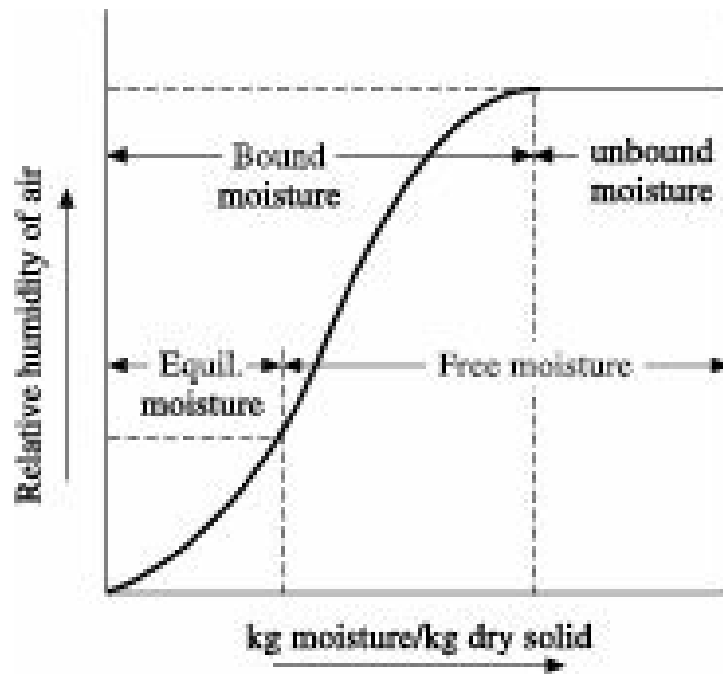


Figure 12.3 Bound and unbound moisture.

## 12.4 Mechanism and Theory of Drying

In order to design commercial driers and fix up the drying conditions, it is necessary to determine the rate of drying and study the effects of different operating parameters on such rate. In the absence of adequate theoretical knowledge, such data are often based on experimental studies.

The rate of drying of a solid can be determined in the laboratory by suspending a sample of the solid from a balance in a cabinet through which a stream of hot air at constant temperature and humidity is circulated. The weight of the solid is noted at regular intervals of time. At the end of drying, the dry weight of the sample should also be noted. In order to have reliable data, the drying conditions during the experiment, namely, the ratio of drying to nondrying surface, radiant heat transfer conditions, mode

of supporting the sample as well as the temperature, humidity, speed and direction of the drying air should be as close as possible to those expected to prevail in the commercial equipment. Drying in air of constant temperature, humidity and velocity is known as drying under *constant drying conditions*.

## 12.5 Drying Rate Curve

A preliminary curve with moisture content of the solid as a function of time can be plotted from the test data as shown in Figure 12.4.

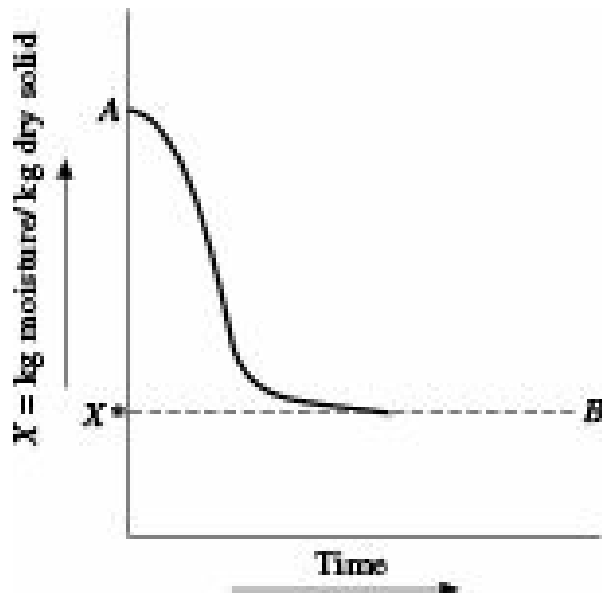


**Figure 12.4** Moisture content of a solid as function of time during batch drying under constant conditions.

This curve can be directly used for determining the time required for drying larger batches under the same drying conditions. However, it is convenient to convert this curve into drying rate curve by plotting drying rate (mass per unit time per unit area) against moisture content and then developing appropriate equations for drying rate. A typical drying rate curve is shown in Figure 12.5. This curve may be drawn by measuring the slopes at different points of the curve AB in Figure 12.4 and plotting them against moisture content.

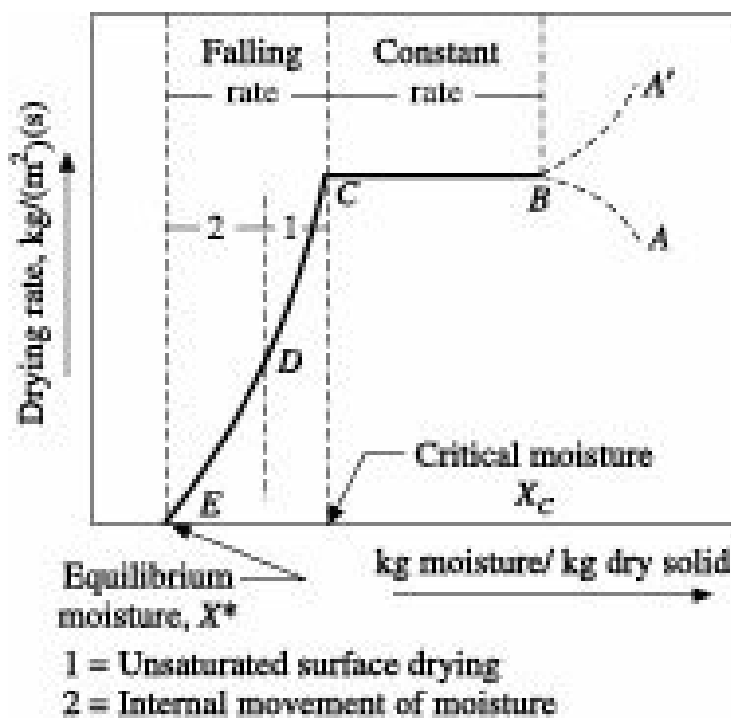


Figure 12.5 Drying rate curve.

Alternatively, the drying rate curve may be drawn by measuring small changes in moisture content DX and the corresponding time Di, and then plotting (DX/Di) as a function of moisture content:

$$R = -\frac{M_S}{A} \frac{\Delta X}{\Delta t} \quad (12.1)$$

where

$R$  = drying rate in mass (amount of moisture) per unit time per unit area

$A$  = drying area, and

$M_S$  = mass of the solid.

It may be seen from Figure 12.5 that the drying rate curve has two distinct parts—the constant rate period and the falling rate period.

### 12.5.1 Constant Rate Period

If a solid with large amount of moisture is exposed to relatively dry air, evaporation of unbound moisture will take place from the surface, the rate of which can be expressed as

$$R_e = k_y(Y_S - Y) \quad (12.2)$$

where,

$R_e$  = rate of evaporation,  $\text{kg}/(\text{m}^2 \cdot \text{s})$

$k_y$  = mass transfer coefficient,  $\text{kg}/(\text{m}^2 \cdot \text{s}) (\square Y)$

$Y_S$  = saturated humidity at surface temperature

$Y$  = humidity of air.

Under constant drying conditions,  $k_y$ ,  $Y_S$  and  $Y$  are constant. The drying rate  $R_e$  therefore remains constant. The capillaries and interstices within the solid being filled up with water can supply the same at a rate fast enough to maintain the constant rate of evaporation at the surface. There may, however, be some initial adjustment at the beginning of drying. If the solid is introduced into the drier at a temperature lower than that prevailing within the drier, its temperature and the rate of evaporation

will rise along  $AB$  before becoming constant as shown in Figure 12.5. If, on the other hand, the temperature of the solid is higher than that within the drier, the temperature and rate of drying will decrease along  $A'B$  before assuming the constant value. The period of initial adjustment is usually very small and can be neglected without any serious error.

The *falling rate period* of drying starts as soon as the critical moisture content is reached and the drying rate decreases with time. There is depletion of moisture at the surface and moisture has to diffuse from within the solid.

The nature of drying during falling rate period and the different theories of moisture diffusion has been discussed later in this chapter.

### 12.5.2 Cross Circulation Drying

During constant rate period of drying, there is a balance between heat supplied to the solid surface and heat required for evaporation.

Figure 12.6 shows a section of a solid being dried in a stream of air with cross circulation of air. Evaporation takes place from the upper surface of the solid having an area  $A$  and a temperature  $t_S$ .

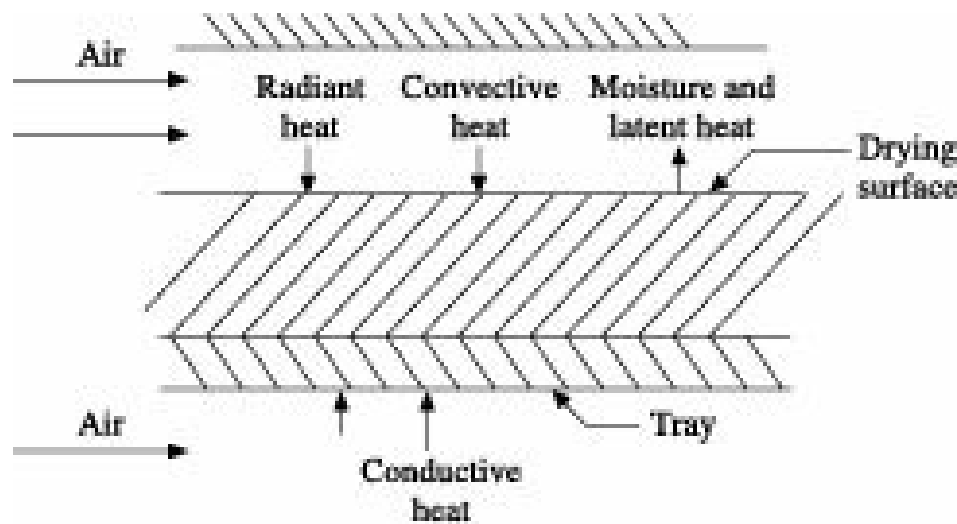


Figure 12.6 Drying with cross circulation of air.

The drying surface may receive heat by convection ( $q_C$ ) from the air, by conduction through the solid ( $q_k$ ) and by radiation from the hot surface of the drier ( $q_R$ ).

Neglecting the small amount of heat required to superheat the evaporated moisture from the surface temperature to the air temperature, the rate of evaporation  $R_C$  is given by

$$R_C m_S = q = q_C + q_k + q_R \quad (12.3)$$

where,  $q_C = h_C(t_G - t_S) \quad (12.4)$

$$q_k = U_k(t_G - t_S) \quad (12.5)$$

and  $q_R = f(5.729 \times 10^{-8})(T_R^4 - T_S^4) = h_R(t_R - t_S) \quad (12.6)$

$$\frac{f(5.729 \times 10^{-8})(T_R^4 - T_S^4)}{t_R - t_S}$$

where,  $h_R = \frac{f(5.729 \times 10^{-8})(T_R^4 - T_S^4)}{t_R - t_S} \quad (12.7)$

and  $m_S$  is the latent heat of vaporisation of water at temperature of the solid surface,  $t_S$ .

$U_k$  in Eq. (12.5) can be estimated from appropriate conduction equation. If the convection coefficient, thermal conductivities of the tray material and the solid being dried as well as areas of the solid being dried and the nondrying surface are known, we have from Eqs. (12.3) to (12.6),

$$R_C = \frac{q}{\lambda_s} = \frac{(h_c + U_k)(t_G - t_S) + h_R(t_R - t_S)}{\lambda_s} = k_y(Y_S - Y) \quad (12.8)$$

The above equation can be used provided the surface temperature  $t_S$  is known for which Eq. (12.8) can be rearranged to give

$$\frac{(Y_S - Y)\lambda_s}{h_c/k_y} = \left(1 + \frac{U_k}{h_c}\right)(t_G - t_S) + \frac{h_R}{h_c}(t_R - t_S) \quad (12.9)$$

For air-water vapour system, the ratio  $h_C/k_y$  may be taken as equal to the humid heat  $C_S$  of the air. During evaporation of unbound moisture,  $Y_S$  is the saturated humidity of the air stream corresponding to the temperature  $t_S$  and both these quantities can be determined by solving Eq. (12.9) simultaneously with the saturated humidity curve on the psychrometric chart.

If conduction through the solid and radiation effects is absent, Eq. (12.9) reduces to that for wet-bulb thermometer and the surface temperature of the drying solid becomes the same as the wet bulb temperature of the drying air.

For flow of gas parallel to solid surface and confined between parallel plates, as between trays in a tray drier with Reynold's number between 2600 and 22000, the transfer co-efficients  $h_C$  and  $k_y$  can generally be expressed as under by equating  $j_H$  and  $j_D$

$$j_H = \frac{h_c}{C_p G} Pr^{2/3} = j_D = \frac{k_y}{G_s} Sc^{2/3} = 0.11 Re^{-0.29} \quad (12.10)$$

where,  $Re = (d_e G/n)$ ,  $d_e$  being the equivalent diameter of the space through which the air or gas is flowing.

With properties of air at 95°C, Eq. (12.10) becomes (Treybal 1985)

$$h_C = 5.90 \frac{G^{0.71}}{d_e^{0.29}} \quad (12.11)$$

Shepherd et al. (1938) suggested the following relation for estimating  $h_C$  during drying of sand in tray driers:

$$h_C = 14.3 G^{0.8} \quad (12.12)$$

The discrepancies between Eqs. (12.11) and (12.12) have been attributed to the variations in several factors such as length of calming sections, differences in leading edges of the drying surfaces, etc.

In case of air flow perpendicular to the drying surface and  $G = 1.08$  to  $5.04 \text{ kg}/(\text{m}^2\text{s})$ , Molstad et al. (1938) have suggested the following expression for  $h_C$

$$h_C = 24.2 G^{0.37} \quad (12.13)$$

The drying rate during constant rate period may be directly estimated from Eqs. (12.8) to (12.13).

These are, however, not as reliable as data from properly conducted experiments. On the basis of the above equations, effects of some important parameters on the rate of drying can be determined.

**Effect of gas velocity:** If conduction through the solid and radiation are neglected, the drying rate becomes proportional to  $G^{0.71}$  for parallel flow and to  $G^{0.37}$  for perpendicular flow. If conduction and radiation are present, effect of air rate will be less important.

**Effect of gas temperature:** Increased air temperature increases the quantity  $(t_G - t_S)$  and hence increases drying rate. Neglecting radiation and the small variation in  $l$ ,  $R_C$  becomes directly proportional to  $(t_G - t_S)$ .

**Effect of gas humidity:** At moderate temperatures the rate of drying varies directly as  $(Y_S - Y)$ , and hence increasing gas humidity reduces drying rate.

**Effect of thickness of drying solid:** If conduction through solid occurs,  $R_C$  decreases as solid thickness increases, but rate of drying may sometimes increase due to higher conduction of heat through the edges.

**EXAMPLE 12.1** (Estimation of convective heat transfer coefficient and hence the rate of drying in a batch cross-circulation dryer): Granular solids are to be dried in a cross-circulation drier. The wet solids are spread uniformly on a rectangular pan, 0.5 m # 0.5 m # 20 mm deep. The pan is placed in an air stream at 70°C and humidity 0.0170 kg water per kg dry air. The air is flowing parallel to the surface of the solid at a velocity of 2.5 m/s. The gap for air flow above the solid surface is 80 mm. Neglecting heat transfer by conduction through solids and by radiation, estimate the rate of drying during constant rate period.

Convection coefficient may be calculated from the relation:

$$h_C = \frac{5.90G^{0.71}}{d_e^{0.29}}$$

where,

$G$  = mass velocity of air,  $\text{kg}/(\text{m}^2)(\text{s})$ , and

$d_e$  = equivalent diameter of air flow space, m.

**Solution:** For air at 70°C with absolute humidity of 0.0170,

Wet-bulb temperature = 32.5°C, Humid volume = 0.996  $\text{m}^3/\text{kg}$  dry air, Density of air =  $(1.017)/(0.996) = 1.02 \text{ kg/m}^3$

$$G = (2.5)(1.02) = 2.55 \text{ kg/(s)(m}^2\text{)}$$

Area of the solid surface =  $0.5 \times 0.5 = 0.25 \text{ m}^2$

Equivalent diameter,  $d_e$  of the space for air flow

$$= \frac{4(0.5)(0.08)}{2(0.5 + 0.08)} = 0.138 \text{ m}$$

From the given relation,

$$h_c = \frac{5.90G^{0.71}}{d_e^{0.29}} = \frac{(5.90)(2.55)^{0.71}}{(0.138)^{0.29}} = 20.37 \text{ W/m}^2 \text{ K}$$

When conduction and radiation are neglected, the surface of the drying solid attains the wet-bulb temperature of the entering air, i.e. 32.5°C. At this temperature, the latent heat of evaporation of water,  $l_s = 2425 \text{ kJ/kg}$ . Therefore, from Eq. (12.8)

$$\text{Rate of drying, } R_C = \frac{h_c(t_G - t_s)}{\lambda_s} = \frac{(20.37)(70 - 32.5)}{2425 \times 10^3}$$

$$= 3.15 \times 10^{-4} \text{ kg/(s)(m}^2\text{)}$$

### 12.5.3 Falling Rate Period

As the critical moisture content  $X_C$  is reached, the liquid film on the solid surface gradually disappears and dry spots appear in its place. Since rate of drying is still calculated on the basis of total drying surface  $A$ , the drying rate appears to fall although the evaporation per unit area remains the same. This phenomenon at the beginning of the falling rate period is called *unsaturated surface drying* as represented by  $CD$  on the drying rate curve (Figure 12.5). At point  $D$ , the solid surface becomes completely dry when drying rate depends on internal diffusion of moisture for which several theories have been proposed. In some cases, the entire falling rate period may be due to internal diffusion of moisture while in some other cases internal diffusion of moisture may not take place at all.

At point  $E$ , the moisture content of the solid reaches the equilibrium moisture content corresponding to the humidity of the drying air and further drying stops. Drying may, however, be continued by reducing the humidity of the drying air.

Several theories have been proposed to throw light on the mechanism of diffusion of moisture to the drying surface. Some of them have been briefly discussed here.

#### **Liquid diffusion**

Moisture moves in liquid state through the solid on account of concentration gradient between the interior of the solid where the concentration is high and the surface where the same is low. In these cases, diffusion controlled falling rate period may start immediately after constant rate period and unsaturated surface drying may not be present (Sherwood 1931). Liquid diffusion is encountered in soap, glue, gelatin, etc. as well as during last phase of drying of clay, textile, paper, wood, etc.

#### **Capillary movement**

Unbound moisture in granular or porous solids moves through the capillaries or interstices of the solid by the action of surface tension (Hougen and McCoulley 1940, Pearse et al. 1949). Initially moisture moves fast enough to keep the surface wet and constant rate drying continues. As drying proceeds, a stage is reached when the surface becomes dry at some spots and falling rate period starts with unsaturated surface drying. The sub-surface water soon dries up and the surface of evaporation gradually recedes into the solid. Evaporation then takes place well within the solid and the vapour thus produced diffuses to the surface.

#### **Vapour diffusion**

If heat is supplied to one surface of the solid and drying takes place from the other, moisture may be evaporated within the solid and the vapour diffuses to the surface (Pearse et al. 1949).

### Pressure action

The solid may shrink on drying and squeeze the moisture to the surface where drying takes place. In some cases the entire falling rate period may be due to unsaturated surface drying. The mechanism of such drying being similar with that for constant rate drying, the effects of temperature, humidity and velocity of drying air and thickness of solid are similar to those for constant rate drying. If, on the other hand, internal diffusion controls drying during the entire falling rate period, the rate is independent of air velocity and the effect of humidity is limited to deciding the equilibrium moisture content.

#### 12.5.4 Through-Circulation Drying

In case of through-circulation drying, the drying rate curve is similar to that shown in Figure 12.5 having both constant rate period and falling rate period.

Figure 12.7 represents a bed of wet granular solids, the bed thickness being quite large in comparison with the size of the solid particles. As the drying air enters the bed, the unbound moisture is first evaporated. The narrow zone where unbound moisture is being dried slowly moves through the bed and unless the bed is internally heated, the gas leaves this zone as saturated at the adiabatic saturation temperature of the entering air. The solid will also attain this temperature. The rate of drying remains constant as long as this zone is fully within the bed. As the zone reaches the end of the bed, the drying rate starts decreasing since the outgoing air leaves the bed unsaturated.

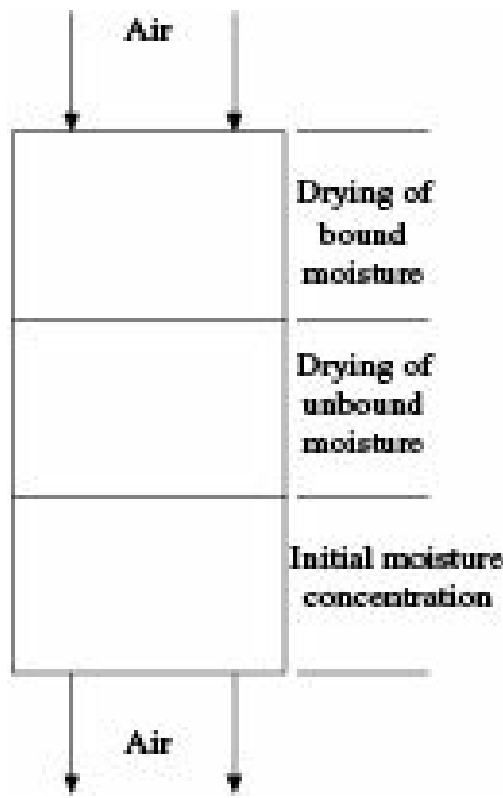


Figure 12.7 Through circulation drying.

#### 12.6 Continuous Drying

The major advantages of continuous drying over batch drying are—the size of equipment is relatively small for the same quantity of material handled, the product is more uniform in moisture content, the

cost of drying is relatively low and the product can be readily sent to subsequent operations, if any without intermediate storage.

The solid and the drying air may flow counter-currently or in parallel. Alternatively, the air may flow across the path of the solid. In adiabatic operations, the air cools down by losing its sensible heat while the evaporated moisture absorbs latent heat of vaporisation from the air. However, the temperature of the air/gas can be kept constant by supplying heat from outside.

As in the case of batch drying, continuous drying may have direct or indirect heating. In direct drying, the hot air may move parallel or counter-current to the moving solid. In parallel adiabatic drying, the wet solid is in contact with the hottest air. Since the solid will be heated only up to the wet-bulb temperature of the air as long as unbound moisture is present in the solid, even heat sensitive solids can be dried by fairly hot air without any damage. Moreover, in parallel drying the moisture content of the dried solid can be better controlled and case hardening can be avoided. In counter-current adiabatic drying, the hottest air is in contact with the driest solid and the discharged solid may reach the temperature of the entering air. Although this permits very rapid drying, there are chances of the solid being damaged by over heating. Also, the heat lost with the discharged solid is very high thereby reducing the thermal efficiency.

In order to decide the flow rates of the solid and the drying air, it is necessary to have material and enthalpy balances for the drying operation.

Figure 12.8 shows a flow diagram for a continuous counter-current drier. The following nomenclatures have been used:

$S$  = mass velocity of dry solid,  $\text{kg}/(\text{m}^2 \text{ s})$

$X$  = moisture content of solid,  $\text{kg}/\text{kg}$  of dry solid

$t_s$  = temperature of solid,  $^\circ\text{C}$

$H_s$  = enthalpy of solid,  $\text{kcal}/\text{kg}$

$G$  = mass velocity of air,  $\text{kg}/(\text{m}^2 \text{ s})$

$Y$  = humidity of air,  $\text{kg}/\text{kg}$  dry air

$t_G$  = temperature of air,  $^\circ\text{C}$

$H_G$  = enthalpy of air,  $\text{kcal}/\text{kg}$

$Q$  = rate of heat flow,  $\text{kcal}/\text{hr}$

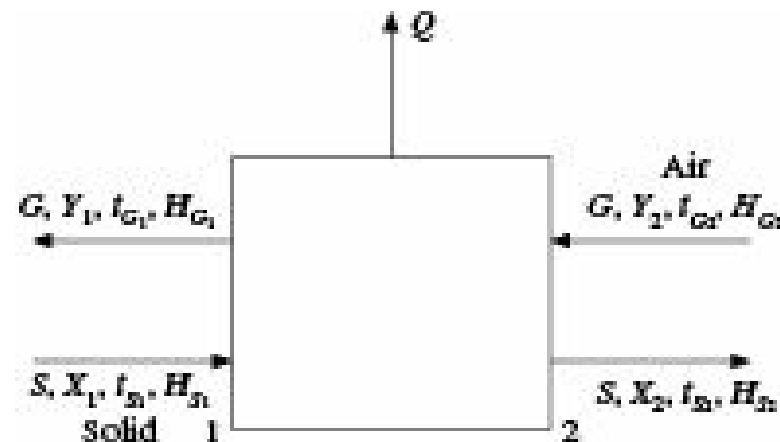


Figure 12.8 Flow diagram of continuous drying.

Suffixes 1 and 2 refer to the two ends of the drier, solid inlet and solid outlet respectively. An overall

material balance for the drier can be written as

$$SX_1 + GY_2 = SX_2 + GY_1 \quad (12.14)$$

or,

$$S(X_1 - X_2) = G(Y_1 - Y_2) \quad (12.15)$$

An enthalpy balance can be written as:

$$SH_{S1} + GH_{G2} = SH_{S2} + GH_{G1} + Q \quad (12.16)$$

For adiabatic operations  $Q = 0$ . If heat is added to the drier and is higher than the heat lost,  $Q$  is negative.

If the solid is placed on trucks or other support, the sensible heat of the support should be taken into account.

The above equations with obvious changes can be used for parallel flow also.

## 12.7 Rate of Batch Drying

### 12.7.1 Cross-Circulation Drying

If a curve with moisture content as a function of time as in Figure 12.4 is available for the exact conditions under which the commercial plant is expected to operate, the time required for drying can be directly determined from the curve by reading the differences in times corresponding to the initial and final moisture contents.

In other cases, the time of drying can be estimated in the following manner.

By definition, the expression for the rate of drying has been given in Eq. (12.1).

Rearranging and integrating Eq. (12.1) over the time interval 0 to  $i$  during which the moisture content changes from  $X_1$  to  $X_2$ ,

$$i = \int_0^i di = \frac{M_s}{A} \int_{X_2}^{X_1} \frac{dx}{R} \quad (12.17)$$

Equation (12.17) can be modified separately for constant rate and falling rate periods.

#### **Constant rate period**

If drying is entirely within the constant rate period, both  $X_1$  and  $X_2$  are greater than  $X_C$  and  $R = R_C$ , Eq. (12.17) then becomes

$$i_C = \frac{M_s(X_1 - X_2)}{AR_C} \quad (12.18)$$

where,  $i_C$  is the time of drying during constant rate period.

#### **Falling rate period**

If  $X_1$  and  $X_2$  are both less than the critical moisture content  $X_C$ , drying is entirely in the falling rate period and the rate of drying changes during drying.

In the general case, for any shape of the falling rate curve, Eq. (12.17) can be integrated graphically by plotting  $(1/R)$  as ordinate against  $X$  as abscissa by taking their values from the drying rate curve

(Figure 12.5) and then determining the area under the curve between the limits  $X_1$  and  $X_2$ .

In the special case where the drying rate  $R$  is linear in  $X$ ,  $R$  may be expressed as

$$R = mX + C \quad (12.19)$$

Substitution of Eq. (12.19) in Eq. (12.17), provides the time ( $i_F$ ) for falling rate drying

$$i_F = \frac{M_S}{A} \int_{X_2}^{X_1} \frac{dX}{mX + C} = \frac{M_S}{mA} \ln \frac{mX_1 + C}{mX_2 + C} \quad (12.20)$$

$$\frac{R_1 - R_2}{X_1 - X_2}$$

Since  $R_1 = mX_1 + C$ ,  $R_2 = mX_2 + C$  and  $m = \frac{R_1 - R_2}{X_1 - X_2}$ ,

Equation (12.20) becomes

$$i_F = \frac{M_S(X_1 - X_2)}{A(R_1 - R_2)} \ln \frac{R_1}{R_2} = \frac{M_S(X_1 - X_2)}{AR_m} \quad (12.21)$$

$$R_m = \frac{(R_1 - R_2)}{\ln(R_1/R_2)}$$

where, logarithmic average of the drying rate

Often, in the absence of detailed data, the entire falling rate curve is assumed to be straight when

$$R = m(X - X^*) = \frac{R_C(X - X^*)}{(X_C - X^*)} \quad (12.22)$$

and Eq. (12.21) becomes,

$$i_F = \frac{M_S(X_C - X^*)}{AR_C} \ln \frac{(X_1 - X^*)}{(X_2 - X^*)} \quad (12.23)$$

When both constant rate and falling rate periods are involved, Eqs. (12.18) and (12.23) may be combined to give the total time,  $i_T$  in second.

$$i_T = i_C + i_F = \frac{M_S}{AR_C} \left( (X_1 - X_C) + (X_C - X^*) \ln \frac{(X_C - X^*)}{(X_2 - X^*)} \right) \quad (12.24)$$

In Eq. (12.24) following changes have been incorporated: (i) the final moisture content  $X_2$  in Eq. (12.18) has been changed by  $X_C$  as the constant rate period proceeds up to the critical moisture content  $X_C$ , and (ii) the initial moisture content  $X_1$  in Eq. (12.23) has been replaced by  $X_C$  due to the fact that the falling rate starts from the critical moisture content  $X_C$ .

**EXAMPLE 12.2** (Estimation of (i) drying time up to a certain moisture content from data on drying up to another moisture content and (ii) moisture content after a given time of drying): A wet solid is dried from 30% to 10% moisture in 5 hr under constant drying conditions. The critical moisture content is 14% and the equilibrium moisture is 4%. Drying rate during falling rate period is proportional to the free moisture content of the solid. Calculate

- (a) the time required to dry the solid to 6% moisture content,  
 (b) the final moisture content of the solid if drying is continued for a total period of 8 hr  
 All moisture contents are on wet basis.

**Solution:**

$$\text{Initial moisture content, } X_1 = \frac{30}{100 - 30} = 0.4286 \text{ kg water/kg dry solid}$$

$$\text{Final moisture content, } X_2 = \frac{10}{100 - 10} = 0.1111 \text{ kg water/kg dry solid}$$

$$\text{Critical moisture content, } X_C = \frac{14}{100 - 14} = 0.1628 \text{ kg water/kg dry solid}$$

$$\text{Equilibrium moisture content, } X^* = \frac{4}{100 - 4} = 0.0417 \text{ kg water/kg dry solid}$$

From Eq. (12.24), we get

$$i_T = i_C + i_F = \frac{M_s}{AR_C} \left( (X_1 - X_C) + (X_C - X^*) \ln \frac{(X_C - X^*)}{(X_2 - X^*)} \right)$$

Substituting the values, we have

$$5 = \frac{M_s}{AR_C} \left( (0.4286 - 0.1628) + (0.1628 - 0.0417) \ln \frac{0.1628 - 0.0417}{0.1111 - 0.0417} \right)$$

$$\text{whence, } \frac{M_s}{AR_C} = 15.006$$

$$(a) \text{ For 6\% moisture, } X'_2 = \frac{6}{100 - 6} = 0.0638$$

$$i_T = 15.006 \left( (0.4286 - 0.1628) + (0.1628 - 0.0417) \ln \frac{(0.1628 - 0.0417)}{(0.0638 - 0.0417)} \right) \\ = 7.08 \text{ hr}$$

The time required to reduce the moisture content to 6% is 7.08 hours.

(b) When drying is continued for a total period of 8 hr,

$$8 = 15.006 \left( (0.4286 - 0.1628) + (0.1628 - 0.0417) \ln \frac{0.1628 - 0.0417}{X''_2 - 0.0417} \right)$$

whence,  $X''_2 = 0.055 \text{ kg water/kg dry solid.}$

$$\text{Moisture content on wet basis} = \left( \frac{0.055}{1.055} \right) \# 100 = 5.21\%$$

Moisture content after 8 hr of drying will be 5.21%

**EXAMPLE 12.3** (Estimation of drying time from data on drying rate with nonlinear falling rate

period curve): Data on drying rate as a function of moisture content for a certain solid are given below. The weight of bone-dry solid per unit surface exposed to drying is  $45.8 \text{ kg/m}^2$ . Estimate the time required to dry the material from 20% to 5% moisture on wet basis.

**Data:**

$X: 0.30\ 0.20\ 0.18\ 0.15\ 0.14\ 0.11\ 0.07\ 0.02$
$R: 1.22\ 1.22\ 1.12\ 0.98\ 0.78\ 0.49\ 0.24\ 0.00$

where,

$X$  = moisture content of solid, kg water/kg dry solid,

$R$  = drying rate,  $\text{kg}/(\text{hr})(\text{m}^2)$ .

**Solution:** The drying rate curve as shown in Figure 12.9, is drawn from the given data by plotting  $R$  as ordinate against  $X$  as abscissa.

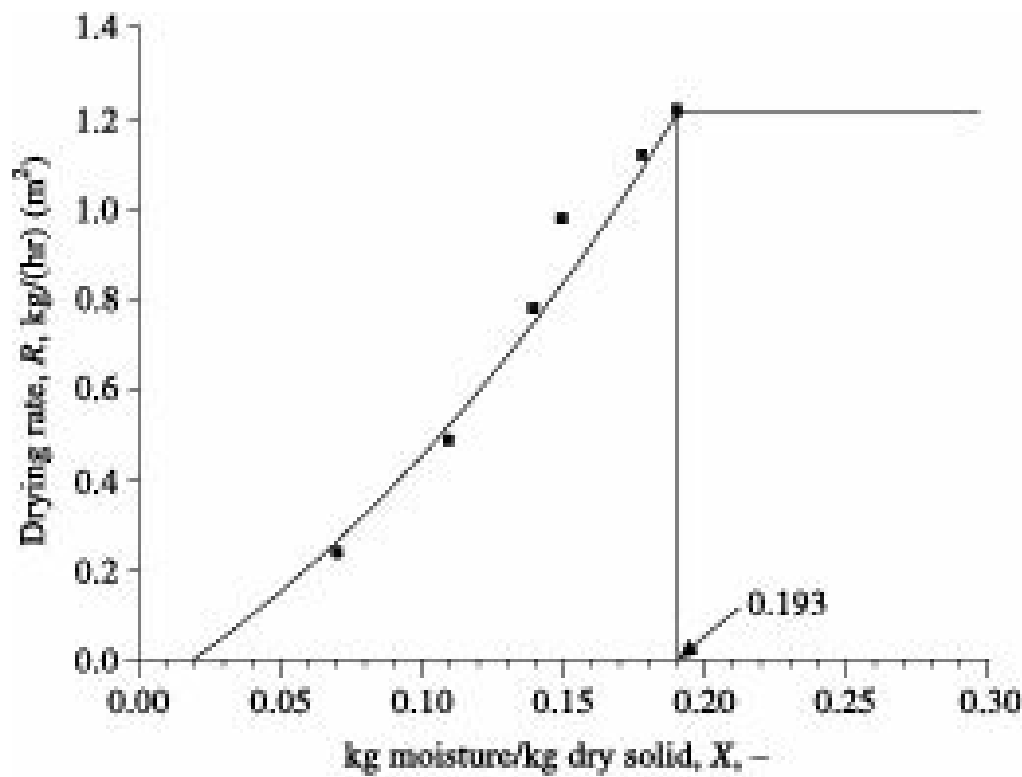


Figure 12.9 Solution to Example 12.3.

From the curve, critical moisture content,  $X_C = 0.193 \text{ kg moisture/kg dry solid}$ ,

Equilibrium moisture content,  $X^* = 0.02 \text{ kg. moisture/kg dry solid}$ .

Drying rate during constant rate period =  $1.22 \text{ kg}/(\text{hr})(\text{m}^2)$

$$X_1 = \frac{20}{100 - 20} = 0.25, X_2 = \frac{5}{100 - 5} = 0.0526$$

Drying from  $X_1 = 0.25$  to  $X_C = 0.193$  will be at constant rate. Hence from Eq. (12.18)

$$t_C = \frac{M_s}{AR_C} (X_1 - X_C) = \frac{45.8}{1.22} (0.25 - 0.193) = 2.14 \text{ hr.}$$

The falling rate curve being nonlinear, drying time should be determined by graphical integration as shown in Figure 12.10 by plotting  $(1/R)$  against  $X$  from the following table.

X:	0.30	0.20	0.18	0.15	0.14	0.11	0.07	0.02
R:	1.22	1.22	1.12	0.98	0.78	0.49	0.24	0.00
1/R:	0.82	0.82	0.89	1.02	1.28	2.04	4.17	¥

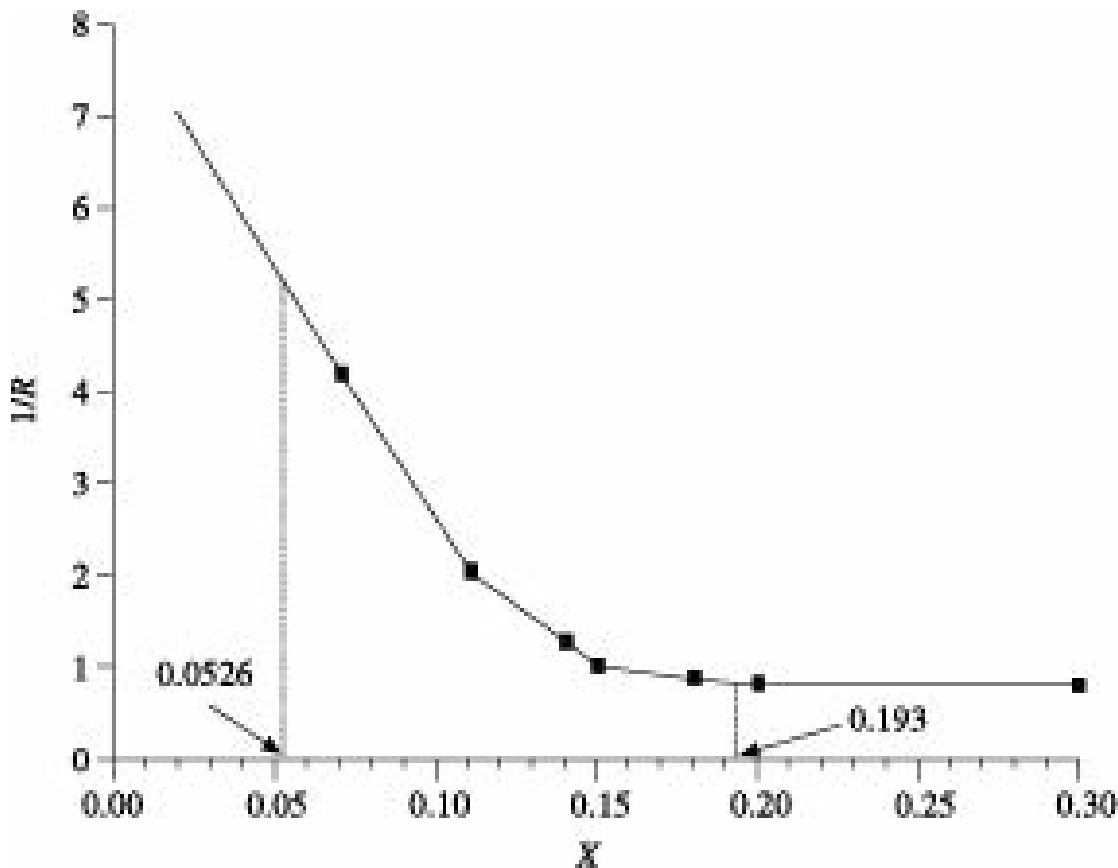


Figure 12.10 Solution to Example 12.3.

Area under the curve within the limits  $X_C = 0.193$  and  $X_2 = 0.0526 = 0.307$  units.

Drying time,  $i_F = (45.8/1) \# 0.307 = 14.06$  hr.

Total drying time  $i_T = i_C + i_F = 2.14 + 14.06 = 16.2$  hr

Alternatively, assuming the falling rate curve to be linear as an approximation, the drying time may be calculated from Eq. (12.23) using  $X_1 = X_C = 0.193$  as the falling rate starts from the critical moisture content

$$i_F = \frac{45.8}{(1)(1.22)} (0.193 - 0.02) \ln \frac{0.193 - 0.02}{0.0526 - 0.02} = 10.84 \text{ hr}$$

Total drying time  $i_T = 2.14 + 10.84 = 12.98$  hr

In this case, if the points representing critical and equilibrium moisture are joined by a straight line, the drying rates obtained are higher than the actual rates. Hence, time required for drying in the falling rate period is less.

**EXAMPLE 12.4** (Determination of drying time from given values of equilibrium moisture, critical moisture and drying rate at critical point): A slab of paper 1.5 m # 1.5 m # 5 mm thick is to be dried under constant drying conditions from 65% to 5% moisture. The equilibrium moisture is 2.5% and the critical moisture content is 46%. All moisture contents are on dry basis. The drying rate at the critical point has been estimated to be  $1.30 \text{ kg}/(\text{hr})(\text{m}^2)$ . Density of the dry pulp is  $220 \text{ kg}/\text{m}^3$ .

Assuming drying to take place from one large face only, estimate the drying time to be provided.

**Solution:**

$$\text{Surface area of the slab} = 1.5 \# 1.5 = 2.25 \text{ m}^2$$

$$\text{Weight of the slab} = 1.5 \# 1.5 \# 0.005 \# 220 = 2.475 \text{ kg}$$

$$X^* = 0.025, X_C = 0.46, X_1 = 0.65, X_2 = 0.05,$$

all expressed in kg water per kg dry pulp.

In the absence of any data on drying rate and any indication regarding the nature of the falling rate curve, it is assumed that the falling rate curve is linear in moisture content. Hence from Eq. (12.24) total drying time,

$$\begin{aligned} i_T &= i_C + i_F = \frac{M_s}{AR_C} \left( (X_1 - X_C) + (X_C - X^*) \ln \frac{(X_C - X^*)}{(X_2 - X^*)} \right) \\ &= \frac{2.475}{(2.25)(1.30)} \left( (0.65 - 0.46) + (0.46 - 0.025) \ln \frac{(0.46 - 0.025)}{(0.05 - 0.025)} \right) \\ &= 1.212 \text{ hr} \end{aligned}$$

**EXAMPLE 12.5** (Percent saving in drying time for drying a material up to a relatively higher moisture content): Woolen cloth is being dried in a hot air drier from initial moisture content of 100% to a final moisture content of 10%. If the critical moisture content is 55% and the equilibrium moisture content is 6%, calculate the saving in drying time if the material is dried to 16% instead of 10%, all other drying conditions remaining the same.

All moisture content are on dry basis.

**Solution:**

$$X_C = 0.55, X^* = 0.06, X_1 = 1.00, X_2 = 0.10,$$

all expressed as kg water per kg of dry cloth.

In the absence of any information regarding the nature of the falling rate drying curve, it is assumed that the same is linear in moisture content of the solid. From Eq. (12.24),

$$i_T = i_C + i_F = \frac{M_s}{AR_C} \left( (X_1 - X_C) + (X_C - X^*) \ln \frac{(X_C - X^*)}{(X_2 - X^*)} \right)$$

Substituting the values, we get

$$\begin{aligned} i_T &= \frac{M_s}{AR_C} \left( (1.0 - 0.55) + (0.55 - 0.06) \ln \frac{(0.55 - 0.06)}{(0.10 - 0.06)} \right) \\ &= 1.68 \frac{M_s}{AR_C} \end{aligned}$$

In the second case, when drying is up to 16% moisture

$$X'_2 = 0.16$$

From Eq. (12.24), we have

$$i'_T = \frac{M_S}{AR_C} \left( (1.0 - 0.55) + (0.55 - 0.06) \ln \frac{(0.55 - 0.06)}{(0.16 - 0.06)} \right)$$

$$= 1.23 \frac{M_S}{AR_C}$$

Therefore, saving in drying time

$$= \frac{1.68(M_S/AR_C) - 1.23(M_S/AR_C)}{1.68(M_S/AR_C)} \# 100$$

$$= 26.79\%$$

### 12.7.2 Through-Circulation Drying

In case of removal of unbound moisture in through-circulation drying, maximum rate of drying will correspond to the situation where the air leaves the drier at its adiabatic saturation temperature with humidity,  $Y_{as}$ . However, in general case, when the gas leaves the bed with humidity  $Y_2$ , the drying rate is given by

$$R = G(Y_2 - Y_1) \quad (12.25)$$

where  $Y_1$  and  $Y_2$  are the inlet and exit humidities, respectively of the drying air.

For a differential section of the bed, the gas undergoes a change in humidity  $dY$  and leaves at a humidity  $Y$ . The drying rate then becomes,

$$dR = G\$dY = k_y ds (Y_{as} - Y) = k_y a dZ (Y_{as} - Y) \quad (12.26)$$

where

$s$  = interfacial area per unit cross section of bed

$a$  = interfacial area per unit bed volume

$Z$  = thickness of the bed

Equation (12.26) can be rearranged as

$$\int_{Y_1}^{Y_2} \frac{dY}{(Y_{as} - Y)} = \int_0^Z \frac{k_y a dZ}{G} \quad (12.27)$$

or,

$$\ln \frac{Y_{as} - Y_1}{Y_{as} - Y_2} = \frac{k_y a Z}{G} = N_t G \quad (12.28)$$

where  $N_t G$  is the number of gas phase transfer units in the bed. Equation (12.28) is similar to the equation for adiabatic humidification of a gas.

### 12.8 Rate of Continuous Drying

Continuous direct heat driers may operate above the boiling point of the moisture to be evaporated when the operation is considered to be high temperature drying. Alternatively, they may operate below the boiling point of the moisture in which case the operation is said to be at low temperature.

During high temperature drying, humidity of air has only minor effect on the rate of drying and calculations are generally based on rate of heat transfer. At low temperatures, mass transfer driving force is considered. These calculations, however, give only rough estimates and experiments should be conducted for obtaining reliable design data.

### Drying at high temperature

In continuous driers, where the solid moves from one end of the equipment to the other end as in rotary driers, the drying gas undergoes a more or less uniform change in temperature. In case of the solids, on the other hand, three different trends in temperature change can be recognized and accordingly the drier is divided into three distinct zones as shown in Figure 12.11.

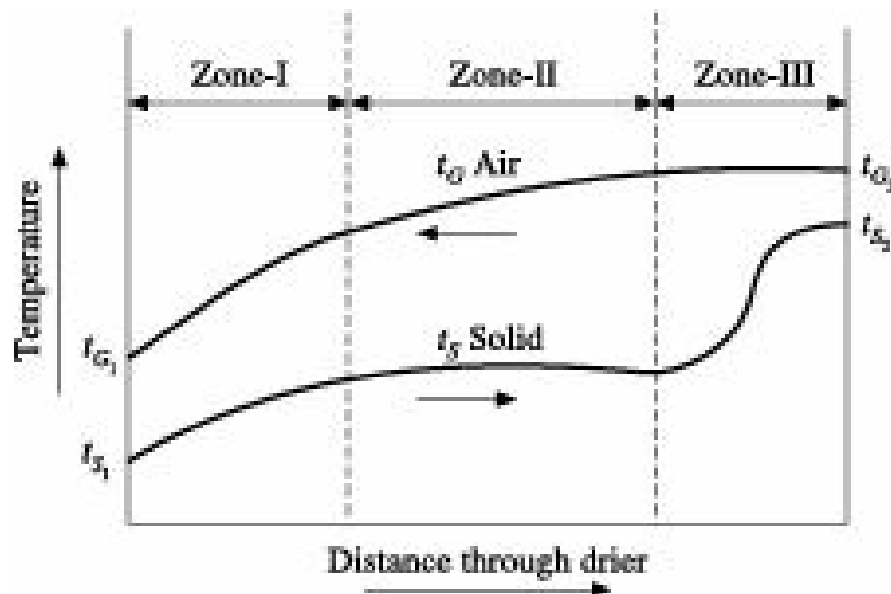


**Figure 12.11** Three zones in a continuous high temperature drier.

Zone-I is the pre-heat zone where the solid is heated by sensible heat transfer from the gas until there is a dynamic balance between the heat required for evaporation and that supplied by the gas. Very little evaporation takes place here.

In Zone-II, surface moisture and unbound moisture are removed and the temperature of the solid remains more or less constant.

In Zone-III, unsaturated surface drying and evaporation of bound moisture take place. The temperature of the solid increases considerably in this zone and it leaves the drier at a temperature very close to that of inlet gas. This zone constitutes the major part of many driers.

Considering heat transfer only between gas and solid, an enthalpy balance for a differential length  $dZ$  of the drier can be written as

$$dq_G = dq + dQ \quad (12.29)$$

where

$q_G$  = heat lost by the gas

$q$  = heat actually transferred to the solid

$Q$  = heat loss to the surrounding

Rearranging Eq. (12.29), we obtain

$$dq = (dq_G - dQ) = Uds (t_G - t_S) = Ua(t_G - t_S) dZ \quad (12.30)$$

where,

$U$  = overall heat transfer coefficient between gas and solid

$(t_G - t_S)$  = temperature difference for heat transfer

$s$  = interfacial surface per unit drier cross section

$a$  = interfacial area per unit drier volume

Equation (12.30) may therefore be written as

$$dq = G C_S dt_G = Ua(t_G - t_S)dZ \quad (12.31)$$

where,  $dt_G$  is the temperature drop in the gas due to heat transfer to the solid alone,  $C_S$  is the humid heat of the gas.

From Eq. (12.31), we get

$$dN_{toG} = \frac{\frac{dt_G}{t_G - t_S}}{G \cdot C_S} = \frac{Ua dZ}{G \cdot C_S} \quad (12.32)$$

and if the heat transfer coefficient is constant,

$$N_{toG} = \frac{Z}{H_{toG}} = \frac{dt_G}{(t_G - t_S)_m} \quad (12.33)$$

$$\text{where, } H_{toG} = \frac{G \cdot C_S}{Ua} \quad (11.34)$$

$N_{toG}$  and  $H_{toG}$  = the overall number and length of heat transfer units

$dt_G$  = change in gas temperature due to heat transfer to solid only

$(t_G - t_S)_m$  = approximate average temperature difference between gas and solid

Assuming the temperature profile to be straight line for each of the three zones separately,  $(t_G - t_S)_m$  becomes the logarithmic mean of the terminal temperature differences for each zone and  $N_{toG}$  becomes the corresponding number of transfer units.

Since the surface of the solid exposed to the drying gas cannot be properly measured, the group  $(Ua)$  has to be considered together. In the absence of reliable experimental data, McCormick (1973) suggested that the value of  $(Ua)$  for a large number of commercial driers may be approximately taken as

$$Ua = \frac{237G^{0.67}}{T_D} \quad (12.35)$$

The approximate average temperature differences in the three zones, particularly in Zone-II are the average wet-bulb depressions in the respective zones since the surface of the solid is at the wet-bulb temperature of the drying gas.

$$\text{For estimation of the total length of the drier, values of } N_{toG} = \frac{dt_G}{(t_G - t_S)_m}$$

for each of the three zones are determined separately, added up and then multiplied by  $H_{toG} = \frac{GC_S}{Ua}$

to yield the approximate length required. Finally, the nearest standard size on the higher side is recommended.

**EXAMPLE 12.6** (Estimation of moisture to be removed and time required using a given correlation for the falling rate period): A compartment drier is to be used to dry rayon yarn from 80% to 1% free moisture on dry basis. The drier will operate at atmospheric pressure under constant drying conditions. The average conditions of the drying air will be 65.5 °C dry bulb temperature, 10% relative humidity. The air will flow at an average velocity 1 m/s. The equilibrium moisture content of the yarn is negligible.

- Determine the amount of water to be evaporated per 100 kg of yarn and
- Estimate the time to be provided for the drying.

Drying will be entirely within the falling rate region for which the data may be correlated by the relation

$$\frac{dF}{d\theta} = 9.89 \times 10^{-4} G^{1.47} (Y_S - Y) F$$

where,

$dF/d\theta$  = rate of drying, kg water/(hr)(kg dry yarn)

$G$  = mass velocity of air, kg/(hr)(m<sup>2</sup>)

$Y_S$  = saturation humidity at wet-bulb temperature of air, kg water/kg dry air

$Y$  = humidity of air, kg water/kg dry air

$F$  = free moisture content of yarn, kg water/kg dry yarn

### Solution:

- Basis: 100 kg of dry yarn

$$\text{Initial moisture} = 0.80 \# 100 = 80 \text{ kg}$$

$$\text{Final moisture} = 0.01 \# 100 = 1 \text{ kg}$$

Hence, moisture evaporated per 100 kg dry yarn

$$= 80 - 1 = 79 \text{ kg}$$

- The equation for correlating drying rate is given as

$$\frac{dF}{d\theta} = 9.89 \times 10^{-4} G^{1.47} (Y_S - Y) F,$$

By readjustment, we get

$$\int_0^{\theta} \frac{d\theta}{d\theta} = \frac{1}{(9.89 \times 10^{-4}) \cdot (G^{1.47}) (Y_S - Y)} \int_{F_1}^{F_2} \frac{dF}{F}$$

On integration, we obtain

$$i = \frac{1}{(9.89 \times 10^{-4}) \cdot (G^{1.47}) (Y_S - Y)} \ln \frac{F_1}{F_2} \quad (i)$$

Absolute humidity of air (65.5°C, 10% RH) = 0.020 kg/kg.

Saturated humidity of air at wet-bulb temperature of 35°C,

= 0.032 kg moisture/kg dry yarn

Specific volume of air at 65.5°C, 10% RH = 0.983 m<sup>3</sup>/kg dry air

$$\text{Density of air, } t_G = \frac{1.02}{0.983} = 1.04 \text{ kg/m}^3$$

Mass velocity of air,  $G = (1 \# 60 \# 60 \# 1.04) = 3744 \text{ kg/(hr)(m}^2\text{)}$

Substituting the values in Eq. (i), we get

$$i = \frac{1}{(9.89 \times 10^{-4})(3744)^{1.47}(0.032 - 0.020)} \ln \frac{0.80}{0.01}$$
$$= 2.06 \text{ hr}$$

## 12.9 Drying Equipment

Different types of driers are used in industry for meeting the specific requirements of a wide variety of solids, slurries and solutions. The performance of a drier depends on how well the drier can make contact between the material to be dried and the drying air or gas.

Driers are broadly classified as batch type and continuous type. Each of these two categories can be further grouped as direct and indirect depending upon whether heat is supplied to the material directly or through some retaining wall.

A classification of some common driers is shown in Figure 12.12.

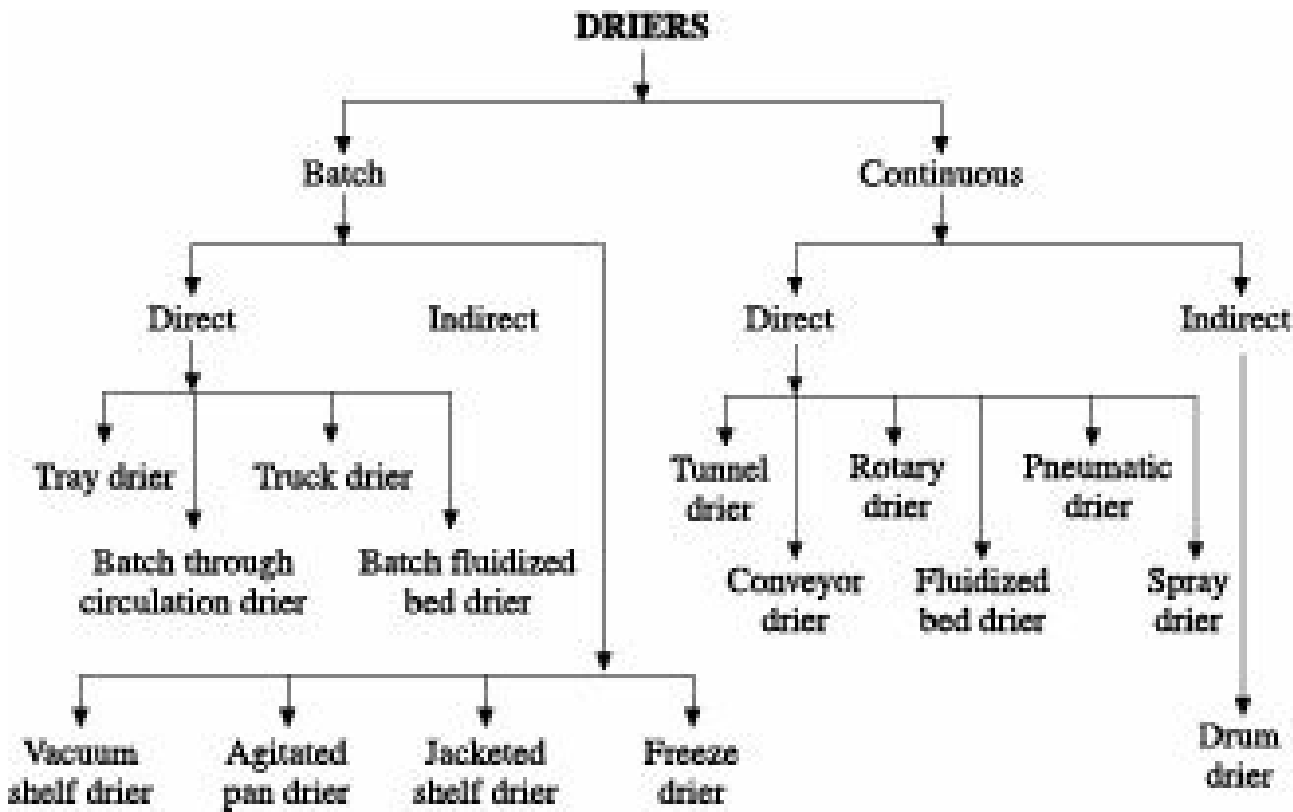


Figure 12.12 Classification of some common driers.

## 12.10 Batch Driers

Batch drying is relatively expensive and is therefore limited to small scale operations, pilot plant and developmental work and drying of valuable materials where the added cost of drying will not have

much effect on the total cost.

### 12.10.1 Direct Driers

#### Tray drier

Tray driers are also called cabinet, compartment or shelf driers. Tray driers are suitable for drying pasty materials such as wet filter cakes, lumpy solids which must be supported on trays. These are also suitable for drying fragile materials.

A schematic diagram of a tray drier is shown in Figure 12.13.

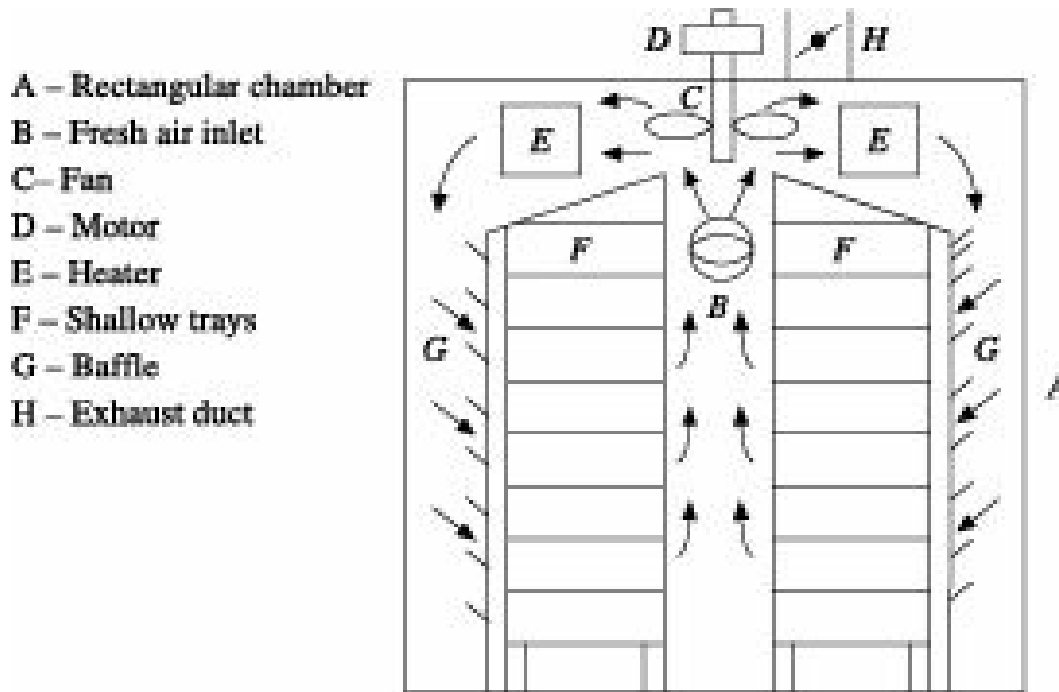


Figure 12.13 Tray drier.

The wet material to be dried is evenly spread on a number of trays, which are then stacked one over the other inside an insulated cabinet. The drying air is heated in contact with steam coils and is blown by a blower inside the cabinet to evaporate the moisture. Inert gas or superheated steam can be used instead of hot air if presence of oxygen has to be avoided. The trays may be rectangular or square, each tray having an area of 0.5 to 1.0 m<sup>2</sup>. The material to be dried is spread on the trays up to a height of 10 to 50 mm. After drying is complete up to the desired moisture content, the trays are removed and a fresh batch of trays is introduced.

In order to have uniform drying and avoid stagnant air or gas pockets, it is necessary to blow a large quantity of air or gas and to have heat economy, a large fraction of the air or gas is recirculated.

The velocity, temperature and humidity of the drying air or gas may be regulated by adjusting the gas flow rate, steam rate and recirculation rate. The recirculation rate is regulated by adjustable vanes on both the ends of the trays.

A major advantage of a tray drier is that the same drier may be used for drying different materials under different drying conditions. Tray driers are relatively cheap and have low maintenance cost. But their operating cost is high due to low heat economy and high labour cost.

In batch 'through circulation drying' the bottoms of the trays are made of screens or perforated plates so that a large fraction of the drying air or gas can pass through the material to be dried and the rate of drying increases appreciably. Granular materials are dried in this way. The solids are spread on the

trays in thin layers.

### Truck drier

A batch truck drier is similar to a tray drier except that the trays are stacked in trucks, which are pushed into the drier cabinet over pairs of rails. Several trucks are usually placed in the same cabinet. It may be mentioned that fluidized bed dryers can be operated in a batch or in a continuous fashion. Microwave drying and heat pump assisted drying processes are also being carried out in either of the modes. Detail discussion of these dryers has been made under Section 12.11.

### 12.10.2 Indirect Driers

#### Vacuum shelf drier

A vacuum dryer consists of a drying chamber, heating media and circulating system, vacuum system, and a solvent recovery system as shown in Figure 12.14.

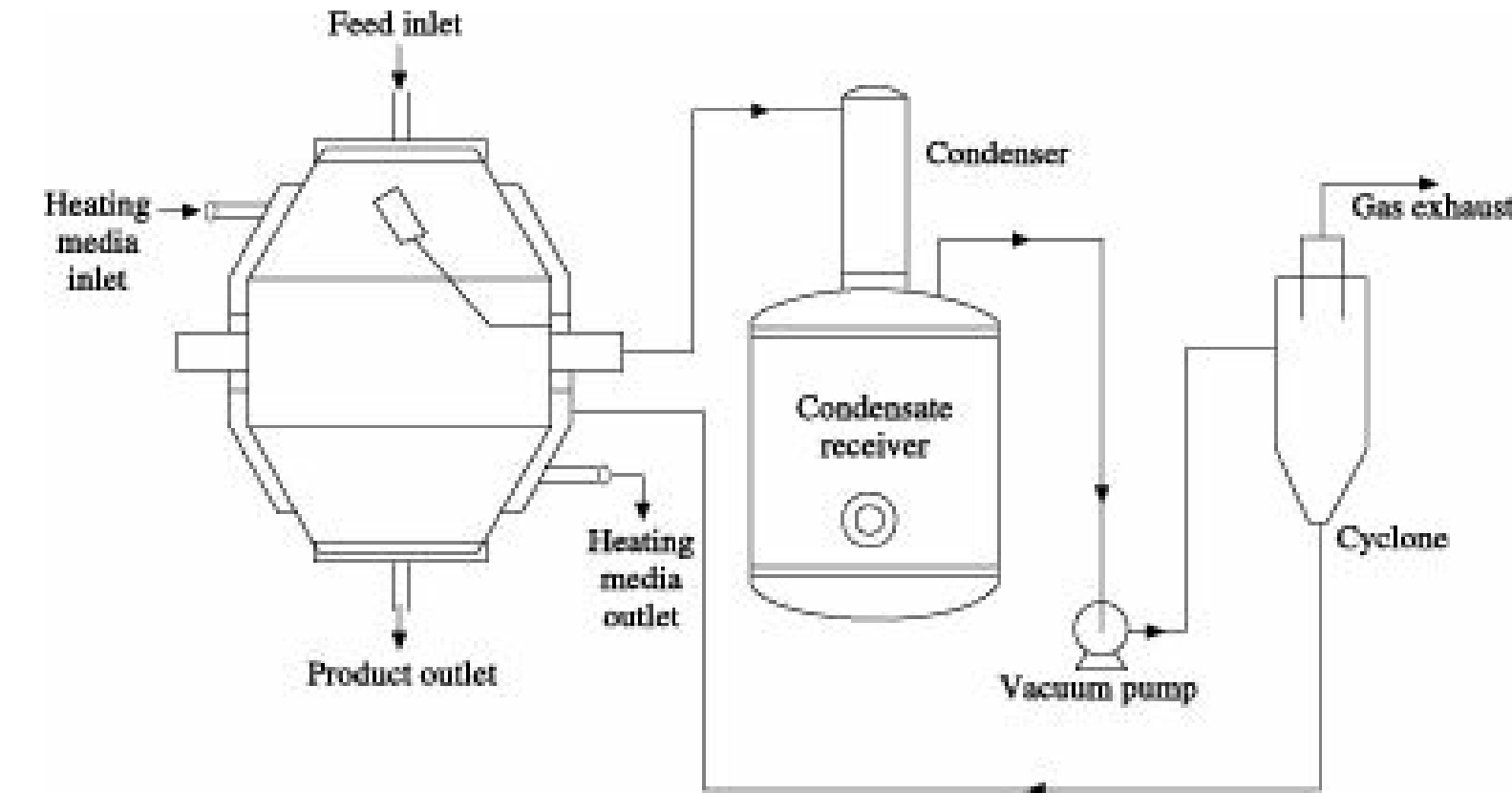


Figure 12.14 Schematic diagram of a vacuum drier.

*Vacuum shelf driers* are tray driers with cast iron, stainless steel or special alloys plate cabinets having closely fitting doors so that they may be operated under vacuum. Its heat transfer mode is conduction or radiation rather than convection as in conventional tray dryer. Trays containing the material to be dried are placed on hollow shelves through which steam or hot water is circulated. If steam is used, condensation may occur. No air or gas is blown over the solid directly. The vapour produced passes to a condenser where they are condensed and are collected. Only the noncondensable gases are removed by a pump. Both shelf and body are heated using controlled circulation of heating media to avoid retrograde condensation. These driers being costly are used only for valuable materials, which must be dried under vacuum. Normally, a vacuum pump is used to create vacuum in the drying chamber. The drying chamber and the vacuum should be properly welded and sealed. There are several types of vacuum pump such as jet pump, rotary pump, ring vacuum

pump, once-through-oil pump.

### Agitated pan driers

These driers consist of shallow circular pans 1 to 2 m in diameter and 0.3 to 0.6 m deep with flat bottom. The pans are jacketed for circulation of steam or hot fluid. The materials on the pan are stirred and scraped by a set of rotating ploughs so that new surface is continuously exposed to heating. In atmospheric pan driers, moisture is evaporated into the atmosphere. Alternatively, the pans may be covered and operated under vacuum, if recovery of solvent is desired.

These driers are used in drying of pastes or slurries in small batches.

### Vacuum rotary drier

*Vacuum rotary driers* are steam jacketed cylindrical shells rotating on a horizontal axis. The materials to be dried are stirred by a set of rotating agitator blades mounted on a horizontal shaft. The vaporised moisture passes out from an opening at the top while the dried solids are discharged from the bottom. Agitation and paddle mixing improves the contacting efficiency between the heat transfer surface and the drying materials. Figure 12.15 shows the schematic diagram of a rotary vacuum paddle dryer.

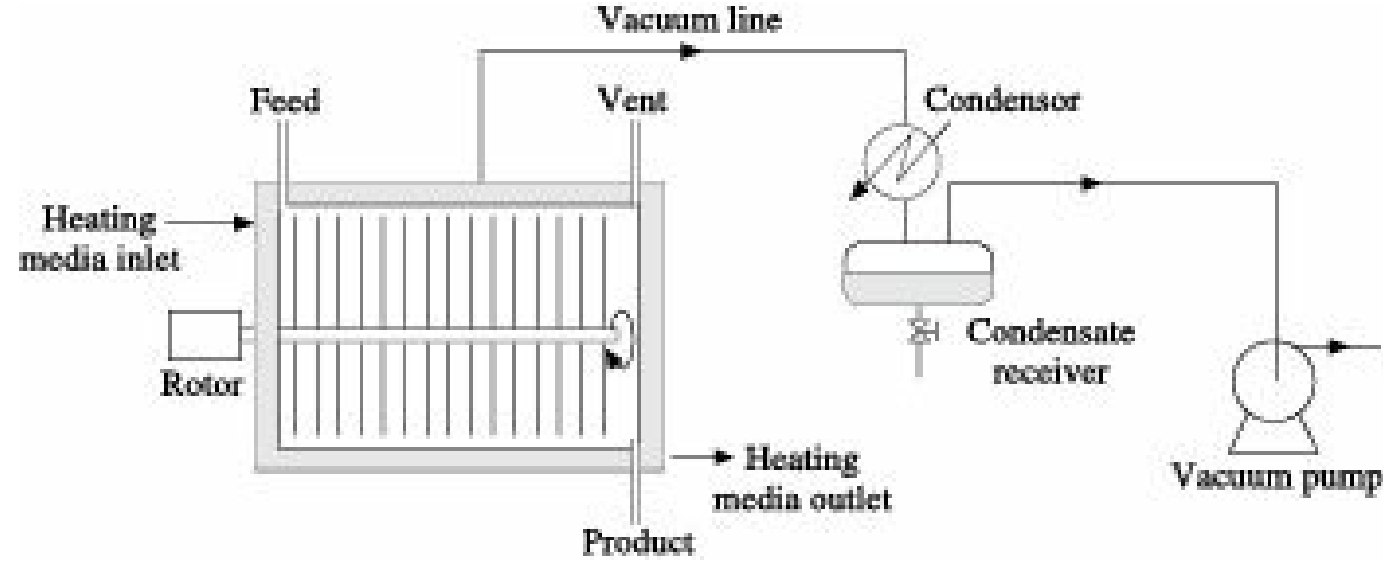


Figure 12.15 Schematic diagram of a rotary vacuum paddle drier.

These driers are usually employed for drying pastes or slurries under vacuum.

The disadvantages of using vacuum drying are the long drying time, wall fouling and potential for case hardening of granular materials. These may be due to the fact that vacuum dryers are indirect dryers and the heat transfer takes place by temperature gradient driven conduction from the heating jacket at the wall of the dryer. The disadvantages can be overcome by combining vacuum drying with the microwave drying. The microwave field allows addition of thermal energy which is in the form of electromagnetic wave besides heat conduction. The microwave vacuum drying permits the higher rate of heat and mass transfer resulting in shortening of drying time. Microwave energy provides thermal energy. The heating jacket can be discarded if the microwave field alone can supply sufficient thermal energy for drying. This helps to eliminate the wall fouling and case hardening of granular materials at the wall of the dryer.

### Freeze drier

Freeze drying is a novel method for drying of heat-sensitive and perishable materials such as fruit,

vegetables, floral products, meat and pharmaceuticals which cannot be heated even to moderate temperatures. It is also used for recovery of water damaged items from fires and floods. The process of freeze drying is a simple one that removes moisture from a frozen material while it remains in a frozen state retaining the material's shape and structure. This process is also known as *lyophilization*. Freeze drying is the most natural means of preservation and it produces a result that favours extended storage of natural items, retaining the material's natural qualities.

Freeze drying, like all other drying processes, is a method to separate liquid water from a wet solid product or from a solution or dispersion of given concentration. There are two general applications:

- (i) long-term preservation or stabilization of perishable products (e.g. foods, biologicals, pharmaceuticals, etc.), and
- (ii) the production of defined porous structures or internal surfaces (e.g. collagen sponges, catalysts, etc.).

Freeze drying is a three step process. These are:

*Step 1:* In this step the material is frozen solid. During the solidification step a phase separation occurs. Most of the water present in the sample is converted to ice crystals whereas the unfrozen water together with solutes form an amorphous or so called *glassy phase*. This phase is the basis for the preservation.

*Step 2:* Under vacuum the water is removed from the frozen sample. Usually, the vacuum drying step is divided in two parts: primary drying means the sublimation of ice crystals. Afterward, only the glassy phase is left having a porous structure. During the secondary drying, the unfrozen water diffuses out of the glassy matrix and is desorbed from its surface. If the sample is sufficiently dry, it can be stored at room temperature without any further loss of quality.

*Step 3:* The rehydration means the reconstitution of the original state by adding water or an aqueous solution. The temperature-concentration diagram in Figure 12.16, shows these three steps from a different point of view.

It is important to keep the temperature of the sample below the glass transition temperature to ensure product stability. The glass transition temperature ( $T_g$ ) itself depends on both water content and material. Therefore, it might be necessary to use certain additives to improve the glass forming properties of the sample. Macromolecules as well as sugars are often used as stabilizers since they form a stable glass and have relatively high glass transition temperatures.

Considering simultaneous heat and mass transfer occurring in the process, the drying time can be calculated using the expression (Geankoplis 2005):

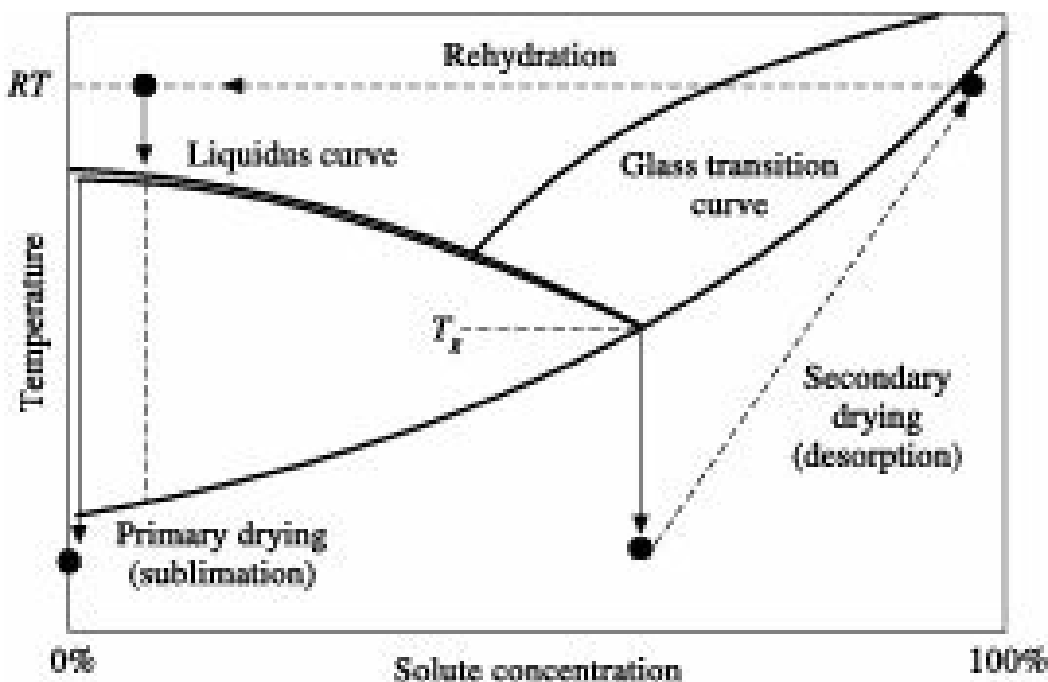


Figure 12.16 Temperature-concentration diagram.

$$\theta = \frac{L^2}{4kV_S} \frac{\Delta H_S}{M_A} \frac{1}{T_e - T_f} \left( x_1 - x_2 - \frac{x_1^2}{2} + \frac{x_2^2}{2} \right) \quad (12.36)$$

where

$\Delta H_S$  = latent heat of sublimation of ice, J/kmol.

$T_e$  = ambient temperature, °C

$T_f$  = temperature of sublimation front or ice layer, °C

$k$  = thermal conductivity of the dry solid, W/(m)(K)

$M_A$  = molecular weight of water

$L$  = thickness of the dry layer, m

$x$  = dimension in the direction of transport of properties, m

$V_S$  = volume of solid material occupied by unit kg of water initially ( $=1/X_0 t_S$ ),  $X_0$  and  $t_S$  being the initial free-moisture content in kg water/kg dry solid, and bulk density of dry solid in kg/m<sup>3</sup> respectively.

A simple freeze-drying equipment is a vacuum shelf type unit operating at an absolute pressure below 0.8 mm Hg. The temperature goes down to -20 °C or even less. The difference between the sublimation pressure and the condenser pressure acts as the driving force for sublimation. Shrinkage of the solid does not normally occur. Freeze dried materials can be rehydrated instantly and fully (Ruthven 1997).

## 12.11 Continuous Driers

### 12.11.1 Direct Driers

#### *Tunnel drier*

A *tunnel drier* consists of a long tunnel through which trucks carrying trays loaded with the solid to be dried are moved while in contact with a current of the drying gas. The trucks are continuously

pulled through the tunnel by a moving chain. Alternatively, the trucks may be pushed periodically at one end, each displacing a truck at the other end. The length of the tunnel and the average speed of the trucks are so adjusted that the solids are dried to the desired moisture content before being discharged from the drier. For low temperature drying, the gas may be steam-heated air. In case of high temperature drying, where slight contamination does not matter, drying may be done by hot flue gases. Both parallel and counter-current flow of solid and gas may be employed. If necessary, the gas may be heated by steam coils so that constant temperature drying may occur. Part of the gas is usually recycled.

Several modifications of the tunnel drier are used for drying special materials such as hide, yarn, etc.

### **Turbo-type drier**

*Turbo-type driers* consist of a series of annular trays arranged in a vertical stack and rotating slowly about a vertical shaft. Each tray is provided with a slot and a levelling rake for spreading the solids. The feed enters at the top and is spread on the top tray. As the tray rotates, the solid is pushed to the next lower tray through the slot. The drying gas enters at the bottom, flows upward and circulated over the trays by a slow turbine fan. The gas is reheated by internal heating pipes. The rate of drying is fairly high in this type of driers.

Turbo-type driers are suitable for granular and powdery materials, heavy sludges and pastes, crystalline solids, etc.

### **Conveyer or belt drier**

A *Conveyer drier* or *belt drier* consists of an endless moving belt made of perforated steel plate or heavy screen having minimum opening of 30 mesh. The width of the belt varies from 0.7 to 4 m and its length varies from 4 to 50 m. The material to be dried is spread up to a thickness of 0.03 to 0.15 m. The superficial velocity of the drying gas usually varies from 0.25 to 1.5 m/s. About 60% to 90% of the drying gas is recycled. Drying takes place by through circulation of the drying gas through the material being dried.

These driers are suitable for coarse materials such as granules, pellets, etc. Some of their common uses are drying of catalyst pellets, pigments, food products such as nuts, fruits, cereals, etc.

### **Rotary drier**

*Rotary driers* are the most widely used driers in the chemical process industry. As shown in Figure 12.17(a), a rotary drier consists of a long circular shell rotating about its central axis with a small angle to the horizontal. The shell is provided with flights to lift the materials to be dried and throw them through the drying gas/air.

Figure 12.17(b) shows a schematic representation of an indirect rotary drier. In this assembly, the solid feed passes through the central tube using of flights and the hot air/gas coming from the combustion chamber flows through the annular space.

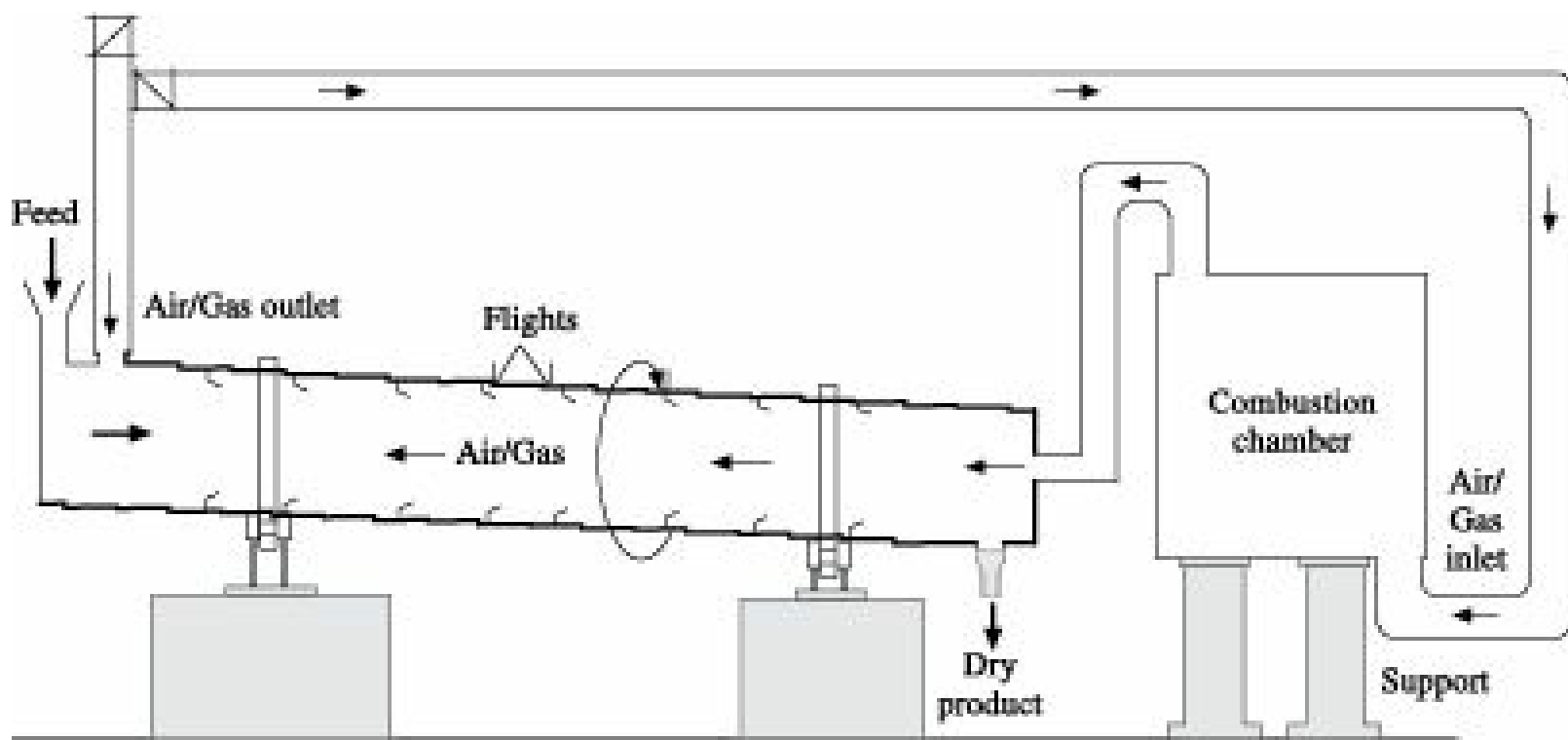


Figure 12.17(a) Counter-current rotary drier.

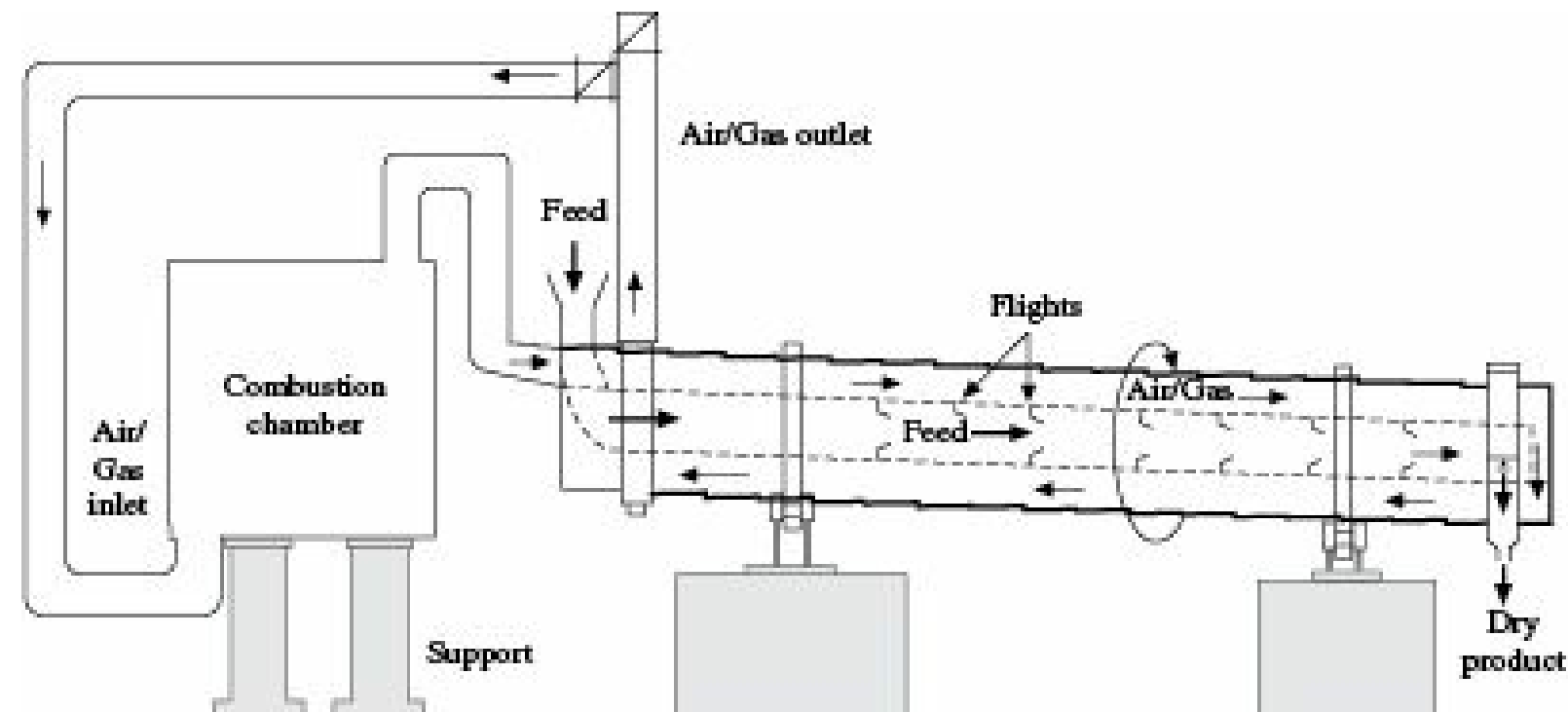


Figure 12.17(b) Indirect rotary drier.

The diameter of the shell depends on the capacity and the length depends on the rate and extent of drying. The length should be just adequate for the material to attain the desired moisture content while leaving the drier. The solids to be dried moves through the drier mainly by two actions—flight action and kiln action. *Flight action* is the lifting and dropping of solids by the flights. *Kiln action* is the forward rolling of the solid particles on the top of each other. In addition, forward movement of solids is enhanced by their bouncing in the forward direction after being dropped by the flights. The forward movement of solids is affected by air or gas flow, being aided by parallel flow and hindered by counter-current flow.

The internal shell diameter varies from 0.30 to 3.0 m. The shell rotates at 4-5 rpm providing a

peripheral speed of 0.2 to 0.5 m/s.

Flights are fixed along the inner wall of the shell and extend up to 8 to 10 percent of the shell diameter. Their number varies from 6 to 10 times the shell diameter in metre. They lift and throw down the solids through a curtain of the drying gas or air thus exposing them to the drying action of the hot gas or air.

Flights are of three types—straight, inclined at 45° and inclined at 90°. Straight flights are preferred for drying slightly pasty or sticky materials. Flights serve three purposes—they expose the solids to be dried to the action of the drying gas or air, help in the forward movement of the solids and prevent agglomeration.

The drier is usually inclined up to an angle of  $\tan^{-1} 0.08$ , i.e. up to 8 cm/m length towards the discharge end. Negative slope is sometimes used in co-current driers.

**Hold-up and retention time in rotary driers:** The hold-up  $z_D$  of solid in a rotary drier is the fraction of the drier volume occupied by the solid at any instant. Although the hold-up depends on the characteristics of the solid being dried, according to Friedman and Marshall (1949), the hold-up of a large number of solids under different operating conditions can be estimated by the simple relation

$$z_D = z_{DO} \pm KG \quad (12.37)$$

where,

$z_{DO}$  = hold-up with no air flow,

$KG$  = correction factor for air or gas flow,  $G$  being the mass velocity of air or gas,  $\text{kg}/(\text{m}^2\text{s})$ .

Positive sign is used for counter-current flow and negative sign is used for co-current flow.

Under typical operating conditions and for  $z_{DO}$  less than 0.08, the authors have recommended the following correlation for  $z_{DO}$ :

$$z_{DO} = \frac{0.3344 S_s}{\rho_s \beta N^{0.9} T_D} \quad (12.38)$$

where,

$b$  = slope of the drier, m/m

$N$  = rotational speed of the drier, rps

$T_D$  = drier diameter, m

For rough estimate,  $K$  may be taken as

$$K = \frac{0.6085}{\rho_s d_p^{0.5}} \quad (12.39)$$

$d_p$  being the average particle diameter.

Hold-ups in the range of 0.05 to 0.15 appear to be best (Treybal 1985).

The retention time  $i$  in seconds of the solids in the drier can be calculated by dividing the hold-up by the volumetric feed rate and is given by

$$i = \frac{\phi_D \cdot Z \cdot \rho_s}{S} \quad (12.40)$$

where,

$S$  = mass velocity of solid,  $\text{kg}/(\text{m}^2)(\text{s})$

$\rho_S$  = density of solid,  $\text{kg}/\text{m}^3$

$Z$  = length of drier, m

$z_D$  = hold-up, i.e. fraction of drier volume occupied by the solid at any time.

Rotary driers are classified into the following four groups:

- **Direct heat counter-current flow:** This is used for materials like minerals, sand, coke, limestone, etc. which can be heated to high temperatures with hot flue gases as heating medium. Hot air may be used for heat-sensitive materials.
- **Direct heat co-current flow:** It is useful for materials for which fear of contamination is not there but which should not be heated to high temperature, for instance, gypsum, iron pyrites, etc.
- **Indirect heat counter-current flow:** This is useful for materials such as white pigment which can be heated to high temperature but must not be contaminated by flue gas.
- **Direct-indirect:** This type of driers are suitable for materials which can be dried by flue gases at high temperature, especially when a large amount of moisture has to be removed and fuel cost is high. In these driers, the hot gas/air enters the central tube at very high temperature and return through the annular drying space. Lignite, coal and coke may be dried in this type of driers. The material to be dried being in an inert atmosphere, chances of explosion are largely reduced. A schematic diagram of a direct-indirect drier is shown in Figure 12.17(c).

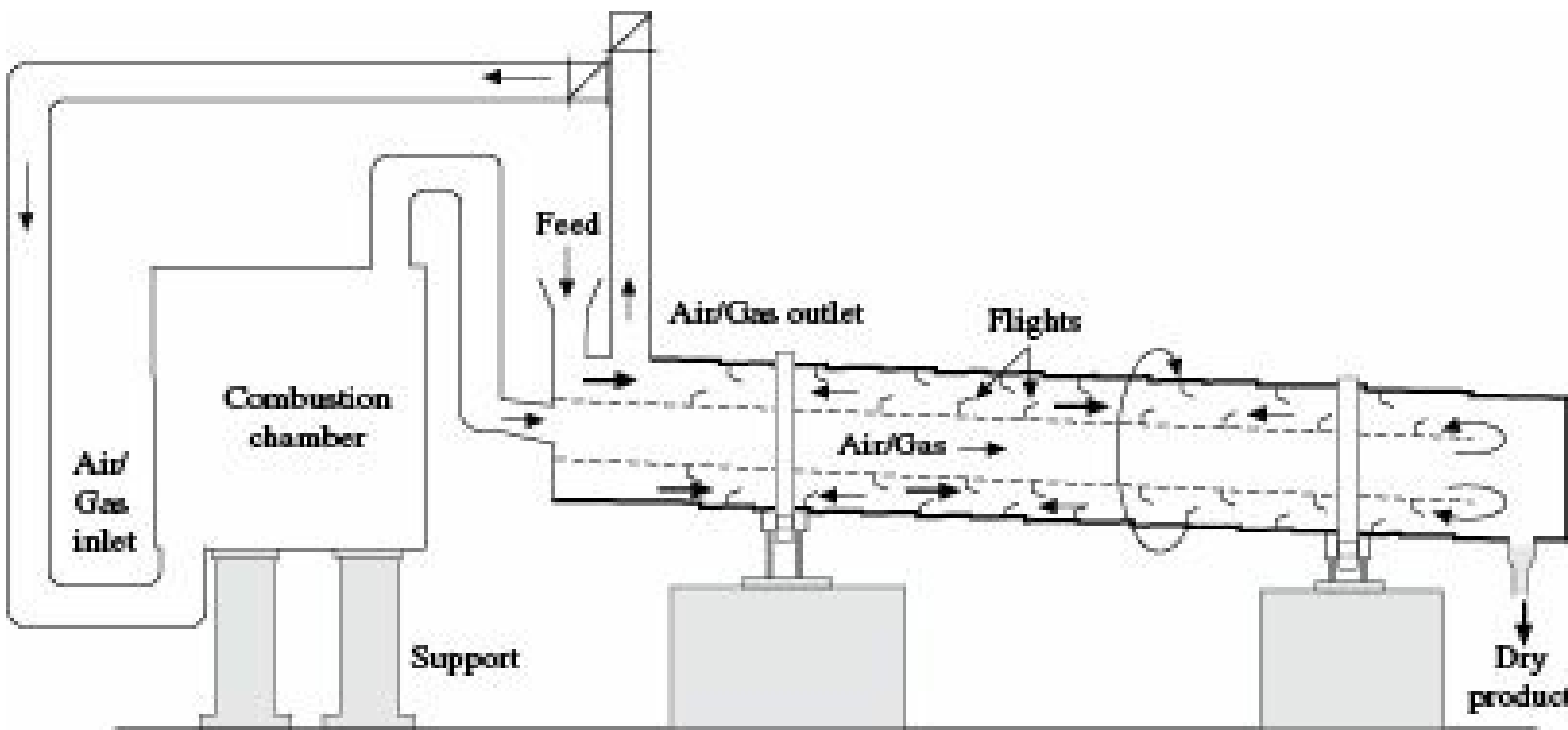


Figure 12.17(c) Indirect-direct rotary drier.

Rotary driers have many applications in the industry. These are very suitable for free flowing granular solids which do not break easily. These are, however, not suitable for sticky or gummy materials.

### **Fluidized and spouted bed driers**

Granular solids can be dried in *fluidized beds* using the drying air or gas as the fluidizing agent. The

advantages of such driers are cross flow of solid and drying gas, precisely controllable residence time for solid and use of any gas temperature. The solid must be free flowing and relatively small in size. Fluidized bed driers are most economically operated at minimum fluidization velocity of the gas. These dryers are used for drying of solids because of their efficiency in promoting high heat and mass transfer rates. Drying time may be reduced from hours or days to minutes. The boiling action of the bed promotes efficient mixing between the gas and the solid phases, which also helps to maintain a more uniform temperature throughout the fluid bed. The fluidized bed dryers give drying efficiency in the range of 40 to 80% (Mujumdar 1995). These dryers are used largely in pharmaceutical and fertilizer industries for drying of wet granules in general. The granules obtained from high shear mixer (HSM) can also be dried using such dryers. It is worthwhile to mention that aqueous-based granules when dried in such dryers, the drying rate is mainly dependent on the humidity of the drying air. The exhaust temperature needs to be recorded during the operation. If the exhaust temperature rises sharply than anticipated, it is an indication that the fluidization is complete.

In *Microwave* or *dielectric* drying, the materials are subjected to electromagnetic radiation (radio frequency from 3 to 150 MHz or microwave frequency at 915 to 2450 MHz). This process has been found to be comparable or superior in terms of efficiency, energy consumption and cost compared to conventional batch or continuous fluid bed drying. Energy savings of as much as 70% in industrial operation have been reported (Thorat and Shinde 2005). Such drying can be conducted in batch or continuous fashion with or without fluidization. In dielectric drying, the rate of drying is proportional to the energy field. If there are large differences between the dielectric constants of the materials, fairly rapid and selective drying is possible. For example, since water has a dielectric constant of 70 and if the dielectric constant of the material itself is around 10, water is heated much more rapidly than the other components of the granules as shown by the equation

$$P = K f E^2 f \tan d \quad (12.41)$$

where

$P$  = power utilized in W/volume

$K$  = geometric constant times the dielectric constant of a vacuum

$f$  = frequency of the applied field

$E$  = field strength in volts per unit distance

$\tan d$  = loss tangent or dissipation factor of the material and

$f$  = relative dielectric constant of the material being heated

In the recent past, microwave vacuum dryers have been recommended as these units offer certain advantages in the drying of solids. Operating under low vapour pressure and combined with molecule selective energy coupling of microwaves, polar solvents may be evaporated at low temperatures. For example, at a typical process pressure of 35 mm Hg, water based granules can be dried at 31°C (Swarbrick and Baylan 1991). Another advantage of combining vacuum and microwaves is that the process is practically independent of ambient atmospheric conditions such as relative humidity and temperature which have dramatic effects on conventional drying techniques.

Drying systems incorporating a dehumidification cycle, called *heat pump dryer* (HPD), have been developed that not only accelerate the drying process but also preserve the quality of the product by facilitating drying at low temperature. The heat pump recovers the sensible and latent heats by condensing moisture from the drying air. Consequently, a partial pressure of solvent in the drying air

decreases thereby increasing the driving potential for mass transfer. The recovered heat is recycled back to the dryer by heating the drying air. Heat pump assisted drying gives high energy efficiency, better quality products especially for heat sensitive materials, and wide range of operating conditions. Its limitations are higher initial cost and maintenance cost due to the need to maintain compressor, refrigerant filters and charging of refrigerants, marginally complex operation relative to simple conventional dryers and additional floor space requirement. Any conventional dryer such as tunnel, fluid bed, spouted bed, rotary, etc. that uses convection as the primary mode of heat transfer can be fitted with a suitably designed heat pump. Heat pump dryer can be installed with different modes of heat input such as convection, conduction and radiation. The efficiency of heat pump assisted dryers are measured in terms of specific moisture evaporation rate which is defined as the amount of water evaporated per unit of energy used. A typical value of the specific moisture evaporation rate achieved by a heat pump is 3 kg/kW h which compares very favourably with conventional drying with values ranging from 0.5 to 1 kg/kW h. Yang et. al (2004) have reported the value of specific moisture evaporation rate as 2.1 kg/kW h for grain drying.

Coarse solids which cannot be readily fluidized can be dried in *spouted bed driers*. The drying gas moves upward through the centre of the bed in the form of a column causing a fountain like spout of solids at the top. The solids then circulate downward around the fluid column. These driers are suitable for drying wheat, peas and the like.

### **Pneumatic driers**

While fluidized bed driers are operated at or near the minimum fluidization velocity of the gas, in *pneumatic driers* the gas velocity is increased to the terminal velocity of the solid particles so that the solids are lifted from the bed and carried away by the gas.

A schematic diagram of a pneumatic drier is shown in Figure 12.18. The wet solid is introduced into the drier by some mechanical feeder like rotating star wheels or by an extrusion machine with a high speed guillotine. Hot gas from an oil burner or a furnace is introduced at the bottom of the drier. The gas picks up the solid particles and carries them up the column. The gas stream, along with the solids is then passed through a cyclone separator where the solids are separated from the hot gas, which leaves the system. In some cases, bag filters are used to collect very fine solids. The time of contact between the solids and the hot gas being very small in this type of drier, the solids do not approach the temperature of the hot gas.

Pneumatic driers are used for drying finely divided solids. Being finely divided, the surface per unit volume of the material becomes very large and a high rate of heat transfer results.

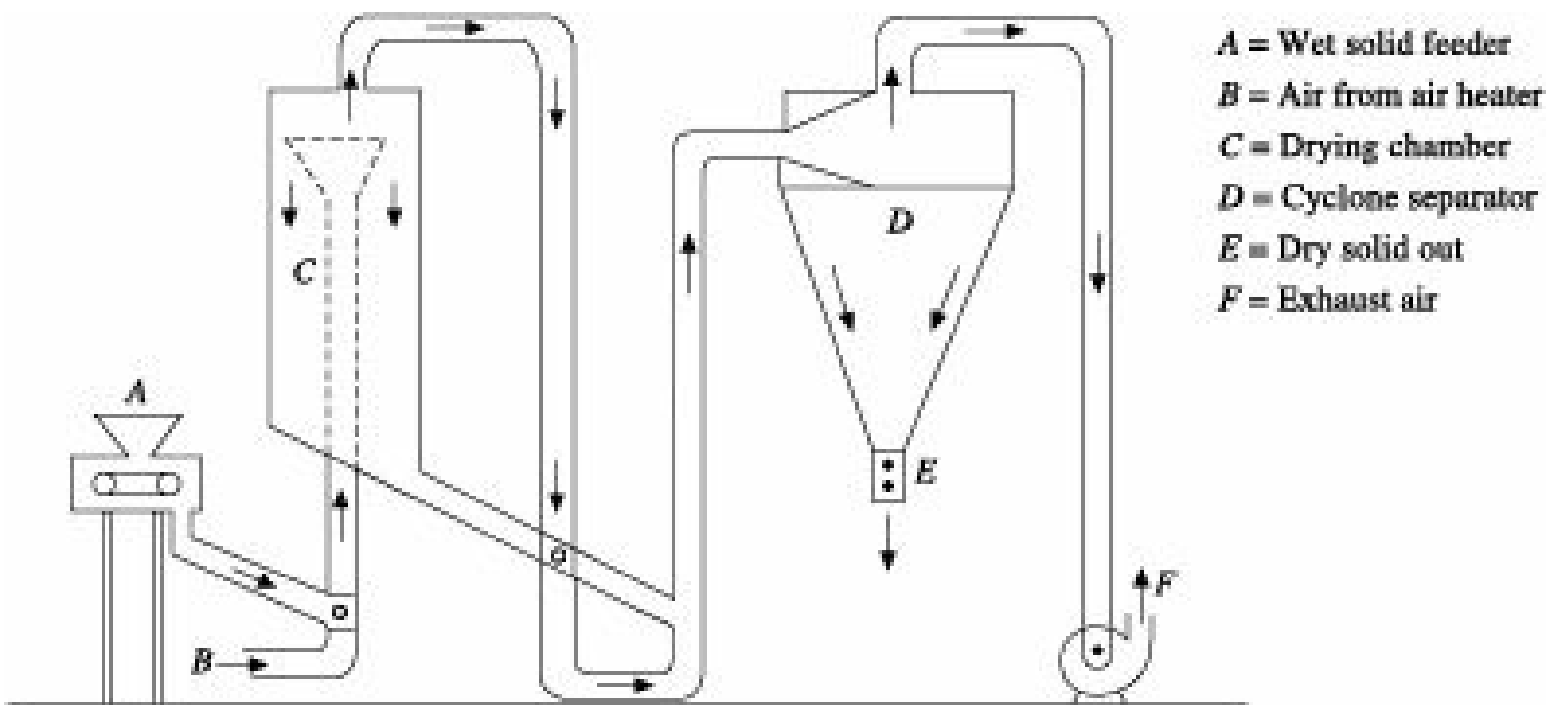


Figure 12.18 Schematic diagram of a pneumatic drier.

### Spray drier

*Spray driers* (Figure 12.19) are suitable for drying of liquids. The liquid to be dried is introduced into a large drying chamber after being atomized into small droplets (Masters 1972). In the chamber, as shown in Figure 12.19, the liquid flowing through the nozzles is dispersed into a stream of hot gas and the liquid evaporates very fast leaving the associated solids as dry powders which settle in the conical bottom of the drier and are pneumatically conveyed to a cyclone separator. The exit gas is also routed through the cyclone separator before being discharged into the atmosphere. Spray driers maybe quite large, up to 12 m in diameter and up to 30 m high.

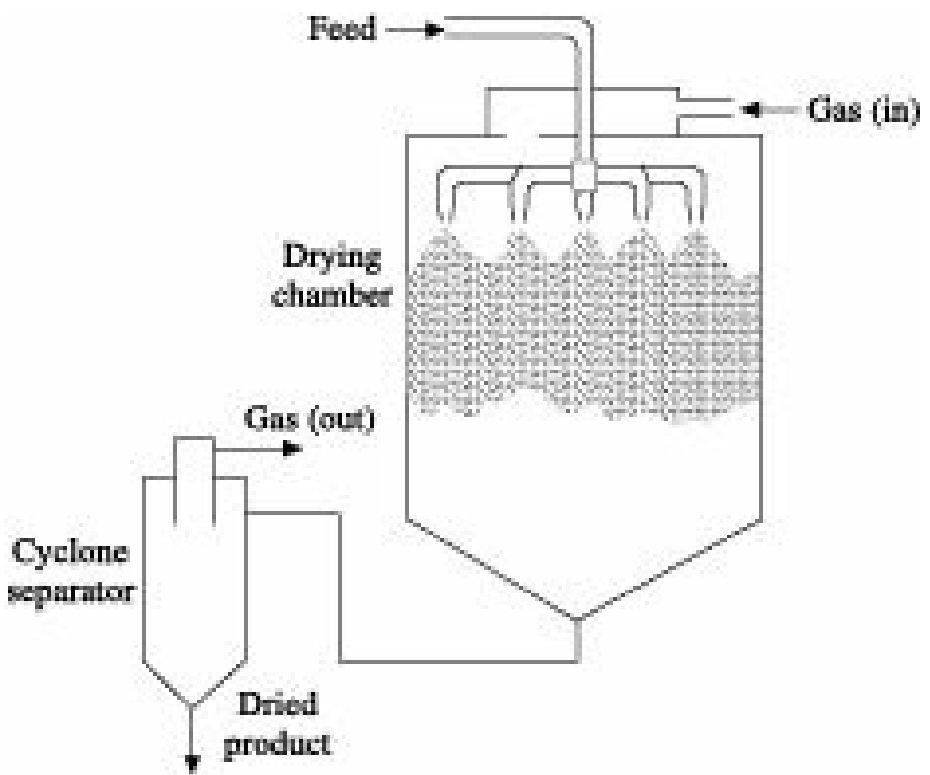


Figure 12.19 Schematic representation of spray drier.

Atomization is done by spray nozzles or by rapidly moving disks. Two types of spray nozzles are in

use, pressure nozzles and two-fluid nozzles.

Spray driers have the advantage of very rapid drying and are therefore recommended for heat-sensitive materials. Moreover, the product size can be controlled within limits. The operating cost is relatively low. However, efficient counter-current action is not ordinarily possible in spray driers and, as a result, sensible heat loss in the waste air is usually high.

### **Filter drier**

Filter driers which allow filtration and drying to be carried out in a single unit, have emerged as combo units used in process industries. A filter drier is typically charged with slurry from a reactor or crystallizer. The slurry is first filtered using gas pressure on one side of the filter medium and vacuum at the other side. The resulting pressure difference drives the filtrate through the filter medium. During drying, heat is supplied to remove liquid that is trapped in the filter cake. Once the filter cake is dried to a certain level of moisture content, it is discharged from the filter and fed into the drier. A thermal drier is required to remove the moisture that adheres strongly to the particulate surfaces. The filter drier based on the location of the filter element, may be of three types—vertical, horizontal and rotary. Detailed descriptions of filter driers are given elsewhere (Mujumdar and Law 2006). These types of filter driers may be assisted with heat-pump system, where the heat-pump evaporator serves as a condenser. The schematic diagram of such driers is shown in Figure 12.20(a)-(c).

As filter drier combines filtration and drying in one unit, floor space, power consumption, spillage and processing time are minimized. Since transport of materials from filter to drier is no longer required, the capital, operating and maintenance costs are reduced appreciably. In addition, processing of materials is simplified and the complexity of manufacturing is eliminated while minimizing product handling procedures.

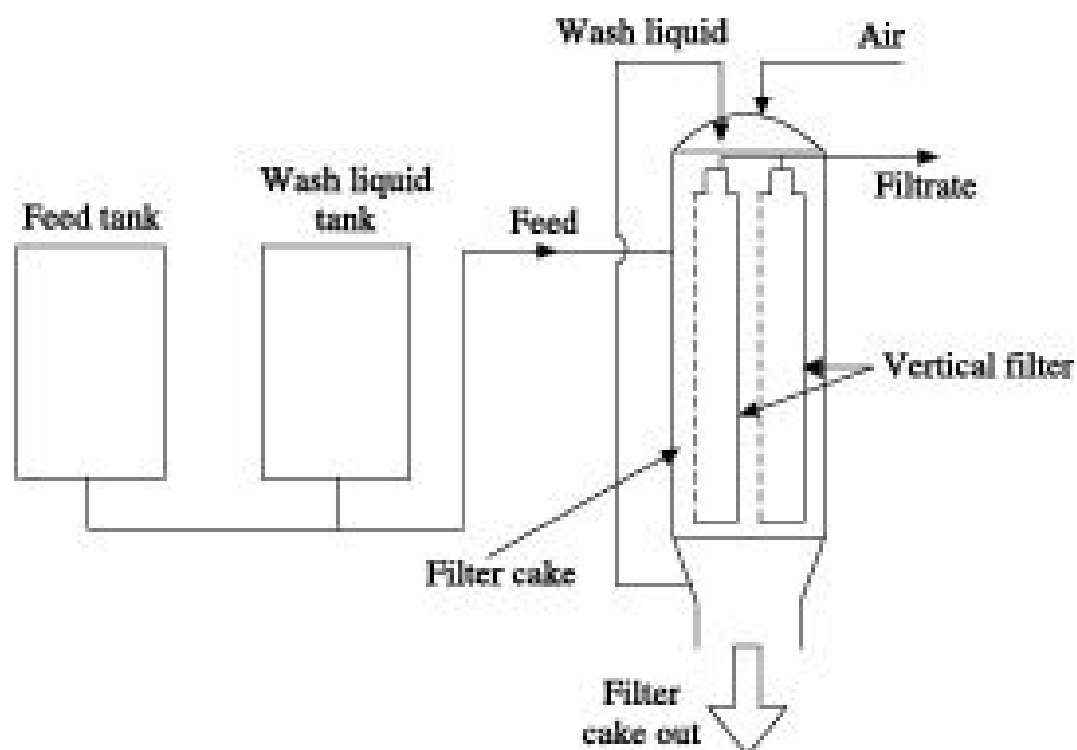


Figure 12.20(a) A typical vertical filter drier.

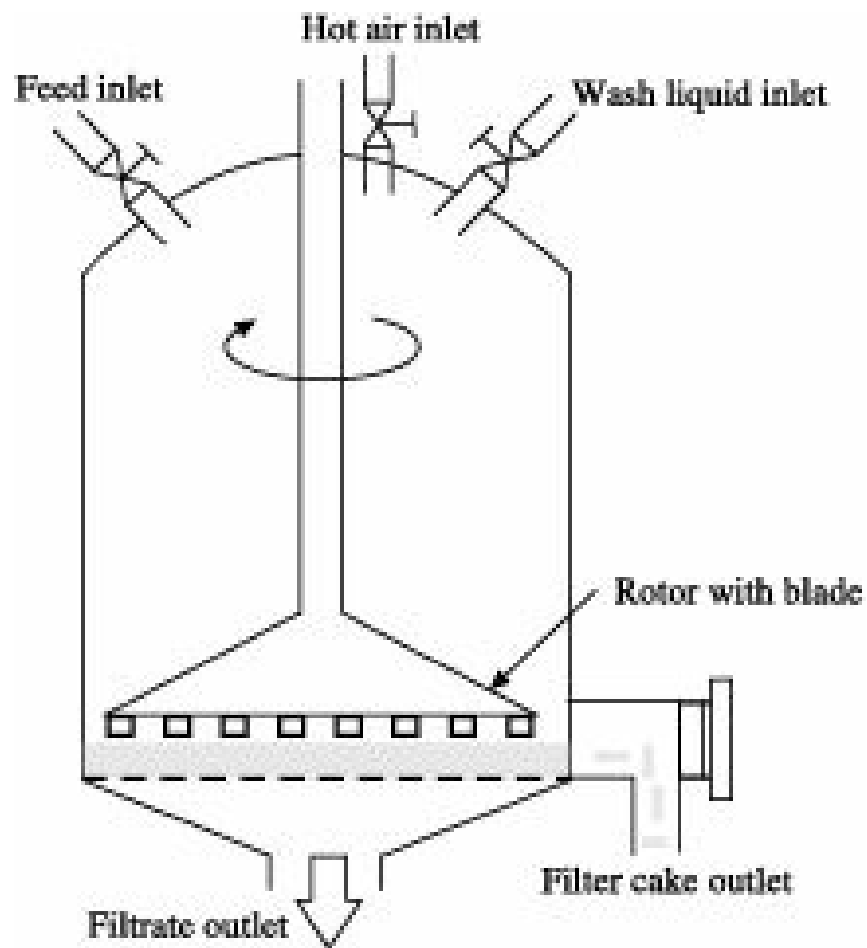
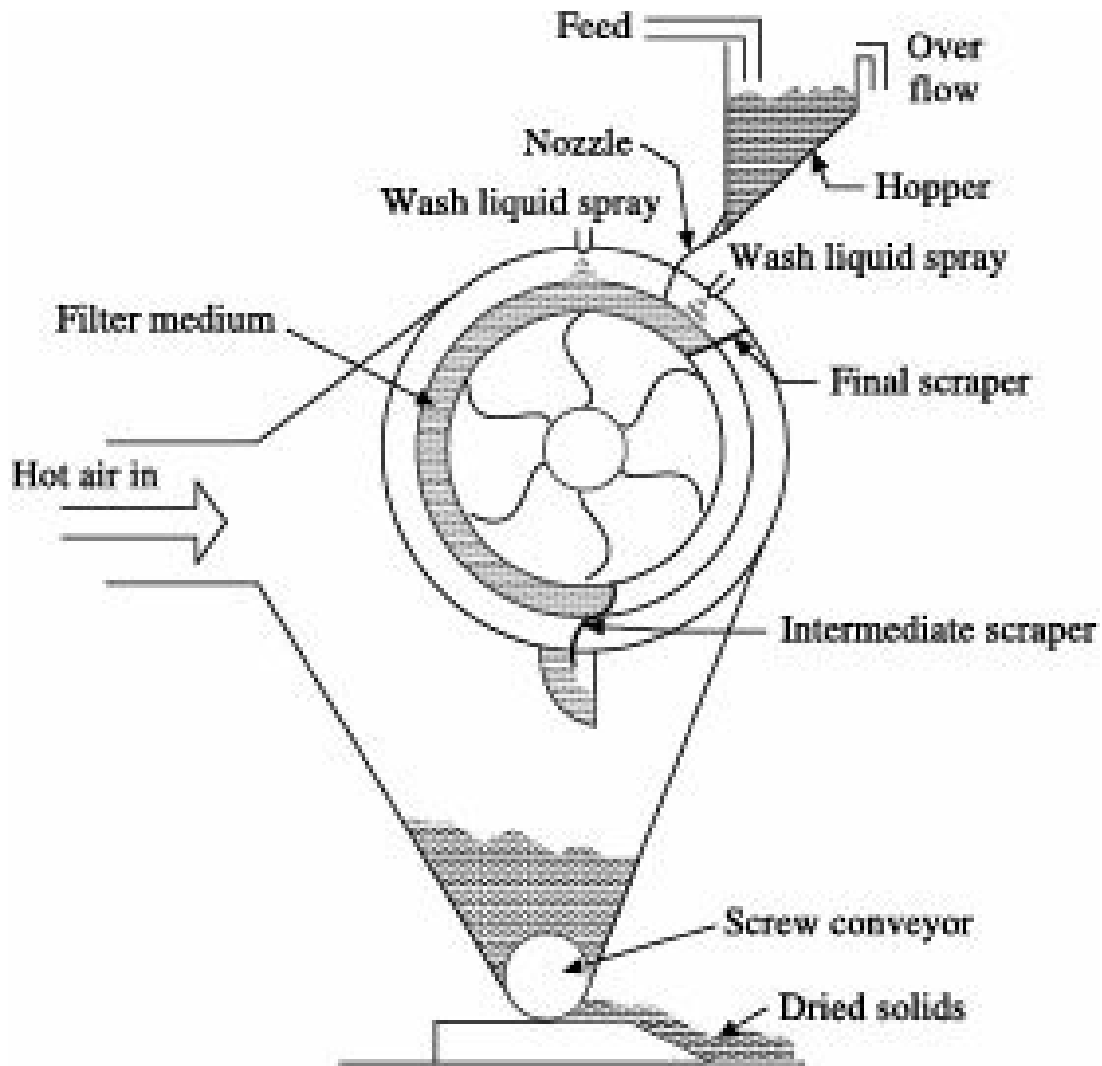


Figure 12.20(b) A typical horizontal filter drier.



**Figure 12.20(c)** Schematic diagram of a typical rotary filter drier.

## 12.11.2 Indirect Driers

### Drum drier

A *drum drier* in its simplest form consists of a slowly rotating metal drum with steam coils inside. About 15-20% of the drum surface dips into a trough containing the liquid to be dried. The drum picks up certain amount of the material, which is then spread uniformly as a film on the outer surface of the drum by a spreader knife. As the drum rotates, moisture is evaporated, the required heat being supplied by steam condensing inside the drum. The dried film is then scraped off by a doctor's knife. For solutions, most of the drying takes place at the boiling point of the solution, while for slurries or pastes of insoluble substances the temperature remains constant at the boiling point of the solvent. In both the cases, however, the temperature rises and approaches the temperature of the drum surface at the end of drying.

Drum driers are suitable for drying solutions, slurries or pastes.

The *double drum drier*, a modified version of the drum drier, consists of two hollow drums of equal size placed side by side with a very small gap and rotating in opposite direction towards each other as shown in Figure 12.21. The feed, usually a solution, is introduced just above the small gap and is picked up by the drums in the form of thin film. Before completion of one revolution, the dried films are scraped by doctor's knives and are collected in receivers placed below.

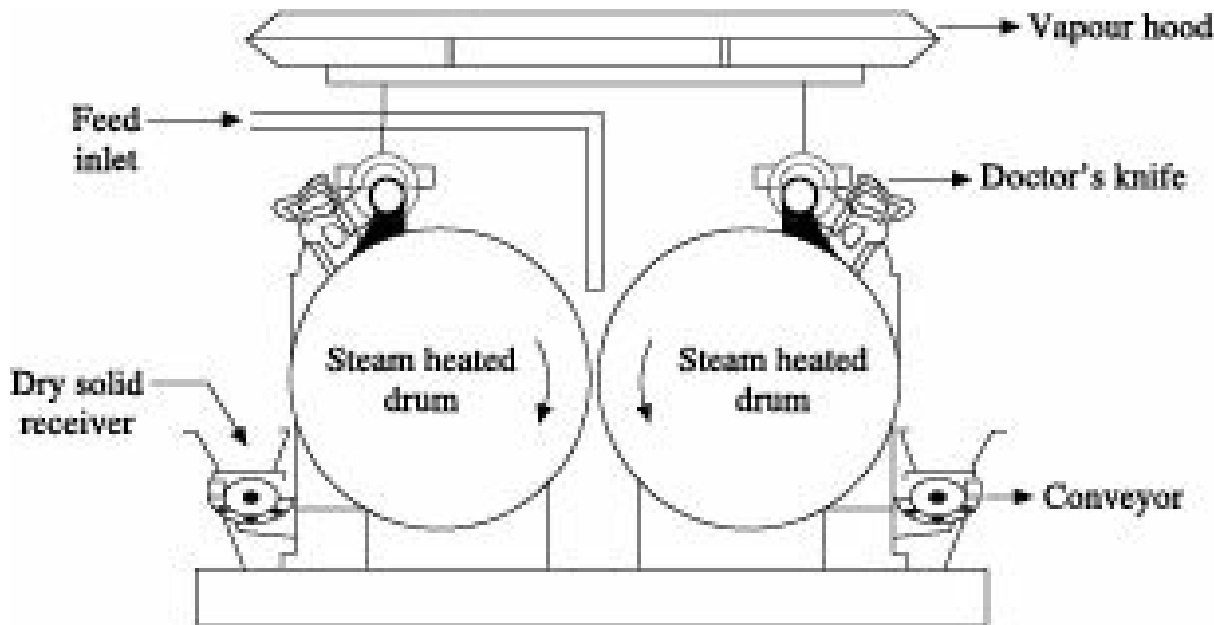


**Figure 12.21** Double drum drier.

The entire operation can be carried out under vacuum. Vacuum double drum driers are suitable for drying milk, fruit juice, etc.

## 12.12 Selection of Drier

Selection of the right drier is one of the most complex areas in the drying technology. Since the life of a drier is typically 25-40 years, selection of inefficient drier can have a long term impact on the economic health of the process plant. The optimal choice can be based on the fact that satisfies all process requirements at minimum cost. The following characteristic information need to be collected for judicious selection of a drier:

- (i) Feed property: liquid, slurry, pasty, free flowing powder, granular, crystalline, etc.
  - (ii) Drier throughput
  - (iii) Particle size and its distribution for a particulate material
  - (iv) Type of operation: batch or continuous
  - (v) Moisture content of the feed and of product
  - (vi) Allowable temperature of the product
  - (vii) Feed cohesiveness
  - (viii) Product fragility
  - (ix) Explosion characteristics
  - (x) Corrosion aspects
  - (xi) Contamination of drying gas
  - (xii) Product value.

Table 12.1 shows the classification of commercial driers based on the materials handled (Wanjari and Thorat 2007).

Product specification may strongly affect the choice of drier. For example, a flaked product is readily obtained from a drum drier while a highly porous, agglomerated product of low bulk density is often produced by spray driers. Sometimes, spray drier is selected if the characteristic spherical particle shape is desired. Typically, the average particle size falls in the range of 50-200 mm. Because of short residence time this driers can be used for heat-sensitive materials, e.g. milk powder. Proper selection of atomizer is vital for the operation of the spray drier as it is affected by the type of feed, abrasive property of the feed, feed rate, desired particle size and size distributions.

Batch driers are usually used of smaller size and are more labour-intensive since each batch must be loaded and unloaded. Hence, the use of batch drier is favoured by a low throughput, low drying rate, batch upstream and downstream equipment and multiple products. If the material is friable, 'layer driers' are preferred, e.g. conveyor drier, tray drier, etc. whereas the 'dispersion driers' can be used if the material is not friable.

Convective driers use higher gas flows and achieve higher heat transfer rates than contact driers. These types of driers can achieve much faster drying. Convective drying are effective in higher temperature applications and can use exhaust gases from burner, furnace, but exhaust heat losses are higher. If containment is required or gaseous particulate emissions are highly restricted, conduction drying is preferable. If feed contains fine particles, the indirect mode of heat transfer is preferred. As the contact with products of combustion from fossil fuels adversely affects the product quality, indirect mode of heat drying like steam-tube rotary drier or multi-coil drier can be used. If the risk of fire, explosion or other oxidative damage is very high, superheated steam drying may be thought of. These types of drying are extensively used in process industries. For drying of very high heat-sensitive materials, freeze drying can be selected; Heat pump assisted drying may be a viable option.

**Table 12.1** Classification based on materials handled

batch operation	<input type="checkbox"/>							
Batch through circulation, direct type, batch operation	<input type="checkbox"/>							
Tunnel, continuous tray direct type, continuous operation	<input type="checkbox"/>							
Continuous through circulation: direct type, continuous operation	<input type="checkbox"/>							
Direct rotary: direct type, continuous operation	<input type="checkbox"/>							
Pneumatic conveying: direct type, continuous operation	<input type="checkbox"/>							
Spray: direct type, continuous operation	<input type="checkbox"/>							
Continuous sheeting: direct type, continuous operation	<input type="checkbox"/>							
Vacuum self: indirect type, batch operation	<input type="checkbox"/>							
Vacuum freeze: indirect type, batch or continuous operation	<input type="checkbox"/>							
Pan: indirect type, batch operation	<input type="checkbox"/>							
Vacuum rotary: indirect type, batch operation	<input type="checkbox"/>							
Screw conveyor & indirect rotary: indirect type, continuous operation	<input type="checkbox"/>							
Fluid bed: batch or continuous, direct or indirect	<input type="checkbox"/>							
Vibrating tray: indirect type, continuous operation	<input type="checkbox"/>							
Drum: indirect type, continuous operation	<input type="checkbox"/>							
Cylinder: indirect type, continuous operation	<input type="checkbox"/>							
Infra red: batch or continuous	<input type="checkbox"/>							
Dielectric: batch or continuous	<input type="checkbox"/>							

When the temperature of the product is required to be kept lower than the ambient temperature, vacuum drying is preferable. If either the product or the removed liquid is toxic, the equipment must be operated in a closed loop. Vacuum drier can provide good service in such situation.

The materials to be dried usually contain bound and unbound moisture. Unbound moisture can readily be removed, i.e. less drying time is required for the purpose. But higher temperature and longer retention time is required for removal of bound moisture. Flash drier may be used for removal of free-moisture. However, for the materials that require longer contact time with the hot gases, direct-heat rotary drier is preferable although crystal breakage may cause problem. Crystal materials or polymers that are relatively fragile can be dried successfully in steam tube rotary drier.

Two-stage drying may be used where either the drying rate or the handling characteristic of the feed change drastically during the drying processes. In the first stage, dispersion drier like spray, pneumatic conveying drier may be used, while in the second stage drier of longer contact time like fluidized bed drier or multistage fluid drier with a well mixed one may be used.

Selection of driers has to be made considering other relevant criteria as well. More information can be available in the literature. Drier selection is a critical issue and has major impact on economic health of plant. The final selection of the drier will therefore depend on cost involved, quality of the desired product, safety aspects and convenience of installation.

## Nomenclature

$a$  : interfacial area of solid/drier volume,  $\text{L}^2/\text{L}^3$

$A$  : drying surface,  $\text{L}^2$

$C_P$  : heat capacity at constant pressure,  $\text{FL}/\text{MT}$

$C_S$  : heat capacity of dry solid,  $\text{FL}/\text{MT}$ , humid heat of air,  $\text{FL}/\text{MT}$

$d_e$  : equivalent diameter,  $\text{L}$

$d_p$  : particle diameter,  $\text{L}$

$G$  : mass velocity of gas,  $\text{M}/\text{L}^2\square$

$G_S$  : mass velocity of dry gas,  $\text{M}/\text{L}^2\square$

$h_C$  : heat transfer coefficient for convection,  $\text{FL}/\text{L}^2\text{T}\square$

$h_R$  : heat transfer coefficient for radiation,  $\text{FL}/\text{L}^2\text{T}\square$

$H'_G$  : enthalpy of wet gas per unit mass of dry gas,  $\text{FL}/\text{M}$

$H_{toG}$  : length of an overall gas transfer unit,  $\text{L}$

$\Delta H_S$  : latent heat of sublimation of ice,  $\text{FL}/\text{kmol}$ .

$i_D, j_H$  : Colburn factor for mass transfer and heat transfer, respectively

$k$  : thermal conductivity of the dry solid,  $\text{W}/\text{LT}$

$k_y$  : gas-phase mass transfer coefficient,  $\text{mol}/\text{L}^2\square$  (mol/mol)

$M$  : mass of the solid,  $\text{M}$

$M_A$  : molecular weight of water

$N$  : rate of revolution,  $\square^{-1}$

$N_{tG}$  : number of gas phase transfer unit

$N_{toG}$  : number of overall gas phase transfer units

$p$  : vapour pressure,  $\text{F}/\text{L}^2$

$p'$  : partial pressure,  $\text{F}/\text{L}^2$

$P$  : total pressure,  $\text{F}/\text{L}^2$

$q$  : heat flux,  $\text{FL}/\text{L}^2\square$

$Q$  : net flux of heat loss,  $\text{FL}/\text{L}^2\square$

$R$  : drying rate in mass per unit time per unit area,  $\text{M}/\text{L}^2\square$

$s$  : interfacial area per unit cross section of the solid,  $\text{L}^2/\text{L}^2$

$S$  : mass velocity of dry solid,  $\text{M}/\text{L}^2\square$

$t$  : temperature,  $^\circ\text{C}$

$T$  : absolute temperature,  $\text{K}$

$T_e$  : ambient temperature, °C

$T_f$  : temperature of the sublimation front or ice layer, °C

$U$  : overall heat transfer coefficient, FL/L<sup>2</sup>T $\square$

$V_S$  : volume of solid material occupied by unit kg of water initially, L<sup>3</sup>

$X$  : moisture content of solid, M/M

$X^*$  : equilibrium moisture content, M/M

$X_0$  : initial free-moisture content, M/M

$x$  : direction of transport of properties, L

$Y$  : moisture content of air/gas, M/M

$Y^*$  : equilibrium moisture content of air/gas, M/M

$Y_S$  : saturated humidity of air/gas, M/M

$Z$  : length of drier/thickness of drying solid, L

### *Greek Letters*

$b$  : slope of drier, m/m

$f$  : emissivity of drier surface, dimensionless

$m_S$  : latent heat of vaporisation at temperature  $t_S$ , FL/M

$\rho$  : density, M/L<sup>3</sup>

$\tau_S$  : bulk density of dry solid, M/L<sup>3</sup>

$\eta$  : viscosity, M/L $\square$

$i$  : time,  $\square$

$\Delta$  : difference/change

$z_D$  : hold-up of solid in a continuous drier, L<sup>3</sup>/L<sup>3</sup>

$z_{DO}$  : hold up of solid at no gas flow, L<sup>3</sup>/L<sup>3</sup>

### *Subscripts*

$c$  : convection

$C$  : constant rate period of drying

$e$  : evaporation

$F$  : falling rate period

$G$  : gas/air

$k$  : conduction

$m$  : mean

$R$  : radiation

$S$  : solid

### **Numerical Problems**

**12.1 Calculation of the Amount of Bone-Dry Air Required for Removal of 100 kg Moisture per Hour and also the Minimum Amount of Dry Air For Varied Humidity of Entering Air:** A drier is to be designed to remove 100 kg moisture per hour from  $\text{CaCO}_3$  slurry. Air at  $20^\circ\text{C}$  and 40% relative humidity enters the drier, and leaves at  $65^\circ\text{C}$  and 65% relative humidity. What is the weight (in kg) of bone-dry air required per hour? The atmospheric pressure is 103 kPa. If the humidity of the air entering the drier can be varied, what is the minimum amount of dry air required? The constants for Antoine equation for vapour pressure of water in mm Hg may be taken as  $A = 18.306$ ,  $B = 3816.44$ , and  $C = -46.13$ .

[Ans: 40000 kg. dry air]

**12.2 Computation of the Flow Rate of Air and also of Steam with Known Dryness Fraction:** A drier with a capacity of 1 tonne/hr (wet basis) is used to dry a material from a moisture content of 55% to one of 8% (wet basis). The atmospheric air available at  $20^\circ\text{C}$  with a relative humidity of 0.75 is heated in an air heater to  $110^\circ\text{C}$ . The drying potential at the outlet from the drier is  $10^\circ\text{C}$ . Determine (i) the rates of flow of the air and (ii) the heating steam if the steam pressure is 2.5 atm (abs) and its dryness fraction is 95%.

[Ans: (i) 20800 kg/hr (ii) 950 kg/hr]

**12.3 Determination of Temperature and Moisture Content of the Exit Air and also the Temperature of the Wet Material During First Period of Drying:** Find the temperature and moisture content of the air leaving a drier if the mean drying potential is  $41^\circ\text{C}$ . Air is fed into the air heater at  $15^\circ\text{C}$  and relative humidity of 70%. The enthalpy of the air fed into the drier from the air heater is 144.2 kJ/kg. Also, find the temperature of the wet material during the first period of drying.

[Ans: Temperature of air =  $53^\circ\text{C}$ , Moisture content = 0.035 kg/kg, Temperature of wet material =  $38^\circ\text{C}$ .]

**12.4 Determination of Rate of Drying and Critical Moisture Content:** A dye paste was dried in a chamber drier with recirculation of the air. An analysis of samples for their moisture content revealed the data shown below:

Time from beginning of drying, hr	Moisture content of material, % (dry basis)
0	104.0
2	84.0
2.5	79.1
4	63.9
5	53.9
6	43.9
8	32.0
10	21.9
12	14.0
14	8.0
16	5.0
18	3.0
20	1.5

Determine the rate of drying depending on the time. Use the data to construct the drying rate curve and find the critical moisture content.

[Ans: Critical moisture content of 43.9% (bone-dry basis) or 30.6% of moisture per total mass of the

product (wet basis) is reached in 6 hr after the beginning of drying]

**12.5 Calculation of Drying Rate and Time Required for Drying of Food:** Drying of food is carried out in an insulated tray. The drying air has a partial pressure of water equal to 2360 Pa and a wet-bulb temperature of 30°C. The product has a drying surface of 0.05 m<sup>2</sup>/kg dry solid. The material having a critical rate in the falling rate period is proportional to moisture content, and mass transfer coefficient is  $5.34 \times 10^{-4}$  kg/(m<sup>2</sup>)(hr)(Pa). Calculate (i) the drying rate in the constant rate period in kg/m<sup>2</sup> hr and (ii) the time required to dry material from a moisture content of 0.22 to 0.08. The vapour pressure of water at 30°C is 4232 Pa.

[Ans: (i) 1.06 kg/(m<sup>2</sup>)(hr) (ii) 14.96 hr]

**12.6 Computation of Drying Time for given Critical and Equilibrium Moisture Contents:** A commercial drier needed 7 hr to dry a moist material from a moisture content of 33% to one of 9% (bone-dry basis). The critical moisture content of the material was 16%, and the equilibrium moisture content was 5%. Determine the time needed to dry this material from a moisture content of 37% to one of 7% if the drying conditions remain unchanged. Neglect the initial starting period.

[Ans: 9.9 hr]

**12.7 Determination of Drying Time to Reduce the Moisture Content to a Certain Value from a Known Drying Time for Another Set of Conditions:** A moist material with an initial moisture content of 33%, a critical one of 17%, and an equilibrium moisture content of 2% is dried in constant conditions to a moisture content of 9% during 8 hr. Determine the time of drying to a moisture content of 3% in the same conditions. The moisture content is indicated on bone-dry basis in mass%.

[Ans: 16.5 hr]

**12.8 Estimation of Time Required for Drying a Material from Drying Rate Curve and Weight of the Dry Material:** Data on drying rate curve of a particular solid are given below:

Moisture content $X$ , kg/kg dry solid: 0.30 0.20 0.18 0.15 0.14 0.11 0.07 0.02
---

Rate, $R$ , kg/(m <sup>2</sup> )(hr): 1.22 1.22 1.12 0.98 0.78 0.49 0.24 0.00
---

The weight of dry material in the solid is 48.8 kg/m<sup>3</sup>. Calculate the time required to dry the material from 20% to 5% moisture (wet basis). [Ans: 13.63 hr]

**12.9 Calculation of Drying Time of a Material for a Specified Moisture Change on Dry Basis:** Data on drying rate curve of a particular solid are given below:

Moisture content $X$ , kg/kg dry solid: 0.30 0.20 0.18 0.15 0.14 0.11 0.07 0.05
---

Rate, $R$ , kg/(m <sup>2</sup> )(hr): 1.22 1.22 1.14 0.90 0.80 0.56 0.22 0.05
---

The weight of dry material in the solid is 48.0 kg/m<sup>3</sup>. Calculate the time required to dry the material from 25% to 8% moisture (dry basis).

[Ans: 10.47 hr]

**12.10 Estimation of Additional Time Required for Further Reduction of Free-Moisture Content of a Material:** A certain material was dried under constant drying condition and it was found that 2 hr

is required to reduce the free moisture content from 20% to 10%. Determine further time required to reduce the free moisture to 4%. Assume that no constant rate period is encountered.

[Ans: 2.39 hr]

**12.11 Estimation of Moisture Content of a Material after Extended Period of Time for Drying:** A certain material having an initial moisture content of 18% is dried to 8% moisture in 5 hr. The equilibrium moisture content of the material is 3%. All the moisture contents are expressed on dry basis. If the material is dried for a further period of 3 hr under the same drying conditions, estimate the moisture content of the material at the end of the extended period.

It may be assumed that the material does not exhibit any constant rate period of drying and that the falling rate period is linear.

[Ans: 5.58%]

**12.12 Time Required for Drying of Slabs of Paper Pulp under Constant Drying Condition:** Slabs of paper pulp 100 cm # 100 cm # 1.5 cm is to be dried under constant drying condition from 66.7 to 30% moisture. The value of equilibrium moisture for the material is 0.5% if critical moisture content is 60% and rate of drying at critical point is  $1.5 \text{ kg}/(\text{m}^2)(\text{hr})$ . Calculate the drying time, the dry weight of the slabs being 2.5 kg. All moisture contents are on wet basis.

[Ans: 1.99 hr]

**12.13 Computation of the Drying Time of a Slab Using the Data on Drying Rate at Critical Moisture Content:** A slab of paper pulp 1.2 m # 1.2 m # 5 cm is to be dried under constant drying conditions from 85% to 15% moisture content on dry basis. The equilibrium moisture content is 2.5% (dry basis) and the critical moisture content is 0.45 kg free-water per kg of dry pulp. The drying rate at the critical point has been estimated to be  $1.40 \text{ kg}/(\text{m}^2)(\text{hr})$ . The dry weight of the slab is 13.0 kg. Assuming drying to take place from two large faces only, estimate the drying time to be provided.

[Ans: 2.96 hr]

**12.14 Determination of Drying Time of a Sheet Material under Constant Drying Condition:** A sheet material measuring 1.5 m # 1 m # 5 cm is to be dried from 40% to 5% moisture under constant drying conditions. The density of dry material is  $450 \text{ kg}/\text{m}^3$  and its equilibrium moisture content is 2%. Experiments showed that the rate of drying was constant at  $4.2 \text{ kg}/(\text{hr})(\text{m}^2)$  between 40% to 20% moisture content below which the rate decreased linearly. If drying takes place from the two large faces only, calculate the time required to dry the material from 40% to 5% moisture content. All the moisture contents are on wet basis. [Ans: 2.35 hr]

**12.15 Calculation of Time for Drying of Coetex Sheets Assuming the Rate of Drying under Linear Falling Rate Period:** Coetex sheets are to be dried by blowing air at  $60^\circ\text{C}$ , 10% relative humidity and a velocity of 10 m/s. The critical moisture content is 0.35 kg free water/kg dry solid. The rate of drying in the falling rate period can be considered linear. Coetex must be dried from 55% to 12%, equilibrium moisture content under the drying condition is 5%. The coetex layer is insulated by 6 cm. The density of dry solid is 1.38 g/cc. Calculate the time of drying the sheets.

The rate of drying,  $R_C$  in  $\text{g}/(\text{cm}^2)(\text{hr})$  during constant rate period is given by

$$R_C = 0.004v^{0.8} (p'_i - p'_g)$$

where,  $v$  is the velocity of air in m/s;  $p'_i$  and  $p'_g$  are the partial pressure of water vapour and that at dew point temperature, respectively. [Ans: 25.14 hr]

**12.16 Estimation of Time for Drying of Fibre Board in Sheets, Assuming the Falling Rate Period Linear:** It is desired to dry a certain type of fibre board in sheets 0.131 # 0.0162 # 0.071 m from 58% to 5% moisture (wet basis) content. Initially from laboratory test data with this fibre board, the rate of drying at constant rate period was found to be  $8.9 \text{ kg}/(\text{m}^2)(\text{hr})$ . The critical moisture was 24.9% and the equilibrium moisture content was 1%. The fibre is to be dried from one side only and has a bone dry density of  $210 \text{ kg}/\text{m}^3$ . Determine the time required for drying. The falling rate may be assumed linear. [Ans: 2.87 hr]

**12.17 Assuming the Rate of Drying Under the Falling Rate Period Directly Proportional to the Free Moisture Content, Determination of the Drying Time of a Material:** Under constant drying conditions, a filter cake takes 5 hr to reduce its moisture content from 30% to 10% on wet basis. The critical and equilibrium moisture contents of the material are 14% and 4% (on dry basis), respectively.

Assuming the rate of drying in the falling rate period to be directly proportional to the free moisture content, estimate the time required to dry the cake from 30% to 6% moisture on wet basis. [Ans: 6.69 hr]

**12.18 Time Required for Drying of Granular Solid under Constant Drying Condition:** 1400 kg (bone dry) of granular solid is to be dried under constant drying conditions from a moisture content of 0.2 kg/kg of dry solid to a final moisture content of 0.02 kg/kg of dry solid. The material has an effective area of  $0.0615 \text{ m}^2/\text{kg}$ . Under the same condition the following rates were previously known:

Moisture content  $X$ ,

kg/kg dry solid	0.3	0.2	0.14	0.096	0.056	0.042	0.026	0.016
Rate, $R$ , $\text{kg}/(\text{m}^2)(\text{hr})$	1.71	1.71	1.71	1.46	1.29	0.88	0.54	0.376

Calculate the time required for drying.

[Ans: 2.26 hr]

**12.19 Estimation of Drying Time of a Material From a Moisture Content of 50% to 3.5% in a Continuous Counter-Current Drier:** A material is dried in a continuous counter-current drier from a moisture content of 50% to one of 3.5% (wet basis). The capacity of the drier (wet basis) is 2260 kg/hr. The density of the drying material is  $640 \text{ kg}/\text{m}^3$ . The evaporation surface area per kg of dry material is  $0.0615 \text{ m}^2$ .

It was found in preliminary experimental drying that the critical moisture content of the material is 20% and the equilibrium moisture content is 1.5% (wet basis). During the first drying period, when the surface of the material is saturated with moisture, the drying rate was 2.44 kg of moisture per hr from  $1 \text{ m}^2$ . The air used had a moisture content of 0.0306 kg/kg. The moisture content of the saturated air at the temperature of the material was 0.0495 kg/kg. The coefficient of

mass transfer has been determined from these data as

$$[2.44/(0.0495 - 0.0306)] = 129 \text{ kg}/(\text{m}^2) (\text{hr}) (\Delta x = 1).$$

Determine the drying time.

[Ans: 5 hr 9 min]

**12.20** Determination of Flow Rates of Air and Steam, as Well as the Heating Surface of an Air Heater: Find the rate of flow of air, rate of flow and required pressure of the heating steam, and surface area of the air heater for a drier whose capacity is 600 kg/hr of moist material with an initial moisture content of 50% and a final moisture content of 9% (wet basis). The readings of the psychrometer for the air entering the air heater are 10 and 5°C. The air leaves the drier at 50°C and a relative humidity of 50%. Assume that the temperature of the heating steam is 15°C above the temperature of the air at the outlet from the heater. The moisture content of the heating steam is 6%. The consumption of heat is 10% higher than that in a theoretical drier. The overall coefficient of heat transfer in the air heater is 35 W/(m<sup>2</sup>)(K).

[Ans: Air flow rate: 6840 kg/hr, Steam flow rate: 565 kg/hr, Steam pressure: 10 atm (abs), Heating surface area: 135 m<sup>2</sup>]

**12.21** Calculation of Heating Surface of the Air Heater and also of the Flow Rate of Heating Steam: A drier having a capacity of 500 kg/hr (dry basis) dries a material from a relative humidity of 70% to 10% (wet basis). The readings of the psychrometer measuring at the atmospheric air are 15 and 20°C. The air leaves the drier at a temperature of 45°C and a relative humidity of 50%. The losses of heat in the drier and the air heater are 8% of the loss of heat in a theoretical drier. Determine the heating surface area of the air heater and the rate of flow of the heating steam if it has a pressure of 2 atm (abs) and a moisture content of 5%. The overall coefficient of heat transfer in the air heater is 35 W/(m<sup>2</sup>)(K). [Ans: 868 m<sup>2</sup>, 1865 kg/hr]

**12.22** Estimation of the Flow Rates of Air and Heating Steam in a Drying System Consisting of Three Air Heaters: A theoretical drier operating with intermediate (by stages) heating of air is supplied with 1800 kg/hr of a moist material having an initial moisture content of 39%. The final moisture content is 8% (wet basis). The air leaves the drier at a temperature of 45°C. The temperature of the atmospheric air is 20°C. The drying system has a total 3 air heaters, in each of which the air is heated to 70°C. After each heater, the air in the drier is saturated with water vapour to a relative humidity of 0.7. Find the rates of flow of the dry air and the heating steam. The pressure of the heating steam is 3 atm (abs), and its moisture content is 5%.

[Ans: Rates of flow of air and steam are 16200 kg/hr and 960 kg/hr, respectively]

**12.23** Comparison of the Consumption of Heat in Vacuum Dryer and Atmospheric Drier: A wet material having an initial moisture content of 50% is dried at a rate of 1000 kg/hr to a final moisture content of 8% (wet basis). Drying is performed (i) in a vacuum drier with the temperature of the material during drying equals to 40°C, and (ii) in an atmospheric air drier at the same temperature of the material (during the first period). The atmospheric air has a temperature of 20°C and a relative humidity of 0.7, the air leaving the drier has a temperature of 55°C. In both cases, the moist material enters the drier at 15°C and leaves it at 40°C. The specific heat capacity of the dried material is 1.26 # 10<sup>3</sup> J/(kg)(K). Neglecting the losses of heat to the surroundings and for heating the conveying means, determine the specific consumptions of heat in

both the driers.

[Ans: (i) 2545 kJ/kg, (ii) 3685 kJ/kg]

**12.24 Calculation of the Heating Surface Area of a Double-Drum Drier:** Determine the consumption of heat for heating the material, and the heating surface area to be provided in a double-drum drier for drying a nickel carbonate paste with a capacity of 90 kg/hr of the paste. The initial and final moisture contents are 75% and 10% (wet basis), respectively. The drier is heated with indirect steam available at 1 atm pressure. The thickness of the layer of material is 1 mm, and the thickness of the wall of iron drum is 10 mm. Air is blown over the surface of the material with a velocity of 1.5 m/s. The temperature of the air is 40°C, the relative humidity being 40%. The temperature of the paste is 15°C. The coefficient of heat transfer from the condensing steam to the drum wall equals to 9280 W/(m<sup>2</sup>)(K). The thermal conductivity of iron is 46.4 W/(m)(K), the mean thermal conductivity of the material being dried is 0.8 W/(m)(K), and its heat capacity is 3.46 kJ/(kg)(K).

[Ans: 46500 W, 5.38 m<sup>2</sup>]

**12.25 Time Required and the Length of a Pneumatic Drier for Drying Crystals of Salicylic Acid:** Determine the time needed to dry crystals of salicylic acid (angular particles) in a pneumatic drier and the required length of the drier for the following conditions:

Capacity of final dry product is 250 kg/hr, Equivalent particle diameter is 1 mm, Density of the material is 1480 kg/m<sup>3</sup>, Temperature of the air entering the air heater is 15°C with relative humidity = 0.7, Temperature of the air leaving the air heater is 90°C, Temperature of the air leaving the drier is 50°C, Temperature of the crystals fed to the drier is 15°C, Temperature of the crystals discharged from the drier is 40°C, Specific heat capacity of dry crystals (final) is 1.16 # 10<sup>3</sup> J/(kg)(K), Initial and final moisture contents of crystals (bone-dry basis) are 15% and 1%, respectively.

[Ans: 11.9 s, 14 m]

**12.26 Calculation of Length and Diameter of a Counter-Current Rotary Drier:** A counter-current rotary drier is to be designed for drying 2 # 10<sup>4</sup> kg/hr of wet salt containing 7.5% (wet basis) water to 0.25% (wet basis) water. The wet salt enters the drier at 30°C and it has a specific heat of 0.25 kcal/kg °C. Heated air at 150°C with a wet-bulb of 40°C is available for drying the salt. If the outlet temperatures of air and salt are 65°C and 80°C, respectively, calculate the length and diameter of the drier.

The humidity of air at entry obtained from psychrometry chart is 0.2418 kg water/kg dry air °C.

[Ans: Length: 25.93 m, Diameter: 3.66 m]

**12.27 Diameter and Length of a Single Shell Direct Counter-Current Rotary Drier:** Design a single shell direct counter-current rotary drier to dry 15 tonne/hr of an ore at 26.5°C with an average particle size of 1.02 mm diameter from an initial moisture content of 0.13 kg moisture per kg of dry solid to a final product with 0.005 kg moisture per kg of dry solid. At these conditions, the critical moisture content will be less than 0.005 kg/kg. The drying medium air initially at 26.5°C and 21.1°C wet-bulb temperature is heated to 138°C before entering the drier.

[Ans: Diameter = 3.45 m, length = 25.33 m]

## **Short and Multiple Choice Questions**

1. Explain the following terms: equilibrium moisture; free moisture; critical moisture; bound moisture and unbound moisture.
2. Under which conditions of drying does the surface temperature of the drying solid become equal to the wet bulb temperature of the drying air?
3. How will the rate of drying during constant rate period be affected if the humidity of drying air is increased?
4. During which stage of drying does surface evaporation of unbound moisture take place?
5. How does the temperature of a drying solid vary during falling rate period of drying?
6. In which materials does liquid diffusion of moisture occur during the falling rate period of drying?
7. Which parameter in a drying operation should be controlled to prevent case hardening of solids during drying?
8. What are the advantages of parallel drying in continuous dryers?
9. How would you construct the drying rate curve from preliminary experiment on drying?
10. Assuming the drying rate curve for the falling rate period to be linear, what is the expression for the total drying time for batch drying of a solid?  
  
11. Moisture in a solid exerting an equilibrium vapour pressure equal to that of the pure liquid at that temperature is  
(a) bound moisture    (b) critical moisture    (c) free moisture    (d) unbound moisture
12. Milk is usually dried in a  
(a) tray drier    (b) spray drier    (c) freeze drier    (d) rotary drier
13. If moisture content of a solid on dry basis is  $X$  then the same on wet basis is  
  
(a)  $\frac{X}{X+1}$     (b)  $\frac{X}{1-X}$     (c)  $\frac{1+X}{X}$     (d)  $\frac{1-X}{X}$
14. Heat sensitive materials like certain food stuff and pharmaceuticals can be dried in  
(a) indirect tray drier    (b) spray drier    (c) freeze drier    (d) pan drier
15. Calcium ammonium nitrate (a fertilizer) is dried in a  
(a) vacuum shelf drier  
(b) rotary drier  
(c) tunnel drier  
(d) tray drier
16. In the constant rate period of the drying rate curve for batch drying  
(a) cracks develop on the surface of the solid  
(b) rate of drying decreases abruptly  
(c) surface evaporation of unbound moisture occurs  
(d) all of these
17. The average retention time ( $q$ ) of solids in a rotary drier is given by

$$(a) \theta = \frac{2\phi_D \rho_s}{S_S}$$

$$(b) \theta = \frac{S_S}{2\phi_D \rho_s}$$

$$(c) \theta = \frac{\phi_D \rho_s}{S_S}$$

$$(d) \theta = \frac{\phi_D}{S_S \rho_s}$$

where,  $z_D$  = hold-up of solid

$S_S$  = flow rate of solid, kg/s

$\rho_s$  = density of solid, kg/m<sup>3</sup>

**18.** Rotary driers are operated with hold-up of solids in the range of

- (a) 0.20 to 0.40    (b) 0.60 to 0.80    (c) 0.40 to 0.50    (d) 0.05 to 0.15

**19.** Synthetic detergent powder is produced by drying detergent slurry in a

- (a) cylinder drier    (b) spray drier    (c) rotary drier    (d) freeze drier

**20.** A solid is being dried in a cross-flow tray drier with air at 60°C and 0.015 humidity. If conduction and radiation are neglected, the approximate surface temperature of the solid will be

- (a) 21°C    (b) 31°C    (c) 41°C    (d) 0°C

**21.** What type of flow is preferred for drying a heat-sensitive material in a continuous drier?

- (a) cross-current flow  
(b) counter-current flow  
(c) co-current flow  
(d) none of these

**22.** Flights are provided in rotary driers to

- (a) lift and shower the solids thus exposing them to the action of the drying gas or air  
(b) reduce the residence time of the solids  
(c) increase the residence time of the solids  
(d) none of these

**23.** All moisture in a nonhygroscopic material is

- (a) free moisture  
(b) equilibrium moisture  
(c) unbound moisture  
(d) bound moisture

**24.** What type of flight is used in a rotary drier drying a sticky material?

- (a) straight flight  
(b) 90° inclined flight  
(c) 45° inclined flight  
(d) all of these

**25.** What type of drier would you recommend for large-scale drying of the following materials?

- (a) sugar crystals    (b) table salt  
(c) soap bars    (d) ammonium sulphate crystals  
(e) streptomycin    (f) green ceramic wares  
(g) milk    (h) refractory bricks

*Answers to Multiple Choice Questions*

11. (d)    12. (b)    13. (a)    14. (c)    15. (b)    16. (c)    17. (a)

## References

- Friedman, S.J. and W.R. Marshall, *Chem. Eng., Prog.*, **45**, 482, 573 (1949).
- Geankoplis, C.J., *Transport Processes and Separation Process Principles*, 4th ed., PHI Learning, New Delhi (2005).
- Hougen, O.P. and H.J. McCoulley, *Trans. AIChE*, **36**, 183 (1940).
- Masters, K., *Spray Drying*, CRC Press, Cleveland, Ohio (1972).
- McCormick, P.Y., in *Perry's Chemical Engineers' Handbook*, 5th ed., Perry, R.H. and C.H. Chilton (Eds.), McGraw Hill, New York (1973).
- Molstad, M.C., P. Farebaag and A. Farrell, *Ind. Eng. Chem.*, **30**, 1131 (1938).
- Mujumdar, A.S., *Handbook of Industrial Drying*, vols. **1 & 2**, Marcel Dekker Inc., New York (1995).
- Mujumdar, A.S. and C.L. Law, *Chem. Ind. Digest*, **XIX** (4), 54 (2006).
- Pearse, J.G., T.R. Oliver and D.M. Newitt, *Trans. Inst. Chem. Engrs.*, London, **27**, 1, 9 (1949).
- Ruthven, D.M. in *Encyclopedia of Separation Technology*, John Wiley, New York (1997).
- Shephard, C.B., C. Haddock and P.C. Boewer, *Ind. Eng. Chem.*, **30**, 1131 (1938).
- Sherwood, T.K., *Trans. AIChE.*, **27**, 190 (1931).
- Swarbrick, J. and J.C. Baylan, *Drying and Dryers* in *Encyclopedia of Pharmaceutical Technology*, vol. **4**, Marcel Dekker Inc., New York (1991).
- Thorat, B.N. and S.S. Shinde, *Chem. Ind. Digest*, **XVIII** (10), 64 (2005).
- Treybal, R.E., *Mass Transfer Operations*, 3rd ed., McGraw Hill, Singapore (1985).
- Wanjari, A.N. and B.N. Thorat, *Chem. Ind. Digest*, **XX** (8), 67 (2007).
- Yang, J., L. Wang, F. Xiang, L. Tang and F. Su, *J. of Univ. of Science and Technology Beijing*, **11** (4), 373 (2004).

# 13

## Crystallization

### 13.1 Introduction

Crystallization is a liquid-solid mass transfer operation in which solid crystals are formed and precipitated from solution or melt. In such separation, the substance being crystallized diffuses from liquid to solid phase and interacts with the solid surface where the crystals grow. A large variety of the products of chemical process industry such as sugar crystals, common salt, ammonium sulphate, sodium chromate and a host of organic and inorganic compounds are marketed as crystals. Crystallization is the reverse of dissolution of a solid in a liquid. This is an age old separation and purification process used in the production of a wide range of materials. In many applications, the product obtained from crystallization is the finished product which is expected to meet the stringent purity and morphology specifications. In addition, many of the impurities present in the solution are discarded during crystallization so that the product is obtained in relatively purer form. Crystallization has been traditionally known to be the best and the cheapest method for obtaining pure solids from impure solutions with desirable properties such as flowability, handling and packaging characteristics, and attractive appearances. In recent times the focus has changed to a very large extent on getting the particles of right morphology. Particle properties like crystal structure, crystal size distribution, polymorphism, etc. are going to be very critical parameters because of their direct bearing with the product quality and performance. Hence, it has become extremely important to get the appropriate morphological form of the desired product.

In case a product mixture forms a high- or low-boiling azeotrope, it is not possible to separate the valuable component from the mixture with distillation. In case the components of a mixture have close boiling points, distillation may require a large number of trays to achieve the purity of the product required. For such cases, extractive distillation may be an alternative but this requires downstream recovery of the extractive agent. Crystallization may be a viable option in such cases. Crystallization takes place at lower temperatures compared to distillation and this is favourable for products which exhibit polymerization or instability at high temperatures.

An important difference with distillation is the energy consumption of a crystallization process. The energy required to transform organic chemicals from liquid to solid is generally 25 to 50% of the amount of energy required to transform from liquid to vapour, resulting in significant energy savings (van der Steen and Nandani 2007). Apart from yield and purity, the size and often the shape of the crystals are important. Uniform sizes not only increase market appeal but also are better suited for packaging, handling and storing. Since most of the crystals directly reach the consumers, market requirements like shape, size range, noncaking properties, etc. limit the product to a narrow range.

#### 13.1.1 Crystal Form

A crystal is a solid body with plane faces in which the atoms are arranged in an orderly manner. The atomic arrangement and the distance between atoms remain constant for crystals of a particular compound irrespective of size. It has been found that even if the relative size of the different faces of two crystals of the same material are widely different, the interfacial angles of corresponding faces of the two crystals are all equal and characteristic of the substance.

Since the crystals of a particular substance have the same interfacial angles in spite of wide variation in their sizes, crystal forms are generally classified on the basis of these angles. Different combinations of angles and lengths of the axes give rise to seven classes of crystals as under:

The cubic system: Three equal rectangular axes.

The triclinic system: Three mutually inclined and unequal axes, all the three angles being different and other than 90, 60 or 30 degrees.

The monoclinic system: Three unequal axes two of which are inclined and the third is perpendicular to the other two.

The orthorhombic system: Three unequal rectangular axes.

The tetragonal system: Three rectangular axes two of which are equal and different in length from the third.

The trigonal system: Three equal and equally inclined axes.

The hexagonal system: Three equal coplanar axes inclined at 60 degrees to each other and a fourth axis perpendicular to the other three axes.

The relative growth of the faces of crystals can be controlled by adjusting a number of parameters such as rate of crystallization, type of solvent, nature of impurities present, etc. (Mullin 2001).

Two or more substances that crystallize in the same form are called *isomorphous*. Ammonium and potassium alums are isomorphous. Substances that can crystallize in more than one form are called *polymorphous*. Graphite and diamond are polymorphous. Crystals may be produced both from solution which is a homogeneous mixture of more than one species such as common salt from brine, and from melt more correctly refers to a pure molten solid such as silicon, the former is called *solution crystallization* while the latter is called *melt crystallization*.

### 13.1.2 Liquid Crystals

Most substances are available in three states, as crystal, liquid and vapour. Some organic substances, on the other hand, form another phase intermediate between crystal and liquid. This new phase is called *crystal-liquid* phase. A few examples of crystal-liquid are: ethyl para-azoxybenzoate, ammonium oleate, para-azoxyphenetol, cholestryl acetate, etc. These materials melt at a definite temperature to form a cloudy viscous liquid (the crystal-liquid) which when further heated to some higher definite temperature is transformed to a clear liquid.

## 13.2 Solid–Liquid Equilibria

If a few particles of a solid are added to a liquid in which the solid is soluble, the particles will undergo dissolution as long as the concentration of the solid in the solution is less than that at saturation, i.e. less than the solubility of the solid in the liquid at that temperature. Conversely, if a few seed crystals are added to a supersaturated solution, the solid will crystallize out of the solution. The extent of supersaturation acts as the driving force for crystallization. Equilibrium data for

crystallization are usually represented by solubility curves in which solubility is expressed as a function of temperature. Solubility can be defined in different ways; the most common one being parts anhydrous salt per 100 parts of solvent.

The curve  $AB$  in Figure 13.1 shows the solubility of sodium nitrate in water as a function of temperature. It is evident that the solubility of sodium nitrate in water increases with increase in temperature, sometimes considerably and sometimes slightly.

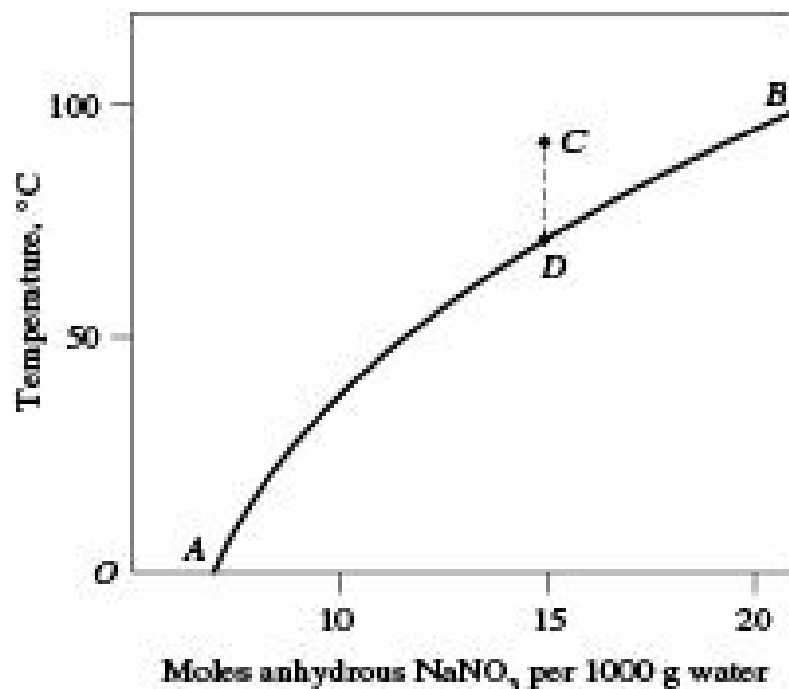
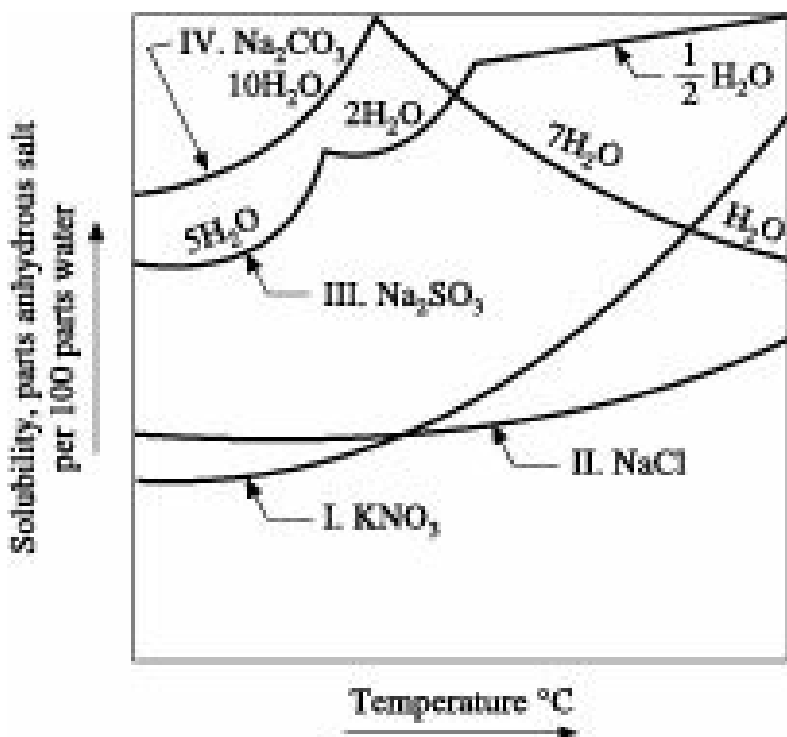


Figure 13.1 Solubility of sodium nitrate in water.

A point on the curve  $AB$  represents the solubility or saturation concentration of sodium nitrate at the corresponding temperature. The region above the curve  $AB$  represents an unsaturated solution. If a solution represented by the point  $C$  is cooled, it becomes saturated on reaching the temperature corresponding to the point  $D$  on the solubility curve vertically below the point  $C$ . On further cooling, sodium nitrate crystallizes and the state of the solution changes along  $DA$  on the curve  $AB$ .

Figure 13.2 exhibits typical solubility curves of some salts in water. Four types are generally encountered in practice. In addition to solubility, these curves in certain cases indicate the crystallization characteristics of the solutes and the method of crystallization to be followed.



**Figure 13.2** Different types of solubility curves.

Substances represented by type-I, for instance, potassium nitrate exhibits rapid increase in solubility with increase in temperature. This type of substances can be easily crystallized only by cooling the solution. Type-II, represented by sodium chloride has only marginal increase in solubility with increase in temperature and therefore requires evaporation and cooling for appreciable yield of crystals. As shown by the curve, type-III substances, for instance, sodium sulphite crystallizes with different proportions of water of crystallization at different temperature ranges. Some systems show a number of transition points over a small range of temperature. For example, 3 forms of Ferrous sulphate may be obtained from aqueous solution depending upon the temperature. Type-IV represented by sodium carbonate initially exhibits increase in solubility with increase in temperature up to a certain temperature after which the solubility decreases with further increase in temperature. The discontinuity in the solubility curve indicates the phase change. Similar observation showing the transition point is obtained during crystallization of sodium sulphate. In fact, the solid deposited from aqueous solution below its transition point remains in hydrated state whereas the solid deposited above the transition temperature contains anhydrous salt.

## 13.3 Material and Energy Balance

### 13.3.1 Material Balance

Material and energy balance equations form the basis of many crystallization calculations. An expression for estimation of crystal yield can be developed by the application of the principles of material balance to crystallization process.

Figure 13.3 shows a simple flow diagram of a cooling type crystallizer. Assuming that the mother liquor is saturated with solute at the final temperature of crystallization and making a solute balance at the inlet and outlet of a crystallizer operating under steady state conditions

$$A = \frac{Y}{R} + \left( W - E - \frac{Y(R-1)}{R} \right) \cdot s \quad (13.1)$$

By rearrangement, we get

$$Y = \frac{R[A - s(W - E)]}{1 - s(R - 1)} \quad (13.2)$$

where

$A$  = weight of anhydrous solute in original solution, kg

$W$  = weight of initial solvent, kg

$E$  = loss of solvent by evaporation during the process, kg/kg of original solvent present

$R$  = ratio of molecular weights of hydrated to anhydrous crystal,

$s$  = solubility (concentration) at particular temperature, kg solute per kg of solvent

$Y$  = yield of crystal, kg

Equation (13.2) can be used directly to estimate the yield of crystals from a given solution under given set of operating conditions.

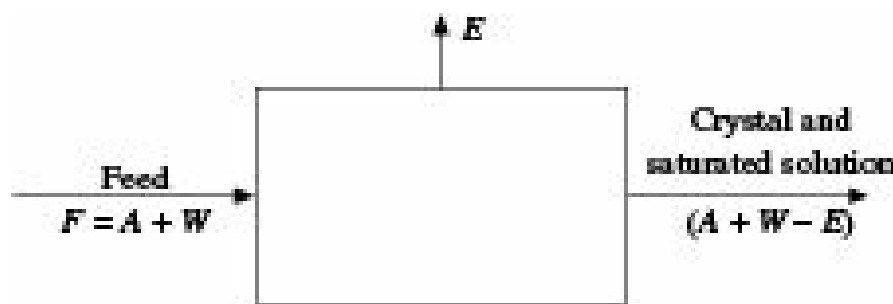


Figure 13.3 Flow diagram of a cooling type crystallizer.

**EXAMPLE 13.1** (Estimation of crystal yield and mother liquor left in a crystallization process): A crystallizer is charged with 5000 kg of an aqueous solution of sodium sulphate containing 29.6%  $\text{Na}_2\text{SO}_4$ . The solution is cooled when  $\text{Na}_2\text{SO}_4 \cdot 10\text{H}_2\text{O}$  is crystallized. 10% by weight of initial water is lost by evaporation. If the mother liquor contains 18.3%  $\text{Na}_2\text{SO}_4$ , calculate

- (i) the weight of salt crystallized and
- (ii) the weight of mother liquor left.

**Solution:** Molecular weight of anhydrous  $\text{Na}_2\text{SO}_4$  = 142 and that of  $\text{Na}_2\text{SO}_4 \cdot 10\text{H}_2\text{O}$  = 322.

From Eq. (13.2), we have

$$Y = \frac{R[A - s(W - E)]}{1 - s(R - 1)}$$

100 kg solution contains 29.6 kg  $\text{Na}_2\text{SO}_4$

$$\therefore 5000 \text{ kg solution contains } \left( \frac{29.6 \times 5000}{100} \right) = 1480 \text{ kg } \text{Na}_2\text{SO}_4 (A)$$

Water present initially =  $(5000 - 1480) = 3520 \text{ kg} (W)$

Water evaporated =  $(3520 \# 0.10) = 352 \text{ kg} (E)$

Mother liquor contains 18.3%  $\text{Na}_2\text{SO}_4$

\ Solubility of  $\text{Na}_2\text{SO}_4 = \frac{100 - 18.3}{100} = 0.224$  parts/part of water ( $s$ )

$$R = \frac{\text{Mol. wt. of hydrated salt}}{\text{Mol. wt. of anhydrous salt}} = \frac{322}{142} = 2.268 (R)$$

Substituting the values in Eq. (13.2), we obtain

$$Y = \frac{2.268[1480 - 0.224(3520 - 352)]}{1 - 0.224(2.268 - 1)} = 2440.2 \text{ kg}$$

- (i) Weight of salt crystallized = 2440.2 kg
- (ii) Amount of mother liquor =  $(5000 - 352 - 2440.2) = 2207.8 \text{ kg}$

### 13.3.2 Heat Balance

Heat balances are useful in estimating the cooling requirements and in determining the final conditions.

Denoting the output stream separately in terms of solid crystals and saturated solution and striking a balance between heat input and heat output,

$$Fh_F = Yh_y + Sh_S + q \quad (13.3)$$

where

$F$  = feed solution

$Y$  = yield of crystals

$S$  = saturated solution in final product

$h_F$ ,  $h_y$  and  $h_S$  = enthalpies of feed, crystals and saturated solution, respectively.

If the temperature and composition of the feed and the final temperature are fixed, then the composition of the yield and of the solution leaving also gets fixed. Thus, the quantities and compositions of all the streams become known. In majority of cases, however, adequate thermal data are not available and approximate methods are to be employed for estimating cooling requirement and the final conditions.

## 13.4 The Crystallization Process

The overall process of crystallization consists of three distinct steps, namely, formation of supersaturated solution, crystal formation or nucleation, and crystal growth. Supersaturation is the common driving force for both nucleation and crystal growth. Supersaturation can be achieved by a variety of ways:

*Temperature change:* The solubilities of most of the materials go down as the temperature is lowered. So, cooling is one of the popular techniques of separation.

*Evaporation of solvent:* A solvent is removed by evaporation in order to reach the point of supersaturation. This is employed for nonaqueous systems with high vapour pressure.

*Chemical reaction:* This is usually used for salt formation which involves acid-base reactions.

*Changing the solvent composition:* A solvent or antisolvent in which the solute has poor solubility, can be added. Supersaturation can also be achieved by changing the pH which is widely used in

commercial practice.

Unless a solution is supersaturated, crystals can neither form nor grow. After the building up of a supersaturated solution, the first step in crystallization is the ‘phase separation’ of solid from liquid giving rise to ‘birth’ of new crystals. Since the supersaturated solution is not in equilibrium and in a meta stable state, crystal formation gets started in order to relieve supersaturation and the process moves towards equilibrium. As a thumb rule more rapid the supersaturation, faster is the nuclei formation, i.e. faster precipitation of the solids out of the solution, resulting in a lower control on crystallization process. Typical supersaturation value defined as a ratio of the concentration of solute at a particular temperature and equilibrium concentration at the same temperature, lies in the range of 1.1 to 1.5. However, supersaturation affects nucleation and crystal growth in radically different manners. The relation of the degree of nucleation with crystal growth controls the crystal size and size distribution of the products, and is crucial for industrial crystallization process.

Nucleation, initiation of a phase change in a small region, can occur under two different circumstances. In the first case, nucleation takes place from a solution which is totally free from any solid particles. If there be any solids in the solution, these should not have any influence on the crystallization. Nucleation from such a solution is said to take place from an unseeded solution. This is known as *primary nucleation*. High degree of supersaturation helps the phenomenon to take place and it is the basic mechanism for precipitation to occur. The primary nucleation may be of two types—homogeneous and heterogeneous. While homogeneous nucleation is not influenced by solids (vessel wall can also act as solid), heterogeneous one occurs due to solid which helps in increasing the rate of nucleation. The presence of small solute crystals, small crystals of foreign materials or even dust lead to the second type of nucleation, namely nucleation from seeded solutions. This is known as *secondary nucleation* which may occur due to shearing of fluid or due to collisions between the existing crystals and the vessel wall or the foreign materials. Most of the commercial crystallizers where crystalline surfaces are present and large sized crystals are desirable, are being operated following the mechanism of secondary nucleation. Except for closed batch crystallizers where the solution is heated much above the saturation temperature, most of the commercial crystallizers use the seeded method of nucleation.

Miers and his associates (Miers 1927) have proposed a theory known as *Miers' theory* regarding crystallization from an unseeded solution. According to this theory, there is a definite relation between the concentration and the temperature at which spontaneous nucleation will take place in an unseeded solution. They conceived the existence of the so called *supersolubility* curve which is roughly parallel to the solubility curve and situated at the supersaturated zone. According to Miers, there will be no spontaneous nucleation in the region between the solubility and supersolubility curves. But as soon as the supersolubility curve is crossed, spontaneous crystallization will start. The relationship is shown in Figure 13.4.

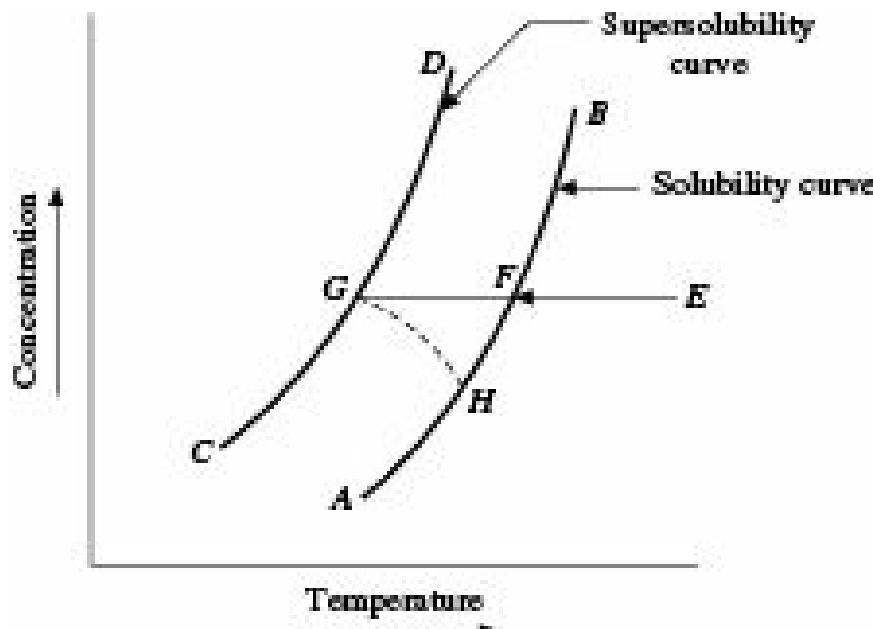


**Figure 13.4** Mier's supersolubility curve.

As shown in Figure 13.4,  $AB$  is the normal solubility curve and  $CD$  is Miers' supersolubility curve. When a solution at  $E$  is cooled, spontaneous nucleation will not occur merely on reaching the point  $F$  on the solubility curve. It will start only when the point  $G$  on the supersolubility curve as conceived by Miers is crossed. In other words, spontaneous nucleation will not occur until a certain degree of supersaturation is attained.

In spite of lot of controversy regarding the existence of such a supersolubility curve, this theory has been useful in analysing many problems on crystallization.

Considering the formation of cluster by an addition mechanism and also the thermodynamic aspect of homogeneous nucleation by Volmer (1929) and others, the rate of nucleation may be expressed in the form of Arrhenius equation as

$$N = A' \exp \left( -\frac{16\pi\sigma^3 M^2}{3R^3 T^3 \rho^2 (\ln S_S)^2} \right) \quad (13.4)$$

where

$N$  = rate of nucleation, no. of nuclei formed/(q)(L<sup>3</sup>)

$A'$  = preexponential factor, constant for a particular type of salt

$M$  = molecular weight of solute, M/mol

$\sigma$  = surface energy, F/L

$\rho$  = density, M/L<sup>3</sup>

$S_S$  = supersaturation ratio [=  $C_A/C_S$ ],  $C_A$  being the concentration of solute in the bulk solution and  $C_S$  being the saturation concentration of solute.

When the value of  $S_S = 1$ , the solution is saturated

$S_S < 1$ , the solution is unsaturated, and

$S_S > 1$ , the solution is supersaturated.

[The change in Gibbs free energy,  $DG$  can be expressed as

$$DG = \frac{4}{3} \pi r^2 v(i)$$

$$\ln S_S = \ln \left( \frac{C_A}{C_S} \right) = \frac{2M\sigma}{RT\rho r} \quad (ii)$$

where  $r$  is the radius of a crystal particle.

Substituting the value of  $r$  in Equation (i), one can have

$$DG = \frac{16\pi\sigma^3 M^2}{3R^2 T^2 \rho^2 (\ln S_S)^2} \quad (iii)$$

The rate of nucleation is related by the expression

$$N = A \square \exp \left( \frac{-\Delta G}{RT} \right) \quad (iv)$$

Substituting the expression of  $DG$  from Eq. (iii) in Eq. (iv), we have Eq. (13.4)

$$N = A \square \exp \left( -\frac{16\pi\sigma^3 M^2}{3R^2 T^2 \rho^2 (\ln S_S)^2} \right) \quad (13.4)$$

In order to find out the relation between the nucleation time and the degree of supersaturation, the time required for spontaneous nucleation of supercooled water vapour was computed (Volmer 1939) as under:

From Table 13.1, it appears that there is a critical level of supersaturation in the region of  $S_S \approx 4$  where spontaneous nucleation would occur within a tangible period of time. But it is also clear that nucleation would occur at any value of  $S_S > 1$ , only if sufficient time is allowed.

**Table 13.1** Time for nucleation of supercooled water vapour

Supersaturation:	1.0	2.0	3.0	4.0	5.0
Time:	$\infty$	$10^{62}$ yr	$10^3$ yr	0.1 s	$10^{-13}$ s

Randolph and Larson (1988) have suggested the following equation for the theoretical rate of nucleation in an unseeded solution (Randolph and Larson 1988, Myerson 2002):

$$N = A' \exp \left( \frac{16\pi\sigma^3 v_M^2}{3k^2 T^2 (\ln \varphi_S + 1)^2} \right) \quad (13.5)$$

where

$N$  = nucleation rate, number of nuclei formed/(m<sup>3</sup>)( s),

$A'$  = a constant

$k$  = Boltzmann constant

$T$  = absolute temperature

$$= \frac{(C_A - C_S)}{C_S} = \frac{C_A}{C_S} - 1 = S_S - 1$$

{ $S$  = relative supersaturation}

$yM$  = volume of a molecule.

Considering classical chemical kinetics of crystallization in conjunction with the Kelvin equation (sometimes known as Gibbs-Thompson and Ostwald equations), the rate of primary homogeneous nucleation as reported, is expressed as

$$N = A' \exp \left( -\frac{16\pi\sigma^3 v_M^2 N_a}{3n^2 R^3 T^3 \rho^2 (\ln S_g)^2} \right) \quad (13.5a)$$

where

$N$  = nucleation rate, number of nuclei formed/(cm<sup>3</sup>)(s)

$N_a$  = Avogadro's number

$n$  = number of ions per molecule of solute

Due to presence of dust or foreign materials, the experimental value of  $A'$  may be different from the theoretically calculated value of  $10^{30}$  nuclei/(cm<sup>3</sup>)(s). However, the equation may be used in primary heterogeneous nucleation when the value of  $A'$  has to be obtained experimentally.

## 13.5 Methods of Nucleation

There are two general methods for providing the required amount of nuclei in the solution so that crystal growth can proceed smoothly. One method is to generate the nuclei *in situ*, i.e. within the solution either spontaneously or by induction. The other method is to add required amount of nuclei from outside.

### 13.5.1 Formation of Nuclei *in Situ*

Nuclei may be formed within the solution by any one of the following methods:

- *Spontaneous nucleation of unseeded solution.* For this the solution must be sufficiently concentrated, either by evaporating the solvent or by cooling the solution so that the required degree of supersaturation can be attained.
- *By attrition of existing crystals.* Small corners and fragments of existing crystals may be broken due to vigorous stirring and act as new nuclei. The damaged parts of the existing crystals soon repair themselves.
- *By mechanical impact.* Mechanical impact in a supersaturated solution give rise to new nuclei in addition to those formed due to attrition.
- New nuclei may be formed by the inoculating effect of the crystals already present. This method is an important one and can be controlled easily.
- By local variation of concentration. For instance, withdrawal of heat through the walls of the crystallizer may cause temperature gradient near the wall as a result of which supersaturation may be increased and nucleation may start.
- Application of ultrasonic vibration to a supersaturated solution gives rise to new nuclei.

### 13.5.2 Addition of Nuclei from Outside

The simplest method of providing nuclei in a crystallizer is to add required amount of nuclei from

outside. This method is generally practiced in industry. Impurities in the solution may inhibit the formation of new nuclei. The effect of a given impurity cannot be precisely predicted. However, high molecular weight materials are usually more effective inhibitors.

## 13.6 Crystal Growth

When some nuclei have been formed in or added to a supersaturated solution, they start growing although crystal growth may take place simultaneously with nuclei formation. Several theories regarding the mechanism of crystal growth have been proposed by different authors. Among these theories, the mass transfer or diffusional theory, originally proposed by Berthoud (1912), Valeton (1923, 1924) is the most widely accepted one.

According to the mass transfer theory, there are two distinct steps in the process of crystal growth. The first step is the transport of the solute from the bulk of the supersaturated solution to the surface of the crystal. The second step is surface integration of the solute molecules with the growing layers of the crystal. Since the transport of solute through the main bulk of the solution is by convective diffusion due to turbulence, the diffusion of solute molecules from the bulk of the solution to the crystal surface is almost entirely controlled by the resistance of the laminar layer around the crystal.

### 13.6.1 Rate of Crystal Growth

The amount of solute transported from the bulk of the solution to the crystal surface may be written as,

$$\frac{dm}{d\theta} = k_L a (C_A - C_B) \quad (13.6)$$

where

$m$  = mass of a single crystal

$a$  = surface area of a single crystal

$i$  = time

$k_L$  = diffusion coefficient of mass transfer of solute from the bulk of the solution to the crystal surface

$C_A$  = solute concentration in the bulk of the solution,

$C_B$  = solute concentration at the solid-liquid interface.

Berthoud (1912) assumed the transfer at the interface to be directly proportional to the supersaturation at the interface,

$$\frac{dm}{d\theta} = k' a (C_B - C_S) \quad (13.7)$$

where,

$k'$  = rate constant for the surface reaction process,

Substituting the expression for  $C_B$  from Eq. (13.6) in Eq. (13.7), we get

$$\begin{aligned} \frac{dm}{d\theta} &= \frac{a}{(1/k_L) + (1 + k')} (C_A - C_S) \\ &= K a (C_A - C_S) \end{aligned} \quad (13.8)$$

where,  $K$  is the overall coefficient for diffusion and surface reaction given by

$$K = \frac{1}{(1/k_L) + (1/k')}$$

$(C_A - C_S)$  is the supersaturation.

Assuming the crystals to be perfect cubes,

$$m = t_S L^3 \text{ and } a = 6L^2 .$$

where

$L$  = linear dimension of the crystal cubes

$t_S$  = density of the crystal.

Substituting these values in Eq. (13.8) and simplifying, one can have

$$\frac{dL}{d\theta} = \frac{2K(C_A - C_S)}{\rho_s} \quad (13.9)$$

Expressing the supersaturation in terms of mole fraction and introducing a shape factor  $m$  for crystal shapes other than cubic, we have

$$\frac{dL}{d\theta} = \frac{2K'm(y - y^*)}{\rho_s \lambda} \quad (13.10)$$

where

$y - y^*$  = supersaturation in terms of mole fraction

$K'$  = overall coefficient in terms of mole fraction driving force, expressed as

$$K' = \frac{1}{(1/k_L) + (1/k')} \quad (13.11)$$

$m$  is the shape factor being 1 for cubes.

**EXAMPLE 13.2** (Determination of growth rate of crystals): Crystals of epsom salt having an equivalent diameter of 1.5 cm are growing in a solution of  $MgSO_4$  at a supersaturation of 0.005 mole fraction  $MgSO_4 \square 7H_2O$  and a temperature of 30°C. For saturated solution of  $MgSO_4$ , the average coefficient of interfacial reaction is 0.18 gmol/(cm<sup>2</sup>)(hr)(mol fraction). The mass transfer coefficient has been estimated to be 1.75 gmol/(cm<sup>2</sup>)(hr)(mol fraction). The average density of the crystals is 1.68 g/cc.

Assuming the crystals to be cubic, estimate their growth rate in cm/hr.

**Solution:**

$$y - y^* = 0.005, t_S = 1.68, M = 246.5$$

Equation (13.10) is used for determination of the rate of crystal growth

$$\frac{dL}{d\theta} = \frac{2(y - y^*) K' M}{\lambda \rho_s}$$

Using Eq. (13.11), the value of  $K'$  is

$$K' = \frac{1}{\left(\frac{1}{k_L} + \frac{1}{k'}\right)} = \frac{1}{\left(\frac{1}{1.75} + \frac{1}{0.18}\right)}$$
$$= 0.1632 \text{ gmol/(cm}^2\text{)(hr)(mol fraction)}$$

Substituting the values in Eq. (13.10), we get

$$\frac{dL}{d\theta} = \frac{(2)(0.005)(0.1632)(246.5)}{(1)(1.68)}$$
$$= 0.239 \text{ cm/hr}$$

### 13.6.2 Effect of Impurities on Crystal Growth

In many cases, impurities present in the solution are discarded during crystallization so that relatively pure products are obtained as crystals. However, in some cases the presence of impurities may adversely affect the rates of both nucleation and crystal growth. This retarding effect is probably due to adsorption of the impurities on the surfaces of the nuclei and the crystals. An example of utilization of such retardation is the addition of small quantities of relatively large molecules such as glue, tannin, dextrin, etc. in boiler feed water which retard crystallization of calcium carbonate and thereby, minimize scaling.

### 13.6.3 Heat Effects

The heat effects in a crystallization process can be determined by a heat balance discussed in Section 13.3.2. Such heat balance can be made in two ways: One way is to compute the individual heat effects like sensible heat, latent heat and heats of crystallization and balance them. The other way is to make an enthalpy balance by subtracting the total enthalpy of all entering streams from the total enthalpy of all leaving streams.

### 13.6.4 Heat of Crystallization

Heat of crystallization is the latent heat accompanying the formation of crystals from a saturated solution. The heat of crystallization is usually exothermic. It varies with both concentration and temperature. The heat of crystallization is related to the heat of solution of the crystals and the heat of dilution of the solution. The heat of solution is the heat evolved when unit mass of the solid is dissolved in a very large quantity of solvent. Large volume of data on heat of solution is available in the literature (Perry et al. 1997). Data on heat of dilution, on the other hand, are very scanty, particularly for concentrated solutions and it is customary to use the negative value of the heat of solution. This is equivalent to neglecting heat of dilution. Heat of dilution usually being very small in comparison with the heat of solution, this approximation does not lead to any serious error.

**EXAMPLE 13.3** (Estimation of heat of crystallization from solubility data): The heat absorbed when 1 g mol of  $\text{MgSO}_4 \cdot 7\text{H}_2\text{O}$  is dissolved isothermally at  $18^\circ\text{C}$  in a large amount of water is 3.18 kcal. What is the heat of crystallization of 1 kg of  $\text{MgSO}_4 \cdot 7\text{H}_2\text{O}$  if heat of solution effect is neglected?

**Solution:** The molecular weight of  $\text{MgSO}_4 \cdot 7\text{H}_2\text{O}$  is 246.5.

The heat of crystallization of  $\text{MgSO}_4 \cdot 7\text{H}_2\text{O}$  is

$$\frac{3.18}{246.5} = 0.0129 \text{ kcal/g}$$
$$= 12.9 \text{ kcal/kg}$$

**EXAMPLE 13.4** (Estimation of cooling water requirement and heat transfer area of a crystallizer): 2000 kg/hr of an aqueous solution of sodium nitrate containing 57.6%  $\text{NaNO}_3$  is being cooled in a continuous crystallizer from 90 to 40°C. Cooling water flows counter currently and its temperature rises from 16 to 21°C. Water amounting to 2% by weight of the initial solution is being evaporated during cooling.

Using the given data (i) estimate the cooling water rate to be used and (ii) the heat transfer area to be provided.

**Given:** A saturated solution of  $\text{NaNO}_3$  at 40°C contains 1.045 kg  $\text{NaNO}_3$  per kg water. The average specific heat of  $\text{NaNO}_3$  solution is 0.59 kcal/(kg) (°C) and that of solid  $\text{NaNO}_3$  is 0.287 kcal/(kg) (°C). The heat of crystallization of  $\text{NaNO}_3$  is 59.17 kcal/kg. The average latent heat of vaporisation of water may be taken as 575 kcal/kg. The overall heat transfer coefficient has been estimated to be 120 kcal/(hr)( $\text{m}^2$ )(°C).

**Solution:** 2000 kg/hr solution contains  $(2000 \# 0.576) = 1152 \text{ kg/hr NaNO}_3$ .

$$\text{Initial water present} = 2000 - 1152 = 848 \text{ kg/hr}$$

$$\text{Water evaporated} = 2000 \# 0.02 = 40 \text{ kg/hr}$$

$$\text{Water present in mother liquor} = 848 - 40 = 808 \text{ kg/hr}$$

$$\text{NaNO}_3 \text{ present in mother liquor} = 808 \# 1.045 = 844.36 \text{ kg/hr}$$

$$\text{NaNO}_3 \text{ crystallized} = 1152 - 844.36 = 307.64 \text{ kg/hr}$$

Heat to be removed during cooling

$$q = (808 + 844.36)(0.59)(90 - 40) + (307.64)(0.287)(90 - 40) + \\ (307.64)(59.17) - (40)(575) \\ = 48362.3 \text{ kcal/hr}$$

(i) Water rate to be used =  $\frac{48362.3}{21 - 16} = 9672.5 \text{ kg/hr}$

(ii)  $\Delta T_1 = 90 - 21 = 69^\circ\text{C}$ ,  $\Delta T_2 = 40 - 16 = 24^\circ\text{C}$

$$DT_{lm} = \frac{(69 - 24)}{\ln(60/24)} = 42.61^\circ\text{C}$$

Surface required =  $\frac{48362.3}{(120)(42.61)} = 9.46 \text{ m}^2$

### 13.6.5 The $\Delta L$ Law

On the basis of large number of experiments, McCabe (1929) had established that all geometrically similar crystals of the same material suspended in the same solution grow at the same rate, if the

growth is measured as the increase in length of geometrically corresponding distances on all the crystals. If  $DL$  is the increase in linear dimension of one of the crystals, the corresponding dimensions of all the crystals in the solution will increase at the same rate during this time. This increase is independent of the initial sizes of any of the crystals provided all the crystals in the suspension are treated exactly in the same way.

## 13.7 Fractional Crystallization

When two or more solutes are present in a solution, it is often possible to crystallize one of the solutes while the other remains in solution. Separation of two or more substances by utilizing this principle is known as *fractional crystallization*. Fractional crystallization is based on the difference in solubilities of the solutes.

The solubility of a material in a solution of another solute is in general widely different from its solubility in the pure solvent. For example, the solubility of sodium chloride in water at 20°C is 36 parts NaCl per 100 parts of water, and the solubility of sodium nitrate in water at 20°C is 88 parts NaNO<sub>3</sub> per 100 parts water. But a saturated solution of these two salts in water at 20°C contains only 25 parts NaCl and 59 parts NaNO<sub>3</sub> per 100 parts of water. Thus, if adequate NaCl is added to a saturated solution of NaNO<sub>3</sub>,  $(88 - 59) = 29$  parts of NaNO<sub>3</sub> will crystallize out per 100 parts of water.

## 13.8 Crystallization and Precipitation

In contrast to crystallization, precipitation is a process that produces a solid from a solution as a result of simultaneous and very rapid nucleation, crystal growth and agglomeration of particles. Sparingly soluble solids produce precipitates at a very high degree of supersaturation. For example, if sodium chloride solution is added to a solution of silver nitrate, a very high degree of supersaturation of silver chloride is created in the solution and silver chloride precipitates out. This is due to extremely high rate of nuclei formation along with moderate rate of crystal growth as a result of which supersaturation is lost very quickly producing very large number of small crystals.

## 13.9 Caking of Crystals

The caking of crystals is a phenomenon which makes crystals moist and form lumps during handling and storage, particularly in relatively humid atmosphere. If crystals are brought into contact with air having humidity higher than the critical humidity, the crystals absorb moisture to form saturated solution around them. When they are removed to relatively dry atmosphere, the moisture reevaporates binding a number of crystals into a compact mass. Caking may also occur during improper stacking, particularly for crystals of nonuniform shape and size when the pressure at some points of contact become very high increasing the solubility. On releasing pressure, the solution recrystallizes forming an agglomerate of several crystals. Caking creates many problems in handling and use of crystals, and needs to be prevented.

The caking of crystals can be avoided by maintaining uniform size of crystals, minimum possible voidage and highest possible critical humidity by removal of impurities like CaCl<sub>2</sub> in case of NaCl, free acids, etc. Caking can also be prevented by dusting, i.e. forming a coating around each crystal.

Good quality table salt for instance is usually coated with magnesia or tricalcium phosphate.

## 13.10 Crystallization Equipment

Crystallization equipment are generally classified into four major groups according to the method of producing supersaturation.

*Group-I:* In equipment belonging to this group, supersaturation is achieved by cooling only. They are suitable for substances whose solubilities decrease appreciably with temperature. Thus being the normal type of solubility for most substances, these equipment are in wide use. Typical equipment in this group are:

Batch— Tank crystallizers, Agitated batch crystallizer

Continuous— Swenson-Walker crystallizer.

*Group-II:* In these equipment, supersaturation is created by evaporation of solvent. They are used for substances whose solubility curves are so flat that yield of crystal by cooling alone would be negligible. Mainly used for common salt.

*Group-III:* In equipment of this group, supersaturation is produced by adiabatic evaporation. In these equipment, a hot solution is introduced in a vacuum space where the total pressure is kept below the vapour pressure of the solvent at that temperature so that the solvent flashes and produces adiabatic cooling.

*Group-IV:* In this group of equipment, salting out is done by adding a substance that reduces the solubility of the material to be crystallized. This method is not generally practised. Indirect application is found in evaporation of electrolytic caustic soda. As the concentration of NaOH increases, that of NaCl decreases and the latter crystallizes out.

## 13.11 Working Principles of Some Important Crystallizers

Many special types of equipment have been developed according to the requirement of the particular industries, possibly extreme examples being the simple open ponds for solar evaporation of brines and recovery of salt, and the specialized vacuum pans of the sugar industry that operate with syrup on the tube side of calandrias and elaborate internals to eliminate entrainment. The working principles of some of the basic equipment have been discussed here.

### 13.11.1 Agitated Batch Crystallizer

As shown in Figure 13.5, an *agitated batch crystallizer* consists of a conical bottom tank with provision for water circulation through cooling coils or jacket, and for agitation by propellers mounted on a central vertical shaft. The agitation serves two purposes; firstly, it increases the rate of heat transfer and keeps the temperature of the solution uniform and secondly, by keeping the fine crystals in suspension, it gives them opportunity to grow uniformly instead of forming large crystals or agglomerates. Agitation also helps in rapid cooling and formation of large number of nuclei so that the product is much finer and more uniform.

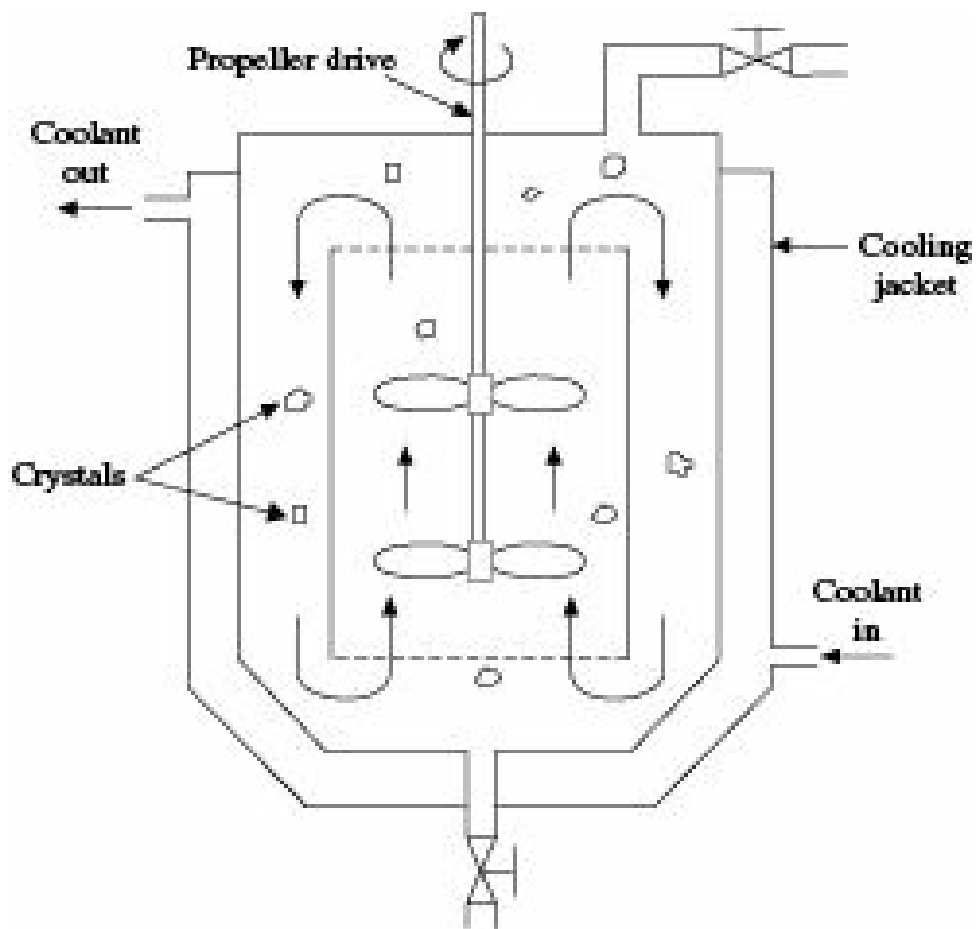


**Figure 13.5 Agitated batch crystallizer.**

The hot feed solution with necessary supersaturation is introduced into the crystallizer, usually by pumping and necessary supersaturation is created by cooling the solution. Requisite amount of nuclei is added to the solution and crystals start growing. On completion of crystal growth, the product is withdrawn and the crystallizer is ready for the next batch.

The capacities of agitated batch crystallizers are usually small ranging from about 100 kg to 15,000 kg/day. They are generally used in production of fine chemicals, pharmaceuticals and speciality chemicals.

### 13.11.2 Swenson–Walker Crystallizer

The standard design consists of an open trough, about 600 mm wide with semicircular bottom, a water jacket welded to the outer surface of the trough and a slow speed, long-pitch spiral agitator set close to the bottom of the trough. Each crystallizer is about 3 m long and a number of units may be joined in series or in cascade to provide for the required length. Feed solution is introduced at one end and cooling water flows through the jacket counter-current to the solution. The slow speed agitator keeps small crystals in suspension and pushes them to the delivery end as they grow. A Swenson-Walker crystallizer is shown in Figures 13.6.

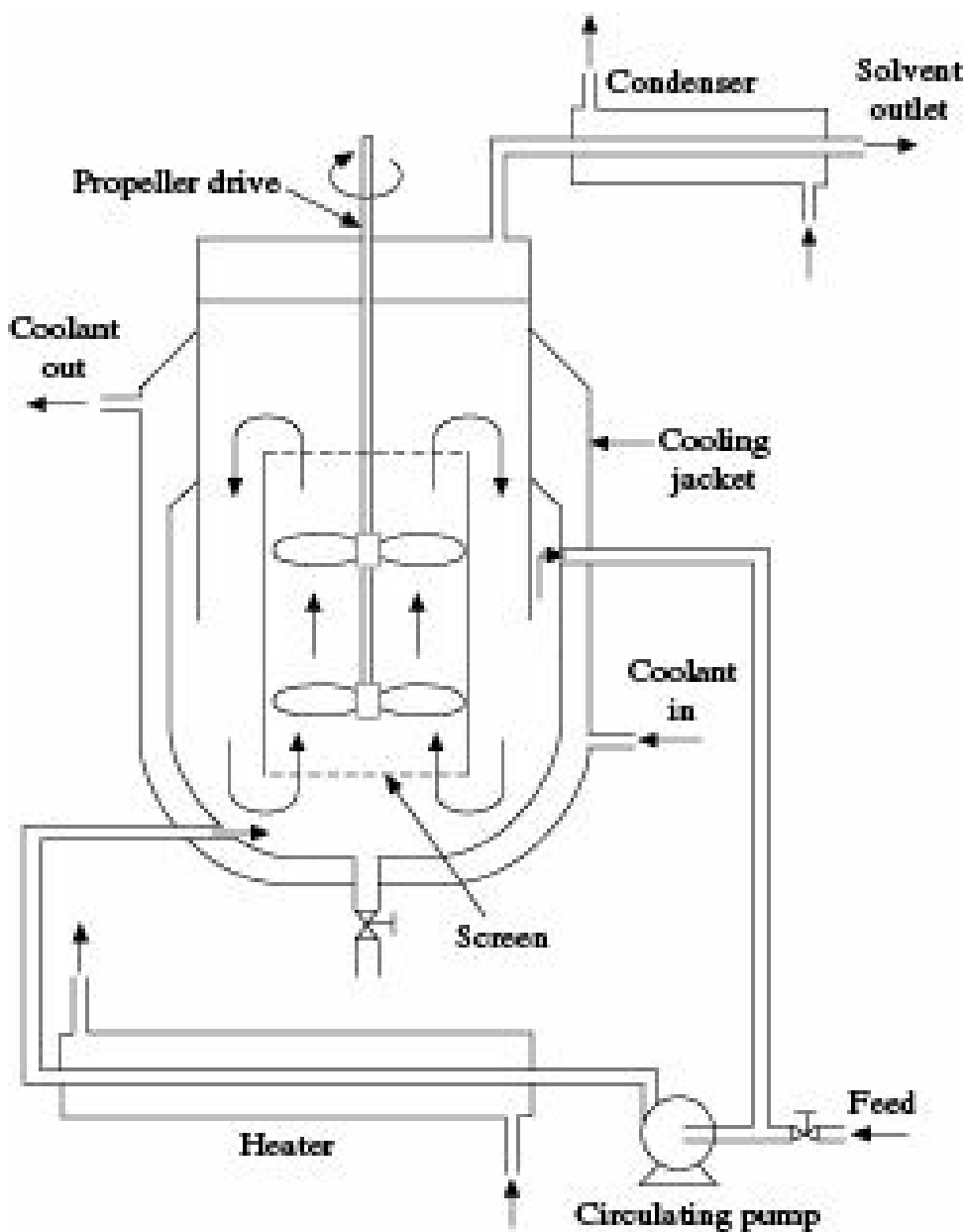


**Figure 13.6** Swenson-Walker crystallizer.

**EXAMPLE 13.5** (Cooling water rate and number of units of a Swenson-Walker crystallizer): A Swenson-Walker crystallizer is to produce 1000 kg/hr of ferrous sulphate crystals by cooling a saturated solution. The solution enters the crystallizer at 55°C and the slurry leaves at 27°C. The cooling water flows counter currently through the jacket and its temperature rises from 16 to 21°C. The overall heat transfer coefficient has been estimated to be 190 W/(m<sup>2</sup>)(K).

- (i) Estimate the cooling water requirement in kg/hr
- (ii) If each crystallizer unit is 3.2 m long and each metre of crystallizer provides 2.5 m<sup>2</sup> surface, how many crystallizer units will be required?

**Given:** Saturated solutions of ferrous sulphate contain 170 and 75 parts FeSO<sub>4</sub> per 100 parts excess water at 55°C and 27°C, respectively.

Specific heat of solution = 2930 J/(kg) (K)

Heat of crystallization of FeSO<sub>4</sub> = 66.2 kJ/kg.

**Solution:**

At 55°C: (100 + 170) = 270 parts saturated solution = 170 parts FeSO<sub>4</sub>•7H<sub>2</sub>O.

At 27°C:  $(100 + 75) = 175$  parts saturated solution = 75 parts  $\text{FeSO}_4 \cdot 7\text{H}_2\text{O}$ .

$(170 - 75) = 95$  parts  $\text{FeSO}_4 \cdot 7\text{H}_2\text{O}$  obtained from 270 parts solution.

$$\frac{270 \times 1000}{95}$$

1000 kg  $\text{FeSO}_4 \cdot 7\text{H}_2\text{O}$  to be obtained from

$$= 2842.1 \text{ kg solution}$$

$$\begin{aligned} q &= (2842.1)(2930)(55 - 27) + (66.2 \times 10^3) \times 1000 \\ &= 2.9937 \times 10^8 \text{ J/hr} \end{aligned}$$

(i) Cooling water requirement

$$\frac{2.9937 \times 10^8}{(4187)(21 - 16)} = 14300 \text{ kg/hr}$$

(ii) Crystallizer units required

$$\square T_1 = (55 - 21) = 34^\circ\text{C}, \square T_2 = (27 - 16) = 11^\circ\text{C}.$$

$$\text{Hence, } \square T_{lm} = \frac{34 - 11}{\ln\left(\frac{34}{11}\right)} = 20.38^\circ\text{C.}$$

$$q = UA\square T_{lm}, \text{ or } A = q/(U\square T_{lm})$$

$$= \frac{2.9937 \times 10^8}{(3600)(190)(20.38)} = 21.48 \text{ m}^2$$

Since 1 m of crystallizer has  $2.5 \text{ m}^2$  of surface,

$$\text{Length of crystallizer required} = \frac{21.48}{2.5} = 8.59 \text{ m}$$

$$\text{Number of crystallizer units required} = \frac{8.59}{3.2} = 2.68 \approx 3.$$

Most of the large scale industrial crystallizers are grouped into two major categories: (i) circulating liquor crystallizers, and (ii) circulating magma crystallizers.

### 13.11.3 Circulating Liquor Crystallizers

In this type of crystallizers, the crystals remain in the crystallization chamber while the solution is circulated through an external heat exchanger in which the liquor is either heated or cooled to attain the necessary supersaturation. Heating is done by passing steam and cooling is effected by passing a suitable cooling agent. Oslo vacuum crystallizers belong to this group.

#### *Oslo vacuum crystallizer*

The *Oslo vacuum crystallizer*, also known as *Krystal crystallizer* produces supersaturation in a circulating stream of solution in one section of the equipment and releases the same in another section. As shown in Figure 13.7, feed is introduced into the flashing chamber through a heater using a pump.

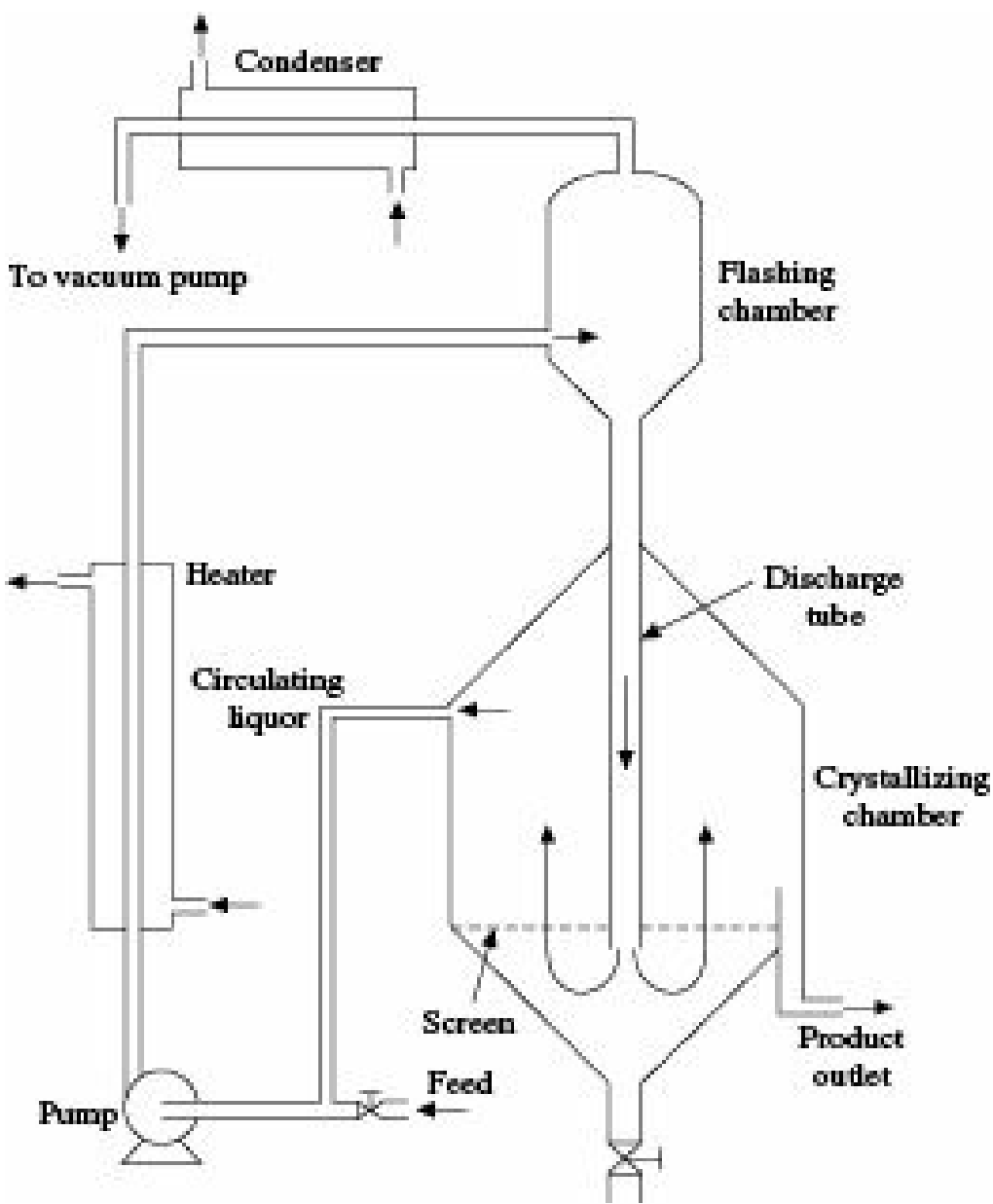


**Figure 13.7 Oslo vacuum crystallizer.**

The vapour released in the flashing chamber is withdrawn and passed to the condenser from where the noncondensed gases are drawn by a vacuum pump. The supersaturated solution moves down through the discharge tube, and then flows upward in the crystallizing chamber through a screen while it loses its supersaturation to the growing crystals there. Large enough crystals settle down and are withdrawn at product outlet for filtration or centrifuging or further processing. Fine crystals and excess nuclei are taken out and mixed with fresh feed, heated and recirculated to the flashing chamber.

These crystallizers are generally used for large scale crystallization of inorganic compounds like sodium nitrate, ammonium nitrate, ammonium sulphate, etc. Such operations are feasible when the solubility falls sharply with decreasing temperature.

#### 13.11.4 Circulating Magma Crystallizers

In the circulating magma type crystallizers, the crystals are kept in suspension (about 20–40% solids) and the slurry is circulated through an external steam-heated heat-exchanger where the desired degree of supersaturation is achieved. The Draft Tube Baffle (DTB) crystallizer, a typical crystallizer belonging to this group is described here.

## The draft tube baffle crystallizer

The Draft Tube Baffle (DTB) crystallizer with elutriation leg is very effective for continuous crystallization and simultaneous classification (Randolph 1961).

Figure 13.8 shows a typical DTB crystallizer provided with a draft tube which also acts as baffle. A propeller type agitator near the bottom of the draft tube provides controllable circulation of the liquor. The elutriation leg below the crystallizing chamber classifies the crystals according to size so that crystals of specified size range are obtained.

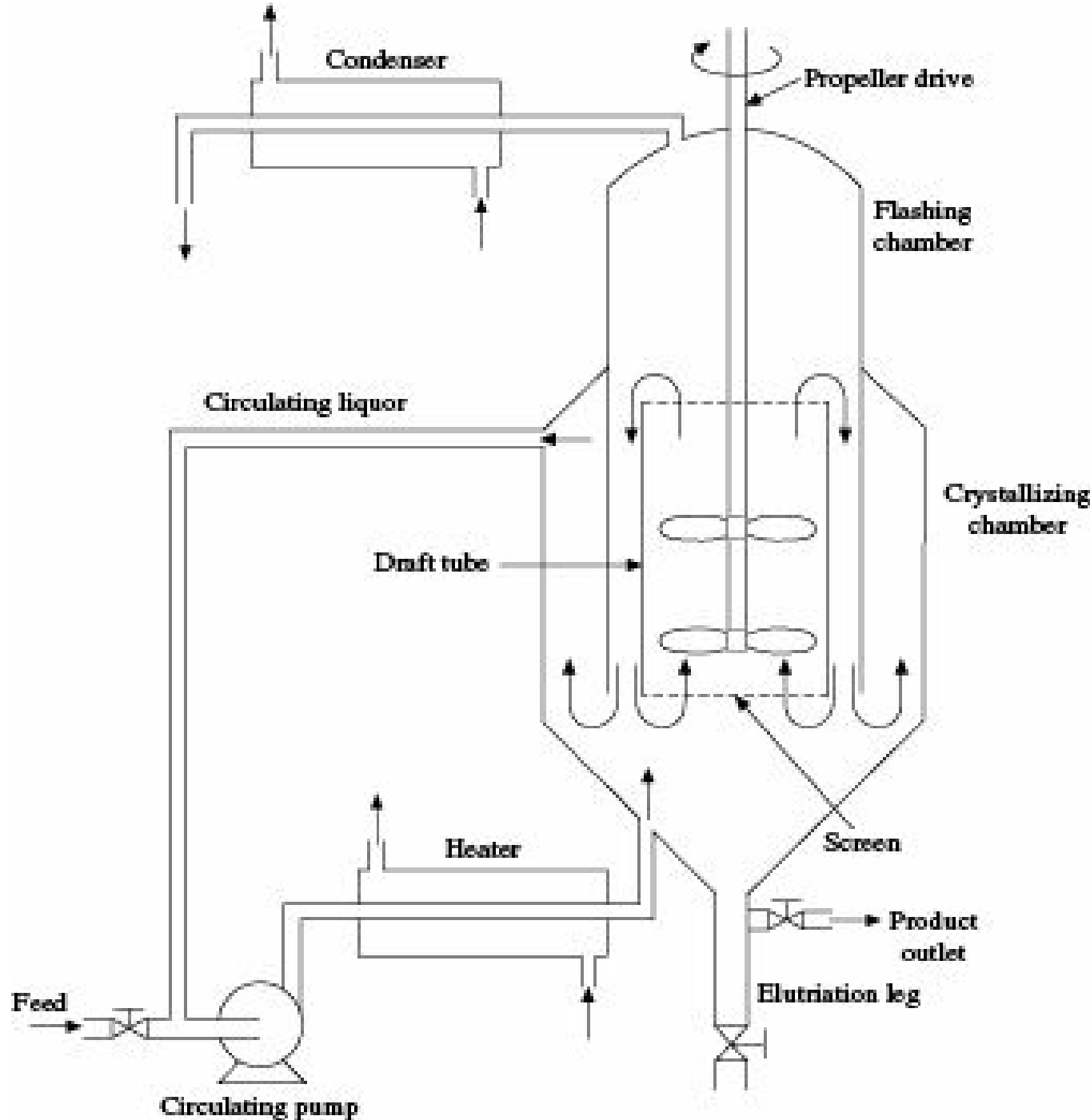


Figure 13.8 Draft tube Baffle crystallizer.

The feed along with the circulating liquor is pumped by the circulating pump through the steam-heated heater and enters the crystallizing chamber. It moves upward through the draft tube and flashes near the liquid surface where the pressure is sufficiently low. Nucleation and crystal growth take place during downward movement of the supersaturated solution through the annular space, large crystals settle down and are removed at the product outlet.

A part of the circulating liquor is pumped through the elutriation leg by the elutriating pump (not shown in Figure 13.8) that acts as hydraulic sorting fluid to carry the small crystals back to the crystallization zone for further growth. Excess nuclei and fine crystals float in the upward stream of mother liquor, and are collected in the annular space between the extended wall of the flashing chamber and the enlarged cone of the crystallizing chamber. They are withdrawn from the top of the settling zone and are recirculated through the heater along with fresh feed. Hold-up time in the equipment is kept sufficient for crystal growth to the desired size. Products such as potassium chloride, ammonium sulphate, and  $(\text{NH}_4)_2\text{PO}_4$  can be made in this equipment in the range of 6-20 mesh. Reaction and crystallization can be accomplished simultaneously in DTB units. The reactants can be charged into the recirculation line or into the draft tube. Example is the production of ammonium sulphate from ammonia and sulphuric acid, and the neutralization of waste acid with lime. The heat of reaction is removed by evaporation of water.

### 13.12 Melt Crystallization

Melt crystallization is a highly efficient process to obtain ultra-pure organic chemicals in a continuous manner. Most organic compounds having melting points in the range of 0–200°C are prime candidates for melt crystallization. This process has certain advantages over solution crystallization:

- (i) in solution crystallization organic solvents are required, the recovery of which is very much expensive and hazardous. But melt crystallization does not require any solvent, rather the impurities are recovered in molten form and can be recycled
- (ii) melt crystallization can be operated at lower temperature compared to that required in solution crystallization
- (iii) melt crystallization processes require considerably less volume of materials for which compact equipment of smaller sizes are required, and hence equipment cost and energy consumption are less compared to that required in solution crystallization
- (iv) melt crystallization can process high viscosity fluids with moderate growth rate and good selectivity whereas solution crystallization can handle only fluids of low viscosity for higher growth rate and better selectivity.

Melt crystallization is now much in use for manufacture of *p*-xylene, *p*-cresol, bisphenol A, *p*-dichlorobenzene, *p*-nitrochlorobenzene, *p*-nitrotoluene, etc. This technology is superficially analogous to distillation with solid-liquid equilibria used to effect separation instead of vapour-liquid equilibria in case of distillation. The resembling phenomena between the two separation processes are that both the processes involve— phase equilibria and phase separation, and mass transfer rates that allow the phases to attain equilibrium. However, some of the differences between the processes are:

- (i) In distillation, both the phases are miscible whereas in crystallization, liquid phases are miscible but solid phases are not miscible
- (ii) Ultra-high purity product can be obtained by crystallization but not by distillation.
- (iii) Adiabatic contact assures phase equilibrium in distillation whereas in crystallization solid phase requires to be melted and refrozen to allow phase equilibrium
- (iv) In distillation, phase separation is rapid and complete but in crystallization, phase separation is low as the surface tension effects prevent its completion

- (v) Phase densities differ by a factor of 100-10,000:1 in distillation but the same is about 10% in crystallization
- (vi) Counter-current contact is quick and complete in distillation but the same is slow and imperfect in crystallization.

Melt crystallization is also a highly selective process, only building blocks of the desired component will fit in the crystal lattice. An important parameter, however, is the crystal growth velocity driven by the temperature difference between the crystal surface and the bulk melt. In case this temperature difference increases, the solid-melt boundary layer temperature will tend towards the equilibrium temperature, while further away from this layer the melt bulk temperature will be lower. This is called *conditional supercooling*. If an irregular shape on the crystal surface enters this area of higher supersaturation, the irregularity will grow proportionally high compared to the rest of the crystal surface and may possibly form dendritic shapes. These shapes can physically include impure mother liquor in which case the crystal is not pure any more. It is therefore of utmost importance to keep temperature differences between crystal surface and melt bulk low. Industrial melt crystallization processes are of the following two categories.

### 13.12.1 Suspension Based Melt Crystallization

There is a conflict with crystal formation capacity which represents the purified product rate. If the temperature differences have to be kept low, another method to increase crystal formation capacity is to provide sufficient surface area. Suspension based crystallization, i.e. crystals are kept in suspension surrounded by mother liquor, provides huge surface area. As a result of this huge surface area, the driving force ( $DT$ ) for the crystals to grow can be kept low; the crystal will grow slowly being even pure without inclusion of impurities. Matsuoka (1977) stated that over 50% of the binary organic mixtures of which phase diagrams can be found, exhibit simple eutectic behaviour. Nearly 85% exhibit peritectic and eutectic behaviour. Crystallization of these mixtures can form pure crystals without the inclusion of impurities in the crystal lattice. The remaining 15% exhibit solid solution behaviour, impurities will be included in the crystal lattice.

The suspension melt crystallization process consists of three main components:

- The crystallizer, where crystals are formed and the mother liquor temperature is slightly subcooled below the equilibrium temperature of the mixture.
- The recrystallizer is a stirred vessel where the crystals are kept in suspension. The crystals formed in the crystallizer are allowed to grow using the subcooled temperature of the mother liquor as a driving force.
- The wash column where the crystals are separated from the mother liquor.

The crystallizer and the recrystallizer are standard equipment. The operating temperatures are moderate, the operating pressure is low at approximately 1 bar (g). Rotating speeds and related maintenance costs are low, general equipment maintenance is simple.

The feed is being circulated from the recrystallizer over the crystallizer where the temperature is gradually lowered. Generally, when the equilibrium temperature is reached, crystals will be formed. The mother liquor will be depleted of the crystallized component and the composition of the mother liquor will shift towards the eutectic composition. The crystal suspension from the recrystallizer is fed to the wash column. The amount of crystals made in the crystallizer and taken from the

recrystallizer to the wash column is balanced to maintain a crystal density between 25 to 35% in the recrystallizer. In the wash column the crystals are compressed to a firm crystal bed with crystal density of approximately 80%. Since in the wash column the pure wash liquid will crystallize on the surface of the supplied crystals, no wash liquid is pushed back to the process. The amount of impurities affects both nucleation rate and crystal growth rate. If the composition of mother liquor shifts towards the eutectic point, nucleation rate will increase which will decrease the average crystal size and reduce the porosity of the compressed crystal bed. The effect is enhanced by the fact that the crystal growth rate will decrease simultaneously. As a result, the wash column has to be operated with a higher pressure in the melting loop.

An advantage of the process is that the total process plant is liquid-filled. There are no gas caps, with problematic interfaces between product and oxygen, and obviously there is no need of blanketing systems. The process is continuous without need for intermediate storage tanks and related pumps, piping, tracing, insulation, space, etc. The crystal that is formed in the crystallizer leaves the process as a pure component, that is named *crystallization effort*, which in this case is unity. For layer crystallization systems, the crystallization effort can be as high as six or higher in order to reach the required product purity, with related high energy cost.

The feasible yield defined as the ratio of the amount of the valuable component in the purified product to the amount of the valuable component in the feed, for the process obviously depends on the feed and achievable mother liquor concentrations. A multistage process design will facilitate a lower mother liquor concentration resulting in increased yield. In order to increase the feed concentration and thus the yield, extractive distillation can be applied upstream the suspension based melt crystallization process, creating a hybrid overall process design.

### **13.12.2 Progressive Freezing Crystallization**

Suspension based melt crystallization processes depend on density difference to promote counter-current transport of crystals and melt. The continuous removal of crystals by sedimentation or centrifuge makes it more complicated. Progressive freezing process may be an alternative because a crystal in this process is grown on a heat transfer surface and phase separation to facilitate counter-current contact occurs by gravity draining irrespective of density difference. In this process, a uniform crystalline layer is allowed to grow instead of scrapping crystals from the heat transfer surface. Impure melt is drained from this layer by gravity and pure product is recovered by remelting the layer.

Progressive freezing crystallization may be of two types—static crystallization and falling film crystallization.

#### ***Static crystallization***

In this technique, the crystal layer is slowly grown on a cooled surface immersed in quiescent melt. Horizontal shell and tube heat exchangers or vertical plates, used with the melt on the shell side is filled with feed. Coolant temperature is then ramped down slowly to grow the crystal layer. After the crystal layer is grown, the shell side of the exchanger is drained leaving crystals on the outside of the tubes. The coolant temperature is then carefully ramped up to sweat the crystals. The sweated crystals are then melted off the tubes as product.

#### ***Falling film crystallization***

In this process, a film of melt is made to fall continuously over the cooled surface on which the crystal layer grows. The resulting shear at the solid-liquid interface transports impurities rapidly into the bulk of the melt, even with viscous melt. This allows much faster crystal growth rates without interphase instabilities. It is possible to grow solid slabs of crystals at faster rates than that obtained in the static crystallization. Figure 13.9 shows schematically the process adapted by *Metallwerk Buchs* (MWB).

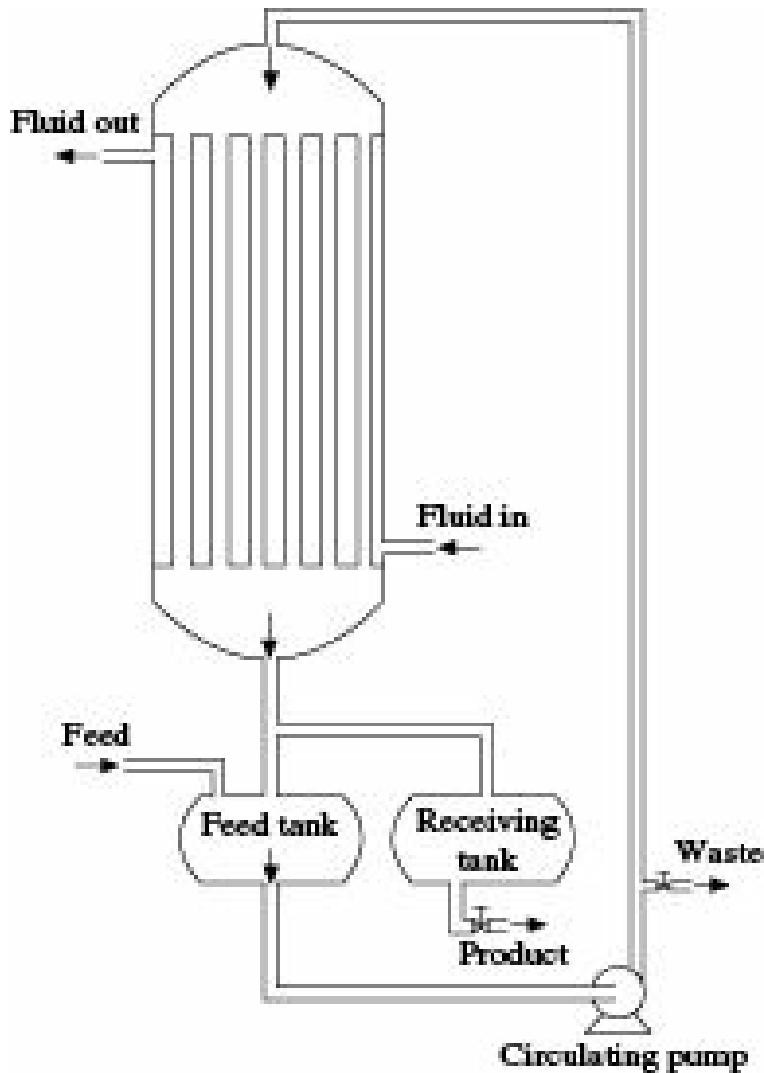


**Figure 13.9** Falling film crystallizer.

The crystallizer contains vertical tubes in which the crystal layers grow as cylinders. The collecting tank beneath the tubes is built integrally with the crystallizer. At the start of the operation, it is filled with a batch of material. The circulating pump is then started to irrigate the tubes and the coolant is introduced simultaneously on the shell side while the temperature ramping is commenced in the crystallizer. The melt circulation rate is kept high compared to the rate of crystal deposition in order to maintain the temperature and composition almost uniform along the length of the tubes. Shell side temperature is ramped down at a constant rate until the level in the collecting tank drops to a preset value indicating the designed amount of product suspended in the tubes. When an appropriate thickness of solid is accumulated at this point, melt circulation ceases and the crystals drain free of residue. Shell side temperature is then ramped up to a value just below the melting point of the product to sweat out the impurities and to assist the draining process.

### 13.13 Purification

Since the impurities remain included in the crystal lattice, purification can only be accomplished in multiple crystallization stages where the product is reprocessed by repeating the crystallization, sweating and melting steps. As an alternative to multistage crystallization processes with their associated problems of material handling and losses, several types of continuous column crystallizers have been developed in which the product crystals are washed with their own melts in counter-current flow (Walas 1988). These are as follows:

**Schildknecht column:** This uses a rotating spiral or screw to move the solids in the direction against the flow of the fluid. The conveyor is of open construction so that the liquid can flow through it but the openings are small enough to carry the solids.

**Philips crystallization process:** The purifying equipment consists of a vessel with a wall filter and a heater at the bottom. Crystals are charged from an external crystallizer and forced downwards with a reciprocating piston or with pulses from a pump. The washing liquid reflux flows from the melting zone where it is formed upward through the crystal bed and out through the wall filter.

**Brodie crystallizer purifier:** This equipment combines a horizontal scraped surface crystallizer with a vertical purifying section.

**TNO bouncing ball purifier:** Figure 13.10 shows a TNO type purifier containing a number of sieve trays attached to a central shaft that oscillates up and down. The slurry from the crystallizer is fed into the column and the crystals are formed during the movement of the slurry through the sieve-trays. Bouncing balls on each tray impact the crystals and break up some of them. The resulting small crystals melt and enrich the liquid phase, thus providing an upward refluxing action on the large crystals that continue to move downward to the melting zone. Reflux is then returned from the melting zone and product is taken out.

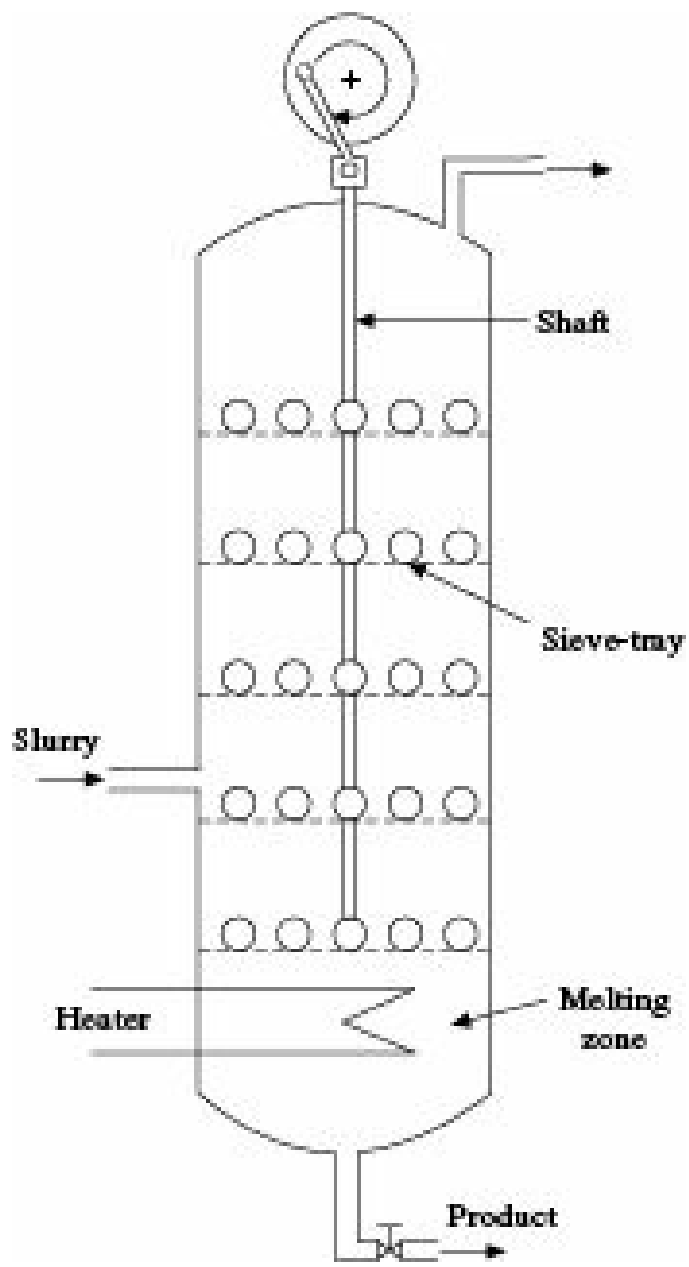


**Figure 13.10 Purifier—TNO type.**

**Kureha double screw purifier:** The unit employs a double screw with intermeshing blades that pull the liquid from the crystal mass as it is conveyed upward. The melt is formed at the top, washes the rising crystals counter-currently, and leaves as residue at the bottom.

**Brennan-Koppers purifier:** Figure 13.11 shows a schematic representation of a Brennan-Koppers type equipment which employs top melting like the Kureha and wall filters like the Philips. The slurry from the crystallizer is drawn by a circulating pump and fed into the column in which the crystals are formed due to ramping of temperature. The upward movement of the crystals thus formed, is caused by drag of the flowing fluid. The crystal bed is held compact with a rotating top plate or piston called a harvester. It has a corrugated surface that scrapes off the top of the bed and also the openings that permit the crystals to enter the melting zone at any desired rate. The melt flows downward through the openings in the harvester, washes the upwardly moving crystals, and leaves through the sidewall filter as residue. The movement of crystals is quite positive and not dependent on particle size as in other kinds of purifiers.

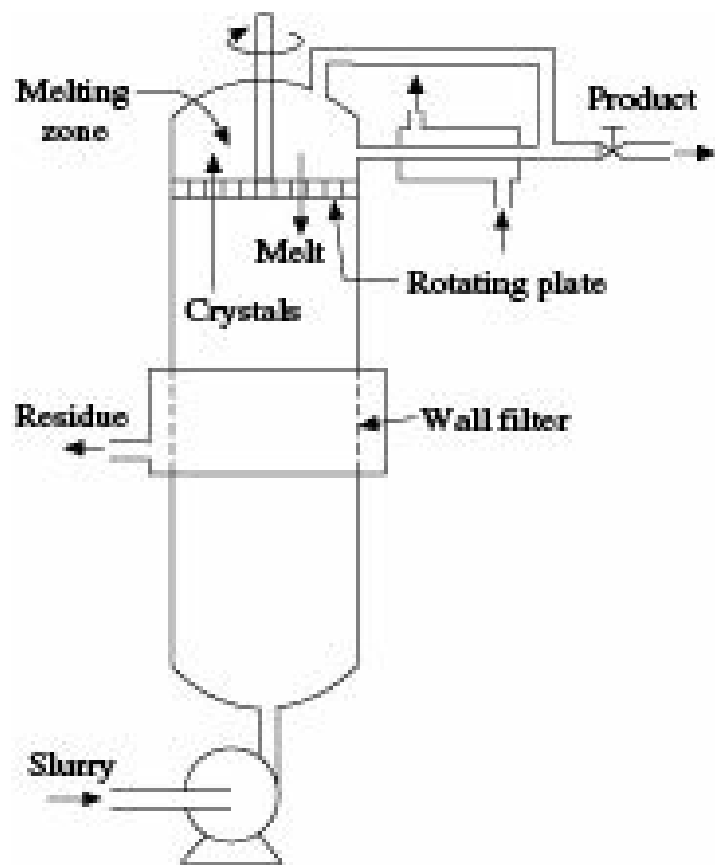


Figure 13.11 Brennan-Koppers type purifier.

### 13.14 Reactive Crystallization

Reactive crystallization is the process where *in situ* product separation by crystallization takes place to enhance the yields or conversions of equilibrium limited reactions. This process is widely used in pharmaceutical industry to facilitate resolution of enantiomers (diastereometric crystallization) by reacting the racemate with a specific optically active resolving agent producing two derivatives easily separated by crystallization. Its uses include liquid-phase oxidation of *p*-xylene to produce technical grade terephthalic acid, hydrolysis of sodium salicylate into salicylic acid in acid medium, absorption of ammonia in aqueous sulphuric acid from ammonium sulphate. The reactive crystallization processes are also used for manufacture of calcium carbonate, magnesium hydroxide, nickel hydroxide, sulphamic acid, procaine benzyl penicillin, magnesium ammonium phosphate, barium carbonate, etc.

Advantage of reactive crystallization over conventional crystallization has been shown by Tamura and Tsuge (2006) using gas-liquid reaction for calcium carbonate. Lin et al. (2006) have explored the mass transfer aspects for calcite nanocrystallization. The limitations of reactive crystallization process are that the reaction and crystallization media should be identical as the mother liquor is recycled to the reaction section, and the solubility of the product should be lower than the solubility of reactants or by-products at crystallization temperature.

### *Nomenclature*

$a$  : surface area of a molecule,  $\text{L}^2$

$A$  : mass of anhydrous solute in original solution,  $\text{M}$

$A'$  : constant

*c* : concentration of solute in solution, M/L<sup>3</sup>

*C<sub>A</sub>,C<sub>B</sub>* : solute concentration in bulk solution and solid-liquid interface respectively, M/L<sup>3</sup>

*E* : evaporation of solvent during crystallization, M, M/□

*F* : feed solution, M, M/□

*h, ΔH* : enthalpy, FL/mol, FL/M

*k* : Boltzman constant

*k<sub>L</sub>* : mass transfer coefficient, mol/L<sup>2</sup>□ (M/L<sup>3</sup>)

*k'* : coefficient of surface integration

*K* : overall coefficient of diffusion and surface reaction

*K'* : overall mass transfer coefficient in terms of mole fraction

*L* : linear dimension of crystal, L

*m* : mass of a single crystal

*M* : molecular weight, M/mol

*N* : rate of nucleation, No/L<sup>3</sup>□

*q* : heat lost from crystallizer, FL, FL/□

*R* : ratio of molecular weights of hydrated to anhydrous salts

*s* : solubility of solute at a particular temperature

*S* : saturated solution in final product

*S<sub>S</sub>* : supersaturation ratio

*T* : absolute temperature, T

*y<sub>M</sub>* : volume of one molecule, L<sup>3</sup>

*W* : mass of solvent, M, M/□

*Y* : yield of crystal, M, M/□

*v* : surface energy, F/L

*m* : shape factor

*t* : density, M/L<sup>3</sup>

*i* : time, i

{*S*} : fractional supersaturation

### *Subscripts*

*F* : feed

*S* : saturated solution

*y* : crystal .

### **Numerical Problems**

**13.1 Estimation of the Amount of Crystals Formed:** Find the amount of crystals to be liberated in a crystallizer when 10 tonnes of saturated aqueous solutions of potash are cooled from 80 to 35°C without evaporation of the water. The potash crystallizes with two molecules of water per

molecule of  $K_2CO_3$ .

The solubility curve gives the concentrations of the saturated aqueous solutions of potash as follows:

at  $80^\circ C$ : 10 mol of  $K_2CO_3$  per 1000 g of water

at  $35^\circ C$ : 8.15 mol of  $K_2CO_3$  per 1000 g of water.

[Ans: 1900 kg]

**13.2 Calculation of the Temperature to Reduce the Concentration of the Mother Liquor by 50% to Freeze Out the Crystals:** To what temperature does a hot 40% aqueous solution of potassium nitrate have to be cooled for the concentration of the mother liquor to be half the initial one after it is cooled and crystals freeze out? Relevant data are to be collected from the solubility curve of potassium nitrate.

[Ans:  $15^\circ C$ ]

**13.3 Formation of Crystals of Soda During Cooling:** How many kilograms of crystals freeze out when 4.2 tonnes of a soda solution containing 2.5 mol of soda per 1000 g of water are cooled from  $30^\circ C$  to  $15^\circ C$ ? The soda crystallizes with 10 molecules of water per soda molecule. [Ans: 1300 kg]

**13.4 Estimation of Capacity of an Open Tank, Cooling Surface requirement and Yield of Crystals:** A saturated solution of potassium chloride at  $90^\circ C$  containing 700 kg potassium chloride is cooled to  $20^\circ C$  in an open tank by circulation of water. The cooling water enters the tank at  $15^\circ C$  through a jacket and leaves at  $25^\circ C$ . The average specific heat and density of the solution are 0.48 cal/g°C and  $1.2 \text{ g/cm}^3$ , respectively.

Assuming the overall heat transfer coefficient to be  $120 \text{ kcal}/(\text{hr})(\text{m}^2)(^\circ\text{C})$ , determine (i) the capacity of the tank, (ii) the weight of crystals obtained, and (iii) the cooling surface of the tank.

[Ans: (i)  $1.67 \text{ m}^3$ , (ii) 249.02 kg, (iii)  $29.02 \text{ m}^2$ ]

**13.5 Computation of the Rate of Growth of Crystals from the Knowledge of Degree of Supersaturation, and Values of Coefficients of Mass Transfer and Surface Interaction:** Estimate the rate of growth of  $MgSO_4 \cdot 7H_2O$  in cm/day from a solution of  $MgSO_4$  having a supersaturation of 0.004 mol fraction  $MgSO_4 \cdot 7H_2O$ . The mass transfer coefficient has been estimated to be  $1.60 \text{ kmol}/(\text{m}^2)(\text{hr})(\text{mol fraction})$  and the coefficient of interaction is 1.40. The crystals may be assumed to be cubes having an equivalent diameter of 0.50 cm. The density of the crystal is  $1.68 \text{ g/cm}^3$ . [Ans: 2.1 cm/day]

**13.6 Determination of Quantity of Heat Withdrawn in a Continuous Crystallizer:** Determine the quantity of heat that must be withdrawn in a continuous crystallizer for cooling an aqueous solution of  $NaNO_3$  from  $90^\circ C$  to  $40^\circ C$  at a rate of 5000 kg/hr. The solution contains 16 mol of  $NaNO_3$  per 1000 g of water at  $90^\circ C$ . Consider that when the solution is cooled in the crystallizer water simultaneously evaporates in an amount equal to 3% of the initial amount of the solution. The concentration of a saturated solution of  $NaNO_3$  at  $40^\circ C$  is 12.3 mol per 1000 g of water.

[Ans: 130 kW]

**13.7 Calculation of the Cooling Surface and the Flow Rate of Water Required:** For the conditions of the preceding Problem 13.6, determine the required cooling surface area and the rate of flow of

water in the crystallizer. Assume that the overall heat transfer coefficient equals  $100 \text{ W}/(\text{m}^2)(\text{K})$ . The water enters the cooling jacket at  $15^\circ\text{C}$  and leaves it at  $20^\circ\text{C}$ . Counter-flow cooling is used.

[Ans: 22400 kg/hr]

**13.8 Requirement of the Cooling Surface in a Counter-Flow Crystallizer:** Determine the required cooling surface area of a counter-flow crystallizer used to cool 10000 kg/hr of a solution containing 7 mol of ammonium sulphate per 1000 g of water from  $85^\circ\text{C}$  to  $35^\circ\text{C}$ . During cooling, water evaporates (5% of the mass of the initial solution). The overall heat transfer coefficient is  $127 \text{ W}/(\text{m}^2)(\text{K})$ . The cooling water is heated from  $13^\circ\text{C}$  to  $24^\circ\text{C}$ . Also, determine the rate of flow of cooling water.

[Ans:  $20.3 \text{ m}^2$ , 7660 kg/hr]

**13.9 Estimation of Cooling Water and Surface Area Requirement for a Given Crystallization Operation in a Swenson-Walker Crystallizer:** A Swenson-Walker crystallizer is to produce 800 kg/hr of  $\text{FeSO}_4 \cdot 7\text{H}_2\text{O}$  crystals. The saturated solution enters the crystallizer at  $49^\circ\text{C}$  and the slurry leaves at  $27^\circ\text{C}$ . Cooling water enters in the jacket of the crystallizer at  $15^\circ\text{C}$  and leaves at  $21^\circ\text{C}$ . The overall heat transfer coefficient has been estimated to be  $175 \text{ kcal}/(\text{hr})(\text{m}^2)(^\circ\text{C})$ . There are  $1.3 \text{ m}^2$  of cooling surface per metre of crystallizer length.

(i) Estimate the cooling water requirement in kg/hr, and

(ii) Determine the number of crystallizer sections to be provided, each section being 3 m long.

*Given:* Saturated solution of  $\text{FeSO}_4$  at  $49^\circ\text{C}$  and  $27^\circ\text{C}$  contain 140 parts and 74 parts of  $\text{FeSO}_4 \cdot 7\text{H}_2\text{O}$  per 100 parts of excess water, respectively. The average specific heat of the initial solution is  $0.70 \text{ kcal}/(\text{kg})(^\circ\text{C})$ , and the heat of crystallization is  $15.8 \text{ kcal/kg}$ .

[Ans: (i) 9571 kg/hr (ii) 6]

## **Short and Multiple Choice Questions**

1. What do you mean by critical humidity of a solid?
2. What is the heat of crystallization? On what factor does it depend?
3. What are the methods of producing supersaturation in a solution prior to crystallization?
4. What is  $\square L$  law for crystal growth?
5. Why agitation is provided during crystallization?
6. Why crystallization in an unseeded solution does not start just on reaching saturation?
7. State the methods of formation of nuclei in situ.
8. What are the causes of caking of crystals? How can caking be prevented?
9. What is polymorphism?
10. What is a liquid crystal? Name two substances that produce liquid crystals.
11. A crystal having three unequal rectangular axes is  
(a) cubical      (b) orthorhombic      (c) trigonal      (d) triclinic
12. Two or more crystals that crystallize in the same form are called  
(a) isomorphous  
(b) amorphous

- (c) polymorphous
- (d) none of these

13. Formation of large crystals is favoured by

- (a) a low nucleation rate
- (b) a high degree of supersaturation
- (c) a high magma density
- (d) a low magma density

14. Caking of crystals can be prevented by

- (a) maintaining a high critical humidity
- (b) maintaining a low critical humidity
- (b) producing crystals of nonuniform size
- (b) all of the above

15. The characteristic length of a crystal increases from 1.5 mm to 1.7 mm when suspended in a supersaturated solution of the same material for 3 hours. The characteristic length of a 3 mm crystal of the same material if allowed to grow for 6 hours in the same solution under similar conditions will be

- (a) 3.2 mm
- (b) 3.4 mm
- (c) 3.6 mm
- (d) 3.8 mm

16. Swenson-Walker crystallizer is a

- (a) batch unit
- (b) semi-batch unit
- (c) continuous unit
- (d) both (b) and (c)

17. Agitation is provided in a crystallizer for

- (a) avoiding deposition on cooler surfaces
- (b) facilitating nuclei formation
- (c) facilitating crystal growth
- (d) all of the above

18. An evaporative crystallizer is preferred for the crystallization of a substance having

- (a) relatively flat solubility curve
- (b) solubility curve that rapidly increases with temperature
- (c) inverse solubility relation
- (d) all of the above

19. The DL law is found to be valid for the crystallization of a certain substance. Which of the following resistances is likely to control the rate of crystal growth?

- (a) diffusional
- (b) surface reaction
- (c) both (a) and (b)
- (d) none of these

20. A DTB crystallizer works on the principle of

- (a) circulating magma crystallizer
- (b) circulating liquor crystallizer
- (c) cooling type crystallizer

(d) all of the above

### Answers to Multiple Choice Questions

- 11. (b) 12. (a) 13. (b) 14. (a) 15. (b) 16. (c) 17. (d)
- 18. (a) 19. (b) 20. (a)

### References

- Berthoud, A., *J. Chem. Phys.*, **10**, 624 (1912).
- Lin, R.Y., J.Y. Zhang and Y.Q. Bai, *Chem. Eng. Sci.*, **61**, 7019 (2006).
- Matsuoka, M., *Sep. Proc. Eng.*, **7**, 245 (1977).
- McCabe, W.L., *Ind. Eng. Chem.*, **21**, 30, 112 (1929).
- Miers, H.A., *J. Inst. Metals*, **37**, 331 (1927).
- Mullin, J.W., *Crystallization*, 4th ed., Butterworth-Heinemann, Boston (2001).
- Myerson, A.S., *Handbook of Industrial Crystallization*, 2nd ed., Butterworth, London (2002).
- Perry, R.H., D.W. Green and J.O. Malony (Eds.), *Perry's Chemical Engineers' Handbook*, 7th ed., McGraw-Hill, New York (1997).
- Randolph, A.D., *Chem. Eng.*, **77**, 86 (May, 1961).
- Randolph, A.D. and M.A. Larson, *Theory of Particulate Processes*, 2nd ed., Academic Press, New York (1988).
- Tamura, K. and H. Tsuge, *Chem. Eng. Sci.*, **61**, 5818 (2006).
- Valeton, J.J.P., *Z. Krist.*, **59**, 135, 335 (1923); **60**, 1 (1924).
- van der Steen, R. and S. Nandani, *Chem. Ind. Dig.*, **XX**(2), 67 (2007).
- Volmer, M., *Z. Electrochem.*, **35**, 555 (1929).
- Volmer, M., *Kinetik der Phasenbildung*, Dietrich Steinkopff Verlag, Dresden and Leipzig (1939).
- Walas, S.M., *Chemical Process Equipment-Selection and Design*, Butterworth, USA (1988).

# Adsorption and Chromatography

## 14.1 Introduction

An adsorption is a fluid-solid mass transfer operation useful in separating components of gaseous or liquid mixtures. It is a surface phenomenon that utilizes the ability of certain solids to preferentially concentrate specific substances on their surfaces. In case of gases, typical applications include dehumidification of air or other gases, removal of impurities or objectionable odours from industrial gases, recovery of valuable solvent vapours from air or other gases and fractionation of hydrocarbon gases. In case of liquids, removal of moisture from gasoline, decolourisation of petroleum products or sugar solution, removal of objectionable odour or taste from water and fractionation of aromatic and paraffinic hydrocarbons are typical examples of adsorption.

The gas or liquid being adsorbed by a solid is called *adsorbate* while the solid that adsorbs is known as *adsorbent*.

The reverse of adsorption is known as *desorption* or *regeneration*. The term desorption also indicates the reverse of absorption. In some cases, the adsorbed material may be valuable and it becomes necessary to separate and recover the same from the adsorbent. In other cases, the substance being adsorbed may not have any value but the adsorbent is costly and it has to be reused after desorption of the adsorbed species followed by regeneration if required.

The amount of an adsorbate adsorbed or desorbed per unit mass of the adsorbent largely depends on the prevailing temperature and pressure. Lower temperature and higher pressure favour adsorption while higher temperature and lower pressure favour desorption. By taking the advantage of these phenomena, both adsorption and desorption are usually carried out in the same vessel in case of batch adsorption. When the adsorbent is nearly saturated, the flow of feed is stopped and the temperature is raised when desorption takes place. A carrier gas or superheated steam may be passed through the bed of adsorbent for carrying away the desorbed substance.

## 14.2 Types of Adsorption

Depending upon the strength of the bond between the adsorbent and the adsorbate, adsorption may be of two broad types—*physical adsorption* and *chemical adsorption*.

In physical adsorption or physisorption or van der Waals adsorption, the adsorbed molecules neither enter the crystal lattice of the solid nor get dissolved in it, but concentrate only on the surface of the solid. If, however, the solid is highly porous, the adsorbed substance may sometimes enter into the pores. Physical adsorption is caused by intermolecular forces of attraction between molecules of the adsorbent and those of the substance adsorbed. During adsorption of gases, heat evolved is of the order of the heat of sublimation of the gas. Physical adsorption is a highly reversible process and the adsorbed substance can be easily desorbed by lowering the pressure or increasing the temperature.

This type of adsorption finds frequent industrial application where the adsorbed substance has to be recovered or the adsorbent has to be reused. Most of the industrial adsorptions come under this category. Classic example is the separation of nitrogen and oxygen from air in the Linde column. Chemical adsorption or chemisorption or activated adsorption is caused by chemical interaction between the adsorbent and the substance being adsorbed (Clark 1970). In this process, the adsorbate molecules or ions are strongly bonded with the adsorbent surface through some involvement of valence electrons. One such example is the adsorption of fluoride ions on activated alumina. The adhesive force is generally much higher than in case of physical adsorption. The strength of the bond varies widely and identifiable chemicals may not be formed. The heat evolved, usually in the range of 10 to 100 kcal/gmol during chemisorption is also much higher than that in physical adsorption, being of the order of heat of reaction. The adsorbents used in chemisorption, cannot be regenerated easily, usually regenerated by more severe thermal or chemical treatments or are discarded after using once. Chemisorption plays an important role in catalysis. The reactant molecules chemisorb on the catalyst surface prior to the formation of product molecules and this step more often controls the rate and selectivity of the catalytic reaction.

Adsorption technology is nowadays used very effectively for separation and purification of many gas and liquid mixtures in chemical, petrochemical and biochemical industries (Keller et al. 1987, Ledoux 1947, Sircar et al. 1998). This is considered to be a cheaper and easier technology compared to distillation, absorption and extraction.

### 14.3 Adsorption Equilibrium

*Adsorption isotherm* is the relationship between the concentration of the solute in the fluid and in the solid adsorbent in equilibrium at a given temperature. In case of gases, concentration is usually expressed in terms of partial pressure or mole percent while for liquids, the same is expressed as weight percent or weight per unit weight. In case of solid adsorbents, the concentration is generally expressed as weight per unit weight of solute-free adsorbent. A plot of the equilibrium concentration of solute in an adsorbent against temperature at constant pressure is called an *isobar*. Similarly, a plot of the logarithm of the concentration or partial pressure of the solute in the fluid against the inverse of the absolute temperature (as abscissa) for a constant loading of the adsorbent is called the *isostere*.

Adsorption isotherm of benzene upon activated carbon is shown in Figure 14.1. In this figure, the concentration of the adsorbed vapour in the solid is plotted as abscissa against the equilibrium partial pressure ( $p^*$ ) of the gas at constant temperature. The curve is analogous to the solubility curves of gases in liquids. The equilibrium adsorption characteristics of a gas or vapour upon a solid have striking similarity with the equilibrium solubility of a gas in a liquid.

The nature of the adsorption isotherm depends on the adsorbent used. Thus, the curve of Figure 14.1 will be quite different if silica gel is used as the adsorbent instead of active carbon. Changes in origin, method of preparation, physical state of aggregation and duration of use of the adsorbent result in significant change in the equilibrium adsorption.

In Figure 14.1, concentration corresponding to any point on the equilibrium curve may be obtained either by adsorption of solute by a fresh adsorbent or by desorption from an adsorbent having higher adsorbate concentration. In some cases, however, different equilibrium curves, at least over a part of the isotherm, are obtained depending upon whether the gas or vapour is adsorbed or desorbed. This phenomenon known as *hysteresis* is shown in Figure 14.2.

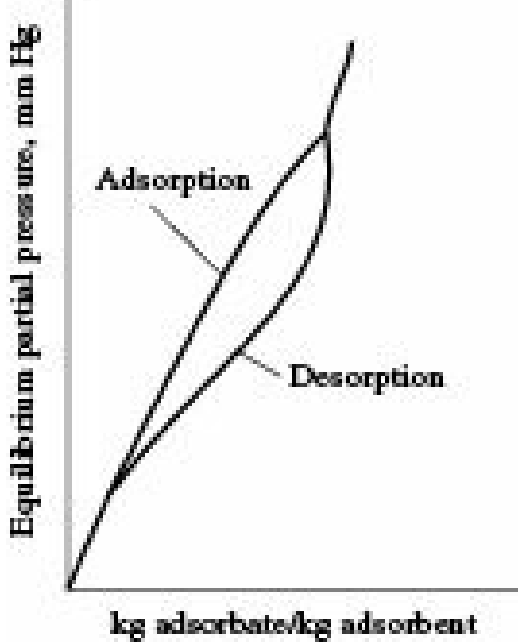
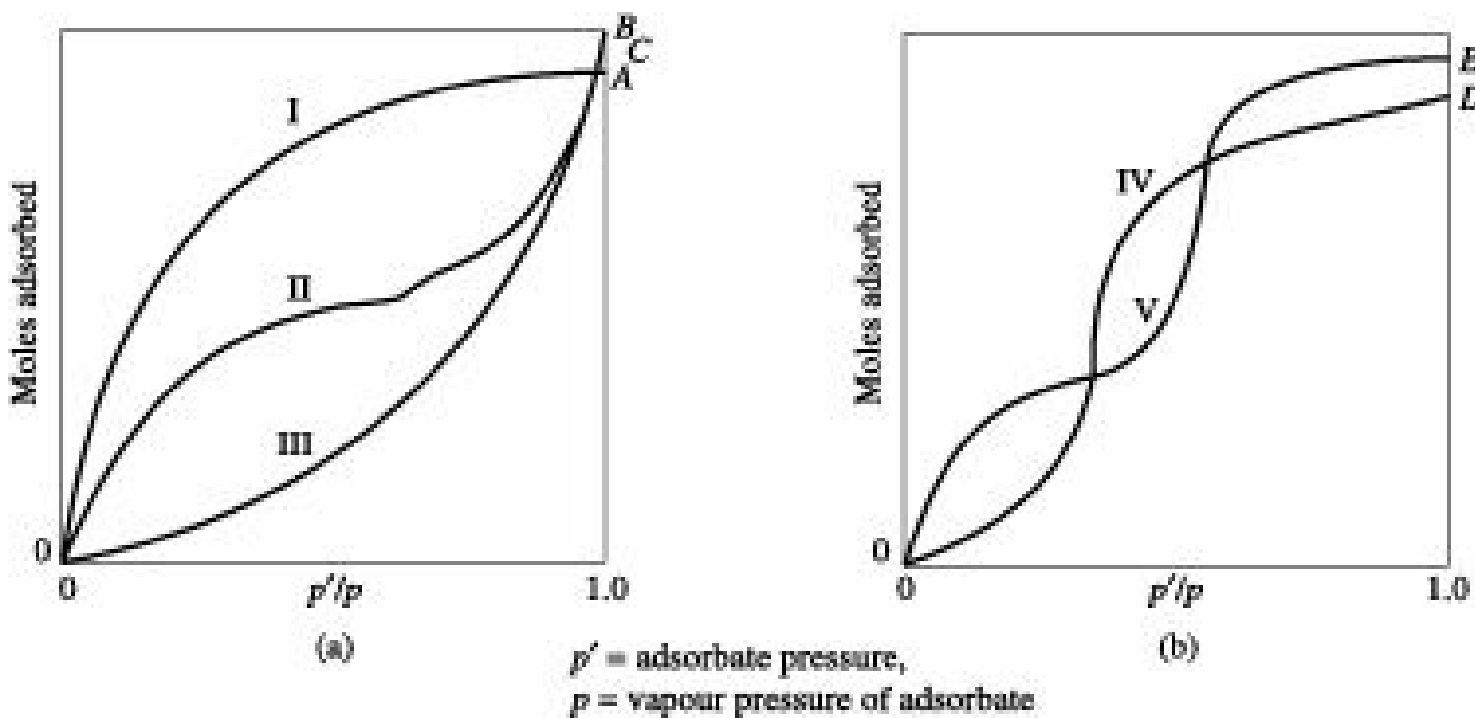


Figure 14.2 Adsorption isotherm with hysteresis.

In case of hysteresis, the equilibrium partial pressure corresponding to a certain amount of solute concentration in the adsorbent is high in case of adsorption than that in case of desorption. Hysteresis may be due to the shape of the openings to the capillaries and pores of the adsorbent or due to nonuniform wetting (Treybal 1985).

Different types of adsorption isotherms are exhibited by different adsorbate-adsorbent combinations. The five types of adsorption isotherms identified by Braunauer et al. (1940) are shown in Figures 14.3(a) and 14.3(b). In these figures, moles adsorbed have been plotted as ordinate against  $(p'/p)$ ,  $p'$  being the partial pressure of the sorbate and  $p$  is its vapour pressure.

In Figure 14.3(a), the curve  $OA$  (Type-I) is concave downwards and represents systems in which adsorption does not proceed beyond the formation of a monomolecular layer of the adsorbate. Many common gas-solid adsorption systems follow this type of adsorption isotherm. Adsorption of oxygen on carbon at about  $-183^{\circ}\text{C}$  is an example. The curve  $OB$  (Type-II) is initially concave downwards and then near the middle of the abscissa it becomes concave upwards. This point indicates the completion of formation of monomolecular layer and beginning of the formation of multimolecular layer of the adsorbate. This type of behaviour is generally exhibited by physical adsorption of water vapour by carbon black at about  $30^{\circ}\text{C}$ . The curve  $OC$  (Type-III) is concave upwards. This is a relatively rare type. The amount of gas or vapour adsorbed increases indefinitely as the relative saturation  $(p'/p)$  approaches unity. The convex downward nature is caused by the heat of adsorption of the first layer becoming less than the heat of condensation due to molecular interaction in the monolayer. The solute loading is low at low concentration of the adsorbate in the fluid. This type of isotherm is obtained when adsorbing bromine on silica gel at  $20^{\circ}\text{C}$ . Adsorption of nitrogen on ice is another example.



**Figure 14.3** Five basic types of adsorption isotherm.

Curve  $OD$  (Type-IV) is a variation of a Type-II, but with a finite multilayer formation corresponding to complete filling of the capillaries. This type of isotherm is found when adsorption of water vapour takes place on active carbon at about  $30^{\circ}\text{C}$ . Curve  $OE$  (Type-V) shown in Figure 14.3(b) is a similar variation of a Type-III obtained, for instance when adsorbing water vapour on activated carbon at about  $100^{\circ}\text{C}$ .

Several mathematical expressions have been proposed to describe adsorption equilibria. While some of them are based on theoretical considerations, others are just empirical. The analysis of data for 18 different pure gases adsorbing on various adsorbents showed that the isotherms for these gases varied considerably with different adsorbents and that adsorbate loading varied essentially inversely with their molecular weights. None of the models can be generalized to describe all the systems realistically (Valenzuela and Meyers 1989). Three commonly used classical expressions considered to be the best because of their simplicity and ability to correlate Type-I isotherms, have been discussed below:

### 14.3.1 Langmuir Isotherm

Most of the solid adsorbents have a limited active area on which the adsorbed molecules can be held tightly by formation of monomolecular layer. For a solid having uniform properties that can hold all the adsorbed molecules with the same bonding strength, Langmuir (1916) correlated (derived from simple mass action kinetics assuming chemisorptions) the total number of gas or vapour molecules and those adsorbed by equating the rate of adsorption and desorption of the gas or vapour molecules by the solid at equilibrium. The rate of adsorption was assumed to be proportional to the fraction  $(1 - \{\})$  of the solid surface that was not occupied by the adsorbed molecules.

$$kp'(1 - \{\}) = k'\{\quad (14.1)$$

where  $k$  and  $k'$  are forward and reverse rate constants respectively, and  $p'$  is the partial pressure of the gas or vapour being adsorbed.

Solving for  $\{\}$  and dividing by the area occupied by one molecule give the number of molecules adsorbed per unit total surface from which the number of molecules of the adsorbate per unit mass of

the solid at equilibrium can be worked out to be

$$X^* = X_{\max} \frac{bp'}{1 + bp'} \quad (14.2)$$

where

$X^*$  = amount of gas adsorbed at equilibrium per unit mass of the adsorbent at a partial pressure of  $p'$

$X_{\max}$  = maximum quantity of gas absorbed per unit mass of the adsorbent

$b = k/k'$ , Langmuir equilibrium constant.

This equation gives a relationship between the concentration of a solute adsorbing to the adsorbent and the fractional occupancy of the adsorbed sites.

At low pressure of the adsorbate ( $bp' \ll 1$ )

$$X^* = X_{\max} bp' = K_H p' \quad (14.3)$$

Equation (14.3) represents Henry's law,  $K_H$  being the Henry's constant. Langmuir isotherm was derived on the basis of the following assumptions:

- Adsorption is limited to the formation of monomolecular layer only.
- The energy of adsorption is the same over the entire surface.
- Gas or vapour molecules are adsorbed at fixed sites and do not migrate to other surface.
- There is no interaction between adjacent molecules on the surface.

### 14.3.2 Freundlich Isotherm

Freundlich Isotherm (1926) for gases or vapours assumes that at equilibrium the amount of solute adsorbed by an adsorbent is a power function of the partial pressure or concentration of the solute in the gas or vapour.

$$X^* = K(p')^{1/n} \quad (14.4)$$

where  $K$  and  $n$  are two constants.

The value of  $n$  usually lies between 1 and 5. For  $n = 1$ , Eq. (14.4) assumes the form of Henry's Law relation. A log-log plot of  $X^*$  against  $p'$  yields a straight line with slope  $(1/n)$  and intercept  $\log K$ . Although Freundlich Isotherm was initially derived as an empirical relation, it was found at a later stage that it has some thermodynamic foundation (Glueckauf 1947).

In spite of being an empirical expression, Freundlich Isotherm fits experimental data fairly well for many systems and is widely used. It is observed that the Langmuir relation predicts an asymptotic limit for  $X^*$  at high pressure, whereas the Freundlich relation does not.

Commercial applications of adsorption involve mixtures rather than pure gases. If only one component in the mixture is selectively adsorbed, the adsorption of that component is estimated from its pure gas adsorption as described earlier. However, if two or more components in the mixture are adsorbed during the adsorption process, the estimation becomes more complex and requires an extension of the Langmuir equation (Markham and Benton 1931). In this development, it was assumed that the only effect of the adsorption of one component from the mixture was a reduction in the available surface area for the adsorption of the other components. For a binary gas mixture in which components  $A$  and  $B$  are being adsorbed on the surface of an adsorbent, the equilibrium loading of each component is given by

$$X_A^* = \frac{(X_A)_{\max} b_A p'_A}{1 + b_A p'_A + b_B p'_B} \quad (14.5a)$$

$$X_B^* = \frac{(X_B)_{\max} b_B p'_B}{1 + b_A p'_A + b_B p'_B} \quad (14.5b)$$

where,  $(X_i)_{\max}$  is the maximum loading of component  $i$  when it covers the entire surface of the adsorbent. Equations (14.5a) and (14.5b) can be extended to a multi-component mixture with

$$X_i^* = \frac{(X_i)_{\max} b_i p'_i}{1 + \sum_j b_j p'_j} \quad (14.6)$$

Similarly, the Freundlich equation can be combined with the Langmuir equation to provide another relation for adsorption of components from gas mixtures, namely,

$$X_i^* = \frac{(X_i')_{\max} b_i (p'_i)^{1/n_i}}{1 + \sum_j b_j (p'_j)^{1/n_i}} \quad (14.7)$$

where,  $(X_i')_{\max}$  is the maximum loading that may differ from the  $(X_i)_{\max}$  value obtained for monolayer adsorption. Even though Eqs. (14.6) and (14.7) lack thermodynamic consistency, their simplicity along with relatively reasonable results encourage their continued use. However, improved results were obtained using the procedures outlined by Yang (1987).

Freundlich also suggested an equation for adsorption of solute from dilute solutions. When a dilute solution is in contact with a solid adsorbent, adsorption of both solute and solvent may take place. In such cases, it is almost impossible to measure the amount of solute adsorbed since there may not be any change in the volume of the liquid, and increase in weight of the adsorbent will be due to both adsorption and mechanical occlusion. As a result, the relative or apparent adsorption is measured in the following way. A definite volume of the solution is added to and thoroughly mixed with a known weight of the adsorbent. Due to preferential adsorption of the solute by the solid, the solute concentration in the solution decreases from its initial value of  $c_0$  to the final equilibrium value of  $c^*$ . Neglecting any volume change of the solution the apparent adsorption of the solute may be represented by  $[v(c_0 - c^*)]$ , mass of solute adsorbed per unit mass of adsorbent,

where,

$v$  = volume of solution added/mass of adsorbent

$c_0$  = initial solute concentration in the liquid

$c^*$  final equilibrium solute concentration in the liquid

The apparent adsorption of a solute depends upon the type of the adsorbent, the solvent, the concentration of the solute and the temperature.

For dilute solutions over a small concentration range, the adsorption isotherm can be represented by

Freundlich equation

$$X^* = k[v(c_0 - c^*)]^n \quad (14.8)$$

where,  $[v(c_0 - c^*)]$  is the apparent adsorption, and  $k$  and  $n$  are constants.

Other concentration units are often used in Eq. (14.8) when different values of  $k$  will be obtained. However for dilute solutions for which the equation is applicable, the value of  $n$  remains unchanged. Plotting the equilibrium solute concentration as ordinate against adsorbate content in the solid as abscissa on logarithmic coordinates will result in a straight line of slope  $n$  and intercept  $k$ .

Liquid phase adsorption has been shown to be an effective way for removing suspended solids, odours, organic matter and oil from aqueous solutions, and appears to offer the best prospect over all the other treatments (Nigam et al. 1996) as the process is inexpensive, simply designed, easy to handle, and provide sludge free cleaning operations. Freundlich isotherm is particularly useful in cases where the actual identity of the solute is not known as in the removal of coloured substances from mineral and vegetable oils or from sugar solutions.

#### 14.3.3 Braunauer-Emmet-Teller Isotherm

The Braunauer-Emmet-Teller (BET) Isotherm (Braunauer et al. 1938) developed over Langmuir expression, is applicable to many systems particularly to systems where multimolecular layers are formed. The BET isotherm has been expressed as

$$X^* = X_{\max} \frac{CK}{(1 - K)[1 + (C - 1)K]} \quad (14.9)$$

where

$X^*$  = quantity of gas or vapour adsorbed, g/g of adsorbent

$X_{\max}$  = quantity of gas or vapour to be adsorbed to form a monomolecular layer on the adsorbent surface, g/g of adsorbent

$K = (p'/p)$ ,  $p'$  being the partial pressure and  $p$  the vapour pressure of adsorbate

$C$  = a temperature dependent constant for a particular gas-solid system.

Equation (14.9) is based on the following assumptions:

- (i) The heat of adsorption remains constant till the formation of monomolecular layer on the adsorbent surface is complete, and
- (ii) The heat of adsorption for the subsequent layer is equal to the heat of liquefaction of the adsorbate.

Despite these limitations, the BET equation is very useful because it enables the numerical determination of surface area. Knowing the area occupied by a single molecule of adsorbent and the number of molecules needed to form a monolayer, it is possible to express the surface area of the adsorbent in  $\text{m}^2/\text{g}$ .

Several other adsorption isotherms like the Toth isotherm, Sips isotherm, UNILAN isotherm have been proposed by different workers (Ismadji and Bhatia 2000; Knaebel 1995).

In most of the gas-solid adsorption systems, the heat of adsorption is greater than the heat of evaporation or condensation of the same substance. This means that the entropy of the molecules when adsorbed on a particular surface will be greater than the entropy of the same molecules in their liquid

or solid state. In the gas-phase adsorption, as the van der Waals forces between different molecules are approximately the geometric mean between the values for each of the two molecules when combined with a molecule of its own kind, it is evident that the van der Waals forces hold it in liquid form. There are some exceptions to the fact that the heat of adsorption is higher than the heat of liquefaction. For instance, when water is adsorbed on activated carbon, the polar character of the water molecule causes only weak bonds. In this case, the heat of adsorption is indeed smaller than the heat of liquefaction. Adsorption nevertheless takes place because the influence of the entropy difference is dominating. The fact that the entropy in the adsorbed state is higher than that in a liquid state indicates that the adsorbed molecules have greater degree of freedom than the molecules in the liquid state.

## 14.4 Heat of Adsorption

The adsorption of gases or vapour by solids is always accompanied by liberation of heat known as *heat of adsorption*.

The heat of adsorption may be of the following three types:

- (i) differential heat of adsorption
- (ii) integral heat of adsorption
- (iii) isosteric heat of adsorption.

The *differential heat of adsorption* is the heat liberated at constant temperature when unit amount of gas or vapour is adsorbed by a large amount of solid already having some adsorbate. The quantity of adsorbent being very large, the adsorbate concentration remains unchanged.

The *integral heat of adsorption* at any concentration of the adsorbate in the adsorbent is defined as the enthalpy of the adsorbate-adsorbent combination minus the sum of enthalpies of unit mass of pure adsorbent and sufficient amount of pure adsorbate required to provide the same concentration, all at the same temperature.

The *isosteric heat of adsorption* at a given temperature, pressure and adsorbate concentration is given by

$$(\Delta H)_{\text{ISO}} = -RT^2 \frac{\frac{d \ln p'}{dT}}{d(1/T)} = R \frac{d \ln p'}{dT} \quad (14.10)$$

where,

$\Delta H$  = enthalpy change

$T$  = absolute temperature, K

$p'$  = partial pressure of the adsorbate, kN/m<sup>2</sup>

$R$  = gas constant, 1.987 cal/(gmol)(K)

## 14.5 Some Desirable Qualities of Adsorbents

The adsorption capacities of solids depend not only on their chemical nature but also on several other factors like physical structure, method of manufacture, pre-treatment, previous use, etc.

Adsorption being a surface phenomenon, large surface per unit volume is the most important criteria of an adsorbent. The effective surface of an adsorbent is not just the superficial area as estimated from the overall dimensions, but includes the surface provided by the large number of pores present

in the solid. For instance, a typical gas mask charcoal may have an effective surface of the order of  $1000\text{ m}^2/\text{g}$  (Gregg and Sing 1967).

The adsorbent must selectively combine with the component(s) to be adsorbed. The selectivity may be due to the difference in affinity or difference in the rate of diffusion between the target species and others. In some cases, selectivity may result from difference in size. The molecules larger in size than the pore size of the adsorbent are prevented from entering the pores of the adsorbent while smaller ones can do so.

The adsorbent should have a reasonably high capacity for adsorption so that adsorbent requirement is relatively small. The adsorption capacity depends on the affinity of adsorption and the specific surface area.

In case the adsorbed substance has to be recovered or the adsorbent has to be regenerated and reused, the adsorption must be reversible.

Particle size and its distribution, porosity and pore size distribution are also to be considered.

Adsorbents must have adequate mechanical strength and hardness so that they may be handled or loaded in beds without breakage. Their resistance to flow of gases or liquids should be as low as possible. In addition, they should be free flowing if they are to be transported frequently.

## 14.6 Some Common Adsorbents

### *Activated clays*

These are bentonite type of clays, activated by treatment with sulphuric or hydrochloric acid followed by washing, drying and grinding to fine powder. These are used for decolourizing petroleum products and are generally discarded after single use.

### *Fuller's earth*

These are naturally occurring clays, mainly magnesium aluminium silicates. The clays are dried and heated to develop a porous structure, ground and screened. Commercial sizes vary from coarse granules to fine powders. Fuller's earth is useful in refining petroleum fractions as well as vegetable and animal oils, fats and waxes, and may be reused after washing and burning.

### *Bone char*

Bone char is obtained by destructive distillation of crushed bones at temperatures between  $600^\circ$  and  $900^\circ\text{C}$ . It is mainly used for refining sugar solution and ash removal from solutions. It may be reused after washing and burning.

### *Decolourising carbon*

Decolourising carbon is manufactured by mixing lignin, lignite, peat, wood, saw dust, etc. with an alkali metal sulphate, carbonate or phosphate or zinc chloride and then calcining at  $500\text{-}900^\circ\text{C}$ . The calcined mass is then washed, filtered and dried. It is useful in decolourising sugar solutions, industrial chemicals and drugs, refining of vegetable and animal oils as well as in water purification.

### *Gas-adsorbent carbon*

These are made by carbonization at  $400\text{-}500^\circ\text{C}$  of coconut shells, fruit pits, coal, lignite and wood. These are then activated by treatment with hot air, steam or carbon dioxide at  $800\text{-}1000^\circ\text{C}$  in order to develop the micropores (pore diameter  $< 2\text{ nm}$ ; other types being mesopore when the diameter in the range  $2\text{-}50\text{ nm}$ , and macropore when diameter  $> 50\text{ nm}$ ). Activated carbon has considerable

hydrophobic character. The process of activation may be considered as slow dehydration and carbonization, usually effected by heating the raw material in the absence of air. The activation process selectively enlarges the pores of the carbon to provide high adsorptive capacity. The surface of activated carbon presents a largely homogeneous distribution of electrical charge. For this reason activated carbon does not show any preferential adsorption of polar molecules such as water, rather desorbs polar materials in favour of nonpolar or materials of higher molecular weight. Because there are many types and grades of activated carbon available commercially, it has become necessary to establish specifications to obtain the proper carbon.

Two types of activated carbon are normally available. Powdered activated carbon is available in the size range of 15-25  $\mu\text{m}$  with specific surface of 200 to above 1000  $\text{m}^2/\text{g}$ . Granular activated carbon on the other hand is available as 4 to 6 mm pellets for gas separation and 12 to 42 mesh pellets for liquid separation. These are used in the recovery of gasoline from natural gas, fractionation of hydrocarbons and in gas masks. These may be reused after removal of the adsorbed gas.

### **Molecular sieves**

Molecular sieves are synthetic zeolite crystals. These are crystalline alumino silicates of metals such as sodium, potassium, magnesium or calcium. Molecular sieves are produced from sodium aluminate, silicate and hydroxide, alumina trihydrate, colloidal silica and silicic acid. After completion of the reaction, gel formation is carried out under controlled conditions. The crystalline gel is then filtered, washed and ion-exchanged to replace sodium by other suitable cation as per requirement. Molecular sieves are of two types; type-*A* and type *X*. Type *A* consists of 3 varieties: type 3*A* has potassium cation, type 4*A* has sodium cation and type 5*A* has calcium cation. Their pore sizes are 3 $\text{\AA}$ , 4 $\text{\AA}$  and 5 $\text{\AA}$ , respectively. Type *X* molecular sieves have two varieties: 10*X* and 13*X* with pore size 8 $\text{\AA}$  and 10 $\text{\AA}$ , respectively. The porous structure of the molecular sieves, which can be controlled by the crystal composition, selectively entrap molecules up to certain size and thus effect separation according to molecular size. They are also capable of separating molecules according to polarity. Molecular sieves are available in the form of pellets, beads and powder with different pore diameter up to 1 #  $10^{-6}$  mm. These are useful in dehydration of gases and liquids, separation of both gaseous and liquid hydrocarbons, etc. These may be regenerated by heating. Molecular sieves have both adsorbing and catalytic properties. The activation of zeolites is a dehydration process accomplished by the application of heat under high vacuum. While the molecular sieve-zeolites are polar-hydrophilic and/or crystalline in nature, the carbon molecular sieve is exclusively hydrophobic in nature. Some zeolite crystals show behaviour opposite to that of activated carbon in that they selectively adsorb water in presence of nonpolar solvents. Zeolites can be made to have specific pore sizes that will increase their selective nature due to the size and orientation of the molecules to be adsorbed. Molecules above a specific size cannot enter the pores and are therefore not adsorbed.

### **Silica gels**

Silica gels are made from gel precipitated by sulphuric acid treatment of sodium silicate solution. They are porous, granular and hard. Silica gels are hydrophilic in nature. However, hydrophobic as well as amorphous nature of the gels are sometimes found. Two types of silica gels are available: Type *A* has pores in the range of 3-5 nm and specific surface of about 650  $\text{m}^2/\text{g}$ . Type *B*, on the other hand, has pores of about 7 nm and specific surface of about 450  $\text{m}^2/\text{g}$ . Silica gels are useful in

dehydration of gases, gas masks and fractionation of hydrocarbons. These may be reused by evaporation of adsorbed material(s).

### **Activated alumina**

Activated alumina,  $\text{Al}_2\text{O}_3$  which includes activated bauxite, is made by removing water from hydrated colloidal alumina. It has a moderately high specific surface area with a capacity for adsorption of water sufficient to dry gases to less than 1 ppm moisture content. Because of its high affinity for water, activated alumina is widely used for the removal of water from gases and liquids. In addition to these commonly used adsorbents, some other materials like coal, wood, agricultural wastes (bagasse pith, maize cob, coconut shell, rice husk, etc.) and cotton wastes have been tried with varying success for colour removal (Mckay et al. 1986, Annadurai et al. 2002).

An adsorbent is selected for a particular application on the basis of its characteristics, such as (i) chemical inertness in the application environment, (ii) favourable adsorption isotherm, (iii) highest separation factor for the desired component, (iv) mechanical stability, (v) hydrodynamic properties such as bulk density, porosity and bed voidage, and (vi) diffusivity. Moreover, an adsorbent is selected for a particular application on the basis of the following considerations:

- the nature of the adsorption isotherm,
- the electrochemical nature of the adsorbent surface and adsorbate, and
- the surface area, pore size distribution of the adsorbent and the diameter (sometimes called *kinetic diameter* derived from the flow properties like viscosity, diffusivity, etc.) of the adsorbate.

The pore size distribution of the adsorbent is more important than the surface area. This is the size and shape selectivity of adsorption which is effectively exploited by molecular sieves due to uniformity in their pore size, but is absent in other adsorbents like activated alumina, silica gel, and activated carbon. Typical physical properties of some of the adsorbents are given in Table 14.1.

**Table 14.1** Properties of some commercial adsorbents

Types of adsorbent	Pore diameter, nm	Particle density, kg/m <sup>3</sup>	Particle porosity	Surface area # $10^{-5}$ , m <sup>2</sup> /kg
Carbon, activated small pore	1-2.5	500-900	0.40 - 0.60	4-12
Carbon, activated large pore	> 3	600-800		2-6
Fuller's earth		480-640	0.50	1-2.5
Molecular sieve 3A	0.3	670-740	0.20	7
Molecular sieve 4A	0.4	660-720	0.30	7
Molecular sieve 5A	0.5	670-720	0.40	6.5
Molecular sieve 13X	0.8	610-710	0.50	6
Mordenite	0.3-0.4	720-800	0.25	7
Silica gel Small pore	2.2-2.6	1000	0.47	8
Silica gel Large pore	10-15	620	0.71	3.2
Activated alumina	1-7.5	800	0.50	3.2

**Table 14.2** Some typical applications of commercial adsorbents

<b>Silica gel</b>	Drying of gases, refrigerants, organic solvents, transformer oils, desiccant in packaging and double glazing, dew point control of natural gas.
<b>Activated alumina</b>	Drying of gases, organic solvents, transformer oils, removal of hydrochloric acid from hydrogen, removal of fluorine and boron-fluorine compounds in alkylation processes.
<b>Carbon</b>	Nitrogen from air, hydrogen from synthetic gas and hydrogenation processes, ethane from methane and hydrogen, vinyl chloride monomer (VCM) from air, removal of odours from gases, recovery of solvent vapours, removal of sulphur dioxide and nitrogen dioxide, purification of helium, cleaning of nuclear off-gases, decolourising of syrups, sugars and molasses; water purification including removal of phenol, halogenated compounds, pesticides, caprolactam, chlorine.
<b>Zeolites</b>	Oxygen from air, drying of gases, removing water from azeotropes, sweetening sour gases and liquids, purifications of hydrogen, separation of ammonia and hydrogen, recovery of carbon dioxide, separation of oxygen and argon, removal of acetylene, propane and butane from air, separation of xylene and ethyl benzene, separation of normal from branched paraffins, separation of olefins and aromatics from paraffins, recovery of carbon monoxide from methane and hydrogen, purification of nuclear off-gases, separation of cresols, drying of refrigerants and organic liquids, separation of solvent systems, purification of silanes, pollution control including removal of Hg, NO <sub>2</sub> and SO <sub>2</sub> from gases, recovery of fructose from corn syrup.
<b>Polymers and Resins</b>	Water purification including removal of phenol, chlorophenol, indene, alcohols, aromatics, aniline, ketones, polynuclear aromatics, nitro and chloro-aromatics, PCB, pesticides, antibiotics, detergents, emulsifiers, wetting agents, kraft mill effluents, dyestuffs; recovery and purification of steroids, amino-acids and polypeptides; separation of fatty acids from water and toluene, separation of aromatics from aliphatics, separation of hydro-quinone from monomers, recovery of proteins from enzymes; removal of colours from syrups, removal of organics from hydrogen peroxide.
<b>Clays (acid treated and pillared)</b>	Treatment of edible oils, removal of organic pigments, refining of mineral oils, removal of polychlorobiphenyl (PCB).

## 14.7 Adsorption Operations

Adsorption operations may be carried out in the following ways:

- Single stage
- Multistage cross-current
- Multistage counter-current
- Continuous counter-current: Moving bed—steady state, Fixed bed—unsteady state

### 14.7.1 Single Stage Operation

A schematic flow diagram for single stage adsorption is shown in Figure 14.4. The operation may be both batch type or continuous. In Figure 14.4, the rectangle represents a stage which

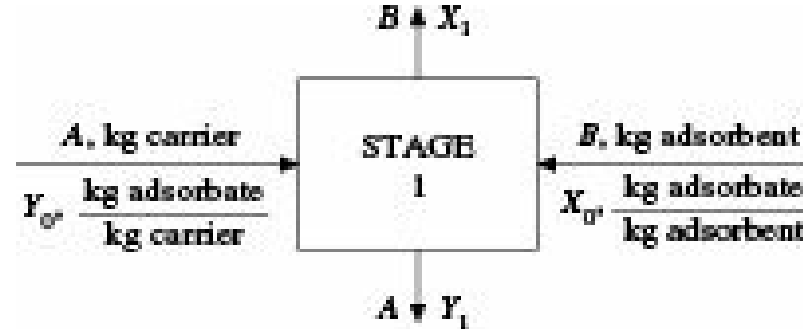


Figure 14.4 Flow diagram of single stage adsorption.

consists of thorough mixing of the fluid and the adsorbent, allowing them to settle and finally separating them. The operation is analogous to single stage gas absorption. Assuming that the carrier fluid is not adsorbed, the adsorbent is not soluble in the solution and no liquid is associated with the

solid, the material balance for the solute may be written as

$$A(Y_0 - Y_1) = B(X_1 - X_0) \quad (14.11)$$

where

$A$  = mass of the carrier fluid (solvent) unadsorbed by the solid

$B$  = mass of pure adsorbent

$Y$  = concentration of solute in fluid, mass per unit mass of  $A$

$X$  = concentration of adsorbate in adsorbent, mass per unit mass of  $B$

For continuous operations,  $A$  and  $B$  are expressed in mass per unit time.

Equation (14.11) is an equation to a straight line on  $X$ - $Y$  co-ordinates passing through the points  $(X_0, Y_0)$  and  $(X_1, Y_1)$  and having a slope  $(-B/A)$ .

The operation is represented graphically in Figure 14.5.  $OA$  is the equilibrium curve and  $BC$  the operating line as per Eq. (14.11). If the stage is a theoretical stage, the operating line will terminate at  $C$  on the equilibrium curve so that  $X_1$  and  $Y_1$  are equilibrium values. If the time is not adequate for equilibrium to attain, the operating line will terminate somewhere before reaching the equilibrium curve, say at  $C'$ .

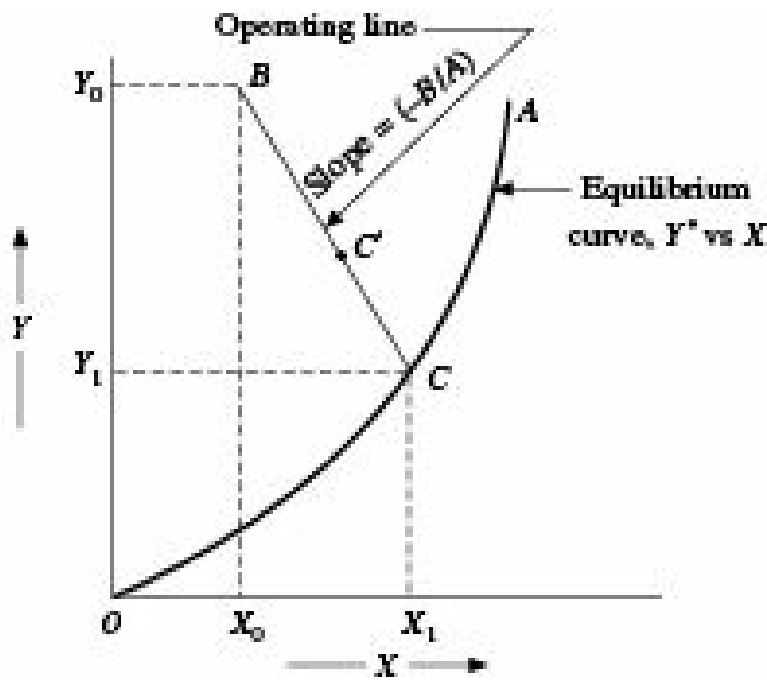


Figure 14.5 Graphical representation of single stage adsorption..

**EXAMPLE 14.1** (Adsorbent requirement for single-stage adsorption): The following equilibrium relationship was obtained during treatment of an aqueous solution of a valuable solute by decolourising carbon for removal of colouring impurities:

$$Y^* = 8.91 \times 10^{-5} X^{1.66}$$

where

$X$  = adsorbate concentration per kilogram of carbon, and

$Y^*$  = equilibrium colour units per kilogram of solution measured on an arbitrary scale proportional to the concentration of the coloured impurity

It is proposed to reduce the colour of the solution to 20% of its original value of 9.0. Determine the quantity of fresh carbon required per 100 kg of the solution for a single stage operation.

**Solution:** From the given equilibrium relation, the following values of  $X$  and  $Y^*$  are determined:

$X$ :	100	200	300	400	600	800	1000
$Y^*$ :	0.18	0.59	1.15	1.86	3.64	5.87	8.51

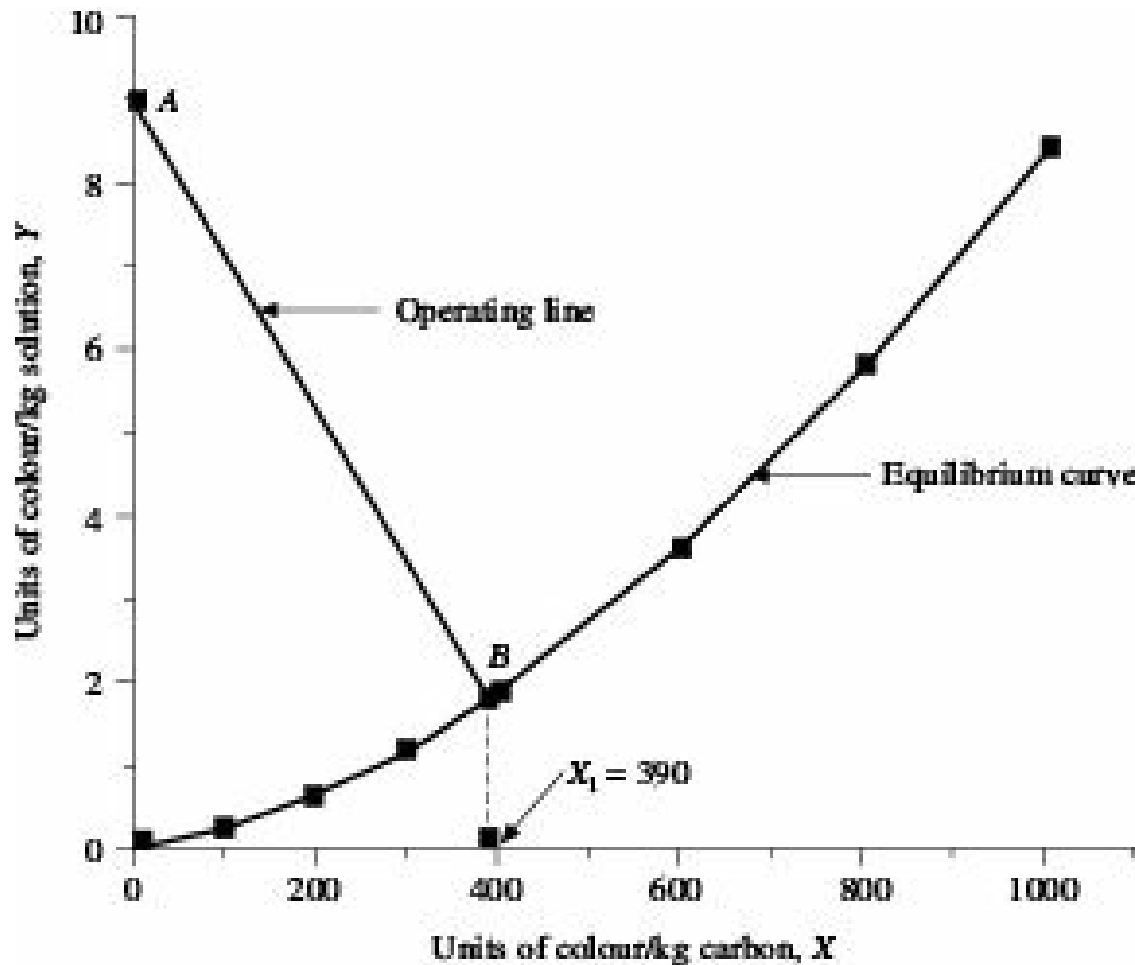


Figure 14.6 Solution to Example 14.1.

The equilibrium curve is plotted in Figure 14.6 from the given data.

$$Y_0 = 9.0 \text{ units of colour per kg solution}$$

$$Y_1 = (0.20)(9) = 1.8 \text{ units of colour per kg solution}$$

$$X_0 = 0.$$

Point  $A$  representing the initial solution ( $Y_0 = 9.0$ ) and fresh adsorbent ( $X_0 = 0$ ) is located. Point  $B$  is then located on the equilibrium curve corresponding to

$$Y_1 = 1.8 \text{ at } B, X_1 = 390.$$

Therefore from Eq. (14.11)

$$B/A = \frac{Y_0 - Y_1}{X_1 - X_0} = \frac{9.0 - 1.8}{390 - 0} = 0.0185 \text{ kg carbon/kg solution}$$

Therefore, carbon required per 100 kg solution =  $0.0185 \times 100 = 1.85 \text{ kg}$ .

In case of desorption, appreciable amount of liquid may be mechanically carried away by the solid and the method of calculation for single stage leaching should be followed. As we are considering only dilute solutions, Freundlich equation is applicable and analytical solution can be developed as

shown below. For the concentration unit being followed here, Freundlich equation may be written as

$$Y^*_1 = kX_1^n \quad (14.12)$$

where,  $X_1$  and  $Y^*_1$  are equilibrium solute concentrations in solid and liquid, respectively. Equation (14.12) may be rearranged as

$$X_1 = \left(\frac{Y^*_1}{k}\right)^{1/n} \quad (14.13)$$

Substituting the value of  $X_1$  from Eq. (14.13) in Eq. (14.11) and noting that usually  $X_0 = 0$ ,

$$\frac{B}{A} = \frac{Y_0 - Y_1}{(Y^*_1/k)^{1/n}} \quad (14.14)$$

The adsorbent to solution ratio for a specified change in solution concentration ( $Y_0 - Y_1$ ) can be directly estimated from Eq. (14.14).

**EXAMPLE 14.2** (Adsorbent requirement by Freundlich equation): A sample of water contains organic colour which has to be extracted with alum and lime, 5 parts of alum and lime per million parts of water will reduce the colour to 25% of its original value and 10 parts will reduce the colour to 3.5%.

Estimate how much alum and lime as parts per million are required to reduce the colour to 0.5% of the original value.

**Solution:** In order to plot the equilibrium data in a suitable form,  $Y$  is defined as units of colour per million parts of solution and  $X$  as units of colour adsorbed per part of alum and lime. The initial colour is assumed to be 1. The calculations are made as under:

Parts, alum and lime per million parts water			$Y^*$ = equilibrium colour units per million parts water	$X$ = adsorbate conc. per part alum and lime
0	1.00			—
5	0.25			$(1 - 0.25)/5 = 0.15$
10	0.035			$(1 - 0.035)/10 = 0.0965$

Values of  $X$  and  $Y^*$  are plotted on logarithmic co-ordinates in Figure 14.7, and a straight line is obtained, so that Freundlich equation is applicable. The value of the slope of the line is  $4.2 = n$ .

At  $X = 0.15$ ,  $Y^* = 0.25$ ,

$$\text{Therefore, } k = \frac{0.25}{(0.15)^{4.2}} = 0.722 \times 10^3 \text{ (using Eq. 14.12)}$$

The Freundlich equation is therefore,

$$Y^* = 0.722 \times 10^3 X^{4.2}$$

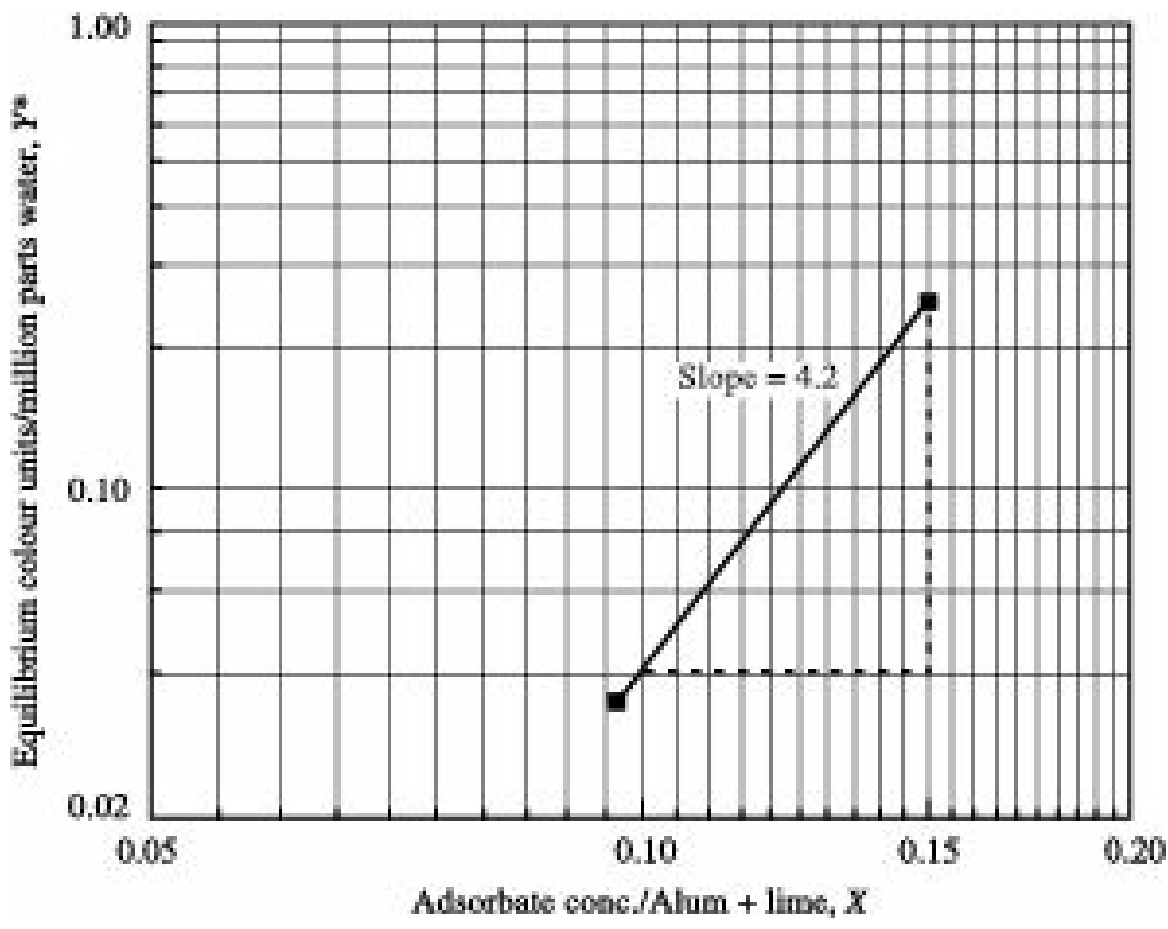


Figure 14.7 Solution to Example 14.2.

Since Freundlich equation applies, from Eq. (14.14), we get

$$\frac{B}{A} = \frac{Y_0 - Y_1}{(Y_1^* / k)^{1/n}}$$

Since  $Y_0 = 1$ ,  $Y_1 = Y_1^* = 0.005$ , defining  $A$  as million parts of water and  $B$  as parts of alum and lime.

$$\left(\frac{B}{A}\right) = \frac{1.0 - 0.005}{\left(\frac{0.005 \times 10^{-3}}{0.722}\right)^{1/(4.2)}} = 16.84$$

16.84 parts of alum and lime will be required to reduce the colour to 0.5% of the original value.

### 14.7.2 Multistage Cross-current Operation

Greater economy of adsorbent may be achieved for removal of a given amount of solute, if the solution is treated with small batches of adsorbent in multiple stage units with filtration in between stages instead of a single stage using the entire adsorbent in one lot. This is generally practised in batch fashion and the number of stages is usually limited to two in order to avoid high handling and filtration costs.

A flow diagram for two stage cross-current adsorption is shown in Figure 14.8.

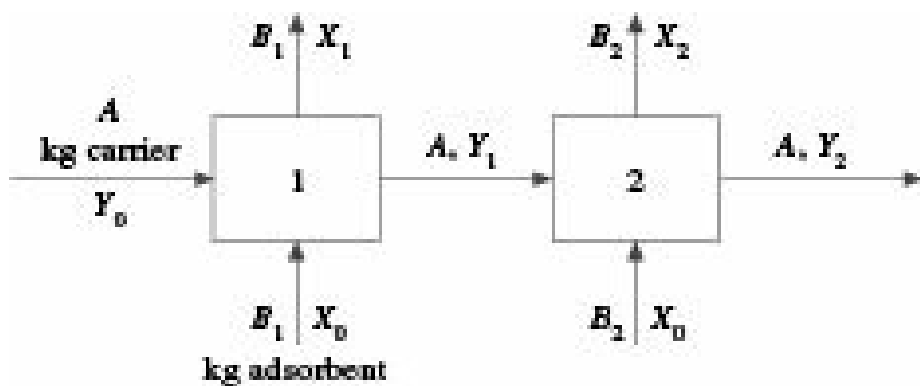


Figure 14.8 Two-stage cross-current adsorption.

Material balance for the two stages can be written as:

For 1st stage:

$$A(Y_0 - Y_1) = B(X_1 - X_0) \quad (14.15)$$

and for 2nd stage:

$$A(Y_1 - Y_2) = B(X_2 - X_0) \quad (14.16)$$

Equations (14.15) and (14.16) are equations to the operating lines for stages 1 and 2 respectively as shown in Figure 14.9.

If equal amount of adsorbent is added in each stage, the operating lines will be parallel to each other.

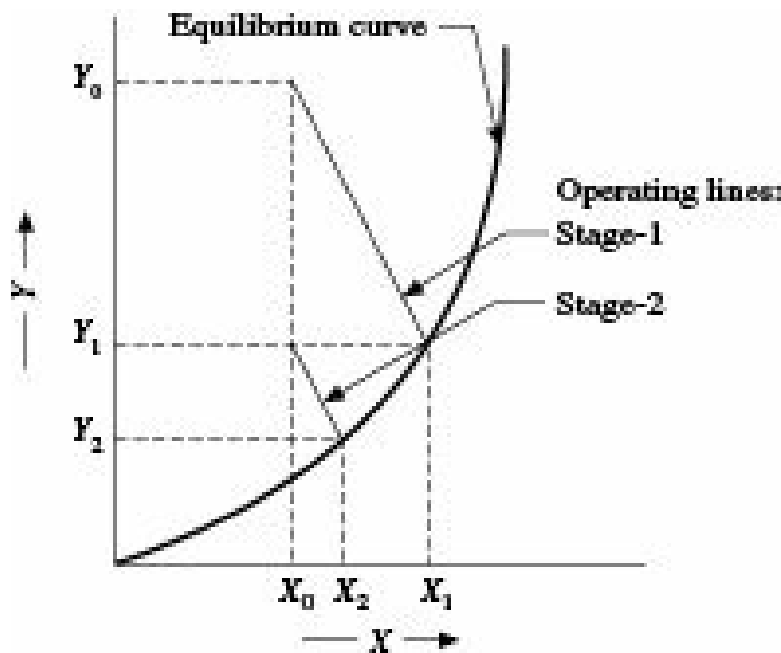
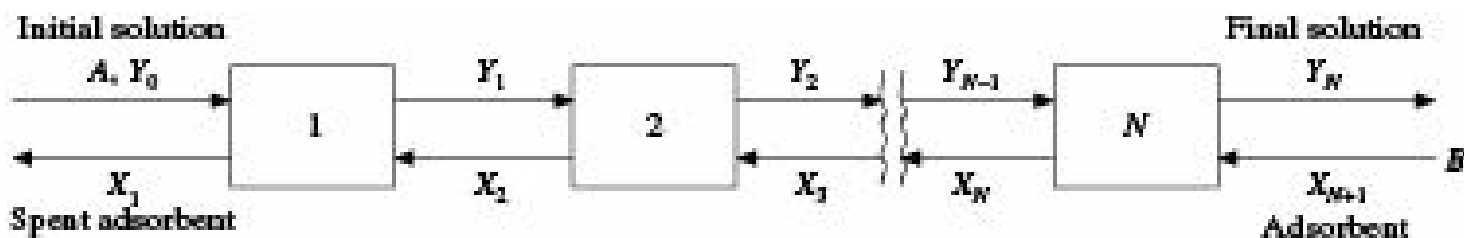


Figure 14.9 Graphical representation of 2-stage cross-current adsorption.

The least amount of adsorbent required for such an operation can be estimated from trial-and-error calculations. If, however, the adsorption equilibrium is satisfactorily represented by Freundlich equation, then the least amount of total adsorbent for two-stage cross-current adsorption can be directly determined.

### 14.7.3 Multistage Counter-Current Operation

Maximum economy of adsorbent can be achieved by counter-current operation. Figure 14.10 shows schematic flow diagram of multistage counter-current adsorption when steady-state has attained after a number of operations.



**Figure 14.10** Multistage counter-current adsorption.

A solute balance about  $N$ -stages gives

$$A(Y_0 - Y_N) = B(X_1 - X_{N+1}) \quad (14.17)$$

Equation (14.17), passing through the points  $(X_1, Y_0)$  and  $(X_{N+1}, Y_N)$  and having a slope of  $B/A$ , is the operating line ( $AB$ ) for the adsorption as shown in Figure 14.11.

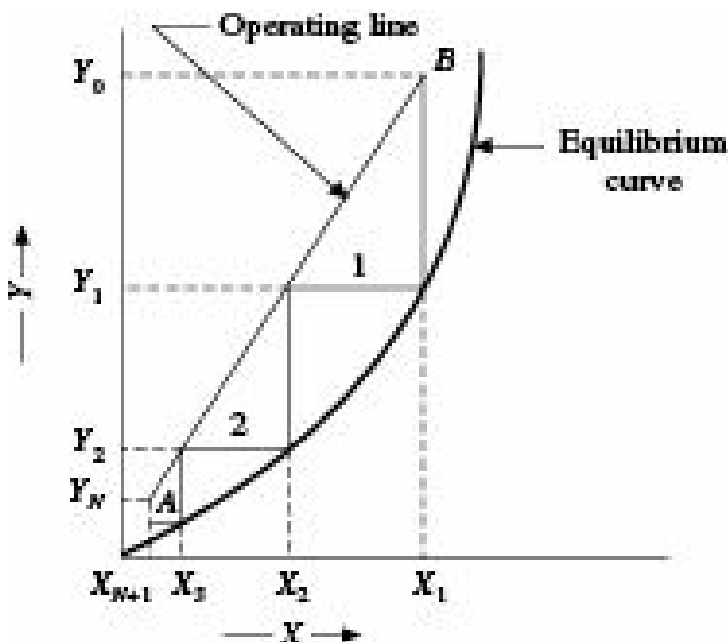


**Figure 14.11** Graphical representation of multi-stage counter-current adsorption.

The number of stages can be determined by drawing steps between the equilibrium curve and the operating line. The adsorbent to solution ratio for a given number of stages can be found by trial and error location of the operating line.

The minimum adsorbent to solution ratio can also be estimated from the largest slope of the operating line for which it touches the equilibrium curve at  $Y = Y_0$  if the equilibrium curve is straight or concave upwards or when it becomes tangent to the equilibrium curve for  $Y < Y_0$ , if the equilibrium curve is concave downwards.

Trial-and-error calculations for the adsorbent/solvent ratio can be avoided if the equilibrium relation can be satisfactorily represented by an algebraic equation. If the equilibrium relation is linear, equations similar to Kremser equation may be used for direct determination of adsorbent/solvent ratio in which case also trial-and-error method may be avoided. However, Freundlich equation is generally useful.

**EXAMPLE 14.3** (Adsorbent requirement for two-stage counter-current adsorption): An aqueous solution of a valuable solute has to be decolourised by treatment with decolourising carbon in a two-stage counter-current adsorption unit.

It is proposed to reduce the colour of the solution to 20% of its original value of 9.0.

The equilibrium relationship of Example 14.1 is applicable and the values of  $X$  and  $Y^*$  are:

$X:$	100	200	300	400	600	800	1000
$Y^*:$	0.186	0.59	1.15	1.86	3.64	5.87	8.51

where

$X$  = adsorbate concentration per kg of carbon, and

$Y^*$  = equilibrium colour units per kg of solution measured on an arbitrary scale proportional to the concentration of the coloured impurity.

Estimate the amount of adsorbent (carbon) required for treating 100 kg aqueous solution.

**Solution:** The equilibrium curve is plotted on  $X$ - $Y$  co-ordinates in Figure 14.12 .

According to the problem, operation has been carried out in 2-stages.

$$Y_0 = 9.0 \text{ units of colour per kg solution}$$

$$Y_2 = (0.20)(9) = 1.80 \text{ units of colour per kg solution}$$

$$X_3 = 0. \text{ (Since the absorbent does not contain any colour)}$$

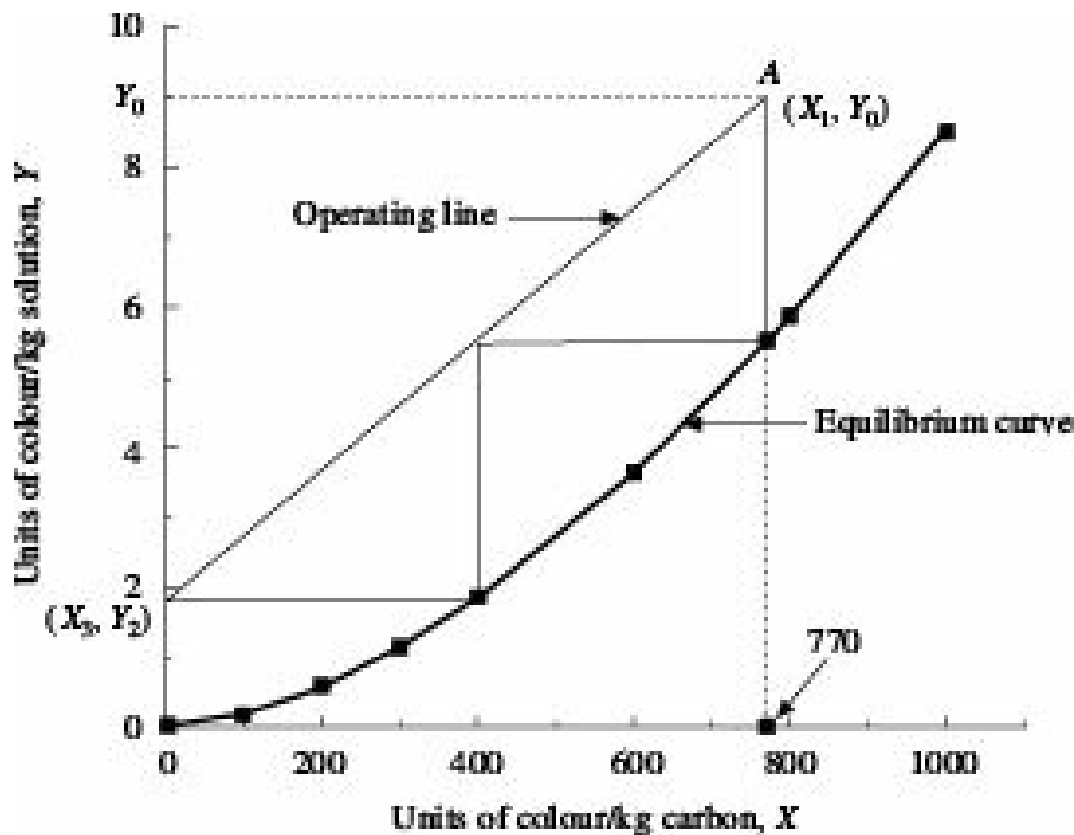


Figure 14.12 Solution to Example 14.3.

For two-stage counter-current operation, the operating line is located by trial so that two stages can be drawn between the operating line and the equilibrium curve within the limits  $Y_0$  and  $Y_2$ .

From the Figure:  $X_1 = 770$

$$\text{Therefore, } (B/A) = \frac{9.0 - 1.80}{770 - 0} = 0.00935 \text{ kg carbon/kg solution.}$$

$$\begin{aligned} \text{Carbon required per 100 kg solution} &= 0.00935 \times 100 \\ &= 0.935 \text{ kg} \end{aligned}$$

**EXAMPLE 14.4** (Theoretical stages for multistage counter-current adsorption): 500 kg/min of dry air at 20°C, carrying 5 kg water vapour per minute are to be dehumidified with silica gel to 0.001 kilogram water per kilogram of dry air. The operation has to be conducted isothermally and counter-currently with 25 kilogram per minute of silica gel.

How many theoretical stages will be required and what will be the water content of the silica gel leaving the bottom stage?

Equilibrium data at 20°C are as follows:

kg water/kg dry silica gel:	0	0.05	0.10	0.15	0.20
kg water/kg dry air:	0	0.0018	0.0036	0.0050	0.0062

**Solution:** 500 kg dry air contains 5 kg water vapour,

$$Y_0 = 5/500 = 0.01 \text{ kg water/kg dry air, and}$$

$$Y_N = 0.001 \text{ kg water/kg dry air}$$

*Overall Material Balance:*

$$A(Y_0 - Y_N) = B(X_1 - X_{N+1}) \quad [\text{Eq. (14.17)}]$$

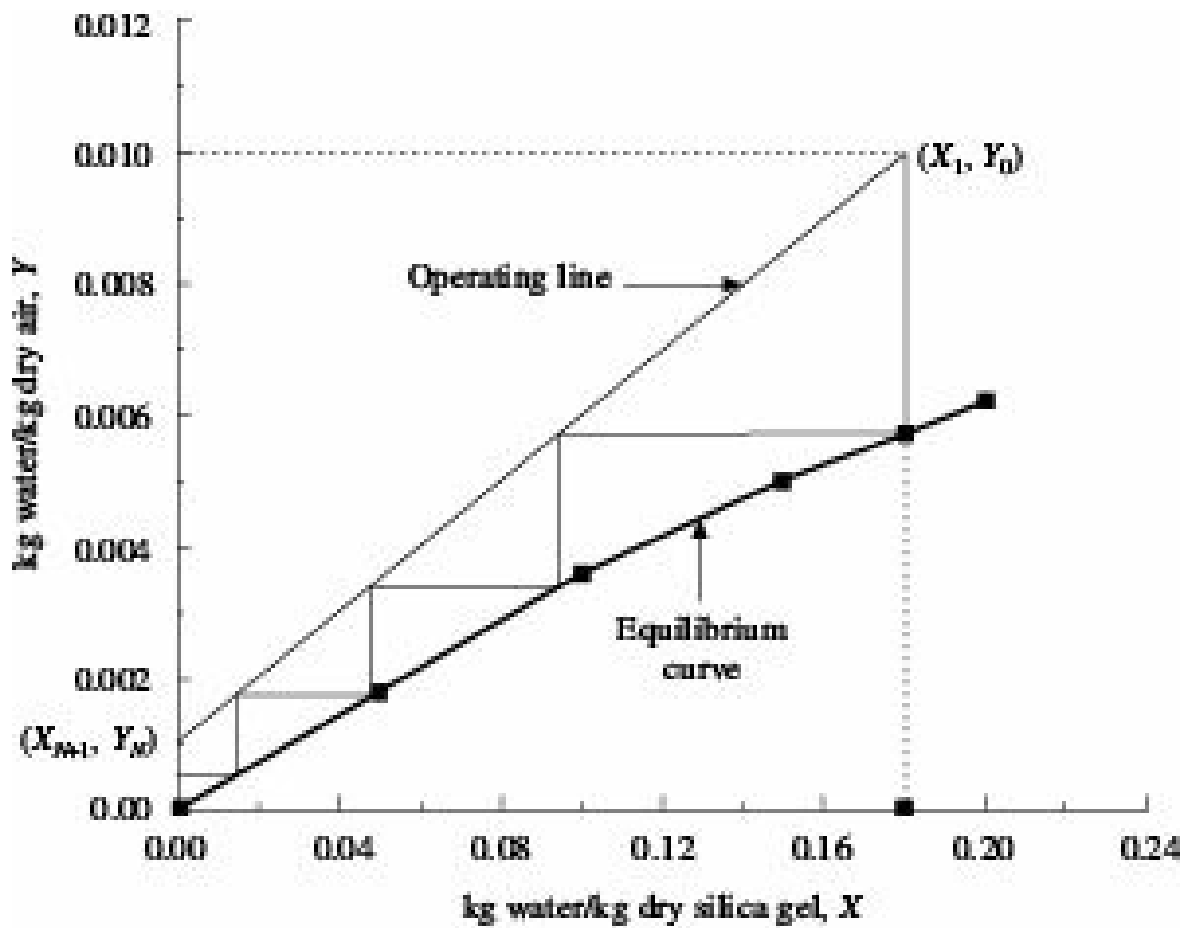


Figure 14.13 Solution to Example 14.4.

Assuming the initial silica gel contains no water,  $X_{N+1} = 0$

$$500(0.01 - 0.001) = 25(X_1 - 0)$$

whence,  $X_1 = 0.18 \text{ kg water/kg dry silica gel.}$

The equilibrium curve is drawn on  $Y$ - $X$  coordinates from the given data as shown in Figure 14.13. The operating line is located by joining the points  $(0, 0.001)$  and  $(0.18, 0.01)$  and then steps are

drawn between the equilibrium and operating lines.

From Figure 14.13, number of stages required = 3.7. Water content of the silica gel leaving the bottom stage

$$= B(X_1 - X_{N+1}) = 25(0.18 - 0) \\ = 4.5 \text{ kg}$$

#### 14.7.4 Continuous Counter-Current Differential Contact Operation

In view of the difficulty and cost involved in continuous steady state movement of solids through equipment, continuous counter-current operation has very limited application in adsorption.

Figure 14.14 depicts a flow diagram showing true continuous counter-current adsorption where only one component is adsorbed. The operation is analogous to gas absorption with the solid adsorbent replacing the liquid solvent. The adsorbent is introduced at the top and moves downwards while the fluid flows from the bottom.

The overall material balance may be written as

$$A(Y_1 - Y_2) = B(X_1 - X_2) \quad (14.18)$$

and for any section above the bottom of the tower,

$$A(Y - Y_2) = B(X - X_2) \quad (14.19)$$

Equations (14.18) and (14.19) are operating lines for adsorption, passing through the points  $(X_1, Y_1)$ ,  $(X_2, Y_2)$  and  $(X_2, Y_2)$ ,  $(X, Y)$ , respectively having a slope of  $B/A$ . This is shown in Figure 14.15 along with the appropriate equilibrium curve for the system at the operating temperature and pressure.

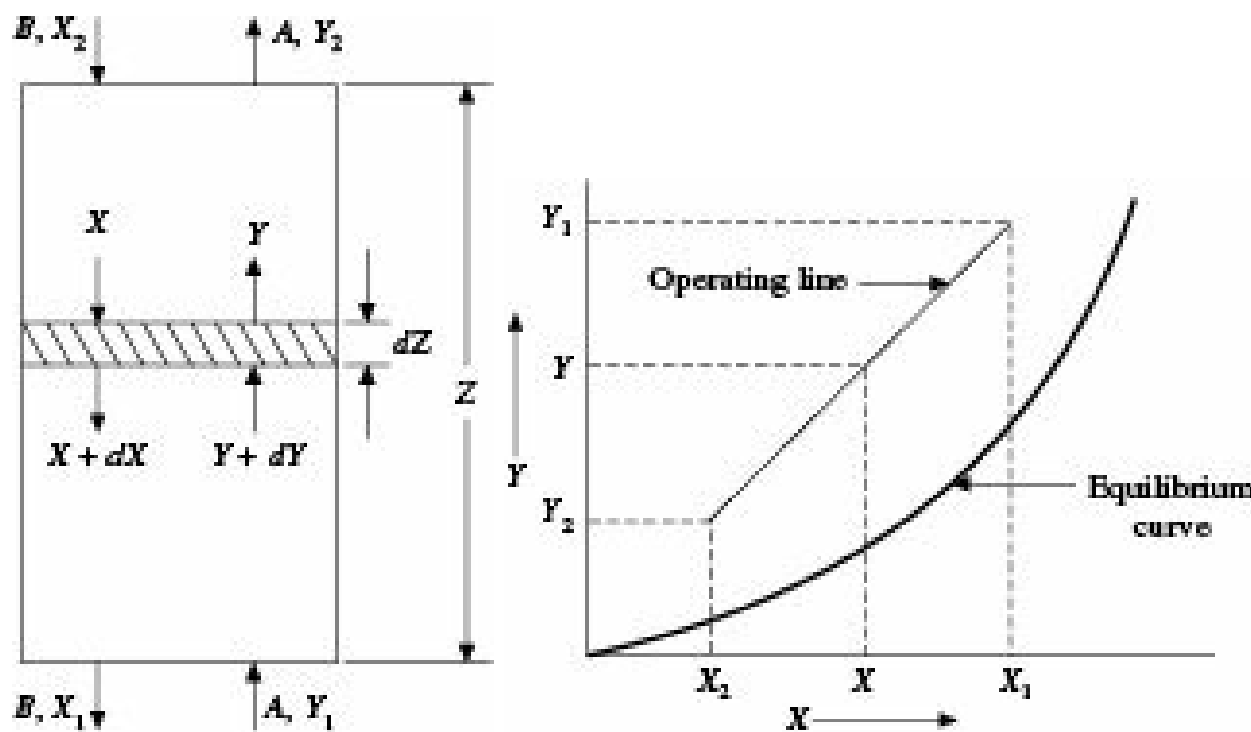


**Figure 14.14** Flow diagram of continuous counter-current differential adsorption.

The rate of solute transfer over a differential height  $dZ$  of the tower is

$$BdX = AdY = K_y a(Y^* - Y)dZ \quad (14.20)$$

where  $K_y$  is the effective overall mass transfer coefficient based on the outside surface of the adsorbent and  $(Y - Y^*)$  is the driving force.

Rearranging Eq. (14.20) and integrating between limits, we have

$$\int_{Y_2}^{Y_1} \frac{dY}{Y - Y^*} = N_{t0}G = \frac{K_y a}{A} \int_0^Z dZ = \frac{K_y a}{A} Z \quad (14.21)$$

whence,  $Z = \frac{A}{K_y a} N_{t0}G = H_{t0}G \# N_{t0}G \quad (14.22)$

where,  $H_{t0}G = \frac{A}{K_y a} \quad (14.23)$

The number of transfer units may be estimated through graphical integration by plotting  $[1/(Y - Y^*)]$  as ordinate against  $Y$  and determining the area under the curve within the limits  $Y_1$  and  $Y_2$ . The height of the tower may then be estimated from knowledge of the height of a transfer unit  $H_{t0}G$  for the system.

#### 14.7.5 Pressure Swing Adsorption

Pressure swing adsorption (PSA) is a novel method of adsorption. It is based on the principle that the adsorbing capacity of an adsorbent increases with increase in the solute pressure. In a pressure swing adsorption system, adsorption is carried out at an elevated pressure. The flow of the gas is stopped as the breakthrough point is reached and the adsorbent is regenerated by reducing the pressure. Sometimes, a hot inert gas is blown through the solid bed to carry away the desorbed solute molecules. Hot air or steam are frequently used for the purpose.

A high dynamic adsorption capacity can be achieved in PSA by reducing the pressure to near vacuum and the PSA system is sometimes modified by putting a vacuum pump in the blow down line. This is called *vacuum swing adsorption* (VSA) or Vacuum pressure swing adsorption (VPSA). Sometimes in a single bed system, the adsorber may be rapidly pressurized and depressurized. It is called *rapid pressure swing adsorption* (RPSA).

The progressive development of the PSA technology over the years has promoted adsorption to become a powerful and versatile tool for separation of bulk gas mixture in the chemical and allied industries (Sircar 2002). Some of the key industrial applications are as follows:

- (i) Gas drying
- (ii) Solvent vapour recovery
- (iii) Fractionation of air to produce oxygen and nitrogen enriched gases
- (iv) Production of hydrogen from steam-methane reformer (SMR) off-gas and petroleum refinery off-gases
- (v) Separation of methane and carbon dioxide from landfill gas
- (vi) Separation of carbon monoxide and hydrogen
- (vii) Normal isoparaffin separation
- (viii) Alcohol dehydration

In fact, PSA has become the state-of-art separation technology for some of the application areas, may

be due to the following reasons (Sircar 2000, 2001):

- (i) An extra degree of thermodynamic freedom for describing the adsorption process introduces immense flexibility in the process design as compared with the other conventional separation processes such as distillation, extraction, absorption, etc.
- (ii) Numerous micro-meso porous families of adsorbents exhibiting different adsorptive properties for separation of gas mixtures are available.
- (iii) The adsorbate is recovered in a relatively concentrated form, and the energy cost is low since no heating is involved.
- (iv) The optimum combination between a material and a process in designing PSA separation scheme promotes innovation.
- (v) Different PSA process cycles.

The RPSA processes are designed to increase the productivity (volume of product/volume of adsorbent/cycle) of separation devices by an order of magnitude or more by using total process cycle times of seconds instead of minutes as in the case of a conventional PSA cycles. It is achieved by simply running a conventional cycle faster using novel hardware or by changing both the adsorber and the process cycle designs. However, separation efficiency and performance may be compromised (lower product purity or recovery) due to time limitations in incorporating the complimentary cyclic steps and limitations caused by adsorption kinetics (Sircar and Hanley 1995). The example of the first type is the hydrogen purification, and that of the second type is production of oxygen enriched air from ambient air.

## 14.8 Mechanism of Adsorption

In fixed bed absorbers, which are mostly used in the industry, the solute concentration in the adsorbent bed as well as in the fluid change both with location and time. Figure 14.16(a) represents the normal operation showing the building up of a saturated zone of adsorbents from the inlet end of the bed. Initially, most adsorption is limited within the narrow zone near the fluid inlet. As more fluid is passed through the adsorber, the adsorbent in this part gets saturated and the saturated zone starts moving forward until the breakthrough point is reached. If the adsorbent is initially free of any adsorbate, the solute content of the fluid exponentially drops to almost zero before reaching the other end of the bed, when the solid near the fluid inlet gets nearly saturated. During the movement of the saturated zone the exit concentration begins to rise rapidly above whatever limit has been fixed as the desirable maximum adsorbate level of the fluid. Further transfer starts taking place away from the inlet within the adsorbent bed. While the concentration is a function of the material used and the operating temperature, the dynamic capacity is also dependent on the operating conditions such as inlet concentration, fluid flow rate and bed length. The dependence of inlet concentration and fluid flow rate arise from heat effect and mass transfer rate. The zone in the adsorbent bed where 95 to 100% adsorption takes place is known as the *mass transfer zone* (MTZ). Within the mass transfer zone the concentration gradient plays a key role. This dynamic adsorption can be explained in terms of the dynamic capacity or breakthrough capacity at given inlet concentrations, temperatures, and flow rate in the bed together with the bed dimensions. It is important that the adsorber bed should be at least as long as the transfer zone-length of the key component to be adsorbed. Therefore, it is necessary to know the depth of this MTZ. Factors that play important roles in dynamic adsorption, and

the length and shape of the mass transfer zone are:

- (i) the type of the adsorbent
- (ii) the particle size of the adsorbent, which is dependent on maximum allowable pressure drop
- (iii) the depth of the adsorbent bed and the fluid velocity
- (iv) the temperature of the fluid stream and the adsorbent
- (v) the concentration of the contaminants to be removed and not to be removed (including moisture)
- (vi) the pressure of the system
- (vii) the removal efficiency required and
- (viii) possible decomposition or polymerization of contaminants on the adsorbent.

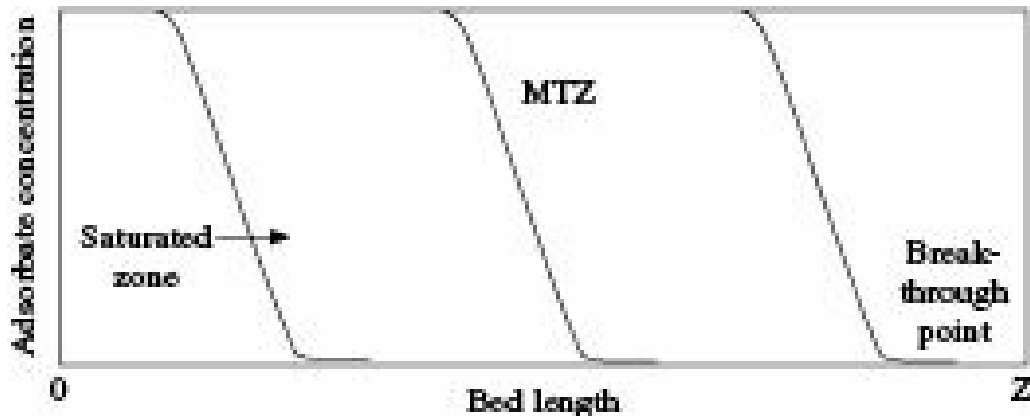


Figure 14.16(a) Formation and movement of the MTZ through an adsorbent bed.

### **Break through curve**

Figure 14.16(b) shows typical change in solute concentration in the fluid with time during adsorption. As shown in the figure, in the initial period, up to time  $q_3$ , the fluid leaves the bed with almost zero solute concentration. After this, the solute concentration in the exit fluid gradually increases. When the solute content of the fluid reaches some predetermined value, called the *break point*, the flow is either stopped or diverted to another unit and the adsorbent is either rejected or subjected to regeneration.

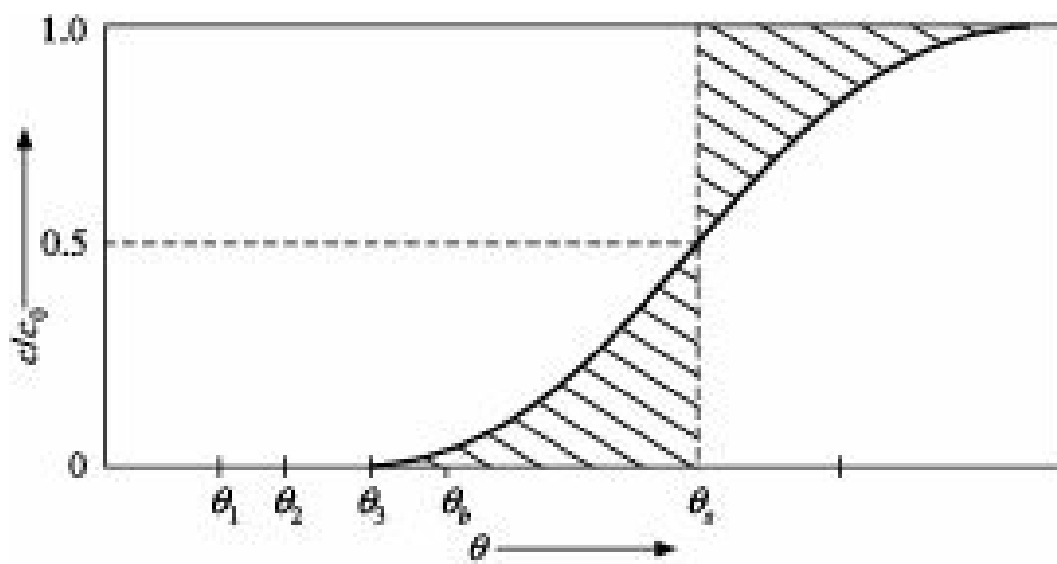


Figure 14.16(b) Breakthrough curve.

The solute content of the fluid at break point usually varies around 5% of the initial value. The total solute removal from the fluid up to the break point may, however, be 99% or more. The *ideal*

*adsorption time* is  $i_s$  by which the solute concentration in the fluid is reduced to 50% of the original value.

The movement of the adsorption zone through the adsorbent bed and the effect of some process variables on the ideal adsorption time can be obtained in the following manner:

The solute fed per unit time per unit area of bed cross section is given by

$$F_A = u_0 c \quad (14.24)$$

where

$F_A$  = flow rate of solute per unit cross sectional area of bed,  $\text{g}/(\text{cm}^2)(\text{s})$ ;

$u_0$  = superficial velocity of the feed (fluid)  $\text{cm}/\text{s}$ ;

$c$  = solute concentration in the solution  $\text{g}/\text{cm}^3$ .

For an ideal break through curve all the solute fed in time  $i_s$  is adsorbed, thereby increasing the solute content of the solid from  $X_0$  to  $X^*$  (saturated concentration). Hence, we have

$$u_0 c i_s = Z t_b (X^* - X_0) \quad (14.25)$$

where,  $Z$  and  $t_b$  are length or height, and bulk density of the bed.

From Eq. (14.25), we get

$$i_s = \frac{Z \rho_b (X^* - X_0)}{u_0 c} \quad (14.26)$$

The actual amount of solute adsorbed at the break point can be determined by integration of the break point curve up to the break point time  $i_s$ . For narrow beds, the break point curve is steep and most of the capacity of the solid adsorbent is utilized. For thicker adsorbent beds, the break point curve extends to the right and the utilization of adsorbent capacity decreases with increase in bed thickness. A shallow bed is therefore preferred in practice, which results in efficient use of adsorbent as well as low regeneration cost.

It is an accepted fact that adsorption takes place at the interphase boundary; the surface area of the adsorbent is therefore an important factor in an adsorption process. Generally, the higher the surface area of the adsorbent, the higher is its adsorption capacity for all compounds. However, the surface area has to be available in a particular pore size within the adsorbent. At low partial pressure (concentration), the surface area in the smallest pores in which the adsorbate can enter is the most efficient. At higher pressures the larger pores become more important while at very high concentrations capillary condensation will take place within the pores, and the total micropore volume is the limiting factor. Thus, the adsorption capacity of certain adsorbents has bearing with its surface area and pore-volume distribution in pores of different diameters. The relationship between adsorption capacity and surface area under conditions of optimum pore-sizes is dependent on concentration. It is very important that any evaluation of adsorption capacity has to be performed under actual concentration. The dimensions and shape of particles affect both the pressure drop through the adsorbent bed and the rate of diffusion into the particles. Pressure drop is lowest when the adsorbent particles are spherical and uniform in size. External mass transfer increases inversely with  $d^{3/2}$ , where  $d$  is the particle diameter, whereas the internal adsorption rate varies inversely with  $d^2$ .

Pressure drop varies with the Reynolds number, and is approximately proportional to the gas velocity through the bed and inversely proportional to the particle diameter. Assuming all other parameters being constant, adsorbent beds comprised of small particles tend to provide higher adsorption efficiencies but at the cost of higher pressure drop, resulting in the sharper and smaller mass transfer zones.

The adsorption bed depth has two effects on mass transfer—firstly, the bed will be deeper than the length of the transfer zone which is unsaturated, and secondly, any multiplication of the minimum bed depth gives more than a proportionally increased capacity. It is therefore advantageous to size the adsorption bed to the maximum length allowed by pressure-drop considerations. The depth of the MTZ or unsaturated depth may be determined using the relationship

$$MTZ = \frac{Z}{\frac{\theta_s}{\theta_s - \theta_b} - f} \quad (14.27)$$

where

$Z$  = total bed length or depth

$i_s$  = ideal adsorption time or time required for saturation

$i_b$  = time required to reach the break point, and

$f$  = degree of saturation in the MTZ

The above expression may be represented in terms of capacity as

$$MTZ = \frac{1}{1-f} Z_1 \left( 1 + \frac{c_{b1}}{c_s} \right) \quad (14.28)$$

where,

$Z_1$  = depth of bed 1

$c_{b1}$  = breakthrough capacity of bed 1

$c_s$  = saturation capacity of the bed

$c_s$  can be obtained by measuring the breakthrough capacities of two beds and using the equation as

$$c_s = \frac{\frac{c_{b2}Z_2 - c_{b1}Z_1}{Z_2 - Z_1}}{1-f} \quad (14.29)$$

where,  $c_{b2}$  is the breakthrough capacity for bed 2. Direct methods for the calculation of the MTZ are also possible using transfer units. However, the calculation of the same for multicomponent systems becomes very much complicated.

As stated, the mass transfer zone directly affects the operation of an adsorbent bed. The continual widening of the mass transfer zone as shown in Figures 14.16(a), is typical of that obtained with a linear adsorption isotherm. However, when the isotherm is either a Langmuir or a Freundlich type, the widening of the MTZ rapidly diminishes within the bed and an asymptotic or constant pattern front is developed in which the MTZ is also constant. For a constant pattern front, Cooney (1990) presents an approximate but convenient method using the Langmuir and Freundlich isotherms to estimate concentration profiles and breakthrough curves when mass transfer and equilibrium parameters are

available.

On the other hand, Collins (1967) has developed a technique for determining the length of a full-scale adsorbent bed when the constant-front assumption is valid, directly from breakthrough curves obtained in small scale laboratory experiments. In this approach the adsorbent bed is considered to be the sum of two sections:

In the first section, the adsorbent is in equilibrium with the adsorbate concentration in the feed and is designated as the length of the equilibrium section (LES). In the second section, the adsorbate loading is zero and is specified as the length of the unused bed (LUB). The length of this section depends on the width of the MTZ and the shape of the concentration profile within the MTZ. The total required bed length,  $Z$  is

$$Z = \text{LES} + \text{LUB} \quad (14.30)$$

Since the LUB is one-half the width of the MTZ for a constant pattern front, it may be determined from the experimental breakthrough curve from the relation

$$\text{LUB} = \frac{\theta_s - \theta_b}{\theta_s} Z \quad (14.31)$$

where

$i_s$  = breakthrough time required to attain the mid-point concentration between the inlet and exit concentrations in the MTZ,

$i_b$  = breakthrough time required to attain the desired exit concentration, and

$Z$  = length of the bed.

For a cylindrical adsorbent bed, the LES value can be determined by assuming an ideal adsorber, where  $\text{LUB} = 0$  and making a solute mass balance. The resulting relation is

$$\text{LES} = \frac{c_0 F \theta_s}{q_p \rho_b} \quad (14.32)$$

where

$c_0$  = concentration of the adsorbate in the feed

$F$  = mass flow rate per unit cross sectional area of the bed

$t_b$  = time for breakthrough at which the LES is evaluated

$q_F$  = loading of the adsorbent during each cycle and

$t_b$  = density of the bed

The length to diameter ratio of vertical cylindrical adsorption bed is usually greater than 1.5. Higher  $L/D$  values may be necessary for liquid feeds to minimize the problem with a large MTZ. To minimize pressure drop through adsorbers, it may be necessary to use either a slanted or a horizontal adsorption unit.

The velocity of the gas stream through adsorbent beds is limited by the adsorbent crushing velocity and varies with different types of adsorbents. The data on crushing velocity may be obtained from the manufacturers of adsorbents. However, the same can be calculated using a relation: crushing velocity = (superficial velocity of the gas) # (molecular weight of the gas) # (system pressure). The length of the MTZ is directly proportional to the velocity. At high velocities, the unsaturated zone gets elongated.

As stated, adsorption decreases with increasing temperature. Since the equilibrium capacity of adsorbent is lower at higher temperatures, the dynamic or breakthrough capacity becomes lower, and the MTZ changes proportionally with temperature. Increase in temperature during adiabatic operation of an adsorption bed can be estimated using appropriate equation.

The adsorption capacity of adsorbents is directly proportional to the concentration of the adsorbate, and the length of the MTZ is inversely proportional to the concentration of the adsorbate. Under identical conditions, a deeper bed will be required to remove a contaminant of lower concentration with equal efficiency than to remove the same contaminant of higher concentration. For combustible gases, the concentration of the adsorbate is to be kept below the lower explosive limit.

### ***Skarstrom cycle***

In a single bed system, the output is not continuous as the bed is to be regenerated separately. However, in a twin bed adsorber the flow of output is kept continuous by operating the twin beds in tandem, one bed acts on adsorption mode while the other on regeneration mode. This is the basic Skarstrom cycle (Skarstrom 1960), the first patent on the subject. Figure 14.17(a) shows the operation of a twin bed adsorber exhibiting the cycle. Each bed operates alternately in two half-cycles of equal duration:

- (i) adsorption followed by pressurization, and
- (ii) purging followed by depressurization or blow down.

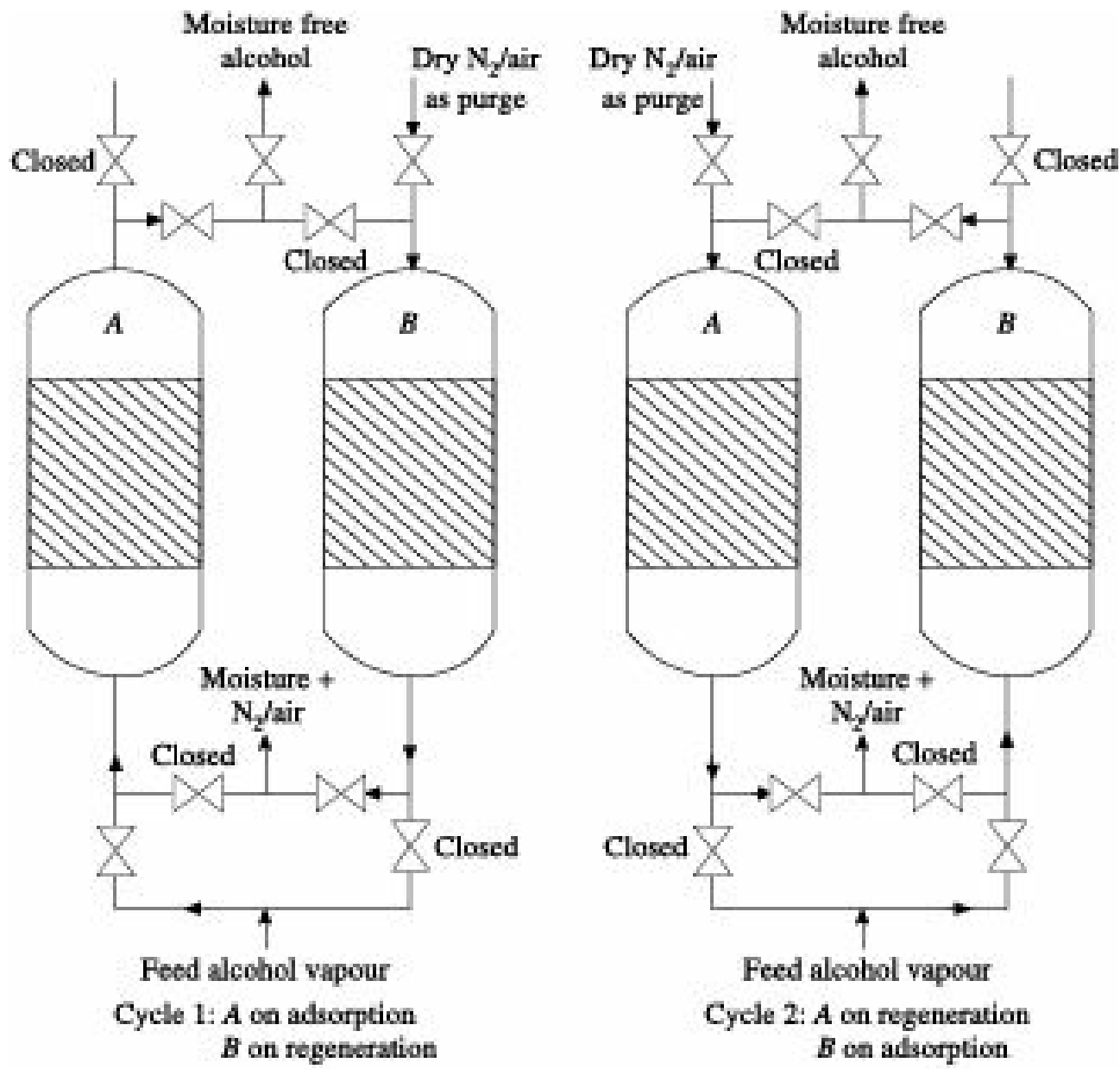


Figure 14.17(a) Schematic diagram of a twin bed adsorber system.

The feed gas is used for pressurization while a part of the effluent product gas is used for purge. As shown in the figure, the adsorption is taking place in bed 1 while a part of the gas leaving the bed 1 is routed to bed 2 to purge that bed in a direction counter-current to the direction of flow of the feed gas during the adsorption step. When moisture is to be removed from air, the dry air product is produced during the adsorption step in each of the beds. The sequence of the steps followed in the cycle is depicted in Figure 14.17(b). The adsorption and purge steps usually take less than 50% of the total cycle time. In many commercial applications of this technology, these two steps consume a much greater fraction of cycle time because pressurization and depressurization (blow down) can be completed rapidly. Therefore, cycle times for PSA and VSA are short, typically seconds to minutes. Thus, small beds have relatively large throughputs.

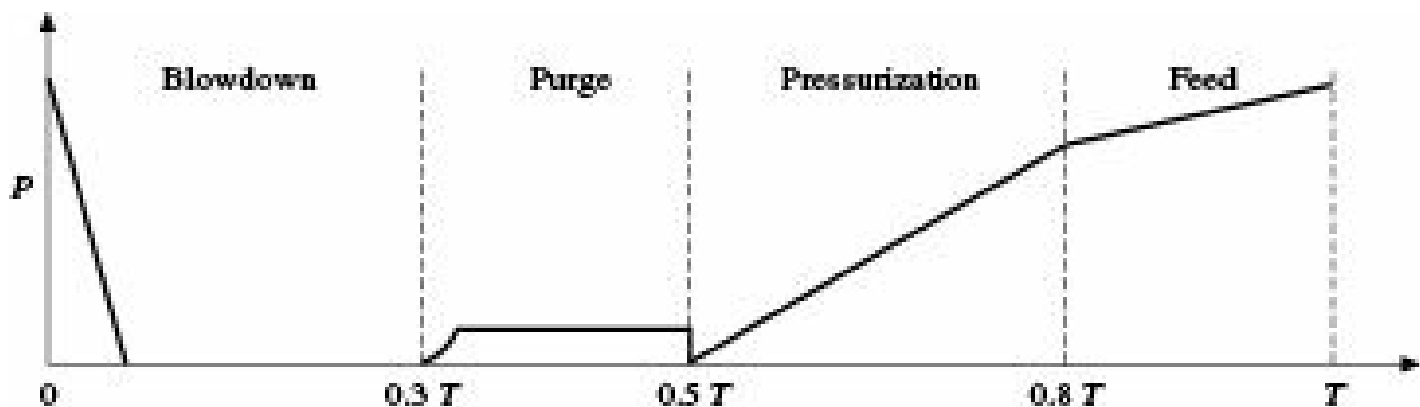


Figure 14.17(b) Sequence of cycle steps in PSA.

Since the introduction of the Skarstrom cycle, numerous improvements have been made to increase product purity, product recovery, adsorbent productivity and energy efficiency (Yang 1987, Ruthven et al. 1994, Crittenden and Thomas 1998). Among these modifications are the use of (i) three, four or more beds, (ii) a pressure equalization step in which both beds are equalized in pressure following purge of one bed and adsorption in the other, (iii) pretreatment or guard beds to remove strongly adsorbed components that might interfere with the separation of other components, (iv) purge with a strongly adsorbing gas, and (v) an extremely short cycle time to approach isothermal operation, if a longer cycle causes an undesirable increase in temperature during adsorption and an undesirable decrease in temperature during desorption.

Separations by PSA and VSA are controlled by adsorption equilibrium or adsorption kinetics, where the latter refers to mass transfer external and/or internal to the adsorbent particle. Both types of control are important commercially. For the separation of air with zeolites, adsorption equilibrium is the controlling factor. Nitrogen is more strongly adsorbed than oxygen and argon. For air with 21% oxygen and 1% argon, oxygen of about 96% purity can be produced. When carbon molecular sieves are used, oxygen and nitrogen have almost the same adsorption isotherms, but effective diffusivity of oxygen is much larger than that of nitrogen. Consequently, nitrogen of very high purity ( $> 99\%$ ) can be produced.

## 14.9 Regeneration of the Adsorbent

Often it becomes necessary to regenerate the adsorbent and reuse the same. This is particularly necessary if the adsorbent is costly or the adsorbate is valuable and has to be recovered to the extent possible. There are several methods for regeneration of adsorbents of which the pressure swing and temperature swing methods are commonly used.

### 14.9.1 Temperature Swing Regeneration

An adsorbate loaded solid can be regenerated by passing a relatively hot inert gas like hot air or steam through the bed. The temperature of regeneration is decided on the basis of adsorption-desorption equilibrium or isotherm and the characteristics of the adsorbent.

In the cycle shown in Figure 14.18(a), a feed stream containing a small quantity of an adsorbate at a partial pressure  $p'_1$  is passed through the adsorption bed at a temperature  $T_1$ . The initial equilibrium loading on the adsorbent is  $X_1$ , generally expressed in weight of adsorbate per unit weight of adsorbent. After equilibrium between the adsorbate and the adsorbent is reached, regeneration requires raising the temperature of the bed to  $T_2$ . Desorption occurs as more feed is passed through

the bed and a new equilibrium loading of  $X_2$  is established. The net removal capacity of the adsorption bed is given by the difference between  $X_1$  and  $X_2$ . When the bed is again cooled to  $T_1$ , purification of the gas stream can be started. Typical adsorbate removal in a temperature swing cycle is generally in excess of 1 kg/100 kg of adsorbent. Since the regeneration time associated with the temperature swing cycle is relatively long, the cycle is used almost exclusively to remove small concentrations of adsorbate from feed streams. This allows the on-stream time to be a significant fraction of the total cycle time of the separation process. In addition, temperature swing cycles may require a substantial quantity of energy per unit of adsorbate. However, if the adsorbate concentration in the feed is small, the energy cost per unit of feed processed can be reasonable.

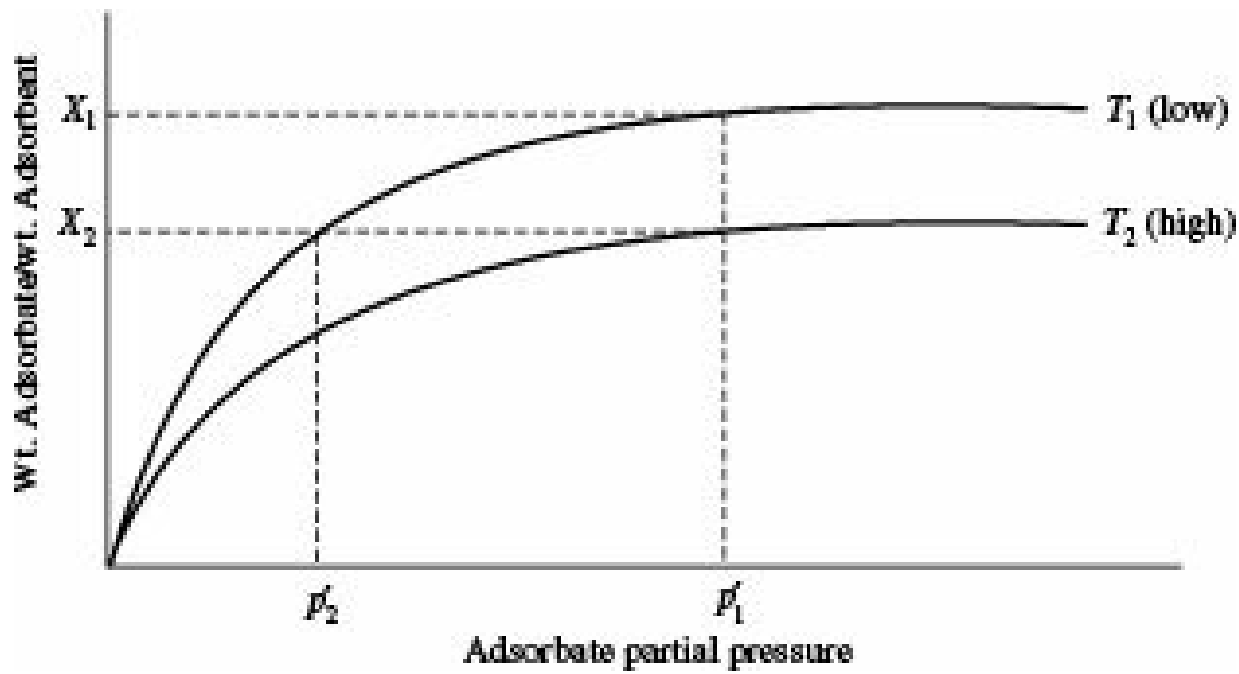


Figure 14.18(a) Temperature swing cycle.

In the inert-purge cycle, the adsorbate during regeneration is removed by passing a nonadsorbing gas containing no adsorbate through the bed. This lowers the partial pressure of the adsorbate and initiates the desorption process. If sufficient pure purge gas is directed through the bed, the adsorbate will be completely removed and adsorption can be resumed. Cycle times, in contrast to temperature swing processes are often only a few minutes rather than hours. However, because adsorption capacity is reduced as adsorbent temperature rise, inert-purge processes are usually limited to 1 to 2 kg of adsorbate/100 kg of adsorbent.

The displacement purge cycle differs from the inert-purge cycle since the cycle uses a gas or liquid in the regeneration step that adsorbs as strongly as the adsorbate. Thus, desorption is facilitated both by adsorbate partial pressure or concentration reduction in the fluid, and by competitive adsorption of the displacement medium. Typical cycle times are usually a few minutes. The use of two different types of purge fluid negatively affects the contamination level of the less adsorbed product. However, since the heat of adsorption of the displacement purge fluid is approximately equal to that of the adsorbate as the two exchange places on the adsorbent, the net heat generated or consumed is essentially negligible and thus maintains nearly isothermal conditions throughout the cycle. The latter condition makes it possible to increase the adsorbate loading of the displacement purge cycle over that for the inert-purge cycle.

One of the important considerations for a TSA system is the temperature of the adsorbent bed during

regeneration, others being quantity and flow of the regenerating gas. The regeneration temperature can be estimated by a simple graphical procedure from the isosteres as shown in Figure 14.18(b). The isosteres are a set of curves which may be drawn from the isotherms by plotting the partial pressures or dew points or concentrations against the corresponding temperature or reciprocal of temperature for a equilibrium loading as parameter. The particular form of the parameters, viz.  $p'$ ,  $\log p'$ ,  $T$ , or  $1/T$  is chosen so as to make the isosteres almost linear for facilitating any interpolation.

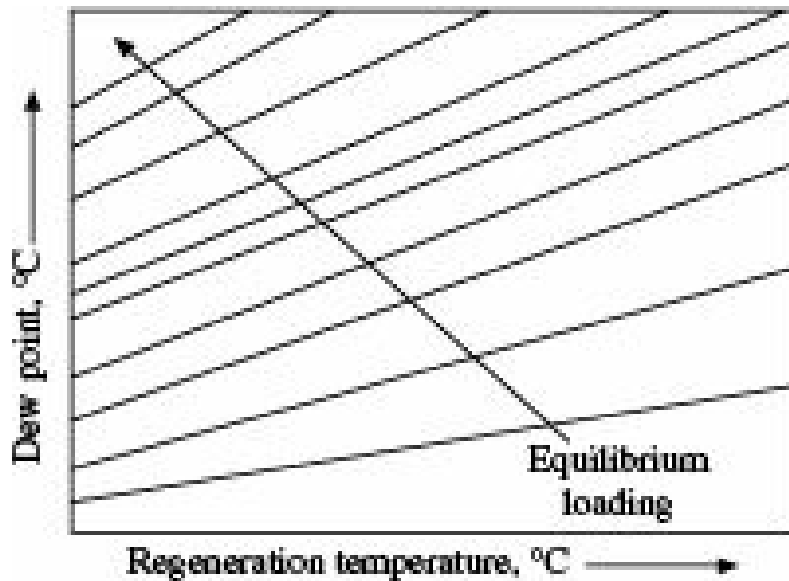
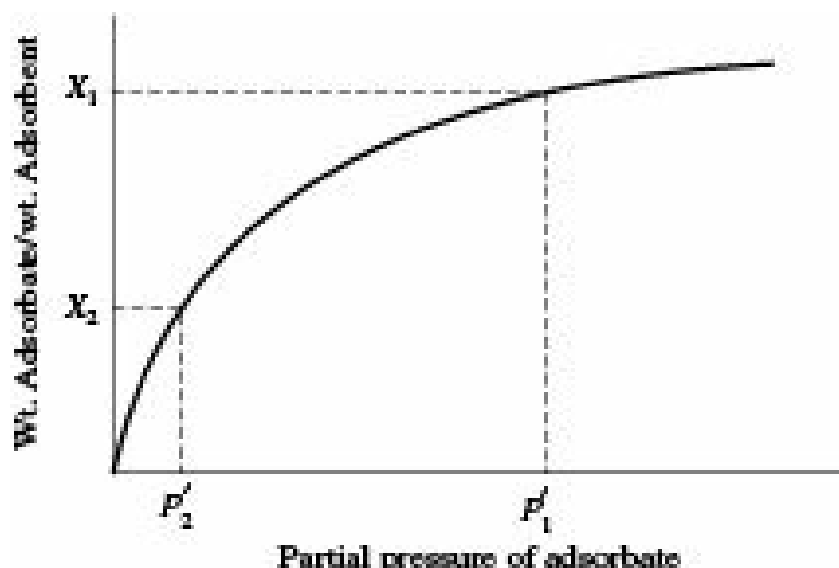


Figure 14.18(b) Use of isosteres to determine regeneration temperature.

#### 14.9.2 Pressure Swing Regeneration

In this method, the adsorbent bed is regenerated by reducing the pressure of the adsorbent bed to atmospheric or even lower pressure when the bed is stripped of the adsorbed solute. If required, the adsorbent bed may be further cleaned by passing hot air or steam through the bed. In the process, the partial pressure of an adsorbate can be reduced by lowering the total pressure of the gas. The lower the total pressure of the regeneration step, the greater is the adsorbate loading during the adsorption step as depicted in Figure 14.18(c). The time required to load, depressurize, regenerate and repressurize a bed is generally only a few minutes. Thus, even though practical adsorbate loadings are almost always less than 1 kg of adsorbate per 100 kg of adsorbent, to minimize thermal gradient problems, the very short times makes the pressure swing cycle a viable option for bulk gas separations.



**Figure 14.18(c)** Pressure swing cycle.

In the pressure swing process one can have 3-12 adsorber vessels, one or more can be used in adsorption step while others are used for various stages of regeneration. Figure 14.19 depicts a schematic representation of a polybed pressure swing adsorption process for commercial production of hydrogen with a purity of 99.99% by steam reforming of methane.

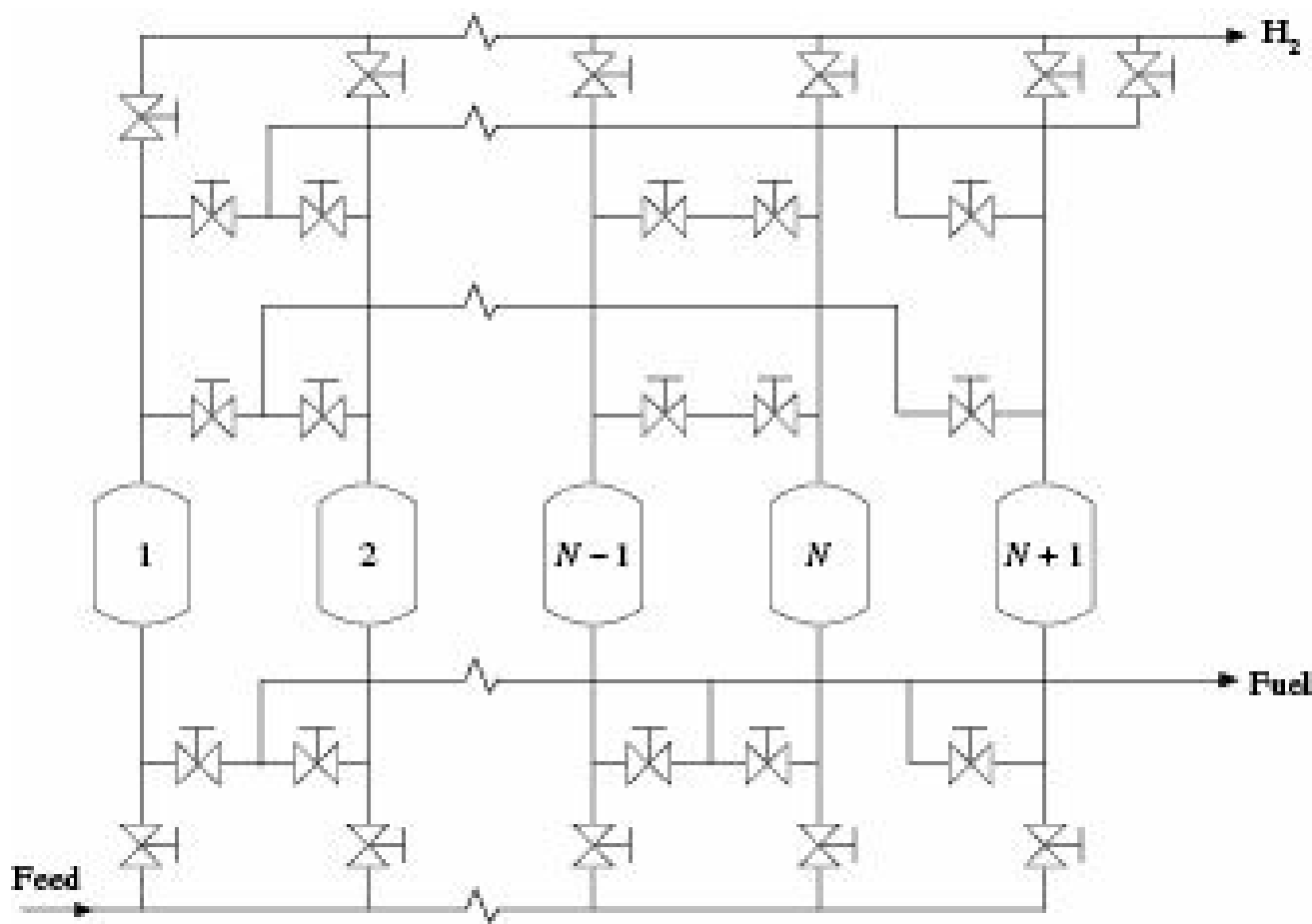


**Figure 14.19** A typical polybed PSA process for steam reforming of methane.

It is quite common in a pressure swing cycle to use a fraction of the less adsorbed gas product as a low pressure purge gas. Often the purge flow is in the opposite direction from that of the feed flow. The simplest version of this process is designated as PSA. Skarstrom (1972) has developed the rules for the minimum fraction of less adsorbed gas product required for displacing the adsorbate. Although the concept of PSA is very simple, the process in commercial application is fairly complex

because it involves a multicolumn design where the adsorbers operate under a cyclic steady-state using a series of sequential nonisothermal, nonisobaric and nonsteady state steps. These include adsorption, desorption and a multitude of complementary steps which are designed to control the purity of product along with its recovery as well as to optimize the overall separation performance. Unique PSA cycles are also used to produce simultaneously two pure products from a multicomponent feed, e.g. oxygen and nitrogen from air, carbon dioxide and hydrogen from SMR off-gas, carbon dioxide and methane from landfill gas, and to produce a product containing a component which is not present in the feed, e.g. ammonia synthesis gas from SMR off-gas.

The RPSA process for hydrogen purification developed by Questar Industries, Canada (Keefer and Doman 1997) utilizes the conventional Hydrogen-PSA process consisting of the following steps:

*Step 1:* adsorption of feed gas over a packed bed of adsorbent at super-ambient pressure in order to produce a hydrogen-enriched gas

*Step 2:* co-current depressurization of adsorber to produce additional amount of hydrogen-enriched gas for pressurizing an accompanied vessel

*Step 3:* further co-current depressurization to produce another stream of hydrogen-enriched gas for counter-currently purging an accompanied vessel

*Step 4:* counter-current depressurization to desorb a part of the feed-gas impurities

*Step 5:* counter-current purge with hydrogen from Step 3 to further desorb the impurities

*Step 6:* counter-current pressurization with hydrogen from Step 2, and

*Step 7:* counter-current pressurization to feed pressure level with hydrogen from Step 1.

The cycle runs rapidly using a total cycle time of ~1 min compared to cycle times of 10-30 minutes in a conventional process. Six parallel adsorbers packed with layers of activated carbons and zeolites are used in conjunction with two rotating flow control valves for introduction and removal of gases to and from the adsorbers. The process produces 99.95% pure hydrogen with a recovery of 67–73% from the feed gas at 8.5 atm pressure.

The peculiarity of a novel adsorber design developed by Air Products and Chemicals, Inc. (Sircar 1991) for production of oxygen-enriched air from ambient air shows the use of two or more (multiples of two) layers of a zeolite adsorbent inside a single vessel separated by a perforated plate (similar to the arrangement of packings or trays in gas/vapour-liquid contacting equipment). The RPSA process consists of the following steps:

- (i) simultaneous pressurization and adsorption of nitrogen from air by one layer of the adsorbent in order to produce the oxygen-enriched gas
- (ii) simultaneous depressurization and purging with oxygen product of the other adsorbent layer of the pair for its regeneration.

Using 5A zeolite as the adsorbent and total cycle time of 10 s (compared to 60-240 s. for a conventional PSA-oxygen process) the process can produce 27.5% oxygen with recovery of 64.1% at feed air pressure of 2.22 atm (Sircar et al. 1998).

### **14.9.3 High Temperature PSA Process**

A chemisorbent,  $\text{Na}_2\text{O}$  supported on alumina, is used in a PSA process for direct removal and recovery of bulk carbon dioxide from a high temperature feed gas (wet) without pre-drying or cooling

of the feed. The adsorbent reversibly chemisorbs carbon dioxide in presence of steam in the temperature range 200-300°C (Sircar 2001, Lee et al. 2007a). A gas stream at ~200°C saturated with water, is treated for simultaneous production of CO<sub>2</sub> depleted stream and CO<sub>2</sub> enriched stream without removing water. The PSA cycle consists of the following steps:

*Step 1:* adsorption at ~125 psia

*Step 2:* co-current CO<sub>2</sub> rinse at ~125 psia with recycle of effluent gas as feed

*Step 3:* counter-current evacuation to ~2.5 psia with simultaneous steam purge at feed gas temperature and

*Step 4:* counter-current pressurization with a part of CO<sub>2</sub> depleted product gas from Step 1.

The effluent gas from Step 3 is partly used as the purge gas in Step 2 after recompression, and the balance is withdrawn as the recovered CO<sub>2</sub> product gas. The inert gas and CO<sub>2</sub> recoveries from the feed gas are ~100 and 78%. This application may be attractive for greenhouse gas emission control, i.e. CO<sub>2</sub> sequestration from a hot gas or CO<sub>2</sub> removal from combustion gases for power generation without cooling the gas and removing the water. This technology is a promising one for future development and possesses high potential for tackling many practical problems in the fields of natural gas supply and conservation, reduction of greenhouse gas emissions, production and conservation of hydrogen, etc. However, considering the present commercial applications, this technology has not been considered in selection of adsorption cycles.

### ***Choice between the adsorption cycles***

The choice of a particular process depends on several factors. The total quantity of adsorbent required for a particular application is equal to the total load of the adsorbate or contaminant in the cycle divided by the dynamic adsorption capacity. The higher is the dynamic adsorption capacity, the less is the size of the bed and hence, less is the capital cost of the equipment as well as the cost of the adsorbent replacement. Thus, *prima facie* PSA appears to be a better choice than TSA. But if the throughput is large, the capital cost of the equipment and the cost of the compression would be very high. Also, in PSA a purge is required to drive off the residual gas from the void spaces of the bed for improving the product quality, and often this purge has to be the product gas itself or a high purity inert gas. Since this cannot be reused due to its level of impurity, it is often vented out which affects the overall recovery or the economics of the operation.

In TSA too, a regenerating gas is required and that has to be heated to a sufficiently high temperature for regenerating the adsorbent bed. In large industries TSA is usually in operation due to having spare resources for use in regeneration. Very large throughputs cannot be handled by PSA. If the feed rate is low or moderate but the feed contains contaminants in large quantity, PSA system is suitable.

PSA and VSA cycles have been modelled successfully for both equilibrium and kinetic controlled processes. The models and computational procedures are similar to those used for TSA. The models are particularly useful for optimizing cycles. Of particular importance in PSA and TSA is the determination of the cyclic steady state. In TSA, following the desorption step the regenerated bed is usually clean. Thus, a cyclic steady state is closely approached in one cycle. In PSA and VSA, this does not often happen where complete regeneration is seldom achieved or necessary. It is only required to attain a cyclic steady-state whereby the product obtained during the adsorption step has the desired purity and at cyclic steady-state, the difference between the loading profiles after

adsorption and desorption is equal to the solute entering in the feed. Starting with a clean bed, the attainment of a cycle steady-state for a fixed cycle time may require tens or hundreds of cycles. For example, ethane and carbon dioxide are separated from nitrogen using 5A zeolite at ambient temperature with adsorption and desorption for 3 min each at 4 atm and 1 atm, respectively, in beds of 0.25 m in length (Mutasim and Bowen 1991). The computation of the loading and gas concentration profiles at the end of each adsorption step for ethane starting with a clean bed, shows that at the end of the first cycle the bed is still clean beyond about 0.11 m and by the end of the 10th cycle, a cyclic steady-state has almost been attained with a clean bed existing only near the very end of the bed. Experimental data for ethane loading at the end of 10th cycle agree reasonably well with the computed profile.

The cycle time in PSA is very short as the adsorbent bed becomes saturated quickly due to large concentration of the contaminant (adsorbate). So the adsorbent must be rugged enough to withstand millions of pressurization and depressurization cycles without disintegration. The carbon molecular sieve in nitrogen generation plant suffers more than 100 million such cycles in its life of 10 years. On the other hand, TSA handles a very large quantity of feed and its cycle time is long because of the sufficient time required to heat and cool the bed. The bed is to be cooled after heating, and brought to adsorption temperature otherwise the adsorption capacity would be less. Naturally, an adsorbent suffers several thousand cycles of thermal expansion and cooling in its life time, and has to be mechanically and chemically rugged enough to withstand such repeated thermal shocks (Datta 2006). For adsorbent like silica gel, the regeneration temperature is very low, usually less than 150°C. But for molecular sieves and activated carbons, the regeneration temperatures are quite high depending on the application. Normally the molecular sieves require regeneration temperatures more than 220°C because of the higher heat of adsorption.

Modelling of PSA and VSA cycles can be carried out in the same fashion as for TSA. However, the assumptions of negligible axial diffusion and isothermal operation may be relaxed. For each cycle, the pressurization and blow down steps are often ignored and the initial conditions for adsorption and desorption are the final conditions for the desorption and adsorption steps, respectively of the previous cycle.

Keller et al. (1987) has developed a simple matrix that can be applied for selection of the appropriate adsorption cycle with essentially no calculation. Table 14.3 contains nine process conditions that can be used to characterize the desired adsorption cycle. It is however, necessary to determine every process condition that applies to the separation being considered. By moving across the matrix, the applicability of a cycle for each specific process condition will indicate one of the four designations. Obviously, a ‘no’ designation eliminates that adsorption cycle from further consideration. A separation indicating a ‘yes’ for each process condition would deserve strong consideration. The other two designations can be used to rank the adsorption cycles if more than one cycle is still a possibility. This selection procedure should be used with some considerations since capital and energy costs can vary from one location to other and can affect the final choice.

**Table 14.3** Matrix for adsorption cycle selection (Peters et al. 2003)

Gas or Vapour Phase	Liquid Phase				
Process condition	Temperature swing	Inert purge	Displacement purge	PSA	Temperature swing†
Feed: gas or vapour	Yes	Yes	Yes	Yes	No

Feed: liquid, vaporise at < 200°C	Unlikely	Yes	Yes	Yes	Yes
Feed: liquid, vaporise at > 200°C	No	No	No	No	Yes
Adsorbate concentration in feed, < 3%	Yes	Yes	Unlikely	Unlikely	Yes
Adsorbate concentration in feed, 3-10%	Yes	Yes	Yes	Yes	No
Adsorbate concentration in feed, > 10%	No	Yes	Yes	Yes	No
High product purity Required	Yes	Yes	Yes	Possible††	Yes
Thermal generation Required	Yes	Yes	No	No	Unlikely
Difficult purge/ adsorbate separation	Possible†††	Unlikely	Unlikely	NA	Possible†††

† includes powered, fixed-bed and moving bed processes.

†† requires very high adsorption pressure and low desorption pressure.

††† only if adsorbate does not need to be recovered.

## 14.10 Adsorption Equipment

### 14.10.1 Stage-wise Contact

#### *Adsorption from gases*

In recent years, *fluidized beds* are widely used for adsorption from gases like recovery of vapours from vapour-gas mixtures, desorption, fractionation of light hydrocarbon vapours and several other applications.

Adsorption is usually carried out at gas velocities just above the quiescent fluidizing velocity when the bed expands and looks like boiling liquid. The solid particles move about freely and are thoroughly circulated. Well defined bubbles of gas rise through the bed.

Only fine particles below 20 mesh are suitable for use in fluidized beds and the superficial gas velocity has to be kept below 0.60 m/s. They can, however, retain large range of particle sizes.

*Teeter beds* are more frequently used for adsorption from gases since they provide better gas-solid contact by accommodating coarser particles, up to 10 mesh at superficial gas velocities in the range of 1.5 to 3 m/s. In these beds, however, there is little gas bubbling and the size range of particles retained is relatively small.

Multistage operations are generally not practised for gas-liquid contact in commercial scale.

#### *Adsorption from liquids*

*Agitated vessels* are commonly used for adsorption from liquids. These are more or less similar to those used for gas-liquid operations. The liquid depths vary between 0.75 to 1.5 tank diameters. The tanks are provided with wall baffles to avoid vortex formation and lift the solid particles through vertical liquid motion.

Flat blade or pitched blade turbines, fitted to an axial shaft are generally used for efficient mixing. Multiple turbines on the same shaft are sometimes used to get more uniform slurry throughout the tank. The clearance of the lowest impeller from the tank bottom should be more than the settled height of the bed, so that the impeller is not embedded if it stops.

A typical batch equipment for liquid-solid contact consists of an agitated vessel as above but having a

filter press and a collection tank. The liquid to be treated and the adsorbent particles are thoroughly mixed in the tank, at the desired temperature for the required length of time. The slurry is then filtered in a filter press to separate the clear liquid from the solid adsorbent containing the adsorbed solute. The operation can be readily converted to multistage one by using additional tanks and filter presses as required. The operation can also be made continuous by using continuous rotary filters or centrifuges instead of a filter press. Alternatively, the adsorbent may be allowed to settle and continuously withdrawn from bottom.

**Multistage contact:** Removal of a given amount of solute can be done with greater economy of adsorbent by treating the solution separately with small batches of adsorbent and filtering between stages rather than employing the entire adsorbent in a single stage. This can be practiced both in batch and continuous operations.

As in other mass transfer operations, greater economy of adsorbent can be achieved by counter-current operation where the solution to be treated and the adsorbent flow in opposite directions, either from stage to stage or in a single equipment.

#### 14.10.2 Continuous Contact

##### *Steady-state moving bed adsorbers*

**Adsorption from gases:** Steady state operation requires continuous movement of both fluid and adsorbent through the equipment at constant rates with no change in conditions at any point with passage of time. In order to have better performance, it is necessary to have counter-current operation so that several stages can be accommodated within a single device, since parallel flow of solids and fluids can at best produce a single stage.

In view of the difficulties in moving solids through equipment continuously and uniformly, it has not been possible to successfully develop continuous flow counter-current adsorber in commercial scale particularly for gas-solid contact.

**Adsorption from liquids:** The difficulties in moving solids continuously and uniformly through equipment, as in case of adsorption from gases, stand in the way of developing successful continuous counter-current equipment for adsorption from liquids also. In case of liquids, however, much less elaborate arrangements are required to overcome the difficulties. For instance, a screw feed or simple gravity flow from a bin may introduce the adsorbent at the top of the tower and the same may be removed from the bottom by a revolving compartmented valve. In the *pulsed* or *moving bed* shown in Figure 14.20, the liquid enters the bottom and leaves through the top of the column. The flow of liquid is stopped periodically, spent adsorbent is withdrawn (pulsed) from the bottom, and virgin or regenerated adsorbent is added into the top of the adsorber.

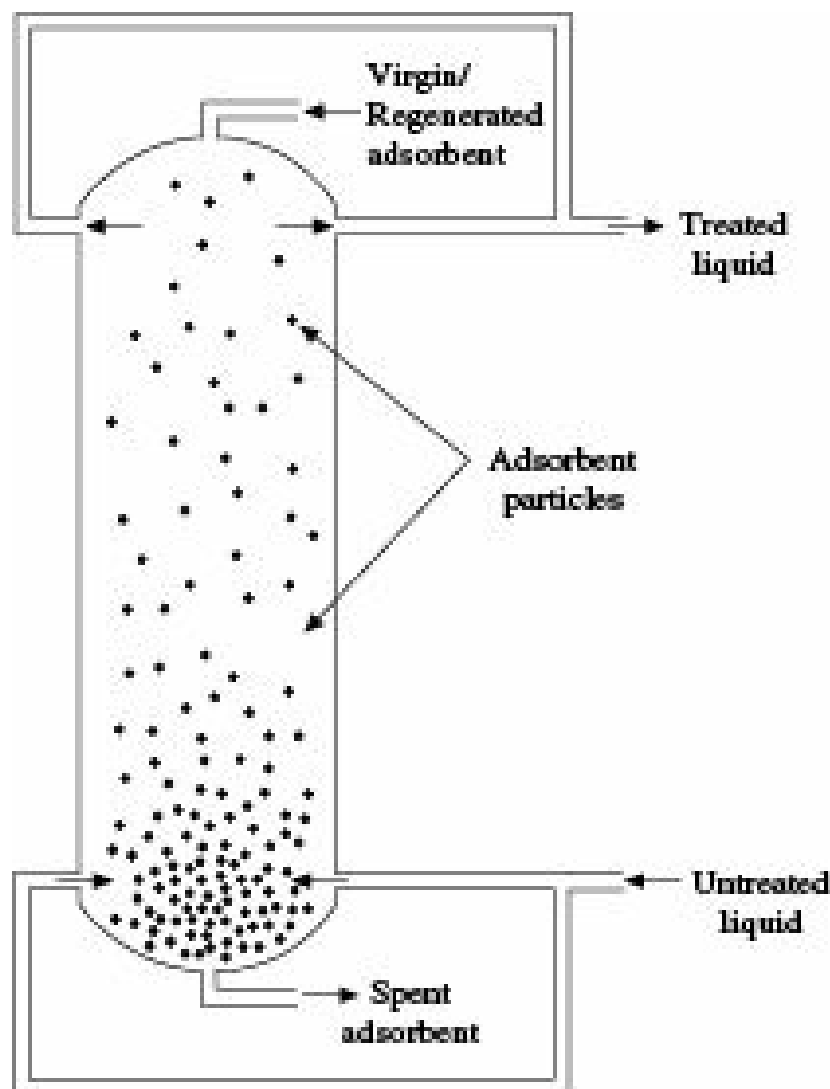


Figure 14.20 Pulsed or moving bed adsorber.

The *Higgins contactor*, originally developed for ion-exchange has been more or less successfully used for adsorption from liquids. The equipment (Figure 14.21), though intermittent and cyclic fashion made by the action of piston, approaches counter-current operation in its performance. Adsorption takes place in the upper part of the equipment where the solution flows down through a stationary bed of the adsorbent. At the end of adsorption, the solid particles are transferred to the lower part for regeneration and the upper part is filled with regenerated adsorbent when the cycle is repeated. Adsorption, regeneration and material shifting from adsorption to regeneration zone are carried out in an intermittent and cyclic way by regulating the valves. Out of three valves in the equipment, one valve remains open for each operation.

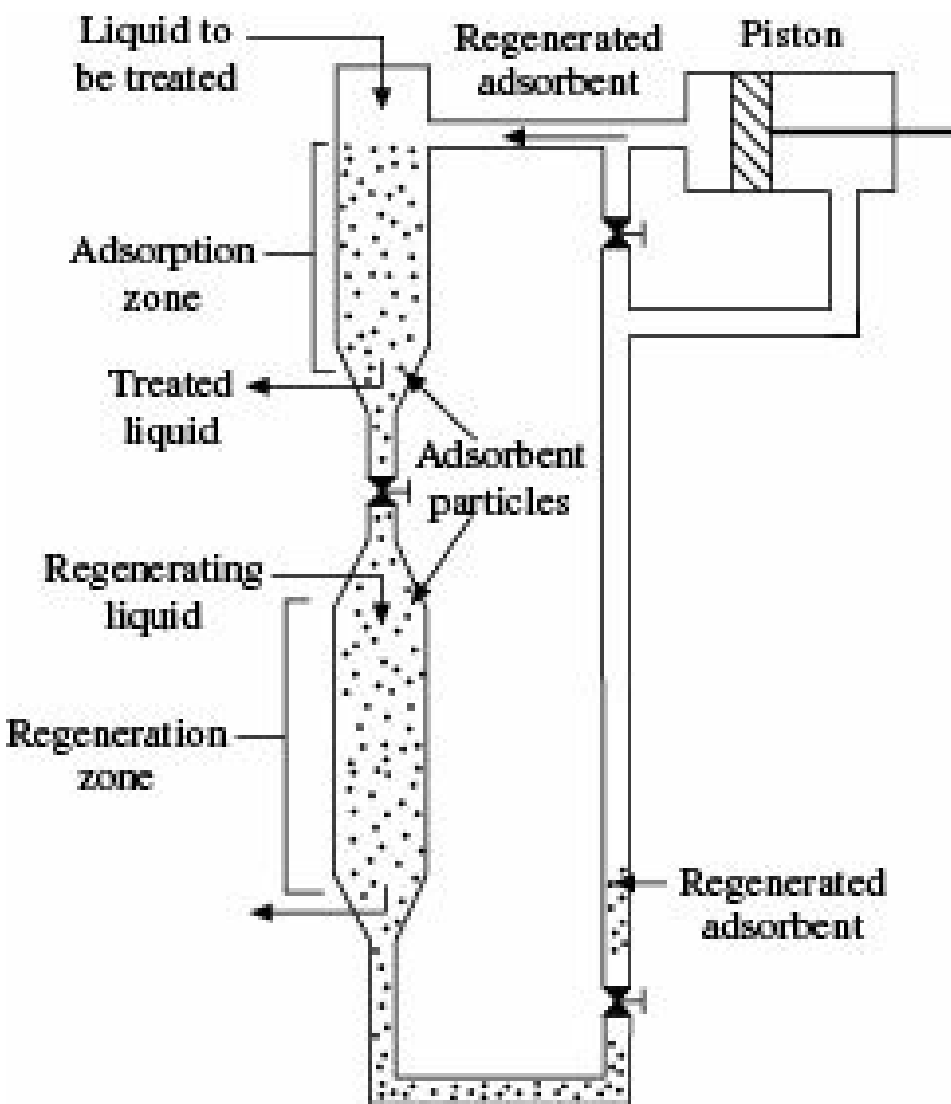


Figure 14.21 Higgins contactor.

### ***Unsteady-state fixed bed adsorbers***

The inconvenience and relatively high cost of moving solid particles as required in steady-state operations often make it more economical to use *fixed bed adsorbers* where the gas or liquid is made to pass through a stationary bed of solid adsorbent. The process is obviously unsteady.

Fixed bed adsorbers are frequently used in recovery of solvent vapours from air or other gases, purification of air in gas masks, dehydration of air or other gases, etc.

The schematic representations of fixed bed adsorbers are depicted in Figure 14.22(a)-(d). Figure 14.22(a) shows a configuration of such an adsorber vertically placed with six trays. A thin bed of adsorbent particles is spread on a screen or perforated plate. The depth of the bed usually varies from 0.3 to 1.3 m. Filtered feed gas is admitted into the chamber and flows through the bed. If the effluent gas is substantially free from solvent vapour, it is discharged into the atmosphere. If, on the other hand, the gas contains appreciable amount of vapour, the same is diverted to a subsequent adsorber in series. When the adsorbent particles in any adsorber become nearly saturated they are subjected to regeneration.

The enclosures for fixed-bed adsorbers may be horizontal or vertical, conical or cylindrical shells shown in Figures 14.22(b)-14.22(c). When multiple fixed beds are needed, the usual configuration is a vertical cylindrical shell as shown in Figure 14.22(d). The type of enclosure used is normally dependent on the gas volume and the permissible pressure drop. The gas flow can be either down or up. Downflow allows for the use of higher gas velocities, while in upflow the gas velocity must be

maintained below the value which causes flooding of the bed. When large volume of gas is to be handled, cylindrical horizontal vessels are suitable. For the continuous operation of fixed bed adsorbers, it is desirable to have two or three units. With two adsorber units, one unit adsorbs while the other regenerates or desorbs. Under most situations, two units are sufficient if the regeneration and cooling of the second bed can be completed prior to the breakthrough of the first unit. The move to three units makes it possible for one bed to be adsorbing, one cooling and the third regenerating. The vapour-free air from the first bed is used to cool the unit which was just regenerated. Occasionally a fourth bed is used, when two units adsorbing in parallel, discharge the exhaust to a third unit on the cooling cycle and a fourth unit is being regenerated. Conical fixed-bed adsorbers are used when a low pressure drop through the cone-shaped bed is less than one-half of that through a conventional flat-bed adsorber, while the air volume is more than double of that through the flat bed.

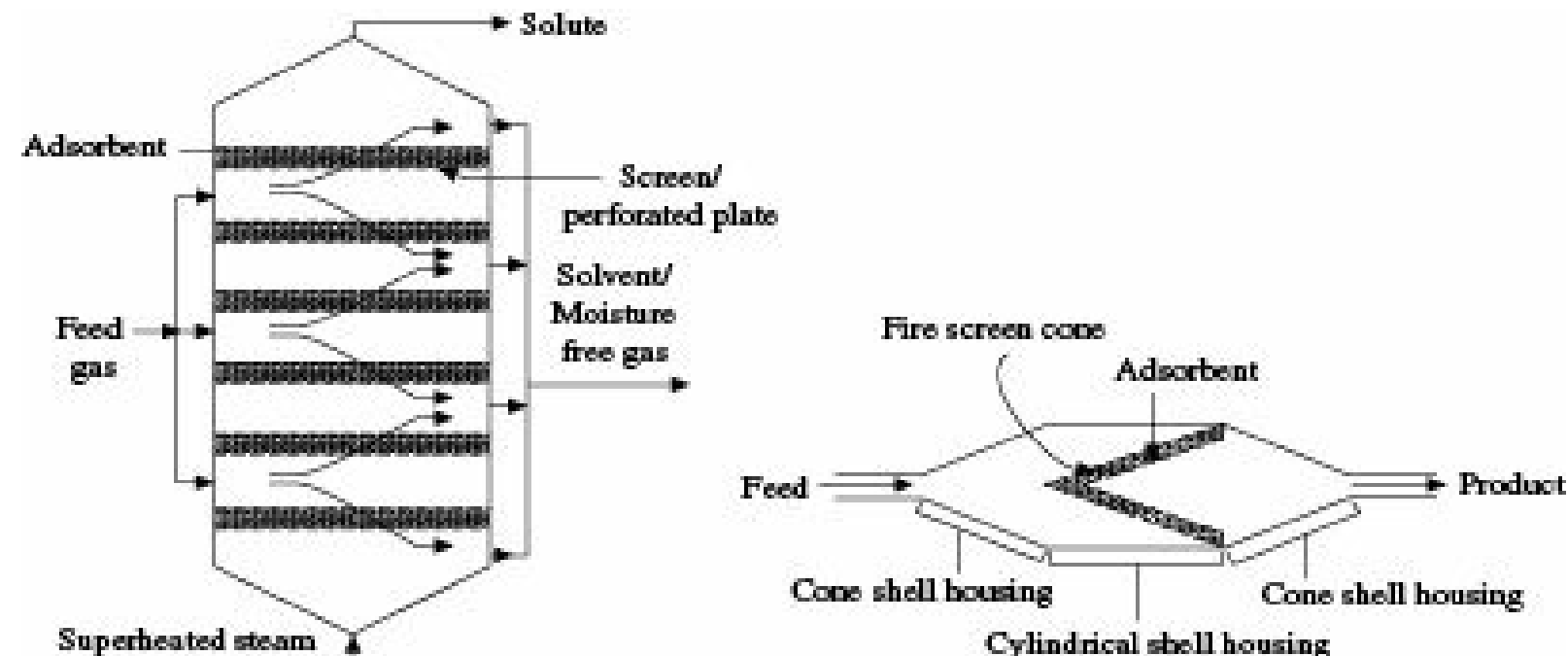


Figure 14.22(a) Fixed-bed adsorber. Figure 14.22(b) Horizontal adsorber configuration.

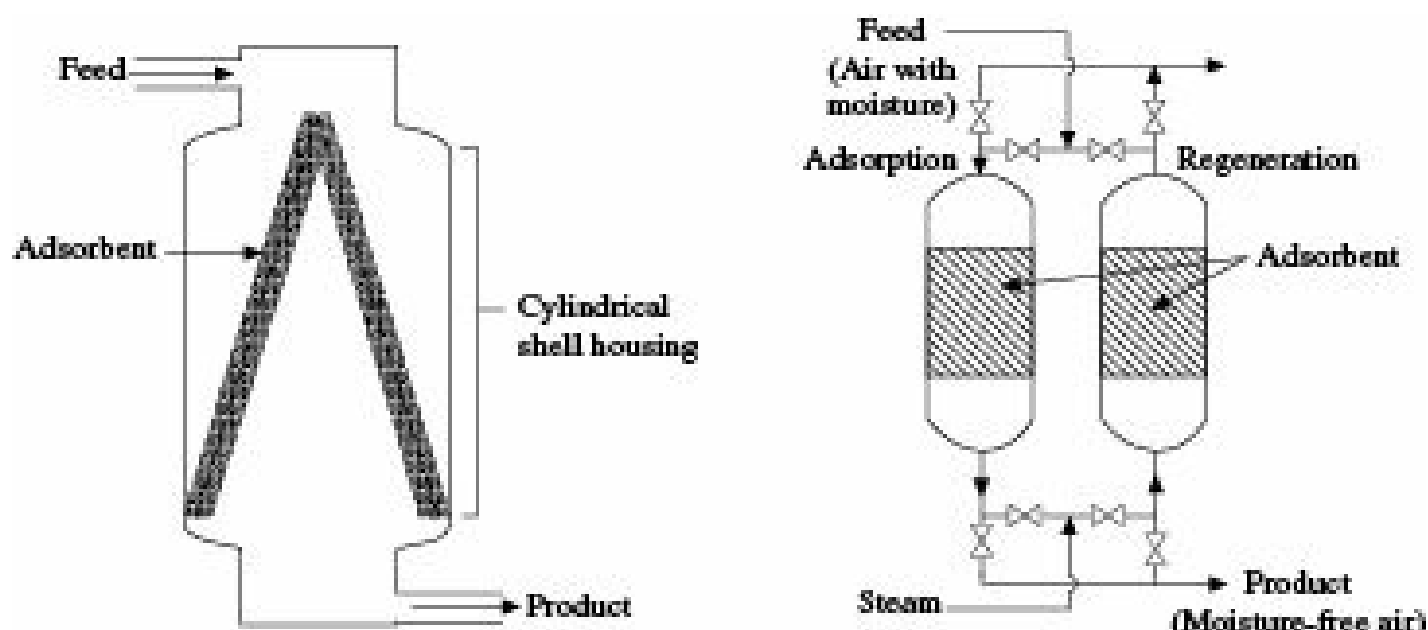


Figure 14.22(c) Vertical adsorber with two cones. Figure 14.22(d) Two unit fixed-bed adsorber.

Regeneration is done by hot inert gas or low pressure steam, the latter being preferred if the solvent is

not miscible with water or if presence of small amount of water is not objectionable. The size of the adsorbent bed is determined on the basis of gas flow rate and desired cycle time. The cross sectional area of the bed is fixed to give a superficial gas velocity of 0.15 to 0.45 m/s. For very large flow rates, rectangular beds in horizontal cylinders are generally used.

The operation can be made more or less continuous by placing the adsorbent particles in several small chambers contained in an inner drum rotating inside a stationary compartmented outer shell. As the inner drum rotate, the adsorbent is successively subjected to adsorption, regeneration, drying and cooling.

Moist gases can be dried by passing them through beds of silica gel, alumina, bauxite or molecular sieves. If the gases are under pressure, towers may be 10 m or more in height, but in such cases, the adsorbent should be supported on trays at intervals of 1 to 2 m in order to minimize compression of the bed.

### ***Adsorption from liquids***

As in case of adsorption from gases, fixed bed adsorbers are often more economical in case of adsorption from liquids also.

Liquids such as gasoline, kerosene, transformer oil, etc., can be dehydrated by activated alumina in fixed bed adsorbers similar to that shown in Figure 14.22. High temperature steam along with vacuum can be used for regenerating the adsorbent.

For the bulk separation of liquid mixtures, continuous counter-current systems are preferred over batch systems because they maximize the mass transfer driving force. This advantage is particularly important for difficult separations where selectivity is not high and/or where mass transfer rates are low. Ideally, a continuous counter-current system involves a bed of adsorbent moving downward in plug flow and the liquid mixture flowing upward in plug flow through the void space of the bed. Unfortunately, such a system has not been successfully developed because of problems of adsorbent attrition, liquid channeling and nonuniform flow of adsorbent particles. Successful commercial systems are based on a simulated counter-current system using a fixed bed.

## **14.11 Reactive Adsorption**

Like other reactive separation processes, *reactive adsorption* process is finding its use in chemical process industries. It is a combination of pressure swing adsorption and a periodic flow reactor. One such configuration is a gas-solid-solid trickle bed reactor where the fine adsorbent trickles through the fixed catalyst bed, removing *in situ* one or more products selectively from the reaction zone. The combo unit operates on Le Chatelier's principle by which the removal of a reaction product by selective adsorption from the reaction zone of an equilibrium controlled reaction increases the conversion and also the rate of formation of the products. This concept is called *pressure swing reactor* when the regeneration of the adsorbent is achieved by using the principles of PSA. Recently, this concept has been used to develop a novel process cycles called *pressure swing sorption enhanced reaction* (PSSER) process for production of hydrogen by reversible steam reforming of methane. The net reaction is highly endothermic and very strongly controlled by reaction thermodynamics. The conversion of methane to hydrogen is relatively moderate and the product gas contains substantial amount of  $\text{CO}_x$ . The PSSER concept permits significant lowering of the SMR reaction from 900 to 400°C without sacrificing conversion, and produces  $\text{CO}_x$  free gas. A reversible

chemisorbent ( $K_2CO_3$  promoted hydrotalcite) has been used in the PSSER process in order to selectively remove  $CO_2$  from the reaction zone at the reaction temperature of 400-500°C (Hufton et al. 1999). A unique property of the chemisorbent is that it exhibits moderately large adsorption capacity for  $CO_2$  in the temperature range in the presence of steam. Consequently, it can be regenerated by using steam purge. The experimental studies and model evaluation have been made (Lee et al. 2007b) for the equilibrium data for chemisorption of  $CO_2$  on sodium oxide promoted alumina and dynamics of  $CO_2$  sorption and desorption on this material. An admixture of the chemisorbent and a reforming catalyst has been used as packing in the PSSER column. The steps being followed are:

- (i) sorption-reaction step where a mixture of steam and methane is passed through the reactor at the reaction temperature and pressure, and a product stream containing hydrogen and methane is withdrawn at reaction pressure
- (ii) counter-current depressurization where the pressure in the reactor is lowered to near ambient
- (iii) the reactor is counter-currently evacuated and simultaneously purged with steam and
- (iv) counter-current depressurization where the reactor pressure is raised back to the reaction pressure by steam.

Simulated moving bed reactors involving chemical reaction and adsorptive separation in a single unit have been explored for production of highly concentrated fructose syrup by glucose isomerization (Zhang et al. 2007), for esterification to synthesize methyl acetate (Lode et al. 2003) and methyl acrylate (Stroehlein et al. 2006), for hydrogenation of trimethyl benzene (Viecco and Caram 2006). Another novel concept called *Thermal Swing Sorption Enhanced Reaction* (TSSER) has been proposed for direct production of fuel cell grade hydrogen by low temperature steam-methane reforming (Lee et al. 2007c). The concept can also be utilized for simultaneous production of the fuel cell grade hydrogen at reaction pressure along with essentially pure and compressed  $CO_2$  byproduct gas for potential sequestration from a synthesis gas produced by gasification of coal.

The compactness of the SER process and its ability to directly produce an essentially pure hydrogen gas (Harrison 2008) may be attractive for its integration with a domestic or industrial hydrogen fuel cell for power generation. This process is a promising one for novel applications of adsorption technology.

### ***Chromatographic separation***

The term ‘Chromatography’ came into existence in mid-19th century. The technology has since then advanced very rapidly and found its multifaceted applications. It is based on the partition coefficient between a mobile phase and a stationary phase. Chromatography techniques have long been used for chemical analysis and separation. Various modifications of the conventional techniques have been carried out to improve the efficiency of separation. The reasons for finding increasing use of chromatographic separation can be as follows:

- (i) Chromatography is the most efficient among the separation methods due to the highest number of theoretical plates it offers per unit length at perhaps the lowest cost per plate
- (ii) Chromatography offers maximum flexibility in designing separation factor for a given separation through selectivity engineering in the form of infinitely possible surface modifications
- (iii) Chromatography is one of the separation methods that give multicomponent separation in a single

operation.

Chromatography separates mixtures into components by passing a fluid mixture through a bed of adsorbent material called stationary phase. The two most common adsorbents used in chromatography are porous alumina and porous silica. Sometimes carbon, magnesium oxide and various carbonates are also used. Alumina is a polar adsorbent and is preferred for the separation of components that are weakly or moderately polar. In addition, alumina is a basic adsorbent preferentially retaining acidic compounds. Silica gel is less polar than alumina and is an acidic adsorbent preferentially retaining basic components such as amines. Carbon is a nonpolar stationary phase with the highest attraction for larger nonpolar molecules. Adsorbent type sorbents are better suited for the separation of a mixture on the basis of chemical type (e.g. olefins, esters, acids, aldehydes, alcohols, etc.) than for separation of individual members of a homologous series. For the latter, partition chromatography is preferred wherein an inert solid support like silica gel, is coated with a liquid phase. For application to gas chromatography the liquid must be nonvolatile. For liquid chromatography, the stationary liquid phase must be insoluble in the mobile phase. The stationary liquid phase may however be bonded to the solid support if required. An example of a bonded phase is the result of reacting silica with a chlorosilane. If the resulting stationary phase is more polar than the mobile phase, the technique is referred to as normal-phase chromatography. Otherwise, the name reverse-phase chromatography is used. In liquid chromatography, the order of elution from the column of the solutes in the mobile phase can also be influenced by the solvent carrier of the mobile phase by matching the solvent polarity with the solutes and using more polar adsorbents for less polar solutes and less polar adsorbents for more polar solutes.

Operation modes for large-scale, commercial application of chromatography are mainly of two types: the first and the most common is a transient mode that is a scaled-up version of an analytical chromatograph, referred to as large scale, batch (elution) chromatography. If properly designed, the batch chromatograph operates somewhat like a distillation column, producing a nearly pure cut for each component in the feed and slop cuts for recycle; the second major type of large scale chromatograph is the counter-current flow or simulated counter-current flow mode as discussed in adsorption. This mode is more efficient but complicated and can only separate a mixture into two products. A third mode not yet commercialized, is the continuous cross-current chromatograph. In this technique, a packed annular bed rotates slowly about its axis, past the feed inlet point. Eluant enters the top of the bed uniformly over the entire cross sectional area. Both feed and eluant are fed continuously and are carried downward and around by the rotation of the bed. Because of the different selectivities of the feed components for the sorbent, each component traces a different helical path since each spends different amount of time in contact with the sorbent. Thus, each component is eluted from the bottom of the packed annulus at a different location. In principle, a multicomponent feed can be separated continuously into nearly pure components following separation of the carrier fluid from each eluted fraction.

The adsorbent materials which may be solid, gel, or liquid phase immobilized in or on a solid phase, are kept in a column. When a mobile phase or fluid phase is injected into the packed column, the pulse generated is followed by a solvent or eluent. The pulse enters as narrow concentrated peak but exits dispersed and diluted by additional solvent. Different solutes in the mixture interact differently with the adsorbent which is considered as stationary phase, some solutes interact weakly while some others act strongly. Solutes that interact weakly with the solid matrix pass out of the column rapidly

while others exit slowly due to their strong interaction with the matrix. The differential rates of migration separate the solutes into different peaks that exit at a characteristic retention time. In fact, chromatographic separation is achieved through unequal partitioning of solutes between two phases, i.e. the stationary and mobile phases.

The *elution chromatography* in which the substances emerge from a column into narrow peaks, is being used to achieve maximum purification of a product due to wide separation of peaks. It is used to purify the product even it is diluted. It is different from fixed-bed adsorption (sometimes called *frontal chromatography*) in which the solute is entrapped in the adsorbent and then eluted as a concentrate.

When huge amounts of material are being processed *displacement chromatography* may be attractive. It works on the principle that a molecule with a high affinity for the chromatography matrix competes effectively for binding sites and thus helps in displacing all molecules having lesser affinities. In this technique, the column is subjected to sequential step changes in inlet conditions, e.g. nature of solvent, and the feed mixture is introduced in the bed followed by a constant infusion of displacer solution. The displacer must have a higher affinity for the stationary phase than any compound in the feed solution. The displacer pushes solute off the stationary phase and back into the mobile phase. If conditions are selected properly, the feed components are forced into adjacent square-wave-like zones of concentrated, pure solutes. These zones then break through the end of the column with the zone having the solute with lowest affinity for the stationary phase exiting first. The advantages of displacement chromatography over elution chromatography are that components are resolved into consecutive zones of pure substances rather than peaks and the potential for higher throughput, but the operation is more difficult and in certain cases high resolution, i.e. separation of solutes can be difficult. These chromatographic processes are almost always run as batch operations although schemes for continuous or semi-continuous operation have been proposed. Some important chromatographic methods are:

**Adsorption chromatography (ADC):** In this chromatography, the stationary bed contains solid particles and the solute molecules get adsorbed on solid particles such as alumina, silica gel, by weak van der Waal forces and steric interactions.

**Gel permeation chromatography:** It is also known as *Size exclusion chromatography* or *Gel filtration chromatography*. It separates molecules according to their sizes and shapes. Solute molecules penetrate into small pores of packing particles, get trapped and are removed from the mobile phase. Unequal rate of migration of charged molecules in a buffer through a gel phase under electric field is the basis of *electrophoresis separations*.

**Affinity chromatography (AFC):** It is based on the selective non-covalent interactions between solute molecules and ligands. It is very specific, e.g. enzyme-substrate interaction which may depend on covalent, ionic forces or hydrogen bond formation, but not very robust. Affinity binding may be molecular size and shape specific.

**Ion-exchange chromatography (IEC):** Adsorption of ions or electrically charged compounds including amino acids, peptides and proteins takes place on the ion-exchange resin particles by electrostatic forces. It is used to separate analytes on the basis of their respective charges.

**Liquid-liquid partition chromatography (LLC):** It is a separation technique while the mobile phase is a liquid. This process is based on the different partition coefficients of solute molecules between

an adsorbed liquid phase and passing solution. The adsorbed liquids used are often nonpolar.

**Hydrophobic chromatography (HC):** The hydrophobic interaction between solute molecules (e.g. proteins) and functional groups (e.g. alkyl residues) on support particles is the criterion of the process. This method is a type of reverse phase chromatography, which requires the stationary phase to be less polar than the mobile phase.

**High performance liquid chromatography (HPLC):** In this technique a liquid (mobile phase) at high pressure is passed through a packed column containing solid particles, porous monolithic layer or porous membrane. It is operated on the principle of chromatography, the only difference being high pressure applied to the packed column. Due to flow of liquid at high pressure (high liquid flow rate) and dense column packing, HPLC provides fast and high resolution of solute molecules. Considerable developments in the fifties and sixties led to the emergence of high performance chromatography through use of adsorbent beads smaller than 10 mm. This has improved the fluid dynamics performance of chromatographic separations by more than three orders of magnitude. A 250 mm long column provides thousand theoretical plates required for separation of molecules having a separation factor close to unity. Recent emergence of ultra performance liquid chromatography (UPLC) using smaller particles is a further step towards improving resolution and speed of separation.

The choice of the stationary phase and consequently the type of chromatography depend on the nature of the solutes and process goals. Ion-exchange chromatography is widely used particularly for recovery of proteins. This method offers good resolution of peaks, high capacity, and good speed. HC and LLC share many of the attributes but are best applied when the aqueous phase is at high ionic strength. Also organic solvents may be needed, which may denature proteins or create environmental problems. Adsorption chromatography is relatively inexpensive but the resolutions are often not very sharp. Gel-filtration chromatography is good for buffer exchange and desalting and offers descent resolution. Because gels are compressible, capacity and throughput are often low; new rigid packing for size exclusion chromatography allows faster flow rates. Affinity method offers the possibility of very high selectivity and good capacity and speed. However, such methods can be extremely expensive especially if based on antibodies. For real bioprocesses like recovery of proteins, multiple types of chromatography are used since greater purity is possible if more than one basis of separation is used. Ion-exchange and Affinity chromatography are the most widely used methods to recover proteins from bioprocesses. Some other chromatographic separation techniques like Pyrolysis gas chromatography, Reverse phase chromatography, Counter-current chromatography and Chiral chromatography are being practiced. Of many separation techniques practiced, perhaps the most powerful is the chromatographic separation. Not surprisingly therefore, chromatography is often combined with mass spectroscopy (LC-GC-MS) for high performance separation and identification.

Figure 14.23 shows a typical chromatography column in which a solution is flowing in downward direction. During the movement of the solution, the solute is adsorbed on adsorbent solids and a band is usually formed. The solvent that carries the solute downwards moves along the axis of the column. It is assumed that a rapid equilibrium is established between the solute and the adsorbent; the radial gradients are considered negligible.

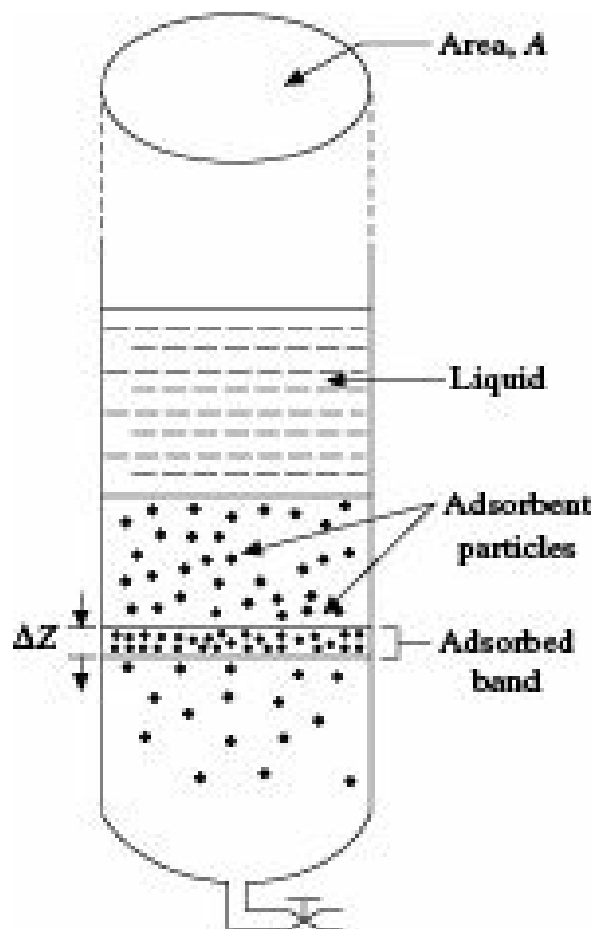


**Figure 14.23** Schematic diagram of a chromatography column.

Consider a small volume ( $DV$ ) of solution introduced into the column containing adsorbent and the solvent carries the adsorbed solute downward in the column. A material balance of the solute over a differential column height,  $DZ$  yields

(Rate of solute (Rate of solute removed (Rate of solute removed removed from solution) = through void space) + through solid)

$$\left( \left[ \frac{\delta c}{\delta Z} \right]_{\Delta Z} \right) \Delta V = \epsilon A \Delta Z \left[ \frac{\delta c}{\delta V} \right]_{\Delta V} + A \Delta Z \left[ \frac{\delta c_s}{\delta V} \right]_{\Delta V} = 0 \quad (14.33)$$

where,  $c_s$  is the amount of solute adsorbed per unit volume of column. The Equation (14.33) can be written as

$$\frac{\delta c}{\delta Z} + A \left( \epsilon \left[ \frac{\delta c}{\delta V} \right] + \left[ \frac{\delta c_s}{\delta V} \right] \right) = 0 \quad (14.34)$$

The amount of solute adsorbed per unit volume of column ( $c_s$ ) is closely related to the adsorption isotherm of the solute as

$$c_s = mf(c) \quad (14.35)$$

where,  $m$  is the amount of adsorbent per unit volume of column and  $f(c)$  is the adsorption isotherm or amount of adsorbed solute per unit amount of adsorbent which is a function of  $c$ . Substituting the derivative of Eq. (14.35) into Eq. (14.34), we get

$$-\frac{\delta c}{\delta Z} = A [(f + mf'(c))] \frac{\delta c}{\delta V} \quad (14.36)$$

Since  $(dc/dZ) = (dc/dV) (dV/dZ)$ , Equation (14.36) can be written as

$$\left(\frac{\delta V}{\delta Z}\right) = A [(f + mf'(c))] \quad (14.37)$$

Integrating Equation (14.37) within the limits  $(Z_0, V_0)$  and  $(Z, V)$ , one can have

$$DZ = \frac{\Delta V}{A[(f + mf'(c))]} \quad (14.38)$$

where  $DV$ ,  $A$ ,  $f$ , and  $m$  are constants. Equation (14.38) shows that  $DZ$  is dependent on  $f'(c)$  which is derivative of  $f(c)$ , or the adsorption isotherm. The location of the solute band formed can therefore be determined knowing the adsorption characteristics of a particular solute on an adsorbent. When the solution contains two solutes  $i$  and  $j$  as in Figure 14.24(a), the solutes form two distinct bands at different axial distances as depicted in Figure 14.24(b) depending on their adsorption characteristics.

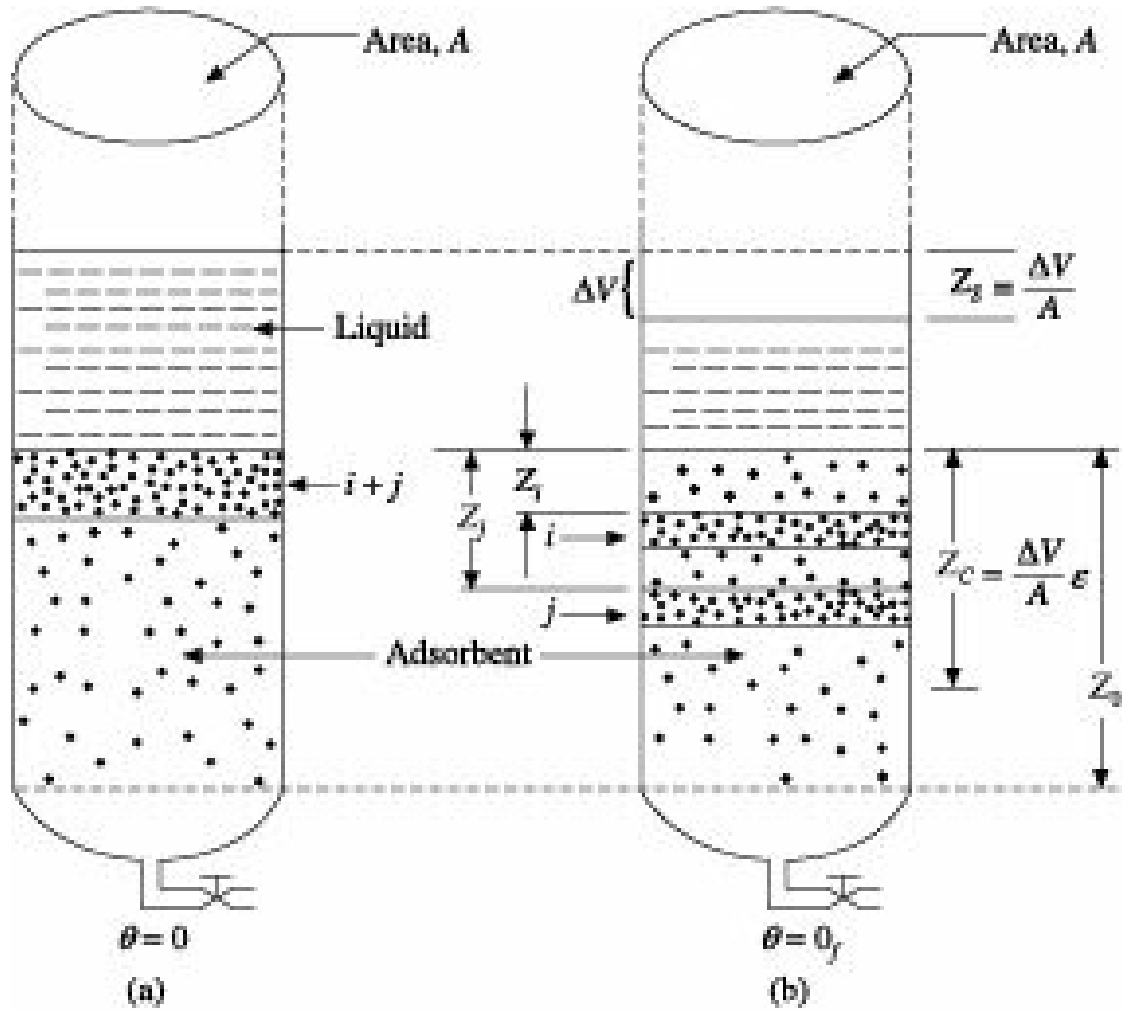


Figure 14.24 Separation of a binary mixture in a chromatographic column.

Let the volume of the solution as in Figure 14.24(a) be  $V_0$  at  $i = 0$ , i.e. initially. After the solute gets adsorbed in the adsorbent, the volume is reduced to  $V$  as shown in Figure 14.24(b), causing a change in volume of  $DV$ . Let us consider  $Z_i$  as the distance (height) travelled by solute  $i$ ,  $Z_S$  representing the height left out due to change in volume in the column caused by the adsorption of solute ( $DV/A$ ), and  $Z_C$  representing the penetration distance of the solvent into the column ( $DV/A f$ ). The resolution ( $R$ ) defined as the ratio of the distance traveled by solute  $i$  to that of solvent in the space above the liquid in the column can therefore be expressed as

$$R = \frac{Z_i}{Z_S} = \frac{1}{1 + mK_D} \quad (14.39)$$

where,  $K_D = f(c_L) = df(c_L)/dc_L$  = partition coefficient. Similarly, the ratio of the travel distance of  $i$  to that of solvent in the column ( $R_f$ ) can be represented as

$$\frac{Z_i}{Z_C} = R_f = \frac{1}{1 + mK_D} \quad (14.40)$$

If the component  $i$  is moved out of the column,  $Z_i$  becomes equal to  $Z_0$  and  $Z_S$  becomes equal to  $V_0/A$ . The ratio of solvent volume to column volume ( $V_r$ ) can therefore be represented as

$$\frac{Z_S}{Z_i} = \frac{V_0}{Z_0 A} = 1 + mK_D \quad (14.41)$$

This principle of chromatography is applicable to fixed column adsorption, partition, ion-exchange and affinity chromatography. The theory of gel-filtration chromatography is somewhat different. In gel-filtration chromatography, solute molecules diffuse into porous structures of support particles depending on their molecular size and shape. Small solute molecules get into the fine pore structures of the support particles and remain in contact with the solid for long period while large molecules are adsorbed on the outer surface and remain in contact with the solid for a short period. When the column is eluted, the largest molecules appear first in the eluant solvent, and the smallest molecules last. Different bands of solute molecules are obtained on the basis of their size and shape.

Consider the case where a buffer with the solute of interest is added to the column, followed by sufficient washes to elute the original buffer solution.

The total volume of the buffer solution eluted from the column over a certain period of time is

$$V_e = V_f + K_D V_i \quad (14.42)$$

where

$V_e$  = total eluant buffer volume

$V_f$  = void volume in the column which is the volume of fluid filling the void space outside the gel particles

$V_i$  = total void volume inside the gel particles, and

$K_D$  = partition coefficient

For large molecules that do not penetrate inside the gel structure,  $K_D = 0$ , for small molecules that completely penetrate inside the gel,  $K_D = 1$ . Equation (14.42) can be rewritten as

$$\frac{V_e}{V_0} = 1 + K_D \frac{V_i}{V_0} \quad (14.43)$$

Gel-filtration chromatography can be used to determine the molecular weight of macromolecules.

Affinity chromatography is based on the highly specific interaction between solute molecules and ligands attached on polymeric or ceramic beads in a packed column. The matrix is usually agarose. However, polyacrylamide, hydroxyethyl methacrylate, cellulose, and porous glass can also be used as

matrix beads. Spacer arms between the matrix and ligand are usually linear aliphatic hydrocarbons. The use of spacer arms may reduce the steric hindrance generated by the matrix. Coupling between the matrix and ligand depends on the functional groups present on the matrix and ligand. Chemically reactive groups on the support matrix usually are —OH, —NH<sub>2</sub> or —COOH groups. If the reactive group on the matrix is an —OH group (polysaccharides, glass, hydroxyalkyl methacrylate), then cynogen bromide is used as coupling agent.

Another type of affinity chromatography is IMAC (immobilized-metal-affinity chromatography) which exploits the different affinities that solutes have for metal ions chelated to a support surface.

The theory of chromatography derived, is based on many simplifying assumptions. Usually the analysis of actual columns is more complicated owing to dispersion, wall effects, and lack of local equilibrium. Wall effects can be reduced by keeping the column diameter to bead diameter ratio larger than 10. But compression can occur under some operating conditions and can further complicate the analysis of the system by causing flow irregularities. Understanding these hydrodynamic and kinetic effects is also critical for scaling-up of chromatographic processes. These effects alter the shape of the peaks exiting the column. In addition, the step controlling the rate of adsorption will alter peak size. For a porous support internal diffusion, diffusion through the external film or external dispersion in laminar flow can control the rate of mass transfer. Recent development in the design of packings for chromatography columns helps in scale-up. Rigid mechanically strong particles with macropores allow convective flow both around and through particles. The macropores are initially connected with the micropores thus resulting in good mass transfer. These particles allow fast flow of solvent and solutes, and reduce problems of bed compression allowing column length to be increased.

Chromatography is one of the few separation techniques that can separate a multicomponent mixture into nearly pure components in a single device, generally a packed column with a suitable sorbent. The degree of separation depends on the length of the column and the differences in component affinities for the adsorbent.

### ***Combo unit in chromatographic separation***

Integration of reaction and adsorption has been explored in chromatographic reactors, and in periodic separating reactors. Simulated moving bed chromatographic reactor where there is continuous counter-current chromatographic separation with chemical reaction, allows higher yields and conversions for an equilibrium reaction. Rotating cylindrical annulus chromatographic reactor is another category of adsorptive reactor investigated for hydrolysis of aqueous methyl formate and dehydrogenation of cyclohexane to Benzene (Krishna 2002). Some other processes investigated in pilot scale are: esterification of glycerine with acetic acid and MTBE synthesis in simulated moving bed chromatographic reactor (SMBCR); hydrogenation of mesitylene and biosynthesis of dextran polymer from sucrose in chromatographic pulse reactor; enzymatic production of *L*-amino acids in centrifugal partition chromatographic reactor; dissociation of dicyclopentadiene in rotating cylindrical annulus chromatographic reactor, etc. It is expected that some of the processes will be commercialized in the near future.

### ***Nomenclature***

$a$  : specific surface, L<sup>2</sup>/L<sup>3</sup>

$A$  : mass or mass velocity of carrier fluid unadsorbed by the solid, M or  $M/L^2$ ; Area of the adsorption column,  $L^2$

$b$  : Langmuir equilibrium constant

$B$  : mass or mass velocity of pure adsorbent, M or  $M/L^2q$

$c$  : solute concentration in fluid,  $M/L^3$

$c^*$  : equilibrium solute concentration in the liquid (feed),  $M/L^3$

$c_0$  : concentration of the adsorbate (solute) in the feed,  $M/L^3$

$c_b$  : breakthrough capacity of the bed

$c_s$  : saturation capacity of the bed; amount of adsorbed solute per unit volume of column

$C$  : temperature dependent constant

$F$  : mass or mass velocity of feed, M or  $M/L^2q$

$F_A$  : flow rate of solute per unit cross section of bed,  $M/L^2q$

$H$  : enthalpy,  $FL/M$

$H_{toG}$  : height of overall transfer unit in terms of gas phase, L

$k, k', K$  : constants

$K_D$  : partition coefficient

$K_y$  : overall gas phase mass transfer coefficient,  $M/L^2q$  (M/M)

$m$  : constant

$n$  : constant

$N_{toG}$  : number of overall transfer unit in terms of gas phase, dimensionless

$p'$  : partial pressure,  $F/L^2$

$p$  : vapour pressure,  $F/L^2$

$P$  : total pressure,  $F/L^2$

$q_F$  : loading of the adsorbent in each cycle, M

$R$  : gas constant, resolution i.e. ratio of the distance travelled by solute to that of solvent in the space above the column

$R_f$  : ratio of travel distance of  $i$  to that of solvent in the column

$T$  : absolute temperature,  $T$

$u_0$  : superficial fluid velocity,  $L/q$

$v$  : volume of solution added per unit mass of adsorbent,  $L^3/M$

$V_0$  : volume of solvent required to displace out of the packed column,  $L^3$

$V_r$  : ratio of solvent volume to column volume, dimensionless

$V_f$  : total void volume outside the gel particles,  $L^3$

$W$  : solute content of solid,  $M/M$

$X$  : concentration of adsorbate in adsorbent,  $M/M$

$X^*$  : amount of gas (solute) adsorbed at equilibrium per unit mass of the adsorbent, M/M

$X_{\max}$  : maximum amount of absorbate adsorbed per unit mass of adsorbent at a given partial pressure of adsorbate, M/M

$Y$ : concentration of solute in fluid, M/M

$Z$  : height or length of bed, L

$Z_C$  : penetration distance of the solvent into the column, L

$Z_i$  : distance travelled by the solute, L

$Z_S$  : distance travelled by the solute above the adsorption zone, L

### Greek Letters

$\tau$  : density of fluid M/L<sup>3</sup>

$\tau_b$  : bulk density of the bed, M/L<sup>3</sup>

$\{\}$  : fraction of solid surface covered by adsorbate, —

$f$  : degree of saturation in MTZ, porosity of the adsorbent bed

$i$  : time for breakthrough at which the LES is evaluated, □

$i_s$  : ideal adsorption time or time required to attain saturation, □

$i_b$  : time required to reach break point, □

### Numerical Problems

**14.1** Estimation of the Amount of Activated Carbon, Depth of the Carbon Bed, and the Diameter of the Adsorber: Determine (i) the required amount of activated carbon, (ii) the depth of the adsorbent bed and (iii) the diameter of a batch adsorber for adsorbing petrol vapour from its mixture with air. The rate of flow of the vapour and air mixture is 3450 m<sup>3</sup>/hr. The initial concentration of the petrol is 0.02 kg/m<sup>3</sup>. The velocity of the vapour and air mixture is 0.23 m/s reduced to the total cross section of the apparatus, the dynamic activity of the carbon relative to petrol is 7% (mass), the residual activity after desorption is 0.8% (mass), the bulk density of carbon is 500 kg/m<sup>3</sup>. The duration of desorption, drying and cooling of the adsorbent is 1.45 hr.

[Ans: (i) 1612 kg (ii) 0.8 m (iii) 2.3 m]

**14.2** Prediction of Isotherm for Adsorption of Papain on Activated Charcoal: Experiments carried out in the laboratory for adsorption of papain from an aqueous solution on the solid matrix of activated charcoal, revealed the following equilibrium data:

$c^*$ , g papain/L solution	9.295	18.667	28.754	38.278	48.355
$q^*$ , g papain/g charcoal	0.3511	0.6109	0.6614	1.1953	1.2626

Evaluate the constants of Langmuir and Freundlich isotherms, and compare the results.

**Hints:** For the stated problem, Equations (14.2) and (14.4) can be rewritten as

$$q^* = q_m \frac{bc^*}{1 + bc^*} \text{ and } q^* = K \cdot c^{*1/n}, \text{ respectively.}$$

[Ans:  $q_m = 2.4588$  g papain/g charcoal;  $b = 0.01765$  L/g papain;  
 $K = 0.266$  g papain/g charcoal; and  $n = 1.1623$  g papain/L solution.  
Langmuir isotherm gives a better fit.]

**14.3 Computation of the Diameter of the Adsorber and the Time of Adsorption:** Determine (i) the charge of activated carbon, (ii) the diameter of the adsorber, and (iii) the duration of the adsorption of 100 kg of octane vapour from its mixture with air. The following data are available: the initial concentration of the octane vapour in the mixture =  $0.012 \text{ kg/m}^3$ , the velocity of the mixture = 20 m/min, the activity of the carbon with respect to benzene = 7%, the bulk density of carbon =  $350 \text{ kg/m}^3$ , and the depth of the carbon bed = 0.8 m.

[Ans: (i) 1430 kg (ii) 2.55 m and (iii) 1 hr 22 min]

**14.4 Calculation of the Velocity of Adsorbent in a Column:** Determine the minimum velocity of type NaA zeolite in a column apparatus for deep drying of air in the following conditions: initial concentration of the adsorbate is  $0.01 \text{ kg/m}^3$ , the value indicating the break-point concentration of the adsorbate is  $2.94 \times 10^{-6} \text{ kg/m}^3$ , the diameter of the zeolite particles is 0.002 m, and the amount of the adsorbate corresponding to equilibrium with the initial concentration of the adsorbate (it is taken from the adsorption isotherm in kg/kg, and is multiplied by the bulk density of the adsorbent particle in  $\text{kg/m}^3$ ) is  $170 \text{ kg/m}^3$ . The velocity of the gas stream related to the total cross section of the apparatus is 0.5 m/s.

[Ans:  $2.94 \times 10^{-5} \text{ m/s}$ ]

**14.5 Estimation of Break-point Coefficient and Loss in the Break-point Time:** Experimental data have revealed that the duration of adsorbing chloropicrin vapour (initial concentration =  $6.6 \text{ g/m}^3$ ) using a bed of activated carbon with a depth of the bed of 0.05 m and a cross-sectional area of  $0.01 \text{ m}^2$  at a volumetric flow rate of  $0.03 \text{ m}^3/\text{min}$  is 336 min. According to the isotherm for chloropicrin, the activity of carbon is  $222 \text{ kg/m}^3$ . The diameter of the carbon particles is 1.5 mm. Find (i) the break-point coefficient of the bed,  $K$ , (ii) the loss in the break-point time (kinetic coefficient),  $x_0$ , and (iii) the value of the dynamic characteristics  $B_1$  and  $B_2$ .

[Ans: (i) 187 hr/m (ii) 224 min (iii) 33600, 259000]

**Hints:** The break-point time,  $x$  is determined by Shilov's equation as  $x = K(H - h)$  in which  $Kh = x_0$ . Hence,  $x = KH - x_0$  where,  $K$  is the break-point coefficient of the sorbent bed, s/m;  $H$  is the depth of the sorbent bed, m,  $h$  is the depth of the unutilized sorbent bed in dynamic conditions, m, and  $x_0$  is the kinetic coefficient, or the loss in the break-point time of the sorbent bed, equal to the time spent for the formation of the adsorption zone, s.

The break-point coefficient of a bed can be found by the equation  $K = (a_0/vc_0)$ ,  $a_0$  being the equilibrium adsorption capacity,  $\text{kg/m}^3$ ;  $v$  being the velocity of the vapour and gas mixture related to the total cross section of the apparatus,  $\text{m/s.}$ ;  $c_0$  being the initial concentration of the adsorbate in the vapour and gas mixture,  $\text{kg/m}^3$ .

The dynamic characteristics,  $B_1$  and  $B_2$ , are observed for the same adsorbent and adsorbate at a

constant concentration and temperature of the vapour and gas stream, and are expressed by the following equations:

$B_1 = Kv$ , and  $B_2 = (x_0 \sqrt{v})/d$ , where  $d$  is the mean diameter of the sorbent grains, m.

**14.6 Determination of Break-Point Coefficient and Time of Adsorption:** In the preceding Problem 14.5, the velocity of the vapour and air mixture is 6 m/min. Find (i) the break-point coefficient of the bed, (ii) the loss in the break-point time, and (iii) the duration of adsorption for a bed having a depth of 0.1 m.

[Ans: (i) 5600 min/m (ii) 159 min (iii) 401 min]

**14.7 Determination of Break-Point Time and Loss in Break-Point Time:** Determine (i) the break-point time and (ii) the loss in the break-point time for the adsorption of carbon tetrachloride vapour by a bed of activated carbon having a depth of 0.10 m. The velocity of the vapour and gas mixture is 5 m/min, the diameter of the carbon particles is 2.75 mm, the dynamic characteristics are 14500 and 52945.

[Ans: (i) 225 min and (ii) 65 min]

**14.8 Computation of the Amount of Adsorbent in a Batch Adsorber, Diameter of the Adsorber and the Break-Point Time:** A batch adsorber processes  $2000 \text{ m}^3$  of a vapour and air mixture having a diethyl ether concentration of  $0.006 \text{ kg/m}^3$  during one cycle. The temperature of the process is  $20^\circ\text{C}$ , the pressure is atmospheric, the velocity of the stream of vapour and gas mixture is 13 m/min, the concentration of the mixture after it leaves the adsorber is  $3 \times 10^{-5} \text{ kg/m}^3$ . The adsorbent is activated carbon with a grain diameter of 0.004 m and a bulk density of  $500 \text{ kg/m}^3$ . The depth of the carbon bed is 0.7 m.

According to benzene isotherm for  $20^\circ\text{C}$  using the same grade of carbon, construct an isotherm of the adsorption of diethyl ether from air at  $20^\circ\text{C}$ . Using this isotherm, find the amount of activated carbon needed for one batch, the diameter of the adsorber, and the break-point time.

Data for benzene isotherm are given as

Concentration of adsorbed benzene, kg/kg:	0.103	0.122	0.208	0.233	0.262	0.276	0.294	0.318	0.338	0.359
Partial pressure of benzene, mm Hg:	0.105	0.223	1	3	8	13	19	33	42	50

**Hints:** You may use the following expression:

$a_2 = (a_1 V_1)/V_2$ , where  $a_1$  and  $a_2$  are the concentrations of benzene and ether, kg/kg and  $V_1$  and  $V_2$  are the molar volumes of benzene and ether in the liquid state,  $\text{m}^3/\text{kmol}$ .

[Ans:  $0.182 \text{ m}^3$ ,  $0.69 \text{ m}$ ,  $3.9 \text{ hr}$ ]

**14.9 Depth of the Bed of Activated Carbon in a Continuous Adsorption Operation:** Using the benzene adsorption isotherm at  $20^\circ\text{C}$ , determine the velocity and the operating depth of the bed of activated carbon in the continuous adsorption of a vapour and gas mixture having an initial concentration of  $0.11 \text{ kg/m}^3$ , a velocity of 20 m/min, and a mass transfer coefficient of  $4 \text{ s}^{-1}$ . The carbon in the process of adsorption is saturated up to 80% of its static activity. The residual activity of the carbon after desorption is 14.5% of the initial static activity. The vapour and gas mixture must be purified to a concentration of not more than  $0.01 \text{ kg/m}^3$ .

[Ans: Velocity: 0.08 m/s and depth of bed: 0.4 m]

**14.10 Determination of Time of Adsorption Using an Adsorption Isotherm:** Using an adsorption isotherm for a mixture of vapours of ethyl alcohol and diethyl ether, determine the duration of adsorption of this mixture by a bed of activated carbon having a depth of 1.0 m. The initial concentration of the mixture is  $0.072 \text{ kg/m}^3$ , the mean concentration at the outlet from the adsorber is  $0.0001 \text{ kg/m}^3$ , the velocity of the vapour and gas mixture related to the total section of the adsorber is 12 m/min, the diameter of the activated carbon particles is 0.004 m, their bulk density is  $500 \text{ kg/m}^3$ , the adsorption temperature is  $20^\circ\text{C}$ ; and the pressure is atmospheric.

[Ans: 1 hr 38 min]

**14.11 Estimation of Depth of the Adsorbent Bed using Adsorption Isotherm:** A continuous adsorber of diameter of 0.32 m processes  $120 \text{ m}^3$  of vapour and gas mixture per hour. The activated carbon supplied to the adsorption zone contains  $4 \text{ kg/m}^3$  of the adsorbate; at the outlet from this zone its adsorbate content reaches  $30 \text{ kg/m}^3$ . The concentration of the vapour and gas mixture entering the adsorber is  $0.105 \text{ kg/m}^3$ , and that of the effluent mixture is  $0.0065 \text{ kg/m}^3$ . The coefficient of mass transfer of the adsorbate in the conditions of the adsorption operation is  $5 \text{ s}^{-1}$ . Using the adsorption isotherm, determine the velocity of the activated carbon and the depth of its bed.

[Ans: Velocity: 0.00128 m/s and depth of bed: 0.5 m]

**14.12 Amount of Heat Liberated During First Adsorption Cycle:** A vertical adsorber 3 m in diameter with a steel tube of 0.35 m diameter is fed with  $170 \text{ m}^3/\text{min}$  of a vapour and gas mixture. The initial concentration of the ethyl alcohol vapour in the mixture is  $0.02 \text{ kg/m}^3$ . The concentration of ethyl alcohol in the discharged gas is  $0.0002 \text{ kg/m}^3$ , the depth of the activated carbon bed is 1.5 m, the bulk density of the carbon is  $500 \text{ kg/m}^3$ , and the duration of one adsorption cycle is 4 hr 37 min. Find the amount of heat liberated in the adsorber during the first cycle.

[Ans:  $228 \text{ kJ/kg of carbon; or } 1.21 \times 10^6 \text{ kJ}$ ]

**14.13 Estimation of Height of Resin Bed:** An antibiotic is separated from a fermentation broth by adsorption on a resin bed in a column. The bed is 5 cm in diameter and contains  $0.75 \text{ cm}^3 \text{ resin/cm}^3$  bed. The overall mass transfer coefficient is  $12 \text{ hr}^{-1}$ . The antibiotic with a concentration of 5 g/L solution is desired to be separated till its concentration in the effluent becomes 0.2 g/L. The superficial velocity of liquid is 1.7 m/hr. The equilibrium line relationship is

$$X = 10Y$$

where  $X$  and  $Y$  are the g solute/L resin and g solute/L solution, respectively.

Determine the height of the column for the desired separation. [Ans: 0.91 m]

**Hints:** Equation (14.21) for the stated operation can be written as

$$Z = \frac{\frac{u_0}{k_p(1-\epsilon)}}{1 - \int_{Y^*}^{Y_e} \frac{dY}{(Y - Y^*)}}$$

where  $(1 - f)$  in  $\text{cm}^3 \text{ resin}/\text{cm}^3 \text{ bed}$ ; and  $K_y$  in  $\text{hr}^{-1}$ ; and  $u_0$ , the superficial velocity of solution in  $\text{m/hr}$ .

**14.14 Determination of Equilibrium Solute Concentrations and the Ratio of Travel Distances of Solute to Solvent:** A solute protein is to be separated from a liquid phase in a chromatographic column. The adsorption isotherm is given by the relation

$$c_S = kc_L^2$$

where,  $c_S$  is the solute concentration in solid phase ( $\text{mg of solute/mg adsorbent}$ ) and  $c_L$  is the liquid phase concentration of solute ( $\text{mg of solute/mL liquid}$ ). Use the following information:

$k = 0.4$ ,  $f = 0.3$ ,  $A = 25 \text{ cm}^2$ , and  $M = 10 \text{ g adsorbent}/100 \text{ mL column} = 100 \text{ mg/mL}$ .

- (i) For  $V = 400 \text{ mL}$  and  $Z = 25 \text{ cm}$ , determine the equilibrium solute concentrations in liquid and solid phases.
- (ii) Determine the ratio of travel distances of solute to solvent,  $R_f$ .

[Ans: (i)  $4.25 \times 10^{-3}$ ,  $7.225 \times 10^{-6}$ , (ii) 0.469]

### ***Short and Multiple Choice Questions***

1. State with reasons whether physical adsorption is a reversible or an irreversible phenomenon.
2. What is the order of heat exchange in chemisorption?
3. Under what conditions can adsorption isotherms be represented by Freundlich Equation?
4. What is the relation between heat of wetting and heat of adsorption in physical adsorption?
5. What is the difference between differential and integral heats of adsorption?
6. How does integral heat of adsorption change with increase in adsorbate concentration?
7. Between adsorption equilibrium and desorption equilibrium, which one is usually higher in adsorption hysteresis?
8. What do you mean by mass transfer zone within an adsorbent?
9. What are molecular sieves?
10. Name three adsorbents which are commonly used for dehydration of air.
11. Chemisorption is
  - (a) same as van der Waals adsorption
  - (b) a reversible phenomenon
  - (c) an irreversible phenomenon
  - (d) none of these
12. Rate of adsorption increases as the
  - (a) temperature increases
  - (b) temperature decreases
  - (c) pressure decreases
  - (d) size of adsorbent increases
13. Molecular sieves are
  - (a) synthetic zeolite crystalline metal alumino silicates

(b) obtained by destructive distillation of wood

(c) porous form of aluminium oxide

(d) porous form of silicon dioxide

14. With increase in temperature at a given equilibrium pressure, the concentration of adsorbed gas in a solid adsorbent

(a) increases                         (b) remains unchanged

(c) decreases                         (d) increases exponentially

15. In case of adsorption hysteresis, the desorption equilibrium pressure is

(a) always lower than that obtained during adsorption

(b) always higher than that obtained during adsorption

(c) same as that obtained during adsorption

(d) can be either higher or lower than that obtained during adsorption

16. Freundlich equation is applicable to adsorption of solute from

(a) dilute solutions over a small concentration range

(b) concentrated solutions

(c) gas mixtures at high pressure

(d) none of these

17. The pore size of molecular sieve  $5\text{\AA}$  is

(a) 5 nm                             (b)                     0.5 nm

(c) 0.05 nm                         (d)                     0.5 m

18. The change in enthalpy per unit weight of gas when adsorbed on gas free or degassed adsorbent to form a definite concentration of adsorbate is called its

(a) integral heat of adsorption

(b) differential heat of adsorption

(c) heat of wetting

(d) heat of normal condensation

19. With the lowering of equilibrium pressure at a given temperature, the amount of adsorbate on adsorbent

(a) increases                         (b) remains the same

(c) decreases                         (d) may increase or decrease

20. Desorption of the adsorbed solute by a solvent is called

(a) leaching                         (b) extraction

(c) dialysis                         (d) elution

21. With increase in concentration of the adsorbate, the integral heat of adsorption

(a) increases                         (b) remains unchanged

(c) decreases                         (d) may increase or decrease

22. As an adsorbent approaches complete saturation, the differential heat of adsorption approaches

(a) heat of normal condensation                         (b) integral heat of adsorption

(c) zero

*Answers to Multiple Choice Questions*

11. (c) 12. (c) 13. (a) 14. (c) 15. (a) 16. (a) 17. (c)

## References

- Annadurai, G., R. Juang and D. Lee, *J. Hazard. Mat.*, **2830**, 1 (2002).
- Braunauer, S., S. Emmet and E. Teller, *J. Am. Chem. Soc.*, **60**, 309 (1938).
- Braunauer, S., L.S. Deming, W.E. Deming and E. Teller, *J. Am. Chem. Soc.*, **62**, 1223 (1940).
- Collins, J.J., *Chem. Eng. Prog. Symp. Series*, **63**(74), 31 (1967).
- Cooney, D.O., *Chem. Eng. Comm.*, **91**, 1 (1990).
- Clark, AJ., *The Theory of Adsorption and Catalysis*, Academy, New York (1970).
- Crittenden, B., *The Chemical Engineer*, No. 452, 21 (Sept. 1988).
- Crittenden, B. and W. J. Thomas, *Adsorption Technology and Design*, Butterworth-Heinemann, Oxford (1998).
- Datta, N.C., *Chem. Ind. Digest*, **XIX**(9), 48 (2006).
- Freundlich, H., *Colloid and Capillary Chemistry*, Methuen (1926).
- Glueckauf, E. and J.I. Coates, *J. Chem. Soc.*, 1315 (1947).
- Gregg, S.J. and K.S.U. Sing, *Adsorption, Surface Area and Porosity*, Academic, New York (1967).
- Harrison, Douglas P., *Ind. Chem Eng. Res.*, **47**, 6486 (2008).
- Hufton, J.R., S. Mayoraga and S. Sircar, *AIChE J.*, **45**, 248 (1999).
- Ismadji, S. and S.K. Bhatia, *Canad. J. Chem. Eng.*, **78**, 892 (2000).
- Keefer, B.G. and D.G. Doman, *WIPO International Publication*, No. WO 97/39821 (1997).
- Keller, G.E., R.A. Anderson and C.M. Yon, *Adsorption* in *Handbook of Separation Process Technology*, R.W. Rousseau (Ed), John-Wiley and Sons, New York (1987).
- Knaebel, K.S., *Chem. Eng.*, 92 (November, 1995).
- Krishna, R., *Chem. Eng. Sci.*, **57**, 1491 (2002).
- Langmuir, I., *J. Am. Chem. Soc.*, **38**, 2221 (1916).
- Ledoux, E., 'Adsorption' in *Kirk-Othmer's Encyclopedia of Chemical Technology*, Vol. 1, (1947).
- Lee, K.B., M.G. Beaver, H.S. Caram and S. Sircar, *Adsorption*, **13**, 385 (2007a).
- Lee, K.B., M.G. Beaver, H.S. Caram and S. Sircar, *AIChE J.*, **53**, 2824 (2007b).
- Lee, K.B., M.G. Beaver, H.S. Caram and S. Sircar, *Ind. Chem. Eng. Res.*, **46**, 5003 (2007c).
- Lode, F., G. Francesconi, M. Mazzotti and M. Morbidelli, *AIChE J.*, **49**, 1516 (2003).
- Markham, E.C. and A.F. Benton, *J. Am. Chem. Soc.*, **53**, 497 (1931).
- Mckay, G., G.R. Prasad and P.R. Mowli, *Water Air Soil Pollut.*, **29**, 273 (1986).
- Mutasim, Z.Z., and J.H. Bowen, *Trans. Inst. Chem. Engrs.*, **69**, Part-A, 108 (March 1991).
- Nigam, P., I.M. Banat, D. Singh and R. Marchant, *Process Biochem.*, **31**, 435 (1996).
- Peters, M.S., K.D. Timmerhaus and R.E. West, *Plant Design and Economics for Chemical Engineers*, 5th ed., McGraw-Hill (2003).
- Ruthven, D.M., S. Farooq and K.S. Knaebel, *Pressure-Swing Adsorption*, VCH, New York (1994).
- Sircar, S., *Gas separation by Rapid Pressure Swing Adsorption*, US Patent 5,071,449 (1991).

- Sircar, S., *Adsorption*, **6**, 359 (2000).
- Sircar, S., *Adsorption Sci. Tech.*, **19**, 347 (2001).
- Sircar, S., *Ind. Eng. Chem. Res.*, **41**, 1389 (2002).
- Sircar, S. and B.F. Hanley, *Adsorption*, **1**, 313 (1995).
- Sircar, S. and C.M.A. Golden, *Process for removal of bulk CO<sub>2</sub> from a wet gas at high temperature by Pressure Swing Adsorption*, US Patent 6,322,612 (2001).
- Sircar, S., M.B. Rao and T.C. Golden, in *Studies in Surface Science and Catalysis*, A. Dabrowski (Ed.), Elsevier Science, New York, Vol. **120A**, 395 (1998).
- Skarstrom, C.W., *Method and Apparatus for fractionating gaseous mixtures by Adsorption*, US Patent 2,944,627 (1960).
- Skarstrom, C.W., in *Recent Developments in Separation Science*, Vol. 2, N.N. Li (Ed.), CRC Press, Cleveland, Ohio (1972).
- Stroehlein, G., Y. Assuncao, N. Dube, A. Bardow, M. Mazzotti and M. Morbidelli, *Chem. Eng. Sci.*, **61**, 5290 (2006).
- Treybal, R.E., *Mass Transfer Operations*, 3rd ed., McGraw-Hill, Singapore (1985).
- Valenzuela, D.P. and A.L. Meyers, *Adsorption Equilibrium Data Handbook*, Prentice Hall, Englewood Cliffs, NJ (1989).
- Viecco, G.A. and H.S. Caram, *Chem. Eng. Sci.*, **61**, 6869 (2006).
- Yang, R.T., *Gas Separation by Adsorption Processes*, Butterworth Boston (1987).
- Zhang, Y., K. Hidajat and A.K. Ray, *Biochem. Eng. J.*, **35**, 341 (2007).

# Membrane Separation

## 15.1 Introduction

The development of separation processes with reduced energy consumption and minimal environmental impact is critical for sustainable operation. The basis of any separation method is exploitation of physico-chemical differences between the molecules. Separation of cell components into major classes like proteins, lipids, minerals, sugars and nucleic acids is rather easy. One has to encounter problems for the separation of chemically and/or biologically similar compounds inevitably found in most instances. In order to describe ease or difficulty of separation of any two such compounds, one has to know the ‘separation factor’. The separation of the materials is impossible when the separation factor becomes unity. Attempts are being made to find a property that gives the separation factor well away from unity. The membrane processes as one of the separation processes are finding wide applications ranging from water treatment to reactors to advanced bioseparations. The use of membranes has become indispensable in production, quality control and research in the several fields. Today, we find, on one hand, the commercial exploitation of the first generation membrane processes and, on the other hand, development of the next generation membrane processes. Although membranes as separating agents have been known for more than 100 years, large-scale applications have only appeared in the last six decades. The first commercial membranes for practical applications were manufactured by the Sartorius in Germany after World War I, the know-how necessary to prepare these membranes originated from the early work of Zsigmondy and Bachmann (1918). The first practical membrane application on haemodialysis using cellophane membranes was introduced by Kolff in 1940 while taking care of casualties after the German invasion of the Netherlands and the recovery of an acute renal failure patient undergone the treatment was reported (Kolff and Berk 1944). In 1940s, porous fluorocarbons were used to separate  $^{235}\text{UF}_6$  from  $^{238}\text{UF}_6$ . As far as industrial membrane applications are concerned, a breakthrough was achieved by the development of an asymmetric membrane (Loeb and Sourirajan 1962). In the mid-1960s, reverse osmosis with cellulose acetate was first used to desalinate seawater to produce potable water (Havens and Guy 1968), and also the ultrafiltration started its use in the commercial scale for concentration of macromolecules in USA. In 1979, a hollow-fibre membrane of polysulphone was introduced by Monsanto Chemical Company for recovery of hydrogen from a gas mixture (Bollinger et al. 1982). The commercialization of alcohol dehydration by pervaporation began in 1980s in Germany and Netherlands, as did the large-scale application of emulsion liquid membranes for the removal of metals and organics from waste water. The replacement of more common separation operations with membrane separations has the potential to save large amount of energy. This replacement requires the production of defect-free, long-life membranes with high mass transfer flux.

on a large scale and the fabrication of the membrane into compact, economic modules of high surface area per unit volume.

Membrane technology undoubtedly is an emerging technology because of its multidisciplinary characteristics. The benefits of such technology can be summarized as

- separation can be carried out continuously
- energy consumption is generally low
- membrane processes can be used in the hybrid processing
- separation can be carried out under mild conditions
- scaling-up is easy
- membrane properties are variable and can be adjusted
- no additives are required

In membrane separation process, a feed consisting of a mixture of two or more components is partially separated by means of a semi-permeable barrier which separates components of a mixture or solution by selectively controlling their movement from one side of the membrane to the other. In some cases, particles or molecules of sizes larger than those of the pores of the membrane are excluded right at the upstream side while in others, they move through the membranes at differential rates depending upon their molecular weights or volumes so that separation becomes possible.

## 15.2 Membranes

A membrane in a very general fashion can be defined as a selective barrier between two phases, the term *selective* being inherent to a membrane or a membrane process. The definition does not say anything about membrane structure or its function (Mulder 1996).

Membranes can be classified in many ways:

According to the resources, membranes may be of two types—natural or biological (living or nonliving) and synthetic (organic or inorganic).

According to morphology or structure, membranes again may be of two types—symmetric (porous or nonporous) and asymmetric as shown in Figure 15.1.

Membranes are of two major types:

- (i) thin layers of rigid materials having numerous micropores such as porous glass or sintered metals, and
- (ii) flexible films of synthetic polymers specially manufactured to have high permeability for specific substances.

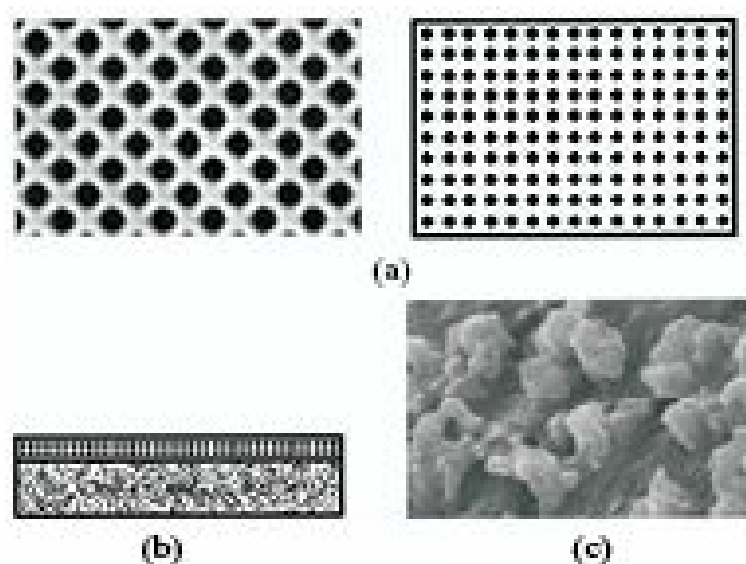


Figure 15.1 (a) Symmetric, (b) asymmetric composite, and (c) asymmetric polymeric membrane.

### 15.3 Transport in Membranes

As mentioned, selective barrier, i.e. membrane accomplishes a separation and hence characterizes a membrane process. The semipermeable barrier helps to transport very fast one or more species than another or other species. Because of differences in physical and/or chemical properties between the membrane and the permeating component(s) as shown in Figure 15.2, a feed mixture is separated. After separation a part of the feed that does not pass through the membrane and is retained, is called *retentate* whereas the other part of the feed that passes through the membrane, is known as *permeate*.

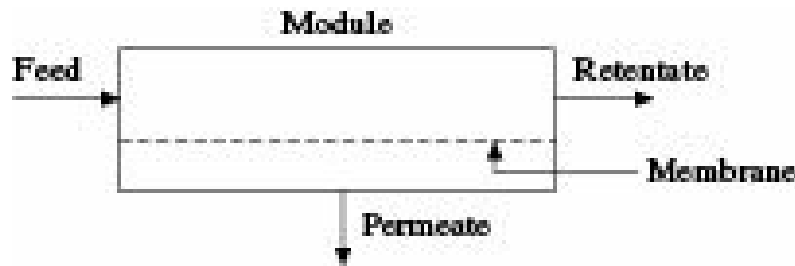


Figure 15.2 Retentate and permeate streams in a membrane separation process.

The *membrane structure* can be considered to be an interface in which a permeating molecule or particle experiences a friction or resistance. Transport through the membrane takes place due to the driving force acting on the components in the feed and the permeation rate through the membrane is proportional to the driving force as

$$J_i = -D_i \frac{\text{Driving force}}{\text{Length}} \quad (15.1a)$$

$$J_{M,i} = -q_i \frac{\text{Driving force}}{\text{Length}} \quad (15.1b)$$

where,

$J_i$  and  $J_{M,i}$  = permeation mass or volumetric flux of component  $i$ , respectively

$D_i$  = diffusivity of component  $i$

$q_i$  = the permeability coefficient of component  $i$ , the phenomenological constant

driving force may be temperature, concentration or pressure and length means the distance traversed

in perpendicular direction to the transport barrier.

The analogous equations used for transport of some properties are given in Table 15.1.

**Table 15.1** Phenomenological equations

Mass flux	$J_A = -D_{AB} \frac{dc}{dz}$ (Fick's law, $D_{AB}$ is the mass diffusivity)
Volume flux	$J_V = -q_A \frac{dp}{dz}$ (Darcy's law, $q_A$ is the permeability coefficient)
Heat flux	$J_h = -\alpha \frac{dT}{dz}$ (Fourier's law, $\alpha$ is the thermal diffusivity)
Momentum flux	$J_m = -\nu \frac{dy}{dz}$ (Newton's law, $\nu$ is the momentum diffusivity)
Electrical flux	$J_e = -(1/R) \frac{de}{dz}$ (Ohm's law, $1/R$ is the electrical conductivity)

An overview of various membrane processes and driving forces is given in Table 15.2 (Mulder, 1996).

**Table 15.2** Some membrane processes and driving forces

Membrane process	Phase 1	Phase 2	Driving force
Microfiltration	L	L	DP
Ultrafiltration	L	L	DP
Nanofiltration	L	L	DP
Reverse osmosis	L	L	DP
Piezodialysis	L	L	DP
Gas separation	G	G	Dp
Vapour permeation	G	G	Dp
Pervaporation	L	G	Dp
Electrodialysis	L	L	DE
Membrane electrodialysis	L	L	DE
Dialysis	L	L	Dc
Diffusion dialysis	L	L	Dc
Membrane contactors	L	L	Dc
	G	L	Dc/Dp
	L	G	Dc/Dp
Thermo-osmosis	L	L	DT/Dp
Membrane distillation	L	L	DT/Dp

## 15.4 Membrane Materials

The industrial membranes are usually fabricated from natural or synthetic polymers. Natural polymers include wool, rubber and cellulose. Some of the commonly used materials are cellulose acetate, cellulose triacetate, cellulose nitrate, regenerated cellulose, nylon 66, polyacrylonitrile, polyimide, polypropylene, polystyrene, polyisoprene, polycarbonate, polytetrafluoroethylene (PTFE), aromatic polyamide, polyamide hydrazide, polyvinyl alcohol derivatives, polyvinylidene difluoride (PVDF), polysulphone, poly ether block amide (PEBA), PDMS/aromatic PA laminated, mordanite with ZSM-5 zeolite, Ge-substituted ZSM-5, and polyurea-polyamide composite. Cellulose compounds having uniform honeycomb structure all throughout are very useful as membrane material. Polymeric membranes are widely used in membrane processes because they are well developed and quite competitive. The pore size may be held to very narrow tolerances within each filter and many sizes can be manufactured for different uses. The commercially available sizes vary from 8 micron to 0.01

micron. The most commonly used pore sizes are—0.2 micron for sterilizing filtration, 0.45 micron for bacterial reduction and particle removal and 0.65 micron for yeast removal. Smaller pore sizes are used for myco-plasma removal and for concentration of proteins and viruses while larger pore sizes are used in clarifying filtration. Such membranes have high initial cost and while mechanically strong, are sometimes brittle. While most membranes are usually made of polymeric compounds, ceramic membranes are gaining popularity due to its mechanical stability, chemical stability, interactions with proteins, flux rates, ease of sterilization (e.g. thermal stability), biocompatibility and cost. These membranes have a high level of chemical resistance, can be sterilized by steam, and have a longer life time. The actual choice of membrane depends on the application, the composition of the feed streams, and required product characteristics.

Gas separation membranes are made in the form of sheets, tubes or hollow fibres as small as 40 microns in diameter. Hollow fibres have the advantage of withstanding high pressures without any support while flat sheets require additional support. Flux through dense polymer films being inversely proportional to the thickness of the membrane, the membrane should be as thin as possible. At the same time, the membrane films should be strong enough to withstand the operating pressure difference, which is usually in the range of 7-140 kN/m<sup>2</sup>. For this reason, thin membrane films, when operated as sheets, are provided with proper support made of porous ceramic, metal or polymer, but more frequently the support is of the same material as that of the membrane and form an integral part of the membrane. Typical gas separation membranes are 50 to 200 microns thick with the active part made of 0.1 to 1 micron polymer film. Gas separation membranes generally utilize the difference in solubility and diffusivity of gases through nonporous polymers. However, a few membranes operate by sieving, Kundsen flow and chemical complex action. Microfiltration membranes are often used for separation of gases from liquids and solids.

Porous membranes are used in microfiltration and ultrafiltration while nanofiltration and reverse osmosis generally employ nonporous membranes. However, some ultrafiltration membranes have *anisotropic* structure. In anisotropic membrane, a thin skin with small pores is formed on top of a thick and highly porous structure. The thin layer provides selectivity while the thicker layer provides mechanical support. With the development of newer membrane materials, anisotropic membranes are used less frequently. Microporous membranes are usually isotropic and have an open, tortuous path structure which causes particle entrapment within the filter or have well defined pores of uniform size. According to some authors (Rameshbabu 1998), nanofiltration membranes are probably charged porous structures.

The factors which promote the formation of a porous membrane are:

- (i) low polymer concentration
- (ii) high mutual affinity between solvent and nonsolvent
- (iii) addition of nonsolvent to the polymer solution
- (iv) lowering of activity of nonsolvent (vapour phase instead of coagulation bath)
- (v) addition of a second polymer to the polymer solution, such as polyvinylpyrrolidone.

The use of a thin layer of a nano-porous adsorbent material as a semipermeable membrane which allows continuous gas separation like the conventional polymeric membrane, has attracted much attention in recent years. The ‘sorption-diffusion’ mechanism of gas transport through an adsorbent membrane permits them to simultaneously offer high permeance and high selectivity for the

preferentially diffusing component.

Membrane processes offer one step separation for all the dissolved constituents on a molecular or ionic level without chemical reaction. However, fouling and degradation of surfaces of polymeric membranes under adverse chemical and thermal conditions have often been a limiting factor for its varied applications. These fouling phenomena plague many biological, environmental and chemical engineering systems such as medical implants, environmental sensors, and membrane processes. Understanding and controlling surface fouling in aquatic systems require knowledge of colloid and surface chemistry, chemical equilibrium and kinetics, momentum and mass transfer, and interfacial engineering. Biofouling is often referred to as the ‘Achilles heel’ of water treatment membrane processes as it cannot be eliminated completely by feed water treatment, membrane surface modification, module hydrodynamic improvements, process optimization, or chemical cleaning.

The advantages of membrane filters over other methods of separation are:

- Availability of wide range of pore sizes
- Sharpness of separation
- Relatively low separation cost
- Minimum product loss
- Retention unaffected by air bubbles or pressure surges
- Surface tension reduces resistance to flow thereby increasing flow rate per unit area
- Low adsorption effects
- Except electro-dialysis, all membrane processes are pressure driven.

Membranes are generally sized according to their ‘molecular weight cut-off’ which is the molecular weight of a globular protein that is 90% retained by the membrane. An ideal membrane filter will retain all molecules larger than its cut-off and allow the smaller ones to pass freely.

A number of techniques are available to prepare synthetic membranes. Some of these techniques can be used to prepare polymeric as well as inorganic membranes. The most important techniques are sintering, stretching, track-etching, phase inversion, sol-gel process, vapour deposition, and solution coating. Details of these processes are given in the literature (Mulder 1996).

The development of macroporous membranes with tunable properties provide added opportunities in permeate flux and separation selectivity control. Membranes in general prevent ordinary hydrodynamic flow and movement of substances through them is by diffusion. Some of such developments are presented here.

### **Polymer nanocomposite membranes**

A new method of synthesizing super hydrophilic nanoparticles and incorporating the same into a polyamide thin film has been developed, is known as ‘*thin film nanocomposite* (TFN)’. Unlike all other membrane surface modifications, it can be immediately incorporated into existing commercial manufacturing facilities. In addition, nanoparticle properties can be selected or modified to impart a wide array of advantageous membrane surface properties such as chemical reactivity, antimicrobial activity and vibratory motion. The process involves a thin polyamide film with relatively hydrophobic pores periodically interrupted by nanoparticles having super hydrophilic pores. While water diffuses through the polyamide pores only under high pressure, water penetrates through the nanoparticle pores with very little applied pressure. As the nanoparticle pore walls are more negatively charged than the membrane surface, ion exclusion is enhanced along with increased water

permeability. The super-hydrophilic nanoparticles enhance fouling resistance by making the membrane more hydrophilic. This membrane has not only increased permeability of water by 75% but also improved rejection characteristics. The concept was developed at UCLA, USA and is being commercialized by a company NanoH<sub>2</sub>O. TFN membranes can be used to produce water of good or better quality with significantly less pressure requirements and these are more resistant to microbial adhesion and easier to clean. In a nanocomposite membrane formed from super-hydrophilic and antimicrobial nanoparticles, adhered cells are rapidly inactivated due to the intrinsic and regenerative biocidal properties of the synthesized membranes. This new class of membrane promises to provide a viable commercial technology in the field of separation.

### **Carbon membranes**

Two types of nano-porous carbon membranes—*Molecular Sieve Carbon* (MSC) and *Selective Surface Flow* (SSF) membranes, have been successfully developed and scaled-up. These membranes consist of a thin layer (< 10 µm) of a nano-porous (3-10 Å) carbon film supported on a meso-macroporous inorganic solid like alumina or on a carbonized polymeric structure. These are produced by pyrolysis of polymeric films. These membranes exhibit somewhat different characteristics from that of a conventional polymeric membrane due to a reciprocal relationship between permeance and selectivity for following the ‘solution-diffusion’ mechanism of transport.

The MSC membranes are produced by carbonization of polyacrylonitrile, polyimide and phenolic resin films.

The SSF membranes are produced by carbonization of polyvinylidene chloride-acrylate terpolymer latex films. Both the surface polarity and pore sizes of SSF membrane can be controlled by post treatments like oxidation. A highly H<sub>2</sub>O selective SSF membrane has been produced for gas drying application by adding polar groups to the pore walls of the membrane. Other highly polar and nonpolar, noncarbon adsorbent membranes (alumina and zeolites) have also been synthesized and tested for gas separation.

The *carbon nanotube* assembly developed at Lawrence Livermore National Laboratory, can reduce the cost of desalination significantly. This system has the potential to separate various gases leading to the economical methods to capture carbon dioxide emitted from power plants. Recent advances in material sciences have led to the development of carbon aerogels and carbon nanotube which have been proven to be ideal for capacitance deionization. This assembly requires less energy and can withstand high temperatures. The carbon aerogel-carbon paper composites are attractive materials for many applications, most notably, as electrodes in electrochemical double layer capacitors and capacitive deionization. These high density composites (< 0.4 g/ml) have high electrical conductivity, high surface area and favourable microporous structure. The carbon aerogel phase in the composite is derived from an organic aerogel precursor made by the aqueous polycondensation of resorcinol and formaldehyde. These high density cross-linked gels have sufficient strength to retain a large fraction of the porous structure from collapsing due to capillary forces associated with solvent evaporation. The simpler preparation procedure makes the composite aerogel materials more economically attractive than monolithic modules.

In general, carbon membranes are available in four major configurations—flat sheet, membrane supported on tube, capillary and hollow fibre. Permeation properties of carbon membranes have been improved greatly during the last two decades.

## **Organic-inorganic composite membrane**

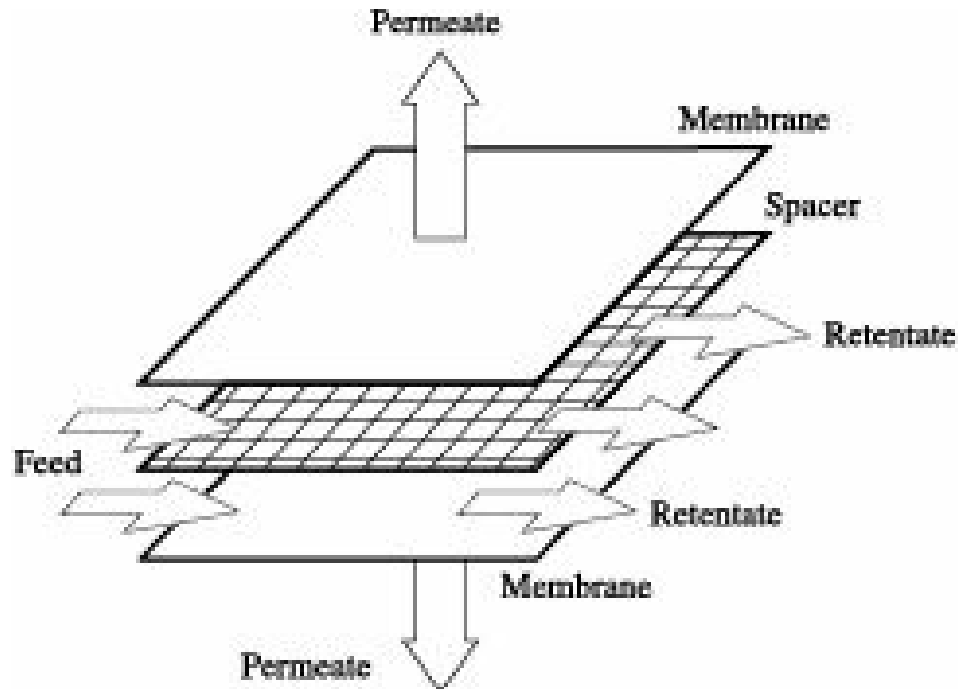
New inorganic-organic nanocomposite membranes involve the incorporation of oxide nanoparticles into ion-conducting polymers to form new nanocomposites. The chemical stabilities of these composite materials are greatly enhanced by the presence of nanoparticles in the polymer framework. The porosity and surface hydrophilic/hydrophobic property and the fouling tendency of the nanocomposites can be easily controlled by incorporating inorganic materials. Organic-inorganic polymer nanocomposites have attracted wide interest as the addition of inorganic particles to polymers can enhance conductivity, mechanical toughness, optimal activity and catalytic activity. This type of nanocomposite membrane finds application in the electrodialysis process for desalination of water.

## **15.5 Membrane Modules**

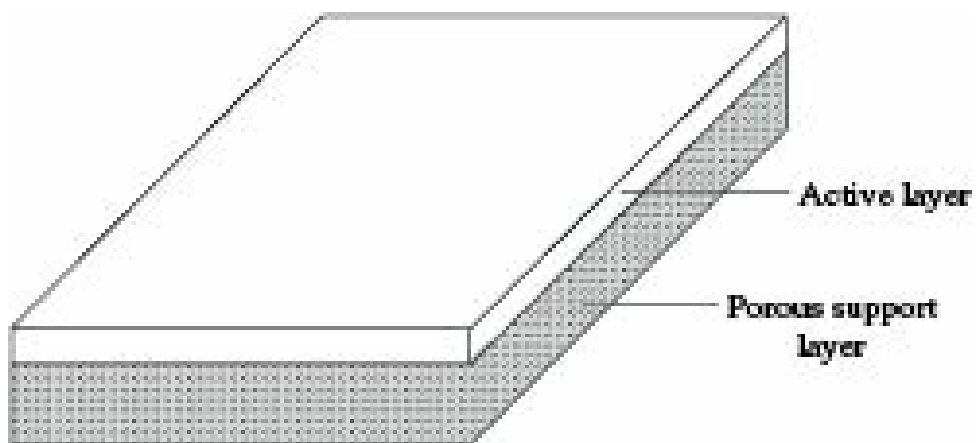
The compact membrane modules with certain advantageous characteristics stated earlier are the requirements in commercial applications. Nearly, all industrial membranes are fabricated from natural or synthetic polymers. The more common membrane modules are: Plate and frame, Spiral-wound, Hollow fibre and Tubular.

### ***Plate and frame module***

A schematic view of a plate and frame module is depicted in Figure 15.3, and the configuration provided in the representation is closest to a flat membrane shown in Figure 15.3(a).



**Figures 15.3** Plate and frame module.



**Figures 15.3(a)** Asymmetric or thin-composite sheet.

Sets of two membranes are placed in a sandwich-like fashion with their feed sides facing each other. A suitable spacer is placed in each feed and permeate compartment thus obtained. The number of sets needed for a given membrane area furnished with sealing rings and two end plates then builds up to a plate and frame stack. The packing density (membrane surface per module volume) of such module is about  $30\text{--}500 \text{ m}^2/\text{m}^3$ . Figure 15.3(b) shows

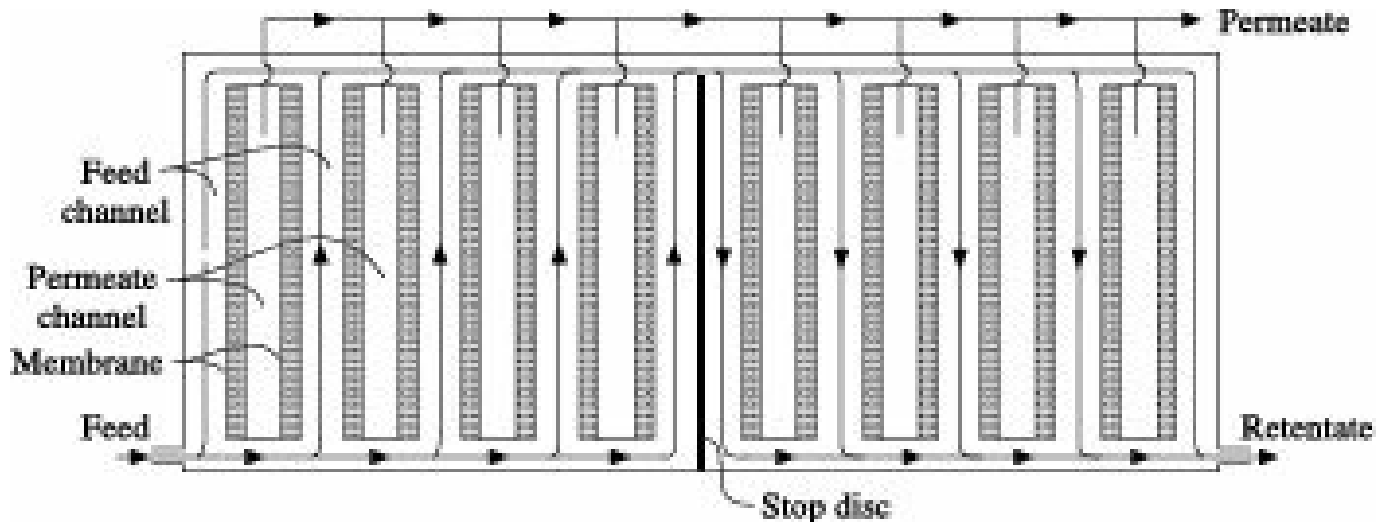


**Figure 15.3(b)** Flow path in a plate and frame module.

a schematic flow path in a plate and frame module. In order to reduce channeling, i.e. the tendency to flow along a fixed pathway and to establish an uniform flow distribution, the so called *stop discs* have been introduced. By applying a high cross flow velocity the residence time of the feed in a feed channel would be quite low. A gasket is used to transform the flat plate into long tortuous narrow channel as represented in Figure 15.3(c).

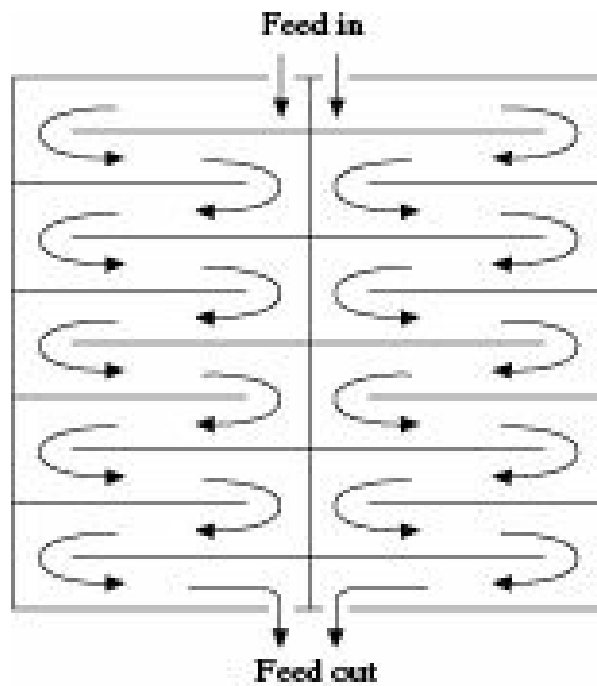


Figure 15.3(c) A flat plate transformed into a long tortuous narrow channel.

### **Spiral wound module**

It is in fact a plate and frame system wrapped around a central collection pipe, in a similar fashion to a sandwich roll. Membrane and permeate-side spacer materials are then glued along three edges to build a membrane envelope. The feed side spacer separating the top layer of the two flat membranes also acts as a turbulent promoter. This module is shown in Figure 15.4(a) and a module with four leaf is depicted in Figure 15.4(b).

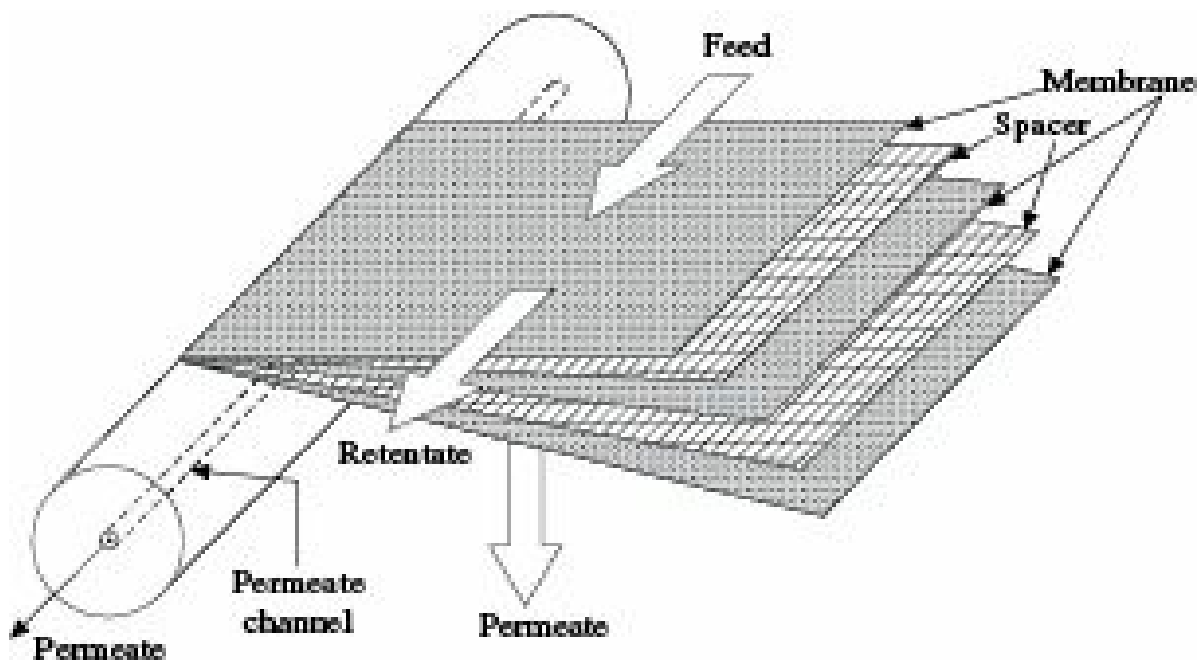


Figure 15.4 Spiral wound module.

The feed flows through the cylindrical module parallel along the central pipe whereas the permeate flows radially toward the central pipe. The packing density of this module ( $200-800 \text{ m}^2/\text{m}^3$ ) is greater than that of the plate and frame module but depends very much on the channel height, which in turn is determined by the permeate and feed side spacer material. The presence of such spacer has a large influence on the mass transfer and the pressure drop.

### **Hollow fibre module**

The hollow fibre module is the replica of capillary module consisting of a large number of capillaries assembled together in a module as shown in Figure 15.5(a).

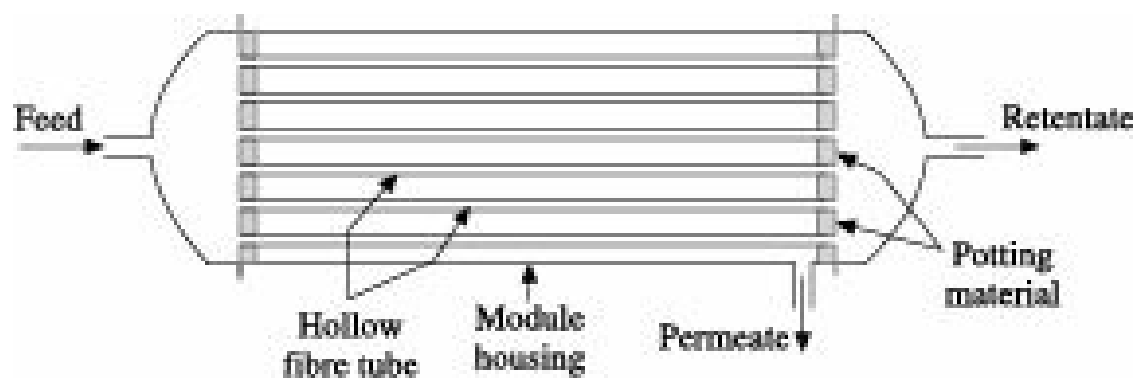
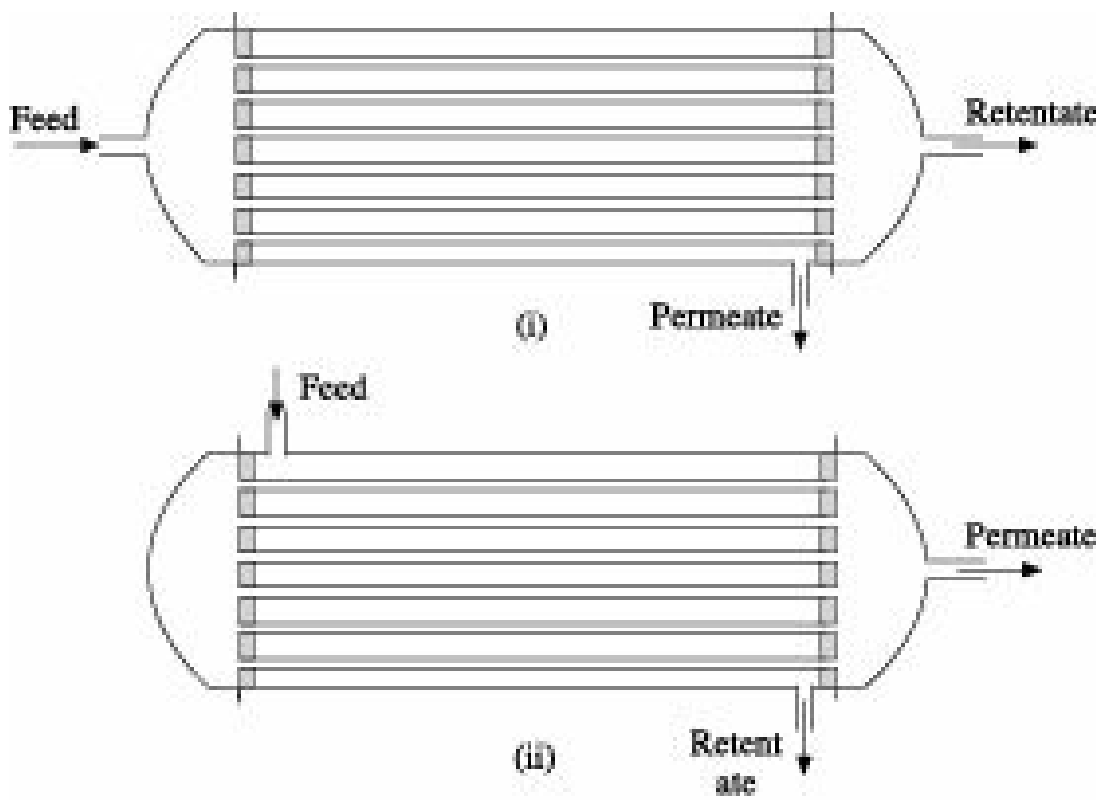


Figure 15.5(a) Hollow fibre module.

The free ends of the fibres (the permeate end) are potted with agents such as epoxy resins, polyurethanes or silicon rubber. The capillaries are self supporting. Two types of module arrangement are available:

- (i) the feed solution passes through the bore of the capillary and the permeate gets collected on the outer side of the capillaries i.e. from the shell-side of the module and
- (ii) the feed solution enters into the shell side of the module while the permeate passes into the bore of the capillaries and gets collected from the tube side. These arrangements are almost similar to 1-1 shell and tube heat exchanger. The choice between the two types is mainly based on the application where parameters such as pressure, pressure drop, type of membrane available, etc. are important. The difference between the capillary and hollow fibre modules is simply the dimensions. When porous ultra-filtration or microfiltration membranes are employed, the capillaries mostly have a gradient in pore size across the membrane. A packing density of about  $600-1200 \text{ m}^2/\text{m}^3$  is obtained with modules containing capillaries of requisite dimensions.

The hollow fibre module can be configured with the highest packing density of about  $9000 \text{ m}^2/\text{m}^3$ . A perforated central pipe is located in the centre of the module through which the feed solution enters. The fibres are arranged in a loop and are potted on one side, the permeate side. One of the disadvantages of the 'outside-in' type is that channeling may occur which means the feed has a tendency to flow along a fixed path thus reducing the effective membrane surface area. With a central pipe, the feed solution is more uniformly distributed throughout the module (inside-out) so that the whole surface area is more effectively used.



**Figure 15.5(b)** Various hollow fibre module (i) Inside-out, and (ii) Outside-in.

The hollow fibre module is used when the feed stream is relatively clean, as in gas separation and pervaporation. Hollow fibre module has also been used for sea water desalination, another relatively clean feed stream as a very effective pretreatment is usually done.

New module concepts have been developed mainly to reduce fouling and concentration polarization as much as possible. One way to achieve this is by changing the flow geometry e.g., transversal flow instead of tangential flow. In this module, the feed flows perpendicular to the fibre thus resulting in an enhancement of mass transfer in the boundary layer. In this concept, the fibres act as turbulence promoters. This type of module design is not only of interest for the pressure driven processes but also for pervaporation, liquid membranes and membrane contactors where the boundary layer resistance may become very important.

### Tubular module

In contrast to capillaries and hollow fibres, tubular membranes are not self-supporting. Such membranes are placed inside a porous stainless steel, ceramic or plastic tube with the diameter of the tube being more than 10 mm. The number of tubes put together in the module normally vary from 4 to 18. Figure 15.6(a) shows a tubular module.

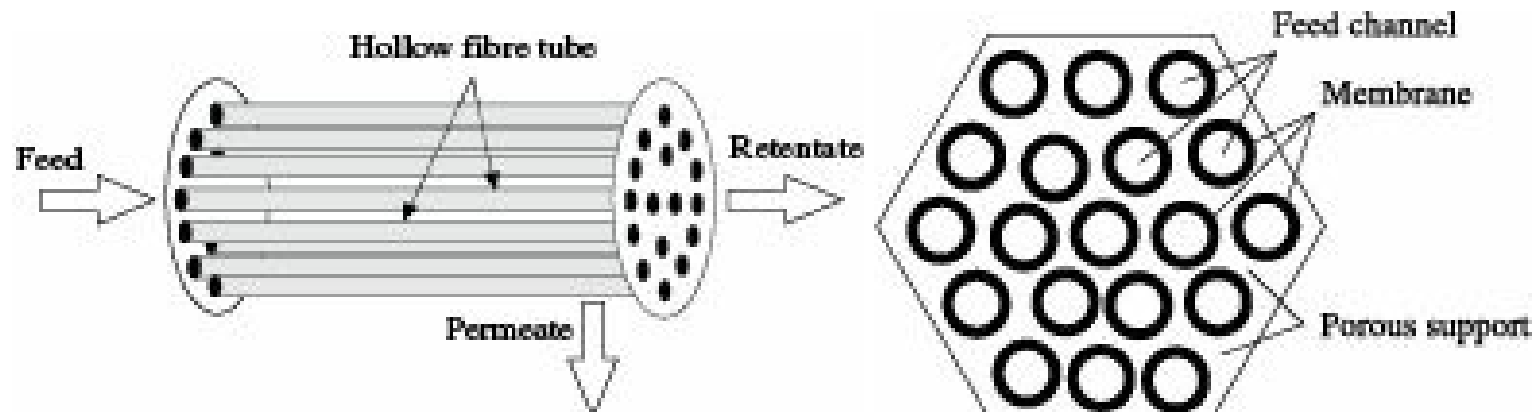


**Figure 15.6(a)** Tubular module. **Figure 15.6(b)** Monolithic module.

The feed solution always flows through the centre of the tubes while the permeate flows through the porous supporting tube into the module housing. Ceramic membranes are mostly assembled in such tubular module configuration. However, the packing density of the tubular module is rather low, being less than  $200 \text{ m}^2/\text{m}^3$ . The monolithic module shown in Figure 15.6(b) is a special type of ceramic module. In this system, a number of tubes have been introduced in a porous ceramic block e.g., an a-Al<sub>2</sub>O<sub>3</sub> the inner surfaces of these tubes are covered by a thin top layer of c-alumina or zirconia by a sol-gel process.

### **Choice of the module**

The choice of the module is mainly determined by economic considerations. This does not mean that the cheapest configuration is always the best choice because the type of application is also very important. In fact, the functioning of a module is determined by the type of application. The characteristics of the modules are given in Table 15.3.

**Table 15.3** Typical characteristics of different membrane modules,

Membrane module	Packing density, $\text{m}^2/\text{m}^3$	Fouling resistance	Cleaning ease	Relative cost	Principal application
Plate and frame	30-500	Good	Good	High	RO, PV, UF, MF
Spiral-wound	200-800	Moderate	Fair	Low	RO, GP, UF, MF
Hollow fibre	500-9000	Poor	Poor	Low	RO, GP, UF
Tubular	30-200	Very good	Very good	High	RO, UF,

## **15.6 Membrane Processes**

In their early stage of development, membrane processes were classified as follows:

- (i) *gaseous diffusion* or *effusion* and *permeation* in separation of gases
- (ii) *dialysis* and *permeation* in separation of liquids.

According to present practice, membrane processes are classified in terms of different types of pressure driven membrane filtration as (Ho and Sirkar 1992, Nunes and Peinemann 2001): microfiltration (MF) for separation of colloidal to micron particles and microorganisms, ultrafiltration (UF) for separation of organics with molecular weight of above 5000, nanofiltration (NF) for separation of divalent salts and organics while permeating monovalent salts such as NaCl, and reverse osmosis (RO) for very high degree of salt separation including NaCl and soluble organics. Reverse osmosis membranes are classified further into three categories: Sea water type membranes for 99.9% rejection of all salts even from 3 to 4% salts with high osmotic pressures, and high separation of organics of low molecular weight such as chlorobenzenes, etc., Brackish water type membranes (low to moderate osmotic pressures, salt < 5000 ppm and high separation of organics of low molecular weight); Ultra low pressure (Ozaki and Li 2002) reverse osmosis (purification of water from low ppm to ppb range). Solvent transport (such as hexane) through RO/NF membranes, on the other hand, requires cross-linked hydrophobic (such as siloxane, polyamide) materials.

A brief discussion about different types of membrane separation processes has been discussed below. The classical method of classification has been taken up first.

### **15.6.1 Separation of Gases**

## Gaseous diffusion or effusion

When a gas mixture having two or more components, is allowed to pass through a porous membrane from a zone of higher pressure to that of lower pressure, the down-stream gas gets enriched in lower molecular weight components since they diffuse at faster rates. This phenomenon is known as *gaseous diffusion* or *effusion*. If the pores are much smaller than the mean free path of the gas, then the gas diffuses independently by Kundsen diffusion. Because of tortuous micropores within the membrane, the diffusivity of the gas gets appreciably reduced. The effective diffusivity is given by the relation.

$$D_{AE} = \frac{D'_A f}{\tau} \quad (15.2)$$

where

$D_{AE}$  = effective diffusivity of component  $A$  through the membrane

$D'_A$  = Kundsen diffusivity

$f$  = porosity of the membrane, and

$\tau$  = tortuosity of the pores

For cylindrical pores,  $D'_A$  depends on the pore size as well as the average velocity and can be expressed as

$$D'_A = 4.85 \times 10^3 d_p \left( \frac{T}{M} \right)^{0.5} \quad (15.3)$$

where

$d_p$  = mean pore diameter

$T$  = temperature in K

$M$  = molecular weight of component  $A$

If the membrane structure is uniform and the gases do not interact, then the concentration gradient through the membrane becomes uniform and the flux of each gas through the membrane is given by

$$J_{M,i} = D_{iE} \left( \frac{\Delta c_i}{\Delta Z} \right) = D_{iE} \left( \frac{\Delta P_i}{RT\Delta Z} \right) \quad (15.4)$$

For a binary system, the composition of the downstream gas is represented by

$$y_A = \frac{J_A}{J_A + J_B} \quad (15.5)$$

Figure 15.7 shows typical pressure gradient for an equimolar binary gas mixture. The diffusivity of gas  $A$  is higher than that of gas  $B$ .

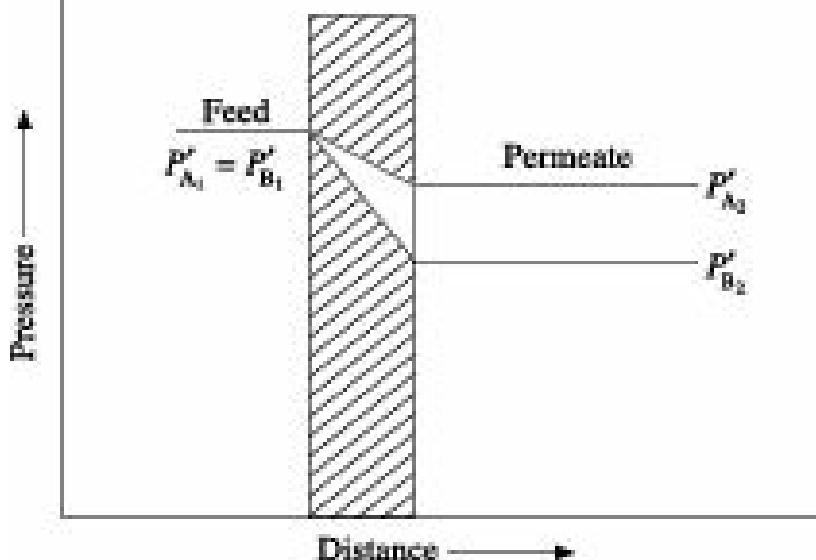


**Figure 15.7** Typical pressure gradient in porous membrane.

Since the gas is binary and equimolal, the partial pressures of both *A* and *B* are the same at the feed end. But the concentration and hence the partial pressure of *A* in the permeate becomes higher due to its higher diffusivity. The concentration of *A* in the permeate can be slightly increased by increasing the pressure differential between the two faces of the membrane. The separation of uranium isotopes using hexa-fluorides of U<sup>235</sup> and U<sup>238</sup> is an example of gas separation by porous membranes.

### Permeation of gases

Transport of gases through dense nonporous polymeric membranes is known as *permeation*. Permeation occurs by the mechanism of solution diffusion, which is more or less similar to that involved in structure insensitive diffusion. The gas gets dissolved in the polymer at the high pressure side, diffuses through the membrane and is released at the low pressure side. The rate of mass transfer is a function of the concentration gradient within the membrane, which in turn is proportional to the pressure gradient if solubility depends on pressure.

If the gas film resistance at the gas-polymer interface is neglected, then the partial pressures of the diffusing components at the gas-polymer interface are same as those in the bulk gas. The flux for gas *A* is given by

$$J_A = -D'_A \frac{dc_A}{dz} = D'_A \frac{c_{A_1} - c_{A_2}}{Z} \quad (15.6)$$

If the system obeys Henry's law, then

$$p'_A = H_A c_A$$

where,  $H_A$  = Henry's law constant for *A*

From Eq. (15.6), we have

$$J_{MA} = \frac{D_A (p'_{A_1} - p'_{A_2})}{H_A Z} \quad (15.7)$$

( $D_A/H_A$ ) is the flux of component *A* per unit pressure gradient and is called the *permeability coefficient* ( $q_A$ ). Since the actual membrane thickness is not always known, it is customary to express

flux per unit pressure difference, which is called *permeability* ( $Q_A$ ).

$$J_{MA} = \frac{q_A (P'_{A_1} - P'_{A_2})}{Z} = Q_A (p'_{A_1} - p'_{A_2}) \quad (15.8)$$

The ratio of permeabilities for a binary mixture is known as membrane selectivity and is denoted by  $a$ ,

$$a = \frac{\frac{Q_A}{Q_B}}{\frac{D_A H_B}{D_B H_A}} \quad (15.9)$$

High selectivity may be obtained either from a favourable diffusivity ratio or from a large difference in solubilities. Diffusivities in membrane depend more strongly on the size and shape of the molecules than gas-phase diffusivities do. Gas solubilities also vary widely with the nature of the gas and the type of polymer.

For most gases, permeability increases with temperature since the increase in diffusivity caused by temperature rise, outweighs any decrease in solubility. The change in permeability may be correlated by Eq. (15.10):

$$Q = a \exp\left(\frac{-E}{RT}\right) \quad (15.10)$$

where,  $E$  is the activation energy.

Membrane selectivity usually decreases at elevated temperature. The operating temperature should therefore be determined by striking a balance between high flux and high selectivity.

The compositions of the permeate and the residue depend on feed composition, permeabilities of the components present, pressure difference across the membrane and the ratio of permeate to feed. Equations have been developed (Fane et al. 1981) which show the effect of these parameters on permeate composition and are useful in estimation of the amount of permeate, its composition and the required membrane area.

In case of multicomponent mixtures, performance of a membrane separator can be estimated by writing flux equations for each component and then by trial and error method.

Membrane separators have also proved to be very successful in gas separation. One of their major applications is in production of 95-99% pure nitrogen for units with capacities up to 1000 m<sup>3</sup>/hr. Enriched oxygen for medical use and for improved combustion, containing up to 50% oxygen, are easily obtained by membrane separation. Higher percentage of oxygen can also be produced but the cost of re-compression makes the process uneconomical.

Recovery of helium from natural gas is an important application of membrane technology. Using a membrane with high He/CH<sub>4</sub> selectivity, 50% He may be recovered in a single stage from a feed having very low concentration of He, giving a permeate 30 times richer in Helium than the feed (Pan 1983).

Membrane separators are also used to recover hydrogen from purge streams involved in ammonia, methanol and hydrogenation plants. Permeate considerably enriched in hydrogen can be obtained in a single stage. Carbon dioxide is being easily removed from natural gas with the aid of gas separation membranes. Selective polymeric membranes offer an edge over other technologies because all the

undesired components -CO<sub>2</sub>, H<sub>2</sub>S and H<sub>2</sub>O- have much higher permeabilities than CH<sub>4</sub>. Removal of carbon dioxide from flue gases and natural gas streams are probably two of the largest applications in process industries so far as carbon dioxide removal is concerned. Polymeric gas separation membranes are extensively used for carbon dioxide removal. Ceramic membranes which have the potential to offer superior performance are still under development. Polymeric membranes which are selective to carbon dioxide are also selective to water transport. The feed streams need to be compressed and the compressor can be coupled with an expander to recover energy. The polymers have high glass transition temperature, high permeability for both water and carbon dioxide, and offer a higher CO<sub>2</sub>/N<sub>2</sub> or CO<sub>2</sub>/CH<sub>4</sub> selectivity. Gas absorption membranes are used as contacting device between a gas and a liquid. The separation is caused by the presence of an absorption liquid on one side of the membrane which selectively removes certain components of the gas stream. Hydrophobic microporous membranes can be used as gas-liquid contactors between the carbon dioxide-rich gas stream and a scrubbing liquid. The feed gas need not be compressed or dried for acid gas separation. Carbon dioxide diffuses through the membrane pores and reacts with the absorbing liquid. The gas separation membranes have inherently superior selectivity to polymeric membranes due to the absorption process. A properly designed membrane gas-liquid contactor offers a high mass transfer coefficient (0.01-0.1 unit) than the conventional packed beds. Membrane absorbers can make an integrated process which can be highly energy efficient. However, further developments of superior gas-liquid contactor membranes and superior absorption liquids, which can be used at higher concentrations and lower circulation rates, will make this technology more attractive.

Another important industrial application of membrane filters is in the production of ultra pure particle-free inert gas, indispensable for manufacture of chips.

Membrane based gas separation systems are now widely accepted and employed unit operations in the industry. Worldwide annual installed gas handling capacity of membranes since 1977, when the first commercial installation was made, has risen from a fraction of million m<sup>3</sup>/day to over 10 million m<sup>3</sup>/day. The technology has also witnessed a number of advances over the past decade and polymeric membranes, in particular, are undergoing a renaissance as a low cost, energy efficient, environment-friendly means for separating gases on the basis of both size and solubility. The use of membranes in gas separation has, however, been limited by the difficulty of preparing membranes with the desirable combination of high selectivity which yields high product purity at low operating cost, and high permeability which reduces the membrane area and capital cost. However, in conventional polymeric membranes as the selectivity increases, permeability invariably decreases and vice versa. As nanostructured polymers continue to develop, many of the insights gained from these multifunctional materials can be exploited in the molecular-level design of selective membranes. Recent efforts have demonstrated that the incorporation of dispersed nanoparticles within a polymer matrix can alter the local free volume of polymeric membranes as well as improve the affinity for one penetrant gas species over another.

Moreover, chemical cross-linking of such membranes can further influence the available free volume of a polymer selectively altering the diffusion of larger gas molecules. The development of cross-linked hydrogen-selective polymers containing palladium nanoparticles grown *in situ* can greatly reduce the permeabilities of larger gases, e.g., carbon dioxide, nitrogen, etc. without hindering the permeabilities of smaller gases, e.g., hydrogen, helium, etc. thereby increasing the ideal

selectivity of hydrogen. Nanoparticles of palladium are integrated into the polymer membrane not only to reduce the free volume available for molecular transport but also to increase the solubility of hydrogen.

The addition of micron-sized porous zeolite particles into organic polymers so as to combine the mechanical elasticity and processibility of polymers with the strong size selectivity characteristics of spatially well-defined zeolite pores, have been explored. However, commercialization of this approach has been hampered by poor polymer-zeolite adhesion and inadequate particle dispersion. Conventional or size-selective polymer membranes preferentially allow small molecules to permeate relative to larger ones. Another class of membranes, reverse-selective membranes preferentially allows larger species to permeate in a mixture. This counterintuitive property is possible because molecular transport in dense polymeric membranes is governed by both penetrant solubility and diffusivity. These reverse-selective membranes are used in the industrial separations in which the smaller, less soluble gas component in a mixture is required at high pressure because it is the larger molecules that preferentially pass through to the low pressure side. This process is being used for the removal of higher hydrocarbons from methane in the purification of natural gas, for separation of organic monomer from nitrogen in the production of polyolefins and for removal of hydrocarbons from hydrogen in refinery applications. Reverse-selective membranes are not subjected to the permeability/selectivity trade-off inherent in conventional size-selective polymeric membranes, more permeable reverse-selective membranes are found to be more selective.

Two types of nanoporous carbon membranes namely, molecular sieve carbon (MSC) and selective surface flow (SSF) are extensively used for gas separation.

Figure 15.8(a) shows the mechanism of gas transport through MSC membranes. The pores of the membrane are smaller (usually 4-5 Å) than some of the feed gas molecules. Consequently, only the smaller-sized components of the feed gas mixture (component *B*) can enter the pores of the membrane at the high pressure side. These molecules adsorb on the pore walls and they migrate to the low pressure side of the membrane by surface diffusion. Thus, the separation is primarily based on the differences in the sizes of the feed gas molecules to be separated. Table 15.4 gives some examples of the separation performance of the MSC membranes (Sircar and Rao 2000).

**Table 15.4** Separation performance of various MSC membranes

<i>Feed gas</i> <sup>*</sup>	<i>Permeance of component 1 (GPU)</i> <sup>†</sup>	<i>Selectivity of comp. 1</i>
O <sub>2</sub> (1) + N <sub>2</sub> (2)	16.0	13.6
H <sub>2</sub> (1) + CH <sub>4</sub> (2)	365.5	500.0
CO <sub>2</sub> (1) + CH <sub>4</sub> (2)	91	50.0
C <sub>3</sub> H <sub>6</sub> (1) + C <sub>3</sub> H <sub>8</sub> (2)	183	12-15
Air(1) + SF <sub>6</sub> (2)	365	>1000

\* component 1 is the smaller species

† gas permeation unit (GPU) = [SCC/(cm<sup>2</sup> s cm Hg)] # 10<sup>-6</sup>

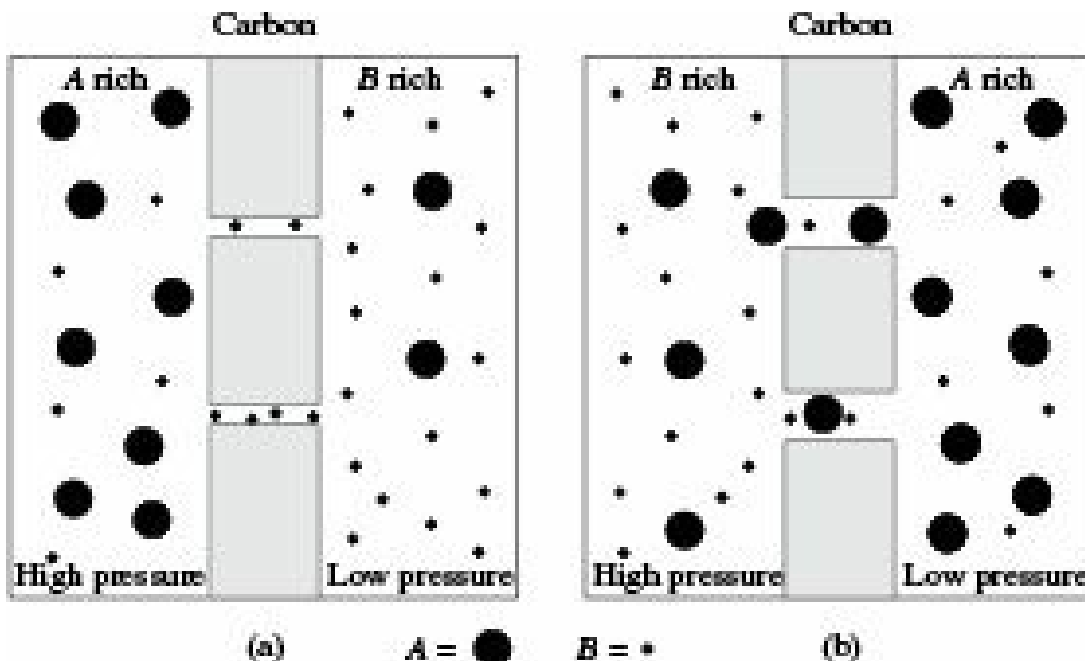


**Figure 15.8** Mechanism of gas transport through (a) Molecular sieve carbon, (b) Selective surface flow (SSF) membrane.

Figure 15.8(b) shows the mechanism of gas transport through SSF membranes. The pores of the membrane are large enough (usually 6-7 Å) to allow all the molecules of the feed gas mixture to enter the pores. However, only the larger (higher polarisability) and more polar molecules (component *A*) are selectively adsorbed on the pore walls. The adsorbed molecules then selectively diffuse to the lower pressure side of the membrane. The adsorbed molecules also hinder the transport of smaller molecules through the void space between the pore walls. The net result is that the SSF membranes selectively permeate the larger and more polar molecules of the feed gas mixture through them. A key feature of this membrane is that the less strongly adsorbed components of the feed gas (smaller molecules) are enriched in the high pressure-side of the membrane. This can be a key practical advantage because the smaller molecules of a gas mixture are often the desired product, and their production at the feed gas pressure reduces or eliminates further recompression. Another key advantage of SSF membrane is that the ‘sorption-diffusion’ mechanism will allow the operation of the membrane with a low pressure gradient across the membrane. This is caused by preferential and substantial adsorption of the selectively permeating component at the feed gas side of the membrane even at a relatively low pressure. SSF membranes have been scaled-up in the tubular form and tested for recovery of hydrogen from refinery and hydrogen-PSA waste gases. These membranes preferentially permeate  $C_3^+$  hydrocarbons and  $CO_2$  from mixtures with hydrogen and methane. These types of membranes are also used for separation of  $H_2S$  and  $H_2$ , and  $H_2S$  and  $CH_4$  binary mixtures.

### **Combo unit for gas separation**

One of the uses of SSF membrane is for recovering hydrogen (~50%) from a refinery waste gas which contains low concentration of  $H_2$  (~20%) along with a variety of  $C_1 - C_3$  impurities and is available at a relatively low pressure (~0.3 MPa). Usually, this gas is being burnt out to recover its fuel value whereby the hydrogen is lost. However, using a SSF membrane in conjunction with PSA unit hydrogen of the order of 50% can be recovered from the waste gas. The gas without compression is fed to a single-stage SSF membrane and the permeate side of the membrane is maintained at near atmospheric pressure. The hydrogen enriched gas (containing mainly ~51.6%  $H_2$ , 41.5%  $CH_4$ )

coming out from the membrane is then compressed to about 20 atmospheric pressure and fed into a conventional PSA unit to produce an essentially pure hydrogen. A novel two-stage SSF membrane arrangement can be used to produce a pure CH<sub>4</sub> or H<sub>2</sub> stream with an overall recovery of 73-77% and H<sub>2</sub>S rejection of 98.3% from an equimolar H<sub>2</sub>S-H<sub>2</sub> (or CH<sub>4</sub>) feed gas mixture at 4.34 atmospheric pressure. The stage-I membrane is operated with low H<sub>2</sub> recovery (high H<sub>2</sub>S rejection) and stage-II membrane is operated with high H<sub>2</sub> recovery (low H<sub>2</sub>S rejection). The high pressure effluent gas from stage-I of the membrane system contains ~ 98% H<sub>2</sub> or CH<sub>4</sub>, which is further purified by a conventional TSA unit. This application of the SSF membrane may be attractive for desulphurisation of natural gas containing bulk quantities of H<sub>2</sub>S.

Selection of appropriate gas separation method is determined by its end use application. A phase change adds a significant energy cost to the separation cost while membrane gas separation does not require phase change and its systems do not have extra mechanical complexity making an ideal choice for gas separation. However, membrane gas separation is not ideally suited in all instances.

## 15.6.2 Separation of Liquids

Several processes have been developed for separation of liquids using both porous and polymeric membranes. In dialysis, porous membranes are used and separation generally depends on diffusivity difference between the solutes of different molecular weights. In liquid-liquid extraction, which also employs porous membranes, the raffinate and extract phases are separated by the membrane. Differences in equilibrium solute distribution and diffusivity determine the extract composition. In permeation of liquids, dense polymeric membranes are used for separation of components of liquids.

### Dialysis

Dialysis is a membrane separation operation used for removal of low molecular weight solutes such as organic acids (100 < molecular weight < 500) and inorganic ions (10 < molecular weight < 100) from a solution. In dialysis, thin porous membranes are employed for selective removal of low molecular weight solutes from a solution. As the molecular weight cut-off of the membrane used in dialysis is very small, solutes of low molecular weight move from a high- to a low-concentration region. Pressure difference across the membrane being negligible, the flux of each component is proportional to the concentration difference at the two ends of the membrane, which acts as the driving force. Solutes of high molecular weight are mostly retained by the feed solution because of their low diffusivities and the high resistance encountered by them during diffusion through pores of almost their own size. At equilibrium, the chemical potentials of the diffusing component on both sides of the membrane are equal.

$$n_1 = n_2 \quad (15.11)$$

In terms of concentration, the above equation can be written as

$$c_1 c_1 = c_2 c_2 \quad (15.12)$$

$\Pi$ ,  $c$  and  $\gamma$  being the chemical potential, concentration and activity coefficient of the diffusing component, respectively. 1 and 2 refer to the two opposite sides of the membrane.

For ideal solutions (very dilute)  $\gamma$  becomes unity, and

$$c_1 = c_2 \quad (15.13)$$

This dialysis equilibrium is based on the assumption of uncharged solute molecules. If macromolecules are polyelectrolytes such as protein and nucleic acids, the charge equilibrium of the macromolecules has to be considered. This equilibrium is known as the *Donnan equilibrium*.

Typical concentration gradients during dialysis are shown in Figure 15.9. The feed contains three species, solute *A* of smallest size, solute *B* of intermediate size and a colloid *C* having large molecules which cannot pass through the pores of the membrane. Concentration boundary layers are formed on both sides of the membrane. Concentration drops through the boundary layers are less than those within the membrane since the effective diffusivities within the membrane are less than the respective bulk diffusivities.

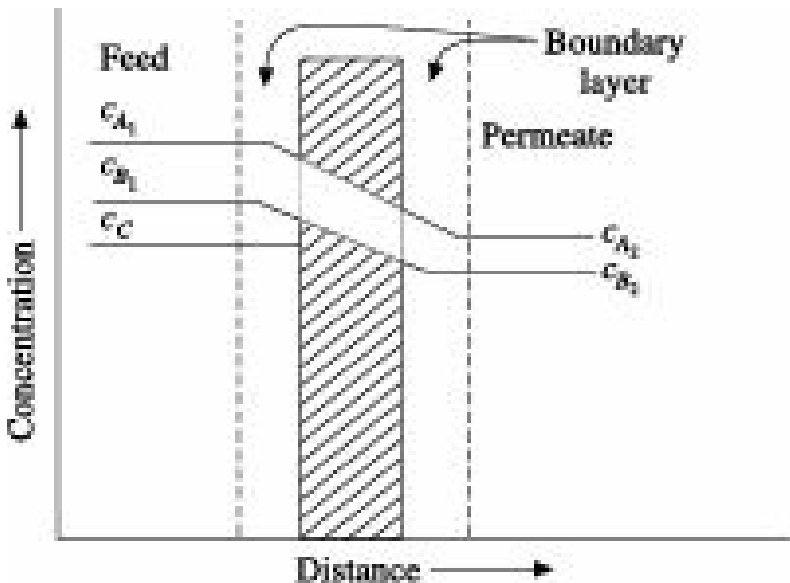


**Figure 15.9** Typical concentration gradient during dialysis.

The flux of solute *A* through the membrane can be represented by

$$J_A = K_A(c_{A1} - c_{A2}) \quad (15.14)$$

and

$$\frac{1}{K_A} = \frac{1}{k_{1A}} + \frac{1}{k_{M_A}} + \frac{1}{k_{2A}} \quad (15.15)$$

where,  $k_1$ ,  $k_2$  and  $k_M$  are the local coefficients of mass transfer for the feed, product and membrane, respectively.

The most important application of dialysis is in artificial kidneys for removal of urea and other waste products from blood. Hollow-fibre cellulosic membranes are used for the purpose, which allow urea, and other impurities to pass through them while proteins and cells are retained in the blood. Other application includes removal of salts from a protein solution which is often a step in resolubilizing the proteins that were initially in inclusion bodies. Dialyses using flat sheet membranes are useful in recovery of caustic soda from hemi-cellulose solutions produced in viscose rayon plants.

### **Electrodialysis**

Electrodialysis is a membrane separation process used for the separation of charged molecules from a solution by application of direct electrical current. The membranes contain ion-exchange groups and have a fixed electrical charge. Positively charged membranes (anion membranes) allow the passage of anions and repel cations, negatively charged membranes (cation membranes) allow the passage of

cations and repel anions. This method is very effective in the concentration of electrolytes and proteins.

The electrodialysis process is driven by electrostatic forces and can be used to transfer salts from low to high concentration. Salt solutions can be concentrated or diluted by this method. The electrodialysis method is much faster than dialysis and is more efficient desalting method.

Ion-exchange membranes used in electrodialysis units are in essence ion-exchange resins in sheet form. Ion-exchange membranes contain mobile counterions that carry electric current. The cation-exchange membranes consist of polystyrene with negatively charged sulphonate groups bonded to phenyl groups in polystyrene. Anion membranes contain positively charged quaternary ammonium groups ( $-N_3R^+$ ) chemically bonded to the phenyl groups in the polystyrene. Mobile counterions account for the low electrical resistance of the membranes. To control swelling of sulphonated polystyrene, some cross-linking agents such as divinyl benzene are included in the polymer. A typical electrodialysis membrane has a pore size of 10 to 20 Å. Membrane thickness is of the order of 0.1 to 0.6 mm, and electrical resistance is approximately 3 to 30 ohm/cm<sup>2</sup>.

Electrodialysis units can be used for (i) concentration and dilution of salts, (ii) ion substitution, and (iii) electrolysis. In electrodialysis units, electrodes play an important role. Two electrode compartments are separated by a membrane in electrolytic units. An example of electrodialysis unit is a chlor-alkali cell in which a sodium chloride solution is electrolysed and converted to sodium hydroxide and chlorine.

### ***Permeation of liquids***

In permeation of liquids, dense polymer membranes are used and transport is by solution-diffusion mechanism. Selectivity depends on solubility ratio and diffusivity ratio, both of which in turn depend on the chemical structure of the polymer and the liquid. Activity gradients within the membrane act as driving force for the transport. The driving force, however, cannot be changed over a wide range by increasing the pressure difference since pressure has very little effect on activity in the liquid phase.

## **15.7 Membrane Filtration**

Industrial membrane filtration was initially developed for treatment of waste water and sewage to remove particulate and macromolecular materials. Its applications have now increased considerably and include such diverse fields as production of high grade injection water, harvesting of microbial cells, production of up to 99% pure nitrogen, production of particle free inert gases and for manufacture of chips. Membrane filtration has a number of important industrial applications in separation of liquids. Some of them are:

- Waste water treatment particularly for removal of stable oil-water emulsions to meet today's effluent standards
- Production of chlorine-and bacteria-free water.
- Production of ultra pure water for electronic and pharmaceutical industries.
- Preparation of sterile fluids for medicinal uses.
- Dairy industry particularly in fractionation of cheese, whey and pre-concentration of milk for production of cheese.
- Clarification of fermentation products by removing suspended solids such as husk, cells, colloids

and macromolecules like proteins and poly saccharides.

- Electro coat paint industry for removal of loose paints after electro deposition.

Membrane Filtration processes are classified as microfiltration, ultrafiltration, nanofiltration and reverse osmosis arranged in order of decreasing pore size. The smallest particles or molecules which can be retained by the techniques are (Mandal 1998):

Microfiltration : 0.02-10 micron

Ultrafiltration : 0.001-0.02 micron

Nanofiltration (Pore size) : 0.001-0.002 micron

Reverse Osmosis : 0.0001-0.001 micron

### 15.7.1 Microfiltration

Microfiltration is the oldest and most widely used membrane filtration. It separates fine particles from true solutions of liquids and gases. Filtration of suspensions of fine particles or colloids with approximate linear dimension of 0.02 to 10 microns is generally done by microfiltration. This size range covers a large variety of natural and industrial particles like silt, clay, colloidal silica, mist fog, carbon black, paint pigments, viruses, bacteria, red blood cells, yeast cells, etc. These particles usually being fairly large, the pressure drop which acts as the driving force, lies within the range of 7 to 350 kN/m<sup>2</sup>. This pressure drop causes the suspending of fluid and very small solute species to pass through the membrane this being collected as permeate. The mechanism by which the particles are separated, depends on the type of membrane and the nature of its interaction with the particles being filtered.

Microfiltration is carried out in two types of configurations, cross flow and dead-end. In cross flow operation the suspension is made to flow tangential with respect to the surface of the membrane. In dead end microfiltration, on the other hand, clarified fluid is forced perpendicularly through the filter while all or most of the particles are retained.

Traditionally, microfiltration (MF) membrane separations have been performed on the basis of size exclusion and are typically used for filtration of suspended solids, bacteria, viruses, etc. However, microfiltration membranes (e.g., celluloses, silica, polysulphone) can be functionalized with a variety of reagents. Depending on the type of functionalized groups (such as chain length, charge of groups, bimolecules, etc.), these microfiltration membranes can be used in applications ranging from metal (or oxyanions) separation to chlorinated organic detoxification to biocatalysis. The use of microfiltration membrane based sorbents containing multifunctional groups is a novel technique to achieve high metal sorption under convective flow conditions. This can be achieved by attachment of various polyamino acids (molecular weight 2500-100000) directly on the membrane pore surfaces. Helix-coil formation ability (for example, with polyglutamic acid) of the attached polyligands can also be used for providing tunable NF type separation and flux control at low transmembrane pressures. Microfiltration membranes are widely used in the pharmaceutical, chemical and food industries for the separation of vaccines, fermentation products, enzymes and other proteins.

### 15.7.2 Ultrafiltration

Ultrafiltration retains soluble macromolecules and anything larger while allowing solvents, ions and other small soluble species to pass through. They are capable of rejecting species in the molecular weight range of 2000 to 5,00,000 (300 to 50000 Dalton). Ultrafiltration membranes are often

characterized by a molecular weight cut-off based on measurements of fraction rejected versus molecular weight (Fane et al. 1981).

Ultrafiltration is widely used to concentrate oil-in-water emulsions, the by-product of many metal working processes. The membrane retains stable emulsified oil while water with very dilute dissolved oil and free surfactants pass through it. Other important applications of ultrafiltration include concentration of dilute latex, removal of virus from solutions in vaccine manufacture and protein recovery in several fermentation processes. Ultrafiltration reduces cost, minimizes disposal problems, increases product recovery and improves product purity.

Ultrafiltration has been in commercial use for almost two decades and is now primarily used for production of ultrapure water for electronic and pharmaceutical industries. It is also used for production of sterile fluids for medicinal purposes. An important use of ultrafiltration membranes is as substrate for composite reverse osmosis membranes.

Typical UF and MF operations are pressure driven processes in which low molecular weight solutes and water pass through the filter, and high molecular weight solutes are retained on the membrane surface. Therefore, a concentration gradient builds up between the surface of the membrane and the bulk fluid. This gradient results in the concentration polarisation. As a result, solute diffuses back from the membrane surface to the solution as shown in Figure 15.10(a).

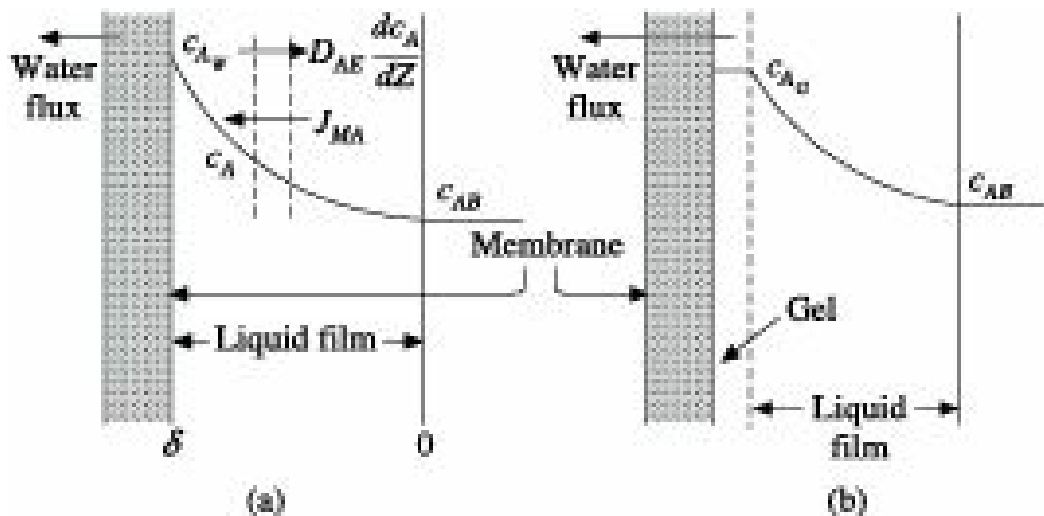


**Figure 15.10** Back diffusion of solute from membrane surface to solution (a) without gel formation and (b) with gel formation.

At steady-state, the rate of convective transfer of solute (*A*) towards the membrane is equal to the rate of diffusion of solute in the opposite direction because of concentration polarisation.

$$D_{AE} \frac{dc_A}{dz} = J_{M,A} c_A \quad (15.16)$$

where

$D_{AE}$  = effective diffusivity of the solute (*A*) in liquid film in  $\text{cm}^2/\text{s}$

$J_{M,A}$  = volumetric filtration flux of *A* in liquid in  $\text{cm}^3/(\text{cm}^2)(\text{s})$

$c_A$  = concentration of solute *A*,  $\text{mol}/\text{cm}^3$  liquid.

Integration of Eq. (15.16) with the boundary conditions of  $c_A = c_{AB}$  at  $Z = 0$ , and  $c_A = c_{AW}$  at  $Z = d$  yields

$$J_{M,A} = \frac{D_{AE}}{\delta} \ln \frac{c_{AW}}{c_{AB}} \quad (15.17)$$

whence,

$$J_{M,A} = k \ln \frac{c_{AW}}{c_{AB}} \quad (15.18)$$

where,  $k = D_{AE}/d$  is the mass transfer coefficient and  $d$  is the film thickness.

The mass transfer coefficient is a function of fluid and solute properties and flow conditions and is correlated with Reynold's number,  $Re$  and Schmidt number,  $Sc$  as

$$Sh = \frac{Ik}{D_{AE}} = aRe^b Sc^b \quad (15.19)$$

where,  $Re = (Lut/d)$  and  $Sc = (n/tD_{AE})$ . The value of  $a$  is  $1/3$  according to the boundary layer theory,  $b$  is approximately  $0.5$  for laminar flow and  $1.0$  for turbulent flow.

A gel layer is formed on the surface of the UF membrane as shown in Figure 15.10(b), when slowly diffusing large macromolecules accumulate on the surface. The solute concentration in the gel  $c_{AG}$  is the maximum value of  $c_{AW}$ . In this case the liquid flux through the filter is

$$J_{M,A} = k \ln \frac{c_{AG}}{c_{AB}} \quad (15.20)$$

A gel layer forms if the protein concentration in the solution exceeds  $0.1\%$ . For biological fluids, protein accumulation is usually dominant. Gel formation depends on the nature and concentration of the solute, pH and pressure. Once gel is formed,  $c_{AG}$  becomes constant and liquid flux decreases logarithmically with increasing solute concentration in the bulk fluid. The gel layer causes a hydraulic resistance against flow and acts somewhat like a second membrane. Figure 15.11 depicts the variation of liquid flux with the log of solute concentration in the absence and presence of gel formation.

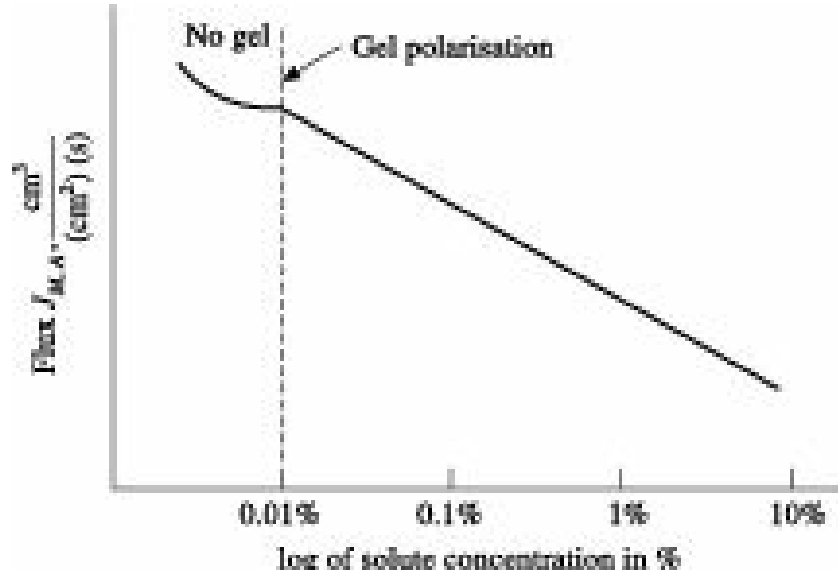
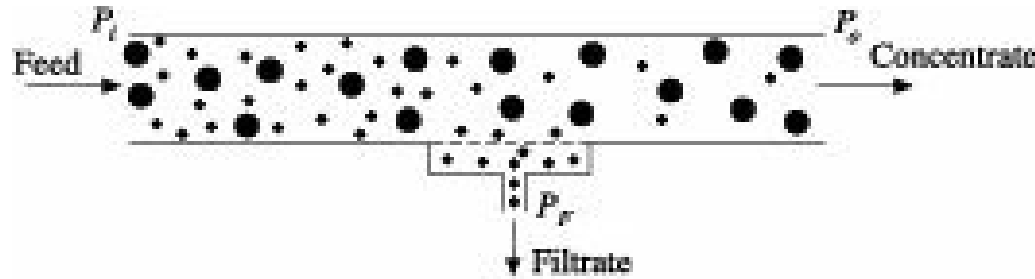


Figure 15.11 Variation of liquid flux with the log of solute concentration with and without gel formation.

Gel formation can be partially eliminated by *cross-flow filtration* where pressure is not applied directly perpendicular to the membrane, but parallel to the membrane surface. This process is also

called *tangential flow filtration* (Shuler and Kargi 2002). In this process fluid flows parallel to the membrane surface and passes through the membrane leaving solutes in a liquid phase above the membrane. Mechanical agitation or vibration of the membrane surface can also be used to alleviate gel formation.

A schematic cross-flow filtration is shown in Figure 15.12.



**Figure 15.12** Schematic diagram of cross-flow filtration.

The pressure drop driving fluid flow is

$$DP = P_i - P_o \quad (15.21)$$

For laminar flow using the Hagen Poiseuille equation, one can have the following expression:

$$P_i - P_o = DP = \frac{C_1 \mu L u}{d^2} = \frac{C_2 \mu L Q}{d^4} \quad (15.22)$$

where,  $L$  is the length of the tube,  $\mu$  is the viscosity of the fluid,  $Q$  is the volumetric flow rate of the liquid, and  $d$  is the diameter of the tube.

For turbulent flow the following equation may be used for  $\square P$ :

$$P_i - P_o = DP = \frac{C_3 \mu L u^2}{d} = \frac{C_4 f L Q^2}{d^5} \quad (15.23)$$

where,  $f$  is the Fanning's friction factor. For cross-flow filtration, turbulent flow is desired. The average transmembrane pressure drop is given by

$$DP_M = \frac{P_i + P_o}{2} - P_F \quad (15.24)$$

where,  $P_F$  is the pressure in the filtrate which is usually near atmospheric pressure.

Assuming that  $P_F = P_{atm}$  or  $P_F$  is zero gauge pressure, the following correlation can be obtained

$$DP_M = P_i - \frac{1}{2} DP \quad (15.25)$$

High inlet pressure and low fluid velocities need to be applied to obtain high  $DP_M$ .

The filtration flux as a function of transmembrane pressure drop is given by

$$J_M = \frac{\Delta P_M}{R_G + R_M} \quad (15.26)$$

where  $R_G$  and  $R_M$  are gel and membrane resistances, respectively.  $R_M$  is constant whereas  $R_G$

varies with solute concentration and the tangential velocity across the membrane which can retard or eliminate gel formation. Also, the filtration flux ( $J_M$ ), is a function of fluid velocity as given in Eqs. (15.25) and (15.26). Usually there is an optimal fluid velocity range maximizing the filtration rate. At low velocities, the mass transfer coefficient is low resulting in high gel resistance ( $R_G$ ) and low filtration flux. At high fluid velocities  $DP$  is high resulting in low  $DP_M$  and therefore low flux ( $J_{MA}$ ) values. Also, there is an optimal value of  $DP_M$  resulting in maximum flux, may be due to a maximum pressure limitation on  $P_i$ . The maximum value of  $DP_M$  is therefore  $P_i$  which is limited by the physical properties of the membrane. With modern membranes, especially the new ceramic membranes it may be possible to push  $P_i$  to high levels. Hence, at low  $DP_M$  values, flux increases with  $DP_M$ , however, at high  $DP_M$  values, filtration flux drops as a result of the decrease in velocity. Hence, the optimal values of  $DP_M$  result in the maximum UF or MF rate for various solute concentrations.

In the absence of gel formation, the filtration flux ( $J_M$ ) increases linearly with  $DP_M$  due to the absence of gel polarisation. However, at high  $DP_M$  gel formation takes place and gel resistance ( $R_G$ ) increases with increasing  $DP_M$ , resulting in constant filtration flux over a large range of high  $DP_M$  values. At higher solute concentrations, flux levels off at lower  $DP_M$  values.

The rejection coefficient ( $\{\}$ ) of an ultrafilter is defined as

$$\phi = \frac{c_{AB} - c_{AF}}{c_{AB}} = 1 - \frac{c_{AF}}{c_{AB}} \quad (15.27)$$

where  $c_{AF}$  is the concentration of the solute  $A$  in the filtrate. When  $c_{AF} = 0$ ,  $\{\} = 1$  indicating that only water passes through the filter and there is complete solute rejection. If  $c_{AF} = c_{AB}$ ,  $\{\} = 0$  which indicates complete solute transfer to the filtrate and no rejection of solute. Usually,  $0 < \{\} < 1$  and is closer to 1. The value of  $\{\}$  is a measure of the selectivity of the membrane for certain solutes. Selective separations of various compounds can be achieved using membranes with the right molecular weight cut-off. For molecular weight  $> 10^5$  and molecular weight  $< 10^3$ ,  $\{\} = 1$  and  $\{\} = 0$ , respectively which means the membrane allows complete passage of compounds having molecular weight  $< 10^3$ , retains compounds with molecular weight  $> 10^5$ , and partially retains compounds of  $10^3 < \text{molecular weight} < 10^5$ .

### 15.7.3 Nanofiltration

Nanofiltration is becoming more and more important in waste water treatment as a pressure driven membrane separation process. The operating range of nanofiltration is intermediate between ultrafiltration and reverse osmosis. Nanofiltration membranes have pores of approximate size range of 0.001 to 0.002 micron and retain sugars, some multivalent salts, etc. but allow free passage to univalent salts. The membrane rejection is a function of concentration and valency type of the feed electrolyte, ion-exchange capacity of the membrane and pH of the feed. The limitation in the operation of polymer membranes occurs when the chemical, thermal and mechanical stability of the membrane is exceeded by the medium to be treated. The long term resistance of the polymeric membranes with

the high chemical and mechanical resistance often proved inadequate for being used in separation techniques in industries.

Ceramic membranes have the combined advantage of high chemical, mechanical and thermal resistance due to which many companies and research institutes have been working on the development of ceramic membranes. Retention of salt is controlled by the charge on these membranes. This charge is determined by measuring the zeta potential at different pH. Negligible salt retention values are noted for the ceramic nanofiltration membrane at pH 6.5 whereas retention in high charge ranges, i.e. at high and low pH values, increased greatly. Besides dependence on pH, membrane retention was also strongly influenced by nature of the electrolyte as well as electrolyte concentrations. As ceramic nanofiltration membranes are generally more expensive than standard commercial polymeric membranes, their use is restricted to applications which demand greater thermal or chemical resistance.

#### 15.7.4 Reverse Osmosis

In osmosis, miscible solutions of different compositions are separated by a membrane, which allows the solvent but not the solutes to pass through its pores. Thus, the spontaneous passage of a liquid from a dilute to a more concentrated solution across an ideal semipermeable membrane takes place by diffusion, where the activity of the solvent is relatively low. Osmotic transfer of water occurs in many plants and animal cells.

If an external force is executed on the more concentrated solution, the equilibrium is disturbed and the activity of the solvent at this end increases. As a result, the flow of solvent is reversed. Thus, the process selectively restricts flow of solute while permitting flow of solvent only. This phenomenon is known as *reverse osmosis* (RO), and depicted in Figure 15.13. Basic RO system with the required components is shown in Figure 15.14.

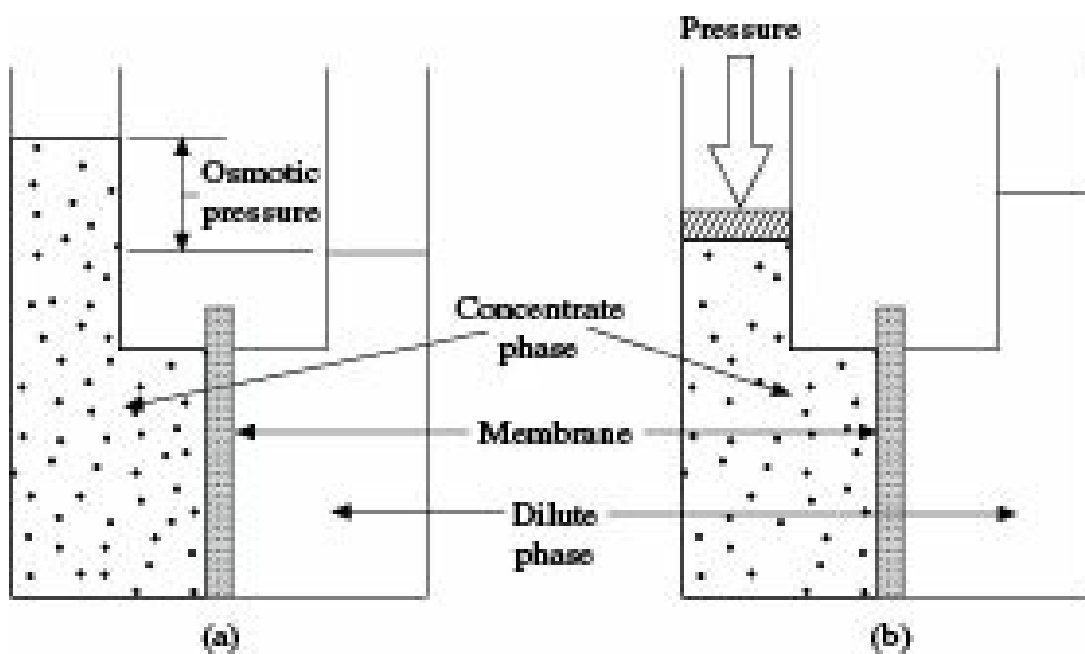


Figure 15.13 (a) Reverse osmosis, (b) Flow reversal principle.

Feed water to the RO system is pumped first through a micrometer filter following a sedimentation tank. This is a replaceable cartridge element filter. The purpose of this filter is to remove any turbidity and particulate matter from the feed water before it enters the RO system. The filtered raw water then flows to a high-pressure pump (not shown in figure),

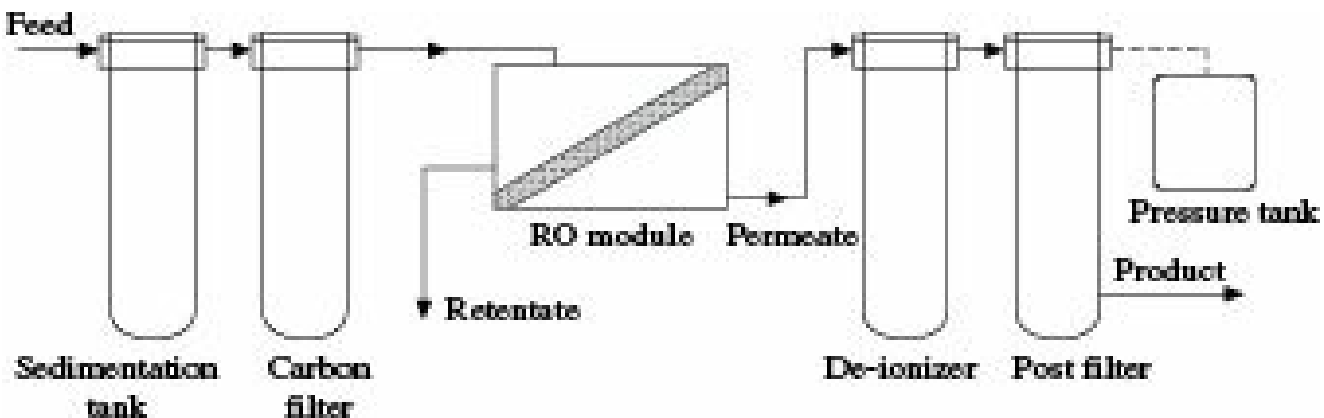


Figure 15.14 Basic components of a RO system.

which feeds the raw water through the RO membrane system. Valves and pressure gauzes between the micrometer filter, the high-pressure pump and membrane modules control the flow of water through the system and monitor its operation. The RO system consists of two stages. The raw water is pumped through the first stage, which contains twice the number of membrane modules as the second stage. The first stage purifies 50% of the water fed to the system and rejects the remaining 50%, which contains all contaminants. This reject water from the first stage is then passed through the second stage, which purifies 50% of the water fed to it and rejects the remaining 50% to waste. This second stage reject contains all of the contaminants removed by both stages. Thus, the total flow through the system is 75% purified product water and 25% reject water.

The RO system removes 90-95% of the total dissolved solids in the raw water, together with suspended matter (including colloidal and organic materials). The exact percent of product purity, product recovery and reject water depends on the amount of dissolved solids in the feed water and the temperature at which the system operates.

RO membrane performance in the utility industry is a function of two major factors—the membrane material and the configuration of the membrane module. Most utility applications use either spiral-wound or hollow-fibre elements. Hollow-fibre elements are particularly prone to fouling and, once fouled, are hard to clean. Thus, applications that employ these fibres require a great deal of pretreatment to remove all suspended and colloidal material in the feed stream. Spiral-wound modules due to their relative resistance to fouling, have a broader range of applications. Two common types of membrane materials used are cellulose acetate and aromatic polyamide membranes. Cellulose acetate membrane performance is particularly susceptible to annealing temperature, with lower flux and higher rejection rates at the higher temperatures. Such membranes are prone to hydrolysis at extreme pH, are subject to compaction at operating pressures, and are sensitive to free chlorine above 1.0 ppm. These membranes generally have a useful life of 2 to 3 years. Aromatic polyamide membranes are prone to compaction. These fibres are more resistant to hydrolysis than are cellulose acetate membranes.

Reverse osmosis membranes are capable of retaining ionic species like sodium chloride or magnesium sulphate, which can freely pass through microfiltration or ultrafiltration membranes. Because of retention of small ionic species having fairly high osmotic pressure, reverse osmosis is operated at relatively high pressure, generally in the range of  $(2.8-7.0) \times 10^3 \text{ kN/m}^2$ , in order to overcome the high osmotic pressure opposing separation of solute from solvent.

Reverse osmosis (RO) for water and waste-water treatment is a well-established process. Typical applications include desalination of sea water to make it potable, removal of salts and minerals for

water recycling in power generating plants, preparation of high quality water supplied for boiler make-up, preparation of high quality drinking water, in the manufacture of spirits, treating wet sulphur dioxide scrubber waste. The main advantage of this process is that it can operate at room temperature and there is no phase change, which would require large amount of heat to be added or removed. The use of RO for desalination of sea water for boiler make-up is a typical application in parts of the Middle East. The availability of this system has opened up the use of heretofore unavailable water supplies and it has been used by the industry as a pretreatment to ion-exchange demineralization. Reverse osmosis acts as an economical roughing demineralizer, bringing down the overall cost and improving the life of resins and operation of the ion exchange equipment.

Two primary membrane separation methods of water desalination are reverse osmosis and electrodialysis. The ED process has many advantages over RO process as it requires a lower level of water pretreatment and reduced membrane replacement frequency but its practicability is hindered by the limited membrane materials and membrane quality available. Polymer membranes used in ED have poor thermal and chemical stability, high sensitivity and a fouling tendency towards organic contaminants. Recently nanotechnology is being exploited to develop new membranes for ED process which would lead to cost effective and highly efficient water recovery systems.

## 15.8 Pervaporation

Pervaporation is the only rate governed membrane separation process where phase transfer occurs. It is a term derived from two major integral operations involved in the separation process—*permeation* and *evaporation*. In the process, a liquid feed mixture is separated by means of selective diffusion-vaporisation through a nonporous membrane (Satyanarayana et al. 2004). It is the separation by partial vaporisation through a semi-permeable membrane. Two models are often used to describe the transport processes through the membrane—One is the ‘solution-diffusion’ model (Binning et al. 1961, Wijmans and Baker 1995) which assumes that the selective component gets dissolved in the selective layer of the membrane and then diffuses through the membrane to the lower pressure side which is usually maintained at vacuum. The other model, the ‘pore flow’ model (Okada and Matsuura 1991), has the following three consecutive steps:

- (i) the liquid transport from the pore inlet to the liquid-vapour phase boundary,
- (ii) evaporation at the phase boundary, and
- (iii) vapour transport from the phase boundary to the pore outlet.

In pervaporation, both driving force and permeability coefficient are dependent on temperature and concentration. Two process configurations are generally encountered in industries: (i) complete mixing at feed side and permeate side, and (ii) cross-flow at the feed side and complete mixing at the vapour side. Commercial pervaporation systems normally operate under conditions similar to the latter configuration.

### ***Complete mixing in pervaporation***

Complete mixing implies that the concentrations at the feed side are constant at each point in the module and are equal to the retentate concentrations. Also at the permeate side, the concentrations are same at any point. The schematic representation is depicted in Figure 15.15.

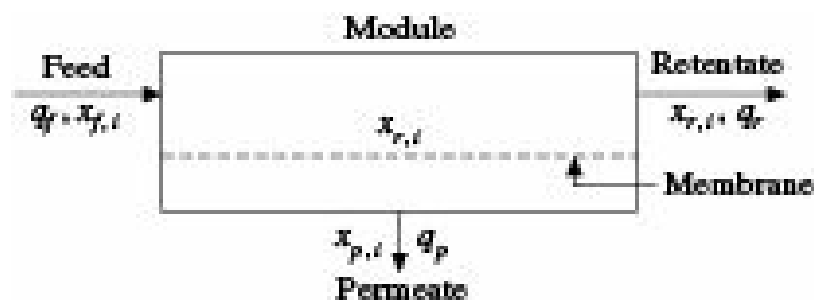


Figure 15.15 Pervaporation with perfect mixing.

The overall material balance is

$$q_f = q_p + q_r \quad (15.28)$$

where  $q_f$ ,  $q_p$  and  $q_r$  represent the volumetric flow rates of the feed, permeate and retentate, respectively.

The mass balance for component  $i$  is

$$q_{f,i} = q_{p,i} + q_{r,i} \quad (15.28a)$$

or,

$$q_f \cdot x_{f,i} = q_p \cdot x_{p,i} + q_r \cdot x_{r,i} \quad (15.28b)$$

where,  $q_{f,i}$ ,  $q_{p,i}$  and  $q_{r,i}$  are the volumetric flow rate of component  $i$  in the feed, permeate and retentate, respectively,

$x_{f,i}$ ,  $x_{p,i}$  and  $x_{r,i}$  are the concentrations of the component  $i$  in the feed, permeate and retentate, respectively in mole fraction.

The recovery,  $S$  defined as the fraction of the feed that has permeated through the membrane, is

$$S = \frac{q_p}{q_f} \quad (15.29)$$

Dividing Eq. (15.29) by  $q_f$  gives the following equations for the concentrations of permeate and retentate, respectively:

$$x_{p,i} = \frac{x_{f,i} - x_{f,i}(1-S)}{S} \quad (15.30)$$

and

$$x_{r,i} = \frac{x_{f,i} - S \cdot x_{p,i}}{1-S} \quad (15.31)$$

The selectivity,  $a_{i,j}$  for a perfect mixing system with components  $i$  and  $j$  can be expressed as

$$a_{i,j} = \frac{x_{p,i}/x_{p,j}}{x_{r,i}/x_{r,j}} = \frac{x_{p,i}/(1-x_{p,i})}{x_{r,i}/(1-x_{r,i})} \quad (15.32)$$

$$x_{p,i} = \frac{\alpha_{i,j} \cdot x_{r,i}}{\alpha_{i,j}(\alpha_{i,j}-1)+1} \quad (15.33)$$

where  $i$  has been assumed to be more permeable component. Combining Eqs. (15.31) and (15.33), we get

$$[S(a_{i,j} - 1)] x_{p,i}^2 - [x_{f,i} (a_{i,j} - 1) + (1 - S) + a_{i,j} \cdot S] x_{p,i} + a_{i,j} \cdot x_{f,i} = 0 \quad (15.34)$$

Analysis of Eq. (15.34) gives rise to

$$S = \frac{\alpha_{i,j} \cdot x_{p,i} - (\alpha_{i,j} - 1)x_{f,i}x_{p,i} - x_{p,i}}{(\alpha_{i,j} - 1)(x_{p,i} - x_{p,i}^2)} \quad (15.35)$$

$$x_{f,i} = \frac{(1 - \alpha_{i,j})x_{p,i} - (\alpha_{i,j} - 1)S \cdot x_{p,i}^2 + \alpha_{i,j} \cdot S \cdot x_{p,i}}{\alpha_{i,j} - (\alpha_{i,j} - 1)x_{p,i}} \quad (15.36)$$

When the concentrations of the feed and permeate are known, the recovery  $S$  can be determined using Eq. (15.35), and the concentration of the feed can be estimated using Eq. (15.36) if the recovery and the permeate concentration are known.

The recovery can also be obtained from the energy balance. For the complete mixing, the temperature at the feed side is constant, and the energy balance can be written as

$$q_f c_{p,f}(T_f - T_0) = q_r c_{p,r}(T_r - T_0) + q_f c_{p,p}(T_p - T_0) + DH_v q_p \quad (15.37)$$

where,  $DH_v$  is the heat of vaporisation,

$c_{p,f}$ ,  $c_{p,r}$  and  $c_{p,p}$  are the specific heats of the feed, retentate and permeate, respectively.

Since there is thermal equilibrium between the feed side and permeate side,  $T_r = T_p$ . Equation (15.37) can further be simplified as a reference temperature  $T_0$  can be chosen arbitrarily. Hence,  $T_r = T_p = T_0$ . Equation (15.37) can therefore be written as

$$q_f c_{p,f}(T_f - T_r) = DH_v q_p \quad (15.38)$$

$$S = \frac{c_{p,f}(T_f - T_r)}{\Delta H_v} \quad (15.39)$$

and

$$J_{M,i} = \frac{q_i}{Z} D p_i \quad (15.40)$$

The flux of component  $i$  is given by

$$J_{M,i} = \frac{q_i}{Z} (x_{r,i} c_i p_i^0 - x_{p,i} p_p) \quad (15.41)$$

where

$J_{M,i}$  = volumetric flux of the component  $i$

$c_i$  = activity coefficient of component  $i$

$p_i^0$  = saturation pressure of the pure component  $i$

$p_p$  = pressure on the permeate side

$q_i$  = permeability coefficient of component  $i$

$Z$  = thickness of the membrane.

The flux can be calculated using Eq. (15.41) provided the values of  $x_{r,i}$  and  $x_{p,i}$  are known.

### Cross-flow in pervaporation

A more realistic flow pattern is cross-flow at the feed side and perfect mixing at the permeate side. The difference between the complete mixing and the cross-flow is that the concentration of the component  $i$  at the feed changes gradually across the system from feed inlet to retentate. Moreover, the temperature decreases as well across the feed side and finally the permeability coefficient depend on concentration and temperature. A system can be divided into a number of segments where the permeability coefficient is supposed to be constant but may be different in the next stage. Therefore, the concentration dependency of the permeability coefficient should be determined experimentally. The number of stages is mainly dependent on the concentration dependency of the permeability coefficient and of the flux. The flux in a certain stage can be calculated using the expression as used for gas separation under cross-flow conditions:

$$J_{M,i} = \frac{q'_i}{Z} (x_{i,lm} c_i p_i^0 - x_{p,i} p_p) \quad (15.42)$$

where

$x_{i,lm}$  = log mean concentration of component  $i$

$q'_i$  = average permeability coefficient of component  $i$ .

Knowing the value of flux either from Eq. (15.41) or Eq. (15.42), the area of the membrane ( $A_M$ ) can be calculated using the expression

$$A_M = \frac{q_{p,i}}{J_{M,i}} = \frac{q_p x_{p,i}}{J_{M,i}} \quad (15.43)$$

Pervaporation is a commercially competitive, membrane based separation process for selective separation of component(s) from a solution. If the proper membrane material is selected, pervaporation can separate azeotropic mixture and close boiling mixtures which cannot be separated by traditional distillation methods. Although, the discovery of pervaporation dates back to 1917, it is getting more commercial importance and most of the research work on this process has been done in the past two decades. A large volume of experimental data is available for the dehydration of ethanol-water system and the behaviour of the system has been well predicted and commercialization is very much successful (Morigami et al. 2001). Other systems like propanol, butanol, acetic acid, etc. have also been investigated for dehydration application. The pervaporation process looks attractive for removing volatile organic compounds (VOCs) from waste water systems and dilute streams from various industries and for separation of aroma components from natural resources.

Separation of FCC gasoline containing 500 ppm sulphur into two product streams i.e. sulphur and gasoline can be achieved using pervaporation technology. The gasoline feed passes over a special polymeric membrane that is selective for sulphur containing hydrocarbon molecules. As gasoline passes over the membrane, sulphur containing molecules and some hydrocarbon molecules enter in membrane structure while other molecules are rejected and lower sulphur retentate product is obtained. Vacuum is applied on the other side of the membrane. Once through the membrane, the

permeated stream is condensed and further processed. The product gasoline retains most of the olefins in the feed and therefore preserves its octane value. The retentate containing about 70-90% of the inlet gasoline will have a sulphur level of less than 30 ppm and can be directly blended with gasoline pool. The other stream, i.e. the permeate contains the bulk of sulphur and requires to be treated in a relatively small hydrodesulphurizer.

## 15.9 Design Procedure for Membrane Separation

When two components are separated, the permeance for a given component diffusing through a membrane is defined as the flow rate of that component per unit cross sectional area of the membrane per unit driving force per unit thickness.

The molar transmembrane flux  $J_{M,i}$  for component  $i$  is given by

$$J_{M,i} = \frac{q_i}{Z} DF_i = Q_i DF_i \quad (15.44)$$

where,  $\Delta F_i$  is the driving force of component  $i$  across the membrane

For a given application, the calculation of the required membrane surface area is generally based on laboratory data for the selected membrane. Although permeation can occur by one or more of the transport mechanisms, all are consistent with Eq. (15.44). For example, the mechanisms for the transport of liquid or gas molecules through a porous membrane can involve bulk flow through the pores, diffusion through the pores, and solution diffusion through dense membranes.

In terms of the bulk flow of a gas through a porous membrane, subjected to a pressure difference, Eq. (15.44) takes the form of

$$J_{M,i} = \frac{q_i (p_f - p_p)}{Z} \quad (15.45)$$

where,  $p_f$  and  $p_p$  are the pressures on the feed and permeate surfaces of the membrane respectively, and  $q_i$  is given by

$$q_i = \frac{\rho t^3}{4.16(1-\epsilon)^2 a_v^2 \mu} \quad (15.46)$$

where,

$a_v$  = pore surface area per unit volume of membrane

$t$  = density of the gas, and

$\mu$  = viscosity of the gas

The porosity of the membrane is obtained from

$$f = \frac{n\pi}{4} \frac{d_p^2}{4} \quad (15.47)$$

where,  $n$  is the number of pores per unit cross section of the membrane.

When the pores are assumed to be cylindrical,  $a_v$  is simply equal to  $6/d_p$ .

If the bulk flow is in the laminar region ( $Re < 2100$ ), which is almost always the case for flow in

small-diameter pores, the bulk-flow flux with the above assumption reduces to

$$J_{M,i} = \frac{\rho \epsilon^3 (p_f - p_p)}{4.16(1-\epsilon)^2 a_v^2 Z \mu} \quad (15.48)$$

Equation (15.48) can be used as a first approximation to obtain the pressure drop for flow through a porous membrane with a tortuosity factor greater than 2. For gas flow, the density may be taken as the arithmetic average of the densities at the feed and permeate surfaces of the membrane.

In liquid diffusion, the solute transmembrane flux is obtained from a modified form of Fick's law as

$$J_{M,i} = D_i \left(\frac{f}{x}\right) (c_f - c_p) K_{r,i} \quad (15.49)$$

where,

$D_i$  = diffusivity of solute  $i$  in the feed mixture

$f$  = porosity of the membrane defined by Eq. (15.47)

$x$  = tortuosity factor

$c_f, c_p$  = concentrations of solute  $i$  in the membrane pores at the feed and permeate surfaces of the membrane, respectively and

$K_{r,i}$  = a restrictive factor that accounts for the effect of pore diameter when the ratio of molecular diameter  $d_m$  to pore diameter  $d_p$  exceeds about 0.01, may be evaluated from

$$K_{r,i} = \left(1 - \frac{d_m}{d_p}\right)^4 \text{ for } \frac{d_m}{d_p} \leq 1 \quad (15.50)$$

In general, transmembrane fluxes for liquids through microporous membranes are very small because diffusivities themselves are very low.

In gas diffusion, the rate of component diffusion can also be expressed in terms of Fick's law. If pressure and temperature on either side of the membrane are equal and the pressure is low to validate use of the ideal gas law, the transmembrane flux relation can be written as

$$J_{M,i} = \frac{D_{iE}}{RTZ} (p'_f - p'_p) \quad (15.51)$$

where,  $D_{iE}$  = effective diffusivity of component  $i$  including both ordinary diffusion and Knudsen diffusion and

$p'_f$  and  $p'_p$  = partial pressures of component  $i$  in the membrane pores at the feed and permeate surfaces of the membrane, respectively.

When Knudsen flow predominates, as it usually does in the micropores of many membranes, the permeability ratio of the two components being separated is inversely proportional to the ratio of the molecular weights of the two components. Except for gaseous components with widely differing molecular weights, the permeability ratio is not very large. This indicates that separation by gaseous diffusion without an accompanying driving force in most cases is not very promising.

The transport of components through nonporous membranes, however, is the mechanism of membrane separators for reverse osmosis, gas permeation, and pervaporation. Liquid diffusivities are several

orders of magnitude less than gas diffusivities and diffusivities of solutes in solids are a few orders of magnitude less than diffusivities in liquids.

Because of the low separation efficiencies obtained with simple liquid or gas diffusion, most membrane systems utilize solution diffusion separations. The solution diffusion model developed by Lonsdale et al. (1965) is most often used to design membrane separators. This model is based on Fick's law for diffusion through solid nonporous membranes subjected to a driving force in which the concentrations are those of the solute dissolved in the membrane. The concentrations in the membrane are related to the concentrations or partial pressures in the fluid adjacent to the membrane faces by assuming thermodynamic equilibrium at the fluid/membrane interfaces.

Comparisons of typical solute profiles for liquid mixtures and for gas mixtures with porous and nonporous membranes are shown in Figure 15.16. For porous membranes the concentration and partial pressure profiles are continuous from the bulk feed side to the bulk permeate side. In nonporous membranes there are film resistances to mass transport at both surfaces of the membrane. Assuming that thermodynamic equilibrium exists at these two fluid/membrane interfaces, the concentrations in Fick's law can be related through the use of thermodynamic equilibrium partition coefficients,  $K_{D_i}$  in the case of liquid mixtures and through the use of Henry's law constant  $H_i$  for gas mixtures.

When the mass-transfer resistances in the two boundary layer films are negligible, the solute transmembrane flux for liquid mixtures is given by

$$J_{M,i} = \frac{K_{D_i} \cdot D_i}{Z} (c_{f,i} - c_{p,i}) \quad (15.52)$$

where the product ( $K_{D_i} \cdot D_i$ ) is the permeance  $q_i$ . In the solution diffusion model,  $K_{D_i}$  accounts for the solubility of the solute  $i$  in the membrane, and  $D_i$  accounts for the diffusion of component  $i$  in the membrane. Since  $D_i$  is generally very small, it is critical that the membrane material provides a large value for  $K_{D_i}$  and/or a small membrane thickness.

Using the same approach with similar assumptions, the solution diffusion model for gas mixtures provides a comparable relation for the solute transmembrane flux of the solute

$$J_{M,i} = \frac{D_i}{H_i Z} (p'_{f,i} - p'_{p,i}) \quad (15.53)$$

The latter depends on both the solubility of the solute in the membrane and the diffusivity of that component in the feed. An acceptable rate of transport through the membrane can only be achieved by using a very thin membrane and a high-pressure difference across the membrane.

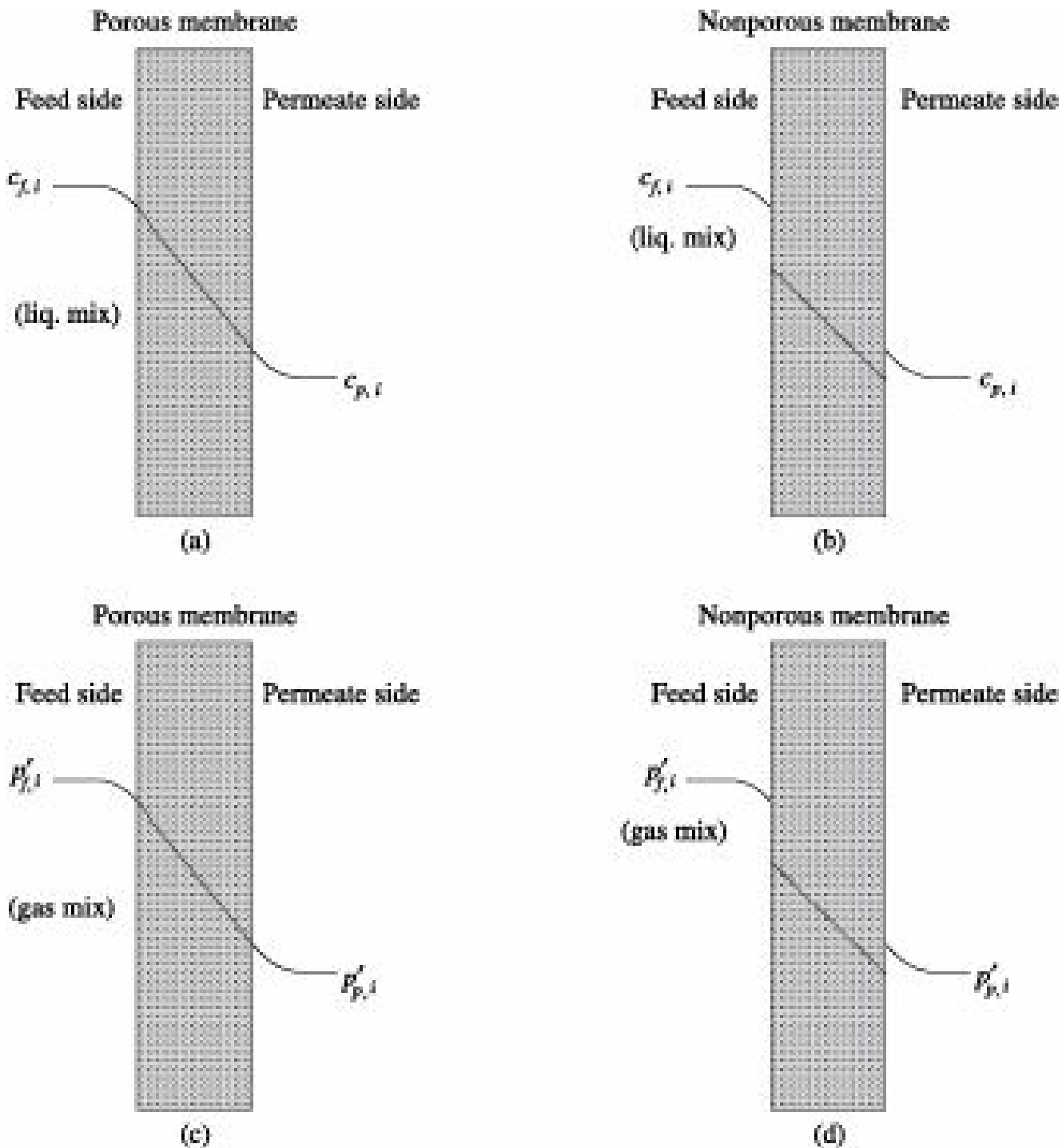


**Figure 15.16** Typical solute profiles for liquid and gas mixtures with porous and non-porous membranes. Liquid mixture with (a) porous and (b) non-porous membranes; Gas mixture with (c) porous and (d) non-porous membranes.

The ideal nonporous membrane exhibits a high permeance for the penetrant molecule and a high separation factor or selectivity,  $a_{i,j}$  between the components to be separated. The separation factor,  $a_{i,j}$  is defined as

$$a_{i,j} = \frac{y_{p,i}/y_{p,j}}{x_{r,i}/x_{r,j}} \quad (15.54)$$

where,  $y_{p,i}$  is the mole fraction of component  $i$  in the permeate leaving the membrane and  $x_{r,i}$  is the mole fraction of component  $i$  in the retentate on the feed side of the membrane. The subscripts  $i$  and  $j$  refer to the components being separated. When the film mass-transfer resistances are negligible on both sides of the membrane and the permeate pressure is very small compared to the feed pressure,

the ideal separation factor can be simplified to

$$a_{i,j}^* = \frac{D_i H_j}{D_j H_i} = \frac{q_i}{q_j} \quad (15.55)$$

The transport of components  $i$  and  $j$  through the membrane, because of perfect mixing, can be written as

$$y_{p,i} n_p = A_M Q_i (x_{r,i} p_r - y_{p,i} p_p) \quad (15.56)$$

and

$$y_{p,j} n_p = A_M Q_j (x_{r,j} p_r - y_{p,j} p_p) \quad (15.57)$$

where

$A_M$  = membrane area normal to the flow

$n_p$  = mols in the permeate

$p_r$  = pressure at the retentate side of the membrane.

When the permeate pressure is not negligible, an expression for  $a_{i,j}$  can be expressed in terms of the pressure ratio ( $p_p/p_f$ ) as

$$a_{i,j} = a_{i,j}^* \frac{x_{r,j}(\alpha_{i,j} - 1) + (1 - \alpha_{i,j})(p_p/p_f)}{x_{r,i}(\alpha_{i,j} - 1) + 1 - (p_p/p_f)} \quad (15.58)$$

where  $x_{r,i}$  is the mol fraction in the retentate on the feed side of the membrane corresponding to the partial pressure  $p'_{f,i}$  in Figure 15.16. Equation (15.58) is an implicit equation for  $a_{i,j}$  in terms of the ( $p_p/p_f$ ) ratio and  $x_i$  that can be solved for  $a_{i,j}$  by using the expression for a quadratic equation. Generally, the permeabilities are high and the separation factors are low in rubbery polymers. The opposite is also true for the glassy polymers. For a given feed composition, however, the separation factor limits the degree of separation that can be attained. A listing of ideal separation factors is available in the *Membrane Handbook* (Ho and Sirkar 1992).

Discussions on this point have assumed a flow pattern with perfect mixing of both the retentate and permeate streams as shown in Figure 15.17(a). Three other flow patterns shown in Figures 15.17(b)-15.17(d) are also used in membrane separation processes. These are the flow patterns of counter-current, co-current, and cross-flow, all assume no fluid mixing and are comparable with the idealized flow patterns used in heat-exchanger design. For a given type of equipment discussed earlier, it is not always obvious which idealized flow pattern to assume. For example, hollow-fiber membrane separation systems may be designed to approximate counter-current, co-current, or cross-flow patterns.

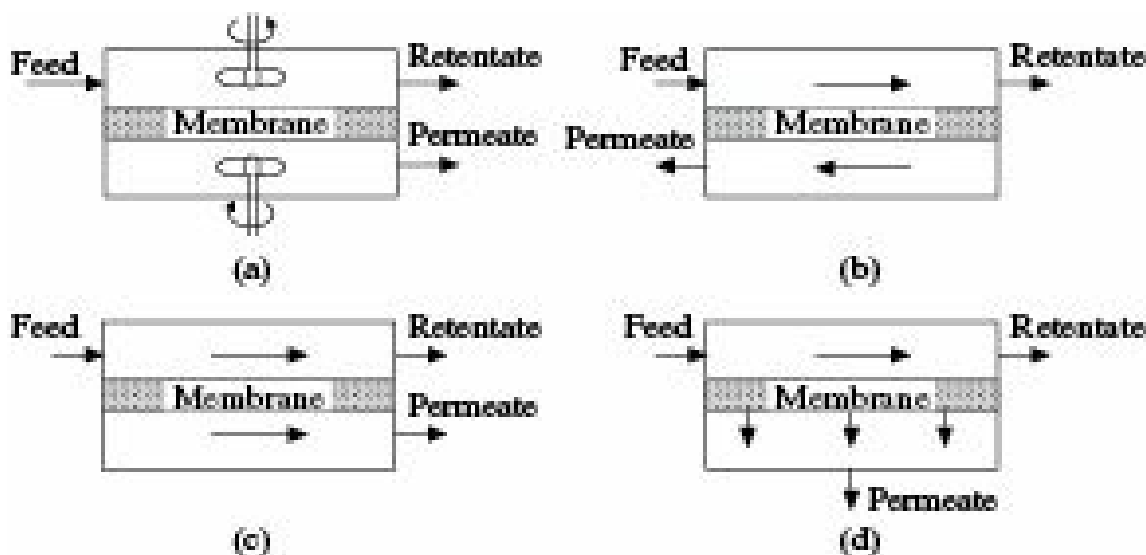


**Figure 15.17** Flow pattern in membrane modules with (a) perfect mixing, (b) counter-current flow, (c) co-current flow and (d) cross-flow.

Solution methods for all four flow patterns are presented by Walawender and Stern (1972) under the assumptions of a binary feed with constant ( $p_p/p_f$ ) ratio and constant ideal separation factor. Exact analytical solutions are available for the situations involving perfect mixing and the cross-flow. Numerical solutions of the ordinary differential equations with appropriate computer codes are required for the situation involving counter-current and co-current flow.

The extent to which a feed mixture can be separated in a single stage is determined by the separation factor  $a$ . The latter depends on the existing flow pattern, the permeability ratio, the driving force for mass transfer and the stage cut  $Q$ , defined as the ratio of the moles in the permeate to the moles in the feed ( $n_p/n_f$ ). Achieving a higher degree of separation will require a counter-current cascade of stages. For a cascade, additional factors that affect the degree of separation of the feed are the number of stages and the recycle ratio, defined as the ratio of permeate recycle rate to permeate product rate. Studies have shown that it is best to manipulate the stage cut and reflux rate at each membrane stage so that the compositions of the two streams entering each stage will be the same.

Generally, it is assumed that the pressure drop on the retentate side of the membrane in a cascade arrangement is negligible. Thus, only the permeate must be pumped when it is a liquid, or compressed when it is a gas, in order to transfer to the next stage. In the case of gas permeation, compression costs can be quite high. Therefore, membrane cascades for gas permeation are often limited to just two or three stages. Common recycle cascades normally involve a two-stage stripping cascade, a two-stage enriching cascade, or a two-step enriching cascade with an additional premembrane stage.

Since design procedures for counter-current and co-current flow patterns necessitate developing a series of differential equations requiring computer solution, the design procedures discussed will be limited to the perfect mixing and cross-flow patterns in membrane modules. For the perfect mixing flow pattern, the initial step is to establish the operating conditions of temperature, pressure and flow rate of the feed. Using the guidelines presented earlier, select the most appropriate membrane for the separation, noting the need for a high separation factor, that is, the membrane must possess a high permeance and a high permeance ratio for the two components being separated by the membrane.

Next, a material balance must be made equating the molar flow rate of each component in the feed to the sum of the molar flow rates in the permeate and retentate streams. Upon substitution of the stage cut definition into the material balance equations, the resulting equations can be expressed in terms of

mole fraction in the retentate streams.

Since both fluid sides are well mixed, the ideal separation factor  $a_{i,j}^*$  may be obtained using Eq. (15.55). The actual separation factor may then be calculated from Eq. (15.58) if the permeate pressure is not negligible. Solution of Eqs. (15.56) and (15.57) will determine the required membrane area for the desired stage cut Q.

In the cross-flow pattern, the feed flows across the upstream membrane surface in plug flow with no longitudinal mixing. In the analytical solution developed by Naylor and Backer (1955), the pressure ratio and the ideal separation factor are assumed constant. The film mass-transfer coefficients on both sides of the membrane are assumed to be negligible. If a differential element within the membrane is considered, the local mole fractions in the retentate and the permeate are  $x_i$  and  $y_i$ , respectively; and the penetrant molar flux is  $(dn/dA_M)$ .

The local separation factor can be obtained with Eq. (15.58) in terms of the local  $x_i$ ,  $(p_p/p_f)$  and  $a_{i,j}^*$ . An alternative expression for the local permeate composition is given by

$$\frac{y_i}{1-y_i} = \frac{\alpha_{i,j}^*[(x_i - y_i)(p_p/p_f)]}{1-x_i - (1-y_i)(p_p/p_f)} \quad (15.59)$$

A material balance around the differential element within the membrane for component  $i$  results in

$$y_i dn = d(nx_i) = n dx_i + x_i dn \quad (15.60)$$

Equation (15.54) can be used to eliminate the  $y_i$  term in Eq. (15.60) to give

$$\frac{dn}{n} = \frac{[1 + (\alpha_{i,j} - 1)x_i]dx_i}{x_i(\alpha_{i,j} - 1)(1-x_i)} \quad (15.61)$$

When the pressure ratio  $(p_p/p_f)$  is small, the separation factor remains relatively constant over much of stage cut range. With this assumption, Eq. (15.61) can be integrated from the local point within the differential element to the final retentate flow rate and composition. The integration results in

$$n = n_r (1 - Q) \left( \frac{x_i}{x_{r,i}} \right)^{1/(\alpha_{i,j} - 1)} \left( \frac{1 - x_{r,i}}{1 - x_i} \right)^{\alpha_{i,j}/(\alpha_{i,j} - 1)} \quad (15.62)$$

The mole fraction of component  $i$  in the final permeate is obtained by integrating the following relation:

$$y_{p,i} = \int_{x_i}^{x_{r,i}} \frac{y_i}{\Theta n_f} dn \quad (15.63)$$

This integral in terms of  $n$  can be transformed into an integral in  $x_i$  by utilizing Eqs. (15.54), (15.59) and (15.62). Integration of the resulting integral for component  $i$  gives

$$y_{p,i} = x_{r,i}^{1/(1-a)} \frac{1-\Theta}{\Theta} [(1-x_{r,i})^a/(a-1) \left( \frac{x_{f,i}}{1-x_{f,i}} \right)^{\omega/(a-1)} - x_{r,i}^{1/(1-a)}] \quad (15.64)$$

where the  $a_{i,j}$  represented as  $a$  can be estimated from Eq. (15.58) by assuming  $x_i = x_{f,i}$ . The differential rate of mass transfer of component  $i$  across the membrane is then given by

$$y_i dn = \left( \frac{q_i}{Z} \right) (x_i p_f - y_i p_p) dA_M \quad (15.65)$$

from which the total membrane area can be obtained by integration of the relation

$$A_M = \int_{x_{r,i}}^{x_{f,i}} \frac{y_i Z}{q_i (x_i p_f - y_i p_p)} dn \quad (15.66)$$

## 15.10 Membrane Based Reactive Separation

Membrane based separation processes such as distillation, absorption and extraction have witnessed a large number of applications in the industry. Membrane based reactive separations, commonly referred to as membrane reactors, have attracted interest over the last two decades due to various functions played by a membrane in a reactor system. Some typical functions of membrane in a reactor are shown in Figure 15.18. Many more functions of membrane reactor in a single unit have been described in details elsewhere (Sirkar 1999).

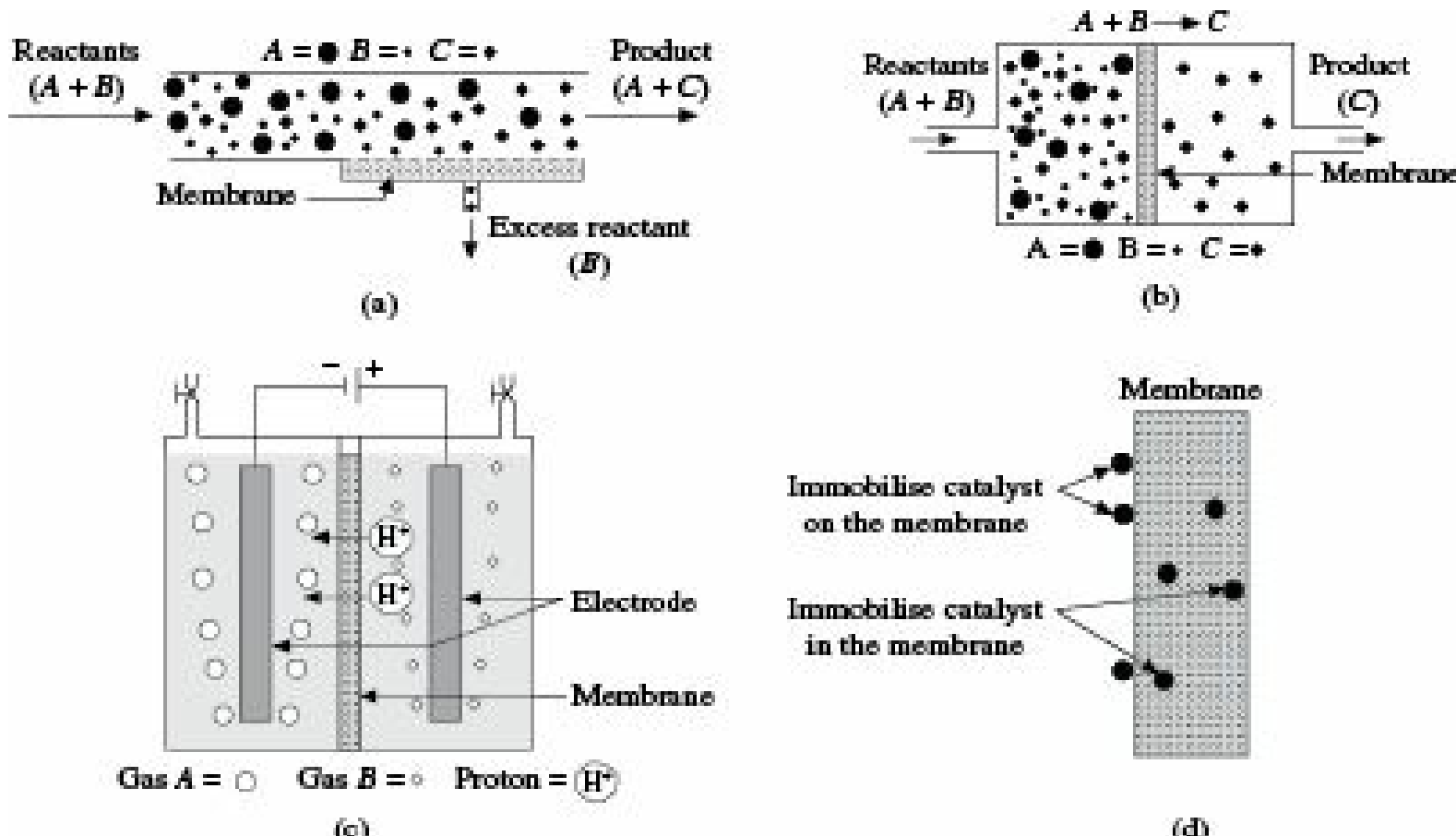


**Figure 15.18** Some functions of membrane in a reactor (a) Separation of a reactant from the reaction mixture, (b) Separation of product from the reaction mixture, (c) In water electrolyzer as proton exchange membrane and (d) Immobilization of catalyst in/on the

membrane.

The heat and mass integrated combination of hydrogenation and dehydrogenation process has been found to be effective in a single membrane unit (Dittmeyer et al. 2001). The use of a membrane pervaporation reactor has been explored for esterification reactions while supra-equilibrium conversions have been achieved (Krishna 2003). The application areas of catalytic membrane reactors include dehydrogenation (ethane to ethene, ethyl benzene to styrene, methanol to formaldehyde), Steam reforming of methane, water gas shift reaction, selective oxidations (propane to acroleine, butane to maleic anhydride, ethylene to ethylene oxide), oxidative dehydrogenation of hydrocarbons, oxidative coupling of methane and methane oxidation to synthesis gas. In an enzymatic membrane reactor with a lipase-immobilised on a polymeric membrane and geranyl acetate, synthesis of ester can be made effectively (Holownia and Noworyta 2007). Another application of enzymatic membrane reactor is the production of S-ibuprofen via hydrolysis of (R,S)-ibuprofen methyl ester coupled with a racemisation of the unwanted enantiomer through removal of the product *in situ* using an ultrafiltration (Krishna 2003). The process helps in avoiding deactivation of the esterase enzyme and leading to a two-fold increase in conversion and production. A two-phase reactor with carbon membrane can be a viable option for production of fatty acid methyl esters (biodiesel) from canola oil and methanol as the process achieves conversions higher than the equilibrium one by *in situ* removal of biodiesel and glycerol along with some methanol from the reaction (Dube et al. 2007). Potential application areas can be nitrate removal in drinking water treatment, removal of endocrine disrupting compounds from water and waste water streams, enhancement of biofuels production using membrane assisted fermentations, and gas extraction and purification in membrane bioreactors. A membrane bioreactor (MBR) with granular activated carbon in enhanced quantity rather than powdered activated carbon can be explored for treatment of industrial waste water containing high organic and other compounds that resist microbial breakage. It is fact that powdered activated carbon causes abrasion on microfiltration membrane resulting in higher operating cost due to shorter life of membrane but granular activated carbon eliminates such abrasion and also keeps the material in suspension state inside the reactor without using extra energy. The advantages of the technology are its considerably reduced carbon uptake and longer service life compared to the powdered activated carbon based system. However, the extensive use of membrane reactors is getting restricted because of relatively high price of membrane units, low permeability, sealing problems, mechanical and thermal agileness of the membranes.

## 15.11 Bioseparations

Separation science forms an integral part of modern chemical and biotechnology. Analysis of mixtures of compounds resulting from synthetic reactions or produced by the diverse cellular factories of nature, is a common problem in both laboratory and industrial sectors. Separation becomes difficult when there are little differences in between the molecules to be separated. Biological activity has been shown to be a highly specific property of a molecule related to its tertiary structure and can be said to be the final stop in the list of differences between two molecules. The process of finding and/or designing intermolecular interactions that can lead to increased separation factor can be termed *selectivity engineering*. Modern separation science or selective engineering aims at devising separation technologies that take advantage of differences in specific biological activities of biomolecules when all other differences fail to provide a healthy separation

factor. Although a plethora of separation related products, machines and technologies are commercially available, each separation problem faced by a molecular biologist, a medicinal chemist or an industrial biotechnologist needs to be studied in details for arriving at an amicable solution. Modern separation problems are challenging the engineers and technologists, particularly biotechnologists. Study of biochemical pathways and system biology requires elucidation of structure-activity relationships of hundreds of proteins and other biological molecules that are to be purified.

It is expected that with increasing understanding of the role of proteins and sugar molecules in cell metabolism, increasing number of drugs will be biomolecules. The development of new biological entities may outplace development of new chemical entities in the coming decades. Characterization and purification of biomolecules are more rigorous and tedious than that of synthetic molecules. Design of inexpensive selective, robust and high throughput adsorbents is the modern day bioseparation challenge to which answers must have to be found through research in industry as well as in academic institutions.

## **Nomenclature**

$a_v$  : pore surface area per unit volume of membrane,  $\text{L}^2/\text{L}^3$

$A_M$  : total membrane area,  $\text{L}^2$

$c$  : concentration,  $\text{mol/L}^3$

$\Delta c$  : concentration difference,  $\text{mol/L}^3$

$d$  : diameter of the tube,  $\text{L}$

$d_p$  : mean pore diameter,  $\text{L}$

$D_i$  : diffusivity of component  $i$ ,  $\text{L}^2/\square$

$D_{AB}$  : mass diffusivity of component  $A$  in  $B$ ,  $\text{L}^2/\square$

$D_{AE}$  : effective diffusivity of component  $A$  through the membrane,  $\text{L}^2/\square$

$D'_A$  : Knudsen diffusivity,  $\text{L}^2/\square$

$E$  : electromotive force, activation energy

$\Delta E$  : difference in e.m.f, volt

$H$  : Henry's law constant

$J_M$  : permeation volumetric flux,  $\text{L}^3/\text{L}^2\square$

$J_i$  : permeation mass flux of component  $i$ ,  $\text{L}^3/\text{L}^2\square$

$J_{M,i}$  : volumetric permeation/filtration flux,  $\text{L}^3/\text{L}^2\square$

$K_D$  : equilibrium partition coefficient

$K$  : overall mass transfer coefficient,  $\text{L}^3/\text{L}^2\square$  ( $\text{mol/L}^3$ )

$k$  : local mass transfer coefficient,  $\text{L}/\square$

$M$  : Molecular weight, M/mol  
 $P$  : total pressure, atm.  
 $\Delta P$  : pressure difference, atm.  
 $p'$  : partial pressure, atm.  
 $p$  : vapour pressure, atm.  
 $\Delta p$  : vapour pressure difference, atm.  
 $p_i^0$  : saturation pressure of the pure component  $i$ , atm.  
 $q_A$  : permeability coefficient of component  $i$ , the phenomenological coefficient  
 $q_f, q_p, q_r$  : volumetric flow rate of the feed, permeate and retentate, respectively, L<sup>3</sup>/q  
 $Q$  : volumetric flow rate of the liquid, L<sup>3</sup>/□  
 $Q_i$  : permeability of component  $i$   
 $R$  : resistance, universal gas constant  
 $Re$  : Reynolds number, —  
 $Sc$  : Schmidt number, —  
 $Sh$  : Sherwood number, —  
 $T$  : temperature, K  
 $\Delta T$  : temeperature difference, K  
 $x_f, x_p, x_r$  : concentrations in the feed, permeate and retentate, respectively, mole fraction  
 $Z$  : thickness of the membrane, L

### *Greek Letters*

$a$  : thermal diffusivity, L<sup>2</sup>/q; membrane selectivity  
 $c$  : activity coefficient  
 $n$  : chemical potential, viscosity of fluid,  
 $t$  : density of fluid, M/L<sup>3</sup>  
 $o$  : momentum diffusivity, L<sup>2</sup>/□  
 $f$  : porosity of the membrane, —  
 $x$  : tortuosity of the pores  
 $\{\}$  : rejection coefficient  
 $\Delta \square$  : driving force across the membrane

### *Subscripts*

$M$  : permeation, Membrane  
 $A$  : component  $A$   
 $G$  : gas phase, gel

*L* : liquid phase

*v* : volume

*h* : heat

*i* : input, component *i*

*m* : momentum

*o* : output

*e* : electric

*f* : feed

*F* : filtrate

*p* : permeate

*r* : retentate

1 : feed

2 : product

## Numerical Problems

**15.1** (Prediction of Diffusion Flux Through Membrane): The molar concentrations of helium on the two opposite surfaces of a plastic membrane of thickness 0.001 m are 0.02 kmol/m<sup>3</sup> and 0.005 kmol/m<sup>3</sup>, respectively. The diffusivity of helium in the membrane is 10<sup>-9</sup> m<sup>2</sup>/s. Find the molar and mass fluxes of helium into the membrane assuming one-dimensional and steady-state diffusion.

[Ans: Molar flux: 1.5 # 10<sup>-8</sup> kmol/m<sup>2</sup> s, Mass flux: 6 # 10<sup>-8</sup> kg/m<sup>2</sup> s]

**15.2** (Estimation of Flux and Diffusivity of Hydrogen Through Membrane): A thin metallic membrane of palladium (0.1 mm thick) is permeable to the diffusion of hydrogen only. On one side of the membrane placed horizontally is a mixture of 50 mol% hydrogen and the rest nitrogen, on another side air flows at high velocity in order to maintain the concentration of hydrogen as zero. At 293 K and 1 atm, the diffusion coefficient of the hydrogen-nitrogen system is 7.63 # 10<sup>-5</sup> m<sup>2</sup>/s. The operation is carried out at 313 K and 1 atm pressure, at which it can be assumed that the resistance to mass transfer in the gas phase occurs through a hypothetical film of thickness 1.0 mm, immediately adjacent to the original side. Further, it is known that the concentration of hydrogen between the solid and the film is 20 mol%. Calculate (i) the flux in kmol/m<sup>2</sup>s of hydrogen through Pd membrane, and (ii) the diffusion coefficient of hydrogen through the membrane.

[Ans: (i) 1.567 # 10<sup>-3</sup> kmol/(m<sup>2</sup>)(s) (ii) 7.835 # 10<sup>-7</sup> m<sup>2</sup>/s]

**15.3** (Calculation of Molar Flux and Concentrations of Oxygen Outside the Rubber Membrane): The oxygen is diffusing through a rubber membrane of 0.05 mm thickness. The pressure on opposite sides of the membrane are 2 bar and 1 bar, respectively. For oxygen-rubber at 298 K:  $D_{AB} = 0.21 \# 10^{-9}$  m<sup>2</sup>/s and  $s = 3.12 \# 10^{-3}$  kmol/m<sup>3</sup> bar. The concentration of oxygen ( $c_A$ ) on the

surface of the membrane is given by  $c_A = s.p_A$ . Calculate the (i) molar diffusion flux of  $O_2$  and (ii) molar concentrations of  $O_2$  outside the rubber membrane assuming that the perfect gas law is being obeyed.

[Ans: (i)  $1.31 \times 10^{-9}$  kmol/(m<sup>2</sup>)(s), (ii)  $c_{A1} = 0.0807$  kmol/m<sup>3</sup> and  $c_{A2} = 0.0404$  kmol/m<sup>3</sup>]

**15.4 (Prediction of Permeation Flux Through Membrane):** An air-ammonia mixture containing 4% ammonia is being passed through an ammonia-selective membrane of thickness 5 mm at a pressure of 100 atm and a temperature of 30°C to recover 90% of ammonia. The permeability is  $1.2 \times 10^{-4}$  cm<sup>2</sup>/s. Find the permeation flux of ammonia through the membrane.

[Ans:  $3.475 \times 10^{-5}$  gmol/(cm<sup>2</sup>)(s) or,  $5.91 \times 10^{-4}$  g/(cm<sup>2</sup>)(s)]

**15.5 (Estimation of Molar Flux of an Electrolyte Through a Membrane):** An electrolyte is diffusing at 20°C from 0.1 M aqueous solution through a water insoluble membrane of 0.0015 cm thickness into 0.01 M aqueous solution. The partition coefficient of the electrolyte between water and membrane is  $6.2 \times 10^{-4}$  and the diffusion coefficient is  $1.72 \times 10^{-5}$  cm<sup>2</sup>/s. Calculate the flux of electrolyte across the membrane.

[Ans:  $6.4 \times 10^{-10}$  mol/(cm<sup>2</sup>)(s)]

**15.6 (Determination of Transmembrane Pressure Drop, Flux of Liquid Through Membrane, and Cake Resistance in Cross-flow Ultrafiltration):** In a cross-flow ultrafiltration unit, a protein of molecular weight  $3 \times 10^5$  da is separated from the fermentation broth by using a UF membrane. The flow rate of liquid through a tube of diameter 2 cm and length 50 cm is 2 L/min. The flow regime is turbulent, the Fanning's friction factor,  $f = 0.0005$  and a constant,  $C_4 = 2$  [atm (s/cm)<sup>2</sup>]. The inlet pressure is 2 atm. Protein concentrations in the solution and on gel film are 30 mg/L and 100 mg/L, respectively.

(i) Determine the exit pressure, (ii) Estimate the transmembrane pressure drop, (iii) Calculate the flux of liquid through the UF membrane, if the mass transfer coefficient for protein flux is 5 cm/s and (iv) Find the cake resistance assuming the resistance of the filter to be 0.002 atm. cm<sup>2</sup>. s/cm<sup>3</sup>.

[Ans: (i) 1.99375 atm (ii) 1.996875 atm (iii)  $40.56$  cm<sup>3</sup>/cm<sup>2</sup> s (iv) 0.047 atm cm<sup>2</sup> s/cm<sup>3</sup>]

**15.7 (Calculation of Pressure Drop Across the Membrane, Filtration Flux, and Rejection Coefficient in a Cross-Flow Ultrafiltration):** In a cross-flow ultrafiltration system used for filtration of proteins from a fermentation broth, gel resistance ( $R_G$ ) increases with increase in protein concentration obeying the following relation:

$$R_G = 0.5 + 0.01C, \text{ where } C \text{ is in mg/L.}$$

Pressure at the entrance and exit of the system are 6 atm and 2 atm, respectively. The shell-side of the filter is open to atmosphere resulting in the filtrate pressure to be 1 atm. The resistance across the membrane is 0.5 atm/(mg/m<sup>2</sup> hr), and the concentration of the protein in the broth is 100 mg/L. Determine (i) the pressure drop across the membrane, (ii) Filtration flux, and (iii) Rejection coefficient of the membrane for protein concentration of 5 mg/L in the effluent.

[Ans: (i) 3 atm (ii)  $1.5 \text{ cm}^3/\text{cm}^2 \text{ s}$  (iii) 0.95]

### 15.8 (Estimation of Transmembrane Pressure Required for Separation of Pure Water from Sea Water):

Typical sea water containing 3.45% (by weight) of dissolved salts has a vapour pressure 1.84% below that of pure water. Estimate the minimum possible transmembrane pressure required to produce pure water if the membrane is ideally selective.

[Ans: 25 atm]

### ***Short and Multiple Choice Questions***

1. What are the two major types of membranes? Give examples.
2. What is gaseous diffusion or effusion?
3. What is dialysis? What are its major applications?
4. Why do diffusivities of gases through membranes get appreciably reduced?
5. What is permeation? Discuss briefly about its mechanism.
6. What do you mean by membrane selectivity?
7. What are the advantages of membrane filters over other similar methods of separation?
8. What are the different types of membrane filtrations? What are the approximate sizes of smallest particles that can be retained by them?
9. Name some common materials that are used as membrane filters.
10. What do you mean by molecular weight cut-off?
11. Name some important applications of ultrafiltration.
12. What is reverse osmosis? Why does it require relatively high pressure?
13. Which of the following membrane processes would you recommend for desalination of water?  
(a) micro-filtration                          (b) reverse osmosis  
(c) pervaporation                              (d) ultrafiltration
14. The smallest particle that can be retained by an ultrafiltration membrane lies in the range of  
(a) 0.001 to 0.02 micron                      (b) 0.001 to 0.002 micron  
(c) 0.0001 to 0.001 micron                    (d) 0.05 to 0.10 micron
15. The effect of concentration polarisation is less important in  
(a) gas separation                                (b) reverse osmosis  
(c) haemodialysis                                 (d) electrodialysis
16. With increase in membrane thickness, the selectivity of separation  
(a) increases                                        (b) decreases  
(c) remains unchanged                            (d) either (a) or (b)
17. With increase in bulk concentration, the flux of ultrafiltration  
(a) increases                                        (b) decreases  
(c) remain unchanged                              (d) either (a) or (b)
18. Which of the following processes is suitable for removing traces of moisture from Methyl isobutyl ketone (MIBK)?  
(a) reverse osmosis                                (b) microfiltration

(c) pervaporation

(d) none of these

### Answers to Multiple Choice Questions

13. (b) 14. (c) 15. (a) 16. (a) 17. (b) 18. (c)

## References

- Binning, R.C., R.J. Lee, J.F. Jennings and E.C. Martin, *Ind. Eng. Chem.*, **53**, 45 (1961).
- Bollinger, W.A., D.L. MacLean and R.S. Narayan, *Chem. Eng. Prog.*, **78**(10), 27 (1982).
- Dittmeyer, R., V. Höllein and K. Daub, *J. Molecular Catal. A-Chem.*, **173**, 135 (2001).
- Dube, M.A., A.Y. Tremblay and J. Liu, *Bioresource Technol.*, **98**, 639 (2007).
- Fane, A.G., C.J.D. Fell, and A.G. Waters, *J. Membrane Sci.*, **9**, 245 (1981).
- Havens, G.G. and D.B. Guy, *Chem. Eng. Prog. Sym. Ser.*, **64**(90), 299 (1968).
- Ho, W.S.W. and K.K. Sirkar, *Membrane Handbook*, Chapman Hall, New York (1992).
- Holownia, A.T. and A. Noworyta, *J. Biotechnol.*, **30**, 47 (2007).
- Kolff, W.J. and H.T. Berk, *Acta. Med. Scand.*, **117**, 121 (1944).
- Krishna, R., in *Reactive Distillation—Status and Future Directions*, Sundmacher, K. and A. Kienle (Eds.), Wiley-VCH (2003).
- Loeb, S. and S. Sourirajan, *Adv. Chem. Ser.*, **38**, 117 (1962).
- Lonsdale, H.K., U. Merten and R.L. Riley, *J. Appl. Polym. Sci.*, **9**, 1341 (1965).
- Mandal, D., Membrane-based Separation Process and their Industrial Applications, *Chemical Product Finder*, p. 69 (June 1998).
- Morigami, Y., M. Kondo, J. Abe, H. Kita and K. Okamoto, *Sep. and Purification Tech.*, **25**, 251 (2001).
- Mulder, M., *Basic Principles of Membrane Technology*, 2nd ed., Kluwer Academic Publishers, Dordrecht (1996).
- Naylor, R.W. and P.O. Backer, *AIChE J.*, **1**, 95 (1955).
- Nunes, S.P. and K.V. Peinemann, *Membrane Technology in the Chemical Industry*, Wiley-VCH (2001).
- Okada, T. and T. Matsuura, *J. Mem. Sci.*, **59**, 133 (1991).
- Ozaki, H. and H. Li, *Water Research*, **36**, 123 (2002).
- Pan, C.Y., *AIChE J.*, **29**, 545 (1983).
- Rameshbabu, P.V., Various Membrane Fillers, *Chemical Product Finder*, p. 85 (June 1998).
- Satyanarayana, S.V., A. Sharma and P.K. Bhattacharya, *Chem. Eng. J.*, **102**, 171 (2004)
- Shuler, M.L. and F. Kargi, *Bioprocess Engineering - Basic Concepts*, 2nd ed., PHI Learning, New Delhi (2002).
- Sircar, S. and M.B. Rao, in *Recent Advances on Gas Separation by Microporous Membranes*, N. Kanellopoulos (Ed.), Elsevier, New York, p. 473 (2000).
- Sirkar, K.K., P.V. Shanbhag and A.S. Kovvali, *Ind. Eng. Chem. Res.*, **38**, 3715 (1999).
- Walawender, W.P. and A. Stern, *Sep. Sci.*, **7**, 553 (1972).

Wijmans, J.G. and R.W. Baker, *J. Mem. Sci.*, **107**, 1 (1995).

Zsigmondy, R. and W. Bachmann, *Z. Anorg. Chem.*, **103**, 119 (1918).

# Appendix A

## A.1 Physical Constants

Gas (ideal) constant, $R$	$82.057 \text{ atm cm}^3 \text{ mol}^{-1} \text{ K}^{-1}$	$1.9872 \text{ cal mol}^{-1} \text{ K}^{-1}$
	$0.082057 \text{ atm m}^3 \text{ kmol}^{-1} \text{ K}^{-1}$	$1.9872 \text{ Btu lb mol}^{-1} \text{ R}^{-1}$
	$8.31452 \square 10^3 \text{ kgm}^2 \text{s}^{-2} \text{ kmol}^{-1} \text{ K}^{-1}$	$0.7302 \text{ atm ft}^3 \text{ lb mol}^{-1} \text{ R}^{-1}$
	$8.31452 \square 10^7 \text{ g cm}^2 \text{ s}^{-2} \text{ g mol}^{-1} \text{ K}^{-1}$	$1.5443 \square 10^3 \text{ ft lb}_f \text{ lb mol}^{-1} \text{ R}^{-1}$
	$8.31451 \text{ J g mol}^{-1} \text{ K}^{-1}$	$10.731 \text{ lb}_f \text{ in}^{-2} \text{ ft}^3 \text{ lb mol}^{-1} \text{ R}^{-1}$
	$8.31451 \text{ kJ kmol}^{-1} \text{ K}^{-1}$	$1.5453 \square 10^3 \text{ ft lb}_f \text{ lb mol}^{-1} \text{ R}^{-1}$
	$8.31451 \text{ kPa m}^3 \text{ kmol}^{-1} \text{ K}^{-1}$	$4.9686 \square 10^4 \text{ lb}_m \text{ ft}^2 \text{ s}^{-2} \text{ lb mol}^{-1} \text{ R}^{-1}$
Acceleration due to gravity, $g$	$32.174 \text{ ft s}^{-2} = 980.665 \text{ cm s}^{-2} = 9.80665 \text{ m s}^{-2}$	
Gravitational Conversion factor, $g_c$	$32.174 \text{ lb}_m \text{ ft lb}_f^{-1} \text{ s}^{-2}$	
	$980.665 \text{ g}_m \text{ cm gf}^{-1} \text{ s}^{-2}$	
	$9.80665 \text{ kg}_m \text{ m kgf}^{-1} \text{ s}^{-2}$	
Farady's constant, $F$	$96485.3 \text{ C g equiv}^{-1}$	
Electron charge, $e$	$1.60218 \square 10^{-19} \text{ C}$	
Speed of light in vacuum, $c$	$2.99792 \square 10^8 \text{ m s}^{-1}$	
Stefan-Boltzmann constant, $\sigma$	$5.67051 \square 10^{-8} \text{ W m}^{-2} \text{ K}^{-4}$	
	$1.7124 \square 10^{-9} \text{ Btu hr}^{-1} \text{ ft}^{-2} \text{ R}^{-4}$	
	$1.3553 \square 10^{-12} \text{ cal s}^{-1} \text{ cm}^{-2} \text{ K}^{-4}$	
Planck's constant, $h$	$6.62608 \square 10^{-27} \text{ erg s molecule}^{-1}$	
	$6.62608 \square 10^{-34} \text{ J s molecule}^{-1}$	
Joule's constant, $J_c$	$778.16 \text{ ft lb}_f \text{ Btu}^{-1} = 4.184 \square 10^7 \text{ erg cal}^{-1} = 4.184 \text{ J cal}^{-1}$	
Avogadro's Number, $N$	$6.02214 \square 10^{23} \text{ molecules g mol}^{-1}$	
Boltzmann's constant, $k$ ( $= R/N$ )	$1.38066 \square 10^{-16} \text{ erg K}^{-1} = 1.38066 \square 10^{-23} \text{ J K}^{-1}$	
Atmosphere (standard)	$1 \text{ atm} = 1.01325 \square 10^5 \text{ N m}^{-2}$	
Pi (r)	3.1415926 -----	
Base of natural logarithms, $e$	2.71828 -----	

## A.2 Conversion Factors

**Acceleration due to gravity:** SI unit ( $\text{m s}^{-2}$ )

$$1 \text{ ft s}^{-2} = 0.3048 \text{ m s}^{-2}$$

$$1 \text{ in s}^{-2} = 0.0254 \text{ m s}^{-2}$$

**Angle:** SI unit (rad)

$$1 \text{ degree} = (\pi/180) \text{ rad}$$

$$1 \text{ revolution} = 2\pi \text{ rad} = 6.28 \text{ rad}$$

**Angular velocity:** SI unit ( $\text{rad s}^{-1}$ )

$$1 \text{ rpm} = (\pi/30) \text{ rad s}^{-1}$$

$$1 \text{ rps} = 2\pi \text{ rad s}^{-1} = 6.28 \text{ rad s}^{-1}$$

**Area:** SI unit ( $\text{m}^2$ )

$$1 \text{ ft}^2 = 0.0929 \text{ m}^2$$

$$1 \text{ in}^2 = 6.451 \times 10^{-4} \text{ m}^2$$

$$1 \text{ Acre} = 4046.85 \text{ m}^2 = 43560 \text{ ft}^2$$

**Density:** SI unit ( $\text{kg m}^{-3}$ )

$$1 \text{ kg m}^{-3} = 10^{-3} \text{ g cm}^{-3} = 0.062 \text{ lb}_m \text{ ft}^{-3}$$

$$1 \text{ lb}_m \text{ ft}^{-3} = 16.02 \text{ kg m}^{-3}$$

$$1 \text{ lb}_m \text{ in}^{-3} = 27.68 \times 10^3 \text{ kg m}^{-3}$$

$$1 \text{ ton m}^{-3} = 1 \text{ kg dm}^{-3} = 1 \text{ g cm}^{-3} = 10^3 \text{ kg m}^{-3} = 62.43 \text{ lb}_m \text{ ft}^{-3} = 8.345 \text{ lb}_m \text{ gal}^{-1} \text{ (US)}$$

**Diffusivity (momentum/ heat /mass):** SI unit ( $\text{m}^2 \text{ s}^{-1}$ )

$$1 \text{ ft}^2 \text{ hr}^{-1} = 25.81 \text{ centistokes (cSt)} = 2.581 \times 10^{-5} \text{ m}^2 \text{ s}^{-1} = 0.2581 \text{ cm}^2 \text{ s}^{-1} = 2.78 \times 10^{-4} \text{ ft}^2 \text{ s}^{-1}$$

$$1 \text{ cm}^2 \text{ s}^{-1} = 10^{-4} \text{ m}^2 \text{ s}^{-1} = 10^2 \text{ centistokes (cSt)} = 3.875 \text{ ft}^2 \text{ hr}^{-1} = 1.076 \times 10^{-3} \text{ ft}^2 \text{ s}^{-1}$$

$$1 \text{ m}^2 \text{ s}^{-1} = 10^4 \text{ cm}^2 \text{ s}^{-1} = 3.875 \times 10^4 \text{ ft}^2 \text{ hr}^{-1} = 10^6 \text{ centistokes (cSt)} = 10.764 \text{ ft}^2 \text{ s}^{-1}$$

$$1 \text{ centistokes (cSt)} = 3.875 \times 10^{-2} \text{ ft}^2 \text{ hr}^{-1} = 10^{-2} \text{ cm}^2 \text{ s}^{-1} = 10^{-6} \text{ m}^2 \text{ s}^{-1} = 1.07 \times 10^{-5} \text{ ft}^2 \text{ s}^{-1}$$

**Force, Weight:** SI unit (N)

$$1 \text{ kgf} = 9.81 \text{ N}$$

$$1 \text{ N (kgms}^{-2}\text{)} = 10^5 \text{ g cm s}^{-2} \text{ (dynes)} = 0.22488 \text{ lb}_f = 7.233 \text{ lb}_m \text{ ft s}^{-2} \text{ (poundals)}$$

$$1 \text{ dyne} = 10^{-5} \text{ N} = 7.233 \times 10^{-5} \text{ poundals}$$

$$1 \text{ poundals} = 0.13826 \text{ N} = 1.3826 \times 10^4 \text{ dynes}$$

$$1 \text{ lb}_f = 4.4482 \text{ N} = 32.174 \text{ poundals} = 4.4482 \times 10^5 \text{ dynes}$$

**Frequency:** SI unit (Hz)

$$1 \text{ Hz} = 1 \text{ s}^{-1} = 1 \text{ rps}$$

$$1 \text{ rpm} = (1/60) \text{ Hz}$$

**Heat:** SI unit (J)

$$1 \text{ erg} = 10^{-7} \text{ J}$$

$$1 \text{ kcal} = 4.1868 \text{ kJ} = 4.1868 \times 10^3 \text{ J}$$

$$1 \text{ ft lb}_f \text{ lb}_m^{-1} = 2.989 \text{ J kg}^{-1}$$

$$1 \text{ cal} = 3.9657 \times 10^{-3} \text{ Btu} = 3.086 \text{ ft lb}_f = 4.184 \text{ J} (\text{kg m}^2 \text{ s}^{-2} = \text{N m}) = 4.184 \times 10^7 \text{ ergs}$$

$$(\text{g cm}^2 \text{ s}^{-2}) = 99.287 \text{ ft poundals} (\text{lb}_m \text{ ft}^2 \text{ s}^{-2}) = 1.1622 \times 10^{-6} \text{ kW hr} = 1.5586 \times 10^{-6} \text{ hp hr}$$

$$1 \text{ Btu} = 252.16 \text{ cal} = 1055 \text{ J} (\text{kg m}^2 \text{ s}^{-2} = \text{N m}) = 1.055 \times 10^{10} \text{ ergs} (\text{g cm}^2 \text{ s}^{-2}) = 778.16 \text{ ft lb}_f =$$

$$2.5036 \times 10^4 \text{ ft poundals} (\text{lb}_m \text{ ft}^2 \text{ s}^{-2}) = 2.9307 \times 10^{-4} \text{ kW hr} = 3.93 \times 10^{-4} \text{ hp hr}$$

$$1 \text{ J} (\text{kg m}^2 \text{ s}^{-2} = \text{N m}) = 0.239 \text{ cal} = 9.4783 \times 10^{-4} \text{ Btu} = 107 \text{ ergs} (\text{g cm}^2 \text{ s}^{-2}) = 0.73756 \text{ ft lb}_f =$$

$$23.73 \text{ ft poundals} (\text{lb}_m \text{ ft}^2 \text{ s}^{-2}) = 2.7778 \times 10^{-7} \text{ kW hr} = 3.725 \times 10^{-7} \text{ hp hr}$$

$$1 \text{ kW hr} = 1.341 \text{ hp hr} = 3.6 \times 10^6 \text{ J} (\text{kg m}^2 \text{ s}^{-2} = \text{N m}) = 8.6042 \times 10^5 \text{ cal} = 3.4122 \times 10^3 \text{ Btu} = 3.6 \times 10^{13} \text{ ergs} (\text{g cm}^2 \text{ s}^{-2}) = 2.6552 \times 10^6 \text{ ft lb}_f = 8.5429 \times 10^7 \text{ ft poundals} (\text{lb}_m \text{ ft}^2 \text{ s}^{-2})$$

**Heat flux:** SI unit ( $\text{W m}^{-2}$ )

$$1 \text{ kcal m}^{-2} \text{ hr} = 1.163 \text{ W m}^{-2}$$

**Heat transfer coefficient:** SI unit ( $\text{W m}^{-2} \text{ K}^{-1}$ )

$$1 \text{ kcal m}^{-2} \text{ hr}^{-1} \text{ K}^{-1} = 1.163 \text{ W m}^{-2} \text{ K}^{-1}$$

$$1 \text{ Btu ft}^{-2} \text{ hr}^{-1} \text{ F}^{-1} = 0.2162 \text{ lb}_f \text{ ft}^{-1} \text{ s}^{-1} \text{ F}^{-1} = 6.9546 \text{ lb}_m \text{ s}^{-3} \text{ F}^{-1} = 5.6782 \times 10^3 \text{ g s}^{-3} \text{ K}^{-1} = 1.3571 \times 10^{-4} \text{ cal cm}^{-2} \text{ s}^{-1} \text{ K}^{-1} = 5.6782 \times 10^{-4} \text{ W cm}^{-2} \text{ K}^{-1} = 5.6782 \text{ W m}^{-2} \text{ K}^{-1} (\text{J m}^{-2} \text{ s}^{-1} \text{ K}^{-1} = \text{kg s}^{-3} \text{ K}^{-1})$$

$$1 \text{ lb}_f \text{ ft}^{-1} \text{ s}^{-1} \text{ F}^{-1} = 4.6263 \text{ Btu ft}^{-2} \text{ hr}^{-1} \text{ F}^{-1} = 32.174 \text{ lb}_m \text{ s}^{-3} \text{ F}^{-1} = 2.6269 \times 10^4 \text{ g s}^{-3} \text{ K}^{-1} = 6.2784 \times 10^{-4} \text{ cal cm}^{-2} \text{ s}^{-1} \text{ K}^{-1} = 2.6269 \times 10^{-3} \text{ W cm}^{-2} \text{ K}^{-1} = 26.269 \text{ W m}^{-2} \text{ K}^{-1} (\text{J m}^{-2} \text{ s}^{-1} \text{ K}^{-1} = \text{kg s}^{-3} \text{ K}^{-1})$$

$$1 \text{ lb}_m \text{ s}^{-3} \text{ F}^{-1} = 3.1081 \times 10^{-2} \text{ lb}_f \text{ ft}^{-1} \text{ s}^{-1} \text{ F}^{-1} = 0.14379 \text{ Btu ft}^{-2} \text{ hr}^{-1} \text{ F}^{-1} = 816.47 \text{ g s}^{-3} \text{ K}^{-1} = 1.9514 \times 10^{-5} \text{ cal cm}^{-2} \text{ s}^{-1} \text{ K}^{-1} = 8.1647 \times 10^{-5} \text{ W cm}^{-2} \text{ K}^{-1} = 0.81647 \text{ W m}^{-2} \text{ K}^{-1} (\text{J m}^{-2} \text{ s}^{-1} \text{ K}^{-1} = \text{kg s}^{-3} \text{ K}^{-1})$$

$$1 \text{ g s}^{-3} \text{ K}^{-1} = 1.2248 \square 10^{-3} \text{ lb}_m \text{ s}^{-3} \text{ F}^{-1} = 3.8068 \square 10^{-5} \text{ lb}_f \text{ ft}^{-1} \text{ s}^{-1} \text{ F}^{-1} = 1.7611 \square 10^{-4} \text{ Btu ft}^{-2} \text{ hr}^{-1} \text{ F}^{-1} = 2.3901 \square 10^{-8} \text{ cal cm}^{-2} \text{ s}^{-1} \text{ K}^{-1} = 10^{-7} \text{ W cm}^{-2} \text{ K}^{-1} = 10^{-3} \text{ W m}^{-2} \text{ K}^{-1} \\ (\text{J m}^{-2} \text{ s}^{-1} \text{ K}^{-1} = \text{kg s}^{-3} \text{ K}^{-1})$$

$$1 \text{ cal cm}^{-2} \text{ s}^{-1} \text{ K}^{-1} = 4.184 \text{ W cm}^{-2} \text{ K}^{-1} = 4.184 \square 10^4 \text{ W m}^{-2} \text{ K}^{-1} (\text{J m}^{-2} \text{ s}^{-1} \text{ K}^{-1} = \text{kg s}^{-3} \text{ K}^{-1}) = 4.184 \square 10^7 \text{ g s}^{-3} \text{ K}^{-1} = 5.1245 \square 10^4 \text{ lb}_m \text{ s}^{-3} \text{ F}^{-1} = 1.5928 \square 10^3 \text{ lb}_f \text{ ft}^{-1} \text{ s}^{-1} \text{ F}^{-1} = 7.3686 \square 10^3 \text{ Btu ft}^{-2} \text{ hr}^{-1} \text{ F}^{-1}$$

$$1 \text{ W cm}^{-2} \text{ K}^{-1} = 10^4 \text{ W m}^{-2} \text{ K}^{-1} (\text{J m}^{-2} \text{ s}^{-1} \text{ K}^{-1} = \text{kg s}^{-3} \text{ K}^{-1}) = 0.239 \text{ cal cm}^{-2} \text{ s}^{-1} \text{ K}^{-1} = 10^7 \text{ g s}^{-3} \text{ K}^{-1} = 1.2248 \square 10^4 \text{ lb}_m \text{ s}^{-3} \text{ F}^{-1} = 380.68 \text{ lb}_f \text{ ft}^{-1} \text{ s}^{-1} \text{ F}^{-1} = 1.7611 \square 10^3 \text{ Btu ft}^{-2} \text{ hr}^{-1} \text{ F}^{-1}$$

$$1 \text{ W m}^{-2} \text{ K}^{-1} (\text{J m}^{-2} \text{ s}^{-1} \text{ K}^{-1} = \text{kg s}^{-3} \text{ K}^{-1}) = 10^{-4} \text{ W cm}^{-2} \text{ K}^{-1} = 2.39 \square 10^{-5} \text{ cal cm}^{-2} \text{ s}^{-1} \text{ K}^{-1} = 10^3 \text{ g s}^{-3} \text{ K}^{-1} = 1.2248 \text{ lb}_m \text{ s}^{-3} \text{ F}^{-1} = 3.8068 \square 10^{-2} \text{ lb}_f \text{ ft}^{-1} \text{ s}^{-1} \text{ F}^{-1} = 0.17611 \text{ Btu ft}^{-2} \text{ hr}^{-1} \text{ F}^{-1} = 0.17611 \text{ Btu ft}^{-2} \text{ hr}^{-1} \text{ R}^{-1}$$

**Mass:** SI unit (kg)

$$1 \text{ lb}_m = 453.6 \text{ gm} = 0.4536 \text{ kg} = 7000 \text{ grains} = 16 \text{ oz}$$

$$1 \text{ kg} = 2.2046 \text{ lb}_m$$

$$1 \text{ ton (short)} = 2000 \text{ lb}_m; 1 \text{ ton (long)} = 2240 \text{ lb}_m; 1 \text{ ton (metric)} = 1000 \text{ kg}$$

**Mass flux:** SI unit ( $\text{kg m}^{-2} \text{ s}^{-1}$ )

$$1 \text{ lb}_f \text{ s} \text{ ft}^{-3} = 1.1583 \square 10^5 \text{ lb}_m \text{ ft}^{-2} \text{ hr}^{-1} = 32.174 \text{ lb}_m \text{ ft}^{-2} \text{ s}^{-1} = 15.71 \text{ g cm}^{-2} \text{ s}^{-1} = 1.571 \square 10^2 \text{ kg m}^{-2} \text{ s}^{-1}$$

$$1 \text{ kg m}^{-2} \text{ s}^{-1} = 0.1 \text{ g cm}^{-2} \text{ s}^{-1} = 0.2048 \text{ lb}_m \text{ ft}^{-2} \text{ s}^{-1} = 737.34 \text{ lb}_m \text{ ft}^{-2} \text{ hr}^{-1} = 6.3659 \square 10^{-3} \text{ lb}_f \text{ s} \text{ ft}^{-3}$$

$$1 \text{ lb}_m \text{ ft}^{-2} \text{ hr}^{-1} = 8.336 \square 10^{-6} \text{ lb}_f \text{ s} \text{ ft}^{-3} = 2.7778 \square 10^{-4} \text{ lb}_m \text{ ft}^{-2} \text{ s}^{-1} = 1.3562 \square 10^{-4} \text{ g cm}^{-2} \text{ s}^{-1} = 1.3562 \square 10^{-3} \text{ kg m}^{-2} \text{ s}^{-1}$$

$$1 \text{ lb}_m \text{ ft}^{-2} \text{ s}^{-1} = 3600 \text{ lb}_m \text{ ft}^{-2} \text{ hr}^{-1} = 3.108 \square 10^{-2} \text{ lb}_f \text{ s} \text{ ft}^{-3} = 0.48824 \text{ g cm}^{-2} \text{ s}^{-1} = 4.8824 \text{ kg m}^{-2} \text{ s}^{-1}$$

$$1 \text{ g cm}^{-2} \text{ s}^{-1} = 10 \text{ kg m}^{-2} \text{ s}^{-1} = 7.3734 \square 10^3 \text{ lb}_m \text{ ft}^{-2} \text{ hr}^{-1} = 6.3659 \square 10^{-2} \text{ lb}_f \text{ s} \text{ ft}^{-3} = 2.0482 \text{ lb}_m \text{ ft}^{-2} \text{ s}^{-1}$$

**Length:** SI unit (m)

$$1 \text{ in} = 2.54 \text{ cm} = 0.0254 \text{ m}$$

$$1 \text{ m} = 100 \text{ cm} = 10^6 \square \text{m} = 10^9 \text{ nm} = 3.2808 \text{ ft} = 39.37 \text{ in}$$

1 mile = 5280 ft

1  $\square$ m = 1 micron

1 Å (angstrom) =  $10^{-10}$  m =  $10^{-1}$  nm =  $10^{-4}$   $\square$ m

### Power: SI unit (W)

$1 \text{ kg}_f \text{ m s}^{-1} = 9.81 \text{ W}$ ;  $1 \text{ J s}^{-1} = 1 \text{ W}$ ;  $1 \text{ erg s}^{-1} = 10^{-7} \text{ W}$

$1 \text{ kcal hr}^{-1} = 1.163 \text{ W}$ ;  $1 \text{ Btu hr}^{-1} = 0.293 \text{ W}$

$1 \text{ hp} = 0.746 \text{ W}$ ;  $1 \text{ lb}_f \cdot \text{ft s}^{-1} = 1.356 \text{ W}$

### Pressure: SI unit (Pa)

$1 \text{ bar} = 10^5 \text{ Pa}$ ;  $1 \text{ dyne cm}^{-2} = 1 \square \text{ bar} = 0.1 \text{ Pa}$ ;

$1 \text{ kg}_f \text{ cm}^{-2} = 1 \text{ atm} = 1.0133 \square 10^5 \text{ Pa}$ ;  $1 \text{ kg}_f \text{ m}^{-2} = 10.133 \text{ Pa}$

$1 \text{ lb}_f \text{ in}^{-2}$  (psi) = 6894.76 Pa;  $1 \text{ lb}_f \text{ ft}^{-2} = 47.88 \text{ Pa}$

$1 \text{ mm H}_2\text{O} = 10.133 \text{ Pa}$

$1 \text{ mm Hg} = 133.3 \text{ Pa}$

$1 \text{ atm} = 760 \text{ mm Hg} = 29.92 \text{ in Hg} = 14.696 \text{ psia} (\text{lb}_f \text{ in}^{-2}) = 2.1162 \square 10^3 \text{ lb}_f \text{ ft}^{-2} = 6.8087 \square$

$10^4 \text{ poundals ft}^{-2} (\text{lb}_m \text{ ft}^{-1} \text{ s}^{-2}) = 1.0133 \square 10^3 \text{ Pa} (\text{N m}^{-2} = \text{kg m}^{-1} \text{ s}^{-2}) = 1.0133 \square 10^6 \text{ dyne cm}^{-2} (\text{g cm}^{-1} \text{ s}^{-2})$

$1 \text{ Pa} = 10 \text{ dyne cm}^{-2} (\text{g cm}^{-1} \text{ s}^{-2}) = 9.8692 \square 10^{-6} \text{ atm} = 7.5006 \square 10^{-3} \text{ mm Hg} = 2.953 \square 10^{-4}$

$\text{in Hg} = 1.4504 \square 10^{-4} \text{ psia} (\text{lb}_f \text{ in}^{-2}) = 2.0886 \square 10^{-2} \text{ lb}_f \text{ ft}^{-2} = 0.67197 \text{ poundals ft}^{-2} (\text{lb}_m \text{ ft}^{-1} \text{ s}^{-2})$

### Specific enthalpy: SI unit (J kg<sup>-1</sup>)

$1 \text{ kcal kg}^{-1} = 1 \text{ cal g}^{-1} = 4190 \text{ J kg}^{-1}$

$1 \text{ Btu lb}^{-1} = 2326 \text{ J kg}^{-1}$

### Specific entropy: (J kg<sup>-1</sup> K<sup>-1</sup>)

$1 \text{ kcal kg}^{-1} \text{ K}^{-1} = 1 \text{ Btu lb}^{-1} \text{ F}^{-1} = 4190 \text{ J kg}^{-1} \text{ K}^{-1}$

### Specific heat: SI unit (J kg<sup>-1</sup>)

$1 \text{ kcal kg}^{-1} = 1 \text{ cal g}^{-1} = 4190 \text{ J kg}^{-1}$

$1 \text{ Btu lb}^{-1} = 2326 \text{ J kg}^{-1}$

### Specific heat capacity: SI unit (J kg<sup>-1</sup> K<sup>-1</sup>)

$1 \text{ erg g}^{-1} \text{ K}^{-1} = 10^{-4} \text{ J kg}^{-1} \text{ K}^{-1}$

### Specific volume: SI unit (m<sup>3</sup> kg<sup>-1</sup>)

$$1 \text{ L kg}^{-1} = 1 \text{ cm}^3 \text{ g}^{-1} = 10^{-3} \text{ m}^3 \text{ kg}^{-1}$$

**Thermal conductivity:** SI unit ( $\text{W m}^{-1} \text{ K}^{-1}$ )

$$1 \text{ kcal m}^{-1} \text{ hr}^{-1} \text{ K}^{-1} = 1.163 \text{ W m}^{-1} \text{ K}^{-1}$$

$$1 \text{ Btu hr}^{-1} \text{ ft}^{-1} \text{ F}^{-1} = 0.21616 \text{ lb}_f \text{ s}^{-1} \text{ F}^{-1} = 6.9546 \text{ lb}_m \text{ ft s}^{-3} \text{ F}^{-1} = 1.7307 \square 10^5 \text{ erg s}^{-1} \text{ cm}^{-1}$$

$$\text{K}^{-1} (\text{g cm s}^{-3} \text{ K}^{-1}) = 4.1365 \square 10^{-3} \text{ cal s}^{-1} \text{ cm}^{-1} \text{ K}^{-1} = 1.7307 \text{ W m}^{-1} \text{ K}^{-1} (\text{kg m s}^{-3} \text{ K}^{-1})$$

$$1 \text{ cal s}^{-1} \text{ cm}^{-1} \text{ K}^{-1} = 418.4 \text{ W m}^{-1} \text{ K}^{-1} (\text{kg m s}^{-3} \text{ K}^{-1}) = 4.184 \square 10^7 \text{ erg s}^{-1} \text{ cm}^{-1} \text{ K}^{-1} (\text{g cm s}^{-3} \text{ K}^{-1}) = 241.75 \text{ Btu hr}^{-1} \text{ ft}^{-1} \text{ F}^{-1} = 52.256 \text{ lb}_f \text{ s}^{-1} \text{ F}^{-1} = 1.6813 \square 10^3 \text{ lb}_m \text{ ft s}^{-3} \text{ F}^{-1}$$

$$1 \text{ W m}^{-1} \text{ K}^{-1} (\text{kg m s}^{-3} \text{ K}^{-1}) = 10^5 \text{ erg s}^{-1} \text{ cm}^{-1} \text{ K}^{-1} (\text{g cm s}^{-3} \text{ K}^{-1}) = 2.39 \square 10^{-3} \text{ cal s}^{-1} \text{ cm}^{-1} \text{ K}^{-1} = 0.5778 \text{ Btu hr}^{-1} \text{ ft}^{-1} \text{ F}^{-1} = 0.12489 \text{ lb}_f \text{ s}^{-1} \text{ F}^{-1} = 4.0183 \text{ lb}_m \text{ ft s}^{-1} \text{ F}^{-1}$$

$$1 \text{ erg s}^{-1} \text{ cm}^{-1} \text{ K}^{-1} (\text{g cm s}^{-3} \text{ K}^{-1}) = 2.39 \square 10^{-8} \text{ cal s}^{-1} \text{ cm}^{-1} \text{ K}^{-1} = 10^{-5} \text{ W m}^{-1} \text{ K}^{-1} (\text{kg m s}^{-3} \text{ K}^{-1}) = 5.778 \square 10^{-6} \text{ Btu hr}^{-1} \text{ ft}^{-1} \text{ F}^{-1} = 1.2489 \square 10^{-6} \text{ lb}_f \text{ s}^{-1} \text{ F}^{-1} = 4.0183 \square 10^{-5} \text{ lb}_m \text{ ft s}^{-3} \text{ F}^{-1}$$

**Temperature:** SI unit (K)

$$1 \text{ K} = 1.8 \text{ R}$$

**Viscosity:** SI unit (Pa s)

$$1 \text{ poise} = 1 \text{ dyne s cm}^{-2} = 0.1 \text{ Pa s}$$

$$1 \text{ cp} = 1.09 \square 10^{-4} \text{ kgf s m}^{-2} = 10^{-3} \text{ Pa s}$$

$$1 \text{ Pa s} (\text{kg m}^{-1} \text{ s}^{-1} = \text{N s m}^{-2}) = 10 \text{ g cm}^{-1} \text{ s}^{-1} (\text{poises}) = 1000 \text{ cp} = 0.67197 \text{ lb}_m \text{ ft}^{-1} \text{ s}^{-1} = 2.4191 \square 103 \text{ lb}_m \text{ ft}^{-1} \text{ hr}^{-1} = 2.0886 \square 10^{-2} \text{ lb}_f \text{ s ft}^{-2}$$

$$1 \text{ g cm}^{-1} \text{ s}^{-1} (\text{poise}) = 10^2 \text{ cp} = 0.1 \text{ Pa s} (\text{kg m}^{-1} \text{ s}^{-1} = \text{N s m}^{-2}) = 6.7197 \square 10^{-2} \text{ lb}_m \text{ ft}^{-1} \text{ s}^{-1} = 2.4191 \square 10^2 \text{ lb}_m \text{ ft}^{-1} \text{ hr}^{-1} = 2.0886 \square 10^{-3} \text{ lb}_f \text{ s ft}^{-2}$$

$$1 \text{ cp} = 10^{-2} \text{ g cm}^{-1} \text{ s}^{-1} (\text{poises}) = 10^{-3} \text{ Pa s} (\text{kg m}^{-1} \text{ s}^{-1} = \text{N s m}^{-2}) = 6.7197 \square 10^{-4} \text{ lb}_m \text{ ft}^{-1} \text{ s}^{-1} = 2.4191 \text{ lb}_m \text{ ft}^{-1} \text{ hr}^{-1} = 2.0886 \square 10^{-5} \text{ lb}_f \text{ s ft}^{-2}$$

$$1 \text{ lb}_m \text{ ft}^{-1} \text{ hr}^{-1} = 2.7778 \square 10^{-4} \text{ lb}_m \text{ ft}^{-1} \text{ s}^{-1} = 8.6336 \square 10^{-6} \text{ lb}_f \text{ s ft}^{-2} = 0.41338 \text{ cp} = 4.1338 \square 10^{-3} \text{ g cm}^{-1} \text{ s}^{-1} (\text{poises}) = 4.1338 \square 10^{-4} \text{ Pa s} (\text{kg m}^{-1} \text{ s}^{-1} = \text{N s m}^{-2})$$

$$1 \text{ lb}_m \text{ ft}^{-1} \text{ s}^{-1} = 3600 \text{ lb}_m \text{ ft}^{-1} \text{ hr}^{-1} = 3.1081 \square 10^{-2} \text{ lb}_f \text{ s ft}^{-2} = 1.4882 \square 10^3 \text{ cp} = 14.882 \text{ g cm}^{-1} \text{ s}^{-1} (\text{poises}) = 1.4882 \text{ Pa s} (\text{kg m}^{-1} \text{ s}^{-1} = \text{N s m}^{-2})$$

**Volume:** SI unit ( $\text{m}^3$ )

$$1 \text{ L} = 10^{-3} \text{ m}^3$$

$$1 \text{ m}^3 = 10^6 \text{ cm}^3 = 10^3 \text{ L} = 35.316 \text{ ft}^3 = 264.17 \text{ gal (US)}$$

$$1 \text{ in}^3 = 16.387 \text{ cm}^3 = 16.39 \square 10^{-6} \text{ m}^3$$

$$1 \text{ ft}^3 = 28.316 \text{ L} = 28.3 \text{ dm}^3 = 0.028317 \text{ m}^3 = 7.481 \text{ gal (US)}$$

$$\begin{aligned}1 \text{ gal (US)} &= 3.7854 \text{ L} = 3.7854 \square 10^3 \text{ cm}^3 = 0.13368 \text{ ft}^3 \\&= 231 \text{ in}^3 = 0.8327 \text{ gal (British)} = 3.8754 \square 10^{-3} \text{ m}^3\end{aligned}$$

### Work, Energy, Quantity of heat: SI unit (J)

$$1 \text{ kgf m}^{-1} = 9.81 \text{ N m}^{-1} = 9.81 \text{ J m}^{-2}$$

$$1 \text{ erg cm}^{-2} = 1 \text{ dyne cm}^{-1} = 10^{-3} \text{ N m}^{-1}$$

$$1 \text{ kW hr} = 3.6 \square 10^6 \text{ J}$$

$$1 \text{ kcal} = 4.1868 \text{ kJ} = 4.1868 \square 10^3 \text{ J}$$

$$1 \text{ lbf ft} = 1.356 \text{ J}$$

$$1 \text{ lbf in} = 0.113 \text{ J}$$

### Miscellaneous

$$\text{Molecular weight of air} = 28.966 \text{ kg kmol}^{-1}$$

$$\text{Molecular weight of water} = 18.015 \text{ kg kmol}^{-1}$$



# Appendix B

## B.1 Physical Properties of Air at 1 Atmosphere

Temperature T, °C	Density t, kg m <sup>-3</sup>	Viscosity n, kg m <sup>-1</sup> s <sup>-1</sup>	Kinematic viscosity v, m <sup>2</sup> s <sup>-1</sup>
0	1.2930	17.20	13.30
5	1.2699	17.44	13.74
10	1.2473	17.69	14.18
15	1.2256	17.93	14.63
20	1.2047	18.17	15.08
25	1.1845	18.41	15.54
30	1.1650	18.64	16.00
35	1.1460	18.88	16.47
40	1.1277	19.11	16.95
45	1.1101	19.34	17.43
50	1.0928	19.57	17.91
55	1.0762	19.80	18.39
60	1.0600	20.02	18.89
65	1.0445	20.24	19.40
70	1.0291	20.47	19.89
75	1.0144	20.71	20.42
80	1.0000	20.91	20.91
85	0.9862	21.13	21.43
90	0.9724	21.34	21.95
95	0.9594	21.56	22.48
100	0.9463	21.77	23.01

## B.2 Physical Properties of Saturated Water

Temperature T, °C	Vapour pressure p <sup>sat</sup> , N m <sup>-2</sup>	Density t, kg m <sup>-3</sup>	Viscosity n □ 10 <sup>6</sup> , kg m <sup>-1</sup> s <sup>-1</sup>
0	611	1000	1790
5	872	1000	1519
10	1228	1000	1310
15	1703	999	1131
20	2336	998	1001
25	3165	997	892
30	4240	996	804
35	5620	994	724
40	7373	992	657
45	9582	990	599
50	12320	988	549
55	15729	985	506
60	19930	983	470
65	24994	981	436
70	31182	978	406
75	38537	975	380
80	47325	972	355

85	57799	968	336
90	70125	965	315
95	84499	962	299
100	101330	958	282

### B.3 Physical Properties of Water (on saturation line)

Temperature T, °C	Pressure $\# \times 10^{-4}$ , N m $^{-2}$	Density $t, \text{kg m}^{-3}$	Enthalpy $\text{kJ kg}^{-1}$	Specific heat $\text{kJ kg}^{-1} \text{K}$
0	10.133	1000.0	4.23	
10	10.133	1000.419	4.19	
20	10.133	998.838	4.19	
30	10.133	996.126	4.18	
40	10.133	992.168	4.18	
50	10.133	988.210	4.18	
60	10.133	983.251	4.18	
70	10.133	978.293	4.19	
80	10.133	972.335	4.19	
90	10.133	965.377	4.19	
100	10.437	958.419	4.23	
110	14.794	951.461	4.23	
120	20.469	943.503	4.23	
130	27.866	935.545	4.27	
140	37.289	926.587	4.27	
150	49.145	917.629	4.32	
160	63.838	907.671	4.36	
170	81.875	897.713	4.40	
180	103.661	887.755	4.44	

### B.4 Physical Properties of Saturated Ammonia Vapour

Temperature T, °C	Pressure (abs.) $\times 10^{-4}$ , N m $^{-2}$	Density of vapour $t \times 10^1, \text{kg m}^{-3}$	Density of liquid $t \times 10^2, \text{kg dm}^{-3}$
-50	4.22	3.82	70.20
-45	5.64	5.00	69.60
-40	7.42	6.45	69.00
-35	9.63	8.23	68.39
-30	12.35	10.38	67.77
-25	15.67	12.97	67.14
-20	19.66	16.04	66.50
-15	24.42	19.66	65.85
-10	30.05	23.90	65.20
-5	36.67	28.83	64.53
0	44.37	34.52	63.86
+5	56.02	41.08	63.17
+10	63.54	48.59	62.47
+15	75.30	57.18	61.75
+20	88.57	66.94	61.03
+25	103.61	77.95	60.28
+30	120.53	90.34	59.52
+35	139.48	104.31	58.75

+40	160.61	120.05	57.95
+45	184.07	127.74	57.13
+50	210.03	157.56	56.29

## B.5 Physical Properties of Some Organic Liquids

Liquid	Formula	Molecular weight kg kmol <sup>-1</sup>	Density, kg m <sup>-3</sup>	Boiling point, °C	Melting point, at 20°C, mm Hg	Saturated vapour pressure
Acetone	CH <sub>3</sub> COCH <sub>3</sub>	58.08	810 56	– 94.3	186	
Benzene	C <sub>6</sub> H <sub>6</sub>	78.11	900 80.2	5.5	75	
Butyl alcohol	C <sub>4</sub> H <sub>9</sub> OH	74.12	810 117.7	– 90	4.7	
Carbon disulphide	CS <sub>2</sub>	76.13	1290 46.3	– 112	298	
Carbon tetrachloride	CCl <sub>4</sub>	153.84	1630 76.7	– 22.8	90.7	
Chloroform	CHCl <sub>3</sub>	119.38	1530 61.2	—	160	
Dichloroethane	CH <sub>2</sub> Cl-CH <sub>2</sub> Cl	99.00	1250 83.7	—	65	
Diethyl ether	C <sub>2</sub> H <sub>5</sub> OC <sub>2</sub> H <sub>5</sub>	74.12	710 34.5	– 116.3	442	
Ethyl acetate	CH <sub>3</sub> COOC <sub>2</sub> H <sub>5</sub>	88.10	900 77.15	– 83.6	73	
Ethyl alcohol	C <sub>2</sub> H <sub>5</sub> OH	46.07	790 78.3	– 114.5	44	
Isoamyl alcohol	C <sub>5</sub> H <sub>11</sub> OH	88.15	810 132	– 117	2.2	
Isobutyl alcohol	C <sub>4</sub> H <sub>9</sub> OH	74.12	800 108	– 108	8.8	
Isopropyl acetate	CH <sub>3</sub> COOC <sub>2</sub> H <sub>5</sub>	130.18	870 142.5	—	6	
Isopropyl alcohol	C <sub>3</sub> H <sub>7</sub> OH	60.09	785 82.4	– 89	32.4	
Methyl acetate	CH <sub>3</sub> COOCH <sub>3</sub>	74.08	930 57.5	—	170	
Methyl alcohol	CH <sub>3</sub> OH	32.04	800 64.7	– 98	95.7	
Propyl acetate	CH <sub>3</sub> COOC <sub>2</sub> H <sub>5</sub>	102.13	890 101.6	—	25	
Propyl alcohol	C <sub>3</sub> H <sub>7</sub> OH	60.09	800 97.2	– 126	14.5	
Toluene Xylenes (o-, m-, p-)	C <sub>6</sub> H <sub>5</sub> CH <sub>3</sub>	92.13	870 110.8	– 95	22.3	
	C <sub>6</sub> H <sub>4</sub> (CH <sub>3</sub> ) <sub>2</sub>	106.16	860 136-145	– 13 to – 48	10	

## B.6 Density of Some Organic Liquids, kg m<sup>-3</sup>

Liquid	Temperature °C									
	0	20	40	60	80	100	120	140	160	180
Acetic acid	1049	1028	1006	984	960	936	909	883	856	—
Acetone	813	791	767	745	721	—	—	—	—	—
Aniline	1037	1023	1007	990	972	952	933	914	896	878
Benzene	900	879	858	836	815	793	769	744	719	691
Carbon tetrachloride	1634	1595	1555	1517	1477	1435	1391	1344	1297	1247
Ethyl alcohol	806	790	772	754	735	716	693	663	633	598

Ethyl ether	736	714	689	666	640	611	576	539	495	—
Glycerine	1267	1259	1250	1238	1224	1208	1188	1163	1126	—
n-Hexane	677	660	641	622	602	581	559	534	504	475
Methyl alcohol	810	792	774	756	736	714	690	664	634	598
Propyl alcohol	819	804	788	770	752	733	711	688	660	629
Toluene	885	866	847	829	810	791	773	754	—	—
m-Xylene	882	865	847	831	813	796	777	759	—	—

## B.7 Surface Tension of Organic Liquids, Dyne cm<sup>-1</sup>

Liquid	Temperature °C											
	-196	-183	0	10	15	17	19	20	30	40	46	60
Acetic acid									27.8			
Acetone			26.2				23.7		21.2		18.6	
Aniline							42.9					
Benzene			31.6				27.6				23.7	
Carbon disulphide					33.6							
Carbon tetrachloride							26.8		29.4			
Chloroform			28.5						21.7			
Diethyl ether							17.0					
Ethyl acetate					23.9							
Ethyl alcohol			24.1				22.8		20.2		18.4	
Formic acid					37.5				30.8			
Methyl alcohol					22.6							
Nitrogen (liquid)	8.5											
Oxygen (liquid)	13.2											
Propyl alcohol					23.8							
Toluene					28.8							
Water			75.6				72.8					

## B.8 Values of Henry's Coefficient for Aqueous Solutions of Some Gases H # 10<sup>-5</sup>, mm Hg

Gas	Temperature, °C										
	0	5	10	15	20	25	30	40	60	80	100
Air	328	371	417	461	504	547	586	661	765	817	816
Acetylene	5.5	6.4	7.3	8.2	9.2	10.1	11.1	-	-	-	-
Bromine	0.162	0.209	0.278	0.354	0.451	0.560	0.688	1.01	1.91	3.07	-
Carbon dioxide	5.53	6.66	7.92	9.3	10.8	12.4	14.1	17.7	25.9	-	-
Carbon monoxide	267	300	336	372	407	440	471	529	625	643	643
Chlorine	2.04	2.50	2.97	3.46	4.02	4.54	5.02	6.00	7.31	-	-
Ethane	96	118	144	172	200	230	260	322	429	502	526
Ethylene	41.9	49.6	58.4	68.0	77.4	86.7	96.2	-	-	-	-
Hydrogen	441	462	483	502	520	537	554	571	581	574	566
Hydrogen sulphide	2.03	2.39	2.78	3.21	3.67	4.14	4.63	5.66	7.82	10.3	11.2
Methane	170	197	226	256	285	314	341	395	476	518	533
Nitrogen	402	454	508	561	611	657	702	792	909	959	954
Oxygen	193	221	249	277	304	333	361	407	478	522	533

## B.9 Equilibrium Composition of Liquid and Vapour for Some Binary Systems at 1 Atmosphere

(i) Nitrogen–Oxygen (ii) Acetone–Methanol (iii) Benzene–Ethylbenzene

Mole% of Nitrogen T, K	Mole% of Acetone Liquid Vapour	Mole% of Benzene T, °C
77.3	100	56.1
100	77.3	100

78	91.9	97.8	55.05	81.1	96.6	99.3
79	78.4	93.2	55.3	81.6	94.5	98.9
80	66.6	88.0	56.0	83.0	90.1	98.0
81	56.6	82.3	56.7	88.0	75.2	93.8
82	47.8	76.4	57.55	94.0	60.0	88.0
83	40.5	70.1	58.65	101.9	43.9	78.5
84	33.8	63.1	60.2	109.6	30.2	66.5
85	27.7	55.7	62.5	120.0	16.5	45.8
86	22.2	47.8	63.6	133.0	3.0	10.5
87	17.1	39.7	64.5	134.5	1.6	6.0
88	11.5	30.4		135.3	1.0	3.3
89	6.2	20.2		136.2	0	0
89.5	3.5	13.0				
90.1	0	0				

**(iv) Water–Acetic Acid (v) Methyl Alcohol–Water (vi) Chloroform–Benzene**

Mole% of water T, °C	Liquid	Vapour	Mole% of Methyl Alcohol T, °C	Liquid	Vapour	Mole% of Chloroform T, °C	Liquid	Vapour
100	100	100	64.5	100	100	61.4	100	100
100.6	90	93.0	66.0	90	95.8	68.9	79	90
101.3	80	86.4	67.5	80	91.5	72.0	66	80
102.1	70	79.5	69.3	70	87.0	74.0	54	70
103.2	60	71.6	71.2	60	82.5	75.3	44	60
104.4	50	62.6	73.1	50	77.9	76.4	36	50
105.8	40	53.0	75.3	40	73.0	77.3	29	40
107.5	30	42.5	78.0	30	66.5	78.2	22	30
110.1	20	30.2	81.7	20	58.0	79.0	15	20
113.8	10	16.7	87.7	10	41.8	79.8	8	10
115.4	5	9.2	91.2	6	30.4	80.6	0	0
118.1	0	0	93.5	4	23.0			
			96.4	2	13.4			
			100	0	0			

**(vii) Benzene–n-Propylbenzene**

Mole% of Benzene

T, °C	Liquid	Vapour
80.08	100	100
81.2	96.5	99.7
82.0	94.4	99.5
85.6	84.6	98.4
93.3	66.8	95.5
96.5	60.4	93.8
122.7	24.9	72.6
138.3	12.6	49.6
150.4	5.0	24.0
156.6	1.4	7.8
154.4	0.5	2.8
159.2	0	0

**B.10 Vapour Pressure of Ethylbenzene and Toluene, mm Hg**

Liquid	Temperature, °C							
	50	60	70	80	90	100	110	110.8

Ethylbenzene	53.8	78.6	113.0	160.0	223.1	307.0	414.1	-	545.9
Toluene	-	139.5	202.4	289.4	404.6	557.2	-	760.0	-

(*Contd.*)

(*Contd.*)

# Index

$\Delta L$  law, 516  
Absolute humidity, 335  
Absorption  
counter-current, 137, 213  
differential contact for, 234  
equilibrium relations, 210  
equipment for, 215  
factor, 222  
flooding, 218  
gas-liquid equilibrium, 210  
individual mass transfer coefficients, 225  
material balance, 213  
methanol wash tower, 216  
solvent selection, 215  
stage calculations, 221  
stripping, 209, 214, 244  
Activity coefficient, 260, 613  
Adiabatic humidification, 346, 350  
Adiabatic operation, 344  
Adiabatic saturation curve, 338  
Adiabatic saturation temperature, 338  
Adsorbents  
activated alumina, 545  
activated clays, 543  
bone char, 544  
carbon, 546  
loading, 543  
molecular sieve, 544  
polymers, 547  
quality of, 543  
regeneration, 535, 564  
resins, 547  
silica gel, 545  
types of, 543  
Adsorber  
agitated vessel, 572  
conical, 575  
cylindrical, 575  
fixed bed, 574  
fluidized bed, 571  
Higgins contactor, 573  
moving bed, 572, 577  
pulsed bed, 573  
steady-state, 572  
Teeter bed, 572  
unsteady-state, 574  
Adsorption  
activated adsorption, 536  
adsorbate loading, 560  
adsorbate, 535  
adsorbent, 535, 543  
adsorbent loading, 562  
batch operation, 572  
BET isotherm, 541

blow down, 563  
break point, 559  
break through capacity, 561  
breakthrough curve, 559  
chemisorption, 535  
concentration of solute, 548, 559  
continuous operation, 572  
counter-current operation, 553  
cross-current operation, 522  
density (bulk) of bed, 560  
design methods for, 552  
desorption, 535  
differential contact operation, 556  
equilibrium, 536  
equilibrium line, 548  
fixed bed operation, 558, 574  
*Adsorption (continued)*  
fraction of solid covered, 539  
Freundlich isotherm, 539  
Higgins contactor, 573  
high temperature PSA process for, 569  
hysteresis, 537  
isobar, 536  
isostere, 547  
isotherm of benzene, 537  
isotherms, 536  
Langmuir isotherm, 538  
length of equilibrium bed/section (LES), 562  
length of unused bed (LUB) 562  
mass transfer coefficient, 557  
mass transfer zone, 558  
moving bed operation, 572  
multi-stage operation, 552  
pressure swing adsorption (PSA), 557  
pressure swing regeneration, 566  
pressure swing sorption enhanced reaction (PSSER), 576  
pressurization, 563  
pulsed bed, 573  
purging, 563  
reactive, 576  
regeneration, 535, 564  
single-stage operation, 548  
Skarstrom cycle, 563  
steady-state, 572  
swing adsorption (RPSA), 557, 568  
temperature swing regeneration, 565  
thermal swing sorption enhanced reaction (TSSER), 577  
unsteady-state, 574  
vacuum swing adsorption (VSA), 557  
vapour pressure, 536  
Affinity chromatography, 579  
Agitated crystallizer, 518  
Agitated vessel, 159, 441  
Air-water system, 338  
Anisotropic membrane, 598  
Antoine constant, 264  
Antoine equation, 263  
Approximate methods, 300

Apron (in Tray column), 168  
Arc downcomer (in Tray column), 168  
Asymmetric membrane, 594, 602  
Atmolysis, 62  
Atmospheric cooling tower, 356  
Atomic diffusion volume, 30  
Average velocity of fluid, 8  
Azeotrope  
    azeotropic mixture, 261  
    distillation of, 308  
    maximum boiling, 262  
    minimum boiling, 261  
    separation of, 308  
Ballast tray, 171  
Batch distillation, 257, 272  
Batch drier, 473  
Batch drying, 463  
Batch operation, 126  
Belt drier, 479  
Berl saddles, 182, 185  
BET isotherm, 541  
Beta ring, 184  
Bioseparation, 635  
Bodenstein number, 412  
Boiling point diagrams, 257  
Bollman extractor, 445  
Bone-dry solid, 454  
Bonotto extractor, 446  
Bottom product, 273, 279  
Bound moisture, 455  
Boundary layer theory, 115  
Breakthrough curve, 559  
Brennan-Koppers purifier, 529  
Brodie crystallizer-Purifier, 528  
Bubble-cap column, 159, 164  
Bubble-cap tray, 165  
Bubble point, 258, 268  
    curve, 258  
Capillary module, 604  
Capillary movement in drying, 461  
Capillary number, 145  
Cascade mini ring, 184, 216  
Catalytic distillation, 314  
Catalytic membrane reactor, 634  
Centrifugal extractor, 410  
Chapman and Enskog equation, 30  
Chemical extraction, 427  
Chemical potential, 613  
Chemisorption, 535  
Chromatography  
    adsorption, 579  
    affinity, 579  
    displacement, 579  
    elution, 579  
    *Chromatography (continued)*  
        frontal, 579  
        gas, 579  
        gel filtration, 579

high performance liquid, 580  
hydrophobic, 580  
immobilized, 584  
liquid, 580  
molecular sieving, 580  
reverse phase, 581  
size exclusion, 579  
ultra performance liquid, 580  
Chromatographic separation  
column for, 581  
combo unit for, 584  
principle of, 583  
resolution, 582  
Circulating liquor magma crystallizer, 521  
Clusius-Dickel column, 62  
Co-current absorption, 135  
Co-current wet scrubber, 197  
Colburn equation, 134, 222, 237  
Collision integral, 31  
Concentration boundary layer, 116  
Concentration of adsorbate, 548, 559  
Concentration profiles in adsorption, 558  
Conditional supercooling, 525  
Conical adsorber, 575  
Constant drying, 456  
Constant molal overflow in distillation, 286  
Constant molal vaporization in distillation, 286  
Constant rate period in drying, 457, 464  
Continuous adsorption, 572  
Continuous distillation, 279, 297  
Continuous drying, 462, 469  
Continuous extraction, 392  
Continuous phase in extraction, 399  
Cooling range, 352  
Cooling tower, 356  
Counter-current adsorption, 553  
Counter-current decantation unit, 443  
Counter-current extraction, 382, 389  
Counter-current wet scrubber, 197  
Counter-flow cooling tower, 358  
Critical moisture content in drying, 455, 460  
Critical Reynold's number, 116  
Cross flow membrane filtration, 619, 631  
Cross-circulation drying, 457, 463  
Cross-current adsorption, 522  
Cross-current extraction, 380, 386, 389  
Cross-flow absorption, 127  
Cross-flow cascade, 127  
Cross-flow cooling tower, 358  
Cross-flow tray, 161  
Cryogenic distillation, 312  
Crystals  
caking of, 517  
forms of, 504  
growth of, 513  
liquid, 504  
purification of, 528  
shape factor, 514

yield of, 507  
Crystallization  
conditional supercooling, 525  
diffusional mass transfer, 513  
effort for, 526  
energy balance for, 508  
equipment for, 518  
falling film crystallization, 527  
formation of nuclei, 512  
fractional supersaturation, 510  
fractional, 517  
heat balance, 508  
heat of, 515  
isomorphous, 515  
magma, 522  
melt crystallization, 504, 524  
methods of nucleation, 512  
phase separation, 509  
Philips crystallization process, 528  
polymorphous, 504  
precipitation, 517  
progressive freezing crystallization, 526  
purification process, 528  
rate of crystal growth, 513  
ratio of supersaturation, 510  
saturated solution, 505, 508, 510  
saturation concentration, 509  
solid-liquid equilibria, 505  
solubility, 505  
solution crystallization, 504  
static crystallization, 527  
supersaturation, 505, 508, 510, 514  
supersolubility, 509  
surface reaction, 513  
suspension based melt crystallization, 525  
Volmer equation, 511  
Crystallizer  
agitated, 518  
circulating liquor, 521  
circulating magma, 521  
Crystallizer (*continued*)  
draft Tube Baffle, 523  
Krystal, 521  
Oslo vacuum, 521  
recrystallizer, 536  
Swenson Walker crystallizer, 530  
wash column, 525  
Cycles of adsorption, 563  
Cyclohelix spiral ring, 184  
Cylindrical adsorber, 575  
Decantation, 443  
Decoction, 427  
Decolorising carbon, 544  
Degree of saturation, 561  
Degrees of freedom, 123  
Dehumidification, 334, 344  
Density (bulk) of bed, 560  
Depressurization, 563

Design methods  
for adsorption, 552  
for gas(vapour)/liquid-liquid systems, 133  
Desorption, 3, 209, 214, 454  
factor, 222  
Dew point, 258, 268, 336  
curve, 258  
Dialysis, 5, 606, 613  
Differential contact operation  
in adsorption, 556  
in extraction, 393  
in gas(vapour)-liquid systems, 135  
Differential distillation, 272, 279  
Diffusion  
atmolysis, 62  
atomic diffusion volume, 30  
average velocity of fluids, 8  
Clusius-Dickel column, 62  
concentration, 8  
through constant area, 16  
diffusion coefficient (also diffusivity), 11, 26, 612  
diffusion volumes of molecules, 30  
diffusional velocity, 13  
Dufour effect, 62  
eddy diffusion, 46  
equimolar counter-diffusion, 19, 41  
Fick's law, 12  
forced diffusion, 62  
frames of reference, 9  
heat flux, 12  
Hottel's theory for molecular, 15  
kinetic theory of gases, 15  
Knudsen, 60  
mass flux, 9  
mean free path, 15  
models of, 11  
molar flux, 9  
molecular, 7, 60  
molecular in gases, 14  
molecular in liquids, 39  
momentum flux, 13  
multicomponent, 21  
Newman's curve, 57  
non-equimolar counter-diffusion, 21  
Prandtl mixing length, 48  
pressure, 62  
Soret effect, 62  
from a sphere, 25  
steady-state in binary system, 16  
steady-state in solids, 50  
Stephan tube method, 36  
Stokes-Einstein equation, 43  
structure insensitive, 50  
structure sensitive, 50  
surface, 61  
through surface of a slab, 54  
sweep, 5, 62  
thermal, 5, 62

thermo-gravitational column, 62  
transient, 51  
transition, 60  
in turbulent stream, 46  
unsteady-state, 51  
through variable area, 23  
Diffusional extraction, 427  
Diffusivity (or Diffusion coefficient)  
atomic diffusion volume, 30  
Chapman and Enskog equation, 30  
collision integral, 33  
of common gas pairs, 28  
determination of  
gas phase, 28, 36  
liquid phase, 46  
diaphragm cell method, 46  
diffusion volumes of molecules, 30  
eddy, 48  
of electrolytes, 45  
of non-electrolytes, 43  
equivalence of, 27  
Fuller's equation, 30  
of gases, 26  
Diffusivity (or Diffusion coefficient) (*continued*)  
Gilliland equation, 29  
Lennard-Jones potential, 31  
liquid phase, 42  
self, 44  
Stefan tube method, 36  
Wilke and Chang equation, 44  
Dilute gas mixtures, 130  
Dilute solution, 241, 541  
Dimensional groups, 38  
Dispersed phase in extraction, 399  
Distillate, 272, 279  
Distillation  
activity coefficient, 260  
Antoine constant, 264  
Antoine equation, 263  
approximate methods for number of stages, 300  
azeotrope, 261, 263  
azeotropic, 308  
batch, 257, 272  
binary systems, 279  
boiling point diagrams, 257  
bottom product, 273, 279  
bubble point, 258, 268  
bubble point curve, 258  
catalytic, 314  
condensate, 271  
condenser, 279  
constant boiling mixture, 261, 263, 307  
constant molal overflow, 286  
constant molal vaporization, 286  
continuous, 279, 297  
cryogenic, 312  
differential, 272, 279  
distillate, 272, 279

divided wall column, 305  
energy balance for, 280  
energy conservation practices in, 303  
enriching section, 279  
entrainer, 308  
equilibrium, 269  
equilibrium data prediction, 263  
equilibrium stage, 281  
equipment for, 303  
exact methods for number of stages, 301  
extractive, 308  
feed conditions, 289  
feed plate, 279  
Fenske equation, 300  
Fenske-Undrwood equation, 281, 292  
flash vaporization, 269  
fractionation, 279  
fugacity, 265  
Gibbs-Duhem equation, 265  
Gilliland equation, 301  
heavy key, 299  
ideal plate, 281  
ideal solution, 271, 274  
intermediate reboilers and condensers, 306  
Lewis-Matheson method, 301, 303  
light key, 299  
mass transfer coefficient, 298  
material balance for, 280  
maximum boiling mixture, 262  
McCabe-Thiele method, 281, 285  
molecular, 310  
multicomponent, 299  
multicomponent equilibria, 267  
for multicomponent system, 271  
multiple effect heat cascading, 307  
Murphree plate efficiency, 295  
open steam, 278, 294  
optimum reflux, 293  
Othmer still, 257  
overall plate efficiency, 295  
packed tower for, 297  
partial condensation, 271  
partial pressure, 260  
plate efficiency, 295  
Ponchon-Savarit method, 281  
pressure swing, 309  
q-line, 287  
Raoult's law, 259  
Rayleigh equation, 273  
RDWC, 315  
reactive, 314  
reboiler, 279  
rectification, 279  
rectified spirit, 261  
rectifying section, 279  
reflux ratio, 281, 287  
relative volatility, 260  
residue in, 279

side stream, 295  
simple, 272  
single-stage, 269  
split tower arrangement, 307  
steam, 277  
stripping section, 279  
theoretical plate, 281  
Thiele-Geddes method, 301  
Distillation (*continued*)  
tie line, 284  
total reflux, 285  
two stage condensation, 306  
two-column, 309  
Underwood equation, 301  
UNIFAC, 266  
van Laar equation, 265  
vaporisation at constant pressure, 257  
vaporisation at constant temperature, 259  
vaporisation efficiency, 278  
vapour pressure, 260  
vapour recompression, 305  
vapour-liquid equilibrium, 256  
Wilson equation, 266  
Distribution coefficient, 376  
Divided wall column, 305  
Donnan equilibrium, 614  
Dorr agitator, 448  
Downcomer, 161, 166  
Downcomer area, 162  
Downcomer flooding, 162  
Draft Tube Baffle crystallizer, 523  
Drier (or Dryer)  
agitated pan, 476  
batch, 473  
belt, 479  
cabinet, 474  
co-current flow in, 482  
compartment, 474  
continuous, 478  
conveyer, 479  
counter-current flow in, 482  
diameter of rotary, 481  
dielectric, 483  
direct, 474, 478, 482  
direct-indirect, 482  
double drum, 488  
drum, 488  
filter, 486  
flight action, 480  
fluidized bed, 483  
freeze, 477  
heat pump, 484  
hold-up in rotary, 481  
horizontal filter, 486  
indirect, 475, 479, 482, 488  
kiln action, 480  
microwave, 483  
number of transfer unit, 471

pneumatic, 484  
retention time in rotary, 481  
rotary filter, 486  
rotary, 479  
selection of, 488  
shelf, 474  
spouted bed, 483  
spray, 485  
tray, 474  
truck, 475  
tunnel, 478  
turbo-type, 479  
UNIQUAC, 266  
vacuum rotary, 476  
vacuum shelf, 475  
vertical filter, 486  
Drift eliminators, 361  
Dry bulb temperature, 335  
Drying  
absorption, 454  
adiabatic saturation temperature, 461  
batch, 463  
bone-dry solid, 454  
bound moisture, 455  
capillary movement, 461  
case hardening, 462  
constant drying conditions, 456  
constant rate period, 457, 464  
continuous, 462, 469  
critical moisture, 455, 460  
cross-circulation, 457, 463  
deliquescence, 454  
desorption, 454  
enthalpy balance in, 464, 470  
equilibria, 453  
equilibrium moisture content, 455  
equipment for, 473  
falling rate period, 457, 460, 464  
free moisture, 455  
gas humidity effect on, 459  
gas temperature effect on, 459  
gas velocity effect on, 459  
glassy phase, 477  
heat transfer coefficient, 458  
latent heat of vaporization, 458  
length of heat transfer unit, 471  
length of, 470  
liquid diffusion, 461  
lyophilization, 477  
material balance in, 463  
mechanism of, 455  
moisture content, 455  
Drying (*continued*)  
number of unit, 469  
pressure action, 461  
rate curve, 456  
rate of, 459, 469  
solid thickness effect on, 459

temperature-concentration diagram, 478  
theory of, 455  
thickness of drying bed, 469  
through-circulation, 461, 469, 474  
time of, 463  
unbound moisture, 455  
unsaturated surface, 460  
vapour diffusion, 461  
wet-bulb temperature, 458  
Dofour effect, 62  
Eddy diffusion, 46  
Eddy diffusivity, 48  
Effective diffusivity, 607, 617, 628  
Efficiency  
Murphree local/point, 173, 175  
Murphree overall, 170, 173, 175  
Murphree plate, 173, 295, 352, 392  
Effusion, 5, 607  
Electrodialysis, 5, 615  
Elution chromatography, 579  
Energy conservation practices in distillation, 303  
Entrainment flooding, 162  
Eötvös number, 411  
Equilibrium distillation, 269  
Equilibrium moisture content, 455  
Equilibrium partition coefficient, 629  
Equilibrium relations  
gas-liquid, 210  
solid-liquid, 428  
Equilibrium stage (theoretical plate), 279, 281  
Equipment for air-water contact, 355  
Equipment for leaching, 440  
Equivalence of diffusivities, 27  
Extraction battery, 441  
Extractive distillation, 308  
Equimolar counter-diffusion, 19, 41  
Extractors  
asymmetric rotating disk, 401, 406  
centrifugal, 410  
characteristics of, 400  
classification of, 400  
drop size estimation, 411  
flow mixer, 402  
graesser, 401  
impeller, 403  
impeller power requirement, 413  
impeller speed, 412  
Karr, 401, 409  
mass transfer coefficient, 413  
mixer-settler, 400, 402, 404  
Oldshue-Rushton, 401, 405  
packed tower, 400, 408  
perforated plate, 400, 407  
plate column, 400  
Podbielniak, 400, 410  
power number, 411, 413  
pulsed column, 400, 408  
potating Disk, 400, 406

Sauter-mean drop diameter, 411  
Scheibel, 400, 405  
Settler, 402  
spray tower, 400, 407  
vibrating plate, 409  
Evaporative cooling, 344, 354  
Fair's correlation, 162  
Falling film crystallization, 527  
Falling rate period, 457, 460, 464  
Fanning's friction factor, 85  
Fast reaction with absorption, 242  
Feed conditions in distillation, 289  
Feed plate in distillation tower, 279  
Fenske equation, 300  
Fenske-Underwood equation, 281, 292  
Fick's law, 12  
Film mass transfer coefficients, 74, 106, 143, 177, 225, 413  
Film penetration theory, 115  
Filter drier, 486  
Filtrate, 619  
Fixed bed adsorber, 574  
Fixed bed adsorption, 558, 574  
Flash distillation, 269  
Flexiring, 184  
Flexitray, 171  
Flooding, 190, 218  
Flooding point, 190  
Flooding velocity, 162, 190  
Flow mixer, 402  
Flow pattern of vapour and liquid, 166  
Flow regimes of gas and liquid, 166  
Fluidized bed adsorber, 571  
Fluidized bed drier, 483  
Forced diffusion, 62  
Formation of nuclei, 509  
Forms of crystals, 504  
Fourier number, 57, 83  
Fraction of solid covered, 539  
Fractional crystallization, 517  
Fractional distillation, 311  
Fractional supersaturation, 510  
Fractionation, 279  
Frames of reference, 9  
Free moisture content, 455  
Freeze drier, 477  
Freundlich isotherm, 539  
Froude number, 144, 412  
Fugacity, 265  
Fuller, et al. equation, 30  
Fuller's earth, 543  
Galileo number, 412  
Gas absorption, 3, 209  
Gas adsorbent carbon, 544  
Gas adsorption, 571  
Gas chromatography, 579  
Gas dispersed, 159  
Gas humidity effect on drying, 459  
Gas separation, 598, 606

Gas temperature effect on drying, 459  
Gas velocity effect on drying, 459  
Gaseous diffusion, 5, 606  
Gas–liquid contact, 3, 73, 104, 159, 209  
Gas–liquid equilibrium, 210  
Gel filtration chromatography, 579  
Gel formation, 618  
Gibbs-Duhem equation, 265  
Gilliland equation, 29, 301  
Grashof number, 83  
Growth of crystals, 513  
Hagen Poiseuille equation, 619  
Heat and mass transfer analogy, 86  
Heat flux, 12  
Heat of adsorption, 542  
Heat transfer coefficient, 458  
Heavy key, 299  
Henry's constant, 212, 608  
Henry's law, 212  
HETP, 138  
HETS, 173, 189  
Higgins contactor, 573  
High performance liquid chromatography, 580  
High temperature drying, 470  
High temperature PSA process, 569  
Hilderbrandt extractor, 444  
Hold-up in rotary drier, 481  
Horizontal adsorber, 575  
Hottel's theory for molecular diffusion, 15  
Humidification  
absolute humidity, 335  
adiabatic gas-liquid contact, 345  
adiabatic humidification, 346, 350  
adiabatic operation, 344  
adiabatic saturation curve, 338  
adiabatic saturation temperature, 338  
air-water system, 338  
atmospheric tower, 356  
blowers, 361  
cooling range, 352  
cooling tower, 356  
counter-flow tower, 358  
cross-flow tower, 358  
dehumidification, 334, 344  
dew point, 336  
drift eliminators, 361  
dry bulb temperature, 335  
enthalpy balance, 345  
enthalpy, 337  
equilibrium line, 347  
equipment for air-water contact, 355  
evaporative cooling, 354  
fans, 361  
forced draft cooling tower, 357  
gas cooling, 334, 345  
gas-liquid contact, 344  
heat transfer coefficient, 340, 351  
height of packed bed, 345, 350

height of transfer unit, 347, 351  
humid heat, 336  
humid volume, 336  
induced draft cooling tower, 358  
Lewis number, 340  
Lewis relation, 340  
mass transfer coefficient, 340, 351  
material balance, 345  
mechanical draft tower, 356  
molal absolute humidity, 335  
Murphree stage efficiency, 352  
natural draft tower, 356  
non-adiabatic operations, 344, 354  
percentage saturation, 336  
psychrometric chart, 341  
Humidification (*continued*)  
psychrometric ratio, 341  
relative humidity, 336  
relative saturation, 336  
saturation humidity, 335  
sling thermometer, 339  
spray chamber, 360  
temperature approach, 353  
tower fills, 360  
water conservation, 359  
water cooling, 334, 344, 346  
water loading, 362  
wet bulb depression, 340  
wet bulb temperature, 339, 362  
wet bulb temperature approach, 348  
Hydrodynamic boundary layer, 116  
Hydrophilic membranes, 598  
Hydrophobic chromatography, 580  
Hydrophobic materials, 600  
Hypak, 182, 184  
Hysteresis, 537  
Ideal adsorption time, 560  
Indirect drier, 475, 479, 482, 488  
Induced draft cooling tower, 358  
Intalox packing (IMTP), 183, 185  
Intalox saddle, 182, 185  
Interphase mass transfer  
boundary layer theory, 115  
concentration boundary layer, 116  
critical Reynold's number, 116  
film penetration model, 115  
hydrodynamic boundary layer, 116  
penetration theory, 113  
surface renewal theory, 115  
surface stretch theory, 115  
thermal boundary layer, 116  
two-film theory, 111  
two-resistance theory, 111  
Impeller power requirement, 413  
Impeller speed, 412  
Ion exchange chromatography, 580  
Isobar, 536  
Isostere, 536

Isotherms, 536  
j factor, 88  
Kennedy extractor, 447  
Kinetic theory of gases, 15  
Knudsen diffusion, 60  
Knudsen number, 61  
Kremser equation, 134, 222, 436  
Kremser-Brown-Souders equation, 134, 222, 436  
Kuhni extractor, 400, 405  
Kureha double screw purifier, 528  
Langmuir isotherm, 538  
Latent heat of vaporization, 458  
Leaching, 4, 371, 427  
agitated vessel, 442  
Bollman extractor, 445  
Bonotto extractor, 446  
decoction, 427  
diffusional, 427  
equipment for, 440  
lixiviation, 427  
multi-stage counter-current, 433  
multi-stage cross-current, 432  
operation, 430  
Rotocel, 444  
Shank's system, 440  
single-stage operation, 432  
solid-liquid equilibria, 428  
solid-liquid extraction, 427  
thickeners – CCD units, 443  
Lean gases, 132, 227, 241  
Lennard-Jones potential, 31  
Lessing rings, 182  
Lewis number, 84, 340  
Lewis-Matheson method, 301, 303  
Light key, 299  
Liquid adsorption, 572  
Liquid chromatography, 580  
Liquid crystals, 504  
Liquid diffusion in drying, 461  
Liquid dispersed, 159, 176  
Liquid hold-up, 193  
Liquid phase diffusivity, 42  
Liquid-liquid equilibrium, 373, 375  
Liquid-liquid extraction, 371  
Liquid-solid separation, 371, 427  
Lixiviation, 371, 427  
Loading of adsorbate, 540  
Loading of adsorbent, 543  
Loading point, 190  
Local/point efficiency, 173  
Log mean concentration difference, 235  
Louvers, 361  
Magma crystallizer, 522  
Mass flux, 9, 73  
Mass transfer  
batch operation for, 126  
co-current, 137  
coefficient, 73

convective, 2  
to drops and bubbles, 96  
in flow normal to a single cylinder, 96  
counter-current, 129, 138  
cross-current, 127  
degrees of freedom, 123  
differential contact, 135  
diffusional, 2  
in flow past flat plates, 91  
in flow past solid sphere, 95  
in flow through packed bed, 94  
in fluids through pipes, 93  
gas phase, 74, 106, 143  
individual volumetric, 77, 143  
interphase, 104  
in laminar flow, 78  
liquid phase, 74, 106, 143  
operating line, 137  
through packed bed, 94  
phase rule, 123  
single-stage, 124  
zone, 558

Mass transfer equipment  
agitated vessel, 159  
apron, 168  
arc downcomer, 168  
ballast tray, 171  
beta ring, 184  
bubble-cap column, 159, 164  
bubble-cap tray, 165  
cascade mini rings, 184, 216  
cross-flow tray, 161  
cyclohelix spiral rings, 184  
Fair's correlation, 162  
film mass transfer coefficient, 177  
flexi-ring, 184  
flexi-tray, 171  
flooding point, 190  
flooding velocity, 162, 190  
flow pattern of vapour and liquid, 166  
flow regimes, 167

Mass transfer coefficient  
height of packed bed, 189  
intalox saddle, 182, 185  
lessing rings, 182  
liquid dispersed, 159, 176  
liquid hold-up, 193  
loading point, 190  
Murphree efficiency, 173  
net column area, 162  
orifice scrubber, 196  
overall tray efficiency, 170, 175  
packed tower, 159, 180, 217  
packing, 182  
pall rings, 182, 216  
partition rings, 182  
plate column, 159  
point efficiency, 175

preloading region, 190  
pressure drop, 163, 189  
pulsed column, 159, 199  
random packing, 182  
raschig rings, 182  
reverse jet froth scrubber, 198, 217  
segmental downcomer, 168  
sieve-plate column, 159, 164, 166  
simulated packed tower, 159, 176  
sloped downcomer, 168  
Souders-Brown factor, 162  
sparged vessel, 159  
spray tower, 159, 195, 217  
string-of-disks column, 159, 178  
string-of-spheres column, 159, 179  
structured packing, 182, 187  
tellerette packings, 182, 185  
tray, 161  
tray spacing, 161  
valve cap, 171  
valve tray, 159, 164, 171  
venturi scrubber, 159, 196, 217  
weeping, 164  
wetted wall tower, 159, 176  
Maximum boiling mixture, 262  
McCabe-Thiele method, 281, 285  
Mechanical draft tower, 356  
Mechanism of  
adsorption, 558  
drying, 455  
Melt crystallization, 504, 524  
Membrane  
anisotropic, 598  
asymmetric, 594, 602  
carbon, 600  
carbon nanotube, 601  
diffusivity, 596, 617  
Donnan equilibrium, 614  
Membrane (*continued*)  
hydrophilic, 598  
hydrophobic materials, 600  
materials of, 598  
modules, 601  
molecular sieve carbon, 611, 630  
nano-composite, 600  
nanoporous, 600, 630  
organic-inorganic composite, 601  
permeability, 609  
permeability coefficient, 596  
permeation flux, 596  
permeation of gases, 608, 623  
polymeric, 598, 600  
porosity of, 607, 627  
porous, 598, 630  
pressure gradient, 607  
processes, 5, 597, 606  
selective, 595  
selective surface flow (SSF), 612

semipermeable, 596  
sorption-diffusion mechanism, 600  
structure of, 595  
symmetric, 595  
thin film nanocomposite, 600  
transport through, 596  
types of, 595  
Membrane filtration  
cross flow, 619  
filtrate, 619  
microfiltration, 616  
nanofiltration, 616, 620  
reverse osmosis, 616, 621  
tangential flow, 619  
ultrafiltration, 616  
Membrane modules  
capillary module, 604  
co-current flow in, 631  
counter-current flow in, 631  
cross flow in, 631  
flow path in, 602  
hollow fiber module, 604  
inside-out, 605  
monolithic, 605  
outside-in, 605  
perfect mixing in, 631  
plate and frame module, 601  
spiral wound module, 603  
tortuous narrow channel, 603  
tubular module, 605  
Membrane reactor  
bioreactor, 634  
catalytic, 634  
immobilization of catalyst, 634  
pervaporation reactor, 634  
Membrane separation  
activity coefficient, 613  
bioseparation, 635  
chemical potential, 613  
combo unit for, 612  
concentration gradient, 607, 614  
concentration, 613  
concentration profile, 630  
cross-flow, 619, 626  
design procedure, 627  
dialysis, 606, 613  
effective diffusivity, 607, 617, 628  
effusion, 607  
electrodialysis, 615  
equilibrium partition coefficient, 629  
gaseous diffusion, 606  
gel formation, 618  
Hagen Poiseuille equation, 619  
Henry's constant, 608  
of liquids, 613, 616  
mass transfer coefficient, 614, 618  
membrane area, 633  
perfect mixing in pervaporation, 624

permeate, 596  
permeation, 606, 615, 623  
pervaporation, 594, 623  
pore flow, 623  
pressure profile, 630  
reactive, 633  
rejection coefficient, 620  
retentate, 596  
selectivity engineering, 635  
solution-diffusion, 623  
transmembrane pressure drop, 619  
volumetric filtration flux, 618, 625  
waste water treatment, 623  
Methods of  
absorption, 215  
distillation, 269  
extraction, 377  
nucleation, 509  
Microwave drier, 483  
Mier's theory, 509  
Minimum boiling mixture, 261  
Minimum liquid to gas flow rates, 218  
Minimum number of theoretical plates, 285, 290  
Minimum reflux, 285, 291  
Minimum solvent rate, 217, 391  
Mixer-settler, 400, 402, 404  
Models of diffusion, 11  
Moisture content, 455  
Molal absolute humidity, 335  
Molar flux, 9  
Molecular diffusion, 7, 60  
in gases, 14  
in liquids, 39  
Molecular distillation, 310  
Momentum and heat transfer analogy, 84  
Momentum flux, 13, 73  
Moving bed adsorption, 572  
Moving bed chromatographic reactor, 584  
Multicomponent  
absorption, 238  
diffusion, 21  
distillation, 299  
equilibria, 267  
systems, 21, 277  
Multiple effect heat cascading, 307  
Multistage operation  
in absorption, 221  
in adsorption, 552  
in distillation, 279  
in extraction, 392  
in leaching, 432  
Murphree local/point efficiency, 173, 175  
Murphree overall efficiency, 170, 173, 175  
Murphree plate efficiency, 173, 295, 352, 392  
Nano-composite membrane, 600  
Nanofiltration, 616, 620  
Nanoporous membrane, 600, 630  
Natural draft tower, 356

Net column area, 162  
Newman's curve, 57  
Non-adiabatic operations, 354  
Non-equimolar counter-diffusion, 21  
Nucleation, 509  
rate, 510  
Nusselt number, 82  
Oldshue-Rushton extractor, 401, 405  
Open steam, 278, 294  
Optimum reflux, 293  
Organic-inorganic composite, 601  
Orifice scrubber, 196  
Oslo vacuum crystallizer, 521  
Othmer still, 257  
Outside-in membrane module, 605  
Overall plate/tray efficiency, 170, 175, 295, 352, 392  
Overall volumetric mass transfer coefficient, 145, 225, 231, 347, 394, 413  
Pachuca tanks, 440, 442  
Packed Tower  
flooding, 190, 218  
flooding point, 190  
flooding velocity, 190  
HETP, 138  
packing, 182  
preloading region, 190  
pressure drop, 163, 189  
Packed tower for distillation, 297  
Packed tower for extraction, 400, 408  
Packed tower, simulated  
absorption with chemical reaction in, 176  
co-current flow in, 177  
counter-current flow in, 177  
liquid dispersed in, 159  
mass transfer coefficient, 176  
physical absorption in, 176  
scaling ratio, 180  
string-of-disks column, 179  
string-of-spheres column, 179  
wetted wall tower, 176  
Packing or tower packing  
cascade mini rings, 184, 216  
cyclohelix spiral rings, 184  
lessing rings, 182  
pall rings, 182, 216  
partition rings, 182  
random packing, 182  
raschig rings, 182  
structured packing, 182, 187  
tellerette packings, 182, 185  
Partial condensation, 271  
Partial pressure, 62, 260, 536, 630  
Partition coefficient, 582, 629  
Peclet number, 82  
Penetration theory, 113  
Percentage humidity, 336  
Percentage saturation, 336  
Percolation tank, 440  
Perfect mixing in membrane, 631

Perfect mixing in pervaporation, 624  
Perforated plate extractor, 400, 407  
Permeability coefficient, 596  
Permeability, 609  
Permeate, 596, 619  
Permeation flux, 596  
Permeation of gases, 608  
Permeation, 5, 606, 615, 623  
Pervaporation, 594, 623  
Phase inversion, 399  
Phase rule, 123  
Phase volumetric mass transfer coefficient, 77, 107, 143, 225, 231, 513, 577  
Philips crystallization process, 528  
Physical adsorption, 535  
Physical properties of adsorbent, 546  
Plait point, 374  
Plate and frame module, 601  
Plate calculations in absorption, 221  
Plate column, 159  
Plate efficiency, 173, 295  
Plate tower/column (also see Tray Tower) arc downcomer, 168  
bubble-cap column, 159, 164  
bubble-cap tray, 165  
diameter, 163  
downcomer, 161, 166  
downcomer area, 162  
downcomer flooding, 162  
entrainment flooding, 162  
Fair's correlation, 162  
flow pattern of vapour and liquid, 166  
flow regimes, 167  
gas dispersed, 159  
liquid hold-up, 193  
local efficiency, 173  
Murphree plate efficiency, 173  
overall efficiency, 170, 175  
point efficiency, 175  
pressure drop, 163  
segmental downcomer, 168  
sieve-plate column, 159, 164, 166  
sloped downcomer, 168  
Souders-Brown factor, 162  
tray spacing, 161  
tray, 161  
valve cap, 171  
valve tray, 159, 164, 171  
weeping, 164  
Pneumatic drier, 484  
Point efficiency, 175  
Polymeric adsorbent, 547  
Polymeric membrane, 598, 600  
Ponchon-Savarit method, 281  
Pore flow in membrane, 623  
Porosity of membrane, 607  
Porous membrane, 598, 630  
Power number, 411, 413  
Prandtl mixing length, 48  
Prandtl number, 81

Precipitation, 517  
Preloading region, 190  
Pressure diffusion, 62  
Pressure gradient, 607  
Pressure profile, 630  
Pressure swing adsorption (PSA), 557  
Pressure swing distillation, 309  
Pressure swing regeneration, 566  
Pressure swing sorption enhanced reaction (PSSER), 576  
Pressurization, 563  
Process intensification, 6, 635  
Process of crystallization, 508  
Progressive freezing crystallization, 526  
Psychrometric chart, 341  
Psychrometric ratio, 341  
Pulsed bed adsorber, 573  
Pulsed equipment, 159, 199  
Pulsed extractor, 400, 408  
Purging, 563  
Purification of crystals, 528  
Purifier  
Brennan-Koppers purifier, 529  
Brodie crystallizer-purifier, 528  
Kureha double screw purifier, 528  
Schildknecht column, 528  
TNO purifier, 528  
q-line, 287  
Raffinate phase, 372  
Random packing, 182  
Raoult's law, 211, 259  
Rapid pressure swing adsorption (RPSA), 557, 568  
Raschig rings, 182  
Rate of crystal growth, 513  
Ratio of supersaturation, 510  
Rayleigh equation, 273  
RDWC, 315  
Reactive absorption, 244  
Reactive adsorption, 576  
Reactive crystallization, 529  
Reactive distillation, 314  
Reactive extraction, 414  
Reactive membrane process, 633  
Reboiler, 279  
Recrystallizer, 525  
Rectification, 279  
Rectifying section, 279  
Reflux ratio, 281, 287  
Reflux, 279  
Regeneration, 535, 564  
Rejection coefficient, 620  
Relative humidity, 336  
Relative saturation, 336  
Relative volatility, 260  
Resins, 547  
Resolution, 582  
Retentate, 596  
Retention time in rotary drier, 481  
Reverse jet froth scrubber, 198

Reverse osmosis, 616, 621  
Reverse phase chromatography, 581  
Reynold's analogy, 84  
Reynold's number, 81, 144  
Rotary drier, 479  
Rotating disk contactor, 400, 406  
Rotocel, 444  
Saturated solution, 505, 508, 510  
Saturation concentration, 509  
Saturation humidity, 335  
Sauter-mean drop diameter, 411  
Scheibel extractor, 400, 405  
Schildknecht purifier, 528  
Schmidt number, 81, 144  
Sling thermometer, 339  
Scrubber  
co-current wet, 197  
counter-current wet, 197  
orifice, 196  
packed wet, 196  
reverse jet froth, 198  
venturi, 196  
wet, 196  
Segmental downcomer, 168  
Selection of drier, 488  
Selective surface flow (SSF) membrane, 612  
Selectivity engineering, 635  
Selectivity, 376  
Self diffusivity, 44  
Semipermeable membrane, 596  
Separation factor, 594  
Separation of azeotropes, 308  
Shank's system, 440  
Shape factor of crystals, 514  
Sherwood number, 81, 82, 145, 413  
Side stream, 295  
Sieve-plate column, 159, 164, 166  
Silica gel, 545  
Simulated packed tower  
absorption with chemical reaction in, 176  
co-current flow in, 177  
counter-current flow in, 177  
liquid dispersed in, 159  
mass transfer coefficient, 176  
physical absorption in, 176  
scaling ratio, 180  
string-of-disks column, 179  
string-of-spheres column, 179  
wetted wall tower, 176  
Single-stage adsorption, 548  
Single-stage distillation, 269  
Single-stage extraction, 378, 384  
Single-stage leaching, 432  
Single-stage operation, 124  
Size exclusion chromatography, 579  
Skarstrom cycle, 563  
Sloped downcomer, 168  
Slow reaction with absorption, 243

Solid thickness effect on drying, 459  
Solid-liquid equilibria, 428  
Solid-liquid extraction, 427  
Solubility, 215, 505  
Solution crystallization, 504  
Solutropes, 375  
Solutropic systems, 374  
Solvent extraction, 371  
Solvent selection, 215, 376  
Soret effect, 62  
Souders-Brown factor, 162  
Sparged vessel, 159  
Split tower arrangement, 307  
Spouted bed drier, 483  
Spray drier, 485  
Spray tower, 159, 195, 217  
Stage calculations, 124, 221  
Stage efficiency, 392  
Stage-wise contact, 124, 221, 377, 402, 432  
Stanton number, 82  
Static crystallization, 527  
Steady-state adsorber, 572  
Steady-state adsorption, 572  
Steady-state diffusion in binary system, 16  
Steady-state diffusion in solids, 50  
Steady-state operation, 137  
Steam distillation, 277  
Stefan tube method, 36  
Stokes-Einstein equation, 43  
String-of-disks column, 159, 178  
String-of-spheres column, 159, 179  
Stripping, 3, 209, 214, 244  
Stripping factor, 222  
Stripping section, 279  
Structure insensitive diffusion, 50  
Structure of membrane, 595  
Structure sensitive diffusion, 50  
Structured packing, 182, 187  
Supercritical carbon dioxide, 396  
Supercritical fluid system, 396  
Supersaturation, 508, 510, 514  
Surface diffusion, 61  
Surface reaction, 513  
Surface renewal theory, 115  
Surface stretch theory, 115  
Suspension based melt crystallization, 525  
Sweep diffusion, 5, 62  
Swenson Walker crystallizer, 519  
Symmetric membrane, 595  
Tangential flow filtration, 619  
Tellerette packings, 182, 185  
Temperature approach, 353  
Temperature swing regeneration, 565  
Ternary equilibrium, 373  
Ternary systems, 374  
Theoretical plate, 281  
Theoretical stage estimation, 380, 432  
Theory of drying, 455

Thermal boundary layer, 116  
Thermal diffusion, 5, 62  
Thermal swing sorption enhanced reaction (TSSER), 577  
Thermo-gravitational column, 62  
Thickeners–CCD units, 443  
Thickness of drying bed, 469  
Thiele-Geddes method, 301  
Through-circulation drying, 461, 469, 474  
Tie line, 284  
Time of drying, 463  
TNO purifier, 528  
Tortuous narrow channel, 603  
Total reflux, 285  
Tower diameter, 161  
Tower fills, 360  
Tower packing, 182  
Tower shell, 161  
Transient diffusion, 51  
Transmembrane pressure drop, 619  
Transport through membrane, 596  
Tray, 161  
Tray Column/Tower (also see Plate Column)  
arc downcomer, 168  
bubble-cap column, 159, 164  
bubble-cap tray, 165  
diameter, 163  
downcomer, 161, 166  
downcomer area, 162  
downcomer flooding, 162  
entrainment flooding, 162  
Fair's correlation, 162  
flow pattern of vapour and liquid, 166  
flow regimes, 167  
gas dispersed, 159  
liquid hold-up, 193  
local efficiency, 173  
Murphree plate efficiency, 173  
overall efficiency, 170, 175  
point efficiency, 175  
pressure drop, 163  
segmental downcomer, 168  
sieve-plate column, 159, 164, 166  
sloped downcomer, 168  
Souders-Brown factor, 162  
tower diameter, 161  
tower shell, 161  
tray, 161  
tray spacing, 161  
valve cap, 171  
valve tray, 159, 164, 171  
weeping, 164  
Tray drier, 474  
Tray spacing, 161  
Triangular diagram, 373  
Truck drier, 475  
Tubular module, 605  
Tunnel drier, 478  
Turbo-type drier, 479

Twin bulb method, 38  
Two stage condensation, 306  
Two-film theory, 111  
Two-resistance theory, 111  
Types of adsorption, 535  
Types of mass transfer coefficient, 74  
Types of membrane, 595  
Ultra performance liquid chromatography, 580  
Ultrafiltration, 616  
Unbound moisture, 455  
Underwood equation, 301  
UNIFAC, 266  
UNIQUAC, 266  
Unsteady-state adsorber, 574  
Unsteady-state adsorption, 574  
Unsteady-state diffusion, 51  
Unsteady-state diffusion in a cylinder, 56  
Unsteady-state diffusion in a slab, 52, 54  
Unsteady-state diffusion in a sphere, 54  
Vacuum rotary drier, 476  
Vacuum shelf drier, 475  
Vacuum swing adsorption (VSA), 557  
Valve cap, 171  
Valve tray, 159, 164, 171  
van Laar equation, 265  
Vapour diffusion, 461  
Vapour pressure, 260, 536  
Vapour recompression, 305  
Vapour-liquid equilibrium, 256  
Venturi scrubber, 196  
Vertical adsorber, 574  
Vibrating plate extractor, 409  
Volatility, 215  
Volmer equation, 511  
Volumetric filtration flux, 618, 625  
Wash column, 525  
Waste water treatment, 623  
Water conservation, 359  
Water cooling, 334, 344, 346  
Water loading, 362  
Weber number, 145, 412  
Weeping, 164  
Weir, 163  
Wet bulb depression, 340  
Wet bulb temperature, 339, 362  
Wet bulb temperature approach, 348  
Wet scrubber, 196  
Wetted wall tower, 159, 176  
Wilke and Chang equation, 44  
Wilson equation, 266  
Zeolites, 547